Nitrogen-neighboured single cobalt sites enable heterogeneous oxidase-type catalysis

Yong Cao (yongcao@fudan.edu.cn)
Fudan University
Qi zhang
Mi Peng
Peking University
Zirui Gao
Peking University
Wendi Guo
Fudan University
Zehui Sun
Fudan University
Yi Zhao
Fudan University
Wu Zhou
University of Chinese Academy of Sciences https://orcid.org/0000-0002-6803-1095
Meng Wang
Peking University
Bingbao Mei
Shanghai Institute of Applied Physics
Xianlong Du
Shanghai Institute of Applied Physics
Zheng Jiang
Shanghai Advanced Research Institute https://orcid.org/0000-0003-4297-464X
Wei Sun
Lanzhou Institute of Chemical Physics
Chao Liu
Lanzhou Institute of Chemical Physics, Chinese Academy of Sciences https://orcid.org/0000-0002-2521-924X
Yifeng Zhu
Dalian Institute of Chemical Physics
Yongmei Liu
Fudan University
Heyong He

Fudan University
Zhen Li
Fudan University
Ding Ma
Peking University https://orcid.org/0000-0002-3341-2998

Physical Sciences - Article

Keywords:

Posted Date: January 4th, 2022

DOI: https://doi.org/10.21203/rs.3.rs-1093028/v1

Title: Nitrogen-neighboured single cobalt sites enable heterogeneous oxidase-type catalysis

Authors: Qi Zhang,[1,8] Mi Peng,[2,8] Zirui Gao,[2,8] Wendi Guo,[1,8] Zehui Sun,[1] Yi Zhao,[1] Wu Zhou,[3,4]* Meng Wang,[2] Bingbao Mei,[5,6] Xianlong Du,[5] Zheng Jiang,[5,6] Wei Sun,[7] Chao Liu,[7] Yifeng Zhu,[1] Yongmei Liu,[1] Heyong He,[1] Zhen Hua Li,[1]* Ding Ma,[2]* Yong Cao[1]*

Affiliations:

[1]Shanghai Key Laboratory of Molecular Catalysis and Innovative Materials, Department of Chemistry, Fudan University, Shanghai, 200438, China.

[2]Beijing National Laboratory for Molecular Engineering, College of Chemistry and Molecular Engineering, Peking University, Beijing, 100871, China.

[3]School of Physical Sciences and CAS Key Laboratory of Vacuum Physics, University of Chinese Academy of Sciences, Beijing, 100049, China.

[4]CAS Center for Excellence in Topological Quantum Computation, University of Chinese Academy of Sciences, Beijing, 100049, China.

[5]Shanghai Institute of Applied Physics, Chinese Academy of Sciences, Shanghai, 201204, China.

[6]Shanghai Synchrotron Radiation Facility, Zhangjiang Lab, Shanghai Advanced Research Institute, Chinese Academy of Sciences, Shanghai, 201204, China.

[7]State Key Laboratory for Oxo Synthesis and Selective Oxidation, Suzhou Research Institute, Lanzhou Institute of Chemical Physics, Chinese Academy of Sciences, Lanzhou, 730000, China.

[8]These authors contributed equally to this work: Qi Zhang, Mi Peng, Zirui Gao, Wendi Guo.

*e-mail: yongcao@fudan.edu.cn (Y.C.); dma@pku.edu.cn (D.M.); lizhenhua@fudan.edu.cn (Z.H.L.); wuzhou@ucas.ac.cn (W.Z.)

Development of biomimetic catalytic systems that can imitate or even surpass natural enzymes remains an ongoing challenge [1–3]. This is particularly true in the context of accessing non-natural reactions by bioinspired approaches, which offer intriguing possibilities for benign and affordable chemical synthesis [4]. Exploiting the untapped potential of inorganic solids by translating complex knowledge in (bio)molecular-based systems may constitute a potentially useful strategy for such purpose [5], but efforts to capitalize on the minimum catalytic unit of a versatile solid matrix have been largely unsuccessful. Here, we show how an all-inorganic biomimetic system bearing robust nitrogen-neighboured single cobalt site/pyridinic-N site (Co-N_4/Py-N) pairs can act cooperatively as an oxidase mimic, which renders an engaged coupling of oxygen (O_2) reduction with synthetically beneficial chemical transformations. By developing this broadly applicable platform, the scalable synthesis of greater than 100 industrially and pharmaceutically appealing O-silylated compounds via the unprecedented aerobic oxidation of hydrosilane under ambient conditions is demonstrated. Moreover, this heterogeneous oxidase mimic also offers potential for expanding the catalytic scope of enzymatic synthesis. We anticipate that the strategy demonstrated here will pave a new avenue for understanding the underlying nature of redox enzymes and open up a new class of material systems for artificial biomimetics.

Expansion of mild selective oxidation routes that use O_2 is one of the ultimate goals of chemical research [6]. However, the exquisite control of O_2-consuming reactions still remains a daunting task due to the kinetic non-reactivity of O_2 without catalytic intervention [7]. In nature, evolution has afforded efficient and selective oxidases, which constitute a class of oxygen-utilizing enzymes that can catalyse the oxidation of a substrate via the co-generation of H_2O_2 (or H_2O) using O_2 as the terminal electron acceptor [8]. A particularly compelling scenario across the oxidase superfamilies hinges on the interplay between redox and base centres to drive a reaction cycle via the so-called proton-coupled hydride transfer (PCHT) pathway (Fig. 1A) [9,10].

Despite the fact that natural enzymes are synthetically beneficial in this context, they are expensive and highly sensitive to reaction conditions. Moreover, their inherent poor operational stability severely limits their practical utility. Therefore, it is imperative to develop new chemical approaches that mimic oxidase-like activity. In this regard, the molecular design of metal-ligand complexes as oxidase mimics has attracted attention [11–14]. However, attempts to mimic the remarkable ability of oxidases with organic-free materials have been mainly unsuccessful.

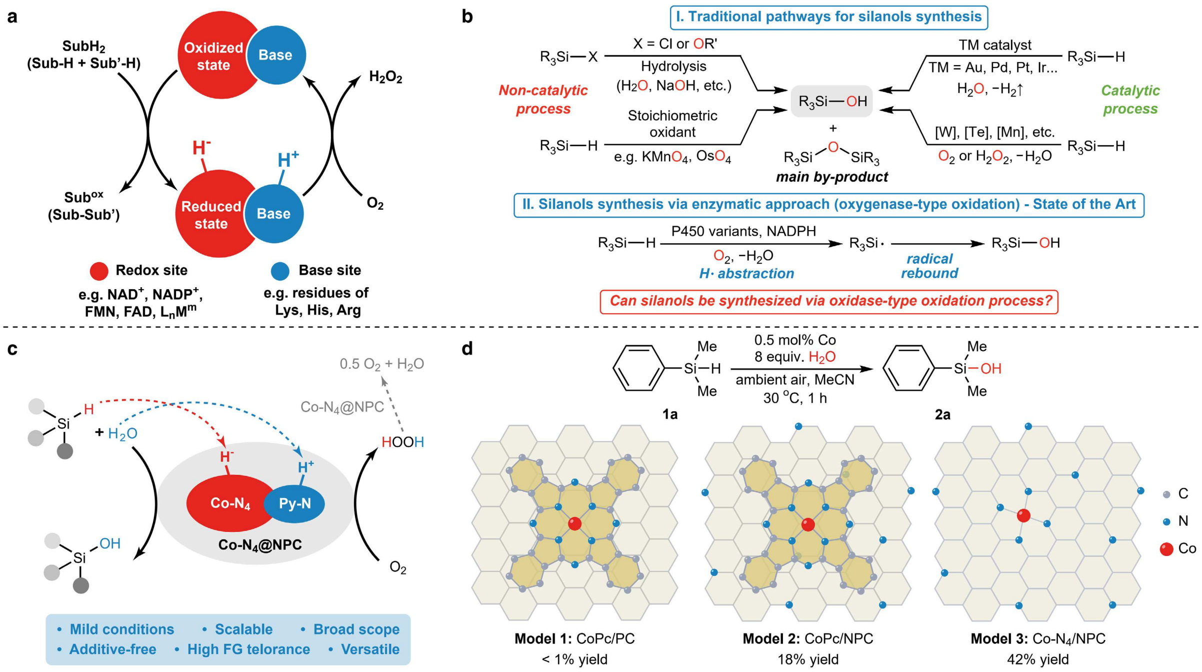

Fig. 1 | Oxidase-inspired aerobic hydrosilane-oxidizing. a, Simplified catalytic cycle of oxidase-catalyzed aerobic oxidation via PCHT pathway. **b**, Classical silanol synthesis methods. **c**, Proposed oxidase-type hydrosilane oxidation process catalyzed by all-inorganic biomimetics bearing independent redox-active Co-N4 sites and basic Py-N sites. **d**, CoPc-based or -derived oxidase-mimicking models for selective silane oxidation. Reactions were performed on 1 mmol scale, see supplementary materials catalytic performance evaluation section for details. Yields were determined by GC using anisole as an internal standard.

In this study, we present a new design of an all-inorganic biomimetic system which exhibits an oxidase-type catalytic activity far superior to that of natural enzymes. Silanols are key precursors for constructing Si-based structural motifs, which are found in a number of advanced functional materials [15]. In addition, silanols have been reported as pivotal intermediates for the synthesis of challenging bioactive agents in experimental pharmacology [16,17] and as catalysts because of their anion recognition ability [18]. Currently, silanols are mainly synthesized by the hydrolysis of chlorosilanes or oxidation of hydrosilanes by using strong oxidants (e.g., permanganate and OsO_4, etc.), which often produces toxic waste and involves tedious procedures (Fig. 1B, I, left paths) [15,19]. The transition-metal-catalysed hydrolytic conversion of hydrosilanes to silanols has been reported often using H_2O_2 as the oxidant (Fig. 1B, I, right paths) [20]. Recently, the selective oxygenase-type oxidation of silanes to silanols using O_2 with engineered cytochrome P450 enzymes has been reported (Fig. 1B, II) [21]. Unfortunately, the reported catalytic activity is extremely dependent on the reaction conditions, and the associated high costs can be a significant limitation for large-scale synthesis.

To realize the selective oxidase-type oxidation of silanes, a reaction that involves the PCHT-initiated co-activation of silane and H_2O and subsequent reaction of the resulting intermediate with O_2 to yield silanols and H_2O_2 was envisioned. By accommodating isolated redox-active centers on a suitably basified surface, such a process was anticipated to be realized (Fig. 1C). Cobalt phthalocyanine (CoPc) complexes are known to activate O_2 under mild conditions [22]. It could be combined with an N-doped carbon matrix bearing Lewis basic N sites to construct a dual-site biomimics, which is the starting point for the development of our catalyst. As a preliminary proof-of-concept, three designs were investigated in which the nature of cobalt sites as well as the availability of N species in the underlying carbonaceous supports derived from zeolitic imidazolate framework-8 (ZIF-8) [i.e. porous carbon (PC) and N-doped PC (NPC)] was changed (Supplementary Fig. 1): (i) CoPc deposited on PC (CoPc/PC), (ii) CoPc deposited on NPC (CoPc/NPC), and (iii) CoPc/NPC subjected to pyrolysis at 600 °C under flowing Ar (Co-N_4/NPC). CoPc/PC and CoPc/NPC were synthesized by the incipient wetness impregnation of the porous supports with N,N-dimethylformamide (DMF) solutions of CoPc and subsequent mild drying at 150 °C. For the last catalyst, the precise location and coordination environment of Co sites were different from those of the CoPc/NPC sample (Supplementary Figs. 2 and 3).

For the aerobic oxidation of dimethylphenylsilane (**1a**, in a mixture of acetonitrile/H_2O under atmospheric air at 30 °C), NPC-containing catalysts (i.e. CoPc/NPC and Co-N_4/NPC) afford the desired product (**2a**) in 18% and 42% yields, respectively (Fig. 1D), whereas the catalyst not doped with N in the corresponding support (CoPc/PC) was inactive. Furthermore, although CoPc/PC or NPC alone was barely active (Supplementary Table 1, entries 3 and 4), the reaction proceeded over a physical mixture of NPC and the CoPc/PC catalyst (Supplementary Table 1, entry 5), albeit with a considerably lower yield. In a set of control experiments conducted without O_2 or H_2O under otherwise similar reaction conditions, the transformation of the hydrosilane substrate was not observed (Supplementary Table 1, entries 6 and 7). In an additional control experiment using an electron-deficient analogue of CoPc/NPC (CoPc-16Cl/NPC), the yield of **2a** noticeably increased (Supplementary Table 1, entry 8). For these experiments, benefits of coupling between **1a**/H_2O and O_2 were identified to be beneficial for this catalytic system. Notably, the high formation efficiency of **2a** required extensive and substantive synergy, which was rendered by the close association of suitable single Co sites and reactive N species embedded in a carbon matrix.

To ensure an intimate proximity between the atomic Co and N sites and clarify the role of different N species, a series of ZIF-derived Co/N co-doped NPC catalysts (Co-N_4@NPC-T, where T denotes the pyrolysis temperature in °C) were prepared by the confined pyrolysis of bimetallic Co_1Zn_{50}-ZIF crystals (see Methods and Supplementary Fig. 4 for catalyst preparation). Co-N_4@NPC-900 exhibited the highest catalytic activity, with a turnover frequency (TOF) of 489 h^{-1} for the conversion of **1a** (Supplementary Fig. 5, metal loading determined by inductively coupled plasma optical emission spectrometry in Supplementary Table 6). Under pressurized air, the reaction rate was further accelerated, and the TOF significantly increased up to 1853 h^{-1} (Fig. 2A, Supplementary Fig. 6). This performance was in contrast to that observed using the nanoparticulate Co catalyst embedded in the NPC matrix (Co-NPs@NPC), the performance of which was independent of O_2 (Fig. 2A). Even under anaerobic conditions, Co-NPs@NPC afforded an equimolar amount of **2a** and H_2 (Supplementary Fig. 7), albeit with an extremely low efficiency. These results underscored the fact that the successful use of Co-N_4@NPC-900 might implicate an O_2-mediated PCHT pathway in lieu of a traditional hydrolytic oxidation process and that the efficiency of the Co site most likely depends on the access to a specific type of neighbouring N species.

The sole presence of isolated Co sites in Co-N_4@NPC-based catalysts was confirmed by aberration-corrected high-angle annular dark-field scanning transmission electron microscopy (HAADF-STEM) (Fig. 2B–D, Supplementary Fig. 8D–F) coupled with electron energy-loss spectroscopy (EELS) measurements (Fig. 2E, Supplementary Figs. 9 and 10). X-ray absorption spectroscopy (XAS) analysis revealed the absence of a Co-Co bond in the Co-N_4@NPC catalysts (Fig. 2F, Supplementary Fig. 11B). The single peak centred at 1.4 Å verified the coordination of cobalt to nitrogen (and possibly carbon as well) in the host. Extended X-ray absorption fine structure (EXAFS) fitting revealed that the Co-N coordination number is ~4 (Supplementary Table 2), indicative of the presence of Co-N_4 motifs. Notably, XAS measurements (Supplementary Fig. 12) and HAADF-STEM imaging revealed that Zn in the sample also was atomically dispersed with the absence of a Zn-Zn bond. Co *2p* X-ray photoelectron spectroscopy (XPS) (Supplementary Fig. 13B) and Co K-edge X-ray absorption near-edge structure (XANES) (Supplementary Fig. 11A) analysis revealed identical results for all Co-N_4@NPC-based samples. The N *1s* XPS featured five species bearing different orders of Lewis basicity, among which Py-N with a binding energy of 398.3 eV [23] was the most relevant N species based on the correlation of the relative N content evolution with the corresponding catalytic performance toward **2a** formation (Fig. 2, G and H, Supplementary Figs. 11 and 13). This characterization provided reasonable verification for our structural hypothesis as well as evidence substantiating the importance of the interplay between neighbouring Py-N and Co-N_4 sites to render oxidative catalysis.

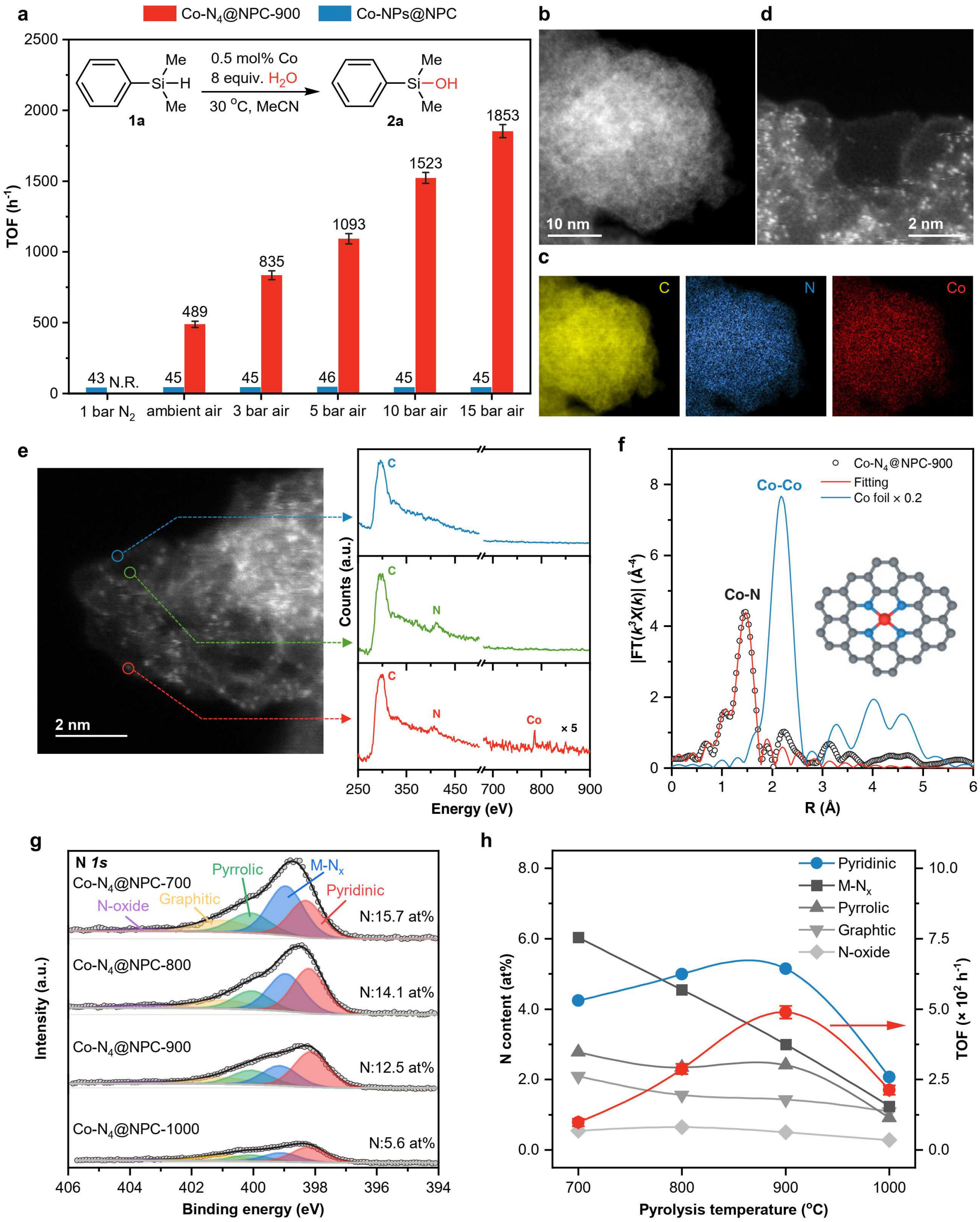

Fig. 2 | Performance and structural characterization of Co-N_4@NPC-based catalysts. a, The performance of Co-N_4@NPC-900 and Co-NPs@NPC in **1a** oxidation under different atmosphere. Reactions were performed on the 1 mmol scale. TOF was measured below 20%

1a conversion based on total Co atoms. Error bars represent standard deviation, calculated from at least three independent experiments. N.R. = no reaction. **b**, **c**, HADDF-STEM image (**b**) and the corresponding elemental maps (**c**) of C (yellow), N (blue) and Co (red) of Co-N_4@NPC-900. **d**, Atomic-resolution HADDF-STEM image of Co-N_4@NPC-900. **e**, EELS point spectra of different regions on Co-N_4@NPC-900. **f**, FT-EXAFS spectra of Co K-edge of Co-N_4@NPC-900. Shown are data (open circle) and fitting curve (red line) for Co-N_4@NPC-900 and corresponding data (blue line) for reference Co foil. The inset shows the schematic of Co-N_4 sites in Co-N_4@NPC-900. The red, blue and grey balls refer to Co, N, and C atoms, respectively. **g**, The high-resolution XPS N *1s* spectra of Co-N_4@NPC-based samples prepared with different pyrolysis temperatures. **h**, Structure-property relationships between the normalized N species content and catalyst effectiveness in Co-N_4@NPC-based samples.

On this basis, the overall reaction efficiency could be improved further by the increase in the surface density of vicinal Co-N_4/Py-N pairs via the re-introduction of Co-N_4 motifs into the Py-N-dominated Co-N_4@NPC matrix (Supplementary Figs. 14–16). The resultant Co-N_4@NPC-re catalyst exhibited an even higher TOF of 595 h^{-1} for **1a** conversion under ambient air, and it effectively facilitated the reaction even under a catalyst loading of 0.01 mol% (Supplementary Fig. 17). Notably, the Co-N_4@NPC-re material readily afforded excellent yields of **2a** at concentrations up to 4.3 M starting with **1a** (Supplementary Fig. 18), corresponding to conditions far better than those used for a natural or genetically engineered enzyme [21]. The robustness and stability of Co-N_4@NPC-re were further investigated in a flow-reaction mode for 300 h (supplementary information, continuous-flow reactions section including Supplementary Figs. 19–23). Notably, the catalyst was stable during the 300-h reaction without any noticeable structural change (Supplementary Figs. 24–27), affording a total turnover number (TON) of 130000 on the basis of the total amount of Co.

Real-time FTIR spectroscopy was employed to gain insights into the possible occurrence of proximity-driven oxidase-type catalysis (Fig. 3A, supplementary information, real-time FTIR experiments section including Supplementary Figs. 28–30). By monitoring the characteristic evolution of Si-OH vs its respective Si-H features during the aerobic oxidation of **1a** in the presence of 2 equiv. $H_2{}^{18}O$ over 0.1 mol% of Co-N_4@NPC-re at 30 °C, FTIR results provided direct molecular-level evidence for the immediate and exclusive incorporation of the ^{18}O-labelled hydroxyl species into the product. With the progress of the reaction, the Si-^{16}O stretching band at 880 cm^{-1} emerged, and it lagged consistently behind that of Si-^{18}O at 865 cm^{-1} (Fig. 3B). This alteration in the oxygen source during the conversion of **1a** to **2a** was interpreted as a sequential H_2O-mediated oxygen-atom transfer. This also considered the O_2-coupled intermediate H_2O_2 formation (Supplementary Figs. 31, 32A and B) and the favourable impact of Co-N_4@NPC-re for rapid H_2O_2 destruction (Supplementary Fig. 32C). Furthermore, based on results of the radical scavenger effect (Supplementary Fig. 33) and kinetic isotope effects associated with **1a** conversion (Supplementary Table 3), this reaction did not involve reactive oxygen species (ROS) and silyl radicals as intermediates, and the rate-limiting step for biomimetic turnover involved the breaking of the Si-H bond.

Density functional theory (DFT) calculations were employed to obtain additional information about the specific nature of oxidase-type PCHT. A CoN_4C_{10} motif in combination with a Py-N moiety was used to represent the Co-N_4@NPC-based catalyst (see computational details in Methods section including Supplementary Fig. 34 in supplementary information). Figure 3C shows the catalytic cycle for the aerobic-hydrolytic oxidation of **1a** in Co-N_4@NPC, and Supplementary Fig. 35 shows the associated free-energy profile. The co-adsorption of **1a** and O_2 on the CoN_4C_{10} motif was the first step in the catalytic reaction, where charge transfer from the axially ligated O_2 to the Co atom enhanced the binding of **1a** to the Co-N_4 site. This aided in the activation of the Si–H bond in a polarised manner. The proposed mechanism for O_2-assisted Si-H bond activation to form adduct **I** was completely supported by **1a**/O_2 adsorption analysis based on *in situ* diffuse reflectance FTIR measurements (Supplementary

Fig. 37). Then, activated **1a** species served as the initial species in the catalytic cycle. The reaction was proposed to proceed in the following four steps. After the formation of adduct **I**, the facile cleavage of the H_2O-assisted Si-H bond to afford **2a** occurred via a concerted linear S_N2-type dehydride mechanism (CLS_N2D, **Step 2** in Fig. 3C), a pathway that required the participation of Py-N species to facilitate the deprotonation of H_2O bonded to the Si atom in adduct **I**.

To further investigate the validity of the proposed CLS_N2D mechanism, an alternative pyrrolic-N or graphitic-N-assisted deprotonation pathway was calculated. The resulting barriers for such processes were elevated (with ΔG = –22.2, 14.5 and 48.0 kcal/mol for initiating the crucial deprotonation step with Py-N, pyrrolic-N and graphitic-N, respectively, Supplementary Fig. 38), providing support for the CLS_N2D mechanism. Moreover, an experiment dealing with the oxidation of an optically active hydrosilane ***R*-1b** (95% *ee*) with O_2 revealed inversion of the configuration at silicon (Supplementary Fig. 39), thereby further supporting the proposed CLS_N2D mechanism as the favoured pathway for silanol formation over a relatively straightforward process involving the hetero- or homolysis of the Si-H bond. Subsequently, the insertion of O_2 into the resulting cobalt hydride **III** to form cobalt hydroperoxide **IV** occurred. The formation of **IV** enabled the rapid formation of HOOH* without any barrier via the transfer of proton to the O atom bonded to the Co atom, ultimately affording H_2O_2 and regenerating the initial Co-N_4 catalyst structure (**Steps 3–5** in Fig. 3C). This reaction was exothermic by 17.3 kcal/mol. The contribution of H_2O_2 to this oxidation reaction was examined. However, on evaluating the reaction efficacy by the experimental replacement of O_2 with a stoichiometric amount of H_2O_2, the reaction barely proceeded (Supplementary Fig. 32D). This result suggested that H_2O_2 exerts a minimal effect on the aerobic oxidation of **1a**, apparently as a result of the rapid disproportionation of H_2O_2 in the presence of Co-N_4@NPC-re under (an)aerobic conditions (Supplementary Fig. 32C).

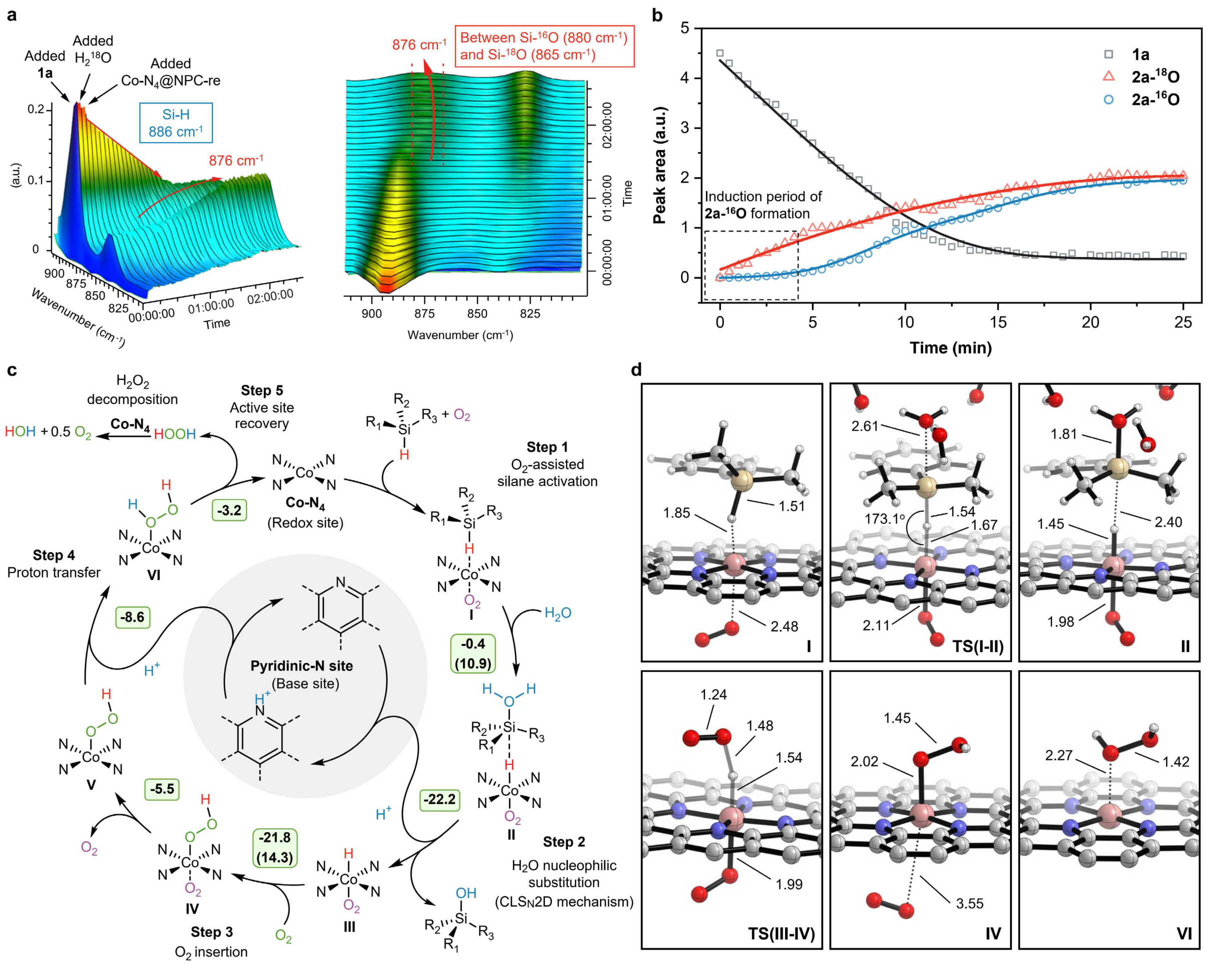

Fig. 3 | Reaction mechanism for Co-N$_4$@NPC-catalyzed selective aerobic hydrosilane oxidation. **a**, Real time FT-IR kinetic studies of the reaction of **1a** in MeCN/H$_2^{18}$O mixture under ambient air using Co-N$_4$@NPC-re as catalyst. Reaction conditions: **1a** (5 mmol), H$_2^{18}$O (10 mmol), Co-N$_4$@NPC-re (Co 0.1 mol%), anhydrous MeCN (15 mL), 30 °C. **b**, Temporal changes of the spectral intensity in Si-^{16}O stretching frequency of **2a-^{16}O** (880 cm^{-1}), Si-^{18}O stretching frequency of **2a-^{18}O** (865 cm^{-1}) and Si-H bending frequency in **1a** (886 cm^{-1}). The spectra were analyzed by deconvolution of the peaks between 840 to 920 cm^{-1}. **c**, A proposed full catalytic cycle of Co-N$_4$@NPC-catalyzed aerobic oxidation of hydrosilanes, as well as the free-energy changes and free-energy barriers (in parentheses) between the corresponding key steps. The energy values are in kcal/mol. **d**, DFT-optimized main intermediates and transition state structures of catalytic cycle. Co, pink; O, red; C, grey; N, blue; H, white. Key distances are given in Å and angles in degrees. For clarity, some hydrogen atoms were hidden.

The general applicability of this catalyst was demonstrated by the selective oxidation of greater than 70 diverse organosilanes with different electronic and steric properties (Fig. 4A and Supplementary Fig. 40). The scope of this chemistry was further extended to the straightforward synthesis of borasiloxanes containing [B-O-Si] motifs by the direct oxidative-hydrolytic conversion of silanes with boranes (Fig. 4B). These motifs are valuable precursors for borosilicate materials, heat- and chemical-resistant polymers, and polymer sensors [24–26]. Moreover, by the application of a single Co-mediated oxidase-type catalyst, selected silyl ethers were prepared starting from silanes and alcohols (Fig. 4C). Silyl ethers are of special interest due to their prevalence in a number of technologically important and functional materials [27]. This class of compounds is routinely prepared either by the dehydrogenative coupling of hydrosilanes with alcohols [28] or by the reaction of halosilanes with alcohols in the presence of a base [29]. Compared with existing Si-alkoxylation processes, the developed single Co-catalysed synthesis of silyl ethers features advantages of more cost-effectiveness or more facile scalability.

Finally, the ability to accomplish oxidase-type oxidation chemistry with these vicinal Co-N_4/Py-N pairs permitted for the oxidation of broader range of substrates without the incorporation of oxygen in the reaction products (Fig. 4D). For example, the oxidative dimerization of 2-naphthol (**7**) to 1,1′-binaphthyl-2,2′-diol (**8**) was successfully achieved. This product comprised binaphthyl backbones, a particularly important scaffold for asymmetric catalysis [30]. Similarly, the oxidative carbonylation of aniline (**9**) to N,N′-diphenyl urea (**10**) was accomplished. Remarkably, the aerobic oxidative cyclization of 2-aminophenol (**11**) also proceeded smoothly under green and mild conditions with an excellent product yield, permitting safe and facile access to biologically and pharmaceutically relevant 2-aminophenoxazin-3-one (**12**). Therefore, inspiration from this developed strategy will exert a key impact on biomimicking chemistry by leading to the discovery of new redox-related pathways as well as enabling the generation of completely green, affordable biomimetic catalytic systems.

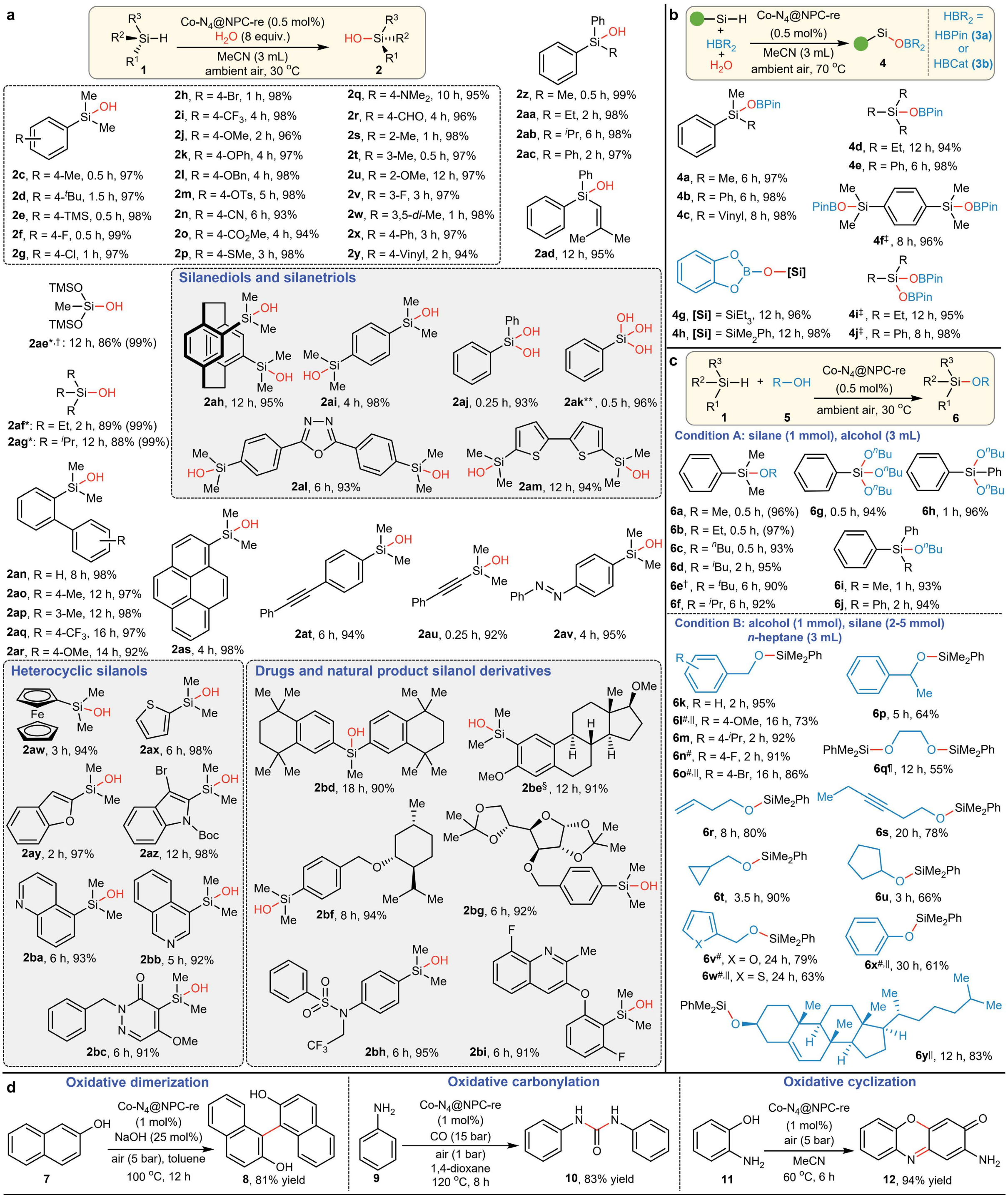

Fig. 4 | Scope of Co-N$_4$@NPC-catalyzed oxidase-type transformations. See supplementary information for experimental details. Reactions were typically performed on 1 mmol scale under air atmosphere. Isolated yields are reported unless otherwise indicated. Yields in parentheses refer to GC yield. **a**, Substrate scope of silane substrates. **b**, Multicomponent synthesis of borosiloxanes. **c**, Oxidative cross-coupling of hydrosilanes and alcohols. **d**, Applications in a variety of other oxidase-like reactions. *10 mmol scale. †Under O_2 (1 bar) atmosphere. **Using acetone as solvent. §Using 5 mL MeCN. ‡2.0 equiv. **3a** and 2.0 equiv. H_2O. #Using toluene as solvent, 3.0 equiv. **1a**. ¶Using toluene/MeCN (v/v = 2:1) as solvent, 5.0 equiv. **1a**. ||60 °C. TMS, trimethylsilyl; Bn, benzyl; Ts, tosyl; Boc, *tert*-butyloxycarbonyl; HBPin, pinacolborane; HBCat, catecholborane.

Main References

1. Chen, J. *et al.* Carbonyl catalysis enables a biomimetic asymmetric Mannich reaction. *Science* **360,** 1438–1442; 10.1126/science.aat4210 (2018).
2. Guan, J. *et al.* Water oxidation on a mononuclear manganese heterogeneous catalyst. *Nat. Catal.* **1,** 870–877; 10.1038/s41929-018-0158-6 (2018).
3. Le Goff, A. *et al.* From hydrogenases to noble metal-free catalytic nanomaterials for H_2 production and uptake. *Science* **326,** 1384–1387; 10.1126/science.1179773 (2009).
4. Liu, W., Lavagnino, M. N., Gould, C. A., Alcázar, J. & MacMillan, D. W. C. A biomimetic S_H2 cross-coupling mechanism for quaternary sp^3-carbon formation. *Science,* eabl4322; 10.1126/science.abl4322 (2021).
5. Ragg, R., Tahir, M. N. & Tremel, W. Solids go bio: Inorganic nanoparticles as enzyme mimics. *Eur. J. Inorg. Chem.* **2016,** 1906–1915; 10.1002/ejic.201501237 (2016).
6. Jiao, N. & Stahl, S. S. (eds.). *Green oxidation in organic synthesis* (Wiley-VCH, 2019).
7. Borden, W. T., Hoffmann, R., Stuyver, T. & Chen, B. Dioxygen: What makes this triplet diradical kinetically persistent? *J. Am. Chem. Soc.* **139,** 9010–9018; 10.1021/jacs.7b04232 (2017).
8. Valentine, J. S., Foote, C. S., Greenberg, A. & Liebman, J. F. *Active oxygen in biochemistry* (Springer US, Boston, MA, 1995).

9. Romero, E., Gómez Castellanos, J. R., Gadda, G., Fraaije, M. W. & Mattevi, A. Same substrate, many reactions: Oxygen activation in flavoenzymes. *Chem. Rev.* **118,** 1742–1769; 10.1021/acs.chemrev.7b00650 (2018).

10. Ghisla, S. & Massey, V. Mechanisms of flavoprotein-catalyzed reactions. *Eur. J. Biochem.* **181,** 1–17; 10.1111/j.1432-1033.1989.tb14688.x (1989).

11. Roux, Y., Ricoux, R., Avenier, F. & Mahy, J.-P. Bio-inspired electron-delivering system for reductive activation of dioxygen at metal centres towards artificial flavoenzymes. *Nat. Commun.* **6,** 8509; 10.1038/ncomms9509 (2015).

12. Largeron, M. & Fleury, M.-B. Bioinspired oxidation catalysts. *Science* **339,** 43–44; 10.1126/science.1232220 (2013).

13. Wang, Y., DuBois, J. L., Hedman, B., Hodgson, K. O. & Stack, T. D. Catalytic galactose oxidase models: Biomimetic Cu(II)-phenoxyl-radical reactivity. *Science* **279,** 537–540; 10.1126/science.279.5350.537 (1998).

14. Chaudhuri, P., Hess, M., Flörke, U. & Wieghardt, K. From structural models of galactose oxidase to homogeneous catalysis: Efficient aerobic oxidation of alcohols. *Angew. Chem. Int. Ed.* **37,** 2217–2220; 10.1002/(SICI)1521-3773(19980904)37:16<2217::AID-ANIE2217>3.0.CO;2-D (1998).

15. Jeon, M., Han, J. & Park, J. Catalytic synthesis of silanols from hydrosilanes and applications. *ACS Catal.* **2,** 1539–1549; 10.1021/cs300296x (2012).

16. Ramesh, R. & Reddy, D. S. Quest for novel chemical entities through incorporation of silicon in drug scaffolds. *J. Med. Chem.* **61,** 3779–3798; 10.1021/acs.jmedchem.7b00718 (2018).

17. Franz, A. K. & Wilson, S. O. Organosilicon molecules with medicinal applications. *J. Med. Chem.* **56,** 388–405; 10.1021/jm3010114 (2013).

18. Kondo, S.-I., Harada, T., Tanaka, R. & Unno, M. Anion recognition by a silanediol-based receptor. *Org. Lett.* **8,** 4621–4624; 10.1021/ol061822p (2006).

19. Chandrasekhar, V., Boomishankar, R. & Nagendran, S. Recent developments in the synthesis and structure of organosilanols. *Chem. Rev.* **104,** 5847–5910; 10.1021/cr0306135 (2004).

20. Wang, K. *et al.* Selective manganese-catalyzed oxidation of hydrosilanes to silanols under neutral reaction conditions. *Angew. Chem. Int. Ed.* **58,** 6380–6384; 10.1002/anie.201900342 (2019).

21. Bähr, S. *et al.* Selective enzymatic oxidation of silanes to silanols. *Angew. Chem. Int. Ed.* **59,** 15507–15511; 10.1002/anie.202002861 (2020).

22. Jasinski, R. A new fuel cell cathode catalyst. *Nature* **201,** 1212–1213; 10.1038/2011212a0 (1964).

23. He, L., Weniger, F., Neumann, H. & Beller, M. Synthesis, characterization, and application of metal nanoparticles supported on nitrogen-doped carbon: Catalysis beyond electrochemistry. *Angew. Chem. Int. Ed.* **55,** 12582–12594; 10.1002/anie.201603198 (2016).

24. Peña-Alonso, R., Mariotto, G., Gervais, C., Babonneau, F. & Soraru, G. D. New insights on the high-temperature nanostructure evolution of SiOC and B-doped SiBOC polymer-derived glasses. *Chem. Mater.* **19,** 5694–5702; 10.1021/cm071203q (2007).

25. Puneet, P., Vedarajan, R. & Matsumi, N. Alternating poly(borosiloxane) for solid state ultrasensitivity toward fluoride ions in aqueous media. *ACS Sens.* **1,** 1198–1202; 10.1021/acssensors.6b00346 (2016).

26. Wu, T. & Chen, B. Synthesis of multiwalled carbon nanotube-reinforced polyborosiloxane nanocomposites with mechanically adaptive and self-healing capabilities for flexible conductors. *ACS Appl. Mater. Interfaces* **8,** 24071–24078; 10.1021/acsami.6b06137 (2016).

27. Kamino, B. A. & Bender, T. P. The use of siloxanes, silsesquioxanes, and silicones in organic semiconducting materials. *Chem. Soc. Rev.* **42,** 5119–5130; 10.1039/c3cs35519e (2013).

28. Asensio, J. M., Bouzouita, D., van Leeuwen, P. W. N. M. & Chaudret, B. σ-H-H, σ-C-H, and σ-Si-H bond activation catalyzed by metal nanoparticles. *Chem. Rev.* **120,** 1042–1084; 10.1021/acs.chemrev.9b00368 (2020).

29. Hatano, B., Toyota, S. & Toda, F. Efficient solvent-free O-silylation of alcohols with R_3SiCl. *Green Chem.* **3,** 140–142; 10.1039/b102447g (2001).

30. Parmar, D., Sugiono, E., Raja, S. & Rueping, M. Complete field guide to asymmetric BINOL-phosphate derived Brønsted acid and metal catalysis: History and classification by mode of activation; Brønsted acidity, hydrogen bonding, ion pairing, and metal phosphates. *Chem. Rev.* **114,** 9047–9153; 10.1021/cr5001496 (2014).

Methods

Chemicals

All materials were used without further purification, unless otherwise stated. Cobalt nitrate hexahydrate ($Co(NO_3)_2·6H_2O$, ≥98.5%), zinc nitrate hexahydrate ($Zn(NO_3)_2·6H_2O$, ≥99.0%), cobalt acetate tetrahydrate ($Co(OAc)_2·4H_2O$, ≥99.5%), ammonium chloride (NH_4Cl, ≥99.5%), ammonium hydroxide ($NH_3·H_2O$, 25.0-28.0%), methanol (MeOH, ≥99.7%), ethanol (EtOH, ≥99.7%) and acetonitrile (MeCN, ≥99.5%) were purchased from Sinopharm Chemical Reagent Co., Ltd. 2-Methylimidazole (2-MeIm, 98%), 1,10-phenanthroline (99%) and dimethylphenylsilane (97%) were purchased from Aladdin.

Preparation of catalysts

Synthesis of Co-N_4@NPC-T catalysts. The Co-N_4@NPC-T catalysts, where T represents the carbonization temperature (T = 700, 800, 900, and 1000 °C), were synthesized by using low Co/Zn ratio bimetallic ZIF (Co_1Zn_{50}-ZIF) as precursor. The molar ratio of metal ions to 2-

MeIm remained at 1:8 and the concentration of metal ions in final mixed solution was controlled at an optimal concentration of 25 mmol/L. The typical synthesis process of Co-N_4@NPC-900 is given as follows. A solution of 2-MeIm (13.4 g, 163.2 mmol) in 408 mL MeOH was added to a solution of $Co(NO_3)_2 \cdot 6H_2O$ (0.116 g, 0.4 mmol) and $Zn(NO_3)_2 \cdot 6H_2O$ (5.95 g, 20 mmol) in 408 mL MeOH. After stirred at room temperature (RT, ~25 ^{o}C) for 24 h, the obtained Co_1Zn_{50}-ZIF precipitates was were collected by centrifugation, wash with MeOH for three times and then dried under vacuum at RT overnight. Subsequently, 1.0 g as-prepared Co_1Zn_{50}-ZIF precursor was heated at 900 ^{o}C for 4 h under the flowing Ar atmosphere (80 mL/min) in a tube furnace, followed by naturally cooling down to RT. Co-N_4@NPC-NL-900 was obtained as a black powder.

Next, ammonia treatment in 2.0 mol/L NH_3/NH_4Cl aqueous solution (sum concentration of initial ammonium ion and ammonia, the molar ratio of ammonium to ammonia was 1:1) at RT for 8 h was carried out to remove Zn species and to generate more favorable open porosity in Co-N_4@NPC-NL-900 samples. Typically, 100 mL leaching solution was used for 100 mg sample. An additional pyrolysis treatment at 900 ^{o}C under the flowing Ar atmosphere for 4 h is necessary to repair the carbon nanostructures. After naturally cooling to RT, Co-N_4@NPC-900 was obtained.

Co-N_4@NPC-700, Co-N_4@NPC-800 and Co-N_4@NPC-1000 were synthesized by using Co_1Zn_{50}-ZIF as precursor following similar procedure to that of Co-N_4@NPC-900 preparation except that the pyrolysis and additional pyrolysis temperature were 700, 800 and 1000 ^{o}C, respectively.

Synthesis of Co-N_4@NPC-re catalyst. For synthesis of Co-N_4@NPC-re, $Co(OAc)_2 \cdot 4H_2O$ (12.7 mg, 0.05 mmol) and 1,10-phenanthroline (27.6 mg, 0.15 mmol) were dissolved in 25 mL EtOH and stirred for 30 min at RT. Then 300 mg ammonia-treated Co-N_4@NPC-NL-900 samples was added and stirred for 4 h at 60 °C. The solvent was removed by rotary evaporation and thus obtained solid was dried under vacuum at RT overnight. A subsequent pyrolysis treatment at 900 °C under the flowing Ar atmosphere (80 mL/min) for 4 h was conducted to obtain the final Co-N_4@NPC-re sample.

Synthesis of Co-NPs@NPC catalyst. Co-NPs@NPC catalysts were synthesized by using high Co/Zn ratio bimetallic ZIF (Co_1Zn_2-ZIF) as precursor. Co_1Zn_2-ZIF was synthesized using similar synthesis procedure of Co_1Zn_{50}-ZIF except that the Zn/Co molar ratio in starting materials was 2:1. Then, as-prepared Co_1Zn_2-ZIF precursor was pyrolysized at 900 °C for 4 h under the flowing Ar atmosphere (80 mL/min) in a tube furnace. After cooling to RT naturally, Co-NPs@NPC was obtained as a black powder without further treatment.

Evaluation of catalytic performance

Normal pressure reactions (ambient air or N_2). Dimethyl-phenylsilane (**1a**, 155 μL, 1 mmol) and water (145 μL, 8 mmol) were mixed with solvent (3 mL) in a 15 mL oven-dried round-bottom tube with steady magnetic stirring (800 rpm) at 30 °C under an ambient atmosphere of air. The reaction was started by the addition of a certain amount of catalyst (metal: 0.5 mol%) and the mixture was allowed to stir for required reaction time. After completion of the reaction, the catalyst was filtered by 0.2 μm syringe filter. For determining conversion and selectivity, anisole (50 μL) used as an internal standard was added to 1 mL filtrate and the mixture was analyzed by GC (Agilent 7820A gas chromatograph with FID detector and 30 m×0.32 mm×0.25 μm HP-INNOWax capillary column). The initial TOF was measured at **1a** conversion below 20% based on total Co atoms.

For evaluating the catalytic performances under N_2 atmosphere, reactions were carried out in a N_2-filled glovebox (MIKROUNA Super; typically < 1 ppm oxygen and water). The catalysts used in such reaction conditions were first evacuated under dynamic vacuum (~ 0.1 torr) at 150 °C for 4 h to remove gas molecules in nanopores and stored under inert atmosphere. Solvent was degassed by three freeze-pump-thaw procedure cycles before used. The reaction procedure and analytical method was the same as that used for catalytic performance evaluation under ambient air atmosphere.

Pressurized reactions. In a N_2-filled glovebox, a mixture of **1a** (155 μL, 1 mmol), water (145 μL, 8 mmol) and degassed solvent (3 mL) was charged into a 25 mL Hastelloy-C high pressure reactor (Beijing Century Senlang Experimental Apparatus Co., Ltd.; contain a stainless steel sampling tube with filter). Then, catalyst (metal: 0.5 mol%) was added and the reactor was sealed. After removing from the glovebox, the reactor was immersed into a pre-heated water bath (30 °C) and connected with a gas cylinder of air. The reaction was started by pressurizing the reactor to given pressure (3-15 bar) and the gas source was kept connected during the reaction. After stirring for a certain period of time, the reaction liquid was taken from the reactor through sampling tube. The conversion and selectivity were determined by GC using anisole as an internal standard.

Catalyst characterization

Element analysis. The contents of metal elements in the samples were measured by inductively coupled plasma optical emission spectroscopy (ICP-OES) using PerkinElmer Optima 2100DV spectrometer. The samples were first digested by hot perchloric acid and then dissolved in hot aqua regia.

XRD analysis. The XRD patterns were collected on a Bruker D8 Advance X-ray diffractometer using a monochromatic Cu Kα (λ=1.5418 Å) source at 40 kV and 40 mA.

Raman spectroscopy. Raman spectra were collected on a HORIBA LabRAM HR Evolution high resolution Raman spectrometer. A 514.5 nm Ar^+ laser was used as the excitation source.

Nitrogen-adsorption and desorption isotherms. The test was performed at 77 K using Micromeritics ASAP 2460 Surface Area and Porosity Analyzer. The specific surface area of sample was estimated by Brunauer-Emmett-Teller (BET) method. The samples were first evacuated under dynamic vacuum (< 10^{-3} torr) at 150 °C for 12 h to remove the guest molecules and adsorbed moisture before re-measuring the accurate sample weight.

FT-IR spectroscopy. FT-IR transmittance spectra were collected on a Nicolet iS10 TF-IR spectrometer with a DTGS detector. The samples were mixed with KBr and made into a small tablet for test. The spectra were obtained by averaging 64 scans with a resolution of 0.5 cm^{-1} over wavenumbers ranging from 400 to 4000 cm^{-1}.

Electron microscopy. The SEM images were acquired on a Zeiss Merlin Compact microscope operated at 10 kV. The samples were prepared by drop-drying the samples from their diluted EtOH suspensions onto silicon slices. The TEM and HRTEM images were acquired on a FEI Tecnai G2 F20 S-Twin operated at 200 kV. Atomic resolution HAADF-STEM images and EELS spectra of samples were captured on a Nion UltraSTEM U100 operated at 60 kV. The HAADF-STEM images were collected with an annular dark field detector in the range of 86-200 mrad with a convergence angle of 30 mrad. EELS was carried out with the same experimental set-up. Samples for TEM were prepared by drop-drying the samples from their diluted EtOH suspensions onto TEM grids.

XPS analysis. The XPS measurements were conducted on a Kratos Axis Ultra Imaging Photoelectron Spectrometer equipped with a monochromatic Al Kα (1486.6 eV) source. The samples were fixed on conductive tapes and introduced into the UHV chamber. The pressure in the analysis chamber was maintained below 5×10^{-9} Torr for data acquisition. The high-resolution spectra were performed at a pass energy of 20 eV and steps of 0.1 eV. The photoelectrons were detected at a takeoff angle of 0° with respect to the surface normal. The binding energy scale was calibrated by assigning the main C 1s peak at 284.6 eV.

XAFS analysis. XAFS measurements at Co K-edge and Zn K-edge under fluorescence mode were performed at the BL14W1 in Shanghai Synchrotron Radiation Facility (SSRF) using a Lytle detector. The electron beam energy was 3.5 GeV and the stored current was 230 mA (top-up). A 38-pole wiggler with the maximum magnetic field of 1.2 T inserted in the straight section of the storage ring was used. The station was operated with a fixed-exit double-crystal Si (111) monochromator. The XAFS samples were prepared by mixing with paraffin wax (Sigma-Aldrich, mp 58-62 °C), then making into a small tablet (8.0 mm diameter) and sealing in a chamber with Kapton tape. Co foil and Zn foil were used as standard reference materials and the X-ray absorption data were recorded in transmission mode using ion chambers. The raw data analysis was performed using IFEFFIT software package [31] according to the standard data analysis procedures. The spectra were calibrated, averaged, pre-edge background subtracted, and post-edge normalized using Athena program in IFEFFIT software package. The Fourier transformation of the k^3-weighted EXAFS oscillations, $k^3 \cdot \chi(k)$, from k space to R space was performed to obtain a radial distribution function. And data fitting was done by Artemis program in IFEFFIT. The wavelet transform (WT) analysis was using FORTRAN program HAMA developed by H. Funke and M. Chukalina [32]. The *k*-space file of each sample which contains the data of exact *k* range of Fourier transformation was processed after running the code, following which the *k* space, *R* space spectra and the continuous wavelet transform figure were generated automatically.

DRIFT spectroscopy. The DRIFT spectra of chemisorbed **1a** were recorded in an in-situ diffuse reflectance cell (Harrick) equipped with a CaF_2 window on a ThermoFisher Nicolet 6700 FT-IR spectrometer, using an MCT detector. Samples (ca. 20 mg) were pretreated at 250 ^{o}C for 1 h with flowing He (20 mL/min), then treated by **1a** at 15 ^{o}C with air (presence of O_2) or He (absence of O_2) gas flow (20 mL/min). The collected spectra were subtracted from the sample background spectra in He to obtain the spectra for chemisorbed **1a**.

Computational details

Quantum chemical calculations were all performed at the density functional theory (DFT) level using the Gaussian 16 software package [33]. The DFT functional used is the MN15 functional [34]. The models of CoPc, CoPc-16Cl, CoN_4C_{10} motif (based on XANES spectra analysis, see Supplementary Figs. 41 and 42 and Supplementary Discussion 1) and N-doped graphene sheets are reported in Supplementary Fig. 4. In this work, the working catalyst, Co-N_4@NPC-based catalyst was modeled by a CoN_4C_{10} cluster model. Cluster and slab models are two commonly used models to approximate the activity centers of heterogeneous catalysts. Using cluster model, we can carefully choose a well-validated DFT functional, MN15, which is very accurate for reaction energetics. This cannot be done if a slab model was used because there are just a few functionals, such as the PBE and PW91 functionals, implemented in the commonly used periodic software packages and these functionals are not very accurate in computing energy barriers. In addition, solvation effect is difficult to deal with if slab model was used but it plays a critical role in our catalytic system. Here we carefully designed the cluster model so that it can well represent the catalytic center. Besides, our experiments showed that there are some similarities between the model CoPc and CoPc-16Cl catalysts and the working catalyst. Because CoPc and CoPc-16Cl are molecular catalysts, the similarity between the CoPc/CoPc-16Cl catalysts and the Co embedded N-doped graphene catalyst indicates that it is reasonable to use the CoN_4C_{10} cluster to model the catalyst.

In the simulation, a moderate basis set (MBS), which was a combined basis set in which the aug-cc-pVDZ basis set [35] was employed to Co atom, the 6-31+G(d,p) basis set [36,37] was employed for the atoms of the reaction center (four N atoms, Si atom, three O atoms on O_2 and H_2O, three hydrogen atoms on Si-H and H_2O, respectively) and the 6-31G(d) basis set [36,37] was employed for the other atoms, was used for geometry optimization. Single-point energies were calculated under a larger basis set (LBS) on the geometries that optimized with the modest basis set to provide more accurate energetic results. For single-point energies calculation, the aug-cc-pVTZ basis set was employed to Co atom, the 6-311++G(3df,2p) basis set [38,39] was employed for the atoms of the reaction center and the 6-311+G(d,p) basis set [38,39] was employed for the other atoms. Except O_2 molecule, DFT calculations for other species were performed in the MeCN solution which was modelled by the polarizable continuum solvation model (IEFPCM) [40] with radii and non-electrostatic terms for Truhlar and coworkers' SMD solvation model [41]. This solvation model is by far the most reliable one in predicting solvation free energies. The convergence criteria used for the geometry optimization were 4.50×10^{-4} au. for gradients, and 1.80×10^{-3} au. for displacements. Harmonic vibrational analyses were carried out to confirm if the optimized structure is a local minimum structure or a first order transition state and to provide zero-point vibrational energy corrections and thermal corrections to various thermodynamic properties. Transition states were further confirmed by IRC calculations. Optimized DFT structures were illustrated using CYLView [42].

The free energy of each species at 298.15 K under standard state (G_{298}) was calculated by:

$$G_{298} = G_{solv} + ZPE + \Delta G_{0\sim298} + \Delta G_C$$

where G_{solv} is the single-point energy of species that calculated under LBS after considering the solvation effect (for O_2, it is the electron energy in the gas phase), ZPE is the zero-point vibrational energy that approximately calculated by harmonic vibration approximation under MBS, $\Delta G_{0\sim298}$ is the Gibbs free-energy change from 0 to 298.15 K calculated under harmonic vibration and rigid rotor approximation and ΔG_C is the free-energy correction for standard state (for O_2 it is 0, for species in solvent it is 1.90 kcal/mol).

Data availability

The data supporting the findings of this study are available within the article and its Supplementary Information files. All other relevant source data are available from the corresponding authors upon reasonable request.

Methods References

31. Ravel, B. & Newville, M. ATHENA, ARTEMIS, HEPHAESTUS: Data analysis for X-ray absorption spectroscopy using IFEFFIT. *J. Synchrotron. Rad.* **12,** 537–541; 10.1107/S0909049505012719 (2005).

32. Funke, H., Scheinost, A. C. & Chukalina, M. Wavelet analysis of extended x-ray absorption fine structure data. *Phys. Rev. B* **71**; 10.1103/PhysRevB.71.094110 (2005).

33. Frisch, M. J. *et al. Gaussian 16.* Gaussian, Inc. (Wallingford CT, 2016).

34. Yu, H. S., He, X., Li, S. L. & Truhlar, D. G. MN15: A Kohn-Sham global-hybrid exchange-correlation density functional with broad accuracy for multi-reference and single-reference systems and noncovalent interactions. *Chem. Sci.* **7,** 5032–5051; 10.1039/c6sc00705h (2016).

35. Woon, D. E. & Dunning, T. H. Gaussian basis sets for use in correlated molecular calculations. III. The atoms aluminum through argon. *J. Chem. Phys.* **98,** 1358–1371; 10.1063/1.464303 (1993).

36. Francl, M. M. *et al.* Self-consistent molecular orbital methods. XXIII. A polarization-type basis set for second-row elements. *J. Chem. Phys.* **77,** 3654–3665; 10.1063/1.444267 (1982).

37. Ditchfield, R., Hehre, W. J. & Pople, J. A. Self-consistent molecular-orbital methods. IX. An extended Gaussian-type basis for molecular-orbital studies of organic molecules. *J. Chem. Phys.* **54,** 724–728; 10.1063/1.1674902 (1971).

38. Krishnan, R., Binkley, J. S., Seeger, R. & Pople, J. A. Self-consistent molecular orbital methods. XX. A basis set for correlated wave functions. *J. Chem. Phys.* **72,** 650–654; 10.1063/1.438955 (1980).

39. McLean, A. D. & Chandler, G. S. Contracted Gaussian basis sets for molecular calculations. I. Second row atoms, Z =11–18. *J. Chem. Phys.* **72,** 5639–5648; 10.1063/1.438980 (1980).

40. Tomasi, J., Mennucci, B. & Cammi, R. Quantum mechanical continuum solvation models. *Chem. Rev.* **105,** 2999–3093; 10.1021/cr9904009 (2005).

41. Marenich, A. V., Cramer, C. J. & Truhlar, D. G. Universal solvation model based on solute electron density and on a continuum model of the solvent defined by the bulk dielectric constant and atomic surface tensions. *J. Phys. Chem. B* **113,** 6378–6396; 10.1021/jp810292n (2009).

42. Legault, C. Y. *CYLview* (Université de Sherbrooke, 2009).

Acknowledgments This work was supported by the National Natural Science Foundation of China (21773033, 21725301, 21972024, 91645201, 21821004, 91645115, 91845201, 22088101, 21961160722), Science & Technology Commission of Shanghai Municipality (19DZ2270100), Beijing Outstanding Young Scientist Program (BJJWZYJH01201914430039) and SINOPEC (X514005). X-ray absorption spectroscopy (XAS) experiments were performed in Shanghai Synchrotron Radiation Facility (SSRF) BL14W. D. M. acknowledges support from the Tencent Foundation through the XPLORER PRIZE.

Author contributions Y.C. and D.M. designed the study. Q.Z. and W.G. performed most of catalyst preparation, characterization, and catalytic tests. Z.S. and Y.Z. assisted with the catalytic tests. M.P., Q.Z., B.M., X.D. and Z.J. performed the X-ray structure characterization (XAS and XPS) and data analysis. Z.G. and W.Z. performed the electron microscopy study. Q.Z., W.S. and C.L. carried out the real-time FT-IR experiments and data analysis. Z.L. finished the DFT calculations. Q.Z., Y.C., W.Z., and D.M. wrote the manuscript. M.P., Z.G., Y.L., M.W., Y.Z. and H.H. assisted in writing and editing the manuscript and provided helpful discussion. All the authors commented on the manuscript and have given approval to the final version of the manuscript.

Competing interests The authors declare no competing interests.

Additional information

Supplementary Information is available for this paper.

Correspondence and requests for materials should be addressed to Yong Cao, Ding Ma, Zhen Hua Li or Wu Zhou.

Supplementary Information for

Nitrogen-neighbored single cobalt sites enable heterogeneous oxidase-type catalysis

Qi Zhang,[1,8] Mi Peng,[2,8] Zirui Gao,[2,8] Wendi Guo,[1,8] Zehui Sun,[1] Yi Zhao,[1] Wu Zhou,[3,4]* Meng Wang,[2] Bingbao Mei,[5,6] Xianlong Du,[5] Zheng Jiang,[5,6] Wei Sun,[7] Chao Liu,[7] Yifeng Zhu,[1] Yongmei Liu,[1] Heyong He,[1] Zhen Hua Li,[1]* Ding Ma,[2]* Yong Cao[1]*

[1]Shanghai Key Laboratory of Molecular Catalysis and Innovative Materials, Department of Chemistry, Fudan University, Shanghai, 200438, China.
[2]Beijing National Laboratory for Molecular Engineering, College of Chemistry and Molecular Engineering, Peking University, Beijing, 100871, China.
[3]School of Physical Sciences and CAS Key Laboratory of Vacuum Physics, University of Chinese Academy of Sciences, Beijing, 100049, China.
[4]CAS Center for Excellence in Topological Quantum Computation, University of Chinese Academy of Sciences, Beijing, 100049, China.
[5]Shanghai Institute of Applied Physics, Chinese Academy of Sciences, Shanghai, 201204, China.
[6]Shanghai Synchrotron Radiation Facility, Zhangjiang Lab, Shanghai Advanced Research Institute, Chinese Academy of Sciences, Shanghai, 201204, China.
[7]State Key Laboratory for Oxo Synthesis and Selective Oxidation, Suzhou Research Institute, Lanzhou Institute of Chemical Physics, Chinese Academy of Sciences, Lanzhou, 730000, China.
[8]These authors contributed equally to this work: Qi Zhang, Mi Peng, Zirui Gao, Wendi Guo.
*Email: yongcao@fudan.edu.cn (Y.C.); dma@pku.edu.cn (D.M.); zhenhuali@fudan.edu.cn (Z.H.L.); wuzhou@ucas.ac.cn (W.Z.)

This PDF file includes:

Table of Contents

Supplementary Methods

Chemcials

All chemicals were used without further purification, unless otherwise stated. cobalt chloride hexahydrate ($CoCl_2·6H_2O$, ≥99.0%), zinc nitrate hexahydrate ($Zn(NO_3)_2·6H_2O$, ≥99.0%), urea ($CO(NH_2)_2$, ≥99.0%), methanol (MeOH, ≥99.7%), ethanol (EtOH, ≥99.7%), N,N-dimethylformamide (DMF, HPLC grade), chloroform ($CHCl_3$, ≥99.0%), acetone ($CO(CH_3)_2$, ≥99.5%), hydrochloric acid (HCl, 36.0-38.0%) and sodium hydroxide (NaOH, ≥96.0%) were purchased from Sinopharm Chemical Reagent Co., Ltd. Tetrachlorophthalic anhydride (98%) was purchased from Aladdin. Ammonium molybdate tetrahydrate ($(NH_4)_6Mo_7O_{24}·4H_2O$, ≥99.0%) were purchased from Sigma-Aldrich. Cobalt (II) phthalocyanine (CoPc, >93.0%) was purchased from TCI. TiO_2 (AEROXIDE P25, specific surface area: 50 m^2/g) was purchased from Evonik.

Synthesis of CoPc-based or -derives catalysts

A) Synthesis of cobalt (II) hexadecachlorophthalocyanine (CoPc-16Cl)

The following procedure is adapted from the literature [1].

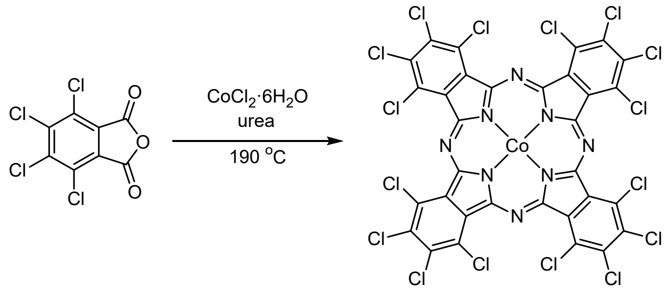

A finely ground mixture of $CoCl_2·6H_2O$ (2.38 g 10 mmol), tetrachlorophthalic anhydride (11.4 g, 40 mmol), urea (24.0 g, 400 mmol) and $(NH_4)_6Mo_7O_{24}·4H_2O$ (0.125 g, 0.1 mmol) was reacted in solid state at 190 °C for 5 h. The resulting solid was ground and further stirred in 500 mL HCl aqueous solution (1 mol/L) and 500 mL NaOH aqueous solution (1 mol/L) at 100 °C for 1 h, respectively. The residue was then filtered, washed with water, and dried under vacuum to obtain crude CoPc-16Cl. The crude product was transferred to a Soxhlet thimble and extracted using $CHCl_3$, EtOH and acetone for 48 h, successively. After drying at 60 °C for 3 h, CoPc-16Cl was obtained as dark green solid.
UV-Vis (DMF, λ_{max} = nm): 660(s), 498(sh), 306(sh).
FT-IR (KBr, cm^{-1}): 1600, 1459, 1393, 1383, 1340, 1315, 1275, 1215, 1201, 1163, 1130, 1103, 1037, 955, 778, 764, 752.

B) Synthesis of PC and NPC supports

PC and NPC supports were synthesized by using ZIF-8 as precursor following one-step thermal activation under different conditions. For synthesis of ZIF-8 precursor, a solution of 2-MeIm (13.1 g, 160 mmol) in 400 mL MeOH was added to a solution of $Zn(NO_3)_2·6H_2O$ (5.95 g, 20 mmol) in 400 mL methanol. After stirred at room temperature (~25 °C) for 24 h, the obtained ZIF-8 precipitates were collected by centrifugation, wash with MeOH for three times and then dried under vacuum at room temperature overnight.

For synthesis of NPC support, 1.0 g as-prepared ZIF-8 precursor was heated at 1000 °C for 4 h with a heating rate of 2 °C/min under the flowing Ar atmosphere (80 mL/min) in a tube furnace, followed by naturally cooling down to room temperature. NPC was obtained as a black powder. The product was used directly without further treatment.

PC support was synthesized using similar procedure but pyrolyzed at 1400 ºC for 8 h.

C) Synthesis of CoPc/PC, CoPc/NPC, CoPc-16Cl/NPC, CoPc/TiO_2 and CoPc-16Cl/TiO_2

A series of supported phthalocyanine cobalt catalysts with the Co loading of 0.25 wt% were prepared by incipient wetness impregnation. The synthesis of CoPc/NPC is given as follows. A certain amount of CoPc was dissolved in 15 mL DMF and 0.5 g NPC was dispersed in the solution. After stirring at room temperature for 12 h, the solvent was removed by rotary evaporation. The sample was dried under dynamic vacuum (~ 0.1 torr) at 150 ºC for 3 h and CoPc/NPC was obtained. Other catalysts were prepared according to the same procedure by using different substituted cobalt phthalocyanines or supports.

D) Synthesis of Co-N_4/NPC

0.5 g as-prepared CoPc/NPC was heated at 600 ºC for 2 h with a heating rate of 2 ºC/min under the flowing Ar atmosphere (80 mL/min) in a tube furnace. After cooling down to room temperature, Co-N_4/NPC was obtained.

Supplementary Figures, Tables and Discussions

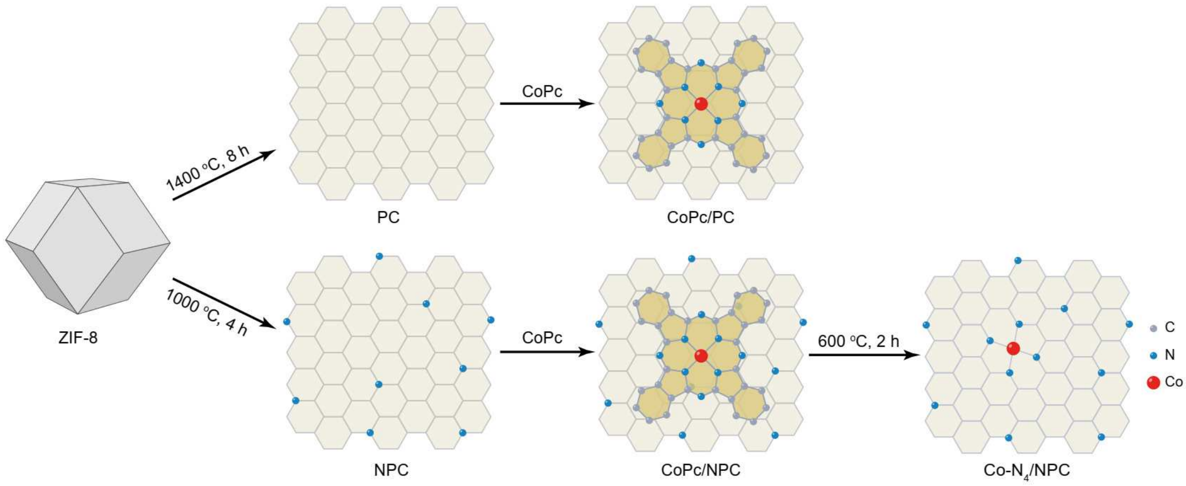

Supplementary Fig. 1 | Procedures for the synthesis CoPc-based or -derived biomimetic catalyst models.

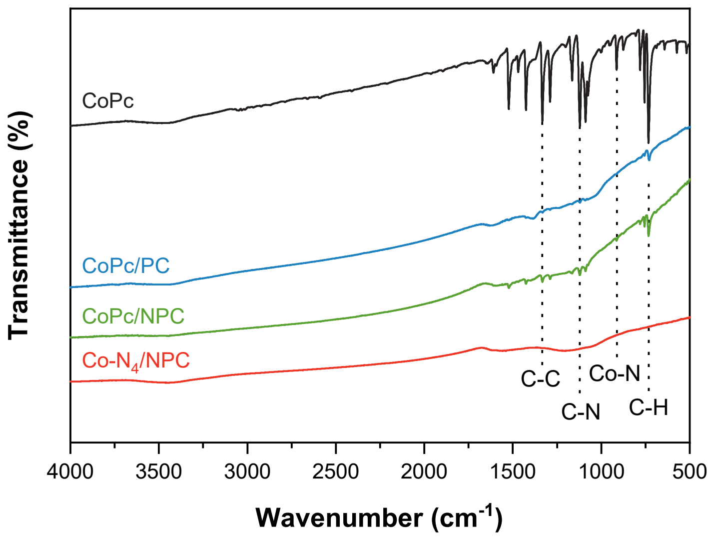

Supplementary Fig. 2 | FT-IR spectra of CoPc, CoPc/PC, CoPc/NPC and Co-N_4/NPC. The characteristic peaks of CoPc could obtain in CoPc/PC and CoPc/NPC samples, confirming the existence of CoPc on the carbon-based supports. While the Co-N_4/NPC sample has no characteristic peak of CoPc, indicating the CoPc molecules were decomposed after pyrolysis step.

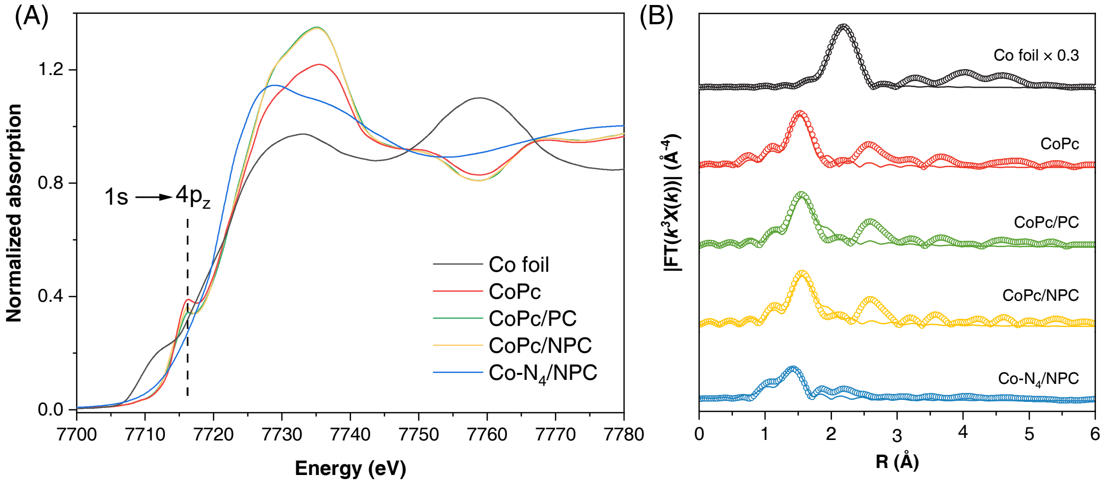

Supplementary Fig. 3 | (A) Co K-edge XANES spectra and (B) R-space Co K-edge EXAFS spectra for CoPc-based or -derived catalysts, CoPc and Co foil (open circles stand for as obtained data and solid lines denote for fitting curves). The fitting results are listed in **Supplementary Table 2**. In **Supplementary Fig. 3A**, the shoulder at 7715.7 eV arising from 1s → $4p_z$ shakedown transition is a straightforward fingerprint for a square-planar $Co-N_4$ configuration with D_{4h} symmetry [2]. However, as this shoulder is relatively weak for $Co-N_4$/NPC as compared to that for CoPc, CoPc/PC and CoPc/NPC, indicating that the D_{4h} symmetry is broken. This result further confirmed that the macrocyclic structure of CoPc was decomposed after pyrolysis step.

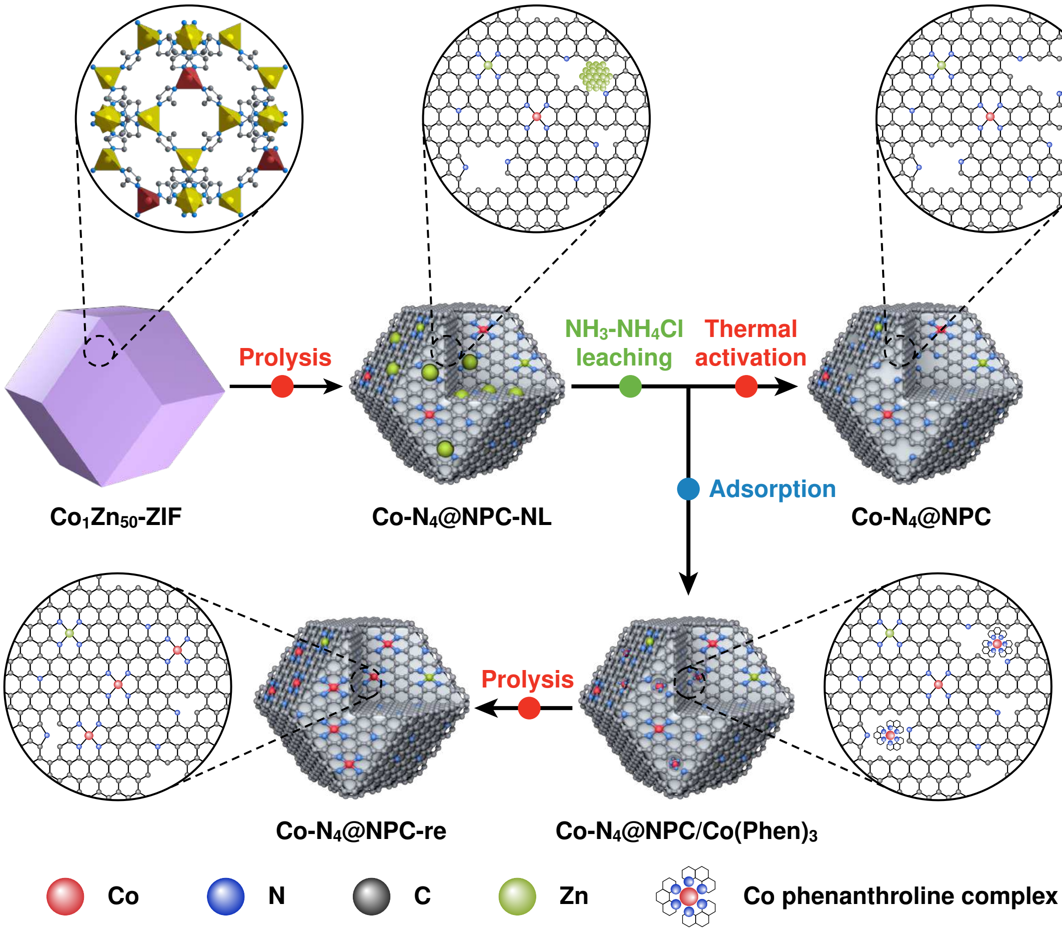

Supplementary Fig. 4 | Procedures for the synthesis of Co-N_4@NPC-based materials.

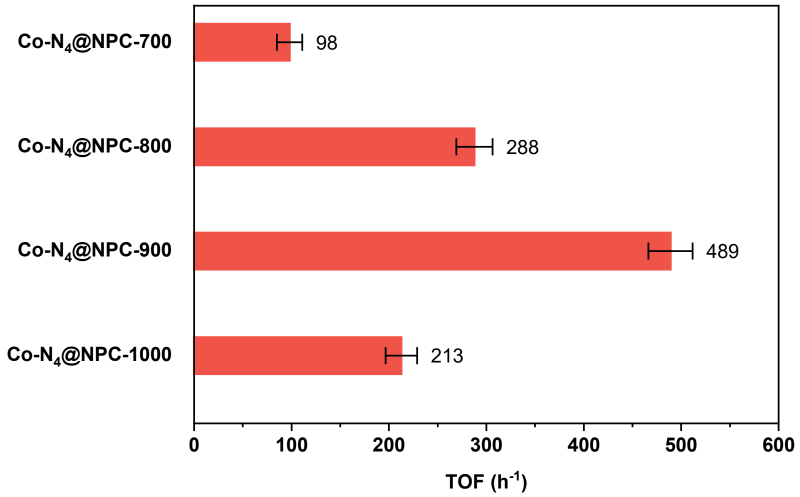

Supplementary Fig. 5 | Catalytic performance for oxidation of **1a** over Co-N_4@NPC-based catalyst prepared with different pyrolysis temperatures. Reaction conditions: **1a** (1 mmol), H_2O (8 mmol), MeCN (3 mL), catalyst (Co 0.5 mol%), air atmosphere, 30 °C. TOF was measured at **1a** conversion below 20% based on total Co atoms. Error bars represent the standard deviation from at least three independent experiments. For all reactions, > 99% selectivity of **2a** were obtained.

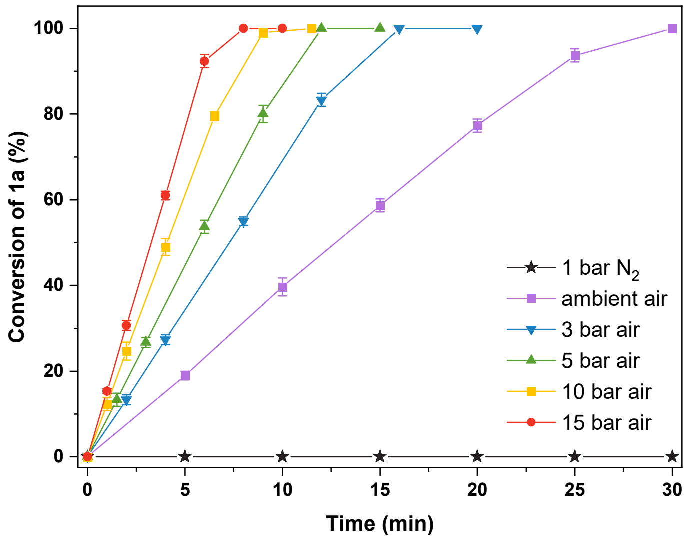

Supplementary Fig. 6 | Reaction profile for oxidation of **1a** under different atmosphere over Co-N_4@NPC-900 catalyst. Reaction conditions: **1a** (1 mmol), H_2O (8 mmol), MeCN (3 mL), Co-N_4@NPC-900 (Co 0.5 mol%), 30 ºC. The conversion was determined by GC using anisole as an internal standard.

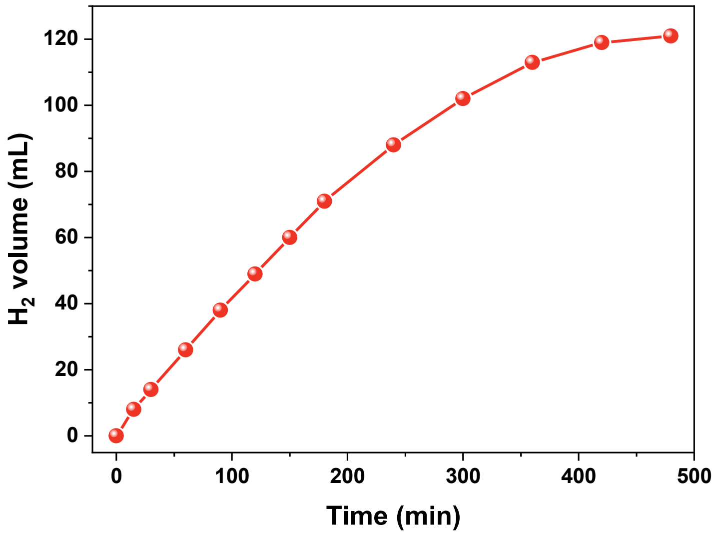

Supplementary Fig. 7 | H_2 evolution by hydrolytic dehydrogenation of **1a** catalyzed by Co-NPs@NPC. Reaction conditions: **1a** (5 mmol), H_2O (40 mmol), MeCN (15 mL), Co-NPs@NPC (0.5 mol%), 30 ºC, N_2 atmosphere. The volume change of H_2 was detected by a gas barrette. After 8 h reaction, 121 mL H_2 was produced.

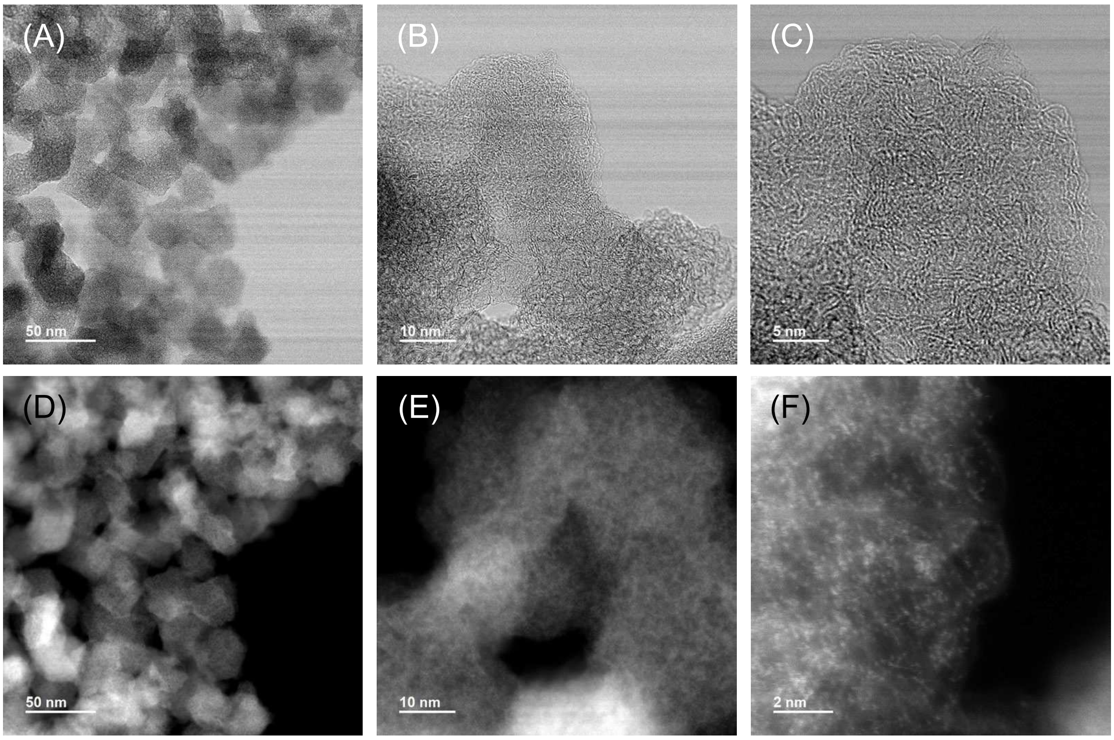

Supplementary Fig. 8 | Additional electron microscopy characterization results of Co-N_4@NPC-900. Low magnifi-cation BF-STEM (bright-field) (A) and HAADF-STEM images (D) showed that Co-N_4@NPC-900 sample has a highly porous appearance, formed by the fusion and aggregation of Co_1Zn_{50}-ZIF precursor (~35 nm) under high-temperature pyrolysis conditions. BF-STEM images (B and C) revealed that Co-N_4@NPC-900 sample has highly disordered carbon structures with randomly oriented graphitic domains. The pore-like structure in carbon species was confirmed by HAADF-STEM image (E). Furthermore, atomic-resolution HAADF-STEM image of different region in Co-N_4@NPC-900 sample (F) also confirmed the uniformly atomic dispersed Co and Zn sites (bright spots).

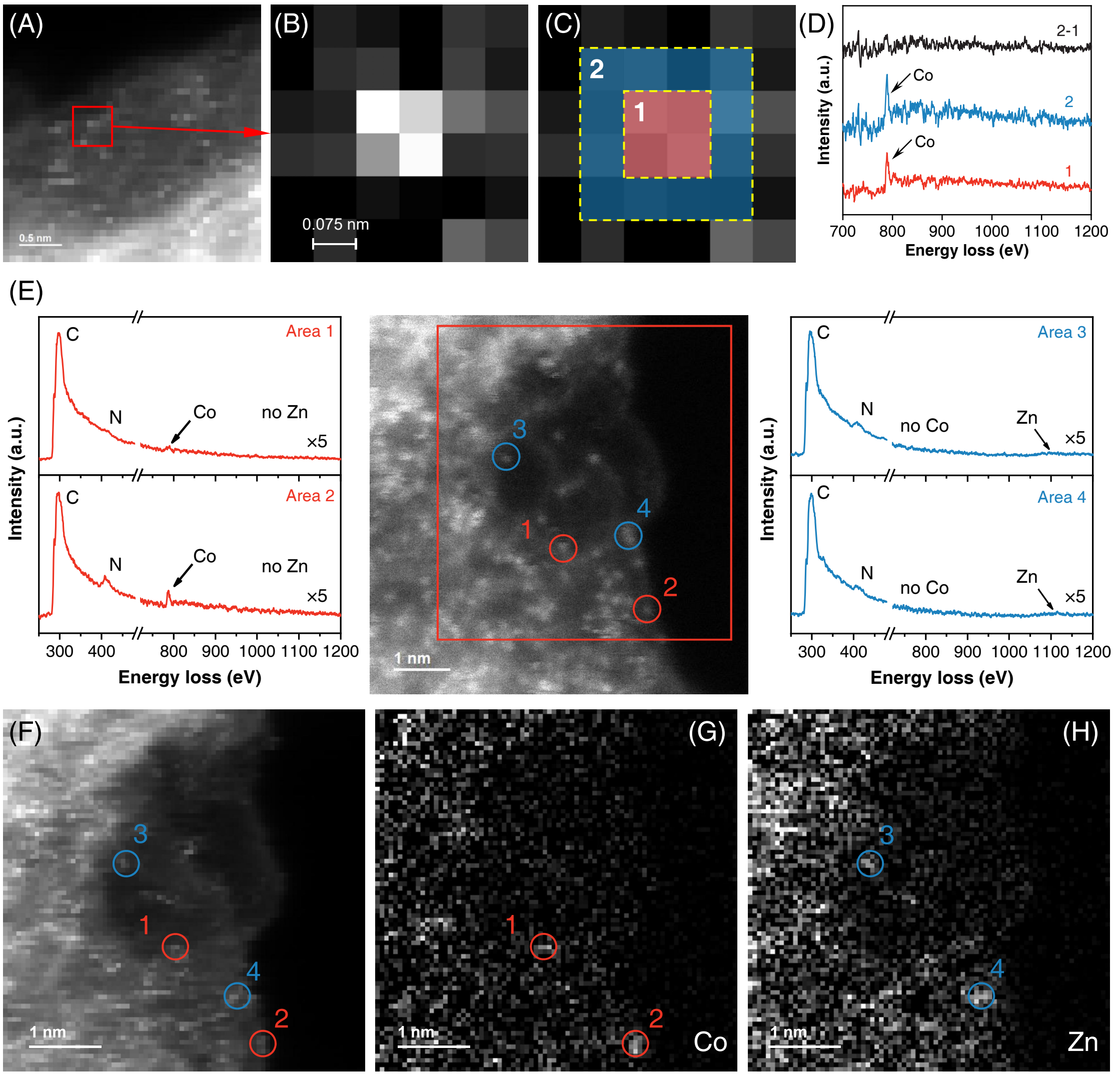

Supplementary Fig. 9 | Identify the M-N$_x$ sites in Co-N$_4$@NPC-900 by EELS analysis. (A) Regions of HAADF spectrum-image for EELS analysis. (B) Local enlarged STEM-EELS spectrum image of the red box in **Supplementary Fig. 9A** with 6×6 pixels. (C) The actual analysis regions with different size (region-1, 0.15×0.15 nm or region-2, 0.30×0.30 nm). (D) The EELS spectra acquired from region-1 (red line), region-2 (blue line) and corresponding difference spectrum (black line) of two areas. The EELS spectra acquired from the same bright spot position with different size (region-1 or region-2) in Co-N$_4$@NPC-900 showing the similar intensity of Co signal. The difference spectrum of region-1 and region-2 further proved that the Co signal only exists in region-1. (E) HADDF-STEM image and EELS spectra of four different regions in the image. EELS spectra acquired from area 1 and 2 (red region) showed the coexistence of Co and N but not Zn; while the EELS spectra acquired from area 3 and 4 (blue region) only showed the coexistence of Zn and N. The STEM-EELS spectrum image of the red box in **Supplementary Fig. 9** (F) and corresponding elemental EELS map of Co (G) and Zn (H) further confirmed the regional distribution of Co and Zn (the Co signal only increases in area 1 and 2; while the Zn signal only increases in area 3 and 4). These results suggested the presence of independent Co-N$_x$ and Zn-N$_x$ sites in Co-N$_4$@NPC-900.

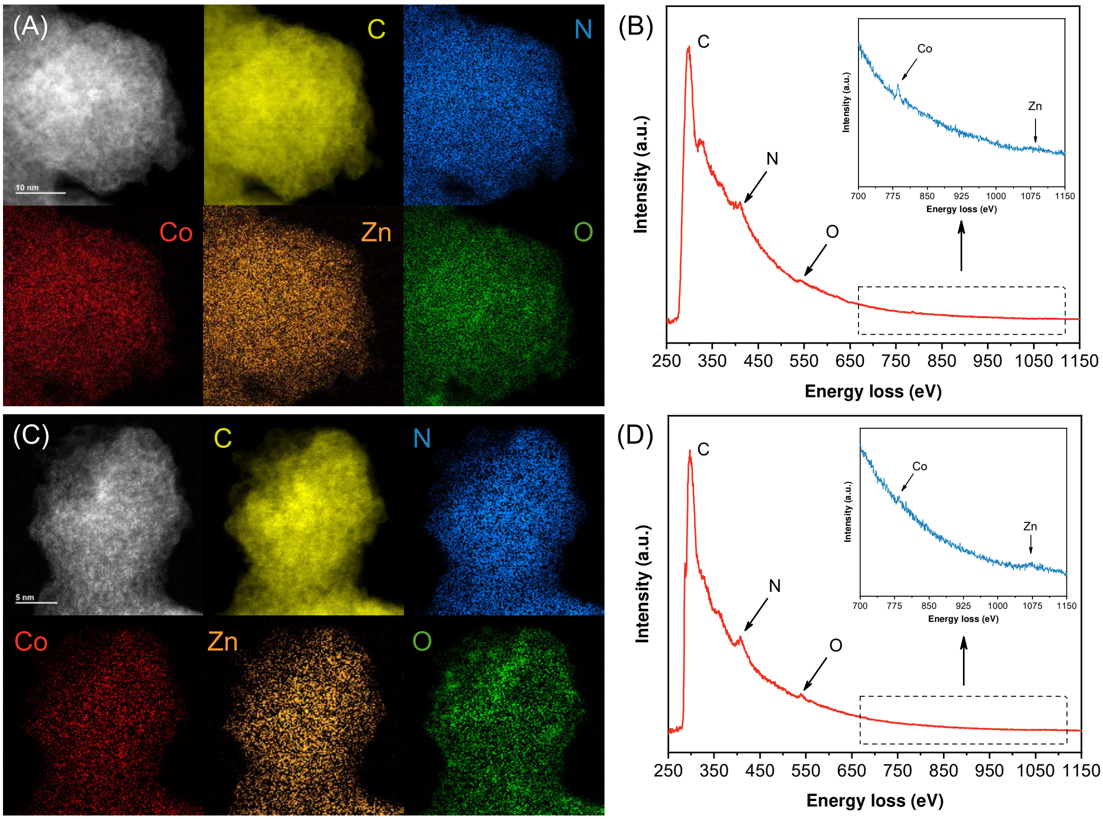

Supplementary Fig. 10 | (A, C) HAADF-STEM images and corresponding EELS elemental maps of C (yellow), N (blue), O (green), Co (red) and Zn (orange) from two different regions in Co-N_4@NPC-900. The **Supplementary Fig. 10A** also shows in **Fig. 2B** in the main text. (B, D) EELS spectra of the entire region in **Supplementary Fig. 10**, A and C, respectively. The inset shows the local enlarged spectrum of 700-1150 eV. Distinguishable signals for C, N, O, Co and Zn were observed in the EELS elemental maps and EELS spectra across the carbon species, indicating the uniform distribution of each element.

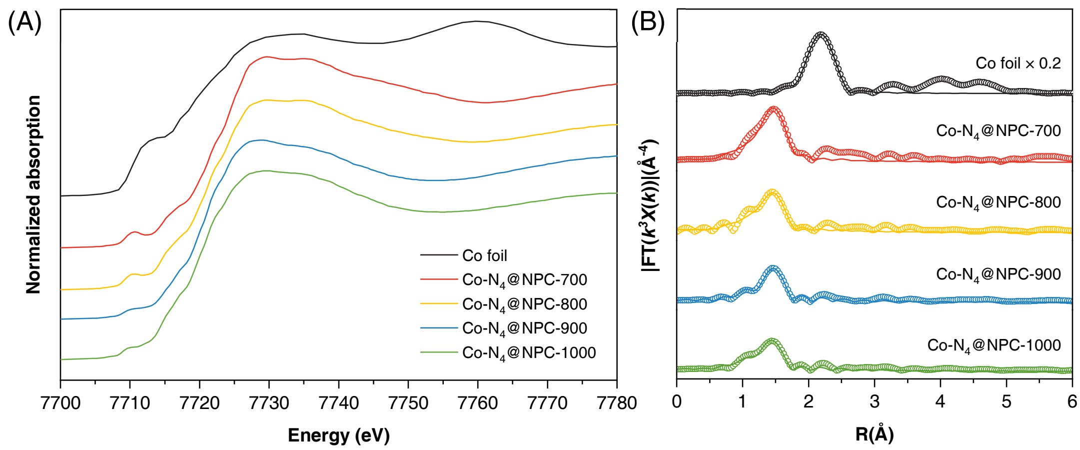

Supplementary Fig. 11 | (A) Co K-edge XANES spectra and (B) R-space Co K-edge EXAFS spectra for Co-N_4@NPC-T catalysts prepared with different pyrolysis temperatures and Co foil (open circles stand for as obtained data and solid lines denote for fitting curves). The fitting results are listed in **Supplementary Table 2**.

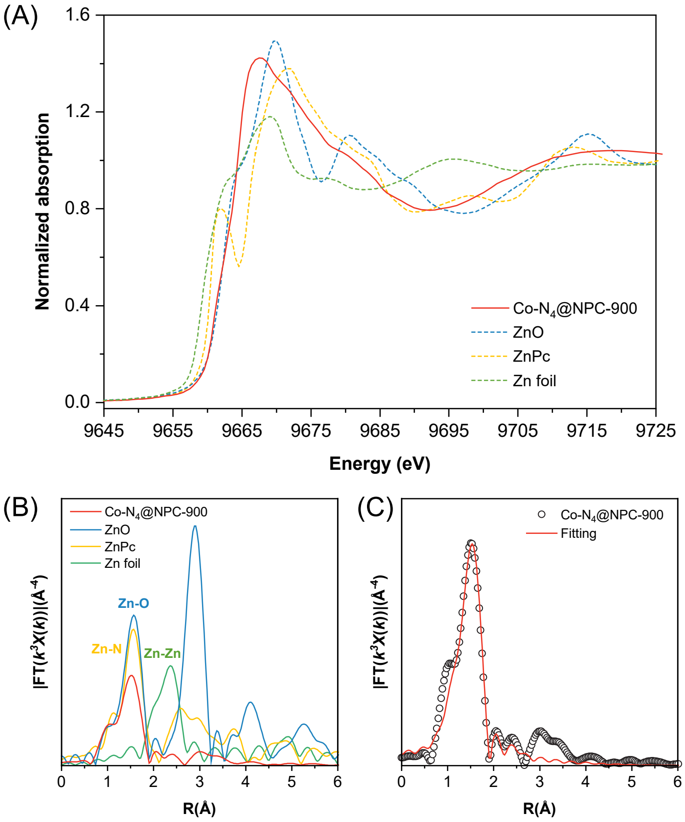

Supplementary Fig. 12 | (A) Zn K-edge XANES spectra and (B) R-space Zn K-edge EXAFS spectra for Co-N_4@NPC-900 catalyst and reference samples. (C) First shell fitting of Zn K-edge EXAFS spectrum for Co-N_4@ NPC-900. The fitting results are listed in **Supplementary Table 2**.

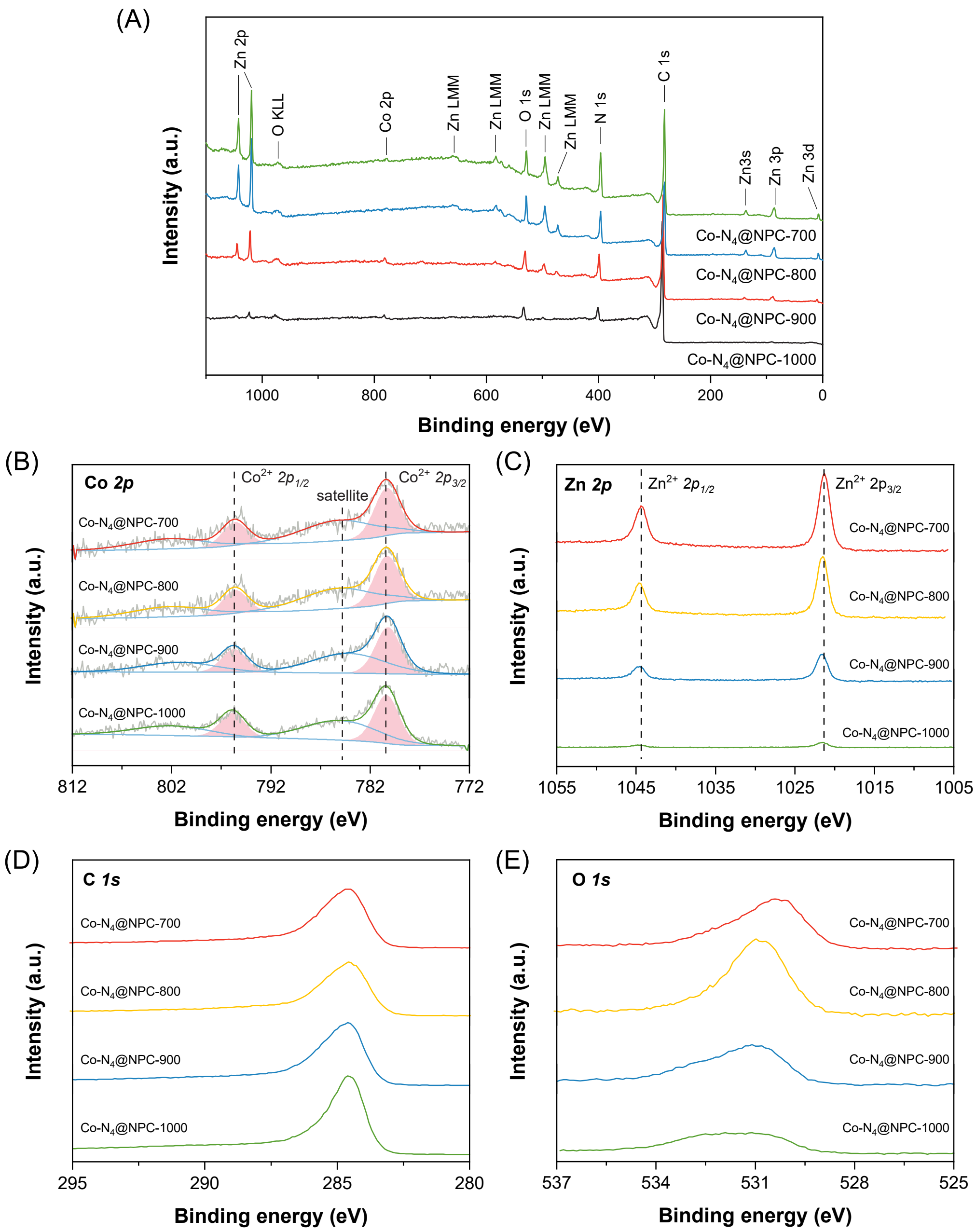

Supplementary Fig. 13 | Survey (A), Co *2p* (B), Zn *2p* (C), C *1s* (D) and O *1s* (E) XPS spectra for Co-N_4@NPC-T samples prepared with different pyrolysis temperatures. It should be noted that only Co^{2+} species (780.3 eV) was found in all the samples, revealing that the majority of Co is in atomically-dispersed Co-N_x sites as evidenced by XAFS results (**Fig. 2F**, **Supplementary Fig. 11**).

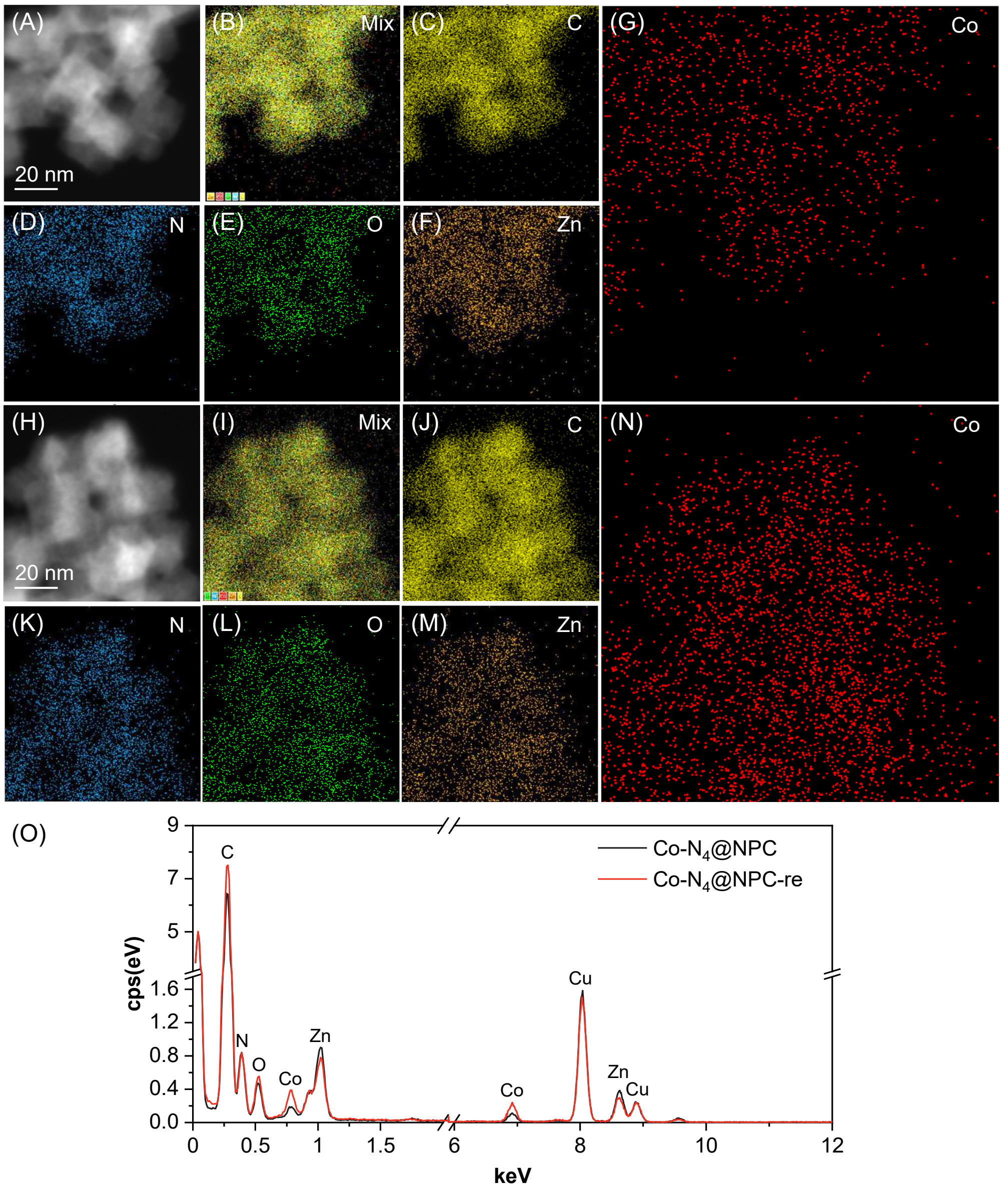

Supplementary Fig. 14 | STEM images and corresponding EDS elemental maps of Co-N_4@NPC-900 (A-G) and Co-N_4@NPC-re (H-N). (O) The corresponding EDS spectra of the region in (A) and (H).

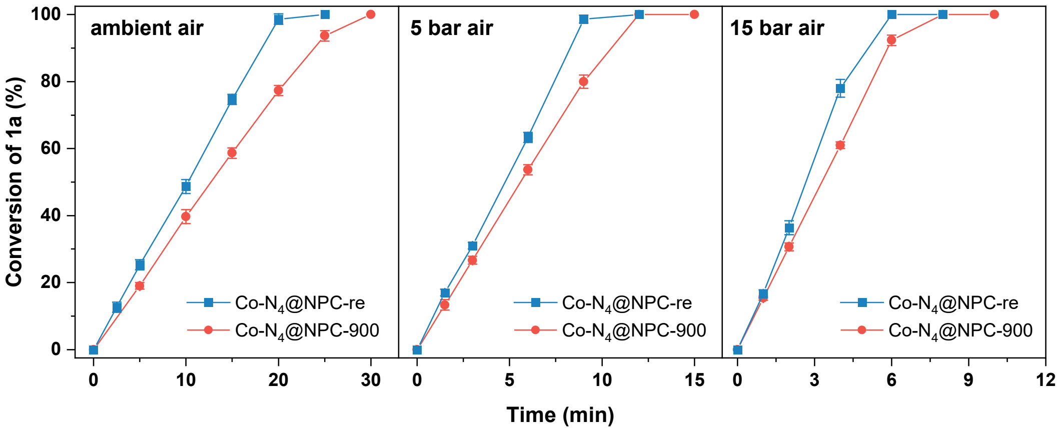

Supplementary Fig. 15 | Reaction profile for oxidation of **1a** under different atmosphere over Co-N_4@NPC-900 and Co-N_4@NPC-re catalyst. Reaction conditions: **1a** (1 mmol), H_2O (8 mmol), MeCN (3 mL), catalyst (Co 0.5 mol%), 30 °C. The conversion was determined by GC using anisole as an internal standard.

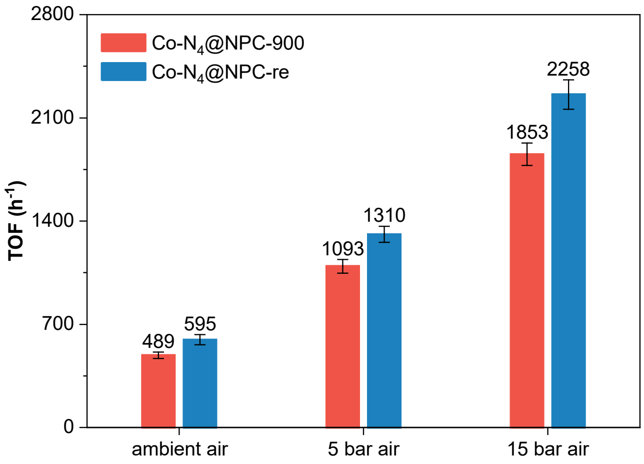

Supplementary Fig. 16 | Catalytic performance for oxidation of **1a** over Co-N_4@NPC-900 and Co-N_4@NPC-re catalysts under different atmosphere. Reaction conditions: Reaction conditions: **1a** (1 mmol), H_2O (8 mmol), MeCN (3 mL), catalyst (Co 0.5 mol%), 30 ºC. TOF was measured at **1a** conversion below 20% based on total Co atoms. Error bars represent the standard deviation from at least three independent experiments. For all reactions, > 99% selectivity of **2a** were obtained.

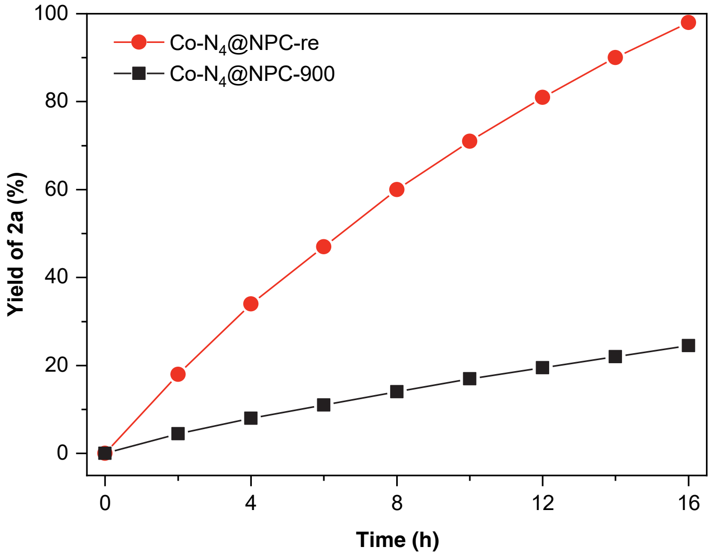

Supplementary Fig. 17 | Comparison of catalytic performance between Co-N_4@NPC-re and Co-N_4@NPC-900 in **1a** oxidation under 0.01 mol% Co level. Reaction conditions: **1a** (50 mmol), H_2O (400 mmol), MeCN (60 mL), catalyst (Co 0.01 mol%), O_2 (15 bar), 30 ºC. The yield of **2a** was determined by GC using anisole as an internal standard.

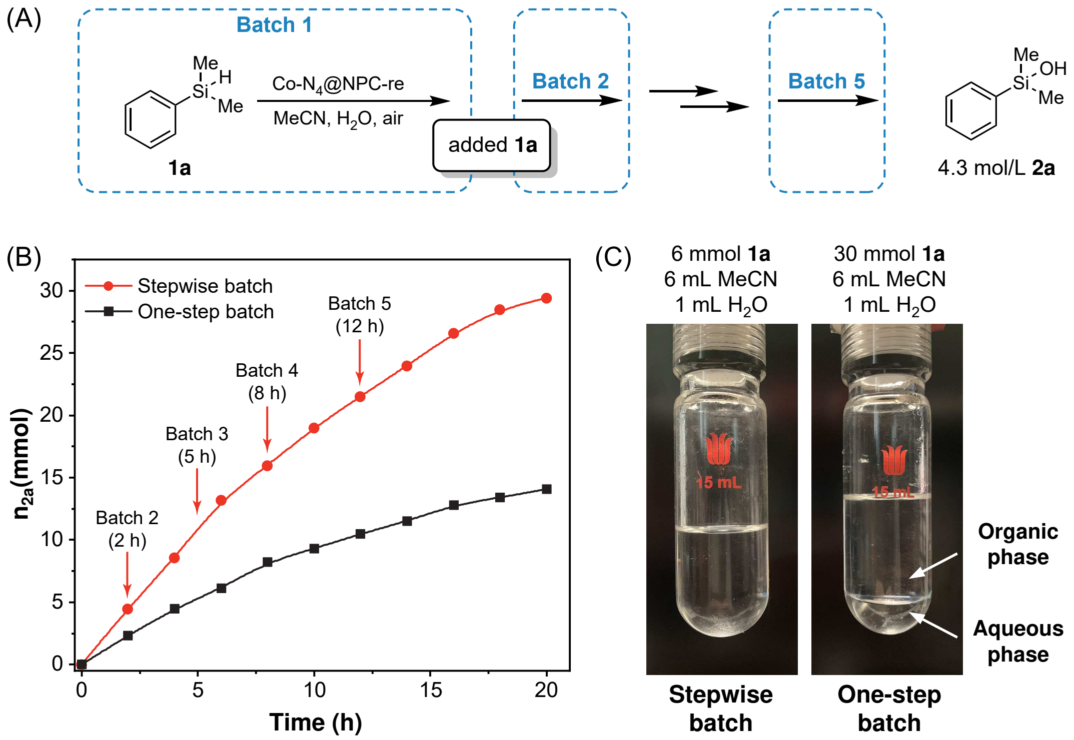

Supplementary Fig. 18 | Development of high-concentration silanol synthesis. (A) Schematic illustration of stepwise approach for high-concentration silanol synthesis. (B) The detail comparison between stepwise and one-step approach. (C) Initial state of reaction solution of stepwise batch (left) and one-step batch (right) approach. Reaction conditions: **1a** (30 mmol), H_2O (1 mL), Co-N_4@NPC-re (Co 0.05 mol%), MeCN (6 mL), 30 °C, air atmosphere. (For the one-step batch, 30 mmol **1a** was added at the beginning of the reaction; for the stepwise batch, 30 mmol **1a** was added repetitively for 5 times during the reaction.)

Although silane (such as **1a**) was usually miscible with MeCN, a phase separation occurred when a large amount of silane added to MeCN-H_2O mixture (**Supplementary Fig. 18**, right). Considering phase separation may reduce mass transfer efficiency of reaction, a semi-continuous procedure was developed, allowing the process-intensified conversion of high-concentration **1a** in MeCN-H_2O mixture. It was thus possible to obtain a solution of 4.3 mol/L **2a** in MeCN/H_2O (6:1) mixture by subjecting Co-N_4@NPC-re catalyst to a five-stage-repetitive injection of 6 mmol **1a** during the reaction. The oxidation of **1a** readily proceeded to give >98% **2a** yield in 20 h and only <1% by-product disiloxane was obtained. In contrast, the conventional one-stage procedure gave only 47% yield after reaction for 20 h. The stepwise reaction mode reduces the working concentration of **1a** in solution, which not only avoids phase separation of reaction system, but also helps to keep optimal silane/H_2O molar ratio for high reaction efficiency.

Continuous-flow reactions

The reactions were performed on a ThalesNano® Phoenix Flow Reactor (**Supplementary Fig. 19**). An HPLC pump was used for substrate solution introduction. Air was introduced by gas module. The liquid and gas were intensively mixed by liquid-gas mixer and flowed by up-flow through the reaction column. The system pressure was regulated by a back pressure valve. While the product solution was mainly collected in product container, the change valve can bypass the product container to sample the reaction mixture.

The stainless steel (SS) reaction column used in research contained a SS tube (110 mm × 2.1 mm I.D. × 1/4 in. O.D.), two nut/ferrule sets, two frits (pore size 50 μm) and two endcaps (**Supplementary Fig. 20**).

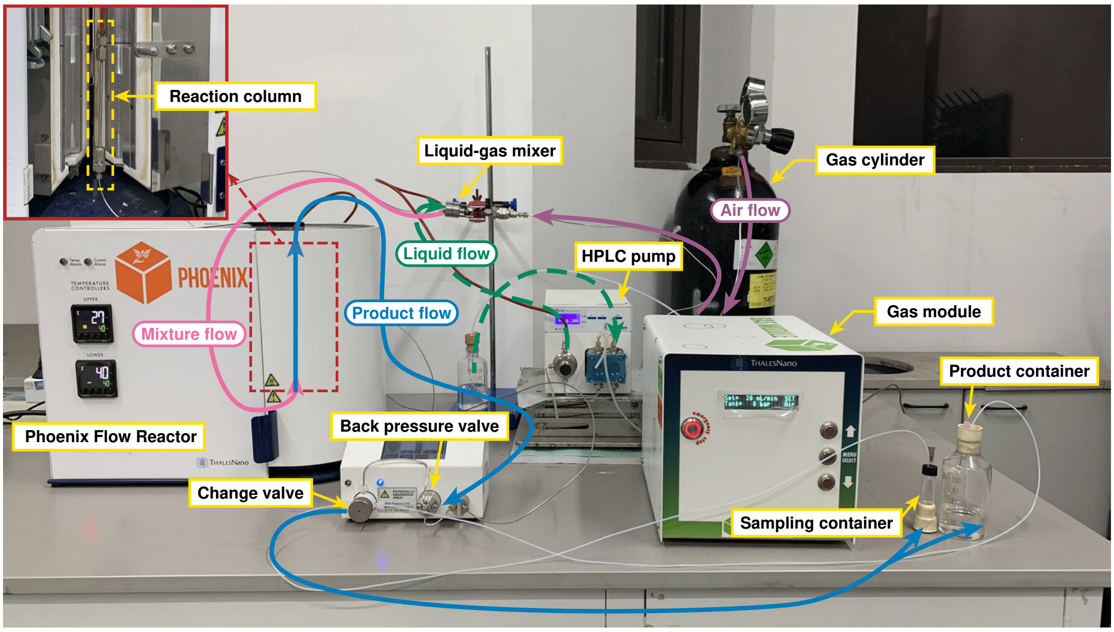

Supplementary Fig. 19 | Photographic image of ThalesNano® Phoenix Flow Reactor.

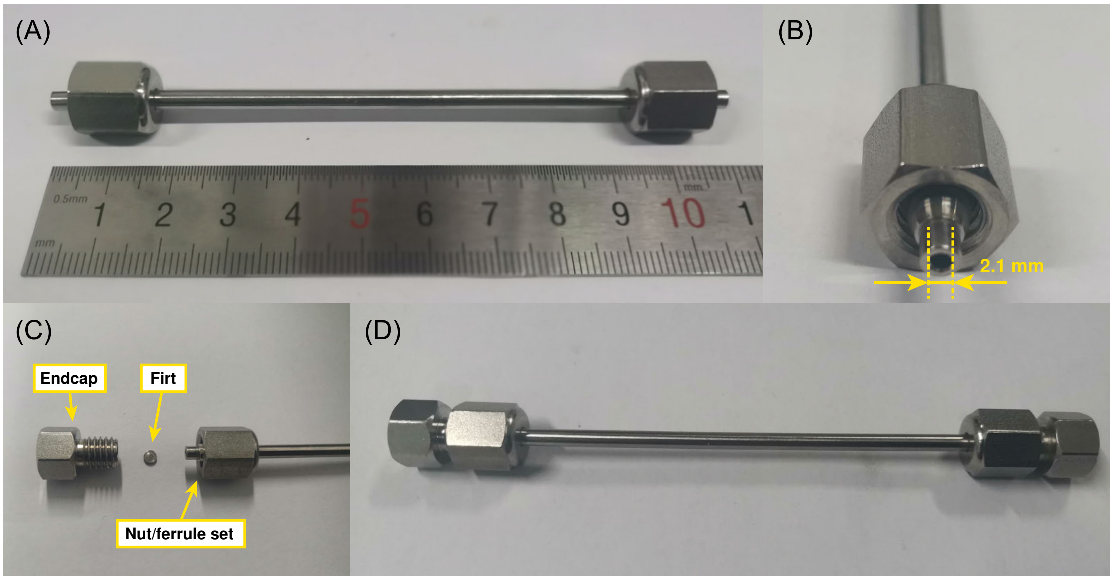

Supplementary Fig. 20 | (A) Stainless steel tube. (B) Close up. (C) End sealing structure. (D) Completely assembled reaction column.

Under a typical continuous-flow procedure (as shown in **Supplementary Fig. 21**), 15 mg Co-N_4@NPC-re was diluted with 135 mg SiO_2 (AEROSIL 380), and then pressed, crushed and sieved to 80-100 mesh. The mixture was packed into reaction column and held in place between quartz sand (80-100 mesh) at either end of the column. The solution (0.3 mol/L **1a** and 2.4 mol/L H_2O in MeCN, 0.20 mL/min) and air (20 mL/min) was introduced simultaneously by up flow. The reaction was carried out under the condition of 30 bar air and 50 °C. After stabilization, the fraction was collected to sampling container every 2 h during the continuous flow and analyzed by GC using anisole as an internal standard. For stability evaluation, the **2a** yield was measured for more than 300 h. The main product solution collected in product container was concentrated on a rotary evaporator and further purified by vacuum distillation (62-64 °C, 0.5 torr) to obtain pure **2a**.

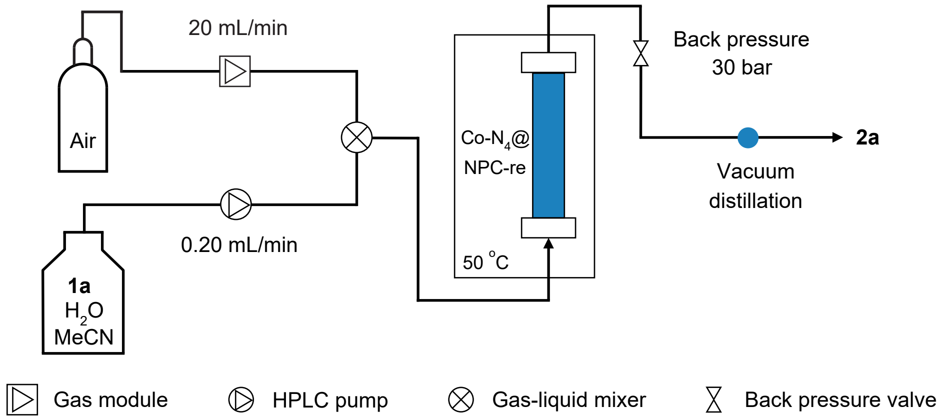

Supplementary Fig. 21 | Diagram of continuous-flow reaction.

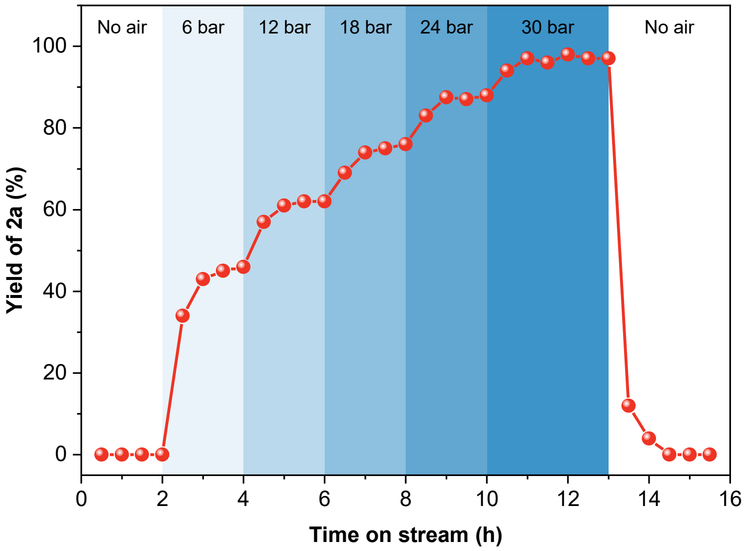

Supplementary Fig. 22 | Catalytic performance of a Co-N_4@NPC-re catalyst for **1a** oxidation under different air pressure in continuous-flow system. Reaction conditions: catalyst (Co-N_4@NPC-re/SiO_2 = 1/9, 150 mg), **1a** (0.3 mol/L), H_2O (2.4 mol/L), MeCN as solvent, liquid flow rate 0.20 mL/min, gas flow rate 20 mL/min (if needed), 50 °C.

The influence of air pressure in continuous-flow system was investigated. As shown in **Supplementary Fig. 22**, when the flow reaction was conducted only using **1a** and H_2O as reactant (0-2 h), no reaction occurred. In contrast, **2a** could be obtained when air was introduced into the flow reaction system simultaneously. Under a certain gas (20 mL/min) and liquid (0.20 mL/min) flow rate, further increasing the air pressure led to a higher yield of **2a** and **2a** reached near quantitative yield under 30 bar air at 50 °C. The catalytic performance in continuous-flow system further confirmed that Co-N_4@NPC-re system for **1a** oxidation followed a O_2-coupled hydrolytic pathway, O_2 was served as another essential reactant.

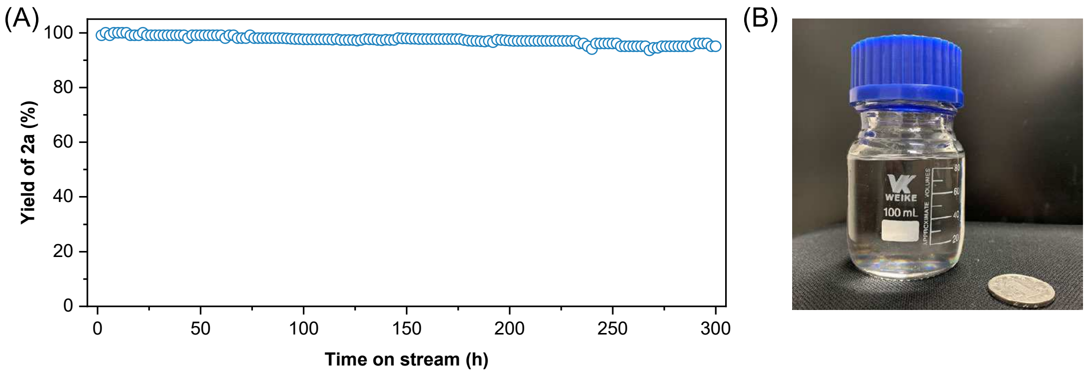

Supplementary Fig. 23 | (A) The stability evaluation of a Co-N_4@NPC-re catalyst for **1a** oxidation under continuous-flow conditions. Reaction conditions: catalyst (Co-N_4@NPC-re/SiO_2 = 1/9, 150 mg), **1a** (0.3 mol/L), H_2O (2.4 mol/L), MeCN as solvent, air (30 bar), liquid flow rate 0.20 mL/min, gas flow rate 20 mL/min, 50 ºC. (B) Image of **2a** after purification.

The Co-N_4@NPC-re catalyst exhibited stable performance over 300 hours. The **2a** yield remained >95% during a 300-hour stability test. The space-time yield of **2a** was ~7.5 $mol_{\mathbf{2a}}/g_{Co}$/h and total turnover number reached up to 130000.

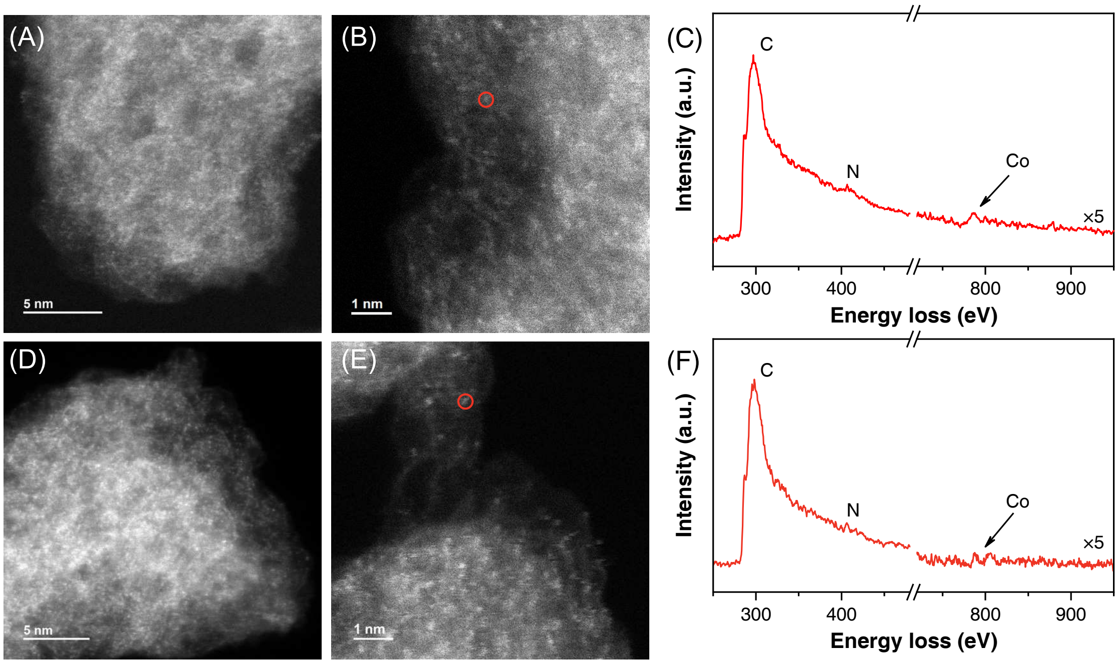

Supplementary Fig. 24 | HAADF-STEM images with accompanying EELS point spectra for Co-N_4@NPC-re catalyst before (A-C) and after (D-F) 300-hour continuous-flow reaction stability test. The microstructure in the catalyst maintained nearly the same and Co-N_x sites could clearly obtained in spent catalyst by EELS point spectra, indicated high stability of Co-N_4@NPC-re catalyst.

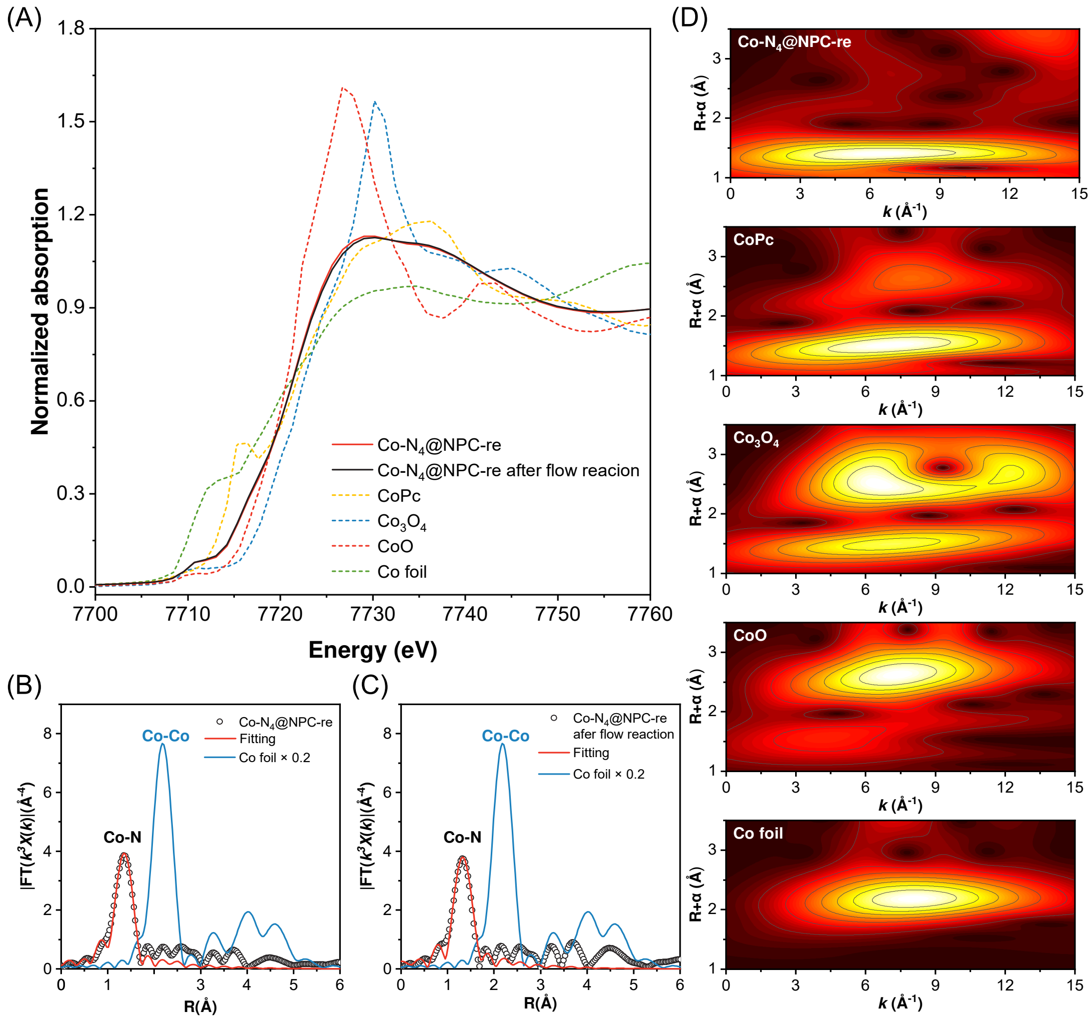

Supplementary Fig. 25 | (A) Co K-edge XANES spectra of Co-N_4@NPC-re catalyst before (red) and after (black) 300-hour continuous-flow reaction stability test and reference samples. (B and C) R-space Co K-edge EXAFS spectra and fittings of Co-N_4@NPC-re catalyst before and after stability test, respectively. The fitting results are listed in **Supplementary Table 2**. (D) WT of Co K-edge for Co-N_4@NPC-re, CoPc, Co_3O_4, CoO and Co foil.

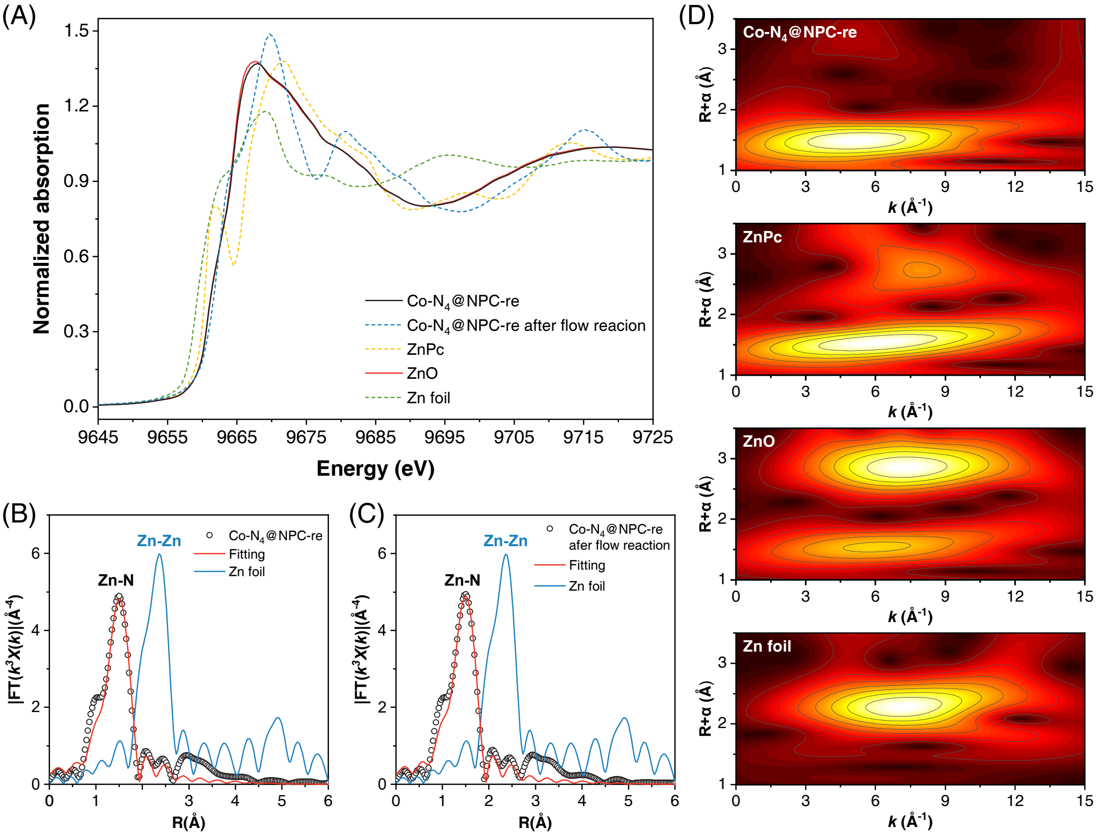

Supplementary Fig. 26 | (A) Zn K-edge XANES spectra of Co-N_4@NPC-re catalyst before (red) and after (black) 300-hour continuous-flow reaction stability test and reference samples. (B and C) R-space Zn K-edge EXAFS spectra and fittings of Co-N_4@NPC-re catalyst before and after stability test, respectively. The fitting results are listed in **Supplementary Table 2**. (D) WT of Zn K-edge for Co-N_4@NPC-re, ZnPc, ZnO and Zn foil.

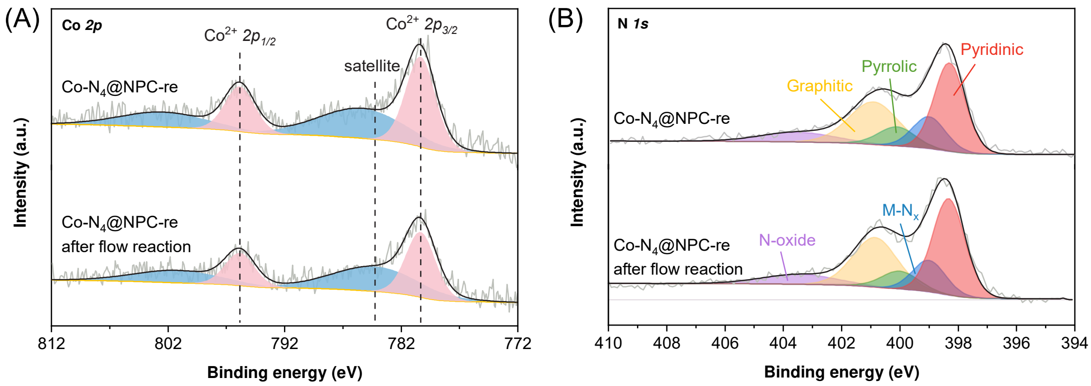

Supplementary Fig. 27 | Co *2p* (A) and N *1s* (B) XPS spectra for Co-N_4@NPC-re catalyst before and after 300-hour continuous-flow reaction stability test. Detailed fitting results of N *1s* XPS spectra are listed in **Supplementary table 5**.

Real-time FT-IR experiments

The reaction spectra were recorded using an IC 15 from Mettler-Toledo AutoChem fitted with a diamond-tipped probe and an MCT detector. Data manipulation was carried out using the iC IR software, version 7.0.

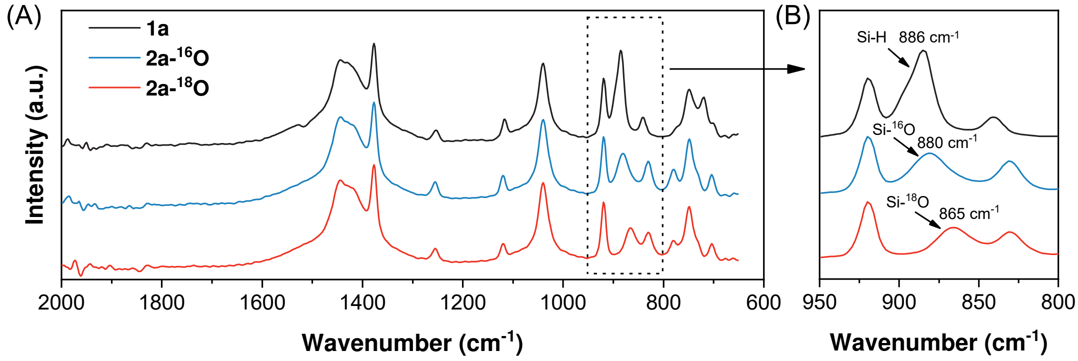

Supplementary Fig. 28 | (A) Characteristic IR band of **1a**, **2a-^{16}O** and **2a-^{18}O** in MeCN. (B) Local enlarged spectra of the region from 950 to 800 cm^{-1}.

As shown in **Supplementary Fig. 28**, the IR band of **1a** at 886 cm^{-1} assigned to bending vibration of Si-H bond. For **2a-^{16}O**, the stretching vibration of Si-^{16}O bond was located at 880 cm^{-1}. While for **2a-^{18}O**, due to the ^{16}O atom was substituted with the higher mass ^{18}O isotope, a downshifted Si-O vibrational frequency occurred and the characteristic stretching vibration of Si-^{18}O bond was obtained at 865 cm^{-1}.

The catalytic reaction was carried out as follows: a three-necked reaction vessel was fitted with a magnetic stirring bar. The IR probe was inserted through an adapter into the middle neck; the other two necks were capped with septa for injections and an air balloon. The reaction vessel was kept at 30 °C. Then, the three-necked vessel was charged with 15 mL anhydrous MeCN and the data collection was started. After 5 min, **1a** (681.5 mg, 5 mmol) was added. Then 5 min later, $H_2{}^{18}O$ (200.2 mg, 10 mmol) was added. After another 5 min, the reaction was initiated by the addition of Co-N_4@NPC-re (9.5 mg, 0.1mol% Co). The IR spectra were recorded over the course of the reaction.

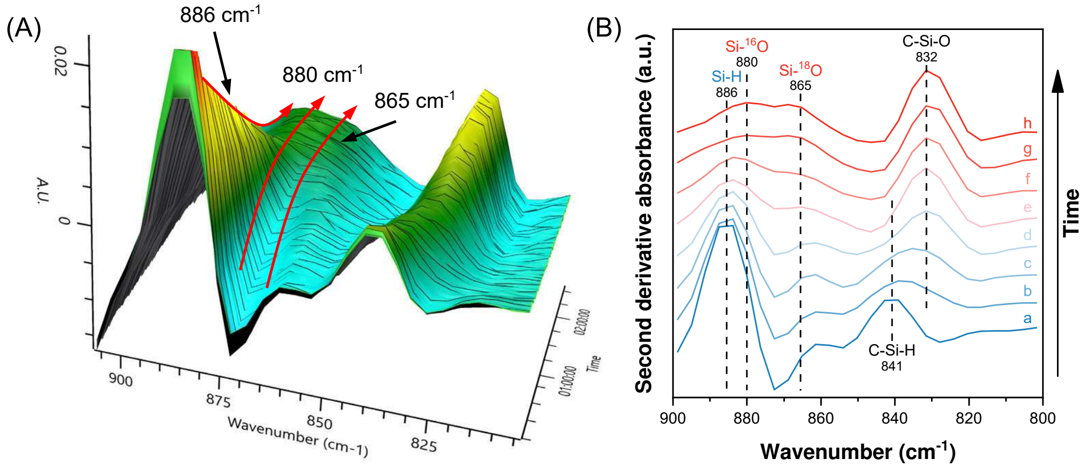

Supplementary Fig. 29 | (A) Three-dimensional (3D) stack plot of the second derivative IR spectra of the oxidation of **1a** in MeCN/$H_2{}^{18}O$ mixture under air atmosphere using Co-N_4@NPC-re as catalyst. The original 3D stack plot of IR spectra was shown in **Fig. 3A**. (B) Selected second derivative spectra of different times. From bottom to top, a-h: 15, 35, 55, 75, 95, 115, 135, and 155 min.

In the real reaction system, due to the partially overlapped of the characteristic band of **1a** (886 cm^{-1}) and **2a** (880 cm^{-1} for **2a-^{16}O** and 865 cm^{-1} for **2a-^{18}O**), second derivative spectroscopy was applied to identify the potential peaks in IR spectra. The second derivative spectra clearly showed the peak at 886 cm^{-1} decreased and the peaks at 880 and 865 cm^{-1} increased during the reaction (**Supplementary Fig. 29**), indicated the consumption of **1a** and the formation **2a-^{16}O** and **2a-^{18}O**. Considering only oxygen molecules contained ^{16}O atoms in the reaction system, these results provided directed evidence that O_2 participates in the reaction as a reactant.

Based on the results of second derivative spectral analysis, a curve-fitting was further used to quantitatively calculate the peak area of each component in the mixture at different reaction times. A part of the fitting results were shown in **Supplementary Fig. 30** and the respective corresponding changes were shown in **Fig. 3B** in the main text. The fitting results indicated that the initially formed product was **2a-^{18}O** accompanied by the delayed appearance of **2a-^{16}O**. Combining the result that in such Co-N_4@NPC-based catalytic system, O_2 could not directly oxidize **1a** in the absence of H_2O (**Supplementary Table 8**, entry 6), the ^{16}O atom in product **2a-^{16}O** should come from the reduction product of O_2 (such as H_2O_2 and H_2O) which was gradually formed during the reaction.

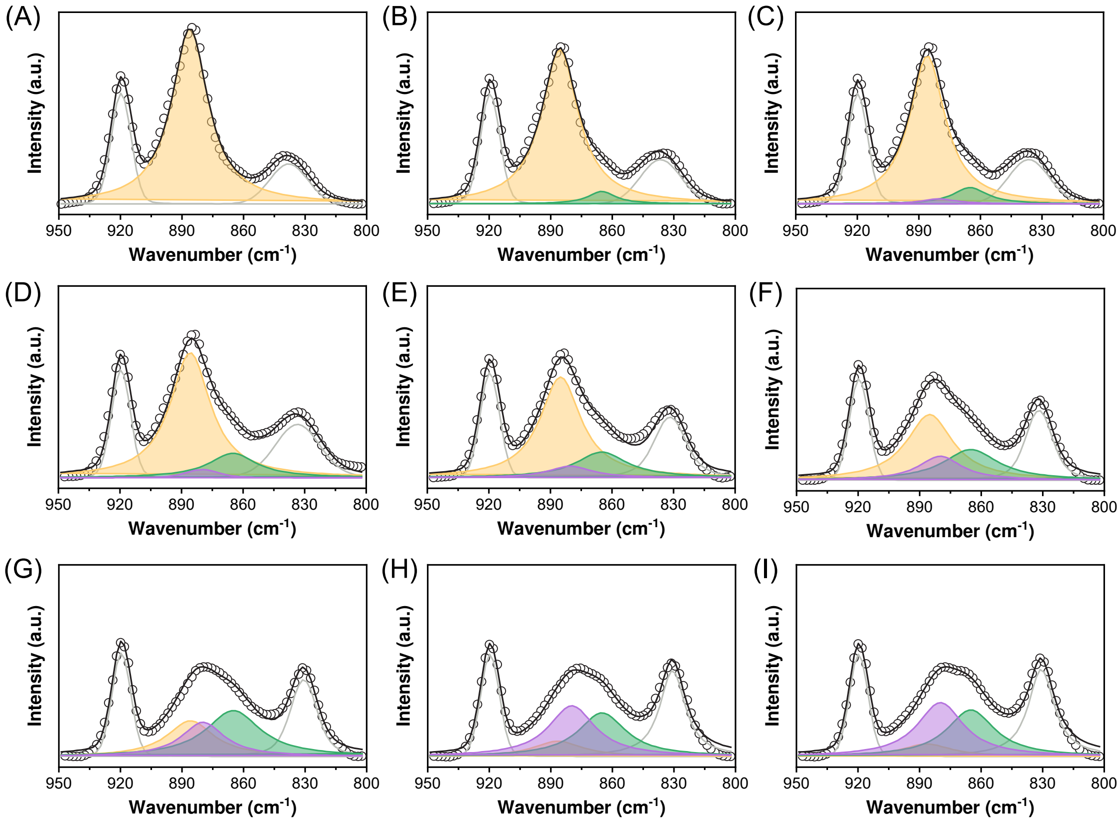

Supplementary Fig. 30 | Raw data and fitting results of selected IR spectra at (A) 15 min, (B) 30 min, (C) 45 min, (D) 60 min, (E) 75 min, (F) 90 min, (G) 105 min, (H) 130 min and (I) 155 min.

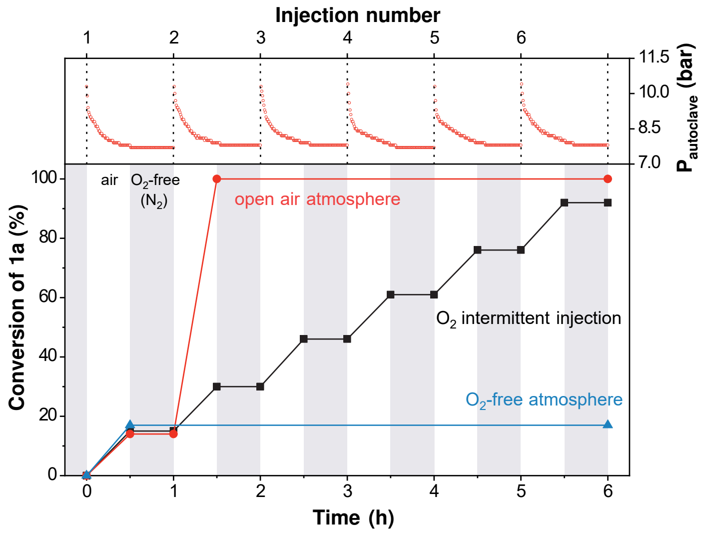

Step	P_i (bar)	P_f (bar)	ΔP (bar)	n_{oxygen} (mol)[a]	ΔConv. of 1a (%)	n_{1a} (mol)	n_{oxygen}:n_{1a}
1	10.3	7.7	2.6	2.06	15.2	3.80	1:1.84
2	10.3	7.8	2.5	1.98	14.9	3.72	1:1.88
3	10.3	7.8	2.5	1.98	15.7	3.92	1:1.98
4	10.4	7.7	2.7	2.14	15.5	3.88	1:1.83
5	10.3	7.8	2.5	1.98	15.3	3.82	1:1.93
6	10.4	7.8	2.6	2.06	16.2	4.05	1:1.97
Sum	-	-	-	12.2	92.8	23.2	1:1.90

[a] Calculated by ideal gas equation, $n_{oxygen} = \frac{\Delta P V_h}{RT}$.

Supplementary Fig. 31 | Intermittent oxygen injection experiments. Reaction conditions: **1a** (25 mmol), H_2O (200 mmol), degassing MeCN (75 mL), Co-N_4@NPC-re (0.1 mol%), 10 bar air (each injection), 30 °C. The table shows the detail pressure and **1a** conversion profile. P_i, initial pressure; P_f, final pressure; Conv., conversion. Conv. determined by GC using anisole as the internal standard.

The capacity of used 120 mL autoclave was determined via water displacement to calculate the injected mole number of oxygen (n_{oxygen}). When equipped with quartz liner, reactants, solvent and stir bar, the surplus volume of headspace (V_h) within the autoclave was 20 mL. During each reaction step, the reactor pressure dropped rapidly at the beginning and finally kept constant. The decreased pressure ΔP roughly equal the partial pressure of O_2 in pressurized air, further GC-TCD analysis showed the O_2 was almost completely consumed after reaction. In addition, by stopping inject oxygen after the first injection, we observed no additional product during the next 5 h (blue line). Contrarily, exposing the solution to open air atmosphere resulting a full conversion of **1a** within 0.5 h (red line). These results further suggested O_2 participates reaction as another reactant, which was in close agreement with the results from real-time FT-IR experiments. Further quantitative analysis showed that the stoichiometry of the overall reaction of O_2 with **1a** was approximately 1:2. Combining the fact of identifying H_2O_2 as an intermediate, the possible pathway for Co-N_4@NPC-re-catalyzed silane oxidation can be described as follows:

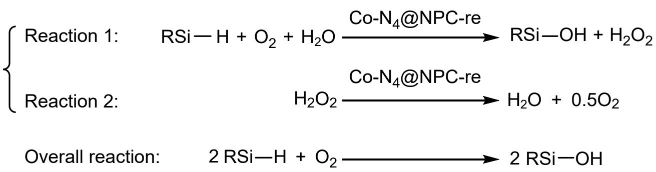

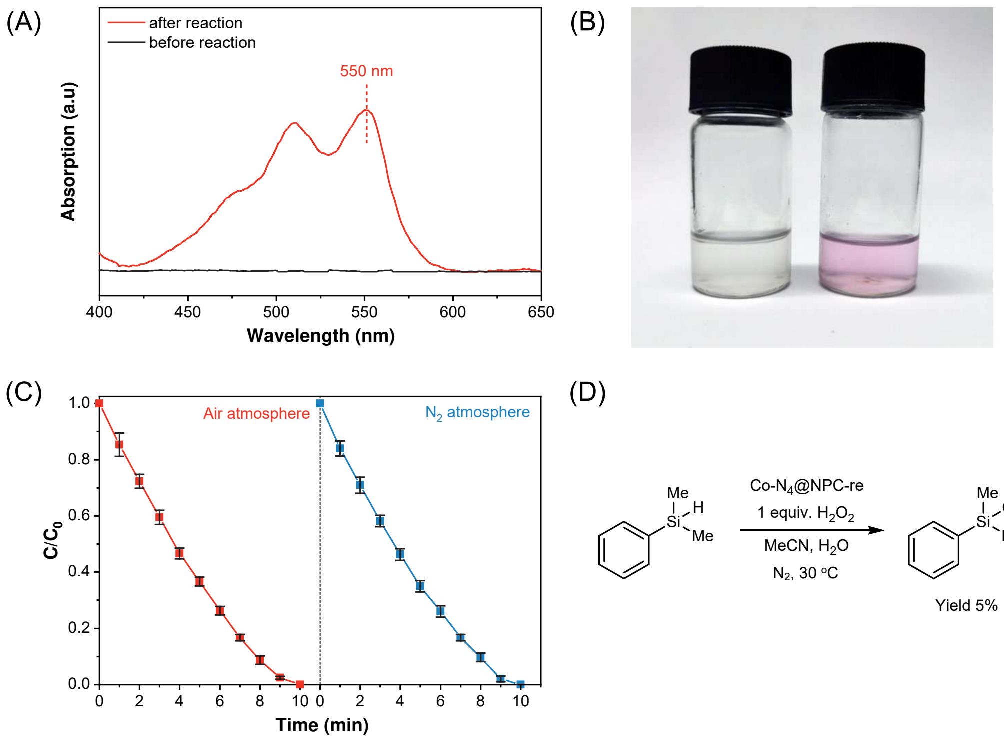

Supplementary Fig. 32 | (A) Colorimetric detection of H_2O_2 in reaction solution. (B) Images of H_2O_2 determination for reaction solution before (left) and after (right) reaction. (C) The evolution of H_2O_2 in Co-N_4@NPC-re-catalyzed H_2O_2 disproportionation under different atmosphere. Reaction conditions: 0.1 mol/L H_2O_2 aqueous solution (100 mL), Co-N_4@NPC-re (Co 0.02 mol%), 30 ºC. Error bars represent the standard deviation from at least three independent experiments. (D) Control experiment with H_2O_2 as oxidant. Reaction conditions: **1a** (1mmol), H_2O (3.5 mmol), Co-N_4@NPC-re (Co 0.5 mol%), MeCN (2.5 mL), 30 ºC, N_2 atmosphere (in a N_2-filled glovebox), 30 min, 100 μL 30% H_2O_2 aqueous solution (contain 1 mmol H_2O_2 and 4.5 mmol H_2O) was dissolved in 0.5 mL MeCN and injected over 5 min via syringe pump.

For determination of H_2O_2, a modified chromogenic method using Fe_3O_4 magnetic nanoparticles as a peroxidase mimetic and *N,N*-diethyl-*p*-phenylenediamine sulfate (DPD) as an indicator was employed [3]. The oxidation product (DPD+) of DPD has a strong absorption maximum at 550 nm. In this way, we were able to clearly identify the formation of H_2O_2 during the reaction (**Supplementary Fig. 32**, A and B).

The essential role of H_2O_2 was further explored via some control experiments. H_2O_2 was found to undergo disproportionation in the presence of Co-N_4@NPC-re under (an)aerobic conditions in the absence of **1a** (**Supplementary Fig. 32C**). The TOF reaches up to more than 44000 h^{-1} in both air and N_2 atmosphere, which is over 70-fold higher than the TOF of catalytic **1a** oxidation. In addition, separate experiment (**Supplementary Fig. 32D**) showed that using H_2O_2 as oxidant only gives very low **2a** yield under actual reaction system (in absence of O_2), while large amounts of O_2 evolution were observed. Together, these results suggest that H_2O_2, formed during the reaction, will undergo rapid disproportionation in preference to oxidizing **1a**.

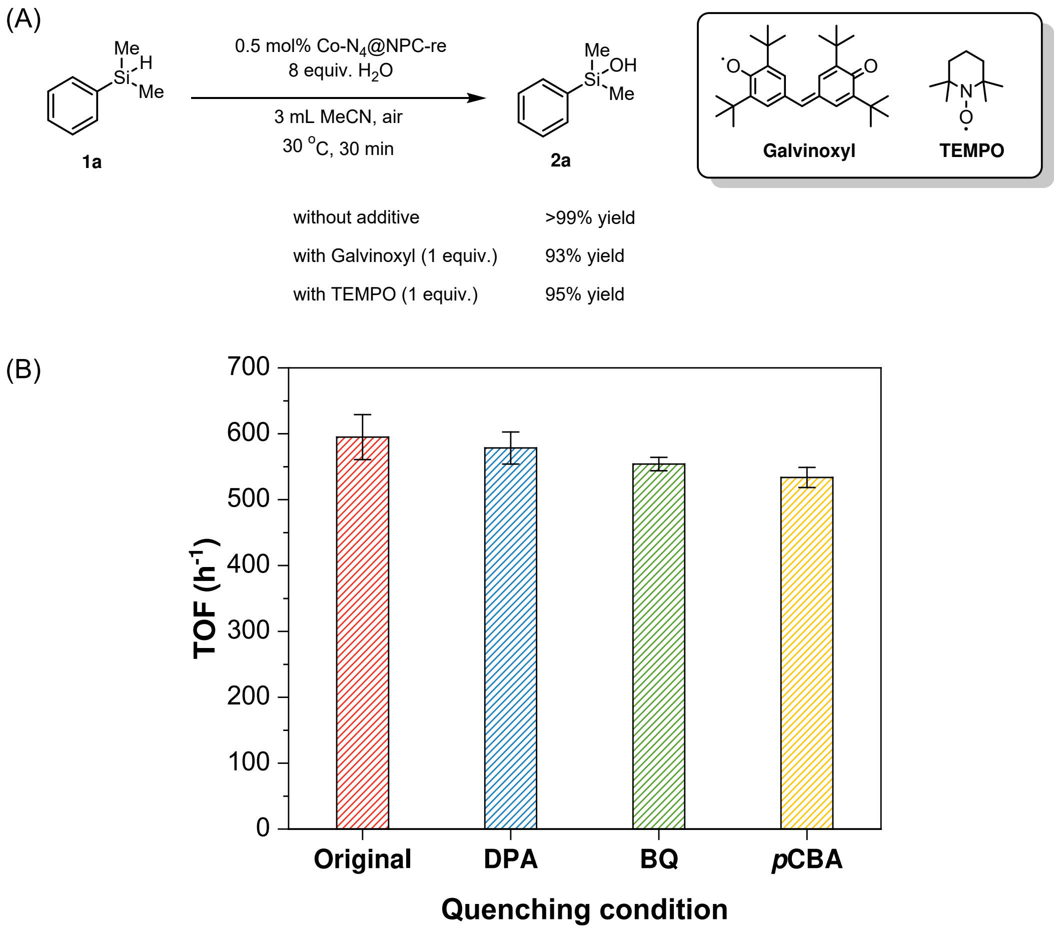

Supplementary Fig. 33 | (A) Control reactions performed in the presence of various radical scavengers. (B) Effect of the addition of various ROS scavengers on **1a** oxidation over Co-N_4@NPC-re catalyst. Reaction conditions: **1a** (1 mmol), H_2O (8 mmol), MeCN (3 mL), Co-N_4@NPC-re (metal 0.5 mol%), Galvinoxyl (1 mmol, if needed), TEMPO (1 mmol, if needed), DPA (0.5 mmol, if needed), BQ (0.5 mmol, if needed), *p*CBA (0.5 mmol, if needed), air atmosphere, 30 °C. The yield was determined by GC using anisole as an internal standard. TOF was measured at **1a** conversion below 20% based on total Co atoms. Error bars represent the standard deviation from at least three independent experiments. DPA, 9,10-diphenylanthracene; BQ, *p*-benzoquinone; *p*CBA, 4-chlorobenzoic acid.

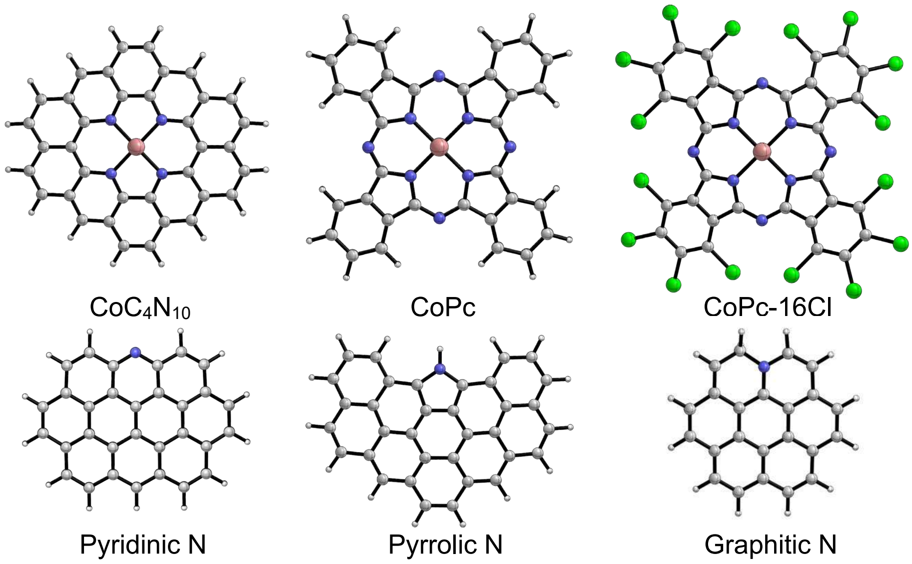

Supplementary Fig. 34 | DFT-optimized cluster models of CoN_4C_{10}, CoPc, CoPc-16Cl and N-doped graphene sheets. Co, pink; C, grey; N, blue; H, white; Cl, green.

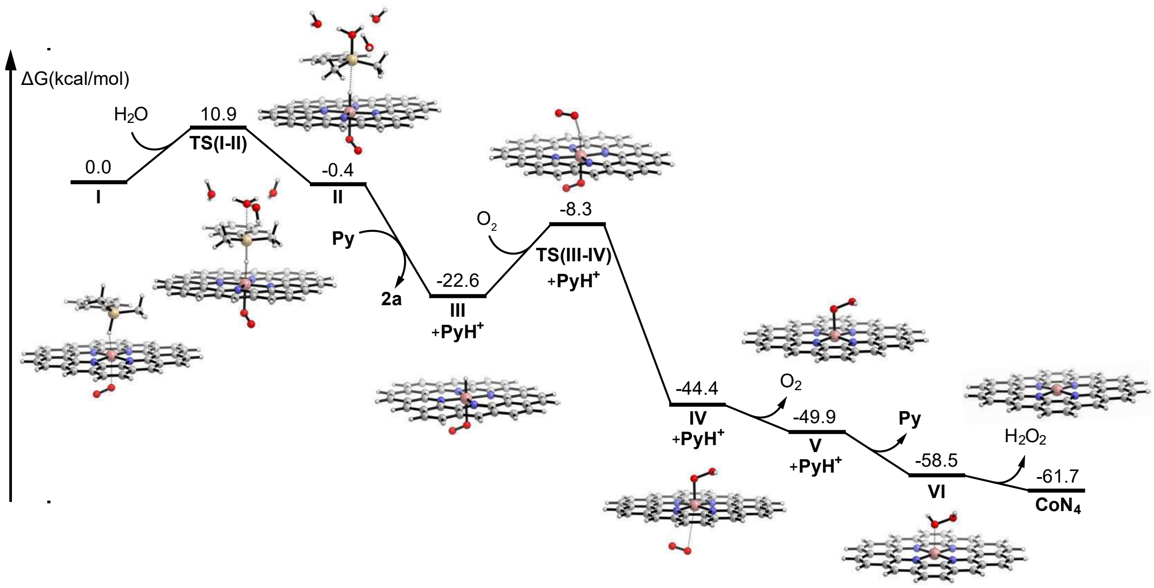

Supplementary Fig. 35 | Free energy profiles for Co-N_4/pyridinic-N catalyzed silane oxidation at 298.15K.

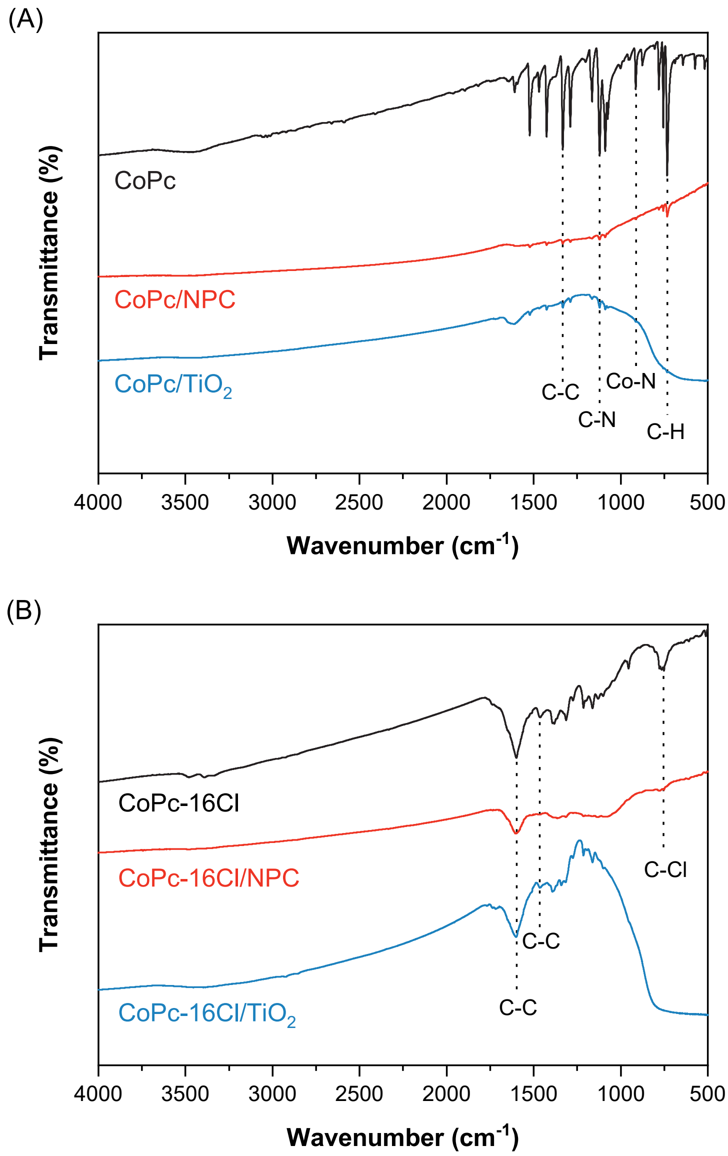

Supplementary Fig. 36 | (A) FT-IR spectra of CoPc, CoPc/NPC and CoPc/TiO_2. (B) FT-IR spectra of CoPc-16Cl, CoPc-16Cl/NPC and CoPc-16Cl/TiO_2.

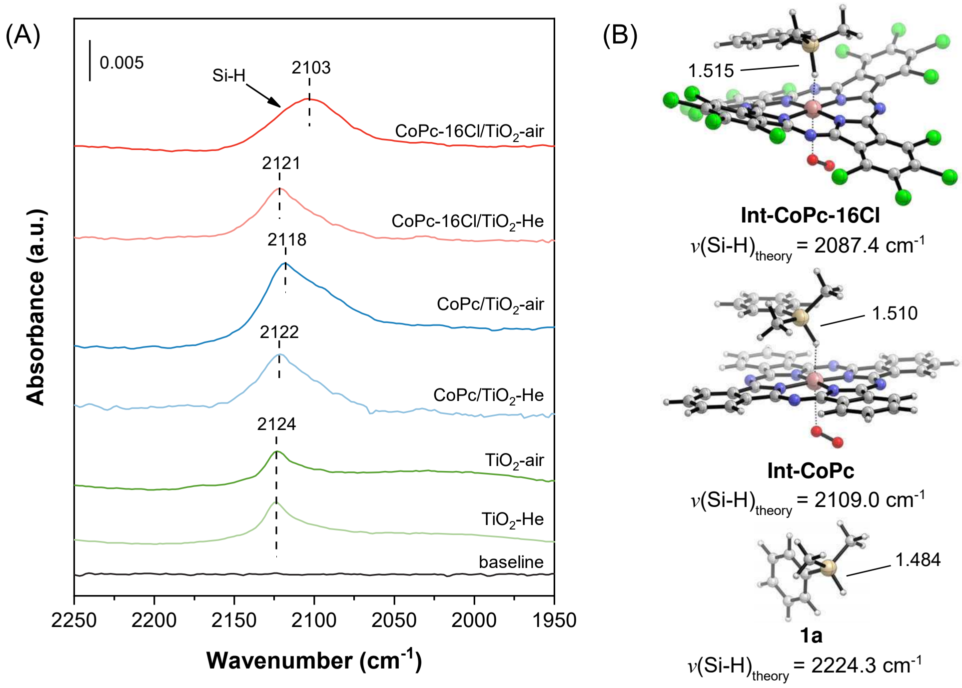

Supplementary Fig. 37 | (A) DRIFT spectra of **1a** adsorbed on TiO_2, CoPc/TiO_2 and CoPc-16Cl/TiO_2 under different atmosphere at 15 ºC. (B) DFT-optimized geometries and corresponding theoretical stretching vibrations of Si-H bond of **1a-CoPc-16Cl-O_2**, **1a-CoPc-O_2** and **1a** structures. Si-H bond lengths are given in Å.

TiO_2-supported CoPc-based samples were chosen as the model of actual catalyst instead of Co-N_4- or CoPc-based carbon catalysts, because the reflectance of such Co-N_4- or CoPc-based carbon catalysts are insufficient for performing IR measurements. As catalytic performance evaluation of CoPc-based or -derived catalyst models (**Supplementary Table 1**) clearly showed that N-coordinated Co atomic site was the reaction site of silane and the reaction behavior of CoPc-based carbon catalysts is similar to that of Co-N_4@NPC-based catalysts, the IR studies of TiO_2-supported CoPc-based samples will reveal the interaction between silane and Co site in some extent.

As shown in **Supplementary Fig. 37A**, the atmosphere during the treatment of TiO_2 with **1a** has no influence for **1a** adsorption. An absorption band assigned to a Si-H bond stretching vibration appeared at ν = 2124 cm^{-1} in the absence or presence of O_2. As a comparison, when CoPc/TiO_2 treated with **1a** in the presence of O_2, slight redshift of stretching band of Si-H bond could be clearly verified. And more importantly, the extent of such redshift was more pronounced on CoPc-16Cl/TiO_2 in the presence of O_2. These phenomena reveal that O_2 promotes the activation of Si-H bond in hydrosilane that adsorbed on N-coordinated Co atomic site. Moreover, electron-deficient Co site can active Si-H bond more efficiently in the presence of O_2, which is in agreement with the higher catalytic activity of CoPc-16Cl/NC-900.

It was reported in electrocatalytic oxygen reduction reaction that O_2 can easily interact with such Co-N_x center through end-on adsorption and cause the electron transfer from Co atom to O atom, which decreases the electron density of Co site [4]. These results make us to propose that in our system, O_2 can act as a ligand to optimize the electronic structure of Co and co-adsorb with silane on Co atom to boost the activation capacity of Co site for the Si-H bond. We employed DFT calculations to study the interaction of O_2, **1a** and CoPc or CoPc-16Cl (**Supplementary Fig. 37B**). The optimal geometries of both adducts **1a-CoPc-16Cl-O_2** and **1a-CoPc-O_2** show a greater Si-H bond length than that of individual **1a**, suggesting the O_2-coordinated Co-N_4 site can active Si-H bond effectively, which is consistent with the observation of DRIFT spectra.

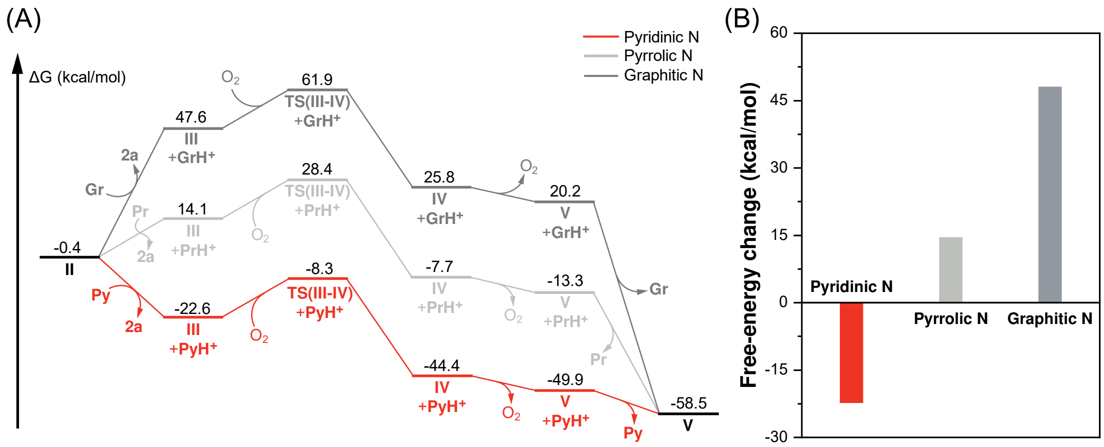

Supplementary Fig. 38 | (A) Free energy profiles for with different N-doped graphene structures at 298.15K. (B) The free-energy changes of the deprotonation step "II→III" with different N-doped graphene structures. Py, Pyridinic N; Pr, Pyrrolic N; Gr, Graphitic N.

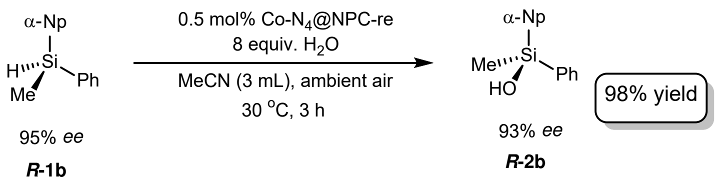

Supplementary Fig. 39 | Oxidation of optically active hydrosilane ***R*-1b** over Co-N$_4$@NPC-re catalyst. As seen from the below Chiral HPLC data, the inversion of the configuration at silicon was obtained.

Chromatogram of **1b**

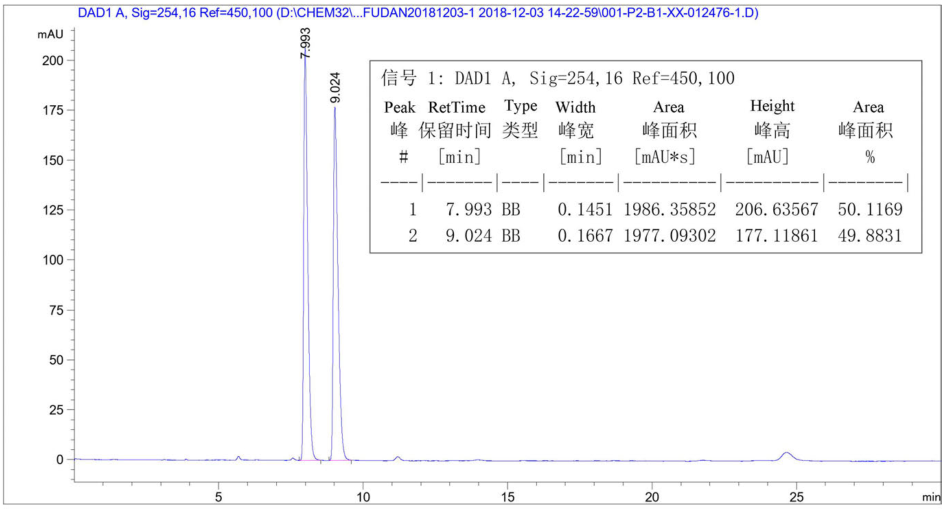

信号 1: DAD1 A, Sig=254,16 Ref=450,100

Peak 峰 #	RetTime 保留时间 [min]	Type 类型	Width 峰宽 [min]	Area 峰面积 [mAU*s]	Height 峰高 [mAU]	Area 峰面积 %
1	7.993	BB	0.1451	1986.35852	206.63567	50.1169
2	9.024	BB	0.1667	1977.09302	177.11861	49.8831

Chromatogram of ***R*-1b**

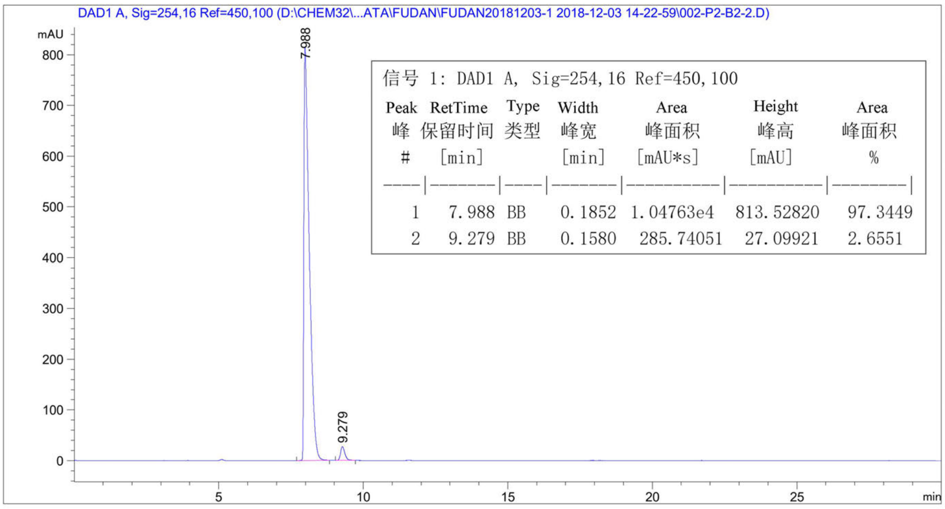

信号 1: DAD1 A, Sig=254,16 Ref=450,100

Peak 峰 #	RetTime 保留时间 [min]	Type 类型	Width 峰宽 [min]	Area 峰面积 [mAU*s]	Height 峰高 [mAU]	Area 峰面积 %
1	7.988	BB	0.1852	1.04763e4	813.52820	97.3449
2	9.279	BB	0.1580	285.74051	27.09921	2.6551

Chromatogram of **2b**

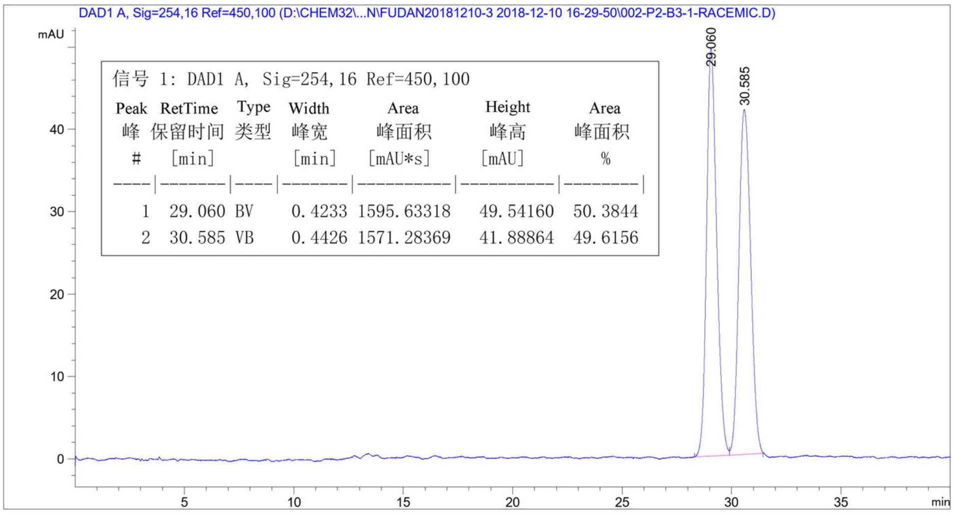

信号 1: DAD1 A, Sig=254,16 Ref=450,100

Peak 峰 #	RetTime 保留时间 [min]	Type 类型	Width 峰宽 [min]	Area 峰面积 [mAU*s]	Height 峰高 [mAU]	Area 峰面积 %
1	29.060	BV	0.4233	1595.63318	49.54160	50.3844
2	30.585	VB	0.4426	1571.28369	41.88864	49.6156

Chromatogram of ***R*-2b**

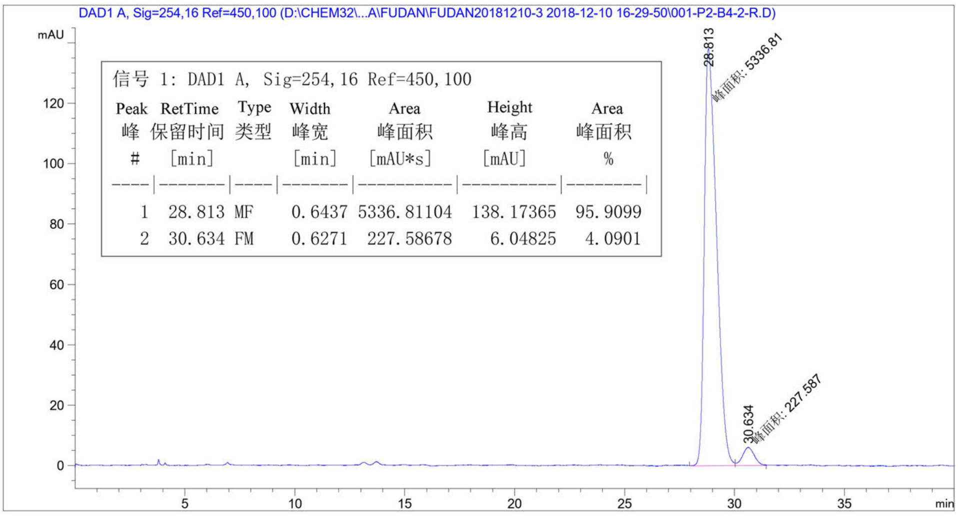

信号 1: DAD1 A, Sig=254,16 Ref=450,100

Peak 峰 #	RetTime 保留时间 [min]	Type 类型	Width 峰宽 [min]	Area 峰面积 [mAU*s]	Height 峰高 [mAU]	Area 峰面积 %
1	28.813	MF	0.6437	5336.81104	138.17365	95.9099
2	30.634	FM	0.6271	227.58678	6.04825	4.0901

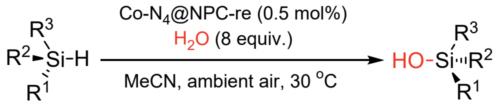

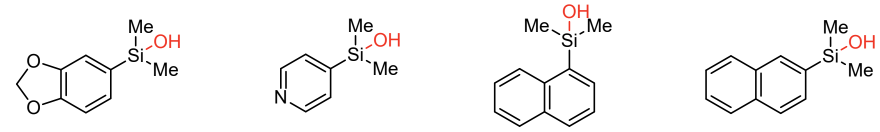

2bj, 3 h, 97% **2bk**, 4 h, 93% **2bl**, 3 h, 98% **2bm**, 1 h, 97%

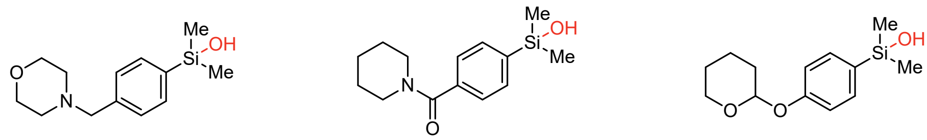

2bn, 6 h, 95% **2bo**, 5 h, 96% **2bp**, 3 h, 97%

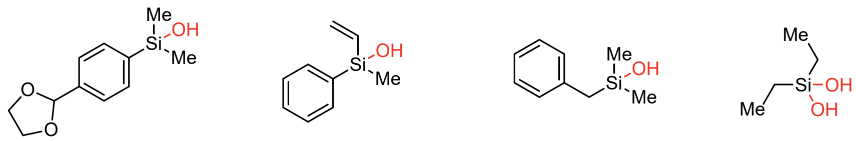

2bq, 4 h, 94% **2br**, 4 h, 97% **2bs**, 4 h, 98% **2bt**, 2 h, 96%

Supplementary Fig. 40 | Extended substrate scope of silane oxidation continued from **Fig. 4A**. Reaction conditions: silane (1 mmol), H_2O (8 mmol), MeCN (3 mL), Co-N_4@NPC-re (Co 0.5 mol%), 30 ºC, air atmosphere. Isolated yields are reported unless otherwise indicated.

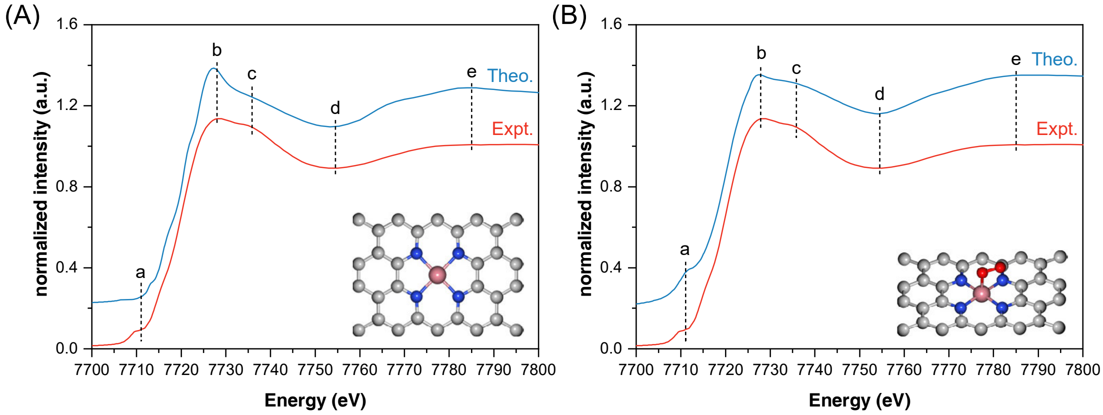

Supplementary Fig. 41 | Comparison between the experimental Co K-edge XANES spectrum of Co-N_4@NPC-re and the theoretical spectra of CoN_4C_{12} and CoN_4C_{12}-O_2 structure.

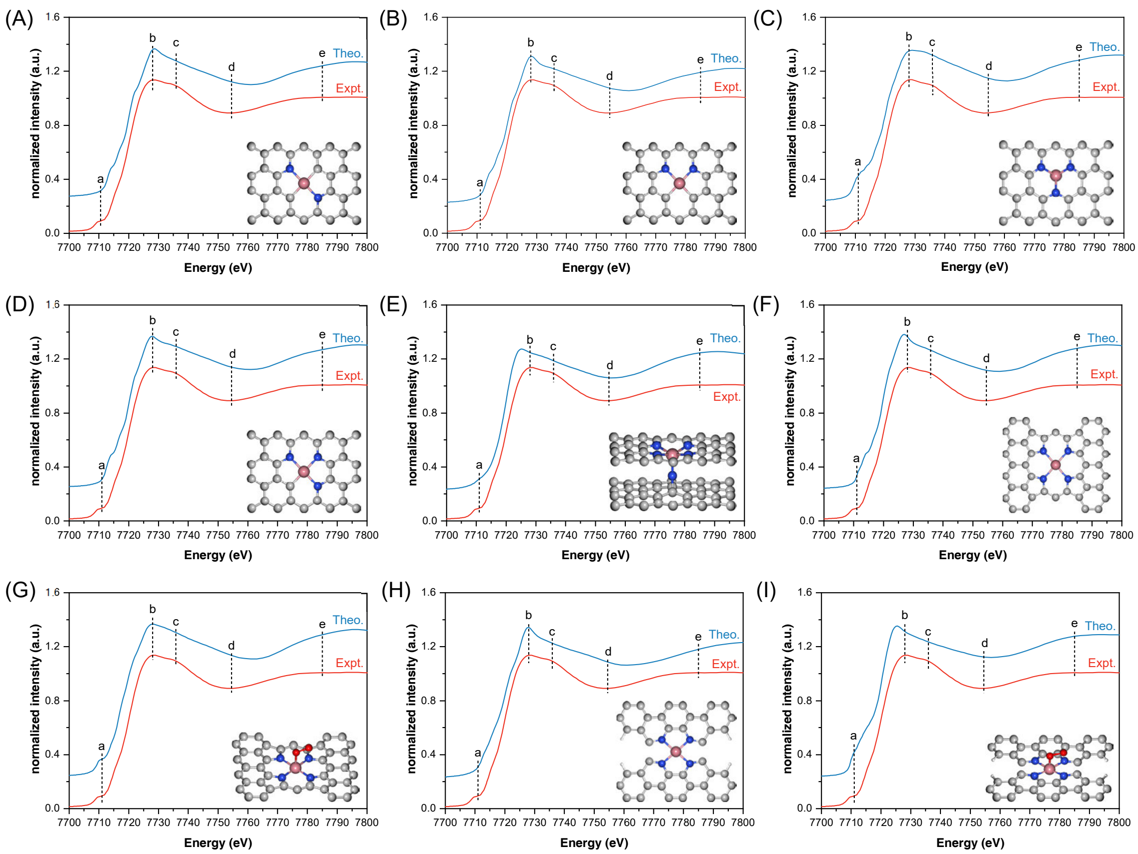

Supplementary Fig. 42 | Comparison between the experimental Co K-edge XANES spectrum of Co-N_4@NPC-re and the theoretical spectra of other potential Co-N-C structures.

The Co K-edge XANES simulation was conducted with the FDMNES code in multiple scattering mode (Green's functions) using the muffin-tin potential. The calculated radius was 6.5 Å with a self-consistent calculated radius of 6.0 Å. Parameter optimization was performed by comparing the theoretical and experimental spectra to acquire the most appropriate convolution parameters. The calculated models were built based on DFT calculations to avoid manual bias.

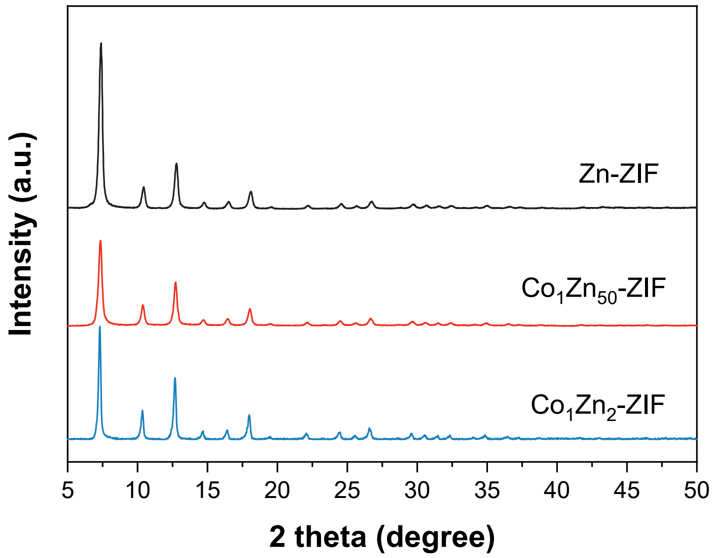

Supplementary Fig. 43 | XRD patterns of ZIF precursors.

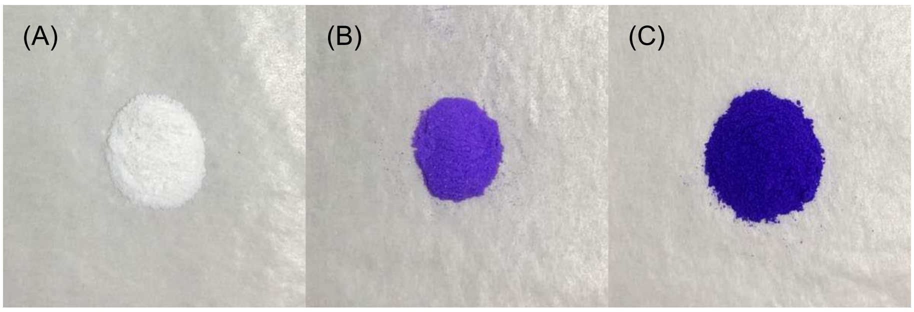

Supplementary Fig. 44 | Photographs of (A) Zn-ZIF, (B) Co_1Zn_{50}-ZIF and (C) Co_1Zn_2-ZIF.

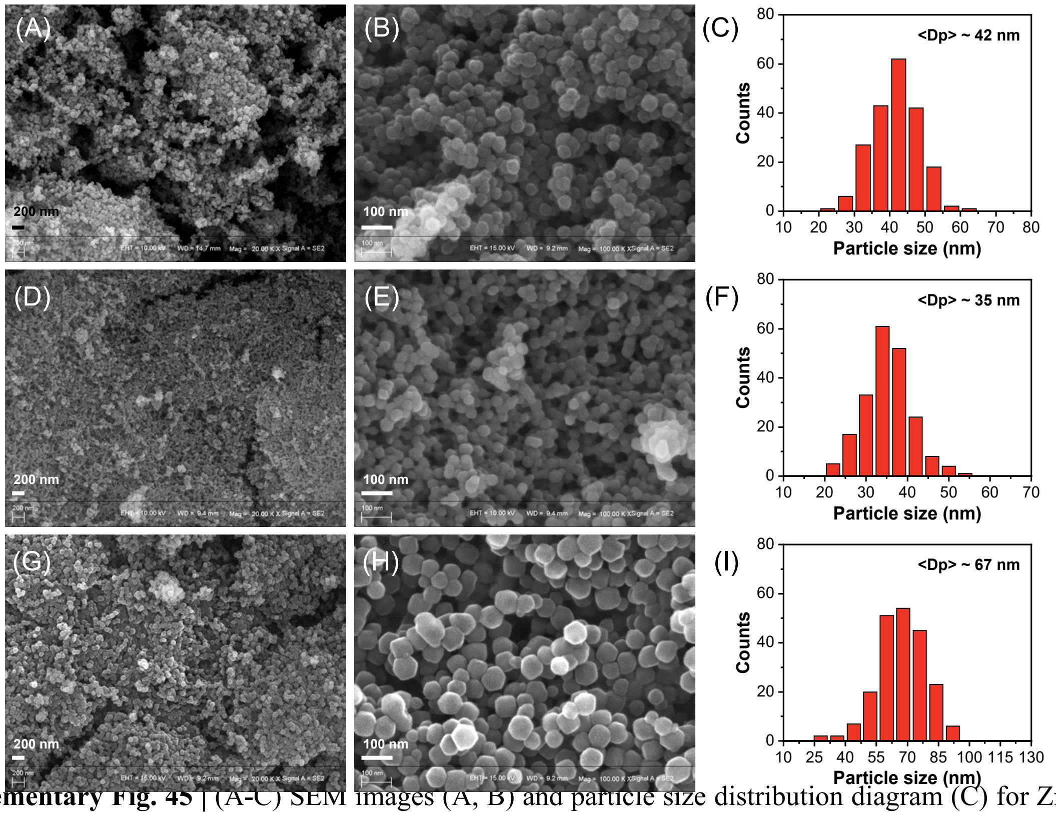

Supplementary Fig. 45 | (A-C) SEM images (A, B) and particle size distribution diagram (C) for Zn-ZIF. (D-F) SEM images (D, E) and particle size distribution diagram (F) for Co_1Zn_{50}-ZIF. (G-I) SEM images (G, H) and particle size distribution diagram (I) for Co_1Zn_2-ZIF.

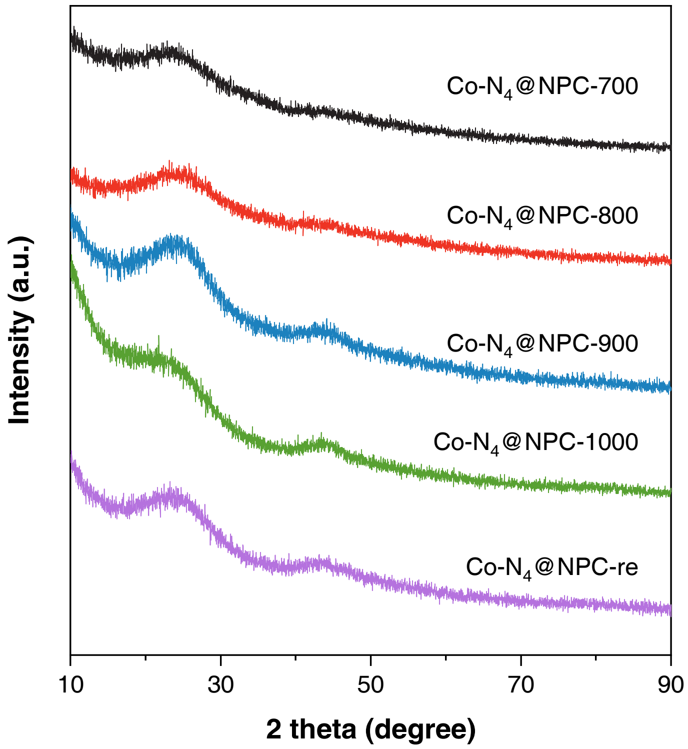

Supplementary Fig. 46 | XRD patterns for Co_1Zn_{50}-ZIF-derived Co-N_4@NPC-based samples with different synthesis conditions.

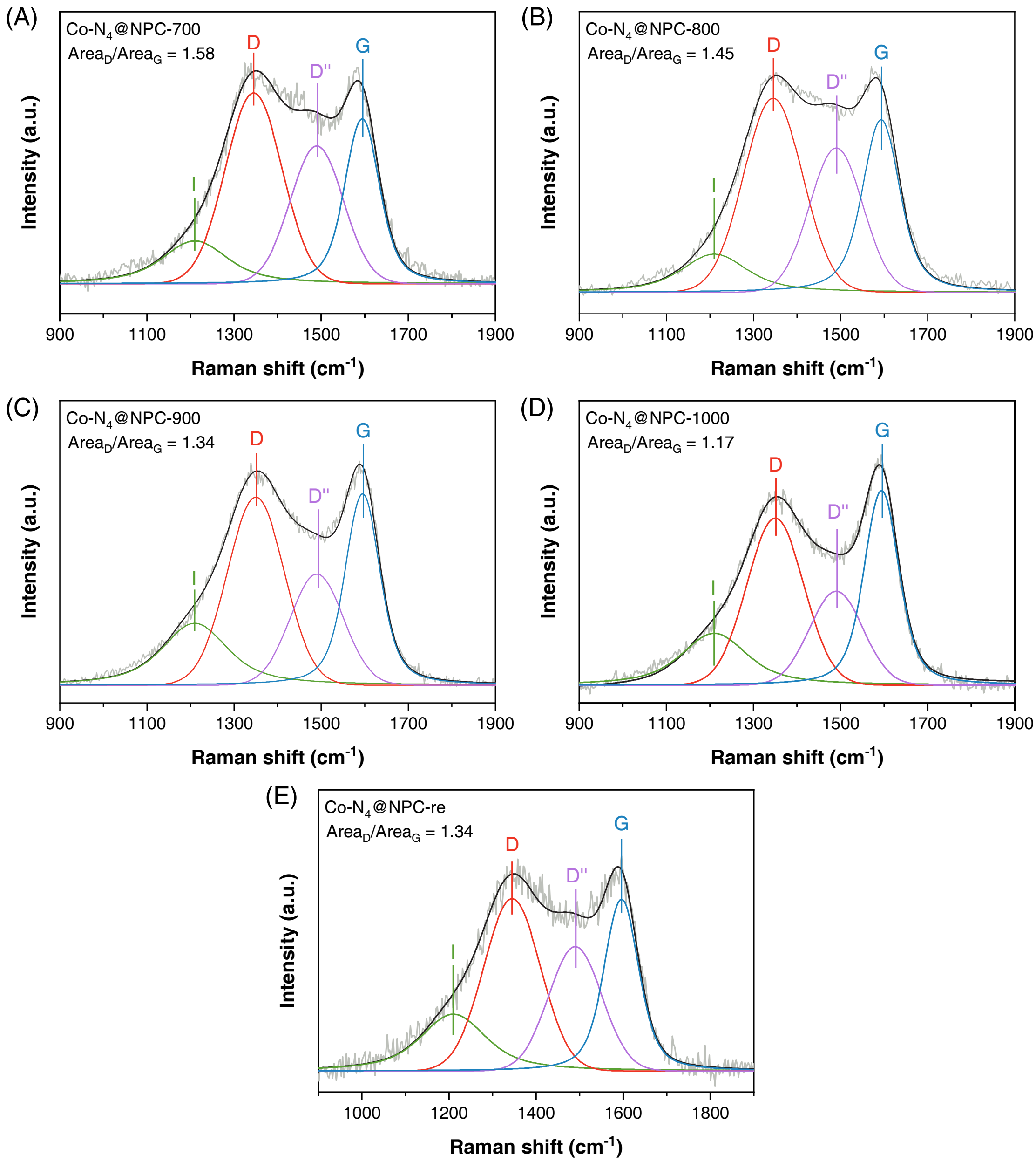

Supplementary Fig. 47 | Raman spectra for Co_1Zn_{50}-ZIF-derived Co-N_4@NPC-based samples with different synthesis conditions. With the increase of pyrolysis temperature, the ratio of $Area_D/Area_G$ decreased gradually, indicating the significant promotion of graphitization degree. In addition, peak around 1490 cm^{-1} becomes obviously smaller with an increase in heating temperatures, suggesting a reduction of nitrogen doping and other irregular carbon structures, i.e. five-side ring [5]. The ratio of $Area_D/Area_G$ in Co-N_4@NPC-re is closed to Co-N_4@NPC-900, revealing the similar partially graphitized carbon structures in such samples.

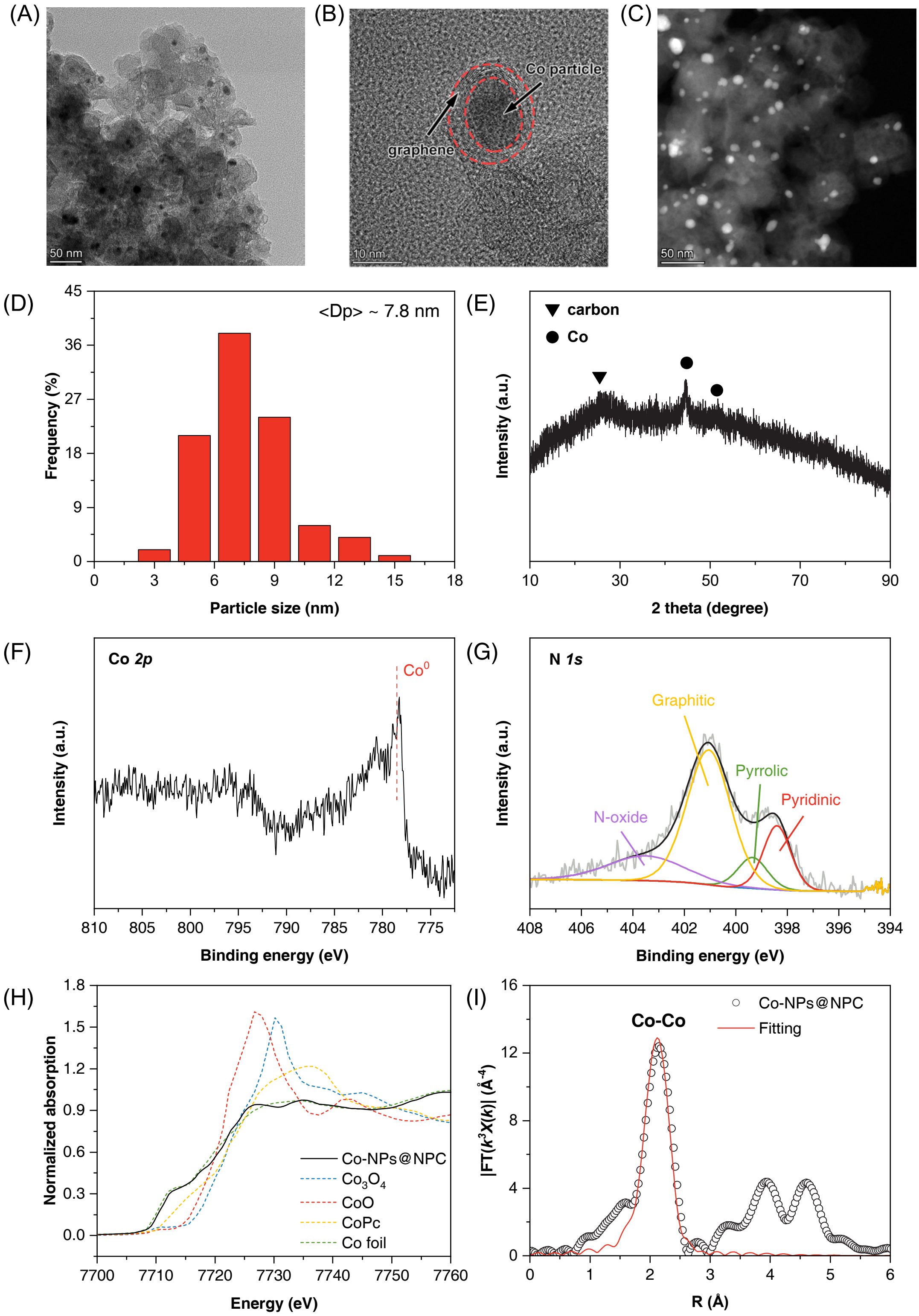

Supplementary Fig. 48 | Characterizations of Co-NPs@NPC. (A) TEM image. (B) High resolution TEM image. The graphene-encapsulated Co nanoparticle was obtained. (C) STEM image. (D) Particle size distribution diagram based on STEM images. The average size of Co particles is 7.8 nm. (E) XRD pattern. (F) Co *2p* XPS spectrum. (G) N *1s* XPS spectrum. (H) Co K-edge XANES spectra of Co-NPs@NPC, Co_3O_4, CoO, CoPc and Co foil. (H) R-space Co K-edge EXAFS spectra and fittings of Co-NPs@NPC. The fitting results are listed in **Supplementary Table 2**.

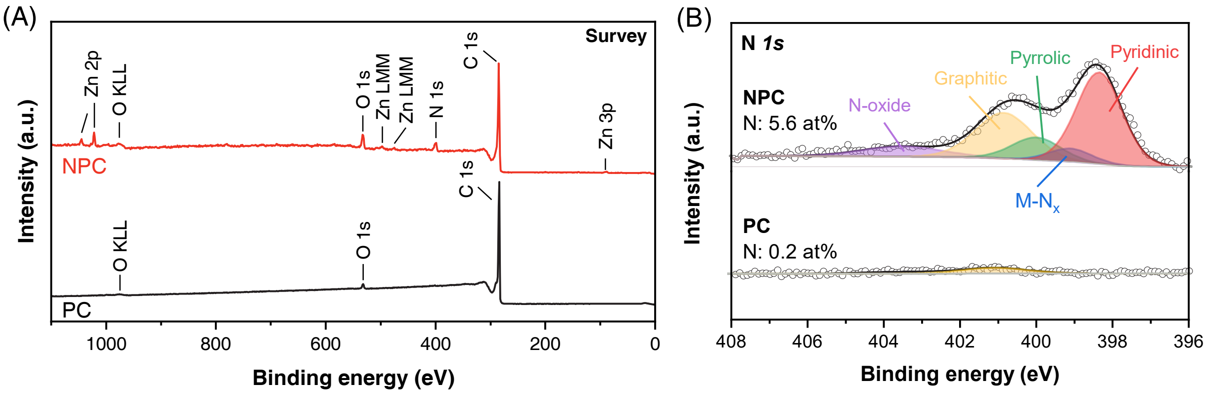

Supplementary Fig. 49 | (A) Survey and (B) N *1s* XPS spectra of PC and NPC. Compared to the N concentration of NPC sample (5.6 at%), that of PC is negligible (0.2 at%). Moreover, analysis for N *1s* spectrum of PC showed the residue N species is mainly graphitic N (401.1 eV)[6]. Thus, the PC sample can be used as a quasi N-free porous carbon.

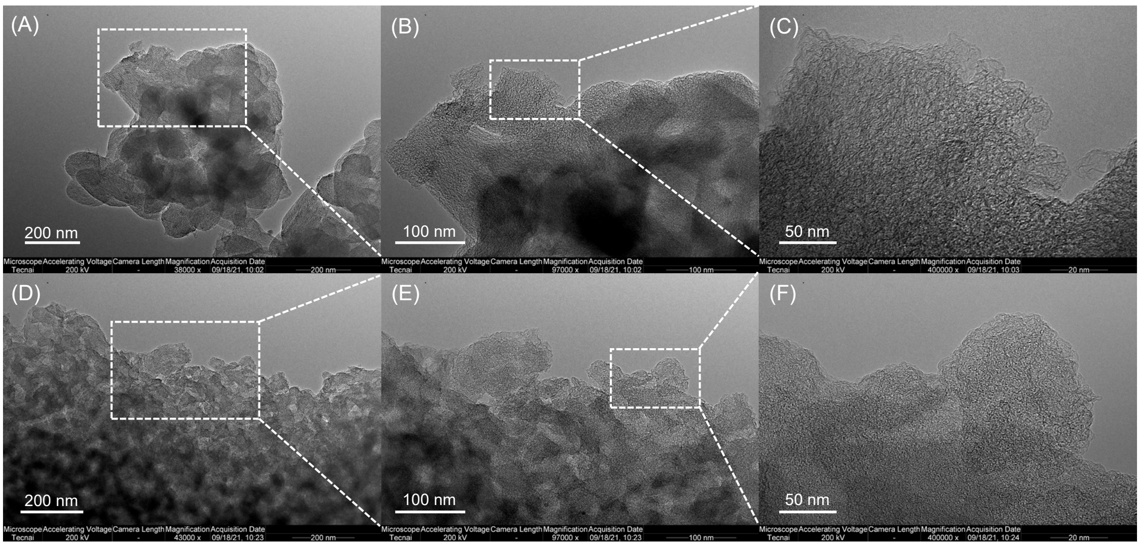

Supplementary Fig. 50 | TEM images of PC (A-C) and NPC (D-F).

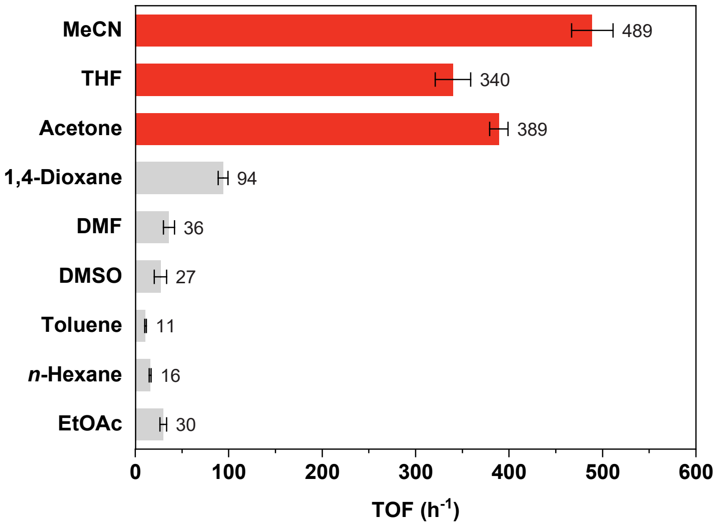

Supplementary Fig. 51 | Catalytic performance for oxidation of **1a** over Co-N_4@NPC-900 catalyst in different solvent media. Reaction conditions: **1a** (1 mmol), H_2O (8 mmol), solvent (3 mL), Co-N_4@NPC-900 (Co 0.5 mol%), 30 °C, air atmosphere. TOF was measured at **1a** conversion below 20% based on total Co atoms. For all reactions, > 99% selectivity of **2a** were obtained.

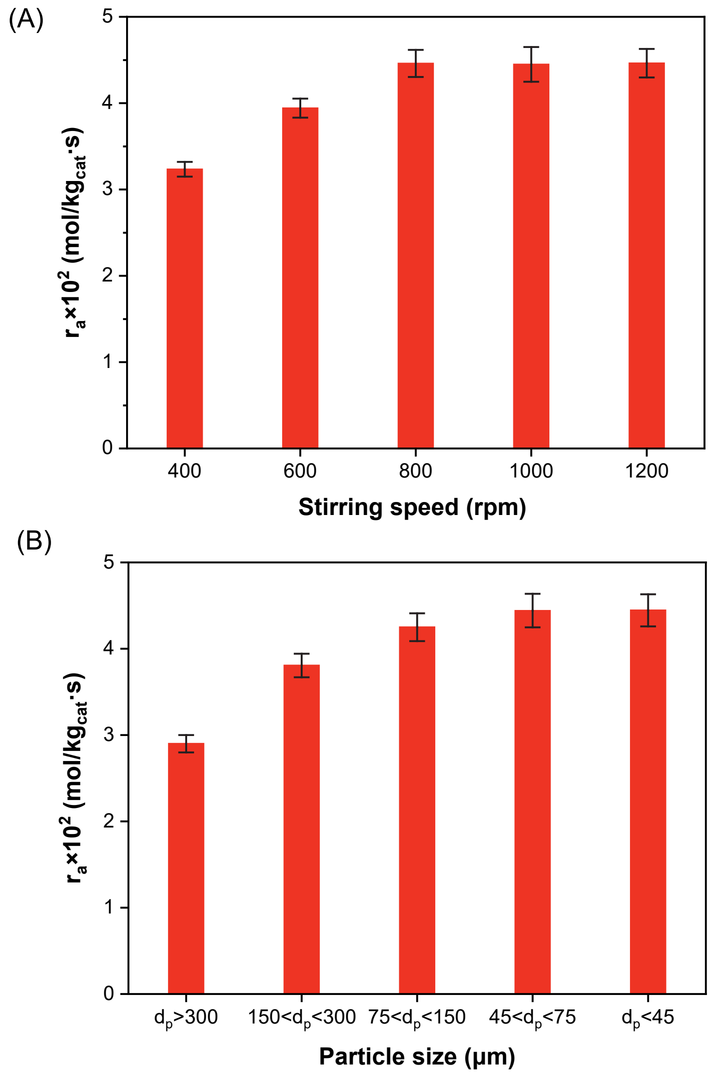

Supplementary Fig. 52 | Dependence of the initial reaction rates (r_a) of Co-N_4@NPC-900-catalyzed **1a** oxidation on (A) stirring speed and (B) particle size. Reaction conditions: **1a** (1 mmol), H_2O (8 mmol), solvent (3 mL), Co-N_4@NPC-900 (Co 0.5 mol%), 30 °C, air atmosphere. Error bars represent the standard deviation from at least three independent experiments. r_a was calculated based on the corresponding TOF values.

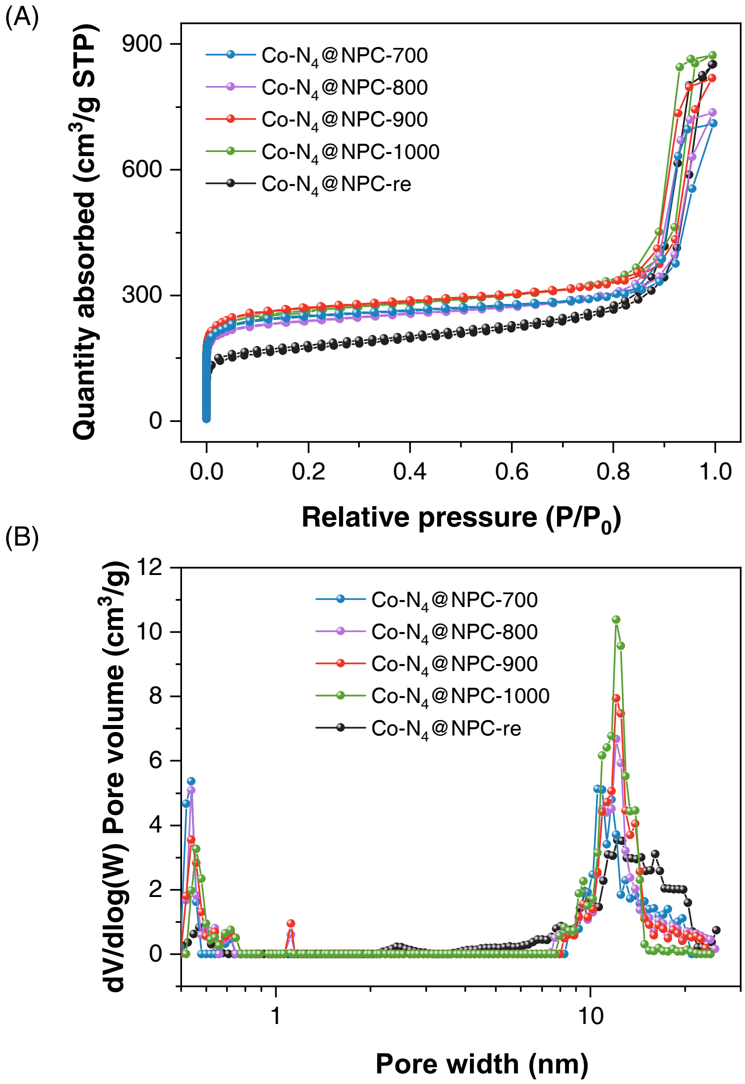

Supplementary Fig. 53 | N_2 adsorption/desorption isotherms (A) and pore size distribution (B) of different Co-N_4@NPC samples. The pore size distribution was determined from non-local density functional theory (NLDFT) model of the N_2 adsorption data.

Supplementary Table 1 | Catalytic results of oxidase-type selective 1a oxidation over CoPc-based or -derived biomimetic catalyst models.

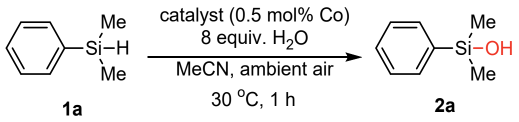

Entry[a]	**Catalyst**	**Yield of 2a (%)**[b]
1	CoPc/NPC	18
2	Co-N_4/NPC	42
3	CoPc/PC	<1
4[c]	NPC	N.R.
5[c]	CoPc/PC + NPC	10
6[d]	Co-N_4/NPC	N.R.
7[e]	Co-N_4/NPC	N.R.
8	CoPc-16Cl/NPC	39

[a] Reaction conditions: **1a** (1 mmol), H_2O (8 mmol), MeCN (3 mL), catalyst (Co 0.5 mol%), air atmosphere, 30 °C, 1 h. [b] The yield was determined by GC using anisole as an internal standard, N.R. = no reaction. [c] Added 120 mg NPC. [d] Under N_2 atmosphere. [e] Without adding H_2O and using anhydrous MeCN (3 mL) as solvent.

Supplementary Table 2 | Structure parameters extracted from the EXAFS fitting[a].

Sample	Edge	Shell	CN	R (Å)	ΔE_0 (eV)	σ^2*10^3 ($Å^2$)	R-factor
Co foil	Co K-edge	Co-Co	12.0	2.49	8.3	6.1	0.002
CoPc	Co K-edge	Co-N	4.0	1.91	1.8	1.3	0.05
Zn foil	Zn K-edge	Zn-Zn	6.0	2.64	-2.5	13.7	0.03
ZnPc	Zn K-edge	Zn-N	4.0	1.97	4.2	3.5	0.02
$Co-N_4$@NPC-700	Co K-edge	Co-N	3.2	1.89	-5.2	0.6	0.004
$Co-N_4$@NPC-800	Co K-edge	Co-N	3.4	1.89	-5.2	3.4	0.005
$Co-N_4$@NPC-900	Co K-edge	Co-N	3.6	1.98	-3.5	10.0	0.03
	Zn K-edge	Zn-N	4.2	2.01	-1.0	10.2	0.003
$Co-N_4$@NPC-1000	Co K-edge	Co-N	3.8	1.94	-6.0	10.3	0.007
$Co-N_4$@NPC-re (fresh)	Co K-edge	Co-N	4.1	1.97	-4.3	4.3	0.02
	Zn K-edge	Zn-N	4.0	2.01	-0.6	10.4	0.004
$Co-N_4$@NPC-re (used)	Co K-edge	Co-N	4.0	2.01	-2.0	3.7	0.02
	Zn K-edge	Zn-N	4.0	2.01	-0.9	8.2	0.004
Co-NPs@NPC	Co K-edge	Co-Co	9.8	2.50	-3.6	6.3	0.003
CoPc/PC	Co K-edge	Co-N	4.2	1.96	-0.1	1.1	0.05
CoPc/NPC	Co K-edge	Co-N	4.3	1.96	-0.1	1.1	0.04
$Co-N_4$/NPC	Co K-edge	Co-N	4.0	2.03	-1.5	9.7	0.01
NPC	Zn K-edge	Zn-N	3.5	2.01	0.2	8.2	0.004

[a] R: absorber-backscatterer distance; CN: coordination number; ΔE_0: inner potential correction, σ^2: Debye-Waller factor. Error bounds (accuracies) that characterize the structural parameters obtained by EXAFS spectroscopy were estimated as CN ± 20%; R ± 1%; ΔE_0 ± 20%; σ^2 ± 20%.

Supplementary Table 3 | Kinetic isotope effect study for oxidation of **1a** over Co-N_4@NPC-re catalyst.

Entry[a]	Silane	Water	TOF (h^{-1})[b]	KIE[c]
1	$PhMe_2SiH$	H_2O	595±34	-
2	$PhMe_2SiD$	H_2O	256±12	2.32±0.17
3	$PhMe_2SiH$	D_2O	572±30	1.04±0.08

[a] Reaction conditions: silane (1 mmol), water (8 mmol), Co-N_4@NPC-re (Co 0.5 mol%), MeCN (3 mL), 30 ºC, air atmosphere. [b] TOF was measured at **1a** conversion below 20% based on total Co atoms. [c] KIE = TOF (entry 1)/TOF (entry 2) or TOF (entry 1)/TOF (entry 3).

Supplementary Table 4 | Elemental quantification (at%) determined by XPS for different Co catalysts.

Sample	C (at%)	N (at%)	O (at%)	Co (at%)	Zn (at%)
Co-N_4@NPC-700	76.3	15.7	6.4	0.1	1.5
Co-N_4@NPC-800	78.6	14.1	5.9	0.1	1.3
Co-N_4@NPC-900	80.5	12.5	6.0	0.2	0.8
Co-N_4@NPC-1000	90.3	5.6	3.7	0.2	0.2
Co-N_4@NPC-re (fresh)	83.7	9.8	5.7	0.3	0.5
Co-N_4@NPC-re (used)	84.1	9.7	5.4	0.3	0.5

Supplementary Table 5 | The total nitrogen content and percentage of different nitrogen species in different Co catalysts derived from XPS analysis.

Sample	N content (at%)	Pyridinic (%)	M-N_x (%)	Pyrrolic (%)	Graphitic (%)	N-oxide (%)
Co-N_4@NPC-700	15.7	27.0	38.4	17.7	13.4	3.5
Co-N_4@NPC-800	14.1	35.4	32.3	16.6	11.1	4.6
Co-N_4@NPC-900	12.5	41.2	24.0	19.3	11.5	4.0
Co-N_4@NPC-1000	5.6	37.0	22.2	16.3	19.4	5.1
Co-N_4@NPC-re (fresh)	9.8	37.2	14.6	9.8	28.6	9.8
Co-N_4@NPC-re (used)	9.7	39.8	13.6	8.7	28.4	9.5

Supplementary Table 6 | ICP-OES results of metal loading amount of different Co-N_4@ NPC-based catalysts.

Sample	Co (wt%)	Zn (wt%)
Co-N_4@NPC-700	1.31	10.55
Co-N_4@NPC-800	1.57	7.88
Co-N_4@NPC-900	1.93	4.18
Co-N_4@NPC-1000	2.11	1.07
Co-NPs@NPC	15.23	0.08
Co-N_4@NPC-re (fresh)	2.75	4.10
Co-N_4@NPC-re (used)	2.74	4.02
Co-N_4/NPC	0.32	1.28

Supplementary Table 7 | TEM-EDS element analysis of Co-N_4@NPC and Co-N_4@NPC-re catalysts.

Element	CoN_4@NPC-900		CoN_4@NPC-re	
	Atomic%	wt%	Atomic%	wt%
C	89.06	83.15	90.25	84.97
N	6.29	6.85	5.97	6.50
O	3.51	4.36	2.82	3.51
Co	0.33	1.50	0.49	2.26
Zn	0.81	4.14	0.54	2.76

Supplementary Table 8 | Reaction condition optimization for oxidation of **1a** over Co-N_4@NPC-900 catalyst.

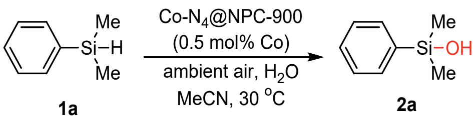

Entry[a]	V_{MeCN} (mL)	V_{water} (μL)	n_{water}/n_{1a}	c_{1a} (mol/L)	Yield of 2a (%)[b]
1	1	145	8	1.0	54
2	2	145	8	0.5	62
3	3	145	8	0.33	71
4	4	145	8	0.25	45
5	5	145	8	0.20	38
6	3	0	0	0.33	N.R.
7	3	55	3	0.33	40
8	3	90	5	0.33	62
9	3	200	11	0.33	46
10	3	270	15	0.33	41

[a] Reaction conditions: **1a** (1 mmol), Co-N_4@NPC-900 (Co 0.5 mol%), 30 °C, air atmosphere, 20 min, N.R.= no reaction. [b] The yield was determined by GC using anisole as an internal standard.

Supplementary Table 9 | N_2 physisorption characteristics of different Co-N_4@NPC-based catalysts.

Sample	**S_{BET} (m^2/g)**	**S_{Micro} (m^2/g)**	**S_{Exter} (m^2/g)**	**V_{Total} (cm^3/g)**	**t-plot V_{Micro} (cm^3/g)**	**V_{Meso} (cm^3/g)**
CoN_4@NPC-700	756	546	210	1.10	0.29	0.81
CoN_4@NPC-800	729	493	236	1.14	0.26	0.88
CoN_4@NPC-900	842	600	242	1.27	0.31	0.96
CoN_4@NPC-1000	804	545	259	1.35	0.29	1.06
CoN_4@NPC-re	636	411	225	1.24	0.18	1.06

Supplementary Table 10 | Raman fitting results of Co-N_4@NPC catalysts with different pyrolysis temperature and synthesis steps.

Sample	**I peak%**	**D peak%**	**D" peak%**	**G peak%**	**$Area_D/Area_G$**
CoN_4@NPC-700	9.4	39.9	25.4	25.3	1.58
CoN_4@NPC-800	10.9	37.8	25.3	26.0	1.45
CoN_4@NPC-900	8.6	35.7	19.8	26.6	1.34
CoN_4@NPC-1000	16.6	35.0	18.5	29.9	1.17
CoN_4@NPC-re	19.9	34.8	21.1	24.1	1.44

Supplementary Table 11 | Reaction condition optimization for Co-N$_4$@NPC-re catalyzed oxidation of 1a and 3g.

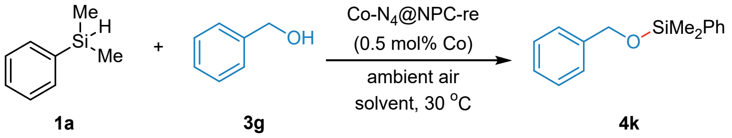

Entry[a]	1a (equiv.)	solvent	Time (h)	Yield of 4k (%)[b]
1	1	*n*-heptane	1	74
2	1	*n*-heptane	1.5	74
3	1.5	*n*-heptane	1.5	87
4	1.5	*n*-heptane	2	91
5	2	*n*-heptane	1	93
6	2	*n*-heptane	1.5	97
7	2	*n*-heptane	2	98
8	3	*n*-heptane	3	99
9[c]	2	*n*-heptane	3	N.R.
10	2	toluene	1.5	68
11	2	toluene	2	68
12	3	toluene	1.5	78
13	3	toluene	2	85
14	2	acetone	2	16
15	2	THF	2	16
16	2	EtOAc	2	31

[a] Reaction conditions: **3g** (1 mmol), Co-N$_4$@NPC-re (Co 0.5 mol%), 30 °C, air atmosphere, N.R.= no reaction. [b] The yield was calculated based on **3g** and determined by GC using anisole as an internal standard. [c] Under N_2 atmosphere.

Supplementary Discussion 1 | Structure identification of Co-N_4@NPC-re

XAFS measurements were carried out to verify the atomic dispersion and precise coordination structure of Co and Zn species in Co-N_4@NPC-re. As shown in **Supplementary Fig. 25**, only one intensity maximum peak located at approximately 1.4 Å was found in FT-EXAFS curve of Co K-edge in Co-N_4@NPC-re, which originates from the interactions between Co and light atoms. This signal was attributed to the contribution of Co-N coordination. In comparison with the Co foil reference, which displayed a main peak at approximately 2.2 Å assigned to the Co-Co bond, it was clear that this metallic interaction was not present in Co-N_4@NPC-re sample, indicating that the Co species in Co-N_4@NPC-re sample are atomically dispersed. The same observation can be made in FT-EXAFS curve of Zn K-edge in Co-N_4@NPC-re with the intensity maximum peak located at 1.5 Å (**Supplementary Fig. 26**), which indicated the existence of Zn-N coordination. Furthermore, the WT plots of Co and Zn K-edge EXAFS spectra both detect only one intensity maximum at approximately 5.0 $Å^{-1}$, which are similar to those in the WT plots of corresponding metal phthalocyanines (**Supplementary Figs. 25** and **26**), providing unequivocal support for the existence of Co-N and Zn-N scattering paths. The fitting results of EXAFS data further suggested that first shell coordination number of Co-N and Zn-N are 4.1 and 4.0, respectively (**Supplementary Table 2**), revealing the metal species in Co-N_4@NPC-re are Co-N_4 and Zn-N_4 sites.

To further identify the geometric configuration of Co-N_4 sites in Co-N_4@NPC-re, we calculated XANES spectra of various Co-N-C structures with different coordination geometries (**Supplementary Figs. 41** and **42**). It turned out that the Co-N_4 sites in the pyridinic coordination environment (labeled as CoN_4C_{10}) could well reproduce the main features of the experimental spectrum. Furthermore, adding an oxygen molecule axial adsorbed on Co center (labeled as CoN_4C_{10}-O_2) caused I_b/I_c ratios in the theoretical and experimental spectra to become more similar and displaying better agreement over the entire XANES energy range. Such structure was also reported in the literatures for Co-N-C catalyst which synthesized using similar ZIF precursors [7]. It was reported that due to the weak interaction of O_2 and Co-N_4 site, the adsorbed O_2 molecule is not very stable [8]. Such CoN_4C_{10} and CoN_4C_{10}-O_2 structures are interconvertible when the sample is placed under different atmosphere (N_2 or O_2). Thus, it is highly likely that in the real sample these two kinds of structure are co-exist and in dynamic equilibrium.

Supplementary Discussion 2 | Re-doping approach for increasing Co-N_4 sites.

As shown in XPS and EDS element analysis (**Supplementary Tables 4** and **7**), in Co-N_4@NPC, the content of pyridinic-N sites is much higher than that of Co-N_4 sites. Thus, we tried to introduce more Co-N_4 sites into Co-N_4@NPC to balance the Co-N_4/pyridinic-N ratio in catalyst for further improving the catalytic activity. Inspired by the recent advances of ORR catalyst in PEMFCs [9], we developed a tandem ammonia-leaching and adsorption approach for re-doping Co-N_4 sites in Co-N_4@NPC matrix (**Supplementary Fig. 4**). In brief, Co-N_4@NPC-NL was first treated NH_3/NH_4Cl aqueous solution. Then the obtained sample was used as a host to adsorb Co phenanthroline complex (Co(Phen)$_3$) to form Co-N_4@NPC/Co(Phen)$_3$. During the following pyrolysis step, Co(Phen)$_3$ transformed to Co-N_4 active sites and doped into porous carbon matrix to generate Co-N_4@NPC-re. The density of Co atoms is approximately 0.44 Co atom/nm^2 (calculated based on BET surface area and loading of Co) in Co-N_4@NPC-re, which is much higher than that of Co-N_4@NPC (0.24 Co atom/nm^2). Catalytic performance evaluation showed that re-doping approach leads to significantly enhanced activity for Co-N_4@NPC sample (**Supplementary Figs. 15** and **16**). Considering the comparable N dopant and carbon structure (**Supplementary Tables 7** and **10**) of Co-N_4@NPC-re and Co-N_4@NPC, the enhanced performance may originate from the optimization of Co-N_4/pyridinic-N ratio caused by the increase of Co-N_4 sites concentration. It should be pointed out that although the re-doping approach has been proved to be an effective means to optimize the Co-N_4/pyridinic-N ratio in sample, the content of pyridinic-N sites in Co-N_4@NPC-re is still excess, suggesting there is still room to further optimize catalyst structure. The possible ways include change solvent during adsorption step, use different Co complexes as Co precursor, and introduce more nanopores in carbon host, etc. These are under investigation now.

Supplementary Discussion 3 | The elimination of mass transfer limitation

To establish the influence of external and internal mass transfer limitations, the effect of agitation speed and particle size on initial reaction rates r_a was examined. **Supplementary Fig. 52A** shows that r_a is independent of stirring speed in the range of 800-1200 rpm, which indicates external diffusion limitation is absent when the stirring speed falls within this range. **Supplementary Fig. 52B** shows that internal diffusion limitation is negligible for particles smaller than 75 μm. Therefore, the catalytic activity testing experiments in this work were carried out at a stirring speed of 1000 rpm with catalyst particles smaller than 45 μm (the catalyst was passed through 325 mesh sifting screen before used) to avoid both external and internal mass transfer limitations.

The importance of internal (intraparticle) diffusion was further evaluated by Weisz-Prater criterion [10]:

$$\Phi = \frac{r_a \rho_p L^2}{C_{s,i} D_{e,i}} = \eta \varphi_i^2$$

where $r_a =$ observed initial reaction rate per unit mass of catalyst, mol/kg·s

$\rho_p =$ density of catalyst, kg/m^3

$L =$ characteristic length of catalyst particle, m

$C_{s,i} =$ surface reactant concentration of specie i, mol/m^3

$D_{e,i} =$ effective liquid phase diffusivity of specie i, m^2/s

If $\Phi \leq 0.3$, the internal diffusion effect can be neglected.

In the current work, the shape of catalyst particle was assumed as sphere and particle size d_p was less than 45 μm, thus $L = d_p/6 = 7.5$ μm. For Co-N_4@NPC-900 catalyst, $\rho_p = 250$ kg/m^3 and $r_a = 4.45 \times 10^{-2}$ mol/kg$_{cat}$·s. A series of correlations [11] were used to estimate the diffusion coefficients D of **1a**, H_2O and O_2. $D_{e,i}$ was further calculated by the expression derived by Ternan [12]:

$$D_{e,i} = D_i \frac{(1-\lambda)^2}{1+P\lambda}$$

where $D_i =$ diffusion coefficients of specie i, m^2/s

$\lambda =$ the ratio of diffusing molecule radius to average pore radius of the catalyst, $r_{molecule}/r_{pore}$

$P =$ fitting parameter

P is an empirical constant which is determined individually for catalysts. Based on the report of Massoth [13], the value of P was calculated to be 11.0, which was employed in this work to estimate $D_{e,i}$ in the Co-N_4@NPC-900 catalyst. The average pore radius of Co-N_4@NPC-900 sample analyzed by BJH method from N_2 adsorption-desorption isotherm was 8.9 nm.

When **1a** was considered as the diffusing reactant, the diffusivity of **1a** in H_2O and MeCN mixture can be estimated using **eq 1-4**.

$$D_{\mathbf{1a}/mix} = \frac{\left(D^0_{\mathbf{1a}/H_2O}\eta^{0.5}_{H_2O}\right)^{x_{H_2O}}\left(D^0_{\mathbf{1a}/MeCN}\eta^{0.5}_{MeCN}\right)^{x_{MeCN}}}{\eta^{0.5}_{mix}} \quad \textbf{eq 1}$$

$$D^0_{\mathbf{1a}/MeCN} = 4.4 \times 10^{-15} \frac{T}{\eta_{MeCN}} \left(\frac{V_{MeCN}}{V_{\mathbf{1a}}}\right)^{1/6} \left(\frac{L^{vap}_{MeCN}}{L^{vap}_{\mathbf{1a}}}\right)^{1/2} \quad \textbf{eq 2}$$

$$D^0_{\mathbf{1a}/H_2O} = \frac{8.621 \times 10^{-14}}{\eta^{1.14}_{H_2O} V^{0.589}_{\mathbf{1a}}} \quad \textbf{eq 3}$$

$$\eta_{mix} = \eta^{x_{MeCN}}_{MeCN} \eta^{x_{H_2O}}_{H_2O} \quad \textbf{eq 4}$$

Due to the low mole fraction of **1a** in reaction solution (1.5 mol%), the influence of **1a** to D_{H_2O} and D_{O_2} can be neglected. The diffusivity of H_2O in MeCN was estimated using **eq 4-7**.

$$D_{H_2O/MeCN} = \frac{\left(D^0_{MeCN/H_2O}\eta_{H_2O}\right)^{x_{H_2O}}\left(D^0_{H_2O/MeCN}\eta_{MeCN}\right)^{x_{MeCN}}}{\eta_{mix}} \quad \textbf{eq 5}$$

$$D^0_{H_2O/MeCN} = 4.4\times10^{-15}\frac{T}{\eta_{MeCN}}\left(\frac{V_{MeCN}}{V_{H_2O}}\right)^{1/6}\left(\frac{L^{vap}_{MeCN}}{L^{vap}_{H_2O}}\right)^{1/2} \quad \textbf{eq 6}$$

$$D^0_{MeCN/H_2O} = \frac{8.621\times10^{-14}}{\eta^{1.14}_{H_2O}V^{0.589}_{MeCN}} \quad \textbf{eq 7}$$

The diffusivity of O_2 in H_2O and MeCN mixture was estimated using **eq 4**, **8-10**.

$$D_{O_2/mix} = \frac{\left(D^0_{O_2/H_2O}\eta^{0.5}_{H_2O}\right)^{x_{H_2O}}\left(D^0_{O_2/MeCN}\eta^{0.5}_{MeCN}\right)^{x_{MeCN}}}{\eta^{0.5}_{mix}} \quad \textbf{eq 8}$$

$$D^0_{O_2/MeCN} = 1.1728\times10^{-16}\frac{T\sqrt{\chi_{MeCN}M_{MeCN}}}{\eta_{MeCN}V^{0.6}_{O_2}} \quad \textbf{eq 9}$$

$$D^0_{O_2/H_2O} = 1.1728\times10^{-16}\frac{T\sqrt{\chi_{H_2O}M_{H_2O}}}{\eta_{H_2O}V^{0.6}_{O_2}} \quad \textbf{eq 10}$$

The definitions of the quantities involved in **eq 1-10** are listed as following:

$D^0_{i/j}$ = diffusivity at infinite dilution of *i* in *j*, m^2/s

$D_{i/j}$ = diffusivity of *i* in the concentrated solution, m^2/s

η_i = viscosity of component *i*, Pa·s

x_i = mole fraction of component *i*

T = system temperature, K

L^{vap}_i = latent heat of vaporization of component *i* at normal boiling point, J/kmol

V_i = molar volume of component *i* at normal boiling point, $m^3/kmol$

χ_i = solvent association parameter

M_i = molecular weight of component *i,* kg/kmol

Subscript: mix = mixture

The properties of the solute and solvents used in calculations are given in **Supplementary table 12** [14–16].

Supplementary Table 12 | Physical properties of **1a**, H_2O, MeCN and O_2

Component	r (nm)	M_i (kg/mol)	V_i (m^3/kmol)	χ_i	η_i@303K ($\times10^{-4}$ Pa·s)	x_i	L^{vap}_i ($\times10^7$ J/kmol)
1a	0.38	136.3	0.153	-	-	-	3.72
H_2O	0.13	18.02	0.0187	2.6	8.01	0.122	4.07
MeCN	-	41.06	0.0574	1	3.25	0.878	3.03
O_2	0.17	32.00	0.0280	-	-	-	-

Supplementary Table 13 | Φ of **1a**, H_2O and O_2 under reaction conditions

Component	λ	$C_{s,i}$ (mol/m^3)	$D_{i/j}$ ($\times10^{-9}$ m^2/s)	$D_{e,i}$ ($\times10^{-9}$ m^2/s)	Φ
1a	0.0427	303	2.69	1.68	2.3×10^{-3}
O_2	0.0191	2.42	5.41	4.30	5.9×10^{-2}
H_2O	0.0146	2424	3.78	3.16	1.5×10^{-4}

As shown in **Supplementary table 13**, the value of Φ for each reactant is less than 0.3, which also proves the absence of mass transfer limitation in Co-N_4@NPC-catalyzed silane oxidation reaction.

Scopes and Limitations Studies

General information

All reactions were carried out under an ambient atmosphere of air using oven-dried glasswares, unless otherwise specified. Anhydrous 2-methyltetrahydrofuran (2-MeTHF), toluene and *n*-heptane were purchased from Sinopharm Chemical Reagent Co., Ltd. and distilled from sodium-benzophenone under N_2 atmosphere. Anhydrous MeCN was purchased from Sinopharm Chemical Reagent Co., Ltd. and distilled from CaH_2 under N_2 atmosphere. Anhydrous alcohols (MeOH, EtOH, *i*-PrOH, *n*-BuOH, *i*-BuOH and *t*-BuOH) were purchased from J&K Scientific (SuperDry) and used as received. Other solvents and reagents were purchased at the highest commercial quality and used directly without further purification. Reactions were monitored by GC (Agilent 7820A gas chromatograph with FID detector and 30 m×0.32 mm×0.25 μm HP-INNOWax capillary column) and/or thin layer chromatography (TLC). TLC was performed using silica gel GF254 pre-coated TLC plates, using short-wave UV light (254 nm) as the visualizing agent, and I_2, or $KMnO_4$ and heating as developing agents. All work-up and purification procedures were carried out with reagent grade solvents. Flash column chromatography was preformed using 300-400 mesh silica gel (Huanghai, Shandong) or 200-300 mesh neutral alumina (Aladdin, Shanghai) as stationary phase. NMR spectra were recorded on Bruker AVANCE III HD 400 and AVANCE NEO 400 instruments and were calibrated using residual undeuterated solvent (chloroform at 7.26 ppm ^{1}H NMR, 77.00 ppm ^{13}C NMR; acetone at 2.05 ppm ^{1}H NMR, 29.84 ppm ^{13}C NMR; DMSO at 2.50 ppm ^{1}H NMR, 39.52 ppm ^{13}C NMR). The following abbreviations (or combinations thereof) were used to explain multiplicities: s = singlet, d = doublet, t = triplet, q = quartet, hept = heptet, m = multiplet, br = broad. Coupling constants, *J*, were reported in Hertz unit (Hz). High-resolution mass spectra (HRMS) were recorded on a Bruker MicrOTOF II mass spectrometer by ESI-TOF (electrospray ionization-time of flight) or APCI-TOF (atmospheric pressure chemical ionization-time of flight) experiments. The enantiomeric excess (*ee*) of chiral compounds was determined on an Agilent 1260 Infinity II LC system using Daicel CHIRALPAK IB analytic column. Optical rotations were recorded on a Rudolph Autopol IV automatic polarimeter.

Preparation of silane substrates

-List of silane substrates

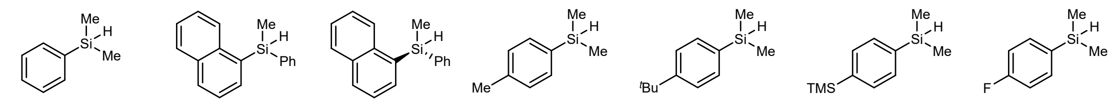

1a **1b** ***R*-1b** **1c** **1d** **1e** **1f**

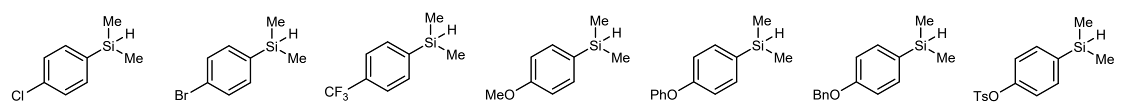

1g **1h** **1i** **1j** **1k** **1l** **1m**

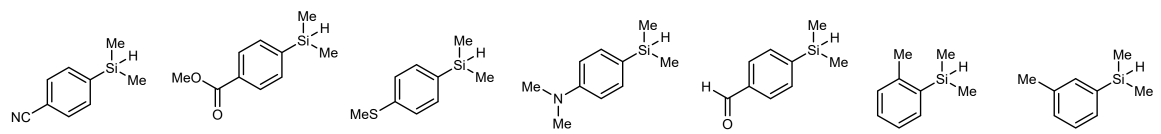

1n **1o** **1p** **1q** **1r** **1s** **1t**

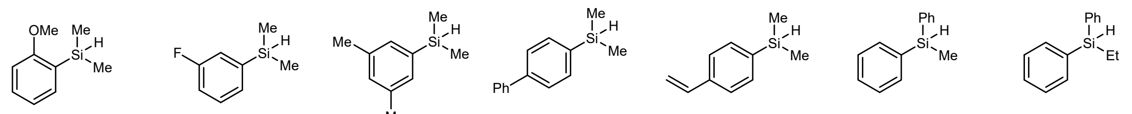

1u **1v** **1w** **1x** **1y** **1z** **1aa**

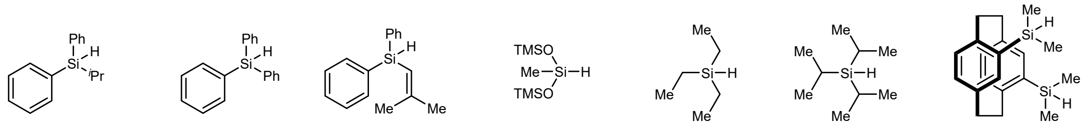

1ab **1ac** **1ad** **1ae** **1af** **1ag** **1ah**

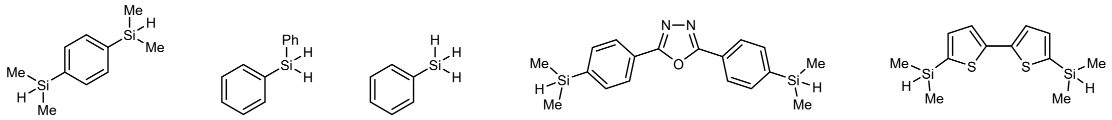

1ai **1aj** **1ak** **1al** **1am**

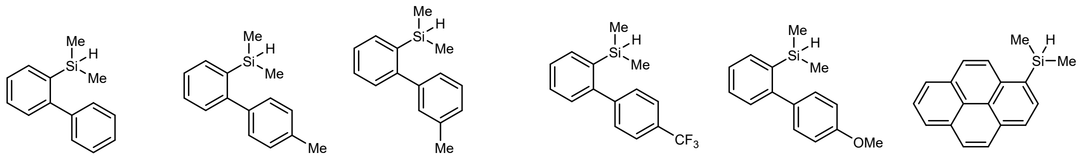

1an **1ao** **1ap** **1aq** **1ar** **1as**

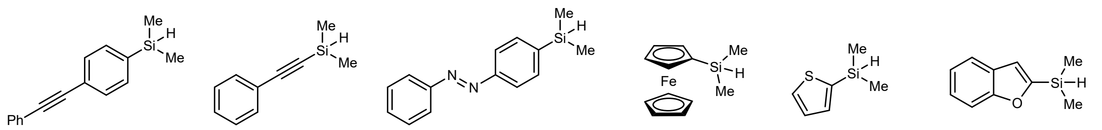

1at **1au** **1av** **1aw** **1ax** **1ay**

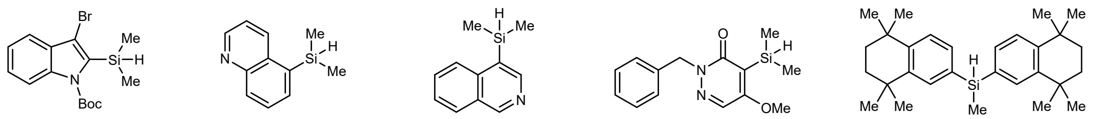

1az **1ba** **1bb** **1bc** **1bd**

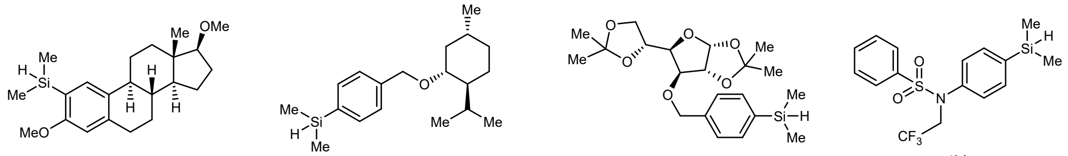

1be **1bf** **1bg** **1bh**

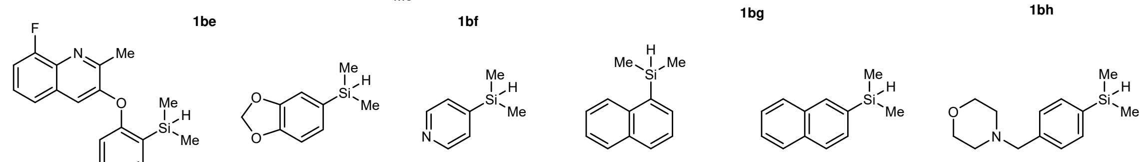

1bi **1bj** **1bk** **1bl** **1bm** **1bn**

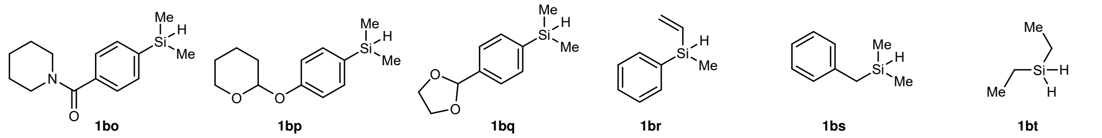

1bo **1bp** **1bq** **1br** **1bs** **1bt**

*A) **1a**, **1z**, **1ac**, **1ae**, **1af**, **1ag**, **1ai**, **1aj**, **1ak**, **1bs** and **1bt** were purchased from commercial suppliers and used without addition purification.*

*B) General procedure for the preparation of **1c**, **1d**, **1e**, **1f**, **1g**, **1i**, **1j**, **1k**, **1p**, **1s**, **1t**, **1u**, **1v**, **1w**, **1x**, **1an**, **1ax**, **1bf**, **1bg**, **1bj**, **1bl**, **1bm**, **1bp** and **1bq** according to a modified literature procedure by Mg insertion [17].*

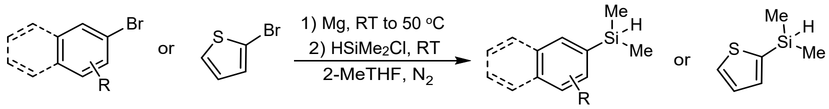

Under N_2 atmosphere, magnesium shavings (0.583 g, 24 mmol, 1.2 equiv.) and 30 mL anhydrous 2-MeTHF was added to a 100 mL two-neck round bottom flask. To this suspension was added 2 drops of 1,2-dibromoethane. A solution of aryl bromide (20 mmol, 1.0 equiv.) in 10 mL anhydrous 2-MeTHF was then added slowly to the suspension of Mg at room temperature. After addition, the resulting mixture was stirred at 50 °C for 3 h and then cooled to room temperature. Chlorodimethylsilane (2.84 g, 30 mmol, 1.5 equiv.) was added and the mixture was stirred overnight. After quenched with saturated aqueous NH_4Cl solution, the mixture was extracted with diethyl ether and the combined organic phases are dried over anhydrous Na_2SO_4. After evaporation of the solvents under reduced pressure, the crude product was purified by flash column chromatography on silica gel using suitable eluents to give the corresponding silane.

Compound 1c

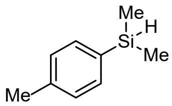

(4-Methylphenyl)dimethylsilane

Physical state: colorless oil.

^{1}H NMR (400 MHz, Chloroform-*d*): δ = 7.44 (d, *J* = 7.6 Hz, 2H), 7.18 (d, *J* = 7.5 Hz, 2H), 4.41 (hept, *J* = 3.8 Hz, 1H), 2.34 (s, 3H), 0.32 (d, *J* = 3.7 Hz, 6H).

^{13}C NMR (101 MHz, Chloroform-*d*): δ = 139.06, 134.03, 128.69, 126.80, 21.46, -3.68.

The characterization data are consistent with that reported in the literature [18].

Compound 1d

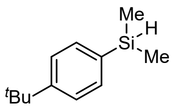

(4-*tert*-Butylphenyl)dimethylsilane

Physical state: colorless oil.

^{1}H NMR (400 MHz, Chloroform-*d*): δ = 7.55 (d, *J* = 6.3 Hz, 2H), 7.46 (d, *J* = 6.3 Hz, 2H), 4.51 - 4.46 (m, 1H), 1.39 (s, 9H), 0.40 (d, *J* = 1.6 Hz, 6H).

^{13}C NMR (101 MHz, Chloroform-*d*): δ = 152.19, 133.93, 124.85, 31.23, -3.72.

The characterization data are consistent with that reported in the literature [19].

Compound 1e

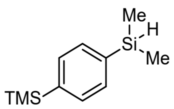

(4-Trimethylphenyl)dimethylsilylsilane

Physical state: colorless oil.

^{1}H NMR (400 MHz, Chloroform-*d*): δ = 7.58 (d, *J* = 5.6 Hz, 4H), 4.47 (tt, *J* = 7.4, 3.6 Hz, 1H), 0.39 (dd, *J* = 5.3, 3.8 Hz, 6H), 0.32 (d, *J* = 5.6 Hz, 9H).

^{13}C NMR (101 MHz, Chloroform-*d*): δ = 141.56, 137.95, 133.29, 132.72, -1.22, -3.85..

The characterization data are consistent with that reported in the literature [20].

Compound 1f

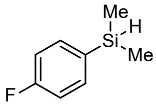

(4-Fluorophenyl)dimethylsilane

Physical state: colorless oil.

^{1}H NMR (400 MHz, Chloroform-*d*): δ = 7.50 (dd, *J* = 8.3, 6.3 Hz, 2H), 7.05 (t, *J* = 8.9 Hz, 2H), 4.41 (dq, *J* = 7.3, 3.7 Hz, 1H), 0.33 (d, *J* = 3.7 Hz, 6H).

^{13}C NMR (101 MHz, Chloroform-*d*): δ = 165.04, 162.58, 135.91, 135.84, 115.11, 114.92, -3.67.

^{19}F NMR (376 MHz, Chloroform-*d*): δ = -111.82.

The characterization data are consistent with that reported in the literature [18].

Compound 1g

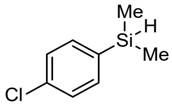

(4-Chlorophenyl)dimethylsilane (1f)

Physical state: colorless oil.

^{1}H NMR (400 MHz, Chloroform-*d*): δ = 7.50 - 7.44 (m, 2H), 7.38 - 7.31 (m, 2H), 4.43 (hept, *J* = 3.8 Hz, 1H), 0.35 (d, *J* = 3.8 Hz, 6H).

^{13}C NMR (101 MHz, Chloroform-*d*): δ = 135.67, 135.49, 135.31, 128.06, -3.86.

The characterization data are consistent with that reported in the literature [21].

Compound 1i

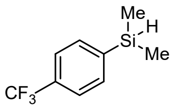

(4-Trifluoromethylphenyl)dimethylsilane

Physical state: colorless oil.

^{1}H NMR (400 MHz, Chloroform-*d*): δ = 7.65 (d, *J* = 7.7 Hz, 2H), 7.59 (d, *J* = 7.7 Hz, 2H), 4.58 - 4.33 (m, 1H), 0.37 (d, *J* = 3.5 Hz, 6H).

^{13}C NMR (101 MHz, Chloroform-*d*): δ = 142.45, 134.29, 131.04, 125.57, 124.41, 124.37, 124.33, 124.30, 122.86, -4.04.

^{19}F NMR (376 MHz, Chloroform-*d*): δ = -62.96.

The characterization data are consistent with that reported in the literature [18].

Compound 1j

(4-Methoxyphenyl)dimethylsilane

Physical state: colorless oil.

^{1}H NMR (400 MHz, Chloroform-*d*): δ = 7.52 (d, *J* = 8.4 Hz, 2H), 6.97 (d, *J* = 8.4 Hz, 2H), 4.53 - 4.40 (m, 1H), 3.86 (s, 3H), 0.37 (d, *J* = 3.7 Hz, 6H).

^{13}C NMR (101 MHz, Chloroform-*d*): δ = 160.55, 135.41, 128.17, 113.64, 55.00, -3.55.
The characterization data are consistent with that reported in the literature [18].

Compound 1k

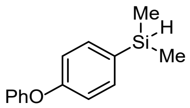

(4-Phenoxyphenyl)dimethylsilane
Physical state: colorless oil.
^{1}H NMR (400 MHz, Chloroform-*d*): δ = 7.53 (dd, *J* = 10.2, 3.4 Hz, 2H), 7.38 (t, *J* = 5.8 Hz, 2H), 7.15 (t, *J* = 6.4 Hz, 1H), 7.04 (dt, *J* = 14.1, 7.0 Hz, 4H), 4.47 (dd, *J* = 6.3, 2.6 Hz, 1H), 0.38 (d, *J* = 3.6 Hz, 6H).
^{13}C NMR (101 MHz, Chloroform-*d*): δ = 158.51, 156.78, 135.62, 131.31, 129.77, 123.49, 119.28, 118.11, -3.59.
The characterization data are consistent with that reported in the literature [22].

Compound 1p

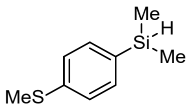

(4-Methylthiophenyl)dimethylsilane
Physical state: colorless oil.
^{1}H NMR (400 MHz, Chloroform-*d*): δ = 7.48 (d, *J* = 8.0 Hz, 2H), 7.29 (t, *J* = 6.6 Hz, 2H), 4.55 - 4.36 (m, 1H), 2.51 (s, 3H), 0.37 (d, *J* = 3.7 Hz, 6H).
^{13}C NMR (101 MHz, Chloroform-*d*): δ = 139.96, 134.34, 128.76, 125.62, 15.28, -3.77.
The characterization data are consistent with that reported in the literature [19].

Compound 1s

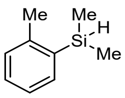

(2-Methylphenyl)dimethylsilane
Physical state: colorless oil.
^{1}H NMR (400 MHz, Chloroform-*d*): δ = 7.48 (d, *J* = 6.6 Hz, 1H), 7.35 - 7.23 (m, 1H), 7.17 (d, *J* = 6.7 Hz, 2H), 4.55 (dd, *J* = 6.6, 3.1 Hz, 1H), 2.46 (d, *J* = 5.5 Hz, 3H), 0.37 (d, *J* = 3.5 Hz, 6H).
^{13}C NMR (101 MHz, Chloroform-*d*): δ =143.68, 136.12, 134.59, 129.54, 129.46, 125.07, 22.34, -3.55.
The characterization data are consistent with that reported in the literature [23].

Compound 1t

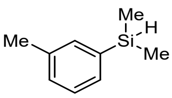

(3-Methylphenyl)dimethylsilane
Physical state: colorless oil.
^{1}H NMR (400 MHz, Chloroform-*d*): δ = 7.38 (d, *J* = 8.1 Hz, 2H), 7.33 - 7.17 (m, 2H), 4.47 - 4.42 (m, 1H),

2.39 (s, 3H), 0.37 (d, J = 3.4 Hz, 6H).
^{13}C NMR (101 MHz, Chloroform-*d*): δ = 137.28, 137.20, 134.67, 130.98, 129.97, 127.80, 21.45, -3.76.
The characterization data are consistent with that reported in the literature [24].

Compound 1u

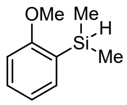

(2-Methoxyphenyl)dimethylsilane
Physical state: colorless oil.
^{1}H NMR (400 MHz, Chloroform-*d*): ^{1}H NMR (400 MHz, Chloroform-d) δ = 7.48 (d, J = 7.2 Hz, 1H), 7.41 (d, J = 7.6 Hz, 1H), 7.00 (d, J = 7.5 Hz, 1H), 6.88 (d, J = 8.2 Hz, 1H), 4.46 (dq, J = 7.8, 3.9, 3.5 Hz, 1H), 3.86 (s, 3H), 0.38 (s, 6H).
^{13}C NMR (101 MHz, Chloroform-*d*): δ = 164.28, 135.73, 131.14, 125.42, 120.52, 109.45, 55.14, -3.83.
The characterization data are consistent with that reported in the literature [21].

Compound 1v

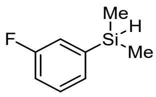

(3-Fluorophenyl)dimethylsilane
Physical state: colorless oil.
^{1}H NMR (400 MHz, Chloroform-*d*): δ = 7.43 - 7.31 (m, 1H), 7.25 (dd, J = 31.7, 8.0 Hz, 2H), 7.04 (t, J = 8.3 Hz, 1H), 4.54 - 4.31 (m, 1H), 0.34 (d, J = 2.6 Hz, 6H).
^{13}C NMR (101 MHz, Chloroform-*d*): δ = 163.80, 161.33, 140.52, 140.48, 129.67, 129.61, 129.51, 129.48, 120.37, 120.19, 116.19, 115.98, -3.93.
^{19}F NMR (376 MHz, Chloroform-*d*): δ = -113.69.
The characterization data are consistent with that reported in the literature [25].

Compound 1w

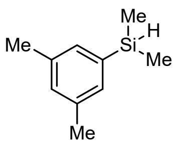

(3,5-Dimethylphenyl)dimethylsilane
Physical state: colorless oil.
^{1}H NMR (400 MHz, Chloroform-*d*): δ = 7.22 (s, 2H), 7.07 (s, 1H), 4.48 - 4.44 (m, 1H), 2.38 (s, 6H), 0.39 (d, J = 4.0 Hz, 6H).
^{13}C NMR (101 MHz, Chloroform-*d*): δ = 137.19, 131.70, 130.94, 21.29, -3.71.
The characterization data are consistent with that reported in the literature [21].

Compound 1x

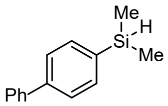

(1,1'-Biphenyl)-4-yldimethylsilane

Physical state: colorless oil.

^{1}H NMR (400 MHz, Chloroform-*d*): δ = 7.70 (dd, *J* = 11.3, 7.1 Hz, 6H), 7.53 (t, *J* = 6.9 Hz, 2H), 7.44 (d, *J* = 6.7 Hz, 1H), 4.91- 4.56 (m, 1H), 0.47 (d, *J* = 3.6 Hz, 6H).

^{13}C NMR (101 MHz, Chloroform-*d*): δ = 141.99, 141.03, 136.13, 134.50, 128.76, 127.39, 127.14, 126.60, -3.73.

The characterization data are consistent with that reported in the literature [26].

Compound 1an

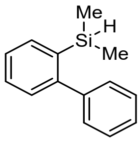

(1,1'-Biphenyl)-2-yldimethylsilane

Physical state: colorless oil.

^{1}H NMR (400 MHz, Chloroform-*d*): δ = 7.70 - 7.62 (m, 1H), 7.50 - 7.29 (m, 8H), 4.37 (hept, *J* = 3.7 Hz, 1H), 0.09 (d, *J* = 3.8 Hz, 6H).

^{13}C NMR (101 MHz, Chloroform-*d*): δ = 149.27, 143.68, 135.10, 129.21, 129.18, 129.09, 127.86, 127.11, 126.38, -3.02.

The characterization data are consistent with that reported in the literature [27].

Compound 1ax

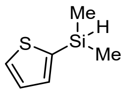

Dimethyl(thiophen-2-yl)silane

Physical state: colorless oil.

^{1}H NMR (400 MHz, Chloroform-*d*): δ = 7.62 (d, *J* = 4.6 Hz, 1H), 7.33 (bd, *J* = 3.3 Hz, 1H), 7.21 (dd, *J* = 4.6, 3.3 Hz, 1H), 4.57 (hept, *J* = 3.7 Hz, 1H), 0.40 (d, *J* = 3.7 Hz, 6H).

^{13}C NMR (101 MHz, Chloroform-*d*): δ = 135.07, 131.05, 128.23, -2.77.

The characterization data are consistent with that reported in the literature [28].

Compound 1bf

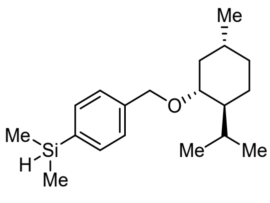

(4-((((1R,2S,5R)-2-isopropyl-5-methylcyclohexyl)oxy)methyl)phenyl)dimethylsilane

Physical state: colorless oil.

^{1}H NMR (400 MHz, Chloroform-*d*): δ = 7.58 - 7.48 (m, 2H), 7.36 (d, *J* = 7.3 Hz, 2H), 4.67 (d, *J* = 11.5 Hz, 1H), 4.48 – 4.37 (m, 2H), 3.19 (td, *J* = 10.6, 4.0 Hz, 1H), 2.32 (p, *J* = 7.3 Hz, 1H), 2.21 (d, *J* = 11.8 Hz, 1H), 1.66 (t, *J* = 11.7 Hz, 2H), 1.38 - 1.24 (m, 2H), 0.93 (dd, *J* = 16.5, 7.7 Hz, 9H), 0.73 (d, *J* = 8.6 Hz, 3H), 0.34 (d, *J* = 3.8 Hz, 6H).
^{13}C NMR (101 MHz, Chloroform-*d*): δ = 140.20, 136.33, 134.01, 127.22, 78.86, 70.31, 48.32, 40.30, 34.57, 31.57, 25.51, 23.25, 22.37, 21.02, 16.06, -3.74.
HRMS (ESI-TOF): calcd for $C_{19}H_{32}OSiNa^+$ $[M+Na]^+$: 327.2115, found: 327.2130.

Compound 1bg

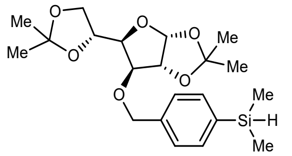

(4-((((3aR,5R,6S,6aR)-5-((R)-2,2-dimethyl-1,3-dioxolan-4-yl)-2,2-dimethyltetrahydrofuro-[2,3-d][1,3]dioxol-6-yl)oxy)methyl)phenyl)dimethylsilane
Physical state: white solid.
^{1}H NMR (400 MHz, Chloroform-*d*): δ = 7.55 (d, *J* = 7.5 Hz, 2H), 7.37 (d, *J* = 5.6 Hz, 2H), 5.92 (d, *J* = 3.3 Hz, 1H), 4.69 (d, *J* = 7.6 Hz, 2H), 4.61 (d, *J* = 3.5 Hz, 1H), 4.49 - 4.43 (m, 1H), 4.42 - 4.37 (m, 1H), 4.15 (dd, *J* = 16.2, 7.8 Hz, 2H), 4.04 (d, *J* = 6.8 Hz, 2H), 1.52 (s, 3H), 1.45 (s, 3H), 1.40 (s, 3H), 1.34 (s, 3H), 0.37 (d, *J* = 3.6 Hz, 6H).
^{13}C NMR (101 MHz, Chloroform-*d*): δ = 138.63, 137.01, 134.10, 127.06, 111.77, 108.95, 105.29, 82.66, 81.72, 81.32, 72.50, 72.27, 67.39, 26.83, 26.76, 26.23, 25.42, -3.80.
HRMS (ESI-TOF): calcd for $C_{21}H_{32}O_6SiNa^+$ $[M+Na]^+$: 431.1860, found: 431.1878.

Compound 1bj

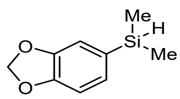

1,3-Benzodioxol-5-yl(dimethyl)silane
Physical state: colorless oil.
^{1}H NMR (400 MHz, Chloroform-*d*): δ = 7.08 - 6.94 (m, 2H), 6.85 - 6.81 (m, 1H), 5.92 (s, 2H), 4.51 - 4.27 (m, 1H), 0.31 (d, *J* = 3.5 Hz, 6H).
^{13}C NMR (101 MHz, Chloroform-*d*): δ = 148.70, 147.55, 130.41, 128.11, 121.75, 113.39, 108.79, 100.67, -3.37.
HRMS (ESI-TOF): calcd for $C_9H_{12}O_2SiNa^+$ $[M+Na]^+$: 203.0499, found: 203.0493.

Compound 1bl

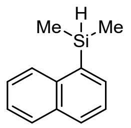

Dimethyl(naphthalen-1-yl)silane
Physical state: colorless oil.
^{1}H NMR (400 MHz, Chloroform-*d*): δ = 8.19 (d, *J* = 7.9 Hz, 1H), 7.97 - 7.68 (m, 3H), 7.64 - 7.39 (m, 3H),

5.01 - 4.92 (m, 1H), 0.56 (d, *J* = 4.0 Hz, 6H).

^{13}C NMR (101 MHz, Chloroform-*d*): δ = 136.92, 135.61, 133.61, 133.17, 129.98, 128.94, 127.59, 125.91, 125.52, 125.16, -3.26.

The characterization data are consistent with that reported in the literature [21].

Compound 1bm

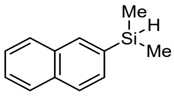

Dimethyl(naphthalen-2-yl)silane

Physical state: colorless oil.

^{1}H NMR (400 MHz, Chloroform-*d*): ^{1}H NMR (400 MHz, Chloroform-d) δ = 8.11 (s, 1H), 7.91 - 7.87 (m, 3H), 7.67 (d, *J* = 8.0 Hz, 1H), 7.56 - 7.52 (m, 2H), 4.66 - 4.60 (m, 1H), 0.50 (d, *J* = 4.0 Hz, 6H).

^{13}C NMR (101 MHz, Chloroform-*d*): δ = 134.85, 134.69, 133.82, 132.96, 130.17, 127.99, 127.74, 127.09, 126.38, 125.95, -3.69.

The characterization data are consistent with that reported in the literature [21].

Compound 1bp

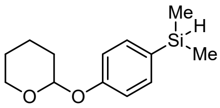

Dimethyl(4-((tetrahydro-2H-pyran-2-yl)oxy)phenyl)silane

Physical state: colorless oil.

^{1}H NMR (400 MHz, Chloroform-*d*): δ = 7.49 (d, *J* = 7.8 Hz, 2H), 7.10 (d, *J* = 7.8 Hz, 2H), 5.49 (s, 1H), 4.44 (dt, *J* = 7.1, 3.5 Hz, 1H), 4.00 - 3.87 (m, 1H), 3.71 - 3.57 (m, 1H), 2.06 (tt, *J* = 15.4, 7.7 Hz, 1H), 1.93 - 1.86 (m, 2H), 1.68 (ddd, *J* = 19.3, 14.6, 7.9 Hz, 3H), 0.35 (d, *J* = 3.6 Hz, 6H).

^{13}C NMR (101 MHz, Chloroform-*d*): δ = 158.06, 135.33, 129.26, 116.04, 96.03, 61.96, 30.31, 25.20, 18.71, -3.58.

HRMS (ESI-TOF): calcd for $C_{13}H_{20}O_2SiNa^+$ $[M+Na]^+$: 259.1125, found: 259.1128.

Compound 1bq

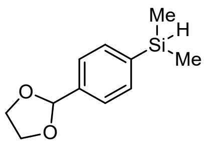

2-(4-(Dimethylsilyl)phenyl)-1,3-dioxolane

Physical state: colorless oil.

^{1}H NMR (400 MHz, Chloroform-*d*): δ = 7.61 (d, *J* = 8.0 Hz, 2H), 7.51 (d, *J* = 8.0 Hz, 2H), 5.87 (s, 1H), 4.52 - 4.47 (m, 1H), 4.16 (s, 2H), 4.07 (s, 2H), 0.38 (d, *J* = 1.9 Hz, 6H).

^{13}C NMR (101 MHz, Chloroform-*d*) δ = 138.86, 138.64, 134.02, 125.73, 103.62, 65.27, -3.85.

The characterization data are consistent with that reported in the literature [29].

*C) General procedure for the preparation of **1m**, **1n**, **1o**, **1bc**, **1bh** and **1bo** according to a modified literature procedure by Grignard reagents exchange* [18]*.*

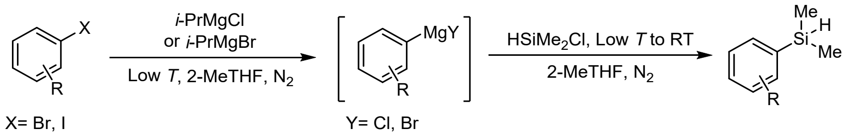

Under N_2 atmosphere, a solution of aryl halogen (10 mmol, 1.0 equiv.) in 15 mL anhydrous 2-MeTHF was cooled to target temperature ***T***. Then Grignard reagents (11 mmol, 1.1 equiv., commercially-available THF solution from J&K Scientific) was slowly added and stirred at ***T*** for appropriate time. Chlorodimethylsilane (1.42 g, 15 mmol, 1.5 equiv.) was added and the mixture was allowed to warm to room temperature and stirred overnight. After quenched with saturated aqueous NH_4Cl solution, the mixture was extracted with diethyl ether, and the combined organic phases are dried anhydrous Na_2SO_4. After evaporation of the solvents under reduced pressure, the crude product was purified by flash column chromatography on silica gel using suitable eluents to give the corresponding silane.

Compound 1m

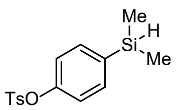

4-(Dimethylsilyl)phenyl 4-methylbenzenesulfonate

Prepared from 4-iodophenyl 4-methylbenzenesulfonate (*Org. Lett.* **2017**, *19*, 2486.) by magnesium-iodine exchange with *i*-PrMgCl (1.1 equiv.) at -20 °C for 2 h and then reacted with chlorodimethylsilane (1.5 equiv.).

Physical state: colorless oil.

^{1}H NMR (400 MHz, Chloroform-*d*): δ = 7.72 (d, *J* = 7.7 Hz, 2H), 7.46 (d, *J* = 7.5 Hz, 2H), 7.32 (d, *J* = 7.7 Hz, 2H), 6.98 (d, *J* = 7.6 Hz, 2H), 4.40 (hept, *J* = 3.5 Hz, 1H), 2.45 (s, 3H), 0.32 (d, *J* = 1.6 Hz, 6H).

^{13}C NMR (101 MHz, Chloroform-*d*): δ = 150.48, 145.30, 136.56, 135.33, 132.47, 129.71, 128.40, 121.68, 21.65, -3.90.

HRMS (ESI-TOF): calcd for $C_{15}H_{19}SO_3Si^+$ $[M+H]^+$: 307.0819, found: 307.0815.

Compound 1n

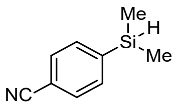

4-(Dimethylsilyl)benzonitrile

Prepared from 4-iodobenzonitrile by magnesium-iodine exchange with *i*-PrMgCl (1.1 equiv.) at -20 °C for 1 h and then reacted with chlorodimethylsilane (1.5 equiv.).

Physical state: yellow oil.

^{1}H NMR (400 MHz, Chloroform-*d*): δ = 7.63 (s, 4H), 4.45 (d, *J* = 3.4 Hz, 1H), 0.37 (s, 6H).

^{13}C NMR (101 MHz, Chloroform-*d*): δ = 144.25, 134.43, 130.99, 118.85, 112.75, -4.22.

The characterization data are consistent with that reported in the literature [18].

Compound 1o

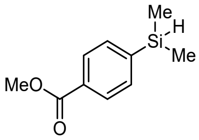

Methyl-4-(dimethylsilyl)benzoate

Prepared from methyl 4-iodobenzoate by magnesium-iodine exchange with *i*-PrMgCl (1.1 equiv.) at -20 ºC for 1 h and then reacted with chlorodimethylsilane (1.5 equiv.).

Physical state: colorless oil.

^{1}H NMR (400 MHz, Chloroform-*d*): δ = 8.03 (d, *J* = 7.4 Hz, 2H), 7.64 (d, *J* = 7.5 Hz, 2H), 4.52-4.44 (m, 1H), 3.94 (s, 3H), 0.39 (d, *J* = 2.9 Hz, 6H).

^{13}C NMR (101 MHz, Chloroform-*d*): δ = 167.13, 143.72, 137.68, 133.95, 128.56, 52.03, -4.05.

The characterization data are consistent with that reported in the literature [30].

Compound 1bc

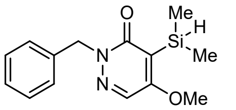

2-Benzyl-4-(dimethylsilyl)-5-methoxypyridazin-3(2*H*)-one

Prepared from 2-benzyl-4-bromo-5-methoxypyridazin-3(2*H*)-one (*J. Org. Chem.* **2009**, *74*, 9440.) by magnesium-bromide exchange with *i*-PrMgCl (1.1 equiv.) at -20 ºC for 10 min in 40 mL anhydrous 2-MeTHF and then reacted with chlorodimethylsilane (1.5 equiv.).

Physical state: white solid.

^{1}H NMR (400 MHz, Chloroform-*d*): δ = 7.73 (s, 1H), 7.44 - 7.38 (m, 2H), 7.34 - 7.24 (m, 3H), 5.27 (s, 2H), 4.47 (hept, *J* = 3.8 Hz, 1H), 3.90 (s, 3H), 0.34 (d, *J* = 3.8 Hz, 6H).

^{13}C NMR (101 MHz, Chloroform-*d*): δ = 164.05, 136.62, 128.68, 128.49, 127.70, 126.35, 117.29, 56.59, 54.58, -4.14.

HRMS (ESI-TOF): calcd for $C_{14}H_{17}N_2O_2Si^+$ $[M-H]^+$: 273.1054, found: 273.1069.

Compound 1bh

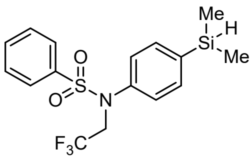

N-(4-(Dimethylsilyl)phenyl)-N-(2,2,2-trifluoroethyl)benzenesulfonamide

Prepared from N-(4-iodophenyl)-N-(2,2,2-trifluoroethyl)benzenesulfonamide (*Angew. Chem. Int. Ed.* **2018**, *57*, 6858., using 4-iodoaniline instead of 4-bromoaniline as starting material) by magnesium-iodine exchange with *i*-PrMgBr (1.1 equiv.) at 0 ºC for 2 h and then reacted with chlorodimethylsilane (1.5 equiv.).

Physical state: white solid.

^{1}H NMR (400 MHz, Chloroform-*d*): δ = 7.61 (t, *J* = 7.7 Hz, 3H), 7.48 (t, *J* = 7.8 Hz, 4H), 7.04 (d, *J* = 7.6 Hz, 2H), 4.53 - 4.32 (m, 1H), 4.23 (q, *J* = 8.2 Hz, 2H), 0.35 (d, *J* = 3.2 Hz, 6H).

^{13}C NMR (101 MHz, Chloroform-*d*): δ = 139.75, 138.79, 138.25, 135.04, 134.02, 133.26, 128.98, 128.39, 127.70, 125.07, 122.29, 52.60, 52.25, 51.91, 51.56, -3.97.

^{19}F NMR (376 MHz, Chloroform-*d*): δ = -70.48 (t).

HRMS (ESI-TOF): calcd for $C_{16}H_{19}NO_2SF_3SiNa^+$ $[M+Na]^+$: 374.0852, found: 374.0843.

Compound 1bo

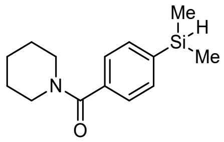

(4-(dimethylsilyl)phenyl)(piperidin-1-yl)methanone

Prepared from (4-iodophenyl)(piperidin-1-yl)methanone (*Angew. Chem. Int. Ed.* **2018**, *57*, 12347.) by magnesium-iodine exchange with *i*-PrMgBr (1.1 equiv.) at -20 ºC for 1 h and then reacted with chlorodimethylsilane (1.5 equiv.).

Physical state: brown oil.

^{1}H NMR (400 MHz, Chloroform-*d*): δ = 7.56 (d, J = 7.4 Hz, 2H), 7.36 (d, J = 7.4 Hz, 2H), 4.43 (hept, J = 3.5 Hz, 1H), 3.52 (two brs, 4H), 1.63 (two brs, 6H), 0.34 (d, J = 3.5 Hz, 6H).

^{13}C NMR (101 MHz, Chloroform-*d*): δ = 170.16, 139.06, 137.07, 133.96, 125.96, 48.50, 43.00, 26.00, 24.52, -3.95.

HRMS (ESI-TOF): calcd for $C_{14}H_{22}NOSi^+$ $[M+H]^+$: 248.1465, found: 248.1468.

D) General procedure for the preparation of ***1h, 1l, 1q, 1y, 1ah, 1al, 1am, 1as, 1at, 1av, 1aw, 1ay, 1ba, 1bb, 1be, 1bi, 1bk*** *and* ***1bn*** *according to a modified literature procedure by lithium-hydrogen/halogen exchange* [18]*.*

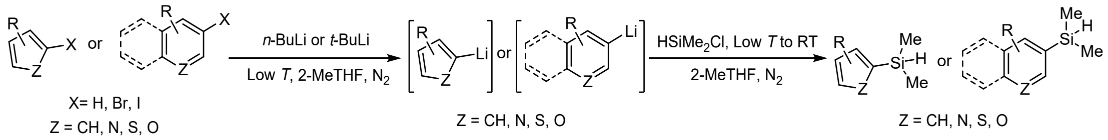

Under N_2 atmosphere, a solution of aryl compound (10 mmol, 1.0 equiv.) in 15 mL anhydrous 2-MeTHF was cooled to target temperature ***T***. Then *n*-BuLi (6.9 mL of a 1.6 M solution in hexane, 11 mmol, 1.1 equiv., commercially-available solution from J&K Scientific) or *t*-BuLi (16.9 mL of a 1.3 M solution in pentane, 22 mmol, 2.2 equiv., commercially-available solution from Aladdin) was slowly added and stirred at ***T*** for appropriate time. **Caution: *t*-BuLi is strongly pyrophoric and should be handled extremely carefully!** Chlorodimethylsilane (1.42 g, 15 mmol, 1.5 equiv.) was then added and the mixture was allowed to warm to room temperature and stirred overnight. After quenched with saturated aqueous NH_4Cl solution, the mixture was extracted with diethyl ether, and the combined organic phases are dried over anhydrous Na_2SO_4. After evaporation of the solvents under reduced pressure, the crude product was purified by flash column chromatography on silica gel using suitable eluents to give the corresponding silane.

Compound 1h

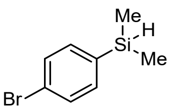

(4-Bromophenyl)dimethylsilane

Prepared from 1,4-dibromobenzene by lithium-bromide exchange with *n*-BuLi (1.1 equiv.) at -78 ºC for 3 h and then reacted with chlorodimethylsilane (1.5 equiv.).

Physical state: colorless oil.

^{1}H NMR (400 MHz, Chloroform-*d*): δ = 7.53 (d, *J* = 8.2 Hz, 2H), 7.43 (d, *J* = 8.2 Hz, 2H), 4.45 (dq, *J* = 7.5, 3.7 Hz, 1H), 0.37 (d, *J* = 3.8 Hz, 6H).
^{13}C NMR (101 MHz, Chloroform-*d*): δ = 136.16, 135.55, 130.99, 123.99, -3.87.
The characterization data are consistent with that reported in the literature [18].

Compound 1l

(4-(Benzyloxy)phenyl)dimethylsilane
Prepared from 1-(benzyloxy)-4-bromobenzene (*J. Am. Chem. Soc.* **2020**, *142*, 13246.) by lithium-bromide exchange with *n*-BuLi (1.1 equiv.) at -78 ºC for 2.5 h and then reacted with chlorodimethylsilane (1.5 equiv.).
Physical state: colorless oil.
^{1}H NMR (400 MHz, Chloroform-*d*): δ = 7.64 - 7.34 (m, 7H), 7.11 (d, *J* = 7.5 Hz, 2H), 5.17 (s, 2H), 4.58 - 4.54 (m, 1H), 0.44 (d, *J* = 1.3 Hz, 6H).
^{13}C NMR (101 MHz, Chloroform-*d*): δ = 159.76, 136.91, 135.42, 132.23, 128.53, 127.90, 127.40, 116.63, 114.51, 69.66, -3.57.
The characterization data are consistent with that reported in the literature [30].

Compound 1q

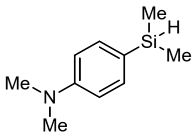

4-(Dimethylsilyl)-N,N-dimethylaniline
Prepared from 4-bromo-N,N-dimethylaniline by lithium-bromide exchange with *n*-BuLi (1.1 equiv.) at -78 ºC for 2 h and then reacted with chlorodimethylsilane (1.5 equiv.).
Physical state: pale yellow liquid.
^{1}H NMR (400 MHz, Chloroform-*d*): δ = 7.57 (d, *J* = 7.5 Hz, 2H), 6.89 (d, *J* = 7.4 Hz, 2H), 4.61-4.57 (m, 1H), 3.09 (s, 6H), 0.47 (d, *J* = 3.7 Hz, 6H).
^{13}C NMR (101 MHz, Chloroform-*d*): δ = 151.10, 134.98, 122.18, 111.96, 40.10, -3.45.
The characterization data are consistent with that reported in the literature [31].

Compound 1y

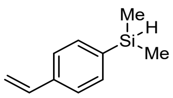

Dimethyl(4-vinylphenyl)silane
Prepared from 1-bromo-4-vinylbenzene by lithium-bromide exchange with *n*-BuLi (1.1 equiv.) at -78 ºC for 2.5 h and then reacted with chlorodimethylsilane (1.5 equiv.).
Physical state: colorless oil.
^{1}H NMR (400 MHz, Chloroform-*d*): δ = 7.56 (t, *J* = 5.6 Hz, 2H), 7.45 (d, *J* = 6.2 Hz, 2H), 6.83 - 6.67 (m, 1H), 5.83 (dd, *J* = 17.6, 3.7 Hz, 1H), 5.31 (dd, *J* = 10.8, 3.5 Hz, 1H), 4.50 - 4.44 (m, 1H), 0.39 (d, *J* = 2.0 Hz, 6H).

^{13}C NMR (101 MHz, Chloroform-*d*): δ = 138.34, 137.03, 136.79, 134.24, 125.63, 114.28, -3.78.
The characterization data are consistent with that reported in the literature [21].

Compound 1ah

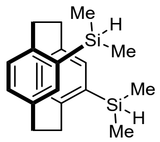

***rac*-4,12-Bis(dimethylsilyl)[2.2]paracyclophane**
Prepared from *pseudo-ortho*-4,12-Dibromo[2.2]paracyclophane (*Eur. J. Org. Chem.* **2017**, 1760.) by lithium-bromide exchange with *t*-BuLi (4.2 equiv.) at -78 ºC for 1 h and then reacted with chlorodimethylsilane (3 equiv.).
Physical state: white solid.
^{1}H NMR (400 MHz, Chloroform-*d*): δ = 6.80 (s, 2H), 6.63 (d, J = 7.8 Hz, 2H), 6.57 (d, J = 7.7 Hz, 2H), 4.66 (m, 2H), 3.45 (m, 2H), 3.18 (m, 6H), 0.42 (d, *J* = 1.2 Hz, 6H), 0.34 (d, *J* = 1.2 Hz, 6H).
^{13}C NMR (101 MHz, Chloroform-*d*): δ = 146.12, 138.03, 137.01, 134.23, 133.31, 35.63, 34.53, -2.64, -4.44.
The characterization data are consistent with that reported in the literature [32].

Compound 1al

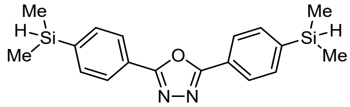

2,5-Bis(4-(dimethylsilyl)phenyl)-1,3,4-oxadiazole
Prepared from 2,5-bis(4-bromophenyl)-1,3,4-oxadiazole (*RSC Adv.* **2017**, *7*, 25444.) by lithium-bromide exchange with *n*-BuLi (3 equiv.) at -78 ºC for 1.5 h and then reacted with chlorodimethylsilane (3 equiv.).
Physical state: white solid.
^{1}H NMR (400 MHz, Chloroform-*d*): δ = 8.14 (d, *J* = 7.5 Hz, 4H), 7.73 (d, *J* = 7.7 Hz, 4H), 4.51 (hept, *J* = 3.6 Hz, 2H), 0.44 (d, *J* = 4.0 Hz, 12H).
^{13}C NMR (101 MHz, Chloroform-*d*): δ = 164.67, 142.48, 134.63, 126.02, 124.41, -3.98.
The characterization data are consistent with that reported in the literature [33].

Compound 1am

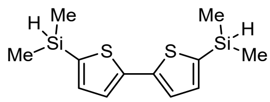

5,5'-Bis(dimethylsilyl)-2,2'-bithiophene
Prepared from 5,5'-dibromo-2,2'-bithiophene by lithium-bromide exchange with *n*-BuLi (3 equiv.) at -20 ºC for 1 h and then reacted with chlorodimethylsilane (3 equiv.).
Physical state: colorless oil.
^{1}H NMR (400 MHz, Chloroform-*d*): δ = 7.27 (d, *J* = 3.2 Hz, 2H), 7.21 (d, *J* = 3.2 Hz, 2H), 4.59 (hept, *J* = 3.6 Hz, 2H), 0.43 (d, *J* = 1.4 Hz, 12H).
^{13}C NMR (101 MHz, Chloroform-*d*): δ = 142.88, 136.01, 135.88, 125.29, -2.88.
The characterization data are consistent with that reported in the literature [34].

Compound 1as

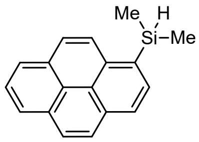

Dimethyl(pyren-1-yl)silane

Prepared from 1-bromopyrene by lithium-bromide exchange with *n*-BuLi (1.1 equiv.) at -78 ºC for 1 h and then reacted with chlorodimethylsilane (1.5 equiv.).

Physical state: white solid.

^{1}H NMR (400 MHz, Chloroform-*d*): δ = 8.43 (t, *J* = 7.9 Hz, 1H), 8.28 - 8.14 (m, 5H), 8.14 - 7.99 (m, 3H), 5.13 (hept, *J* = 2.6 Hz, 1H), 0.65 (d, *J* = 4.2 Hz, 6H).

^{13}C NMR (101 MHz, Chloroform-*d*): δ = 135.67, 132.90, 132.25, 131.26, 130.71, 127.96, 127.48, 127.39, 127.09, 125.81, 125.23, 125.13, 124.43, 124.15, -2.92.

The characterization data are consistent with that reported in the literature [35].

Compound 1at

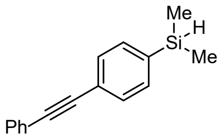

Dimethyl(4-(phenylethynyl)phenyl)silane

Prepared from 1-bromo-4-(phenylethynyl)benzene by lithium-bromide exchange with *n*-BuLi (1.1 equiv.) at -78 ºC for 1 h and then reacted with chlorodimethylsilane (1.5 equiv.).

Physical state: yellow solid.

^{1}H NMR (400 MHz, Chloroform-*d*): δ = 7.60 -7.52 (m, 6H), 7.38 (d, *J* = 4.9 Hz, 3H), 4.50-4.46 (m, 1H), 0.39 (d, *J* = 0.6 Hz, 6H).

^{13}C NMR (101 MHz, Chloroform-*d*): δ = 137.90, 133.89, 131.62, 130.76, 128.32, 128.27, 123.97, 123.21, 89.98, 89.42, -3.90.

HRMS (ESI-TOF): calcd for $C_{16}H_{15}Si^+$ $[M-H]^+$: 235.0938, found: 235.0936.

Compound 1av

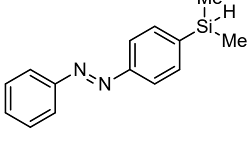

(*E*)-1-(4-(dimethylsilyl)phenyl)-2-phenyldiazene

Prepared from (*E*)-1-(4-iodophenyl)-2-phenyldiazene (*Org. Lett.* **2019**, *21*, 7380.) by lithium-iodine exchange with *n*-BuLi (1.1 equiv.) at -105 ºC for 1 h and then reacted with chlorodimethylsilane (1.5 equiv.).

Physical state: red oil.

^{1}H NMR (400 MHz, Chloroform-*d*): δ = 7.93 (dd, *J* = 13.7, 7.6 Hz, 4H), 7.72 (d, *J* = 7.6 Hz, 2H), 7.58 - 7.46 (m, 3H), 4.51 (hept, *J* = 3.2 Hz, 1H), 0.41 (d, *J* = 3.2 Hz, 6H).

^{13}C NMR (101 MHz, Chloroform-*d*): δ = 153.15, 152.69, 141.36, 134.80, 131.05, 129.08, 122.88, 122.00, -3.82.

HRMS (ESI-TOF): calcd for $C_{14}H_{17}N_2Si^+$ $[M+H]^+$: 241.1156, found: 241.1165.

Compound 1aw

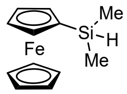

(Dimethylsilyl)ferrocene

Prepared from ferrocene by lithium-hydrogen exchange with potassium *t*-butoxide (0.15 equiv.) and *t*-BuLi (2.1 equiv.) at -78 ºC for 1.5 h and then reacted with chlorodimethylsilane (1.5 equiv.).

Physical state: red oil.

^{1}H NMR (400 MHz, Chloroform-*d*): δ = 4.47 - 4.41 (m, 1H), 4.37 (d, *J* = 16.1 Hz, 2H), 4.22 (s, 2H), 4.18 (s, 5H), 0.34 (d, *J* = 1.5 Hz, 6H).

^{13}C NMR (101 MHz, Chloroform-*d*): δ = 73.40, 71.08, 68.38, 68.10, -3.14.

The characterization data are consistent with that reported in the literature [35].

Compound 1ay

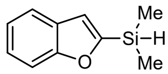

Benzofuran-2-yldimethylsilane

Prepared from benzofuran by lithium-hydrogen exchange with *n*-BuLi (1.1 equiv.) at -78 ºC for 1 h and then reacted with chlorodimethylsilane (1.5 equiv.).

Physical state: colorless oil.

^{1}H NMR (400 MHz, Chloroform-*d*): δ = 7.65 (d, *J* = 7.5 Hz, 1H), 7.59 (d, *J* = 8.0 Hz, 1H), 7.36 (t, *J* = 7.4 Hz, 1H), 7.28 (t, *J* = 7.0 Hz, 1H), 7.11 (s, 1H), 4.61 (hept, *J* = 3.2 Hz, 1H), 0.50 (d, *J* = 3.5 Hz, 6H).

^{13}C NMR (101 MHz, Chloroform-*d*): δ = 160.36, 158.24, 127.85, 124.56, 122.41, 121.04, 117.44, 111.29, -4.77.

The characterization data are consistent with that reported in the literature [30].

Compound 1ba

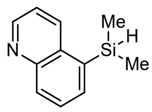

5-(Dimethylsilyl)quinoline

Prepared from 5-bromoquinoline by lithium-bromide exchange with *n*-BuLi (1.1 equiv.) at -78 ºC for 1 h and then reacted with chlorodimethylsilane (1.5 equiv.).

Physical state: brown oil.

^{1}H NMR (400 MHz, Chloroform-*d*): δ = 8.91 (d, *J* = 3.8 Hz, 1H), 8.41 (d, *J* = 8.4 Hz, 1H), 8.13 (d, *J* = 8.3 Hz, 1H), 7.78 - 7.62 (m, 2H), 7.39 (dd, *J* = 8.3, 4.0 Hz, 1H), 4.89 - 4.82 (m, 1H), 0.46 (d, *J* = 3.2 Hz, 6H).

^{13}C NMR (101 MHz, Chloroform-*d*): δ = 149.82, 148.14, 136.46, 135.41, 133.87, 131.71, 131.20, 128.68, 120.72, -3.46.

The characterization data are consistent with that reported in the literature [36].

Compound 1bb

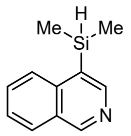

4-(Dimethylsilyl)isoquinoline

Prepared from 4-bromoisoquinoline by lithium-bromide exchange with *n*-BuLi (1.1 equiv.) at -78 ºC for 1 h and then reacted with chlorodimethylsilane (1.5 equiv.).

Physical state: brown oil.

^{1}H NMR (400 MHz, Chloroform-*d*): δ = 9.26 (s, 1H), 8.64 (s, 1H), 8.04 (d, *J* = 8.4 Hz, 1H), 7.97 (d, *J* = 8.1 Hz, 1H), 7.73 (t, *J* = 7.6 Hz, 1H), 7.61 (t, *J* = 7.5 Hz, 1H), 4.85 (hept, *J* = 3.6 Hz, 1H), 0.51 (d, *J* = 3.6 Hz, 6H).

^{13}C NMR (101 MHz, Chloroform-*d*): δ = 154.25, 148.70, 139.27, 130.36, 128.62, 127.88, 127.21, 126.89, 126.37, -3.67.

The characterization data are consistent with that reported in the literature [36].

Compound 1be

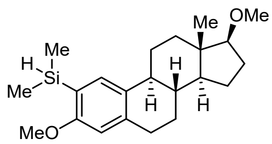

2-Dimethylsilyl-3,17-dimethoxy-β-estra-1,3,5(10)-triene (1bo)

Prepared from 2-bromo-3,17-dimethoxy-β-estra-1,3,5(10)-triene (*Org. Lett.* **2010**, *12*, 3352.) by lithium-bromide exchange with *n*-BuLi (1.1 equiv.) at -78 ºC for 1 h and then reacted with chlorodimethylsilane (1.5 equiv.).

Physical state: white solid.

^{1}H NMR (400 MHz, Chloroform-*d*): δ = 7.37 (s, 1H), 6.57 (s, 1H), 4.38 (h, *J* = 3.4 Hz, 1H), 3.79 (s, 3H), 3.39 (s, 3H), 3.33 (t, *J* = 8.3 Hz, 1H), 2.88 (m, 2H), 2.44 - 1.99 (m, 4H), 1.96 - 1.80 (m, 1H), 1.79 - 1.63 (m, 1H), 1.51 - 1.22 (m, 7H), 0.80 (s, 3H), 0.33 (d, *J* = 2.9 Hz, 6H).

^{13}C NMR (101 MHz, Chloroform-*d*): δ = 162.27, 140.00, 132.93, 126.32, 113.75, 109.91, 90.78, 57.88, 55.21, 50.24, 43.98, 43.22, 38.72, 38.06, 30.20, 27.74, 27.18, 26.44, 23.04, 11.53, -3.63.

HRMS (ESI-TOF): calcd for $C_{22}H_{32}O_3Si^+$ $[M-H]^+$: 357.2244, found: 375.2229.

Compound 1bi

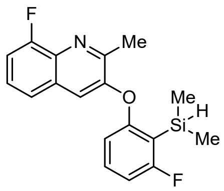

3-(2-(Dimethylsilyl)-3-fluorophenoxy)-8-fluoro-2-methylquinoline

Prepared from 3-(2-bromo-3-fluorophenoxy)-8-fluoro-2-methylquinoline (Patent WO2017/178408) by lithium-bromide exchange with *n*-BuLi (1.1 equiv.) at -78 ºC for 2 h and then reacted with chlorodimethylsilane (1.5 equiv.).

Physical state: pale solid.

^{1}H NMR (400 MHz, Chloroform-*d*): δ = 7.38 (s, 3H), 7.29 (s, 2H), 6.93 (t, *J* = 8.3 Hz, 1H), 6.71 (d, *J* = 8.0 Hz, 1H), 4.52 (dp, *J* = 7.7, 4.1 Hz, 1H), 2.82 (s, 3H), 0.39 (d, *J* = 3.7 Hz, 6H).

Note: Due to an issue with rotational isomers, the ^{13}C NMR spectrum is complex.

^{13}C NMR (101 MHz, Chloroform-*d*): δ = 169.21, 166.79, 160.76, 160.62, 158.90, 156.36, 153.86, 151.24, 132.51, 132.40, 129.88, 126.34, 126.26, 122.22, 122.18, 118.22, 114.44, 112.08, 111.88, 111.67, 111.41, 20.77, -3.29, -3.32.

^{19}F NMR (376 MHz, Chloroform-*d*): δ = -97.13, -125.64 (d).

HRMS (ESI-TOF): calcd for $C_{18}H_{18}NOF_2Si^+$ $[M+H]^+$: 330.1120, found: 330.1130.

Compound 1bk

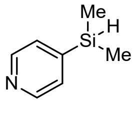

4-(Dimethylsilyl)pyridine

Prepared from 4-bromopyridine by lithium-bromide exchange with *n*-BuLi (1.1 equiv.) at -78 ºC for 2 h and then reacted with chlorodimethylsilane (1.5 equiv.).

Physical state: colorless oil.

^{1}H NMR (400 MHz, Chloroform-*d*): δ = 8.57 (d, *J* = 5.3 Hz, 2H), 7.41 (d, *J* = 5.5 Hz, 2H), 4.69 - 4.10 (m, 1H), 0.37 (d, *J* = 3.8 Hz, 6H).

^{13}C NMR (101 MHz, Chloroform-*d*): δ =148.64, 147.28, 128.68, -4.61.

The characterization data are consistent with that reported in the literature [37].

Compound 1bn

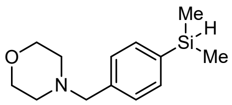

4-(4-(Dimethylsilyl)benzyl)morpholine

Prepared from 4-(4-bromobenzyl)morpholine (*Org. Lett.* **2013**, *15*, 2210.) by lithium-bromide exchange with *n*-BuLi (1.1 equiv.) at -78 ºC for 1 h and then reacted with chlorodimethylsilane (1.5 equiv.).

Physical state: yellow oil.

^{1}H NMR (400 MHz, Chloroform-*d*): δ = 7.53 (d, *J* = 7.3 Hz, 2H), 7.36 (d, *J* = 7.3 Hz, 2H), 4.46 (hept, *J* = 1.6 Hz 1H), 3.74 (t, *J* = 2.0 Hz 4H), 3.53 (s, 2H), 2.48 (t, *J* = 2.0 Hz, 4H), 0.37 (d, *J* = 1.9 Hz, 6H).

^{13}C NMR (101 MHz, Chloroform-*d*): δ = 138.77, 135.96, 133.91, 128.62, 66.90, 63.32, 53.56, -3.80.

HRMS (ESI-TOF): calcd for $C_{13}H_{22}NOSi^+$ $[M+H]^+$: 236.1465, found: 236.1465.

*E) General procedure for the preparation of 1,1'-biphenyl-2-ylsilanes **1ao, 1ap, 1aq** and **1ar** [27].*

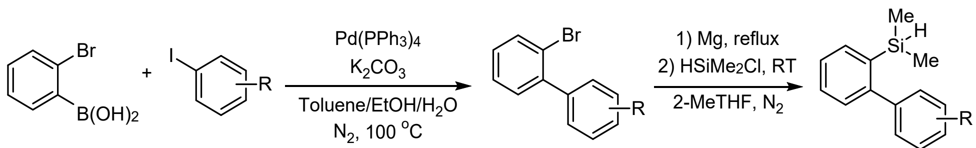

SI-1 2-bromobiphenyl

To a mixture of aryl iodide (10 mmol, 1 equiv.), 2-bromophenylboronic acid **SI-1** (2.21 g, 11 mmol, 1.1 equiv.) and K_2CO_3 (1.73 g, 12.5 mmol, 1.25 equiv.) in a mixed solvents of toluene/EtOH/water (84 mL, v:v:v = 15:7:2) was added $Pd(PPh_3)_4$ (231 mg, 0.2 mmol, 2 mol% Pd) under N_2 atmosphere. The resulting reaction mixture was stirred at 100 °C for 5 h. After cooling to room temperature, the mixture was extracted with EA, and the combined organic phases are dried over anhydrous Na_2SO_4. After evaporation of the solvents under reduced pressure, the crude product was purified by flash column chromatography on silica gel using cyclohexane as eluents to give the corresponding 2-bromobiphenyl.

Under N_2 atmosphere, magnesium shavings (0.144 g, 6 mmol, 1.2 equiv.) and 10 mL anhydrous 2-MeTHF was added to a 50 mL two-neck round bottom flask. To this suspension was added 2 drops of 1,2-dibromoethane. A solution of 2-bromobiphenyl (5 mmol, 1.0 equiv.) in 10 mL anhydrous 2-MeTHF was then added slowly to the suspension of Mg at room temperature. After addition, the resulting mixture was stirred under reflux for 3 h and then cooled to room temperature. Chlorodimethylsilane (0.709 g, 7.5 mmol, 1.5 equiv.) was added and the mixture was stirred overnight. After quenched with saturated aqueous NH_4Cl solution, the mixture was extracted with diethyl ether, and the combined organic phases are dried over anhydrous Na_2SO_4. After evaporation of the solvents under reduced pressure, the crude product was purified by flash column chromatography on silica gel using hexanes as eluent to give the corresponding silane.

Compound 1ao

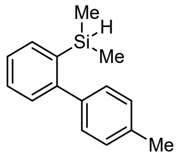

(4'-Methyl-[1,1'-biphenyl]-2-yl)dimethylsilane

Physical state: colorless oil.

^{1}H NMR (400 MHz, Chloroform-*d*): δ = 7.72 (d, *J* = 5.8 Hz, 1H), 7.54 - 7.27 (m, 7H), 4.47-4.42 (m, 1H), 2.50 (s, 3H), 0.18 (d, *J* = 3.6 Hz, 6H).

^{13}C NMR (101 MHz, Chloroform-*d*): δ = 149.29, 140.83, 136.73, 135.97, 135.07, 129.30, 129.07, 128.55, 126.21, 26.91, 21.19, -2.95.

The characterization data are consistent with that reported in the literature [27].

Compound 1ap

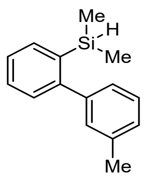

(3'-Methyl-[1,1'-biphenyl]-2-yl)dimethylsilane

Physical state: colorless oil.

^{1}H NMR (400 MHz, Chloroform-*d*): δ = 7.66 (dd, *J* = 7.3, 0.8 Hz, 1H), 7.45 (td, *J* = 7.4, 1.3 Hz, 1H), 7.38 (dd, *J* = 7.3, 6.4 Hz, 1H), 7.35 - 7.29 (m, 2H), 7.19 (t, *J* = 8.4 Hz, 3H), 4.36 (dp, *J* = 7.4, 3.6 Hz, 1H), 2.43 (s, 3H), 0.10 (d, *J* = 3.7 Hz, 6H).

^{13}C NMR (101 MHz, Chloroform-*d*): δ = 149.39, 143.60, 137.39, 135.94, 135.11, 130.01, 129.10, 129.05, 127.76, 126.28, 126.21, 21.41, -2.94.

The characterization data are consistent with that reported in the literature [27].

Compound 1aq

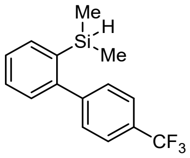

(4'-Trifluoromethyl-[1,1'-biphenyl]-2-yl)dimethylsilane

Physical state: colorless oil.

^{1}H NMR (400 MHz, Chloroform-*d*): δ = 7.74 - 7.69 (m, 3H), 7.49 (dd, *J* = 24.3, 8.7 Hz, 4H), 7.32 (d, *J* = 7.3 Hz, 1H), 4.36 (h, *J* = 3.5 Hz, 1H), 0.14 (d, *J* = 3.2 Hz, 6H).

^{13}C NMR (101 MHz, Chloroform-*d*): δ = 147.71, 147.27, 135.22, 129.55, 129.26, 129.11, 128.98, 128.18, 127.42, 127.28, 127.06, 125.68, 124.92, 124.88, 124.84, -3.06.

^{19}F NMR (376 MHz, Chloroform-*d*): δ = -62.25.

The characterization data are consistent with that reported in the literature [27].

Compound 1ar

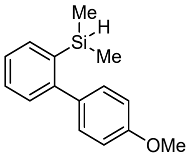

(4'-Methoxy-[1,1'-biphenyl]-2-yl)dimethylsilane

Physical state: colorless oil.

^{1}H NMR (400 MHz, Chloroform-*d*): δ = 7.68 (d, *J* = 7.2 Hz, 1H), 7.51 - 7.29 (m, 5H), 7.03 - 6.95 (m, 2H), 4.43 (dt, *J* = 7.5, 3.7 Hz, 1H), 3.91 (s, 3H), 0.15 (d, *J* = 3.8 Hz, 6H).

^{13}C NMR (101 MHz, Chloroform-*d*): δ = 158.86, 148.94, 136.26, 136.09, 135.08, 130.24, 129.38, 129.10, 126.14, 113.23, 55.25, -3.00.

The characterization data are consistent with that reported in the literature [27].

*F) General procedure for the preparation of **1aa**, **1ab** and **1ad**.*

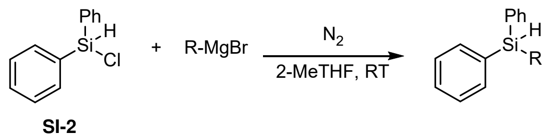

Under N_2 atmosphere, aliphatic magnesium bromide (10 mmol, 1 equiv., commercially-available THF solution from J&K Scientific) was added to 15 mL anhydrous 2-MeTHF at room temperature. Chlorodiphenylsilane **SI-2** (2.73 g, 12.5 mmol, 1.25 equiv.) was then added dropweise, and the mixture was stirred for 6 h. After quenched with saturated aqueous NH_4Cl solution, the mixture was extracted with diethyl ether, and the combined organic phases are dried over anhydrous Na_2SO_4. After evaporation of the solvents under reduced pressure, the crude product was purified by flash column chromatography on silica gel using hexanes as eluent to give the corresponding silane.

Compound 1aa

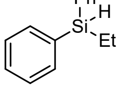

Ethyldiphenylsilane

Physical state: colorless oil.

^{1}H NMR (400 MHz, Chloroform-*d*): δ = 7.59 - 7.49 (m, 4H), 7.41 - 7.27 (m, 6H), 4.82 (t, *J* = 3.3 Hz, 1H), 1.20 - 0.97 (m, 5H).

^{13}C NMR (101 MHz, Chloroform-*d*): δ = 135.14, 134.40, 129.48, 127.94, 8.13, 4.13.

The characterization data are consistent with that reported in the literature [38].

Compound 1ab

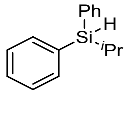

Isopropyldiphenylsilane

Physical state: colorless oil.

^{1}H NMR (400 MHz, Chloroform-*d*): δ = 7.65 - 7.56 (m, 4H), 7.56 - 7.29 (m, 6H), 4.73 (d, *J* = 3.2 Hz, 1H), 1.50 (ddd, *J* = 15.0, 7.6, 3.3 Hz, 1H), 1.13 (d, *J* = 7.4 Hz, 6H).

^{13}C NMR (101 MHz, Chloroform-*d*): δ = 135.48, 133.86, 129.45, 127.88, 18.38, 11.66.

The characterization data are consistent with that reported in the literature [39].

Compound 1ad

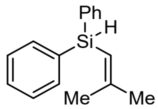

(2-Methylprop-1-en-1-yl)diphenylsilane

Physical state: colorless oil.

^{1}H NMR (400 MHz, Chloroform-*d*): δ = 7.60 - 7.55 (m, 4H), 7.38 - 7.32 (m, 6H), 5.58 - 5.50 (m, 1H), 5.23 (d, *J* = 5.1 Hz, 1H), 1.96 (d, *J* = 1.1 Hz, 3H), 1.85 (d, *J* = 0.5 Hz, 3H).

^{13}C NMR (101 MHz, Chloroform-*d*): δ = 156.93, 135.22, 134.98, 129.35, 127.92, 116.66, 29.46, 23.75.

The characterization data are consistent with that reported in the literature [28].

*G) Preparation of **1r**.*

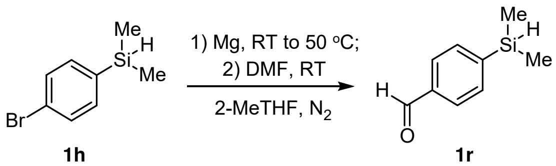

Under N_2 atmosphere, magnesium shavings (0.146 g, 6 mmol, 1.2 equiv.) and 10 mL anhydrous 2-MeTHF was added to a 50 mL two-neck round bottom flask. To this suspension was added 2 drops of 1,2-dibromoethane. A solution of **1h** (1.08 g, 5 mmol, 1.0 equiv.) in 5 mL anhydrous 2-MeTHF was then added slowly to the suspension of Mg at room temperature. After addition, the resulting mixture was stirred at 50 °C for 3 h and then cooled to room temperature. Anhydrous N,N-dimethylformamide (0.439 g, 6 mmol, 1.2 equiv.) was added and the mixture was stirred for 6 h. After quenched with saturated aqueous NH_4Cl solution, the mixture was extracted with EA, and the combined organic phases are dried over anhydrous Na_2SO_4. After evaporation of the solvents under reduced pressure, the crude product was purified by flash column chromatography on silica gel using EA/PE = 1:10 as eluent to give compound **1r**.

Compound 1r

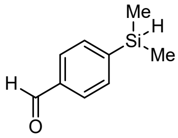

4-(Dimethylsilyl)benzaldehyde

Physical state: colorless oil.

^{1}H NMR (400 MHz, Chloroform-*d*): δ = 10.03 (s, 1H), 7.85 (d, *J* = 7.3 Hz, 2H), 7.72 (d, *J* = 7.4 Hz, 2H), 4.60 - 4.29 (m, 1H), 0.39 (d, *J* = 2.8 Hz, 6H).

^{13}C NMR (101 MHz, Chloroform-*d*): δ = 192.47, 146.03, 136.71, 134.50, 128.65, -4.11.

The characterization data are consistent with that reported in the literature [40].

*H) Preparation of **1au** [28].*

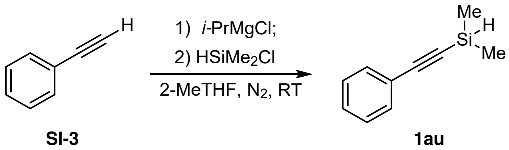

Under N_2 atmosphere, *i*-PrMgCl (24 mmol, 1.2 equiv., commercially-available THF solution from J&K Scientific) was slowly added to a solution of phenylacetylene **SI-3** (2.04 g, 20 mmol, 1 equiv.) in 30 mL anhydrous 2-MeTHF at room temperature and stirred for 2 h. Chlorodimethylsilane (2.84 g, 30 mmol, 1.5 equiv.) was added and the mixture and stirred for another 6 h. After quenched with saturated aqueous NH_4Cl solution, the mixture was extracted with diethyl ether, and the combined organic phases are dried over anhydrous Na_2SO_4. After evaporation of the solvents under reduced pressure, the crude product was purified by flash column chromatography using hexanes as eluent on silica gel to give compound **1au**.

Compound 1au

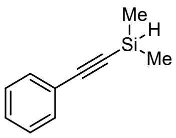

Dimethyl(phenylethynyl)silane

Physical state: colorless oil.

^{1}H NMR (400 MHz, Chloroform-*d*): δ = 7.52 (dd, *J* = 7.1, 1.6 Hz, 2H), 7.35 (t, *J* = 5.8 Hz, 3H), 4.31 (dd, *J* = 7.2, 3.6 Hz, 1H), 0.36 (d, *J* = 3.7 Hz, 6H).

^{13}C NMR (101 MHz, Chloroform-*d*): δ = 131.96, 128.71, 128.22, 122.79, 106.39, 91.06, -2.97.

The characterization data are consistent with that reported in the literature [21].

*I) Preparation of **1az***

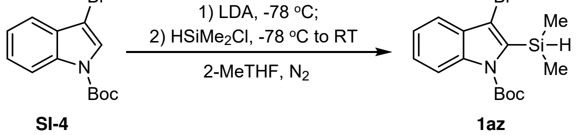

Under N_2 atmosphere, a solution of 1-Boc-3-bromoindolen **SI-4** (1.78 g, 6 mmol, 1.0 equiv.) in 15 mL anhydrous 2-MeTHF was cooled to -78 ºC. Then lithium diisopropylamide (LDA, 3.3 mL of a 2.0 M solution in heptane/THF/ethylbenzene, 5.5 mmol, 1.1 equiv., commercially-available solution from J&K Scientific) was slowly added and stirred at -78 °C for 3 h. Chlorodimethylsilane (0.852 g, 9 mmol, 1.5 equiv.) was added and mixture was allowed to warm to room temperature and stirred overnight. After quenched with saturated aqueous NH_4Cl solution, the mixture was extracted with EA, and the combined organic phases are dried over anhydrous Na_2SO_4. After evaporation of the solvents under reduced pressure, the crude product was purified by flash column chromatography on silica gel using EA/PE = 1:15 as eluent to give compound **1az**.

Compound 1az

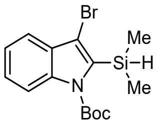

***tert*-Butyl 3-bromo-2-(dimethylsilyl)-1H-indole-1-carboxylate**
Physical state: white solid.
^{1}H NMR (400 MHz, Chloroform-*d*): δ = 7.97 (d, *J* = 8.4 Hz, 1H), 7.59 (d, *J* = 7.8 Hz, 1H), 7.36 (t, *J* = 7.7 Hz, 1H), 7.30 (t, *J* = 7.5 Hz, 1H), 4.99 - 4.91 (m, 1H), 1.73 (s, 9H), 0.47 (d, *J* = 3.0 Hz, 6H).
^{13}C NMR (101 MHz, Chloroform-*d*): δ = 150.84, 136.20, 135.98, 130.94, 125.76, 123.04, 120.01, 115.16, 111.88, 84.79, 28.12, -2.96.
HRMS (ESI-TOF): calcd for $C_{11}H_{11}NO_2Si^{79}Br^+$ $[M-C(CH_3)_3]^+$: 295.9737, found: 295.9745; calcd for $C_{11}H_{11}NO_2Si^{81}Br$ $[M-C(CH_3)_3]^+$: 297.9717, found: 297.9726.

*J) Preparation of **1bd** [41].*

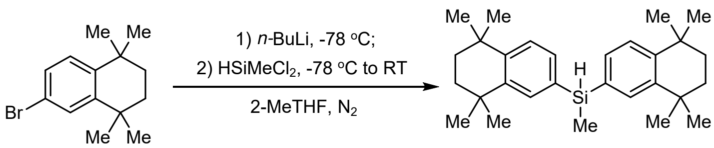

Under N_2 atmosphere, a solution of 6-bromo-1,1,4,4-tetramethyl-1,2,3,4-tetrahydronaphthalene **SI-5** (2.67 g, 10 mmol, 1 equiv.) in 30 mL anhydrous 2-MeTHF was cooled to -78 °C. Then *n*-BuLi (6.9 mL of a 1.6 M solution in THF, 11 mmol, 1.1 equiv.) was slowly added and the mixture was stirred at -78 °C for 2.5 h. Dichloromethylsilane (0.57 g, 5 mmol, 0.5 equiv.) was added and the mixture was allowed to warm to room temperature and stirred overnight. After quenched with saturated aqueous NH_4Cl solution, the mixture was extracted with EA, and the combined organic phases are dried over anhydrous Na_2SO_4. After evaporation of the solvents under reduced pressure, the crude product was purified by flash column chromatography on silica gel using hexanes as eluent to give compound **1bd**.

Compound 1bd

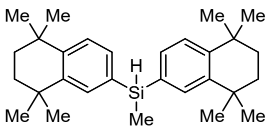

Methylbis(5,5,8,8-tetramethyl-5,6,7,8-tetrahydronaphthalen-2-yl)silane
Physical state: white solid.
^{1}H NMR (400 MHz, Chloroform-*d*): δ = 7.54 (s, 2H), 7.33 (s, 4H), 4.90 (q, *J* = 2.1 Hz, 1H), 1.70 (s, 8H),

1.29 (s, 24H), 0.61 (d, J = 1.8 Hz, 3H).
^{13}C NMR (101 MHz, Chloroform-*d*): δ = 146.16, 144.14, 133.29, 131.94, 131.81, 126.03, 35.17, 35.03, 34.27, 34.17, 31.88, 31.77, -4.78.
The characterization data are consistent with that reported in the literature [41].

*K) Preparation of **1br**.*

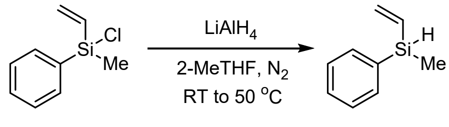

Under N_2 atmosphere, chloromethylphenylvinylsilane **SI-6** (1.83 g, 10 mmol, 2.0 equiv.) was added dropwise to a stirred solution of $LiAlH_4$ (0.190 g, 5 mmol, 1.0 equiv.) in 10 mL anhydrous 2-MeTHF at room temperature. After addition, the resulting mixture was stirred at 50 ºC for 10 h and then cooled to room temperature. After quenched with aqueous solution of NaOH (10 ml, 10 wt%), the mixture was extracted with diethyl ether, and the combined organic phases are dried over anhydrous Na_2SO_4. After evaporation of the solvents under reduced pressure, the crude product was purified by flash column chromatography on silica gel using hexanes as eluent to give compound **1br**.

Compound 1br

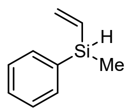

Methyl(phenyl)(vinyl)silane
Physical state: colorless oil.
^{1}H NMR (400 MHz, Chloroform-*d*): δ = 7.60 - 7.49 (m, 2H), 7.35 (dd, J = 9.8, 4.7 Hz, 3H), 6.28 (ddd, J = 20.0, 14.5, 2.7 Hz, 1H), 6.11 (dd, J = 14.5, 3.8 Hz, 1H), 5.85 (dd, J = 20.0, 3.8 Hz, 1H), 4.68 - 4.47 (m, 1H), 0.42 (d, J = 3.8 Hz, 3H).
^{13}C NMR (101 MHz, Chloroform-*d*): δ = 135.31, 134.78, 134.52, 129.40, 127.91, -5.68.
The characterization data are consistent with that reported in the literature [42].

*L) Preparation of **1b** and **R-1b** [43].*

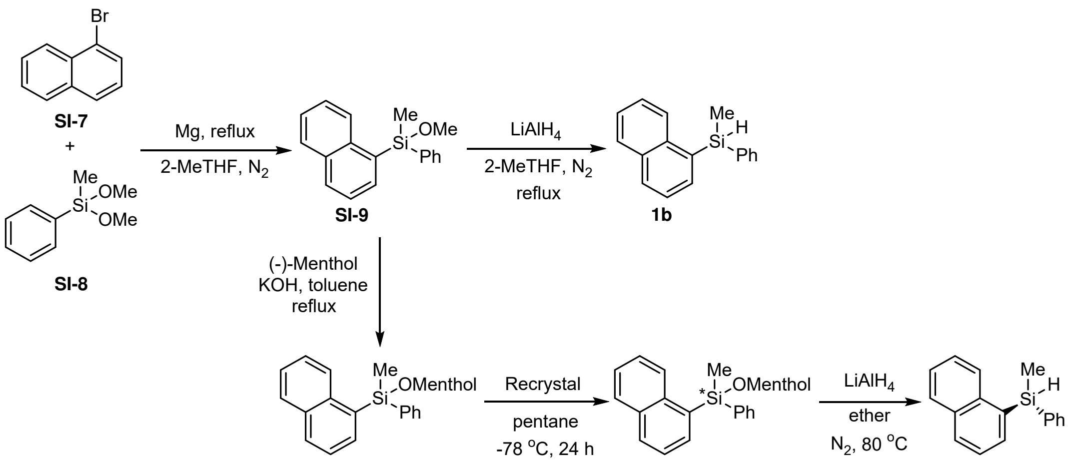

Under N_2 atmosphere, magnesium shavings (2.19 g, 90 mmol, 1.2 equiv.) and 30 mL anhydrous 2-MeTHF was added to a 100 mL two-neck round bottom flask. To this suspension was added 2 drops of 1,2-dibromoethane. A solution of 1-bromonaphthalene **SI-7** (15.53 g, 75 mmol, 1.0 equiv.) in 10 mL anhydrous 2-MeTHF was then added slowly to the suspension of Mg at room temperature. After addition, the resulting mixture was stirred under reflux for 12 h and then cooled to room temperature. A solution of dimethoxymethylphenylsilane **SI-8** (13.67 g, 75 mmol, 1.0 equiv.) was added and the mixture was stirred overnight. After quenched with saturated aqueous NH_4Cl solution, the mixture was extracted with diethyl ether, and the combined organic phases are dried over anhydrous Na_2SO_4. After evaporation of the solvents under reduced pressure, the crude product was purified by fractional distillation followed by crystallization to give 18.21 g (87 % yield) purified methoxy-methyl(1-naphthyl)phenylsilane **SI-9** as colorless crystals.

For synthesis of **1b**, a solution of **SI-9** (2.78 g, 10 mmol, 1 equiv.) in 10 mL anhydrous 2-MeTHF was added dropwise to a stirred solution of $LiAlH_4$ (0.380 g, 10 mmol, 1.0 equiv.) in 10 mL anhydrous 2-MeTHF under N_2 atmosphere at room temperature. After addition, the resulting mixture was stirred at 50 ºC for 12 h and then cooled to room temperature. After quenched with aqueous solution of NaOH (15 ml, 10 wt%), the mixture was extracted with diethyl ether, and the combined organic phases are dried over anhydrous Na_2SO_4. After evaporation of the solvents under reduced pressure, the crude product was purified by flash column chromatography on silica gel using hexanes as eluent to give compound **1b**.

For synthesis of ***R*-1b**, (-)-menthol (6.25 g, 40 mmol, 1 equiv.) and solid NaOH (0.160 g, 4.0 mmol, 0.1 equiv.) were added into a solution of methoxymethyl(1-naphthyl)phenylsilane **SI-9** (11.14 g, 40 mmol) in 20 mL toluene. The reaction mixture was refluxed overnight with a Vigreux column was used to distilled the MeOH-toluene azeotrope. After 12 h, the reaction mixture was cooled down to room temperature and NaOH was removed by passing the reaction mixture through a short column of silica gel with diethyl ether as an eluent. The filtrate was concentrated to afford a pale yellow oil containing a mixture of the diastereomers. The oil was diluted with twice its volume of pentane and chilled under -78 ºC for over 24 h. The white solid were formed, followed by recrystallization from pentane to give 1.54 g (10 % yield) menthoxymethyl(1-naphthyl)phenylsilane **(+)-SI-10** as white solid.

Under N_2 atmosphere, a solution of **(+)-SI-10** (1.21 g, 3 mmol, 1 equiv.) in 5 mL *n*-butyl ether was added dropwise to a stirred solution of $LiAlH_4$ (0.480 g, 12 mmol, 4.0 equiv.) in 5 mL anhydrous 2-MeTHF at room temperature. After addition, the resulting mixture was stirred at 80 ºC for 12 h and then cooled to room temperature. Water was added to quench the excess hydride species and then concentrated hydrochloric acid was also added, the mixture was extracted with diethyl ether, and the combined organic phases are dried over anhydrous Na_2SO_4. After evaporation of the solvents under reduced pressure, the crude product was purified by flash column chromatography on silica gel using hexanes as eluent to give 0.63 g (85 % yield, 95% *ee*) compound ***R*-1b**.

Compound 1b

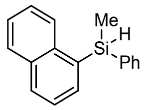

***rac*-Methyl(naphthalen-1-yl)phenylsilane**

Physical state: white solid.

^{1}H NMR (400 MHz, Chloroform-*d*): δ = 8.09 (d, *J* = 8.0 Hz, 1H), 7.95 - 7.86 (m, 2H), 7.77 (d, *J* = 6.7 Hz, 1H), 7.67 - 7.56 (m, 2H), 7.55 - 7.33 (m, 6H), 5.39 (q, *J* = 3.8 Hz, 1H), 0.79 (d, *J* = 3.8 Hz, 3H).

^{13}C NMR (101 MHz, Chloroform-*d*): δ = 137.07, 135.36, 135.21, 134.88, 133.36, 133.24, 130.46, 129.49,

128.87, 128.00, 127.96, 126.05, 125.62, 125.20, -4.53.
The characterization data are consistent with that reported in the literature [43].

Compound *R*-1b

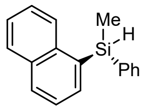

***(R)*-Methyl(naphthalen-1-yl)phenylsilane**
Physical state: white solid.
^{1}H NMR (400 MHz, Chloroform-*d*): δ = 8.09 (d, *J* = 8.0 Hz, 1H), 7.99 - 7.86 (m, 2H), 7.78 (d, *J* = 6.7 Hz, 1H), 7.65 - 7.57 (m, 2H), 7.57 - 7.33 (m, 6H), 5.39 (q, *J* = 3.8 Hz, 1H), 0.80 (d, *J* = 3.8 Hz, 3H).
^{13}C NMR (101 MHz, Chloroform-*d*): δ = 137.10, 135.39, 135.21, 134.88, 133.37, 133.24, 130.47, 129.49, 128.87, 128.01, 127.97, 126.04, 125.62, 125.21, -4.52.
$[\alpha]_D^{24}$ = +32.1 (c = 1.0, cyclohexane).
The characterization data are consistent with that reported in the literature [43].
Chiral HPLC: CHIRALPAK IB (250 mm × 4.6 mm × 5 µm); hexanes: *i*-PrOH (100:0), 1 mL/min, 254 nm; t_R (major) = 8.0 min, t_R (minor) = 9.0 min, 95% *ee*.

*M) Preparation of **1a-d₁*** [44].

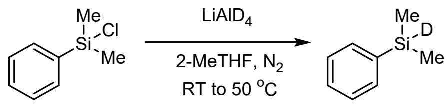

Under N_2 atmosphere, chlorodimethylphenylsilane **SI-11** (1.71 g, 10 mmol, 2.0 equiv.) was added dropwise to a stirred solution of $LiAlD_4$ (0.210 g, 5 mmol, 1.0 equiv.) in 10 mL anhydrous 2-MeTHF at room temperature. After addition, the resulting mixture was stirred at 50 °C for 10 h and then cooled to room temperature. After quenched with aqueous solution of NaOH (10 ml, 10 wt%), the mixture was extracted with diethyl ether, and the combined organic phases are dried over anhydrous Na_2SO_4. After evaporation of the solvents under reduced pressure, the crude product was purified by flash column chromatography using hexanes as eluent on silica gel to give compound **1a-*d₁***.

Compound 1a-*d₁*

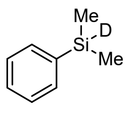

Dimethylphenylsilane-*d₁*
Physical state: colorless oil.
^{1}H NMR (400 MHz, Chloroform-*d*): δ = 7.65 - 7.54 (m, 2H), 7.40 (d, *J* = 4.7 Hz, 3H), 0.39 (s, 6H).
^{13}C NMR (101 MHz, Chloroform-*d*): δ = 137.43, 133.99, 129.17, 127.85, -3.88.
The characterization data are consistent with that reported in the literature [44].

General procedure for Co-N_4@NPC-catalyzed selective oxidation of hydrosilanes under optimized reaction conditions in batch reactors (GP A)

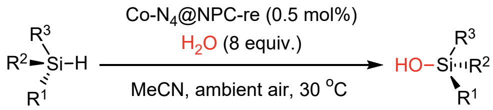

Silane (1 mmol, 1 equiv.) and water (145 µL, 8 mmol, 8 equiv.) were mixed with MeCN (3mL) in a 15 mL oven-dried round-bottom tube with steady magnetic stirring (800 rpm) at 30 °C under an ambient atmosphere of air. The reaction was started by the addition of Co-N_4@NPC-re (0.5 mol% Co) catalyst and the mixture was allowed to stir for given reaction time. After completion of the reaction (monitored by GC and/or TLC), the catalyst was removed by filtration and washed with EA (3 × 5 mL). The combined organics were washed with brine, dried over anhydrous Na_2SO_4 and solvent was removed under reduced pressure. In most cases, correspond silanol was obtained without further purification. If necessary, the product was purified via flash column chromatography or vacuum distillation.

Compound 2a

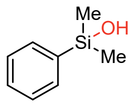

Dimethyl(phenyl)silanol

The reaction was conducted for 0.5 h following **GP A** on 1 mmol scale with **1a**. After dried over anhydrous Na_2SO_4 and evaporated the solvent, the title compound **2a** was obtained in 97% yield (147 mg) without further purification.

Physical state: colorless oil.

^{1}H NMR (400 MHz, Chloroform-*d*): δ = 7.65 - 7.52 (m, 2H), 7.43 - 7.31 (m, 3H), 2.10 (br s, 1H), 0.39 (s, 6H).

^{13}C NMR (101 MHz, Chloroform-*d*): δ = 139.09, 133.03, 129.53, 127.81, -0.10.

The characterization data are consistent with that reported in the literature [21].

Compound 2b

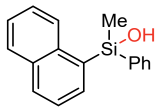

***rac*-Methyl(naphthalen-1-yl)phenylsilanol**

The reaction was conducted for 3 h following **GP A** on 1 mmol scale with **1b**. After dried over anhydrous Na_2SO_4 and evaporated the solvent, the title compound **2b** was obtained in 97% yield (256 mg) without further purification.

Physical state: white solid.

^{1}H NMR (400 MHz, Chloroform-*d*): δ = 8.01 (d, J = 8.2 Hz, 1H), 7.78 (d, J = 8.2 Hz, 1H), 7.73 (d, J = 8.1 Hz, 1H), 7.67 (d, J = 6.7 Hz, 1H), 7.48 (d, J = 7.7 Hz, 2H), 7.26 (m, 6H), 2.99 (br s, 1H), 0.65 (s, 3H).

^{13}C NMR (101 MHz, Chloroform-*d*): δ = 137.60, 136.70, 134.74, 134.65, 133.91, 133.30, 130.66, 129.77, 128.84, 128.41, 127.91, 125.95, 125.47, 124.99, -0.10.

The characterization data are consistent with that reported in the literature [28].

Compound *R*-2b

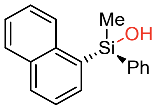

***R*-Methyl(naphthalen-1-yl)phenylsilanol**

The reaction was conducted for 3 h following **GP A** on 1 mmol scale with ***R*-1b**. After dried over anhydrous Na_2SO_4 and evaporated the solvent, the title compound ***R*-2b** was obtained in 98% yield (258 mg) without further purification.

Physical state: white solid.

^{1}H NMR (400 MHz, Chloroform-*d*): δ = 8.10 (d, *J* = 8.2 Hz, 1H), 7.90 (d, *J* = 8.2 Hz, 1H), 7.85 (d, *J* = 9.4 Hz, 1H), 7.78 (d, *J* = 6.8 Hz, 1H), 7.60 (d, *J* = 6.1 Hz, 2H), 7.49 - 7.29 (m, 6H), 2.44 (br s), 0.79 (s, 3H).

^{13}C NMR (101 MHz, Chloroform-*d*): δ = 137.65, 136.75, 134.76, 134.67, 133.94, 133.38, 130.75, 129.87, 128.90, 128.42, 127.98, 126.02, 125.53, 125.02, -0.00.

$[\alpha]_D^{24}$ = -15.6 (c = 1.0, diethyl ether).

The characterization data are consistent with that reported in the literature [28].

Chiral HPLC: CHIRALPAK IB (250 mm × 4.6 mm × 5 µm); hexanes: *i*-PrOH (99:1), 1 mL/min, 254 nm; t_R (major) = 28.8 min, t_R (minor) = 30.6 min, 92% *ee*.

Compound 2c

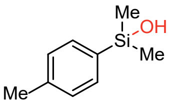

(4-Methylphenyl)dimethylsilanol

The reaction was conducted for 0.5 h following **GP A** on 1 mmol scale with **1c**. After dried over anhydrous Na_2SO_4 and evaporated the solvent, the title compound **2c** was obtained in 97% yield (161 mg) without further purification.

Physical state: colorless oil.

^{1}H NMR (400 MHz, Chloroform-*d*): δ = 7.51 (d, *J* = 7.8 Hz, 2H), 7.23 (d, *J* = 7.7 Hz, 2H), 2.39 (s, 3H), 2.12 (br s, 1H), 0.41 (s, 6H).

^{13}C NMR (101 MHz, Chloroform-*d*): δ = 139.55, 135.51, 133.09, 128.68, 21.48, -0.01.

The characterization data are consistent with that reported in the literature [45].

Compound 2d

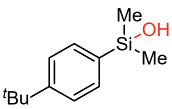

(4-*tert*-Butylphenyl)dimethylsilanol

The reaction was conducted for 1.5 h following **GP A** on 1 mmol scale with **1d**. After dried over anhydrous Na_2SO_4 and evaporated the solvent, the title compound **2d** was obtained in 97% yield (203 mg) without further purification.

Physical state: white solid.

^{1}H NMR (400 MHz, Chloroform-*d*): δ = 7.56 (dd, *J* = 8.0, 1.7 Hz, 2H), 7.44 (dd, *J* = 8.0, 2.0 Hz, 2H), 2.07 (br s, 1H), 1.35 (d, *J* = 4.0 Hz, 9H), 0.41 (s, 6H).

^{13}C NMR (101 MHz, Chloroform-*d*): δ = 152.70, 135.63, 133.01, 124.86, 31.20, -0.02.

HRMS (ESI-TOF): calcd for $C_{12}H_{20}OSiNa^+$ $[M+Na]^+$: 231.1176, found: 231.1175.

Compound 2e

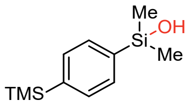

(4-Trimethylphenyl)dimethylsilylsilanol

The reaction was conducted for 0.5 h following **GP A** on 1 mmol scale with **1e**. After dried over anhydrous Na_2SO_4 and evaporated the solvent, the title compound **2e** was obtained in 98% yield (220 mg) without further purification.

Physical state: white solid.

^{1}H NMR (400 MHz, Chloroform-*d*): δ = 7.65 - 7.56 (m, 4H), 2.13 (br s, 1H), 0.42 (s, 6H), 0.30 (s, 9H).

^{13}C NMR (101 MHz, Chloroform-*d*): δ = 142.16, 139.50, 132.75, 132.28, -0.08, -1.25.

The characterization data are consistent with that reported in the literature [46].

Compound 2f

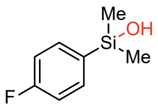

(4-Fluorophenyl)dimethylsilanol

The reaction was conducted for 0.5 h following **GP A** on 1 mmol scale with **1f**. After dried over anhydrous Na_2SO_4 and evaporated the solvent, the title compound **2f** was obtained in 99% yield (168 mg) without further purification.

Physical state: colorless oil.

^{1}H NMR (400 MHz, Chloroform-*d*): δ = 7.51 (t, *J* = 7.1 Hz, 2H), 7.02 (t, *J* = 8.8 Hz, 2H), 2.56 (br s, 1H), 0.34 (s, 6H).

^{13}C NMR (101 MHz, Chloroform-*d*): δ = 165.20, 162.73, 135.11, 135.03, 115.07, 114.88, 0.03.

^{19}F NMR (377 MHz, Chloroform-*d*): δ = -111.02.

The characterization data are consistent with that reported in the literature [47].

Compound 2g

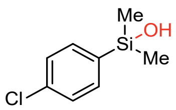

(4-Chlorophenyl)dimethylsilanol

The reaction was conducted for 1 h following **GP A** on 1 mmol scale with **1g**. After dried over anhydrous Na_2SO_4 and evaporated the solvent, the title compound **2g** was obtained in 97% yield (181 mg) without further purification.

Physical state: colorless oil.

^{1}H NMR (400 MHz, Chloroform-*d*): δ = 7.51 (d, *J* = 7.6 Hz, 2H), 7.35 (d, *J* = 7.6 Hz, 2H), 1.92 (br s, 1H), 0.39 (s, 3H).

^{13}C NMR (101 MHz, Chloroform-*d*): δ = 137.26, 135.86, 134.42, 128.06, -0.07.

The characterization data are consistent with that reported in the literature [21].

Compound 2h

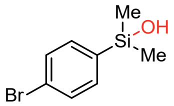

(4-Bromophenyl)dimethylsilanol

The reaction was conducted for 1 h following **GP A** on 1 mmol scale with **1h**. After dried over anhydrous Na_2SO_4 and evaporated the solvent, the title compound **2h** was obtained in 98% yield (226 mg) without further purification.

Physical state: colorless oil.

^{1}H NMR (400 MHz, Chloroform-*d*): δ = 7.51 (d, *J* = 7.6 Hz, 2H), 7.43 (d, *J* = 7.5 Hz, 2H), 2.13 (br s, 1H), 0.38 (s, 6H).

^{13}C NMR (101 MHz, Chloroform-*d*): δ = 137.82, 134.64, 131.04, 124.46, -0.03.

The characterization data are consistent with that reported in the literature [48].

Compound 2i

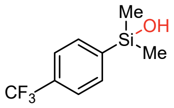

(4-Trifluoromethylphenyl)dimethylsilanol

The reaction was conducted for 4 h following **GP A** on 1 mmol scale with **1i**. After dried over anhydrous Na_2SO_4 and evaporated the solvent, the title compound **2i** was obtained in 98% yield (216 mg) without further purification.

Physical state: colorless oil.

^{1}H NMR (400 MHz, Chloroform-*d*): δ = 7.70 (d, *J* = 7.6 Hz, 2H), 7.62 (d, *J* = 7.7 Hz, 2H), 2.58 (br s, 1H), 0.42 (s, 6H).

^{13}C NMR (101 MHz, Chloroform-*d*): δ = 143.79, 133.34, 133.20, 131.98, 131.66, 131.34, 131.02, 125.49, 124.46, 124.42, 124.38, 124.34, 122.79, 0.05.

^{19}F NMR (376 MHz, Chloroform-*d*): δ = -62.99.

The characterization data are consistent with that reported in the literature[21].

Compound 2j

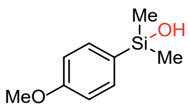

(4-Methoxyphenyl)dimethylsilanol

The reaction was conducted for 2 h following **GP A** on 1 mmol scale with **1j**. After dried over anhydrous Na_2SO_4 and evaporated the solvent, the title compound **2j** was obtained in 96% yield (175 mg) without further purification.

Physical state: colorless oil.

^{1}H NMR (400 MHz, Chloroform-*d*): δ = 7.49 (d, *J* = 8.6 Hz, 2H), 6.90 (d, *J* = 8.6 Hz, 2H), 3.79 (s, 3H), 2.44 (br s, 1H), 0.34 (s, 6H).

^{13}C NMR (101 MHz, Chloroform-*d*): δ = 160.71, 134.59, 130.19, 113.53, 54.98, 0.03.

The characterization data are consistent with that reported in the literature [21].

Compound 2k

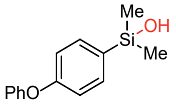

(4-Phenoxyphenyl)dimethylsilanol

The reaction was conducted for 4 h following **GP A** on 1 mmol scale with **1k**. After dried over anhydrous Na_2SO_4 and evaporated the solvent, the title compound **2k** was obtained in 97% yield (237 mg) without further purification.

Physical state: colorless oil.

^{1}H NMR (400 MHz, Chloroform-*d*): δ = 7.56 (d, *J* = 7.6 Hz, 2H), 7.36 (t, *J* = 7.6 Hz, 2H), 7.15 (t, *J* = 7.3 Hz, 1H), 7.04 (t, *J* = 9.3 Hz, 4H), 2.77 (br s, 1H), 0.40 (s, 6H).

^{13}C NMR (101 MHz, Chloroform-*d*): δ = 158.73, 156.60, 134.77, 133.11, 129.74, 123.52, 119.28, 117.94, 0.04.

HRMS (ESI-TOF): calcd for $C_{14}H_{15}O_2Si^-$ $[M-H]^-$: 243.0836, found: 243.0842.

Compound 2l

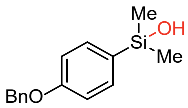

(4-(Benzyloxy)phenyl)dimethylsilanol

The reaction was conducted for 4 h following **GP A** on 1 mmol scale **1l**. After dried over anhydrous Na_2SO_4 and evaporated the solvent, the title compound **2l** was obtained in 98% yield (253 mg) without further purification.

Physical state: white solid.

^{1}H NMR (400 MHz, Chloroform-*d*): δ = 7.55 (d, *J* = 8.5 Hz, 2H), 7.49 - 7.34 (m, 5H), 7.03 (d, *J* = 8.5 Hz, 2H), 5.11 (s, 2H), 2.33 (br s, 1H), 0.41 (s, 6H).

^{13}C NMR (101 MHz, Chloroform-*d*): δ = 159.98, 136.84, 134.62, 130.48, 128.55, 127.93, 127.40, 114.44, 69.68, 0.03.

HRMS (ESI-TOF): calcd for $C_{15}H_{17}O_2Si^-$ $[M-H]^-$: 257.0992, found: 257.0987.

Compound 2m

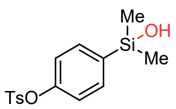

4-(Hydroxydimethylsilyl)phenyl 4-methylbenzenesulfonate

The reaction was conducted for 5 h following **GP A** on 1 mmol scale with **1m**. After dried over anhydrous Na_2SO_4 and evaporated the solvent, the title compound **2m** was obtained in 98% yield (317 mg) without further purification.

Physical state: colorless viscous oil..

^{1}H NMR (400 MHz, Chloroform-*d*): δ = 7.72 (d, *J* = 8.3 Hz, 2H), 7.51 (d, *J* = 8.5 Hz, 2H), 7.33 (d, *J* = 8.0 Hz, 2H), 6.99 (d, *J* = 8.4 Hz, 2H), 2.46 (s, 3H), 2.32 (br s, 1H), 0.37 (s, 6H).

^{13}C NMR (101 MHz, Chloroform-*d*): δ = 150.69, 145.36, 138.31, 134.51, 132.43, 129.74, 128.40, 121.67, 21.65, -0.03.

HRMS (ESI-TOF): calcd for $C_{15}H_{17}SO_4Si^-$ $[M-H]^-$: 321.0611, found: 321.0629.

Compound 2n

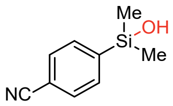

4-(Hydroxydimethylsilyl)benzonitrile

The reaction was conducted for 6 h following **GP A** on 1 mmol scale with **1n**. After purification by flash column chromatography (silica gel, EA/PE = 1:10), the title compound **2n** was obtained in 93% yield (165 mg).

Physical state: colorless oil.

^{1}H NMR (400 MHz, Chloroform-*d*): δ = 7.69 (d, *J* = 8.2 Hz, 2H), 7.59 (d, *J* = 8.2 Hz, 2H), 3.53 (br s, 1H), 0.40 (s, 6H).

^{13}C NMR (101 MHz, Chloroform-*d*): δ = 145.99, 133.47, 130.93, 118.73, 112.51, -0.26.

The characterization data are consistent with that reported in the literature [45].

Compound 2o

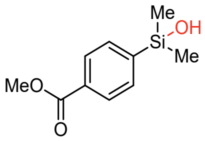

Methyl-4-(hydroxydimethylsilyl)benzoate

The reaction was conducted for 4 h following **GP A** on 1 mmol scale with **1o**. After purification by flash column chromatography (silica gel, EA/PE = 1:10), the title compound **2o** was obtained in 94% yield (198 mg).

Physical state: colorless oil.

^{1}H NMR (400 MHz, Chloroform-*d*): δ = 7.95 (d, *J* = 8.2 Hz, 2H), 7.62 (d, *J* = 8.2 Hz, 2H), 3.89 (s, 3H), 3.42 (br s, 1H), 0.38 (s, 6H).

^{13}C NMR (101 MHz, Chloroform-*d*): δ = 167.33, 145.38, 132.98, 130.59, 128.52, 52.11, -0.16.

The characterization data are consistent with that reported in the literature [49].

Compound 2p

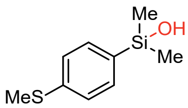

(4-Methylthiophenyl)dimethylsilanol

The reaction was conducted for 3 h following **GP A** on 1 mmol scale with **1p**. After dried over anhydrous Na_2SO_4 and evaporated the solvent, the title compound **2p** was obtained in 98% yield (194 mg) without further purification.

Physical state: colorless oil.

^{1}H NMR (400 MHz, Chloroform-*d*): δ = 7.51 (dd, *J* = 7.9, 1.1 Hz, 2H), 7.28 (d, *J* = 7.5 Hz, 2H), 2.51 (s, 3H), 2.40 (br s, 1H), 0.40 (s, 6H).

^{13}C NMR (101 MHz, Chloroform-*d*): δ = 140.46, 135.02, 133.43, 125.56, 15.22, -0.04.

HRMS (ESI-TOF): calcd for $C_9H_{13}SOSi^-$ [M-H]$^-$: 197.0451, found: 197.0465.

Compound 2q

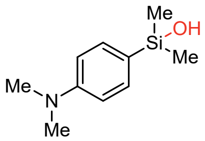

(4-(Dimethylamino)phenyl)dimethylsilanol

The reaction was conducted for 10 h following **GP A** on 1 mmol scale with **1q**. After purification by flash column chromatography (silica gel, EA/PE/NEt_3 = 1:3:0.01), the title compound **2q** was obtained in 95% yield (185 mg).

Physical state: white solid.

^{1}H NMR (400 MHz, Chloroform-*d*): δ = 7.53 (d, *J* = 7.9 Hz, 2H), 6.81 (d, *J* = 8.1 Hz, 2H), 3.02 (s, 6H), 2.63 (br s, 1H), 0.42 (s, 6H).

^{13}C NMR (101 MHz, Chloroform-*d*): δ = 151.36, 134.22, 128.99, 124.63, 111.91, 40.16, 0.00.

The characterization data are consistent with that reported in the literature [50].

Compound 2r

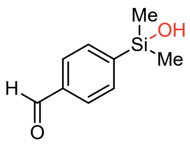

4-(Hydroxydimethylsilyl)benzaldehyde

The reaction was conducted for 4 h following **GP A** on 1 mmol scale with **1r**. After purification by flash column chromatography (silica gel, EA/PE = 1:9), the title compound **2r** was obtained in 96% yield (173 mg).

Physical state: colorless oil.

^{1}H NMR (400 MHz, Chloroform-*d*): δ = 9.99 (s, 1H), 7.84 (d, *J* = 6.4 Hz, 2H), 7.75 (d, *J* = 7.4 Hz, 2H), 2.85 (br s, 1H), 0.43 (s, 6H).

^{13}C NMR (101 MHz, Chloroform-*d*): δ = 192.80, 134.64, 133.57, 132.49, 128.77, -0.08.

HRMS (ESI-TOF): calcd for $C_9H_{11}O_2Si^-$ $[M-H]^-$: 179.0523, found: 179.0523.

Compound 2s

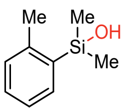

(2-Methylphenyl)dimethylsilanol

The reaction was conducted for 1 h following **GP A** on 1 mmol scale with **1s**. After dried over anhydrous Na_2SO_4 and evaporated the solvent, the title compound **2s** was obtained in 98% yield (163 mg) without further purification.

Physical state: colorless oil.

^{1}H NMR (400 MHz, Chloroform-*d*): δ = 7.56 (d, *J* = 7.2 Hz, 1H), 7.32 (t, *J* = 7.4 Hz, 1H), 7.20 (t, *J* = 7.8 Hz, 2H), 2.52 (s, 3H), 2.36 (br s, 1H), 0.46 (s, 6H).

^{13}C NMR (101 MHz, Chloroform-*d*): δ = 143.23, 137.33, 134.08, 129.86, 129.79, 124.91, 22.72, 0.99.

The characterization data are consistent with that reported in the literature [51].

Compound 2t

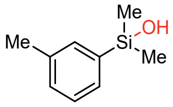

(3-Methylphenyl)dimethylsilanol

The reaction was conducted for 0.5 h following **GP A** on 1 mmol scale with **1t**. After dried over anhydrous Na_2SO_4 and evaporated the solvent, the title compound **2t** was obtained in 97% yield (161 mg) without further purification.

Physical state: colorless oil.

^{1}H NMR (400 MHz, Chloroform-*d*): δ = 7.39 (d, *J* = 10.7 Hz, 2H), 7.28 (t, *J* = 7.3 Hz, 1H), 7.21 (d, *J* = 7.5 Hz, 1H), 2.36 (s, 3H), 2.09 (br s, 1H), 0.39 (s, 6H).

^{13}C NMR (101 MHz, Chloroform-*d*): δ = 138.95, 137.22, 133.66, 130.38, 130.02, 127.81, 21.44, -0.05.

The characterization data are consistent with that reported in the literature [46].

Compound 2u

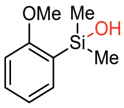

(2-Methoxyphenyl)dimethylsilanol

The reaction was conducted for 12 h following **GP A** on 1 mmol scale with **1u**. After dried over anhydrous Na_2SO_4 and evaporated the solvent, the title compound **2u** was obtained in 97% yield (177 mg) without further purification.

Physical state: colorless oil.

^{1}H NMR (400 MHz, Chloroform-*d*): δ = 7.43 (d, *J* = 7.0 Hz, 1H), 7.39 (t, *J* = 7.9 Hz, 1H), 7.00 (t, *J* = 7.2 Hz, 1H), 6.87 (d, *J* = 8.2 Hz, 1H), 3.85 (s, 3H), 2.47 (br s, 1H), 0.40 (s, 6H).

^{13}C NMR (101 MHz, Chloroform-*d*): δ = 163.80, 134.51, 131.26, 126.83, 120.77, 109.58, 55.16, 0.27.

The characterization data are consistent with that reported in the literature [21].

Compound 2v

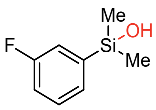

(3-Fluorophenyl)dimethylsilanol

The reaction was conducted for 3 h following **GP A** on 1 mmol scale with **1v**. After dried over anhydrous Na_2SO_4 and evaporated the solvent, the title compound **2v** was obtained in 97% yield (166 mg) without further purification.

Physical state: colorless oil.

^{1}H NMR (400 MHz, Chloroform-*d*): δ = 7.46 - 7.33 (m, 2H), 7.28 (d, *J* = 8.5 Hz, 1H), 7.10 (t, *J* = 7.0 Hz, 1H), 2.51 (br s, 1H), 0.42 (s, 6H).

^{13}C NMR (101 MHz, Chloroform-*d*): δ = 163.84, 161.37, 142.12, 134.43, 129.76, 129.69, 128.54, 128.51, 128.10, 119.48, 119.30, 116.59, 116.38, -0.12.

^{19}F NMR (376 MHz, Chloroform-d): δ = -113.48.

HRMS (ESI-TOF): calcd for $C_8H_{10}FOSi^-$ $[M-H]^-$: 169.0479, found: 169.0472.

Compound 2w

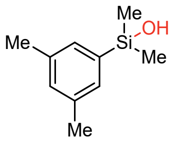

(3,5-Dimethylphenyl)dimethylsilanol

The reaction was conducted for 1 h following **GP A** on 1 mmol scale with **1w**. After dried over anhydrous Na_2SO_4 and evaporated the solvent, the title compound **2w** was obtained in 98% yield (177 mg) without further purification.

Physical state: colorless oil.

^{1}H NMR (400 MHz, Chloroform-*d*): δ = 7.23 (s, 2H), 7.07 (s, 1H), 2.36 (s, 6H), 2.12 (br s, 1H), 0.41 (s, 6H).

^{13}C NMR (101 MHz, Chloroform-*d*): δ = 138.88, 137.22, 131.33, 130.71, 21.29, -0.01.

The characterization data are consistent with that reported in the literature [21].

Compound 2x

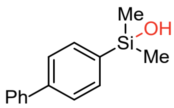

(1,1'-Biphenyl)-4-yldimethylsilanol

The reaction was conducted for 3 h following **GP A** on 1 mmol scale with **1x**. After dried over anhydrous Na_2SO_4 and evaporated the solvent, the title compound **2x** was obtained in 97% yield (223 mg) without further purification.

Physical state: white solid.

^{1}H NMR (400 MHz, Chloroform-*d*): δ = 7.66 (d, *J* = 7.4 Hz, 2H), 7.63 - 7.56 (m, 4H), 7.44 (t, *J* = 7.2 Hz, 2H), 7.36 (d, *J* = 7.3 Hz, 1H), 2.30 (br s, 1H), 0.43 (s, 6H).

^{13}C NMR (101 MHz, Chloroform-*d*): δ = 142.38, 140.96, 137.76, 133.56, 128.77, 127.45, 127.15, 126.62, 0.03.

HRMS (ESI-TOF): calcd for $C_{14}H_{15}OSi^-$ $[M-H]^-$: 227.0887, found: 227.0885.

Compound 2y

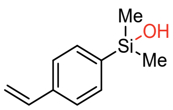

Dimethyl(4-vinylphenyl)silanol

The reaction was conducted for 2 h following **GP A** on 1 mmol scale with **1y**. After purification by flash column chromatography (silica gel, EA/PE = 1:10), the title compound **2y** was obtained in 94% yield (167 mg).

Physical state: colorless oil.

^{1}H NMR (400 MHz, Chloroform-*d*): = 7.53 (d, *J* = 7.9 Hz, 2H), 7.40 (d, *J* = 7.9 Hz, 2H), 6.71 (dd, *J* = 17.6, 10.9 Hz, 1H), 5.78 (d, *J* = 17.6 Hz, 1H), 5.27 (d, *J* = 10.9 Hz, 1H), 2.31 (br s, 1H), 0.37 (s, 6H).

^{13}C NMR (101 MHz, Chloroform-*d*): δ = 138.67, 136.73, 133.30, 125.63, 114.48, -0.04.

HRMS (ESI-TOF): calcd for $C_9H_{11}O_2Si^-$ $[M-H]^-$: 177.0741, found: 177.0746.

Compound 2z

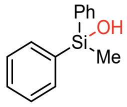

Methyldiphenylsilanol

The reaction was conducted for 0.5 h following **GP A** on 1 mmol scale with **1z**. After dried over anhydrous Na_2SO_4 and evaporated the solvent, the title compound **2z** was obtained in 99% yield (212 mg) without further purification.

Physical state: colorless oil.

^{1}H NMR (400 MHz, Chloroform-*d*): δ = 7.58 (d, *J* = 7.6 Hz, 4H), 7.37 (ddd, *J* = 14.3, 7.6, 2.4 Hz, 6H), 2.56 (br s, 1H), 0.63 (s, 3H).

^{13}C NMR (101 MHz, Chloroform-*d*): δ = 137.16, 134.09, 130.01, 128.04, -1.15.

The characterization data are consistent with that reported in the literature [21].

Compound 2aa

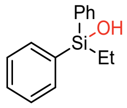

Ethyldiphenylsilanol

The reaction was conducted for 2 h following **GP A** on 1 mmol scale with **1aa**. After dried over anhydrous Na_2SO_4 and evaporated the solvent, the title compound **2aa** was obtained in 98% yield (224 mg) without further purification.

Physical state: colorless oil.

^{1}H NMR (400 MHz, Chloroform-*d*): δ = 7.73 - 7.54 (m, 4H), 7.52 - 7.30 (m, 6H), 2.46 (br s, 1H), 1.22 - 1.02 (m, 5H).

^{13}C NMR (101 MHz, Chloroform-*d*): δ = 136.03, 134.20, 129.80, 127.85, 6.78, 6.62.

The characterization data are consistent with that reported in the literature [52].

Compound 2ab

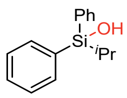

Isopropyldiphenylsilanol

The reaction was conducted for 6 h following **GP A** on 1 mmol scale with **1ab**. After dried over anhydrous Na_2SO_4 and evaporated the solvent, the title compound **2ab** was obtained in 98% yield (237 mg) without further purification.

Physical state: white solid.

^{1}H NMR (400 MHz, Chloroform-*d*): δ = 7.66 (d, *J* = 7.0 Hz, 4H), 7.54 - 7.35 (m, 6H), 2.57 (br s, 1H), 1.61 - 1.39 (m, 1H), 1.13 (d, *J* = 7.4 Hz, 6H).

^{13}C NMR (101 MHz, Chloroform-*d*): δ = 135.23, 134.51, 129.73, 127.78, 17.00, 13.36.

The characterization data are consistent with that reported in the literature [53].

Compound 2ac

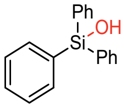

Triphenylsilanol

The reaction was conducted for 2 h following **GP A** on 1 mmol scale with **1ac**. After dried over anhydrous Na_2SO_4 and evaporated the solvent, the title compound **2ac** was obtained in 97% yield (268 mg) without further purification.

Physical state: white solid.

^{1}H NMR (400 MHz, Chloroform-*d*): δ = 7.70 - 7.53 (m, 6H), 7.45 - 7.38 (m, 3H), 7.38 - 7.32 (m, 6H), 2.66 (br s, 1H).

^{13}C NMR (101 MHz, Chloroform-*d*): δ = 135.07, 134.96, 130.08, 127.89.

The characterization data are consistent with that reported in the literature [21].

Compound 2ad

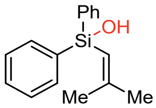

(2-Methylprop-1-en-1-yl)diphenylsilanol

The reaction was conducted for 12 h following **GP A** on 1 mmol scale with **1ad**. After purification by flash column chromatography (silica gel, EA/PE = 1:10), the title compound **2ad** was obtained in 95% yield (242 mg).

Physical state: white solid.

^{1}H NMR (400 MHz, Chloroform-*d*): δ = 7.70 (dd, J = 17.3, 7.0 Hz, 4H), 7.47 - 7.34 (m, 6H), 5.65 (s, 1H), 2.33 (br s, 1H), 2.00 (s, 3H), 1.85 (s, 3H).

^{13}C NMR (101 MHz, Chloroform-*d*): δ = 157.90, 137.10, 134.35, 129.69, 127.85, 119.29, 29.55, 24.19.

The characterization data are consistent with that reported in the literature [28].

Compound 2ae

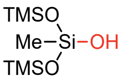

1,1,1,3,5,5,5-heptamethyltrisiloxan-3-ol

The reaction was conducted for 12 h following **GP A** on 10 mmol scale with **1ae** under O_2 atmosphere instead of ambient air. GC analysis showed the yield of title compound **2ae** was 99%. After vacuum distillation (17 Torr, 75-78 °C), 2.05 g (86% yield) **2ac** was obtained.

Physical state: colorless oil.

^{1}H NMR (400 MHz, Chloroform-*d*): δ = 2.08 (br s, 1H), 0.12 (s, 18H), 0.09 (s, 3H).

^{13}C NMR (101 MHz, Chloroform-*d*): δ = 1.60, 1.43.

The characterization data are consistent with that reported in the literature [54].

Compound 2af

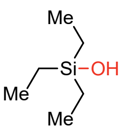

Triethylsilanol

The reaction was conducted for 2 h following **GP A** on 10 mmol scale with **1af**. GC analysis showed the yield of title compound **2af** was 99%. After vacuum distillation (10 Torr, 54-57 ºC), 1.18 g (89% yield) **2ad** was obtained.

Physical state: colorless oil.

^{1}H NMR (400 MHz, Chloroform-*d*): δ = 1.85 (br s, 1H), 1.02 - 0.92 (m, 9H), 0.65 - 0.55 (m, 6H).

^{13}C NMR (101 MHz, Chloroform-*d*): δ = 6.55, 5.74.

The characterization data are consistent with that reported in the literature [21].

Compound 2ag

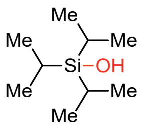

Triisopropylsilanol

The reaction was conducted for 12 h following **GP A** on 10 mmol scale with **1ag** at 60 ºC instead of 30 ºC. GC analysis showed the yield of title compound **2ag** was 97%. After vacuum distillation (0.5 Torr, 42-45 ºC), 1.53 g (88% yield) **2ae** was obtained.

Physical state: colorless oil.

^{1}H NMR (400 MHz, Chloroform-*d*): δ = 1.57 (br s, 1H), 1.08 - 1.00 (m, 21H).

^{13}C NMR (101 MHz, Chloroform-*d*): δ = 17.67, 12.26.

The characterization data are consistent with that reported in the literature [21].

Compound 2ah

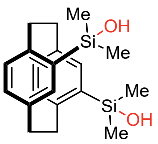

***rac*-4,12-Bis(hydroxydimethylsilyl)[2.2]paracyclophane**

The reaction was conducted for 12 h following **GP A** on 1 mmol scale with **1ah**. After purification by flash column chromatography (silica gel, Et_2O/PE = 1:2), the title compound **2ah** was obtained in 95% yield (338 mg).

Physical state: white solid.

^{1}H NMR (400 MHz, Chloroform-*d*): δ = 6.95 (s, 2H), 6.62 (d, *J* = 7.8 Hz, 2H), 6.55 (d, *J* = 7.7 Hz, 2H), 3.97 (br s, 2H), 3.42 - 3.35 (m, 2H), 3.21 - 3.12 (m, 6H), 0.60 (s, 6H), 0.26 (s, 6H).

^{13}C NMR (101 MHz, Chloroform-*d*): δ = 145.36, 138.01, 137.89, 137.75, 134.57, 133.42, 35.95, 35.52, 2.42, 1.74.

The characterization data are consistent with that reported in the literature [32].

Compound 2ai

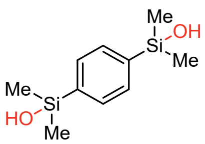

1,4-Phenylenebis(dimethylsilanol)

The reaction was conducted for 4 h following **GP A** on 1 mmol scale with **1ai**. After dried over anhydrous Na_2SO_4 and evaporated the solvent, the title compound **2ai** was obtained in 98% yield (221 mg) without further purification.

Physical state: white solid.

^{1}H NMR (400 MHz, DMSO-*d$_6$*): δ = 7.52 (s, 4H), 5.87 (br s, 2H), 0.23 (s, 12H).

^{13}C NMR (101 MHz, DMSO-*d$_6$*): δ = 141.28, 132.07, 0.57.

The characterization data are consistent with that reported in the literature [21].

Compound 2aj

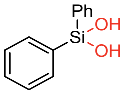

Diphenylsilanediol

The reaction was conducted for 0.25 h following **GP A** on 1 mmol scale with **1aj**. After purification by flash column chromatography (silica gel, EA/PE = 1:2), the title compound **2aj** was obtained in 93% yield (201 mg).

Physical state: white solid.

^{1}H NMR (400 MHz, DMSO-*d$_6$*): δ = 7.59 (dd, *J* = 10.0, 4.9 Hz, 4H), 7.40 - 7.29 (m, 6H), 6.94 (br s, 2H).

^{13}C NMR (101 MHz, DMSO-*d$_6$*): δ = 137.80, 134.07, 129.33, 127.46.

The characterization data are consistent with that reported in the literature [21].

Compound 2ak

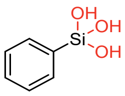

Phenylsilanetriol

The reaction was conducted for 0.5 h following **GP A** on 1 mmol scale with **1ak** using acetone as solvent instead of MeCN. After completion of the reaction, the catalyst was removed by filtration and washed with acetone (3 × 5 mL). The combined organics were dried over anhydrous Na_2SO_4 and solvent was removed by rotary evaporation below 15 °C. The title compound **2ak** was obtained in 96% yield (150 mg) without further purification.

Physical state: white solid.

^{1}H NMR (400 MHz, Acetone-*d$_6$*): δ = 7.75 - 7.68 (m, 2H), 7.39 - 7.28 (m, 3H), 5.81 (br s, 3H).

^{13}C NMR (101 MHz, Acetone-*d$_6$*): δ = 137.01, 135.02, 130.03, 128.05.

The characterization data are consistent with that reported in the literature [55].

Compound 2al

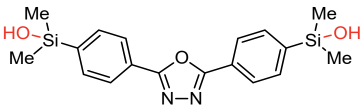

((1,3,4-oxadiazole-2,5-diyl)bis(4,1-phenylene))bis(dimethylsilanol)

The reaction was conducted for 6 h following **GP A** on 1 mmol scale with **1al**. After purification by flash column chromatography (silica gel, CH_2Cl_2), the title compound **2al** was obtained in 93% yield (345 mg).

Physical state: white solid.
^{1}H NMR (400 MHz, Chloroform-*d*): δ = 8.10 (d, *J* = 7.3 Hz, 4H), 7.75 (d, *J* = 7.3 Hz, 4H), 2.39 (br s, 2H), 0.46 (s, 12H).
^{13}C NMR (101 MHz, Chloroform-*d*): δ = 164.63, 144.05, 133.71, 126.05, 124.51, -0.01.
HRMS (ESI-TOF): calcd for $C_{18}H_{21}N_2O_3Si_2^-$ [M-H]$^-$: 369.1085, found: 369.1097.

Compound 2am

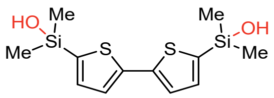

[2,2'-Bithiophene]-5,5'-diylbis(dimethylsilanol)
The reaction was conducted for 12 h following **GP A** on 1 mmol scale with **1am**. After purification by flash column chromatography (silica gel, CH_2Cl_2), the title compound **2am** was obtained in 94% yield (295 mg).
Physical state: white solid.
^{1}H NMR (400 MHz, Chloroform-*d*): δ = 7.28 (d, *J* = 3.3 Hz, 2H), 7.25 (d, *J* = 3.4 Hz, 2H), 2.35 (br s, 2H), 0.49 (s, 12H).
^{13}C NMR (101 MHz, Chloroform-*d*): δ = 142.81, 138.41, 135.45, 125.39, 0.83.
HRMS (ESI-TOF): calcd for $C_{12}H_{17}S_2O_2Si_2^-$ [M-H]$^-$: 313.0203, found: 313.0216.

Compound 2an

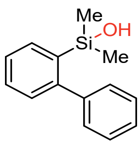

(1,1'-Biphenyl)-2-yldimethylsilanol
The reaction was conducted for 8 h following **GP A** on 1 mmol scale with **1an**. After dried over anhydrous Na_2SO_4 and evaporated the solvent, the title compound **2an** was obtained in 98% yield (224 mg) without further purification.
Physical state: white solid.
^{1}H NMR (400 MHz, Chloroform-*d*): δ = 7.80 (d, *J* = 6.8 Hz, 1H), 7.54 - 7.39 (m, 7H), 7.34 (d, *J* = 7.6 Hz, 1H), 2.55 (br s, 1H), 0.19 (s, 6H).
^{13}C NMR (101 MHz, Chloroform-*d*): δ = 148.35, 144.07, 137.72, 134.20, 129.34, 129.11, 127.95, 127.30, 126.41, 1.45.
The characterization data are consistent with that reported in the literature [27].

Compound 2ao

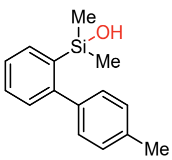

(4'-Methyl-[1,1'-biphenyl]-2-yl)dimethylsilanol
The reaction was conducted for 12 h following **GP A** on 1 mmol scale with **1ao**. After dried over anhydrous Na_2SO_4 and evaporated the solvent, the title compound **2ao** was obtained in 97% yield (236 mg) without further purification.

Physical state: white solid.

^{1}H NMR (400 MHz, Chloroform-*d*): δ = 7.83 (dd, *J* = 7.3, 1.2 Hz, 1H), 7.49 (ddd, *J* = 16.1, 7.3, 1.4 Hz, 2H), 7.36 (dt, *J* = 17.6, 5.0 Hz, 5H), 2.52 (s, 3H), 2.31 (br s, 1H), 0.25 (s, 6H).

^{13}C NMR (101 MHz, Chloroform-*d*): δ = 148.36, 141.19, 137.79, 137.01, 134.11, 129.47, 129.08, 128.97, 128.68, 126.28, 21.13, 1.52.

HRMS (ESI-TOF): calcd for $C_{15}H_{18}OSiNa^+$ $[M+Na]^+$: 265.1019, found: 265.1022.

Compound 2ap

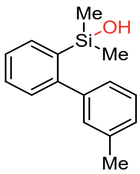

(3'-Methyl-[1,1'-biphenyl]-2-yl)dimethylsilanol

The reaction was conducted for 12 h following **GP A** on 1 mmol scale with **1ap**. After dried over anhydrous Na_2SO_4 and evaporated the solvent, the title compound **2ap** was obtained in 98% yield (237 mg) without further purification.

Physical state: white solid.

^{1}H NMR (400 MHz, Chloroform-*d*): δ = 7.76 (d, *J* = 7.2 Hz, 1H), 7.51 - 7.40 (m, 2H), 7.35 (dd, *J* = 14.3, 7.1 Hz, 2H), 7.23 (dd, *J* = 13.5, 8.7 Hz, 3H), 2.46 (s, 3H), 1.95 (br s, 1H), 0.20 (s, 6H).

^{13}C NMR (101 MHz, Chloroform-*d*): δ = 148.43, 144.99, 137.71, 137.57, 134.11, 129.93, 129.22, 129.04, 128.01, 127.91, 126.34, 126.08, 21.32, 1.53.

HRMS (ESI-TOF): calcd for $C_{15}H_{18}OSiNa^+$ $[M+Na]^+$: 265.1019, found: 265.1018.

Compound 2aq

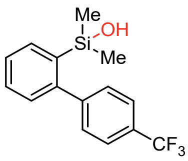

(4'-Trifluoromethyl-[1,1'-biphenyl]-2-yl)dimethylsilanol

The reaction was conducted for 16 h following **GP A** on 1 mmol scale with **1aq**. After dried over anhydrous Na_2SO_4 and evaporated the solvent, the title compound **2aq** was obtained in 97% yield (287 mg) without further purification.

Physical state: white solid.

^{1}H NMR (400 MHz, Chloroform-*d*): δ = 7.80 (d, *J* = 7.0 Hz, 1H), 7.70 (d, *J* = 8.1 Hz, 2H), 7.53 - 7.44 (m, 4H), 7.28 (d, *J* = 8.0 Hz, 1H), 2.35 (br s, 1H), 0.11 (s, 6H).

^{13}C NMR (101 MHz, Chloroform-*d*): δ = 147.73, 146.98, 137.49, 134.54, 129.63, 129.38, 129.33, 127.03, 124.90, 124.86, 124.82, 124.78, 1.42.

^{19}F NMR (376 MHz, Chloroform-*d*): δ = -62.28.

HRMS (ESI-TOF): calcd for $C_{15}H_{15}OF_3SiNa^+$ $[M+Na]^+$: 319.0736, found: 319.0755.

Compound 2ar

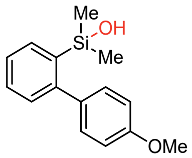

(4'-Methoxy-[1,1'-biphenyl]-2-yl)dimethylsilanol

The reaction was conducted for 14 h following **GP A** on 1 mmol scale with **1ar**. After purification by flash column chromatography (silica gel, EA/PE = 1:10), the title compound **2ar** was obtained in 92% yield (238 mg).

Physical state: white solid.

^{1}H NMR (400 MHz, Chloroform-*d*): δ = 7.75 (d, *J* = 7.2 Hz, 1H), 7.42 (dt, *J* = 23.4, 7.2 Hz, 2H), 7.31 (t, *J* = 8.8 Hz, 3H), 6.99 (d, *J* = 8.4 Hz, 2H), 3.88 (s, 3H), 2.20 (br s, 1H), 0.18 (s, 6H).

^{13}C NMR (101 MHz, Chloroform-*d*): δ = 158.87, 148.04, 137.83, 136.49, 134.19, 130.17, 129.60, 129.09, 126.17, 113.31, 55.18, 1.47.

HRMS (ESI-TOF): calcd for $C_{15}H_{18}O_2SiNa^+$ $[M+Na]^+$: 281.0968, found: 281.0974.

Compound 2as

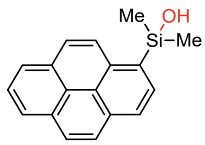

Dimethyl(pyren-1-yl)silanol

The reaction was conducted for 4 h following **GP A** on 1 mmol scale with **1as**. After dried over anhydrous Na_2SO_4 and evaporated the solvent, the title compound **2as** was obtained in 98% yield (271 mg) without further purification.

Physical state: white solid.

^{1}H NMR (400 MHz, Chloroform-*d*): δ = 8.57 (d, *J* = 9.2 Hz, 1H), 8.27 - 8.19 (m, 3H), 8.15 - 8.00 (m, 5H), 2.69 (br s, 1H), 0.72 (s, 6H).

^{13}C NMR (101 MHz, Chloroform-*d*): δ = 135.50, 134.18, 132.42, 131.68, 131.18, 130.57, 128.08, 127.53, 127.39, 125.77, 125.21, 125.13, 124.88, 124.76, 124.51, 124.00, 1.64.

HRMS (ESI-TOF): calcd for $C_{18}H_{15}OSi^-$ $[M-H]^-$: 275.0887, found: 275.0899.

Compound 2at

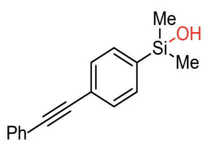

Dimethyl(4-(phenylethynyl)phenyl)silane

The reaction was conducted for 6 h following **GP A** on 1 mmol scale with **1at**. After purification by flash column chromatography (silica gel, EA/PE = 1:10), the title compound **2at** was obtained in 94% yield (237 mg).

Physical state: white solid.

^{1}H NMR (400 MHz, Chloroform-*d*): δ = 7.54 (t, *J* = 6.1 Hz, 6H), 7.33 (s, 3H), 2.28 (br s, 1H), 0.39 (s, 6H).

^{13}C NMR (101 MHz, Chloroform-*d*): δ = 139.38, 132.95, 131.63, 130.82, 128.32, 124.40, 123.17, 90.15,

89.37, -0.08.
HRMS (ESI-TOF): calcd for $C_{16}H_{15}OSi^-$ $[M-H]^-$: 251.0887, found: 251.0896.

Compound 2au

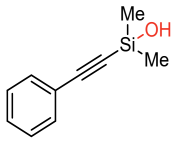

Dimethyl(phenylethynyl)silanol
The reaction was conducted for 0.25 h following **GP A** on 1 mmol scale with **1au**. After purification by flash column chromatography (silica gel, EA/PE = 1:10), the title compound **2au** was obtained in 92% yield (162 mg).
Physical state: colorless oil.
^{1}H NMR (400 MHz, Chloroform-*d*): δ = 7.47 (d, *J* = 6.8 Hz, 2H), 7.36 - 7.23 (m, 3H), 2.35 (br s, 1H), 0.38 (s, 6H).
^{13}C NMR (101 MHz, Chloroform-*d*): δ = 132.03, 128.88, 128.23, 122.42, 104.74, 92.62, 1.50.
The characterization data are consistent with that reported in the literature [21].

Compound 2av

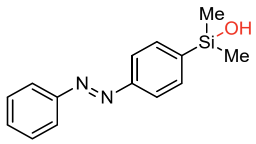

(*E*)-Dimethyl(4-(phenyldiazenyl)phenyl)silanol
The reaction was conducted for 4 h following **GP A** on 1 mmol scale with **1av**. After purification by flash column chromatography (silica gel, EA/PE = 1:10), the title compound **2av** was obtained in 95% yield (243 mg).
Physical state: red oil.
^{1}H NMR (400 MHz, Chloroform-*d*): δ = 7.93 (dd, *J* = 14.4, 7.5 Hz, 4H), 7.74 (d, *J* = 7.6 Hz, 2H), 7.61 - 7.29 (m, 3H), 2.68 (br s, 1H), 0.45 (s, 6H).
^{13}C NMR (101 MHz, Chloroform-*d*): δ = 153.26, 152.61, 142.73, 133.87, 131.10, 129.06, 122.89, 122.02, 0.02.
HRMS (ESI-TOF): calcd for $C_{14}H_{15}NOSi^-$ $[M-H]^-$: 255.0948, found: 255.0957.

Compound 2aw

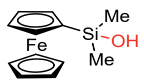

(Hydroxydimethylsilyl)ferrocene
The reaction was conducted for 3 h following **GP A** on 1 mmol scale with **1aw**. After purification by flash column chromatography (silica gel, EA/PE = 1:5), the title compound **2aw** was obtained in 94% yield (244 mg).
Physical state: red soild.
^{1}H NMR (400 MHz, Chloroform-*d*): δ = 4.42 (s, 2H), 4.22 (s, 2H), 4.19 (s, 5H), 1.84 (br s, 1H), 0.39 (s, 6H).

^{13}C NMR (101 MHz, Chloroform-*d*): δ = 73.10, 71.45, 70.50, 68.54, 0.41.
HRMS (ESI-TOF): calcd for $C_{12}H_{15}FeOSi^-$ $[M-H]^-$: 259.0236, found: 259.0242.

Compound 2ax

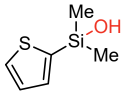

Dimethyl(thiophen-2-yl)silanol
The reaction was conducted for 6 h following **GP A** on 1 mmol scale with **1ax**. After dried over anhydrous Na_2SO_4 and evaporated the solvent, the title compound **2ax** was obtained in 98% yield (155 mg) without further purification.
Physical state: colorless oil.
^{1}H NMR (400 MHz, Chloroform-*d*): δ = 7.62 (dd, *J* = 4.6, 0.8 Hz, 1H), 7.35 (dd, *J* = 3.3, 0.9 Hz, 1H), 7.20 (dd, *J* = 4.6, 3.3 Hz, 1H), 2.65 (br s, 1H), 0.44 (s, 6H).
^{13}C NMR (101 MHz, Chloroform-*d*): δ = 138.53, 134.64, 131.02, 128.15, 0.85.
The characterization data are consistent with that reported in the literature [49].

Compound 2ay

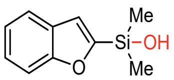

benzofuran-2-yldimethylsilanol
The reaction was conducted for 2 h following **GP A** on 1 mmol scale with **1ay**. After dried over anhydrous Na_2SO_4 and evaporated the solvent, the title compound **2ay** was obtained in 97% yield (186 mg) without further purification.
Physical state: colorless oil.
^{1}H NMR (400 MHz, Chloroform-*d*): δ = 7.62 (d, *J* = 7.6 Hz, 1H), 7.55 (d, *J* = 8.2 Hz, 1H), 7.34 (t, *J* = 7.6 Hz, 1H), 7.26 (t, *J* = 7.4 Hz, 1H), 7.09 (s, 1H), 2.79 (br s, 1H), 0.52 (s, 6H).
^{13}C NMR (101 MHz, Chloroform-*d*): δ = 161.33, 157.84, 127.56, 124.82, 122.47, 121.33, 116.78, 111.41, -0.51.
The characterization data are consistent with that reported in the literature [50].

Compound 2az

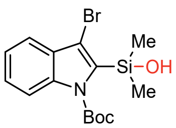

***tert*-Butyl 3-bromo-2-(hydroxydimethylsilyl)-1H-indole-1-carboxylate**
The reaction was conducted for 12 h following **GP A** on 1 mmol scale with **1az**. After dried over anhydrous Na_2SO_4 and evaporated the solvent, the title compound **2az** was obtained in 98% yield (362 mg) without further purification.
Physical state: white solid.
^{1}H NMR (400 MHz, Chloroform-*d*): δ = 7.92 (d, *J* = 8.4 Hz, 1H), 7.56 (dd, *J* = 7.8, 0.5 Hz, 1H), 7.36 (ddd, *J* = 8.5, 7.2, 1.4 Hz, 1H), 7.31 - 7.25 (m, 1H), 3.19 (br s, 1H), 1.71 (s, 9H), 0.57 (s, 6H).
^{13}C NMR (101 MHz, Chloroform-*d*): δ = 151.77, 136.65, 136.06, 130.87, 126.10, 123.27, 120.17, 115.27,

110.61, 85.46, 28.10, 2.28.
HRMS (ESI-TOF): calcd for $C_{10}H_{11}NOSi^{79}Br^-$ [M-Boc]$^-$: 267.9798, found: 267.9792; calcd for $C_{10}H_{11}N$-$OSi^{81}Br^-$ [M-Boc]$^-$: 269.9778, found: 269.9769.

Compound 2ba

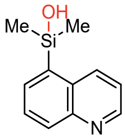

Dimethyl(quinolin-5-yl)silanol
The reaction was conducted for 6 h following **GP A** on 1 mmol scale with **1ba**. After purification by flash column chromatography (silica gel, silica gel, EA/PE = 1:3), the title compound **2ba** was obtained in 93% yield (189 mg).
Physical state: pale yellow solid.
^{1}H NMR (400 MHz, Chloroform-*d*): δ = 8.73 (d, J = 8.4 Hz, 1H), 8.55 (s, 1H), 7.94 (d, J = 8.4 Hz, 1H), 7.75 (d, J = 6.6 Hz, 1H), 7.50 (t, J = 7.5 Hz, 1H), 7.28 - 7.13 (m, 1H), 6.86 (br s, 1H), 0.51 (s, 6H).
^{13}C NMR (101 MHz, Chloroform-*d*): δ = 148.74, 147.31, 139.19, 137.17, 133.52, 131.54, 130.11, 128.67, 120.46, 1.36.
HRMS (ESI-TOF): calcd for $C_{11}H_{12}NOSi^-$ [M-H]$^-$: 202.0683, found: 202.0695.

Compound 2bb

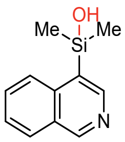

Isoquinolin-4-yldimethylsilanol
The reaction was conducted for 5 h following **GP A** on 1 mmol scale with **1bb**. After purification by flash column chromatography (silica gel, EA/PE = 1:1), the title compound **2bb** was obtained in 92% yield (186 mg).
Physical state: pale yellow viscous oil.
^{1}H NMR (400 MHz, Chloroform-*d*): δ = 9.02 (s, 1H), 8.49 (s, 1H), 8.30 (d, J = 8.4 Hz, 1H), 7.85 (d, J = 8.0 Hz, 1H), 7.77 - 7.65 (m, 1H), 7.57 (t, J = 7.2 Hz, 1H), 5.63 (br s, 1H), 0.54 (s, 6H).
^{13}C NMR (101 MHz, Chloroform-*d*): δ = 153.54, 147.24, 139.20, 130.62, 129.96, 128.64, 127.92, 127.32, 126.96, 1.19.
HRMS (ESI-TOF): calcd for $C_{11}H_{12}NOSi^-$ [M-H]$^-$: 202.0683, found: 202.0689.

Compound 2bc

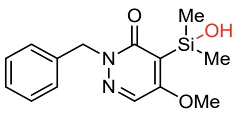

2-Benzyl-4-(hydroxydimethylsilyl)-5-methoxypyridazin-3(2*H*)-one
The reaction was conducted for 6 h following **GP A** on 1 mmol scale with **1bc**. After purification by flash column chromatography (silica gel, EA/PE = 1:2 to 2:1), the title compound **2bc** was obtained in 91% yield (263 mg).

Physical state: white solid.

***2bn** was found by NMR spectroscopy to exist as a pair of isomers (A and B) in a 55:45 ratio due to the tautomerism of amide bond (the major tautomer is represented by A).*

^{1}H NMR (400 MHz, Chloroform-*d*): δ = 7.82 (s, 1H_A), 7.48 (s, 1H_B), 7.43 - 7.39 (m, 2$H_{A/B}$), 7.35 - 7.28 (m, 3$H_{A/B}$), 5.30 (s, 2H_A), 5.23 (s, 2H_B), 5.05 (br s, 1$H_{A/B}$), 3.93 (s, 3H_A), 3.70 (s, 1H_B), 0.36 (s, 6H_A), 0.36 (s, 6H_B).

^{13}C NMR (101 MHz, Chloroform-*d*): δ = 165.64(B), 163.92, 136.67(B), 136.17(A), 128.81(B), 128.60, 128.45(A), 127.91(B), 127.73(A), 126.85(A), 126.40(B), 118.01(A), 117.27(B), 56.58(B), 56.20(A), 54.96(A), 54.63(B), 2.19(A), 0.97(B).

HRMS (ESI-TOF): calcd for $C_{14}H_{19}N_2O_3Si^+$ $[M+H]^+$: 291.1159, found: 291.1141.

Compound 2bd

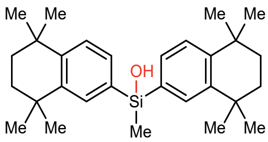

Methylbis(5,5,8,8-tetramethyl-5,6,7,8-tetrahydronaphthalen-2-yl)silanol

The reaction was conducted for 18 h following **GP A** on 1 mmol scale with **1bd**. After purification by flash column chromatography (silica gel, EA/PE = 1:5), the title compound **2bd** was obtained in 90% yield (390 mg).

Physical state: white solid.

^{1}H NMR (400 MHz, Chloroform-*d*): δ 7.60 (s, 2H), 7.39 (d, *J* = 7.7 Hz, 2H), 7.34 (d, *J* = 7.5 Hz, 2H), 2.04 (br s, 1H), 1.71 (s, 8H), 1.30 (d, *J* = 5.0 Hz, 24H), 0.67 (s, 3H).

^{13}C NMR (101 MHz, Chloroform-*d*): δ = 146.59, 144.09, 133.71, 132.39, 131.03, 125.97, 35.14, 34.97, 34.30, 34.17, 31.87, 31.74, -1.09.

The characterization data are consistent with that reported in the literature [41].

Compound 2be

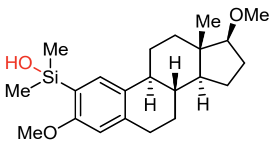

((8R,9S,13S,14S,17S)-3,17-dimethoxy-13-methyl-7,8,9,11,12,13,14,15,16,17-decahydro-6H-cyclopenta[a]phenanthren-2-yl)dimethylsilanol

The reaction was conducted for 12 h following **GP A** on 1 mmol scale with **1be** in 5 mL MeCN. After purification by flash column chromatography (silica gel, CH_2Cl_2/PE = 1:2), the title compound **2be** was obtained in 91% yield (340 mg).

Physical state: white solid.

^{1}H NMR (400 MHz, Chloroform-*d*): δ = 7.36 (s, 1H), 6.59 (s, 1H), 3.82 (s, 3H), 3.39 (s, 3H), 3.33 (t, *J* = 8.4 Hz, 1H), 2.94 - 2.82 (m, 2H), 2.38 - 2.17 (m, 3H), 2.12 - 2.01 (m, 2H), 1.94 - 1.84 (m, 1H), 1.76 - 1.64 (m, 1H), 1.54 - 1.24 (m, 7H), 0.80 (s, 3H), 0.39 (s, 6H).

^{13}C NMR (101 MHz, Chloroform-*d*): δ = 161.78, 140.16, 131.59, 126.29, 113.75, 109.99, 90.76, 57.85, 55.19, 50.23, 43.94, 43.21, 38.69, 38.02, 30.19, 27.72, 27.12, 26.44, 23.02, 11.52, 0.49, 0.44.

HRMS (ESI-TOF): calcd for $C_{22}H_{34}O_3Si^+$ $[M+H]^+$: 375.2350, found: 375.2333.

Compound 2bf

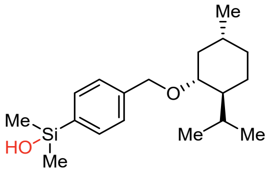

(4-((((1R,2S,5R)-2-Isopropyl-5-methylcyclohexyl)oxy)methyl)phenyl)dimethylsilanol

The reaction was conducted for 8 h following **GP A** on 1 mmol scale with **1bf**. After purification by flash column chromatography (silica gel, EA/PE = 1:5), the title compound **2bf** was obtained in 94% yield (302 mg).

Physical state: viscous oil.

^{1}H NMR (400 MHz, Chloroform-*d*): δ = 7.59 (d, *J* = 7.9 Hz, 2H), 7.39 (d, *J* = 7.8 Hz, 2H), 4.69 (d, *J* = 11.6 Hz, 1H), 4.43 (d, *J* = 11.6 Hz, 1H), 3.20 (td, *J* = 10.5, 4.1 Hz, 1H), 2.33 (dtd, *J* = 14.0, 6.9, 2.5 Hz, 1H), 2.22 (d, *J* = 11.0 Hz, 1H), 2.07 (br s, 1H), 1.74 - 1.62 (m, 2H), 1.43 - 1.28 (m, 2H), 0.95 (dd, *J* = 15.7, 6.8 Hz, 9H), 0.75 (d, *J* = 6.9 Hz, 3H), 0.41 (s, 6H).

^{13}C NMR (101 MHz, Chloroform-*d*): δ = 140.61, 138.06, 133.07, 127.22, 78.90, 70.27, 48.29, 40.27, 34.55, 31.55, 25.50, 23.23, 22.35, 21.00, 16.05, 0.01.

HRMS (ESI-TOF): calcd for $C_{19}H_{31}O_2Si^-$ $[M-H]^-$: 319.2088, found: 319.2096.

Compound 2bg

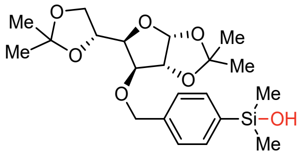

(4-((((3aR,5R,6S,6aR)-5-((R)-2,2-dimethyl-1,3-dioxolan-4-yl)-2,2-dimethyltetrahydrofuro[2,3-d][1,3]dioxol-6-yl)oxy)methyl)phenyl)dimethylsilanol

The reaction was conducted for 6 h following **GP A** on 1 mmol scale with **1bg**. After purification by flash column chromatography (silica gel, EA/PE = 1:3), the title compound **2bg** was obtained in 92% yield (390 mg)..

Physical state: white solid.

^{1}H NMR (400 MHz, Chloroform-*d*): δ = 7.58 (d, *J* = 7.9 Hz, 2H), 7.36 (d, *J* = 7.8 Hz, 2H), 5.89 (d, *J* = 3.6 Hz, 1H), 4.66 (q, *J* = 12.0 Hz, 2H), 4.59 (d, *J* = 3.7 Hz, 1H), 4.36 (dd, *J* = 13.6, 6.1 Hz, 1H), 4.12 (ddd, *J* = 14.8, 8.1, 4.6 Hz, 2H), 4.04 - 3.93 (m, 2H), 2.21 (br s, 1H), 1.49 (s, 3H), 1.42 (s, 3H), 1.37 (s, 3H), 1.31 (s, 3H), 0.39 (s, 6H).

^{13}C NMR (101 MHz, Chloroform-*d*): δ = 139.01, 138.76, 133.16, 127.02, 111.78, 108.97, 105.25, 82.60, 81.72, 81.28, 72.48, 72.21, 67.35, 26.80, 26.74, 26.21, 25.41, 0.02.

HRMS (ESI-TOF): calcd for $C_{21}H_{31}O_7Si^-$ $[M-H]^-$: 423.1834, found: 423.1824.

Compound 2bh

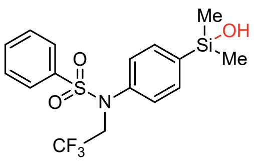

N-(4-(Hydroxydimethylsilyl)phenyl)-N-(2,2,2-trifluoroethyl)benzenesulfonamide

The reaction was conducted for 6 h following **GP A** on 1 mmol scale with **1bh**. After purification by flash column chromatography (silica gel, EA/PE = 1:2), the title compound **2bh** was obtained in 95% yield (368 mg).

Physical state: white solid.

^{1}H NMR (400 MHz, Chloroform-*d*): δ = 7.62 (d, *J* = 7.3 Hz, 3H), 7.54 (d, *J* = 7.7 Hz, 2H), 7.48 (t, *J* = 7.4 Hz, 2H), 7.06 (d, *J* = 7.7 Hz, 2H), 4.23 (q, *J* = 8.2 Hz, 2H), 2.59 (br s, 1H), 0.38 (s, 6H).

^{13}C NMR (101 MHz, Chloroform-*d*): δ = 140.44, 140.00, 138.18, 134.15, 133.28, 128.99, 128.36, 127.66, 125.05, 122.26, 52.56, 52.22, 51.87, 51.52, -0.07.

^{19}F NMR (376 MHz, Chloroform-*d*): δ = -70.47 (t).

HRMS (ESI-TOF): calcd for $C_{16}H_{17}F_3NSO_3Si^-$ $[M-H]^-$: 388.0645, found: 388.0658.

Compound 2bi

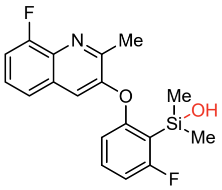

(2-Fluoro-6-((8-fluoro-2-methylquinolin-3-yl)oxy)phenyl)dimethylsilanol

The reaction was conducted for 6 h following **GP A** on 1 mmol scale with **1bi**. After purification by flash column chromatography (silica gel, EA/PE = 1:2), the title compound **2bi** was obtained in 91% yield (315 mg).

Physical state: white solid.

^{1}H NMR (400 MHz, Chloroform-*d*): δ = 7.47 (s, 1H), 7.44 - 7.37 (m, 2H), 7.37 - 7.28 (m, 2H), 6.88 (t, *J* = 8.4 Hz, 1H), 6.55 (d, *J* = 8.1 Hz, 1H), 2.77 (s, 3H), 2.71 (br s, 1H), 0.49 (d, *J* = 1.3 Hz, 6H).

Note: Due to an issue with rotational isomers, the ^{13}C NMR spectrum is complex.

^{13}C NMR (101 MHz, Chloroform-*d*): δ = 168.67, 166.26, 161.26, 161.11, 158.86, 156.31, 154.16, 150.21, 132.61, 132.51, 129.82, 126.57, 126.49, 122.40, 122.36, 120.78, 113.12, 112.60, 112.41, 111.38, 111.11, 20.75, 1.90.

^{19}F NMR (376 MHz, Chloroform-*d*): δ = -99.10, -125.27 (d).

HRMS (APCI-TOF): calcd for $C_{18}H_{18}F_2NO_2Si^+$ $[M+H]^+$: 346.1069, found: 346.1074.

Compound 2bj

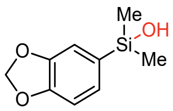

1,3-Benzodioxol-5-yl(dimethyl)silanol

The reaction was conducted for 3 h following **GP A** on 1 mmol scale with **1bj**. After dried over anhydrous Na_2SO_4 and evaporated the solvent, the title compound **2bj** was obtained in 97% yield (190 mg) without further purification.

Physical state: colorless oil.

^{1}H NMR (400 MHz, Chloroform-*d*): δ = 7.19 - 6.96 (m, 2H), 6.87 (d, *J* = 7.5 Hz, 1H), 5.95 (s, 2H), 3.05 (br s, 1H), 0.37 (s, 6H).

^{13}C NMR (101 MHz, Chloroform-*d*): δ = 148.70, 147.31, 132.29, 127.21, 112.45, 108.54, 100.48, 0.01.

The characterization data are consistent with that reported in the literature [46].

Compound 2bk

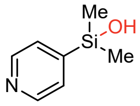

Dimethyl(pyridin-4-yl)silanol

The reaction was conducted for 4 h following **GP A** on 1 mmol scale with **1bk**. After dried over anhydrous Na_2SO_4 and evaporated the solvent, the title compound **2bk** was obtained in 93% yield (142 mg) without further purification.

*Note: **2bi** is unstable and dimerize slowly during storage.*

Physical state: turbid oil.

^{1}H NMR (400 MHz, Chloroform-*d*): δ = 8.57 (d, J = 5.5 Hz, 2H), 7.38 (dd, J = 4.3, 1.3 Hz, 2H), 2.35 (br s, 1H), 0.37 (s, 6H).

^{13}C NMR (101 MHz, Chloroform-*d*): δ = 148.84, 127.67, 0.43.

The characterization data are consistent with that reported in the literature [56].

Compound 2bl

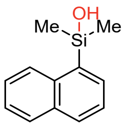

Dimethyl(naphthalen-1-yl)silanol

The reaction was conducted for 3 h following **GP A** on 1 mmol scale with **1bl**. After dried over anhydrous Na_2SO_4 and evaporated the solvent, the title compound **2bl** was obtained in 98% yield (198 mg) without further purification.

Physical state: white solid.

^{1}H NMR (400 MHz, Chloroform-*d*): δ = 8.25 (d, J = 7.8 Hz, 1H), 7.86 (t, J = 7.7 Hz, 2H), 7.74 (d, J = 6.7 Hz, 1H), 7.53 - 7.40 (m, 3H), 2.25 (br s, 1H), 0.55 (s, 6H).

^{13}C NMR (101 MHz, Chloroform-*d*): δ = 136.90, 136.56, 133.36, 133.22, 130.38, 128.99, 128.09, 126.00, 125.50, 125.00, 1.31.

The characterization data are consistent with that reported in the literature [21].

Compound 2bm

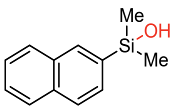

Dimethyl(naphthalen-2-yl)silanol

The reaction was conducted for 1 h following **GP A** on 1 mmol scale with **1bm**. After dried over anhydrous Na_2SO_4 and evaporated the solvent, the title compound **2bm** was obtained in 97% yield (196 mg) without further purification.

Physical state: white solid.

^{1}H NMR (400 MHz, Chloroform-*d*): δ = 8.03 (s, 1H), 7.77 (dd, J = 9.5, 5.5 Hz, 3H), 7.59 (d, J = 8.1 Hz, 1H), 7.51 - 7.39 (m, 2H), 3.00 (br s, 1H), 0.41 (s, 6H).

^{13}C NMR (101 MHz, Chloroform-*d*): δ = 136.46, 133.92, 133.83, 132.77, 129.15, 128.17, 127.66, 127.11, 126.48, 125.92, 0.02.

The characterization data are consistent with that reported in the literature [21].

Compound 2bn

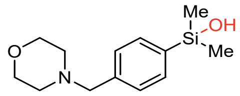

Dimethyl(4-(morpholinomethyl)phenyl)silanol

The reaction was conducted for 6 h following **GP A** on 1 mmol scale with **1bn**. After purification by flash column chromatography (silica gel, EA/PE = 1:3), the title compound **2bn** was obtained in 95% yield (238 mg).

Physical state: white solid.

^{1}H NMR (400 MHz, Chloroform-*d*): δ = 7.56 (d, *J* = 7.5 Hz, 2H), 7.35 (d, *J* = 7.6 Hz, 2H), 3.70 (t, *J* = 4.6 Hz, 4H), 3.51 (br s, 2H), 2.45 (t, *J* = 4.7 Hz, 4H), 0.41 (s, 6H).

^{13}C NMR (101 MHz, Chloroform-*d*): δ = 138.92, 138.09, 133.09, 128.77, 66.84, 63.33, 53.51, 0.04.

HRMS (ESI-TOF): calcd for $C_{13}H_{20}NO_2Si^-$ $[M-H]^-$: 250.1258, found: 250.1279.

Compound 2bo

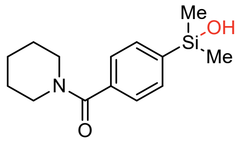

(4-(Hydroxydimethylsilyl)phenyl)(piperidin-1-yl)methanone

The reaction was conducted for 5 h following **GP A** on 1 mmol scale with **1bo**. After purification by flash column chromatography (silica gel, EA/PE = 1:1), the title compound **2bo** was obtained in 96% yield (225 mg).

Physical state: yellow solid.

***2bn** was found by NMR spectroscopy to exist as a pair of isomers (A and B) in a 70:30 ratio due to the tautomerism of amide bond (the major tautomer is represented by A).*

^{1}H NMR (400 MHz, Chloroform-*d*): δ = 7.57 (d, *J* = 4.4 Hz, $2H_B$), 7.56 (d, *J* = 4.6 Hz, $2H_A$), 7.36 (d, *J* = 8.0 Hz, 2 H_A), 7.33 (d, *J* = 7.9 Hz, 2 H_B), 3.71 (br s, $4H_{A/B}$), 3.34 (br s, $4H_{A/B}$), 2.67 (s, 1 H_A), 1.68 (br s, 4H), 1.52 (br s, $2H_{A/B}$), 1.26 (br s, 1 H_B), 0.35 (s, 6 H_B), 0.35 (s, 6 H_A).

^{13}C NMR (101 MHz, Chloroform-*d*): δ =170.34(B), 170.25(A), 141.34(B), 141.18(A), 137.17(A), 137.04(B), 133.05(B), 132.95(A), 125.91(A), 125.85(B), 48.68, 43.05, 26.48, 25.56, 24.52, 0.77(A), -0.03(B).

HRMS (ESI-TOF): calcd for $C_{14}H_{20}NO_2Si^-$ $[M-H]^-$: 262.1258, found: 262.1268.

Compound 2bp

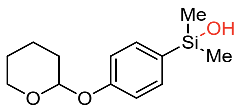

Dimethyl(4-((tetrahydro-2H-pyran-2-yl)oxy)phenyl)silanol

The reaction was conducted for 3 h following **GP A** on 1 mmol scale with **1bp**. After dried over anhydrous Na_2SO_4 and evaporated the solvent, the title compound **2bp** was obtained in 97% yield (244 mg) without further purification.

Physical state: colorless oil.

^{1}H NMR (400 MHz, Chloroform-*d*): δ = 7.53 (d, *J* = 8.5 Hz, 2H), 7.09 (d, *J* = 8.5 Hz, 2H), 5.49 (t, *J* = 2.8 Hz, 1H), 3.96 - 3.87 (m, 1H), 3.71 - 3.54 (m, 1H), 2.29 (br s, 1H), 2.04 (dt, *J* = 16.4, 7.9 Hz, 1H), 1.89 (dt, *J* = 7.5, 3.7 Hz, 2H), 1.76 - 1.61 (m, 3H), 0.40 (s, 6H).

^{13}C NMR (101 MHz, Chloroform-*d*): δ = 158.28, 134.52, 115.95, 95.93, 61.96, 30.25, 25.15, 18.65, 0.04.

HRMS (ESI-TOF): calcd for $C_{13}H_{19}O_3Si^-$ $[M-H]^-$: 251.1098, found: 251.1093.

Compound 2bq

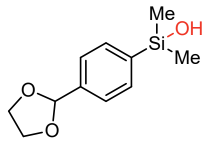

(4-(1,3-Dioxolan-2-yl)phenyl)dimethylsilanol

The reaction was conducted for 4 h following **GP A** on 1 mmol scale with **1bq**. After purification by flash column chromatography (silica gel, EA:PE = 1:3), the title compound **2bq** was obtained in 94% yield (210 mg).

Physical state: colorless oil.

^{1}H NMR (400 MHz, Chloroform-*d*): δ = 7.55 (d, *J* = 8.0 Hz, 2H), 7.43 (d, *J* = 7.9 Hz, 2H), 5.78 (s, 1H), 4.11 - 3.96 (m, 4H), 3.05 (br s, 1H), 0.32 (s, 6H).

^{13}C NMR (101 MHz, Chloroform-*d*): δ = 140.49, 138.81, 133.03, 125.69, 103.53, 65.16, -0.12.

The characterization data are consistent with that reported in the literature [50].

Compound 2br

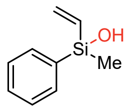

Methyl(phenyl)(vinyl)silanol

The reaction was conducted for 4 h following **GP A** on 1 mmol scale with **1br**. After dried over anhydrous Na_2SO_4 and evaporated the solvent, the title compound **2br** was obtained in 97% yield (160 mg) without further purification.

Physical state: colorless oil.

^{1}H NMR (400 MHz, Chloroform-*d*): δ = 7.64 (dd, *J* = 7.4, 1.7 Hz, 2H), 7.49 - 7.36 (m, 3H), 6.34 (dd, *J* = 20.2, 14.9 Hz, 1H), 6.17 (dd, *J* = 14.9, 3.8 Hz, 1H), 5.92 (dd, *J* = 20.2, 3.9 Hz, 1H), 2.35 (br s, 1H), 0.51 (s, 3H).

^{13}C NMR (101 MHz, Chloroform-*d*): δ = 137.20, 136.50, 134.54, 133.59, 129.80, 127.88, -1.75.

The characterization data are consistent with that reported in the literature [21].

Compound 2bs

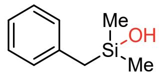

Benzyldimethylsilanol

The reaction was conducted for 4 h following **GP A** on 1 mmol scale with **1bs**. After dried over anhydrous Na_2SO_4 and evaporated the solvent, the title compound **2bs** was obtained in 98% yield (163 mg) without further purification.

Physical state: colorless oil.

^{1}H NMR (400 MHz, Chloroform-*d*): δ = 7.25 (t, *J* = 7.5 Hz, 2H), 7.10 (dd, *J* = 17.8, 7.5 Hz, 3H), 2.19 (s, 2H), 1.91 (br s, 1H), 0.15 (s, 6H).

^{13}C NMR (101 MHz, Chloroform-*d*): δ = 138.98, 128.38, 128.14, 124.25, 28.00, -0.76.

The characterization data are consistent with that reported in the literature [21].

Compound 2bt

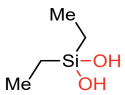

Diethylsilanediol

The reaction was conducted for 2 h following **GP A** on 1 mmol scale with **1bt**. After dried over anhydrous Na_2SO_4 and evaporated the solvent, the title compound **2bt** was obtained in 96% yield (115 mg) without further purification.

Physical state: white solid.

^{1}H NMR (400 MHz, Chloroform-*d*): δ = 3.61 (br s, 2H), 1.05 - 0.88 (m, 6H), 0.71 - 0.44 (m, 4H).

^{13}C NMR (101 MHz, Chloroform-*d*): δ = 6.61, 6.38.

The characterization data are consistent with that reported in the literature [21].

General procedure for Co-N_4@NPC-catalyzed multicomponent synthesis of borosiloxanes (GP B)

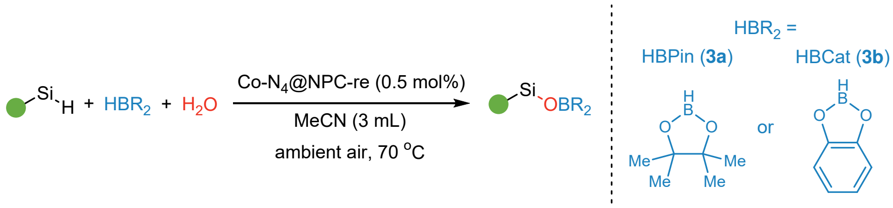

Silane (1mmol), borane (1 mmol) and water (1 mmol) were mixed with MeCN (3mL) in a 10 mL oven-dried round-bottom flask with reflux condenser and steady magnetic stirring (800 rpm) at 30 °C under an ambient atmosphere of air. Then catalyst Co-N_4@NPC-re (0.5 mol% Co) was added and the mixture was heat at 70 °C for given reaction time. After completion of the reaction (monitored by GC), the catalyst was removed by filtration and washed with EA (3 × 5 mL). The combined organics were washed with brine, dried over anhydrous Na_2SO_4 and solvent was removed under reduced pressure. Correspond borosiloxane was obtained without further purification.

Compound 4a

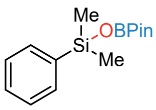

Dimethyl(phenyl)((4,4,5,5-tetramethyl-1,3,2-dioxaborolan-2-yl)oxy)silane

The reaction was conducted for 6 h following **GP B** on 1 mmol scale with **1a** and **3a**. After dried over anhydrous Na_2SO_4 and evaporated the solvent, the title compound **4a** was obtained in 97% yield (269 mg) without further purification.

Physical state: colorless oil.

^{1}H NMR (400 MHz, Chloroform-*d*): δ = 7.67 - 7.59 (m, 2H), 7.38 (tdd, *J* = 3.8, 1.4, 0.7 Hz, 3H), 1.24 (s, 12H), 0.45 (s, 6H).

^{13}C NMR (101 MHz, Chloroform-*d*): δ = 138.15, 133.11, 129.47, 127.64, 82.21, 24.52, -0.27.

The characterization data are consistent with that reported in the literature [57].

Compound 4b

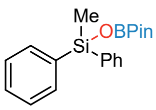

Methyldiphenyl((4,4,5,5-tetramethyl-1,3,2-dioxaborolan-2-yl)oxy)silane

The reaction was conducted for 6 h following **GP B** on 1 mmol scale with **1x** and **3a**. After dried over anhydrous Na_2SO_4 and evaporated the solvent, the title compound **4b** was obtained in 98% yield (334 mg) without further purification.

Physical state: colorless oil.

^{1}H NMR (400 MHz, Chloroform-*d*): δ = 7.68 - 7.61 (m, 4H), 7.43 - 7.32 (m, 6H), 1.23 (s, 12H), 0.74 (s, 3H).

^{13}C NMR (101 MHz, Chloroform-*d*): δ = 136.29, 133.97, 129.67, 127.61, 82.34, 24.45, -1.59.

The characterization data are consistent with that reported in the literature [57].

Compound 4c

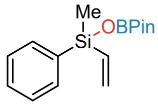

Methyl(phenyl)((4,4,5,5-tetramethyl-1,3,2-dioxaborolan-2-yl)oxy)(vinyl)silane

The reaction was conducted for 8 h following **GP B** on 1 mmol scale with **1bq** and **3a**. After dried over anhydrous Na_2SO_4 and evaporated the solvent, the title compound **4c** was obtained in 98% yield (284 mg) without further purification.

Physical state: colorless oil.

^{1}H NMR (400 MHz, Chloroform-*d*): δ = 7.64 (dd, *J* = 7.3, 1.5 Hz, 2H), 7.44 - 7.34 (m, 3H), 6.32 (dd, *J* = 20.3, 14.9 Hz, 1H), 6.13 (dd, *J* = 14.9, 3.8 Hz, 1H), 5.90 (dd, *J* = 20.3, 3.8 Hz, 1H), 1.25 (s, 12H), 0.53 (s, 3H).

^{13}C NMR (101 MHz, Chloroform-*d*): δ = 136.40, 135.82, 134.49, 133.70, 129.68, 127.67, 82.36, 24.54, -2.02.

The characterization data are consistent with that reported in the literature [57].

Compound 4d

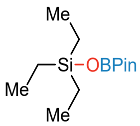

Triethyl((4,4,5,5-tetramethyl-1,3,2-dioxaborolan-2-yl)oxy)silane

The reaction was conducted for 12 h following **GP B** on 1 mmol scale with **1ad** and **3a**. After dried over anhydrous Na_2SO_4 and evaporated the solvent, the title compound **4d** was obtained in 94% yield (243 mg) without further purification.

Physical state: colorless oil.

^{1}H NMR (400 MHz, Chloroform-*d*): δ = 1.23 (s, 12H), 0.95 (t, *J* = 7.9 Hz, 9H), 0.63 (q, *J* = 7.9 Hz, 6H).

^{13}C NMR (101 MHz, Chloroform-*d*): δ = 81.94, 24.53, 6.44, 5.38.

The characterization data are consistent with that reported in the literature [57].

Compound 4e

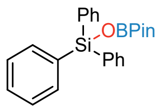

Triphenyl((4,4,5,5-tetramethyl-1,3,2-dioxaborolan-2-yl)oxy)silane

The reaction was conducted for 6 h following **GP B** on 1 mmol scale with **1aa** and **3a**. After dried over anhydrous Na_2SO_4 and evaporated the solvent, the title compound **4e** was obtained in 98% yield (394 mg) without further purification.

Physical state: white solid.

^{1}H NMR (400 MHz, Chloroform-*d*): δ = 7.67 (d, *J* = 6.8 Hz, 6H), 7.41 (dt, *J* = 24.6, 6.9 Hz, 9H), 1.21 (s, 12H).

^{13}C NMR (101 MHz, Chloroform-*d*): δ = 135.22, 134.51, 130.00, 127.68, 82.56, 24.51.

The characterization data are consistent with that reported in the literature [57].

Compound 4f

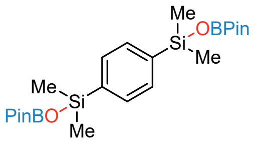

1,4-Bis(dimethyl((4,4,5,5-tetramethyl-1,3,2-dioxaborolan-2-yl)oxy)silyl)benzene

The reaction was conducted for 8 h following **GP B** on 1 mmol scale with **1ag** and 2 mmol **3a** instead of 1 mmol. After dried over anhydrous Na_2SO_4 and evaporated the solvent, the title compound **4f** was obtained in 96% yield (457 mg) without further purification.

Physical state: colorless oil.

^{1}H NMR (400 MHz, Chloroform-*d*): δ = 7.64 - 7.59 (m, 4H), 1.23 (s, 24H), 0.43 (s, 12H).

^{13}C NMR (101 MHz, Chloroform-*d*): δ = 139.47, 132.27, 82.20, 24.52, -0.28.

HRMS (ESI-TOF): calcd for $C_{22}H_{40}B_2O_6Si_2^+$ $[M]^+$: 478.2544, found: 478.2538.

Compound 4g

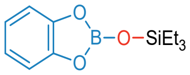

(Benzo[d][1,3,2]dioxaborol-2-yloxy)triethylsilane

The reaction was conducted for 12 h following **GP B** on 1 mmol scale with **1ad** and **3b**. After dried over anhydrous Na_2SO_4 and evaporated the solvent, the title compound **4g** was obtained in 96% yield (240 mg) without further purification.

Physical state: colorless oil.

^{1}H NMR (400 MHz, Chloroform-*d*): δ = 7.12 - 7.06 (m, 2H), 7.04 - 6.97 (m, 2H), 1.04 (t, J = 7.9 Hz, 9H), 0.77 (q, J = 7.9 Hz, 6H).

^{13}C NMR (101 MHz, Chloroform-*d*): δ = 148.29, 122.00, 111.80, 6.37, 5.34.

The characterization data are consistent with that reported in the literature [58].

Compound 4h

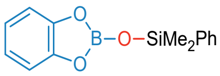

(Benzo[d][1,3,2]dioxaborol-2-yloxy)dimethyl(phenyl)silane

The reaction was conducted for 12 h following **GP B** on 1 mmol scale with **1a** and **3b**. After dried over anhydrous Na_2SO_4 and evaporated the solvent, the title compound **4h** was obtained in 98% yield (264 mg) without further purification.

Physical state: colorless oil.

^{1}H NMR (400 MHz, Chloroform-*d*): δ = 7.74 - 7.61 (m, 2H), 7.42 (d, J = 1.4 Hz, 3H), 7.12 - 7.05 (m, 2H), 7.03 - 6.95 (m, 2H), 0.58 (d, J = 3.1 Hz, 6H).

^{13}C NMR (101 MHz, Chloroform-*d*): δ = 148.00, 136.88, 133.11, 130.04, 127.97, 122.11, 111.90, -0.37.

HRMS (ESI-TOF): calcd for $C_{14}H_{15}BO_3Si^+$ $[M]^+$: 270.0878, found: 270.0869.

Compound 4i

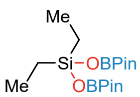

Diethylbis((4,4,5,5-tetramethyl-1,3,2-dioxaborolan-2-yl)oxy)silane

The reaction was conducted for 12 h following **GP B** on 1 mmol scale with **1bs** and 2 mmol **3a** instead of 1 mmol. After dried over anhydrous Na_2SO_4 and evaporated the solvent, the title compound **4i** was obtained in 95% yield (353 mg) without further purification.

Physical state: colorless oil.

^{1}H NMR (400 MHz, Chloroform-*d*): δ = 1.23 (s, 24H), 0.97 (t, *J* = 7.7 Hz, 6H), 0.68 (dd, *J* = 15.9, 8.0 Hz, 4H).

^{13}C NMR (101 MHz, Chloroform-*d*): δ = 82.20, 24.56, 5.95, 5.87.

The characterization data are consistent with that reported in the literature [57].

Compound 4j

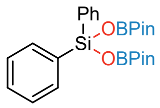

Diphenylbis((4,4,5,5-tetramethyl-1,3,2-dioxaborolan-2-yl)oxy)silane

The reaction was conducted for 8 h following **GP B** on 1 mmol scale with **1ah** and 2 mmol **3a** instead of 1 mmol. After dried over anhydrous Na_2SO_4 and evaporated the solvent, the title compound **4j** was obtained in 98% yield (458 mg) without further purification.

Physical state: colorless oil.

^{1}H NMR (400 MHz, Chloroform-*d*): δ = 7.76 - 7.70 (m, 4H), 7.42 - 7.30 (m, 6H), 1.23 (s, 24H).

^{13}C NMR (101 MHz, Chloroform-*d*): δ = 134.47, 133.17, 130.23, 127.51, 82.54, 24.49.

The characterization data are consistent with that reported in the literature [58].

General procedure for Co-N$_4$@NPC-catalyzed oxidative cross-coupling of hydrosilanes and alcohols in batch reactors

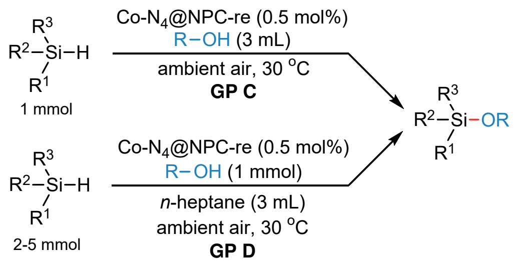

-List of alcohol substrates

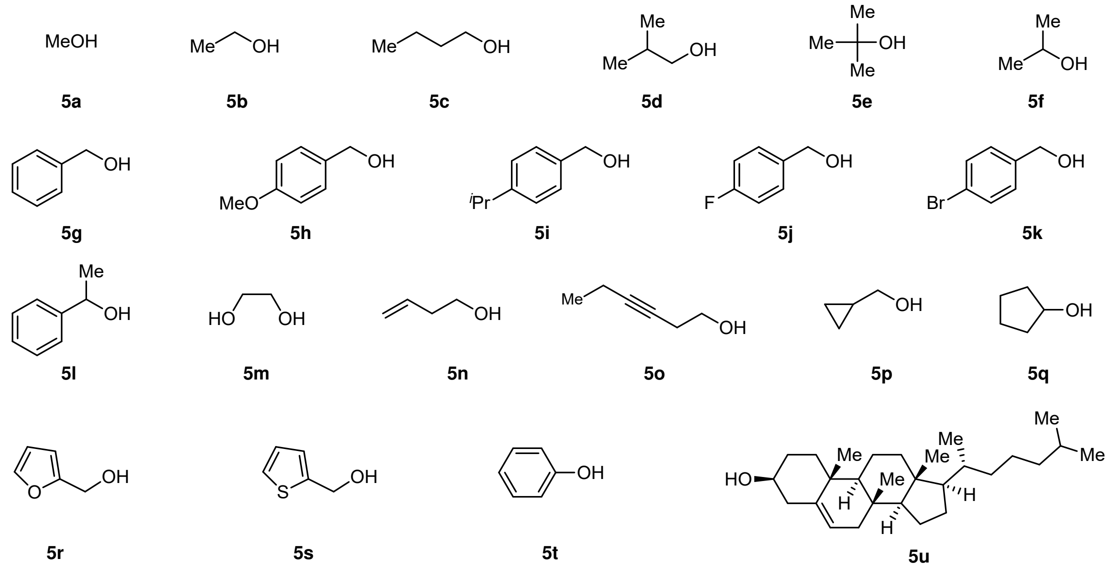

Oxidative cross-coupling of hydrosilanes with simple alkyl alcohols (GP C)

Silane (1 mmol) and anhydrous alcohol (3 mL) were mixed in a 15 mL oven-dried round-bottom tube with steady magnetic stirring (800 rpm) at 30 ºC under an ambient atmosphere of air. The reaction was started by the addition of Co-N$_4$@NPC-re (0.5 mol% Co) catalyst and the mixture was allowed to stir for given reaction time. After completion of the reaction (monitored by GC and/or TLC), the catalyst was removed by filtration and washed with EA (3 × 5 mL). The combined organics were washed with brine, dried over anhydrous Na_2SO_4 and solvent was removed under reduced pressure. The crude product was purified via flash column chromatography or vacuum distillation to obtain corresponding silyl ether.

Note: Drying treatment of alcohols is essential to maximize the yield of silyl ether.

Compound 6a

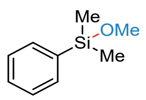

Methoxydimethyl(phenyl)silane

The reaction was conducted for 0.5 h following **GP C** on 1 mmol scale with **1a** and MeOH **5a**. GC analysis showed the yield of title compound **6a** was 96%. For a gram-scale synthesis, the reaction was followed **GP C** with 1.36 g **1a** (10 mmol) and 20 mL **5a** at 30 ºC for 1 h. Purification by vacuum distillation (5 Torr, 51-53 ºC) afforded **6a** in 83% yield (1.38 g).

Physical state: colorless oil.

^{1}H NMR (400 MHz, Chloroform-*d*): δ = 7.60 - 7.55 (m, 2H), 7.40-7.35 (m, 3H), 3.44 (s, 3H), 0.38 (s, 6H).
^{13}C NMR (101 MHz, Chloroform-*d*): δ = 137.36, 133.43, 129.63, 127.85, 50.64, -2.37.
The characterization data are consistent with that reported in the literature [59].

Compound 6b

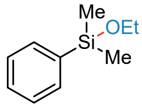

Ethoxydimethyl(phenyl)silane
The reaction was conducted for 0.5 h following **GP C** on 1 mmol scale with **1a** and EtOH **5b**. GC analysis showed the yield of title compound **6b** was 97%. For a gram-scale synthesis, the reaction was followed **GP C** with 1.36 g **1a** (10 mmol) and 30 mL **5b** at 30 °C for 1 h. Purification by vacuum distillation (15 Torr, 82-84 °C) afforded **6b** in 85% yield (1.53 g).
Physical state: colorless oil.
^{1}H NMR (400 MHz, Chloroform-*d*): δ = 7.59 - 7.57 (m, 2H), 7.39-7.36 (m, 3H), 3.67 (q, *J* = 7.0 Hz, 2H), 1.18 (t, *J* = 7.0 Hz, 2H), 0.38 (s, 6H).
^{13}C NMR (101 MHz, Chloroform-*d*): δ = 137.98, 133.44, 129.52, 127.80, 58.66, 18.40, -1.76.
The characterization data are consistent with that reported in the literature [59].

Compound 6c

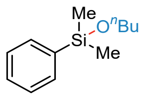

Butoxydimethyl(phenyl)silane
The reaction was conducted for 0.5 h following **GP C** on 1 mmol scale with **1a** and *n*-BuOH **5c**. After purification by flash column chromatography (silica gel, EA:PE = 1:10), the title compound **6c** was obtained in 93% yield (194 mg).
Physical state: colorless oil.
^{1}H NMR (400 MHz, Chloroform-*d*): δ = 7.68 - 7.58 (m, 2H), 7.44 - 7.37 (m, 3H), 3.64 (t, *J* = 6.6 Hz, 2H), 1.61 - 1.49 (m, 2H), 1.38 (q, *J* = 7.4 Hz, 2H), 0.93 (t, *J* = 7.3 Hz, 3H), 0.42 (s, 6H).
^{13}C NMR (101 MHz, Chloroform-*d*): δ = 138.04, 133.43, 129.47, 127.77, 62.82, 34.71, 18.93, 13.83, -1.80.
The characterization data are consistent with that reported in the literature [59].

Compound 6d

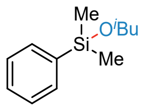

Isobutoxydimethyl(phenyl)silane
The reaction was conducted for 2 h following **GP C** on 1 mmol scale with **1a** and *i*-BuOH **5d**. After purification by flash column chromatography (silica gel, EA:PE = 1:10), the title compound **6d** was obtained in 95% yield (198 mg).
Physical state: colorless oil.
^{1}H NMR (400 MHz, Chloroform-*d*): δ = 7.62 - 7.55 (m, 2H), 7.39 - 7.33 (m, 3H), 3.39 (d, *J* = 6.5 Hz, 2H), 1.93 - 1.67 (m, 1H), 0.90 (d, *J* = 6.6 Hz, 6H), 0.41 (s, 6H).

^{13}C NMR (101 MHz, Chloroform-*d*): δ = 138.15, 133.46, 129.45, 127.76, 69.74, 30.66, 18.99, -1.79.
The characterization data are consistent with that reported in the literature [60].

Compound 6e

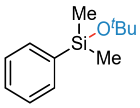

***tert*-Butoxydimethyl(phenyl)silane**

The reaction was conducted for 6 h following **GP C** on 1 mmol scale with **1a** and *t*-BuOH **5e**. After purification by flash column chromatography (silica gel, EA:PE = 1:10), the title compound **6e** was obtained in 90% yield (187 mg).

Physical state: colorless oil.

^{1}H NMR (400 MHz, Chloroform-*d*): δ = 7.61 - 7.59 (m, 2H), 7.36 - 7.34 (m, 3H), 1.25 (s, 9H), 0.38 (s, 6H).

^{13}C NMR (101 MHz, Chloroform-*d*): δ = 140.75, 133.34, 129.02, 127.60, 72.75, 32.06, 1.38.

The characterization data are consistent with that reported in the literature [61].

Compound 6f

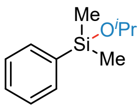

Isopropoxydimethyl(phenyl)silane

The reaction was conducted for 6 h following **GP C** on 1 mmol scale with **1a** and *i*-PrOH **5f**. After purification by flash column chromatography (silica gel, EA:PE = 1:10), the title compound **6f** was obtained in 92% yield (197 mg).

Physical state: colorless oil.

^{1}H NMR (400 MHz, Chloroform-*d*): δ = 7.66 - 7.62 (m, 2H), 7.44 - 7.42 (m, 3H), 4.04 (hept, *J* = 6.1 Hz, 1H), 1.18 (d, *J* = 6.1 Hz, 6H), 0.43 (s, 6H).

^{13}C NMR (101 MHz, Chloroform-*d*): δ = 138.50, 133.47, 129.42, 127.73, 65.27, 25.64, -1.17.

The characterization data are consistent with that reported in the literature [61].

Compound 6g

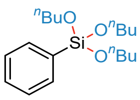

Tributoxy(phenyl)silane

The reaction was conducted for 0.5 h following **GP C** on 1 mmol scale with **1ai** and *n*-BuOH **5c**. After purification by flash column chromatography (silica gel, EA:PE = 1:10), the title compound **6g** was obtained in 94% yield (305 mg).

Physical state: colorless oil.

^{1}H NMR (400 MHz, Chloroform-*d*): δ = 7.72 - 7.68 (m, 2H), 7.47-7.38 (m, 3H), 3.84 (t, *J* = 6.6 Hz, 6H), 1.66 - 1.55 (m, 6H), 1.47 - 1.36 (m, 6H), 0.94 (t, *J* = 7.4 Hz, 9H).

^{13}C NMR (101 MHz, Chloroform-*d*): δ = 134.79, 131.03, 130.20, 127.74, 62.72, 34.51, 18.86, 13.77.

The characterization data are consistent with that reported in the literature [59].

Compound 6h

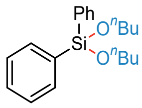

Dibutoxydiphenylsilane

The reaction was conducted for 1 h following **GP C** on 1 mmol scale with **1ah** and *n*-BuOH **5c**. After purification by flash column chromatography (silica gel, EA:PE = 1:10), the title compound **6h** was obtained in 96% yield (315 mg).

Physical state: colorless oil.

^{1}H NMR (400 MHz, Chloroform-*d*): δ = 7.82 - 7.58 (m, 4H), 7.54 - 7.28 (m, 6H), 3.79 (t, *J* = 6.5 Hz, 4H), 1.66 - 1.50 (m, 4H), 1.48 - 1.33 (m, 4H), 0.90 (t, *J* = 7.4 Hz, 6H).

^{13}C NMR (101 MHz, Chloroform-*d*): δ = 134.88, 133.27, 130.08, 127.73, 62.86, 34.59, 18.94, 13.82.

The characterization data are consistent with that reported in the literature [59].

Compound 6i

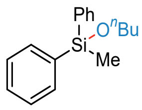

Butoxy(methyl)diphenylsilane

The reaction was conducted for 1 h following **GP C** on 1 mmol scale with **1x** and *n*-BuOH **5c**. After purification by flash column chromatography (silica gel, EA:PE = 1:10), the title compound **6i** was obtained in 93% yield (251 mg).

Physical state: colorless oil.

^{1}H NMR (400 MHz, Chloroform-*d*): δ = 7.64 - 7.59 (m, 4H), 7.43 - 7.36 (m, 6H), 3.71 (t, *J* = 6.5 Hz, 2H), 1.62 - 1.53 (m, 2H), 1.44 - 1.33 (m, 2H), 0.89 (s, 3H), 0.65 (s, 3H).

^{13}C NMR (101 MHz, Chloroform-*d*): δ = 136.29, 134.32, 129.70, 127.79, 63.26, 34.70, 18.96, 13.84, -3.05.

The characterization data are consistent with that reported in the literature [61].

Compound 6j

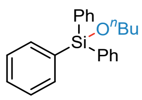

Butoxytriphenylsilane

The reaction was conducted for 2 h following **GP C** on 1 mmol scale with **1aa** and *n*-BuOH **5c**. After purification by flash column chromatography (silica gel, EA:PE = 1:10), the title compound **6j** was obtained in 94% yield (312 mg).

Physical state: colorless oil.

^{1}H NMR (400 MHz, Chloroform-*d*): δ = 7.70 - 7.66 (m, 6H), 7.50 - 7.39 (m, 9H), 3.85 (t, *J* = 6.5 Hz, 2H), 1.69 - 1.57 (m, 2H), 1.50 - 1.39 (m, 2H), 0.91 (t, *J* = 7.5 Hz, 3H).

^{13}C NMR (101 MHz, Chloroform-*d*): δ = 35.36, 134.45, 129.90, 127.79, 63.64, 34.65, 18.95, 13.83.

The characterization data are consistent with that reported in the literature [60].

Oxidative cross-coupling of hydrosilanes with complex alcohols (GP D)

Silane (2 mmol, 2 equiv.) and alcohol (1 mmol, 1 equiv.) were mixed with anhydrous *n*-heptane (3 mL) in a 15 mL oven-dried round-bottom tube with steady magnetic stirring (800 rpm) at 30 ºC under an ambient atmosphere of air. The reaction was started by the addition of Co-N_4@NPC-re (Co 0.5 mol%) catalyst and the mixture was allowed to stir for given reaction time. After completion of the reaction (monitored by GC and/or TLC), the catalyst was removed by filtration and washed with EA (3 × 5 mL). The combined organics were washed with brine, dried over anhydrous Na_2SO_4 and solvent was removed under reduced pressure. The crude product was purified via flash column chromatography to obtain corresponding silyl ether.
Note: Drying treatment of n-heptane is essential to maximize the yield of silyl ether.

Compound 6k

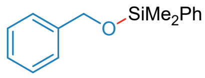

(Benzyloxy)dimethyl(phenyl)silane
The reaction was conducted for 2 h following **GP D** on 1 mmol scale with benzyl alcohol **5g** and **1a**. After purification by flash column chromatography (silica gel, EA:PE = 1:20), the title compound **6k** was obtained in 95% yield (230 mg).
Physical state: colorless oil.
^{1}H NMR (400 MHz, Chloroform-*d*): δ = 7.64 - 7.57 (m, 2H), 7.42 - 7.36 (m, 3H), 7.33 - 7.29 (m, 4H), 7.26 - 7.22 (m, 1H), 4.70 (s, 2H), 0.41 (s, 6H).
^{13}C NMR (101 MHz, Chloroform-*d*): δ = 140.70, 137.58, 133.53, 129.67, 128.25, 127.88, 127.10, 126.53, 64.97, -1.71.
The characterization data are consistent with that reported in the literature [62].

Compound 6l

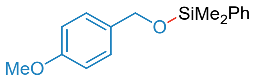

((4-Methoxybenzyl)oxy)dimethyl(phenyl)silane
The reaction was conducted at 60 ºC for 16 h following **GP D** on 1 mmol scale with 4-methoxyphenyl-methanol **5h** and 3 mmol **1a** using toluene as solvent. After purification by flash column chromatography (silica gel, EA:PE = 1:10), the title compound **6l** was obtained in 73% yield (199 mg).
Physical state: colorless oil.
^{1}H NMR (400 MHz, Chloroform-*d*): δ = 7.61 - 7.57 (m, 2H), 7.41 - 7.36 (m, 3H), 7.20 (d, *J* = 8.6 Hz, 2H), 6.84 (d, *J* = 8.6 Hz, 2H), 4.62 (s, 2H), 3.78 (s, 3H), 0.39 (s, 6H).
^{13}C NMR (101 MHz, Chloroform-*d*): δ = 158.79, 137.64, 133.52, 132.82, 129.62, 128.16, 127.84, 113.65, 64.72, 55.22, -1.67.
The characterization data are consistent with that reported in the literature [62].

Compound 6m

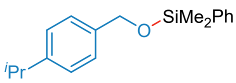

((4-Isopropylbenzyl)oxy)dimethyl(phenyl)silane

The reaction was conducted for 2 h following **GP D** on 1 mmol scale with 4-isopropylphenylmethanol **5i** and **1a**. After purification by flash column chromatography (silica gel, EA:PE = 1:20), the title compound **6m** was obtained in 92% yield (262 mg).

Physical state: colorless oil.

^{1}H NMR (400 MHz, Chloroform-*d*): δ = 7.64 - 7.57 (m, 2H), 7.40 - 7.33 (m, 3H), 7.25 - 7.14 (m, 4H), 4.65 (s, 2H), 2.88 (p, *J* = 6.9 Hz, 1H), 1.23 (d, *J* = 6.9 Hz, 6H), 0.40 (s, 6H).

^{13}C NMR (101 MHz, Chloroform-*d*): δ = 147.81, 138.04, 137.68, 133.54, 129.62, 127.85, 126.74, 126.31, 64.89, 33.82, 24.03, -1.70.

The characterization data are consistent with that reported in the literature [63]).

Compound 6n

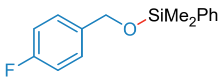

((4-Fluorobenzyl)oxy)dimethyl(phenyl)silane

The reaction was conducted for 2 h following **GP D** on 1 mmol scale with 4-fluorophenylmethanol **5j** and 3 mmol **1a** using toluene as solvent. After purification by flash column chromatography (silica gel, EA:PE = 1:20), the title compound **6n** was obtained in 91% yield (238 mg).

Physical state: colorless oil.

^{1}H NMR (400 MHz, Chloroform-*d*): δ = 7.65 - 7.55 (m, 2H), 7.46 - 7.33 (m, 3H), 7.24 (dd, *J* = 8.0, 5.8 Hz, 2H), 6.99 (t, *J* = 8.7 Hz, 2H), 4.64 (s, 2H), 0.41 (s, 6H).

^{13}C NMR (101 MHz, Chloroform-*d*): δ = 163.25, 160.81, 137.41, 136.43, 133.51, 129.74, 128.27, 128.19, 128.92, 115.15, 114.94, 64.36, -1.75.

^{19}F NMR (376 MHz, Chloroform-*d*): δ = -115.81.

The characterization data are consistent with that reported in the literature [62].

Compound 6o

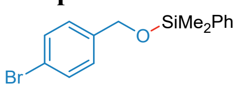

((4-Bromobenzyl)oxy)dimethyl(phenyl)silane

The reaction was conducted at 60 °C for 16 h following **GP D** on 1 mmol scale with 4-bromophenylmethanol **5k** and 3 mmol **1a** using toluene as solvent. After purification by flash column chromatography (silica gel, EA:PE = 1:20), the title compound **6o** was obtained in 86% yield (276 mg).

Physical state: colorless oil.

^{1}H NMR (400 MHz, Chloroform-*d*): δ = 7.68 - 7.59 (m, 2H), 7.52 - 7.25 (m, 5H), 7.22 (d, *J* = 8.4 Hz, 2H), 4.68 (s, 2H), 0.46 (s, 6H).

^{13}C NMR (101 MHz, Chloroform-*d*): δ = 139.77, 137.28, 133.48, 131.31, 129.78, 128.16, 127.93, 120.83, 64.28, -1.76.

The characterization data are consistent with that reported in the literature [62].

Compound 6p

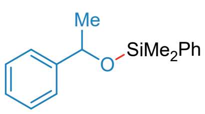

Dimethyl(phenyl)(1-phenylethoxy)silane

The reaction was conducted for 5 h following **GP D** on 1 mmol scale with 1-phenylethan-1-ol **5l** and **1a**. After purification by flash column chromatography (silica gel, EA:PE = 1:20), the title compound **6p** was obtained in 64% yield (164 mg).
Physical state: colorless oil.
^{1}H NMR (400 MHz, Chloroform-*d*): δ = 7.58 - 7.53 (m, 2H), 7.44 - 7.35 (m, 4H), 7.35 - 7.27 (m, 4H), 4.88 (q, *J* = 6.4 Hz, 1H), 1.44 (d, *J* = 6.4 Hz, 3H), 0.36 (s, 3H), 0.31 (s, 3H).
^{13}C NMR (101 MHz, Chloroform-*d*): δ = 146.21, 138.10, 133.51, 129.50, 128.11, 127.75, 126.86, 125.38, 71.06, 26.81, -0.87, -1.42.
The characterization data are consistent with that reported in the literature [64].

Compound 6q

2,7-Dimethyl-2,7-diphenyl-3,6-dioxa-2,7-disilaoctane
The reaction was conducted for 12 h following **GP D** on 1 mmol scale with ethylene glycol **5m** and 5 mmol **1a** using toluene/MeCN (v/v = 2:1) as the solvent. After purification by flash column chromatography (silica gel, EA:PE = 1:20), the title compound **6q** was obtained in 55% yield (182 mg).
Physical state: colorless oil.
^{1}H NMR (400 MHz, Chloroform-*d*): δ = 7.59 - 7.53 (m, 4H), 7.41 - 7.36 (m, 6H), 3.66 (s, 4H), 0.37 (s, 12H).
^{13}C NMR (101 MHz, Chloroform-*d*): δ = 137.76, 133.50, 129.55, 127.79, 64.18, -1.78.
The characterization data are consistent with that reported in the literature [65].

Compound 6r

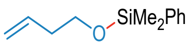

(But-3-en-1-yloxy)dimethyl(phenyl)silane
The reaction was conducted for 8 h following **GP D** on 1 mmol scale with but-3-en-1-ol **5n** and **1a**. After purification by flash column chromatography (silica gel, EA:PE = 1:20), the title compound **6r** was obtained in 80% yield (165 mg).
Physical state: colorless oil.
^{1}H NMR (400 MHz, Chloroform-*d*): δ = 7.60 - 7.56 (m, 2H), 7.40 - 7.37 (m, 3H), 5.79 (ddt, *J* = 17.1, 10.3, 6.8 Hz, 1H), 5.10 - 4.98 (m, 2H), 3.65 (t, *J* = 6.9 Hz, 2H), 2.29 (qt, *J* = 6.9, 1.4 Hz, 2H), 0.38 (s, 6H).
^{13}C NMR (101 MHz, Chloroform-*d*): δ = 137.89, 135.17, 133.47, 129.56, 127.81, 116.45, 62.61, 37.13, -1.77.
The characterization data are consistent with that reported in the literature [66].

Compound 6s

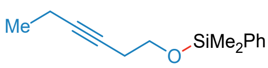

(Hex-3-yn-1-yloxy)dimethyl(phenyl)silane
The reaction was conducted for 20 h following **GP D** on 1 mmol scale with hex-3-yn-1-ol **5o** and **1a**. After purification by flash column chromatography (silica gel, EA:PE = 1:20), the title compound **6s** was obtained in 78% yield (182 mg).

Physical state: colorless oil.

^{1}H NMR (400 MHz, Chloroform-*d*): δ = 7.59 (dq, *J* = 4.7, 2.3 Hz, 2H), 7.41 – 7.37 (m, 3H), 3.68 (t, *J* = 7.3 Hz, 2H), 2.38 (tt, *J* = 7.4, 2.4 Hz, 2H), 2.14 (qt, *J* = 7.6, 2.4 Hz, 2H), 1.10 (t, *J* = 7.5 Hz, 3H), 0.39 (s, 6H).

^{13}C NMR (101 MHz, Chloroform-*d*): δ = 137.66, 133.47, 129.62, 127.83, 82.96, 76.01, 62.14, 22.89, 14.15, 12.38, -1.78.

HRMS (ESI-TOF): calcd for $C_{14}H_{19}N_2O_3Si^+$ $[M+H]^+$: 233.1356, found: 233.1368.

Compound 6t

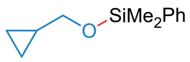

(Cyclopropylmethoxy)dimethyl(phenyl)silane

The reaction was conducted for 3.5 h following **GP D** on 1 mmol scale with cyclopropylmethanol **5p** and **1a**. After purification by flash column chromatography (neutral alumina, Et_2O:hexanes = 1:10), the title compound **6t** was obtained in 90% yield (186 mg).

*Note: **4t** is volatile under high vacuum.*

Physical state: colorless oil.

^{1}H NMR (400 MHz, Chloroform-*d*): δ = 7.62 - 7.56 (m, 2H), 7.42 - 7.35 (m, 3H), 3.44 (d, *J* = 6.7 Hz, 2H), 1.02 (ttt, *J* = 8.1, 6.5, 4.9 Hz, 1H), 0.51 - 0.43 (m, 2H), 0.40 (s, 6H), 0.16 - 0.10 (m, 2H).

^{13}C NMR (101 MHz, Chloroform-*d*): δ = 138.01, 133.51, 129.51, 127.79, 67.81, 13.17, 2.98, -1.65.

The characterization data are consistent with that reported in the literature [62].

Compound 6u

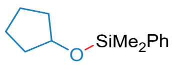

(Cyclopentyloxy)dimethyl(phenyl)silane

The reaction was conducted for 3 h following **GP D** on 1 mmol scale with cyclopentanol **5q** and **1a**. After purification by flash column chromatography (silica gel, EA:PE = 1:20), the title compound **6u** was obtained in 66% yield (145 mg).

Physical state: colorless oil.

^{1}H NMR (400 MHz, Chloroform-*d*): δ = 7.65 - 7.56 (m, 2H), 7.41 - 7.36 (m, 3H), 4.33 - 4.15 (m, 1H), 1.80 - 1.65 (m, 4H), 1.61 - 1.45 (m, 4H), 0.38 (s, 6H).

^{13}C NMR (101 MHz, Chloroform-*d*): δ = 138.67, 133.47, 129.36, 127.72, 74.70, 35.49, 23.13, -1.10.

The characterization data are consistent with that reported in the literature [67].

Compound 6v

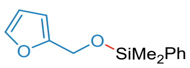

(Furan-2-ylmethoxy)dimethyl(phenyl)silane

The reaction was conducted for 24 h following **GP D** on 1 mmol scale with furfuryl alcohol **5r** and 3 mmol **1a** using toluene as solvent. After purification by flash column chromatography (silica gel, EA:PE = 1:10), the title compound **6v** was obtained in 79% yield (183 mg).

Physical state: colorless oil.

^{1}H NMR (400 MHz, Chloroform-*d*): δ = 7.58 (dd, *J* = 5.0, 2.4 Hz, 2H), 7.38 (dd, *J* = 12.2, 5.9 Hz, 4H), 6.29 (d, *J* = 1.8 Hz, 1H), 6.18 (d, *J* = 3.1 Hz, 1H), 4.59 (s, 2H), 0.39 (s, 6H).
^{13}C NMR (101 MHz, Chloroform-*d*): δ = 153.58, 142.30, 137.28, 133.55, 129.67, 127.85, 110.19, 107.83, 57.71, -1.79.
The characterization data are consistent with that reported in the literature [62].

Compound 6w

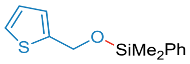

Dimethyl(phenyl)(thiophen-2-ylmethoxy)silane
The reaction was conducted at 60 °C for 24 h following **GP D** on 1 mmol scale with thiophen-2-ylmethanol **5s** and 3 mmol **1a** using toluene as solvent. After purification by flash column chromatography (silica gel, EA:PE = 1:10), the title compound **6w** was obtained in 63% yield (171 mg).
Physical state: colorless oil.
^{1}H NMR (400 MHz, Chloroform-*d*): δ = 7.67 - 7.60 (m, 2H), 7.42 (d, *J* = 7.1 Hz, 3H), 7.26 (dd, *J* = 5.1, 1.3 Hz, 1H), 6.99 - 6.88 (m, 2H), 4.86 (s, 2H), 0.44 (s, 6H).
^{13}C NMR (101 MHz, Chloroform-*d*): δ = 133.57, 129.75, 127.90, 126.53, 124.99, 124.68, 60.32, -1.70.
The characterization data are consistent with that reported in the literature [62].

Compound 6x

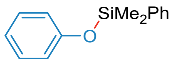

Dimethyl(phenoxy)(phenyl)silane
The reaction was conducted at 60 °C for 30 h following **GP D** on 1 mmol scale with phenol **5t** and 3 mmol **1a** using toluene as solvent. After purification by flash column chromatography (silica gel, EA:PE = 1:20), the title compound **6x** was obtained in 61% yield (139 mg).
Physical state: colorless oil.
^{1}H NMR (400 MHz, Chloroform-*d*): δ = 7.70 - 7.64 (m, 2H), 7.46 - 7.34 (m, 3H), 7.22 (t, *J* = 7.4 Hz, 2H), 6.97 (t, *J* = 7.2 Hz, 1H), 6.85 (d, *J* = 7.7 Hz, 2H), 0.55 (s, 6H).
^{13}C NMR (101 MHz, Chloroform-*d*): δ = 155.04, 137.19, 132.98, 129.88, 129.38, 127.94, 121.48, 120.02, -1.14.
The characterization data are consistent with that reported in the literature [66].

Compound 6y

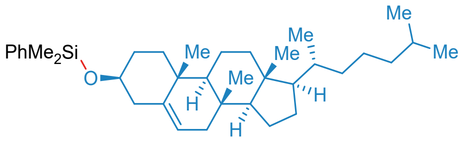

Dimethyl(phenyl)(((3S,8S,9S,10R,13R,14R,17R)-8,10,13-trimethyl-17-((R)-6-methylheptan-2-yl)-2,3,4,7,8,9,10,11,12,13,14,15,16,17-tetradecahydro-1H-cyclopenta[a]phenanthren-3-yl)oxy)silane
The reaction was conducted at 60 °C for 12 h following **GP D** on 1 mmol scale with cholesterol **5u** and **1a**. After purification by flash column chromatography (silica gel, EA:PE = 1:10), the title compound **6y** was obtained in 83% yield (443 mg).
Physical state: colorless oil.

^{1}**H NMR (400 MHz, Chloroform-*d*):** δ = 7.63 - 7.54 (m, 2H), 7.38 - 7.32 (m, 3H), 5.24 (d, *J* = 5.0 Hz, 1H), 3.56 - 3.45 (m, 1H), 2.37 - 2.23 (m, 1H), 2.15 (ddd, *J* = 13.4, 4.6, 1.8 Hz, 1H), 2.03 - 1.90 (m, 2H), 1.86 - 1.74 (m, 2H), 1.69 (d, *J* = 13.0 Hz, 1H), 1.60 - 1.18 (m, 12H), 1.14 - 0.85 (m, 21H), 0.66 (s, 3H), 0.38 (d, *J* = 2.0 Hz, 6H).
^{13}**C NMR (101 MHz, Chloroform-*d*):** δ = 141.18, 138.51, 133.41, 129.41, 127.72, 121.32, 72.73, 56.76, 56.15, 50.14, 42.56, 42.29, 39.78, 39.52, 37.30, 36.49, 36.19, 35.77, 31.86, 28.22, 27.98, 24.27, 23.83, 22.81, 22.56, 21.03, 19.34, 18.72, 11.83, -0.97, -1.06.
The characterization data are consistent with that reported in the literature [68].

Oxidative dimerization

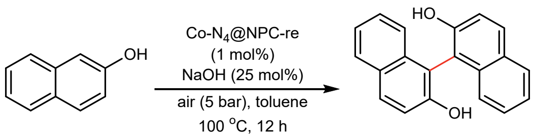

7 8

A mixture of **7** (144 mg, 1 mmol), NaOH (10 mg, 0.25 mmol), Co-N_4@NPC-re (Co 1 mol%) and toluene (3 mL) was charged into a 25 mL Hastelloy-C high pressure Parr reactor. After the reactor was sealed, the reactor was pressured to 5 bar air and then heated to 100 °C. The mixture of substrates and catalyst was stirred at a rate of 800 rpm for 16 h. After completion of the reaction, 5 mL 0.1mol/L HCl aqueous solution was added. Then the mixture was filtered over a short pad of silica and washed with EA (3 × 5 mL). The combined organics were washed with brine, dried over anhydrous Na_2SO_4 and solvent was removed under reduced pressure. The crude product was purified via flash column chromatography (silica gel, EA:PE = 1:10) to afford compound **8** in 81% yield (114 mg).

Compound 8

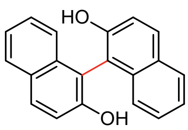

1,1'-Binaphthalene-2,2'-diol
Physical state: white solid.
^{1}**H NMR (400 MHz, DMSO-*d*$_6$):** δ = 9.20 (s, 2H), 7.85 (dd, *J* = 8.6, 3.8 Hz, 4H), 7.33 (d, *J* = 8.9 Hz, 2H), 7.23 (t, *J* = 7.4 Hz, 2H), 7.17 (t, *J* = 7.6 Hz, 2H), 6.94 (d, *J* = 8.4 Hz, 2H).
^{13}**C NMR (101 MHz, DMSO-*d*$_6$):** δ = 152.99, 134.11, 128.62, 128.11, 127.84, 125.81, 124.39, 122.25, 118.53, 115.39.
The characterization data are consistent with that reported in the literature [69].

Oxidative carbonylation

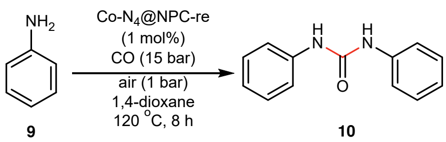

9 10

A mixture of **9** (93 mg, 1 mmol), Co-N_4@NPC-re (Co 1 mol%) and 1,4-dioxane (3 mL) was charged into a 25 mL Hastelloy-C high pressure Parr reactor. After the reactor was sealed, the reactor was charged with 15 bar CO and 1 bar air. The mixture of substrates and catalyst was heated to 120 °C and stirred at a rate of 800 rpm for 8 h. After completion of the reaction, the mixture was filtered over a short pad of silica and washed with EA (3 × 5 mL). The combined organics were washed with brine, dried over anhydrous Na_2SO_4 and solvent was removed under reduced pressure. The crude product was purified via flash column chromatography (silica gel, EA:PE = 1:4) to afford compound **10** in 83% yield (88 mg).

Compound 10

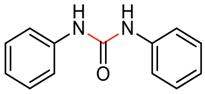

1,3-Diphenylurea

Physical state: white solid.

^{1}H NMR (400 MHz, DMSO-d_6): δ = 8.66 (s, 2H), 7.51 – 7.43 (m, 4H), 7.33 - 7.23 (m, 4H), 7.01 - 6.92 (m, 2H).

^{13}C NMR (101 MHz, DMSO-d_6): δ = 152.55, 139.72, 128.78, 121.80, 118.19.

The characterization data are consistent with that reported in the literature [70].

Oxidative cyclization

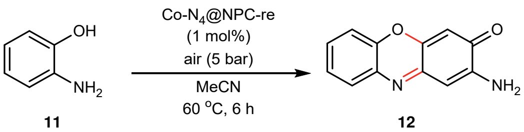

A mixture of **11** (109 mg, 1 mmol), Co-N_4@NPC-re (Co 1 mol%) and MeCN (3 mL) was charged into a 25 mL Hastelloy-C high pressure Parr reactor. After the reactor was sealed, the reactor was pressured to 5 bar air and then heated to 60 °C. The mixture of substrates and catalyst was stirred at a rate of 800 rpm for 6 h. After completion of the reaction, the mixture was filtered over a short pad of silica and washed with THF (3 × 5 mL). The combined organics were washed with brine, dried over anhydrous Na_2SO_4 and solvent was removed under reduced pressure. The crude product was purified via flash column chromatography (silica gel, EA:PE = 3:7) to afford compound **12** in 94% yield (100 mg).

Compound 12

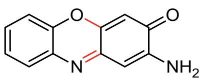

2-Amino-3*H*-phenoxazin-3-one

Physical state: red solid.

^{1}H NMR (400 MHz, DMSO-d_6): δ = 7.71 (dd, J = 7.9, 1.6 Hz, 1H), 7.54 - 7.43 (m, 2H), 7.39 (td, J = 7.5, 1.8 Hz, 1H), 6.81 (br s, 2H), 6.36 (s, 2H).

^{13}C NMR (101 MHz, DMSO-d_6): δ = 180.22, 148.88, 148.25, 147.38, 141.93, 133.74, 128.80, 127.98, 125.28, 115.94, 103.43, 98.35.

The characterization data are consistent with that reported in the literature [71].

NMR Spectra

Compound **1c** ^{1}H NMR

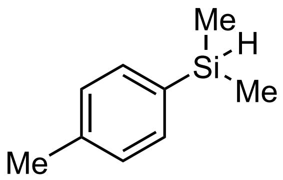

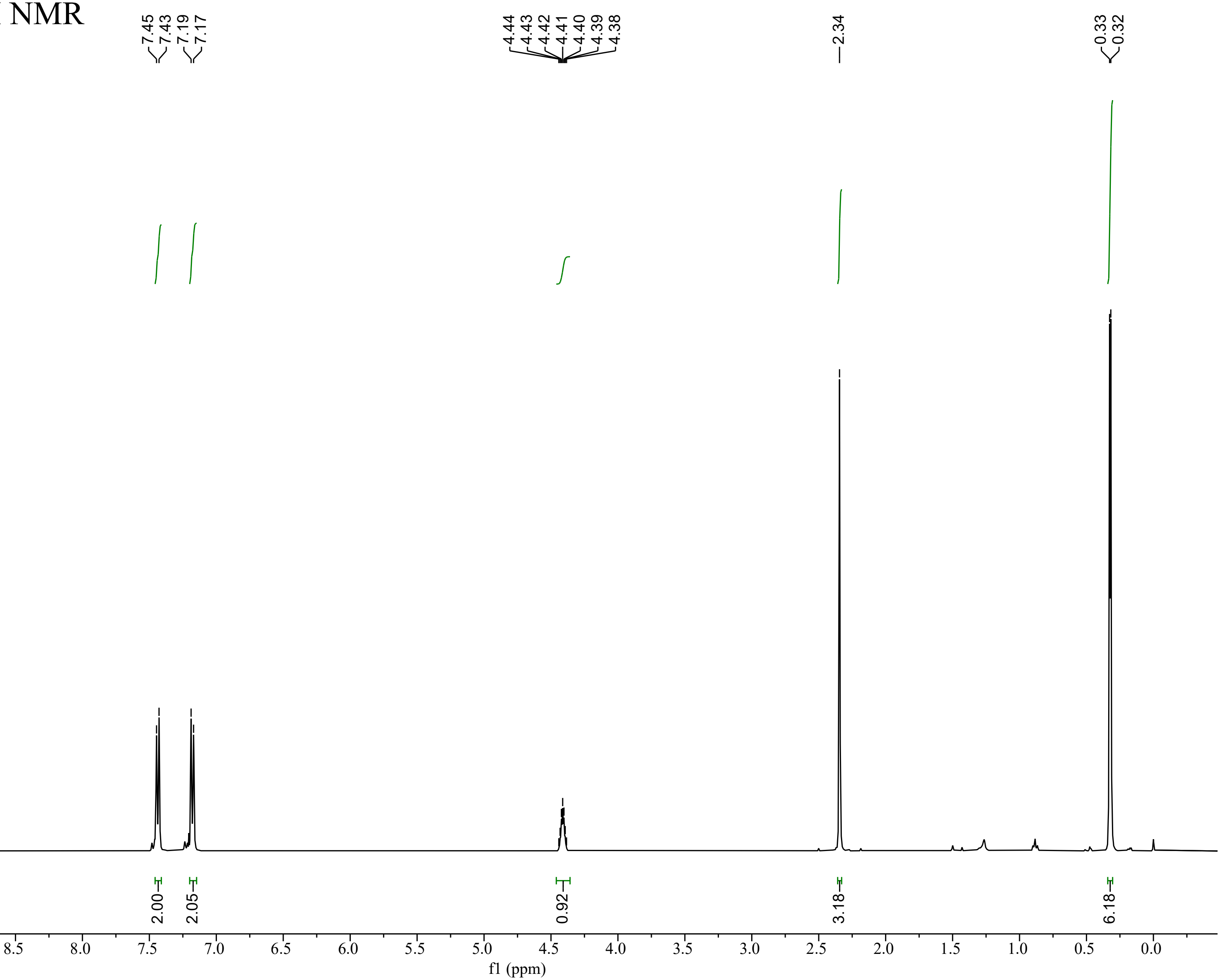

Compound **1c** ^{13}C NMR

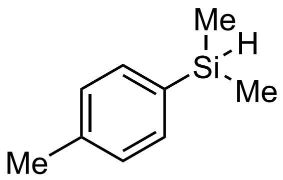

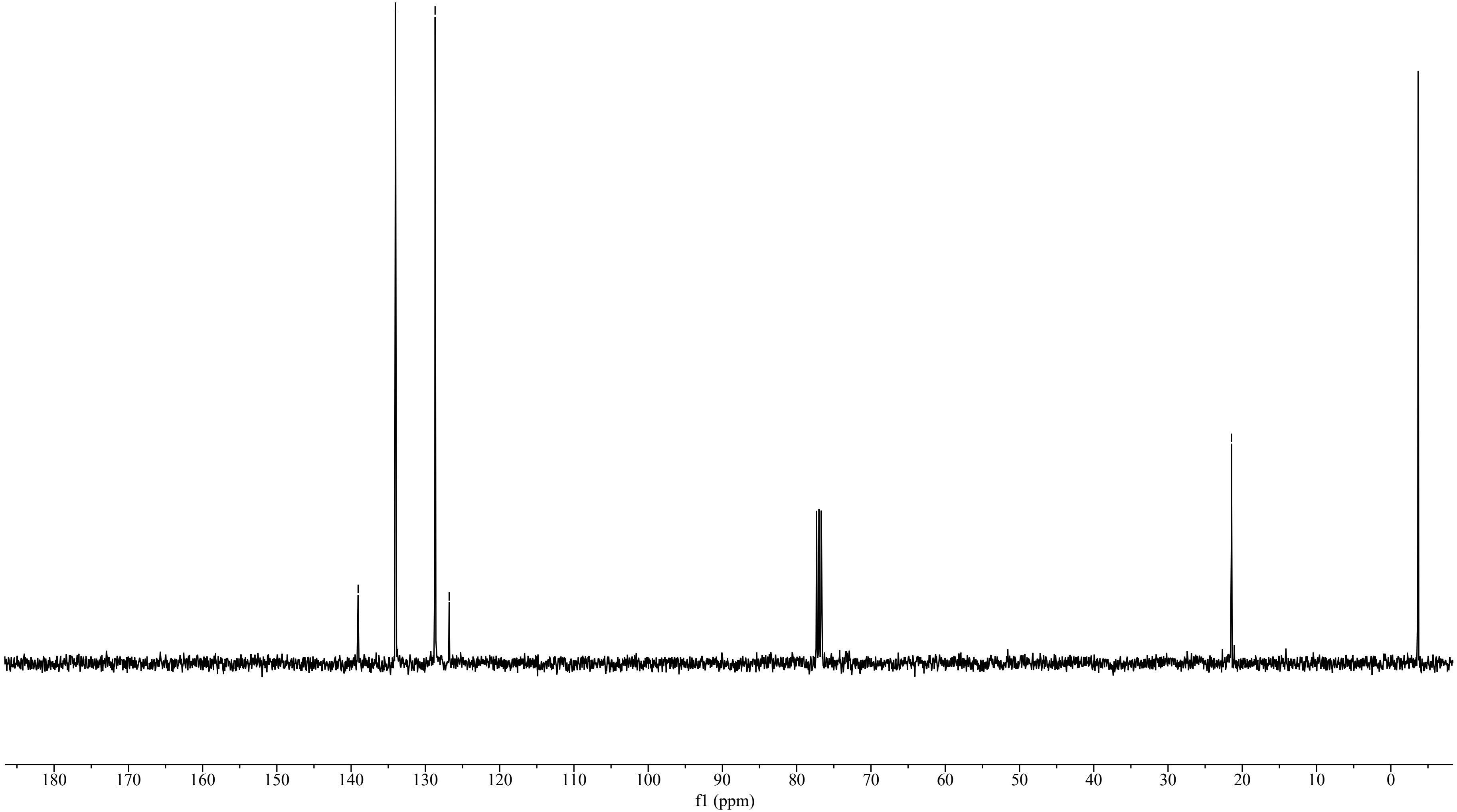

Compound **1d** ^{1}H NMR

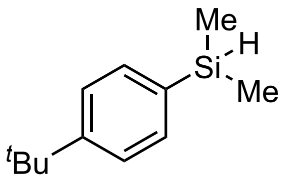

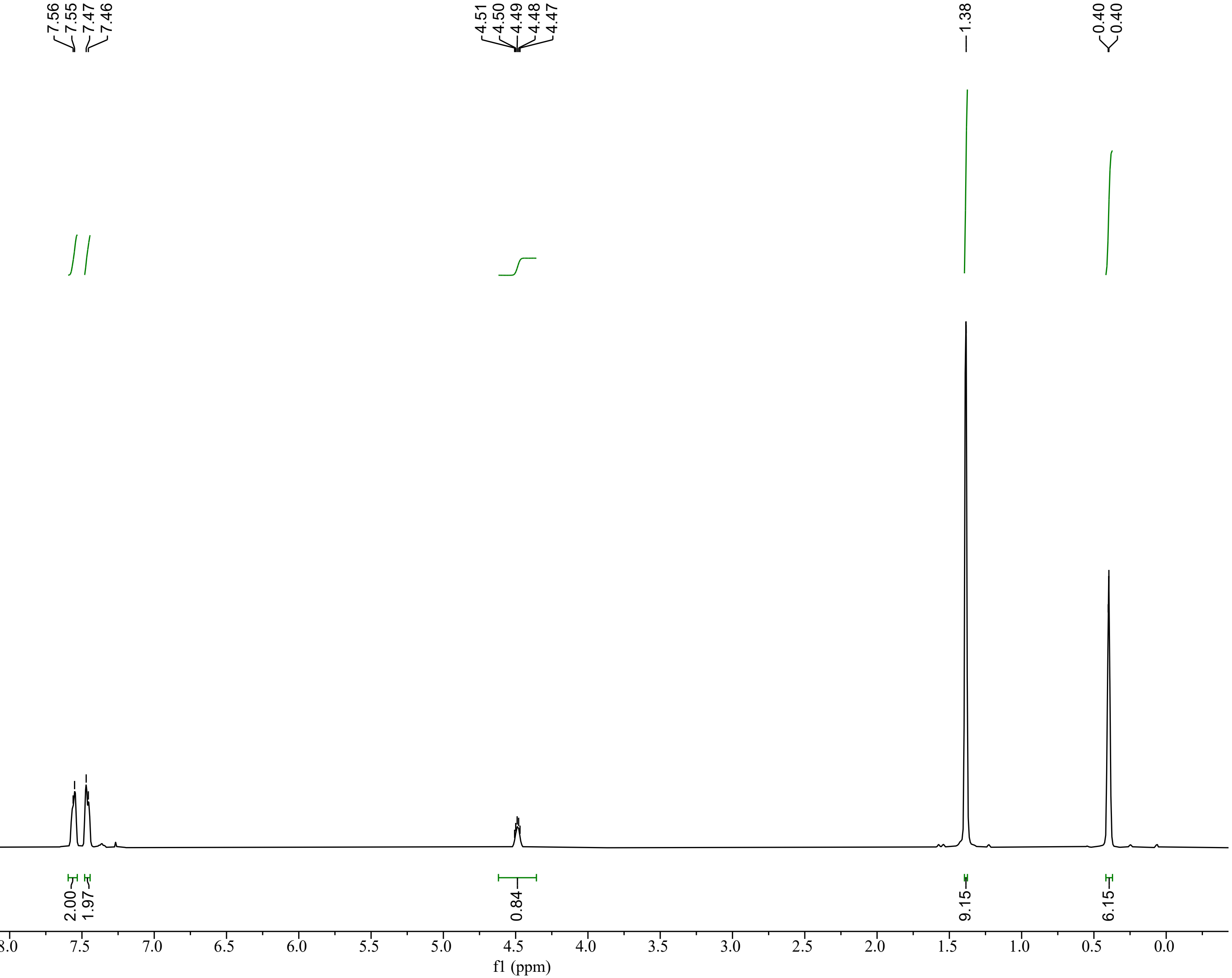

Compound **1d** ^{13}C NMR

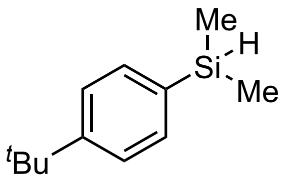

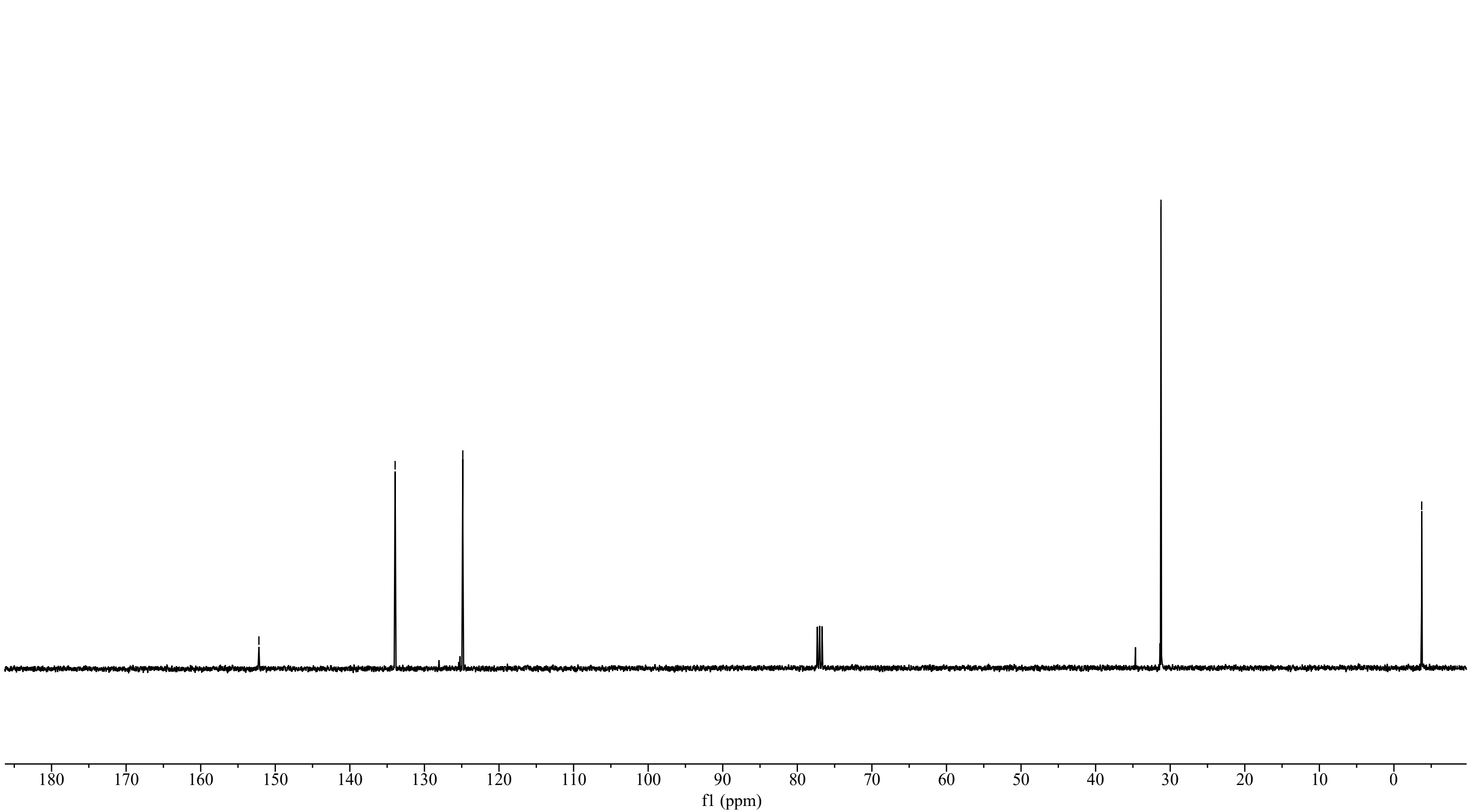

Compound **1e** [1]H NMR

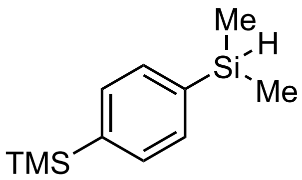

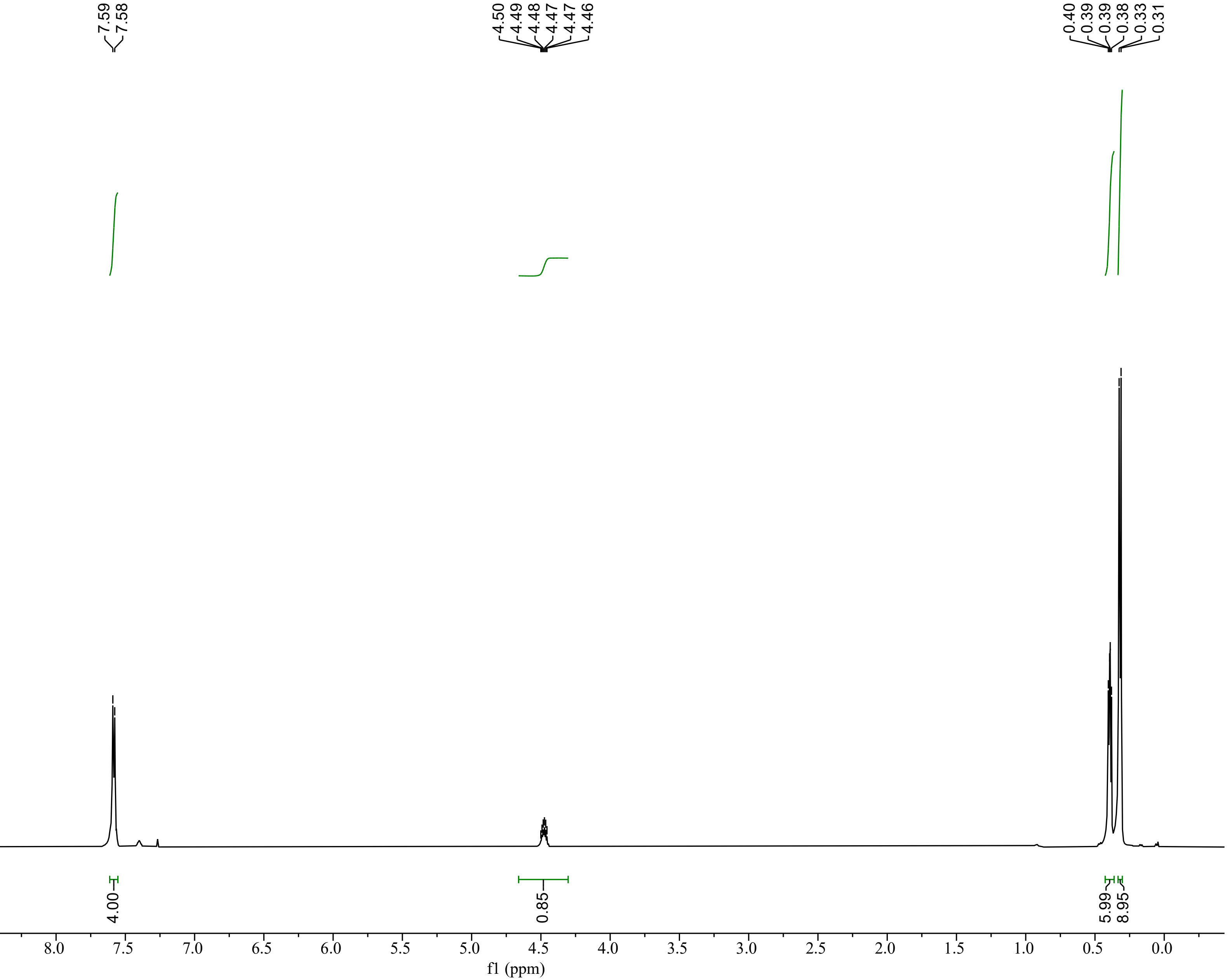

Compound **1e** ^{13}C NMR

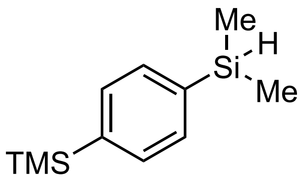

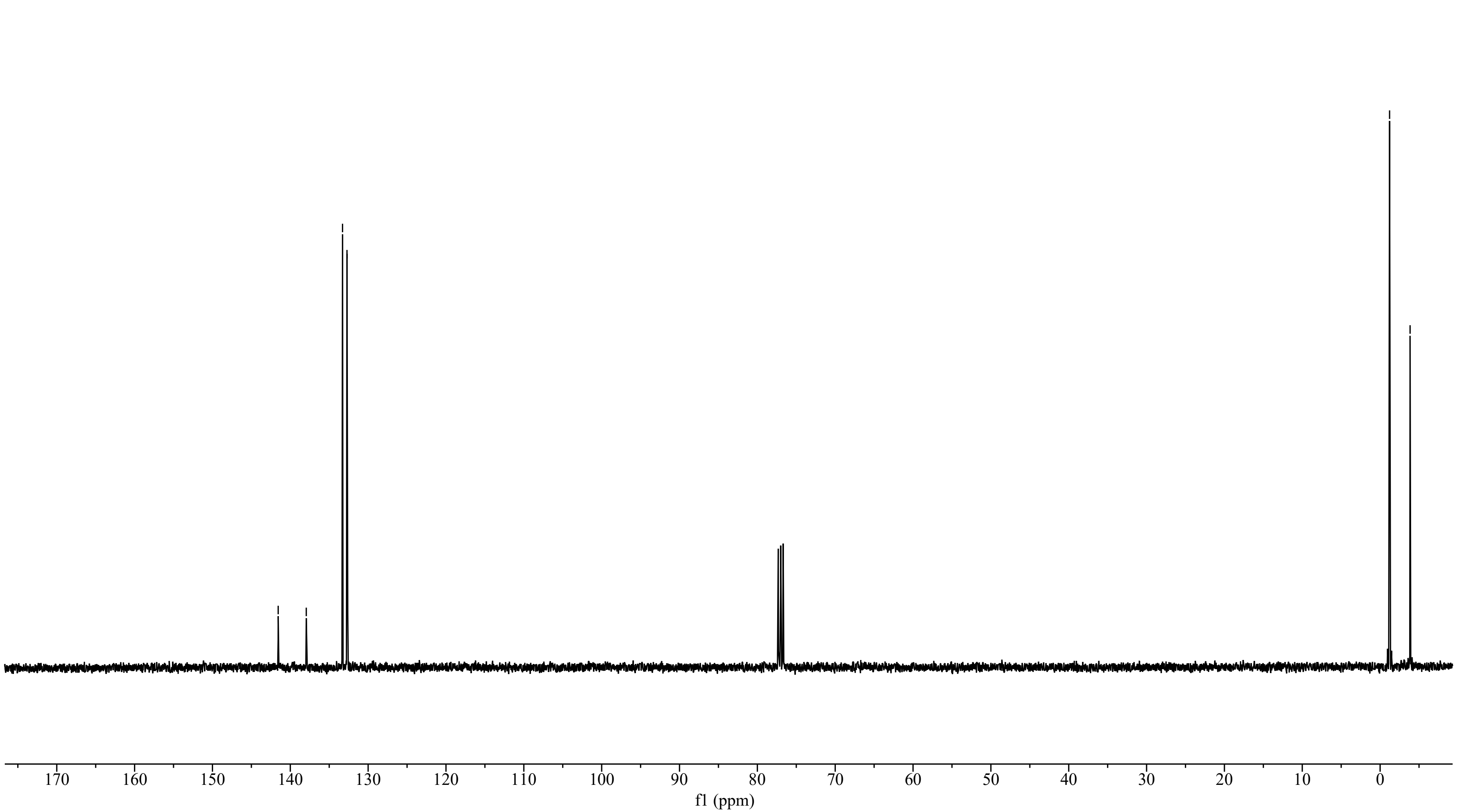

Compound **1f** ^{1}H NMR

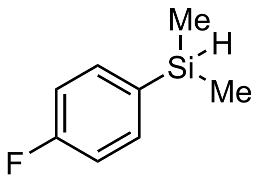

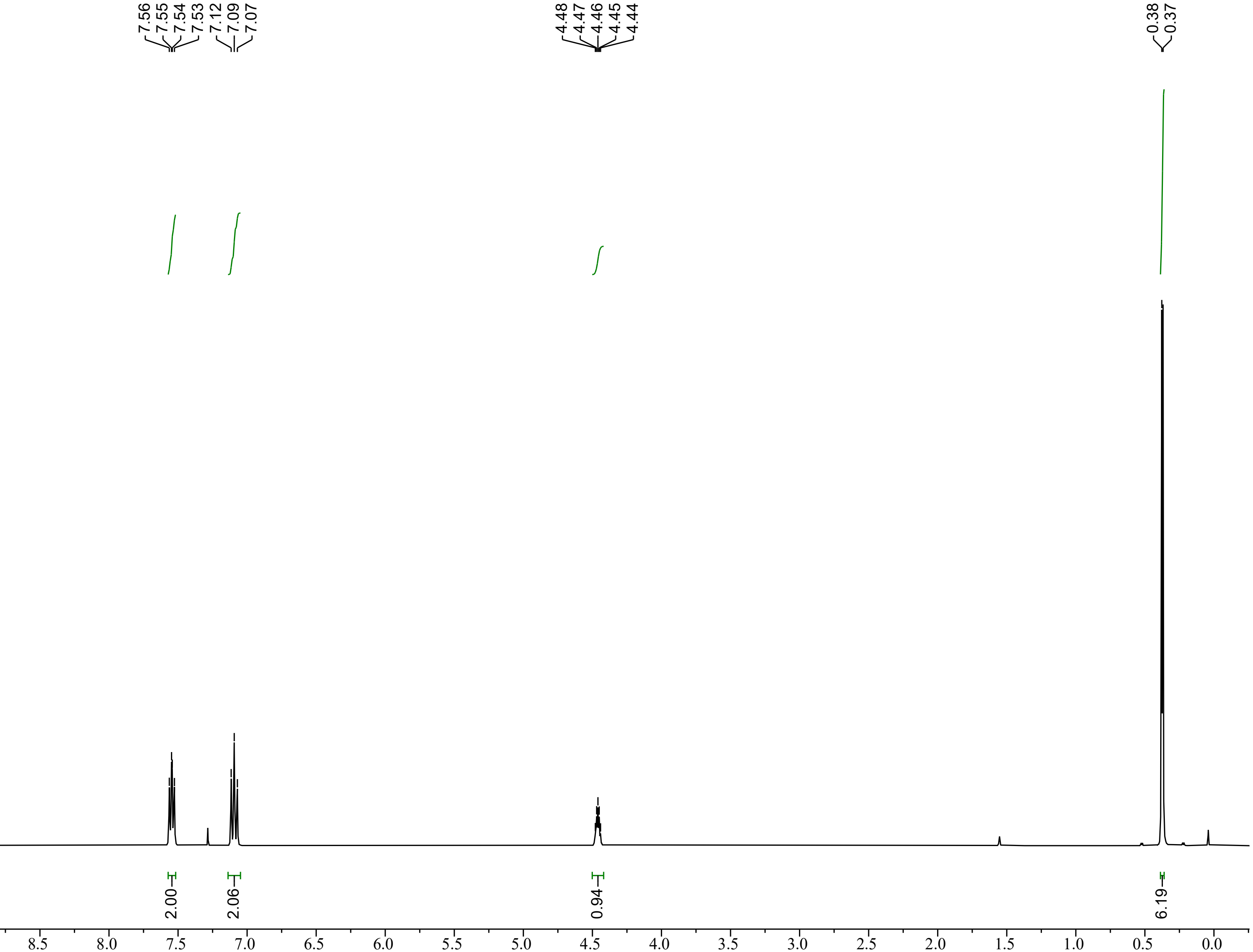

Compound **1f** ^{13}C NMR

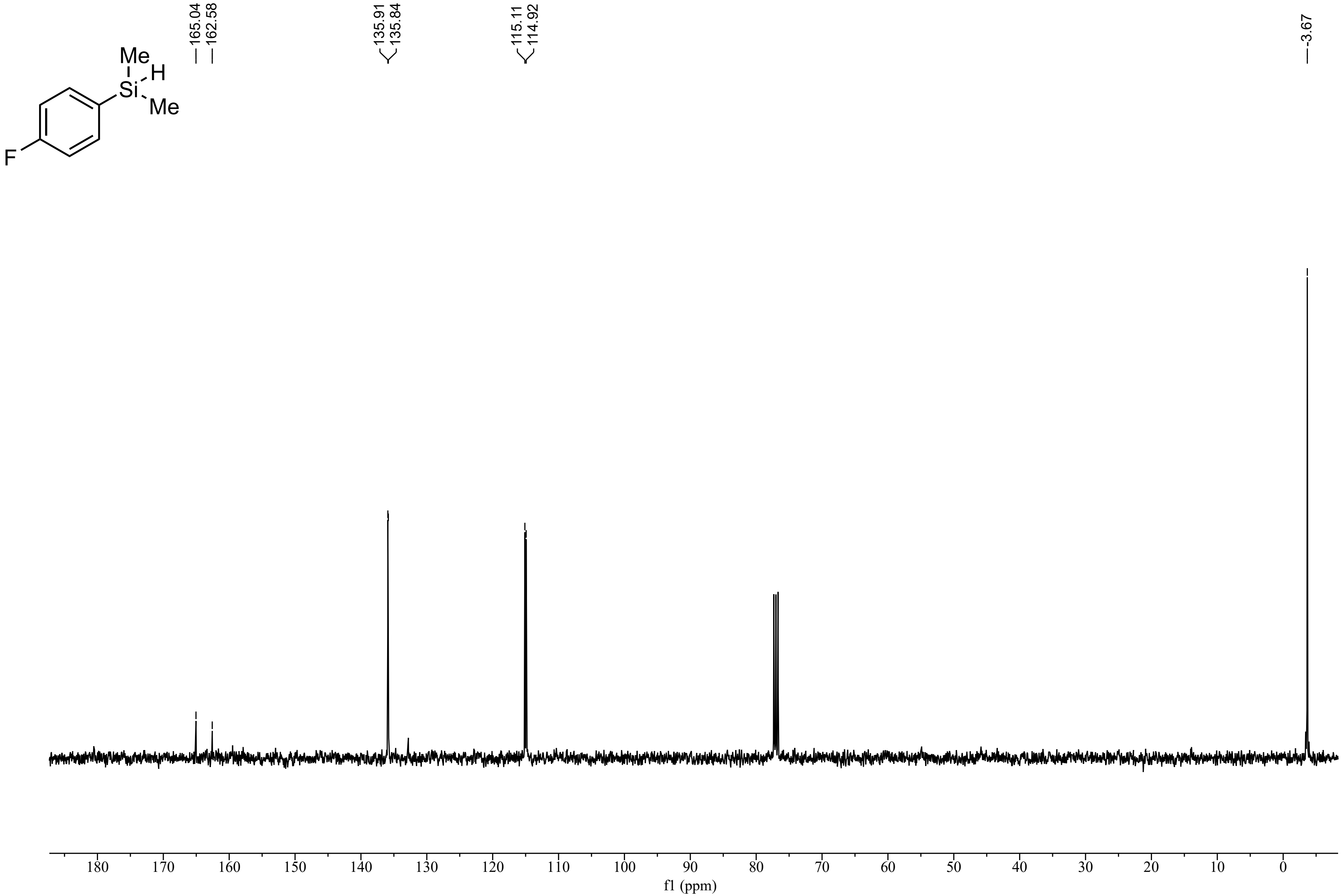

Compound **1f** ^{19}F NMR

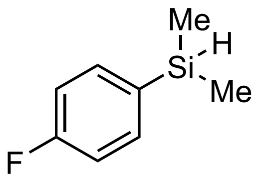

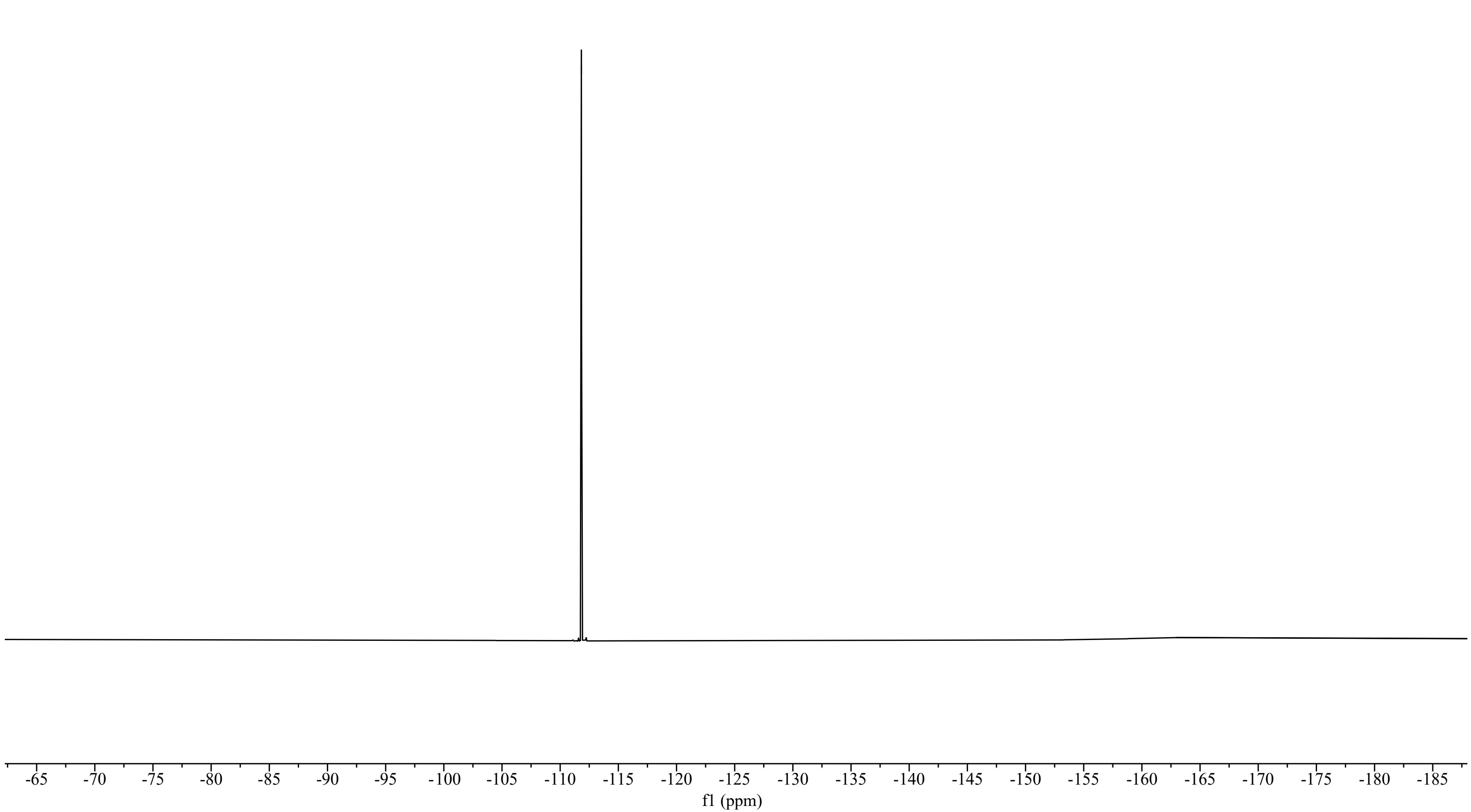

Compound **1g** ^{1}H NMR

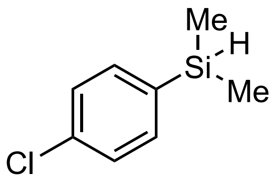

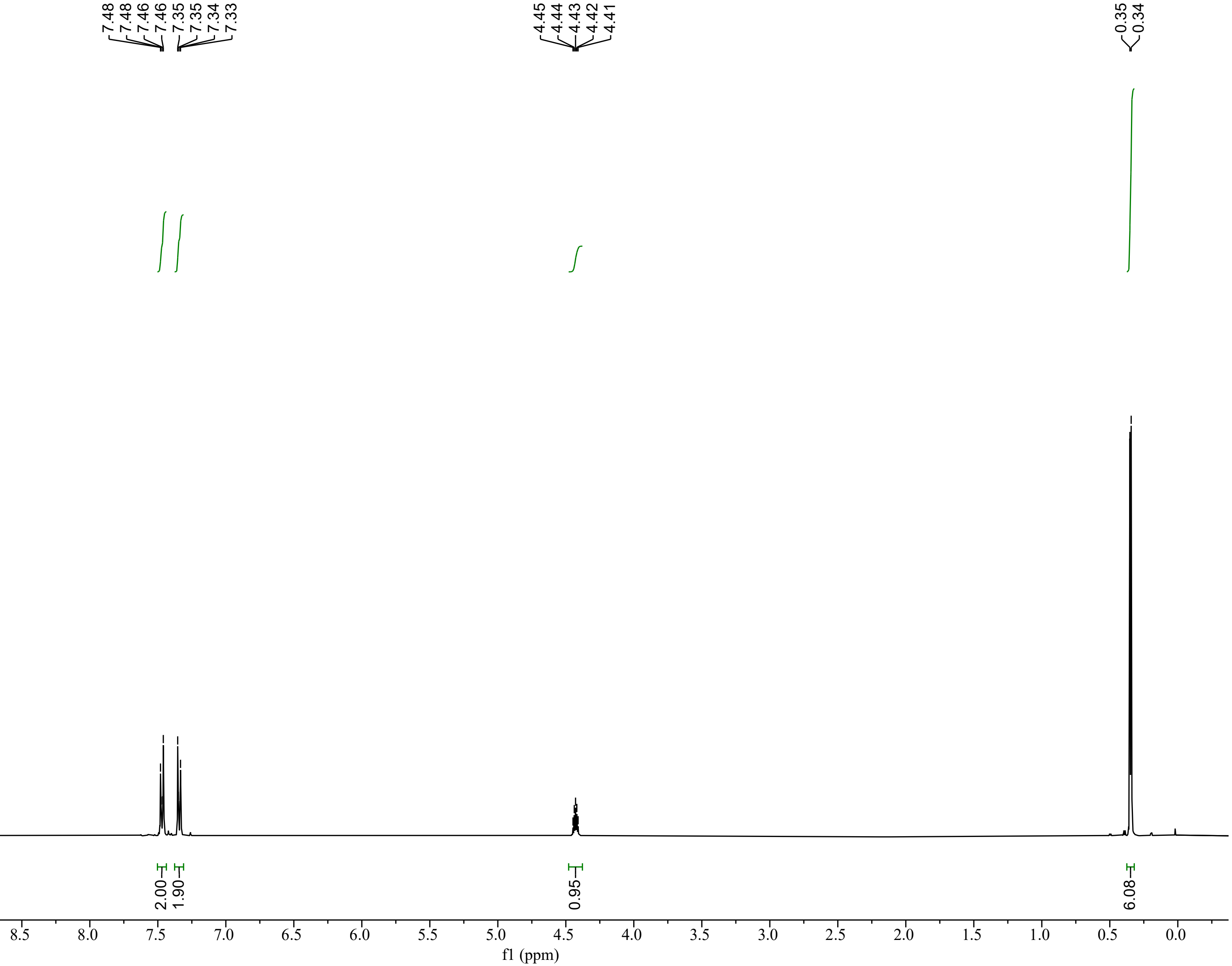

Compound **1g** ^{13}C NMR

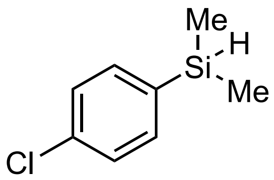

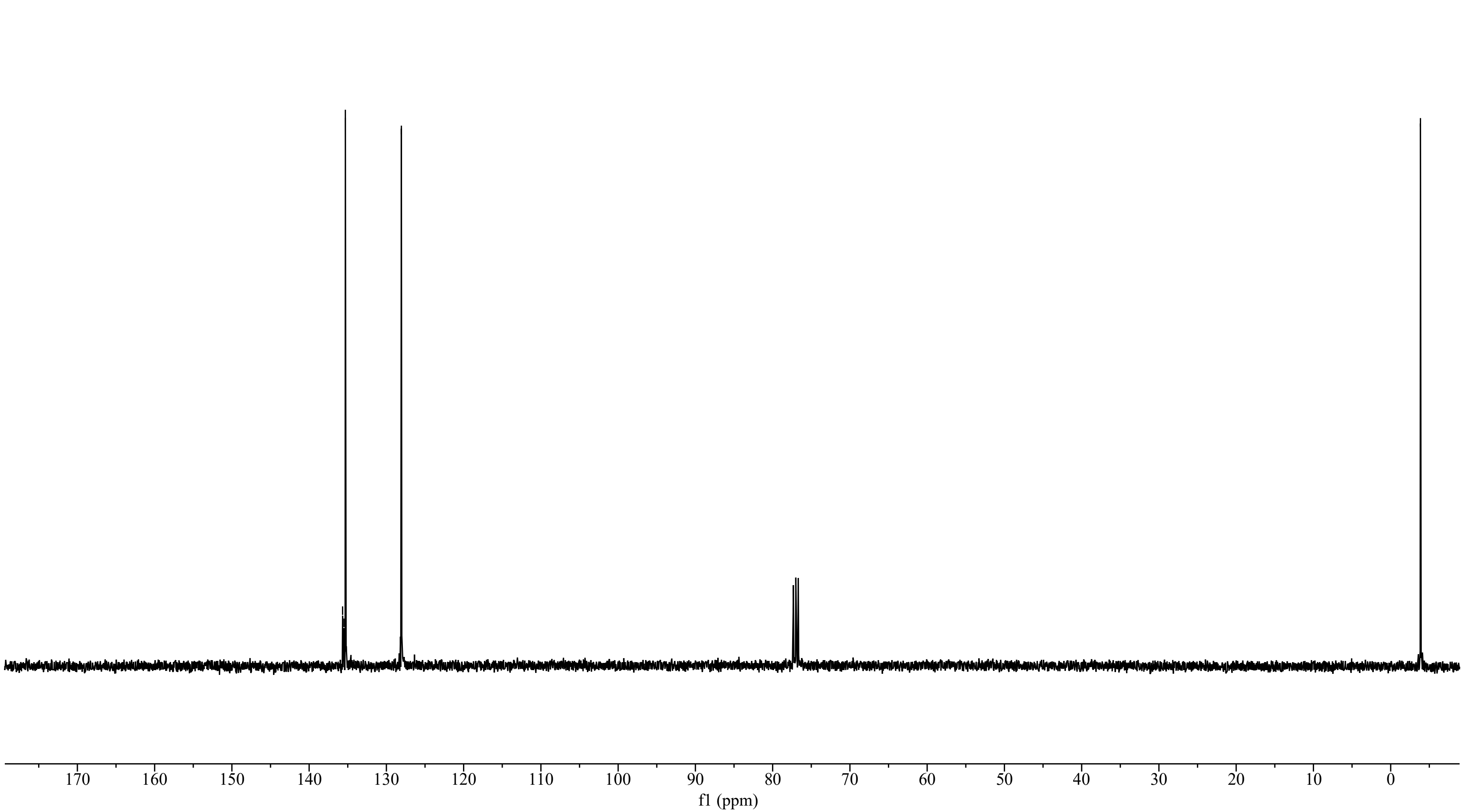

Compound **1h** ^{1}H NMR

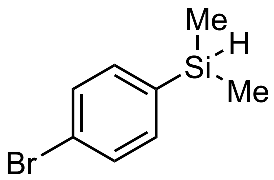

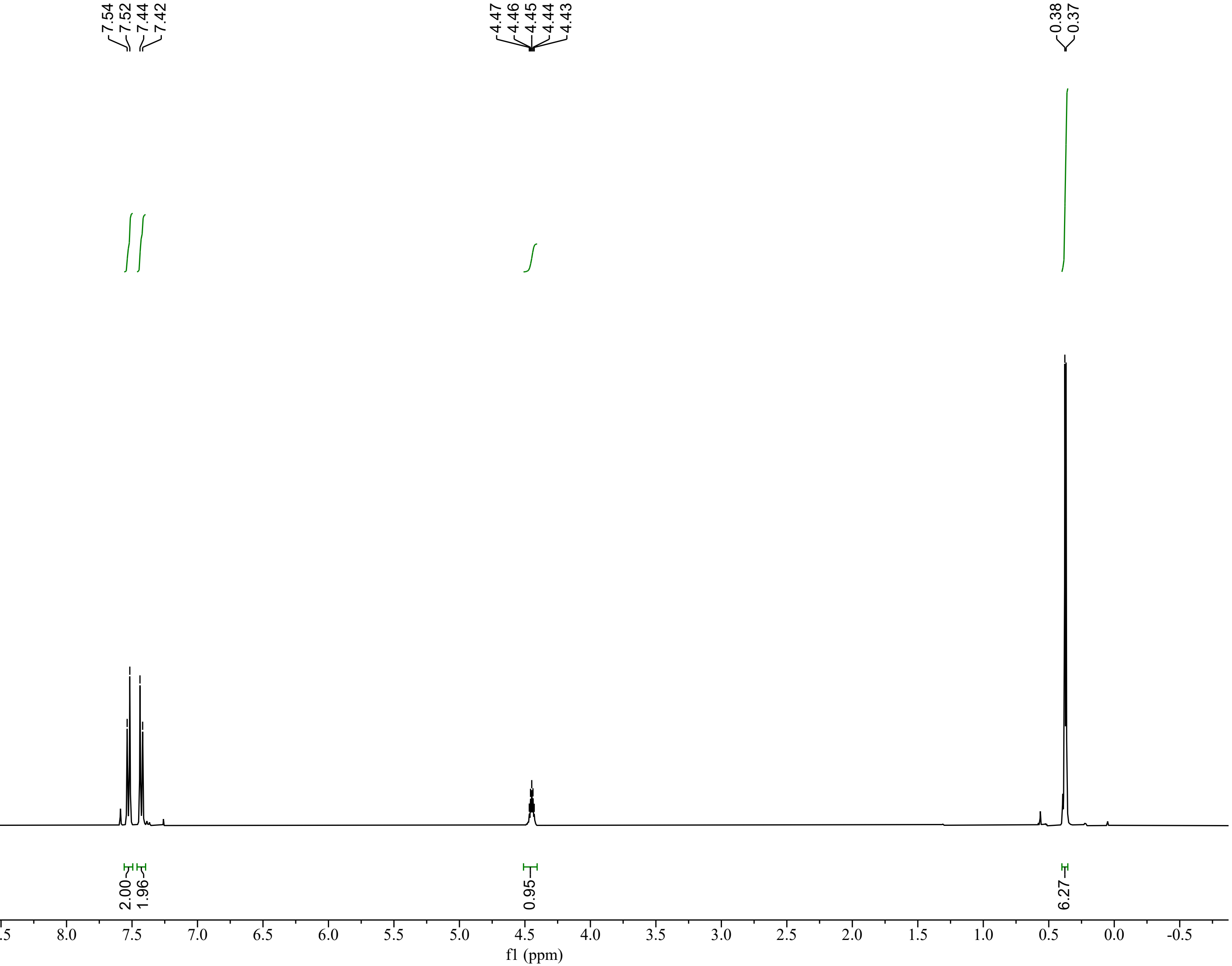

Compound **1h** ^{13}C NMR

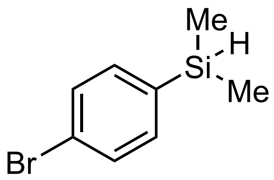

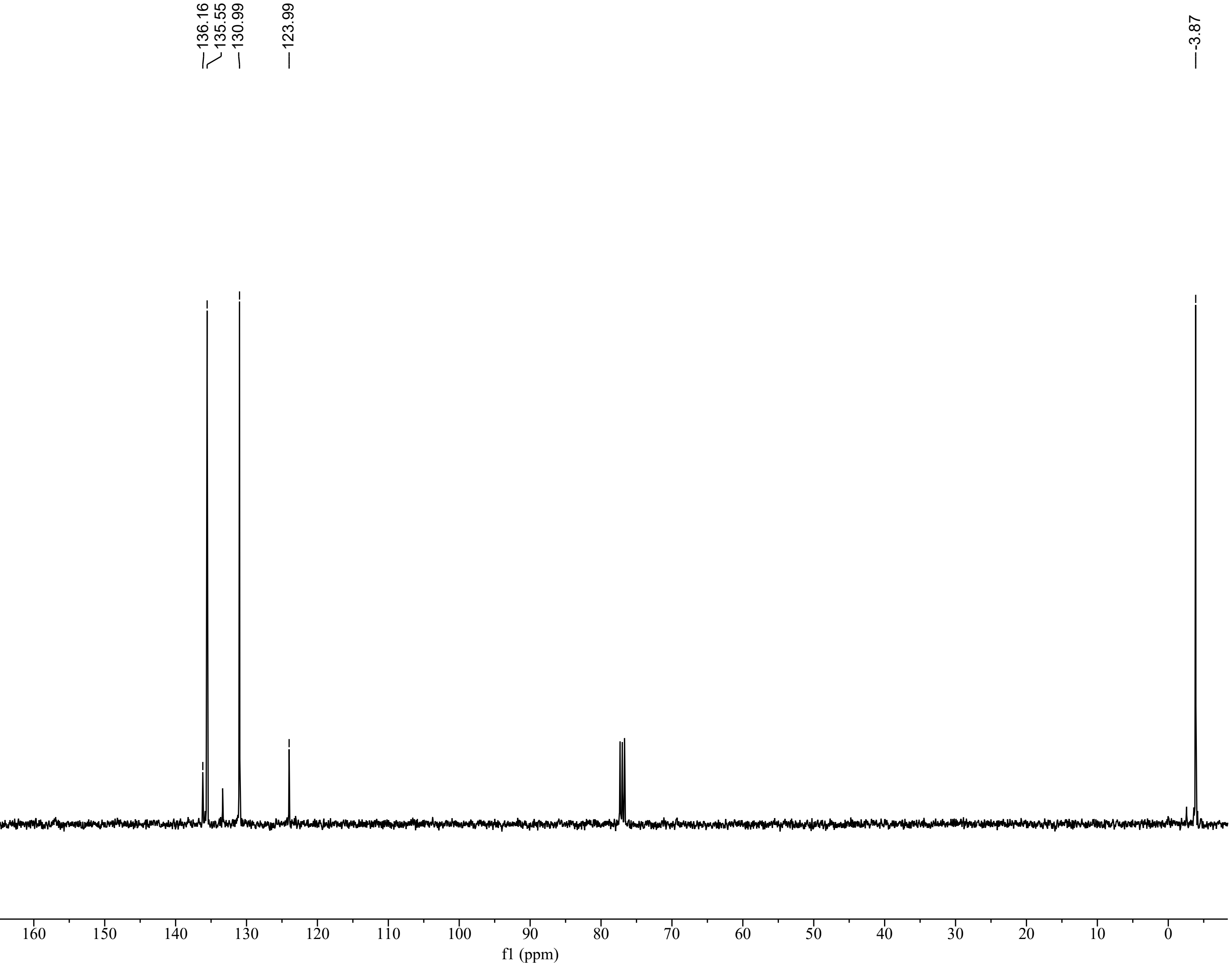

Compound **1i** ^{1}H NMR

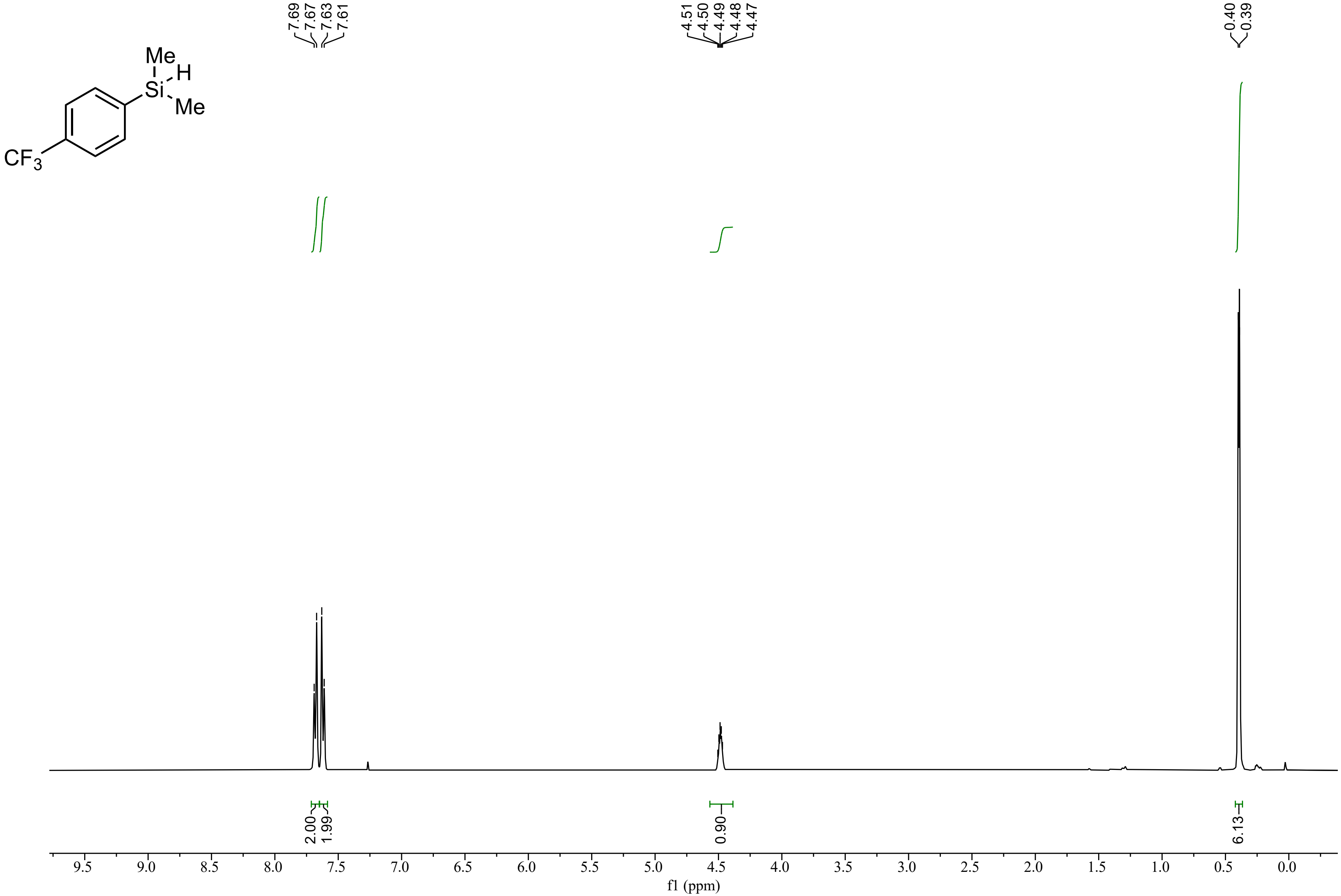

Compound **1i** ^{13}C NMR

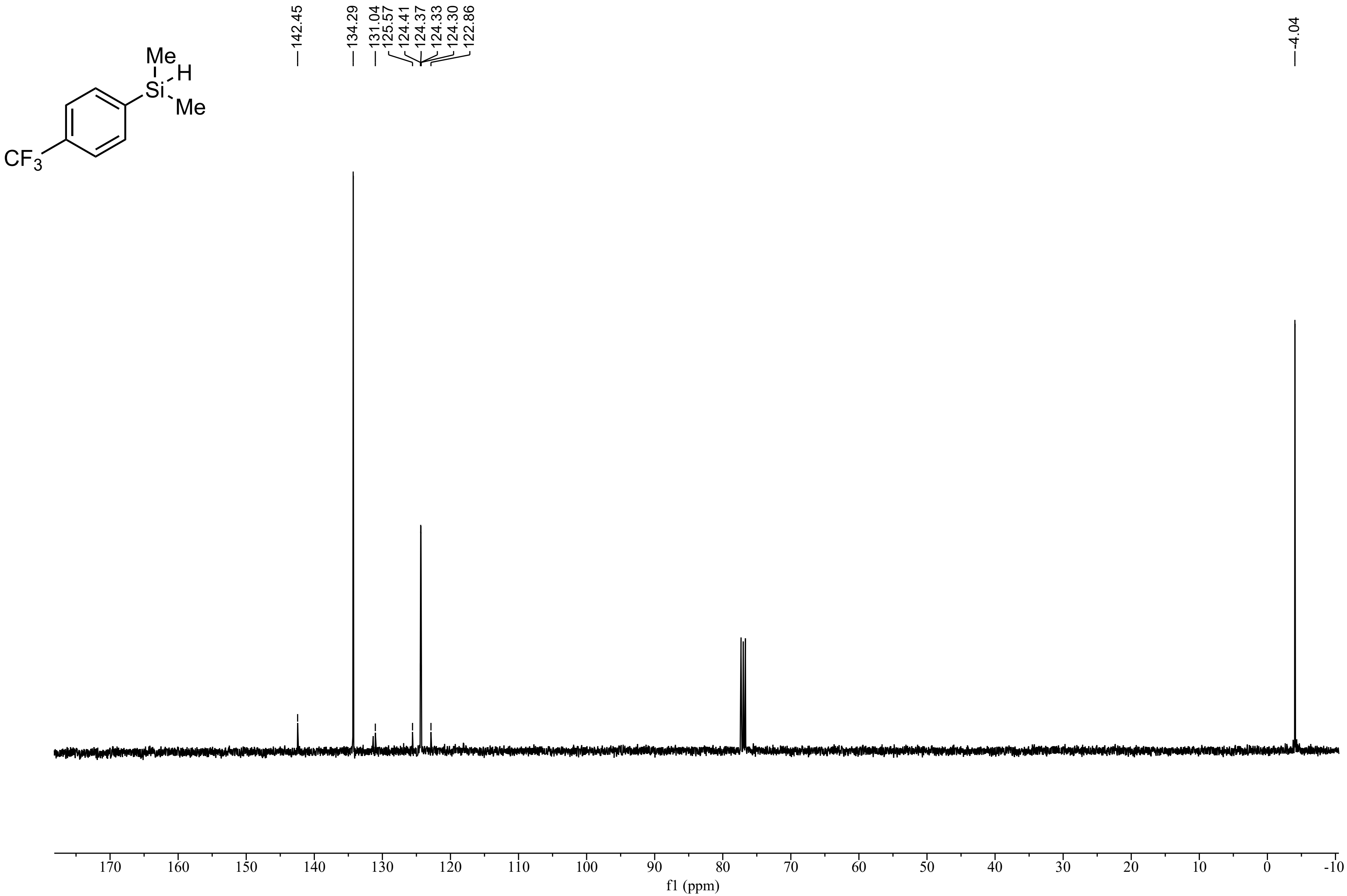

Compound **1i** ^{19}F NMR

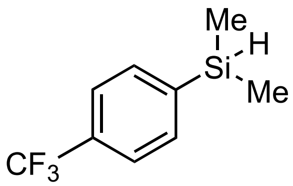

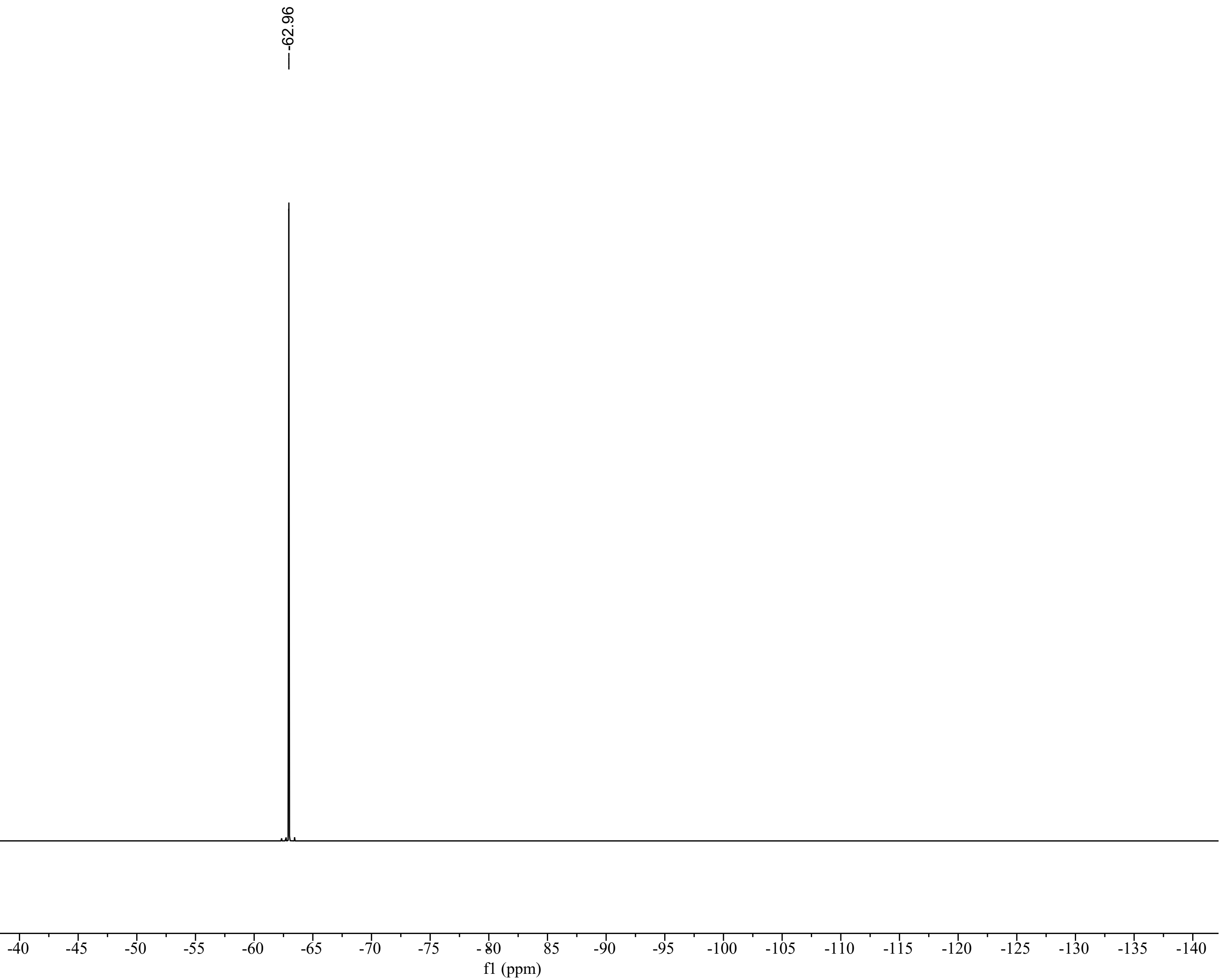

Compound **1j** [1]H NMR

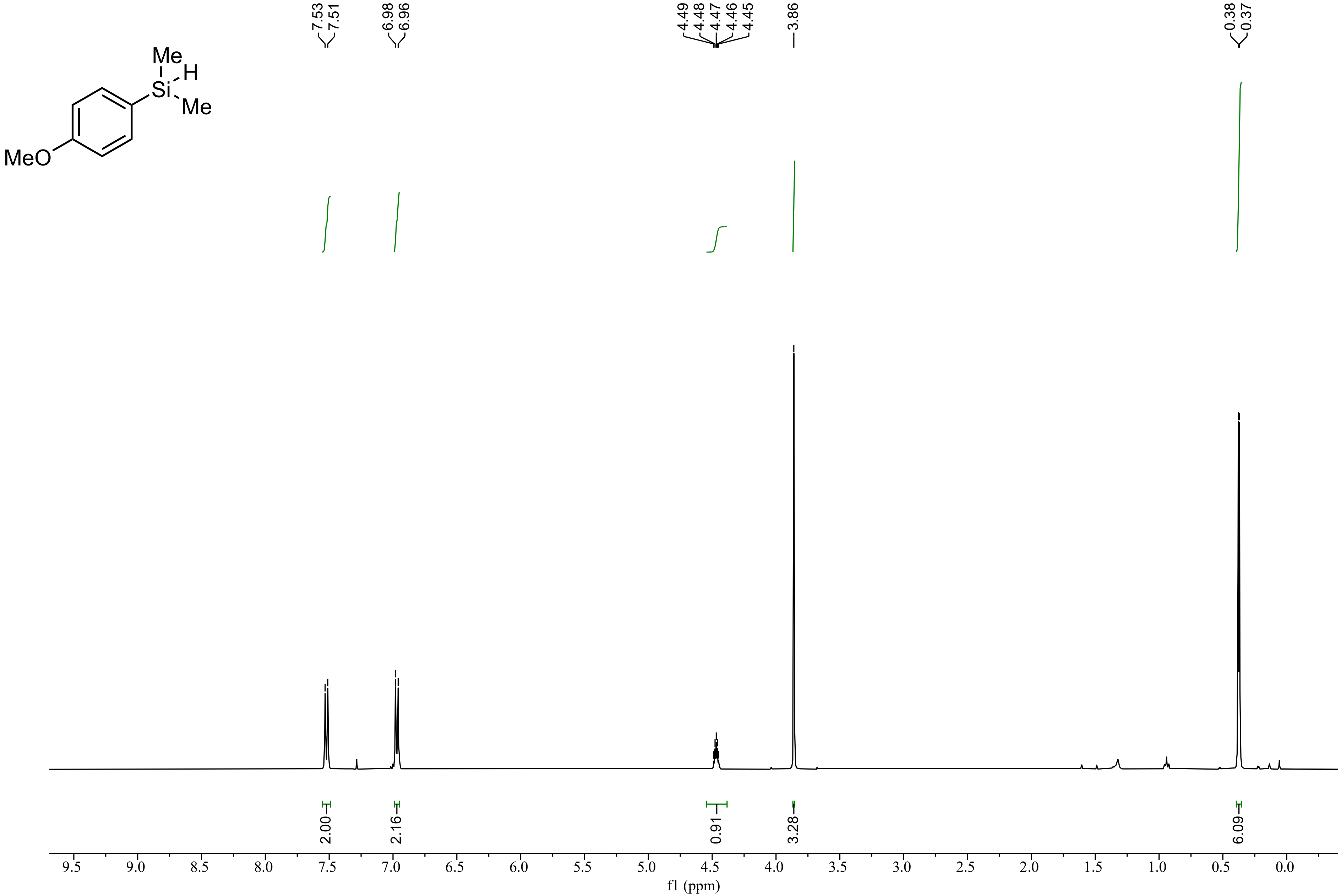

Compound **1j** ^{13}C NMR

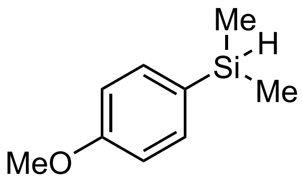

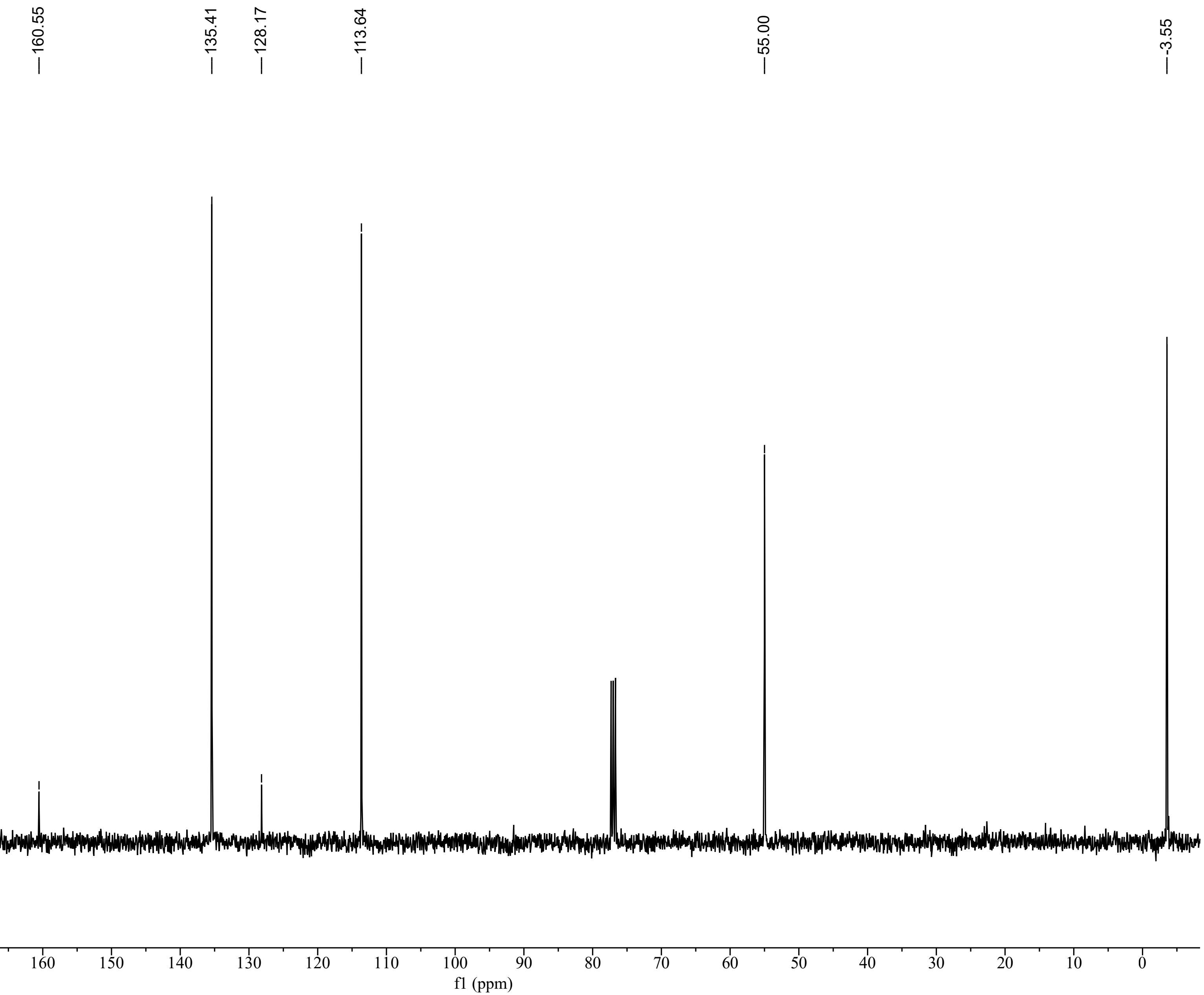

Compound **1k** ^{1}H NMR

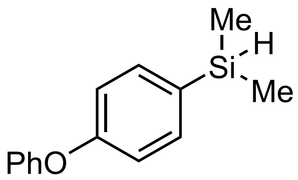

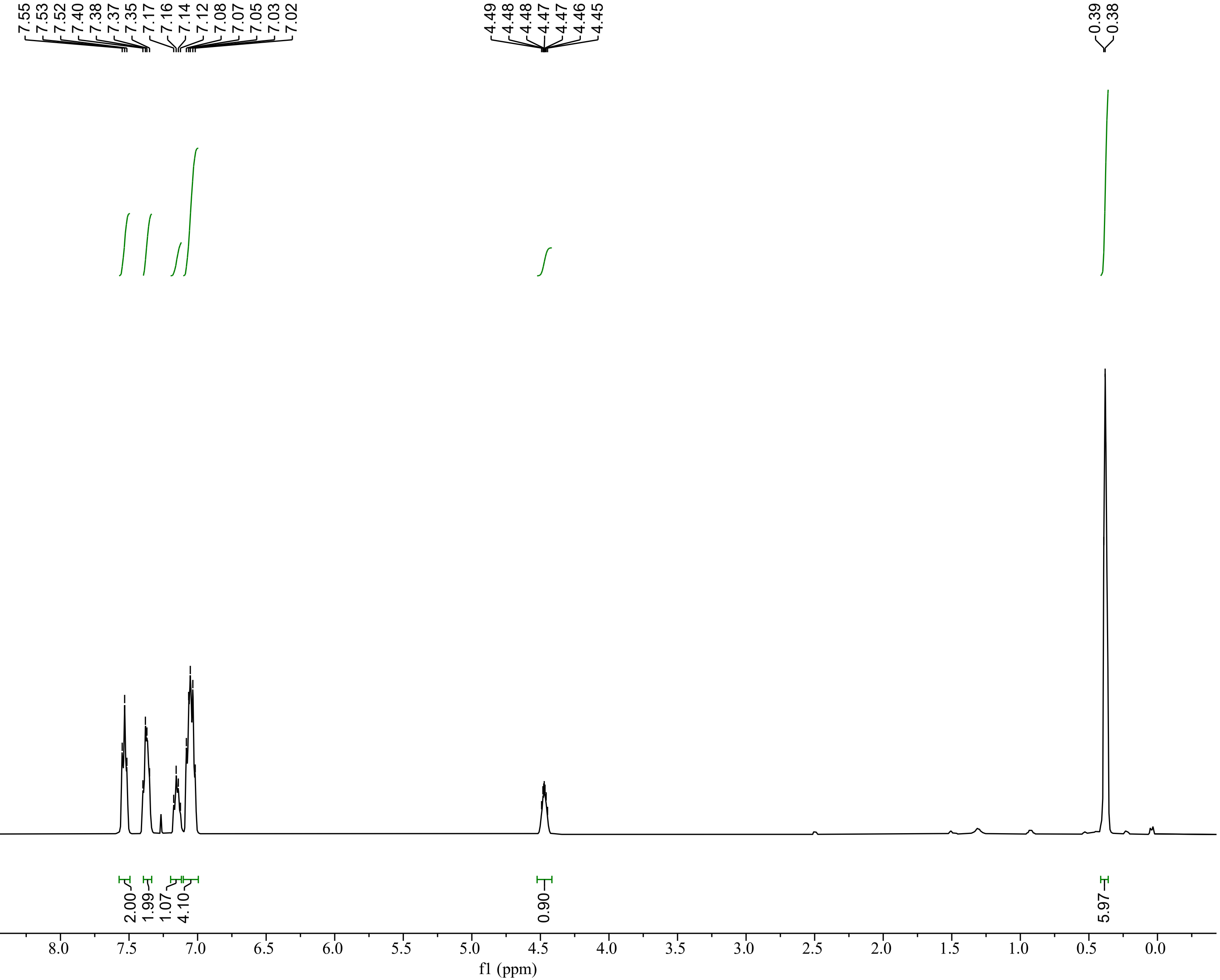

Compound **1k** ^{13}C NMR

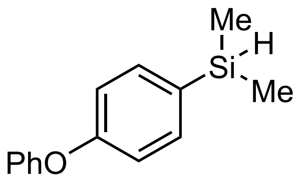

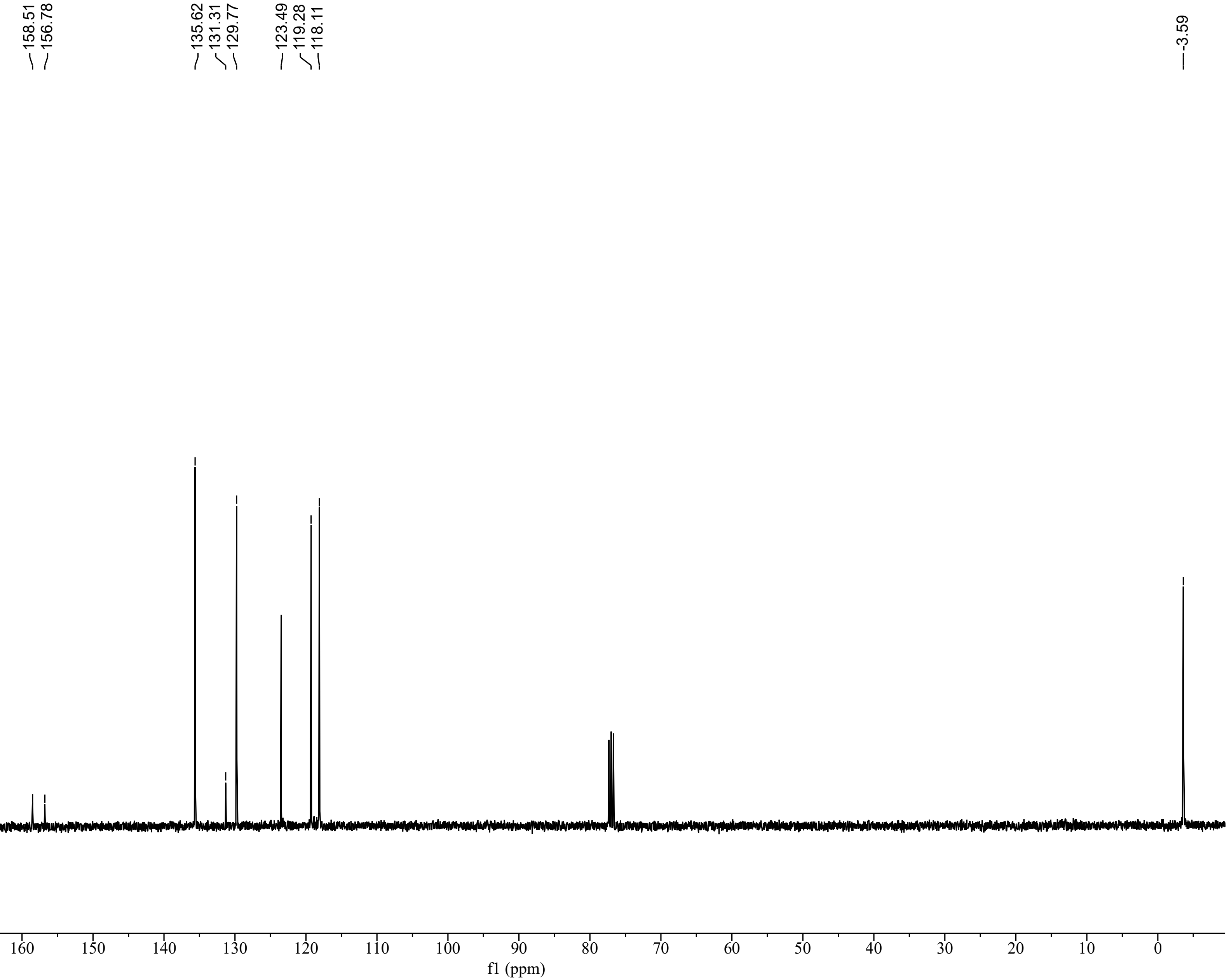

Compound **1l** ^{1}H NMR

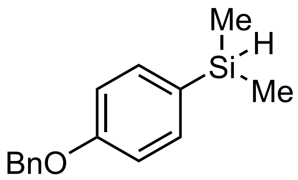

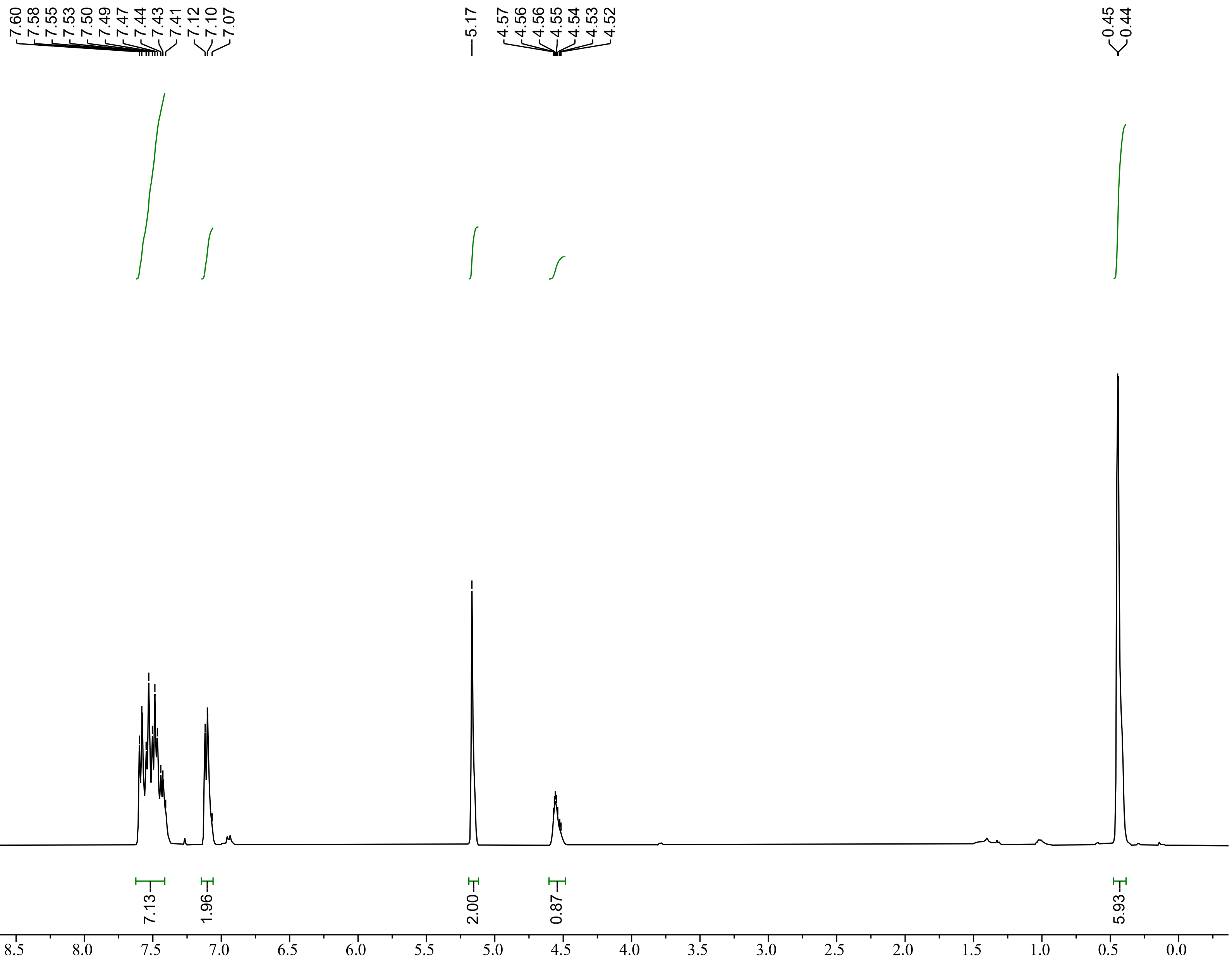

Compound **1l** ^{13}C NMR

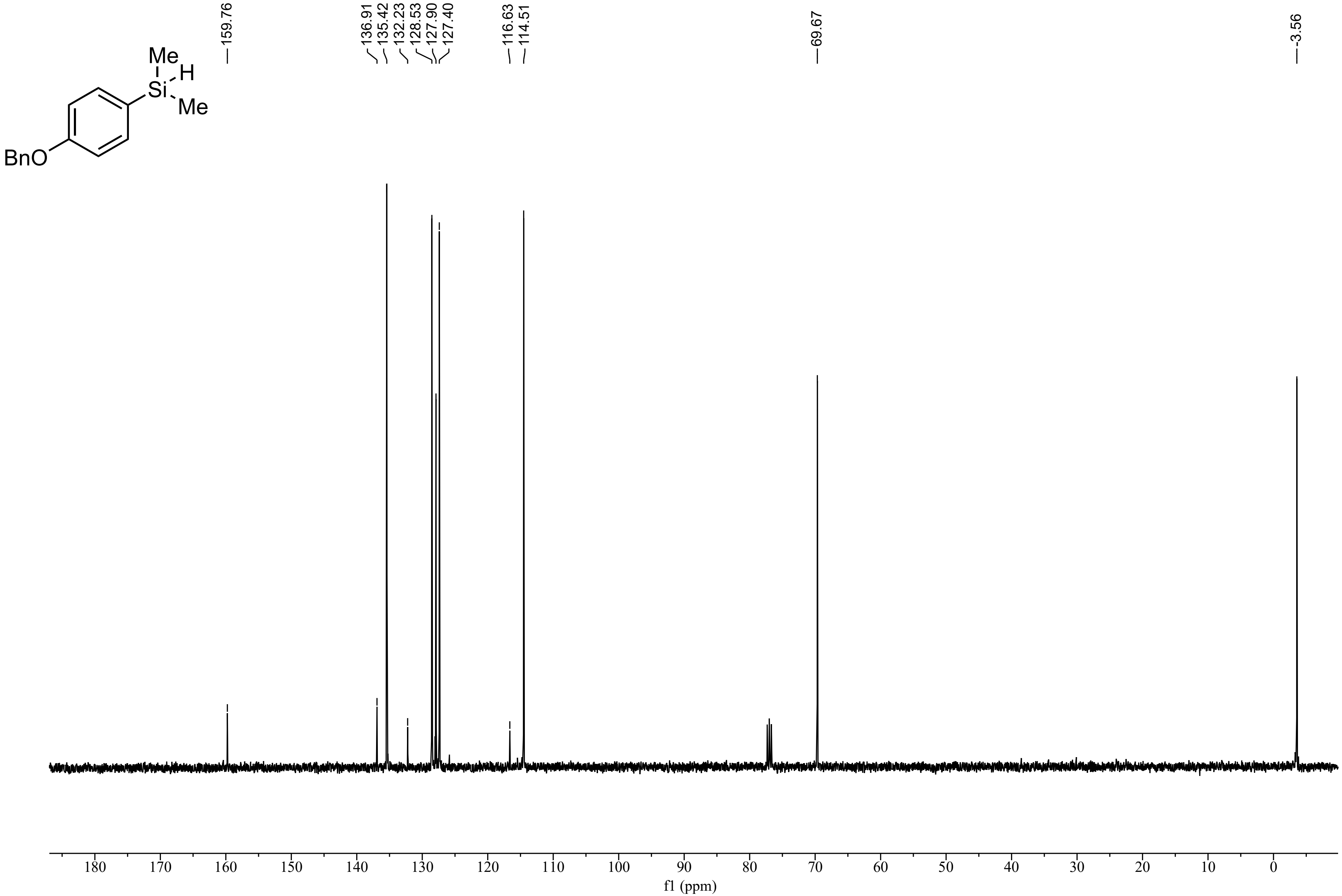

Compound **1m** ^{1}H NMR

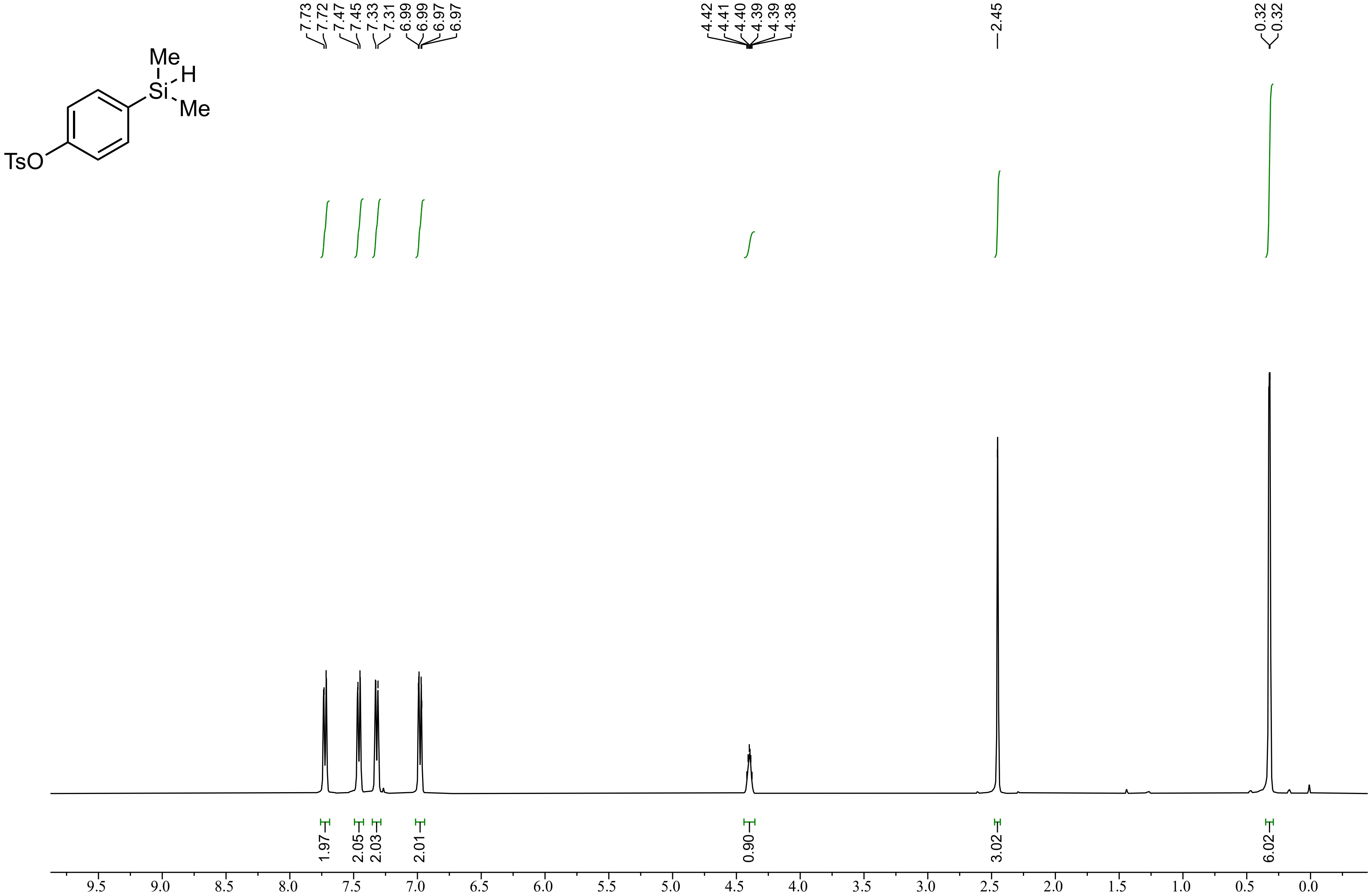

Compound **1m** ^{13}C NMR

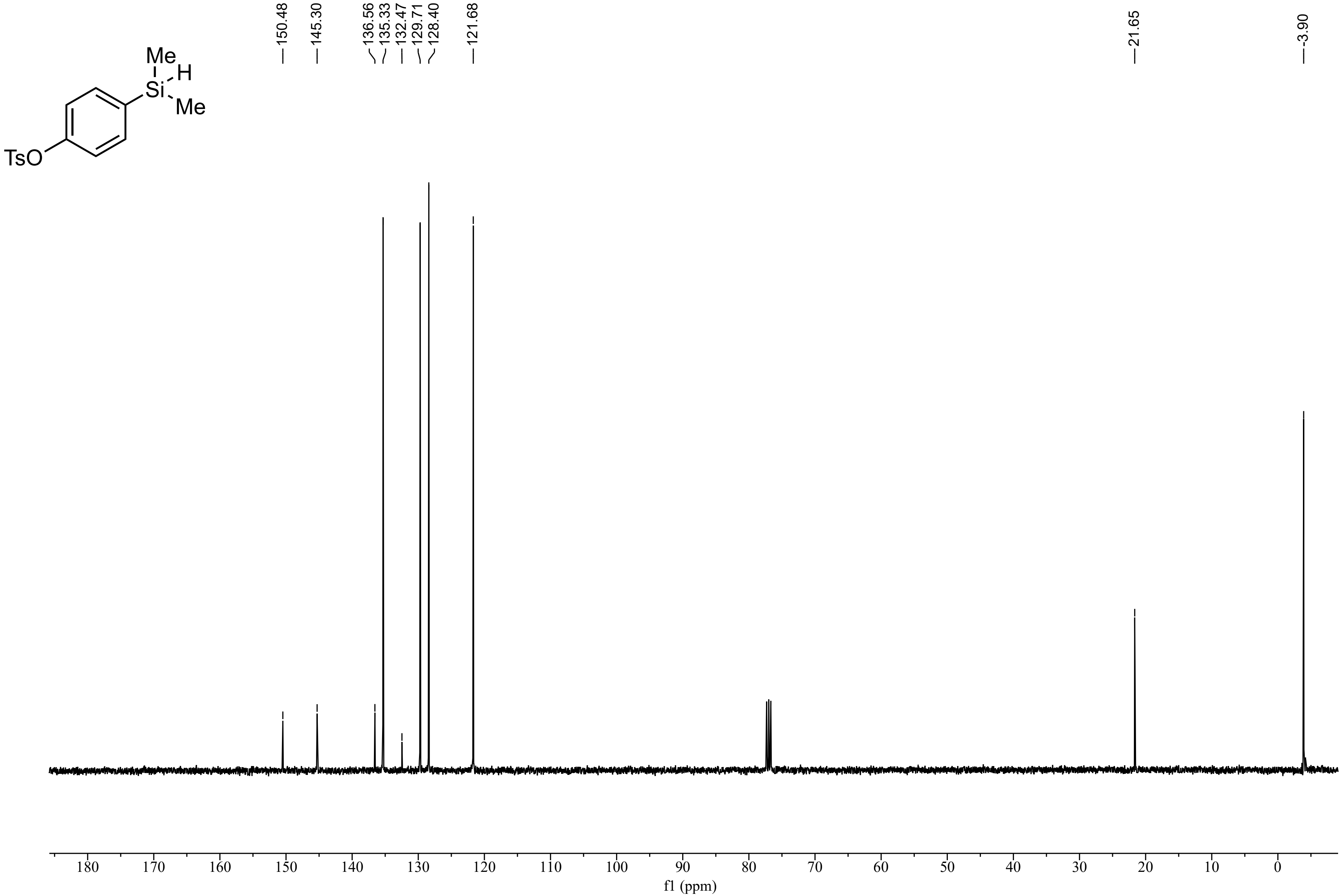

Compound **1n** ^{1}H NMR

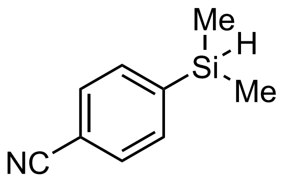

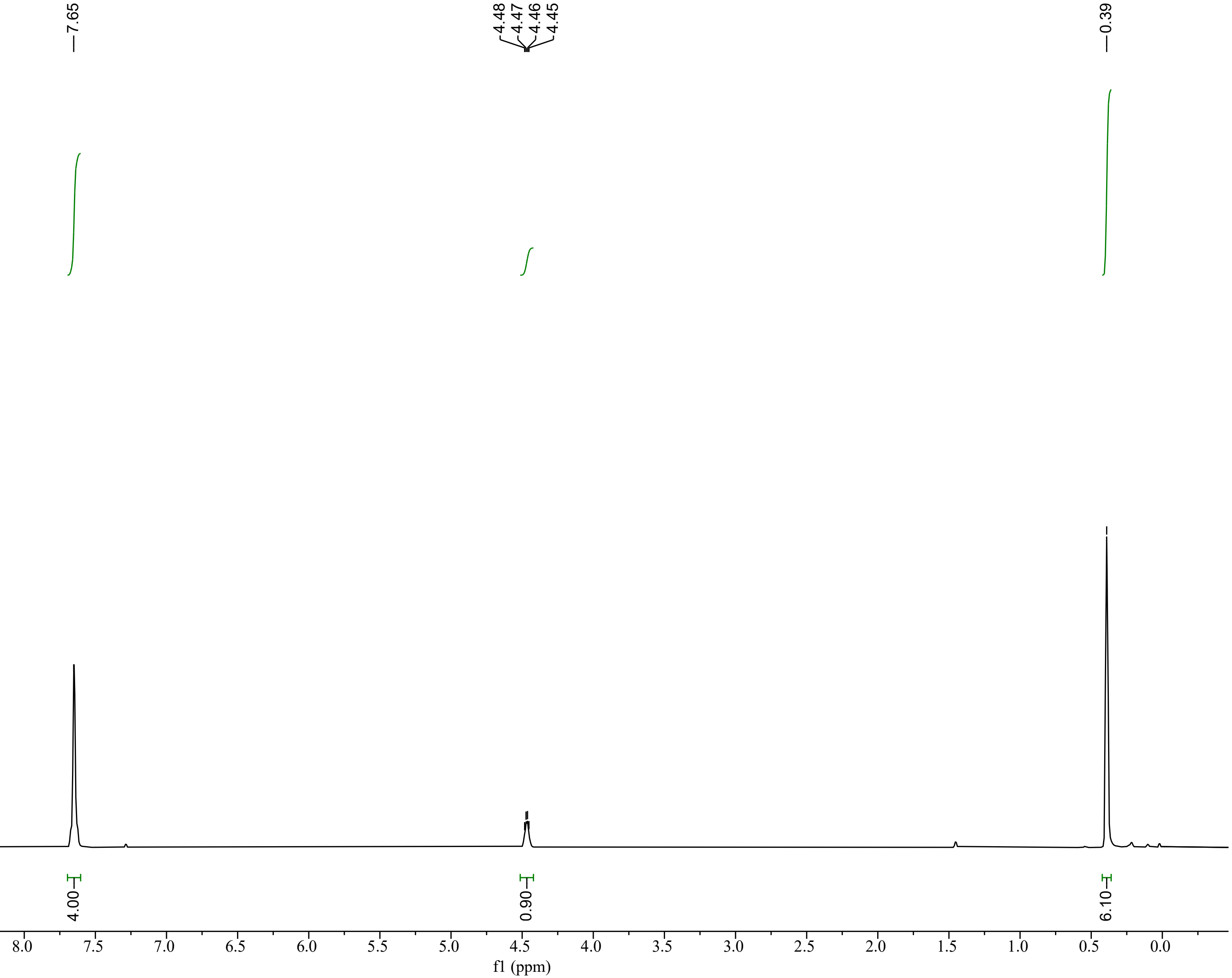

Compound **1n** ^{13}C NMR

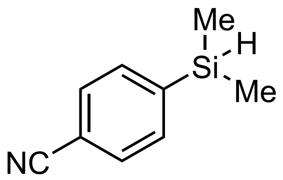

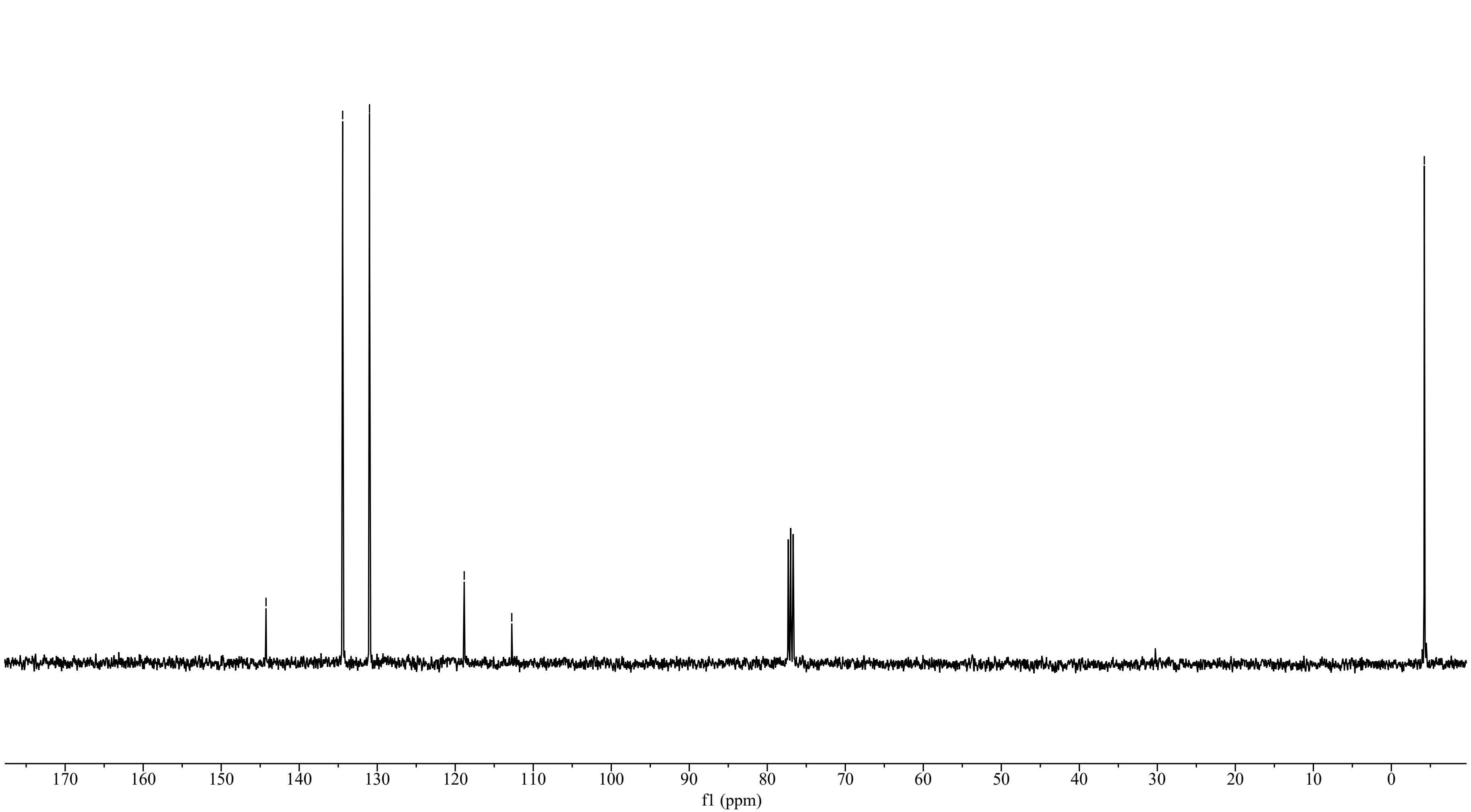

Compound **1o** [1]H NMR

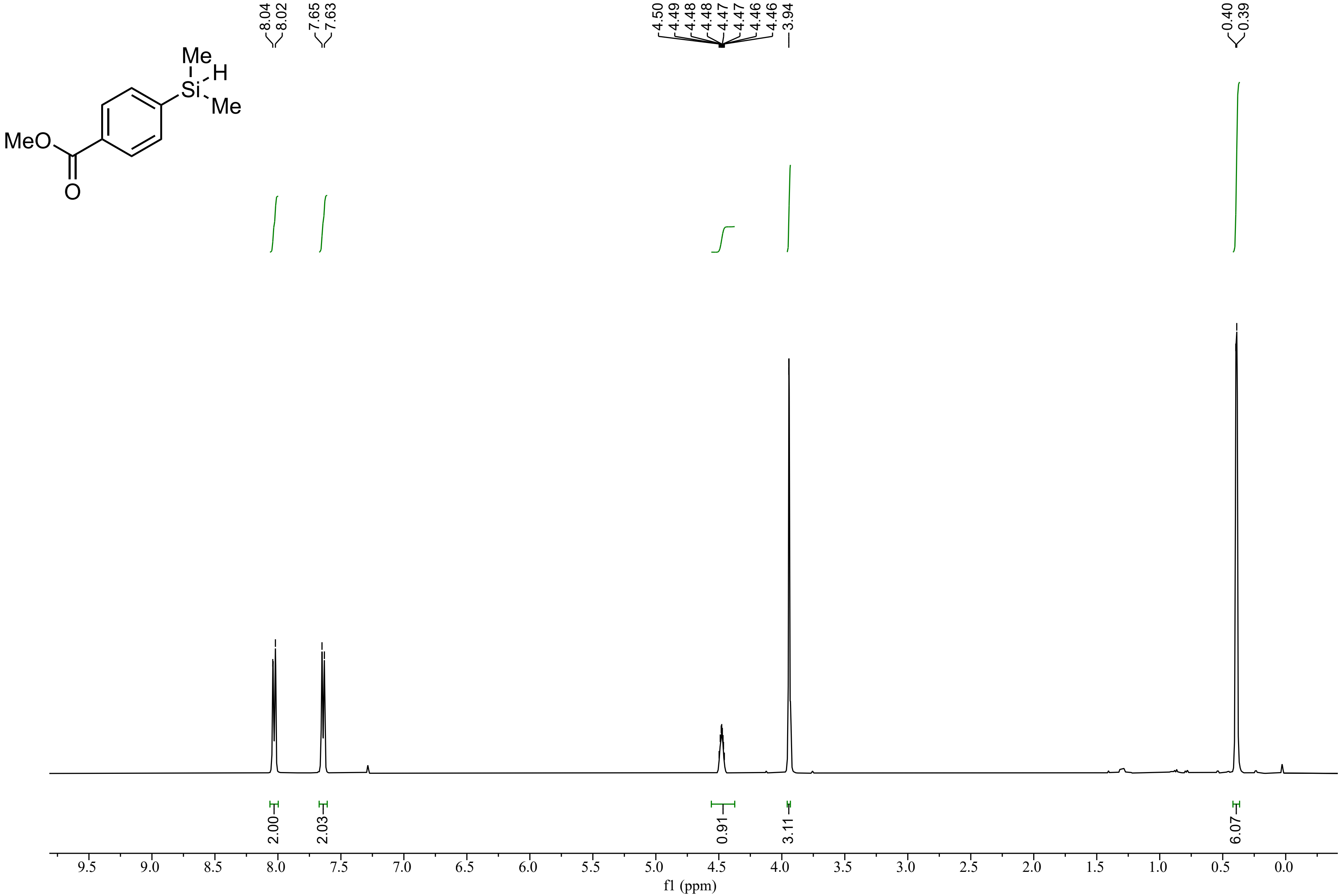

Compound **1o** ^{13}C NMR

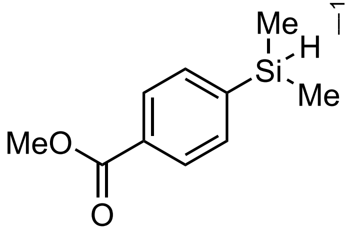

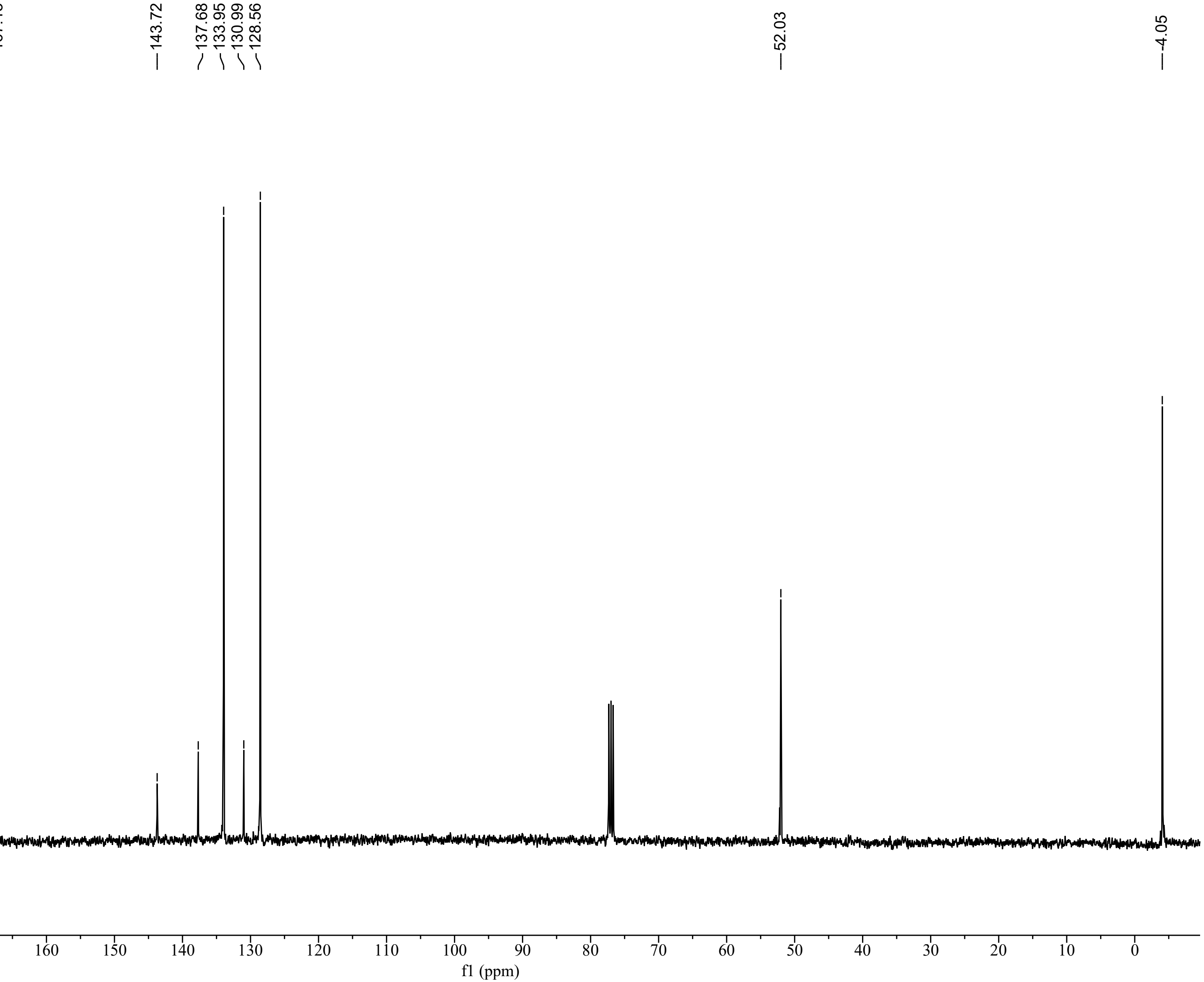

Compound **1p** ^{1}H NMR

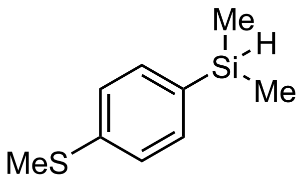

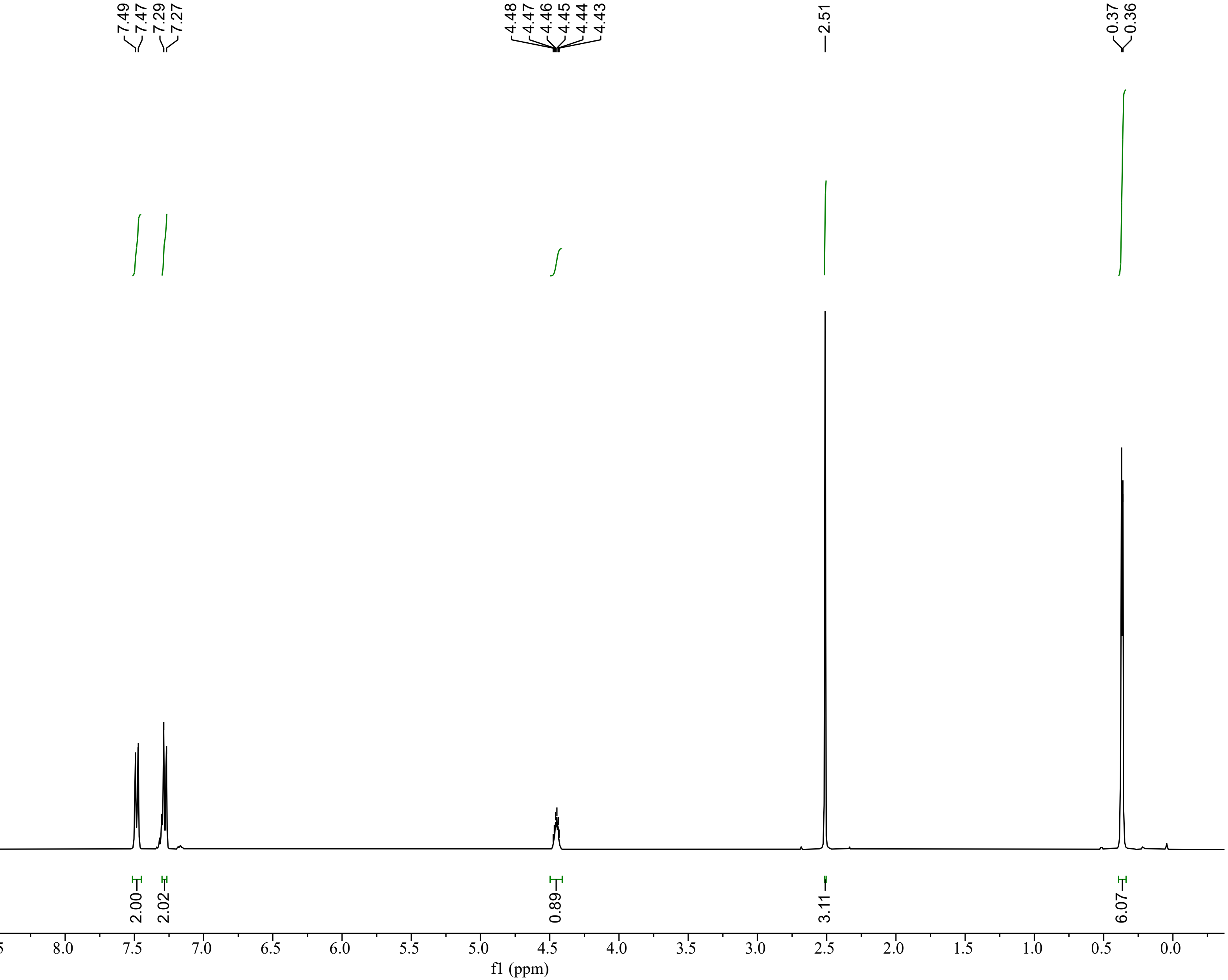

Compound **1p** ^{13}C NMR

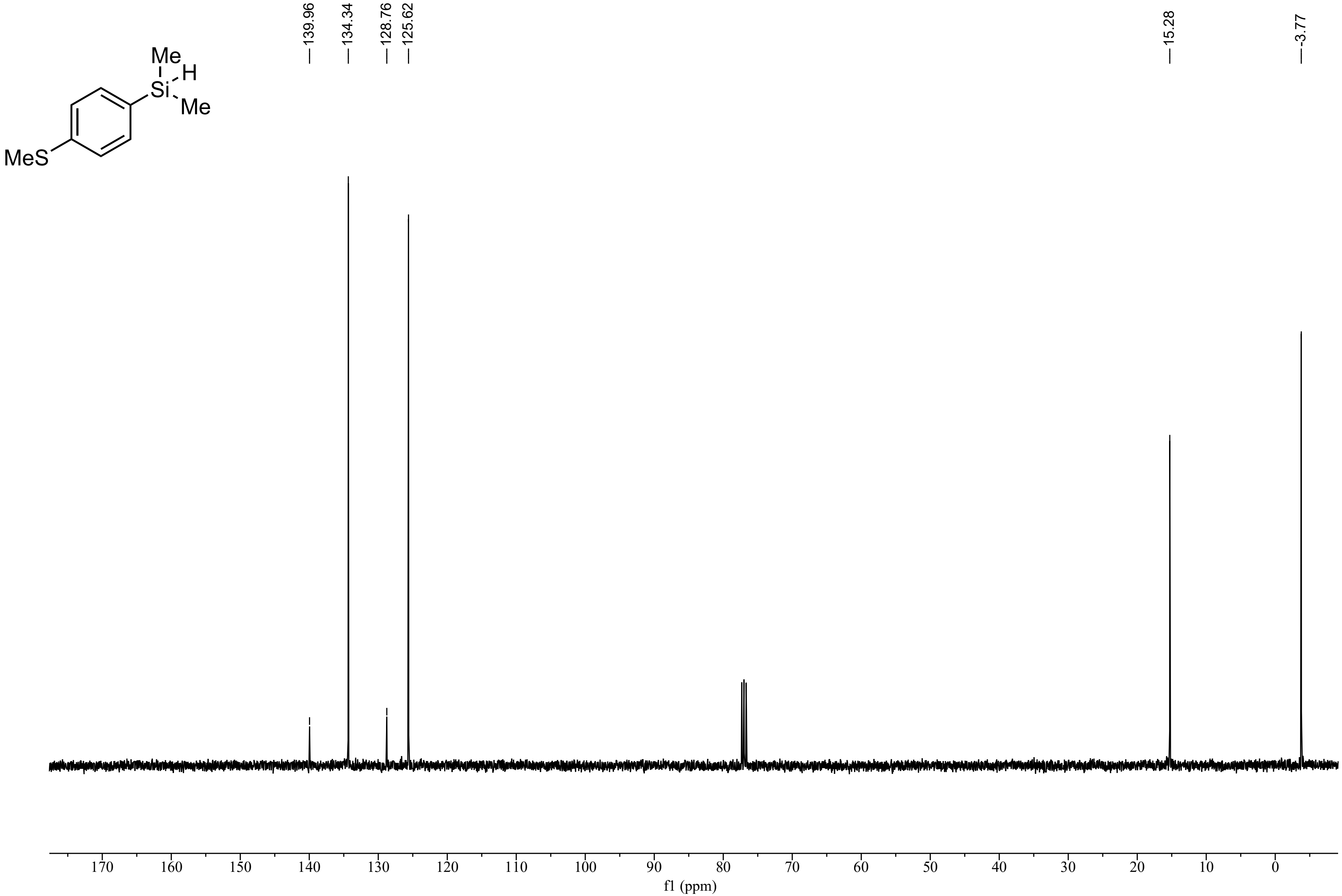

Compound **1q** ^{1}H NMR

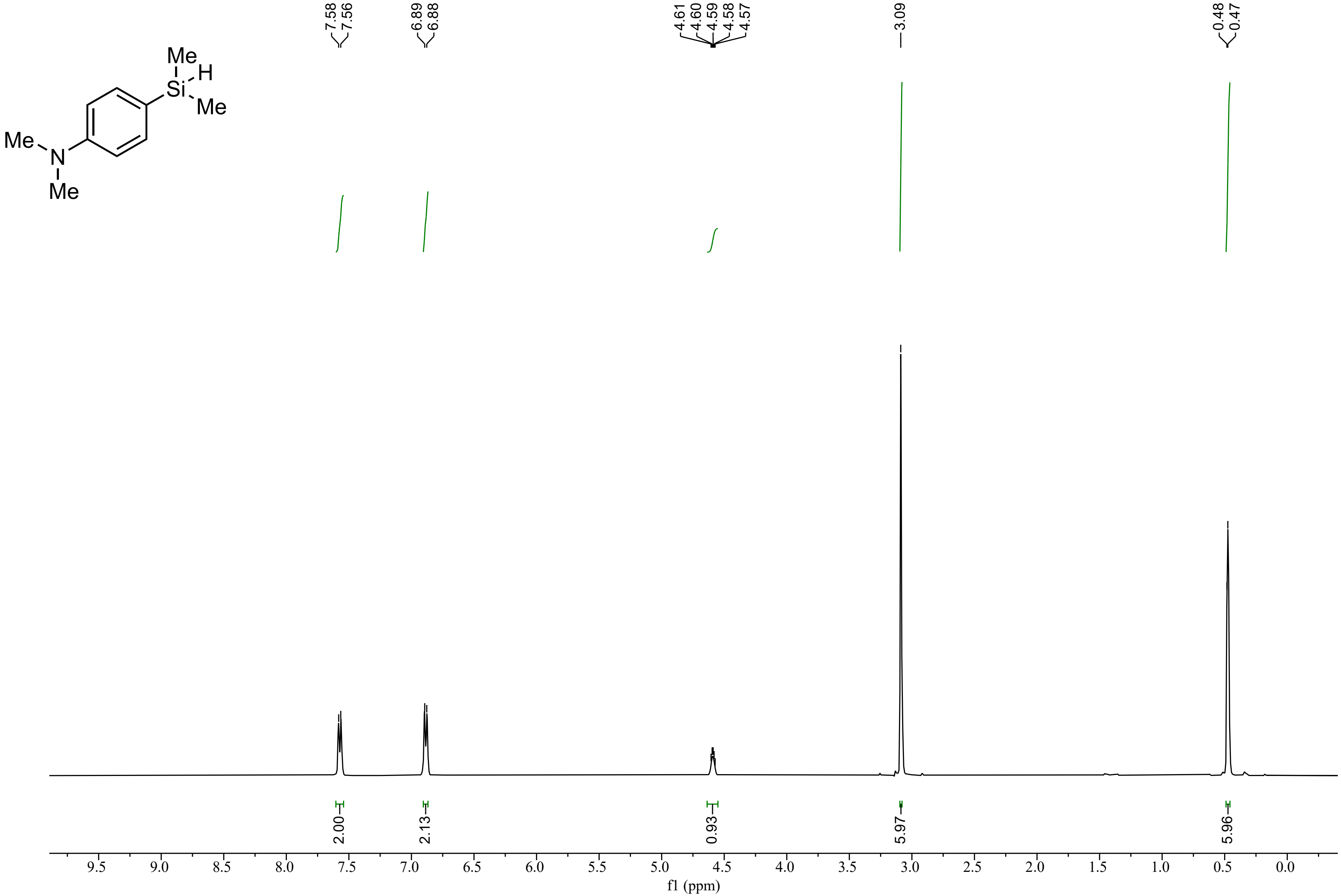

Compound **1q** ^{13}C NMR

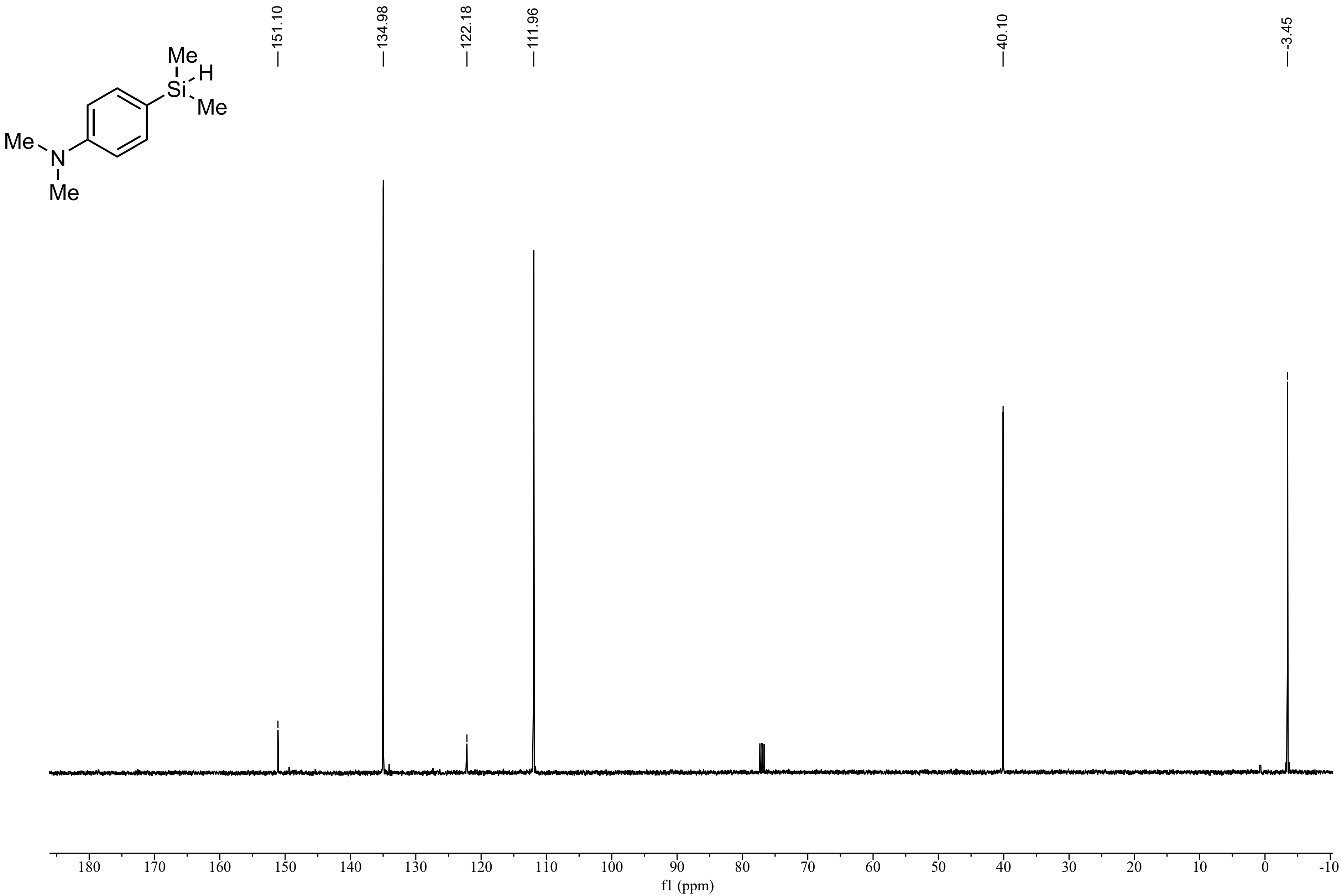

Compound **1r** ^{1}H NMR

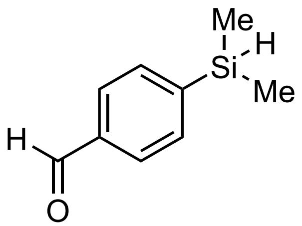

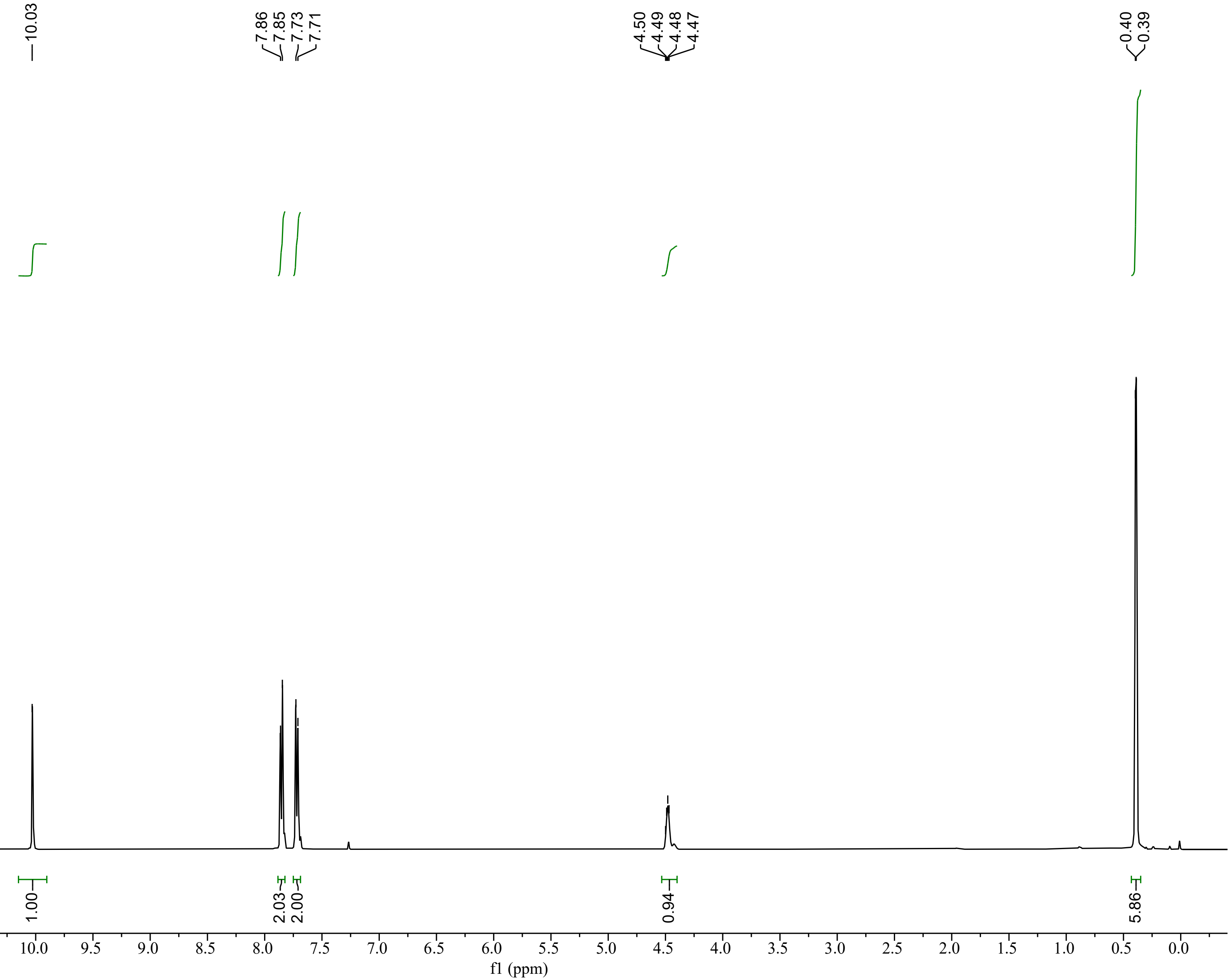

Compound **1r** ^{13}C NMR

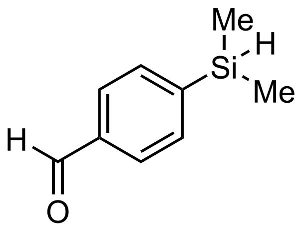

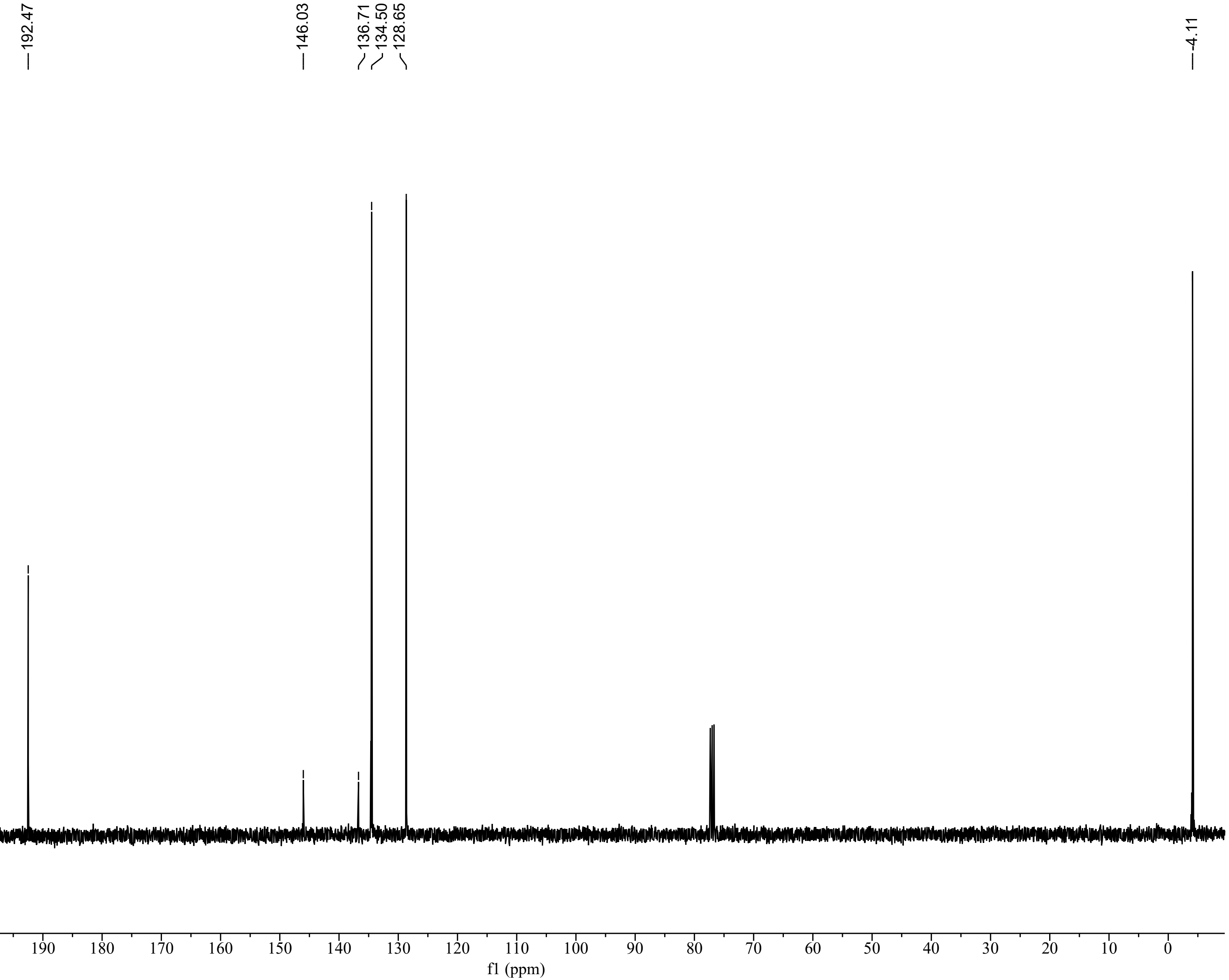

Compound **1s** ^{1}H NMR

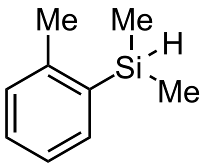

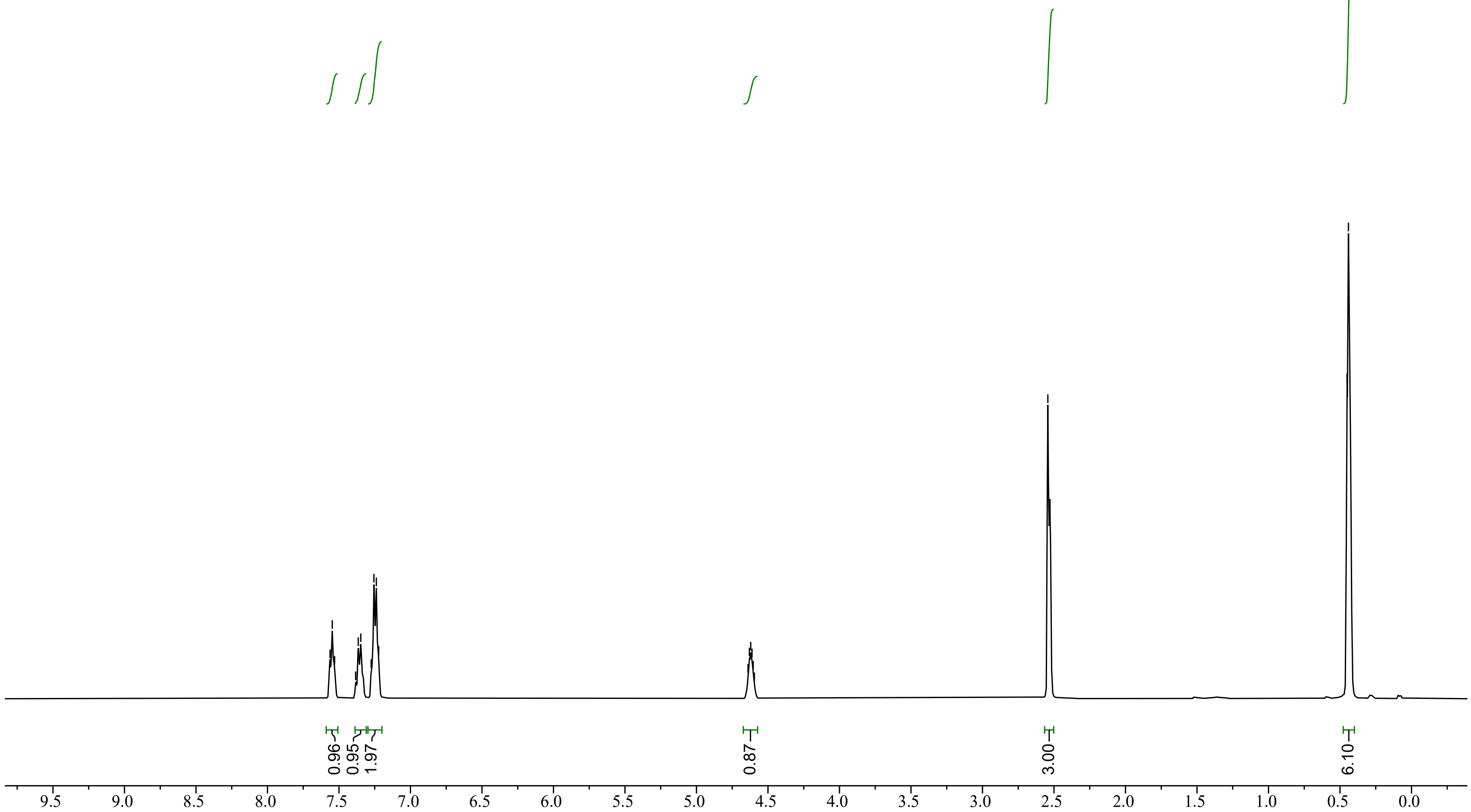

Compound **1s** ^{13}C NMR

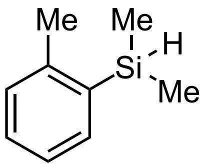

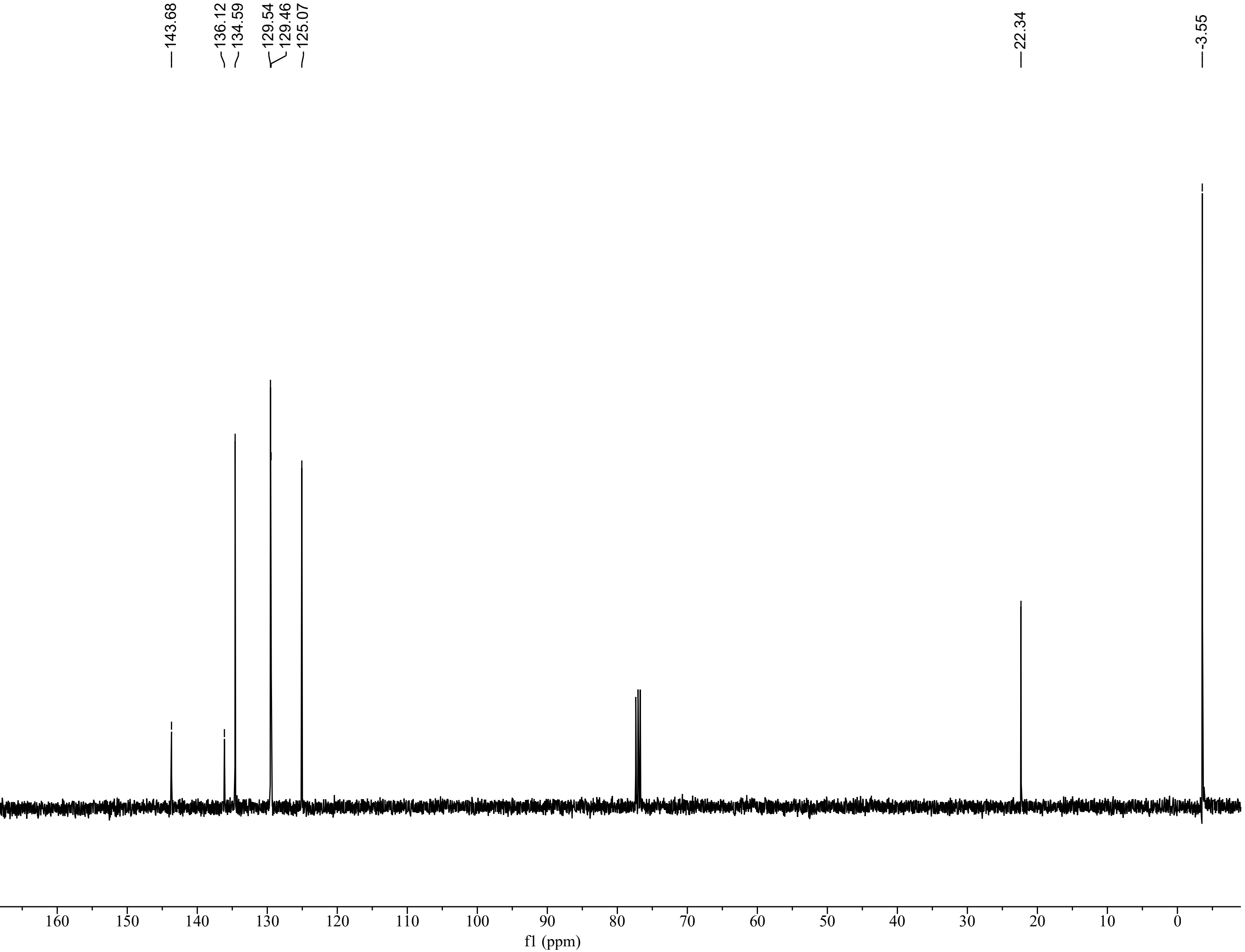

Compound **1t** ^{1}H NMR

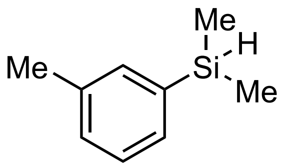

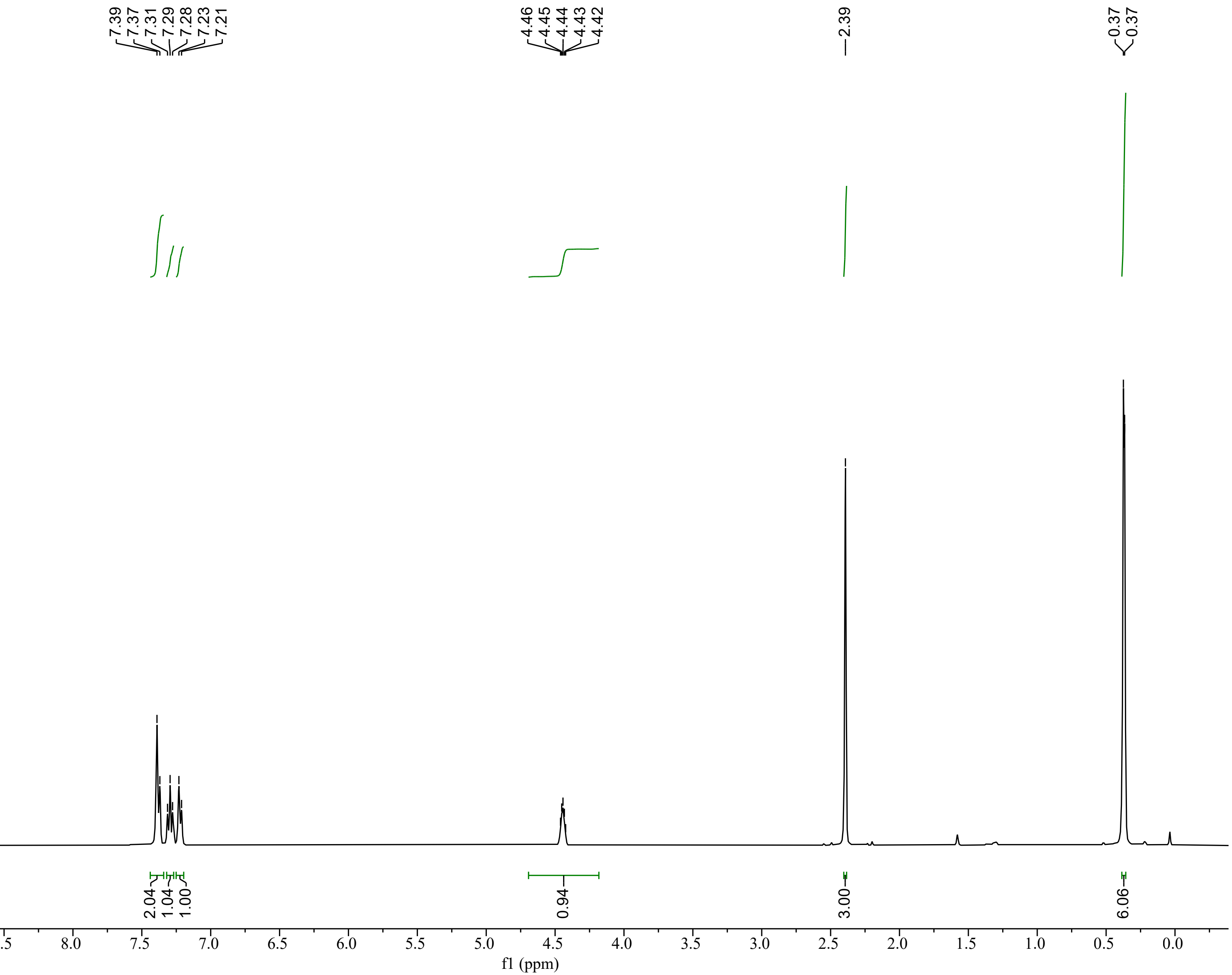

Compound **1t** ^{13}C NMR

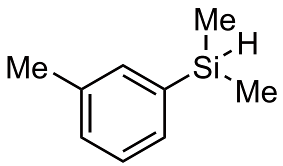

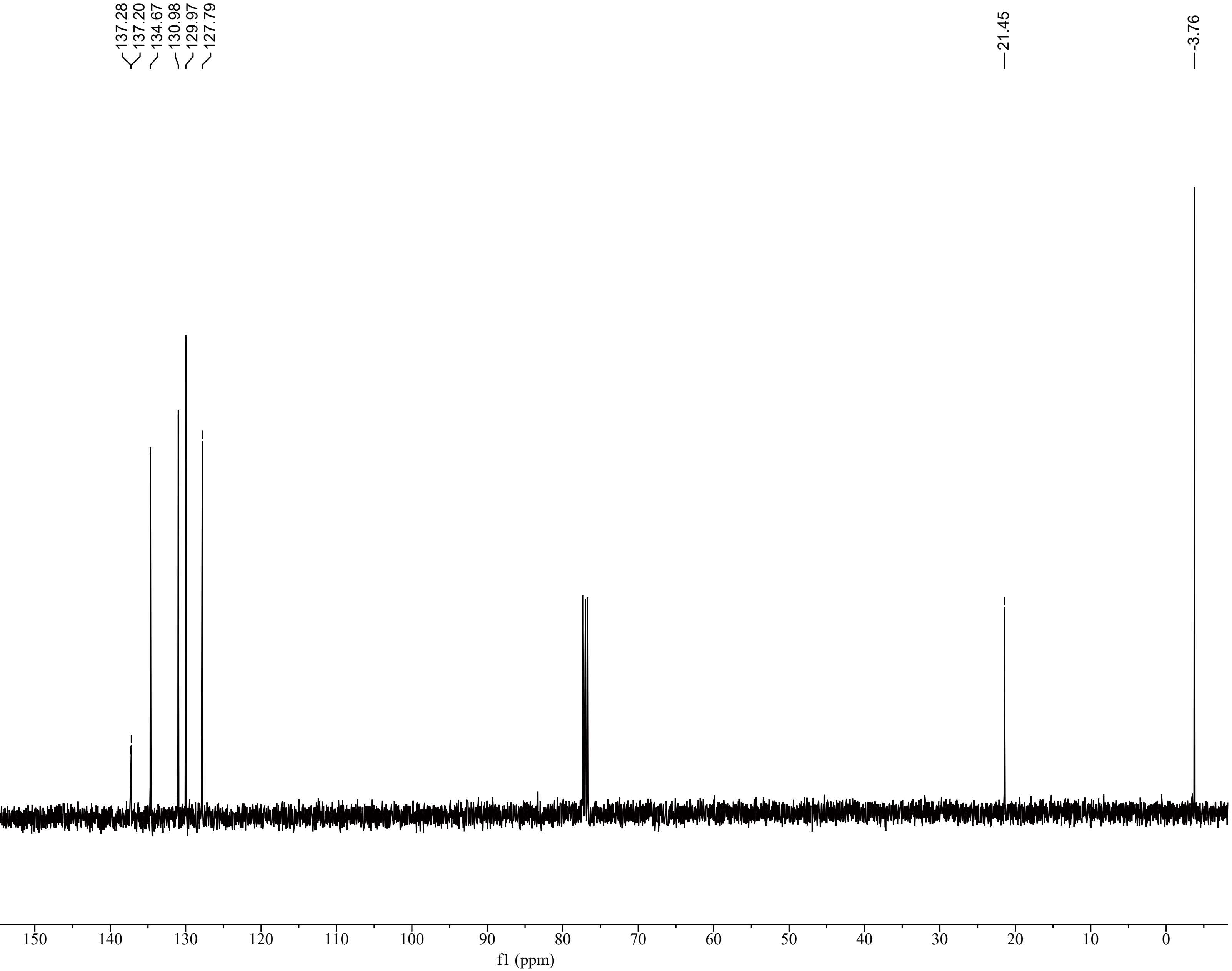

Compound **1u** ^{1}H NMR

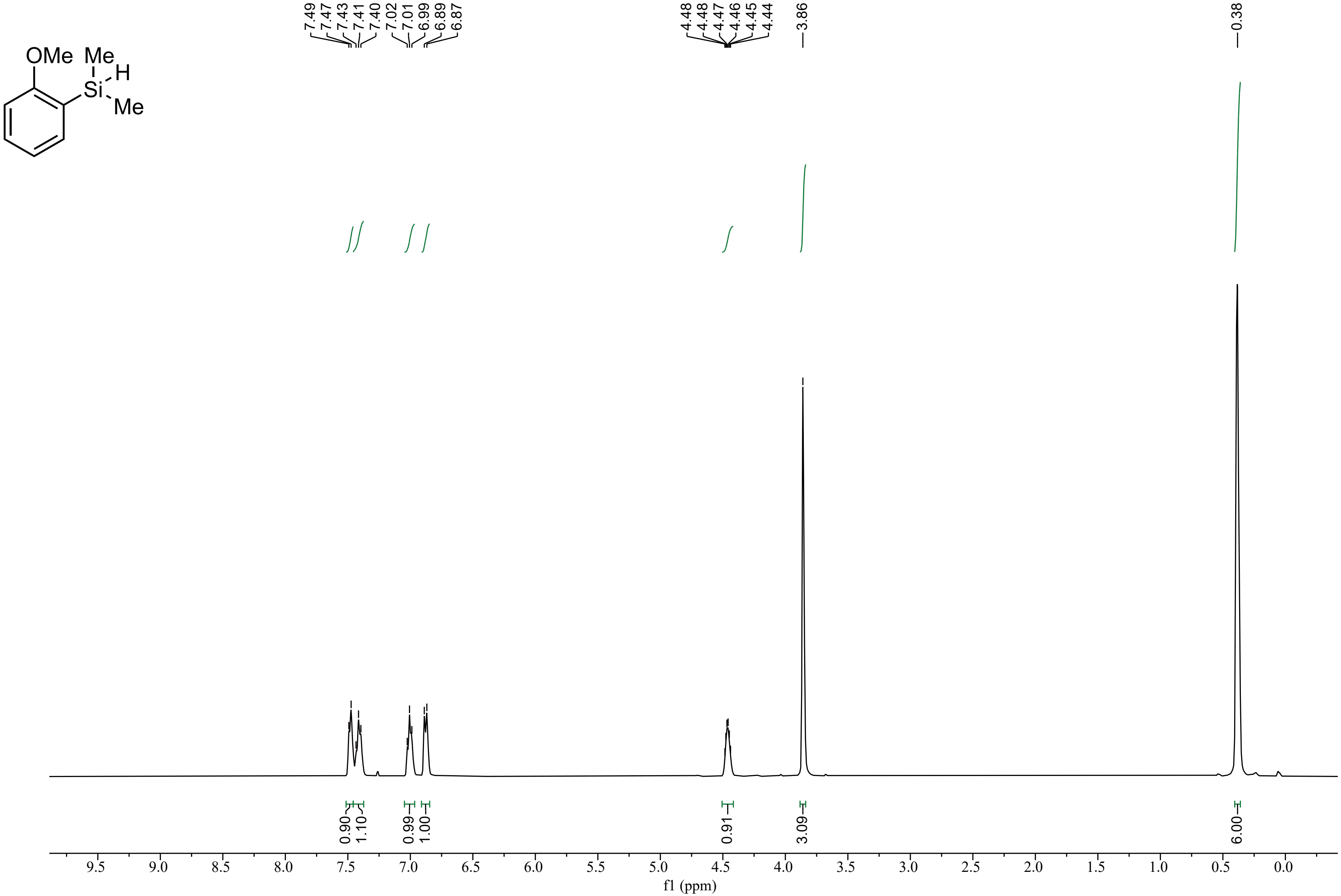

Compound **1u** ^{13}C NMR

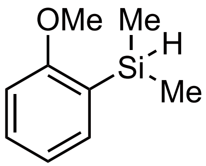

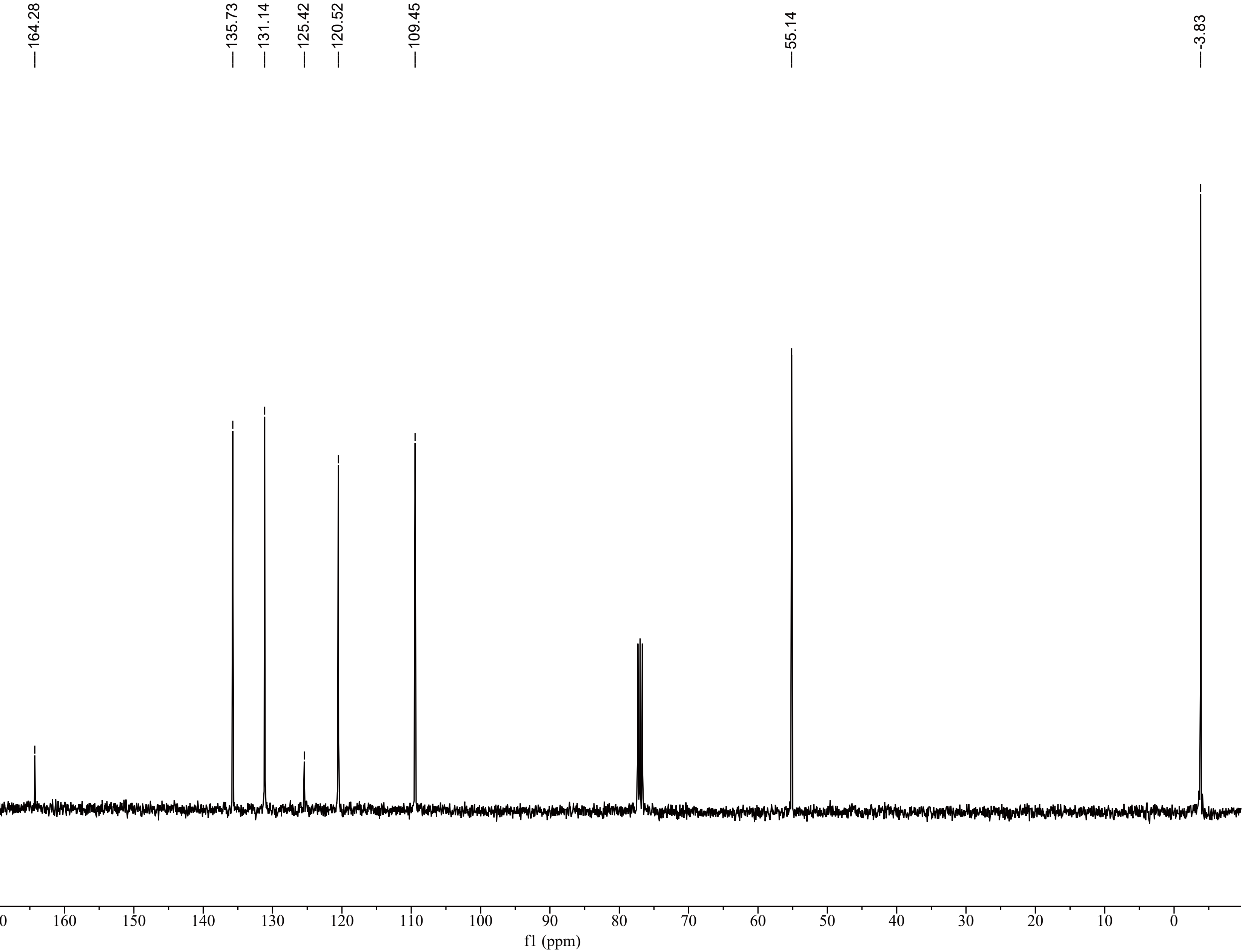

Compound **1v** ^{1}H NMR

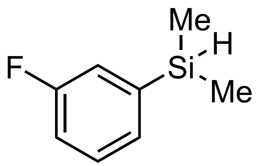

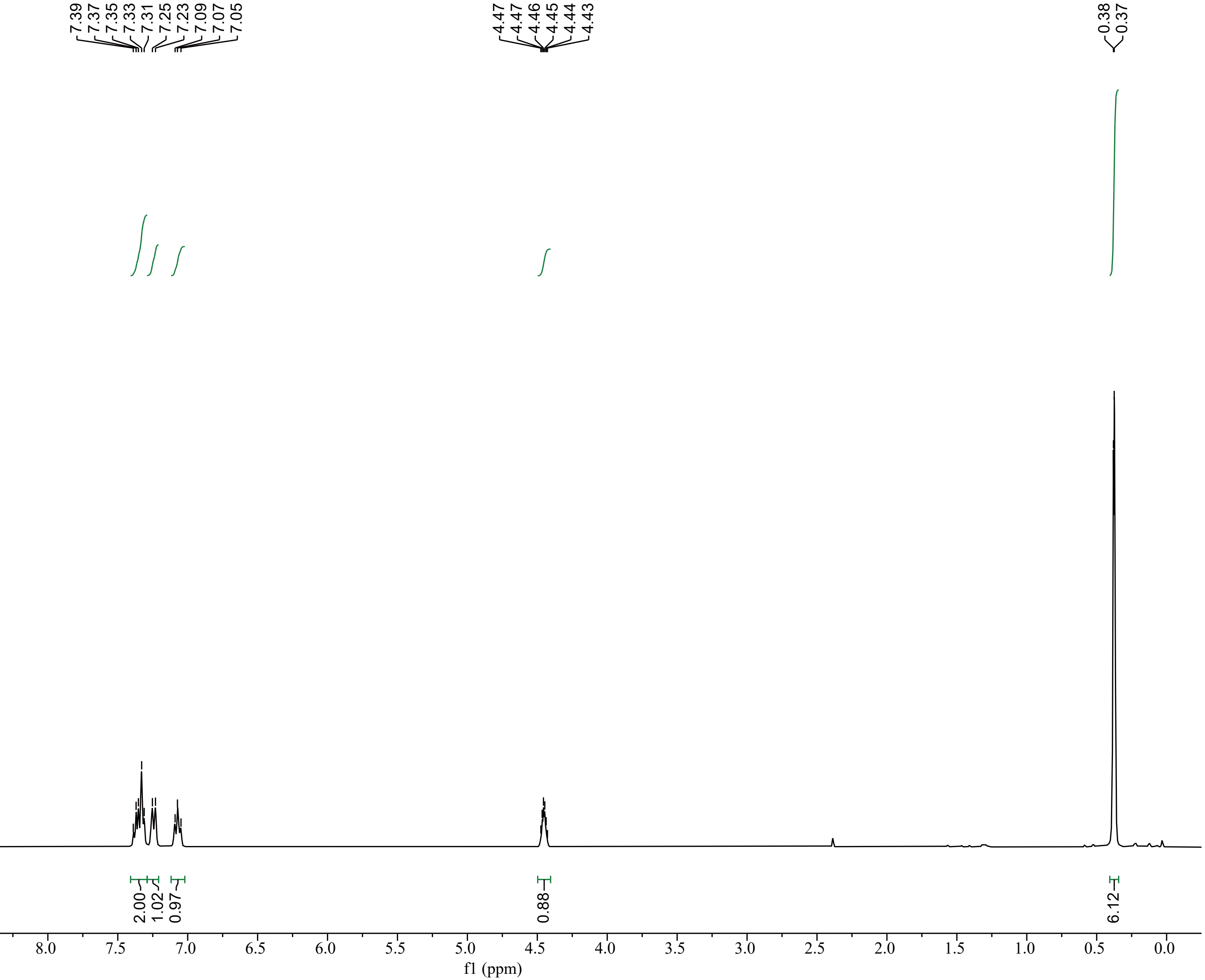

Compound **1v** ^{13}C NMR

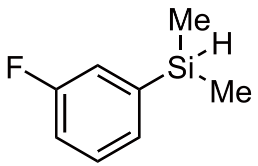

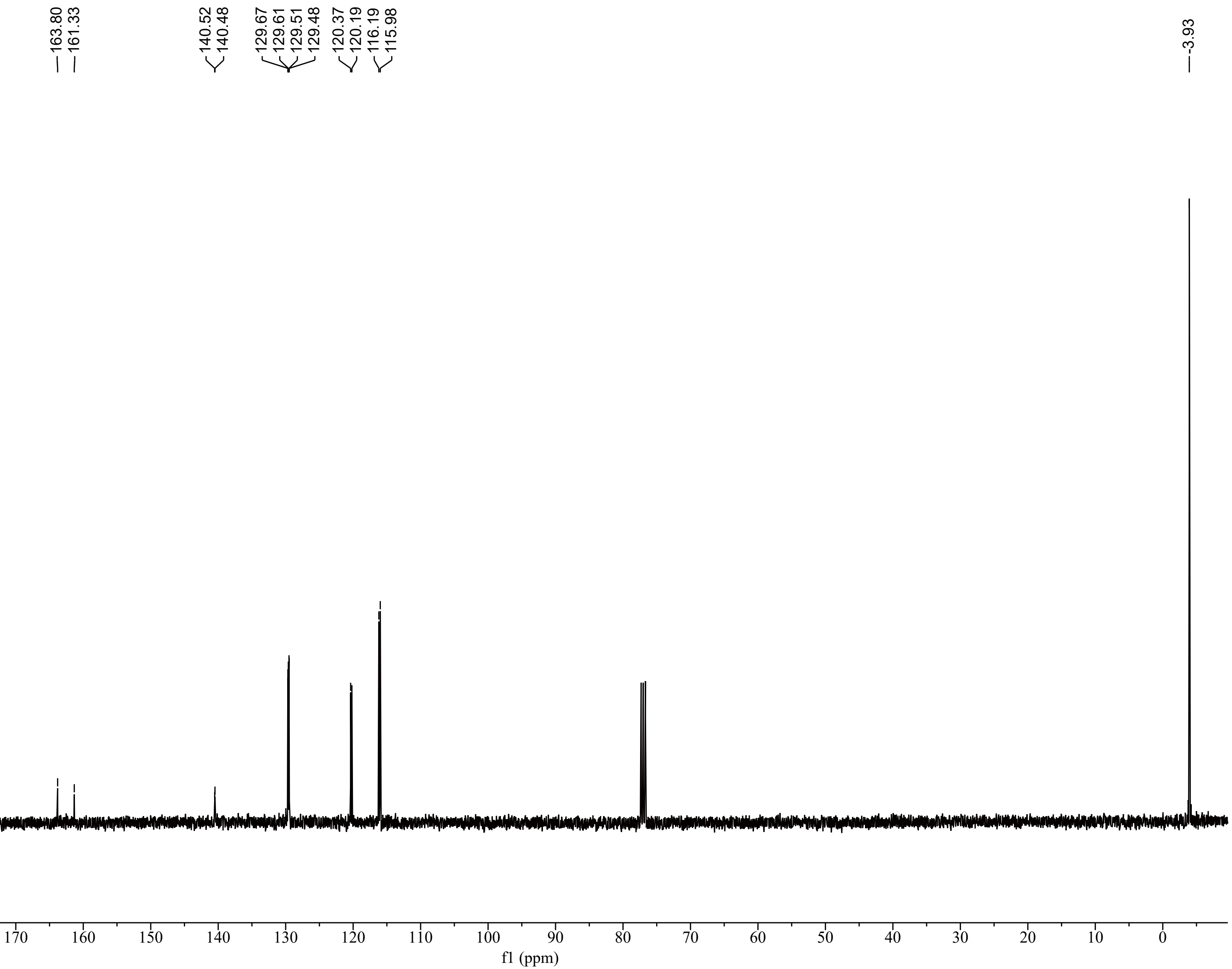

Compound **1v** ^{19}F NMR

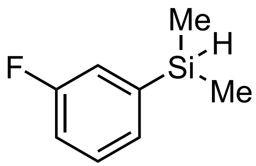

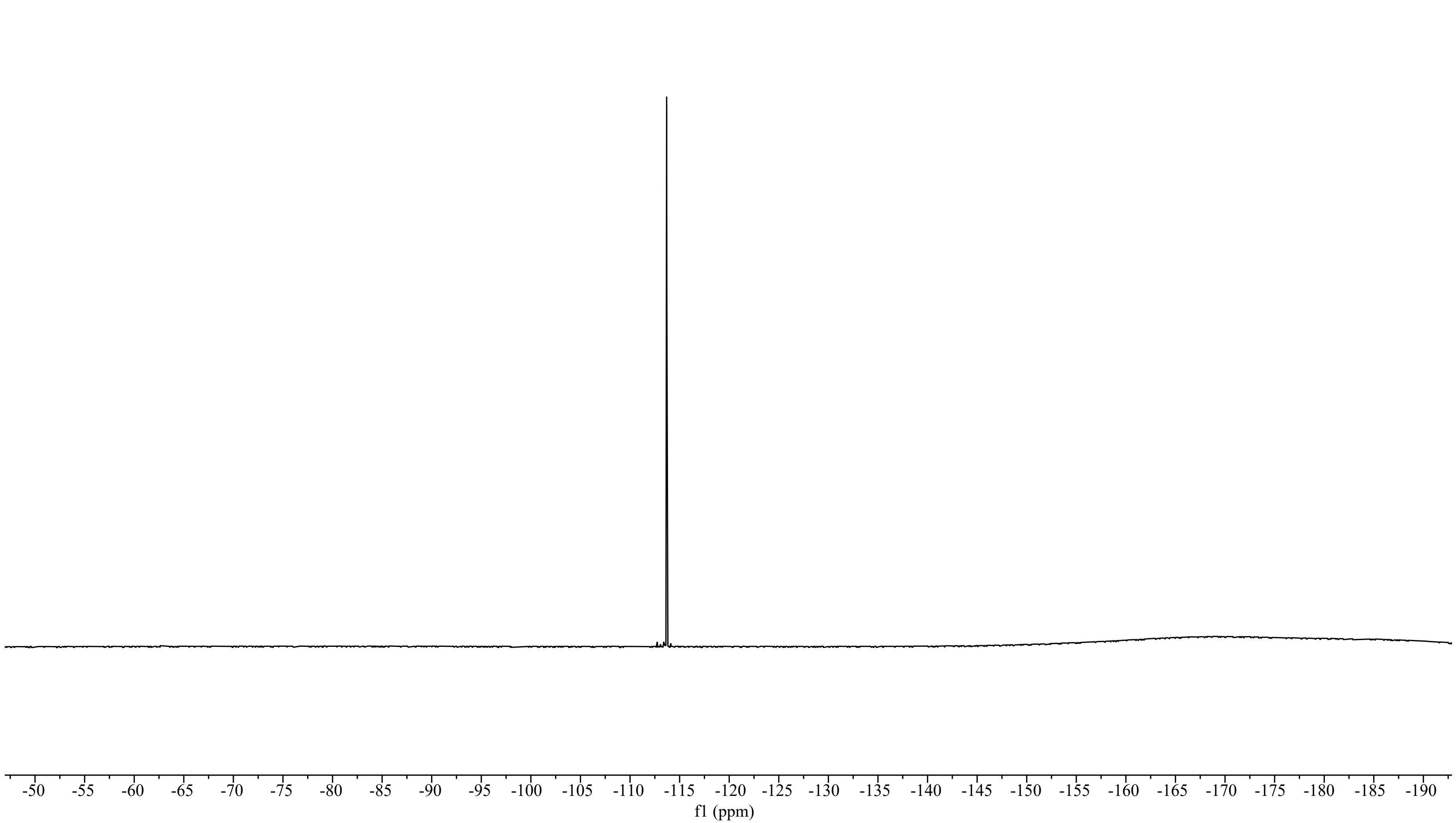

Compound **1w** ^{1}H NMR

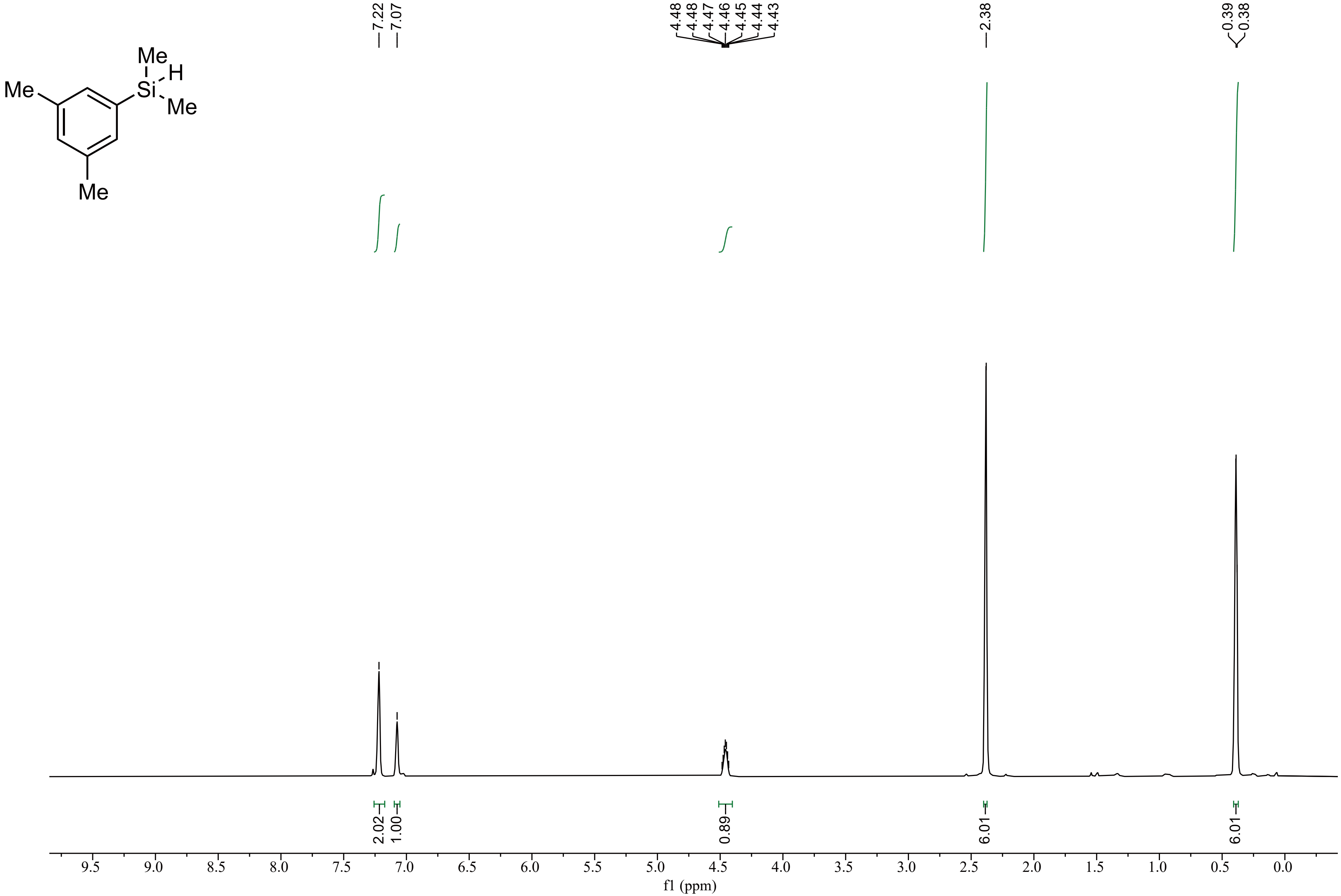

Compound **1w** ^{13}C NMR

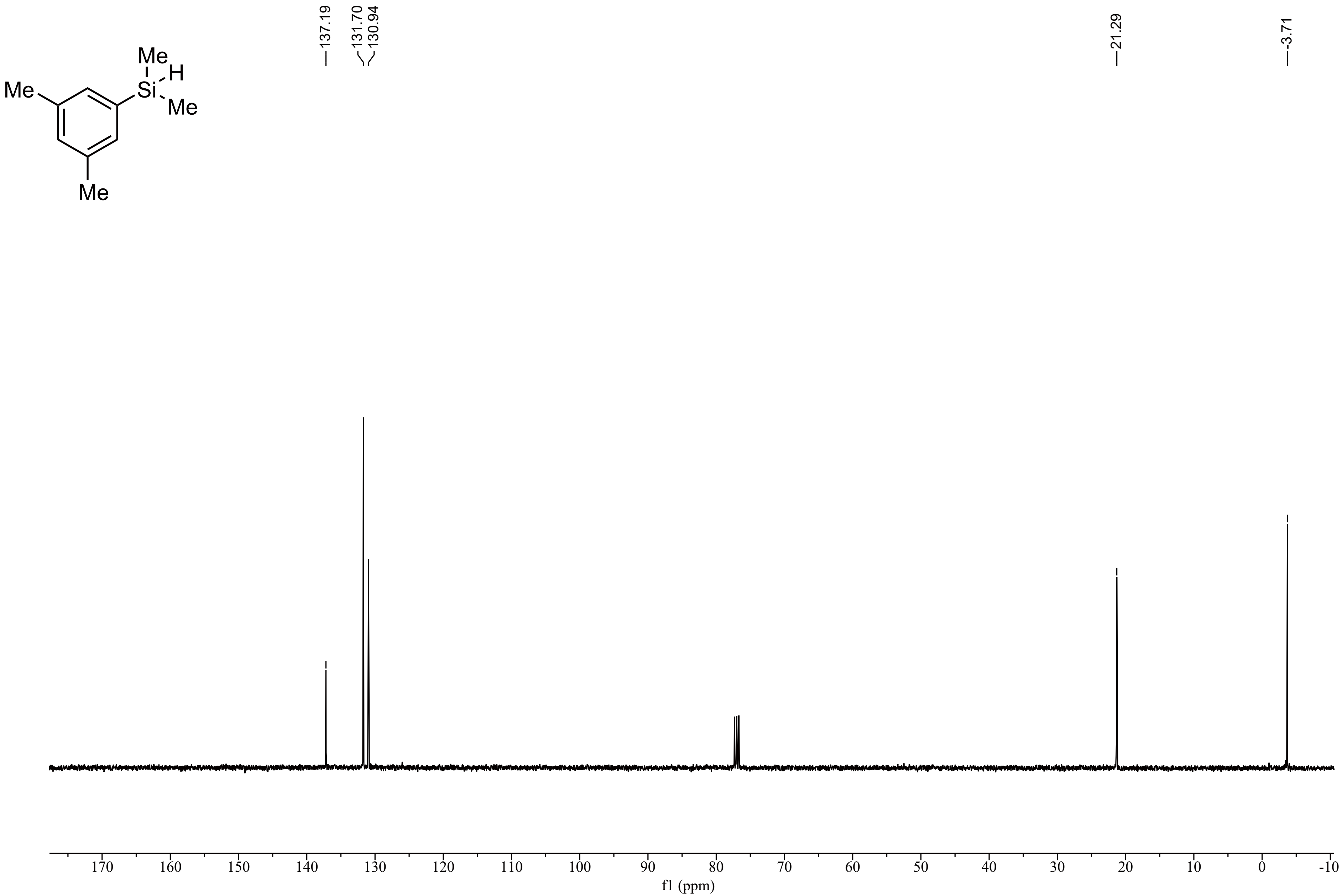

Compound **1x** ^{1}H NMR

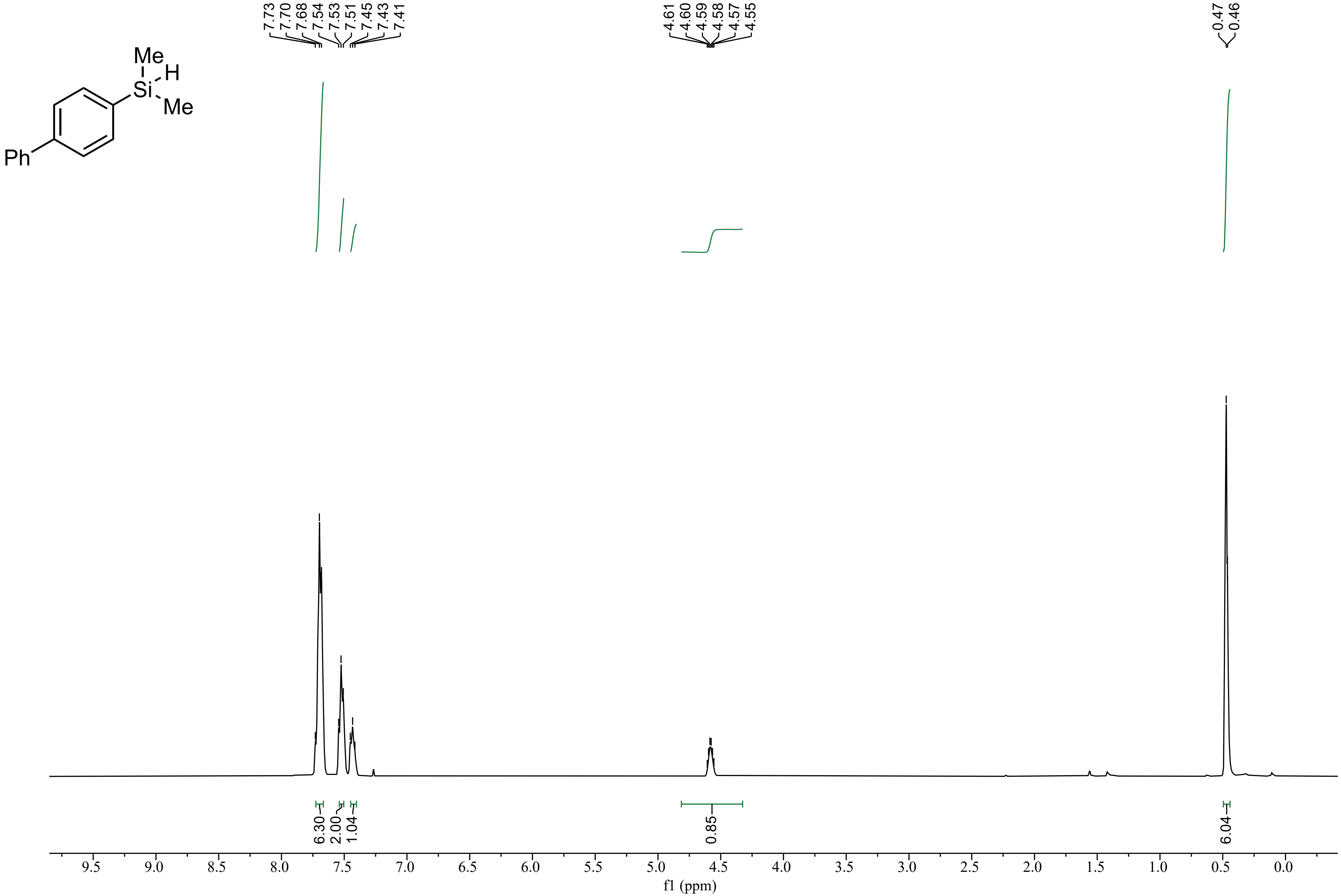

Compound **1x** ^{13}C NMR

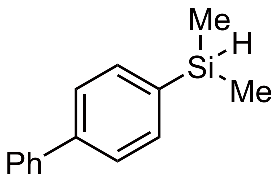

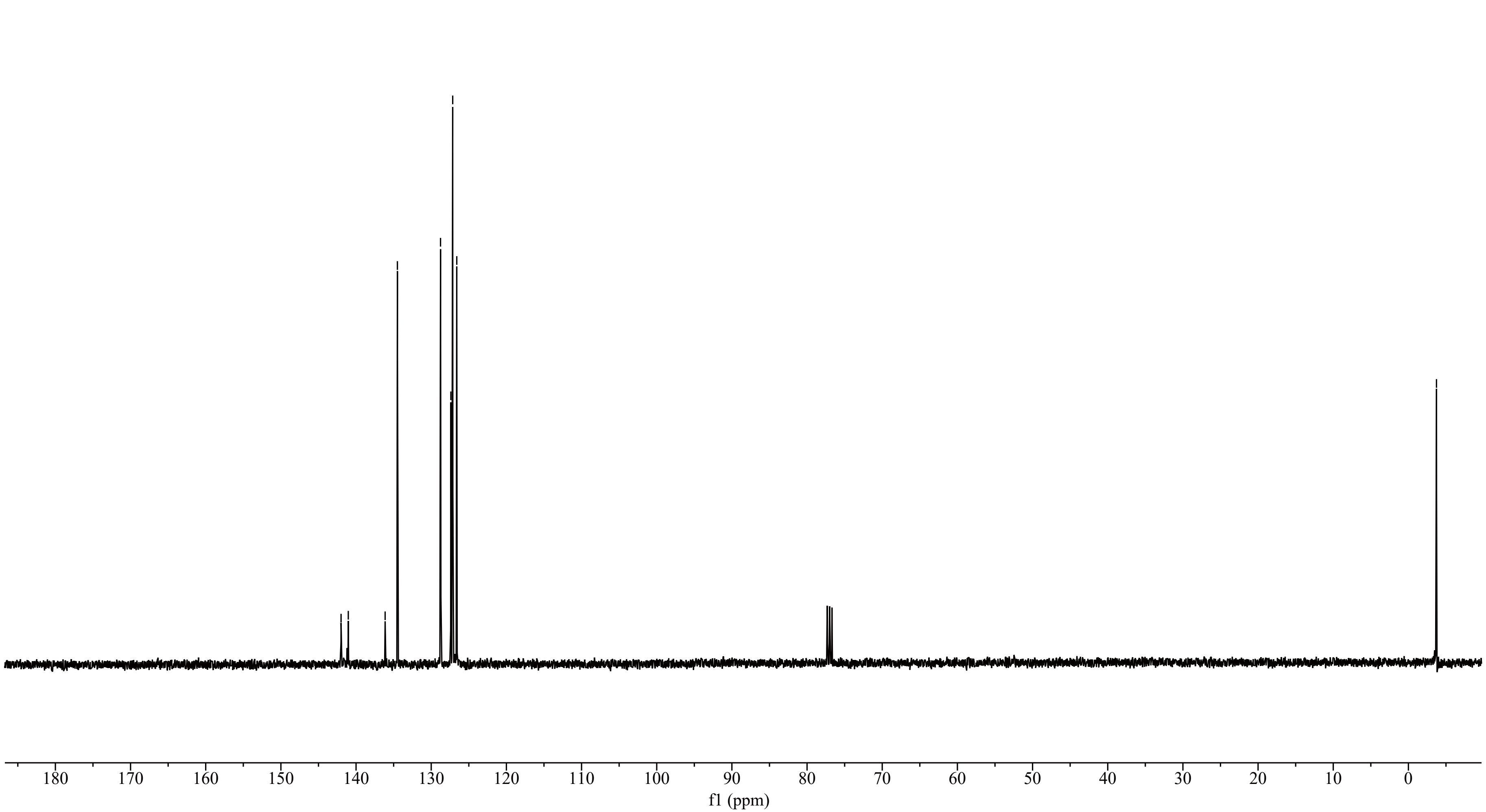

Compound **1y** [1]H NMR

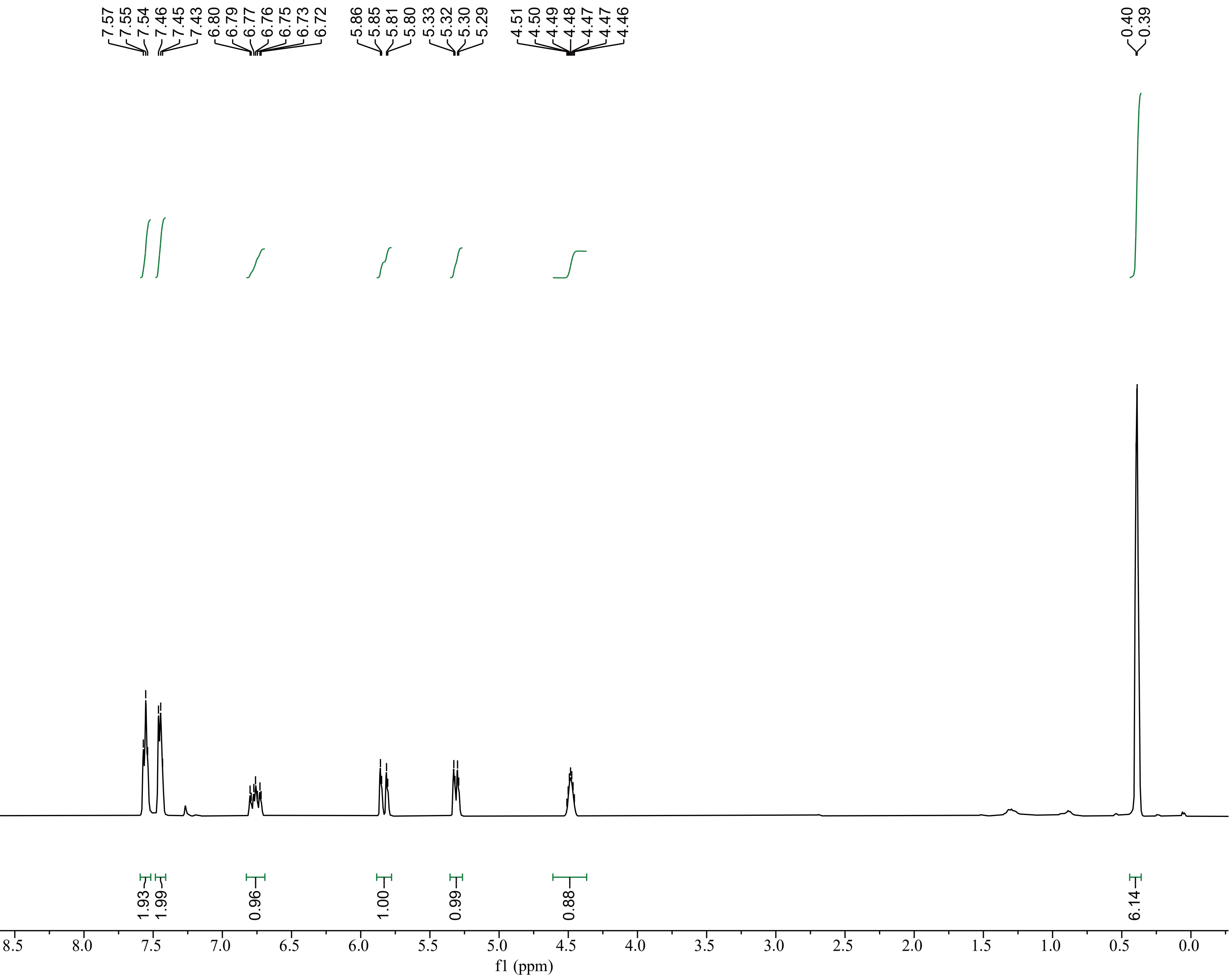

Compound **1y** ^{13}C NMR

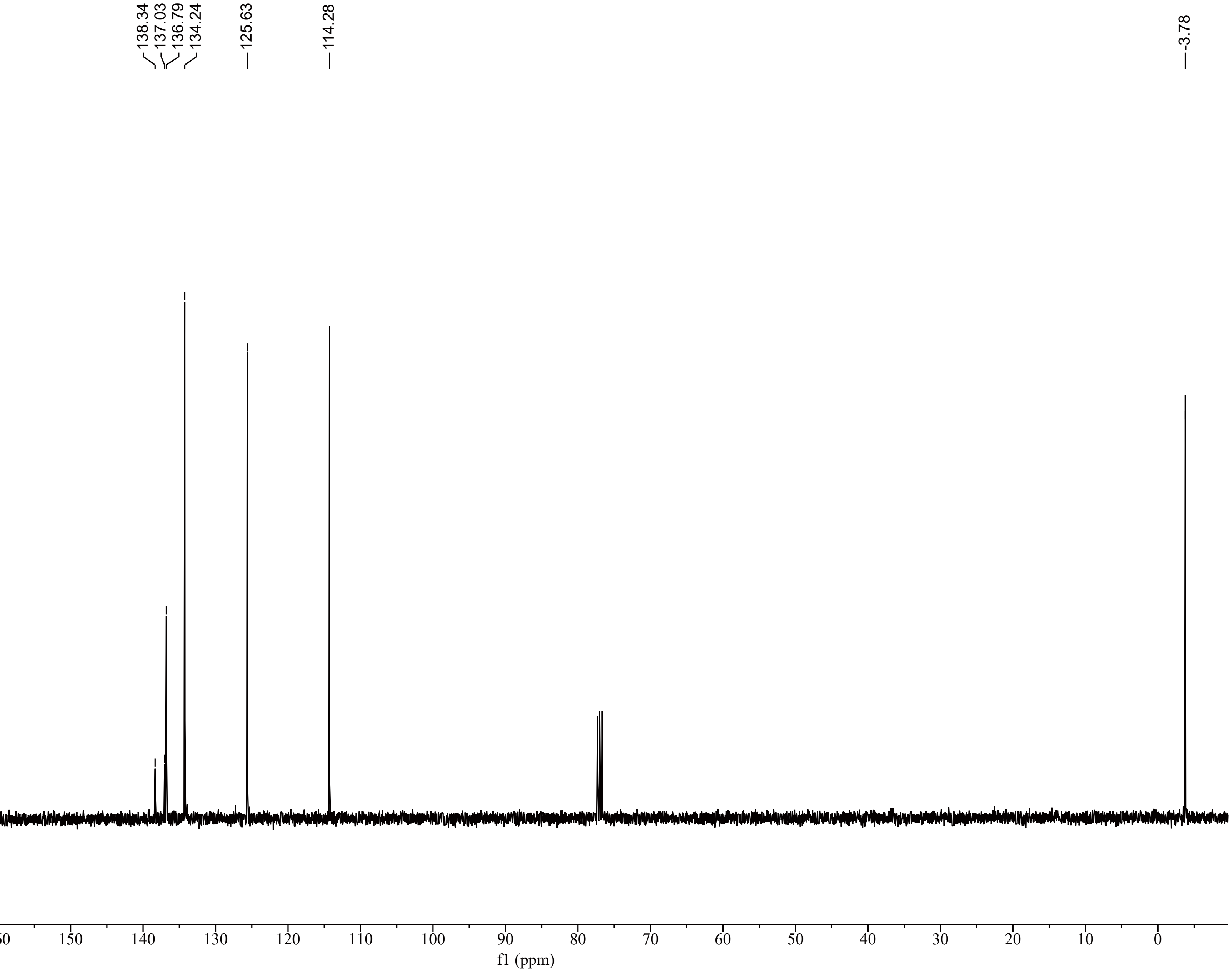

Compound **1aa** ^{1}H NMR

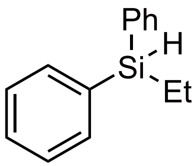

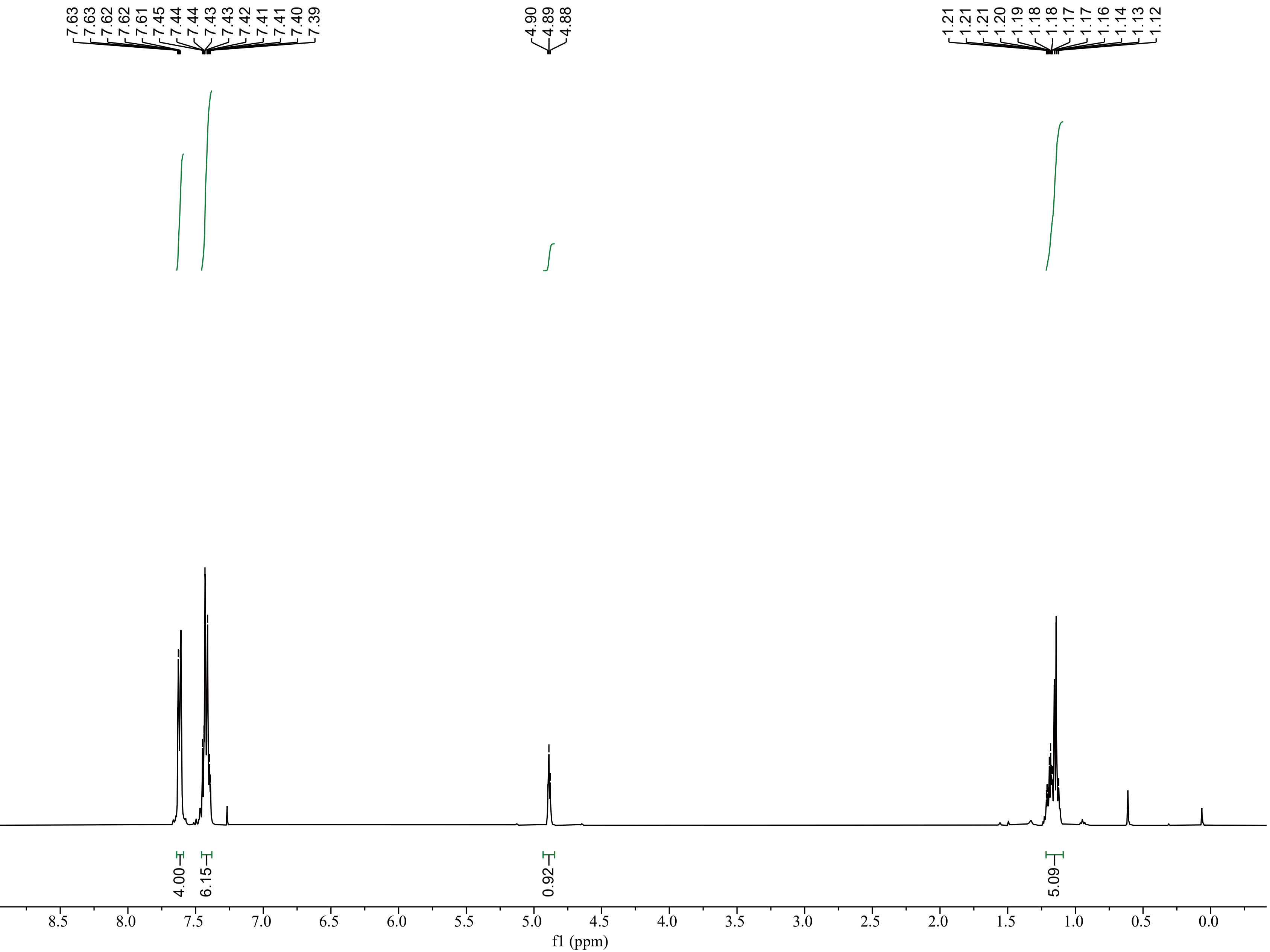

Compound **1aa** ^{13}C NMR

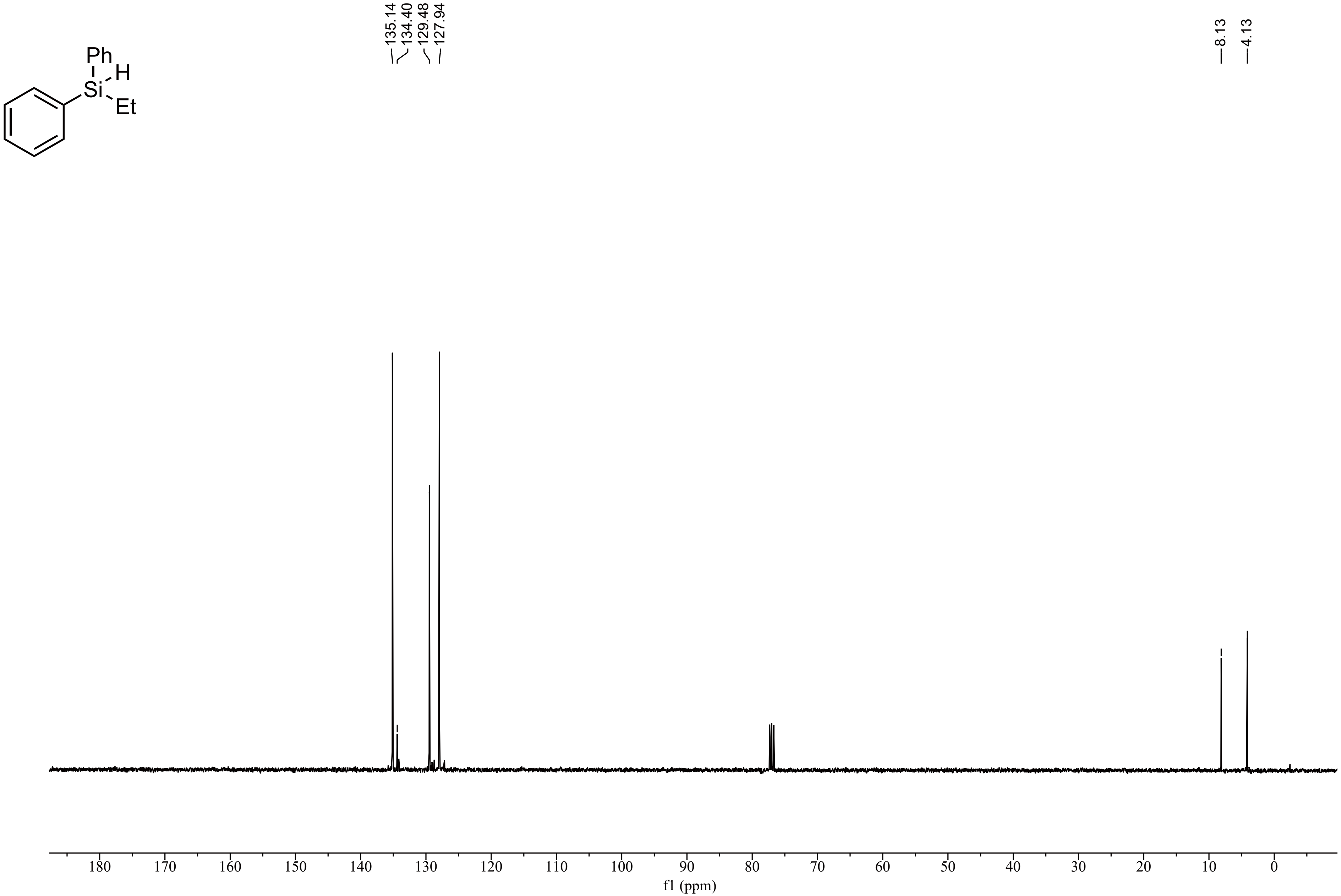

Compound **1ab** ^{1}H NMR

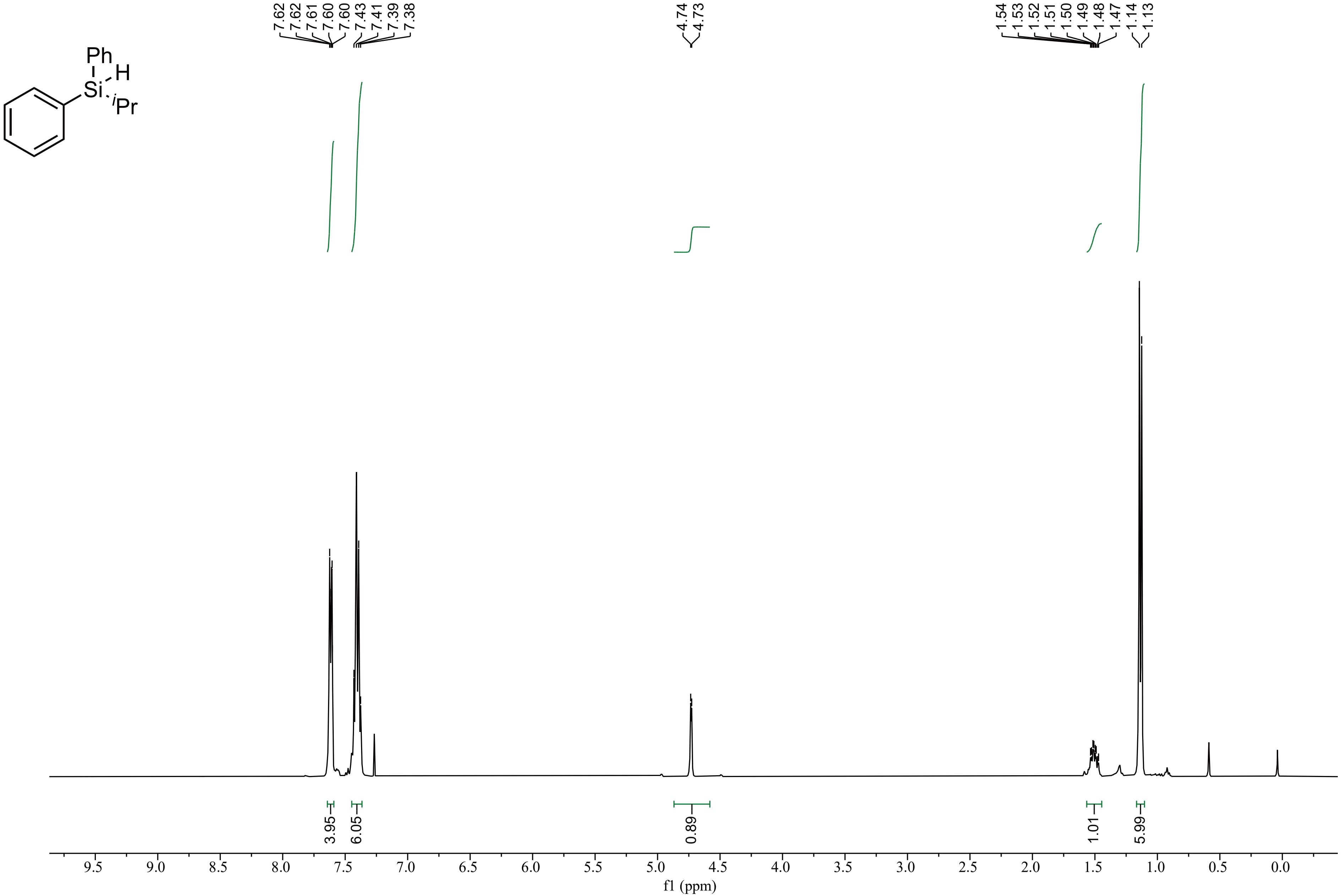

Compound **1ab** ^{13}C NMR

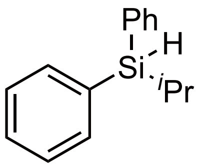

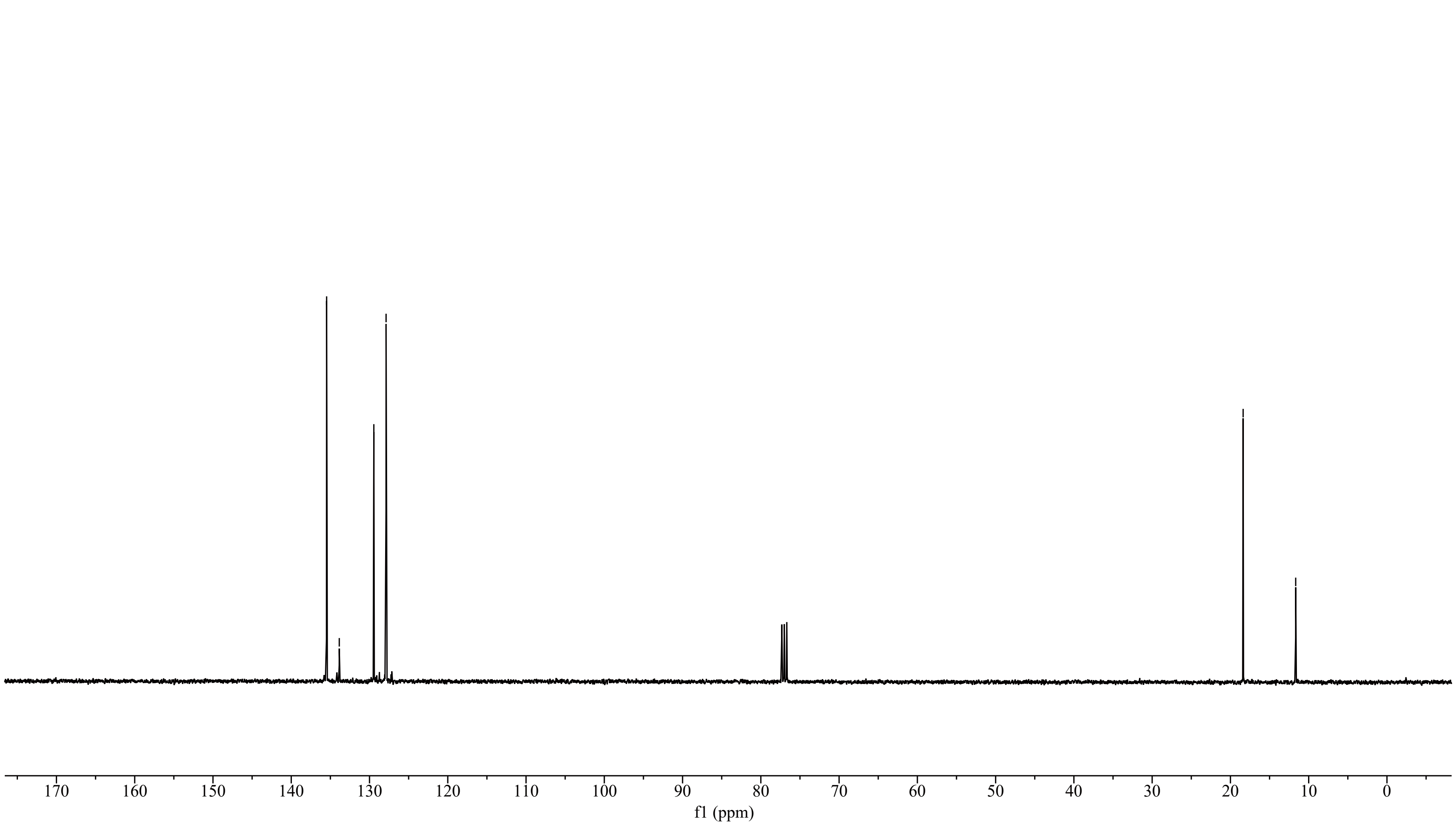

Compound **1ad** ^{1}H NMR

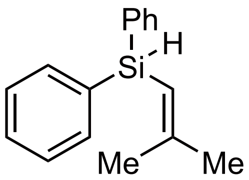

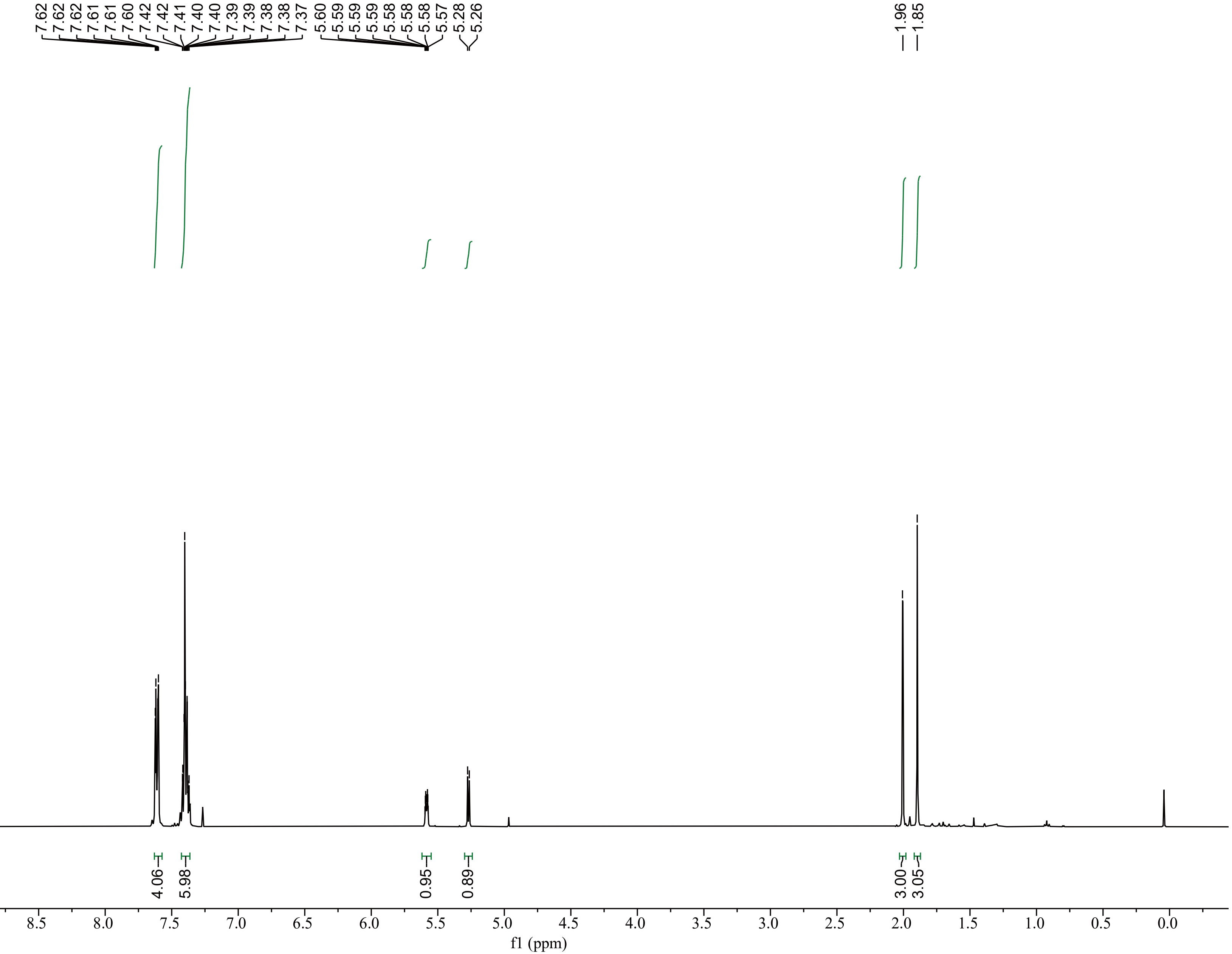

Compound **1ad** ^{13}C NMR

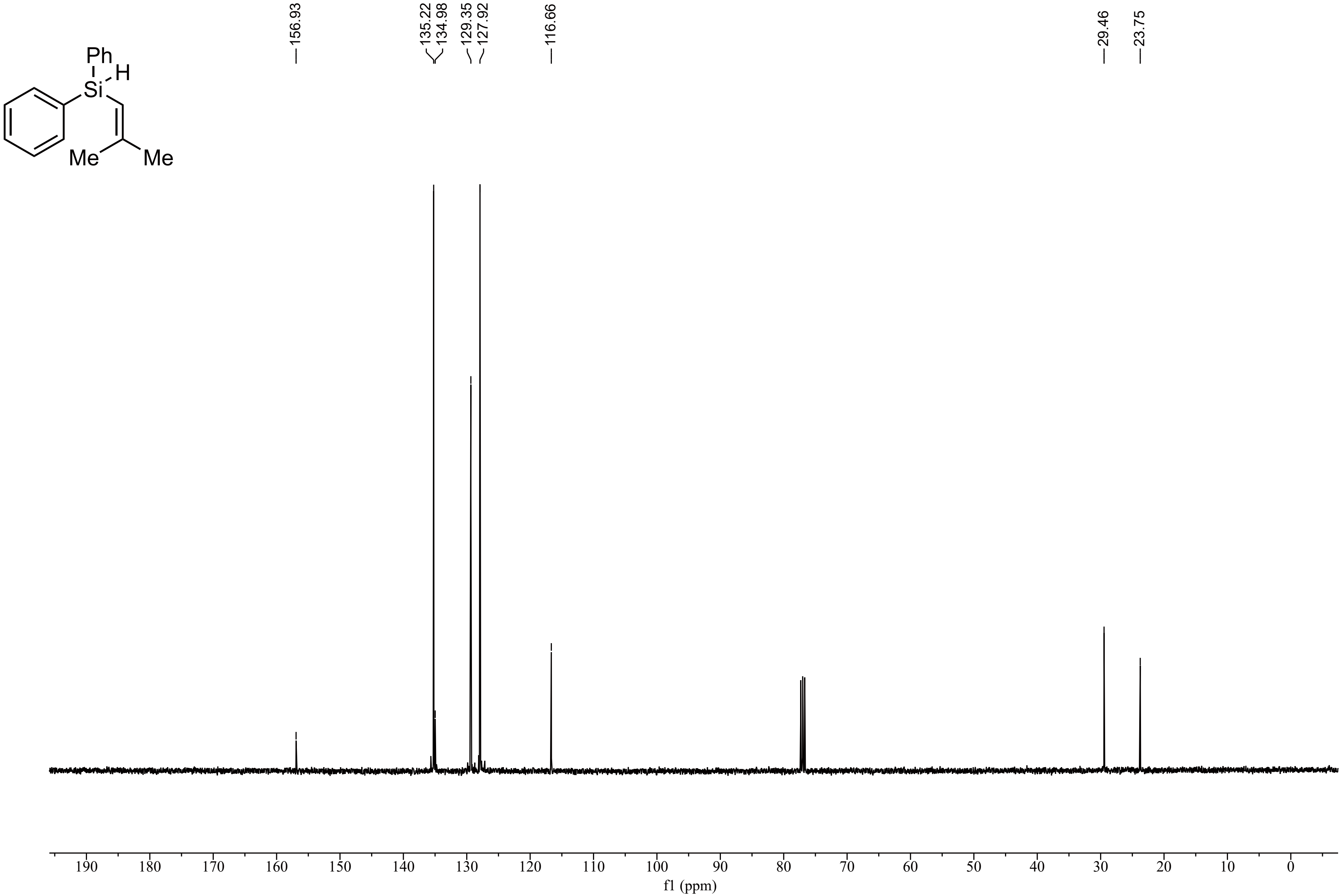

Compound **1ah** ^{1}H NMR

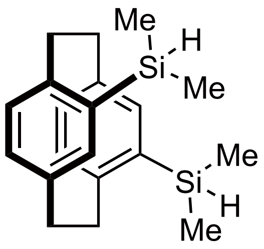

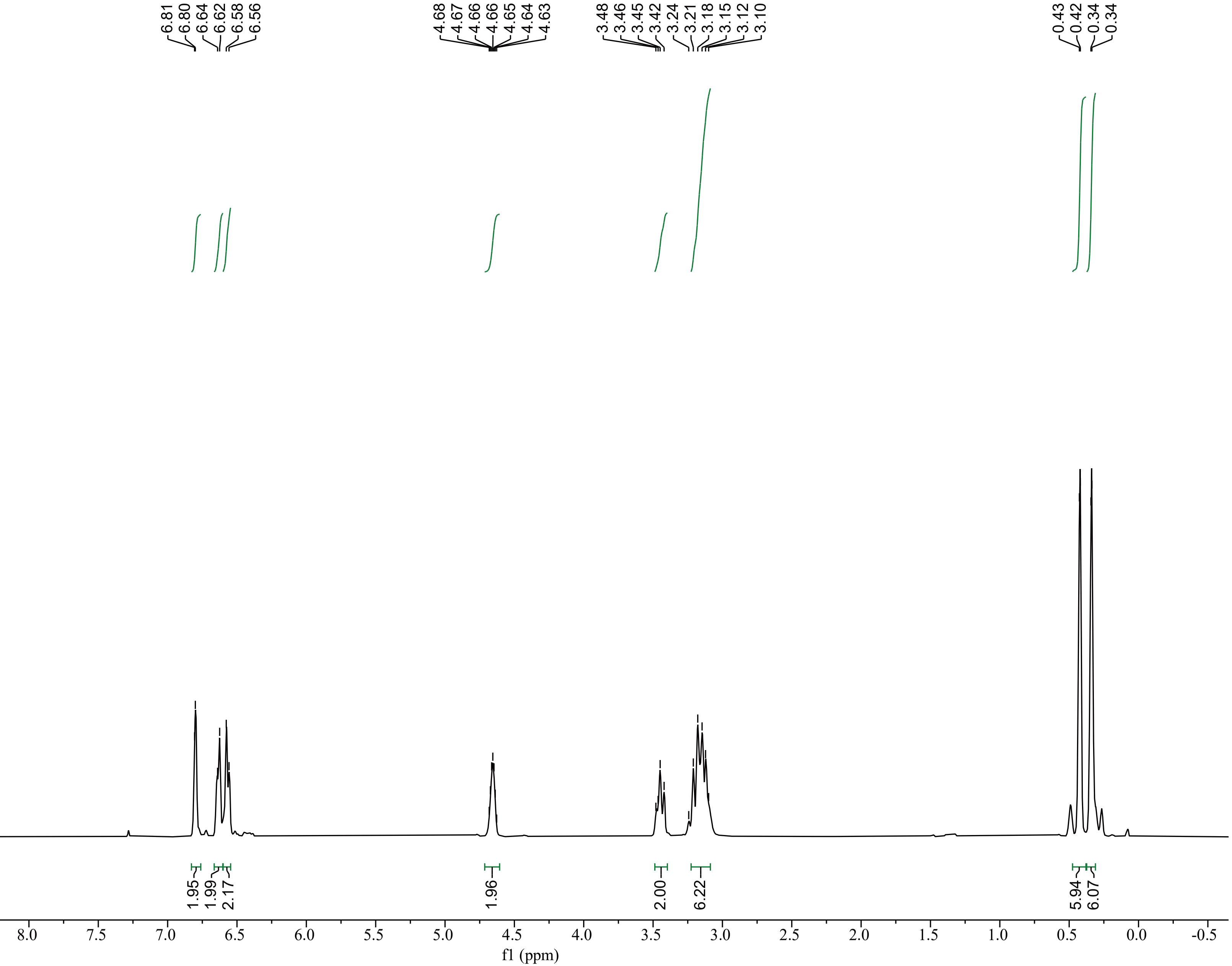

Compound **1ah** ^{13}C NMR

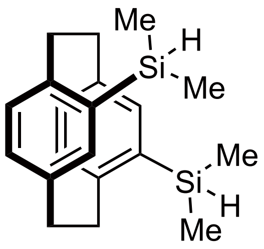

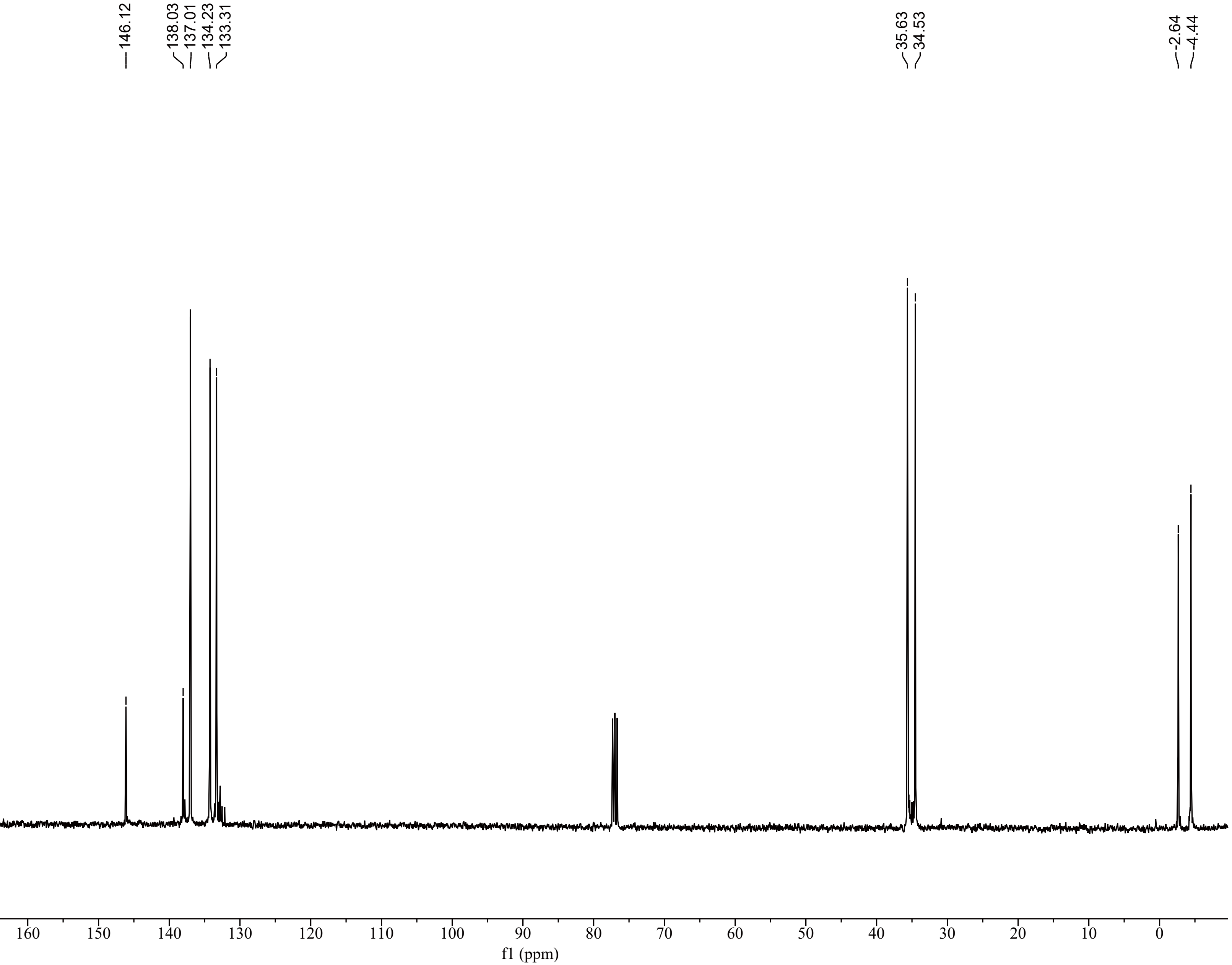

Compound **1al** [1]H NMR

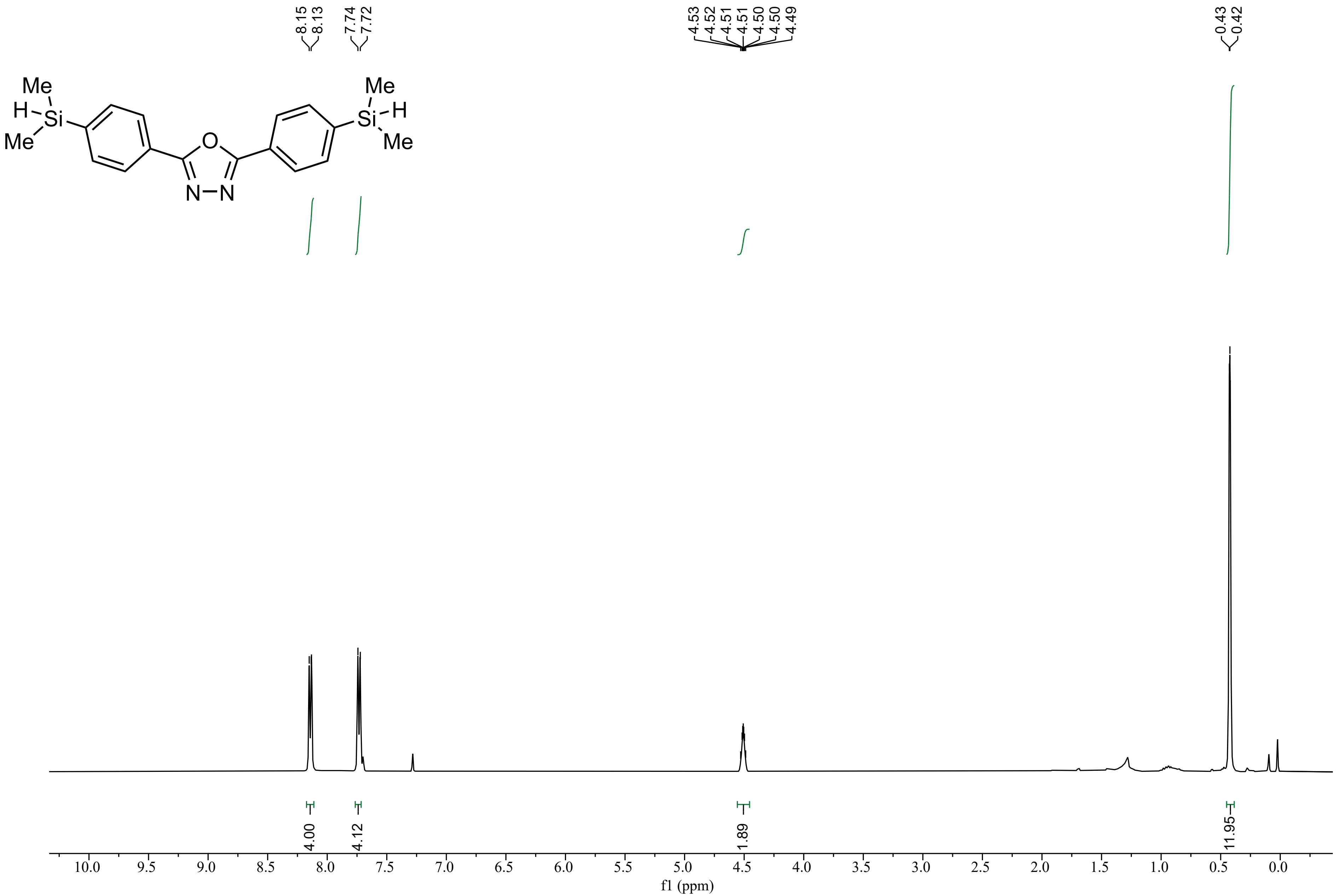

Compound **1al** ^{13}C NMR

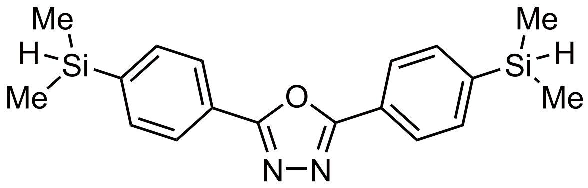

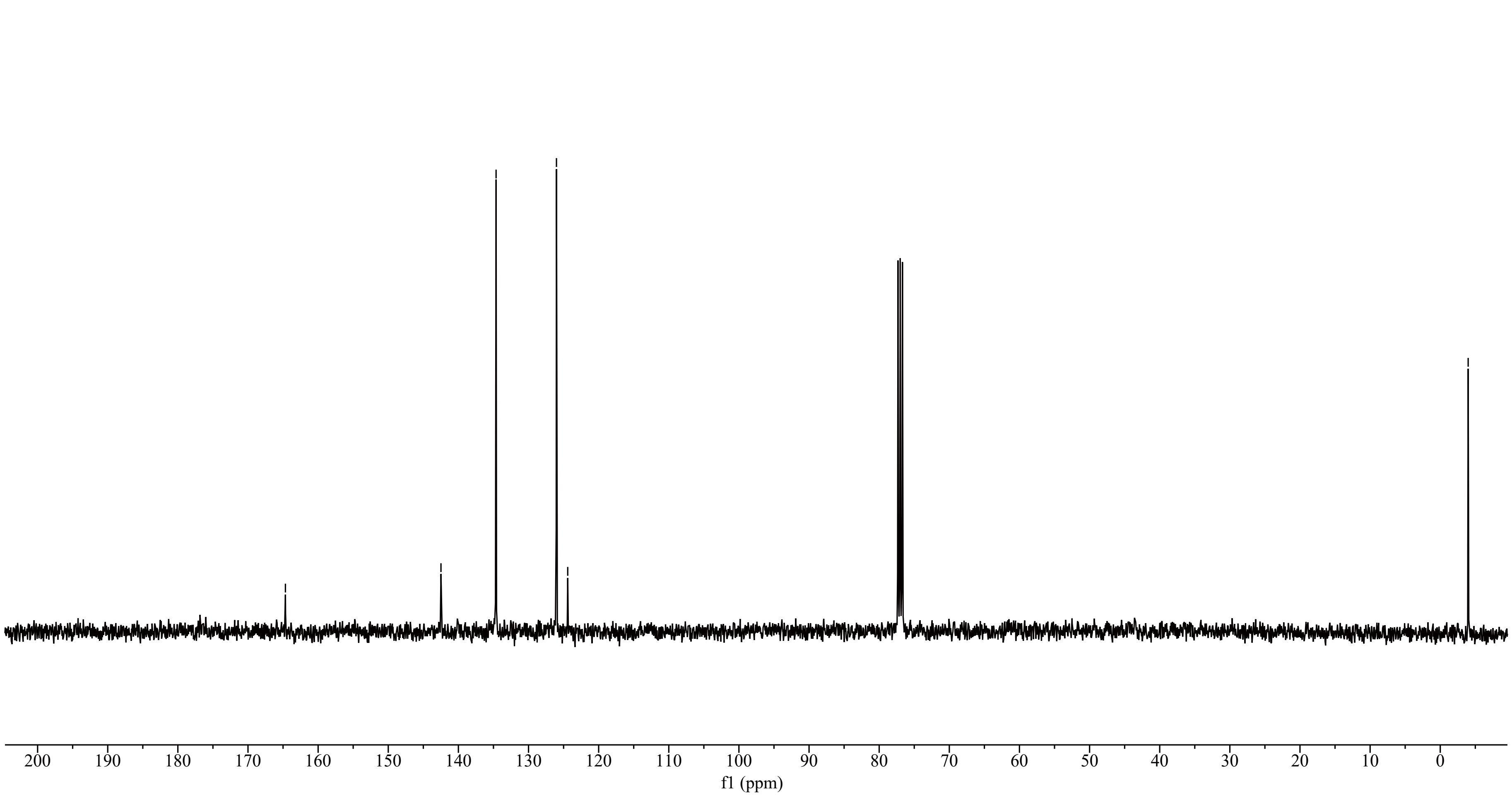

Compound **1am** ^{1}H NMR

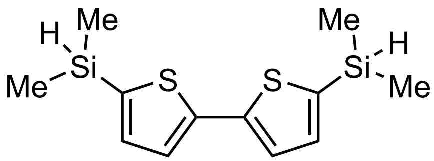

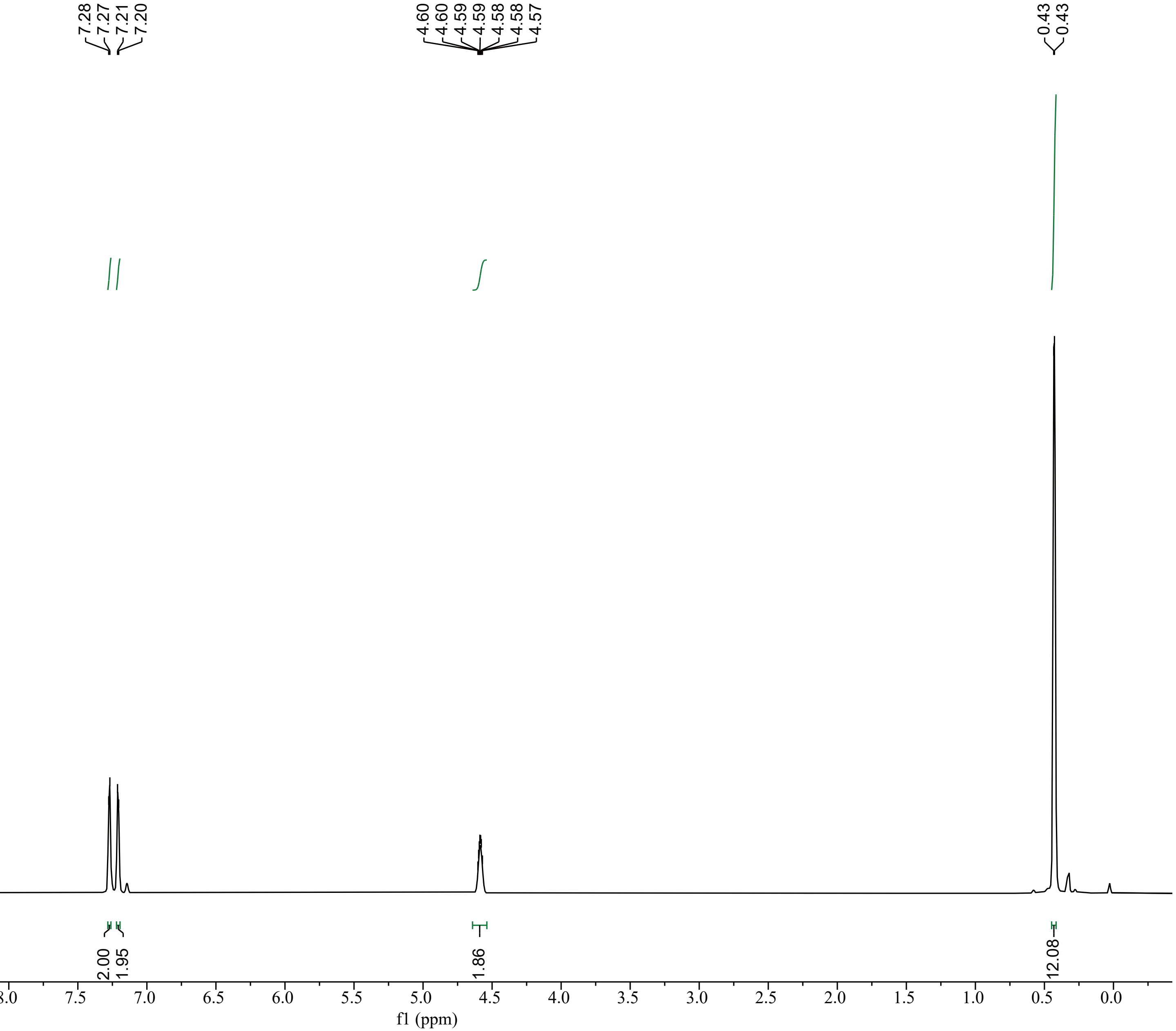

Compound **1am** ^{13}C NMR

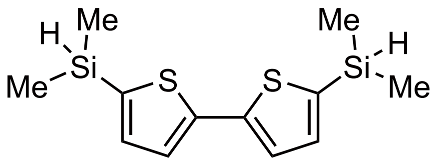

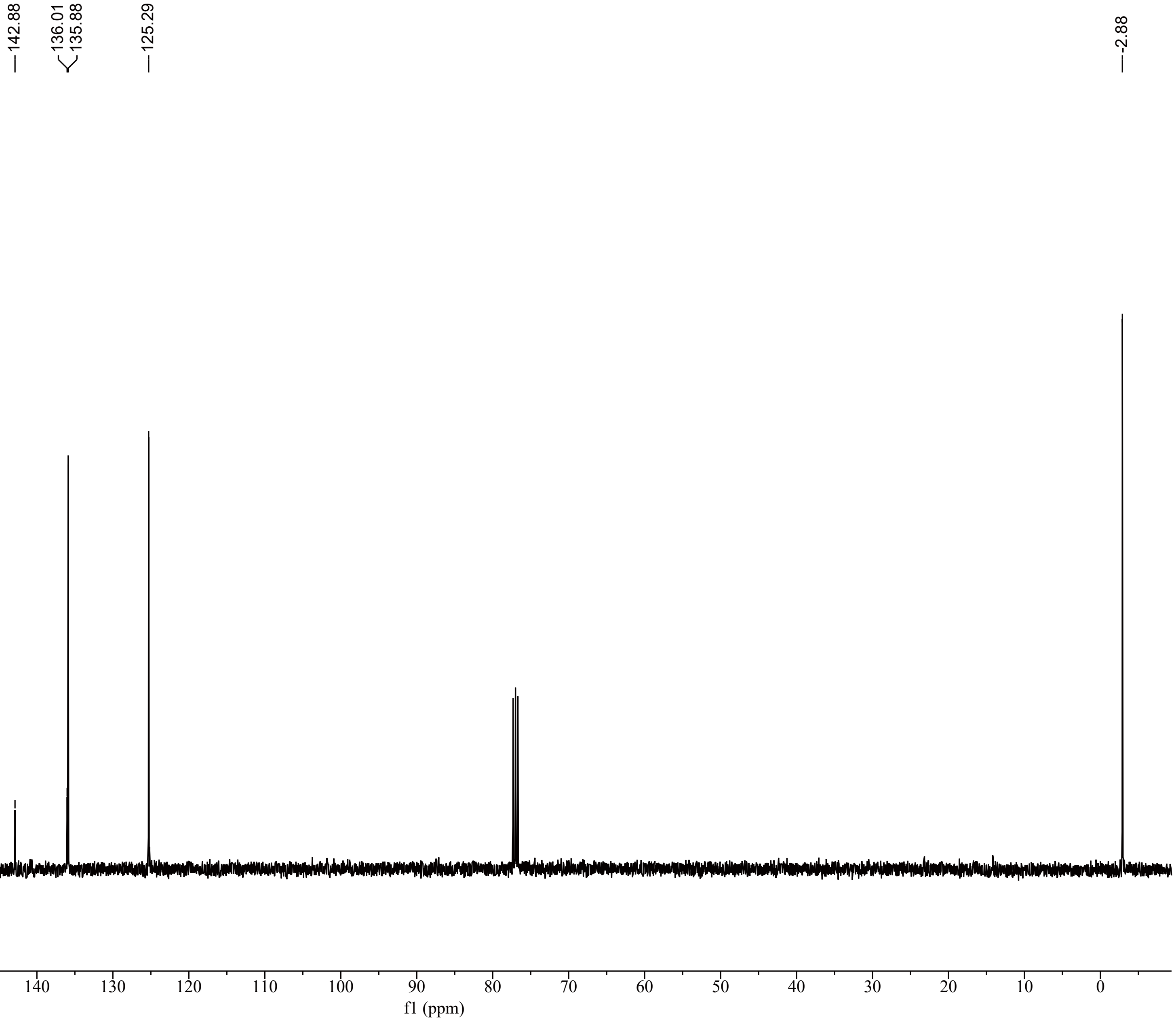

Compound **1an** ^{1}H NMR

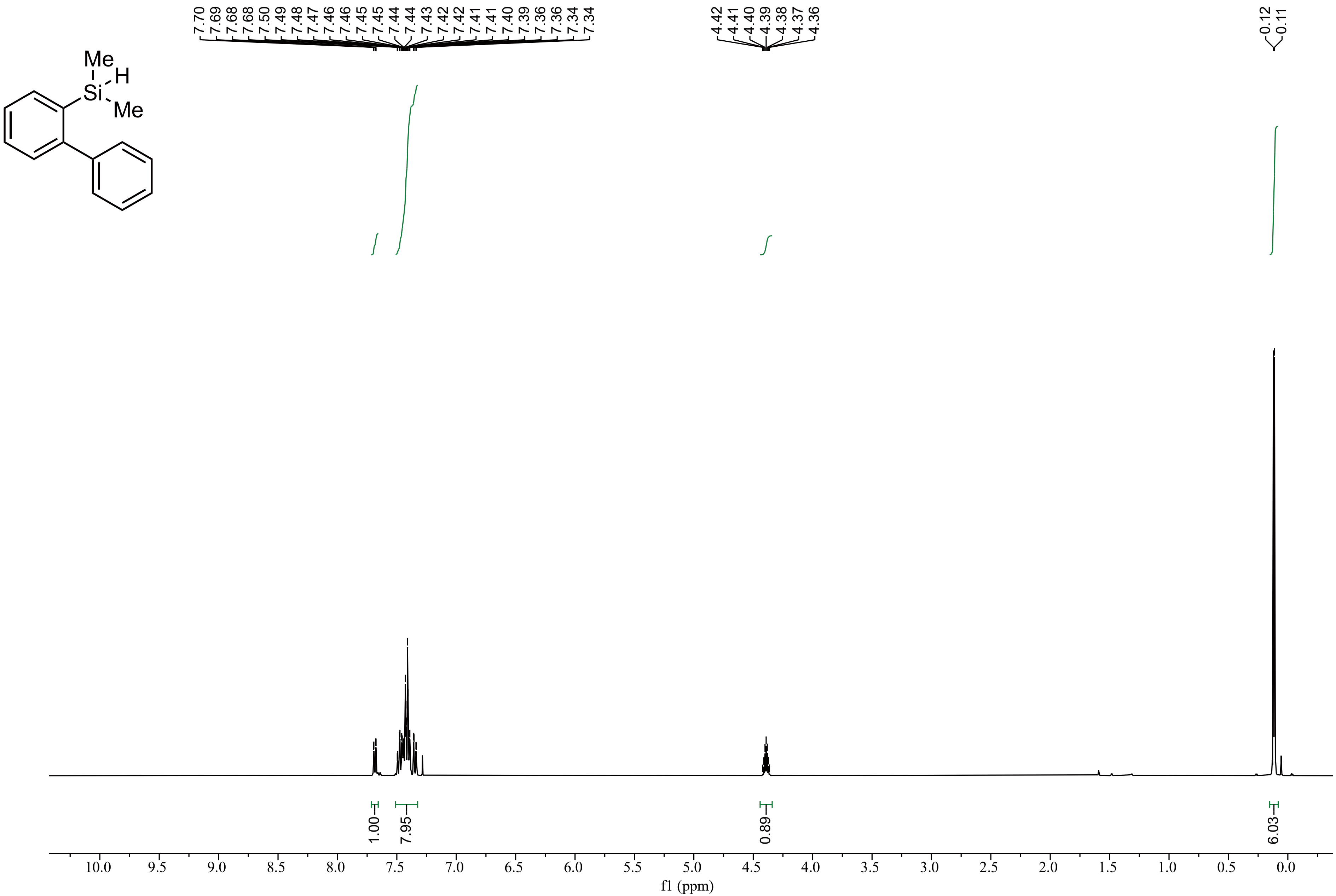

Compound **1an** ^{13}C NMR

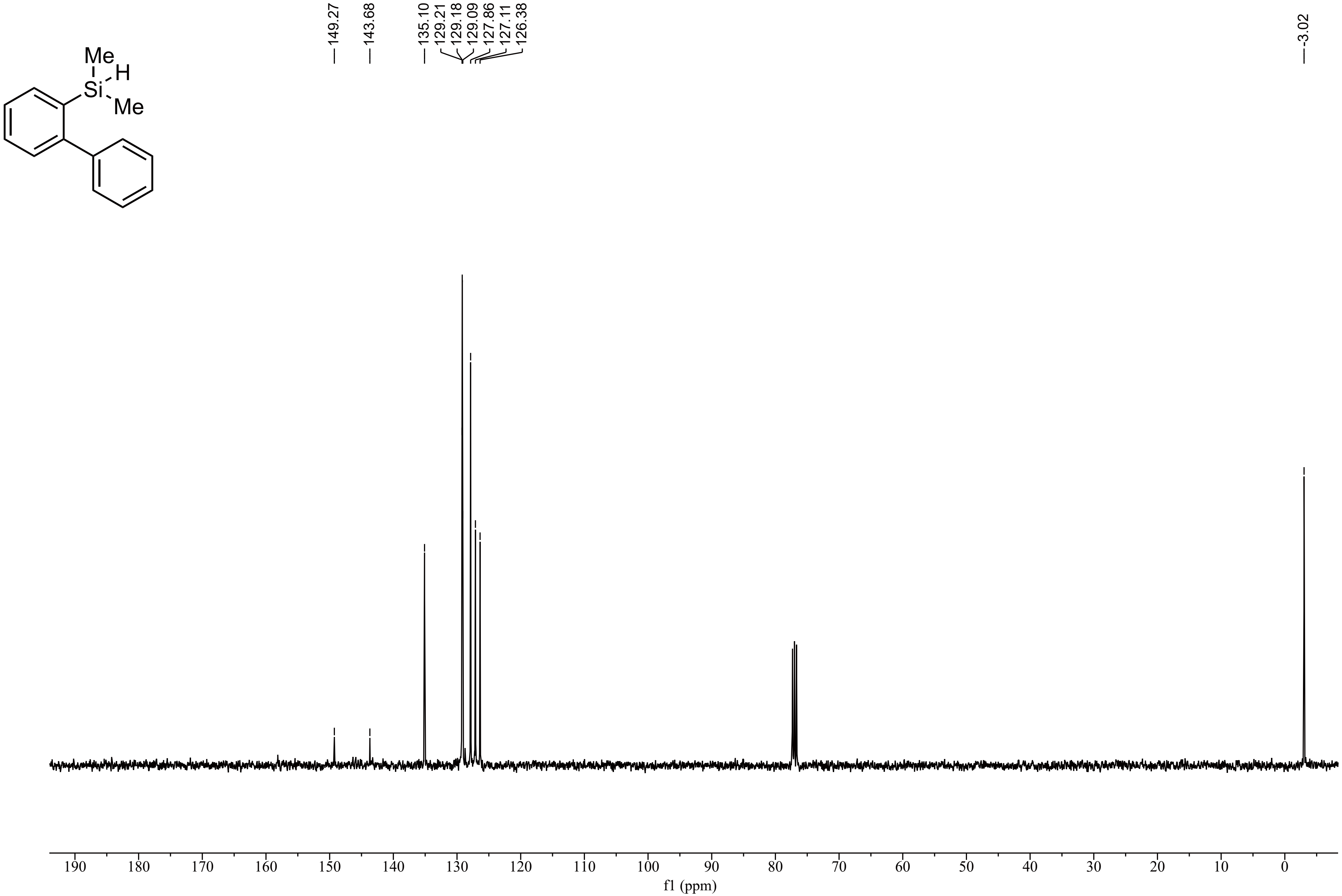

Compound **1ao** [1]H NMR

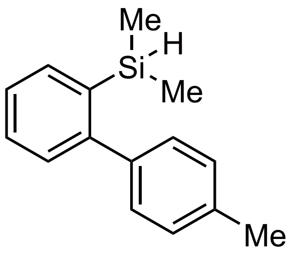

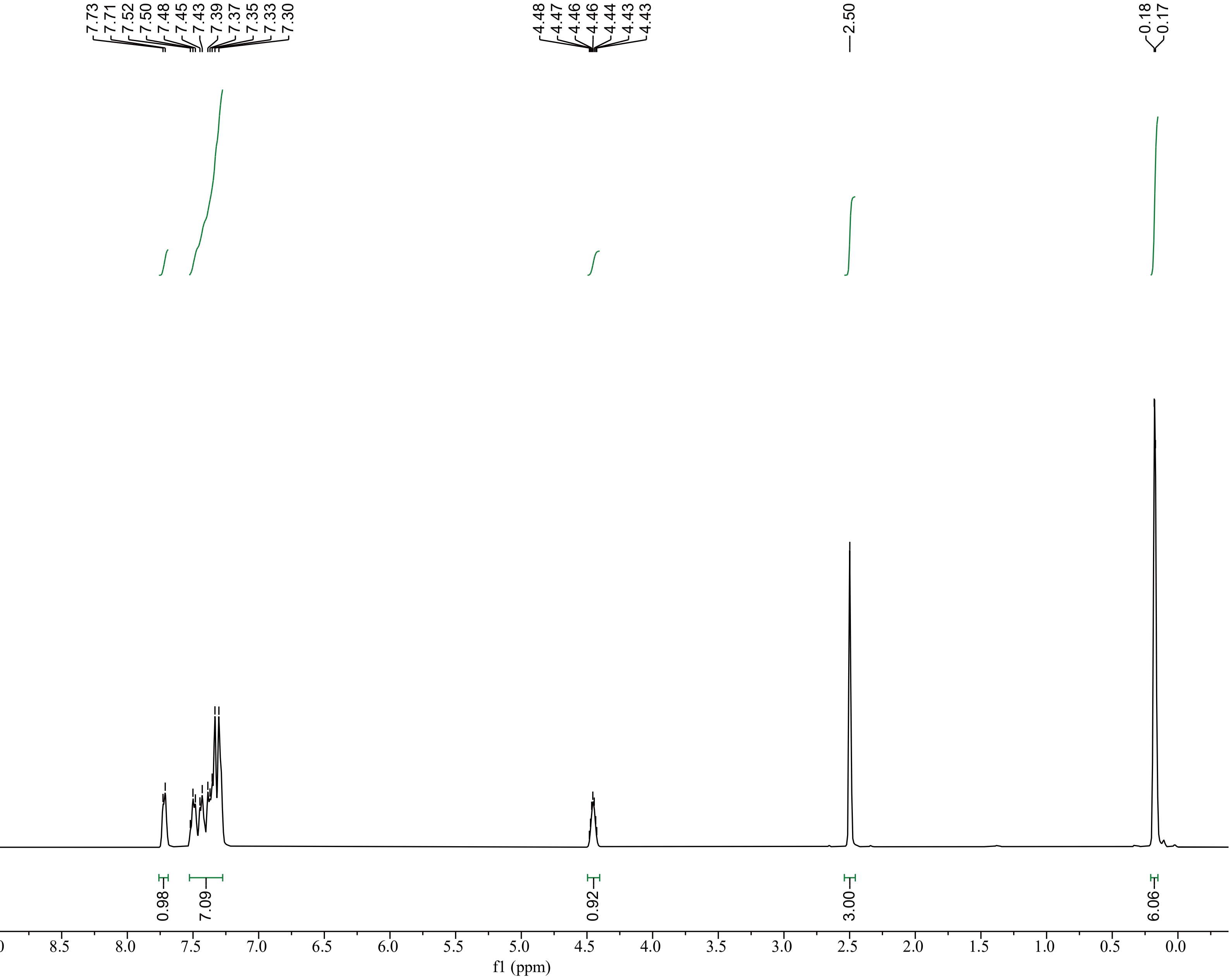

Compound **1ao** ^{13}C NMR

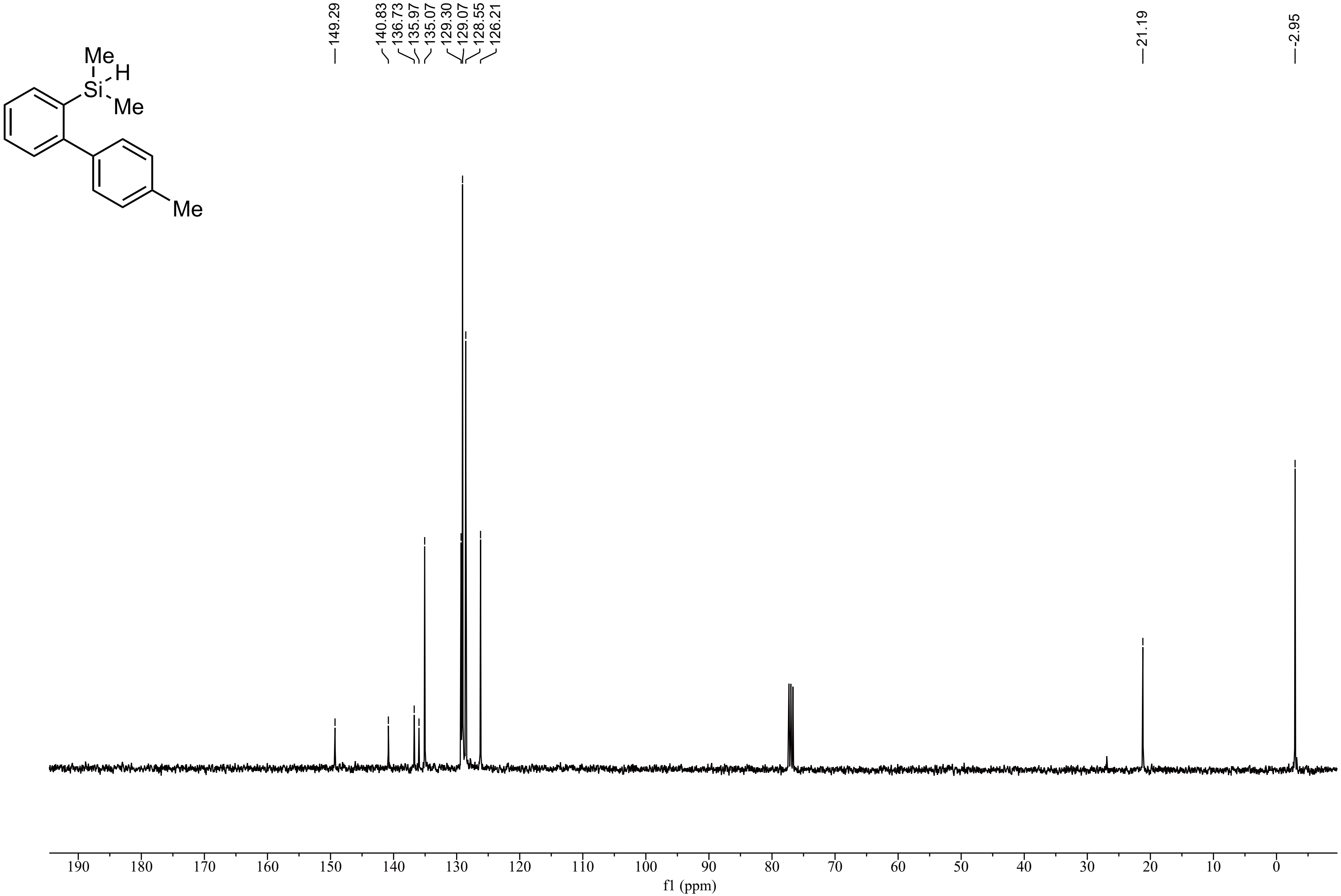

Compound **1ap** ^{1}H NMR

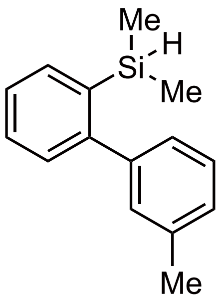

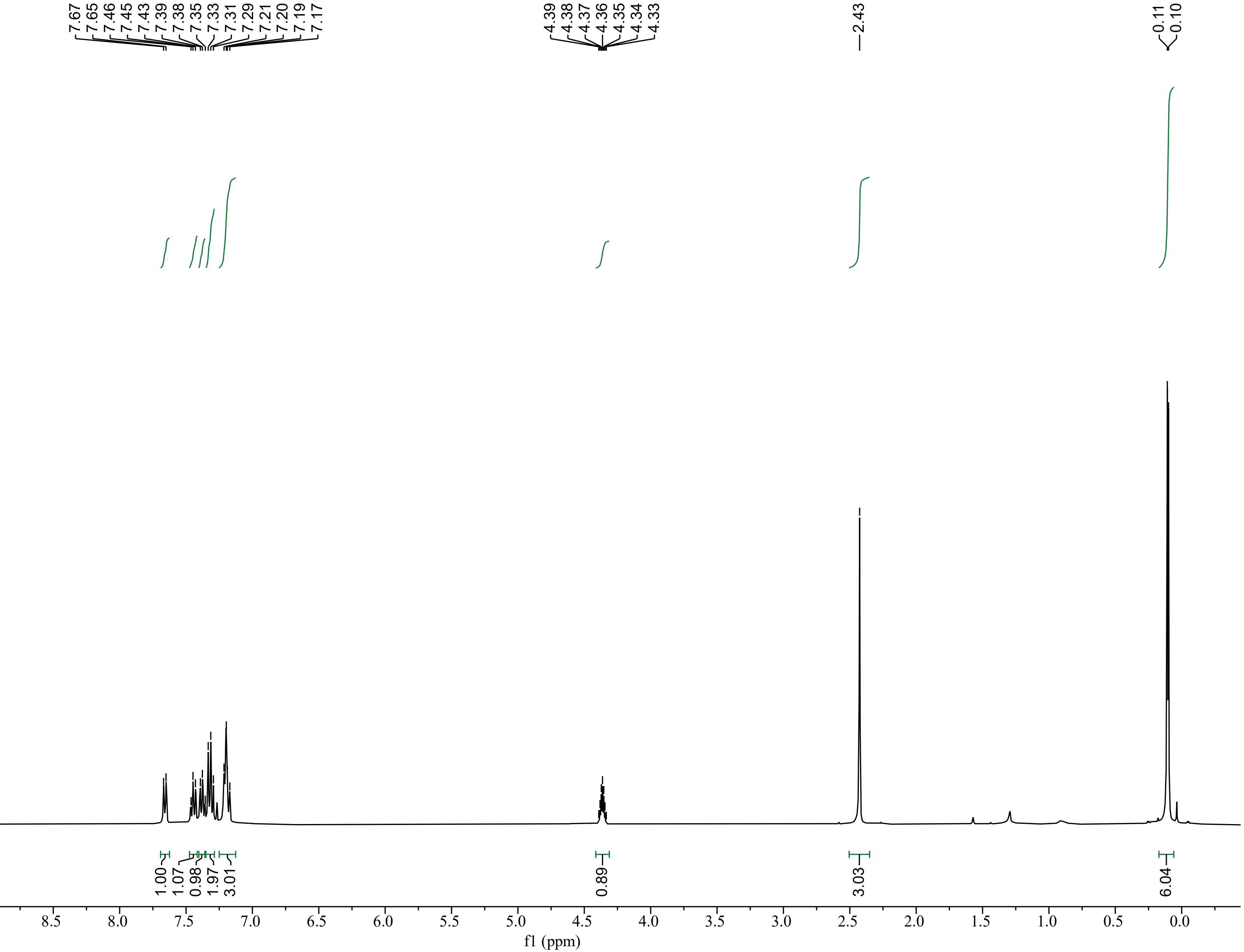

Compound **1ap** ^{13}C NMR

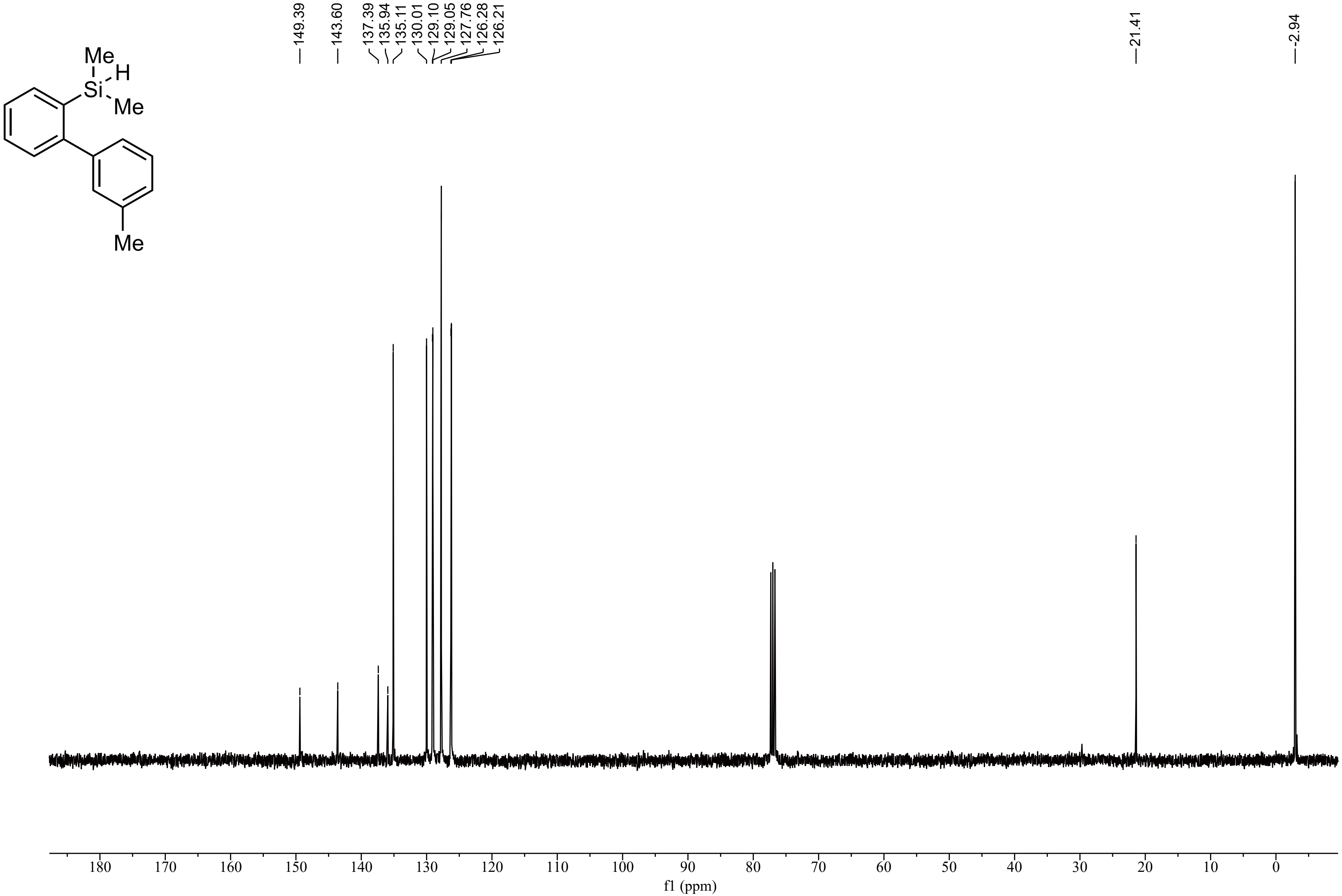

Compound **1aq** ^{1}H NMR

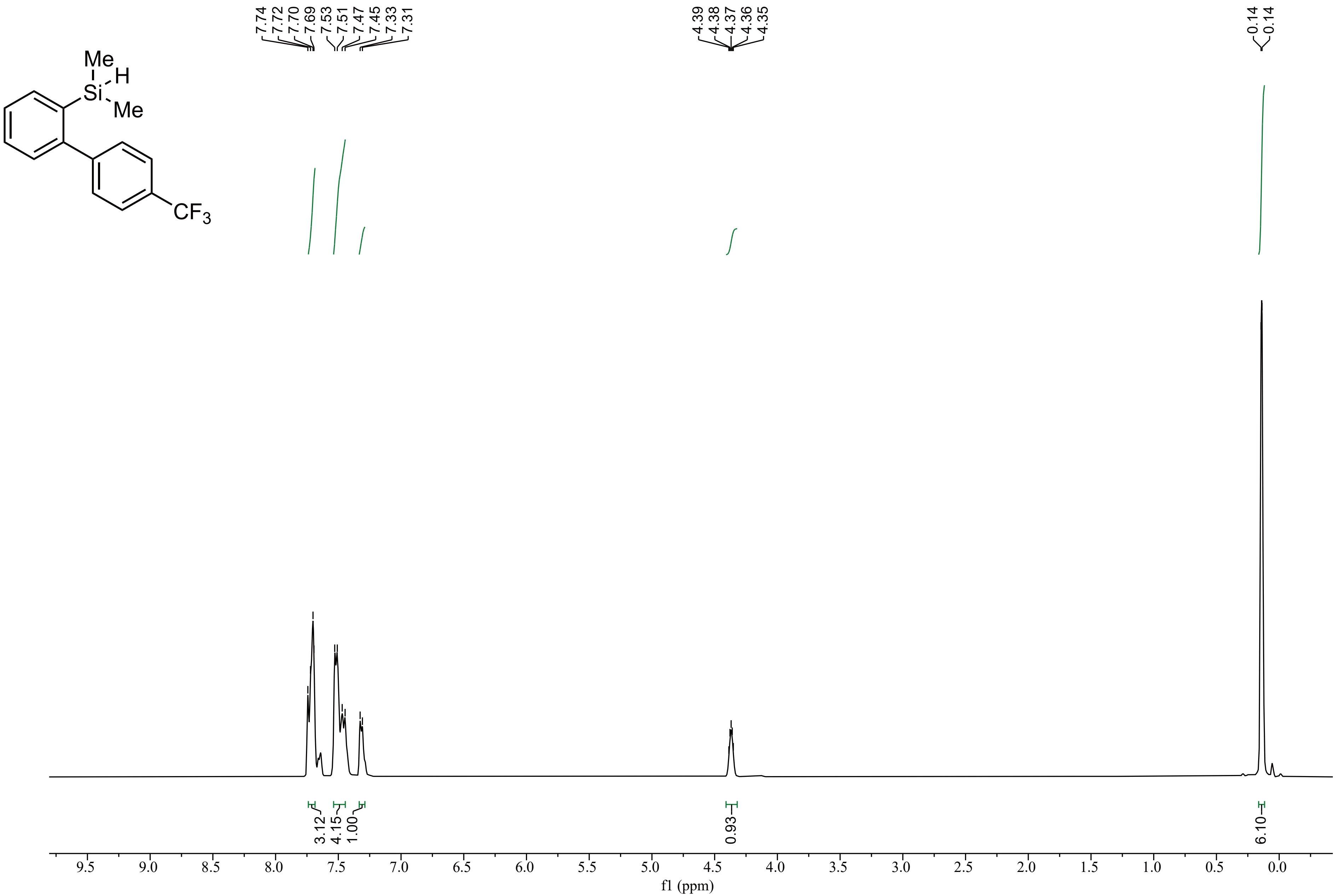

Compound **1aq** ^{13}C NMR

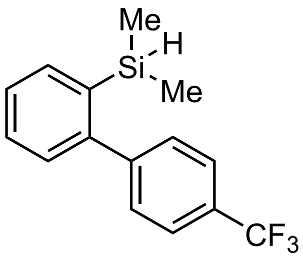

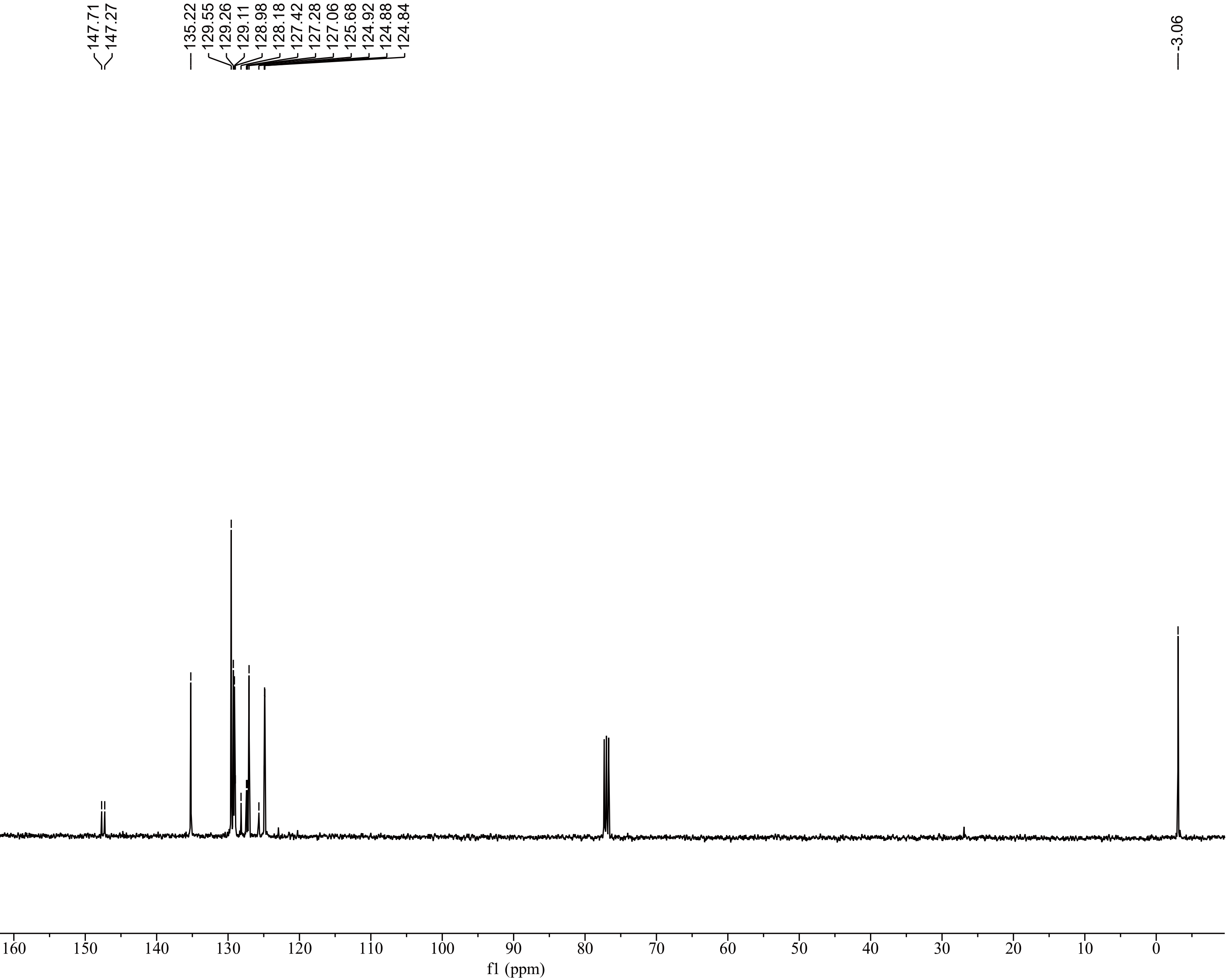

Compound **1aq** ^{19}F NMR

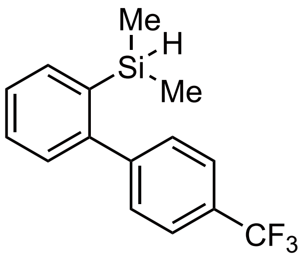

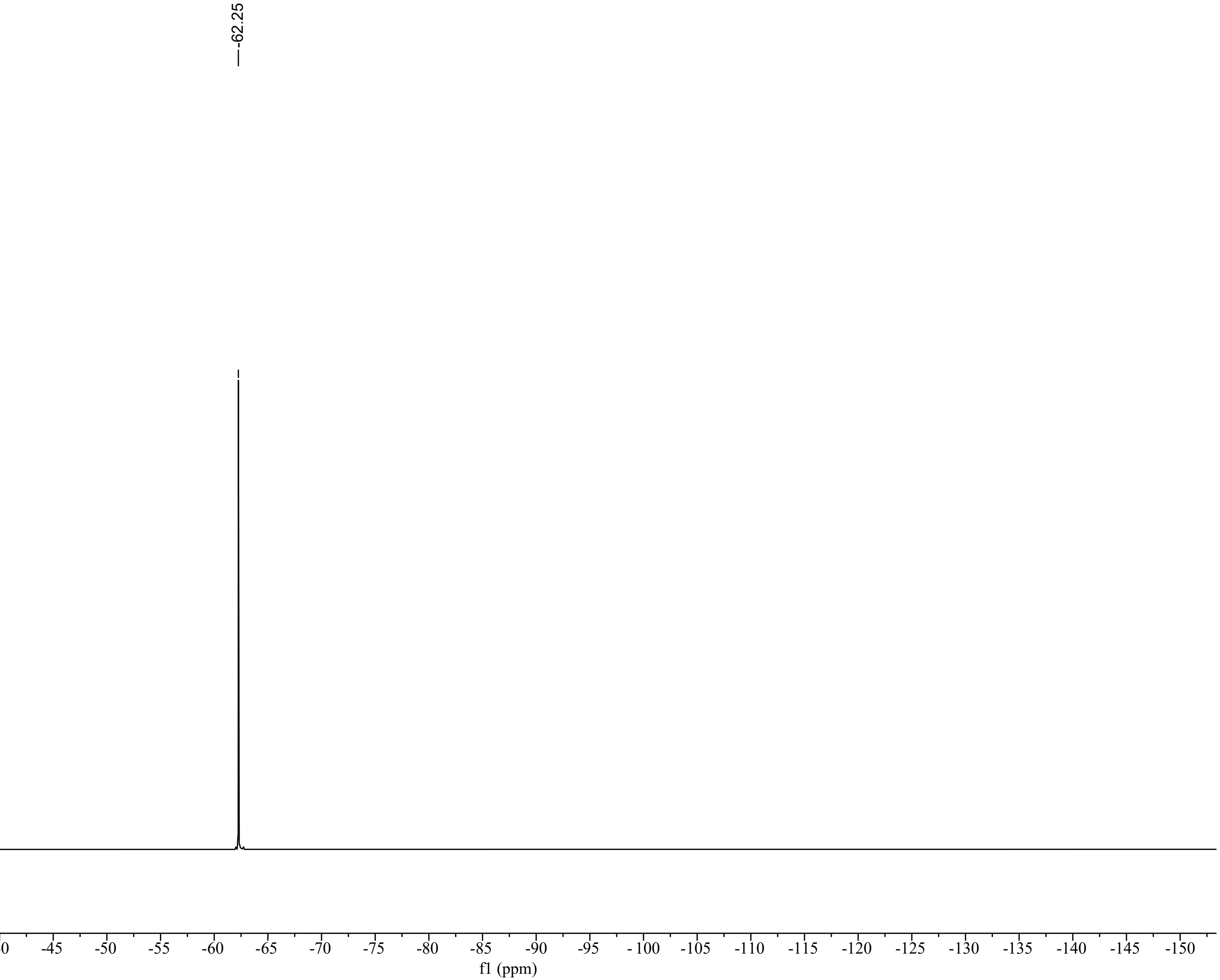

Compound **1ar** ^{1}H NMR

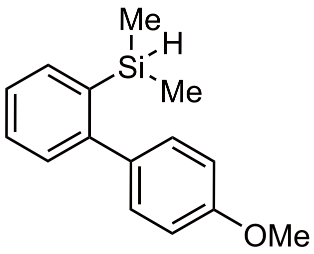

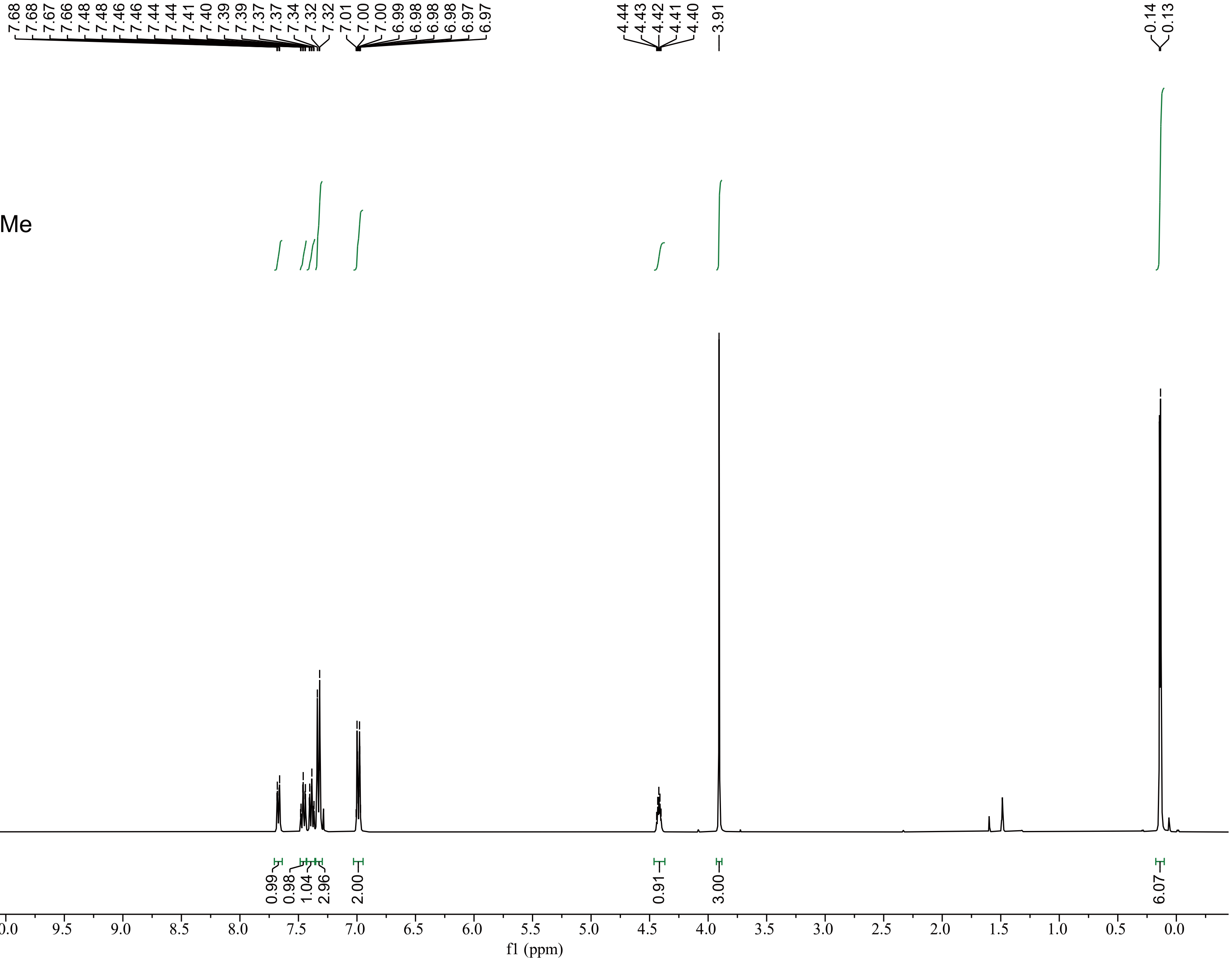

Compound **1ar** ^{13}C NMR

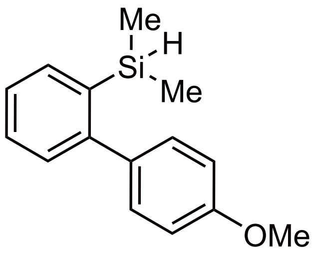

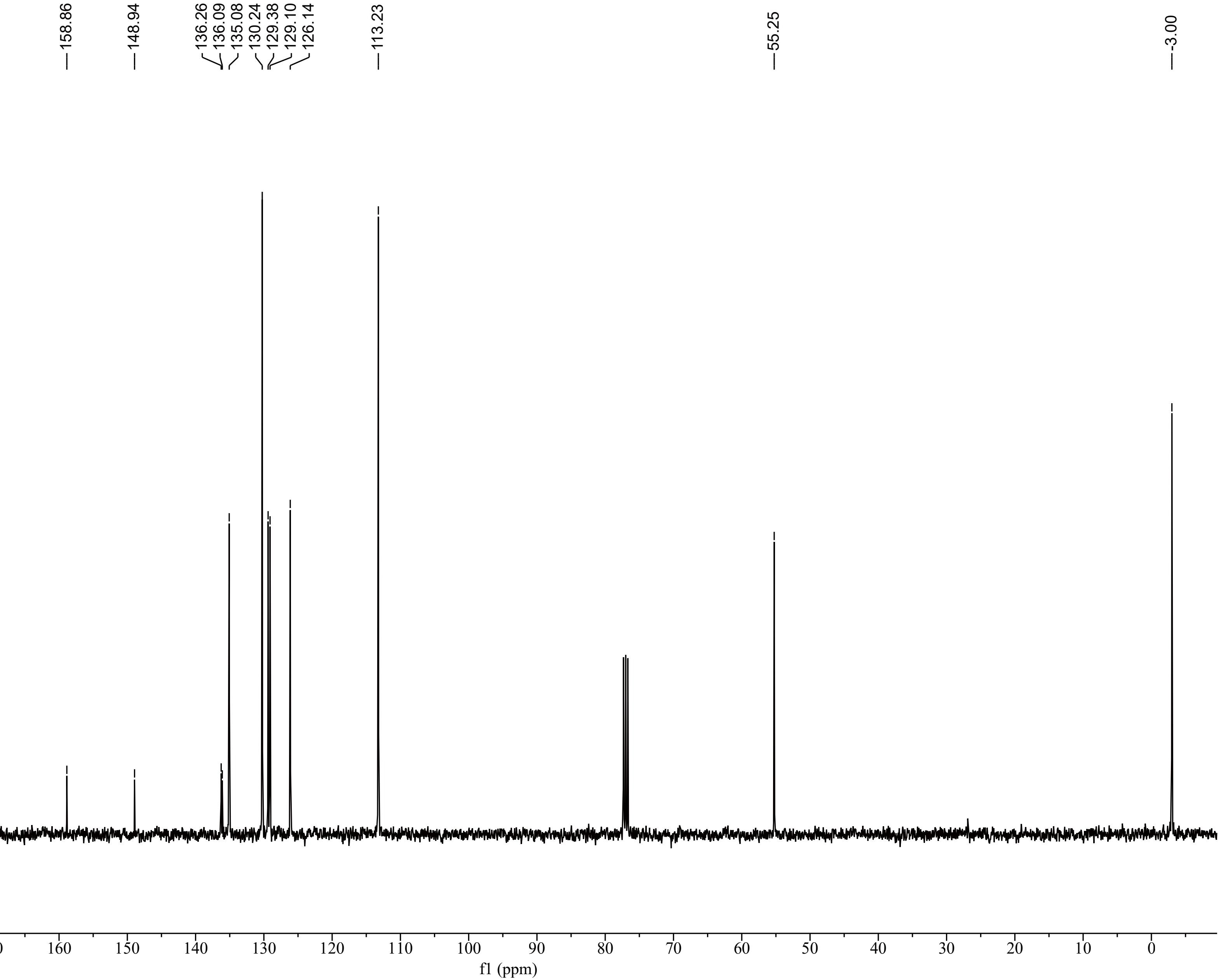

Compound **1as** ^{1}H NMR

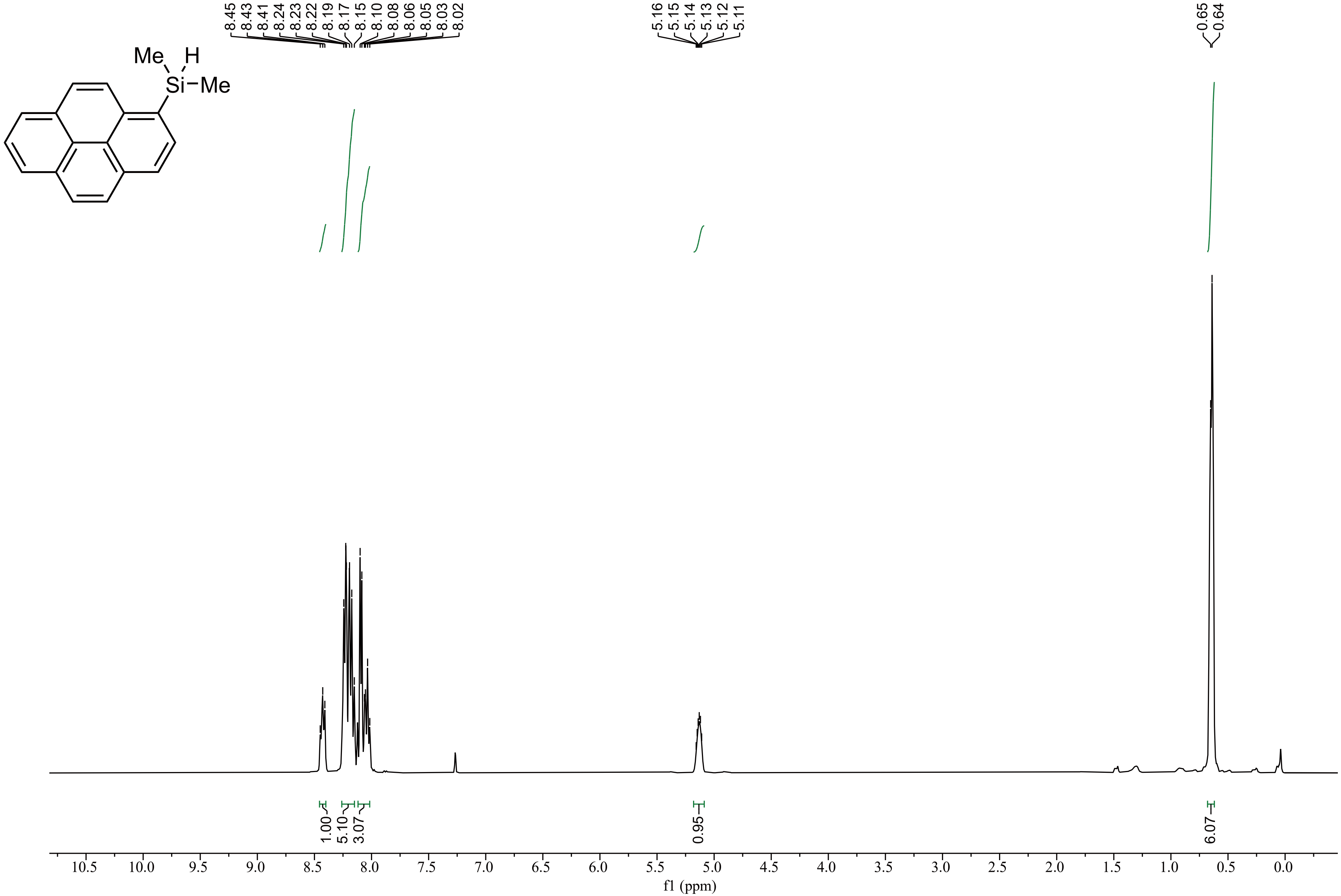

Compound **1as** ^{13}C NMR

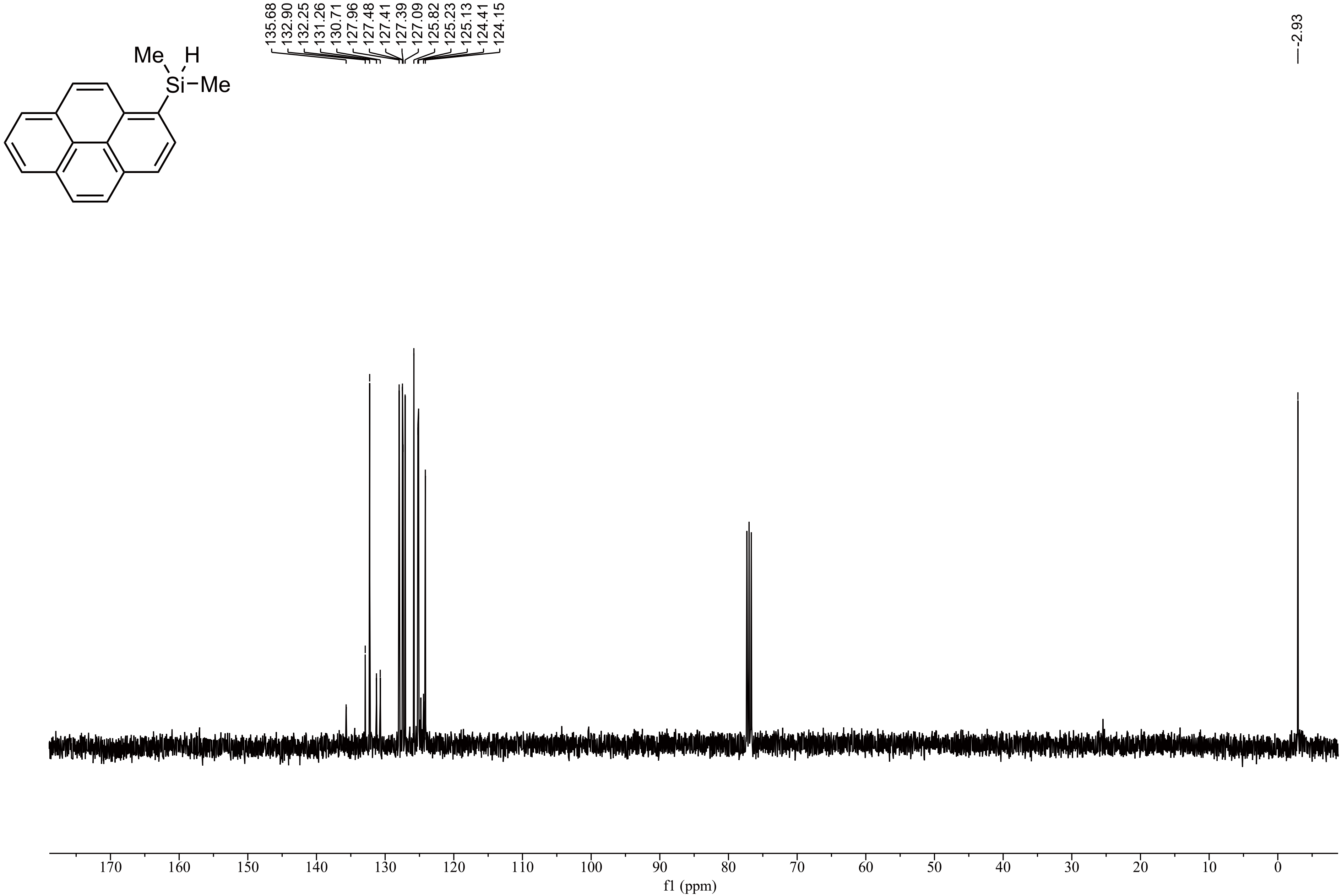

Compound **1at** ^{1}H NMR

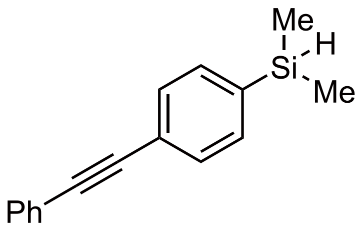

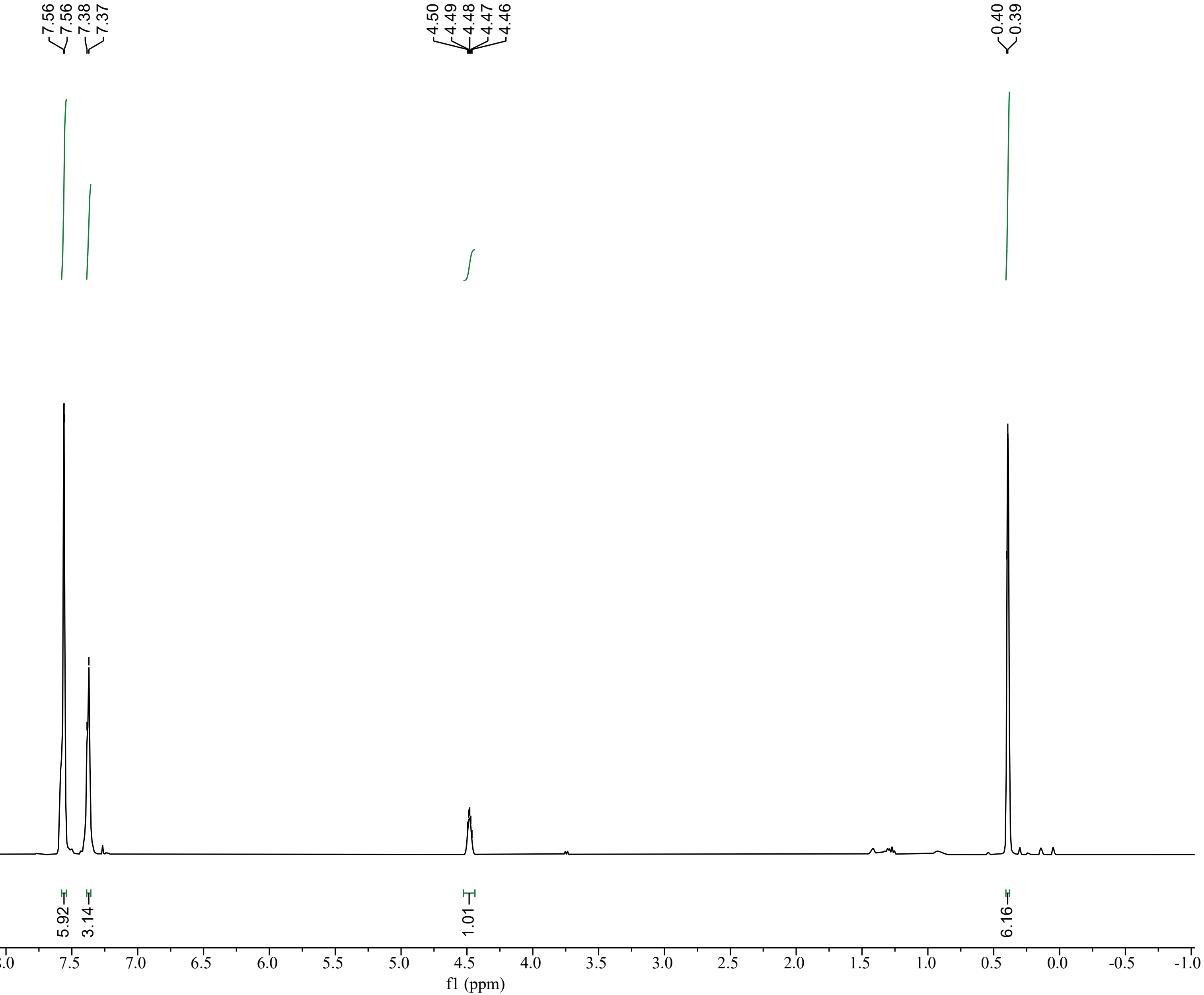

Compound **1at** ^{13}C NMR

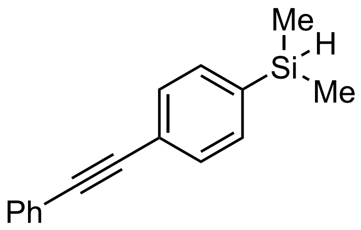

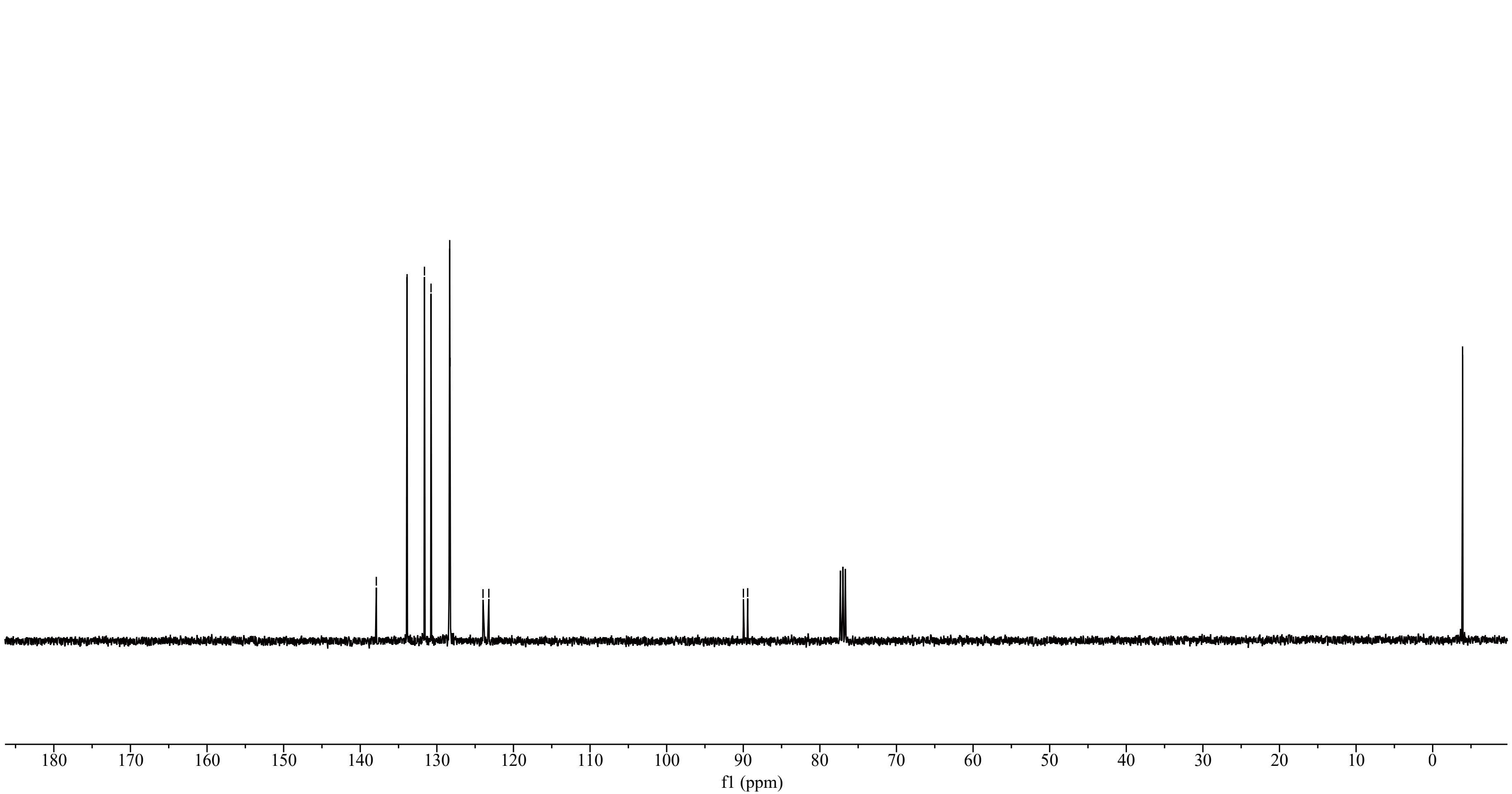

Compound **1au** ^{1}H NMR

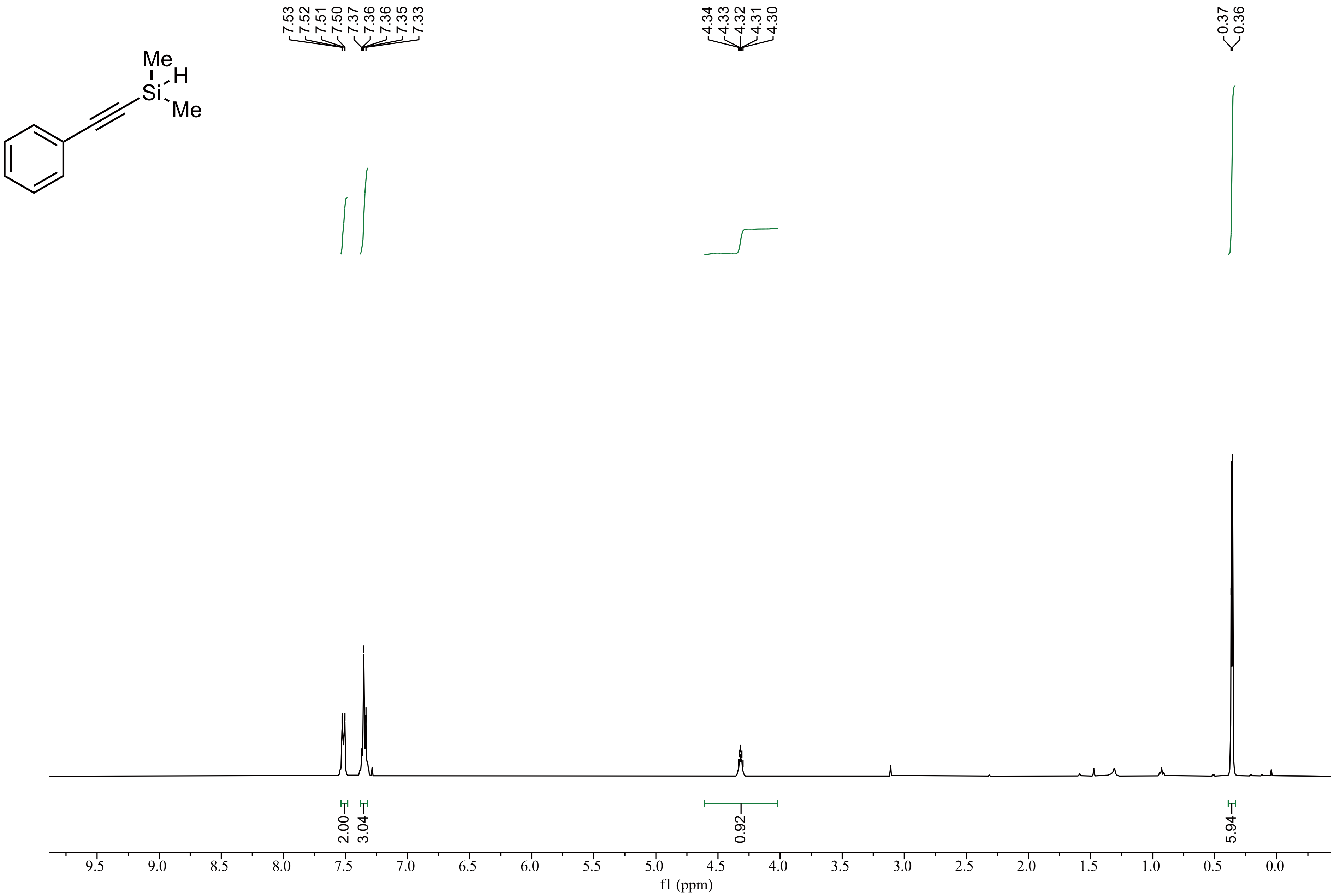

Compound **1au** ^{13}C NMR

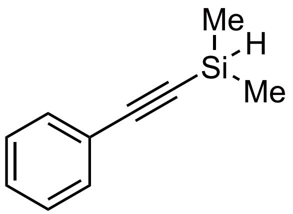

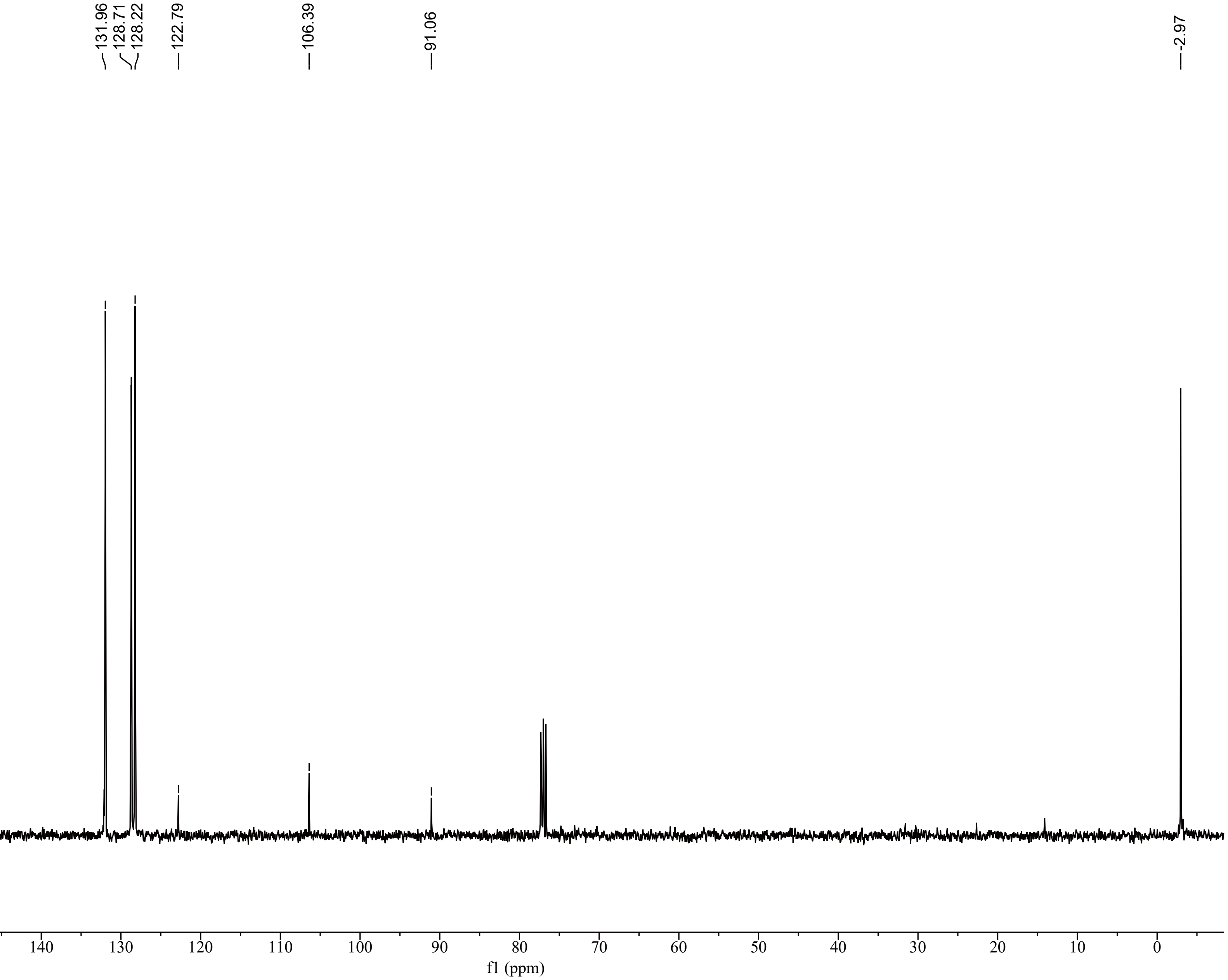

Compound **1av** [1]H NMR

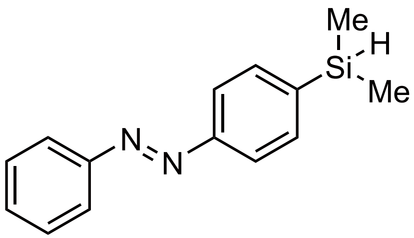

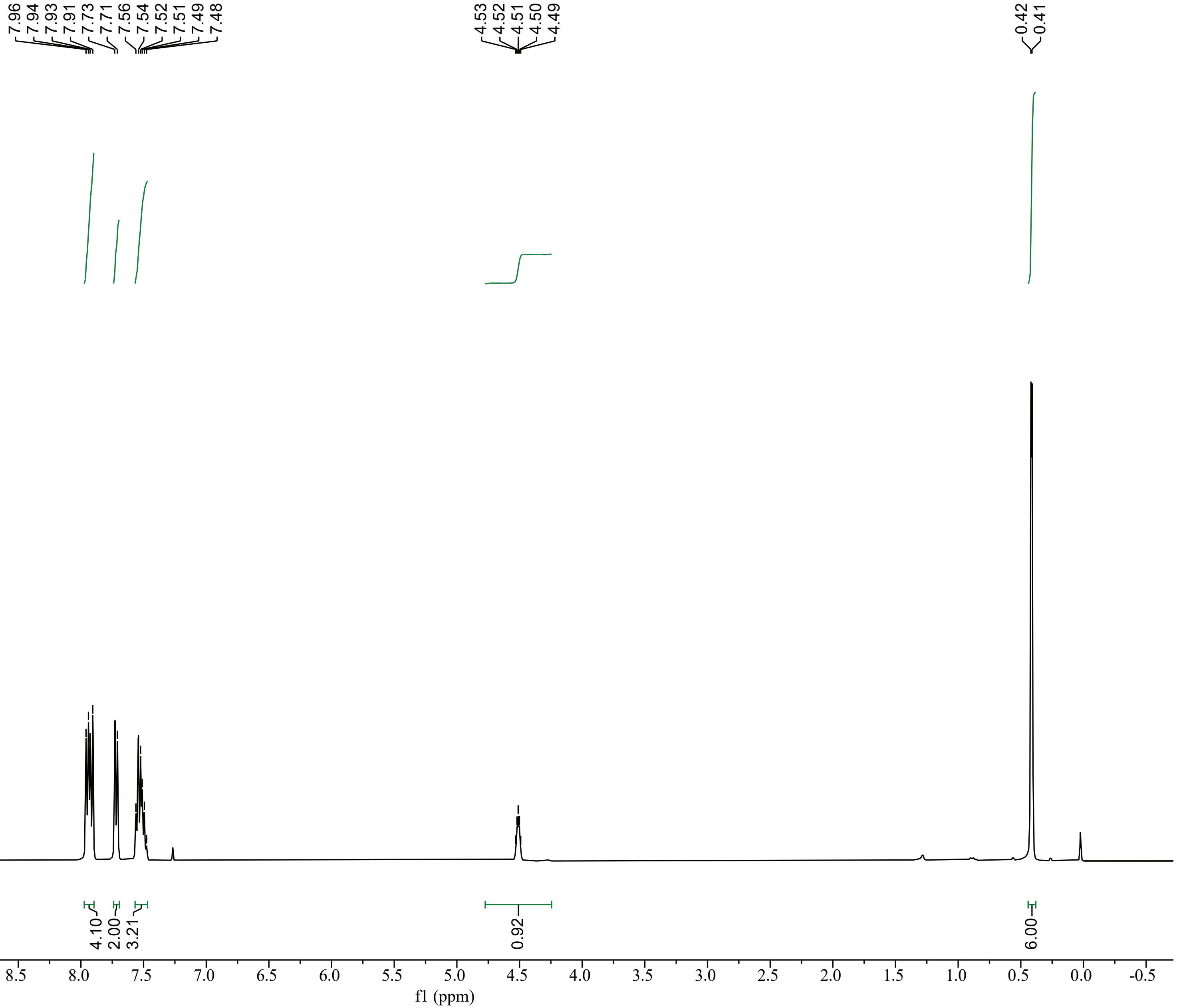

Compound **1av** ^{13}C NMR

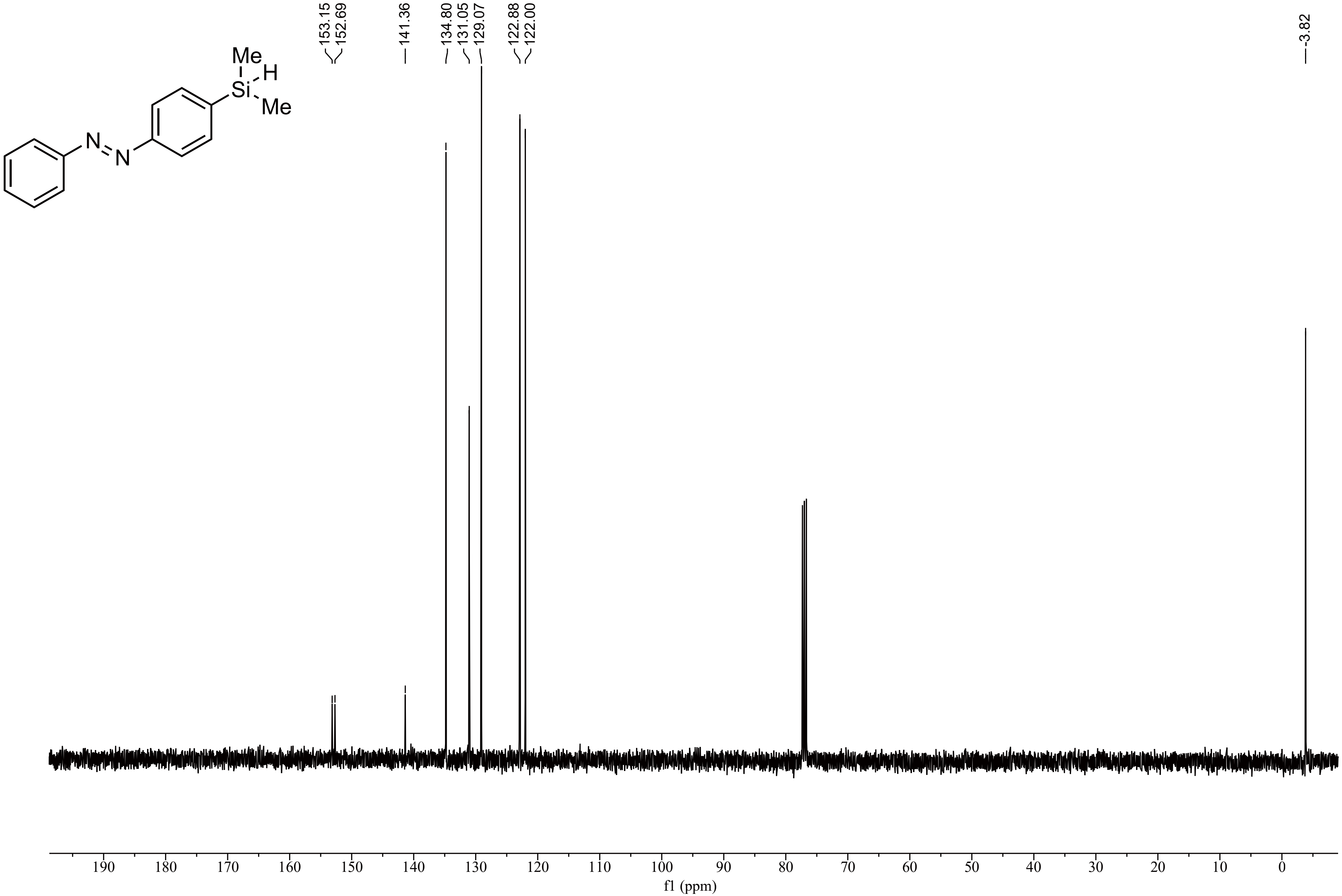

Compound **1aw** ^{1}H NMR

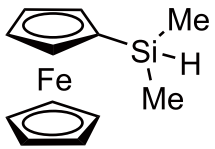

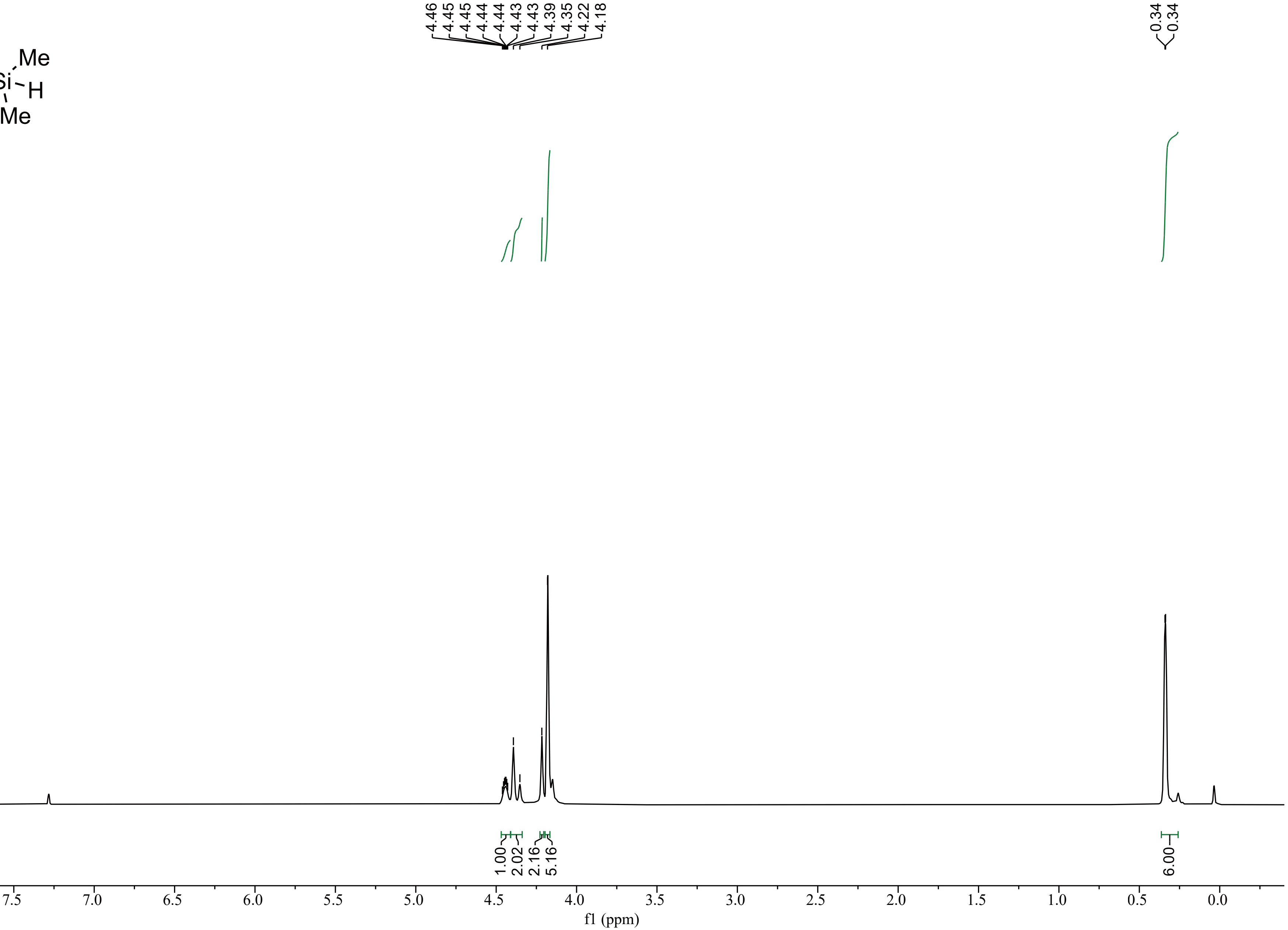

Compound **1aw** ^{13}C NMR

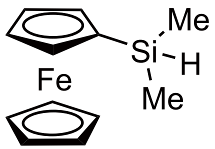

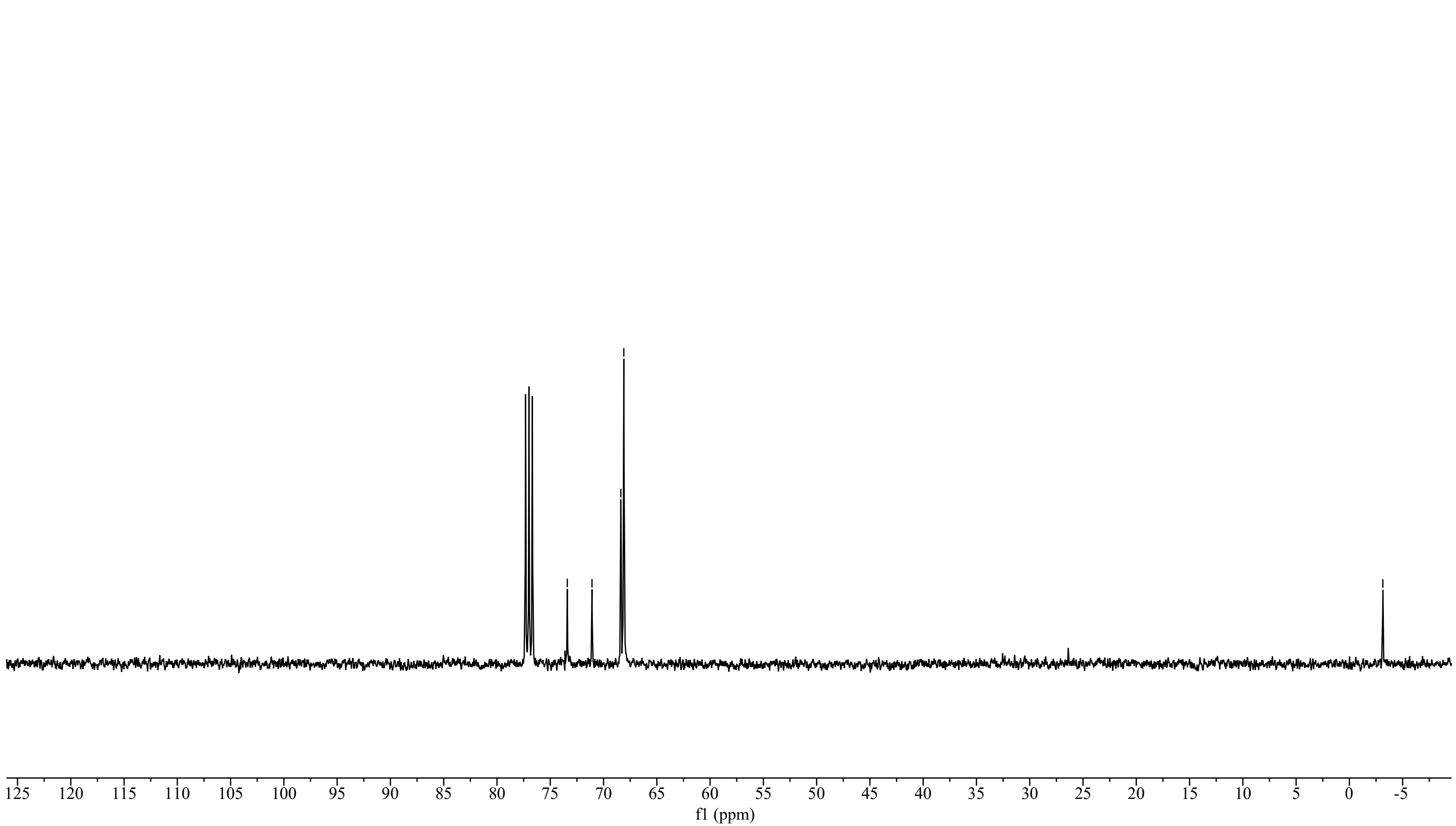

Compound **1ax** ^{1}H NMR

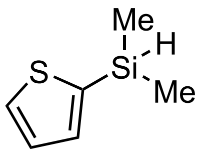

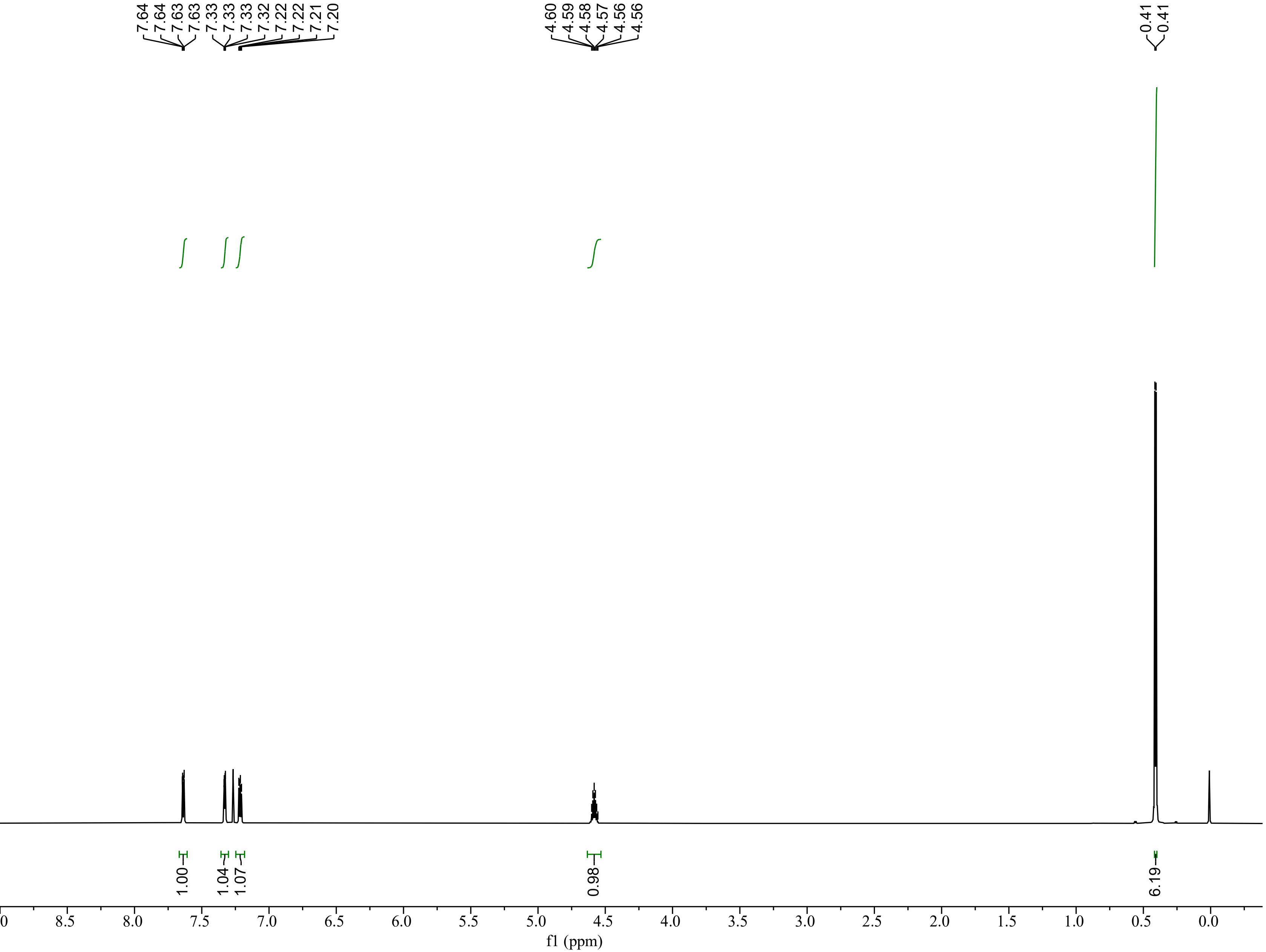

Compound **1ax** ^{1}H NMR

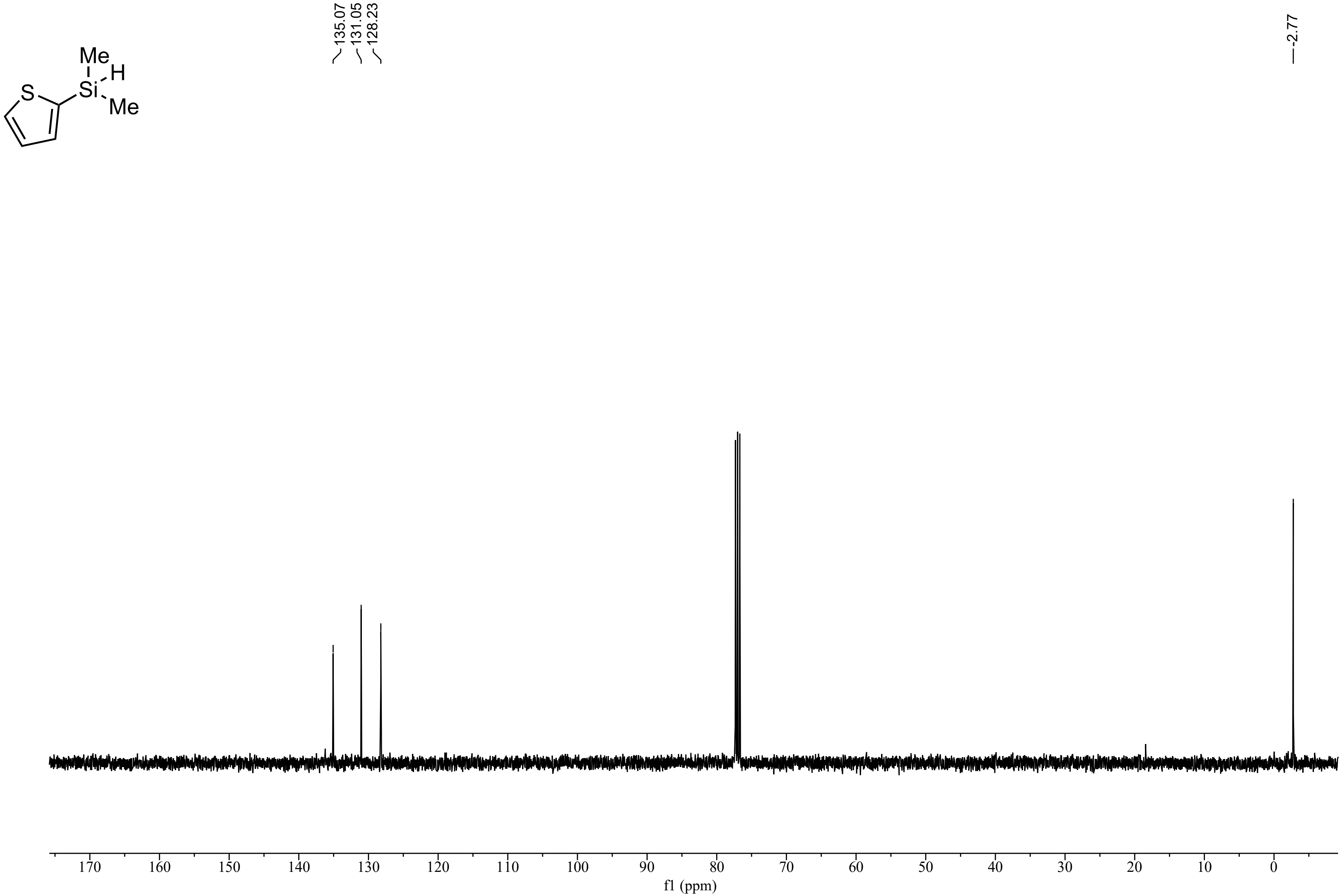

Compound **1ay** ^{1}H NMR

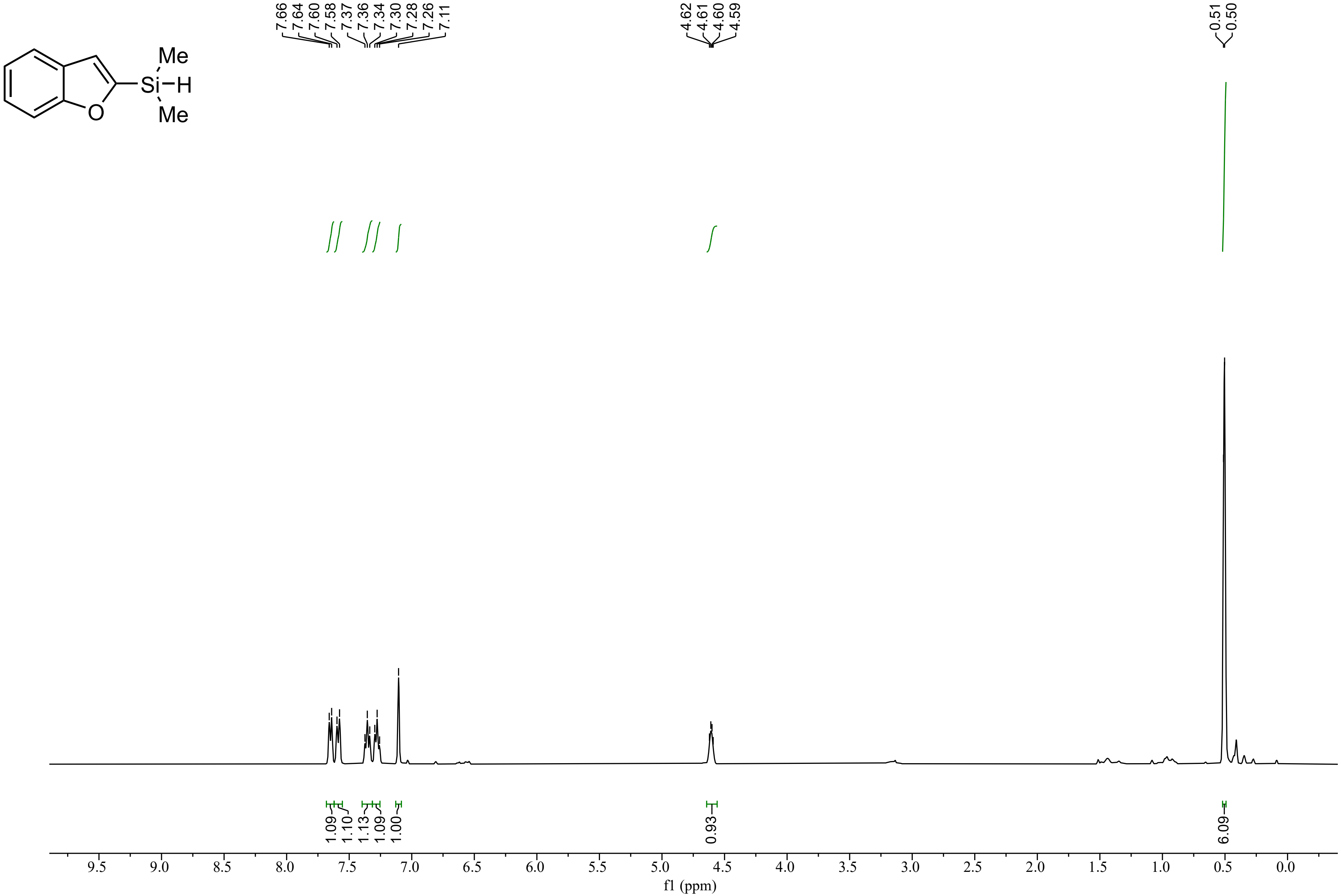

Compound **1ay** ^{13}C NMR

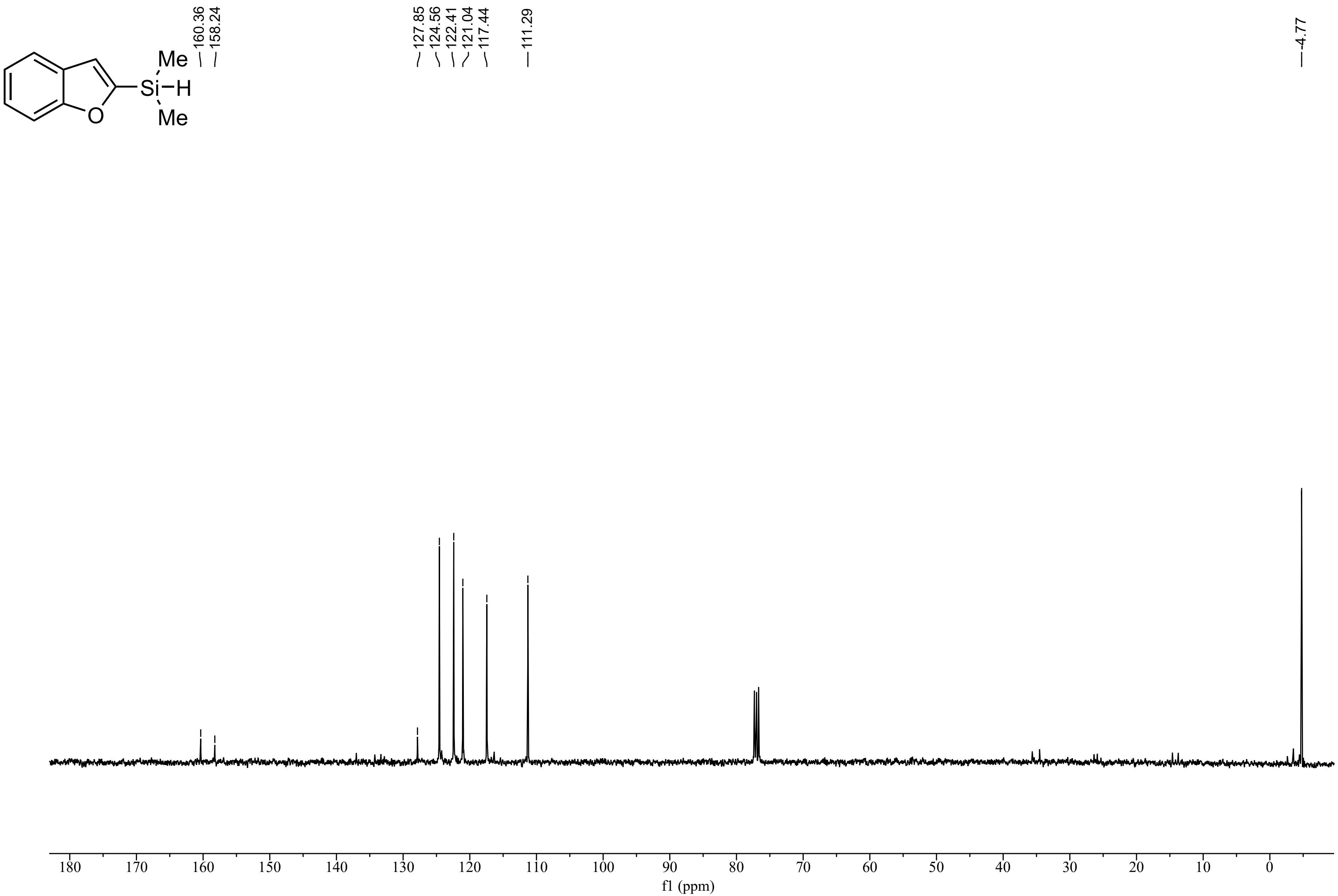

Compound **1az** ^{1}H NMR

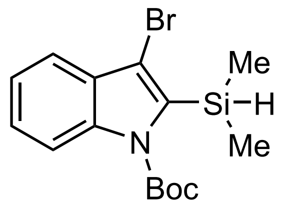

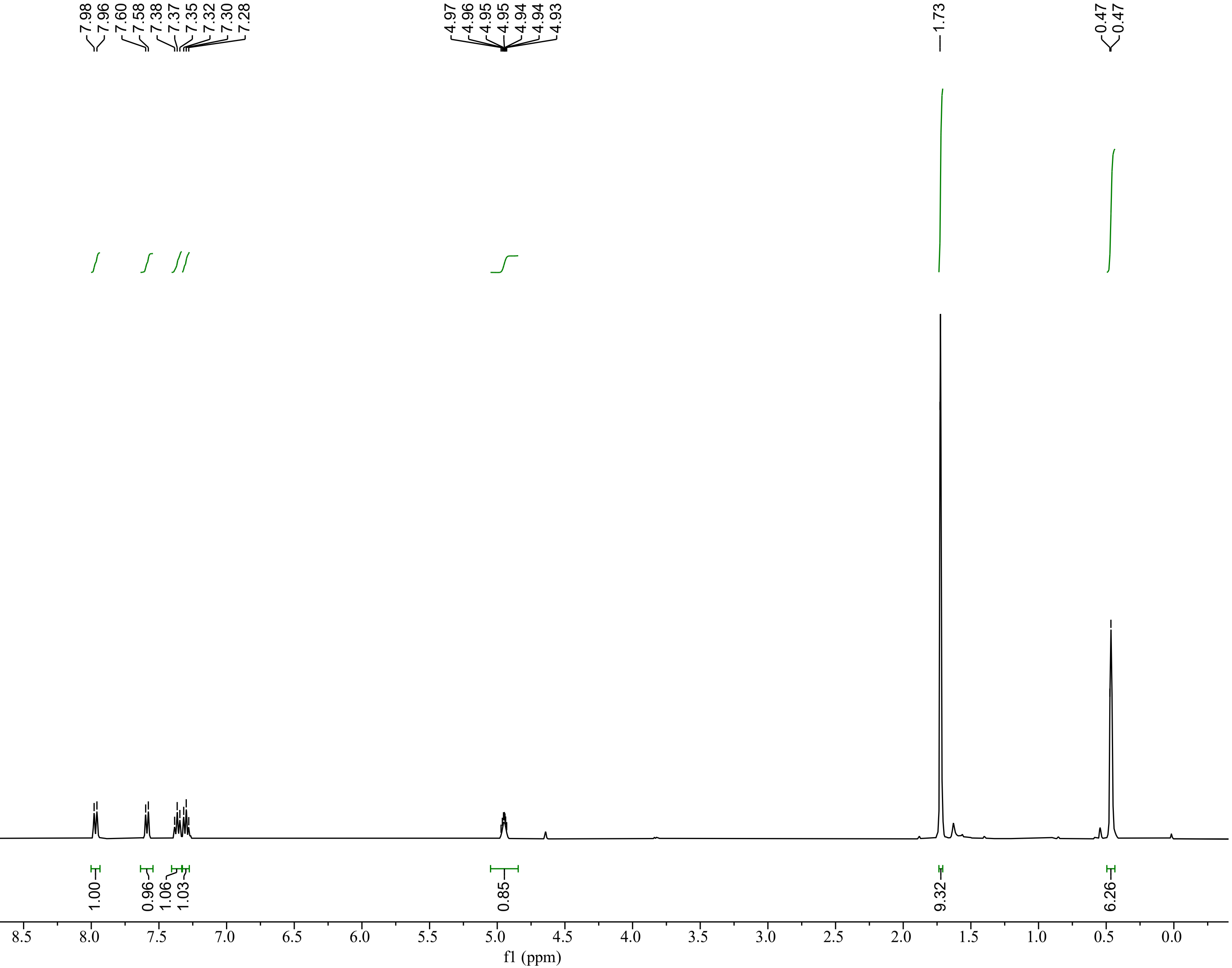

Compound **1az** ^{1}H NMR

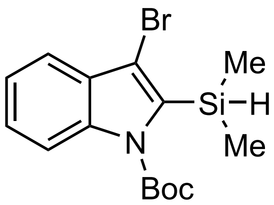

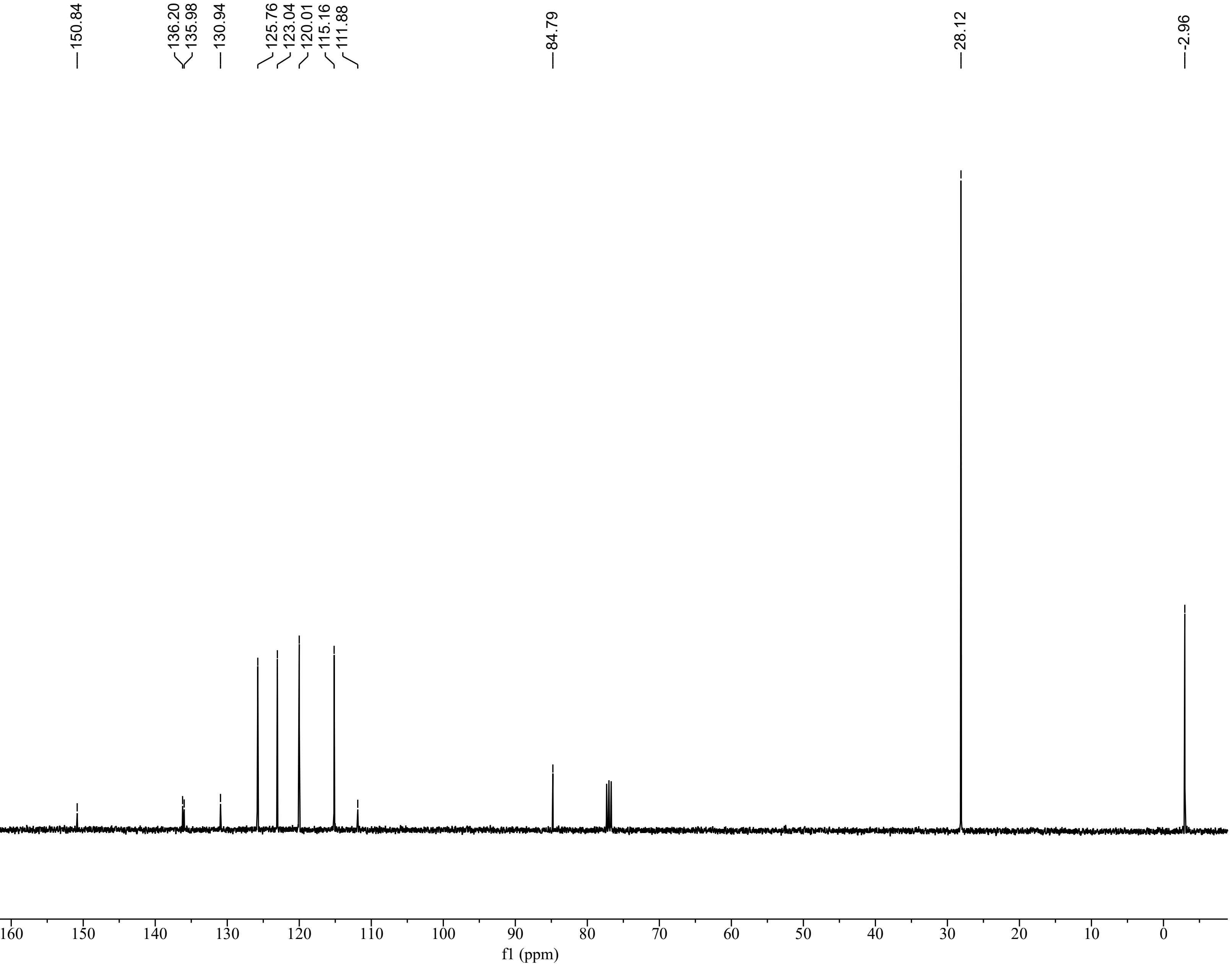

Compound **1ba** ^{1}H NMR

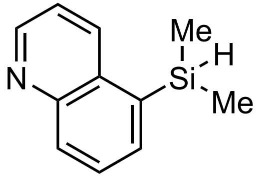

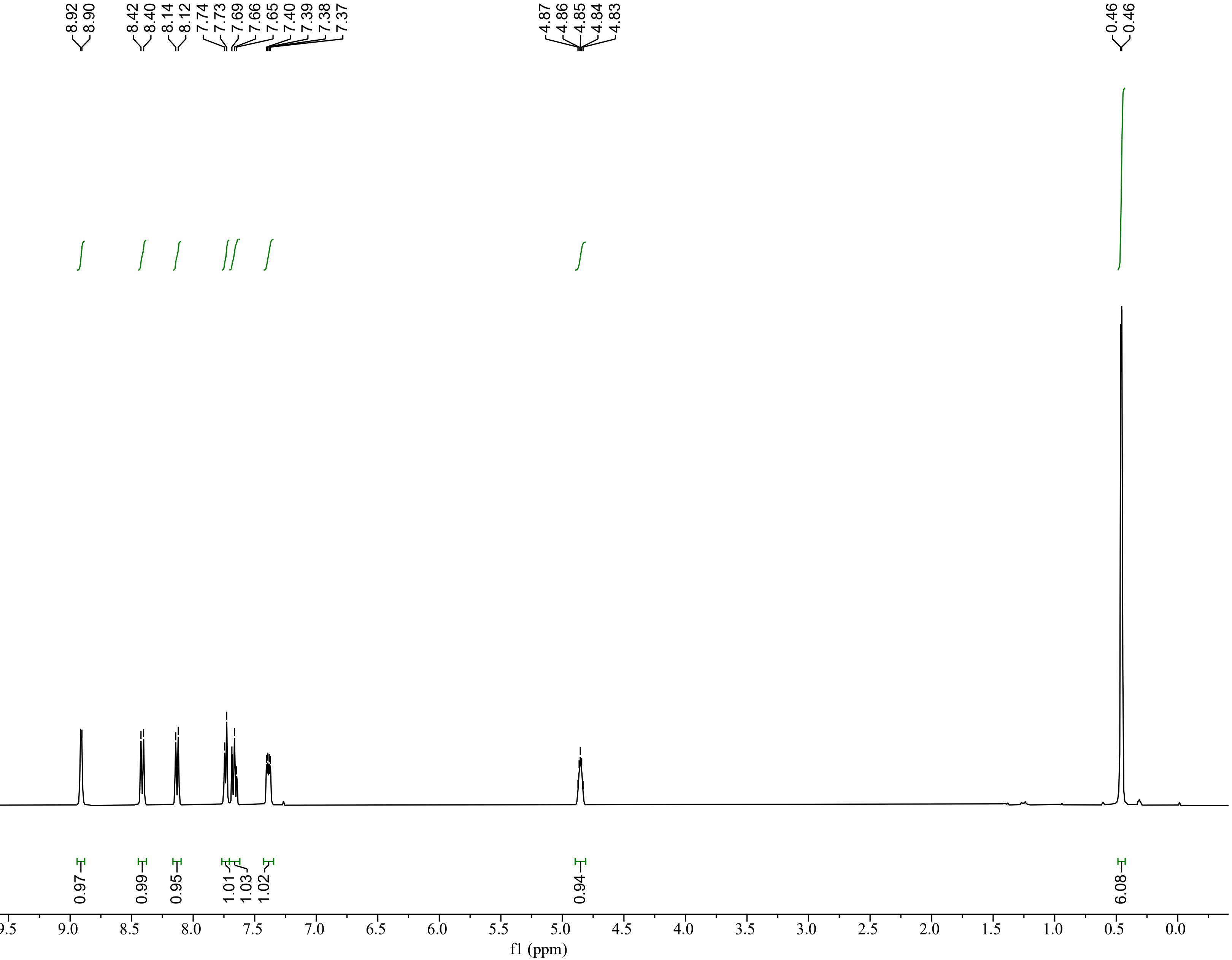

Compound **1ba** ^{13}C NMR

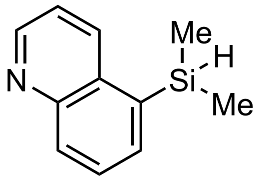

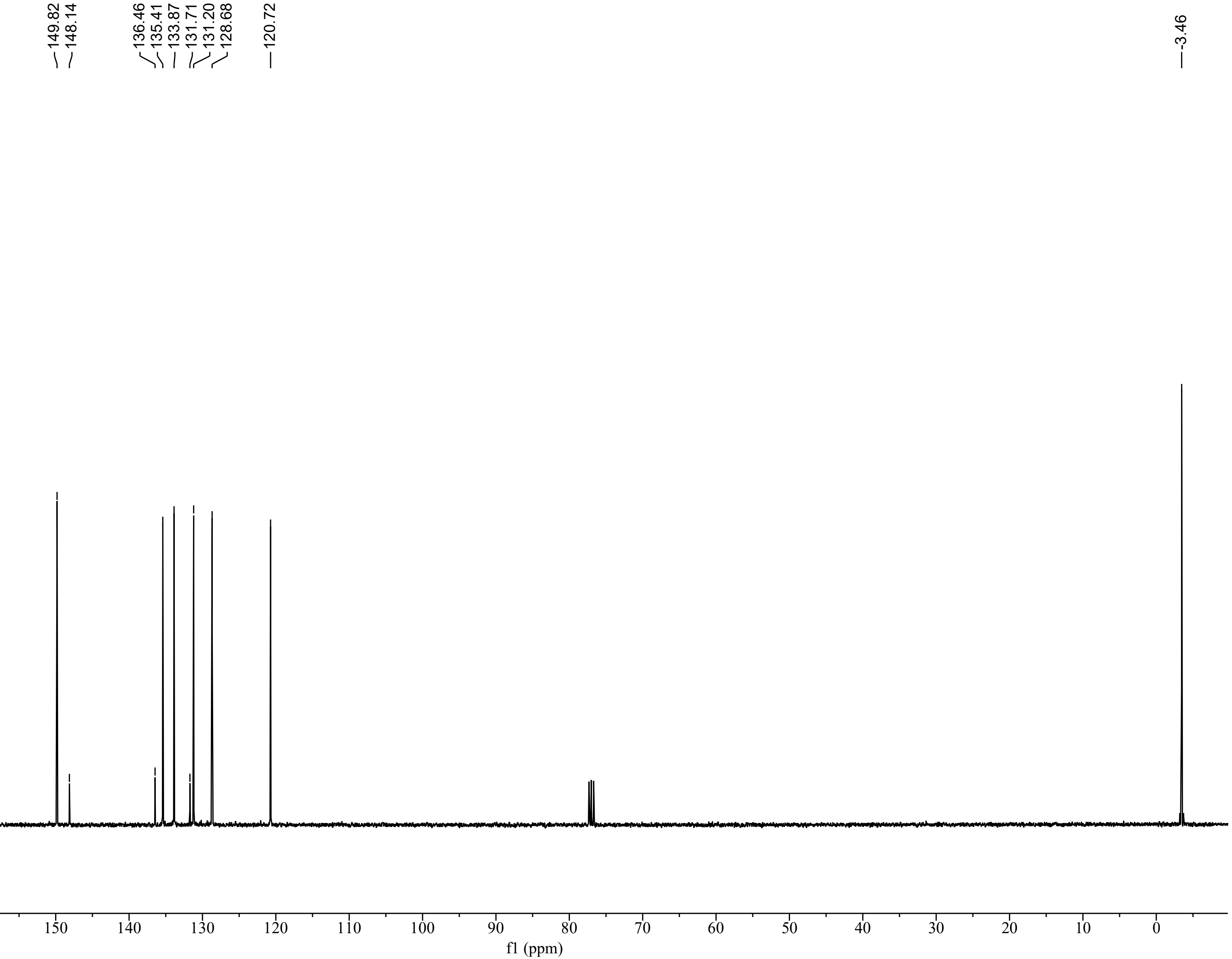

Compound **1bb** ^{1}H NMR

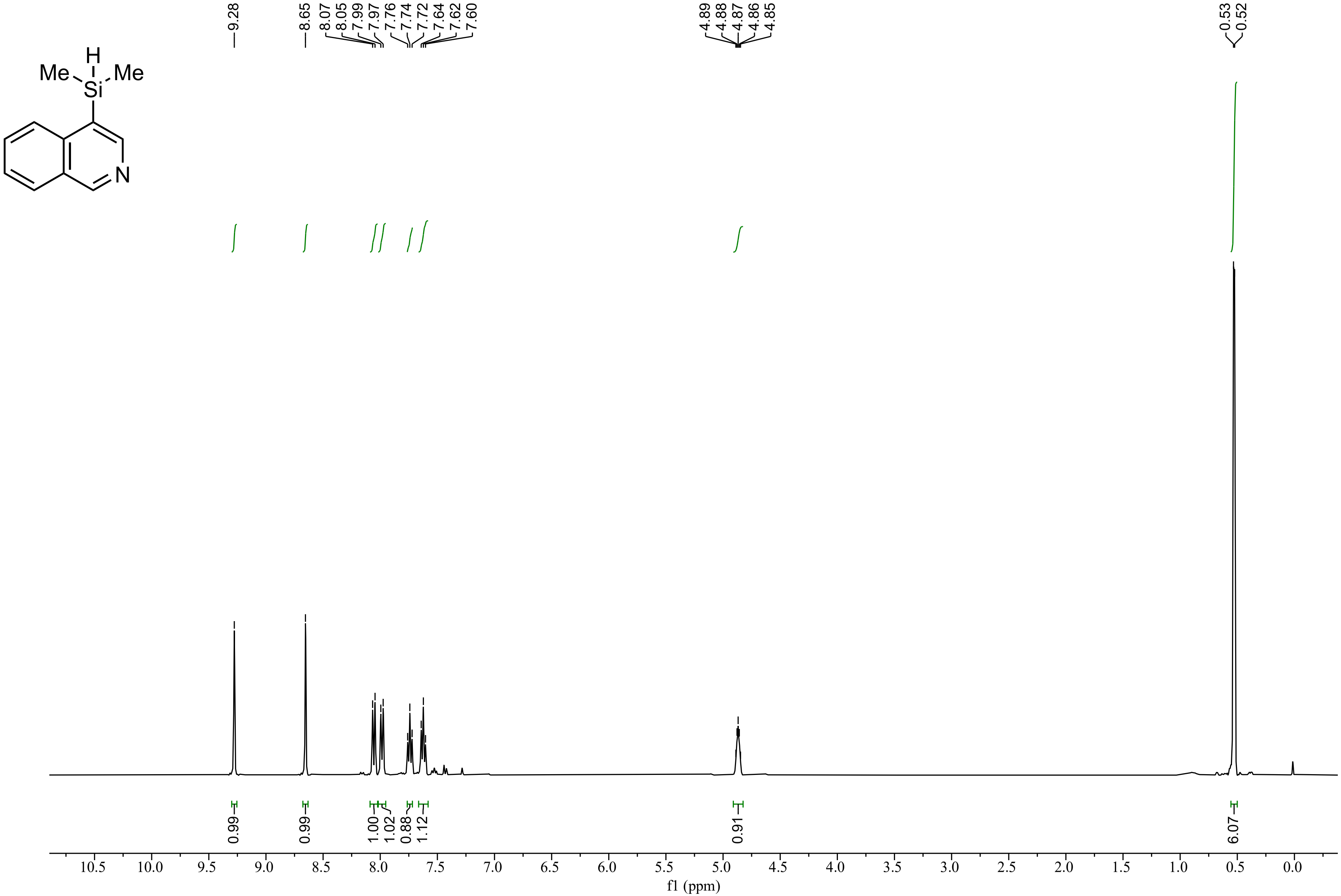

Compound **1bb** ^{13}C NMR

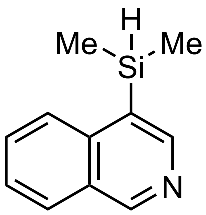

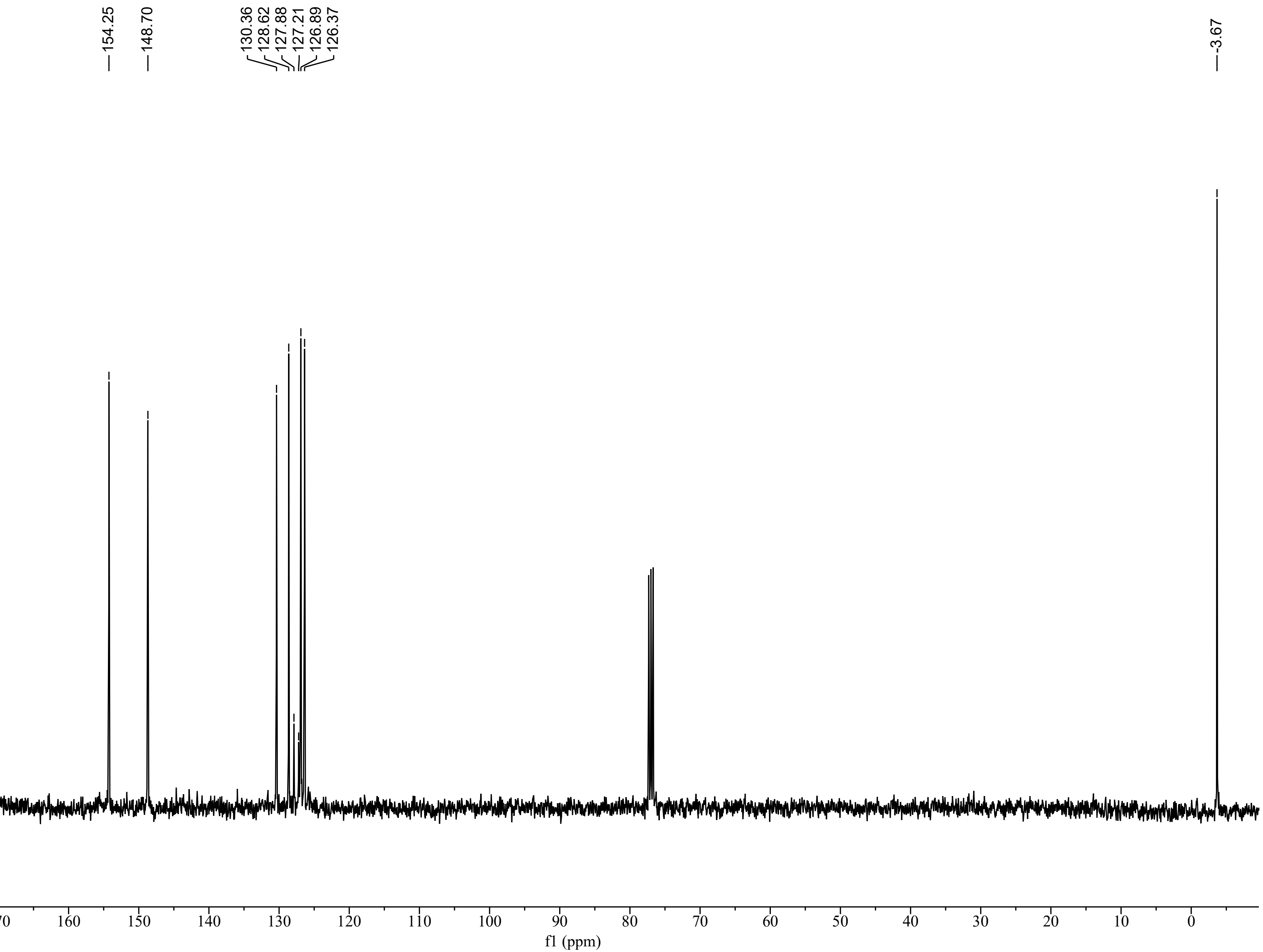

Compound **1bc** ^{1}H NMR

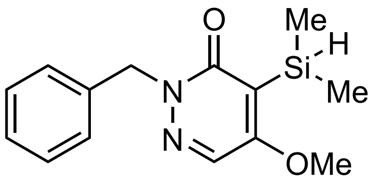

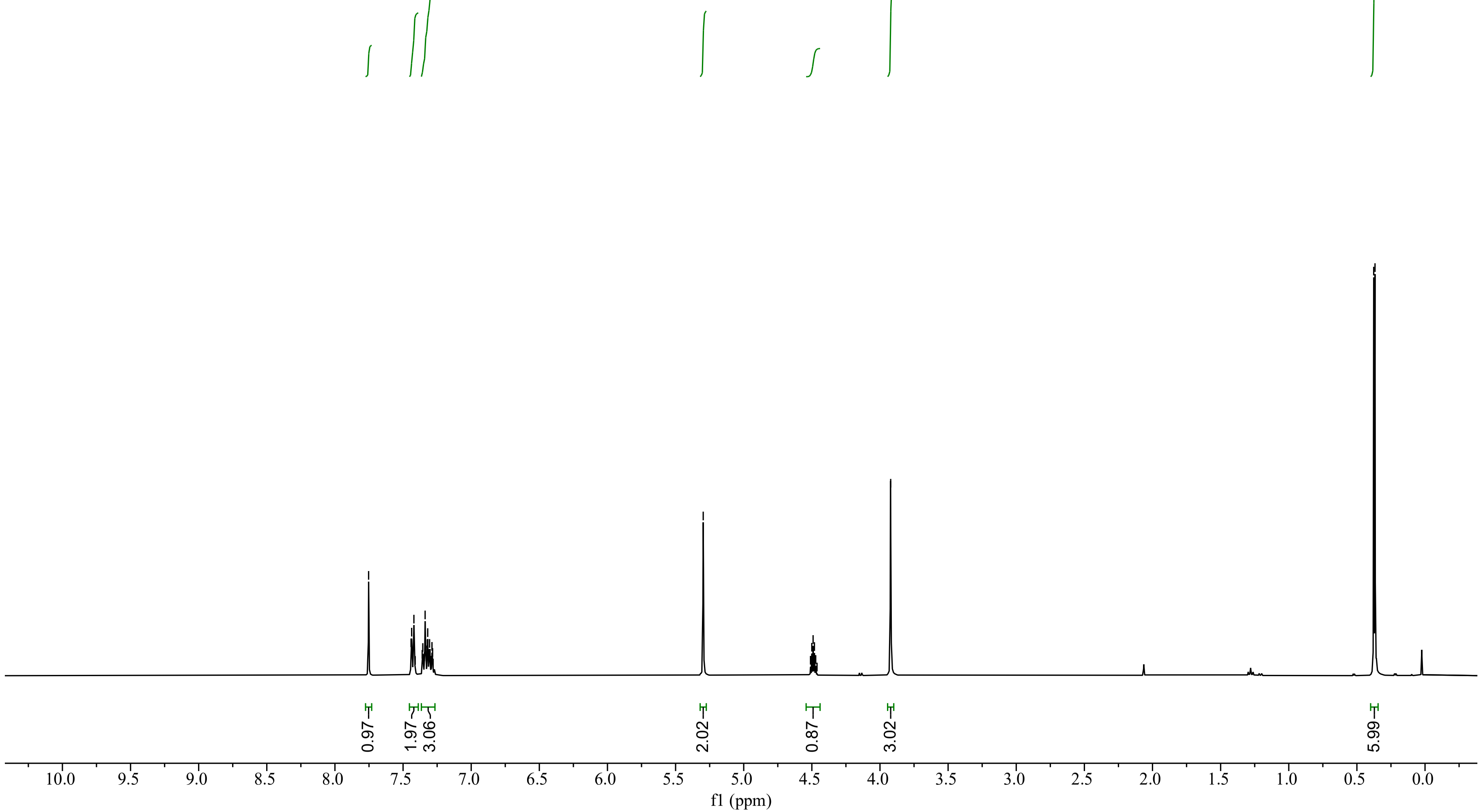

Compound **1bc** ^{13}C NMR

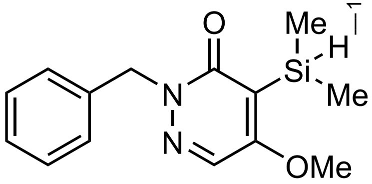

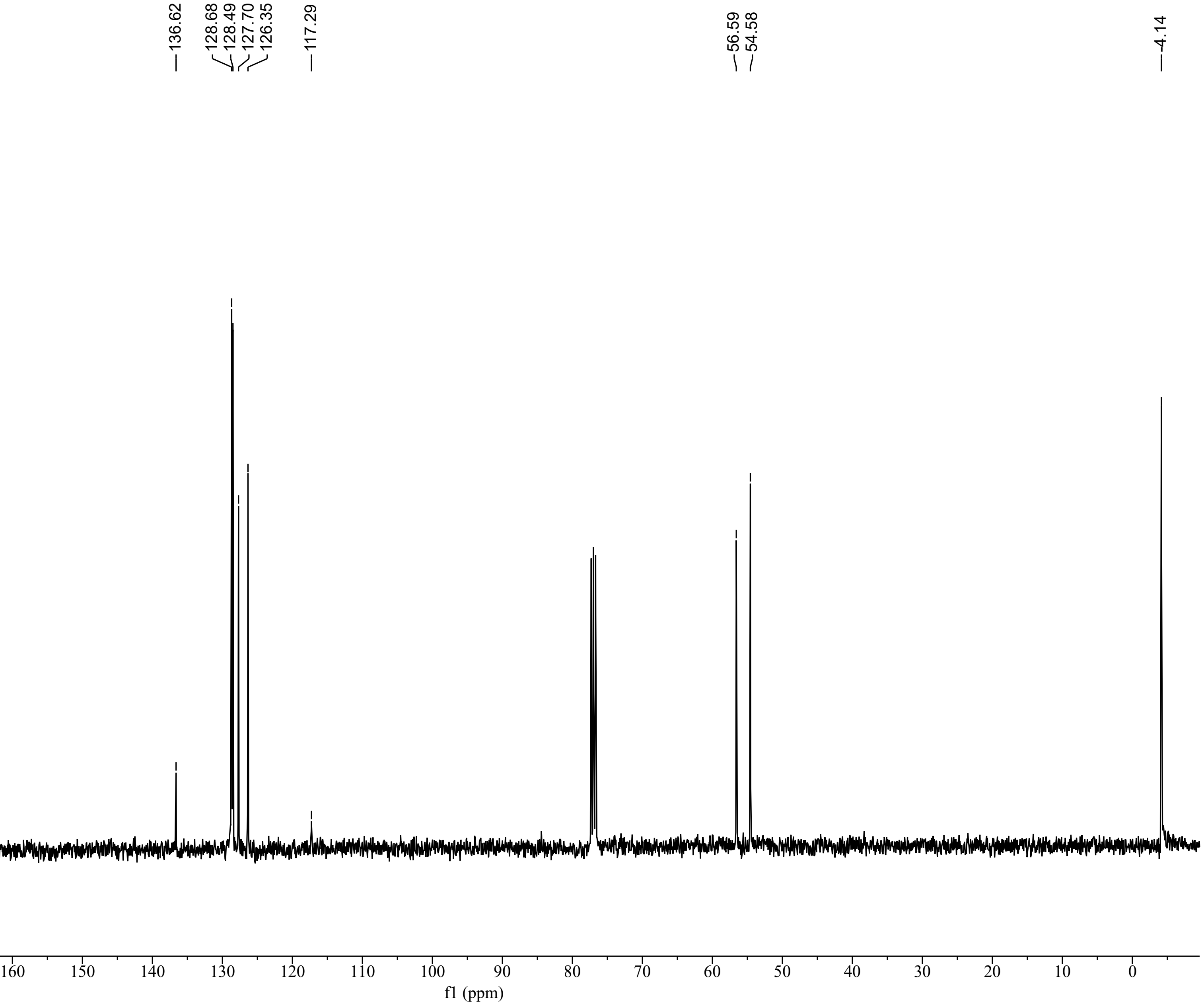

Compound **1bd** ^{1}H NMR

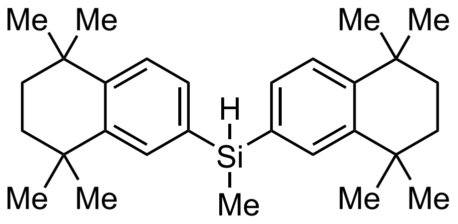

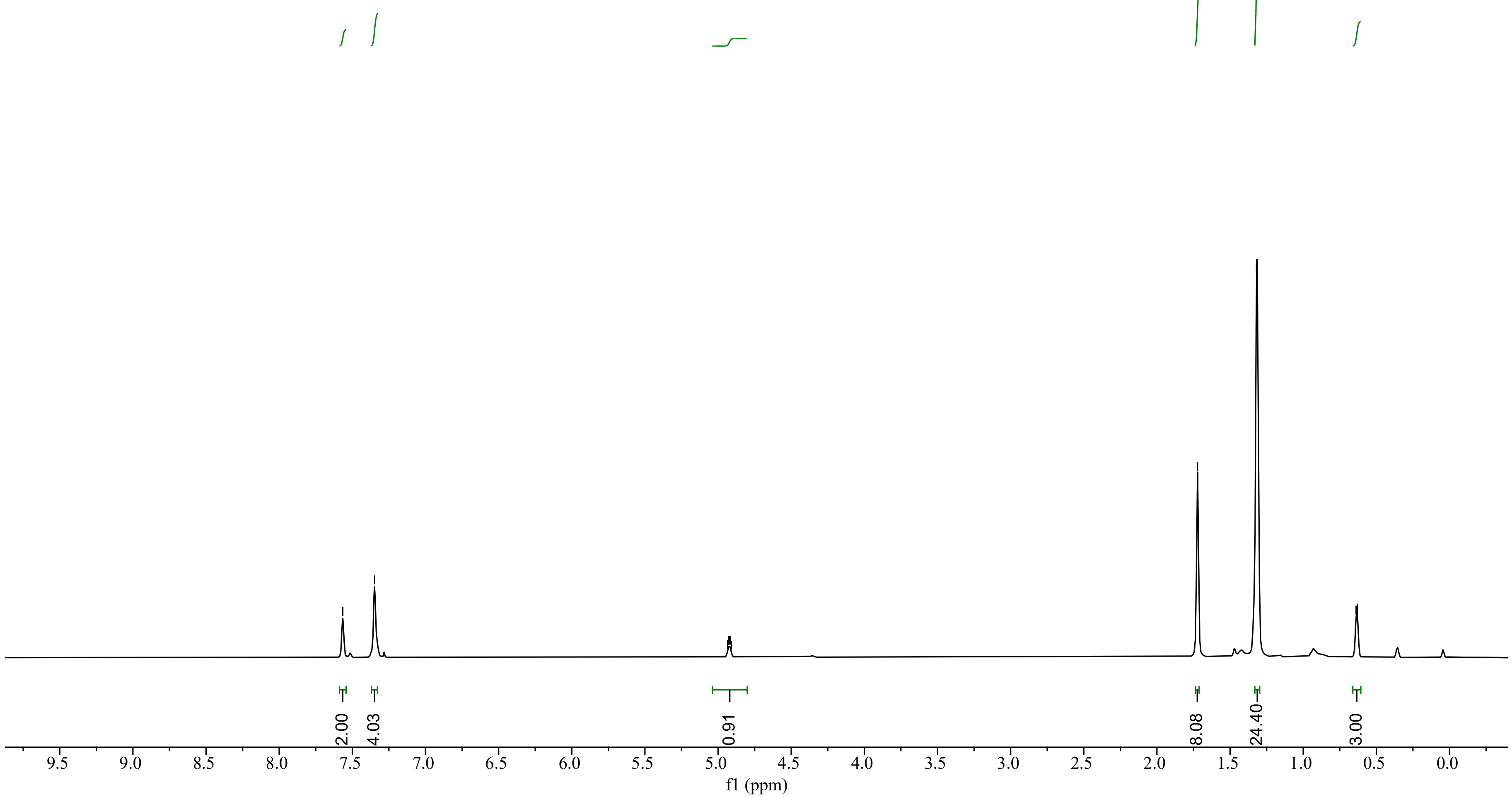

Compound **1bd** ^{13}C NMR

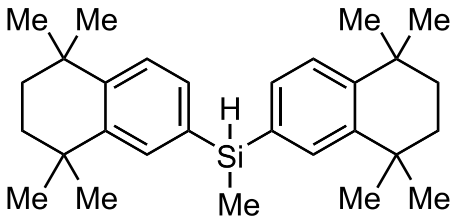

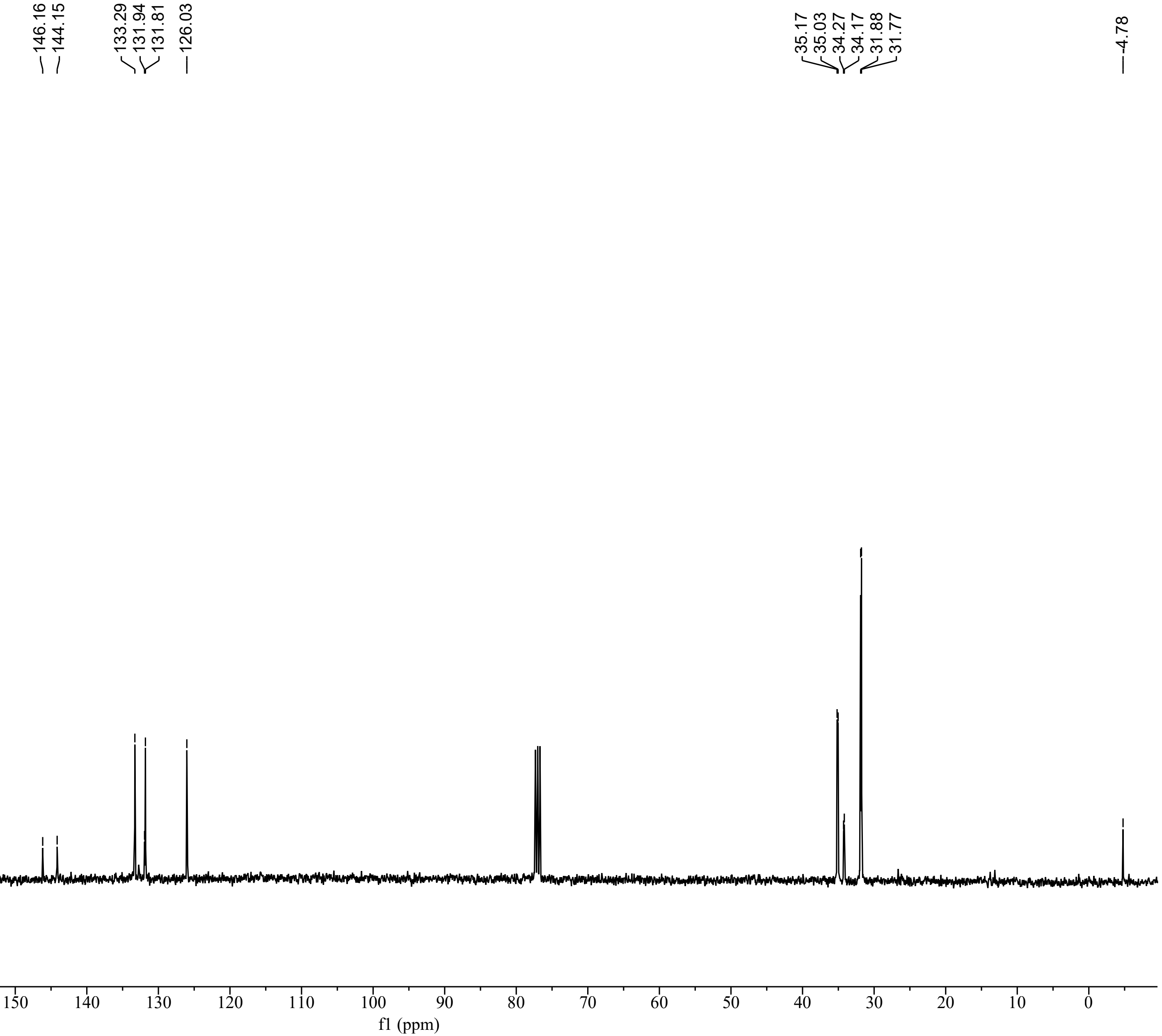

Compound **1be** [1]H NMR

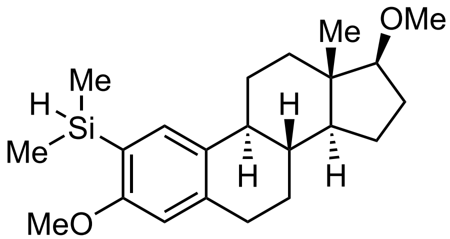

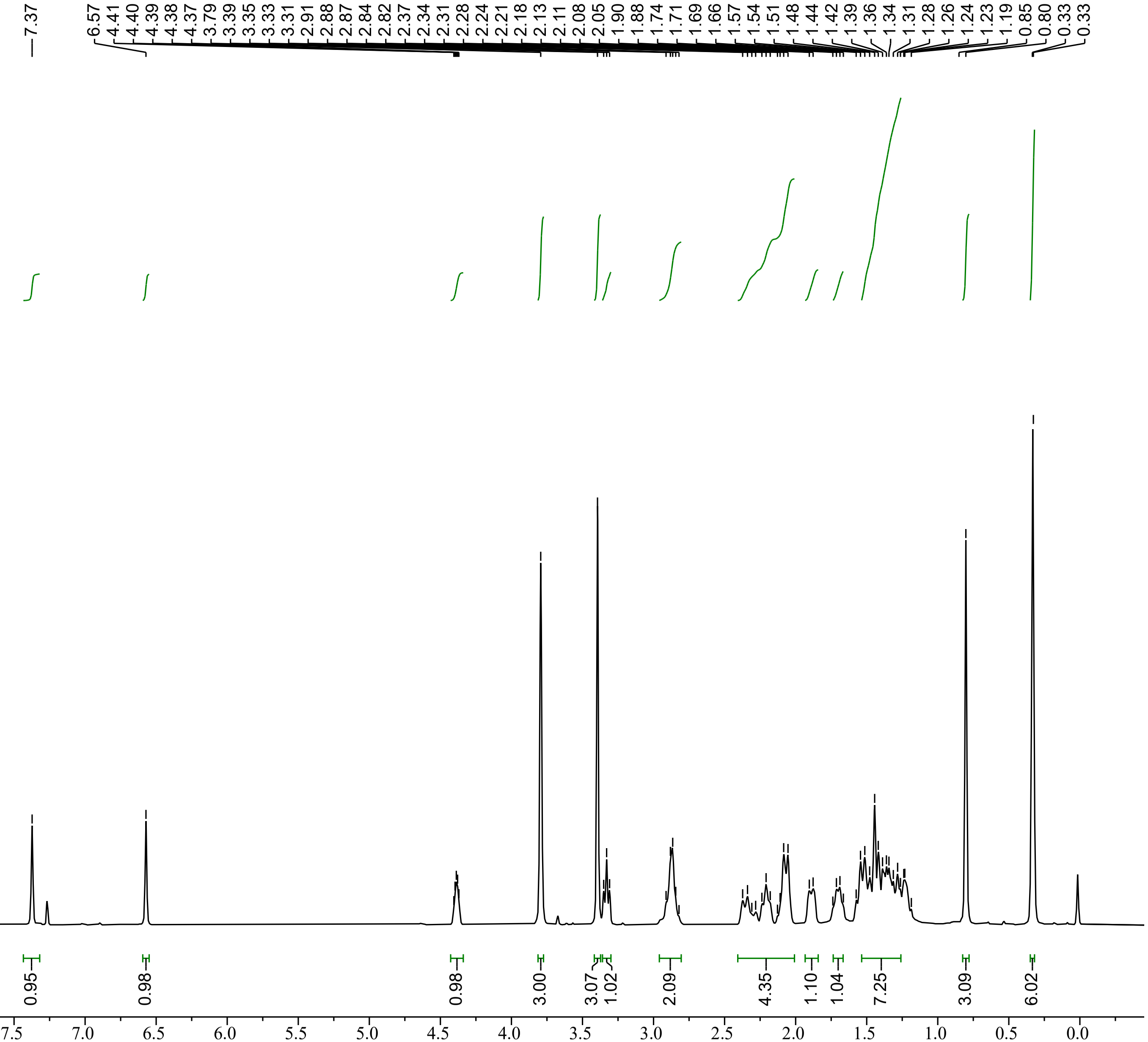

Compound **1be** ^{13}C NMR

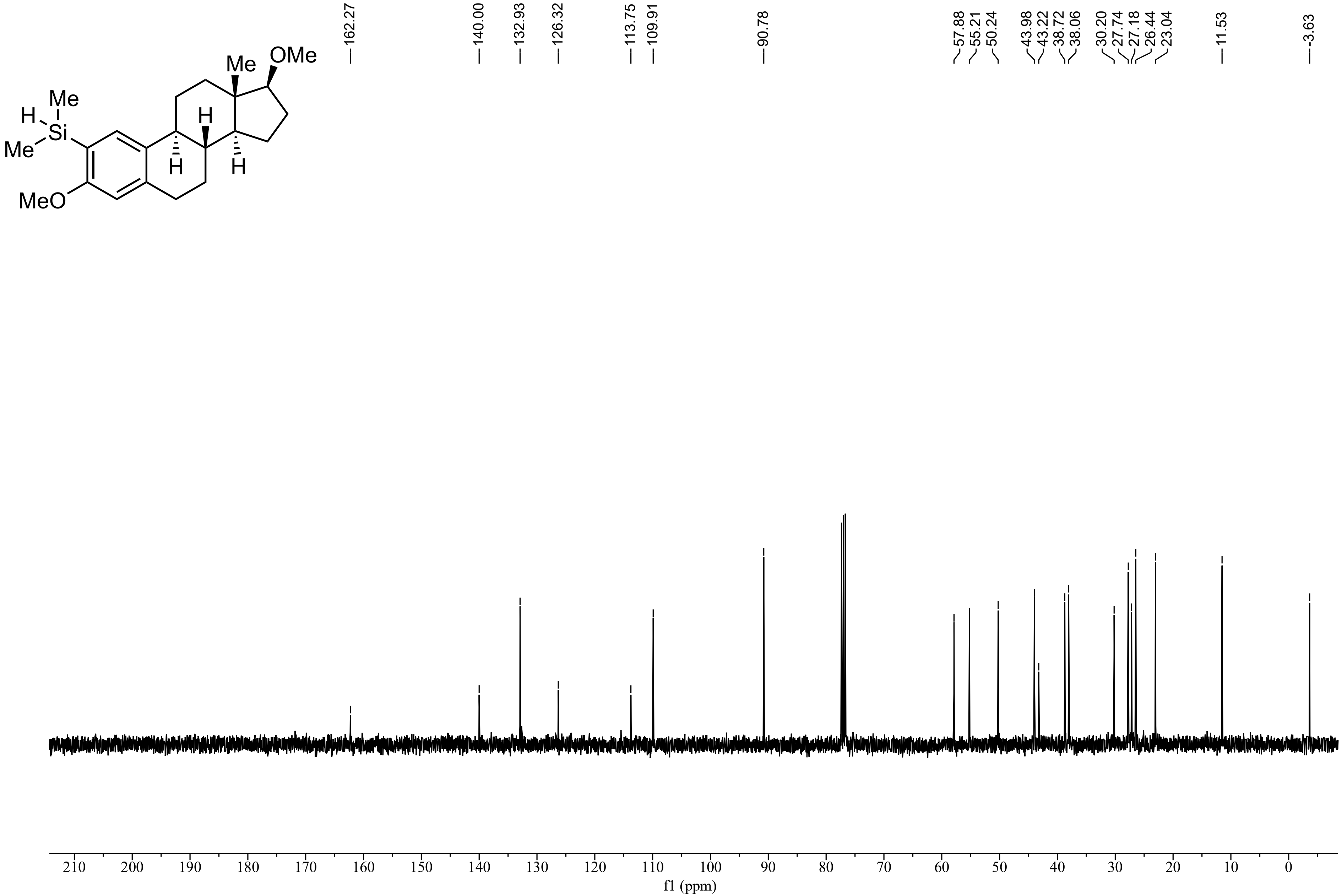

Compound **1bf** ^{1}H NMR

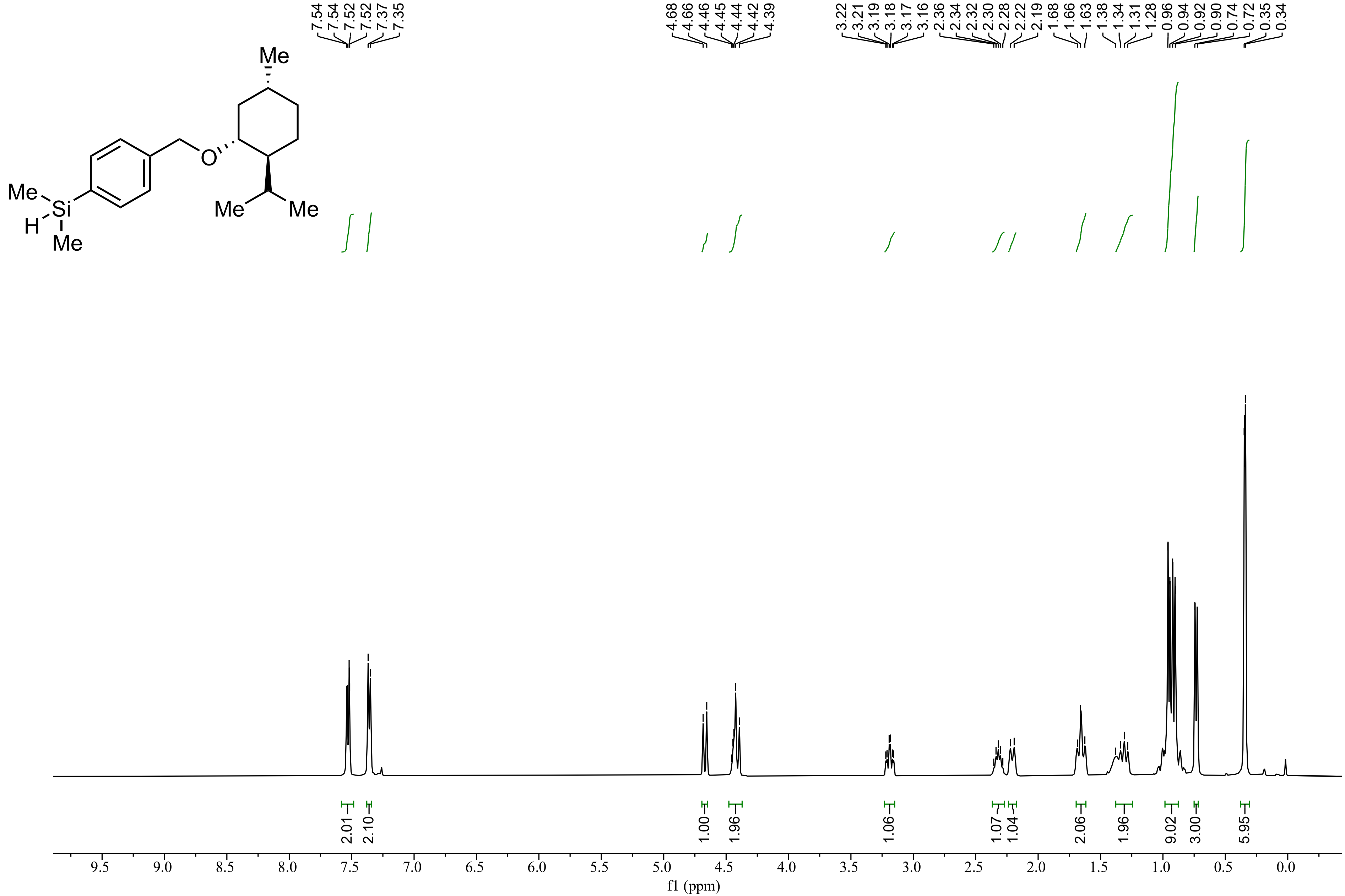

Compound **1bf** ^{13}C NMR

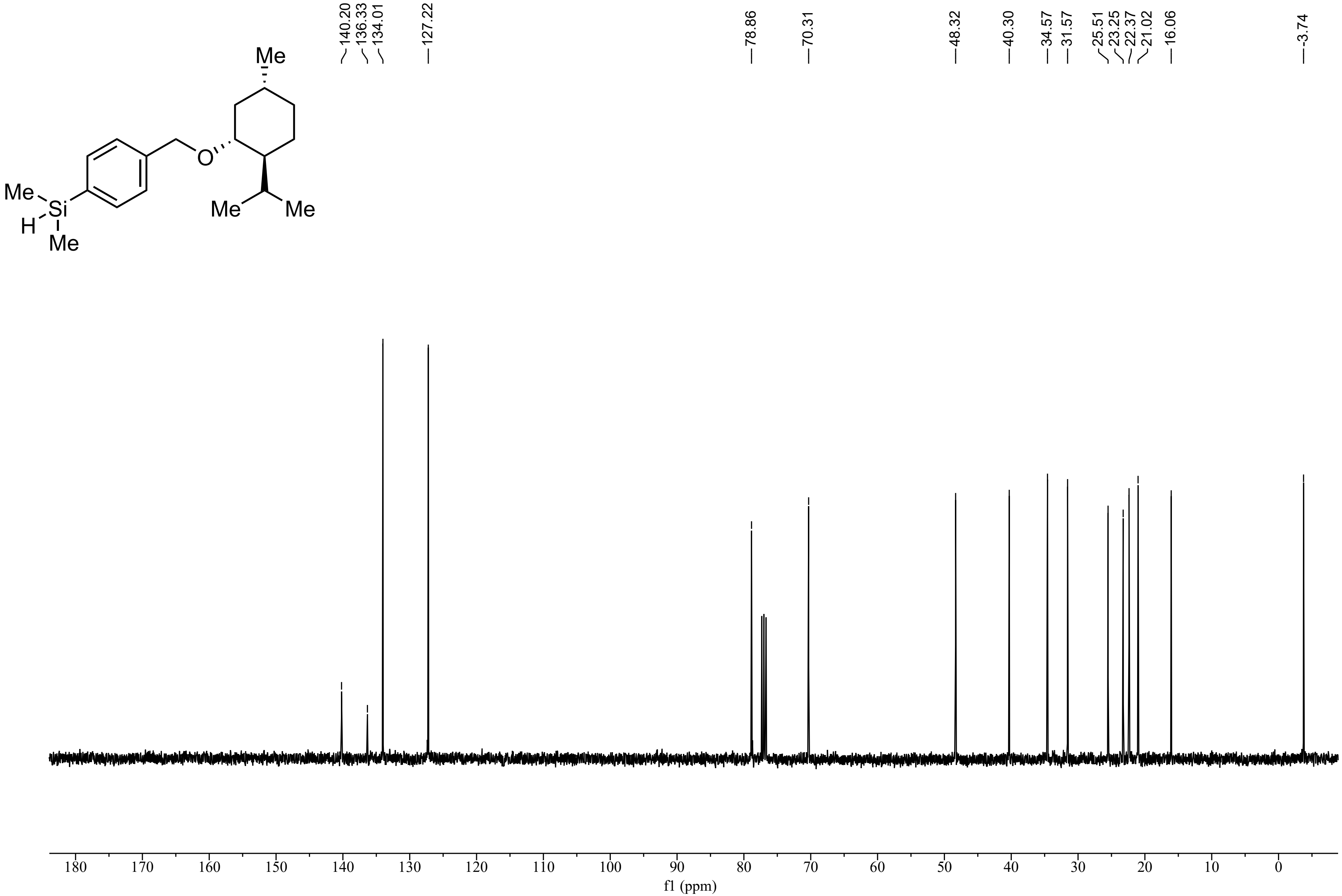

Compound **1bg** ^{1}H NMR

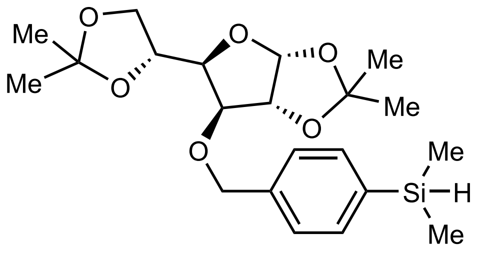

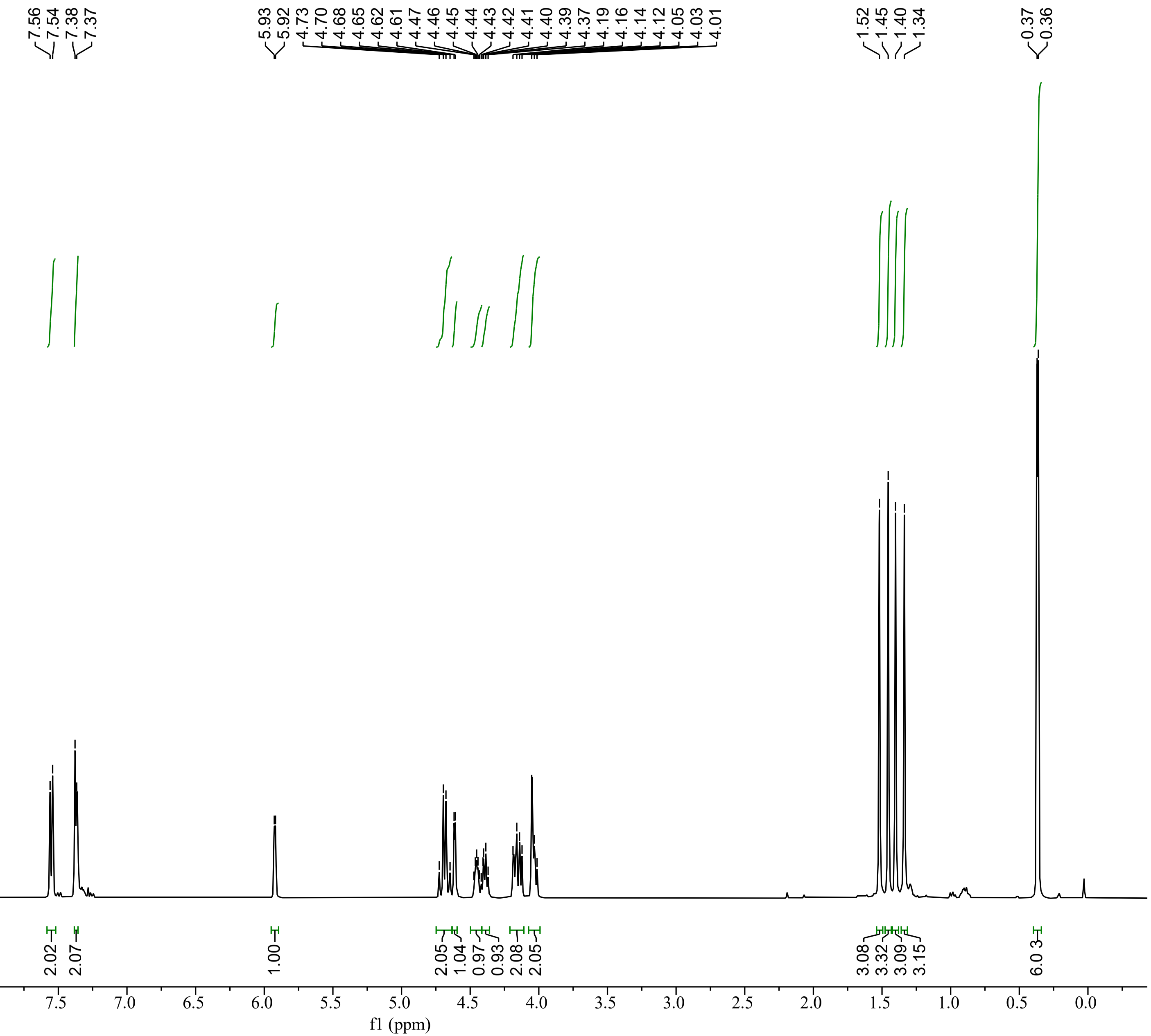

Compound **1bg** ^{13}C NMR

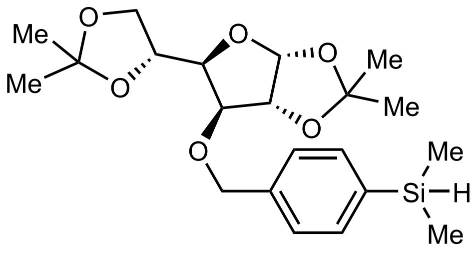

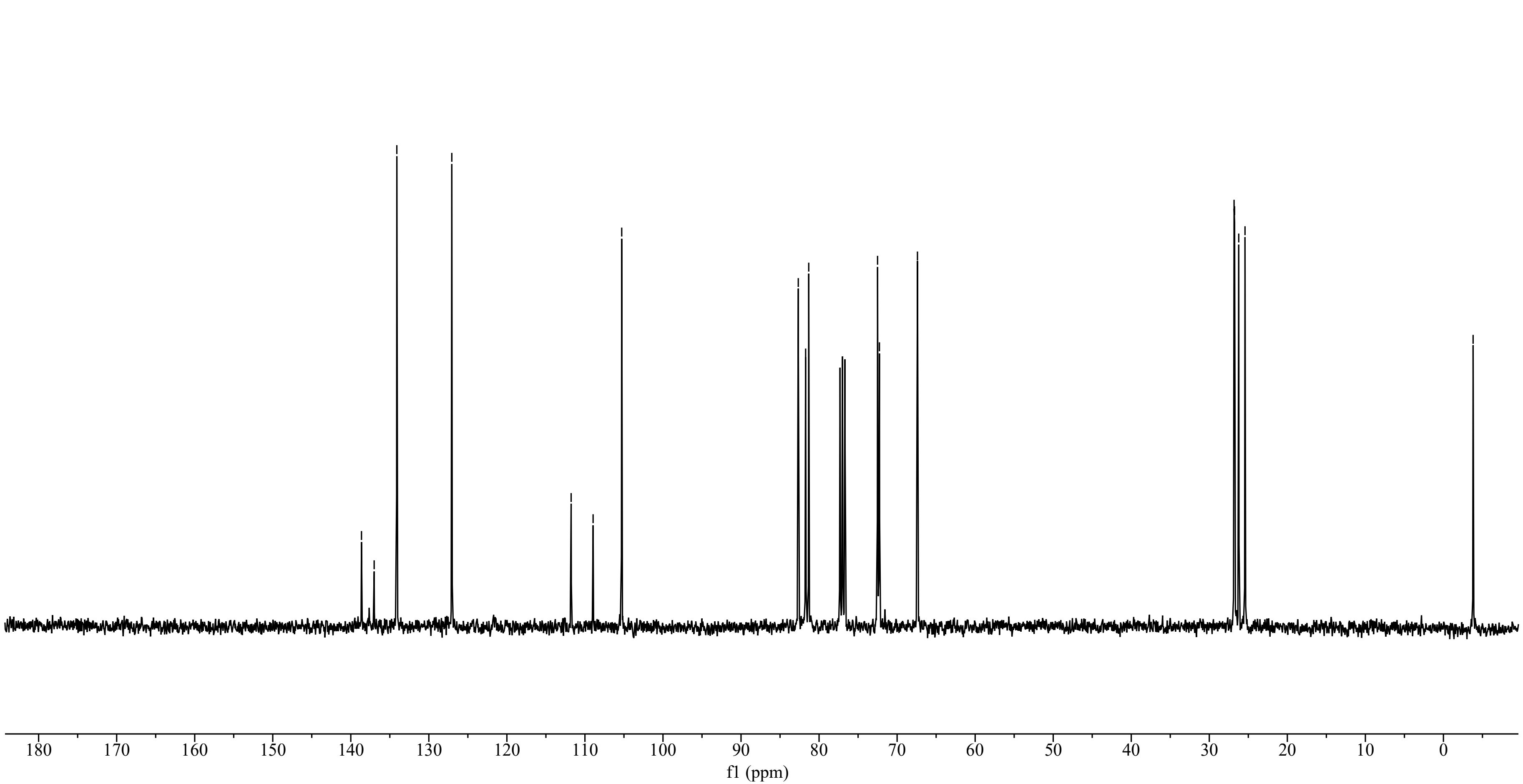

Compound **1bh** ^{1}H NMR

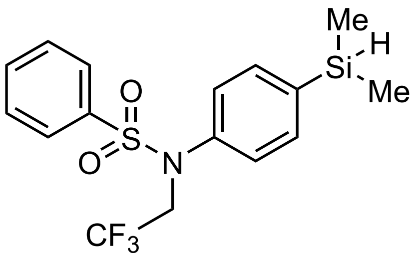

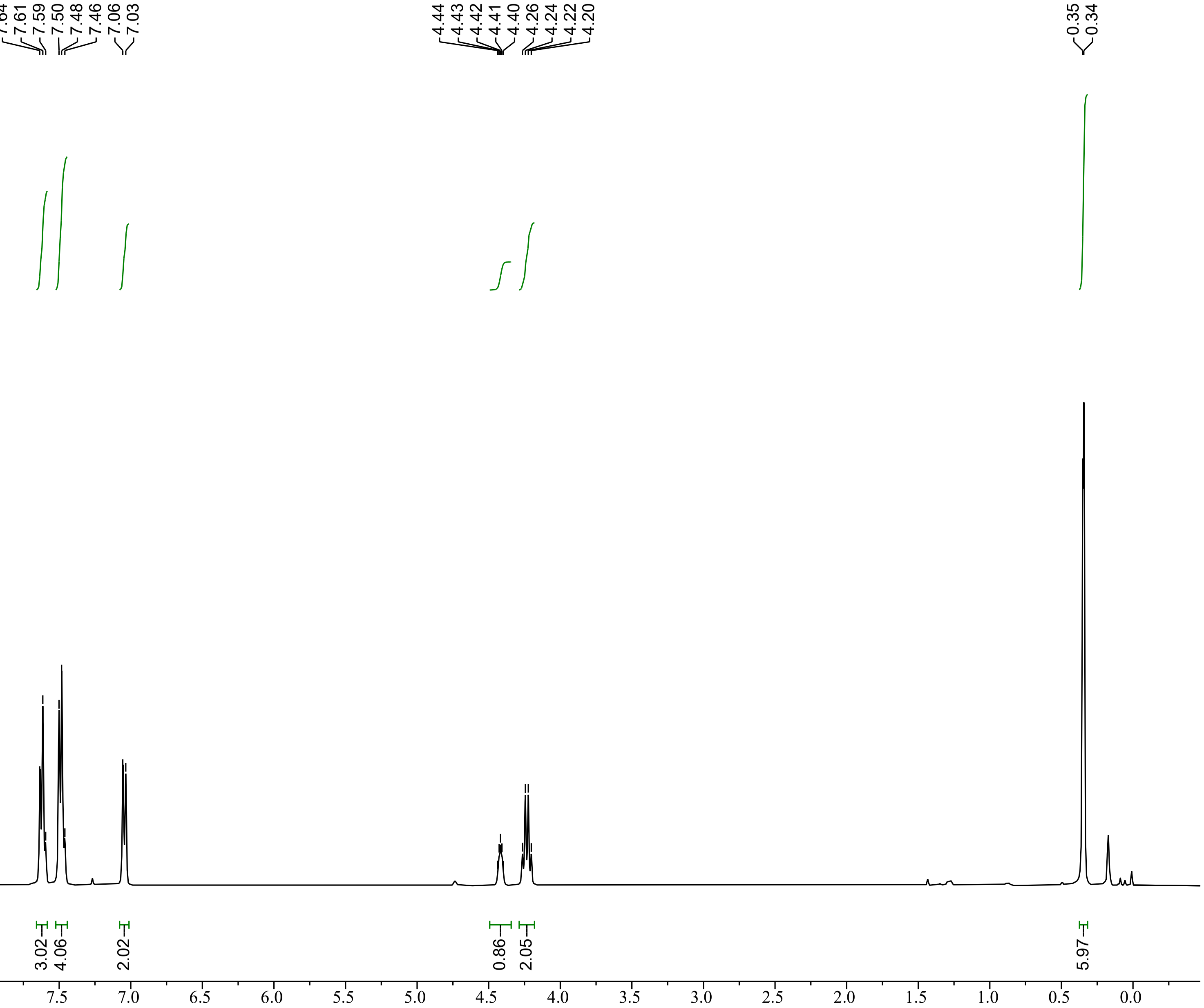

Compound **1bh** ^{13}C NMR

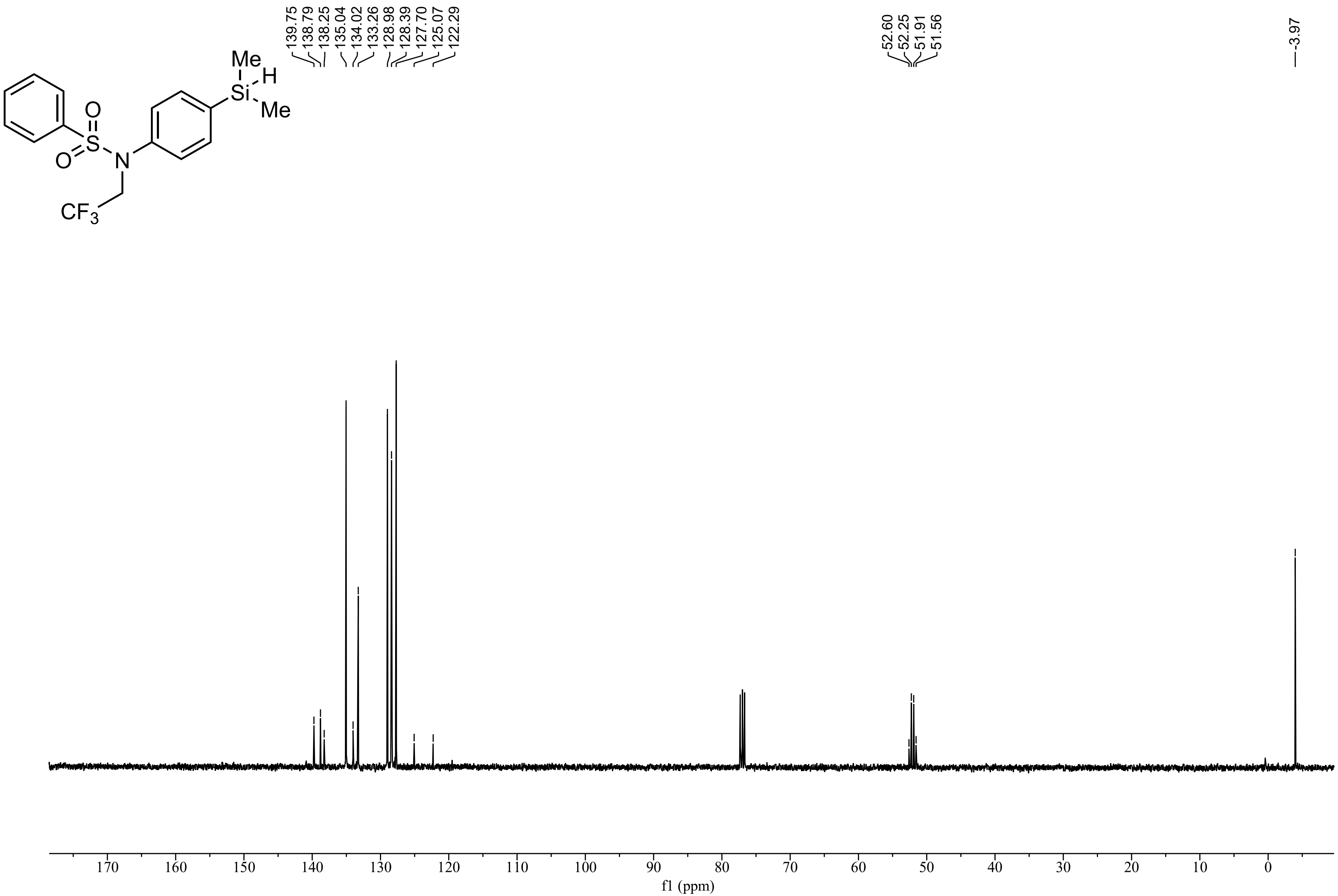

Compound **1bh** ^{19}F NMR

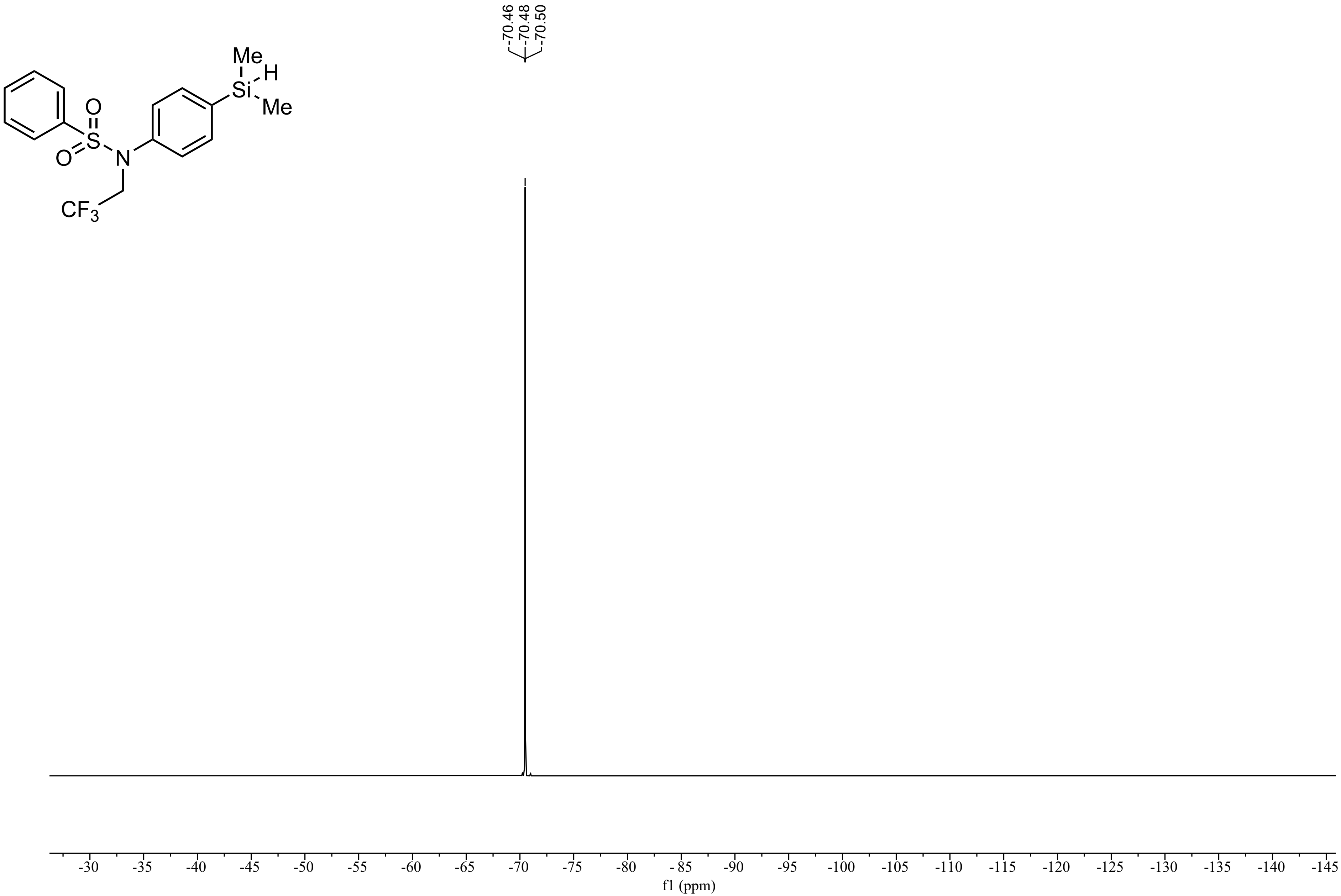

Compound **1bi** ^{1}H NMR

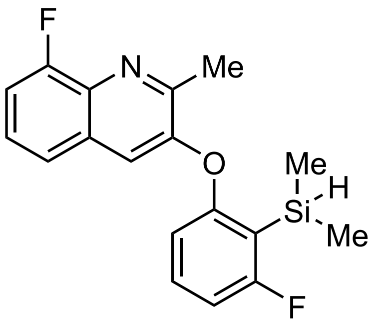

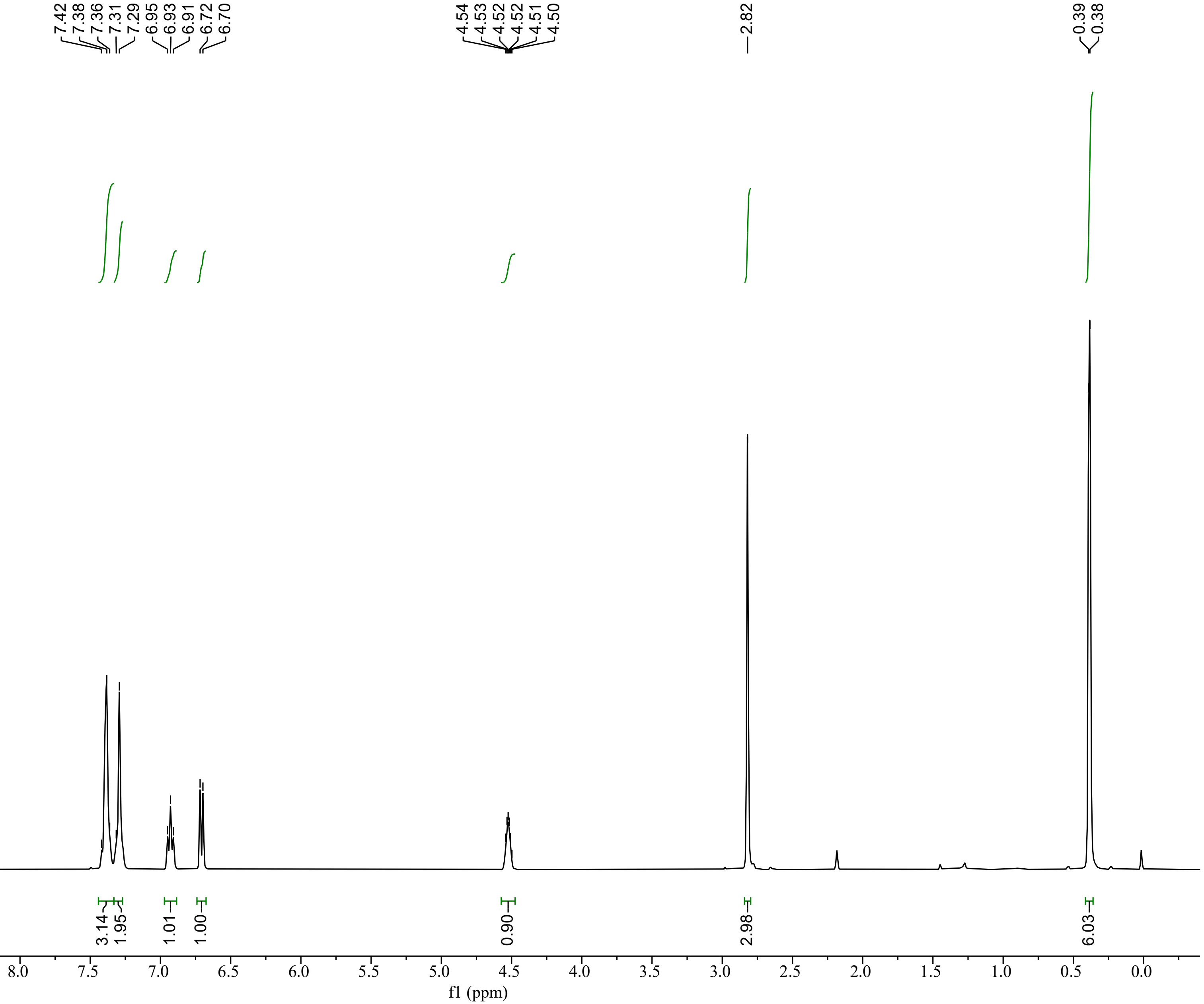

Compound **1bi** ^{13}C NMR

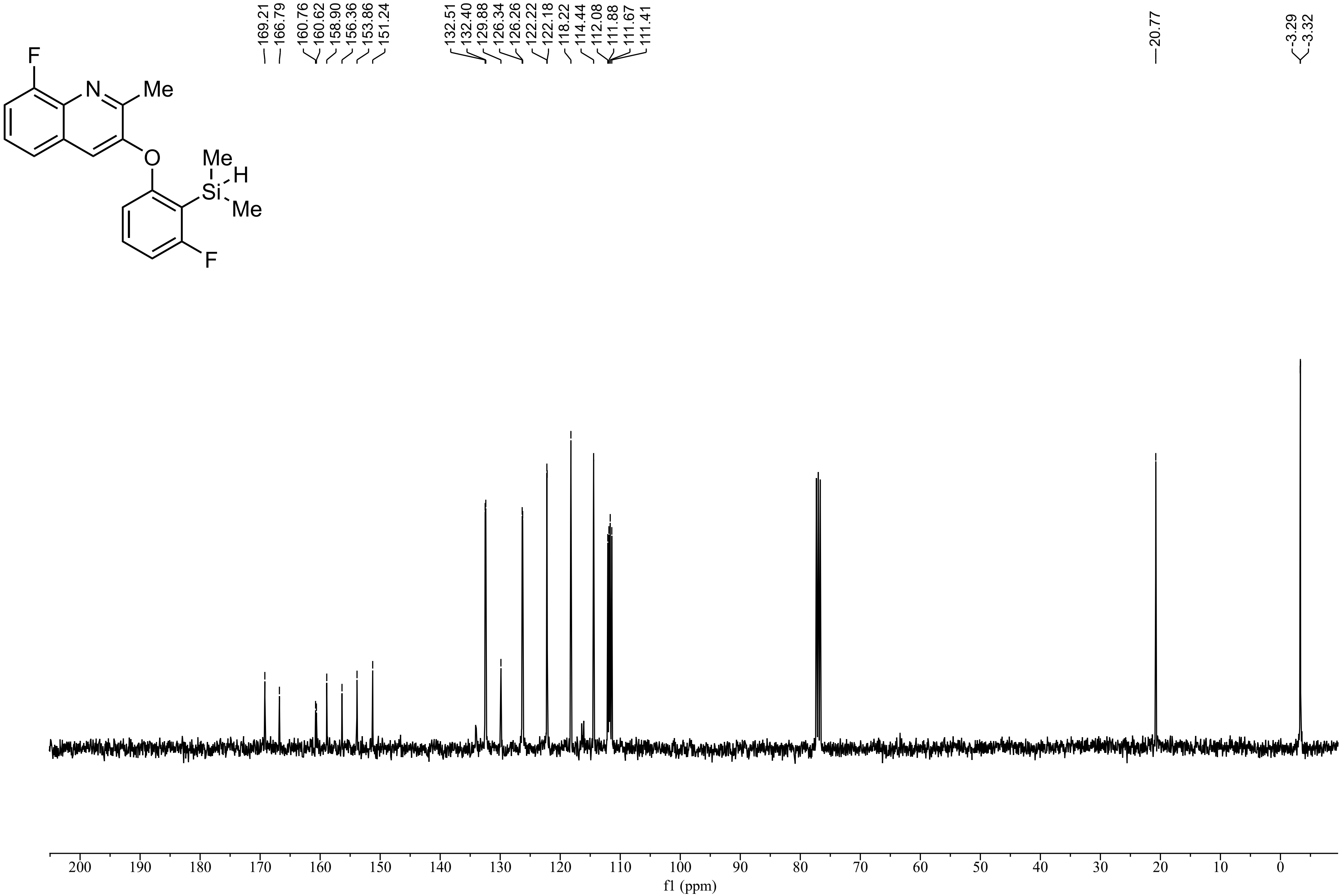

Compound **1bi** ^{13}C NMR

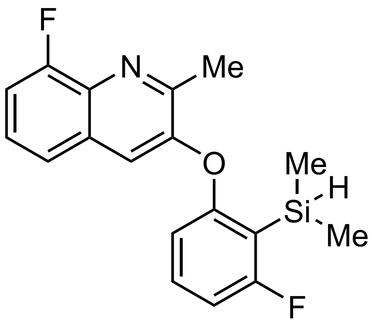

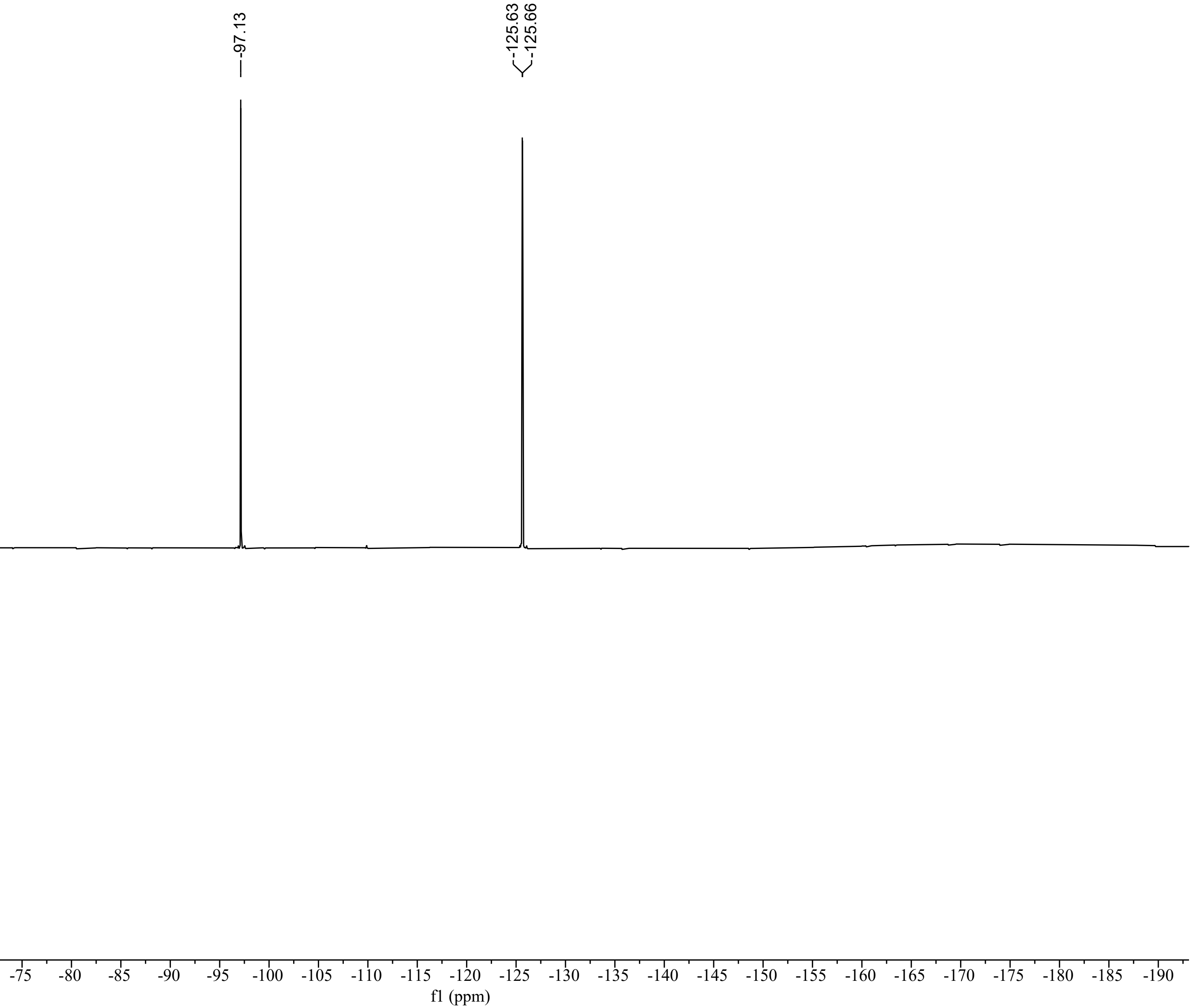

Compound **1bj** ^{1}H NMR

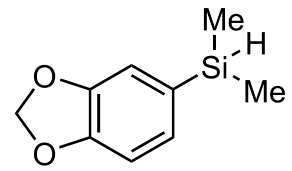

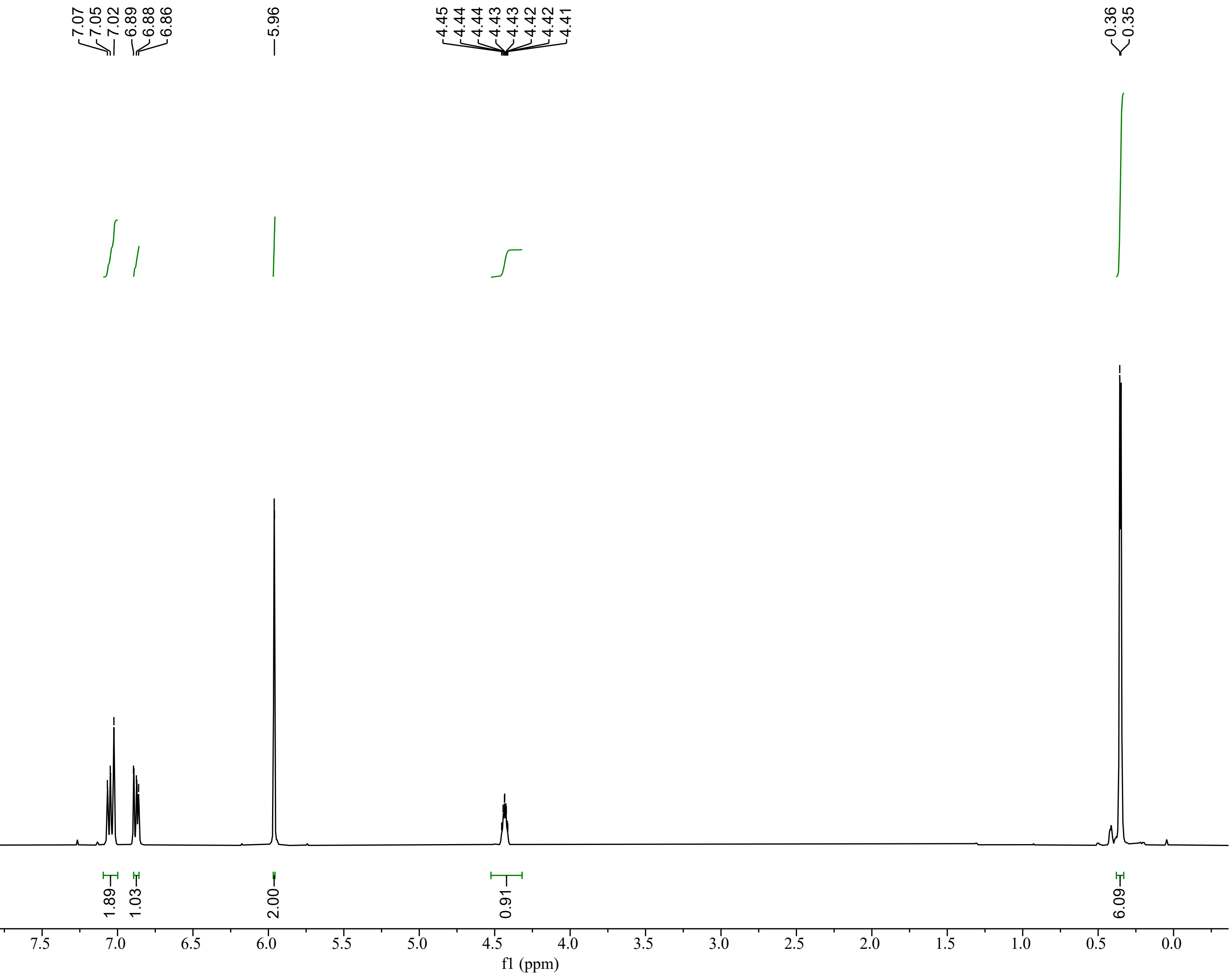

Compound **1bj** ^{13}C NMR

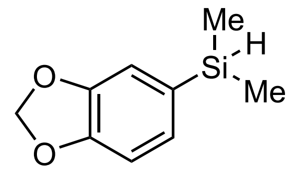

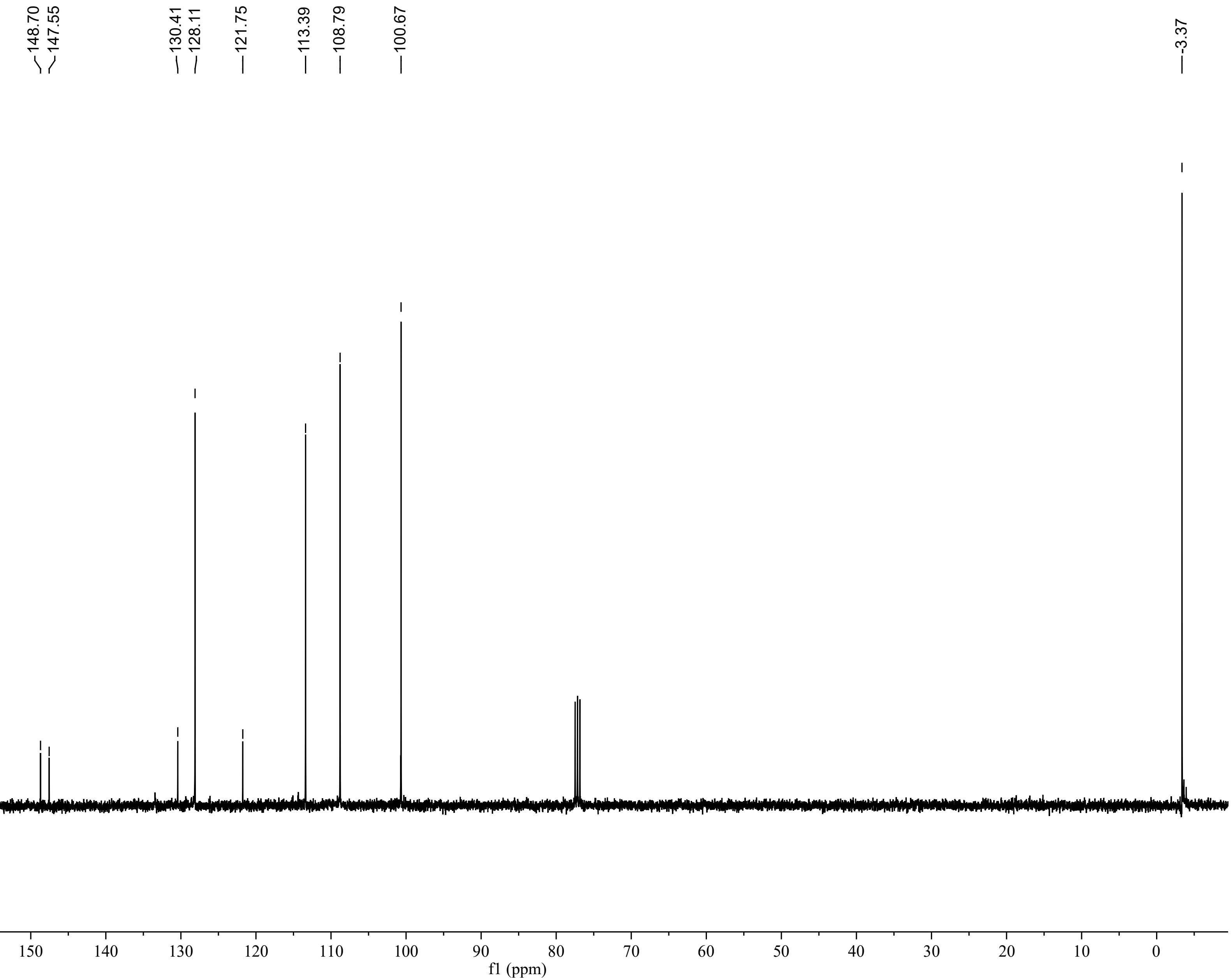

Compound **1bk** ^{1}H NMR

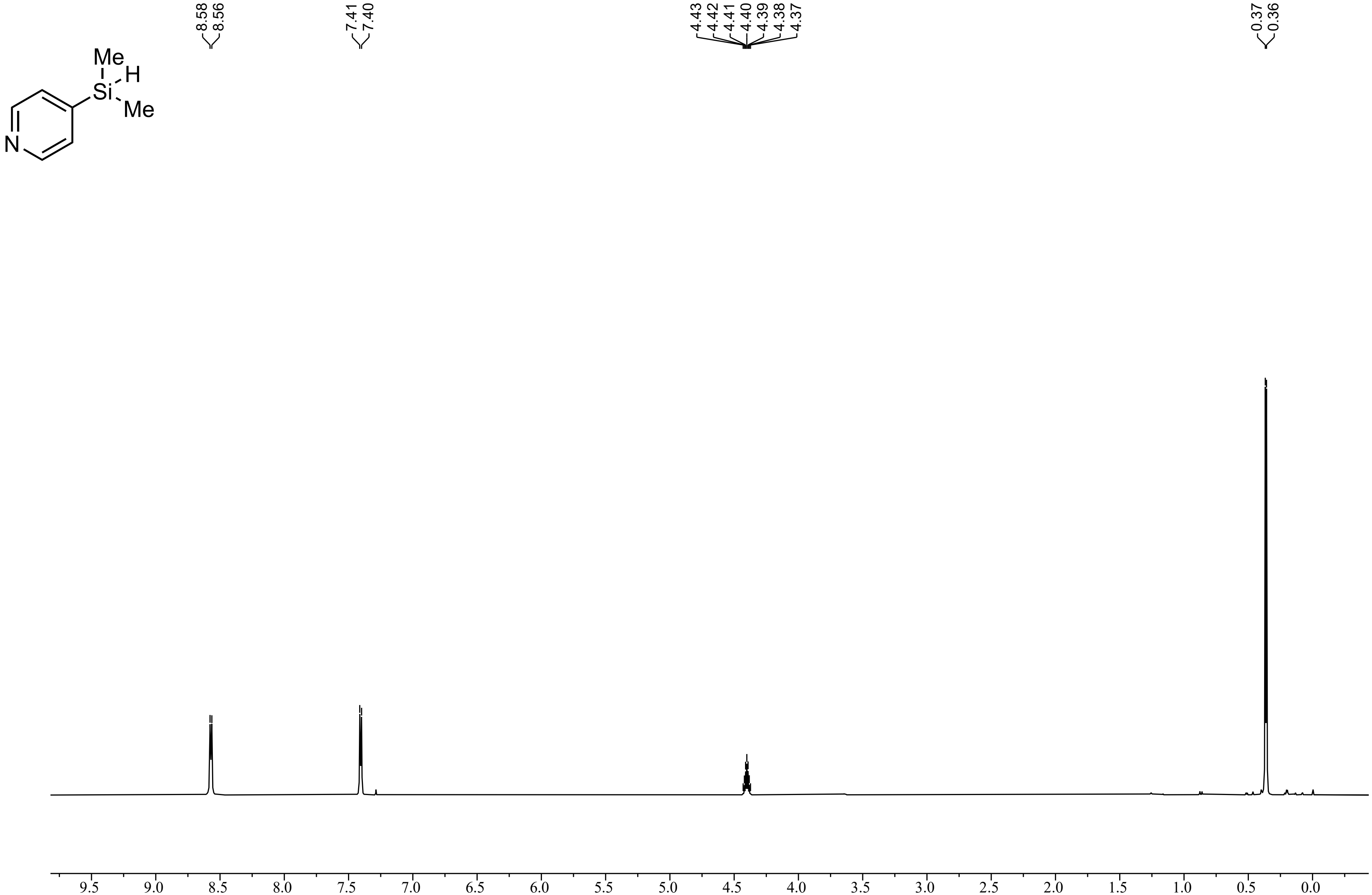

Compound **1bk** ^{13}C NMR

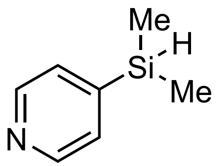

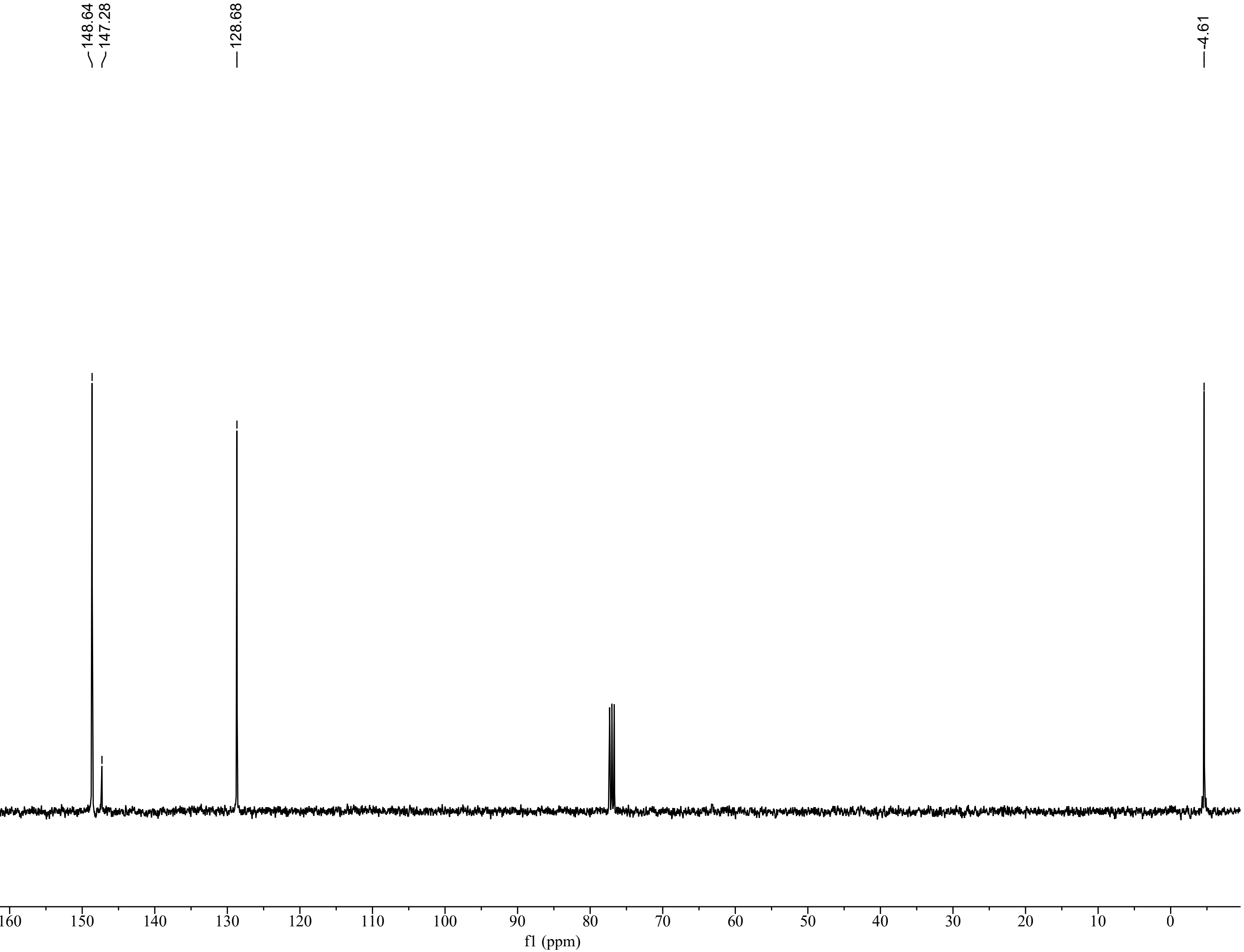

Compound **1bl** ^{1}H NMR

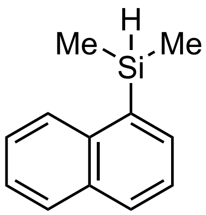

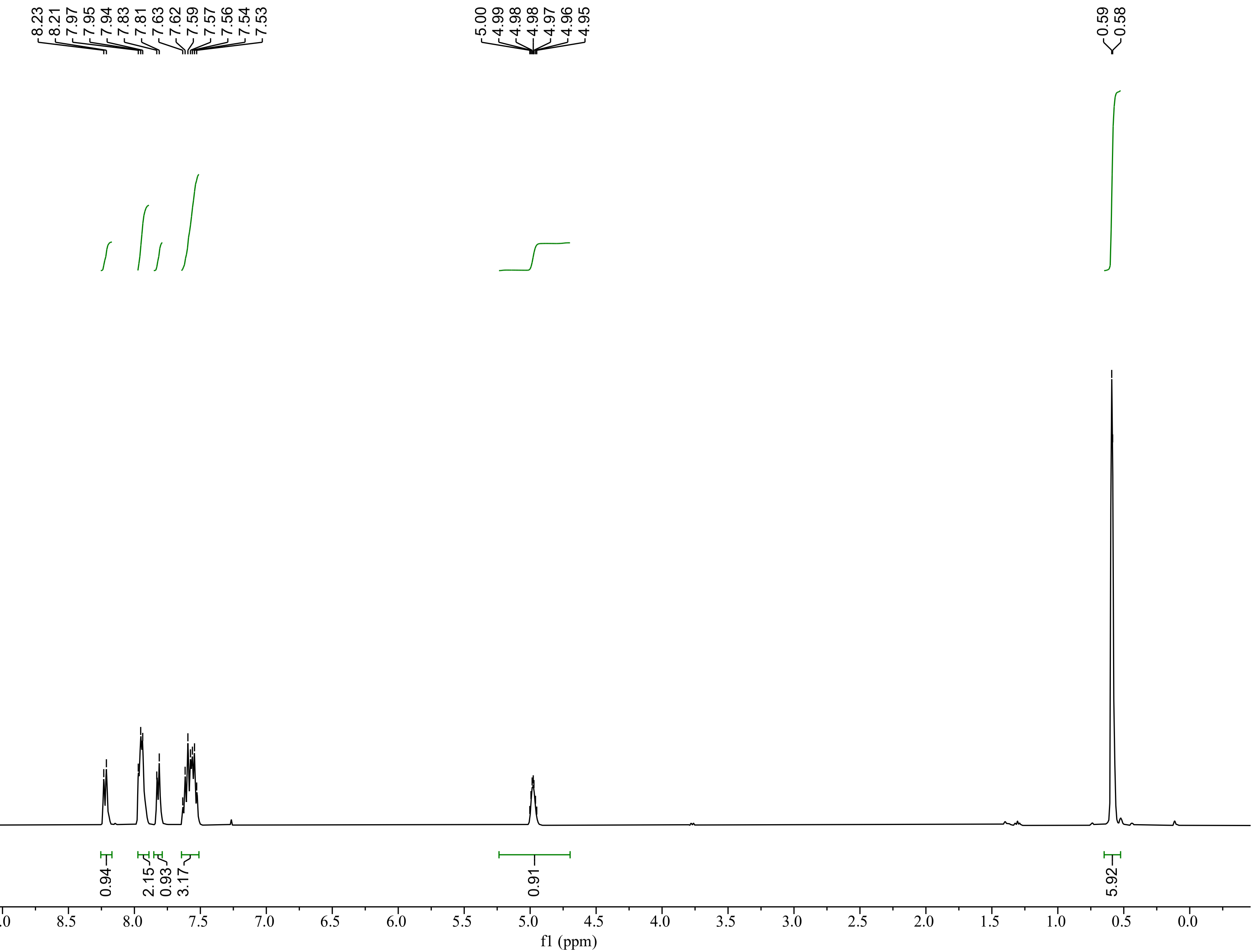

Compound **1bl** ^{13}C NMR

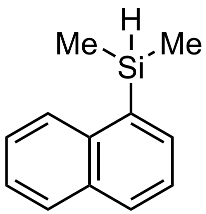

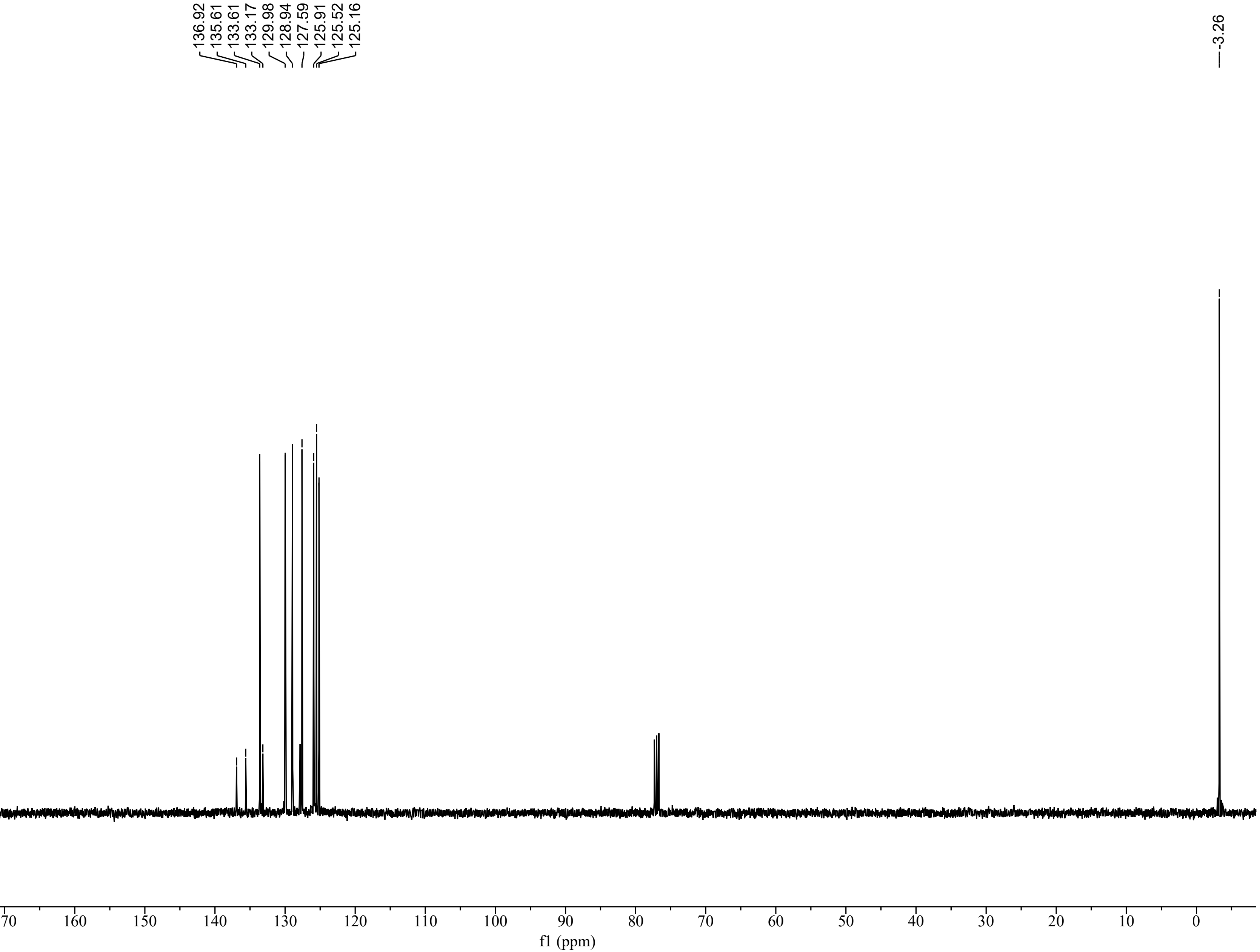

Compound **1bm** ^{1}H NMR

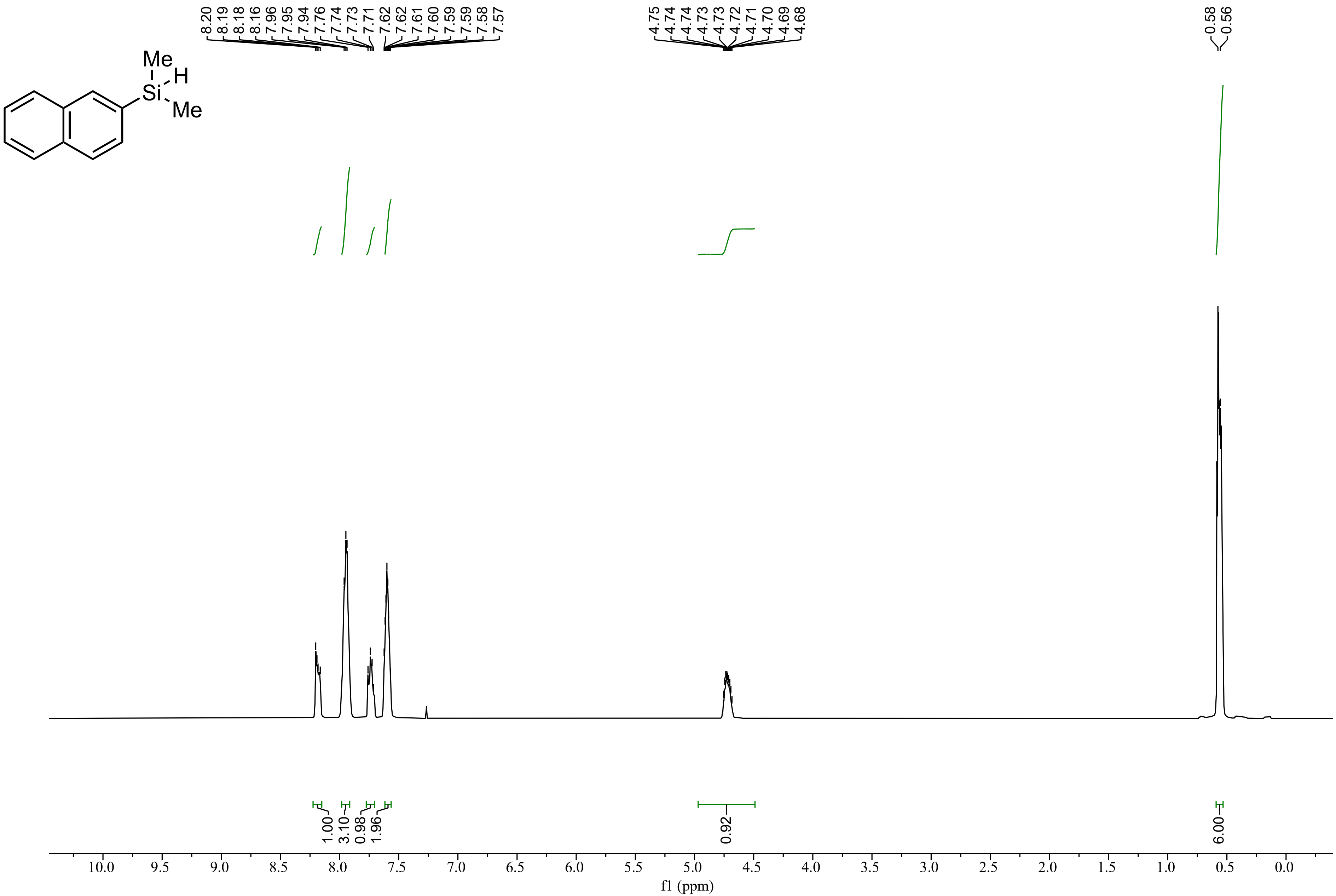

Compound **1bm** ^{13}C NMR

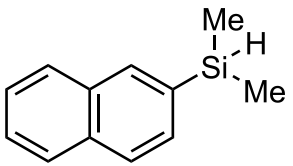

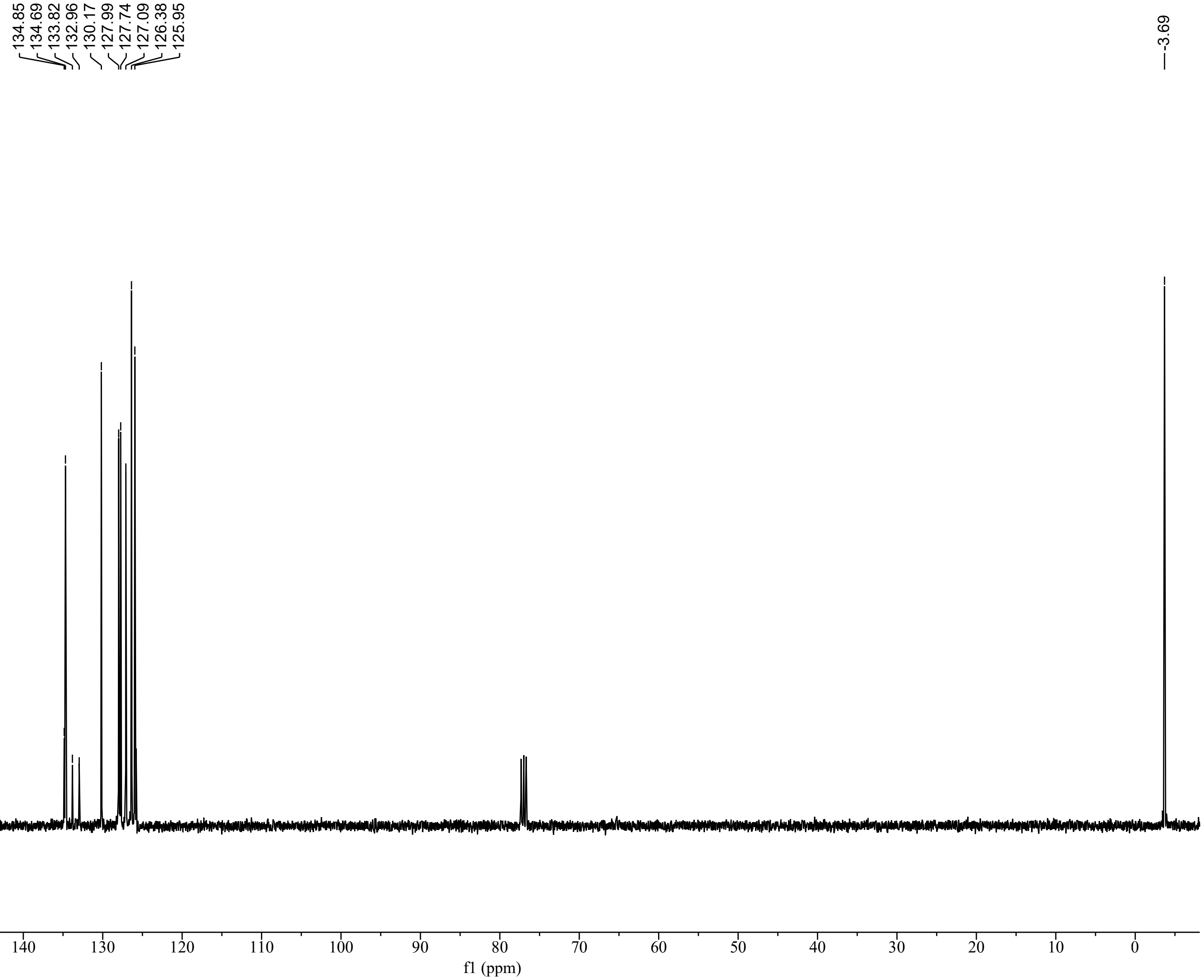

Compound **1bn** ^{1}H NMR

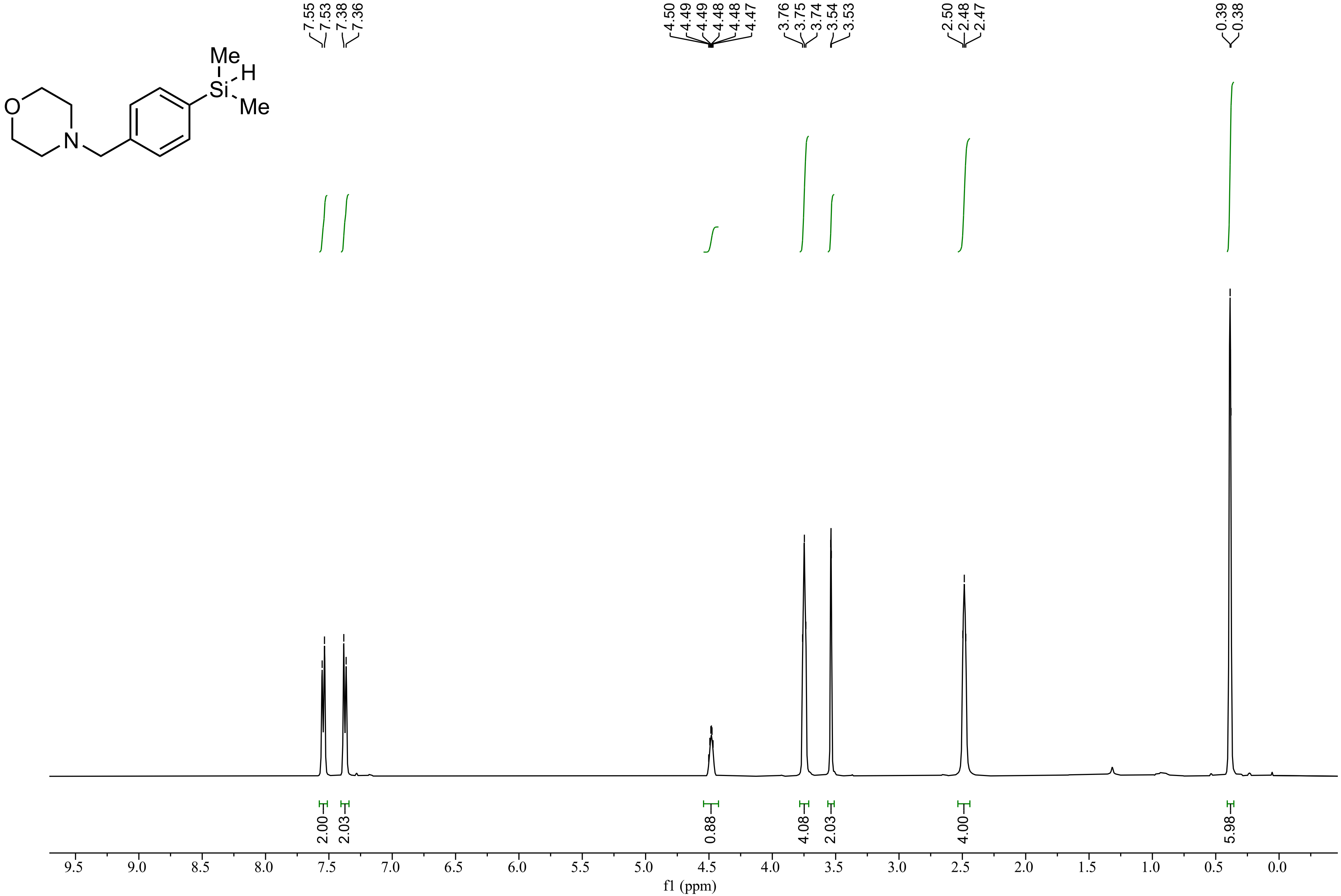

Compound **1bn** ^{13}C NMR

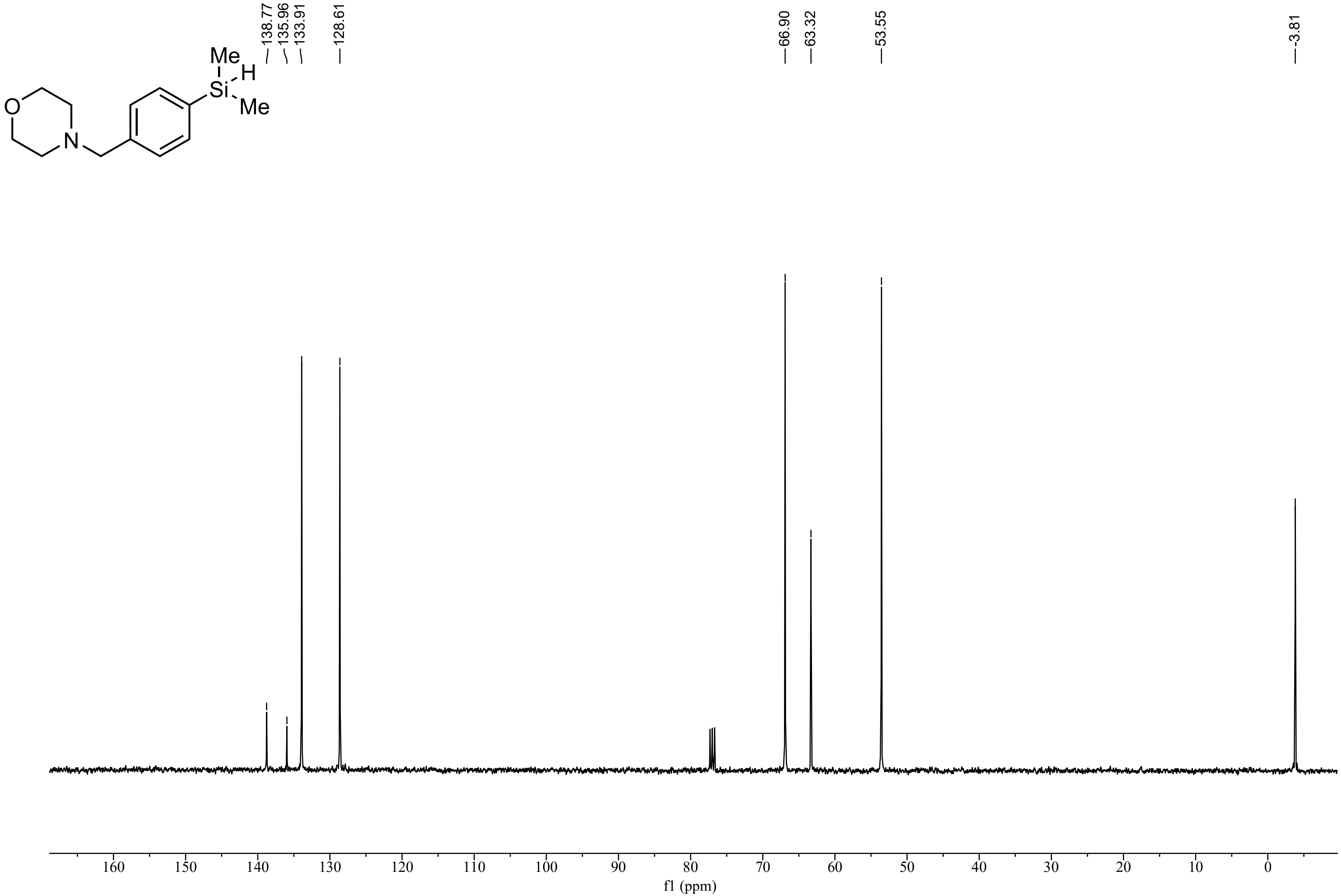

Compound **1bo** ^{1}H NMR

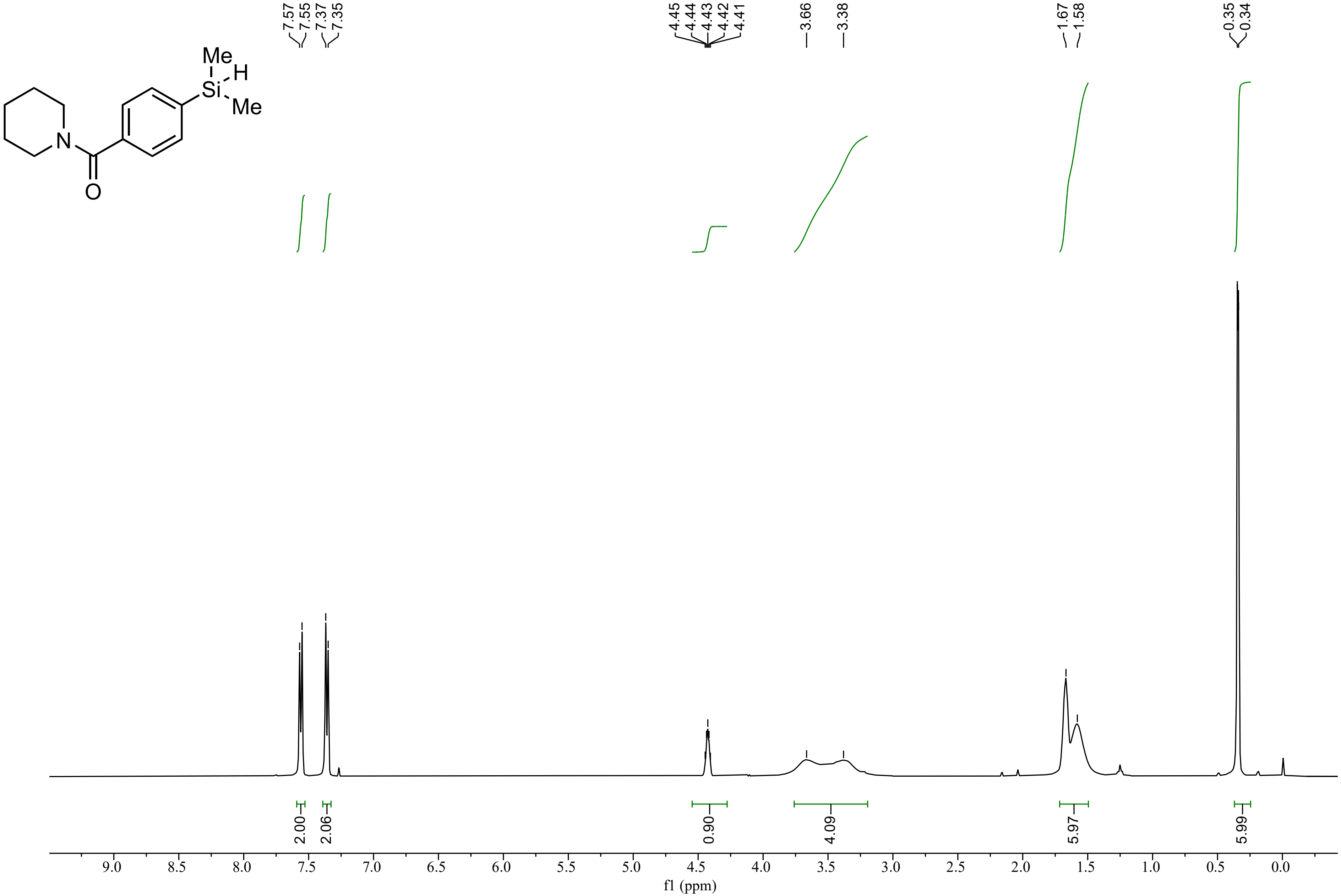

Compound **1bo** ^{13}C NMR

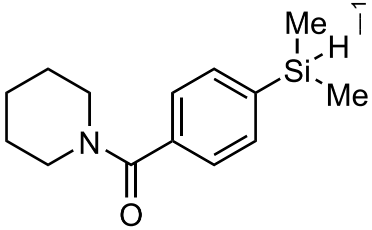

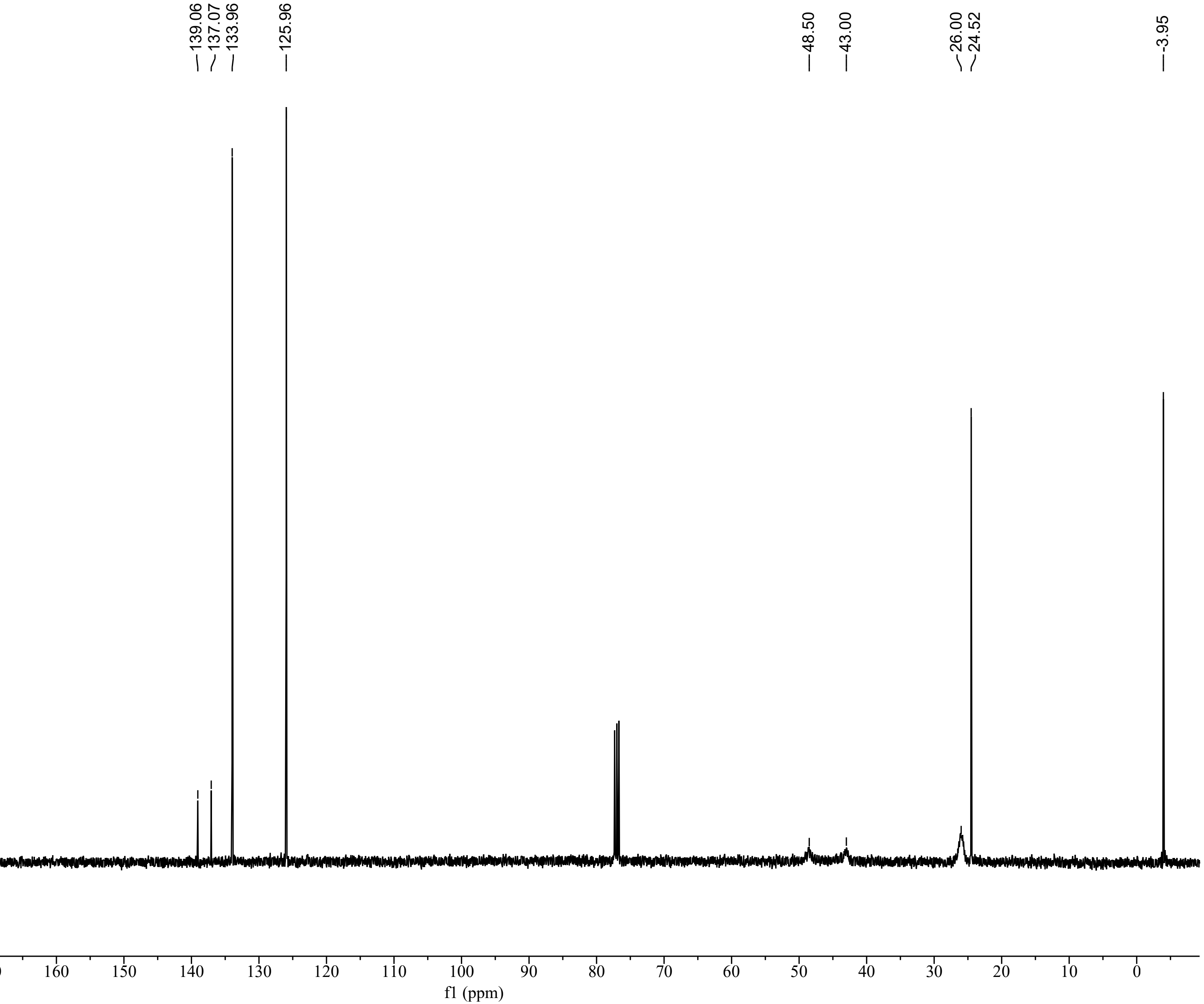

Compound **1bp** ^{1}H NMR

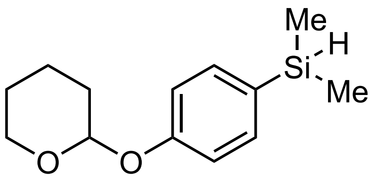

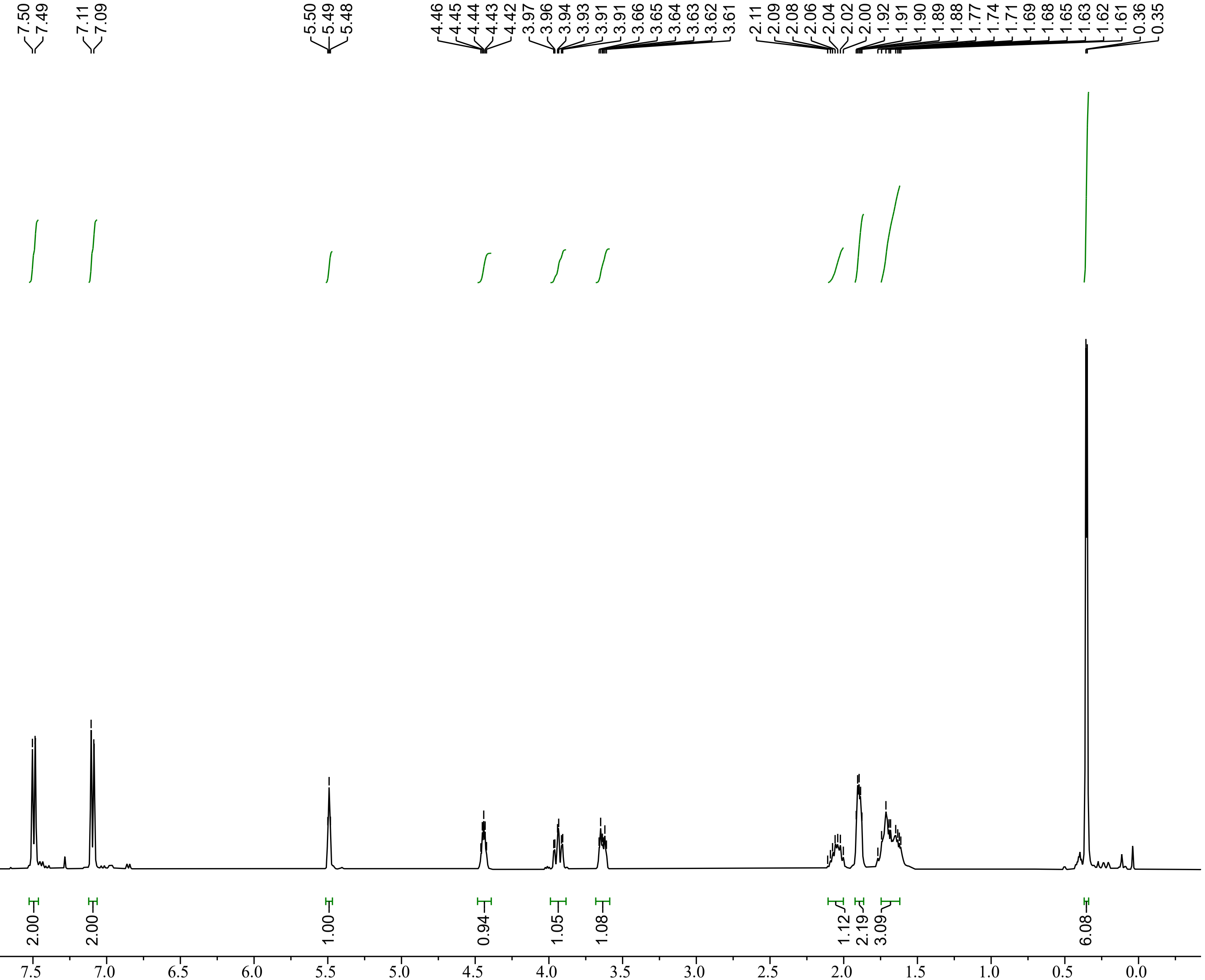

Compound **1bp** ^{13}C NMR

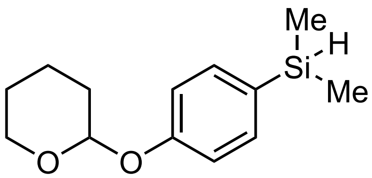

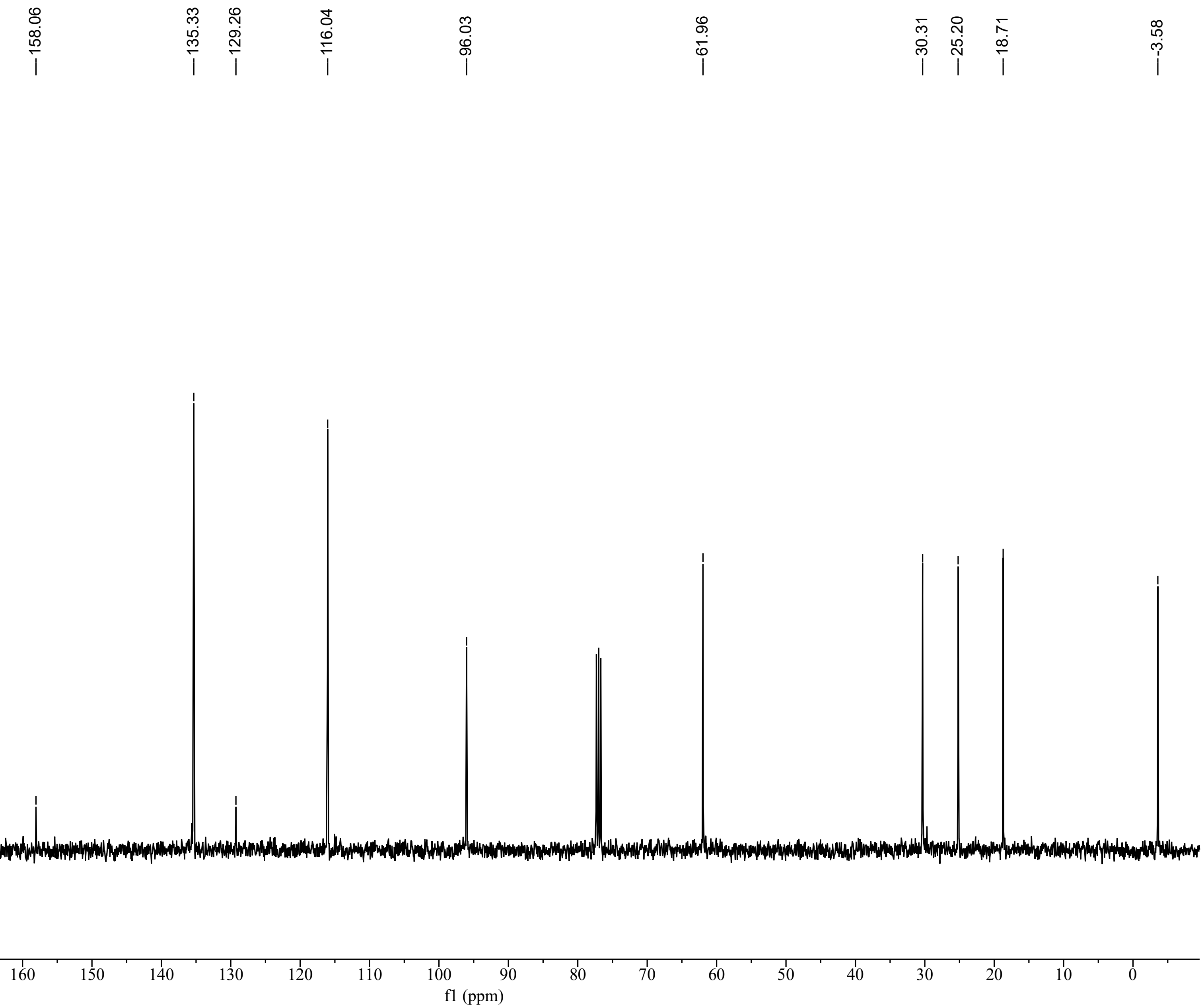

Compound **1bq** ^{1}H NMR

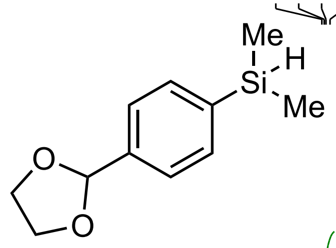

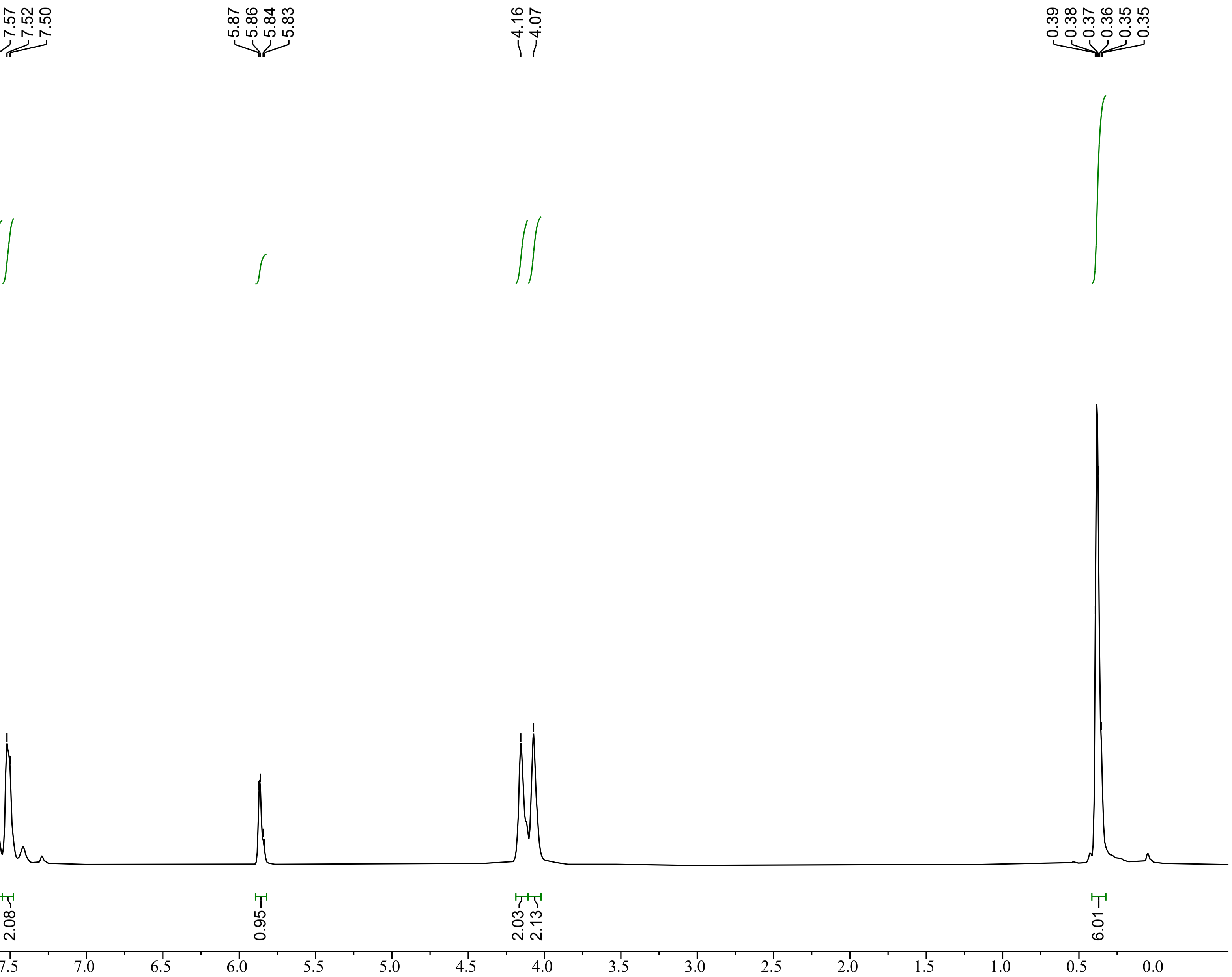

Compound **1bq** ^{13}C NMR

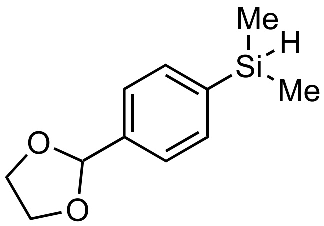

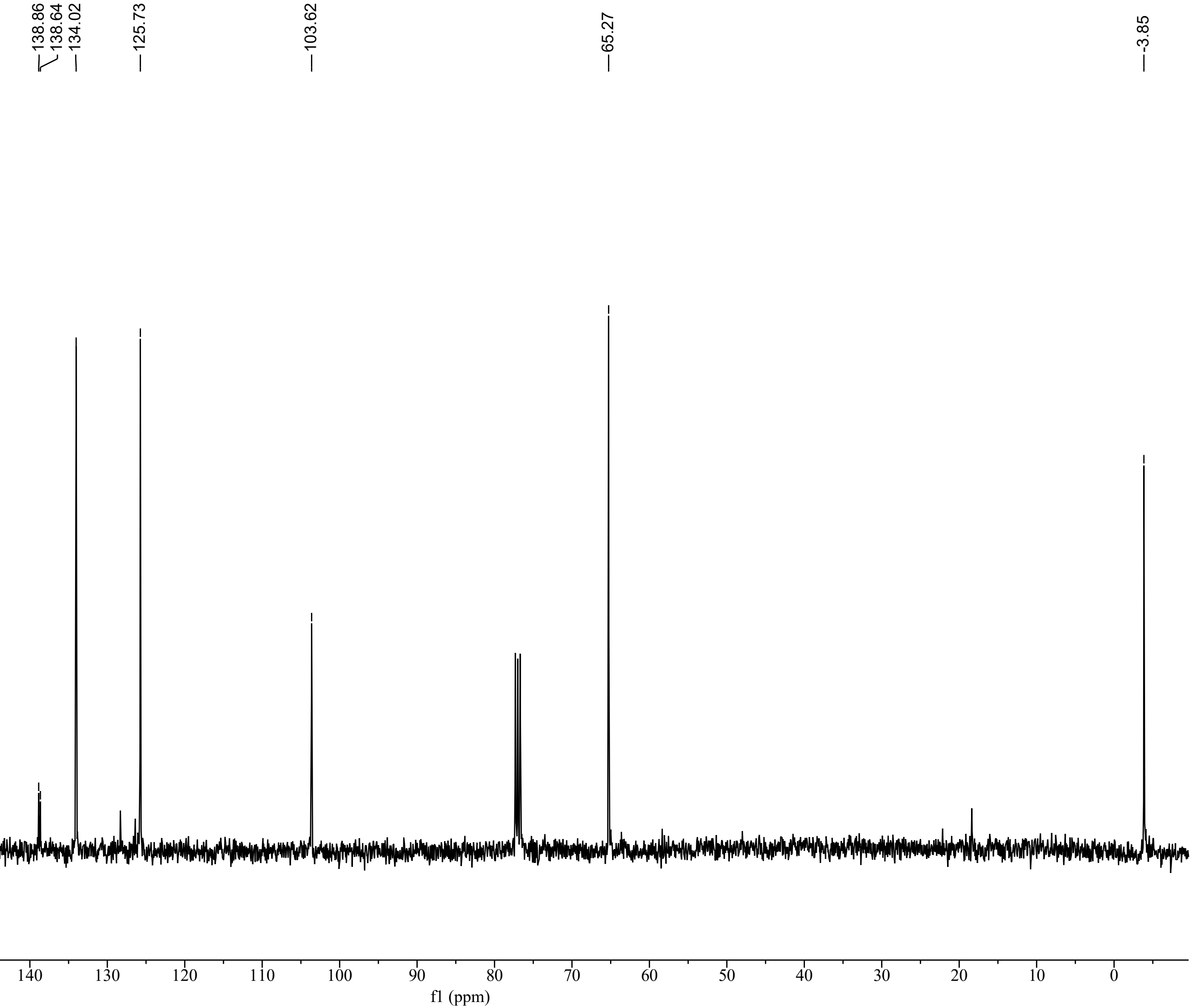

Compound **1br** ^{1}H NMR

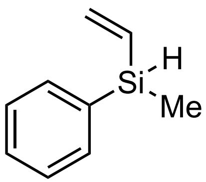

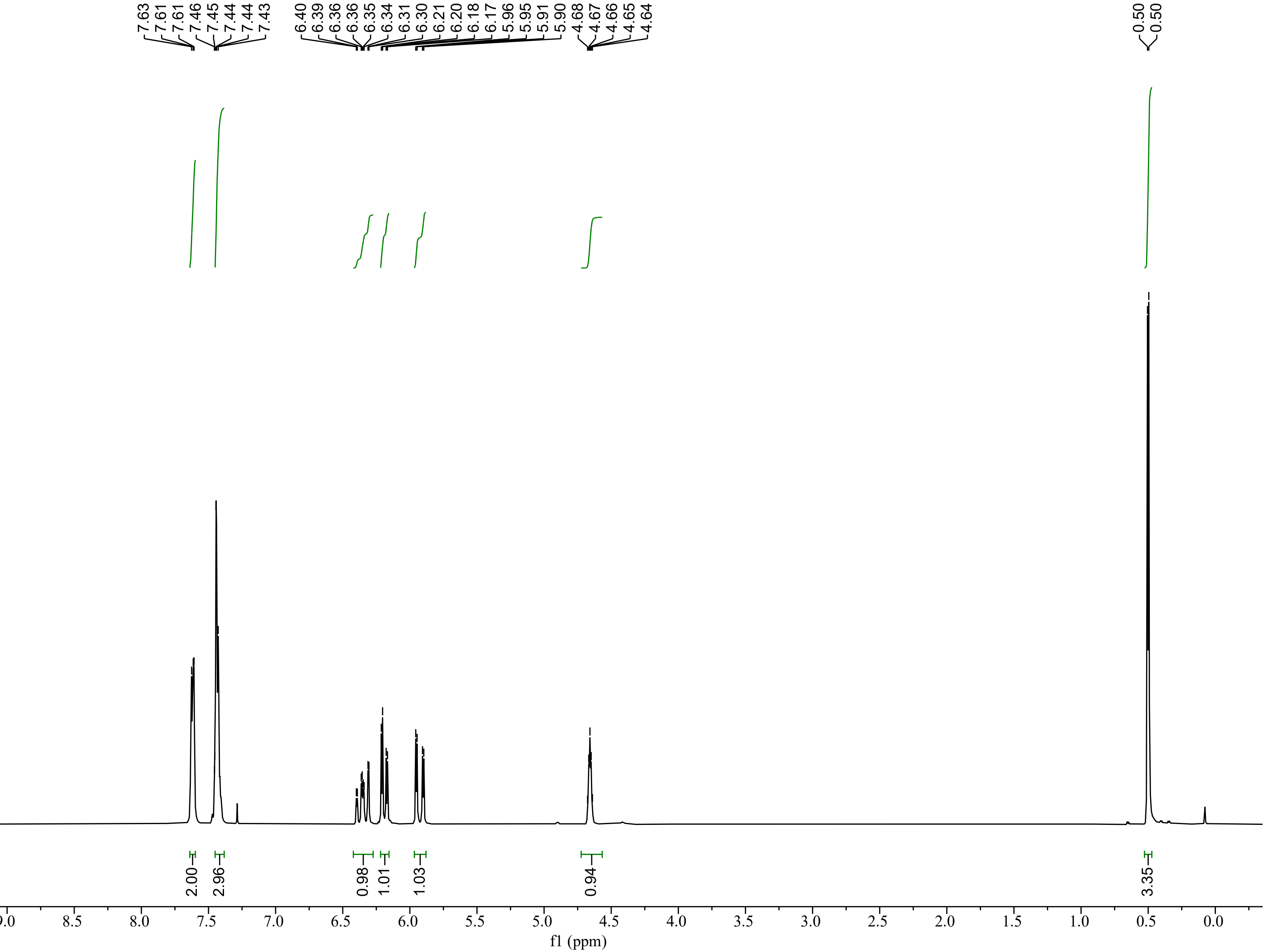

Compound **1br** ^{13}C NMR

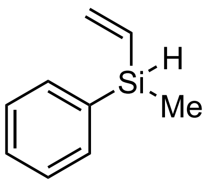

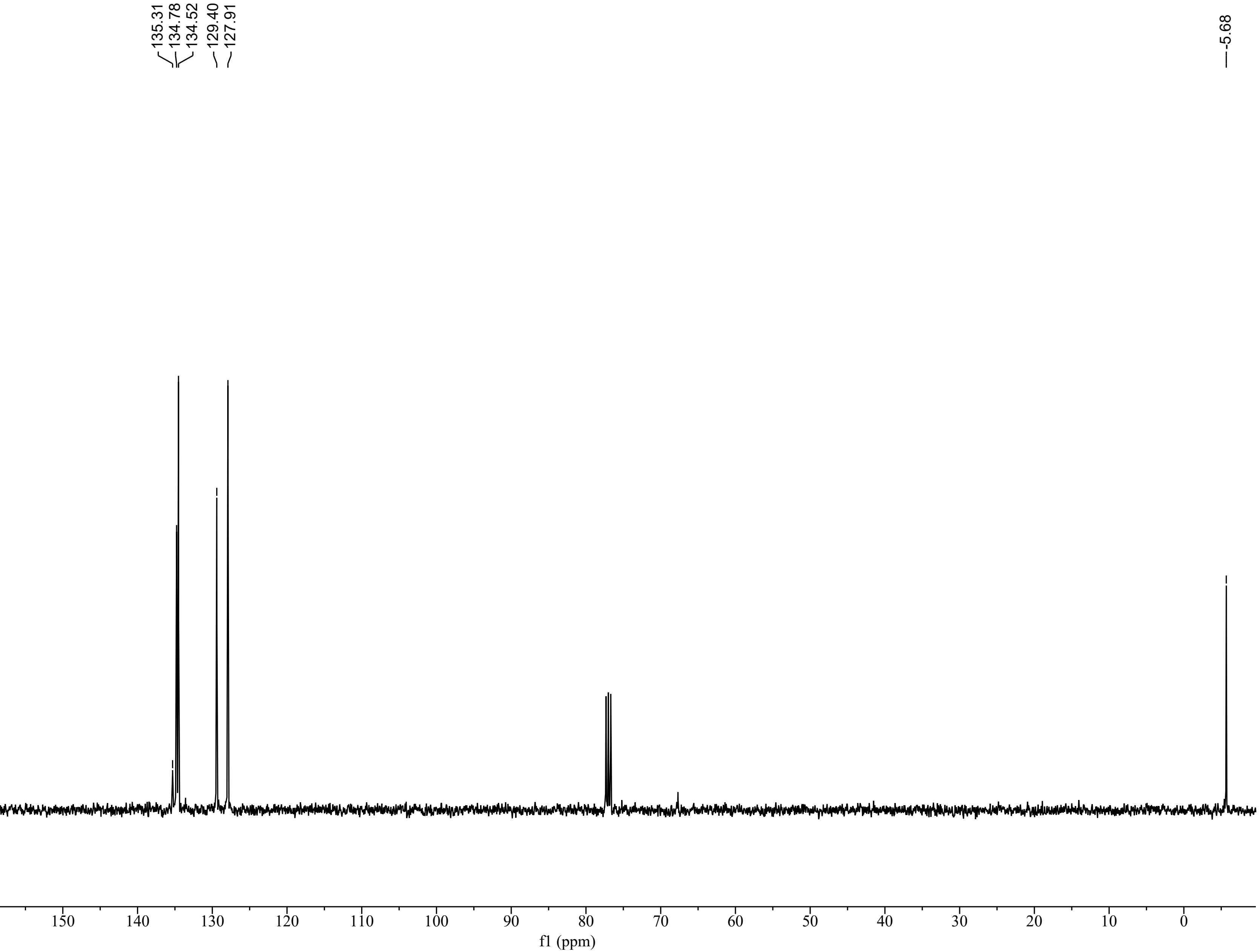

Compound **1b** ^{1}H NMR

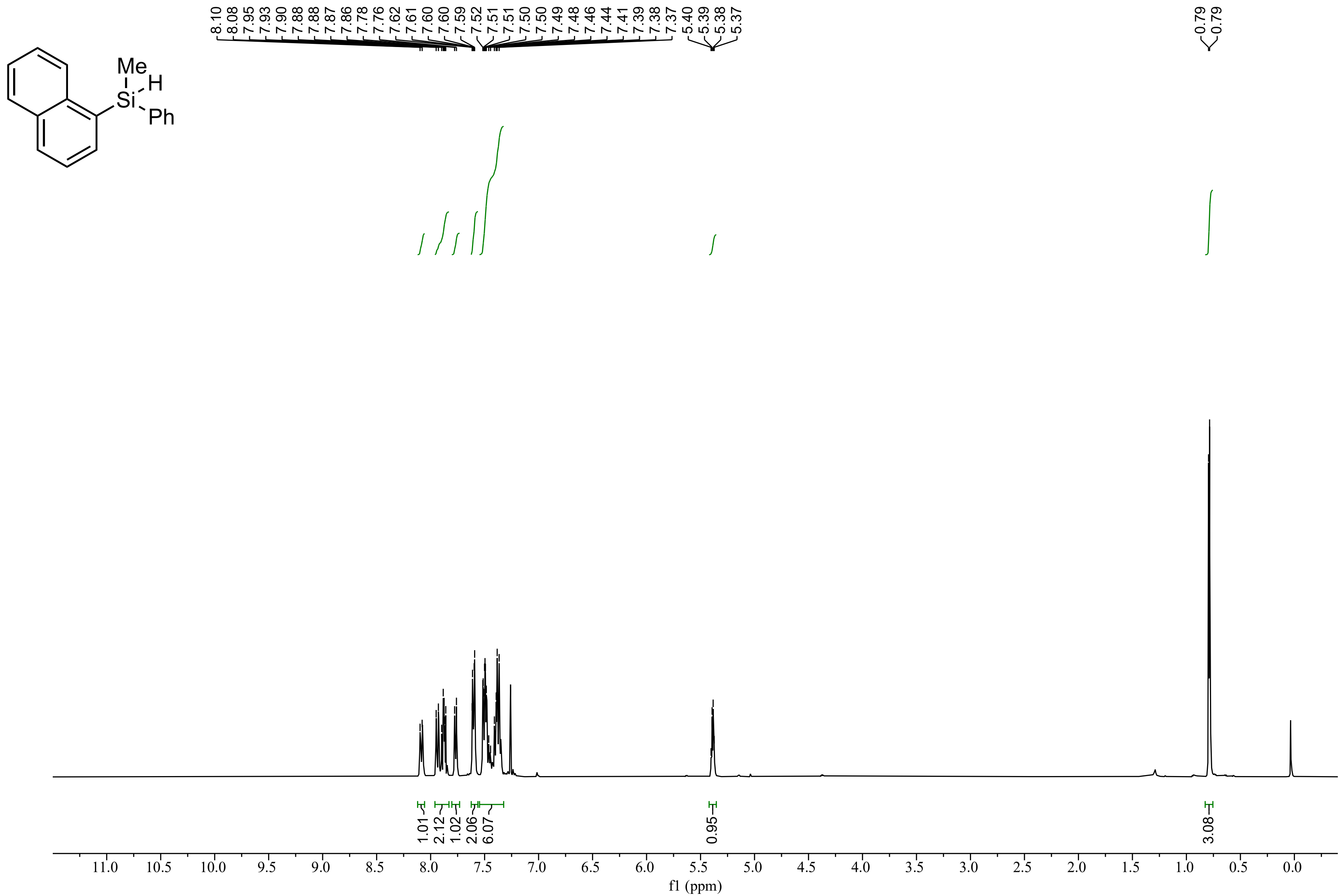

Compound **1b** ^{1}H NMR

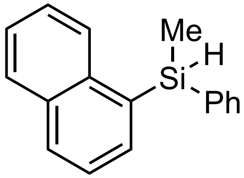

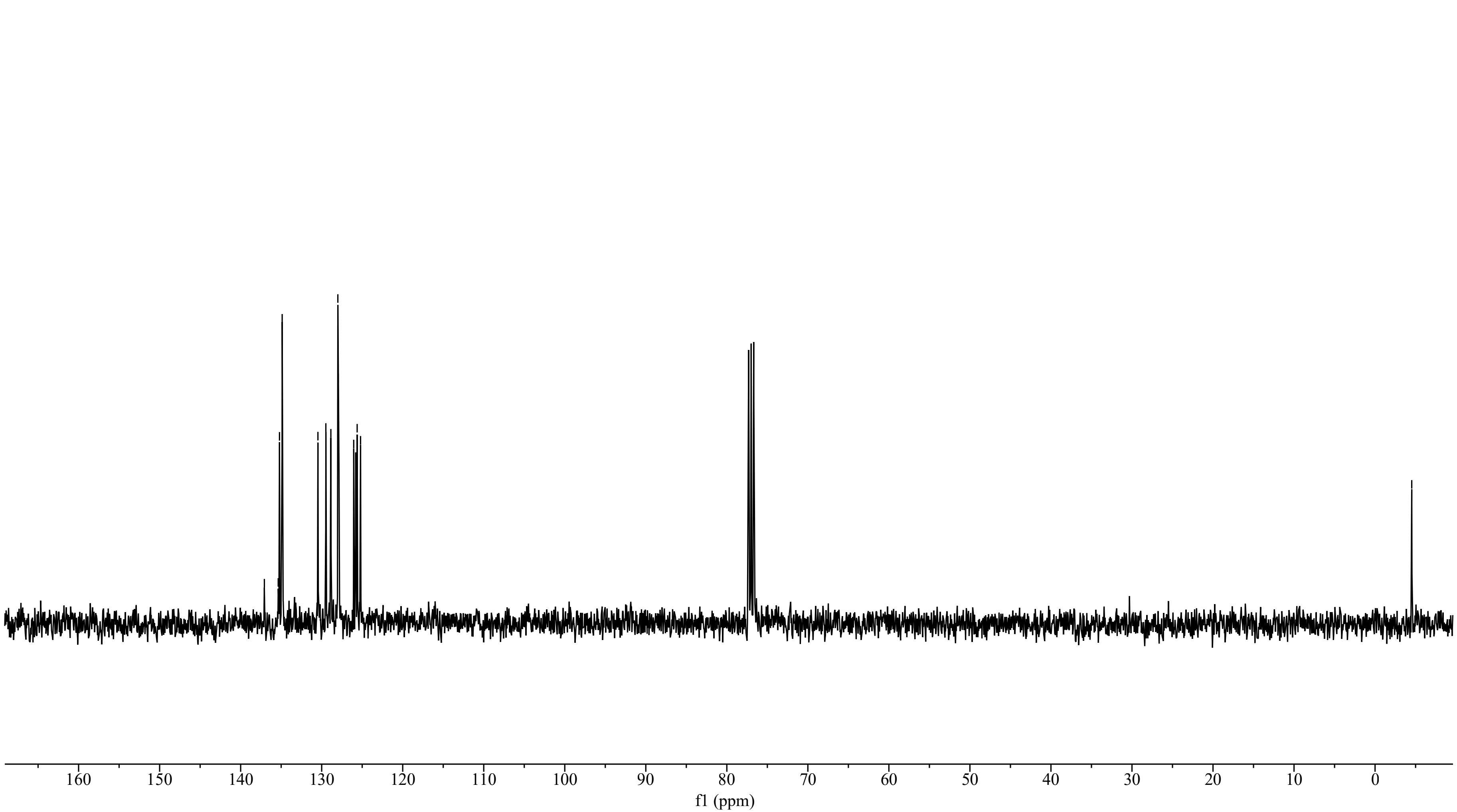

Compound ***R*-1b** ^{1}H NMR

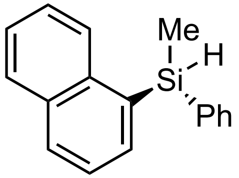

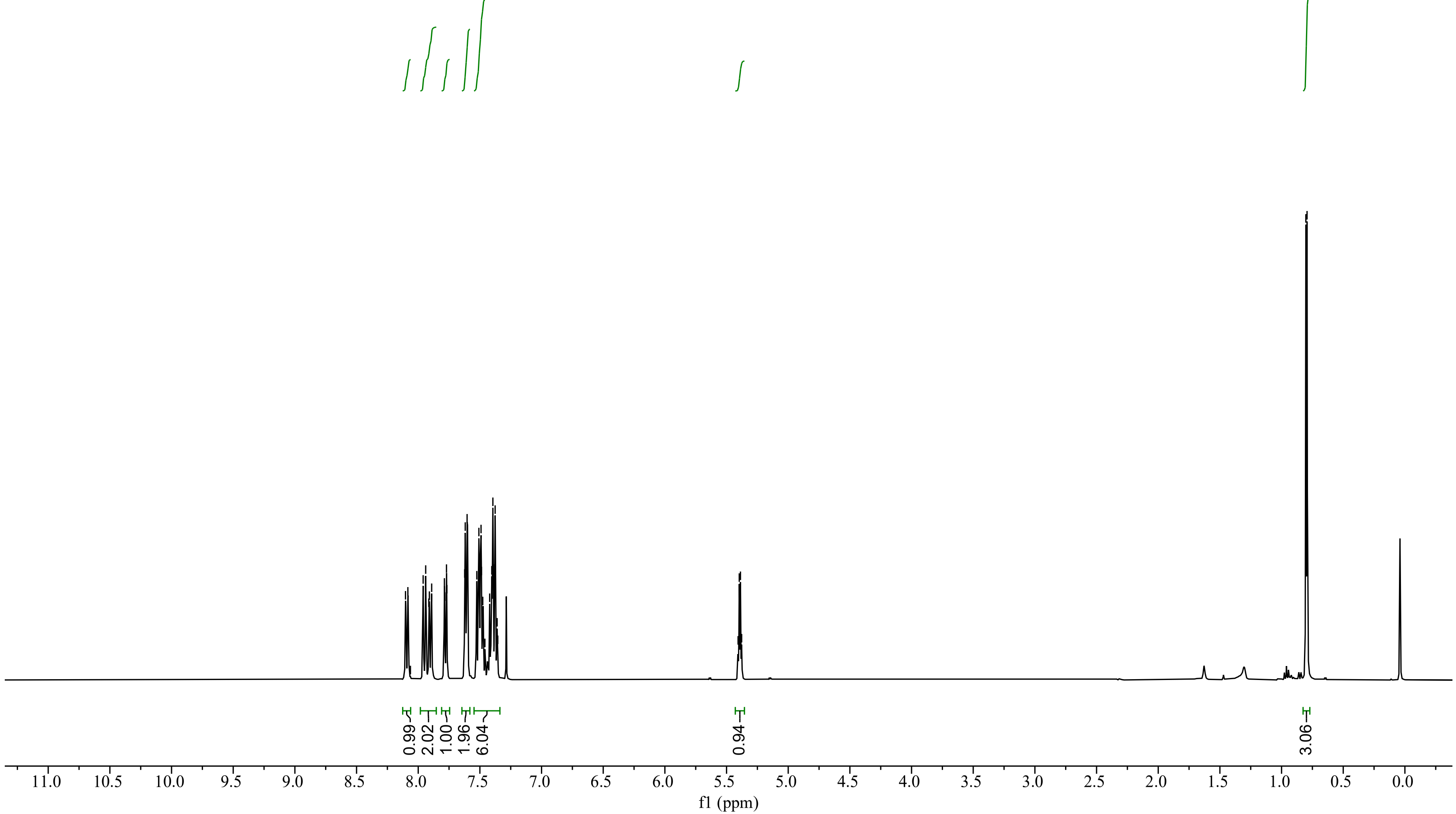

Compound ***R*-1b** ^{13}C NMR

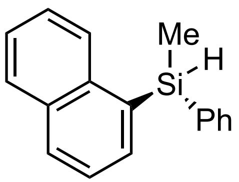

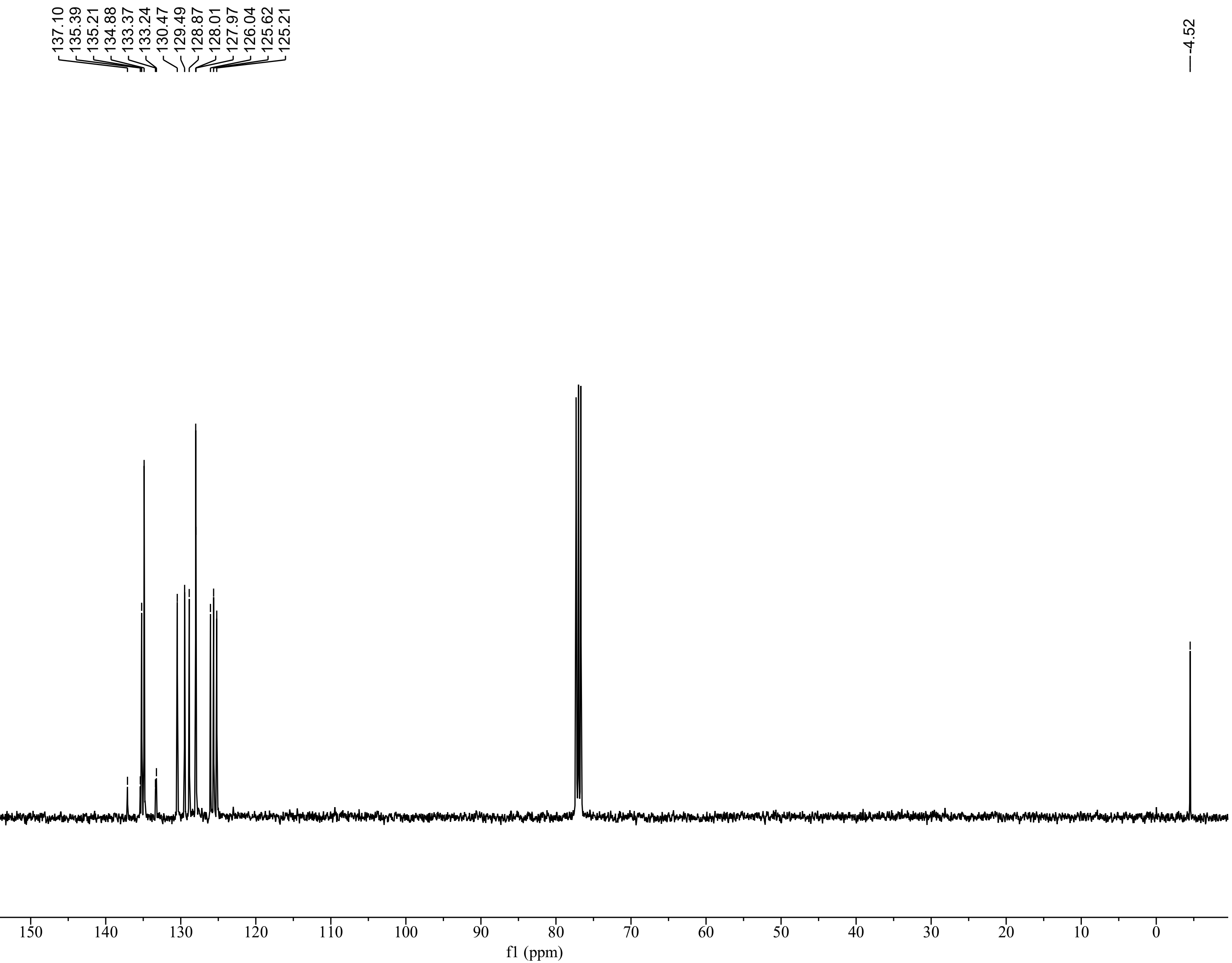

Compound **1a-*d*$_1$** ^{1}H NMR

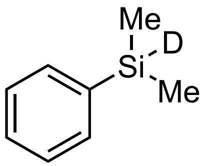

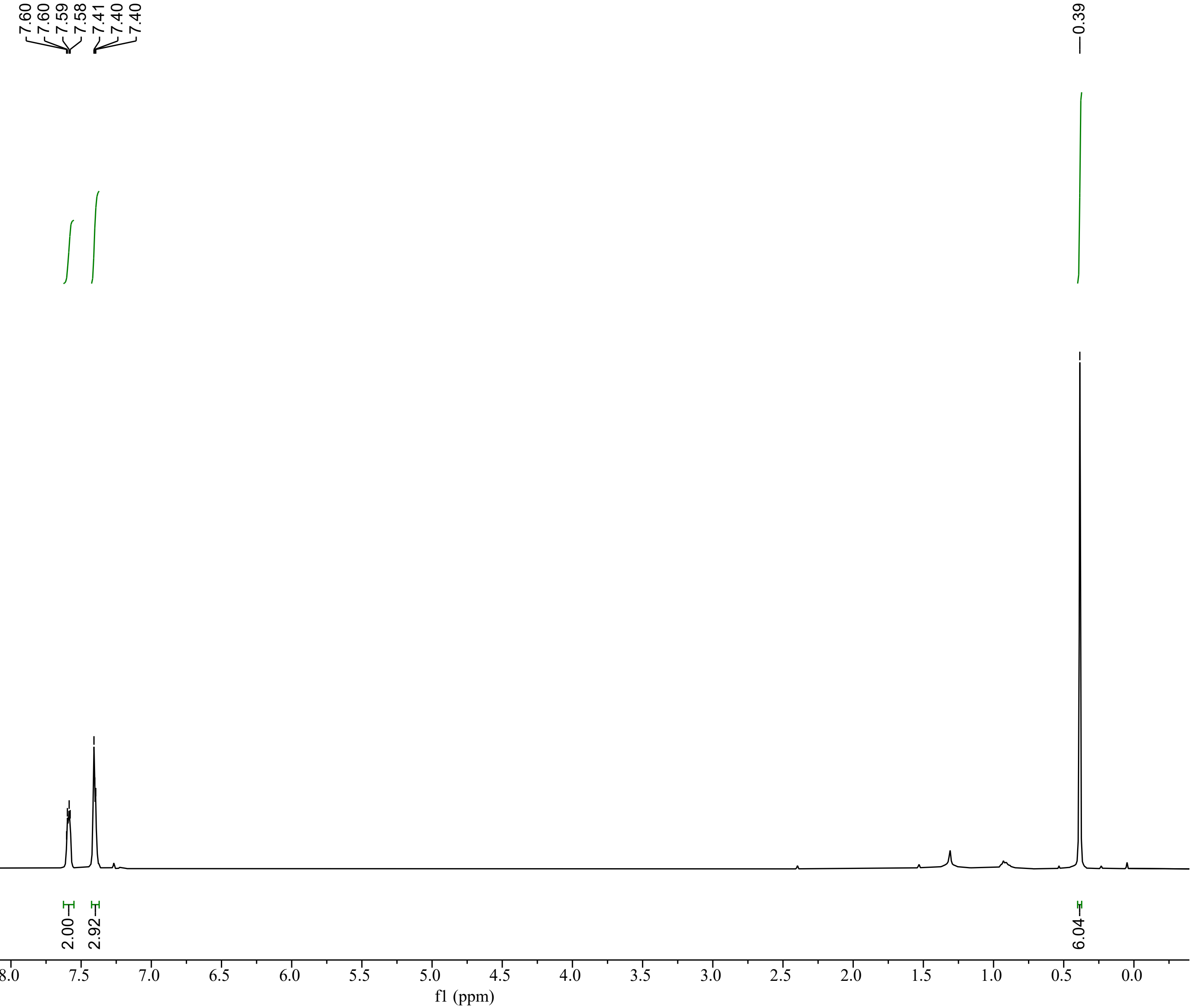

Compound **1a-*d*$_1$** ^{13}C NMR

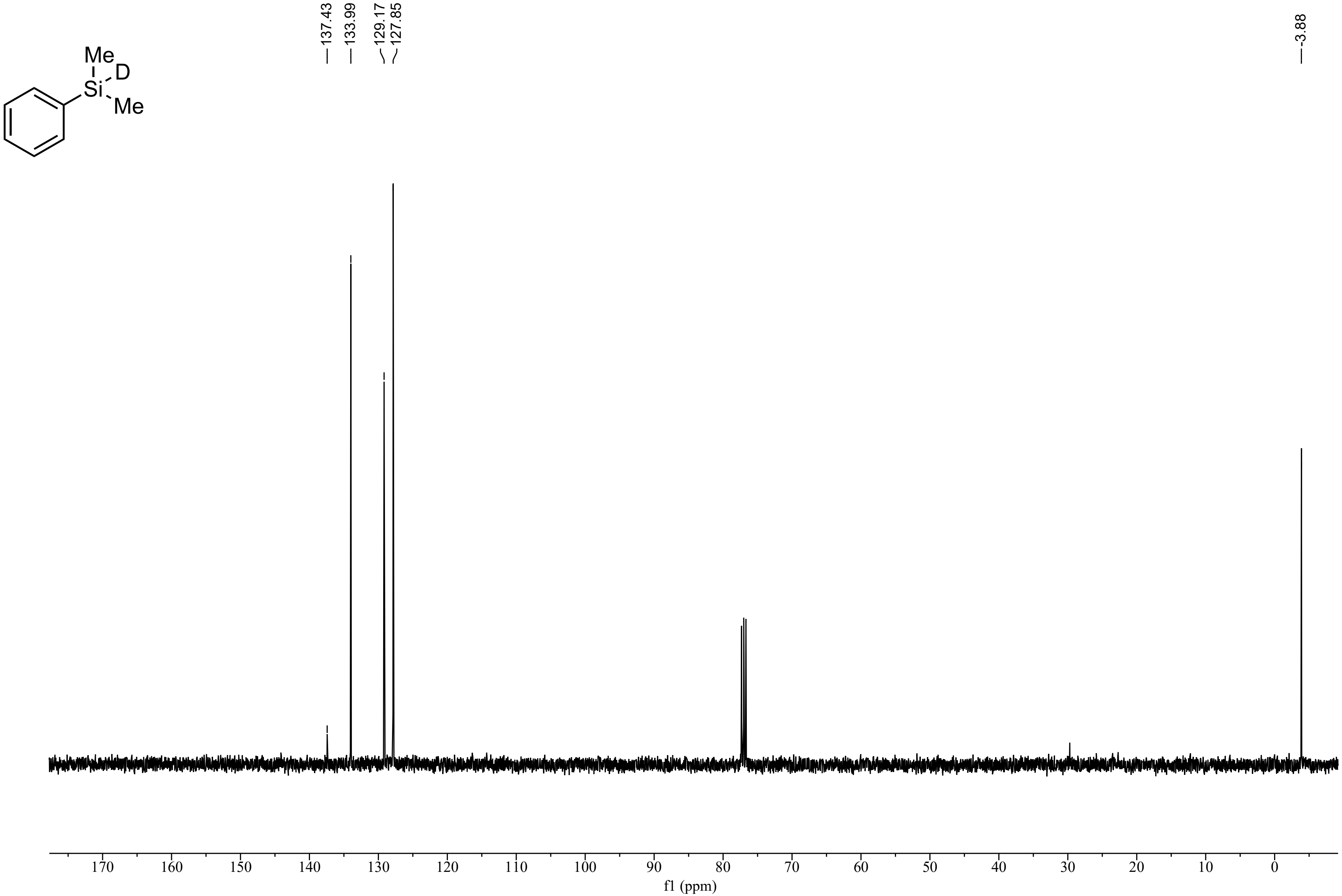

Compound **2a** ^{1}H NMR

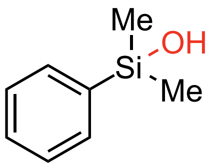

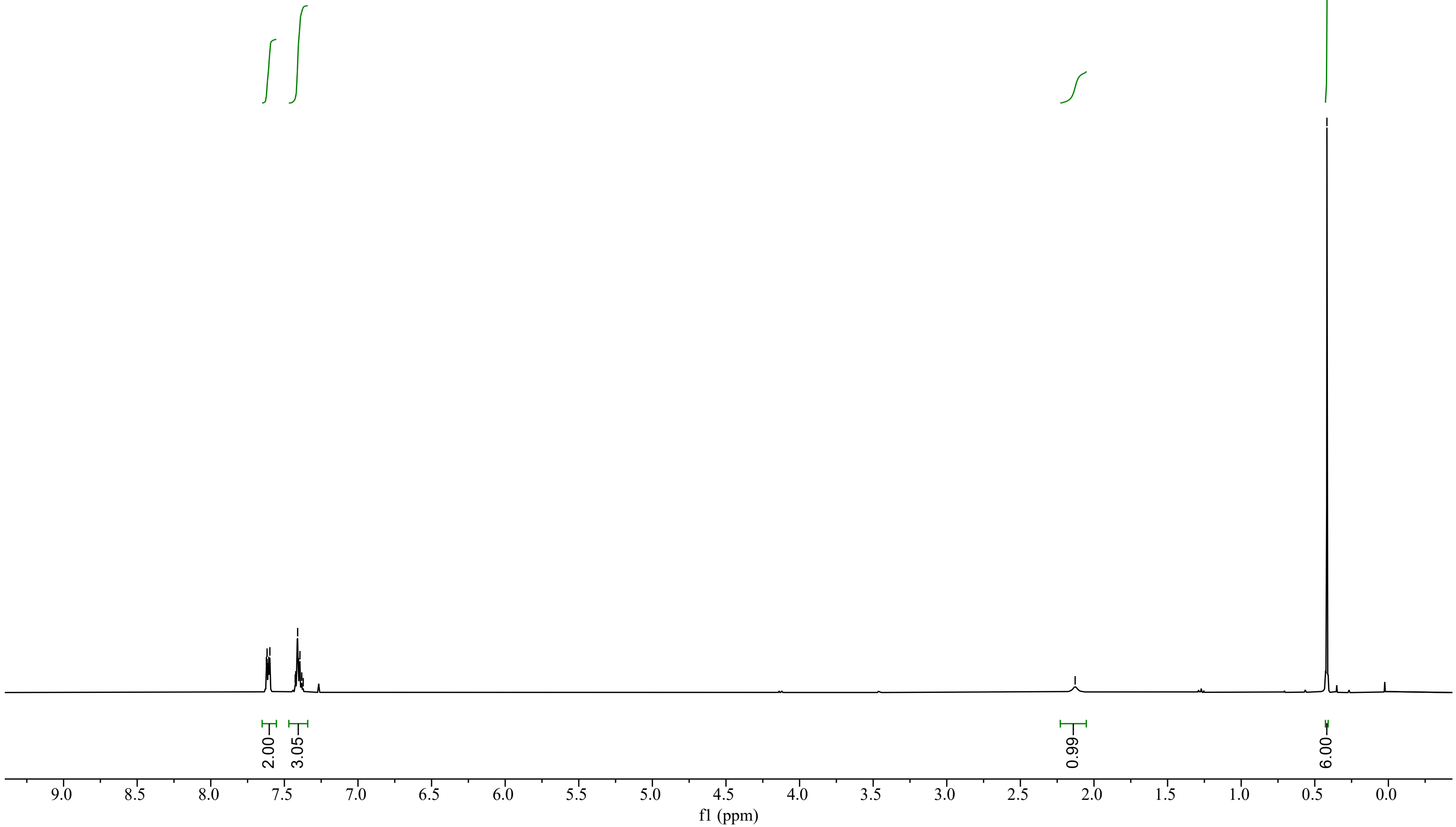

Compound **2a** ^{13}C NMR

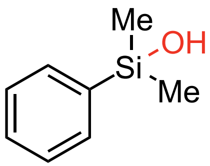

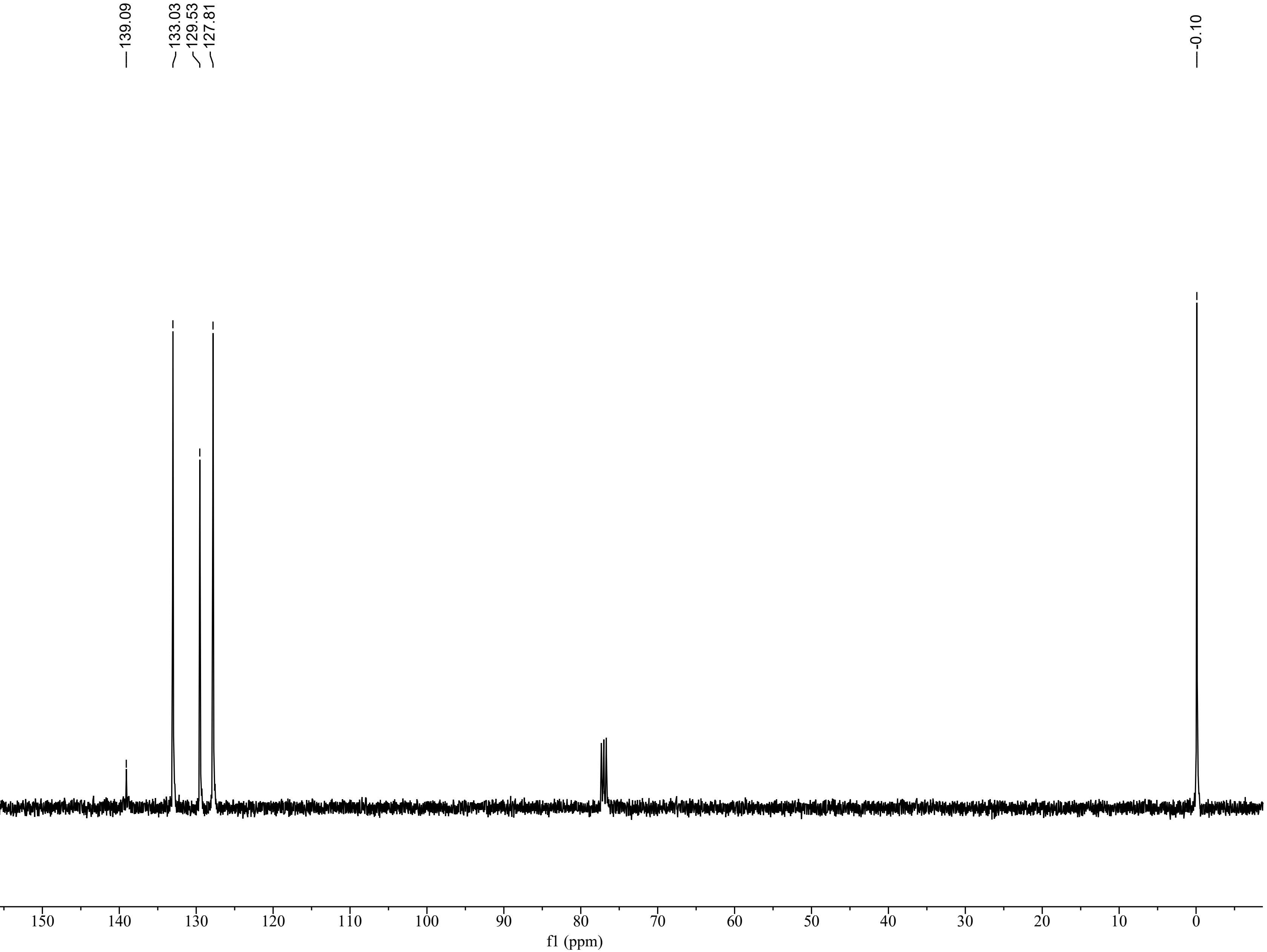

Compound **2b** ^{1}H NMR

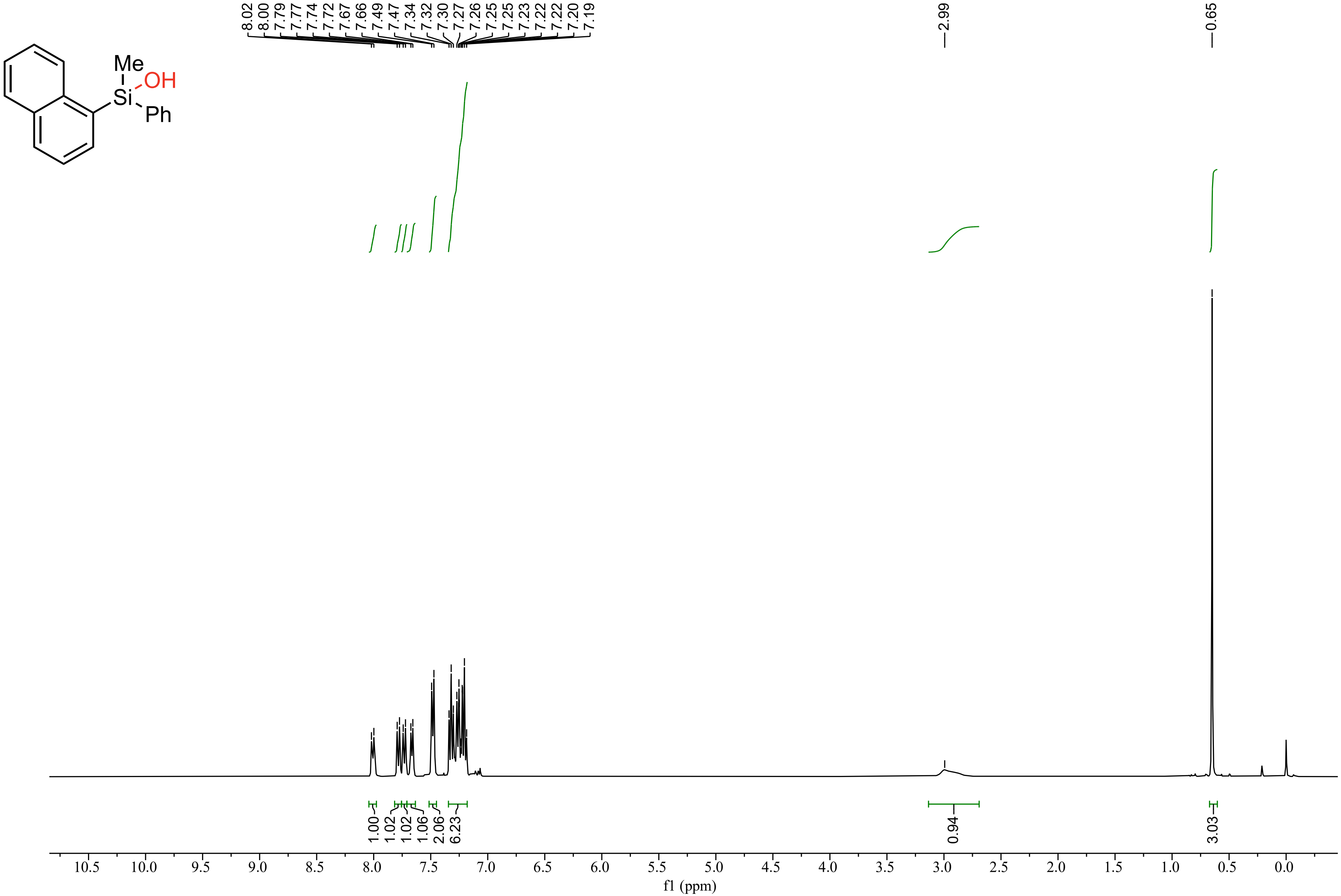

Compound **2b** ^{13}C NMR

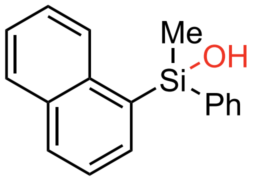

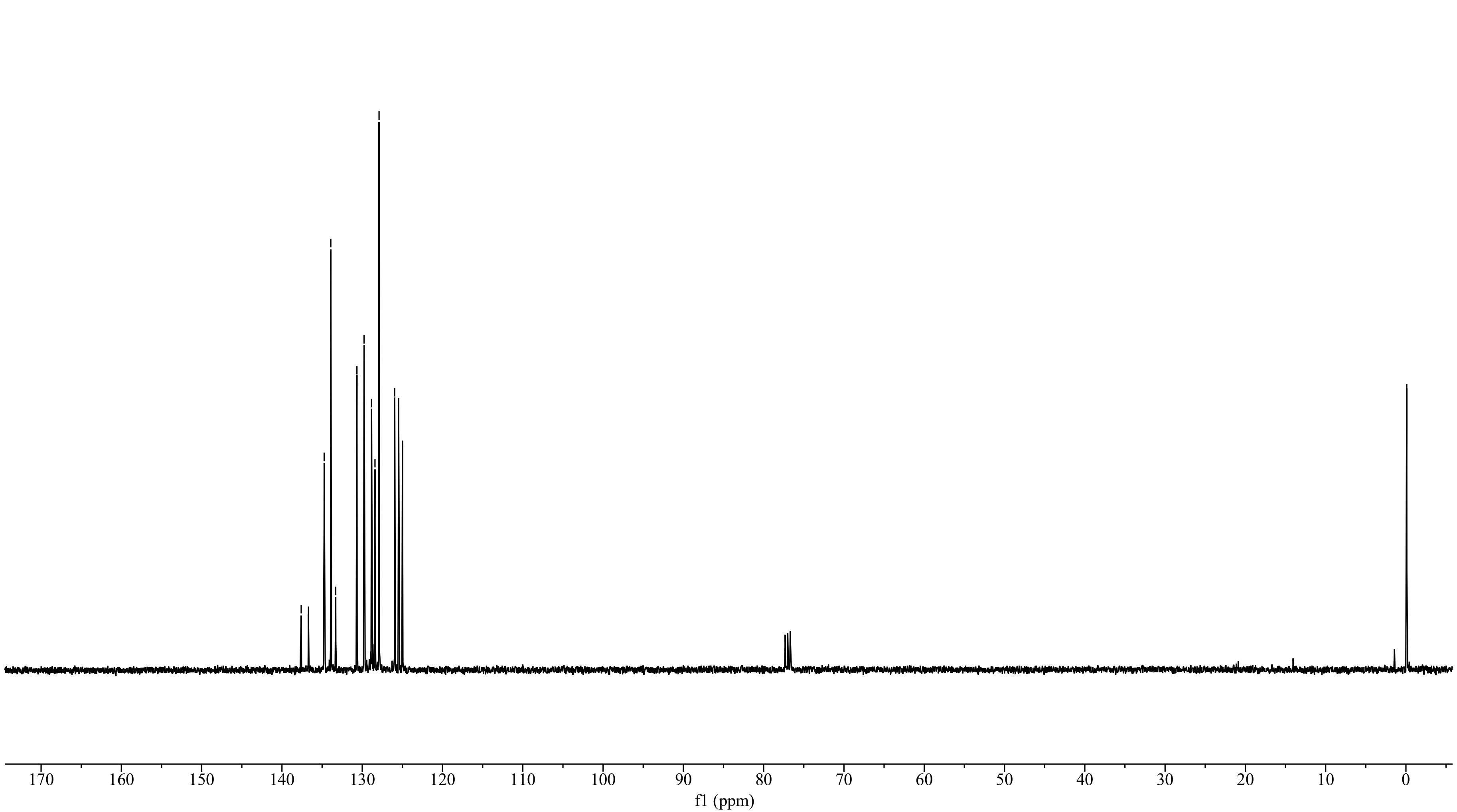

Compound ***R*-2b** ^{1}H NMR

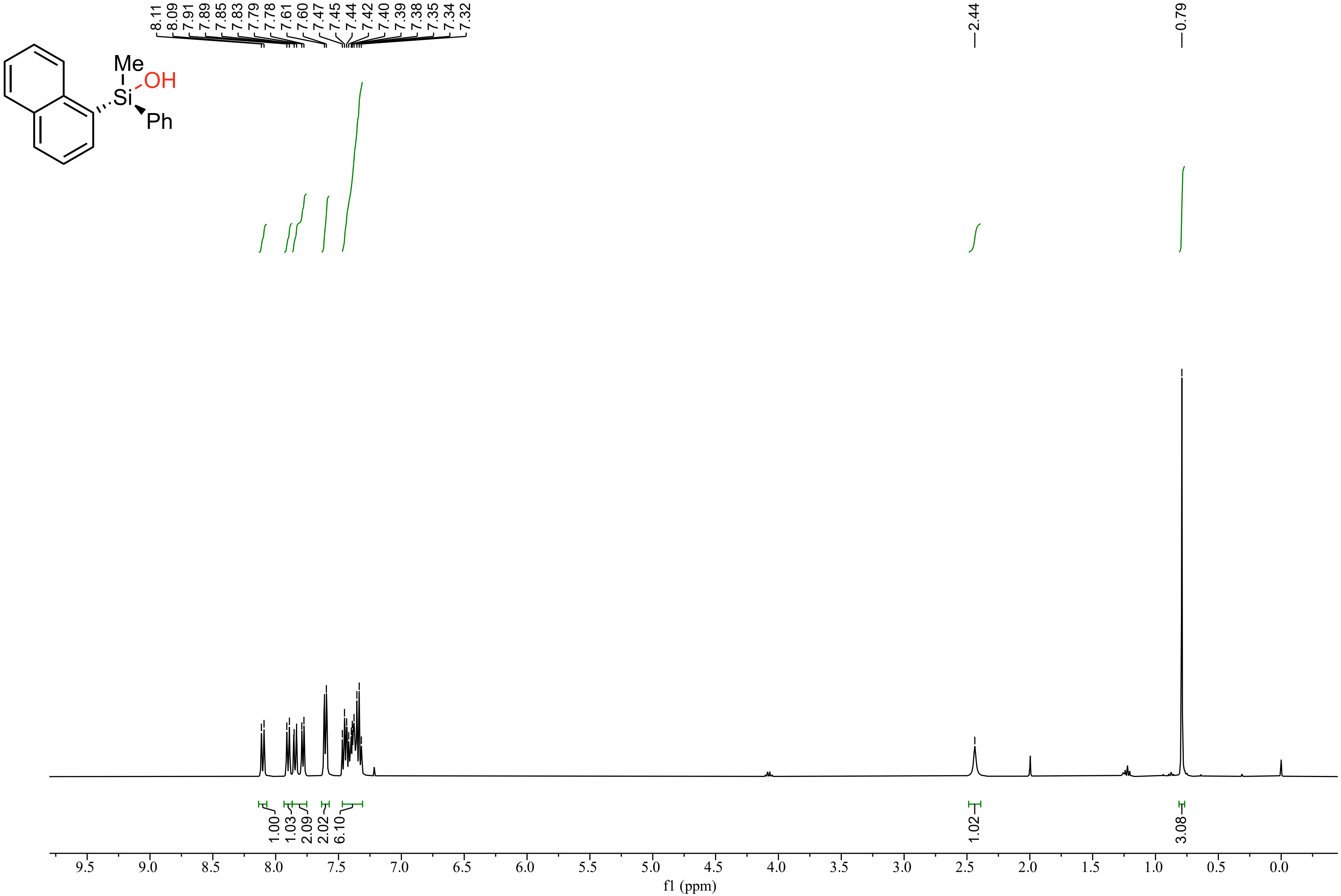

Compound ***R*-2b** ^{13}C NMR

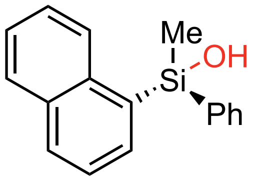

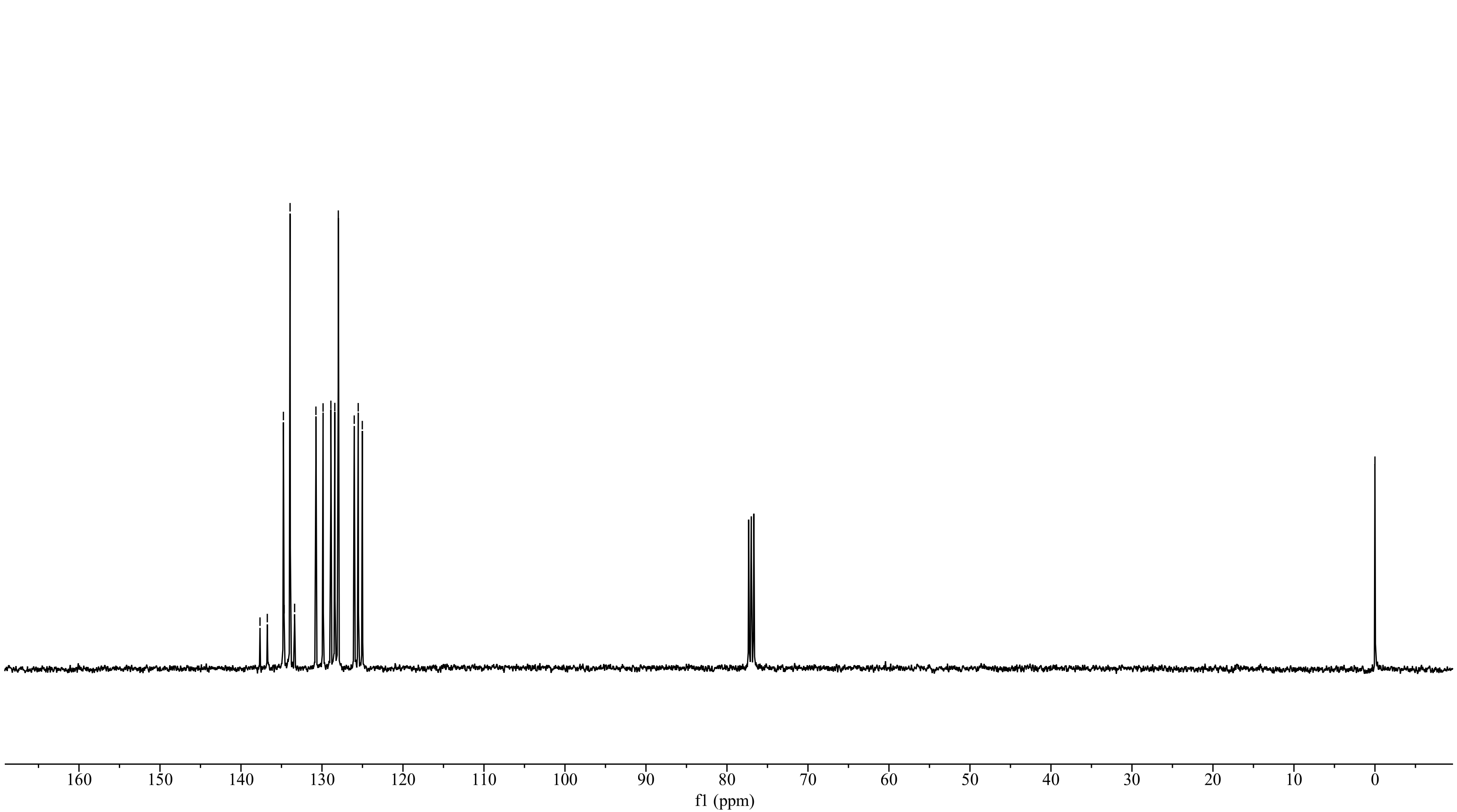

Compound **2c** [1]H NMR

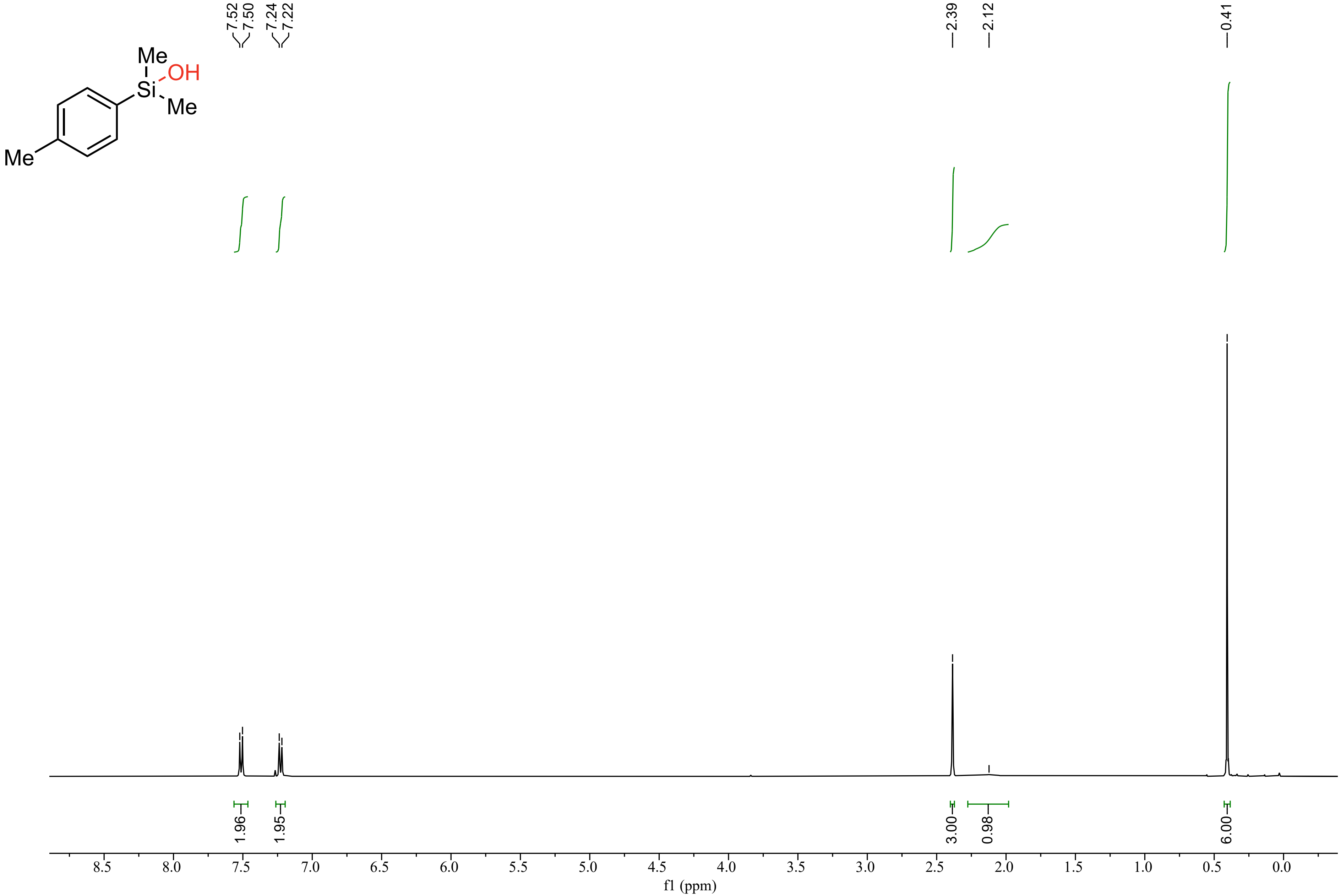

Compound **2c** ^{13}C NMR

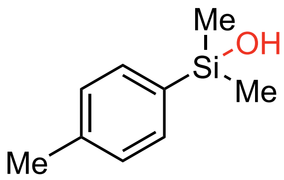

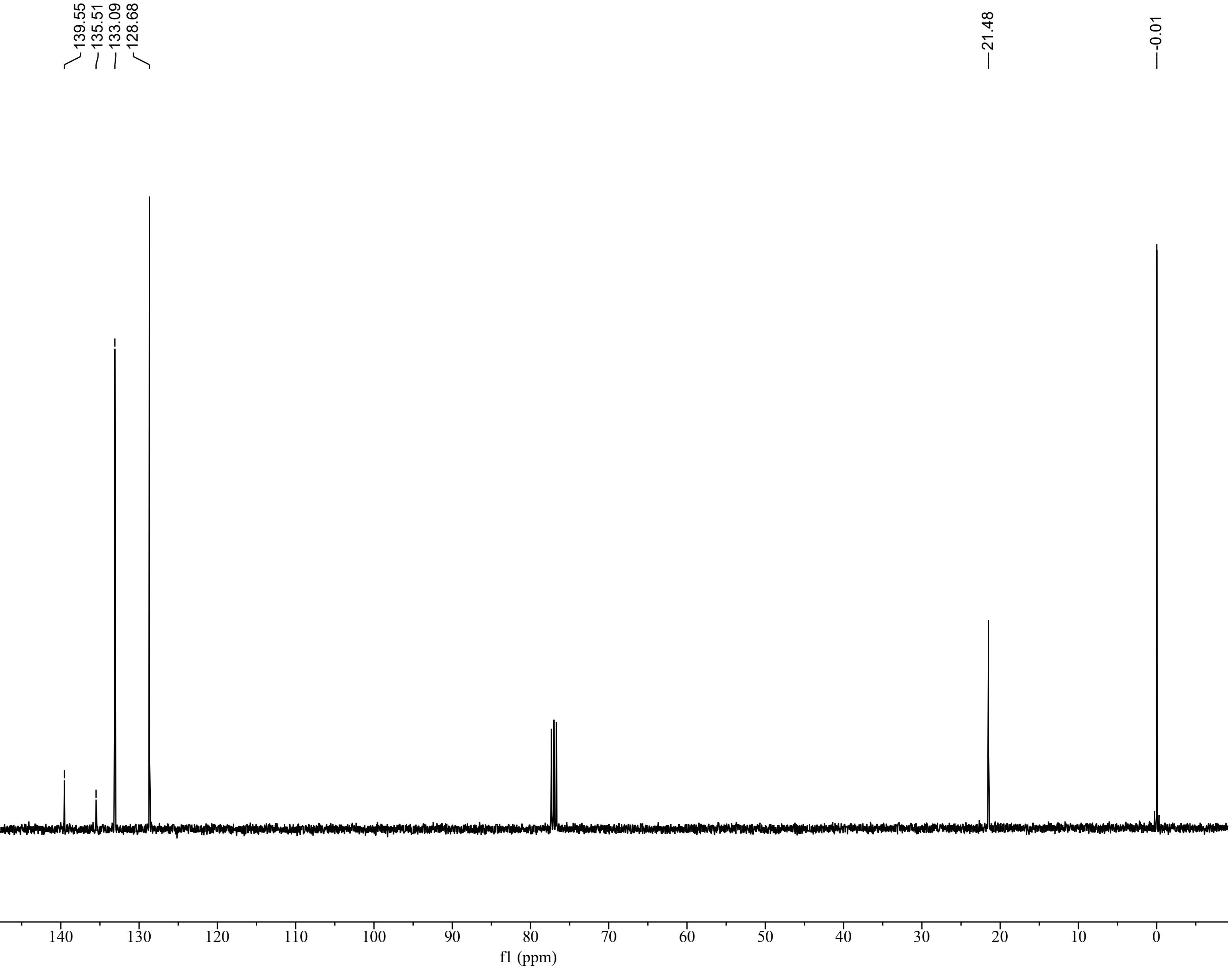

Compound **2d** ^{1}H NMR

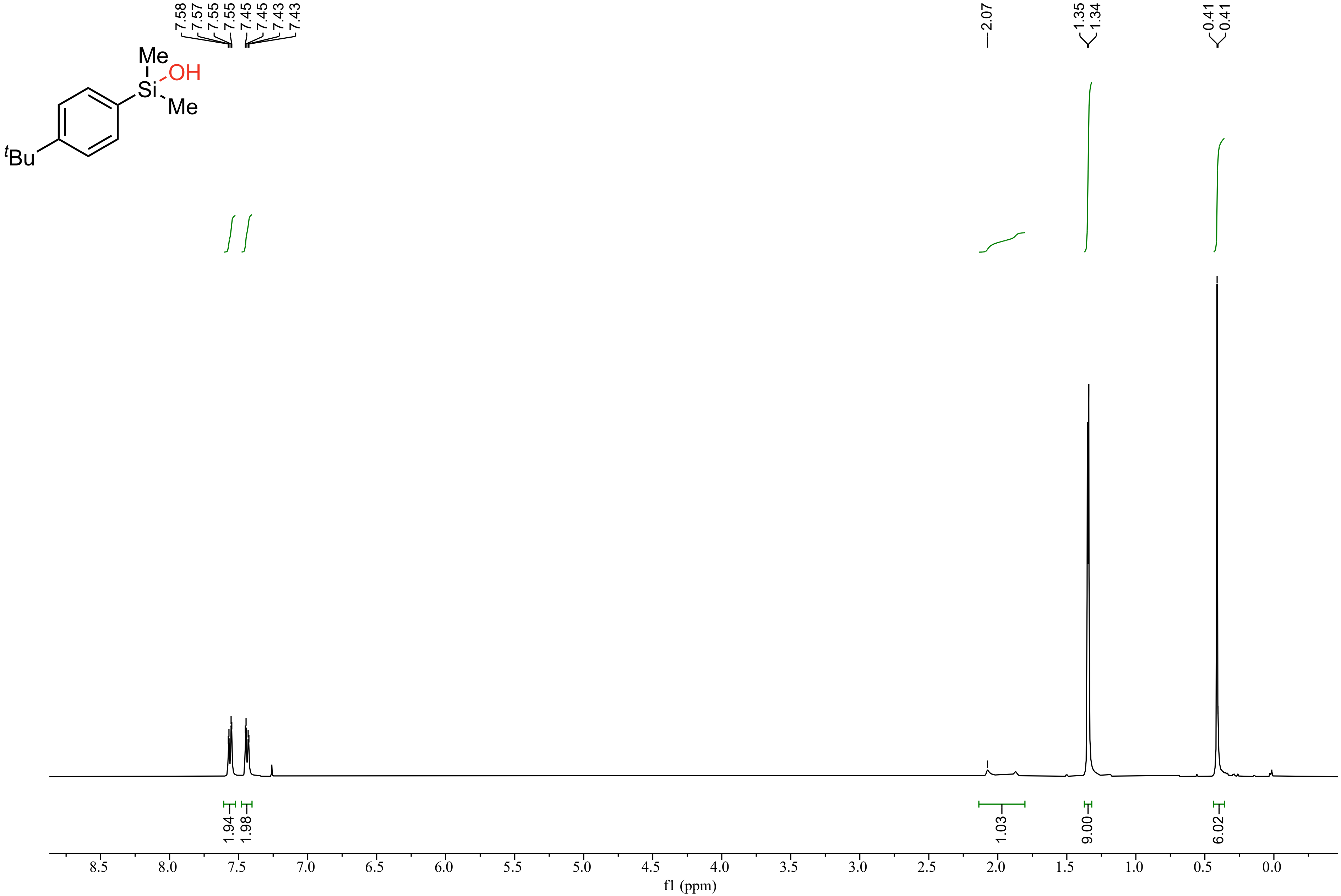

Compound **2d** ^{13}C NMR

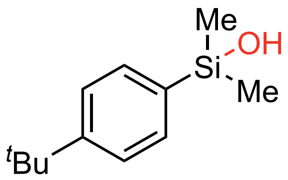

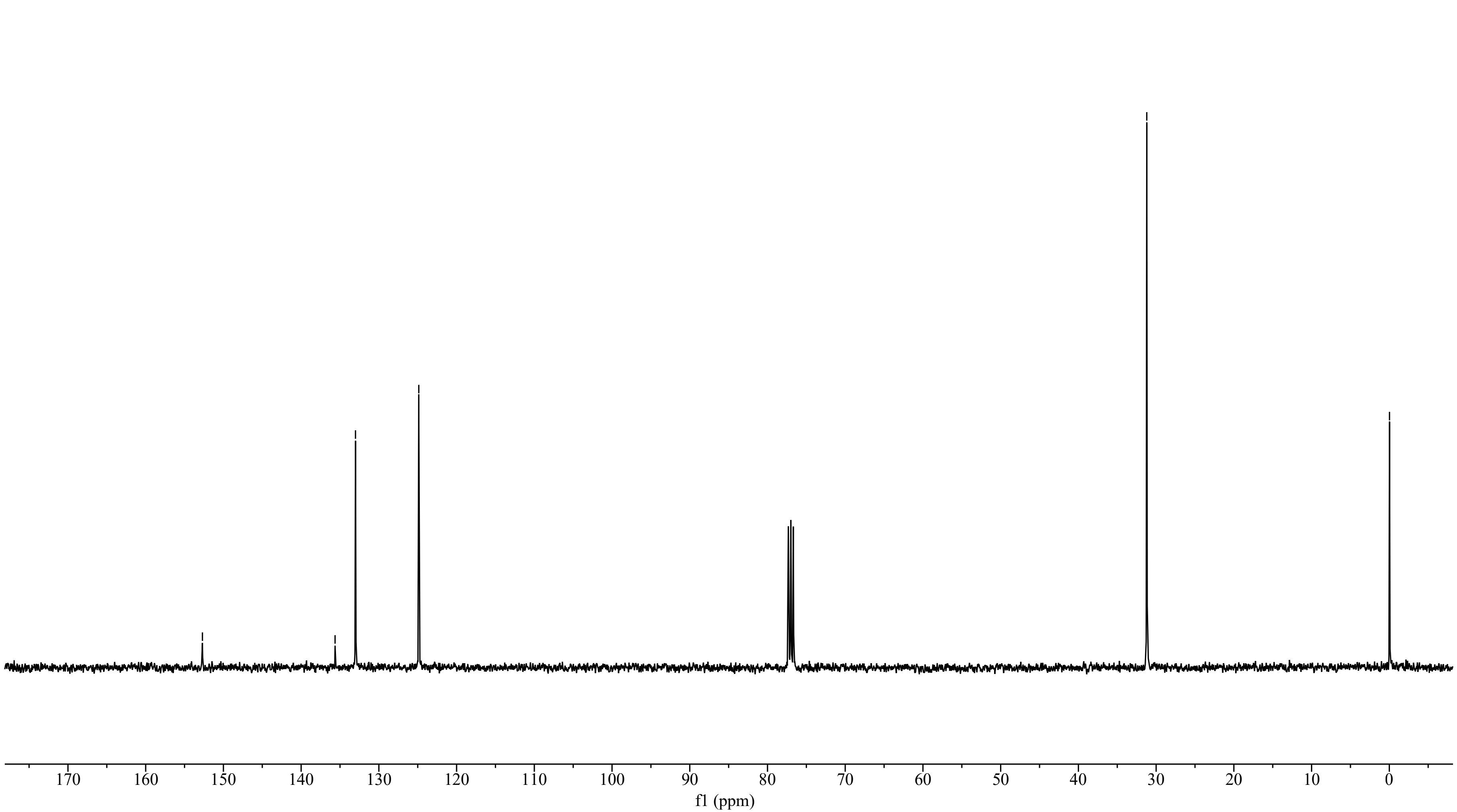

Compound **2e** ^{1}H NMR

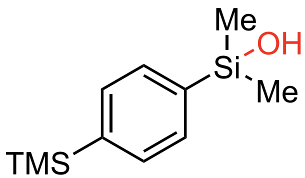

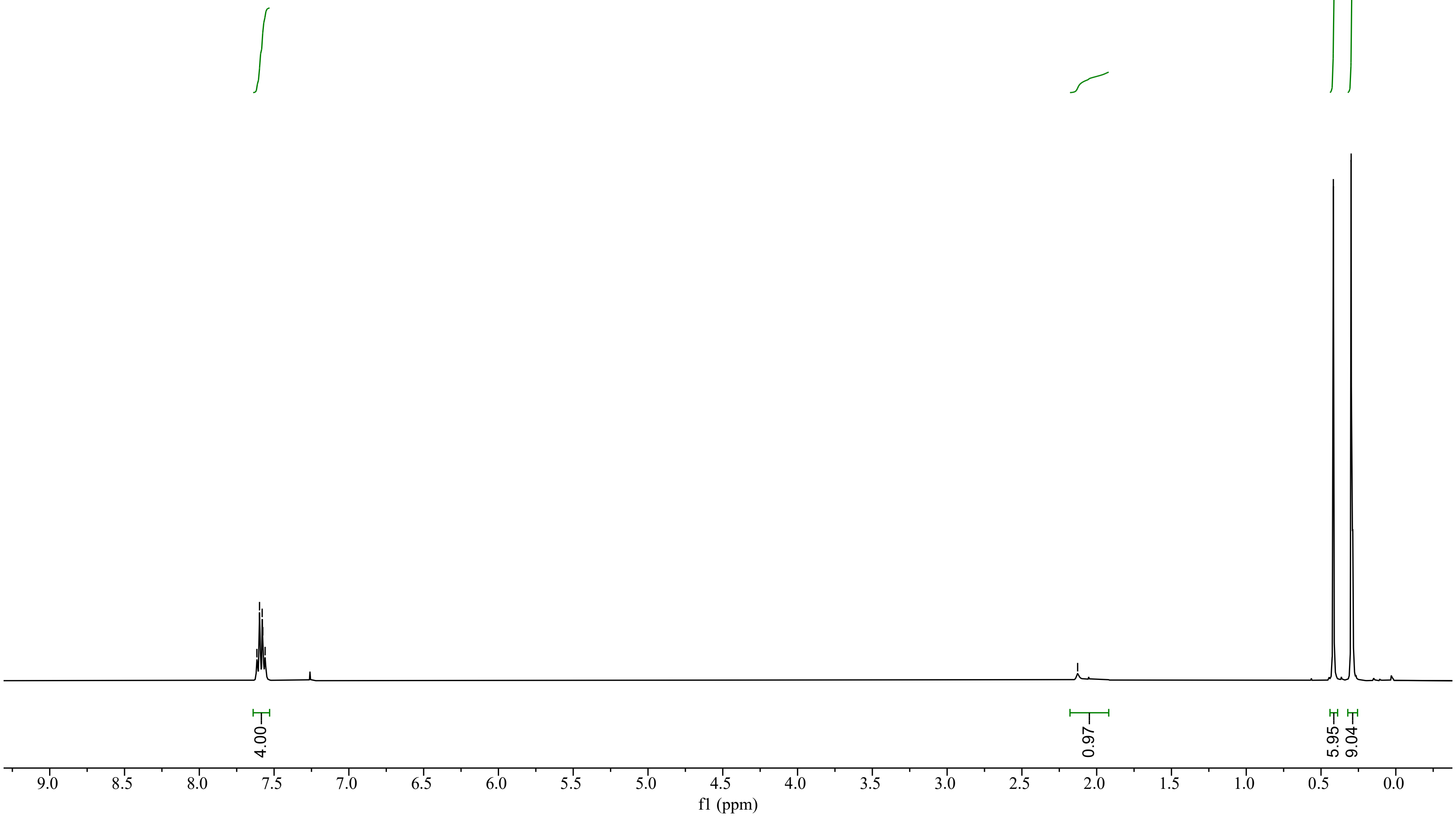

Compound **2e** ^{13}C NMR

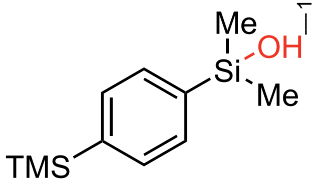

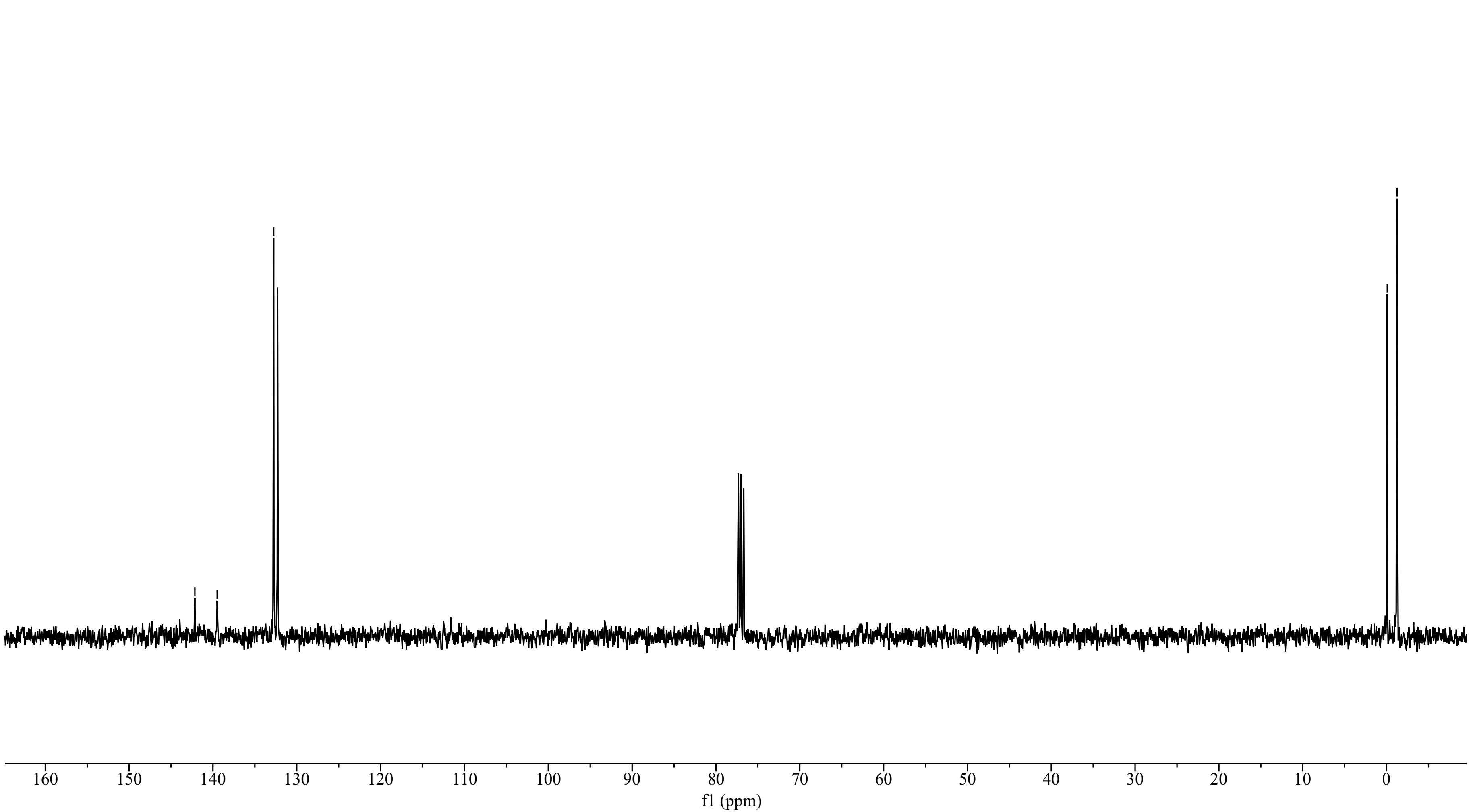

Compound **2f** ^{1}H NMR

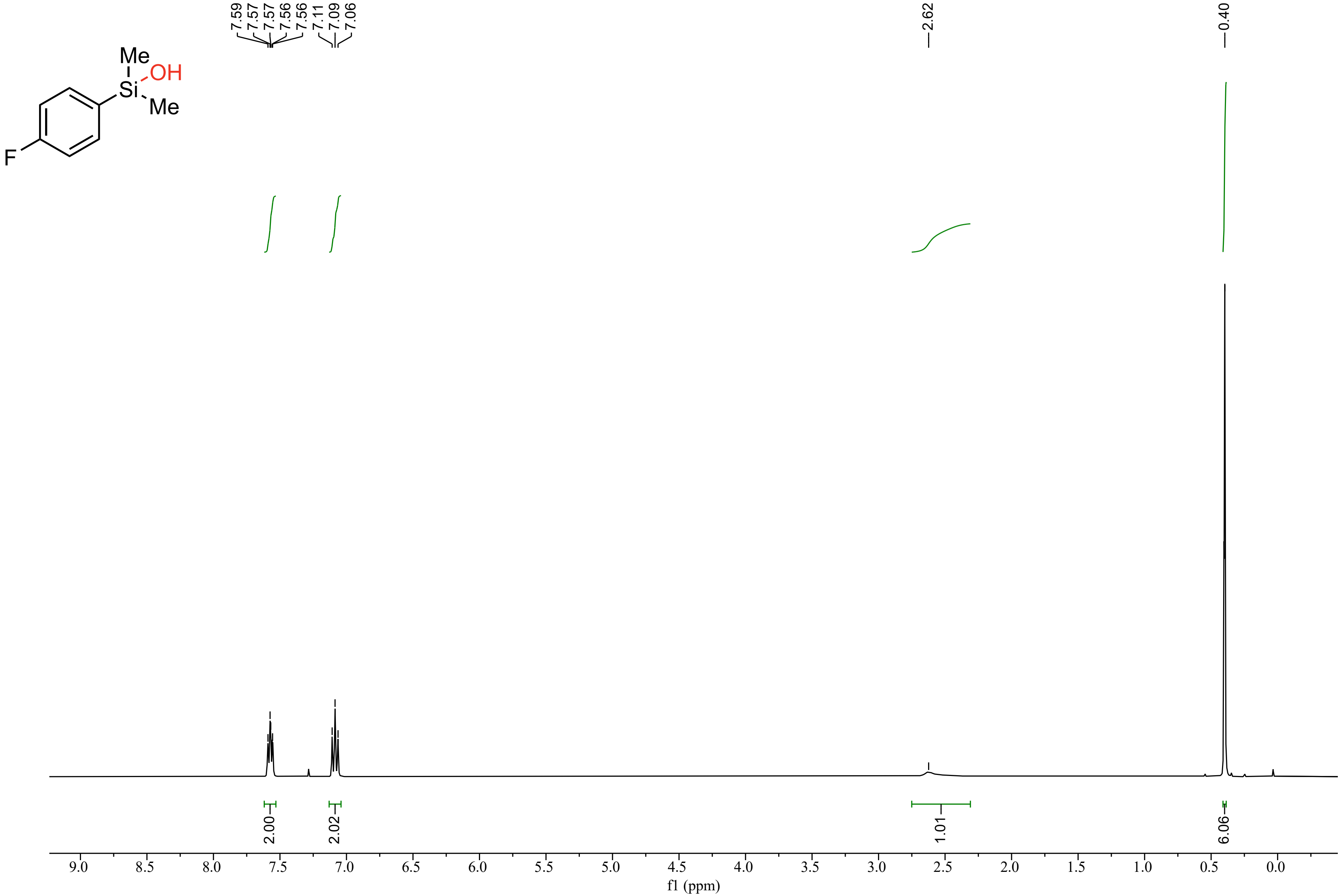

Compound **2f** ^{13}C NMR

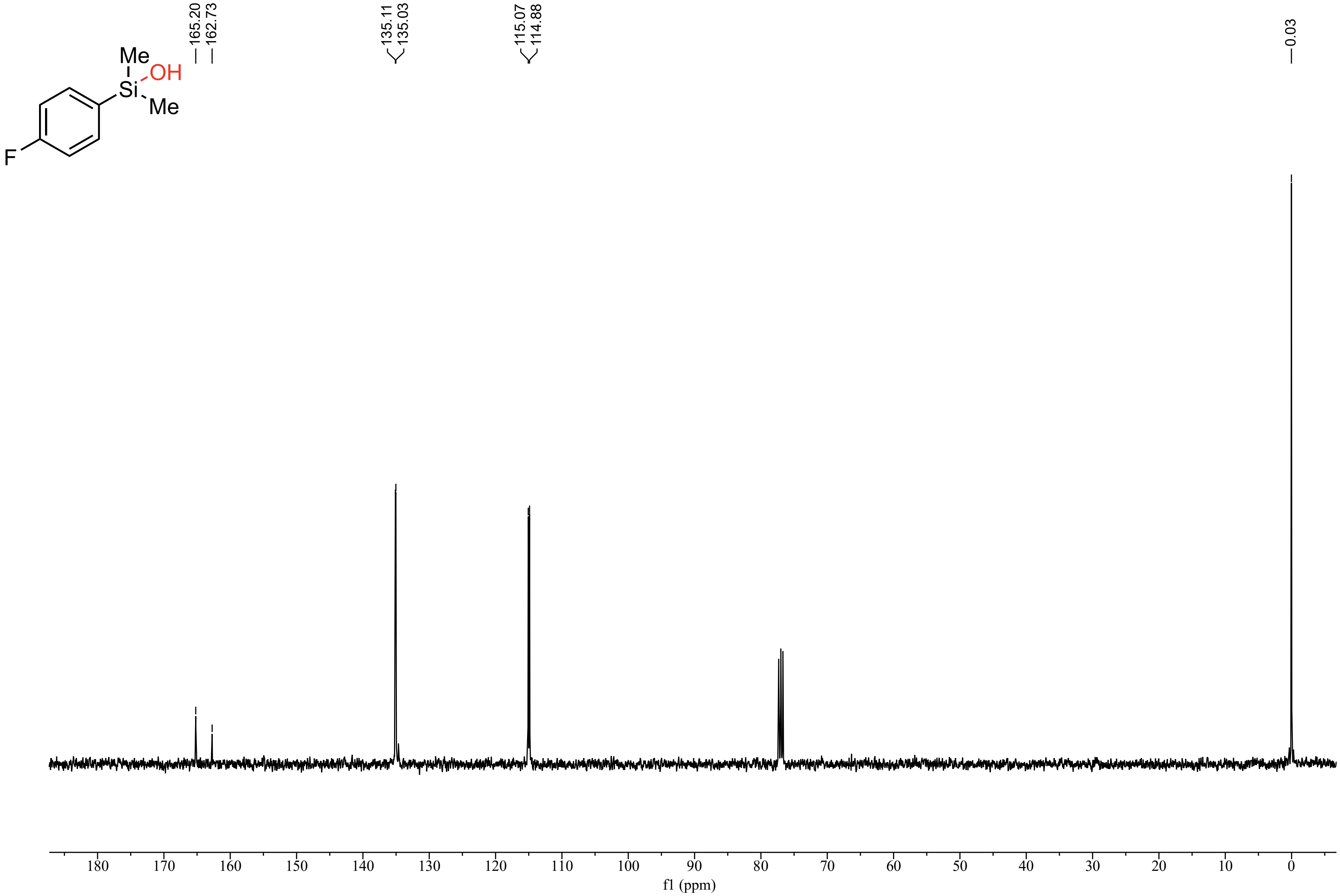

Compound **2f** ^{19}F NMR

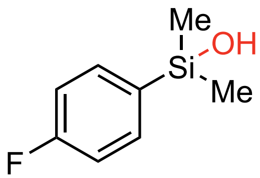

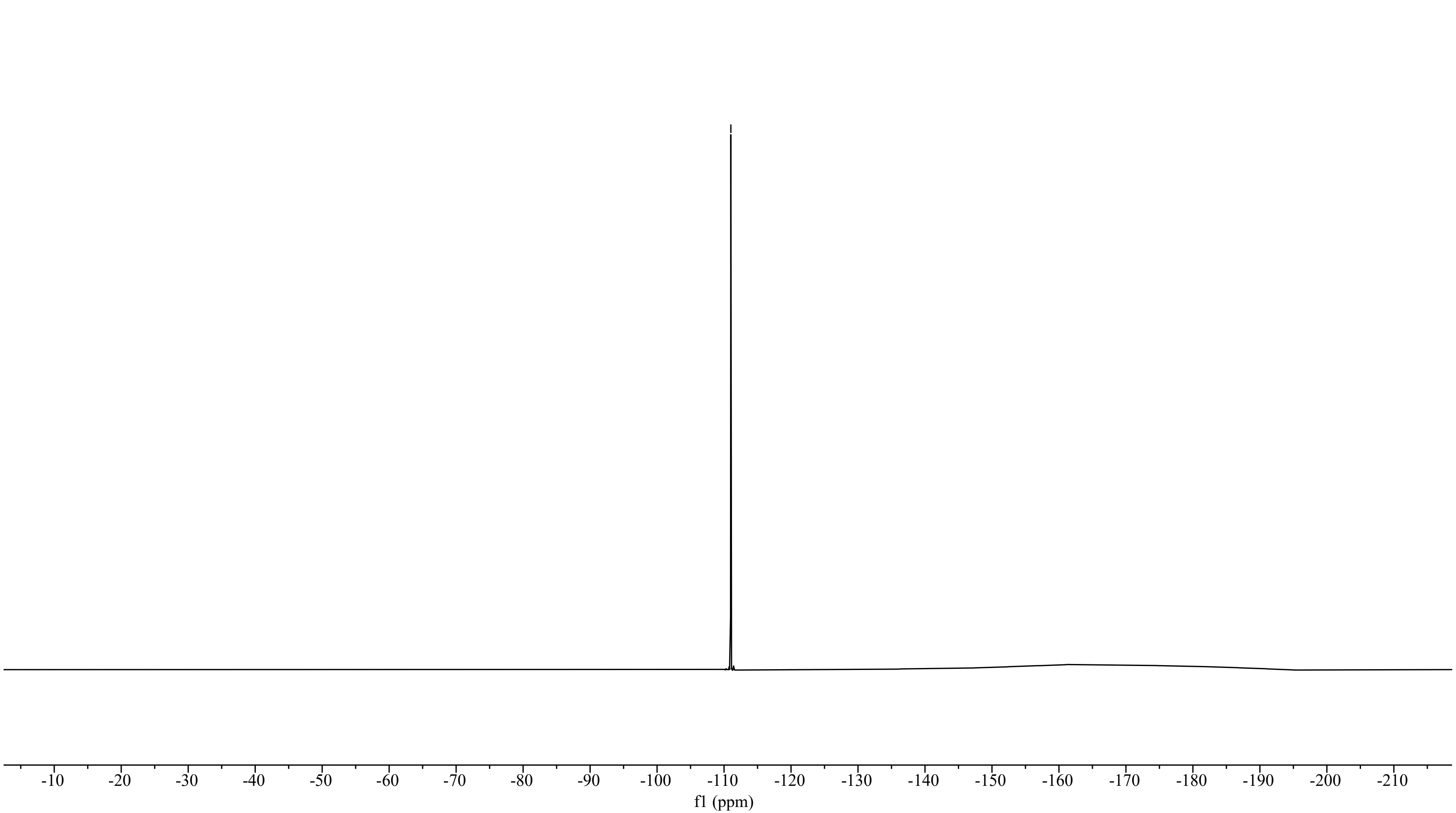

Compound **2g** ^{1}H NMR

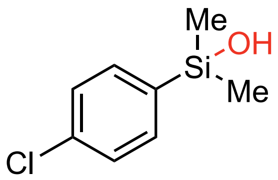

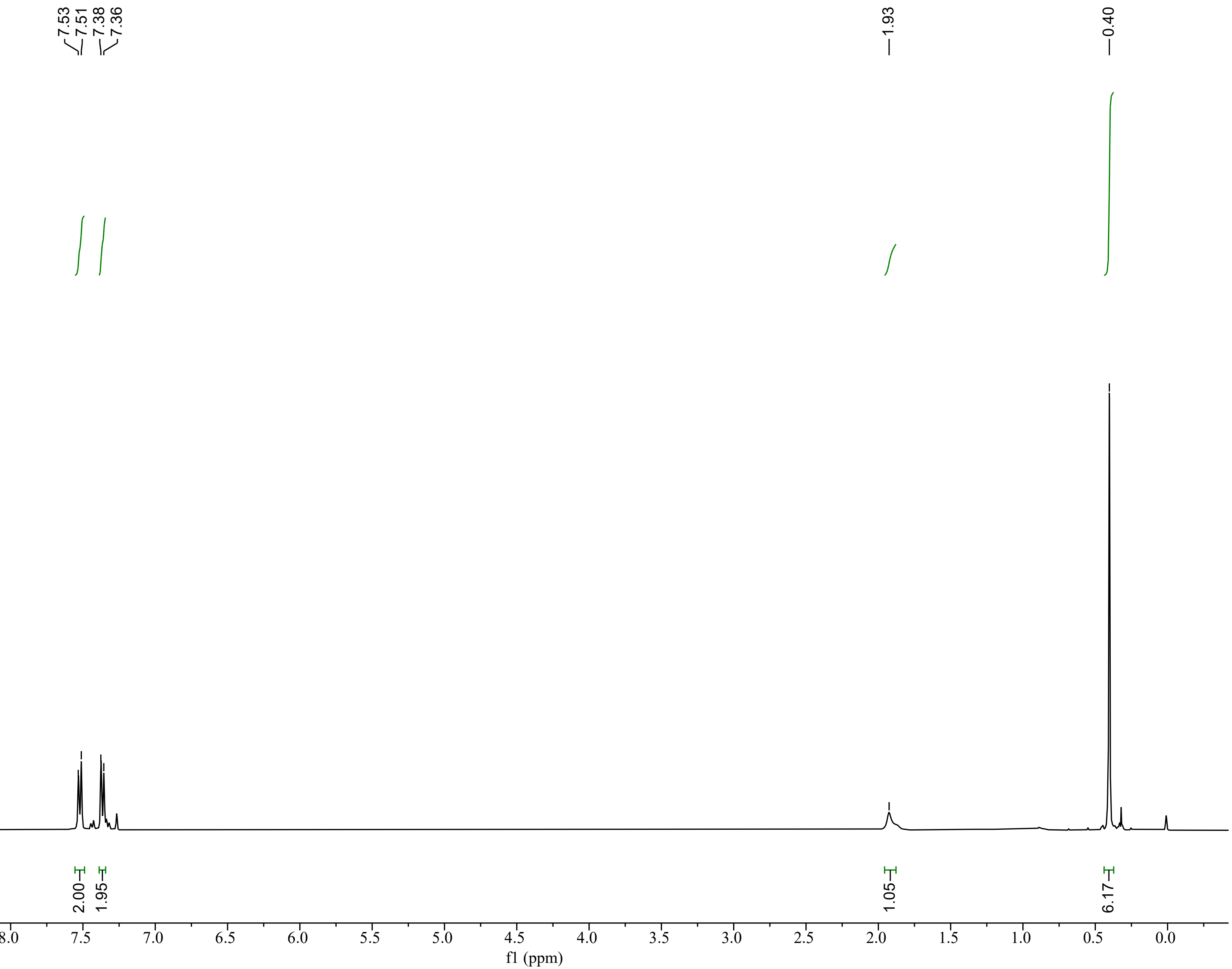

Compound **2g** ^{13}C NMR

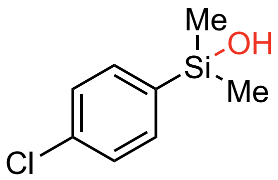

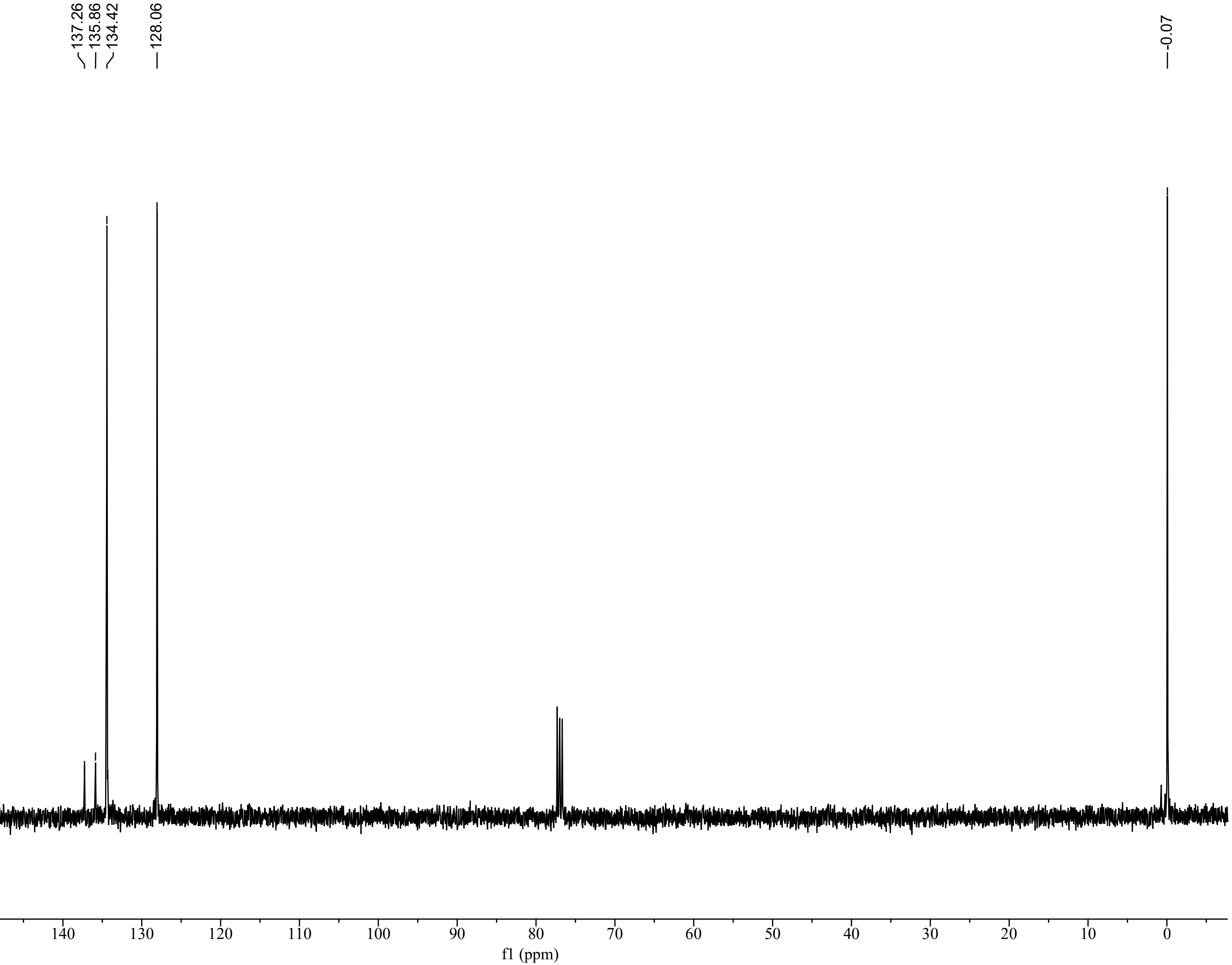

Compound **2h** ^{1}H NMR

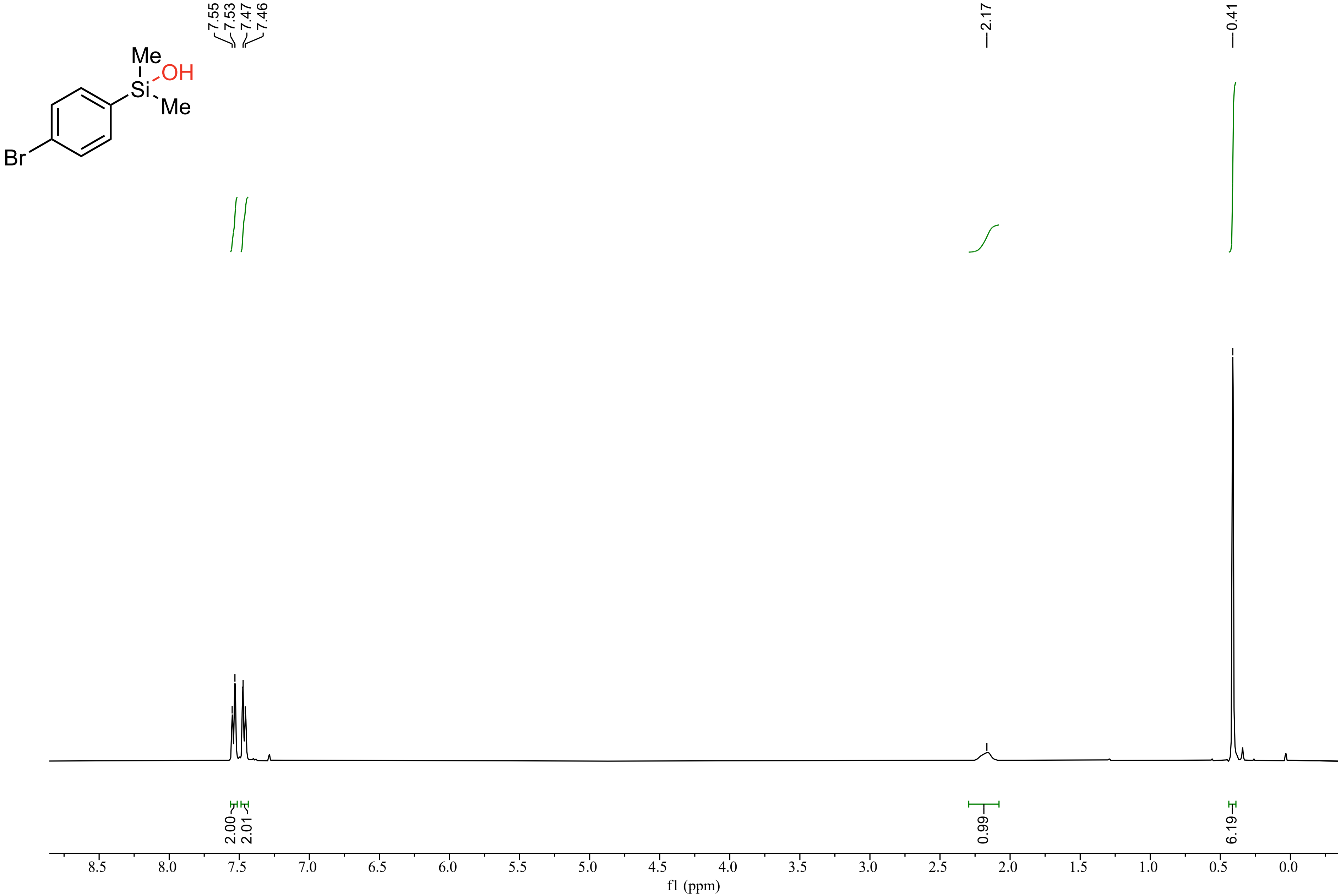

Compound **2h** ^{13}C NMR

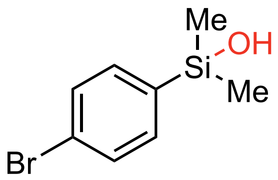

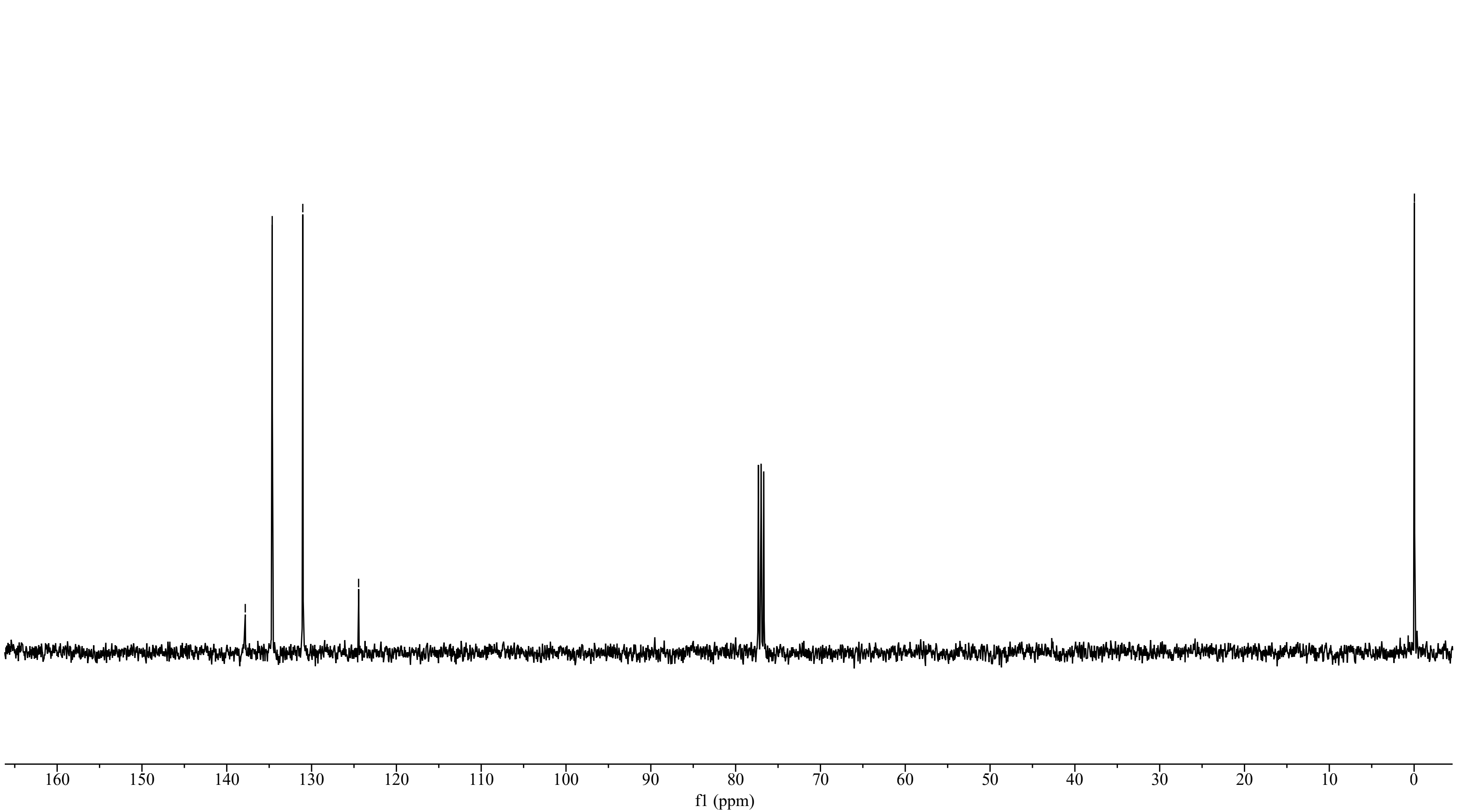

Compound **2i** ^{1}H NMR

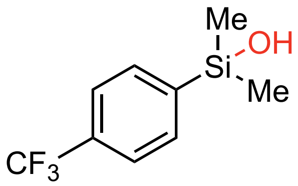

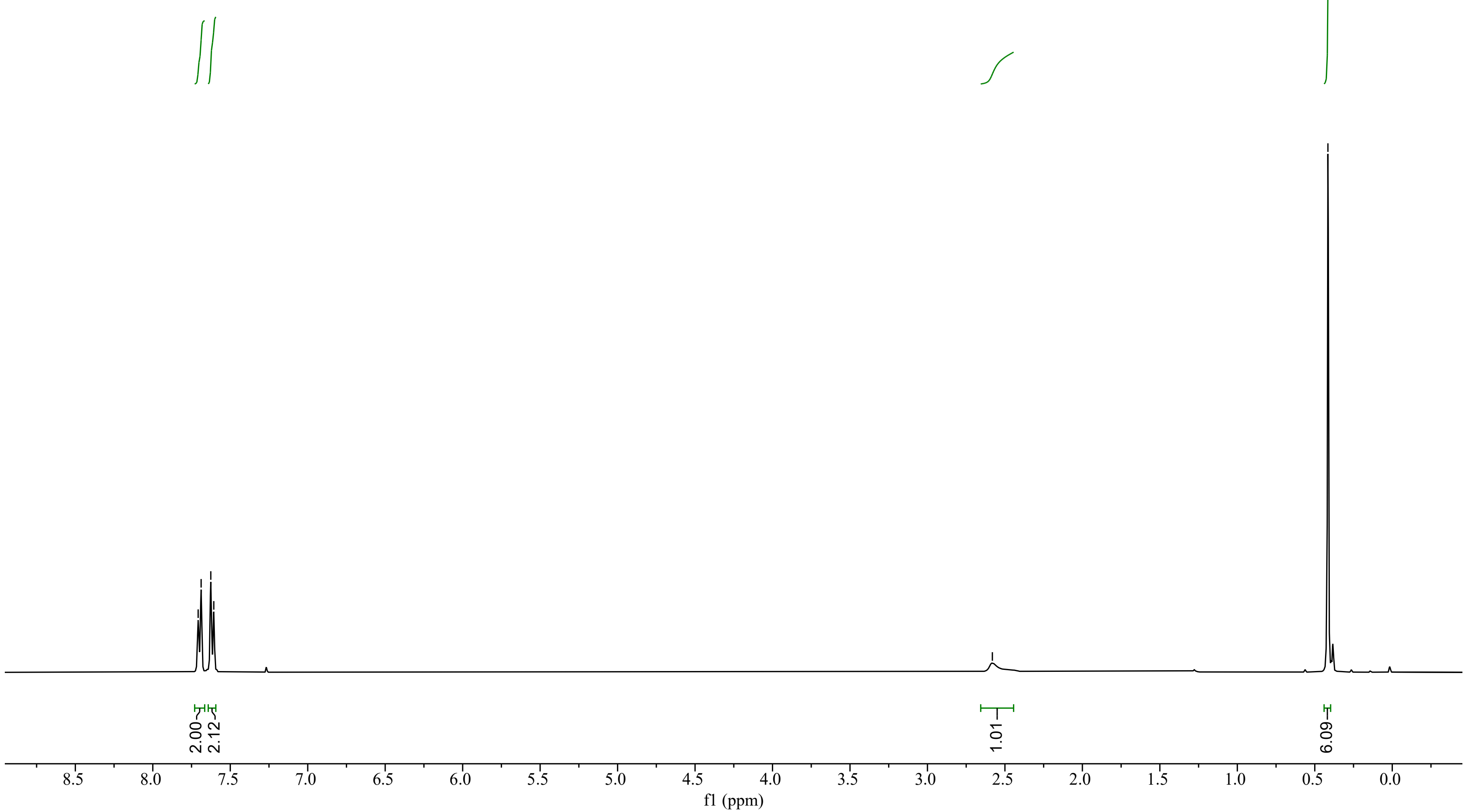

Compound **2i** ^{13}C NMR

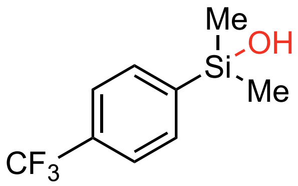

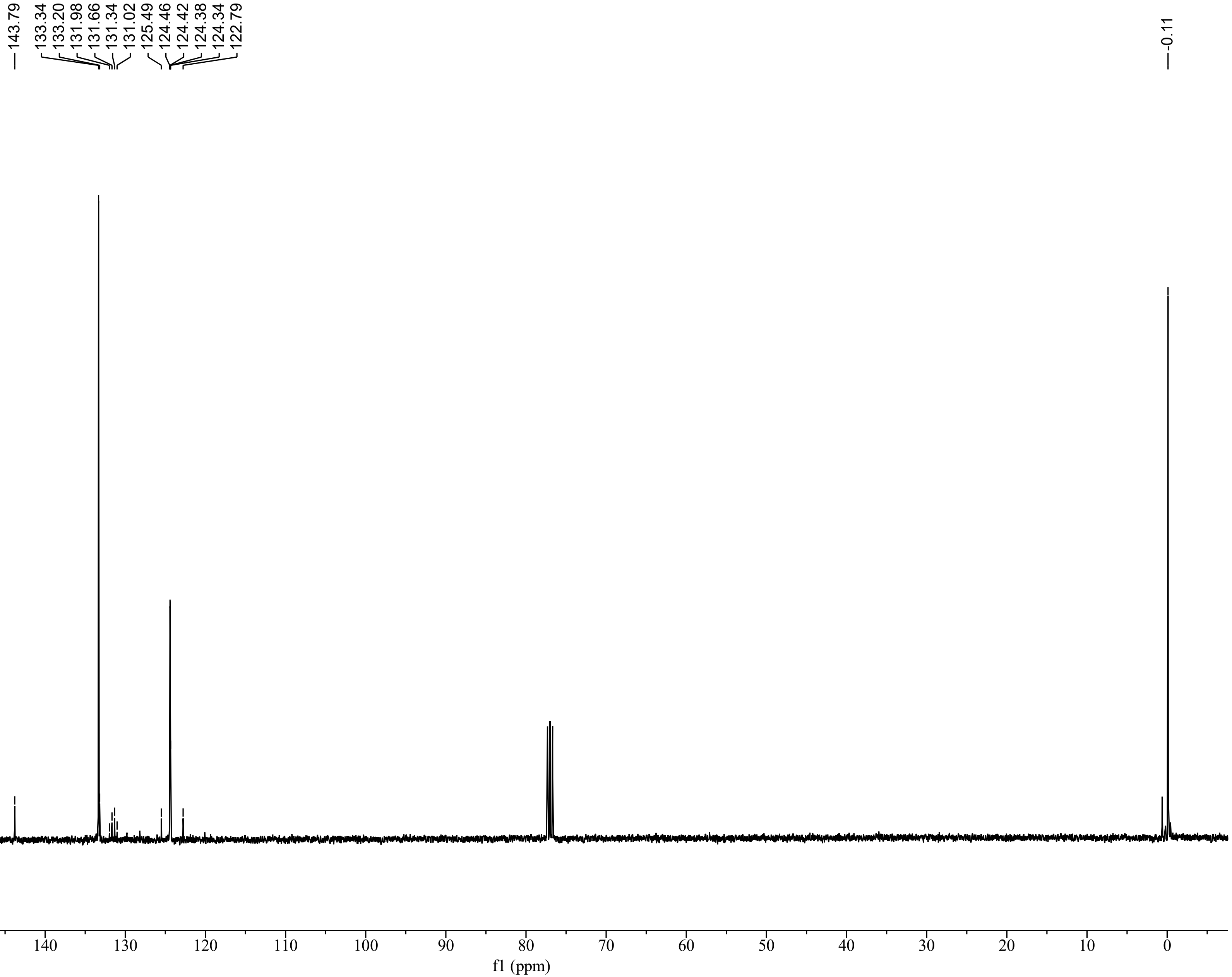

Compound **2i** ^{19}F NMR

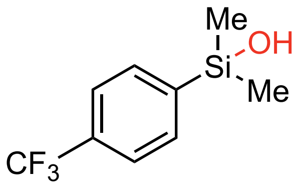

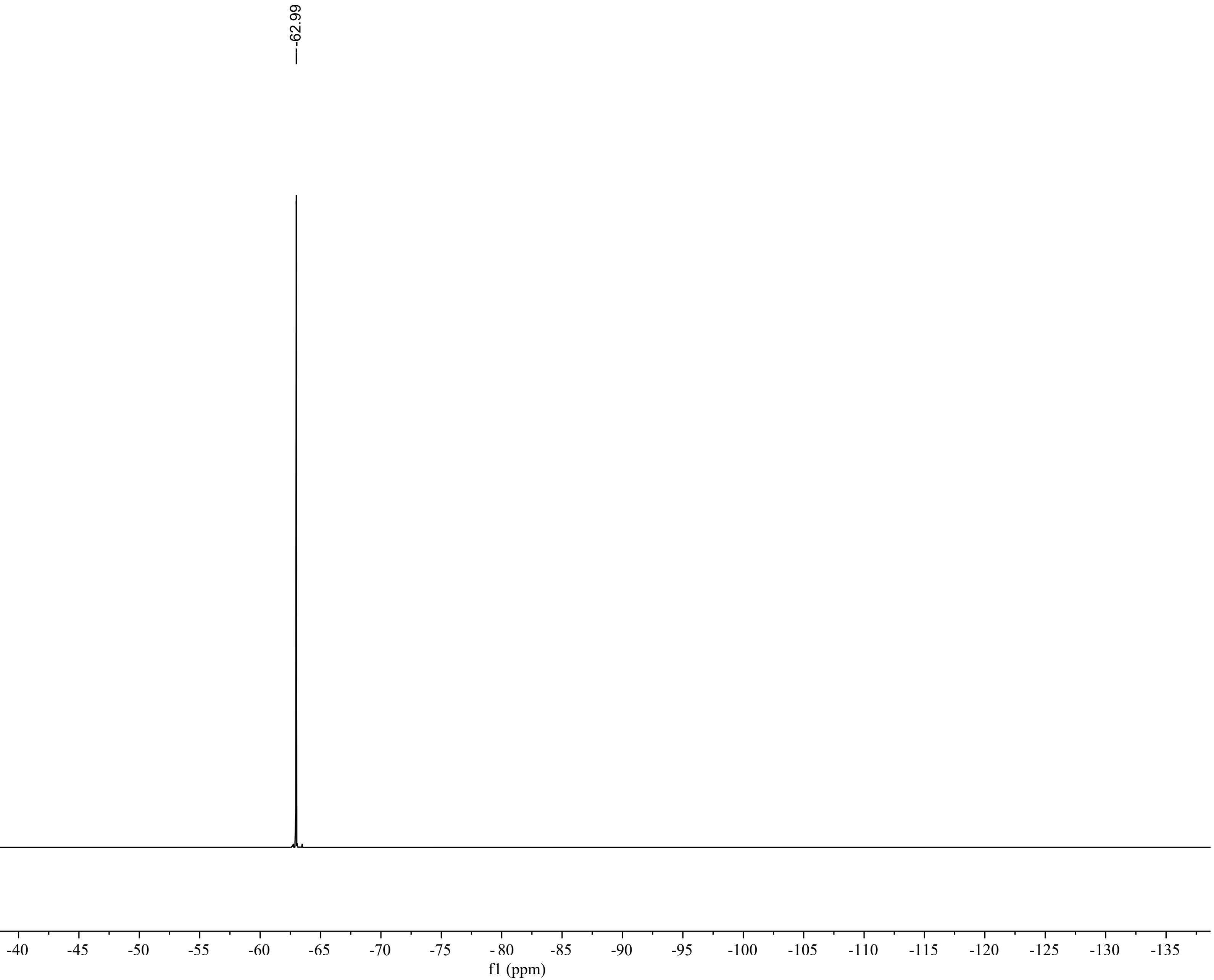

Compound **2j** ^{1}H NMR

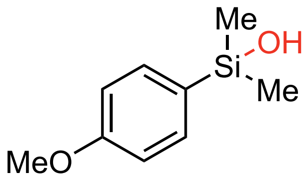

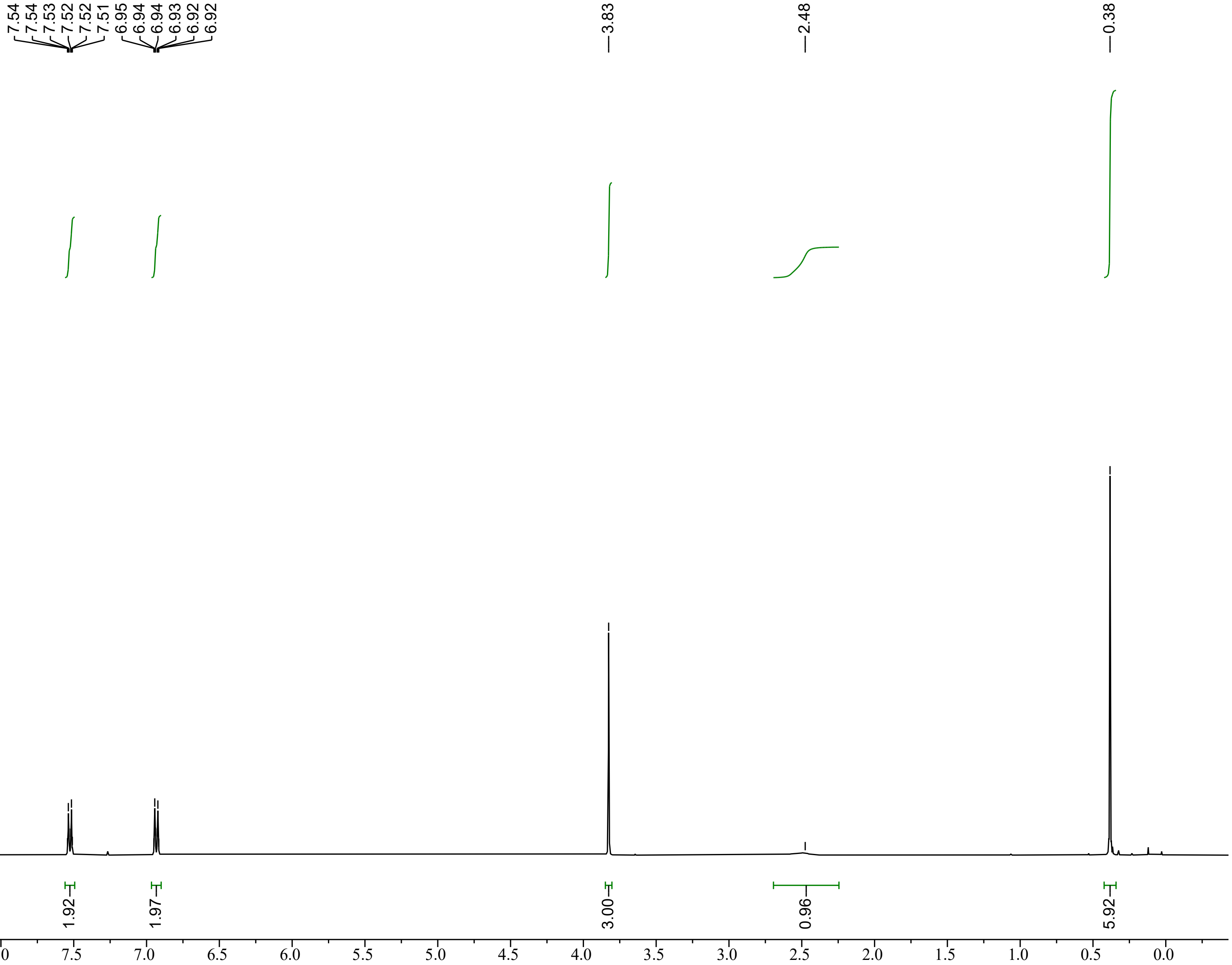

Compound **2j** ^{13}C NMR

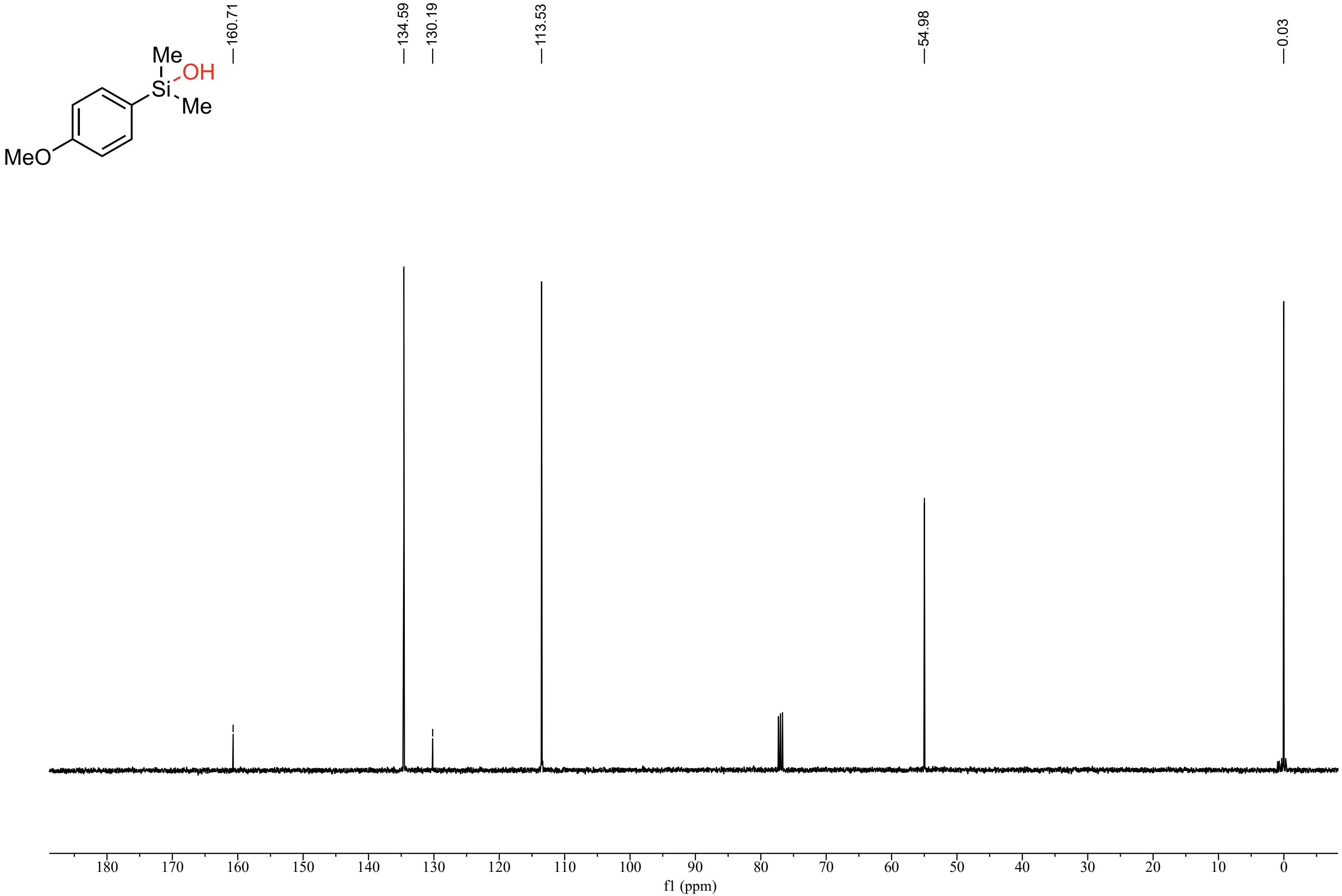

Compound **2k** ^{1}H NMR

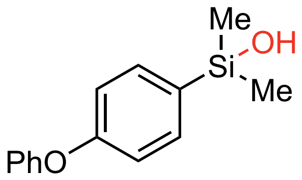

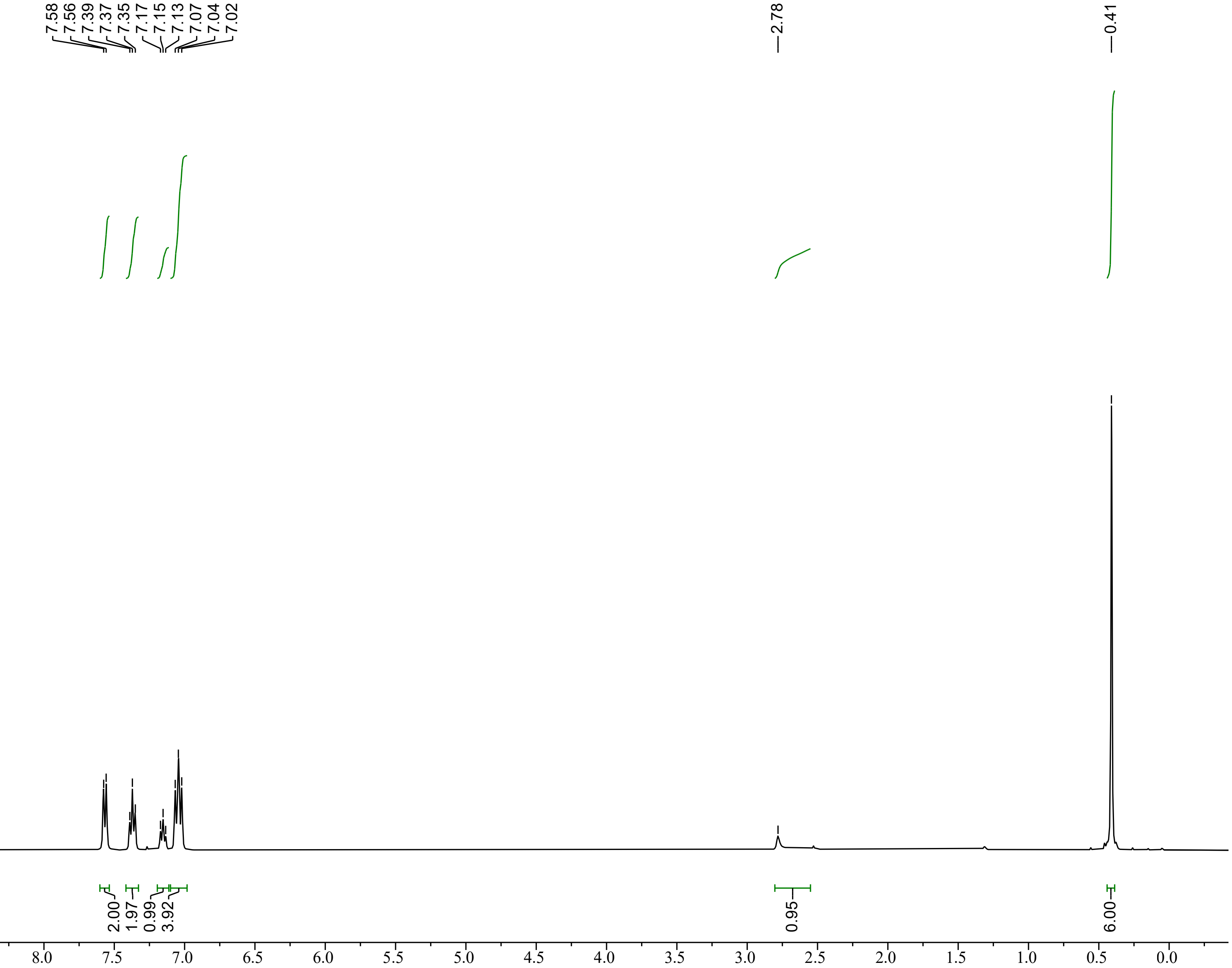

Compound **2k** ^{13}C NMR

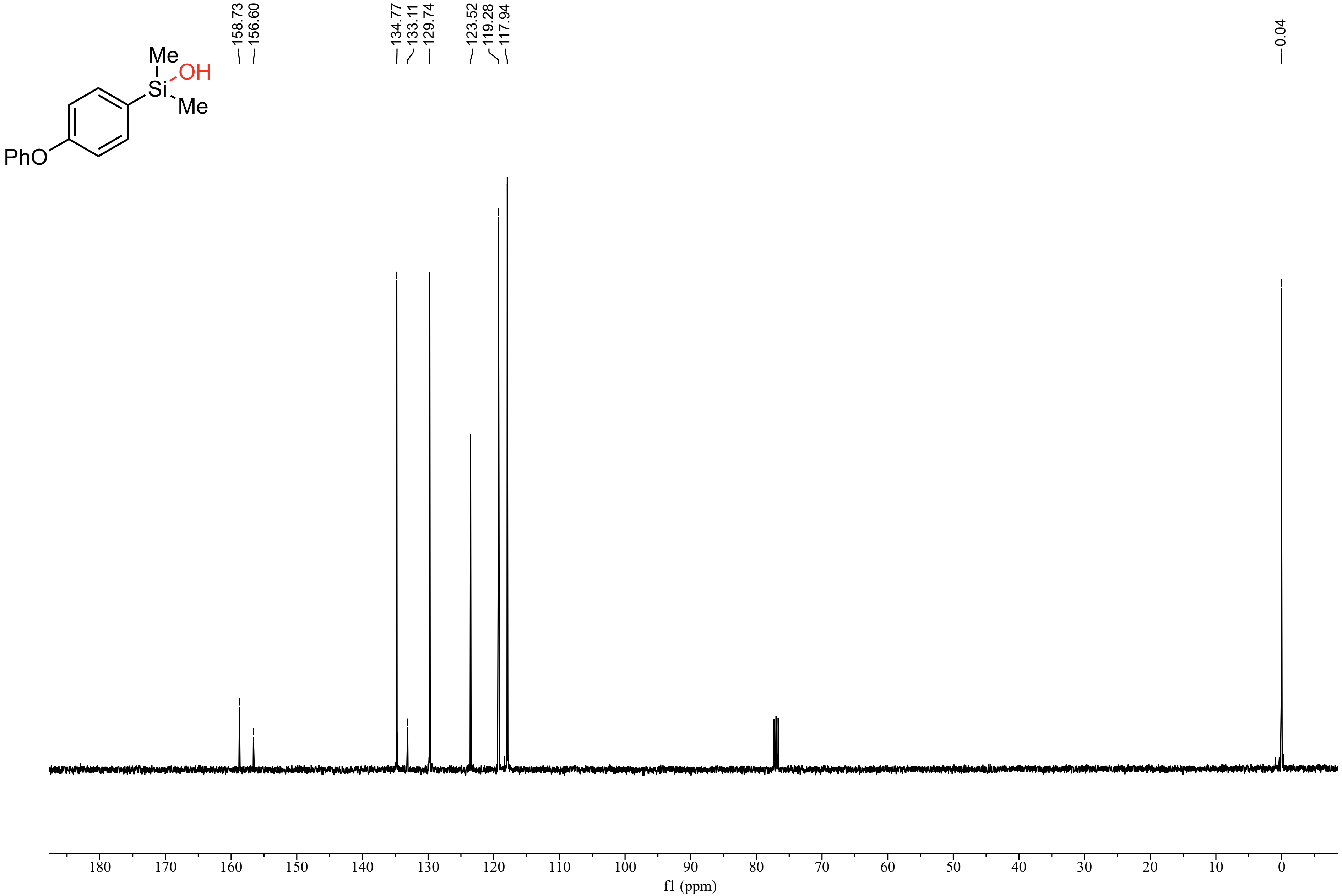

Compound **2l** ^{1}H NMR

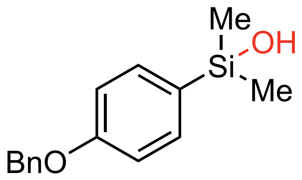

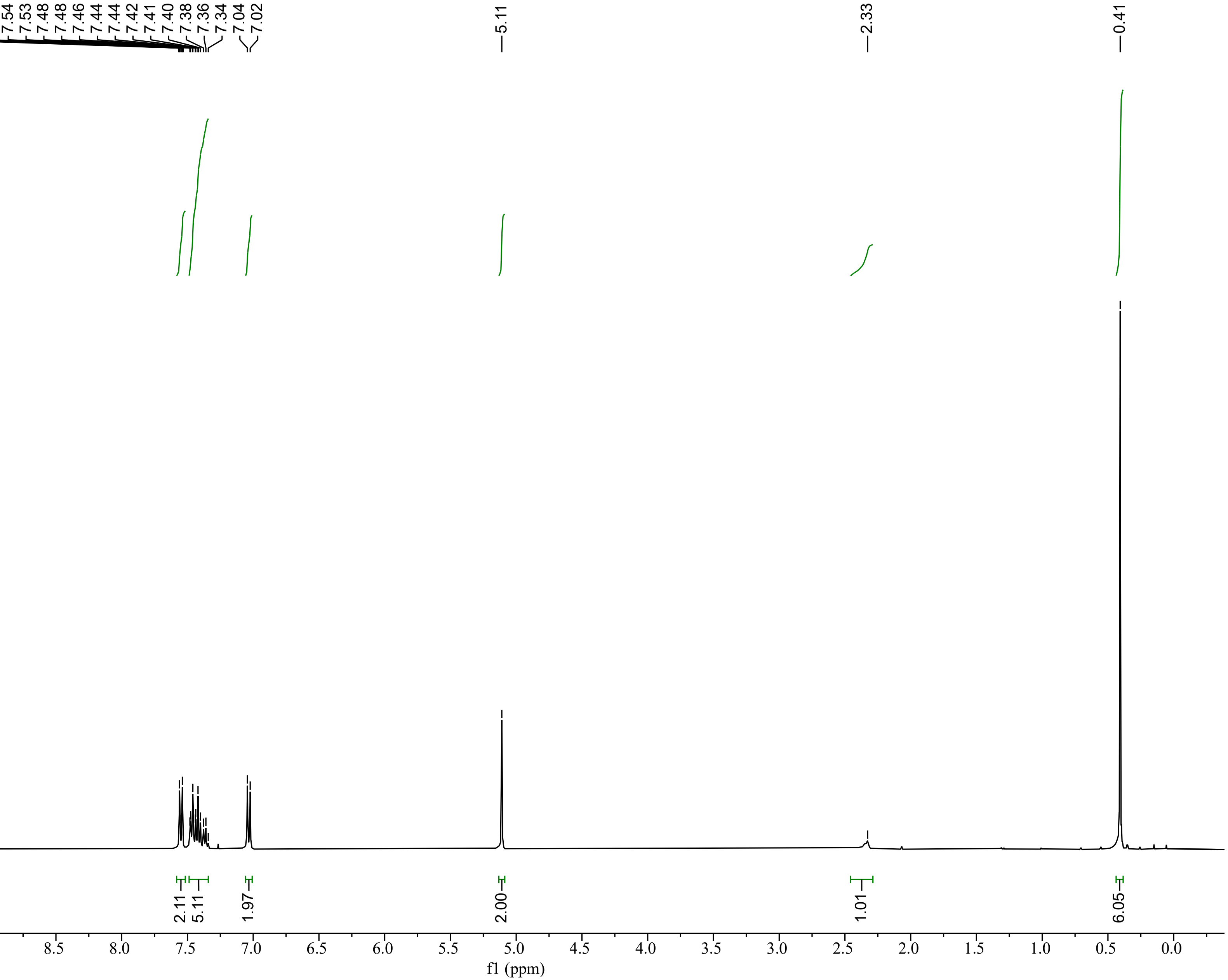

Compound **2l** ^{13}C NMR

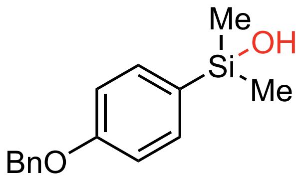

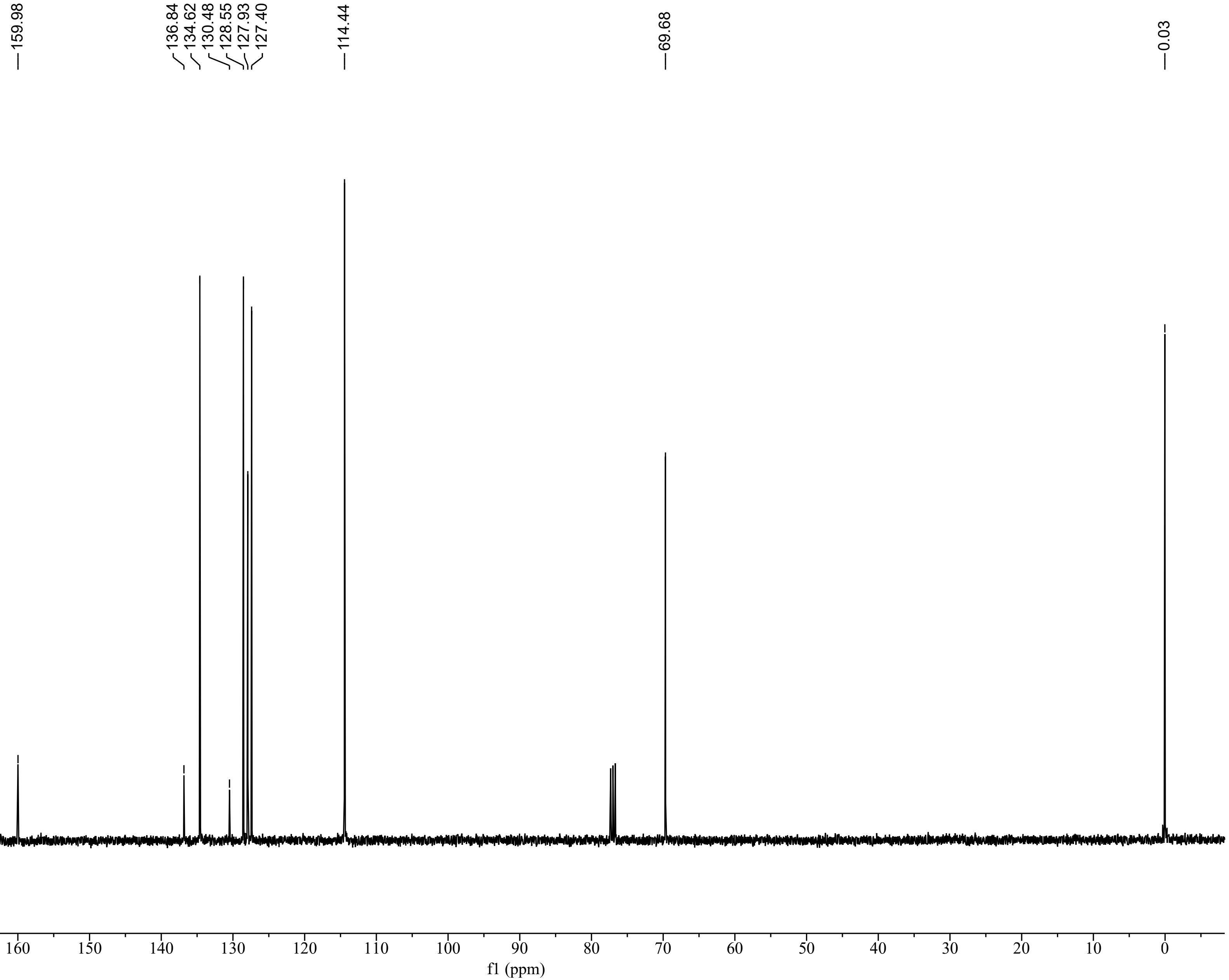

Compound **2m** ^{1}H NMR

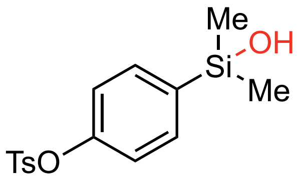

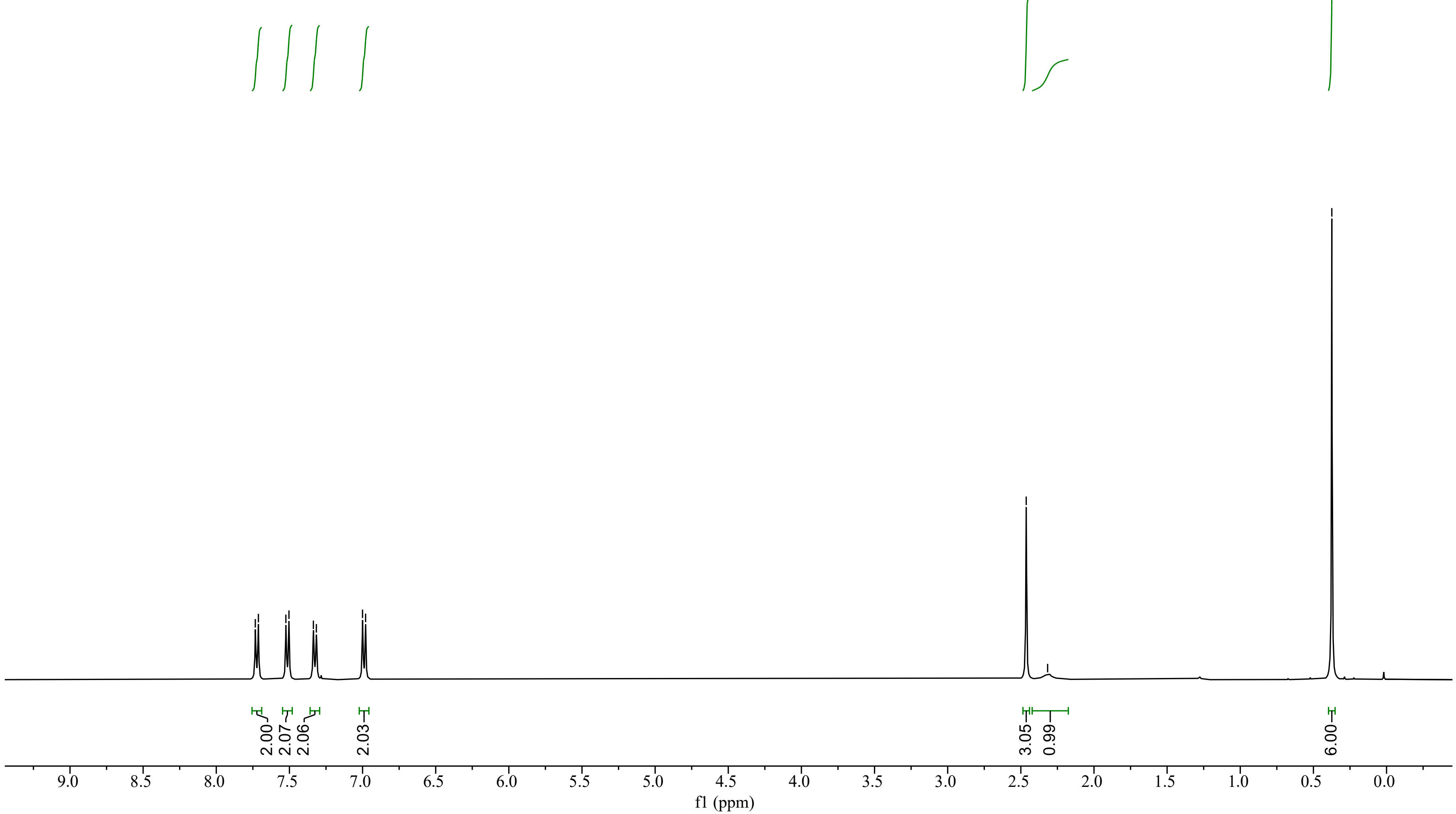

Compound **2m** ^{13}C NMR

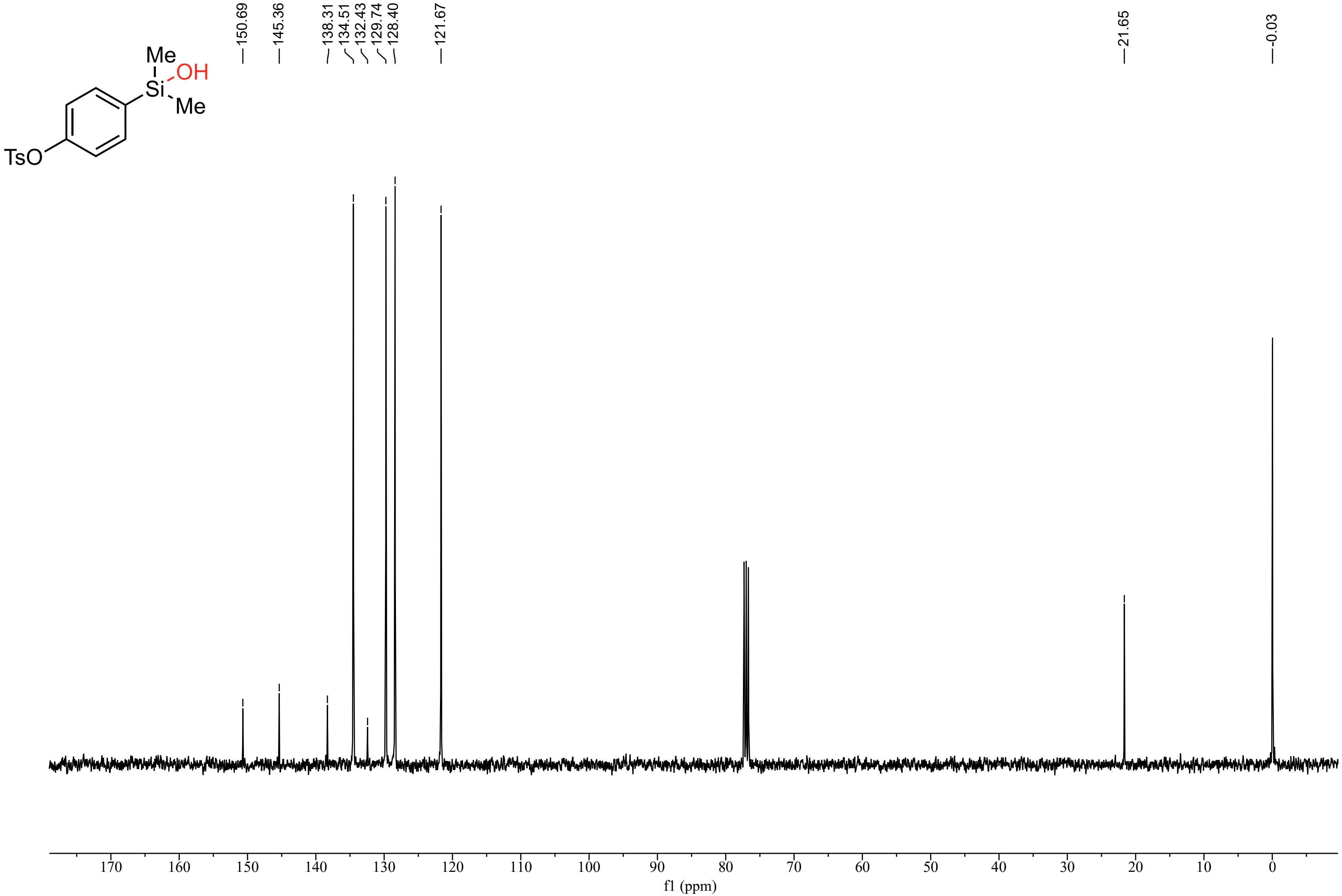

Compound **2n** ^{1}H NMR

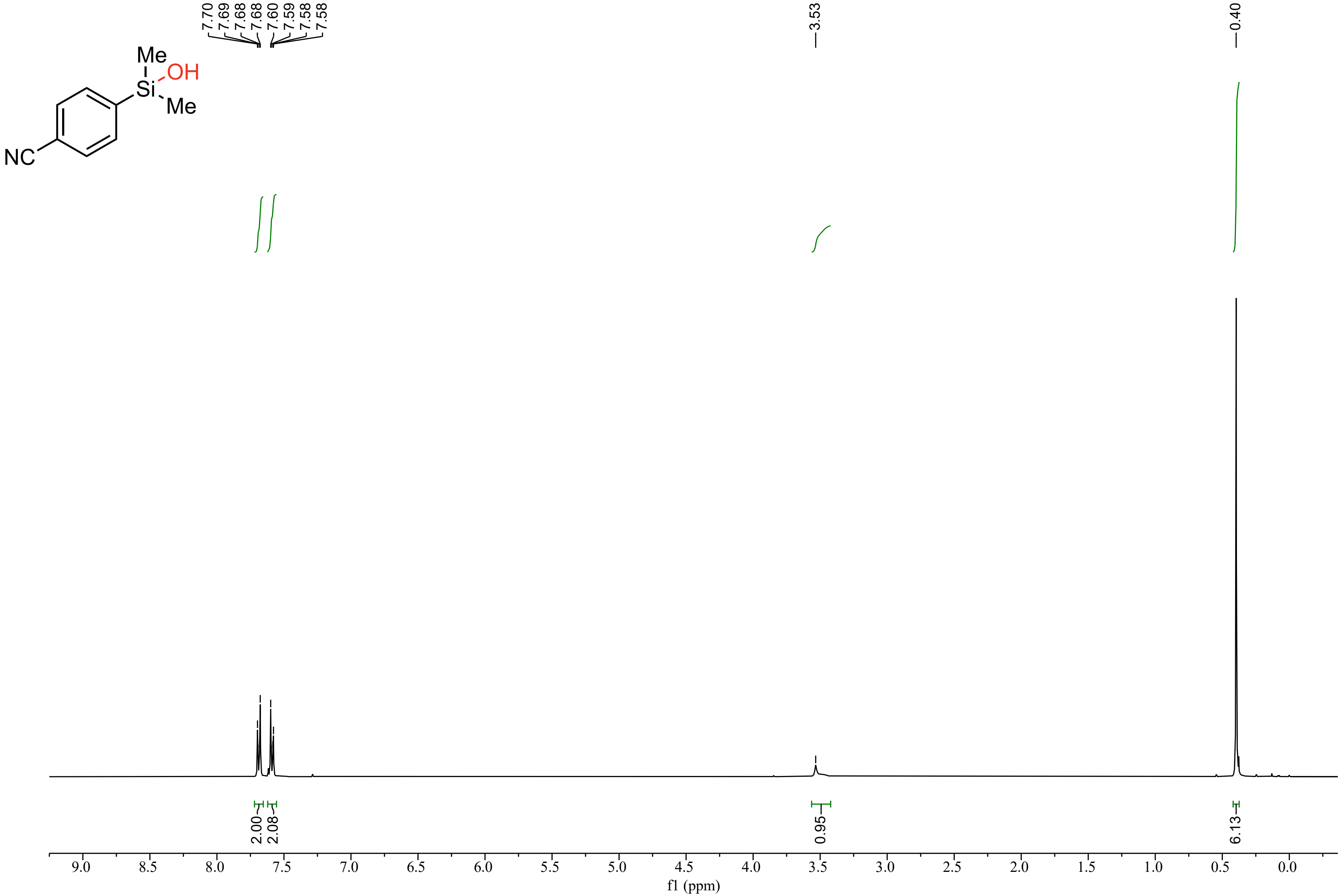

Compound **2n** ^{13}C NMR

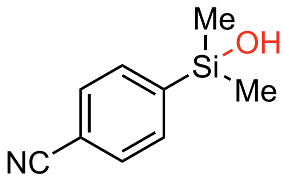

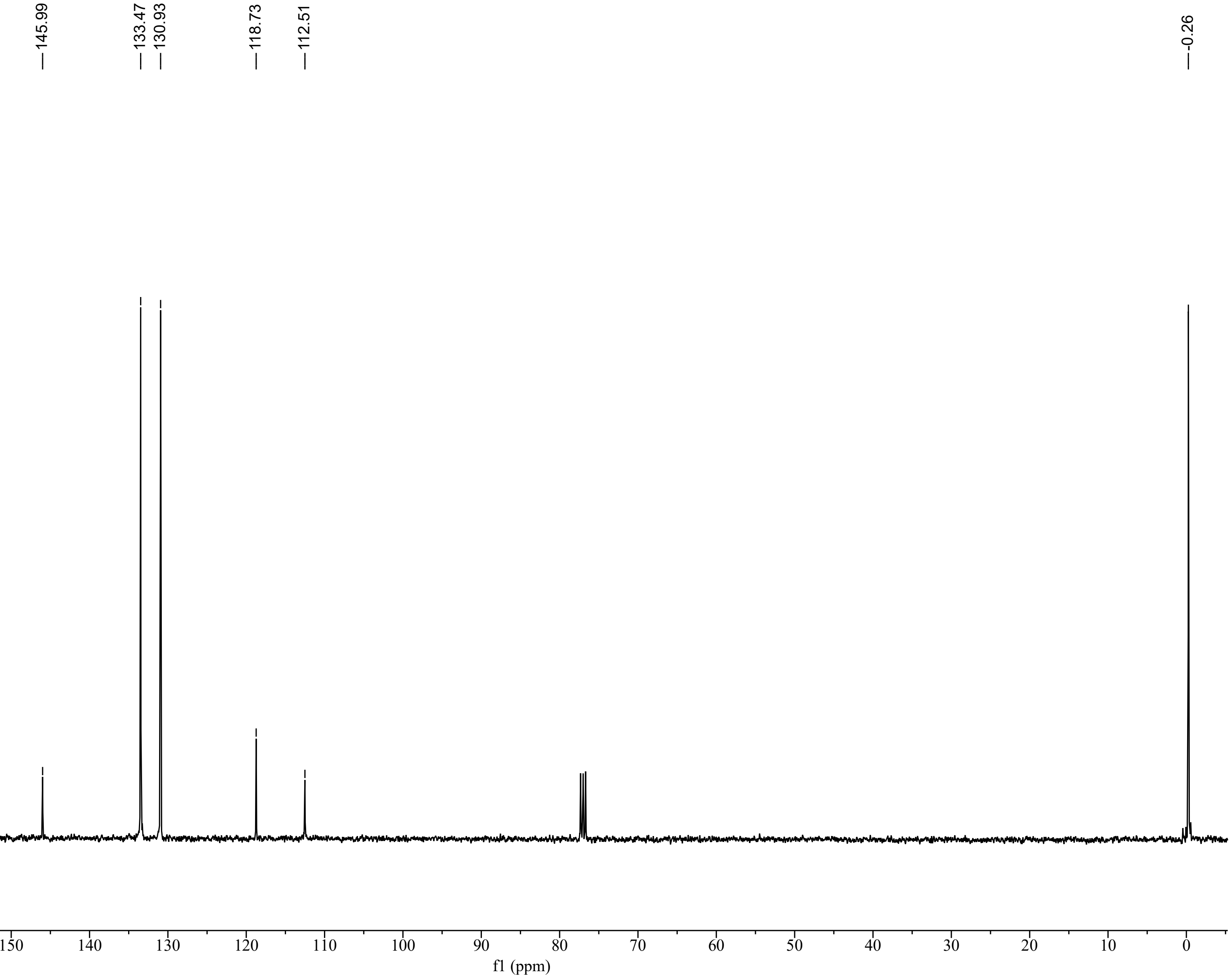

Compound **2o** ^{1}H NMR

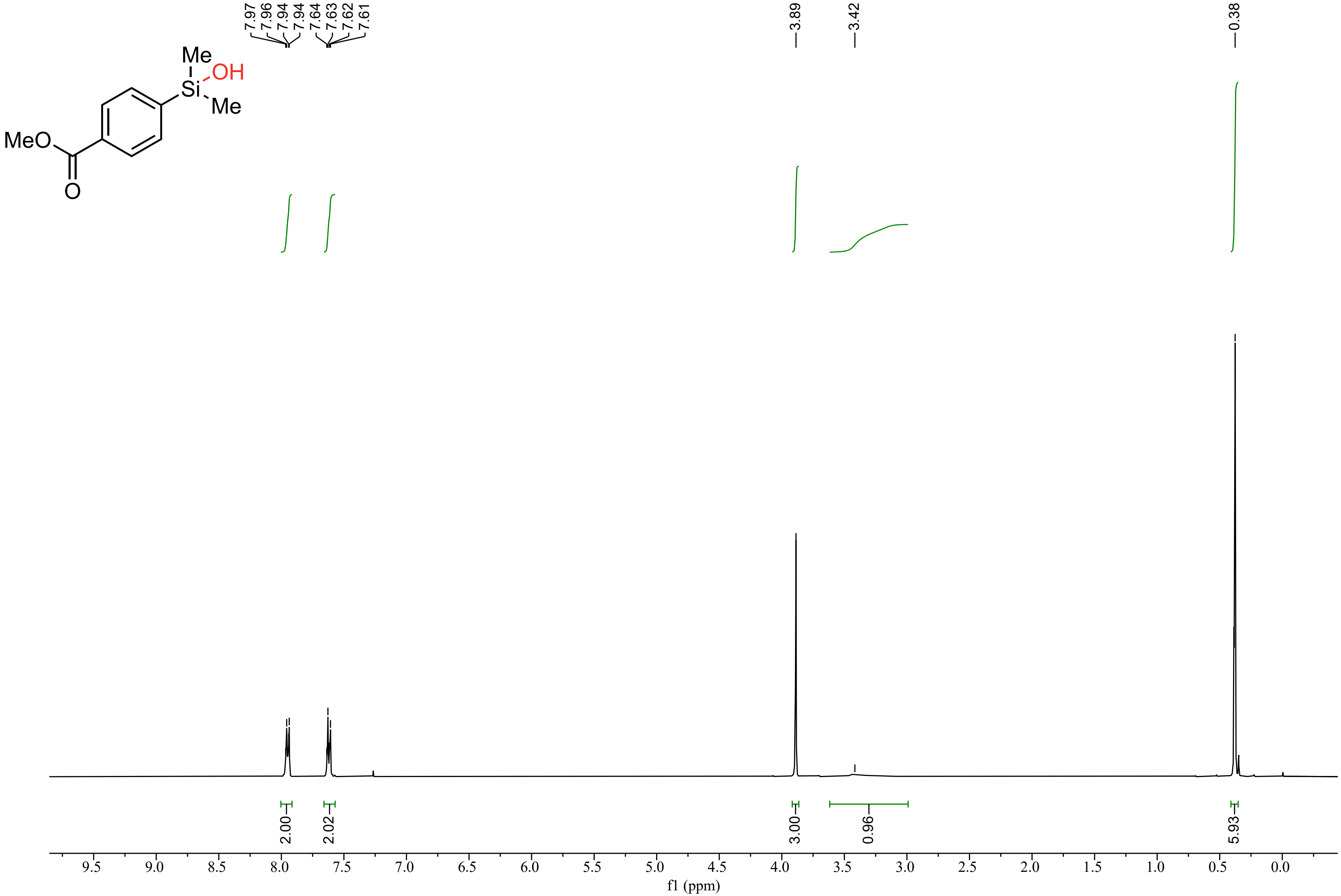

Compound **2o** ^{13}C NMR

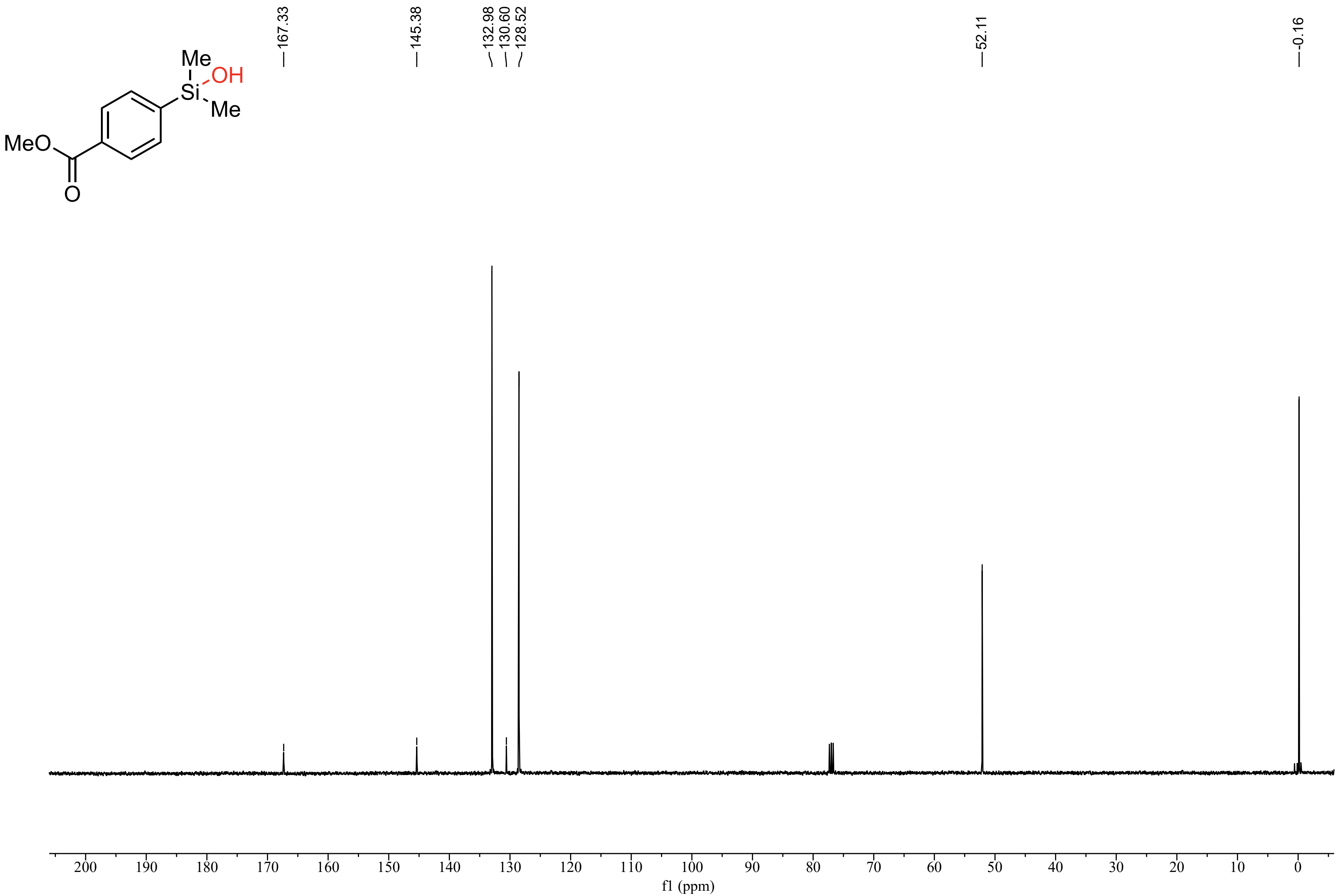

Compound **2p** ^{1}H NMR

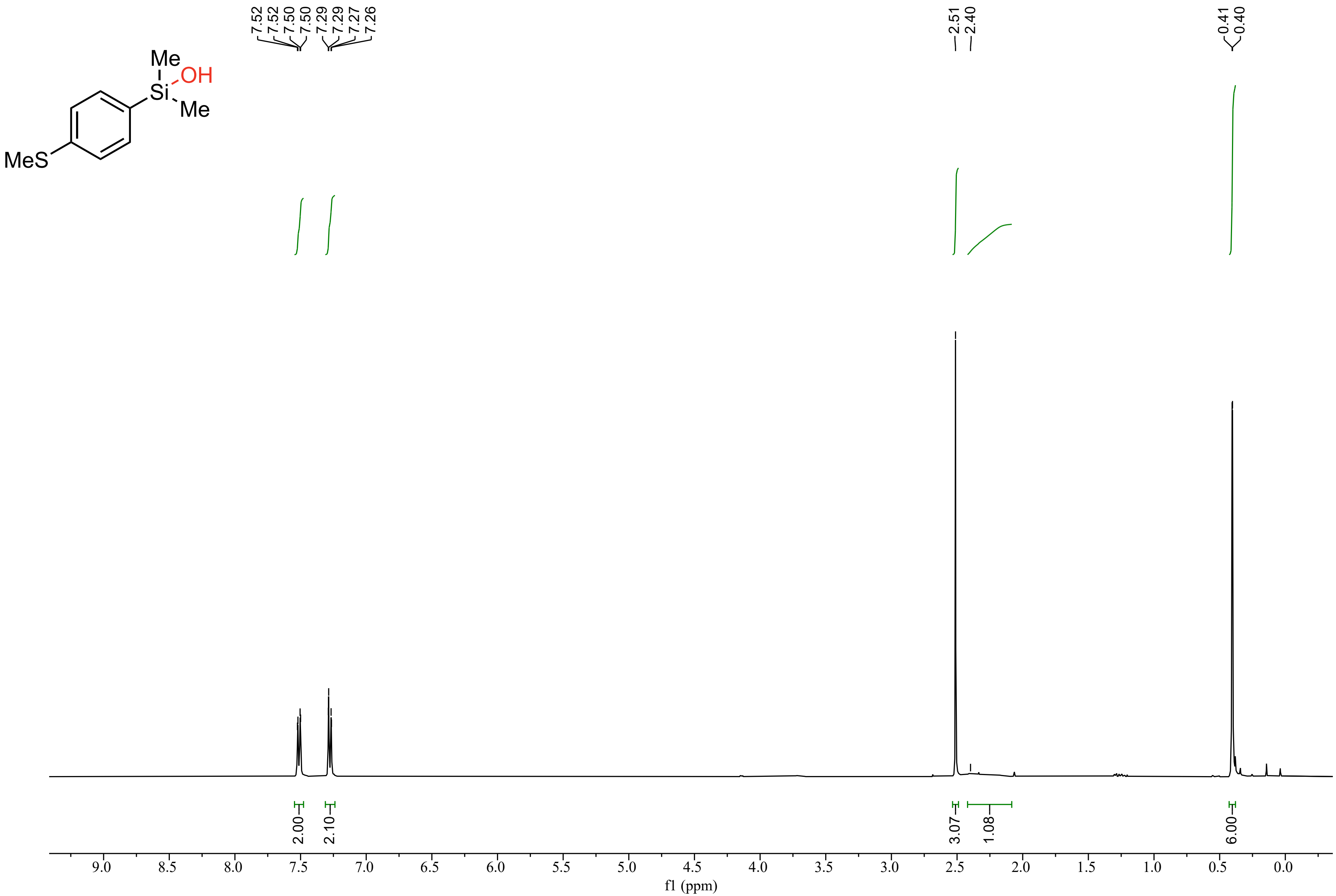

Compound **2p** ^{13}C NMR

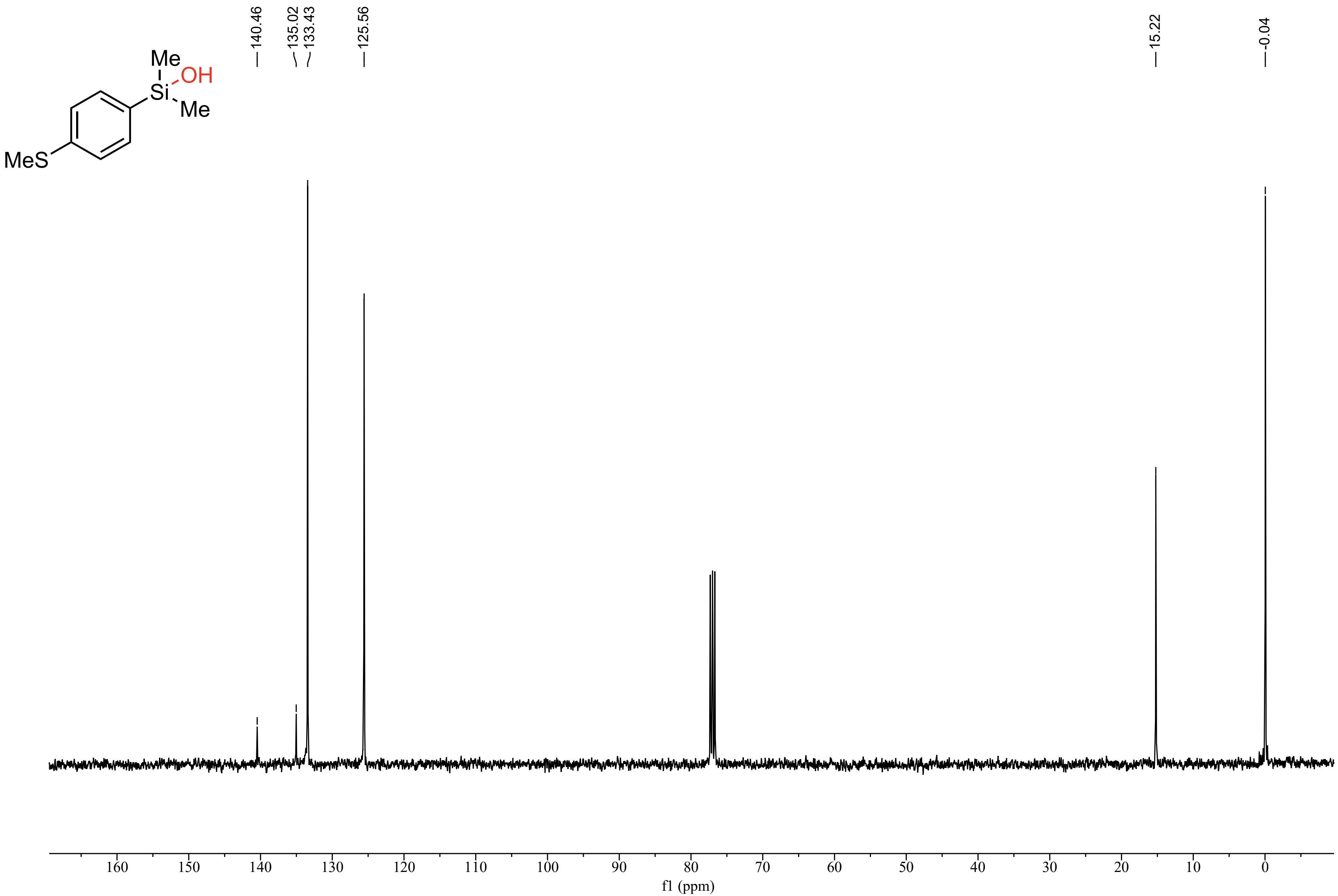

Compound **2q** ^{1}H NMR

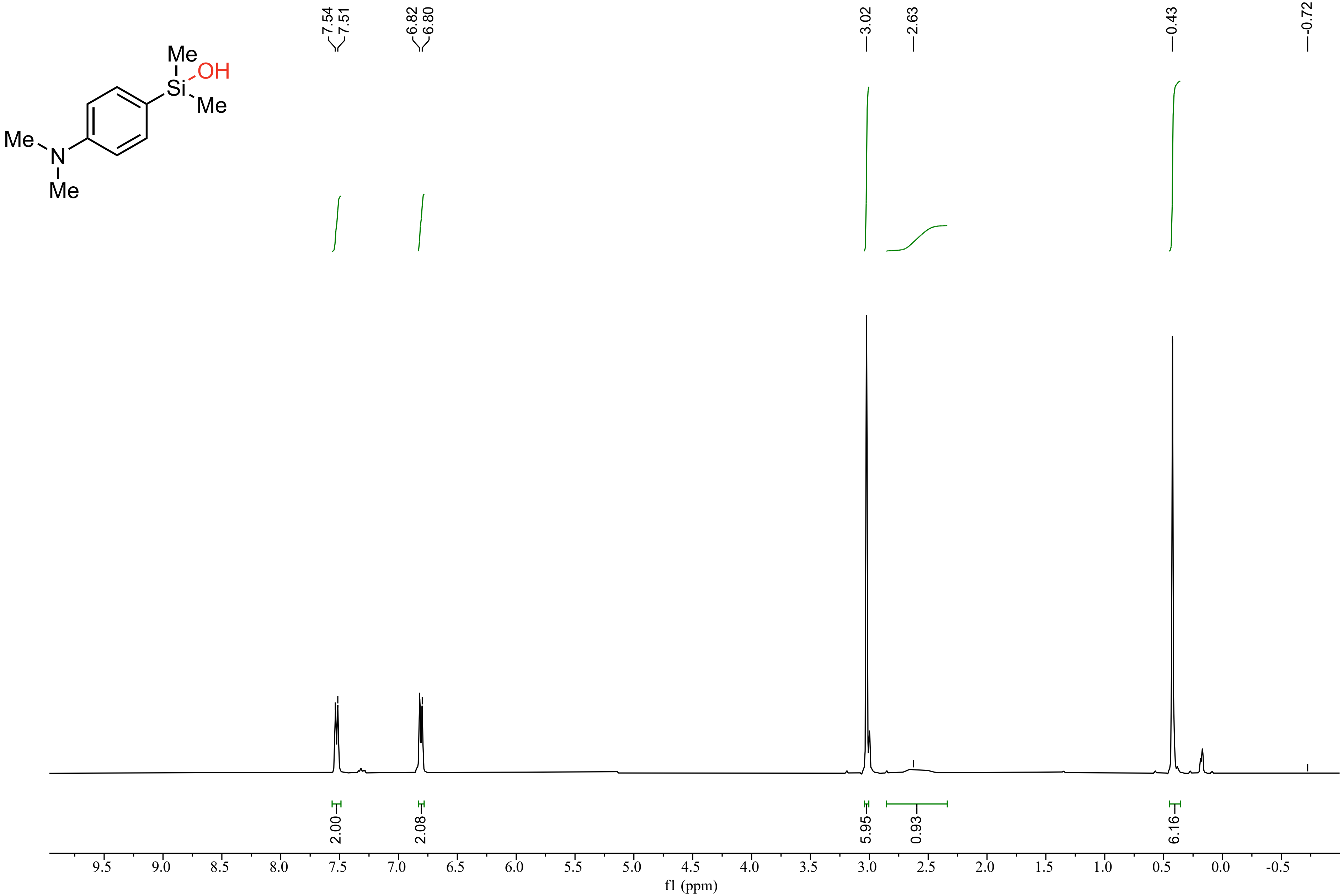

Compound **2q** ^{13}C NMR

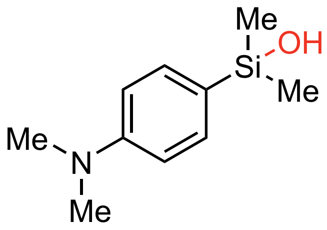

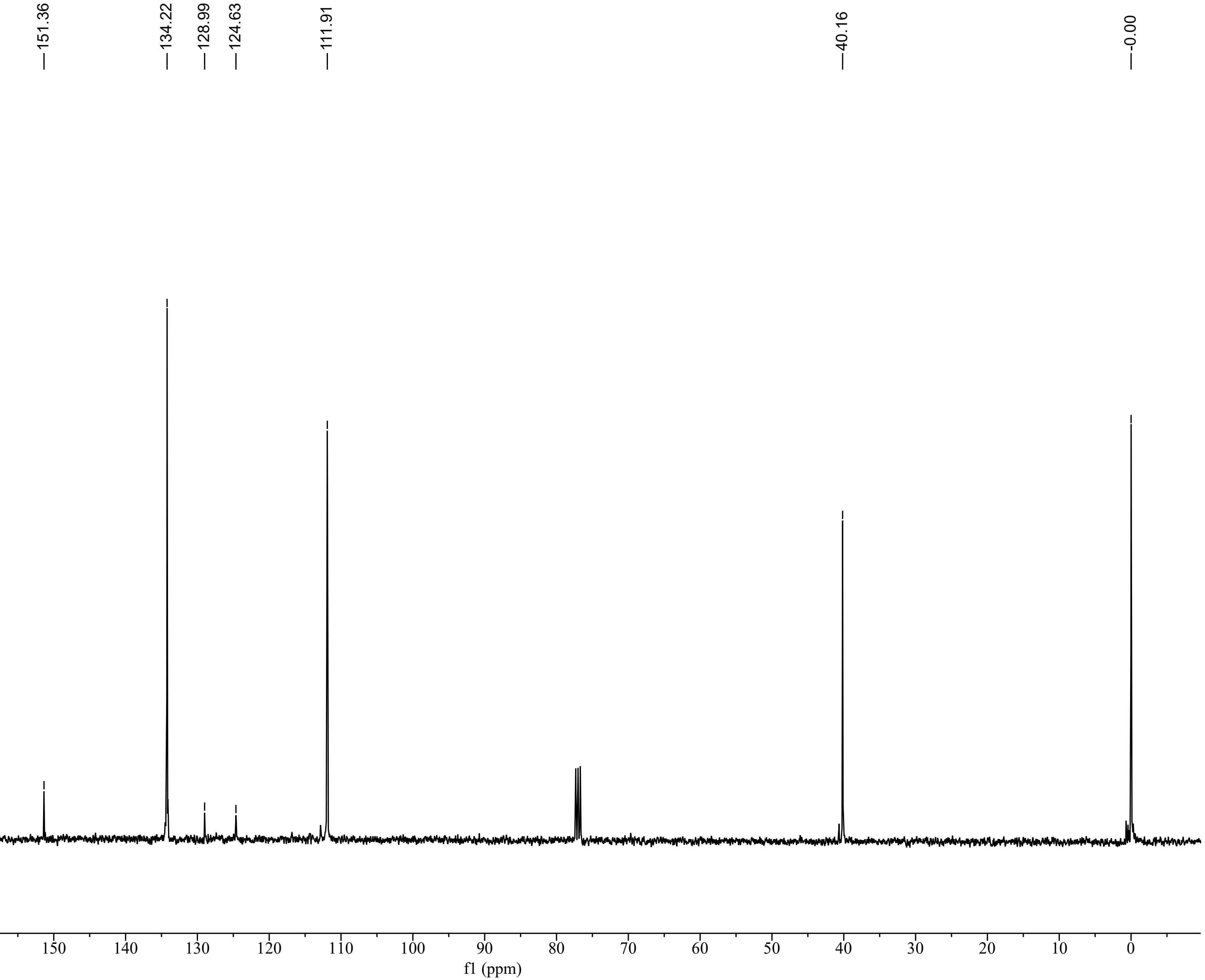

Compound **2r** ¹H NMR

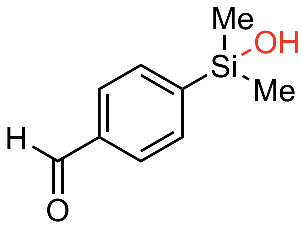

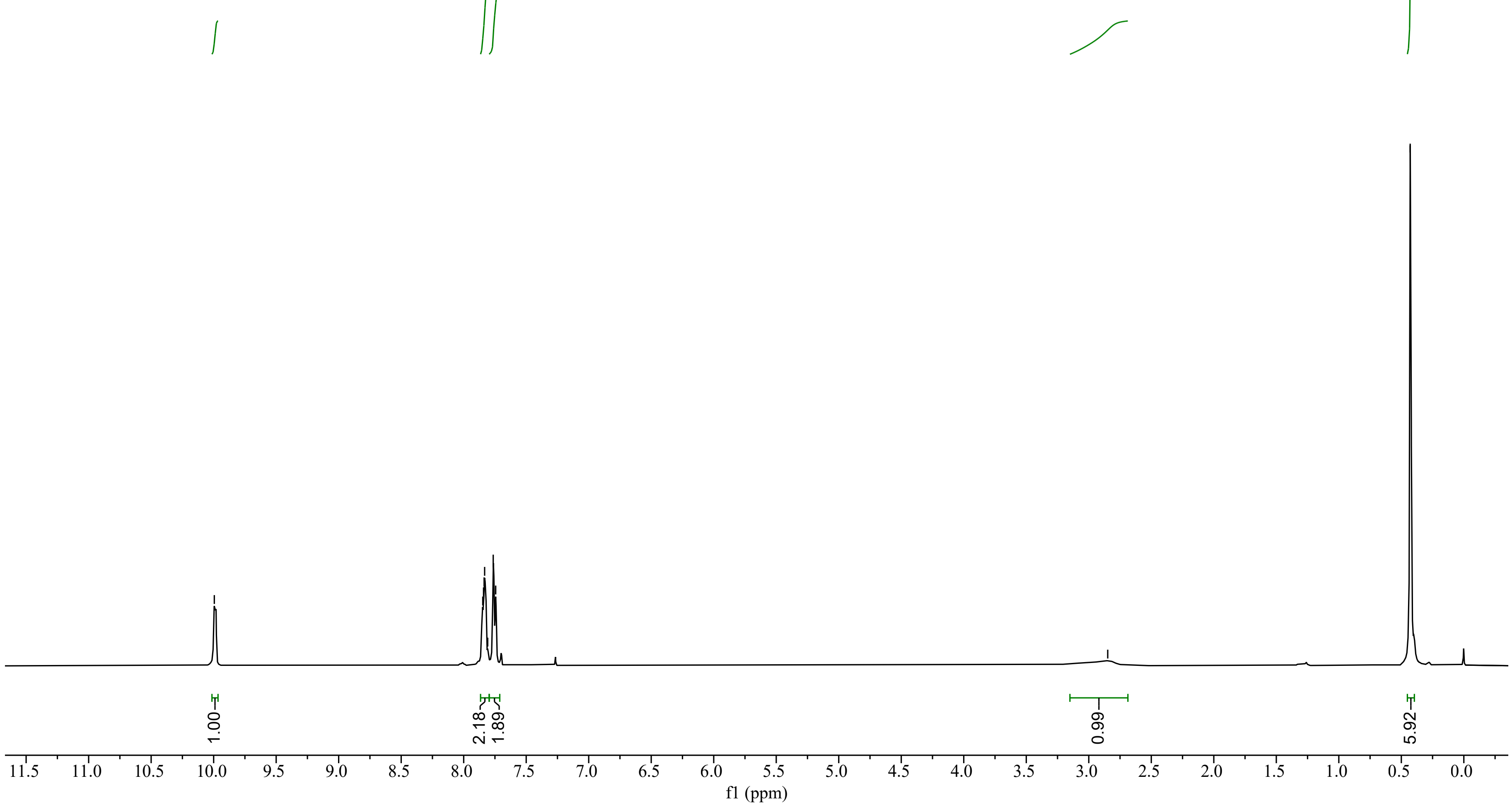

Compound **2r** ^{13}C NMR

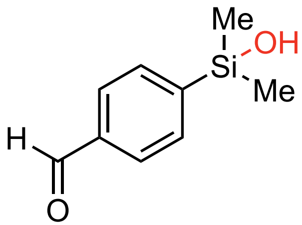

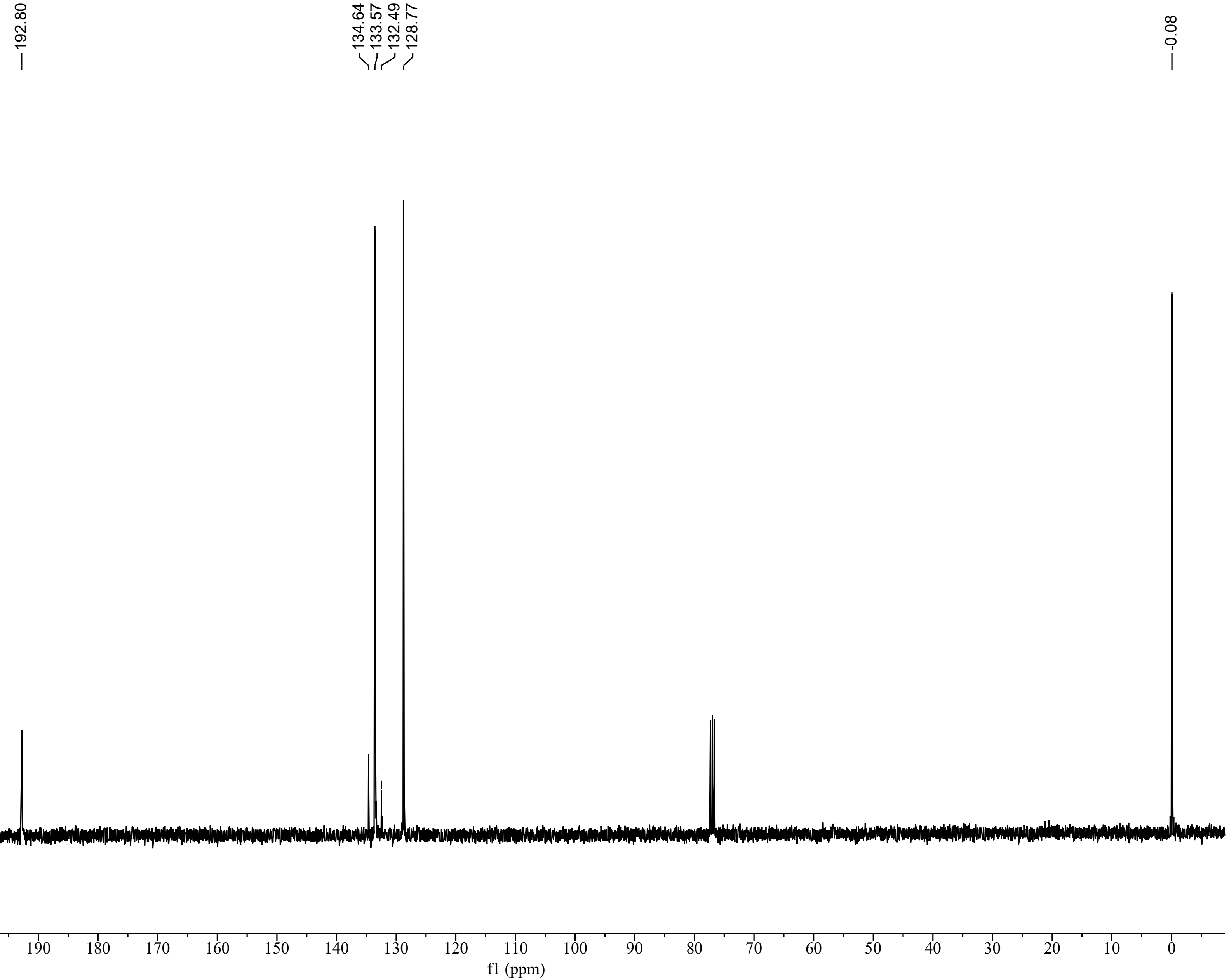

Compound **2s** [1]H NMR

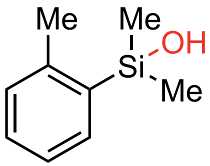

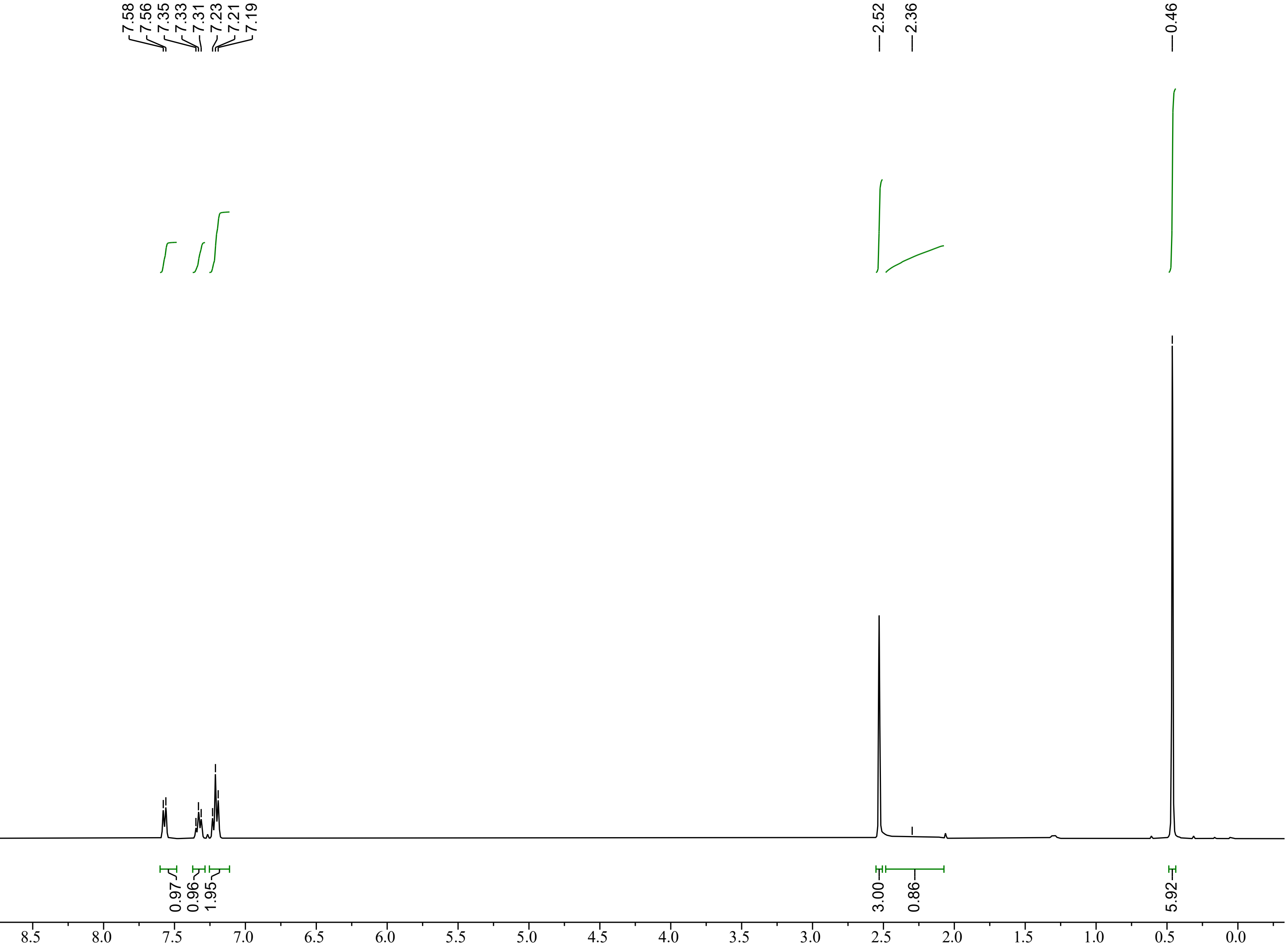

Compound **2s** ^{13}C NMR

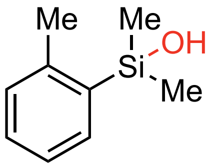

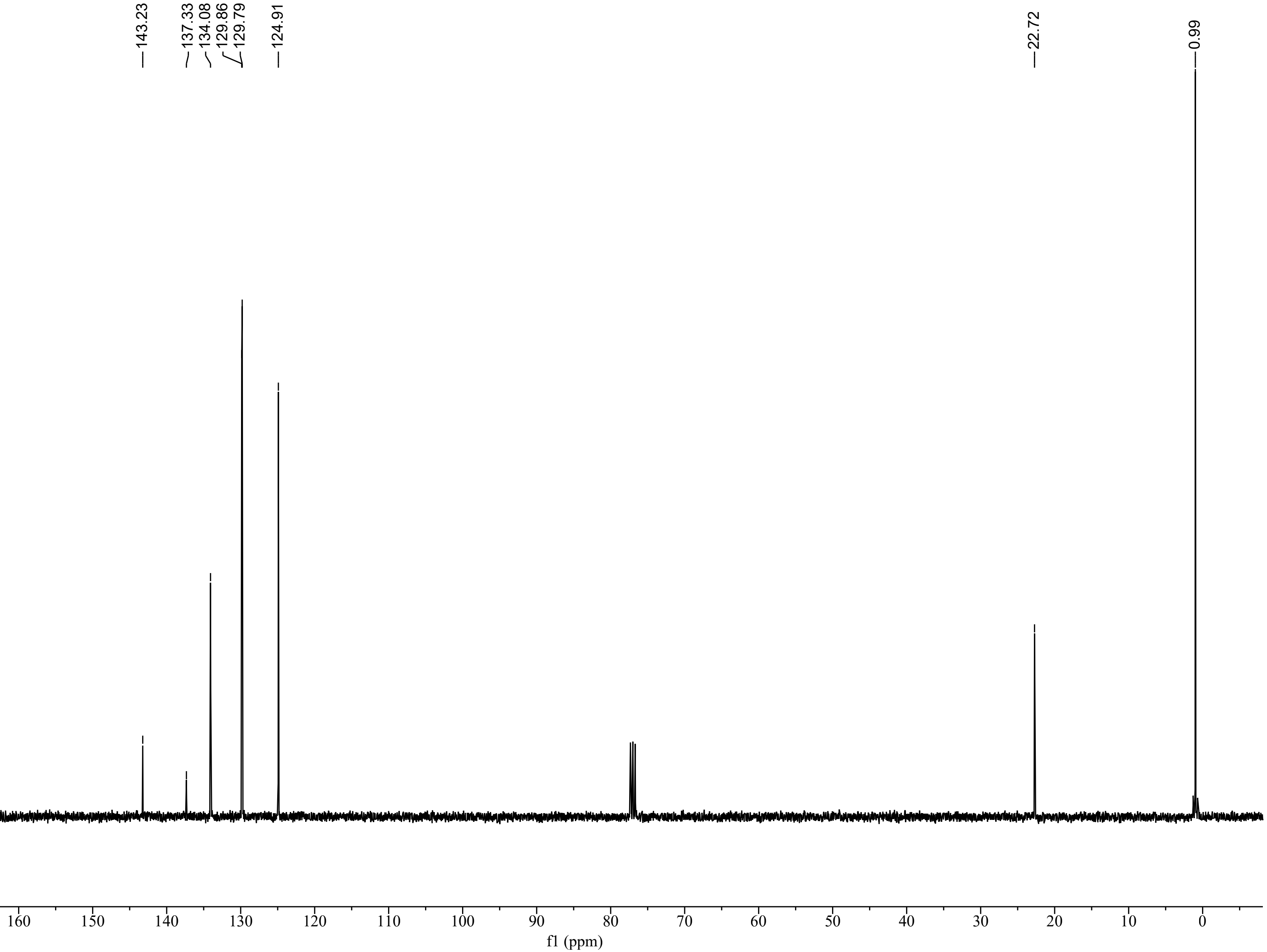

Compound **2t** ^{1}H NMR

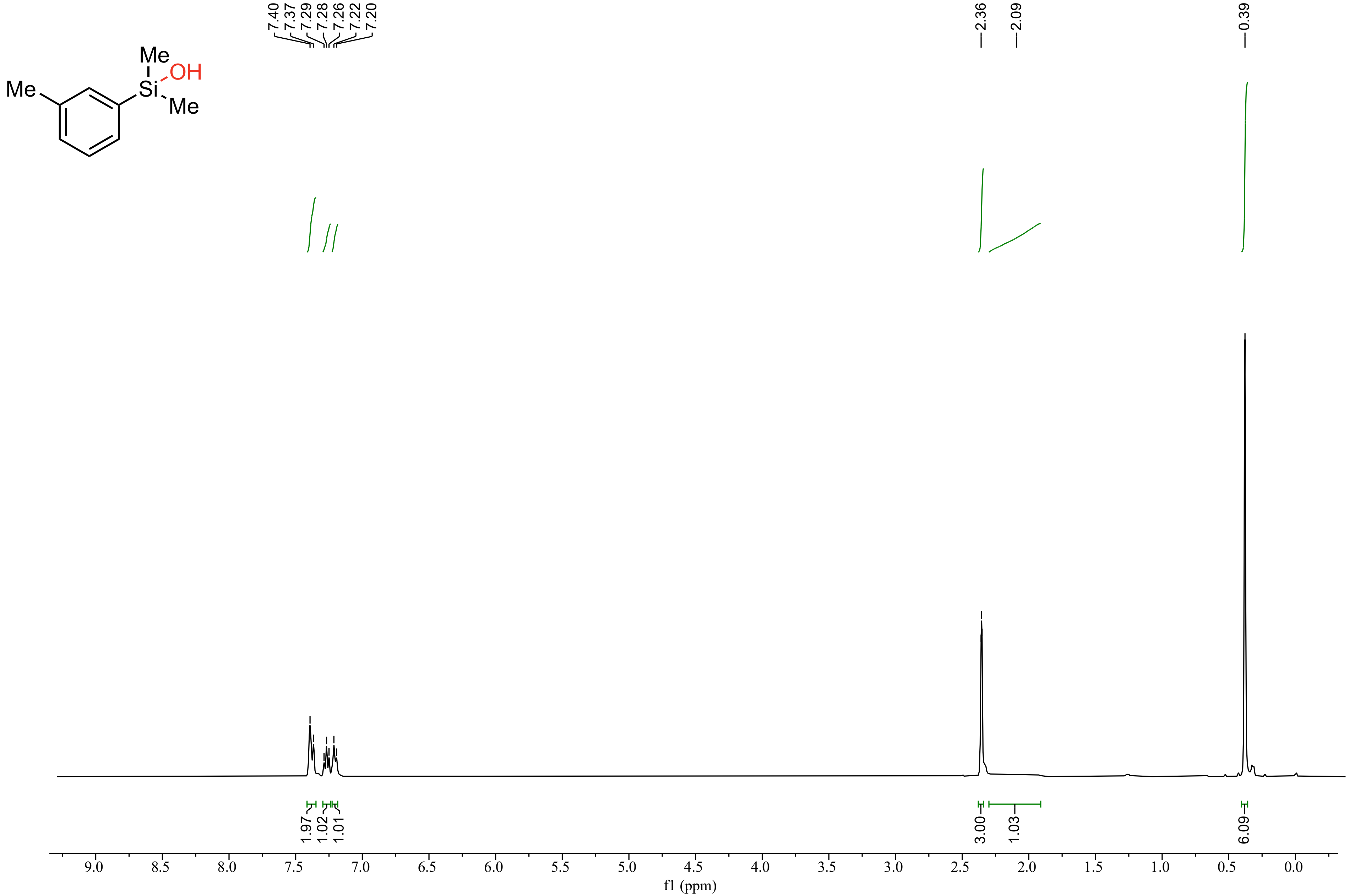

Compound **2t** ^{13}C NMR

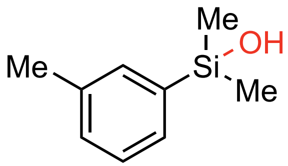

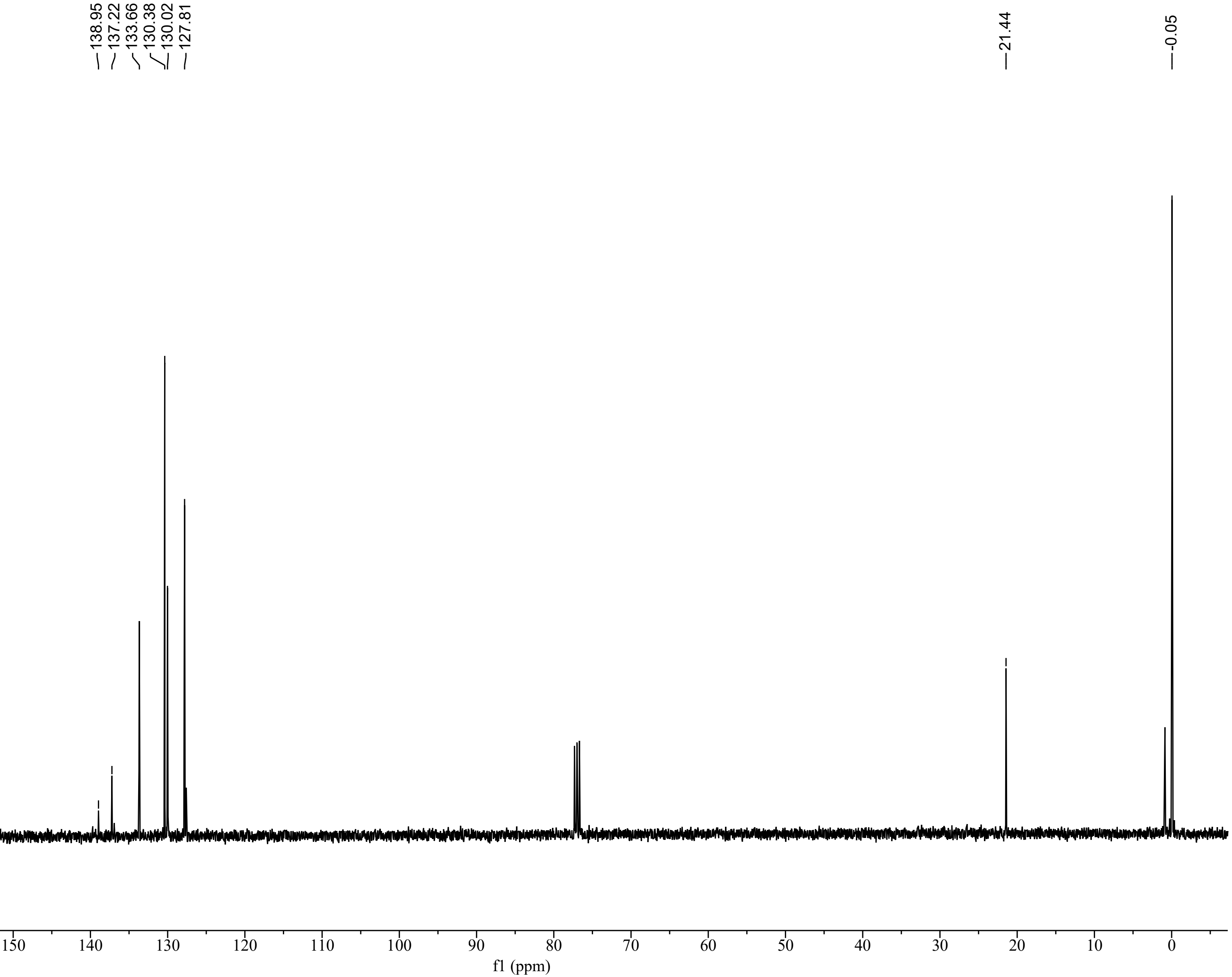

Compound **2u** ^{1}H NMR

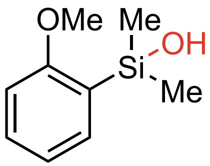

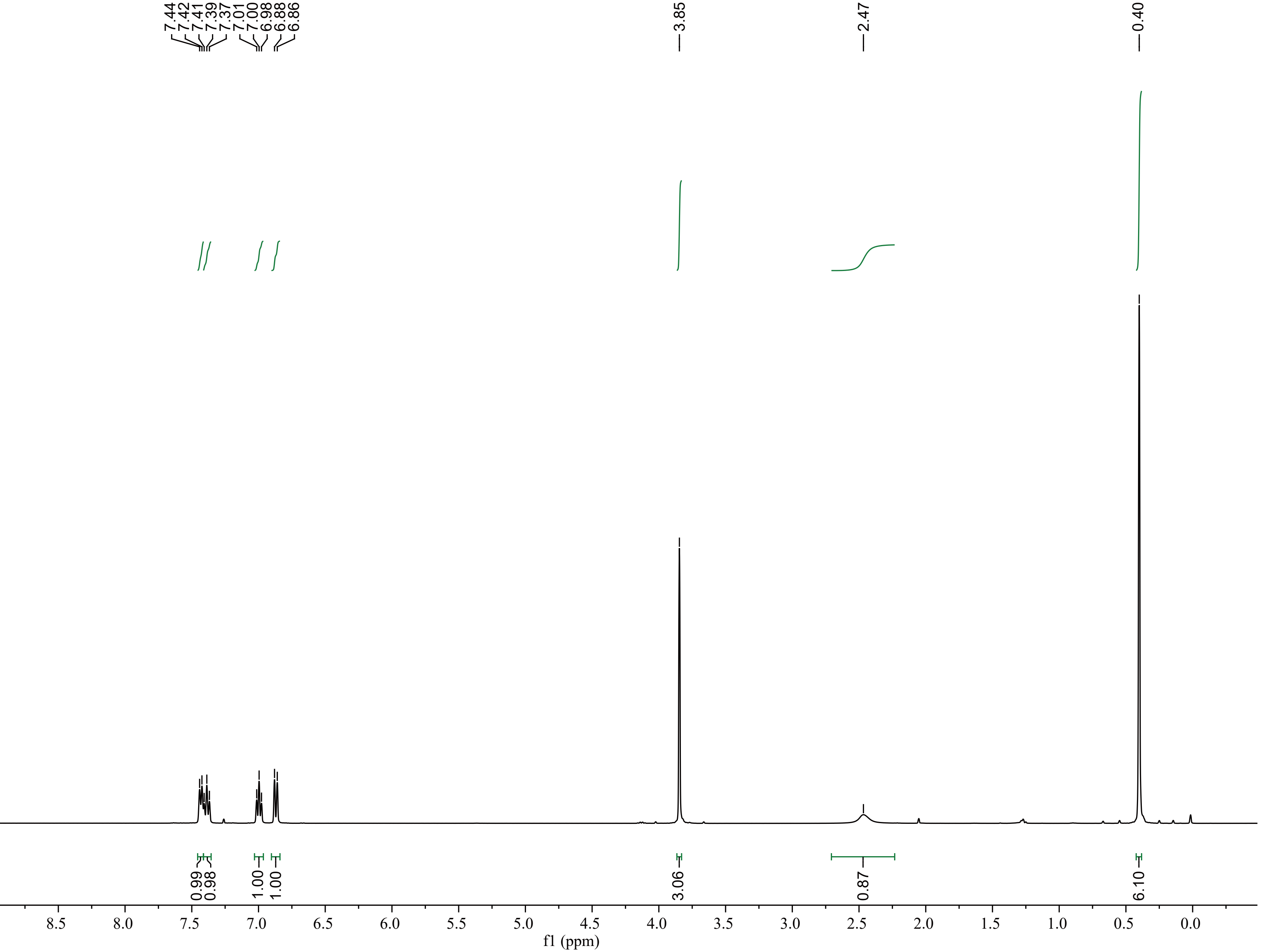

Compound **2u** ^{13}C NMR

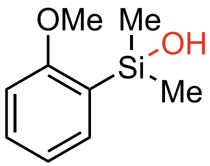

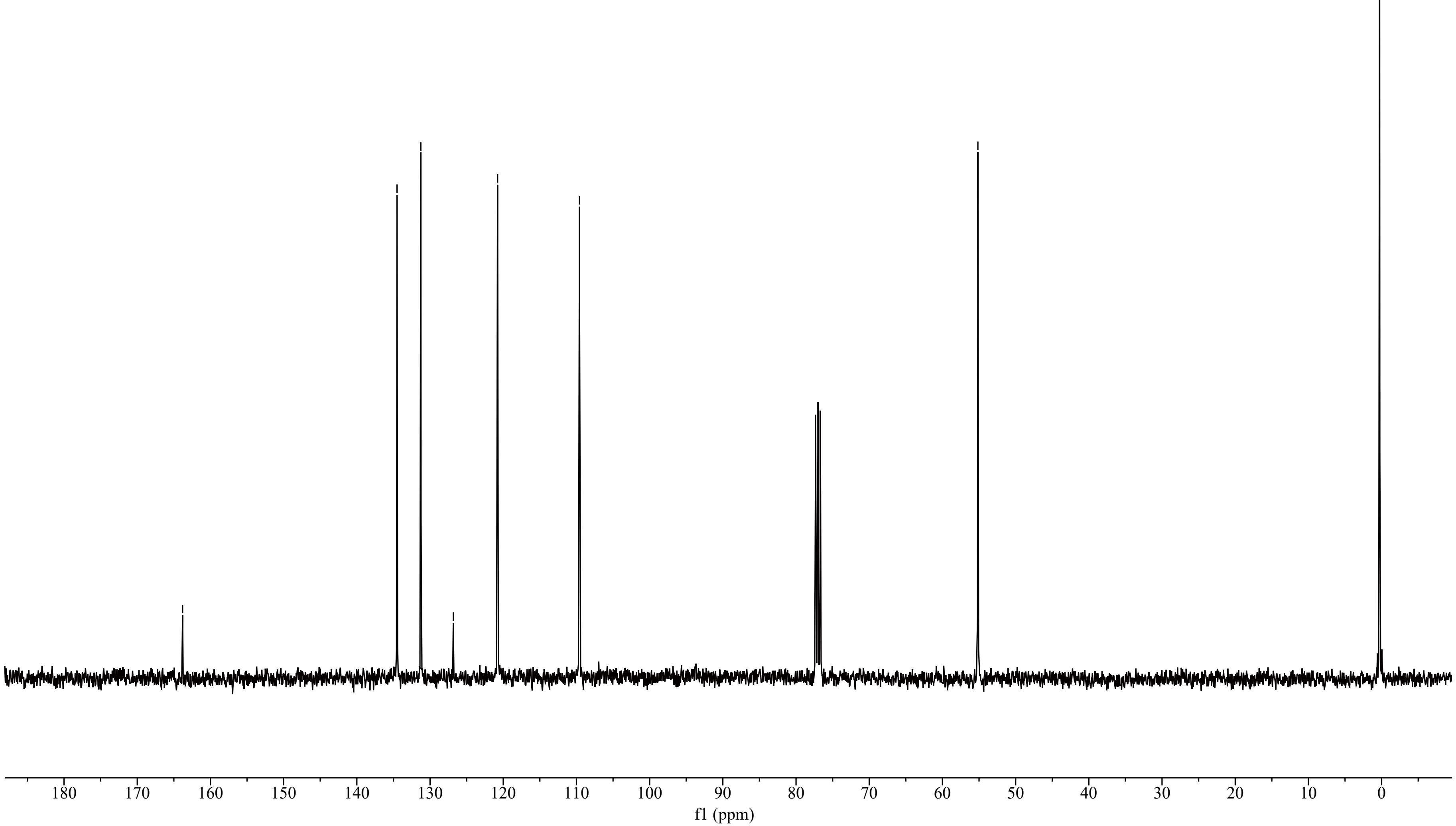

Compound **2v** ^{1}H NMR

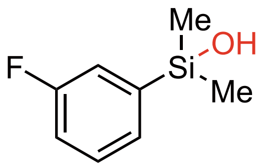

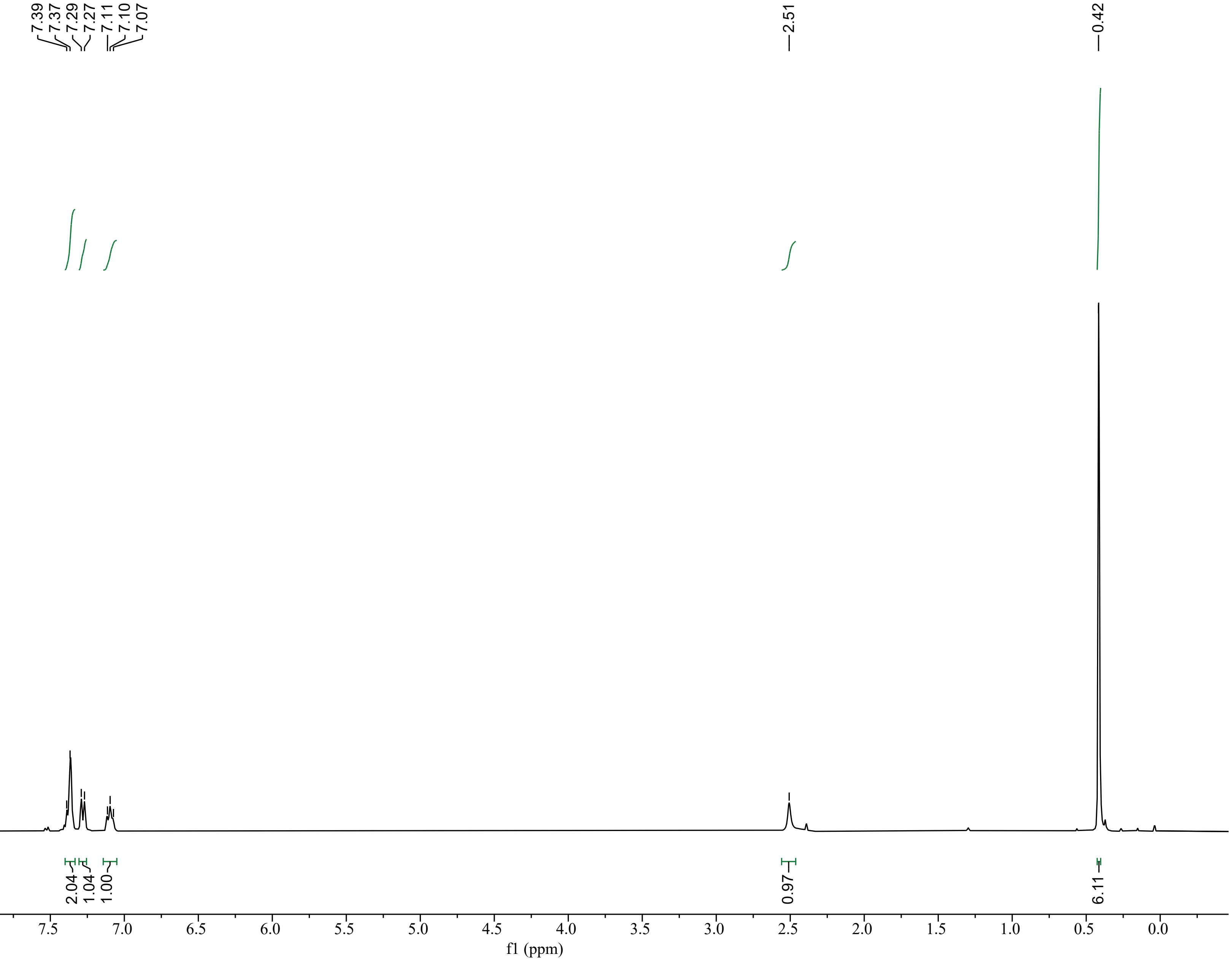

Compound **2v** ^{13}C NMR

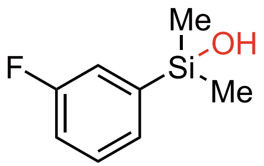

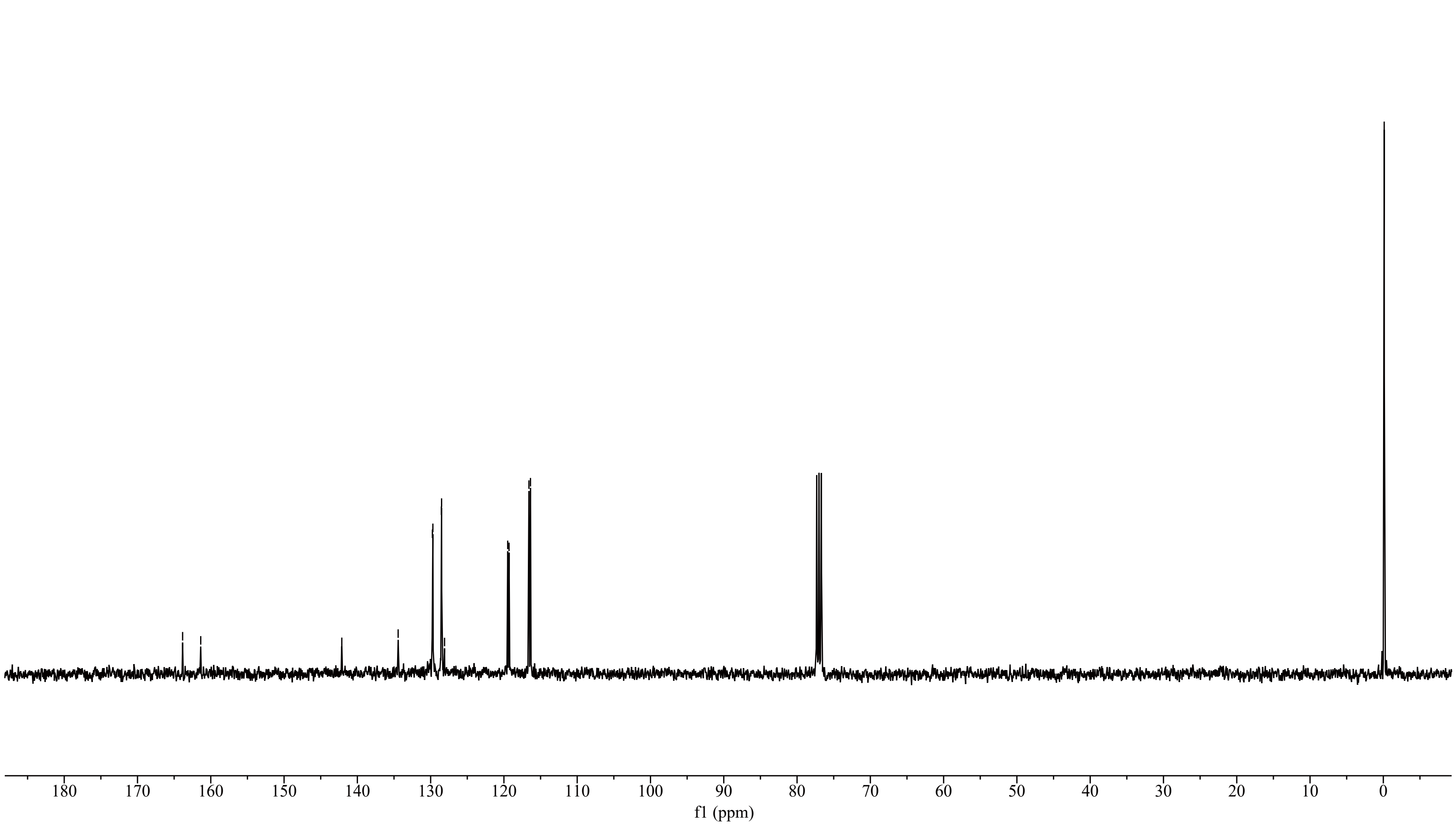

Compound **2v** ^{19}F NMR

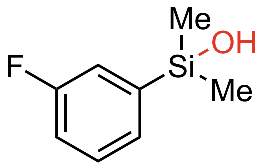

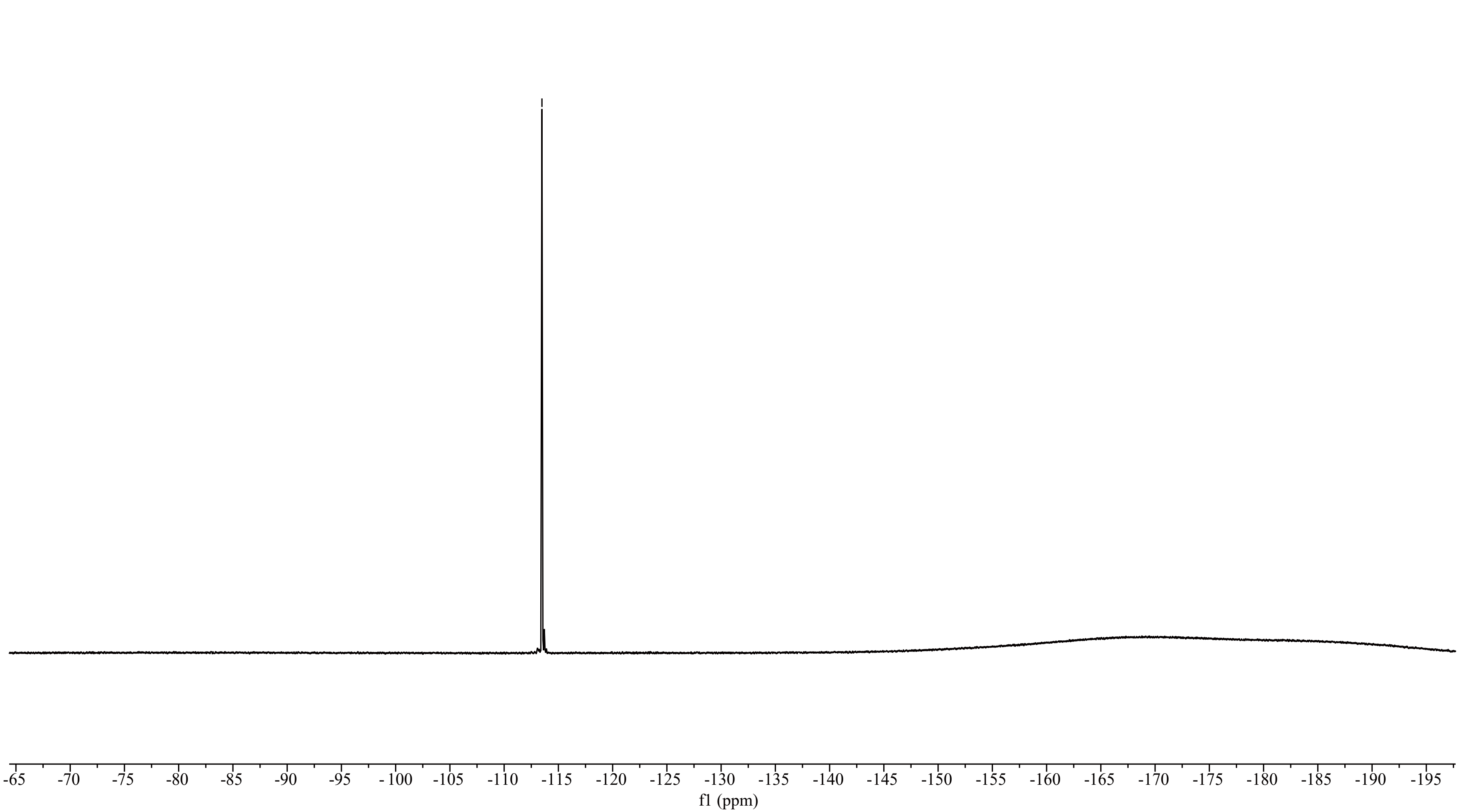

Compound **2w** ^{1}H NMR

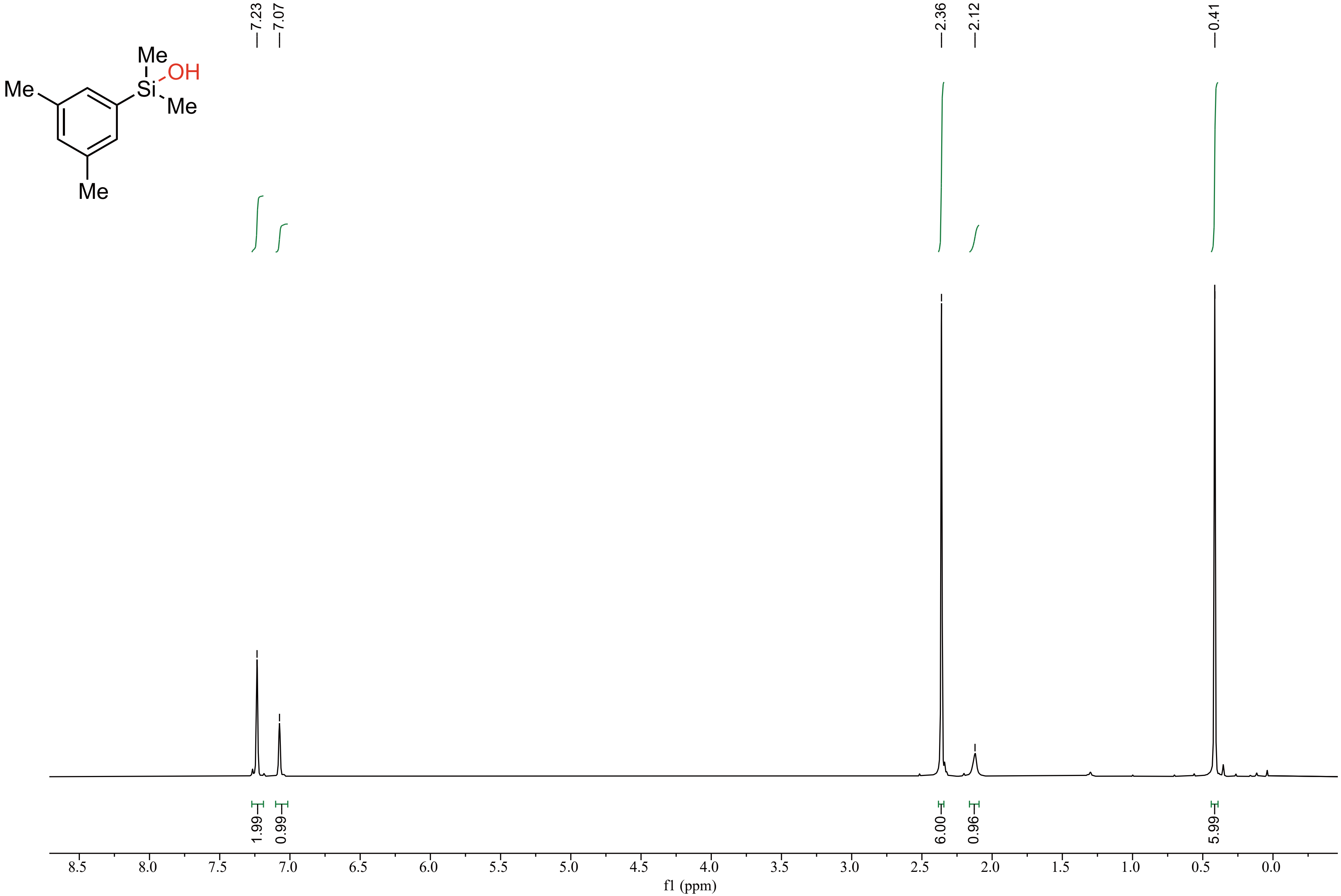

Compound **2w** ^{13}C NMR

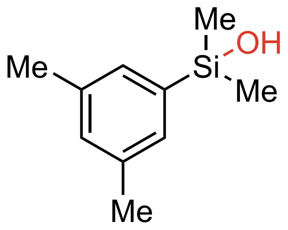

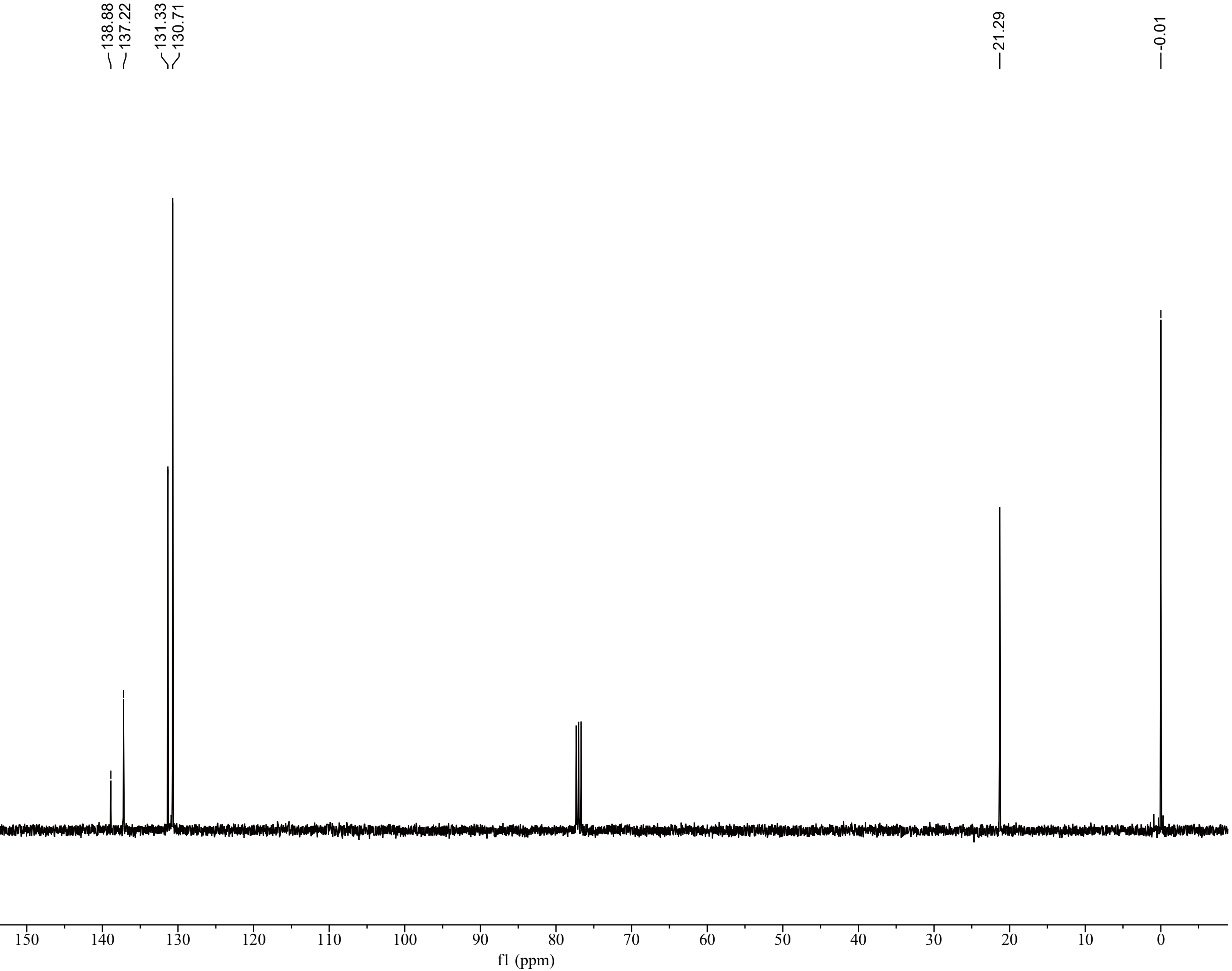

Compound **2x** ^{1}H NMR

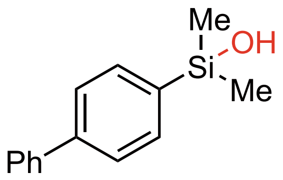

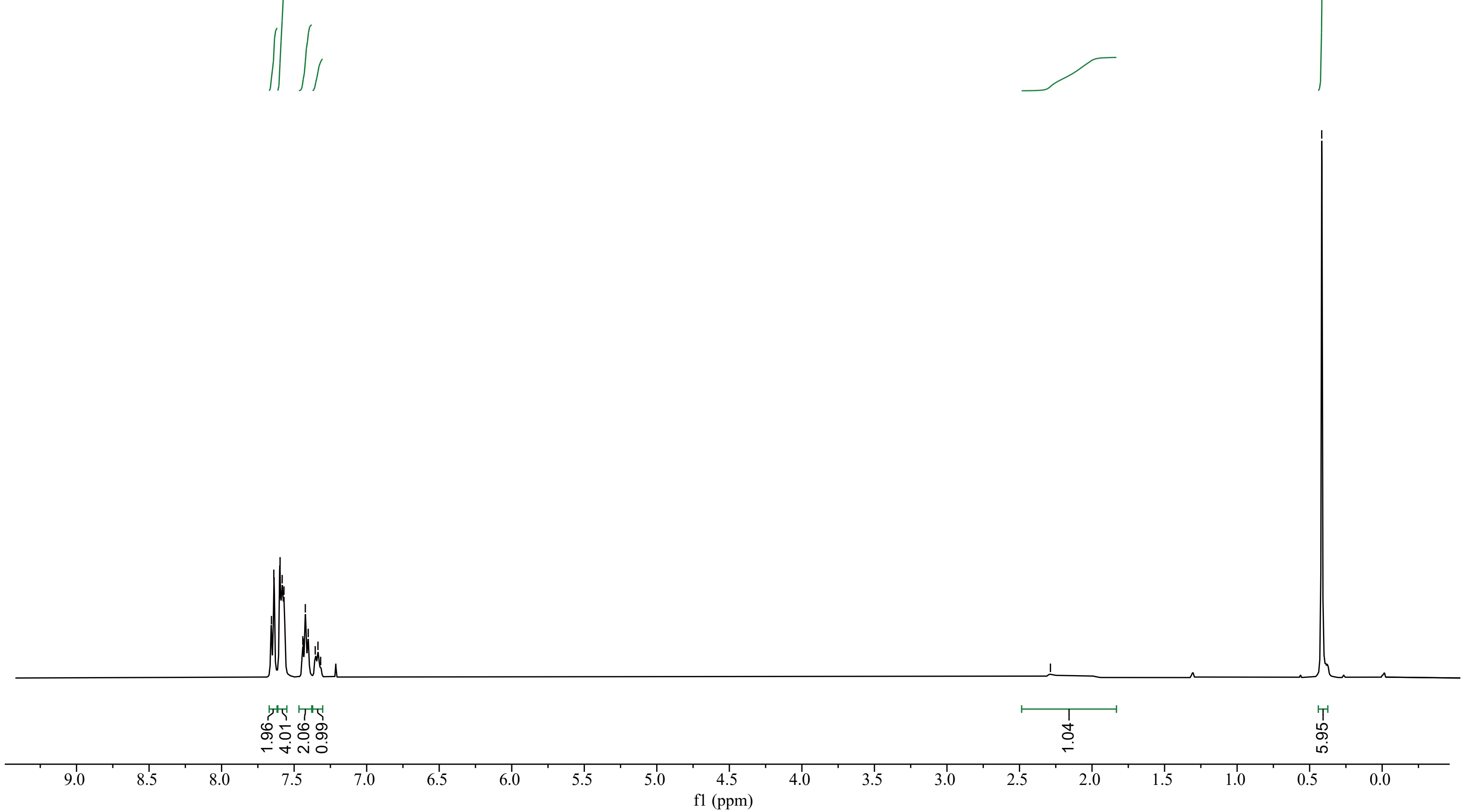

Compound **2x** ^{13}C NMR

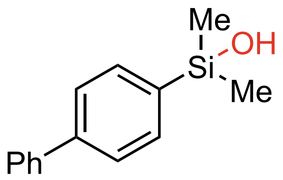

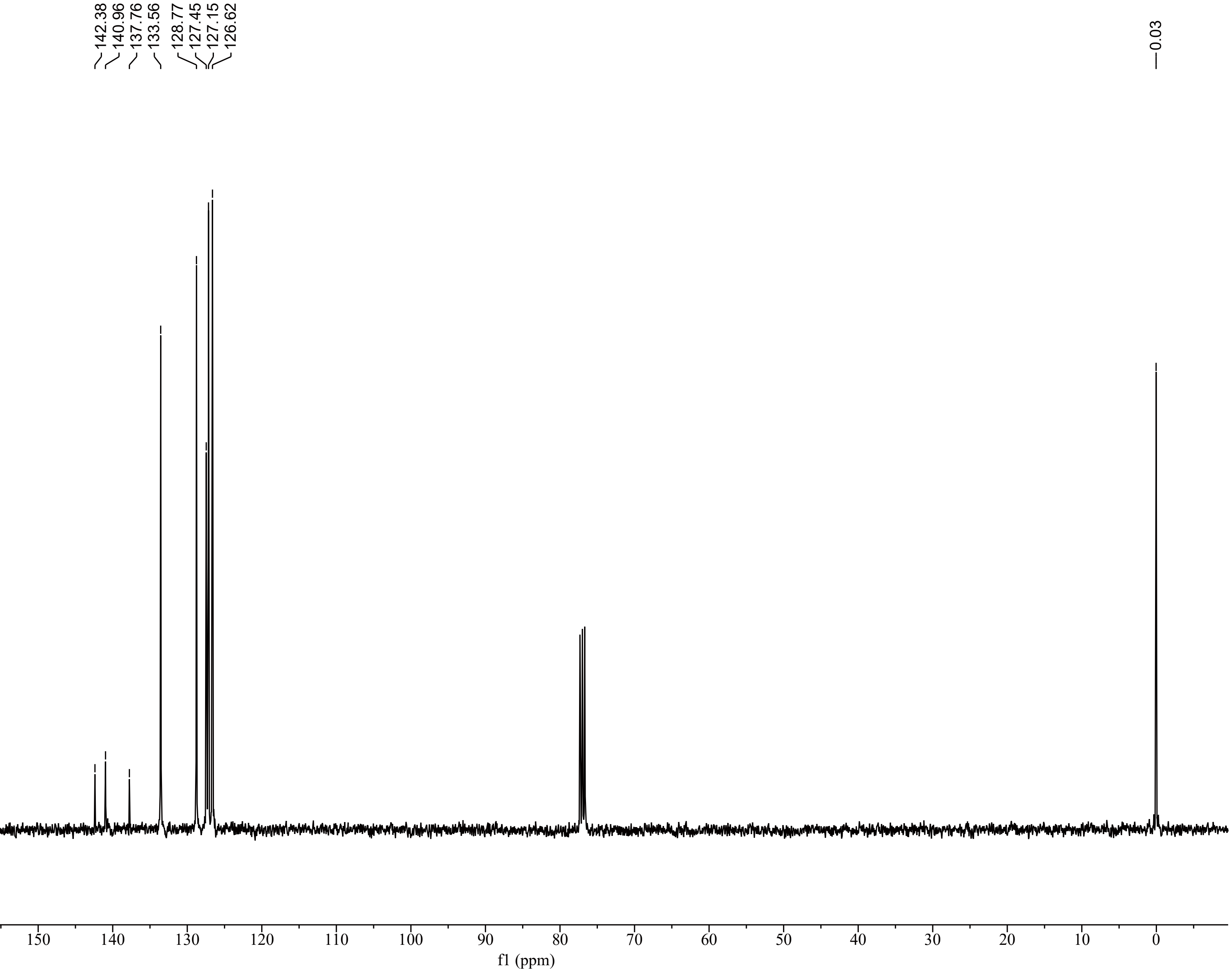

Compound **2y** [1]H NMR

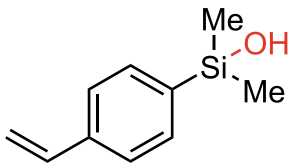

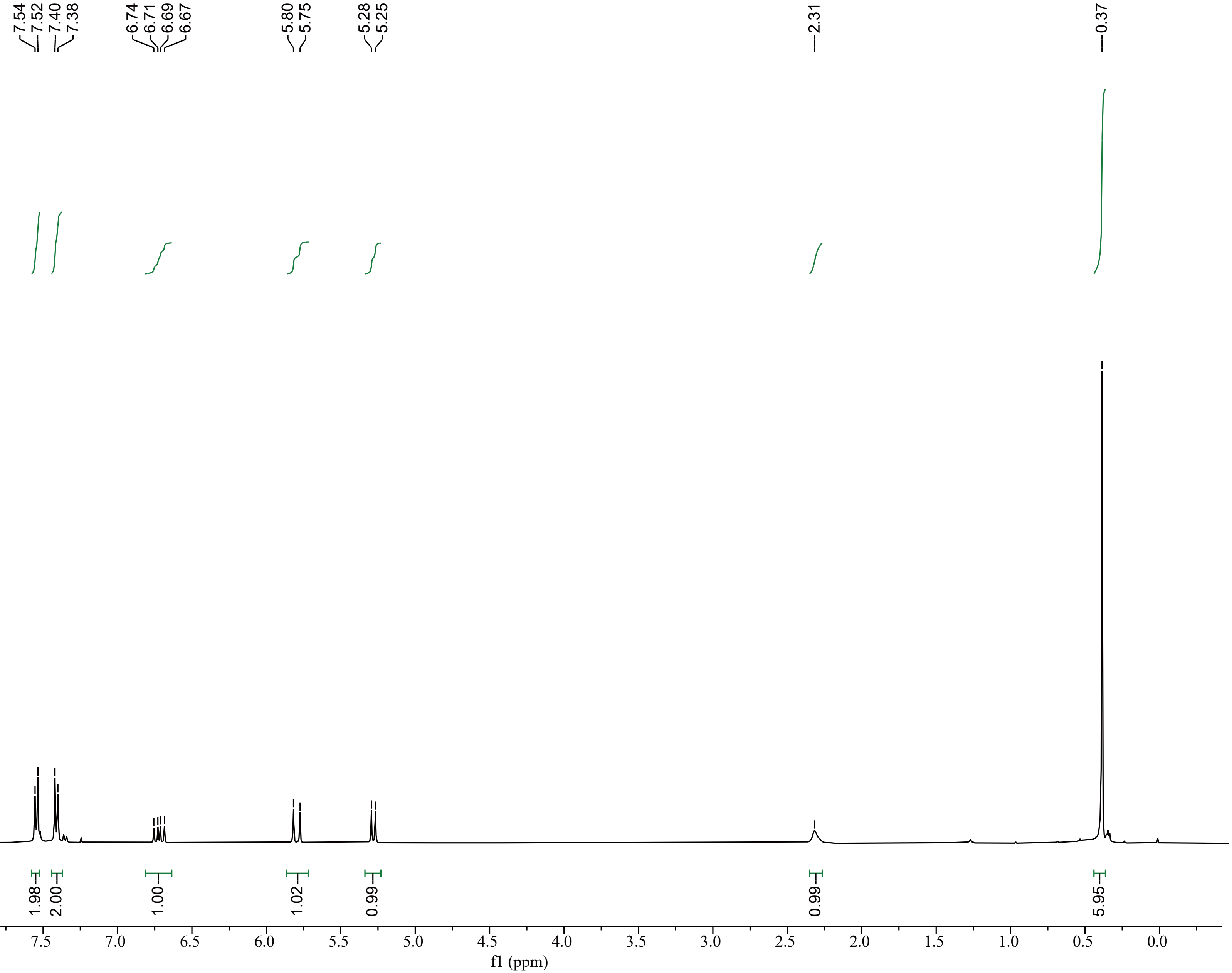

Compound **2y** ^{13}C NMR

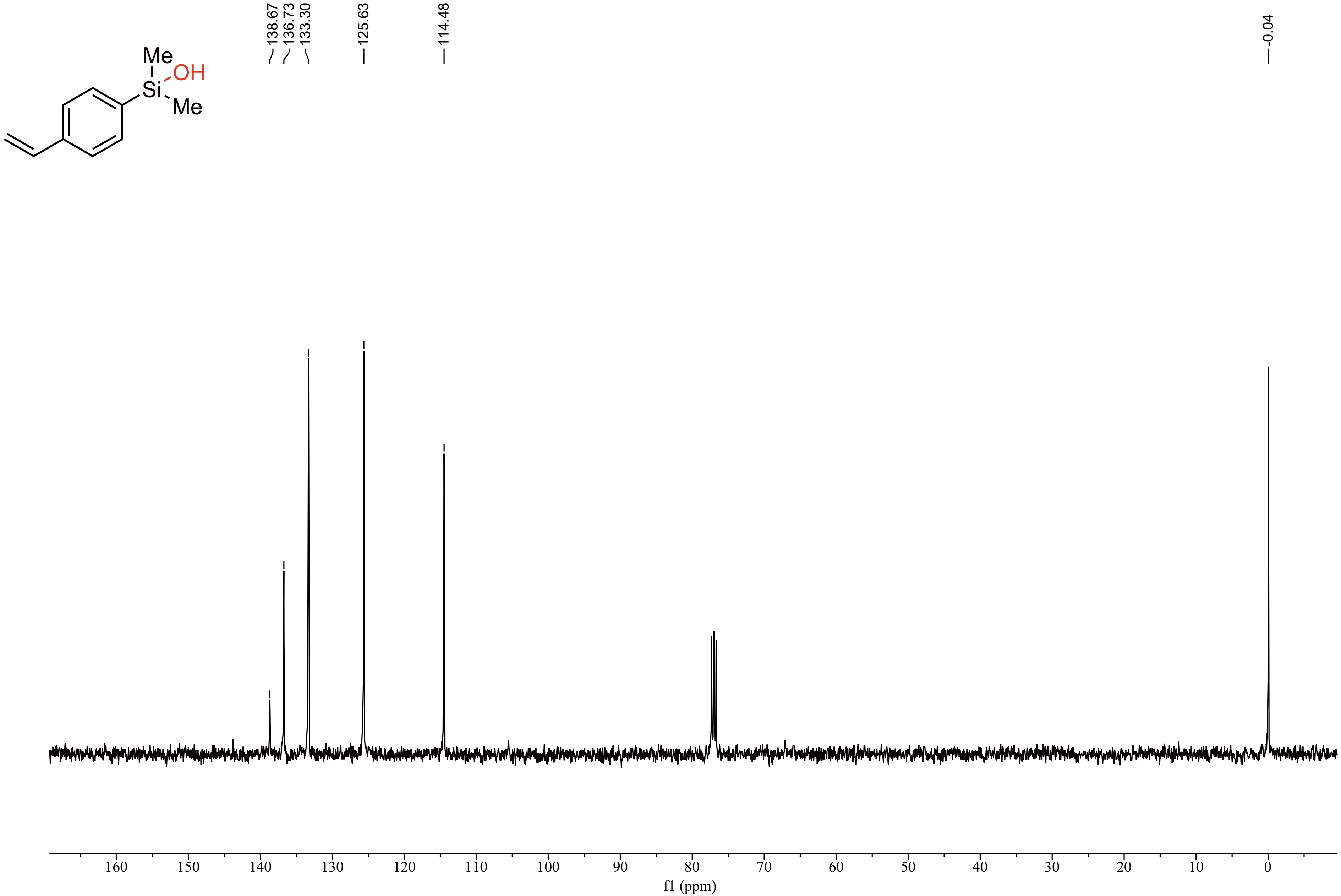

Compound **2z** ^{1}H NMR

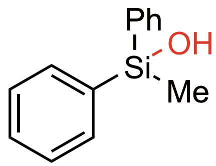

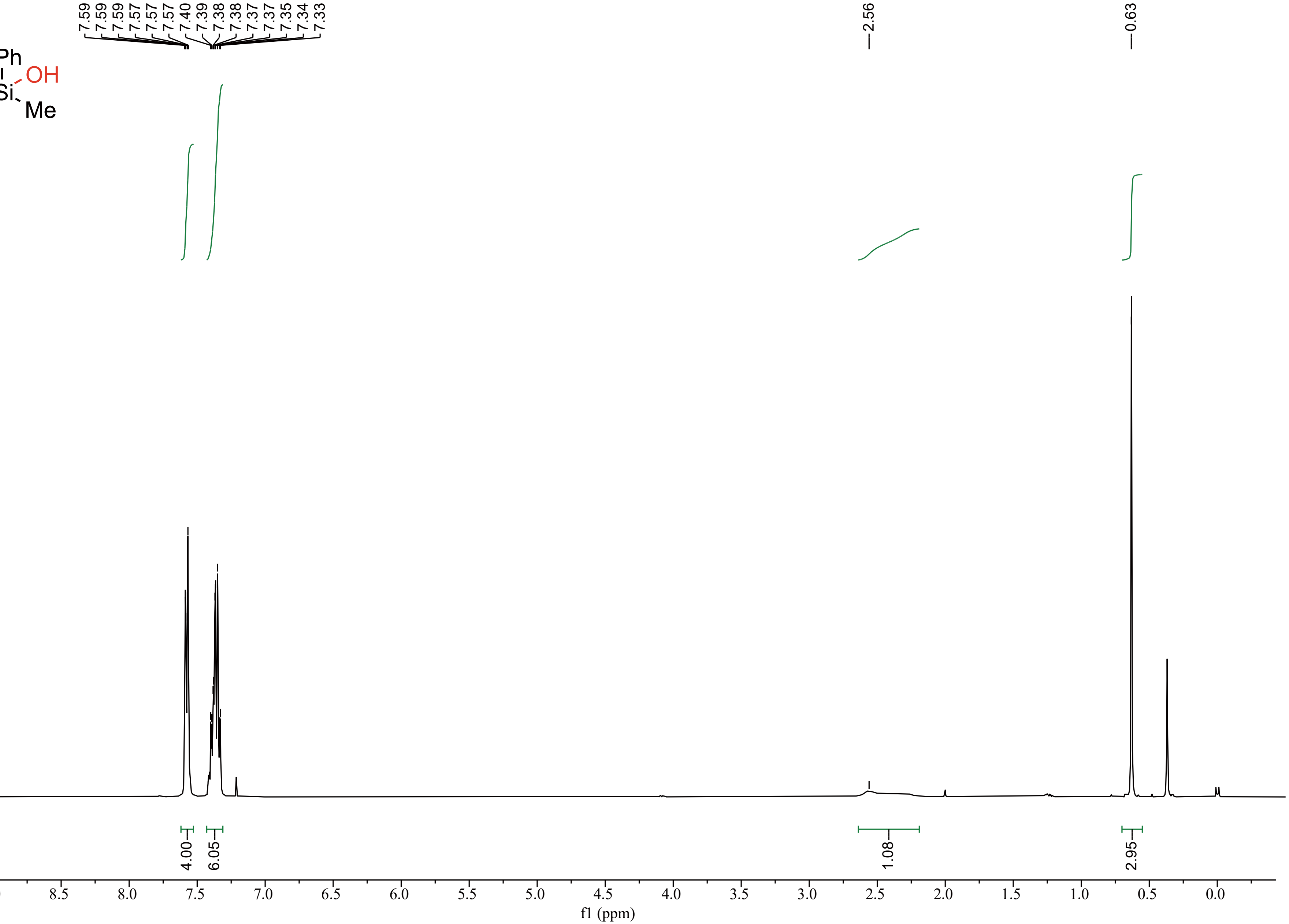

Compound **2z** ^{13}C NMR

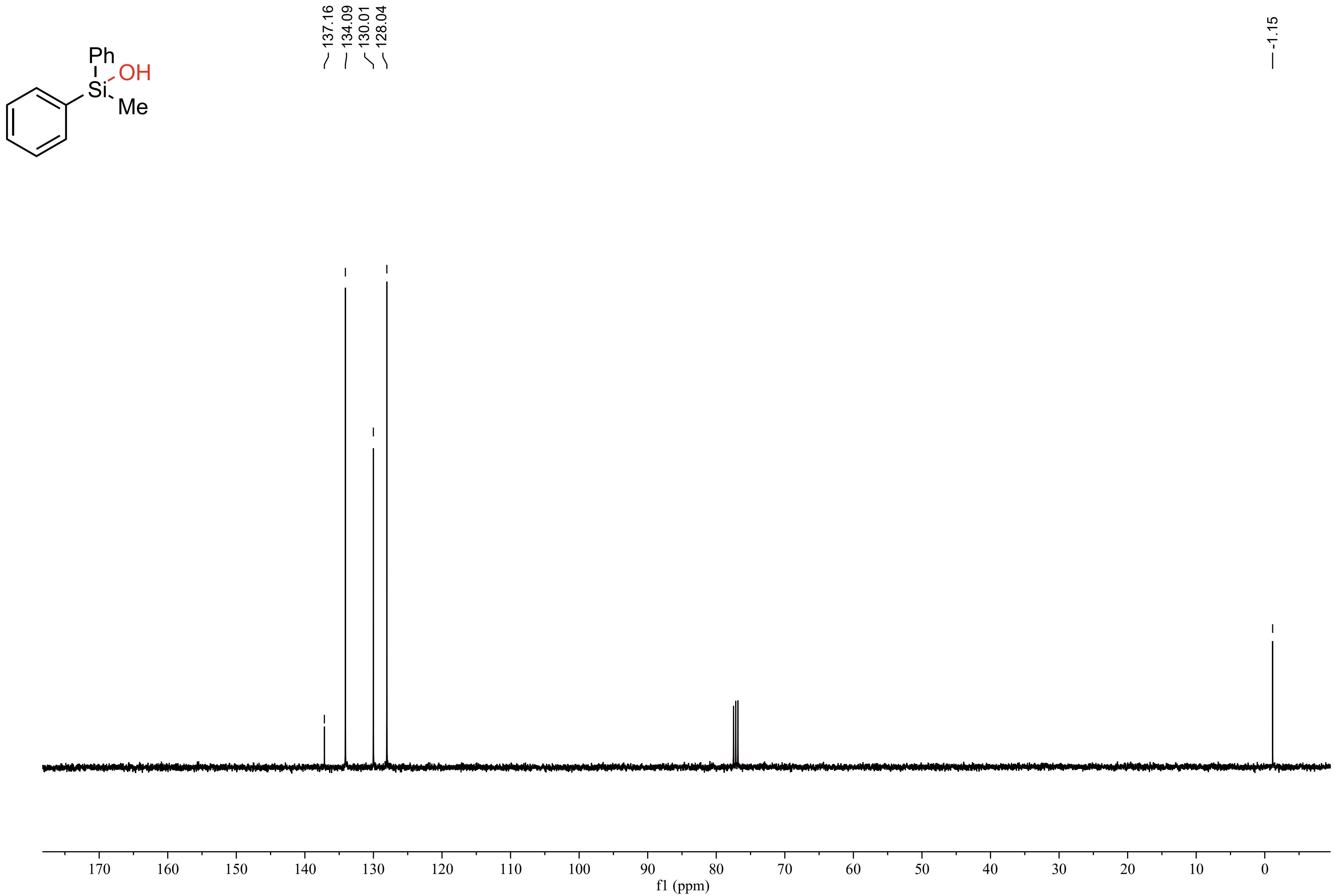

Compound **2aa** ^{1}H NMR

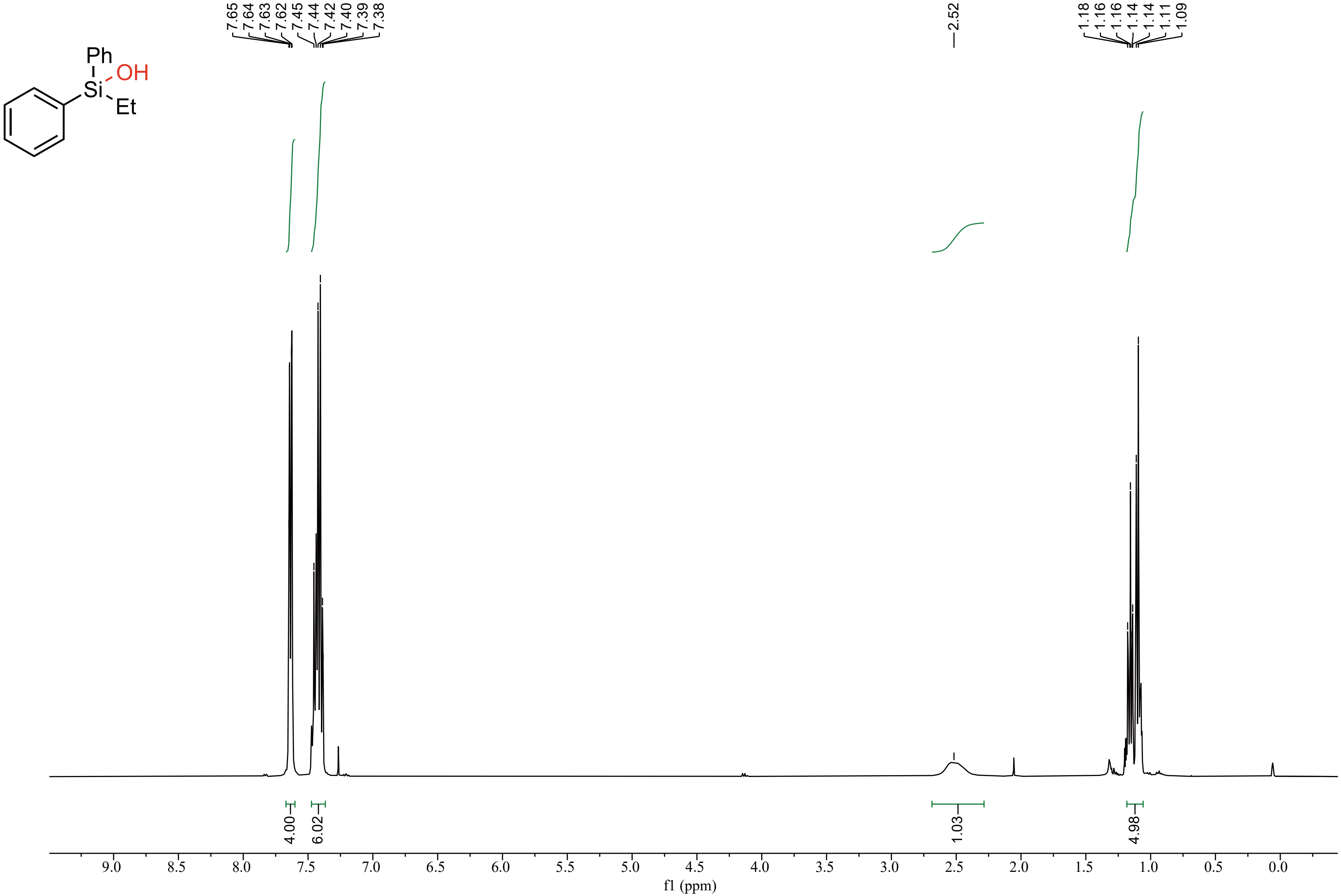

Compound **2aa** ^{13}C NMR

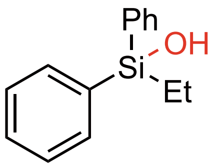

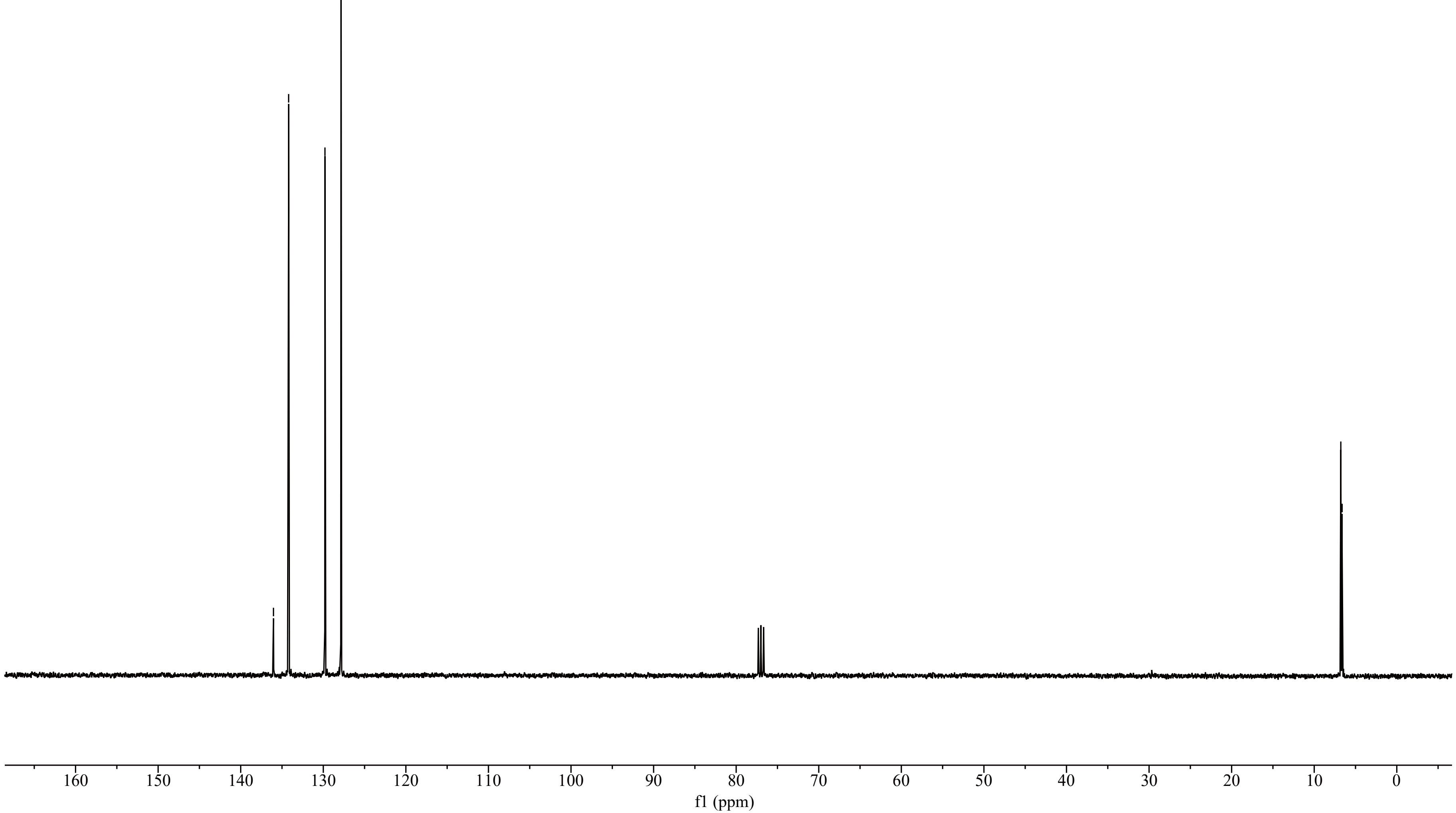

Compound **2ab** ^{1}H NMR

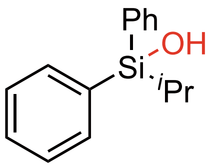

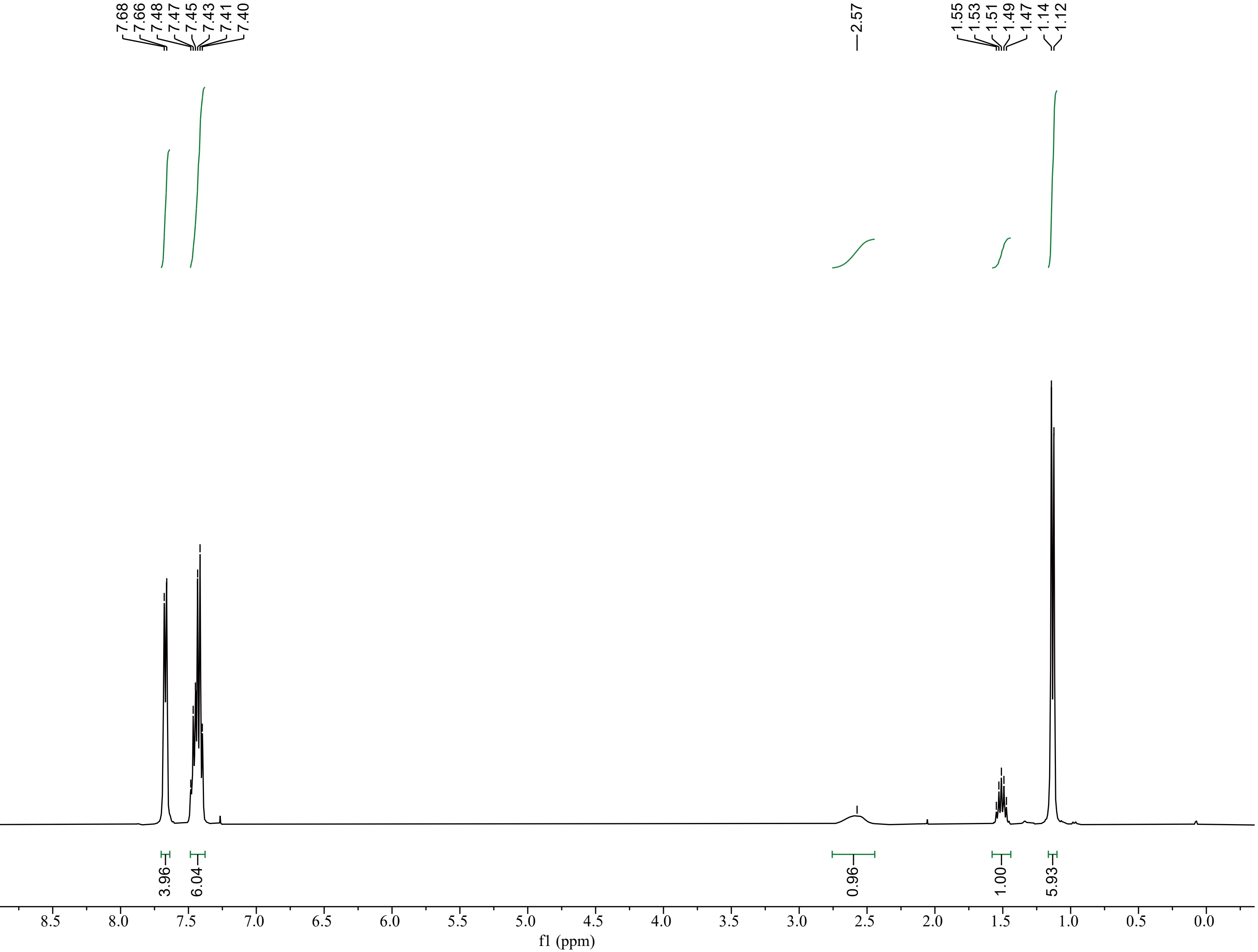

Compound **2ab** ^{13}C NMR

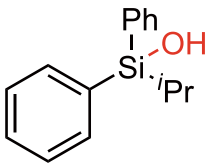

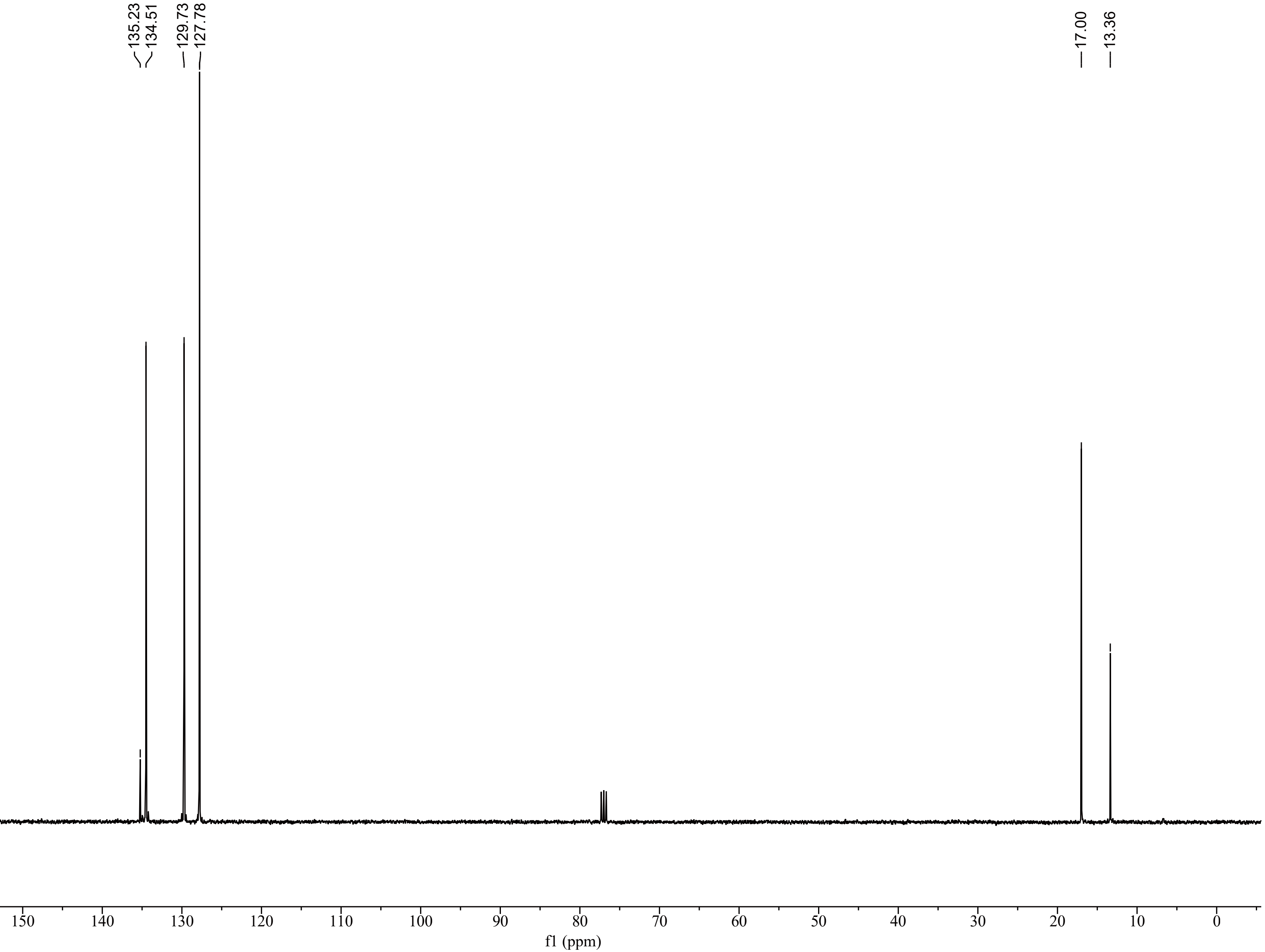

Compound **2ac** ^{1}H NMR

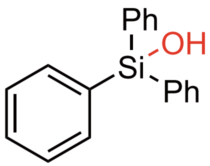

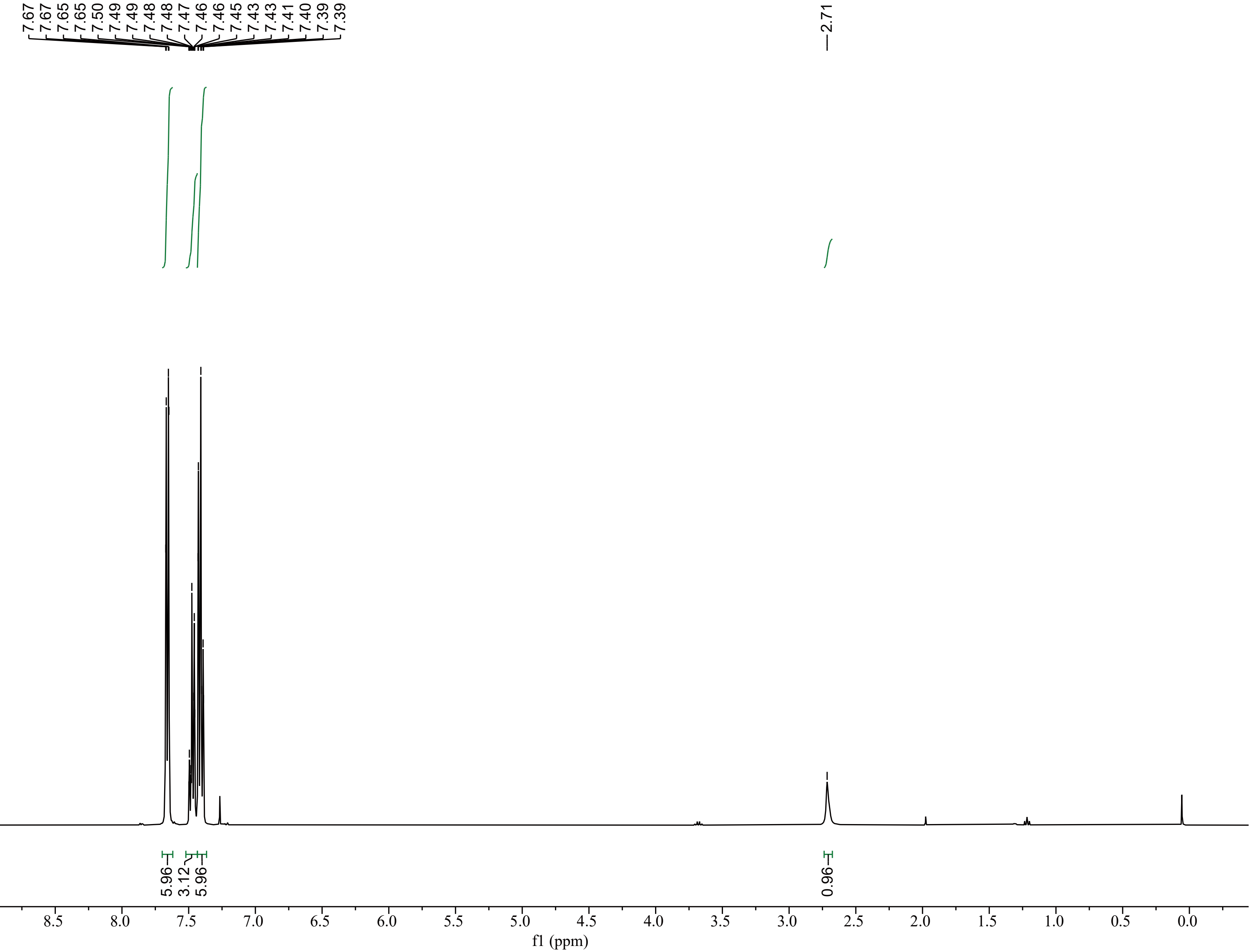

Compound **2ac** ^{13}C NMR

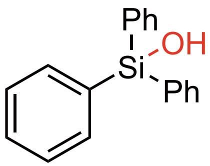

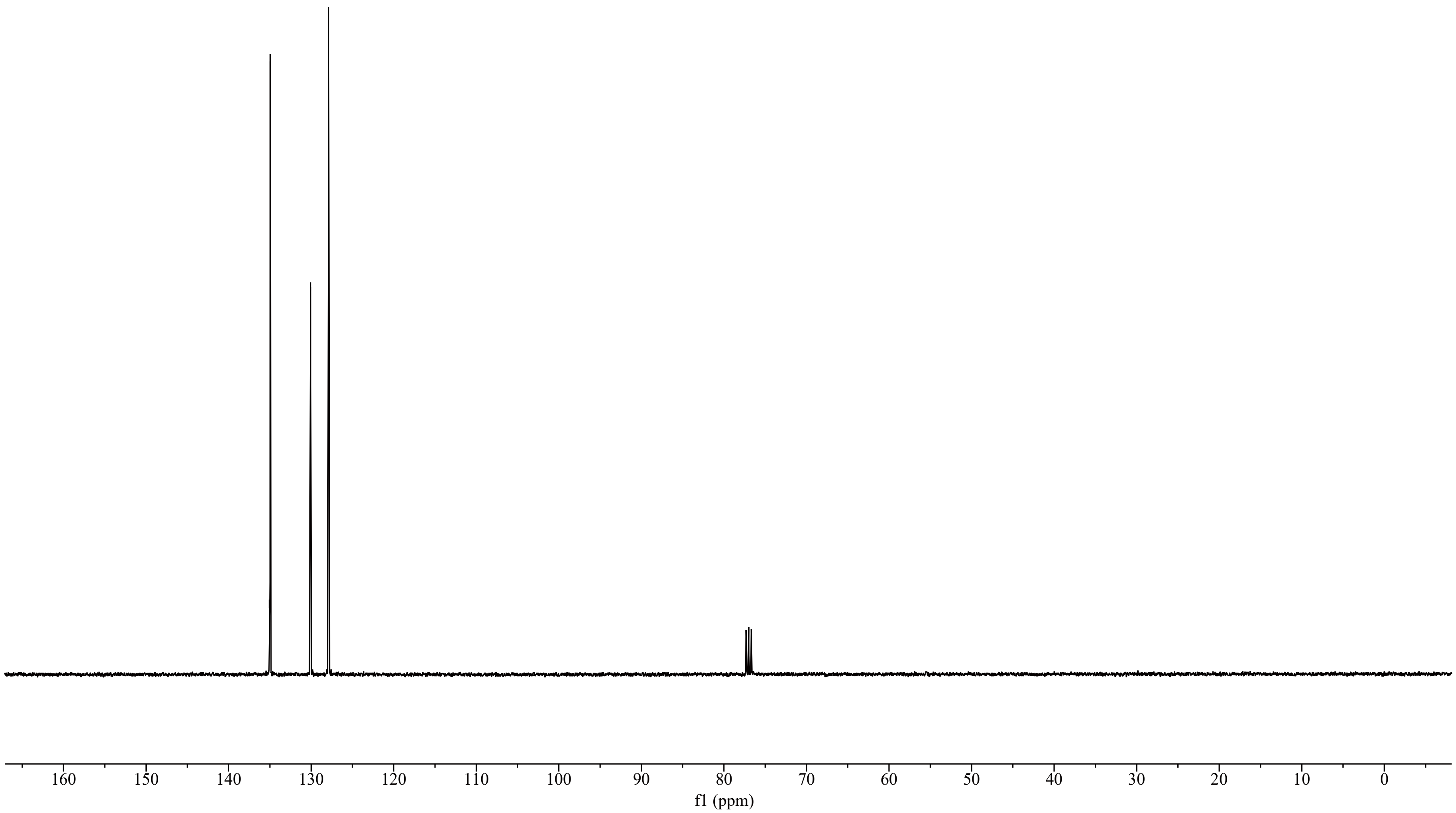

Compound **2ad** [1]H NMR

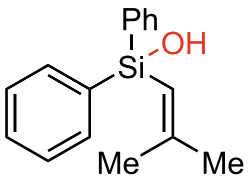

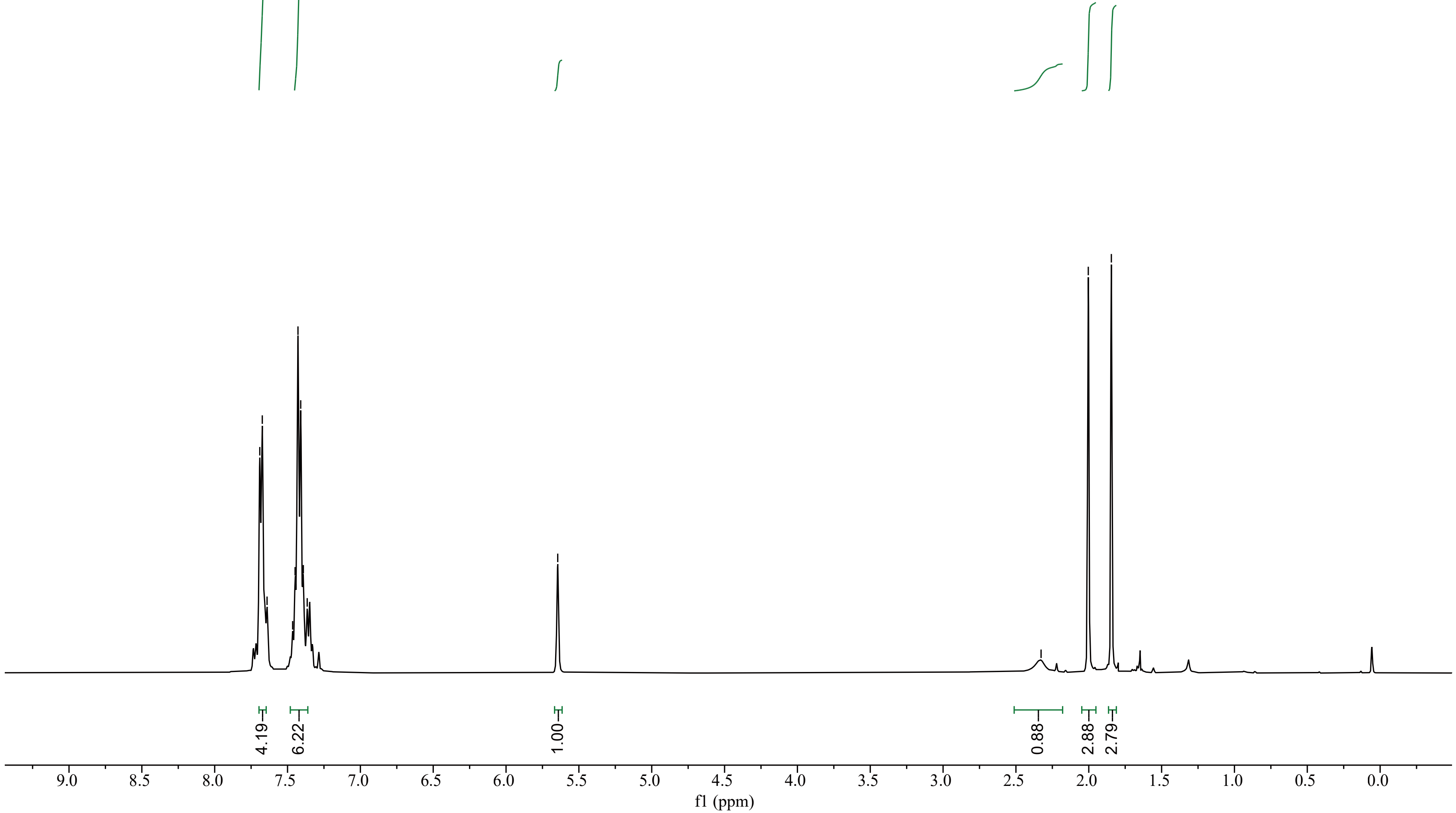

Compound **2ad** ^{13}C NMR

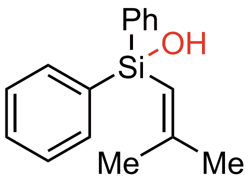

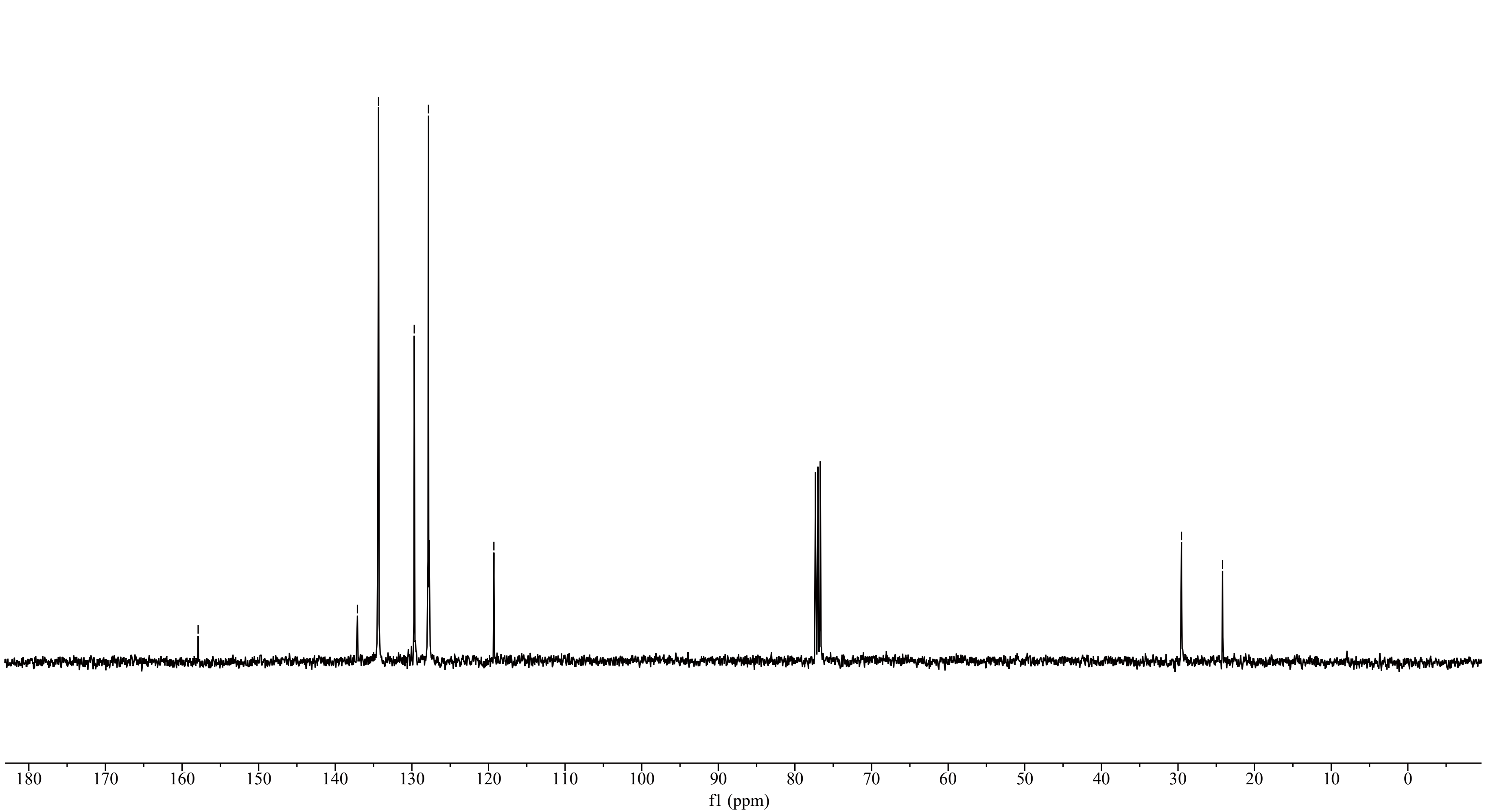

Compound **2ae** [1]H NMR

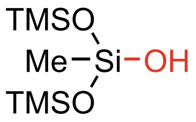

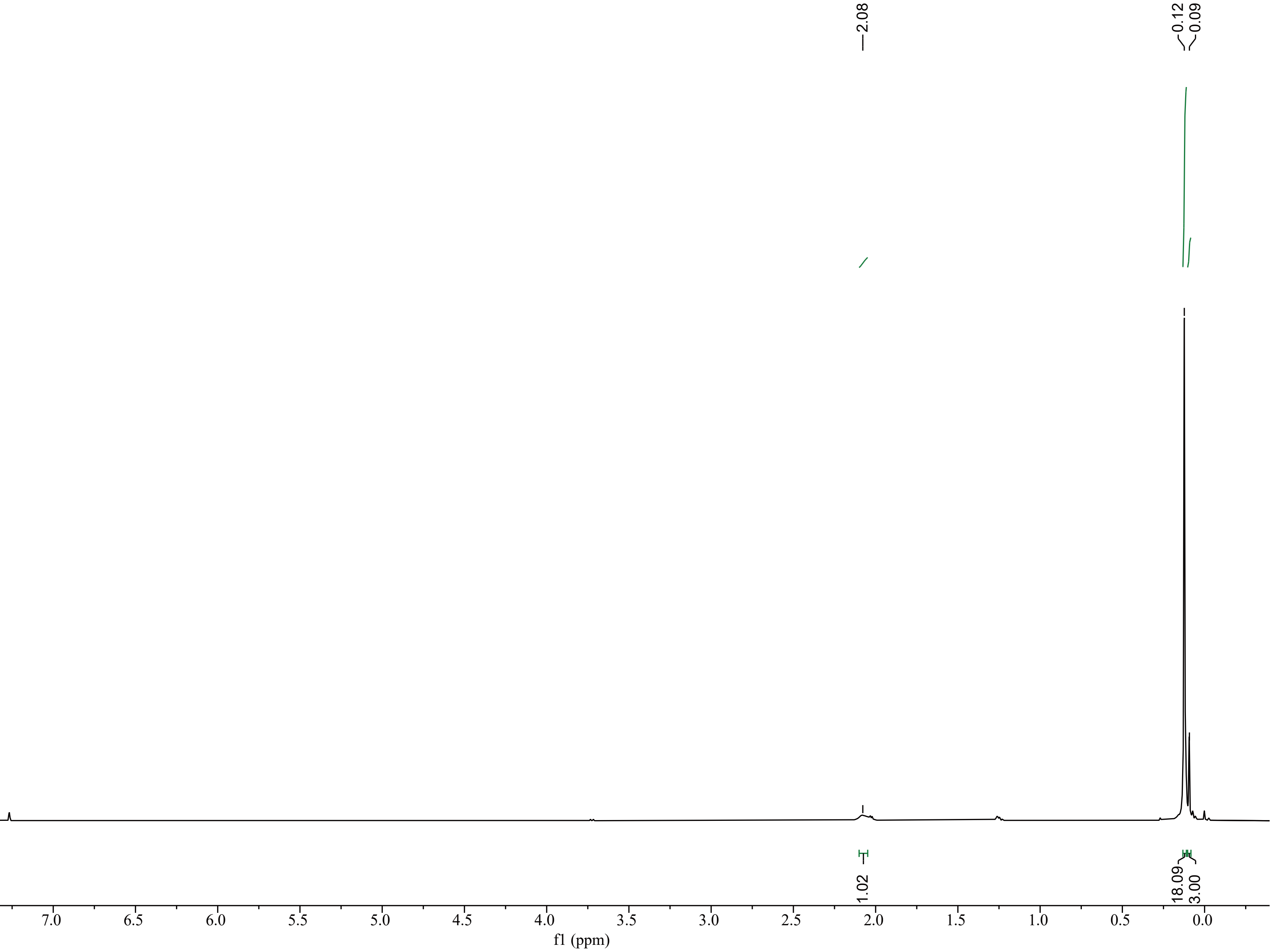

Compound **2ae** ^{13}C NMR

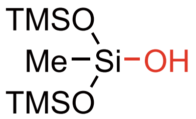

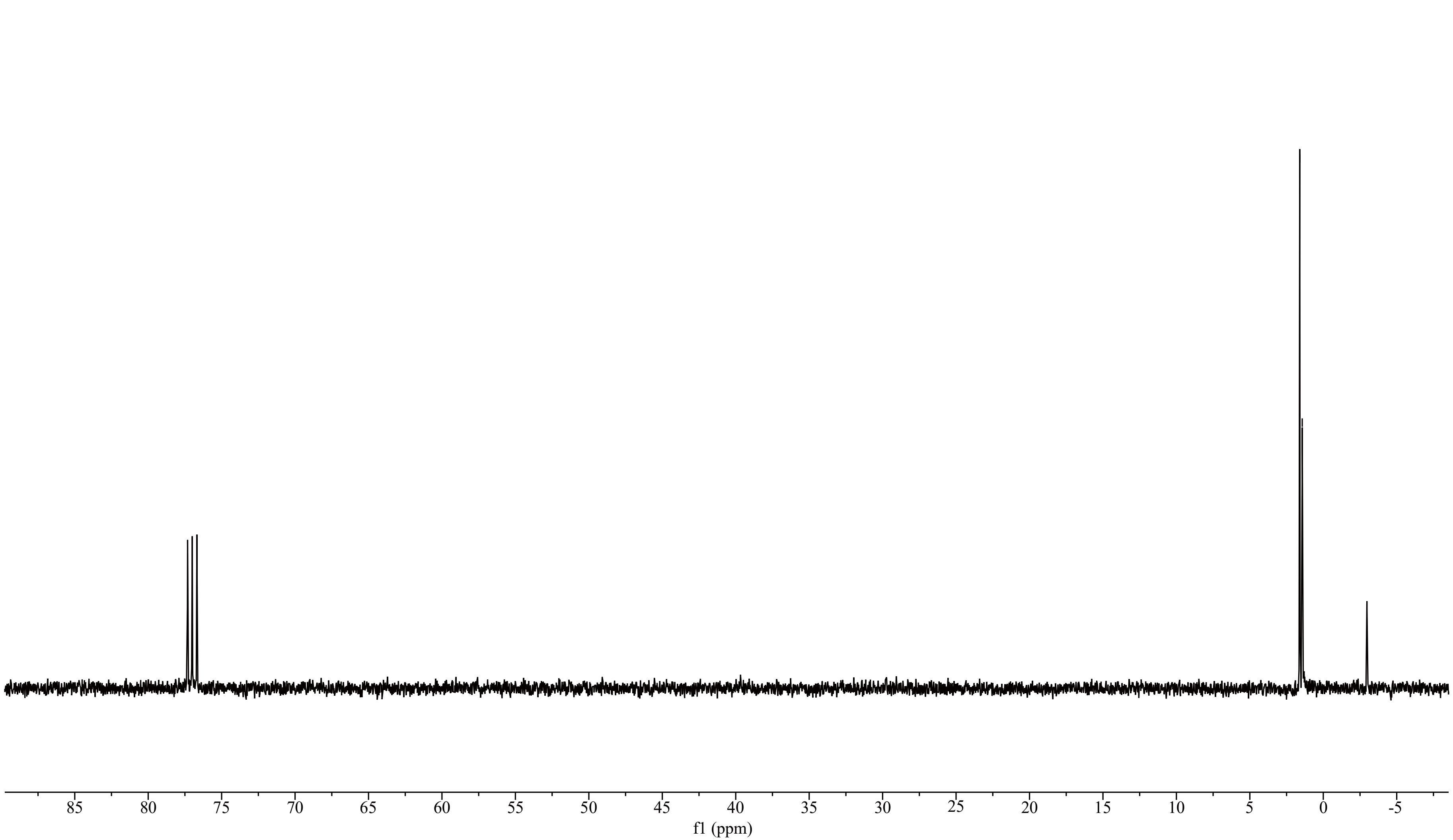

Compound **2af** [1]H NMR

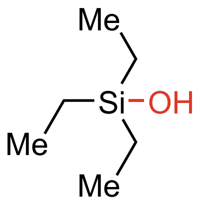

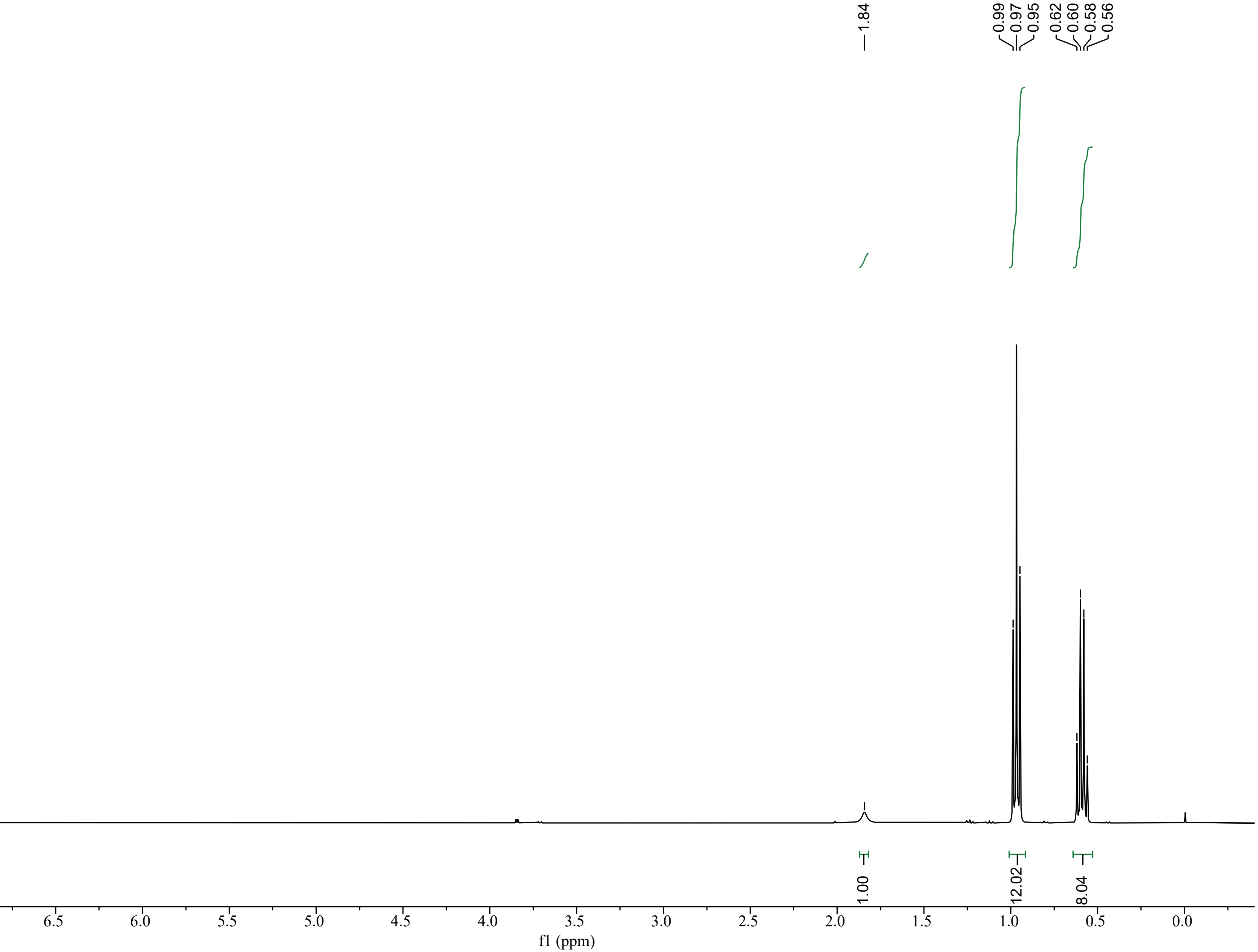

Compound **2af** ^{13}C NMR

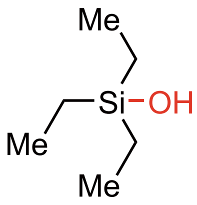

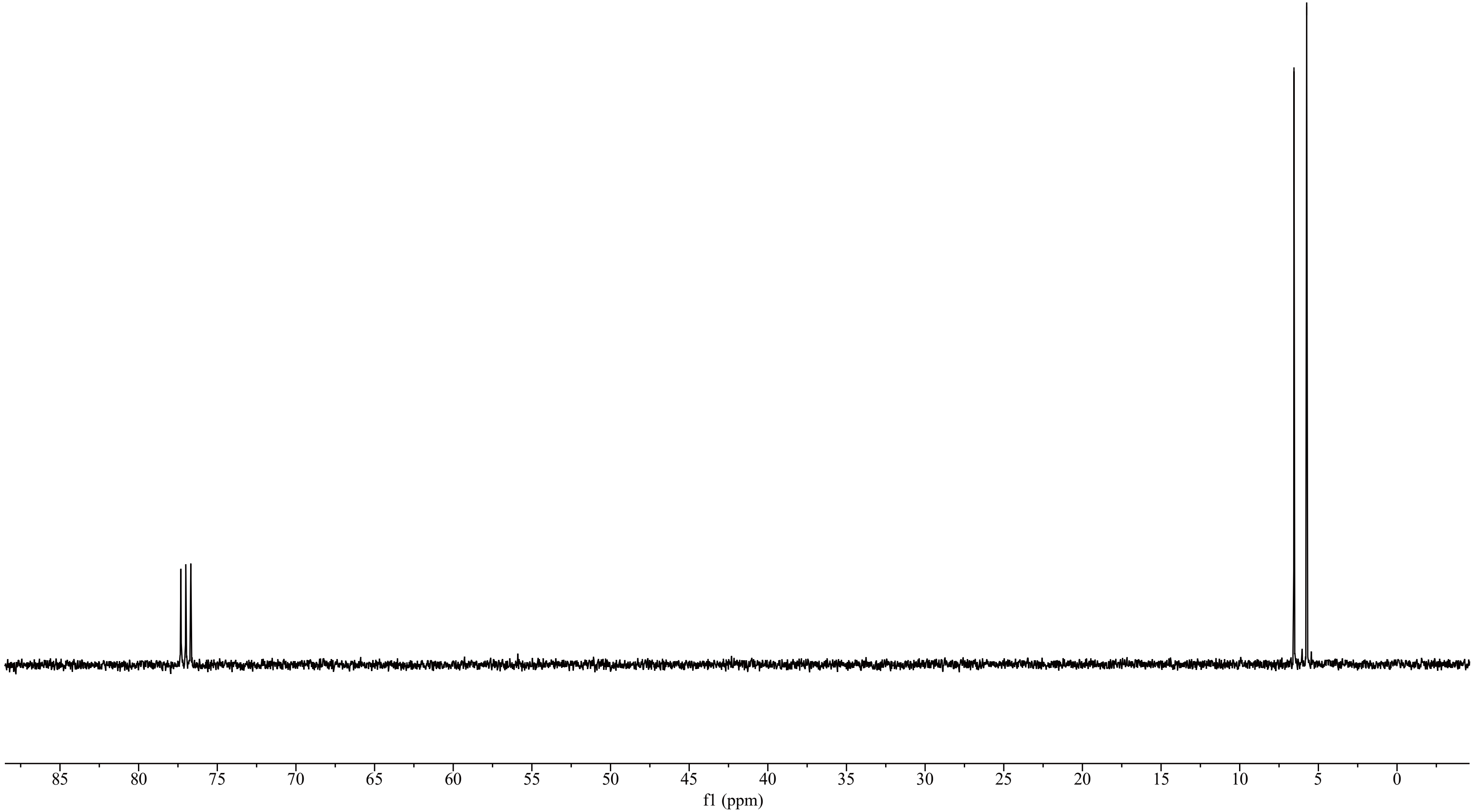

Compound **2ag** ^{1}H NMR

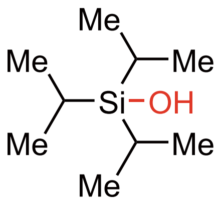

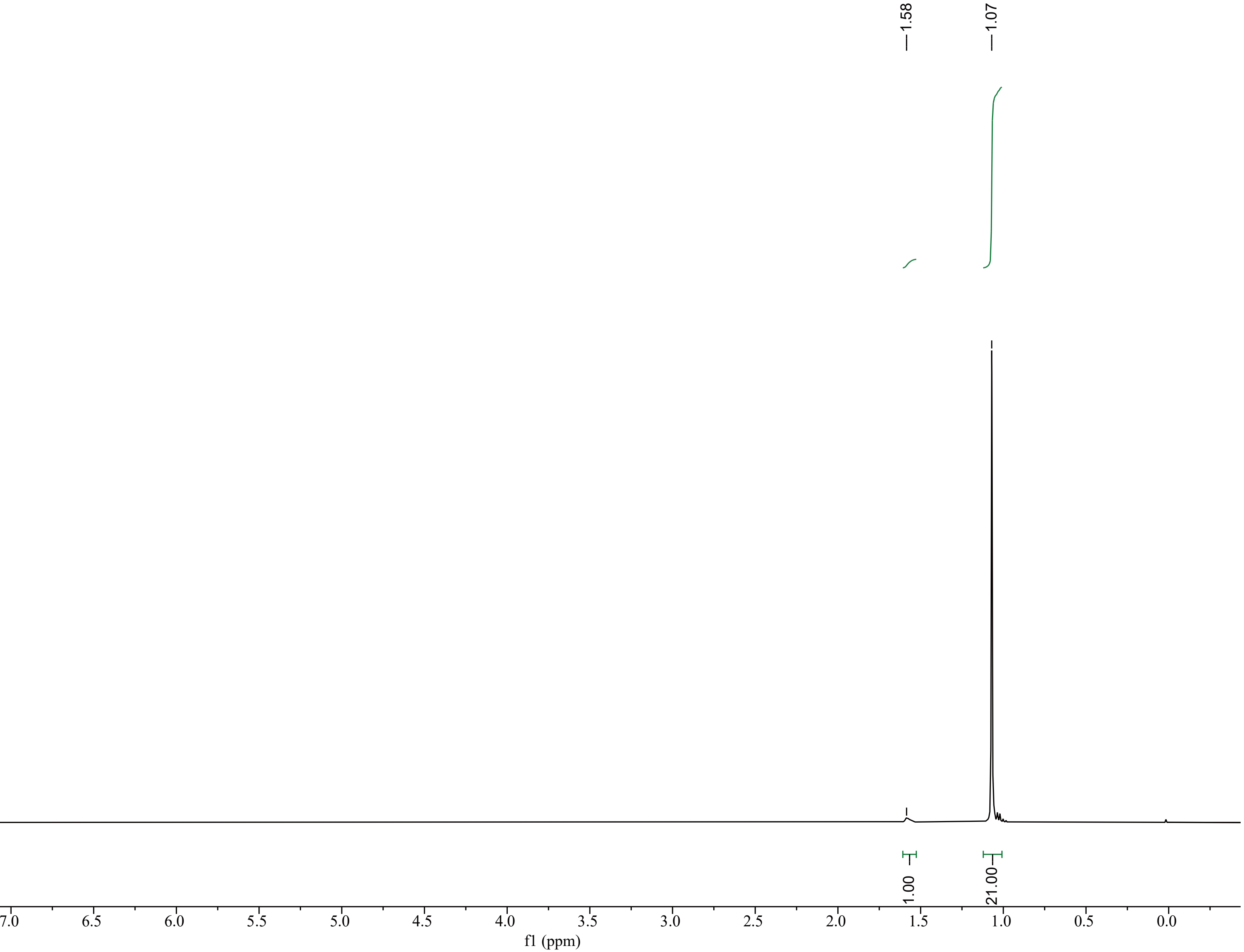

Compound **2ag** ^{13}C NMR

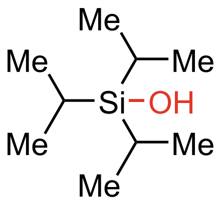

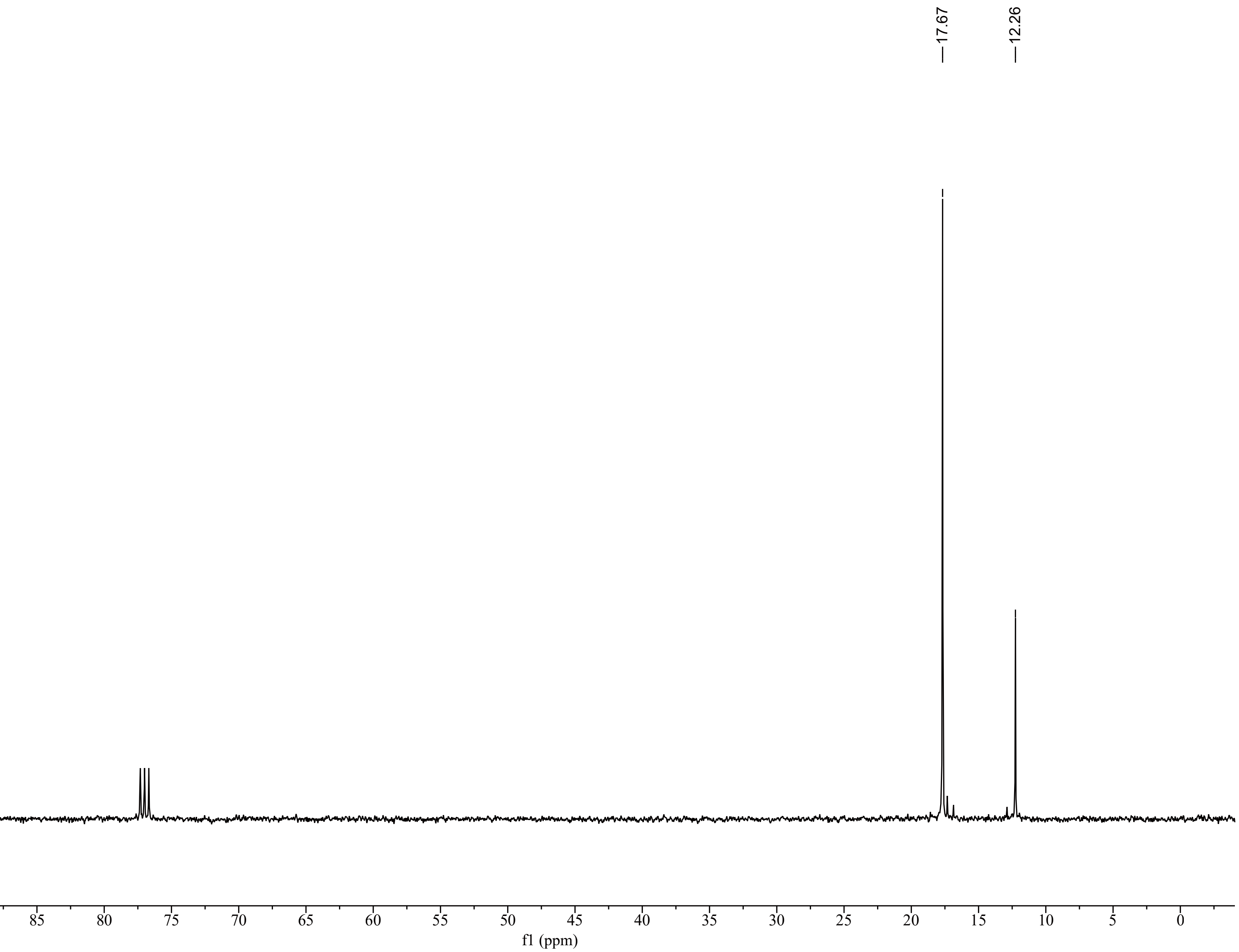

Compound **2ah** ^{1}H NMR

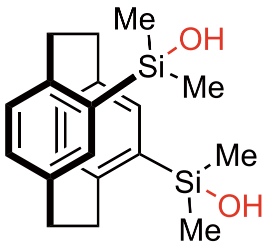

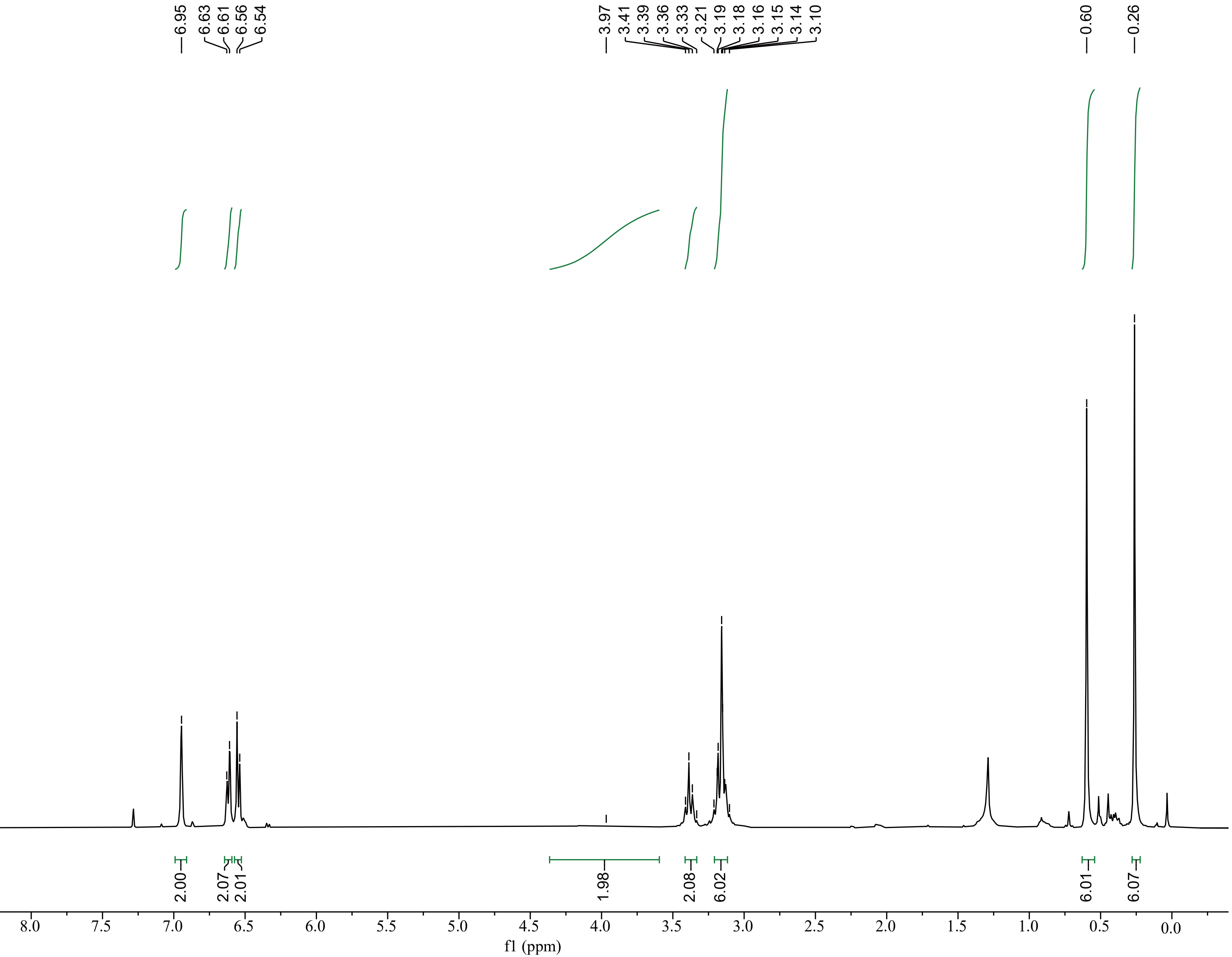

Compound **2ah** ^{13}C NMR

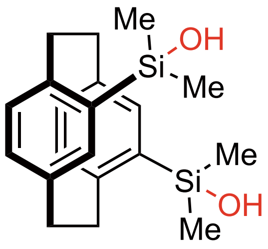

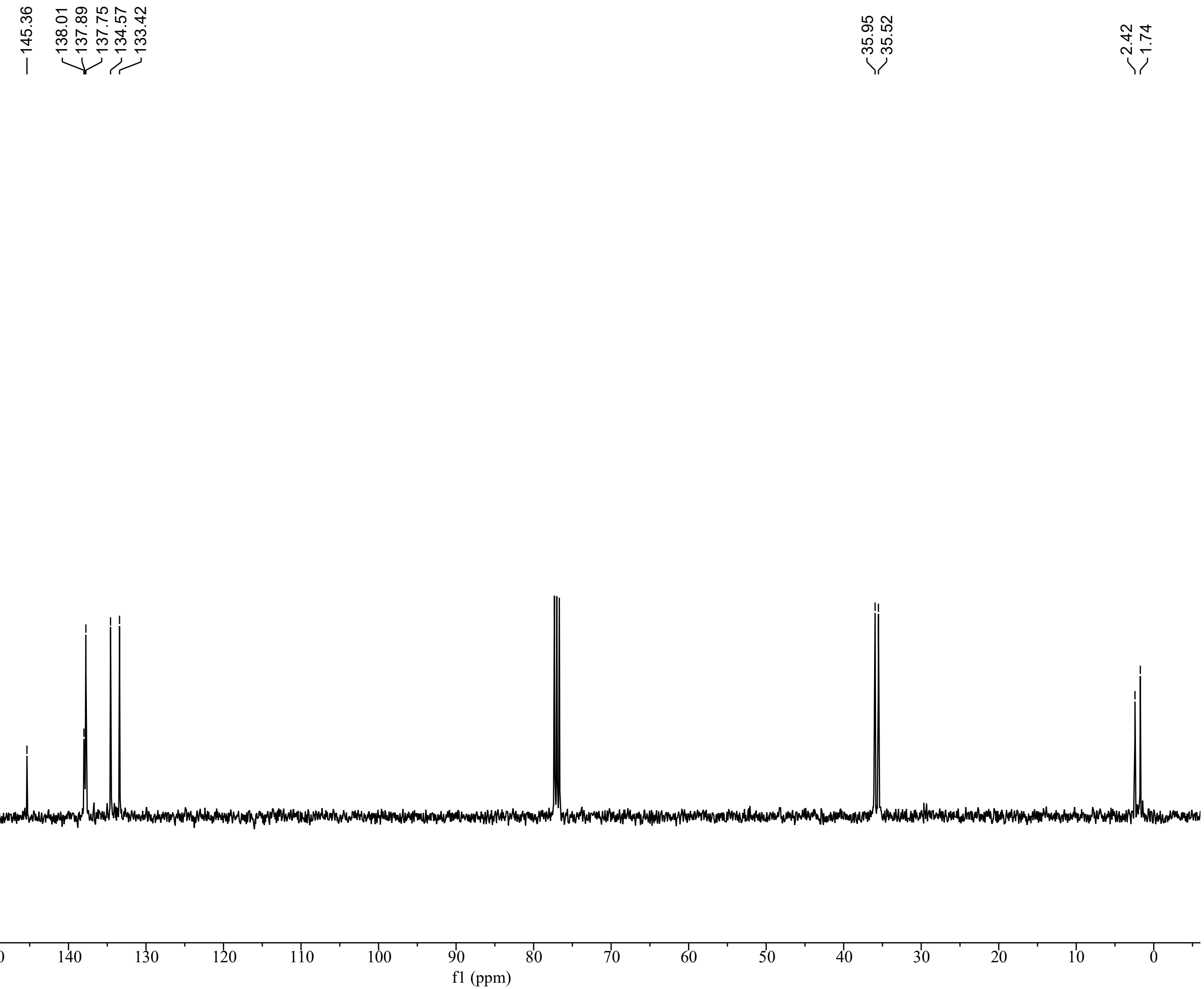

Compound **2ai** ^{1}H NMR

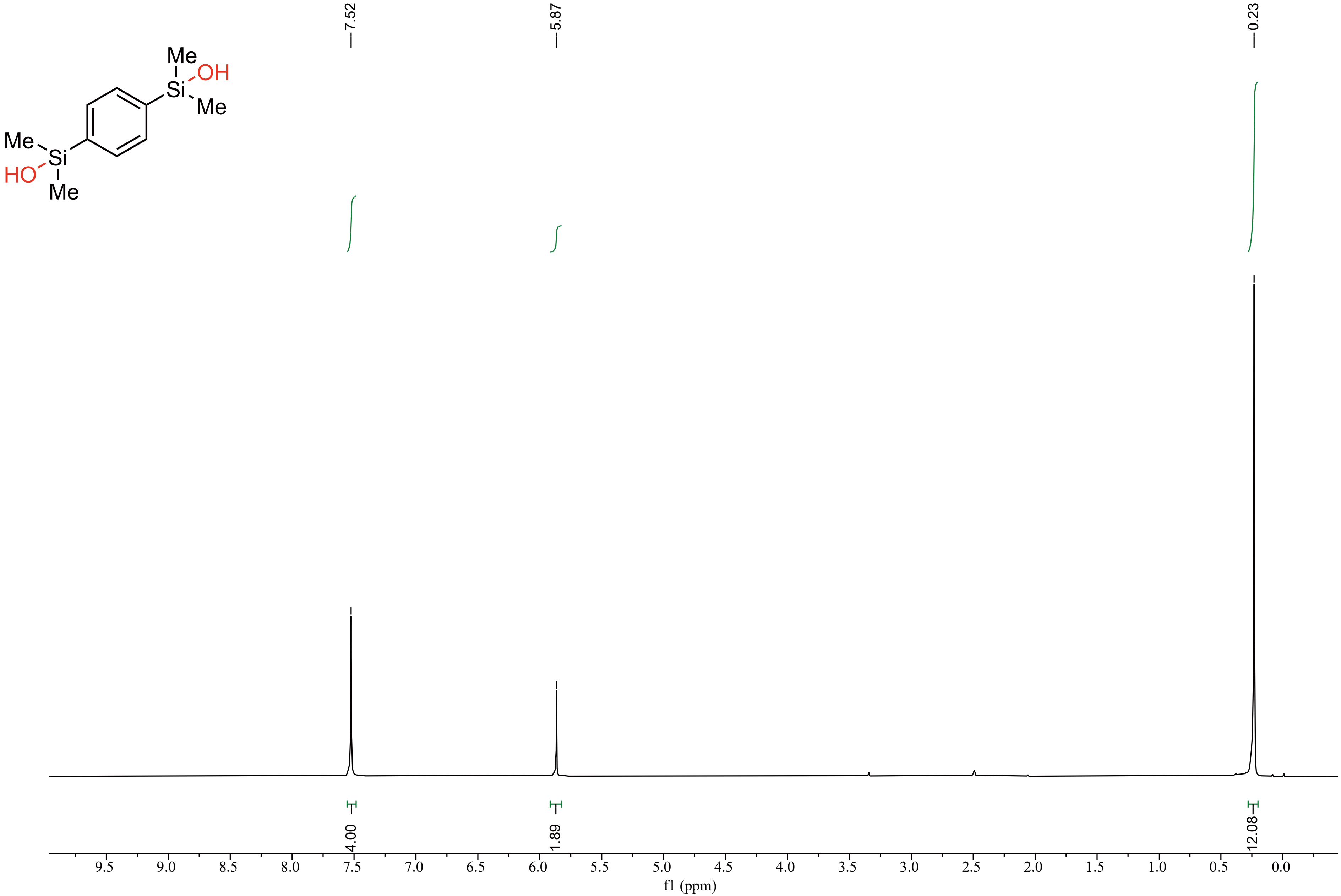

Compound **2ai** ^{13}C NMR

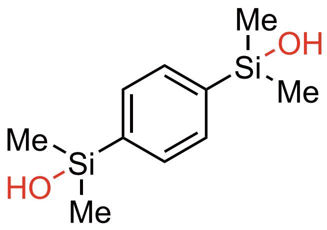

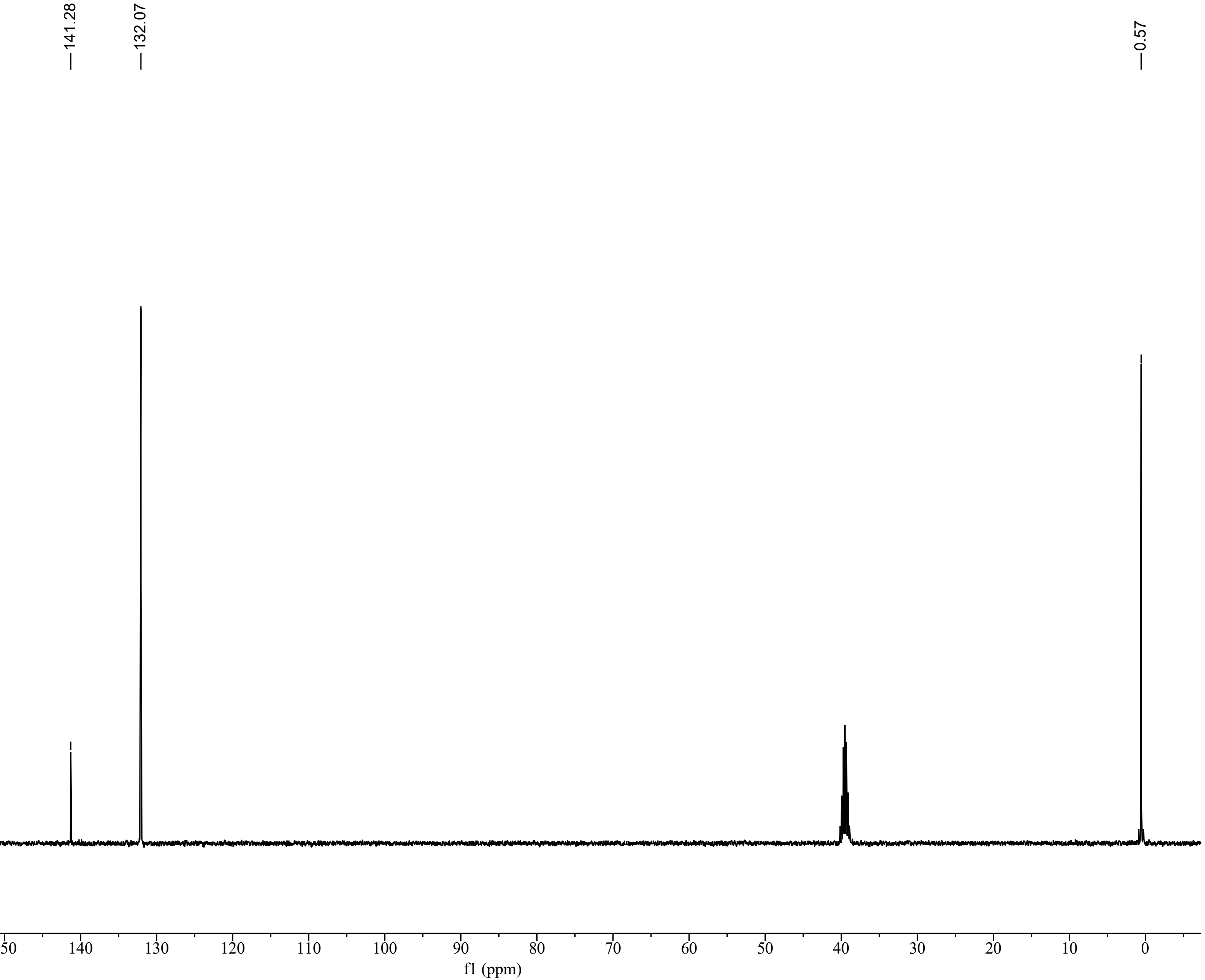

Compound **2aj** ^{1}H NMR

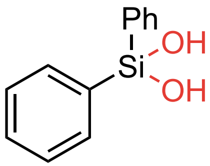

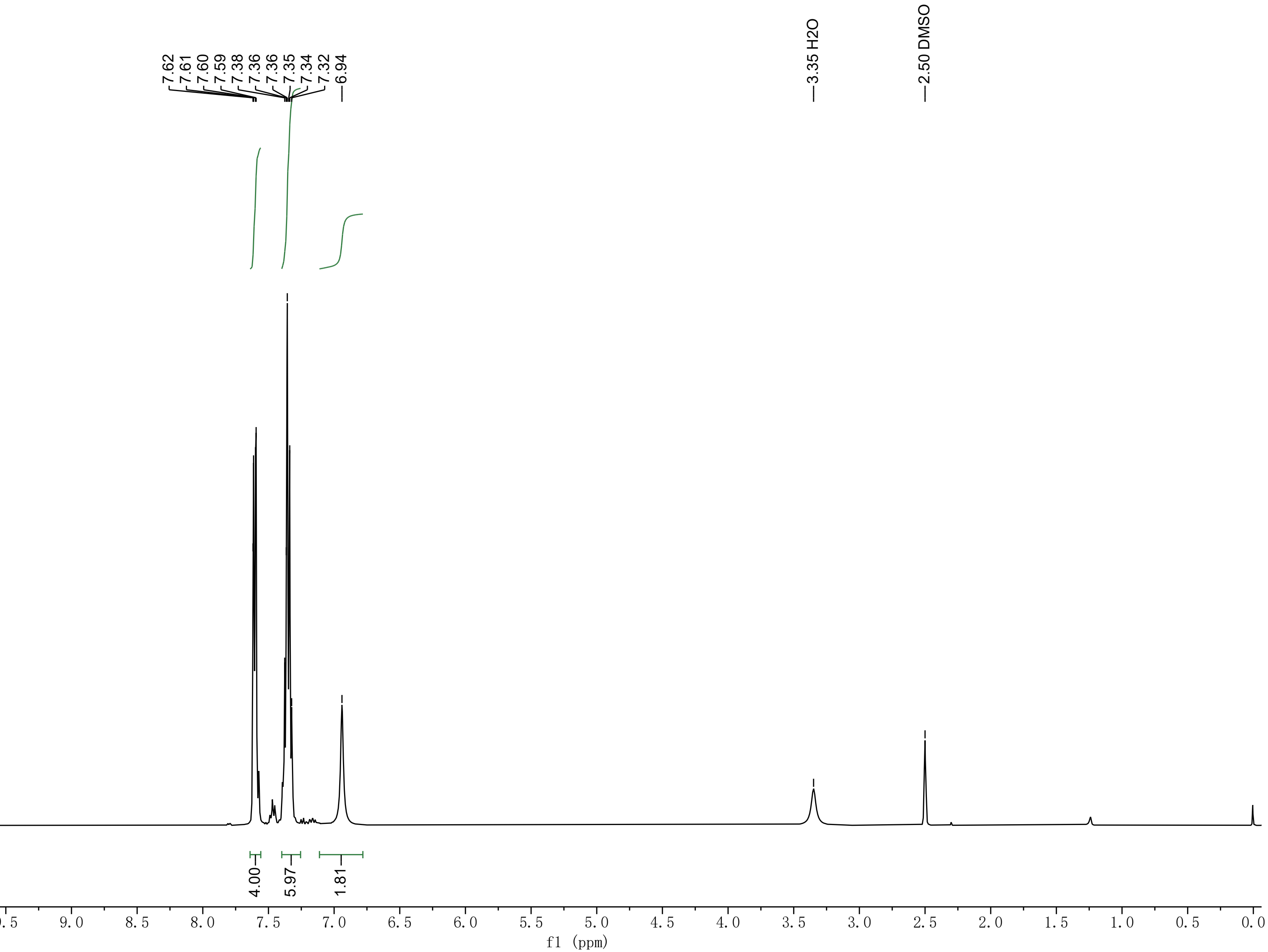

Compound **2aj** ^{13}C NMR

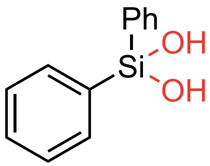

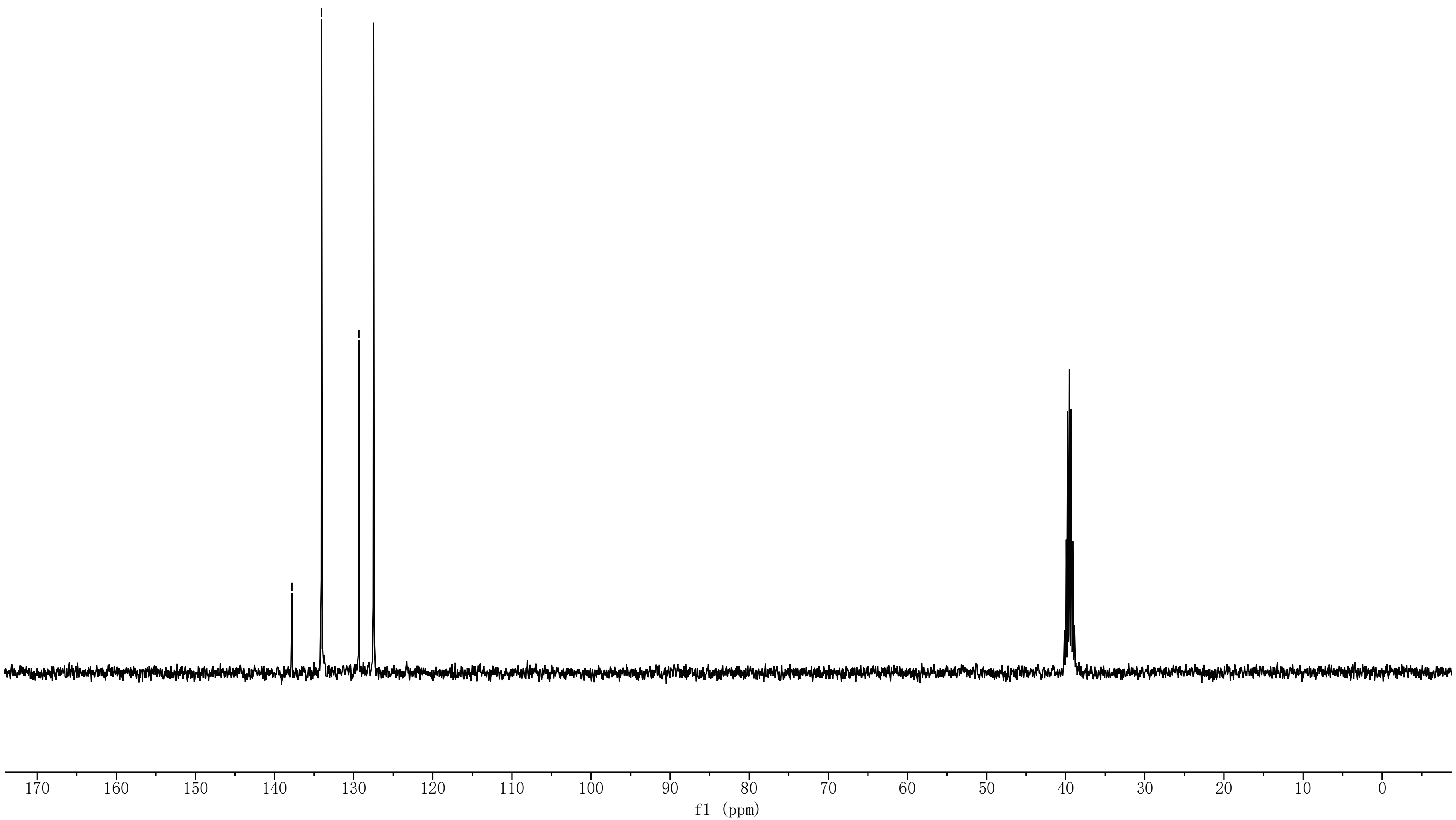

Compound **2ak** ^{1}H NMR

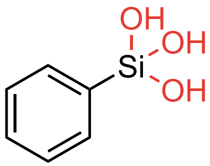

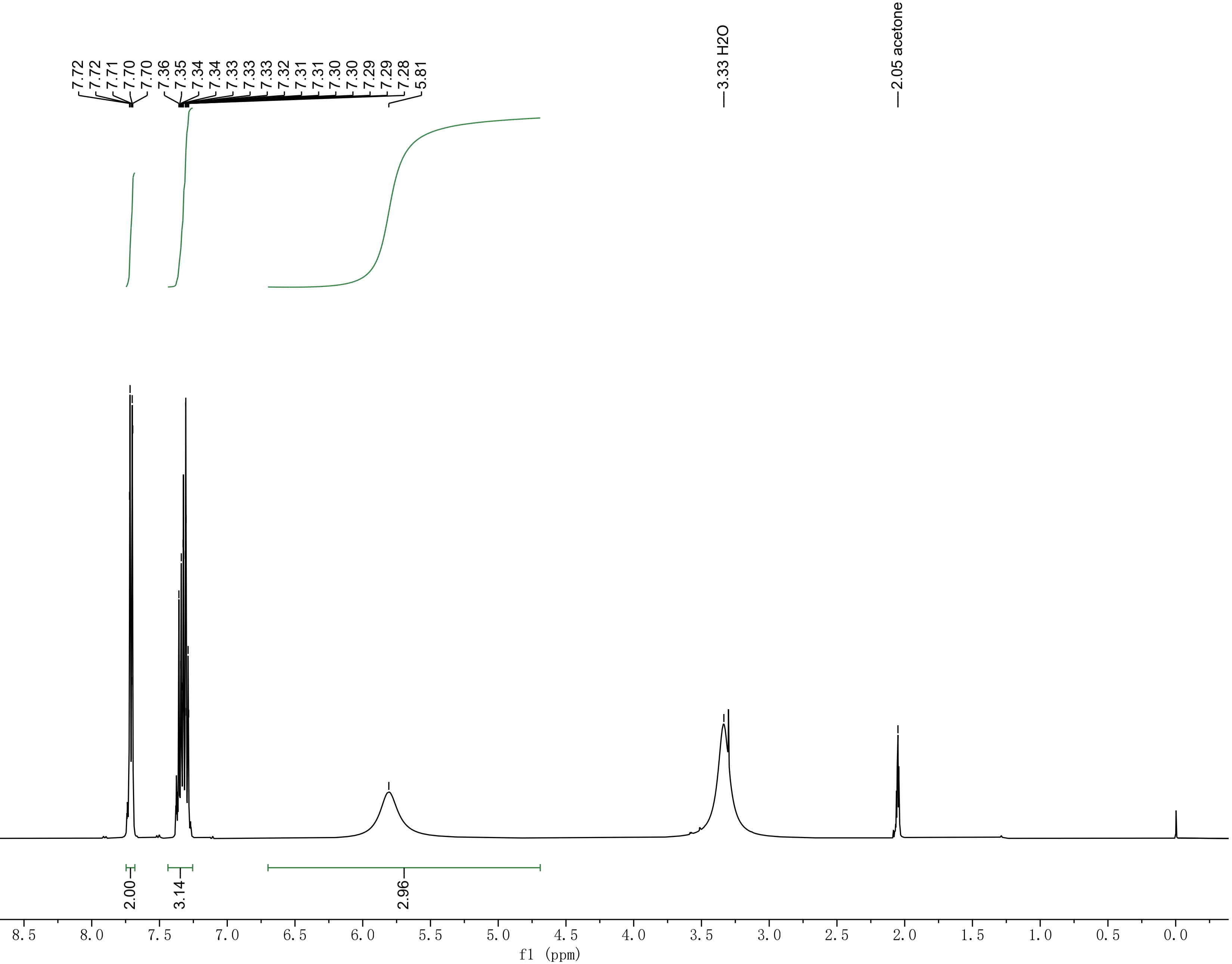

Compound **2ak** ^{13}C NMR

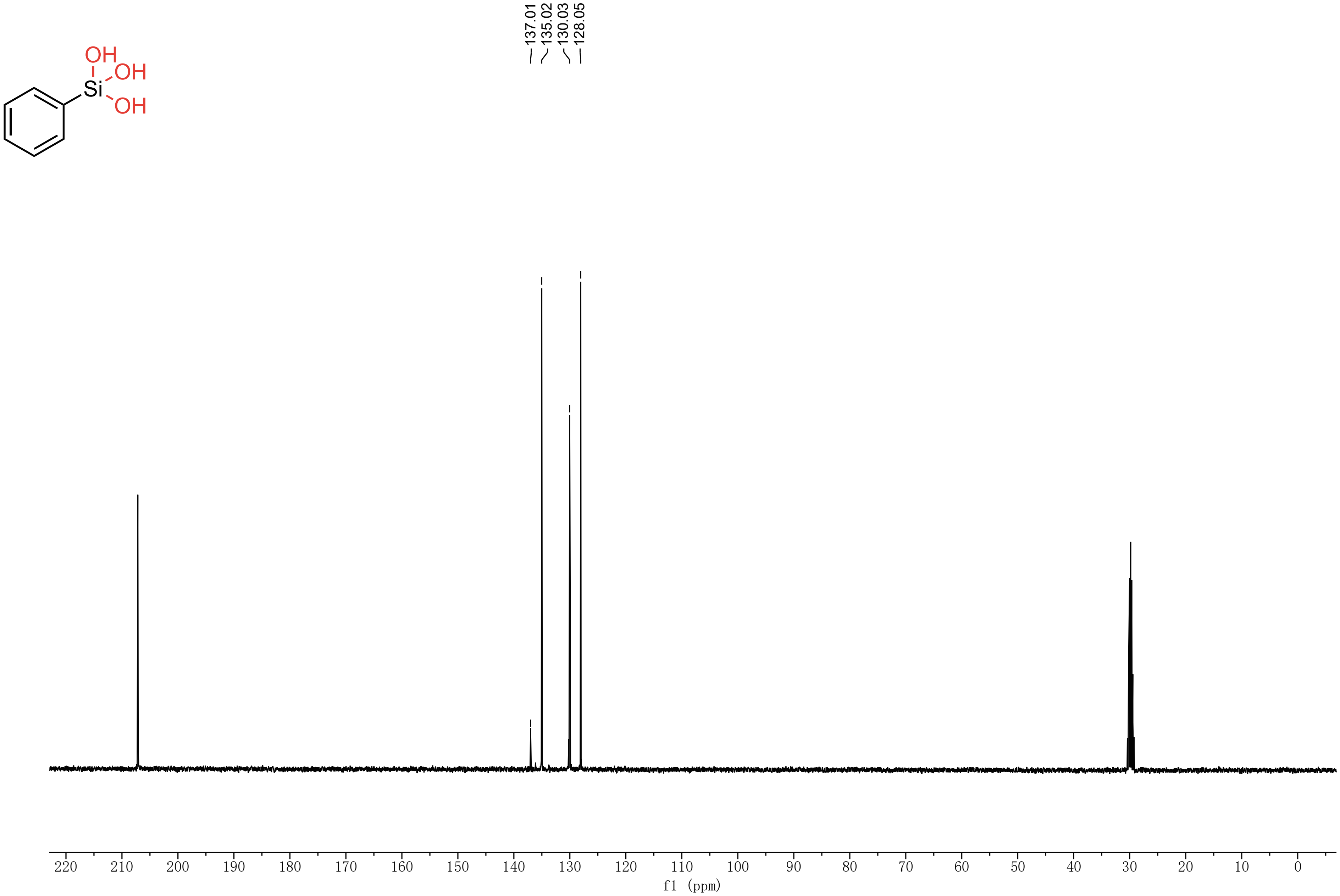

Compound **2al** ^{1}H NMR

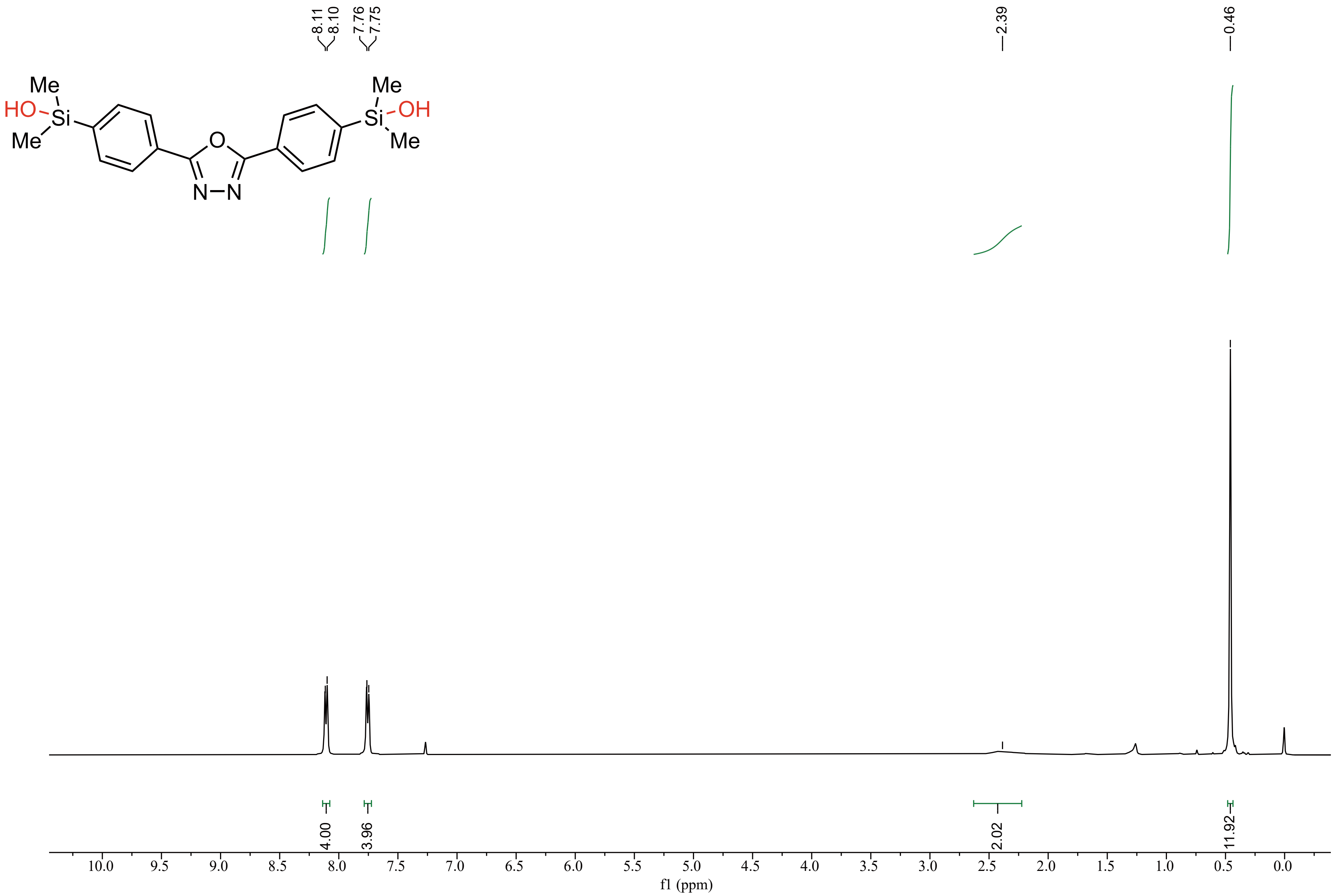

Compound **2al** ^{13}C NMR

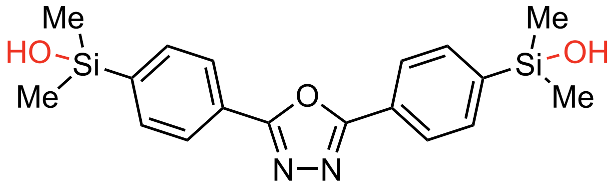

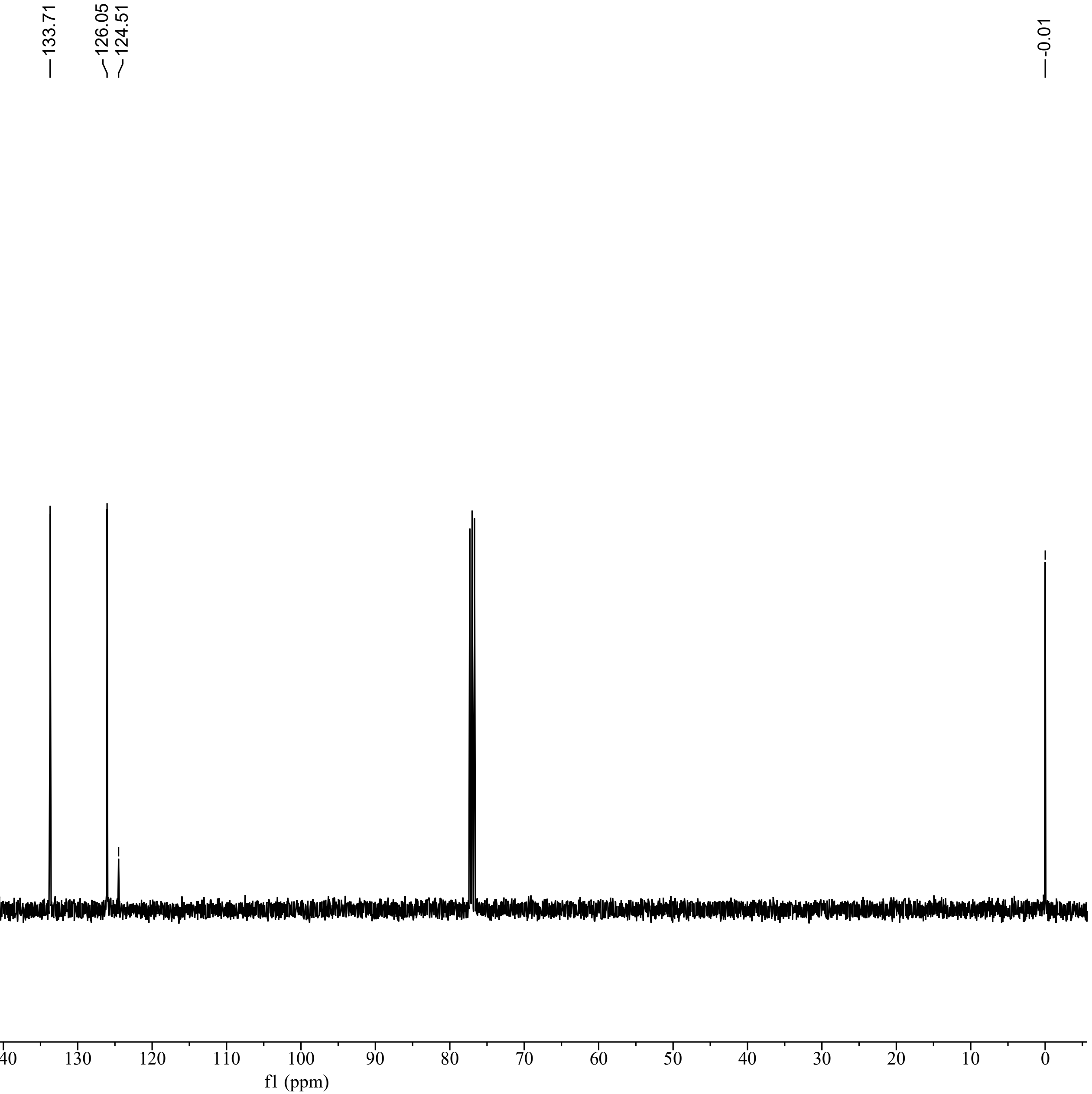

Compound **2am** ^{1}H NMR

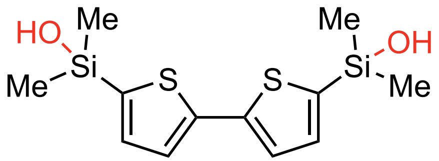

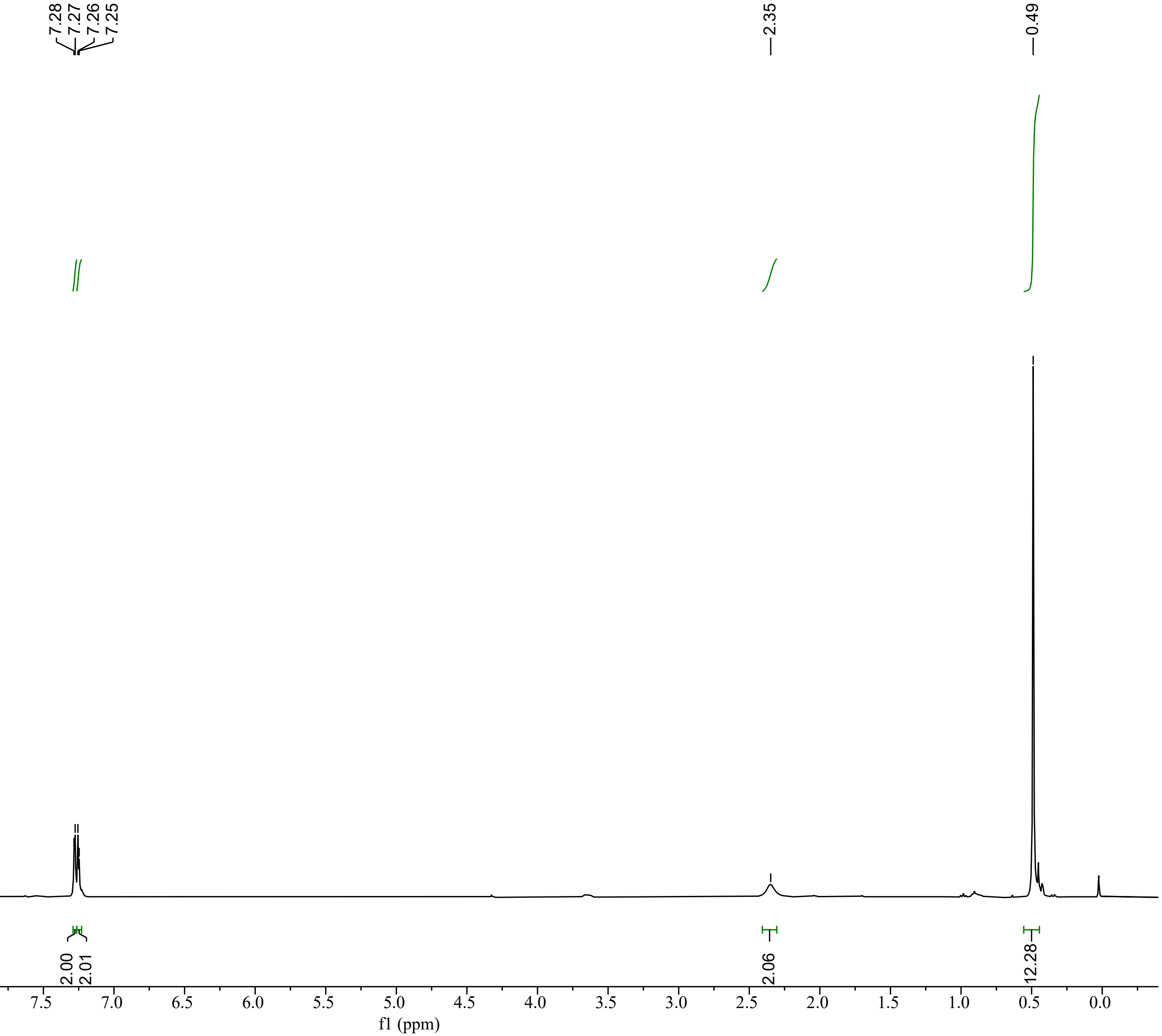

Compound **2am** ^{13}C NMR

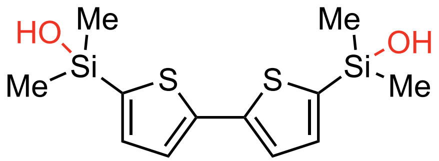

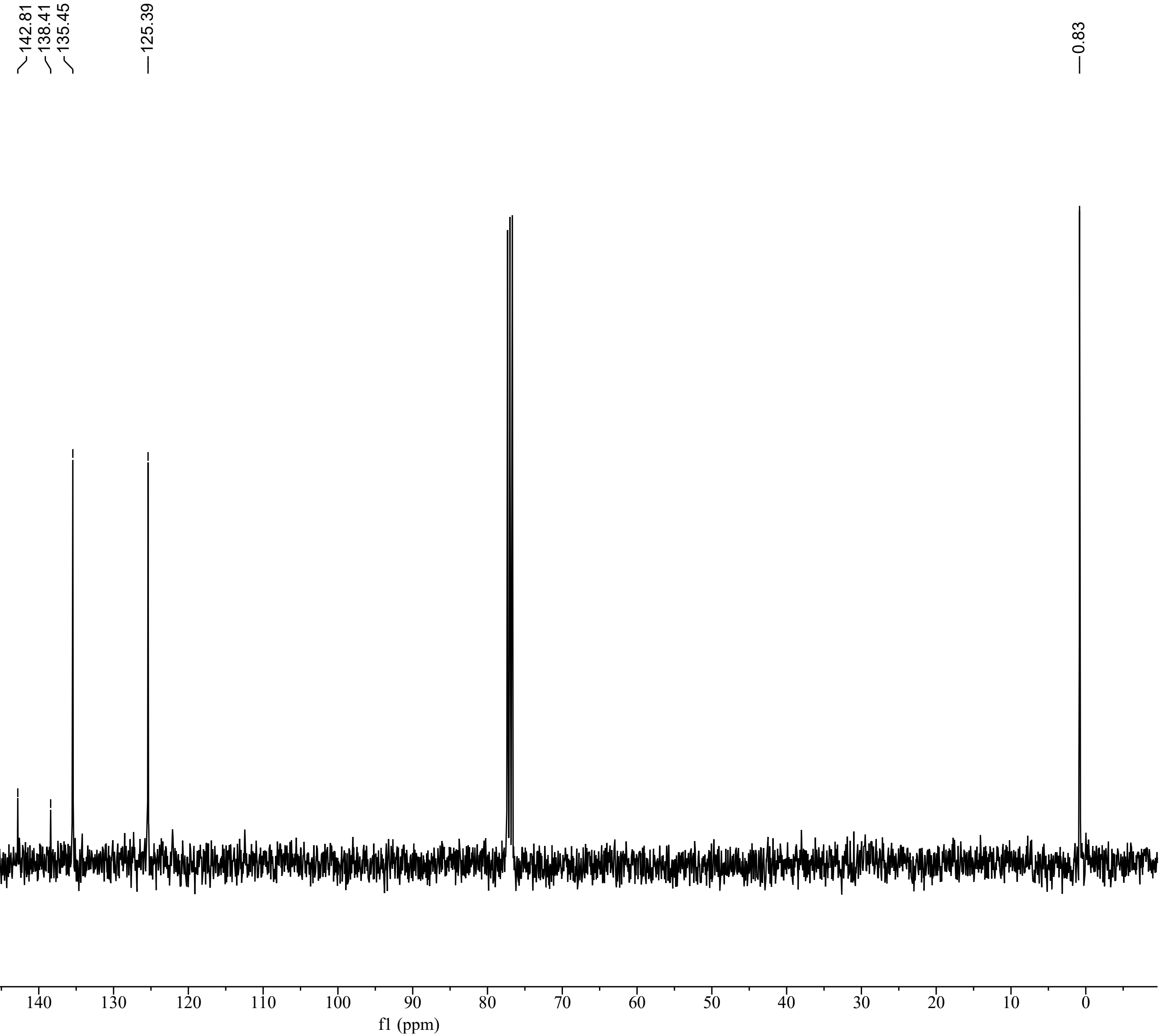

Compound **2an** [1]H NMR

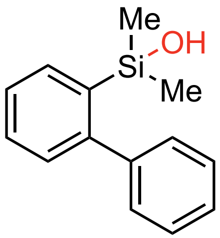

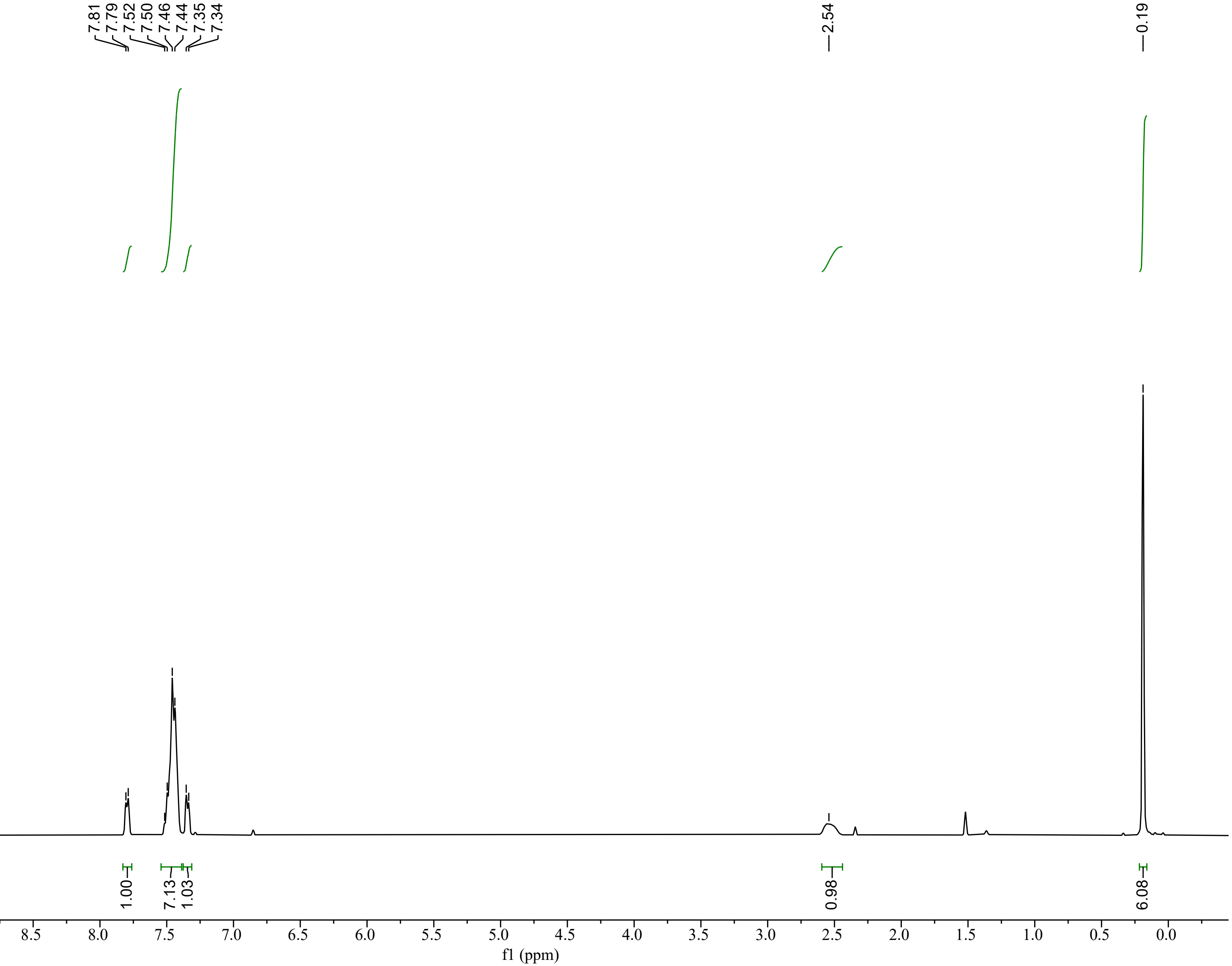

Compound **2an** ^{13}C NMR

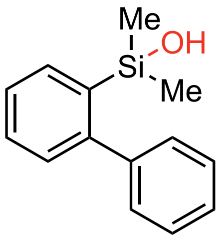

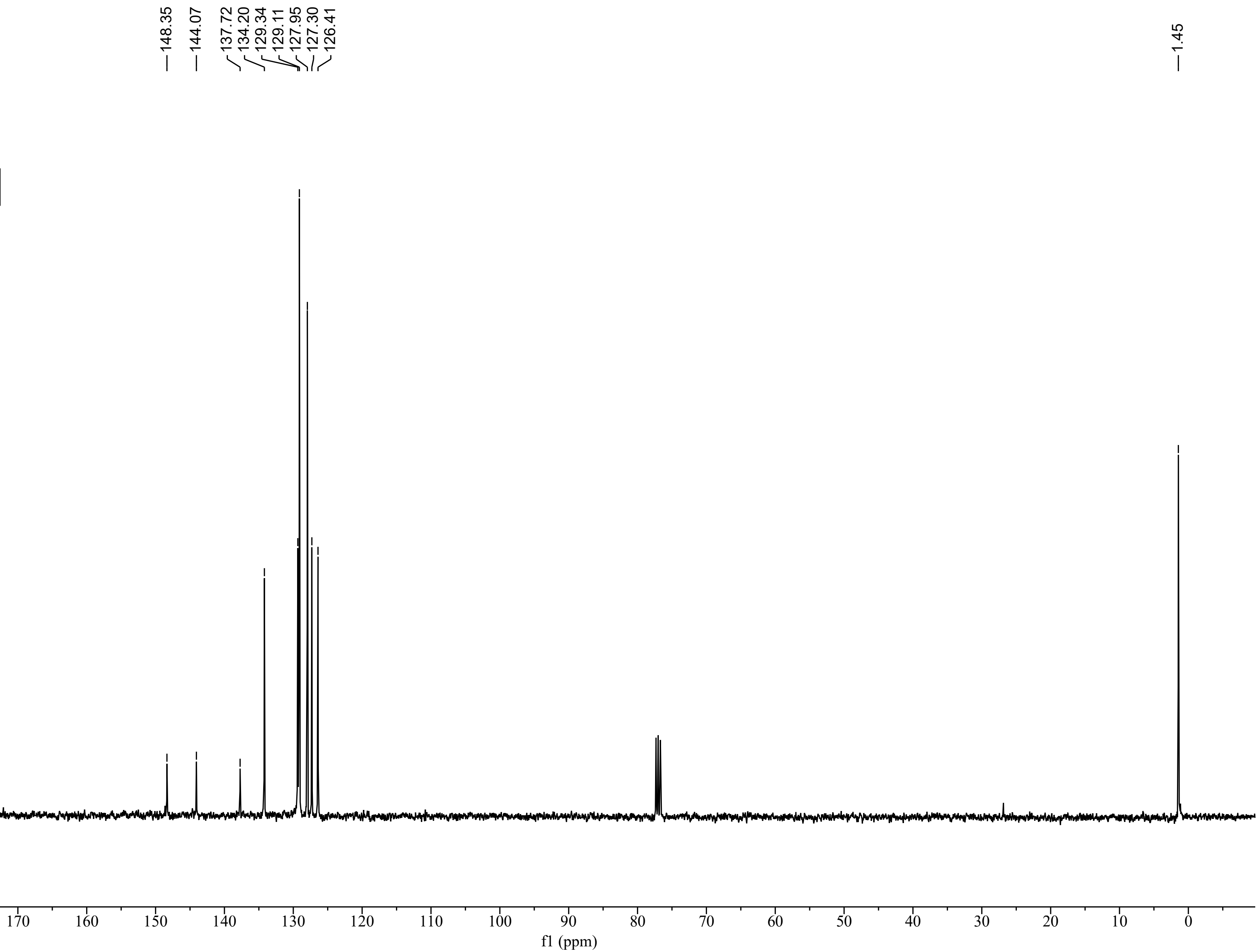

Compound **2ao** ^{1}H NMR

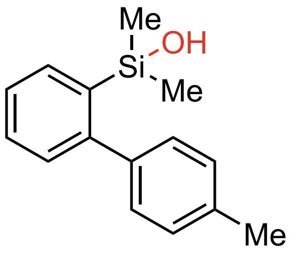

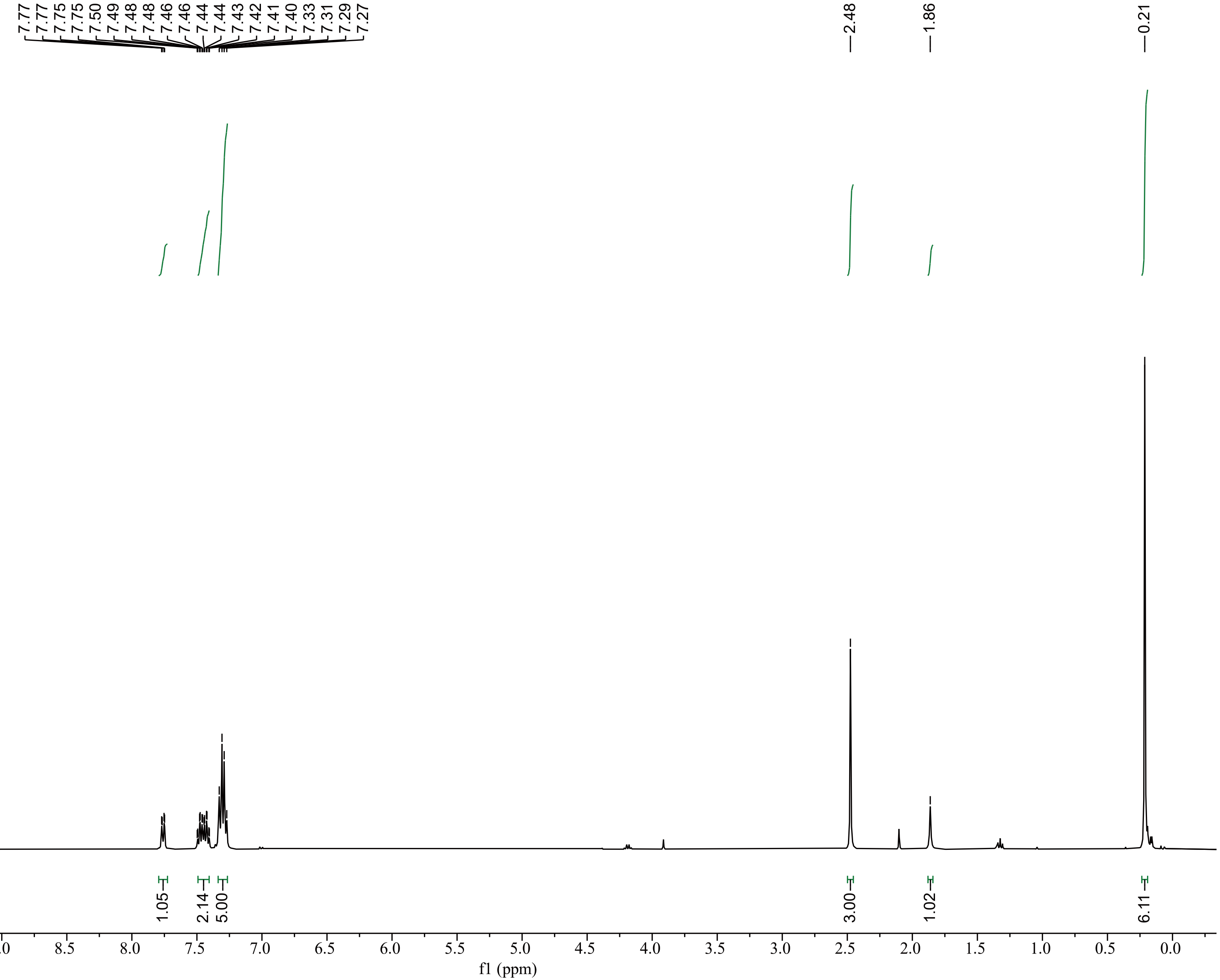

Compound **2ao** ^{13}C NMR

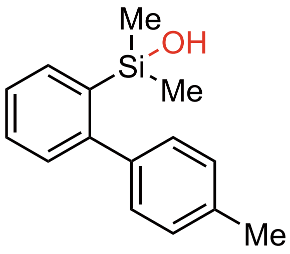

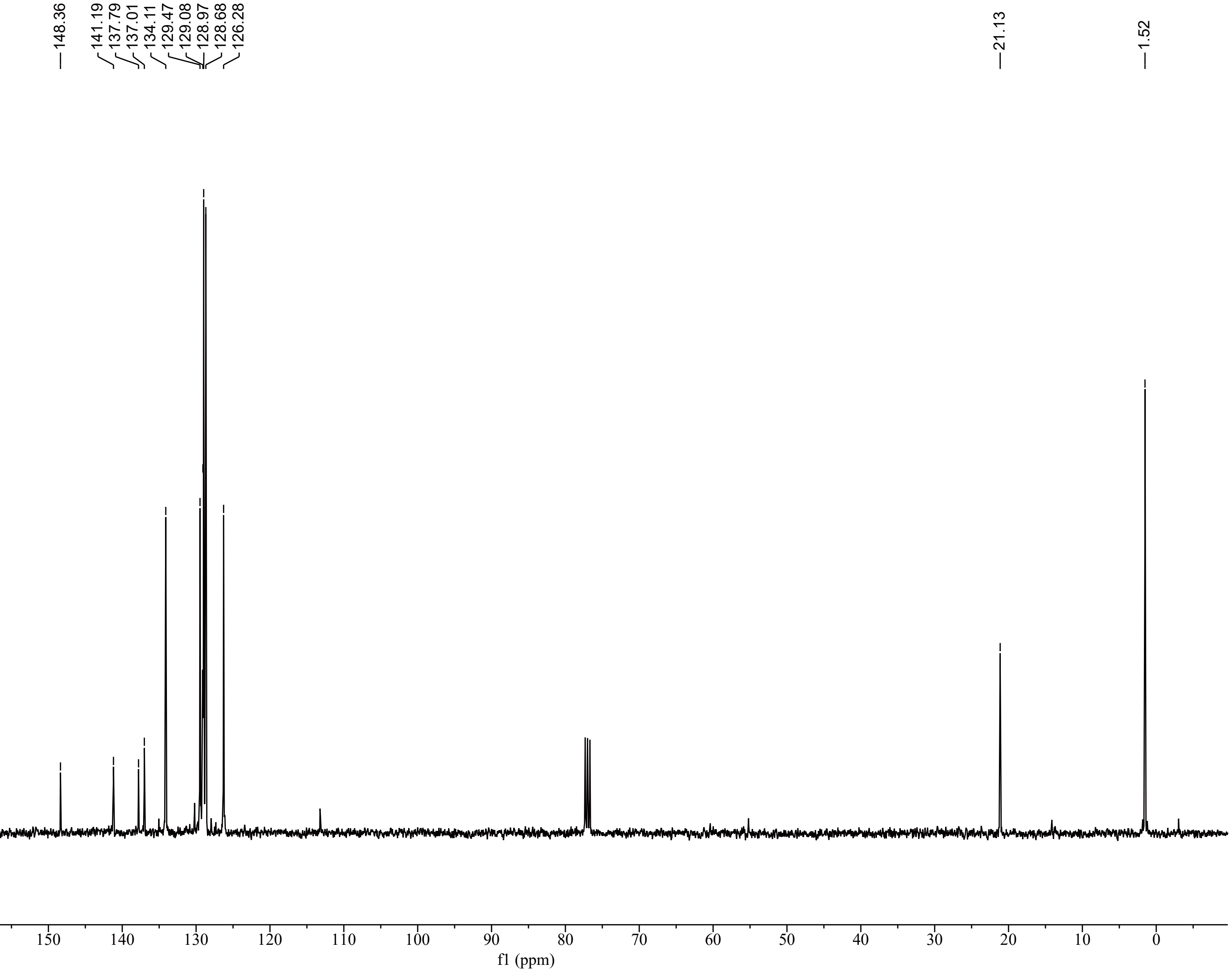

Compound **2ap** ^{1}H NMR

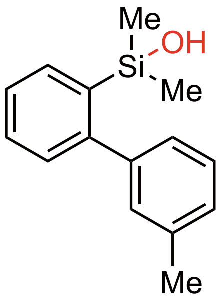

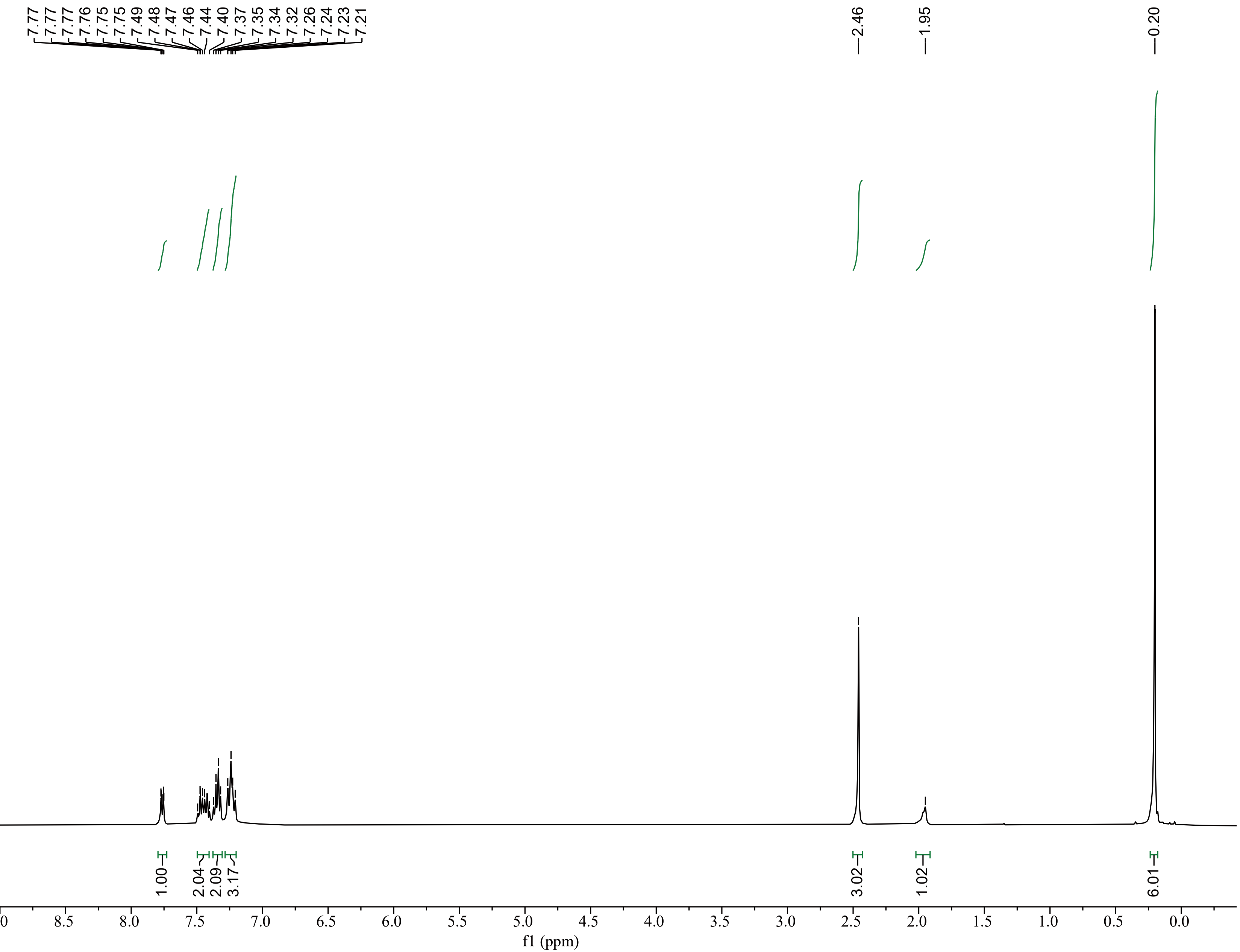

Compound **2ap** ^{13}C NMR

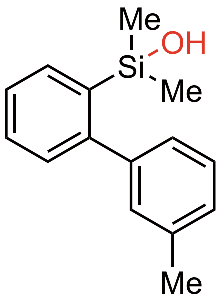

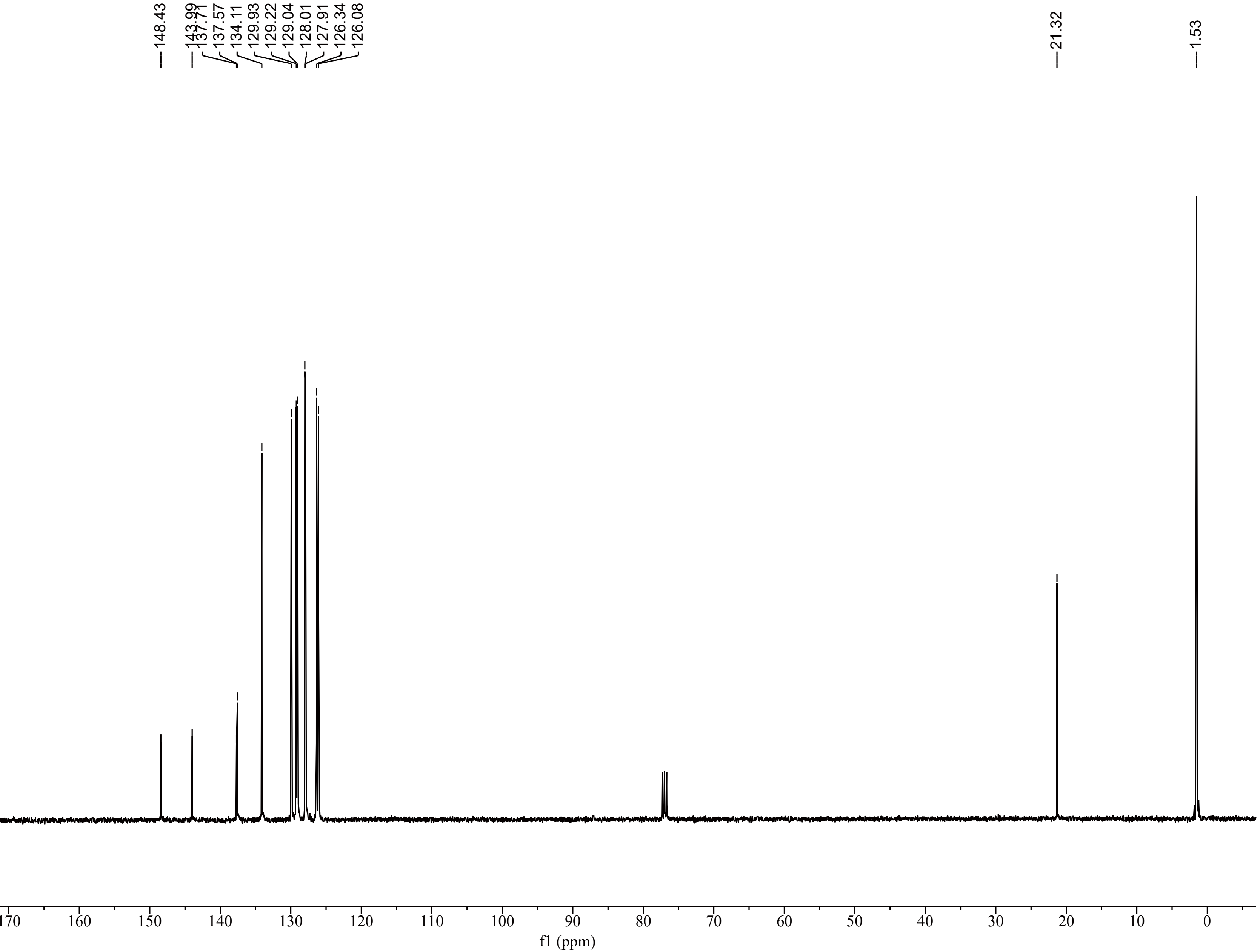

Compound **2aq** ^{1}H NMR

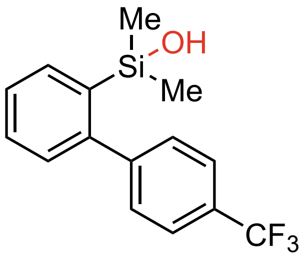

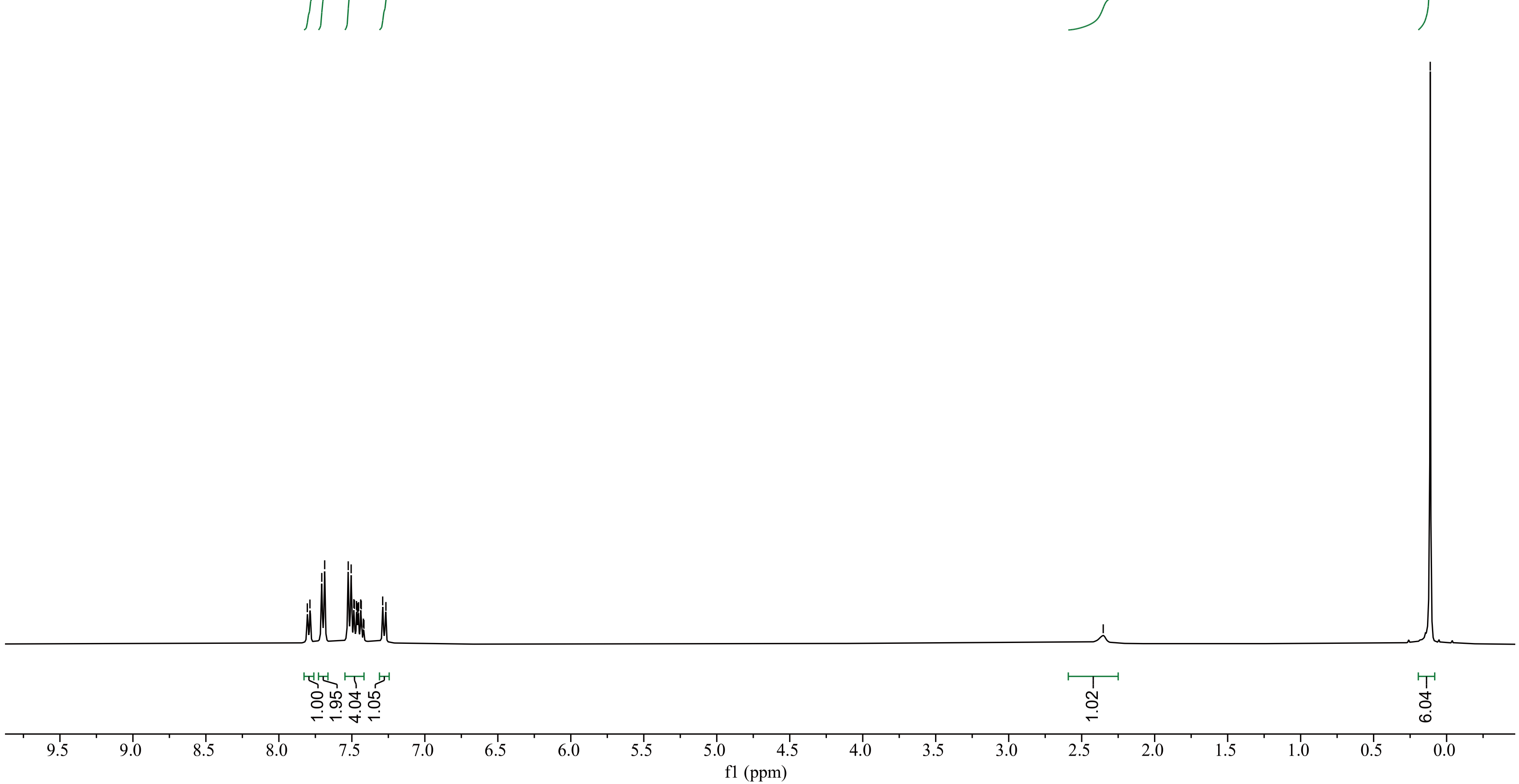

Compound **2aq** ^{13}C NMR

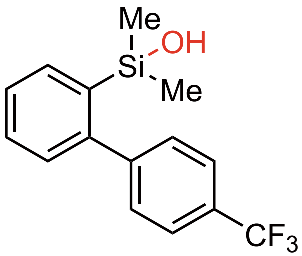

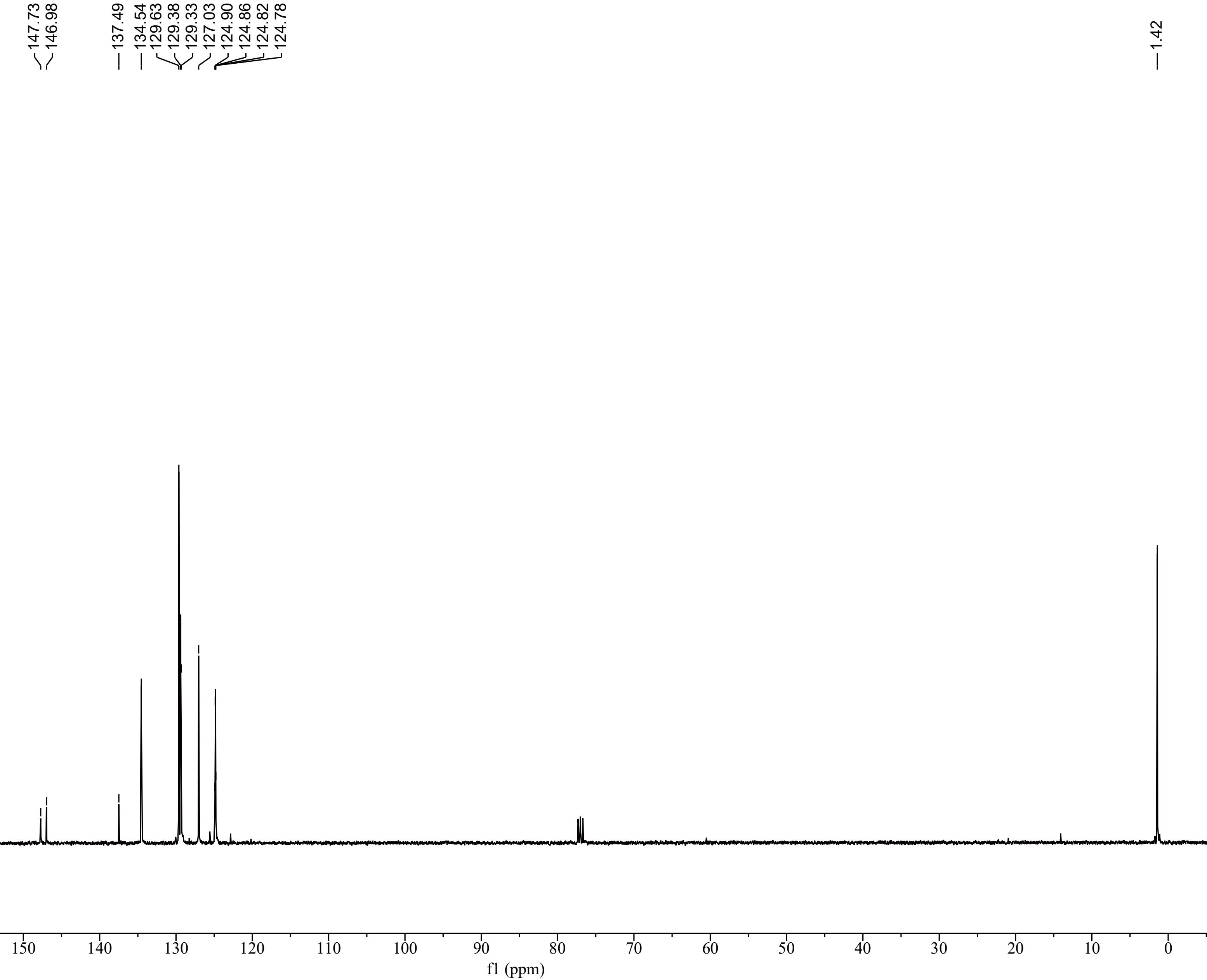

Compound **2aq** ^{19}F NMR

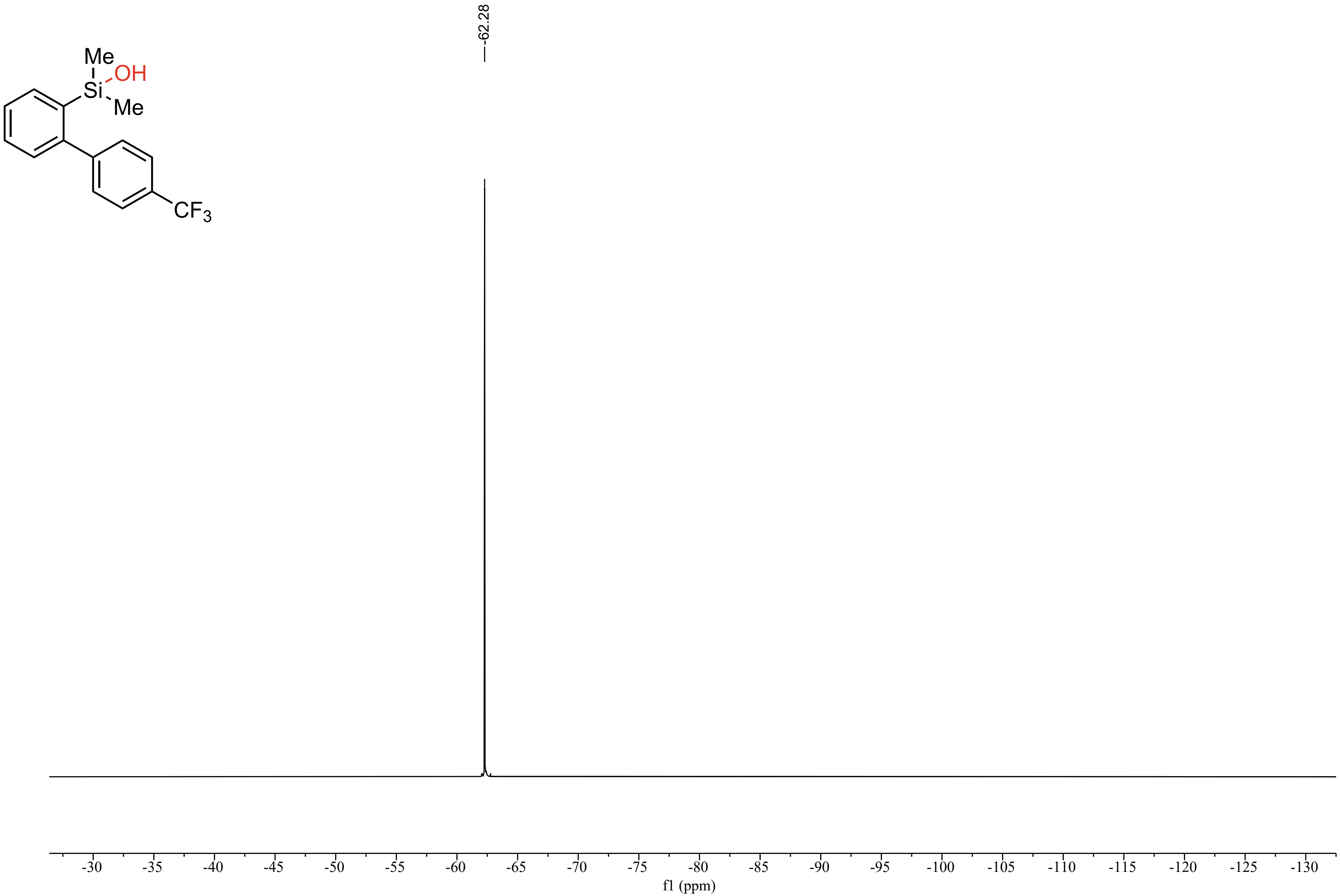

Compound **2ar** ^{1}H NMR

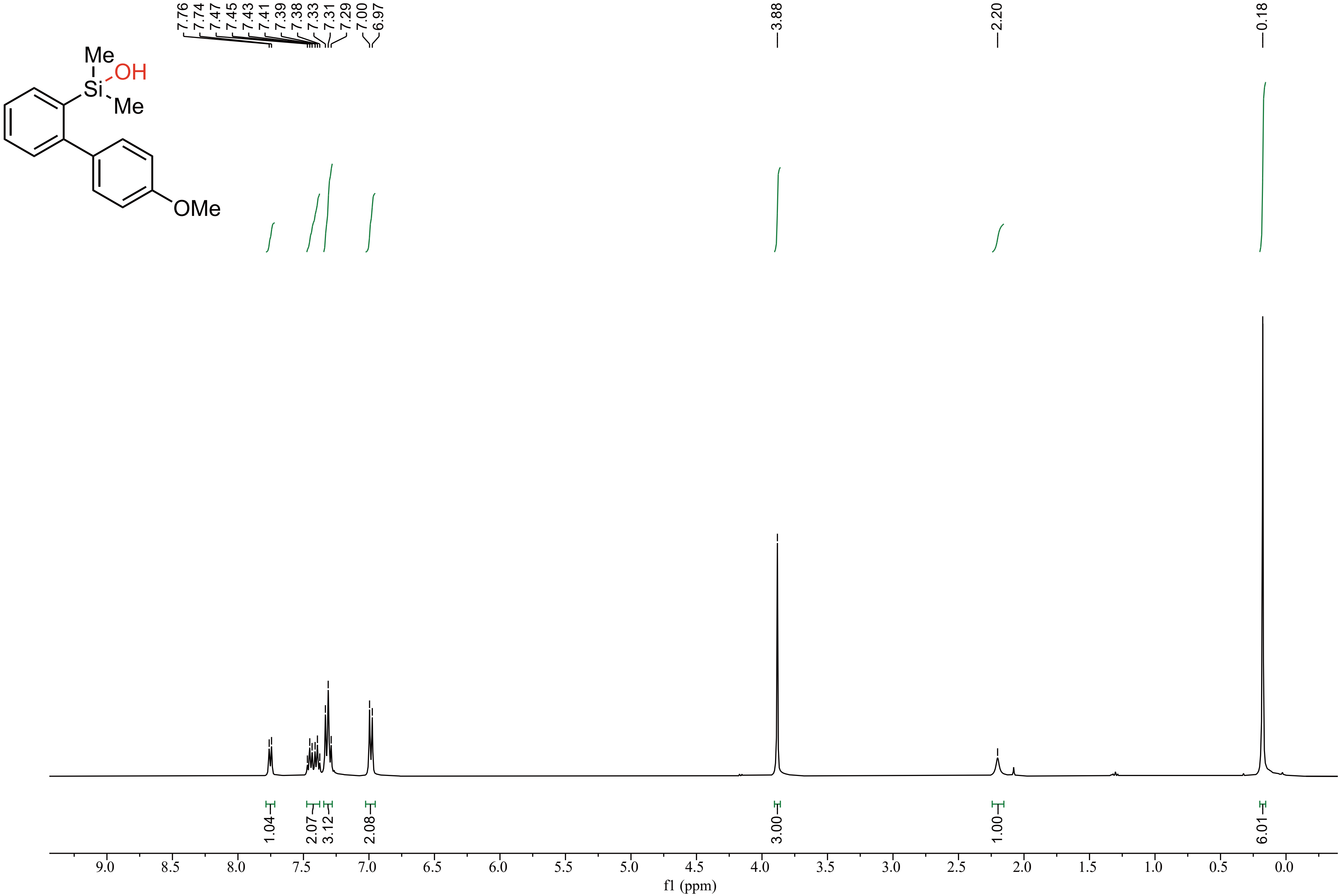

Compound **2ar** ^{13}C NMR

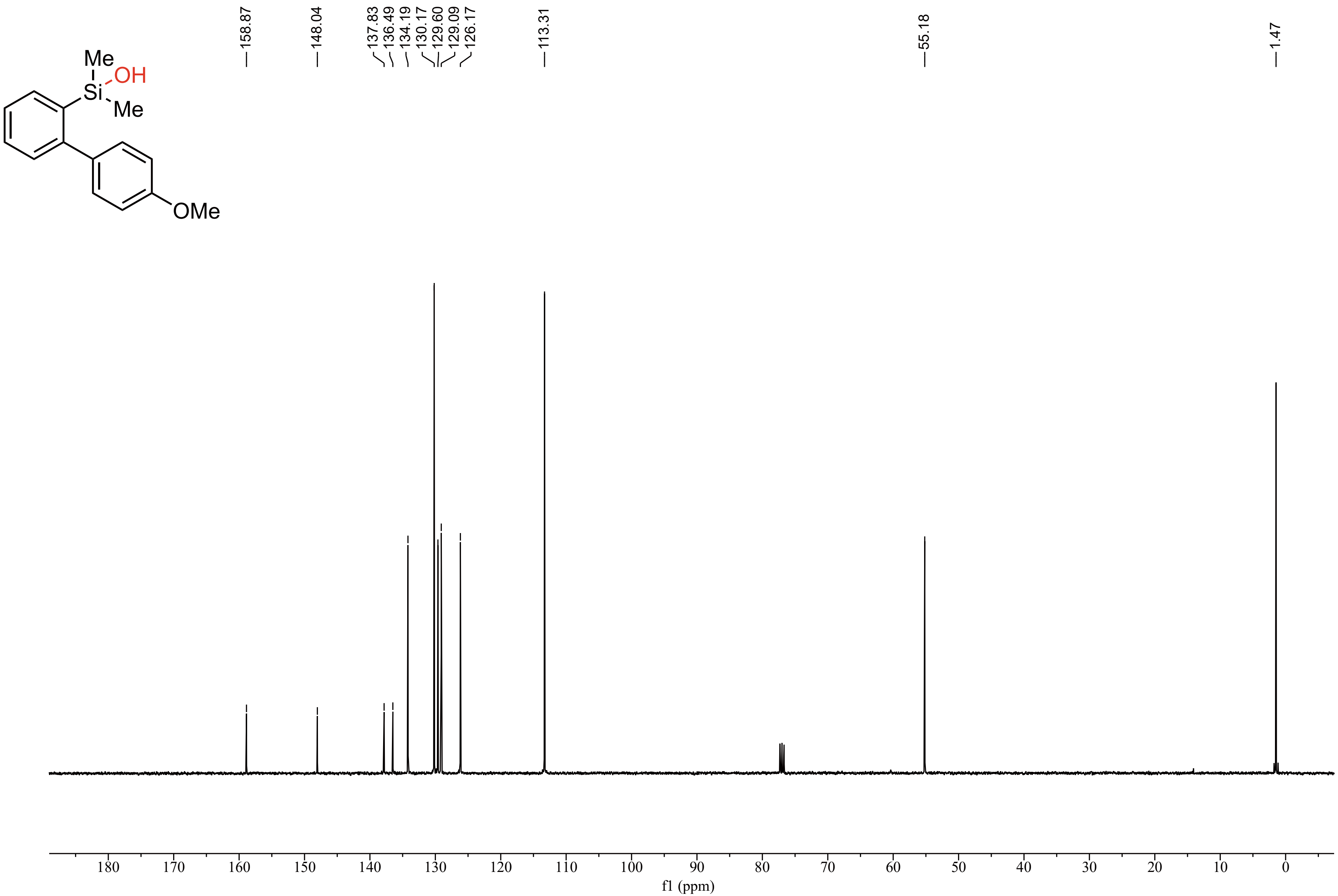

Compound **2as** ^{1}H NMR

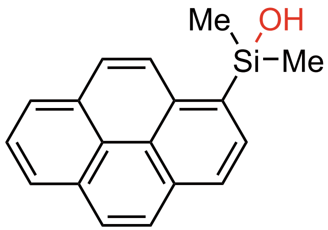

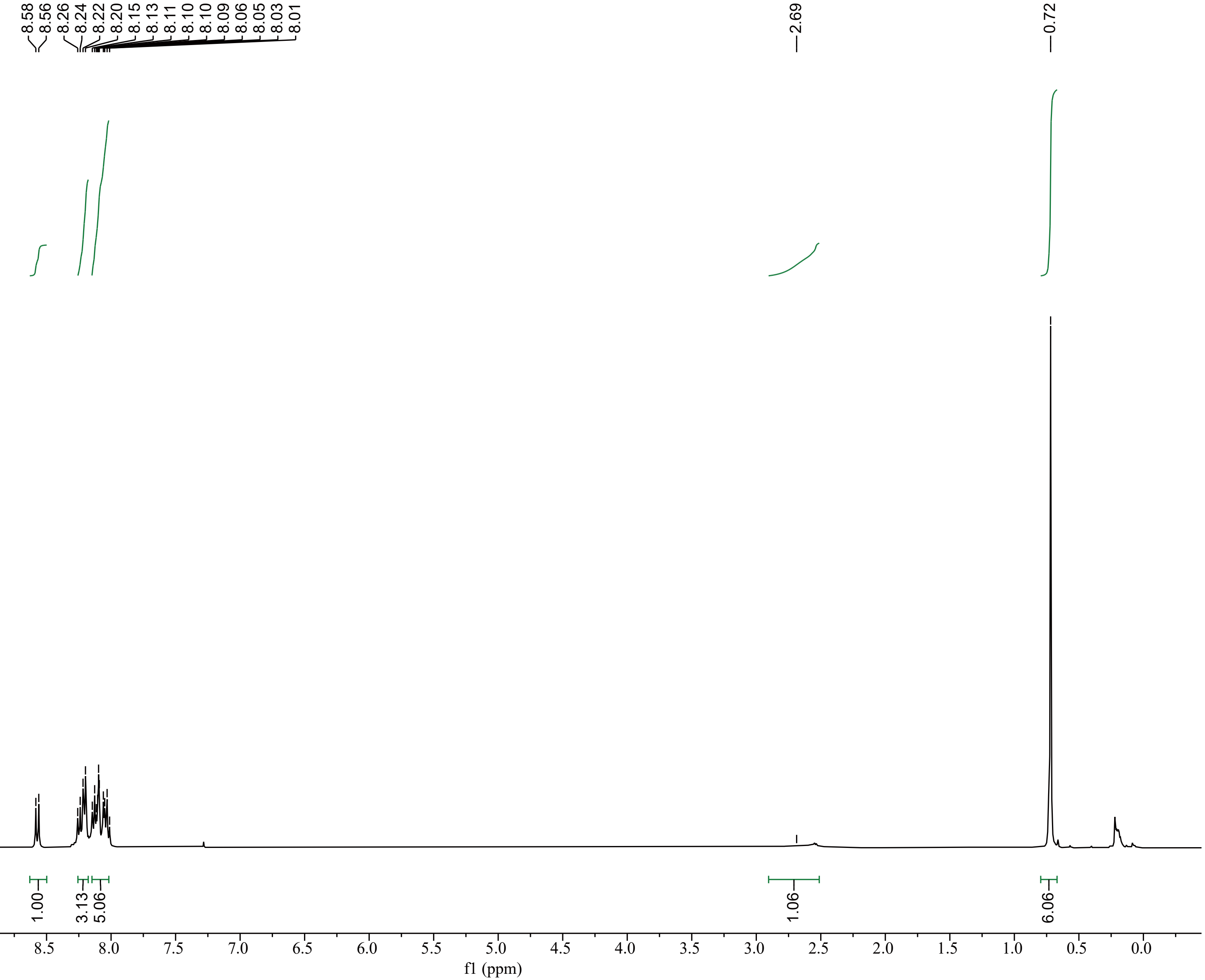

Compound **2as** ^{13}C NMR

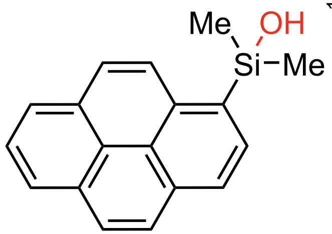

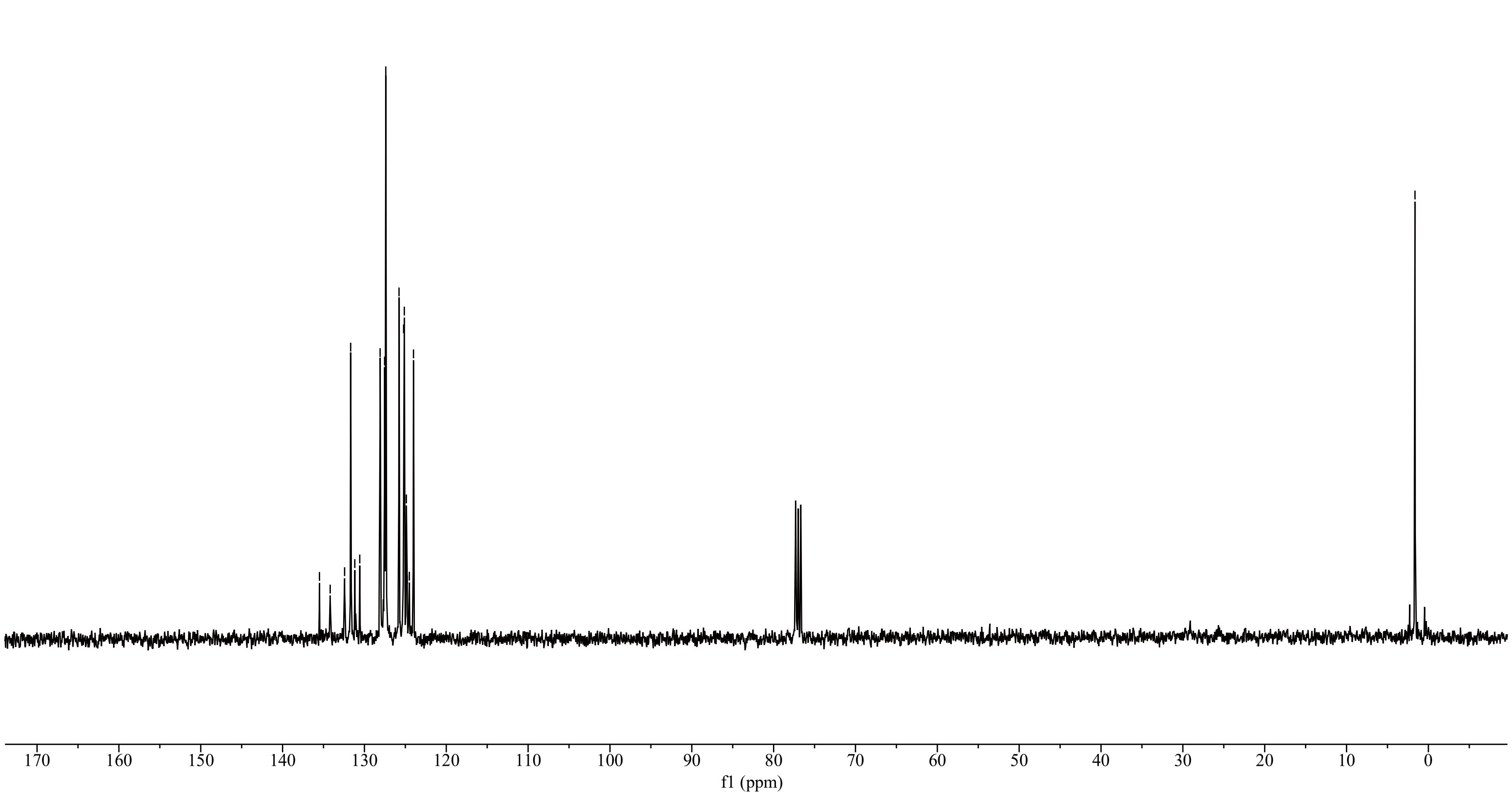

Compound **2at** ^{1}H NMR

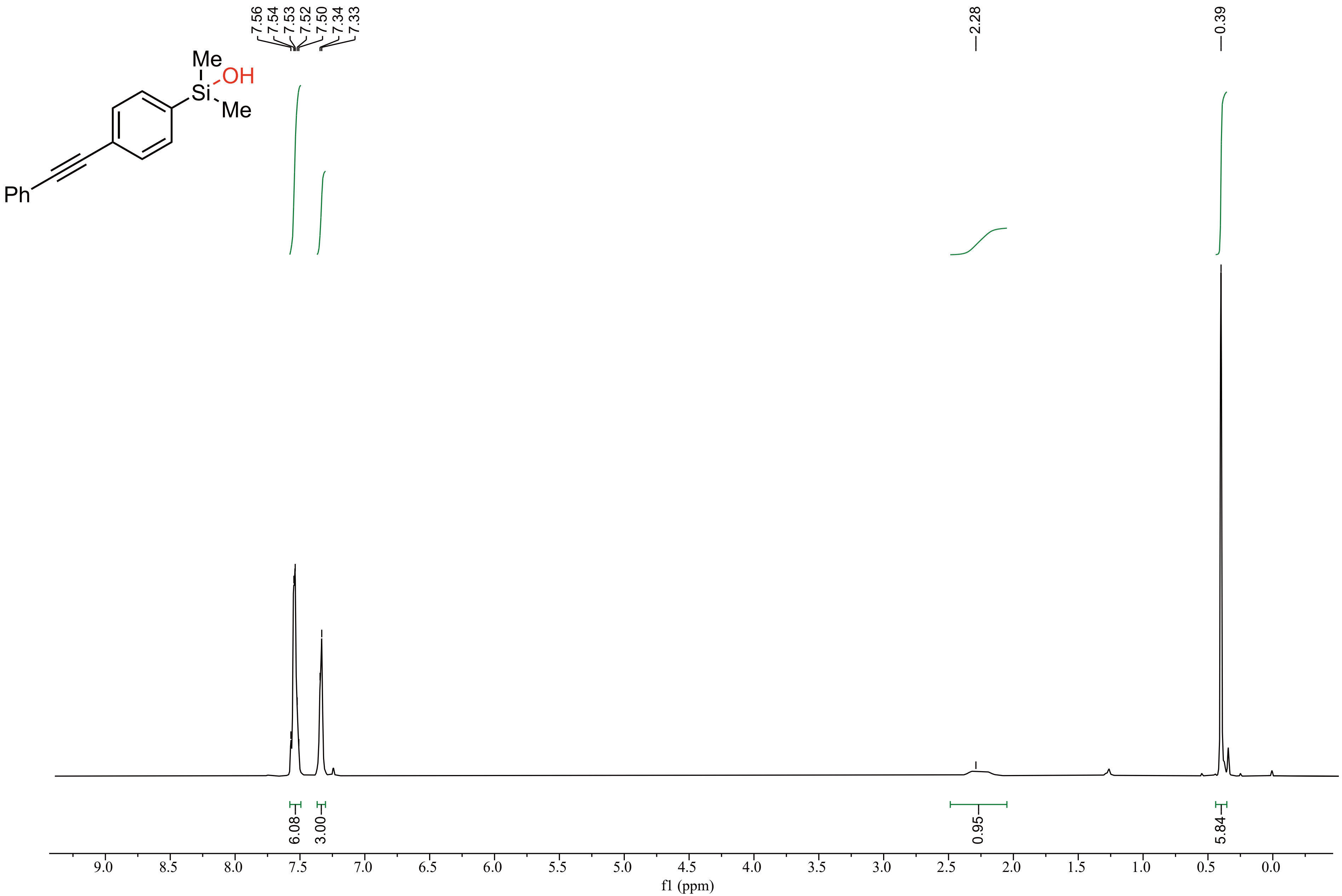

Compound **2at** ^{13}C NMR

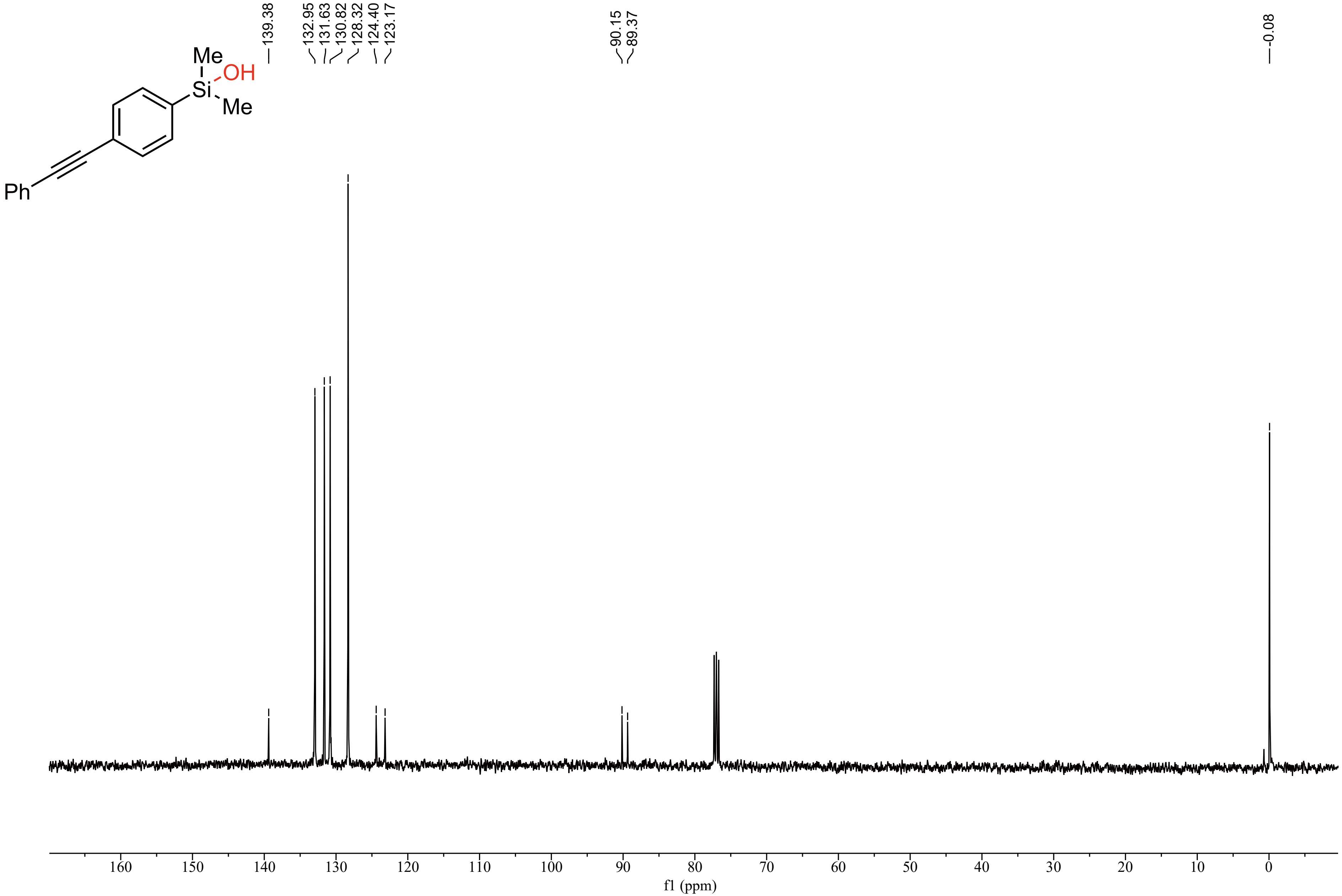

Compound **2au** ^{1}H NMR

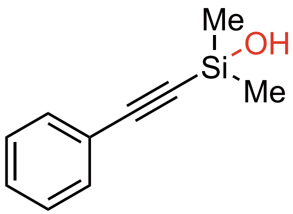

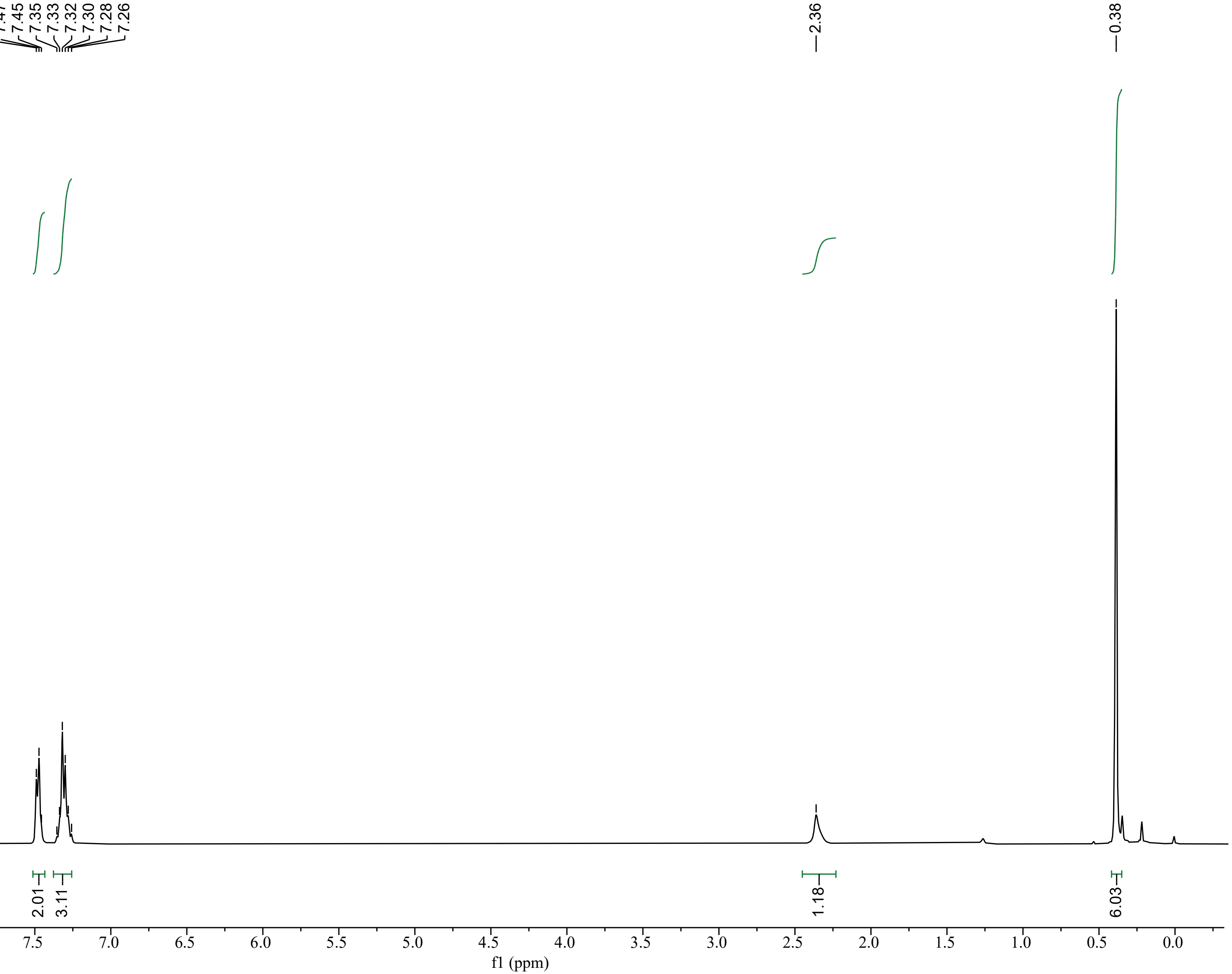

Compound **2au** ^{13}C NMR

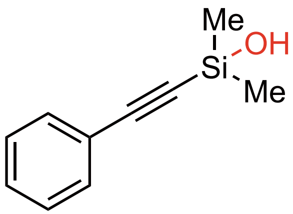

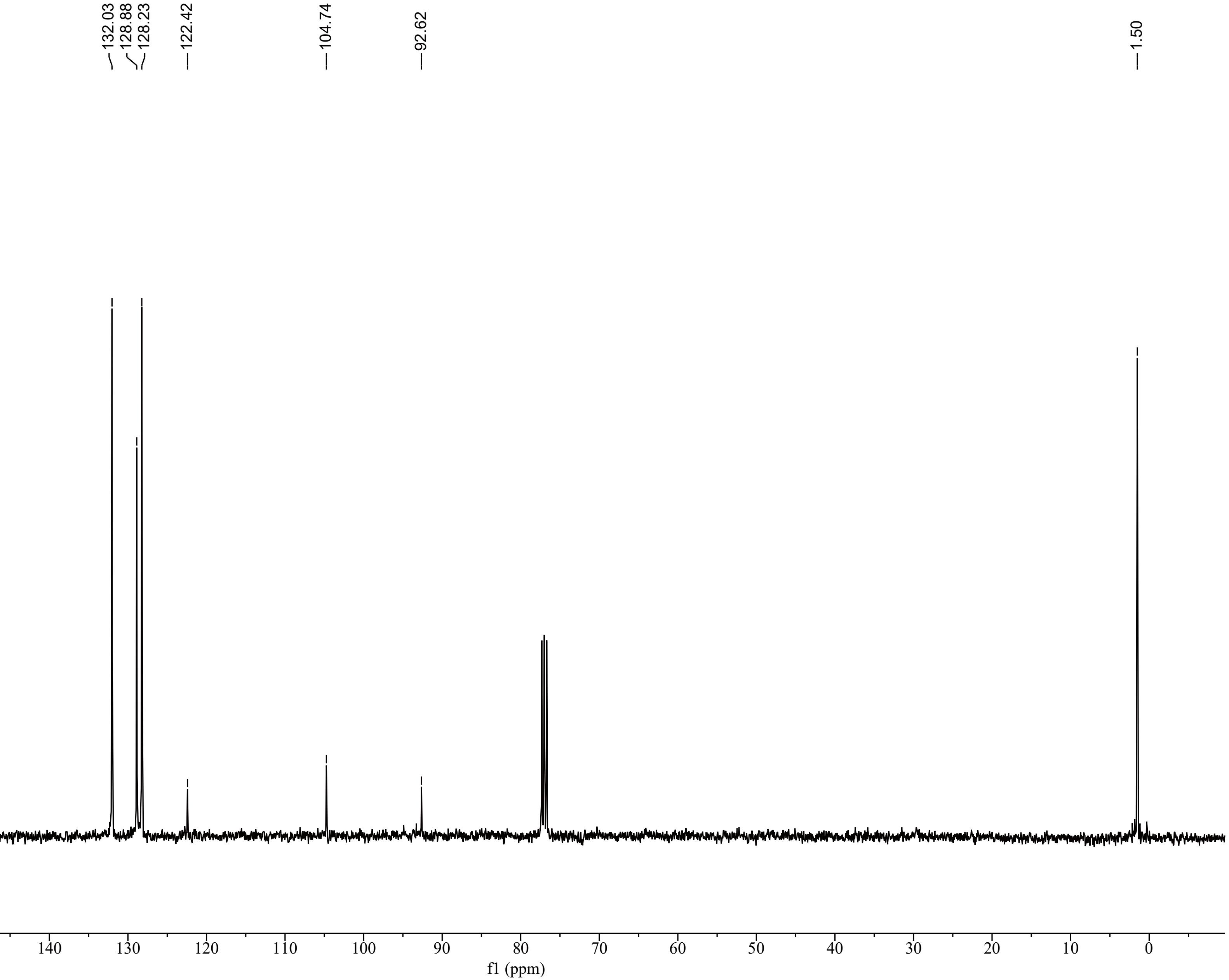

Compound **2av** [1]H NMR

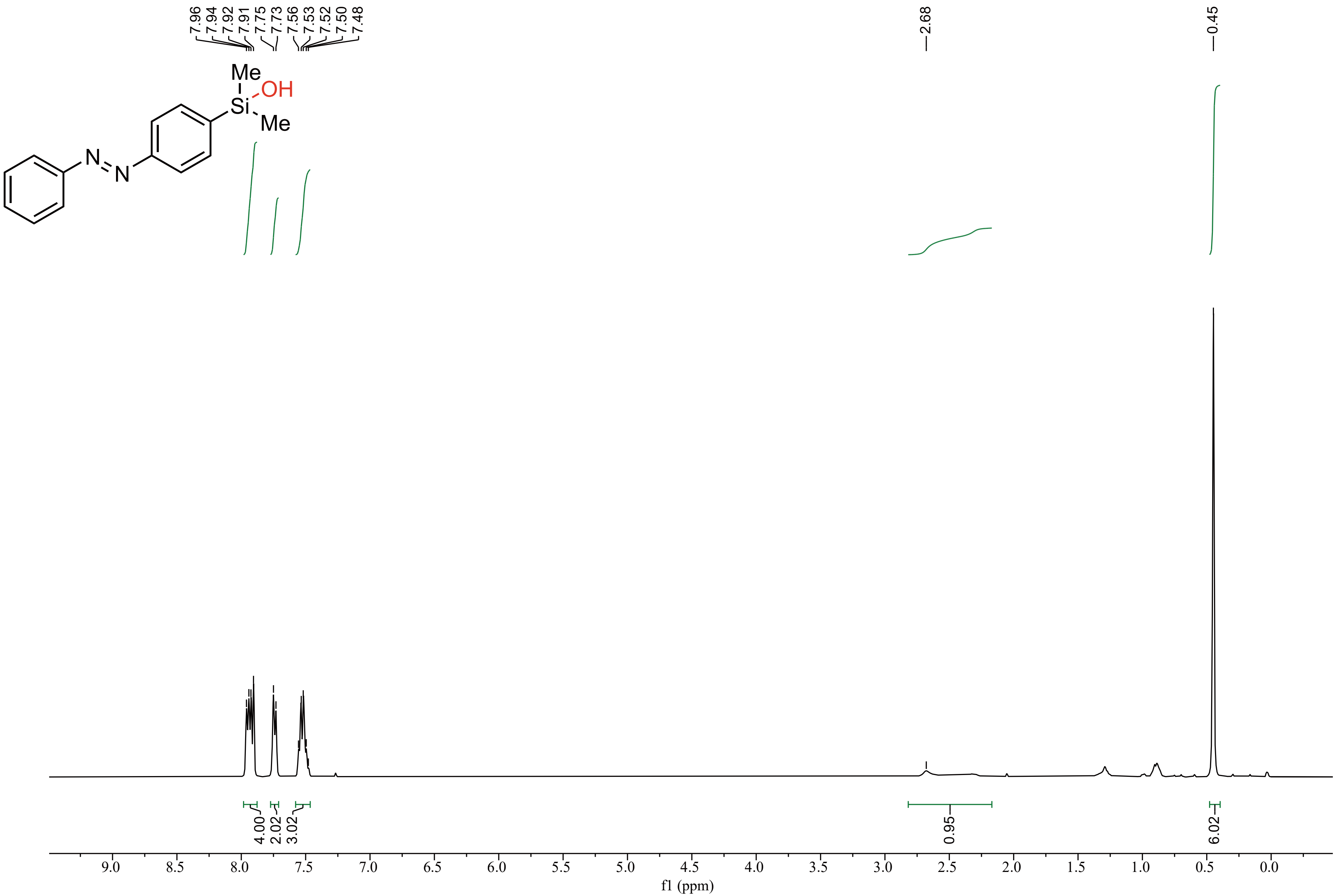

Compound **2av** ^{13}C NMR

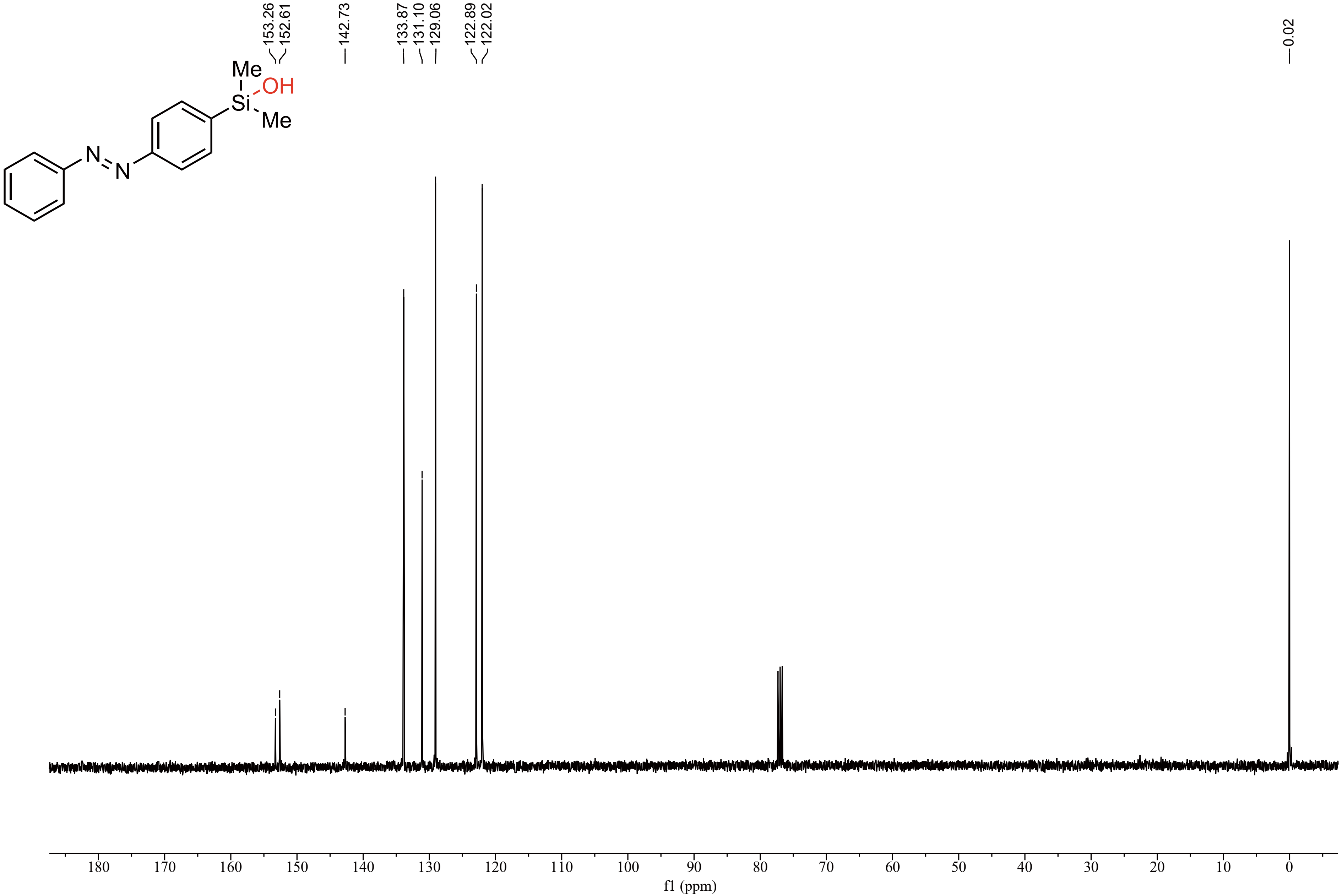

Compound **2aw** ^{1}H NMR

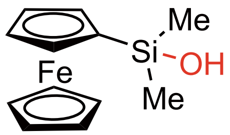

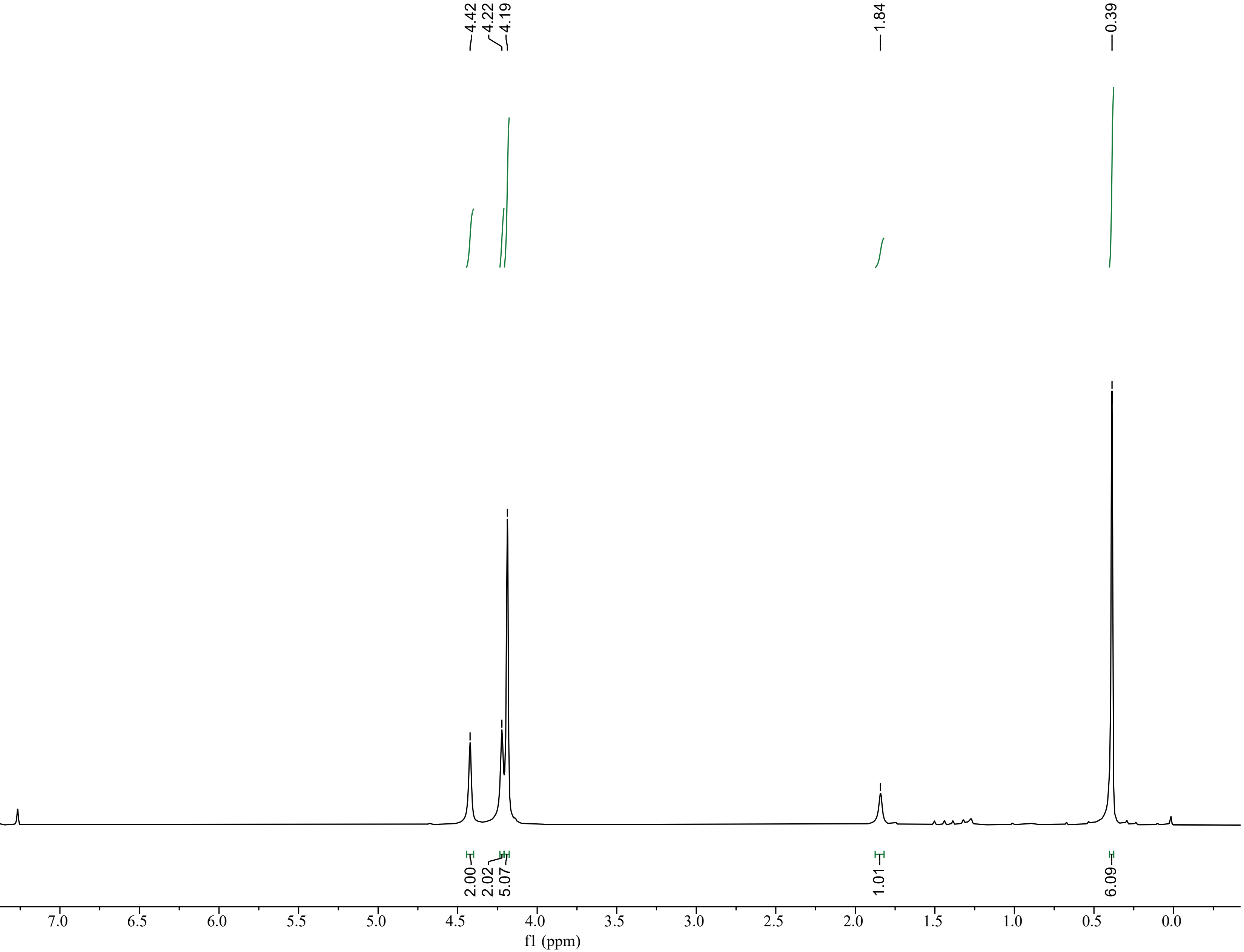

Compound **2aw** ^{13}C NMR

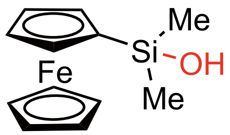

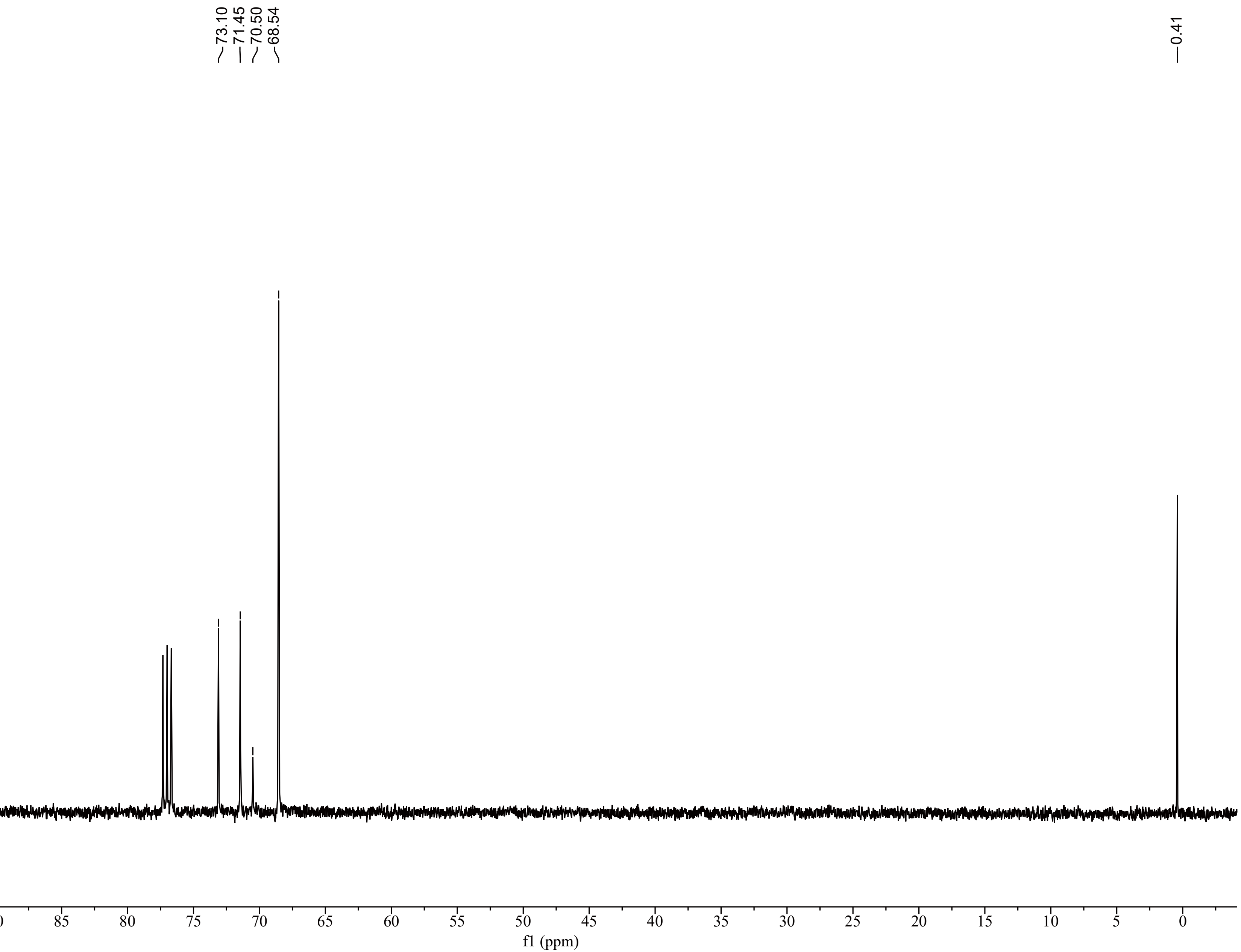

Compound **2ax** ^{1}H NMR

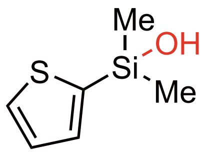

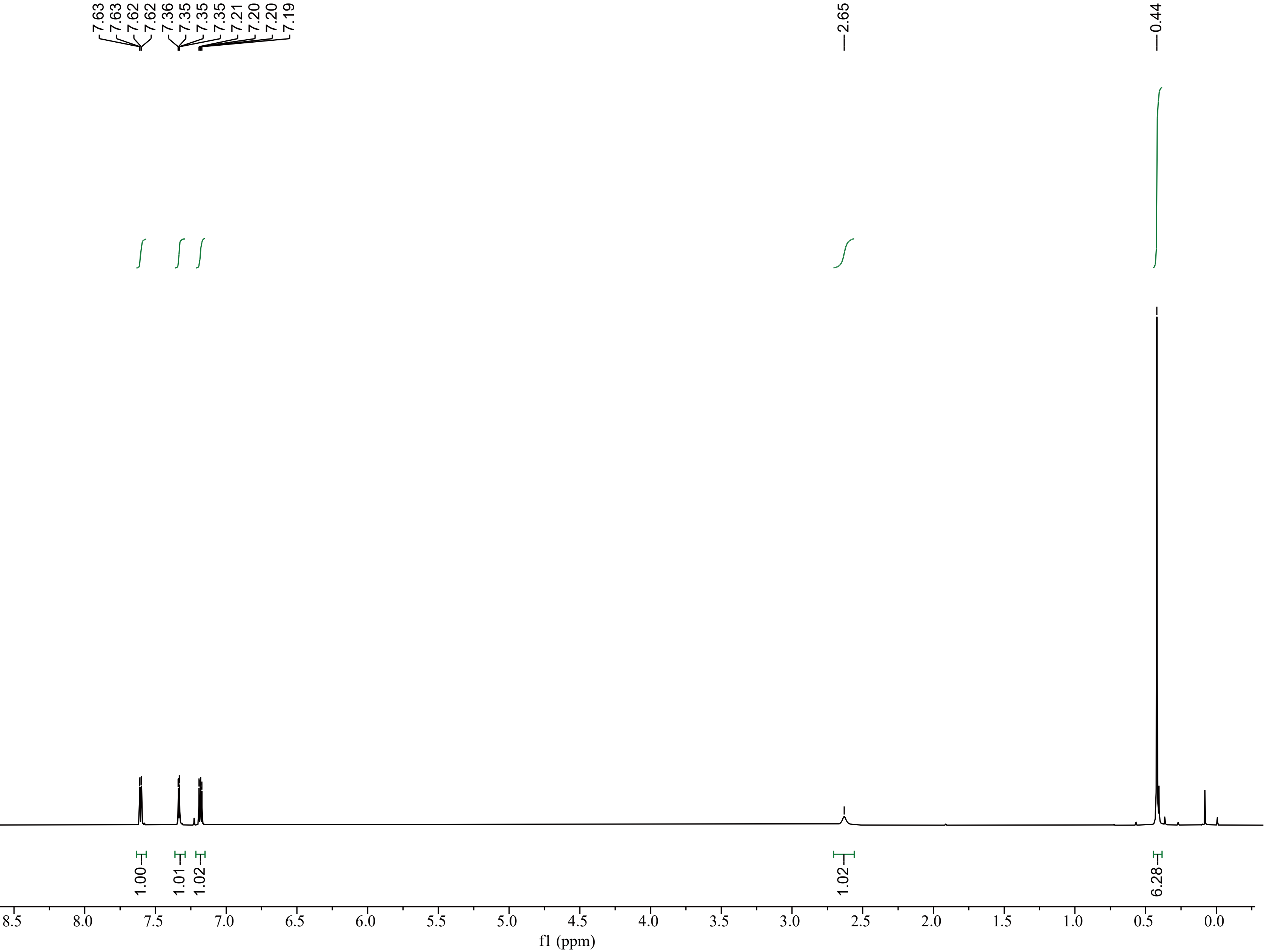

Compound **2ax** ^{13}C NMR

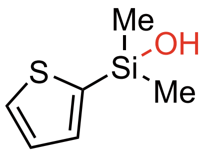

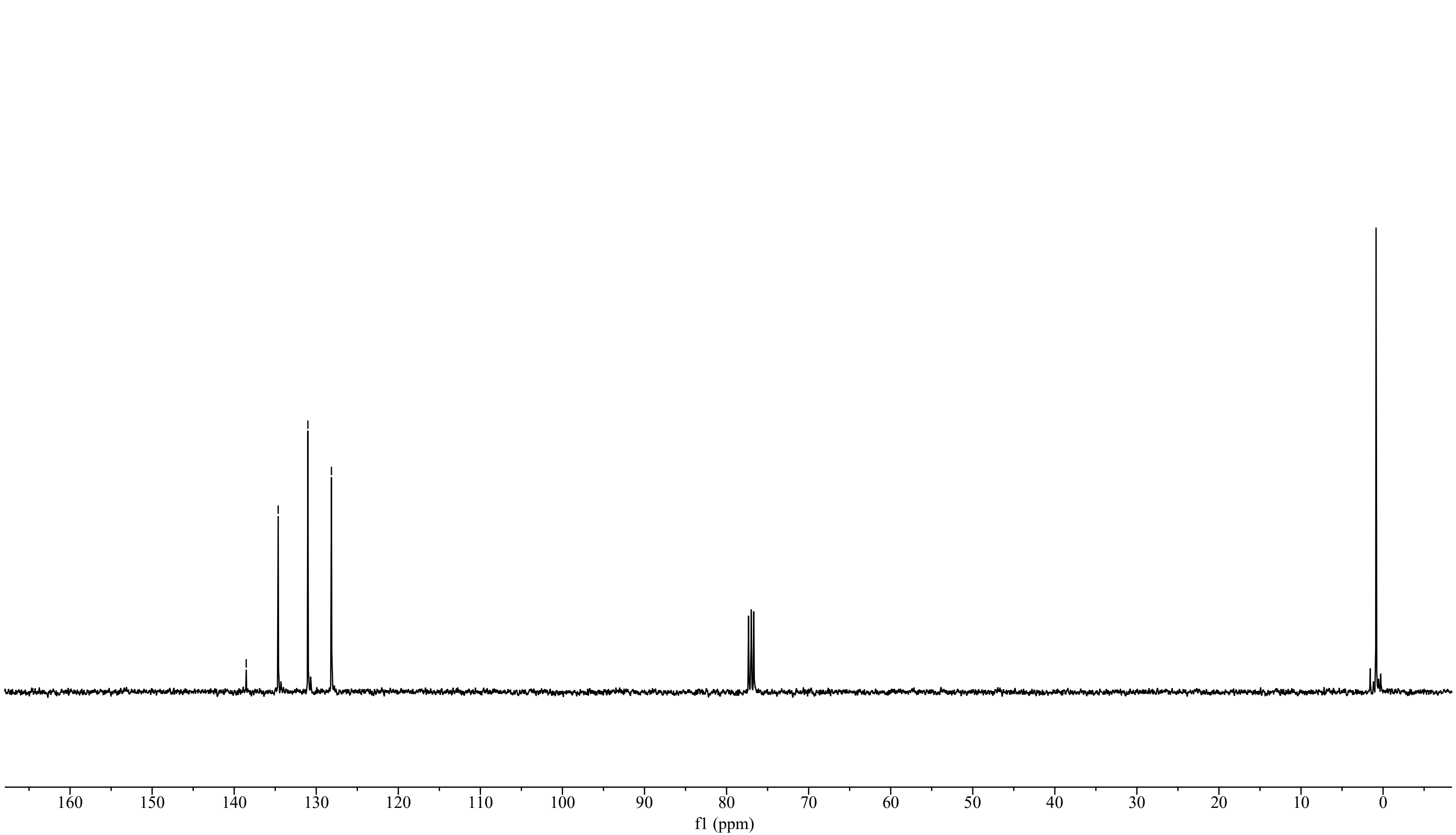

Compound **2ay** [1]H NMR

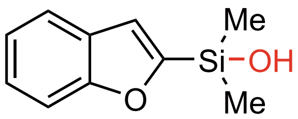

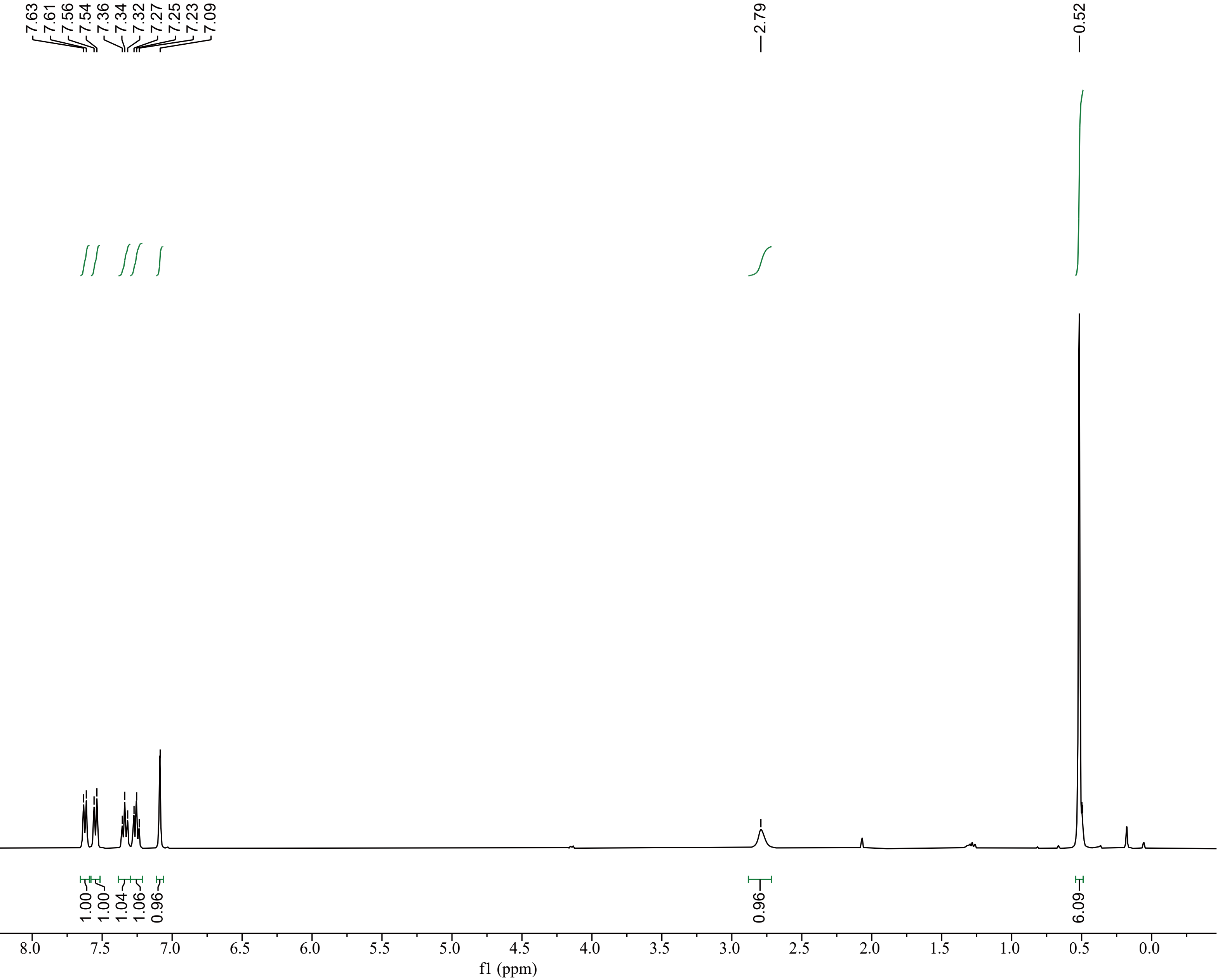

Compound **2ay** ^{13}C NMR

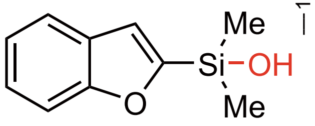

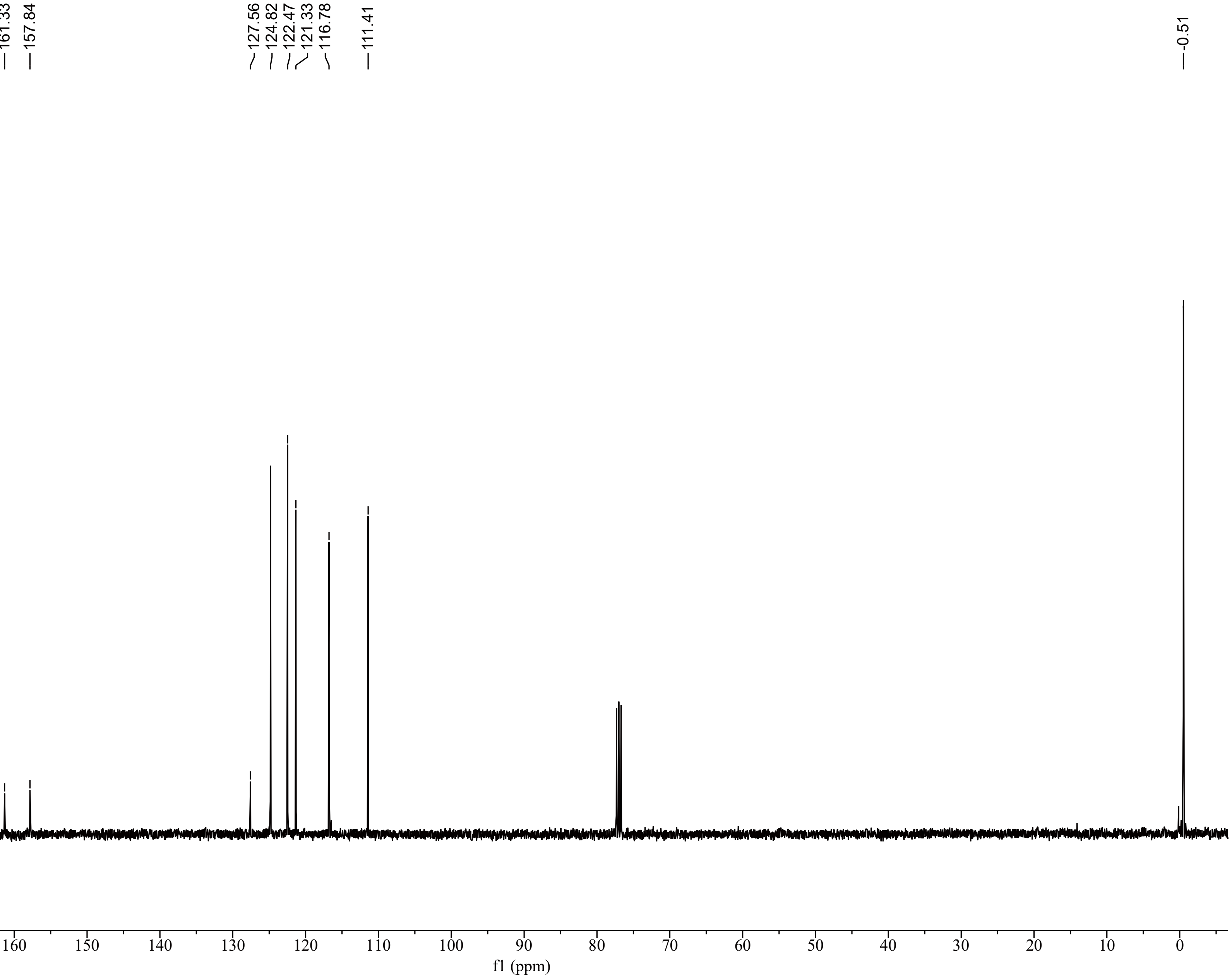

Compound **2az** ^{1}H NMR

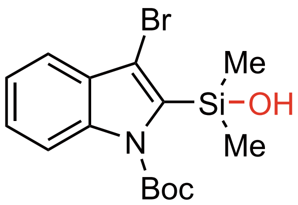

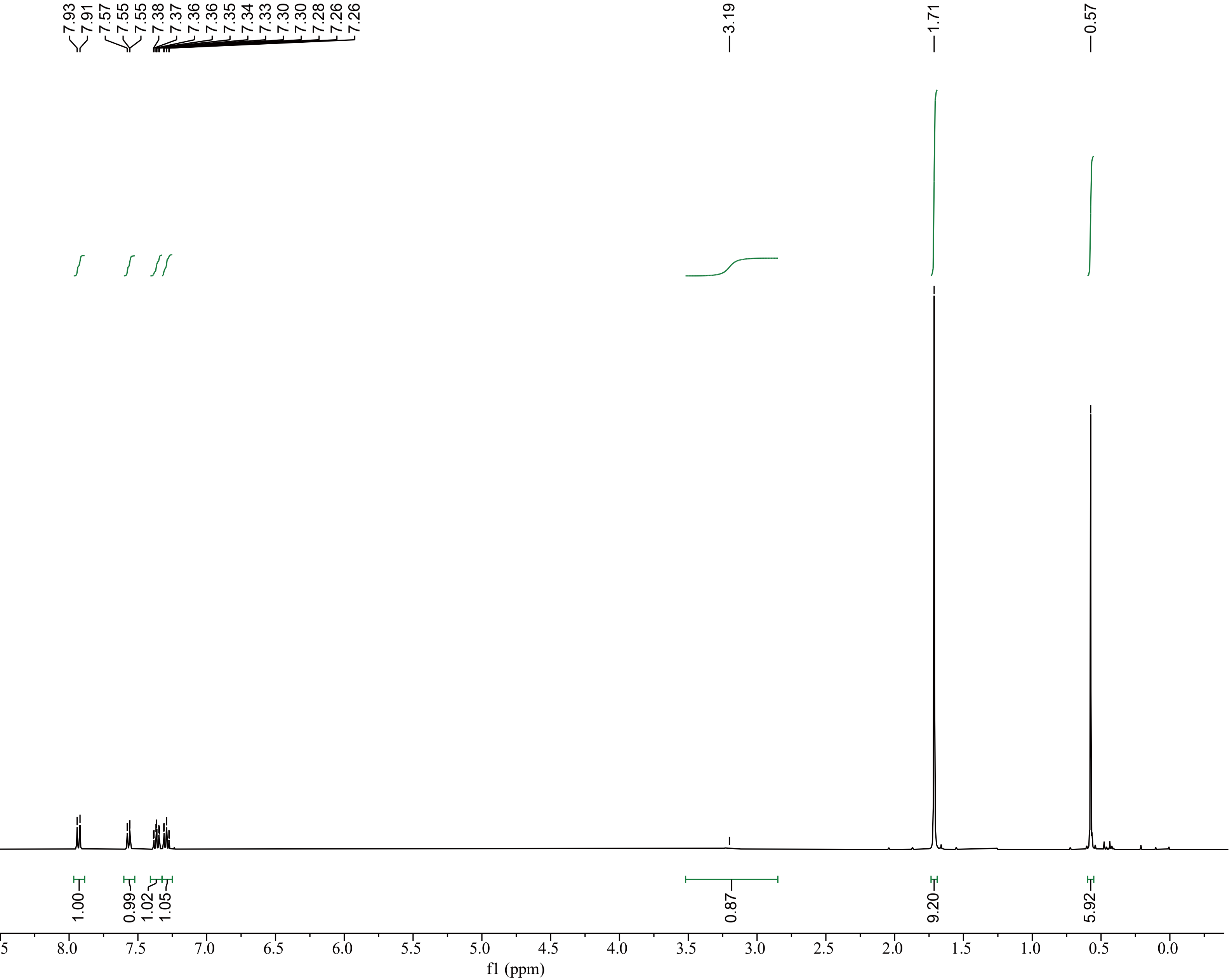

Compound **2az** ^{13}C NMR

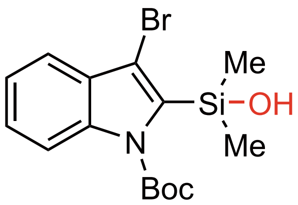

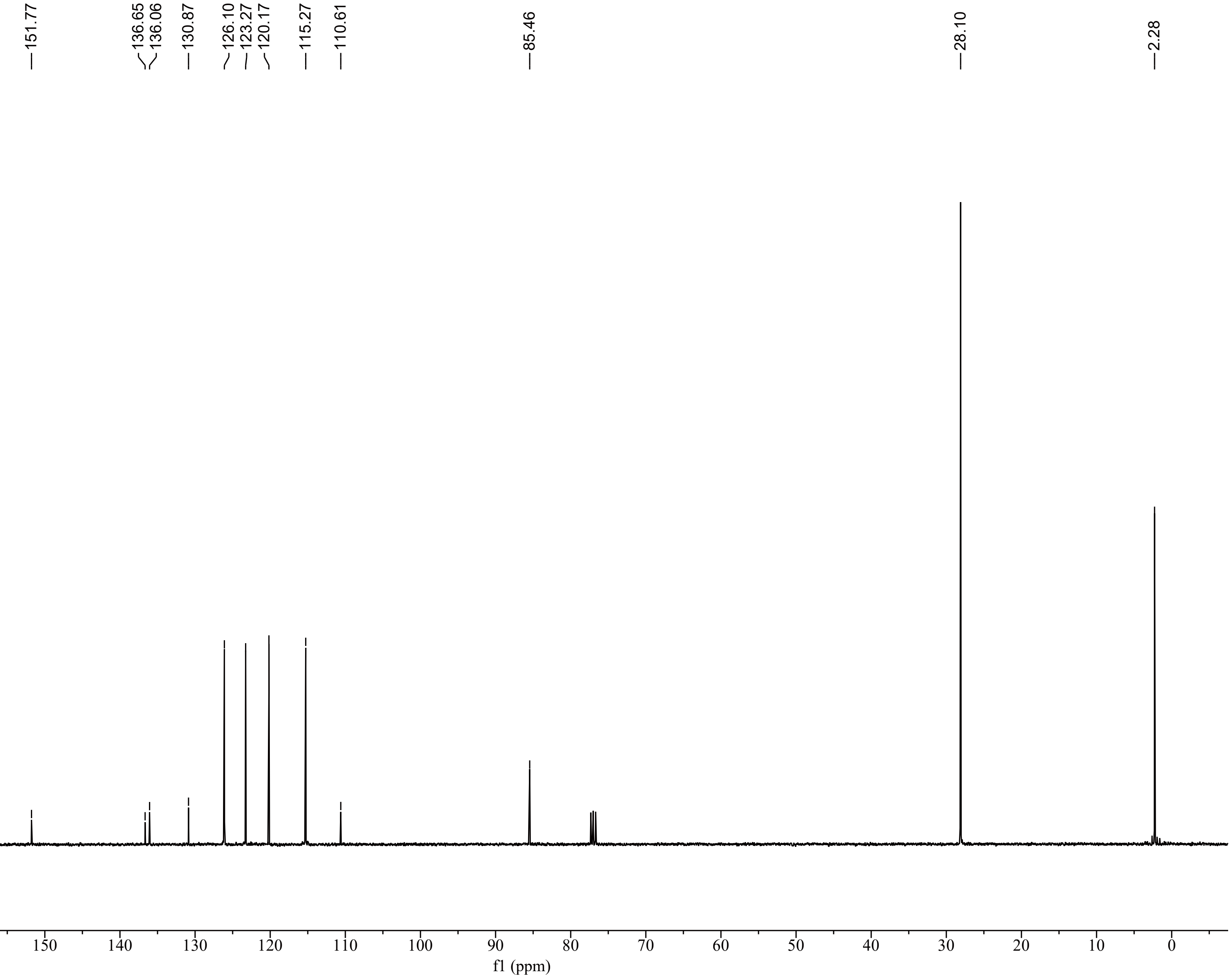

Compound **2ba** ^{1}H NMR

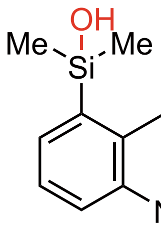

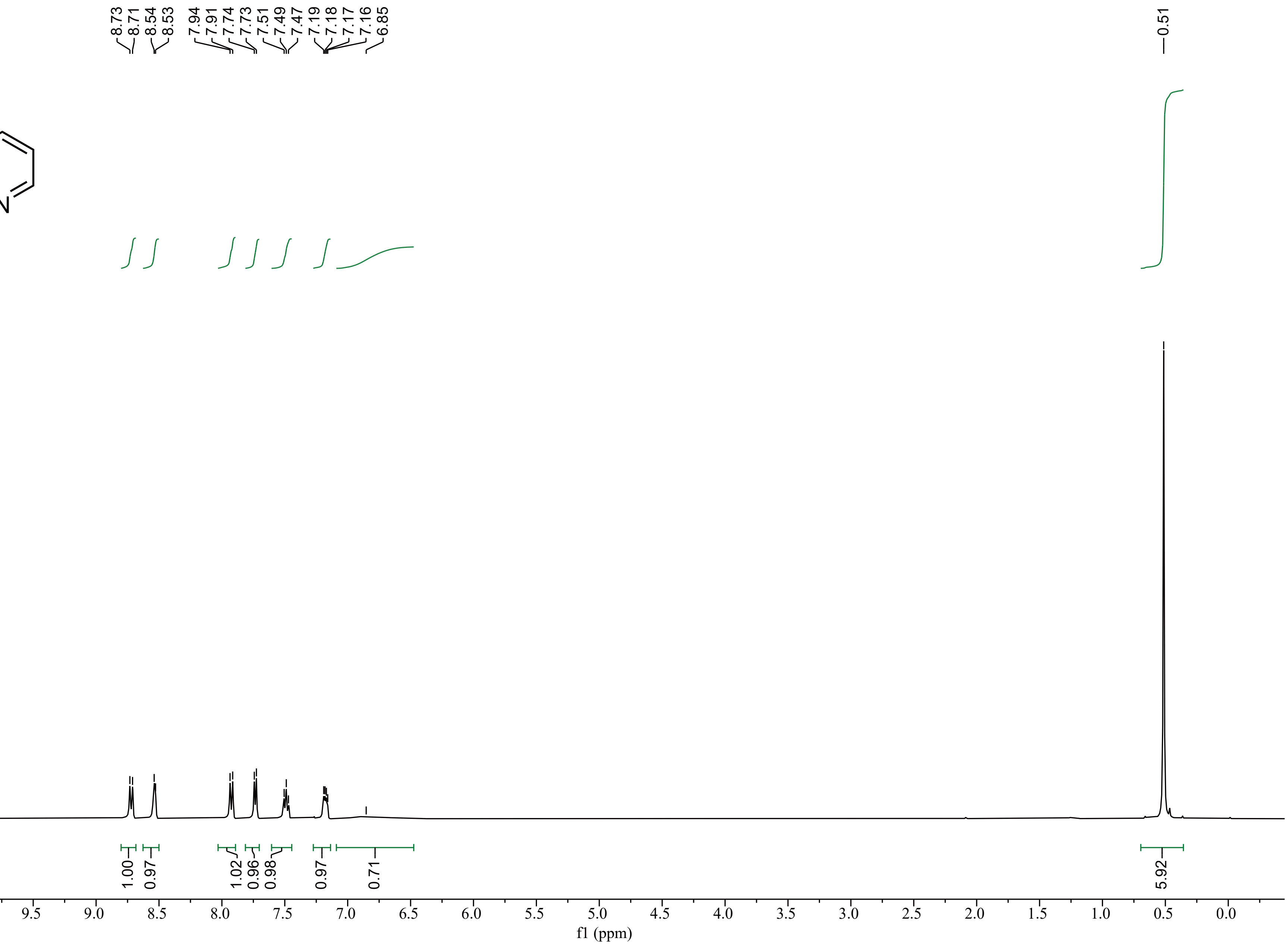

Compound **2ba** ^{13}C NMR

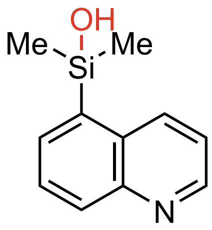

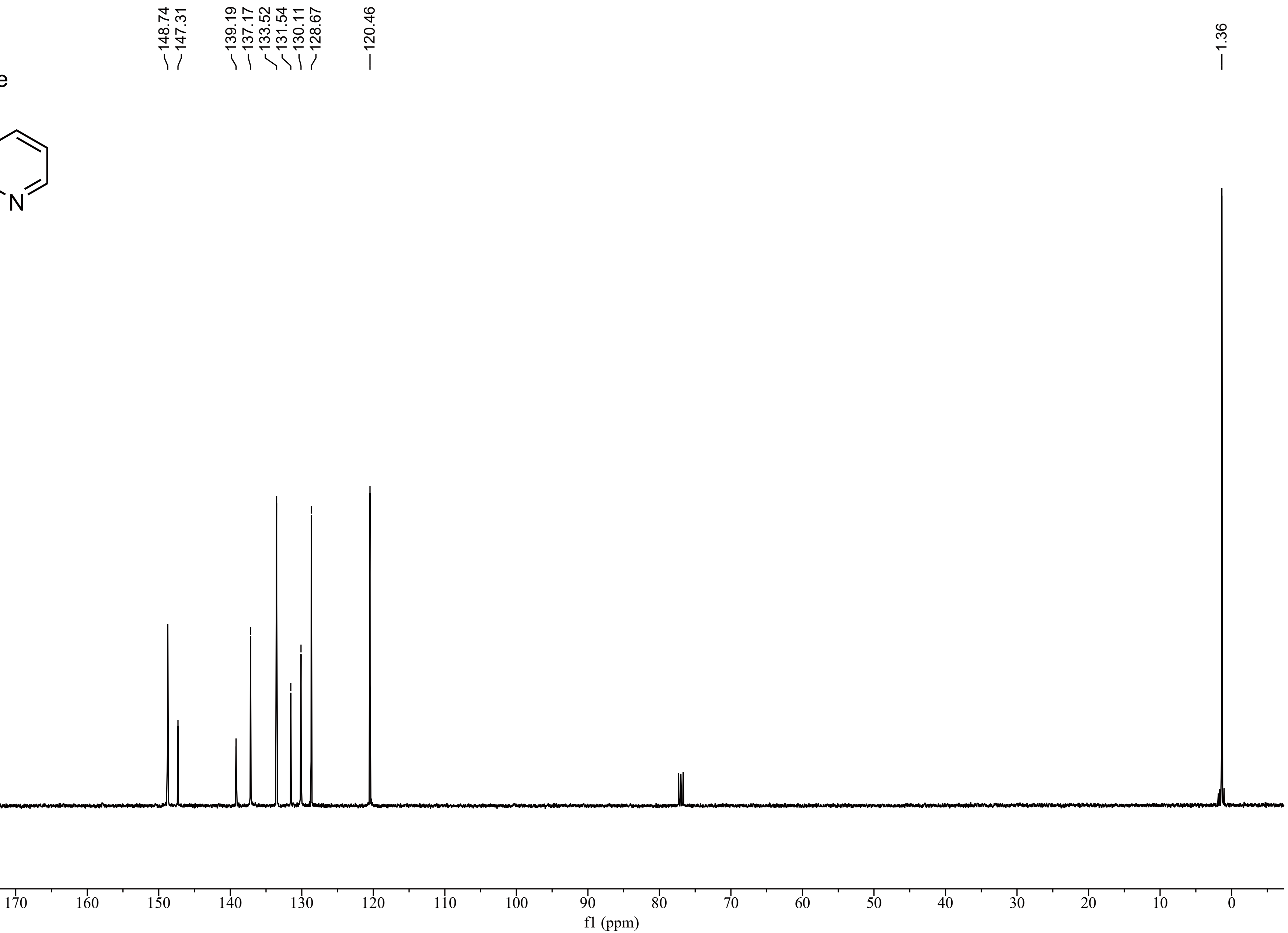

Compound **2bb** ^{1}H NMR

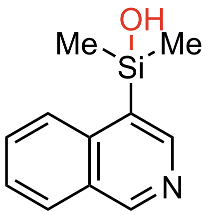

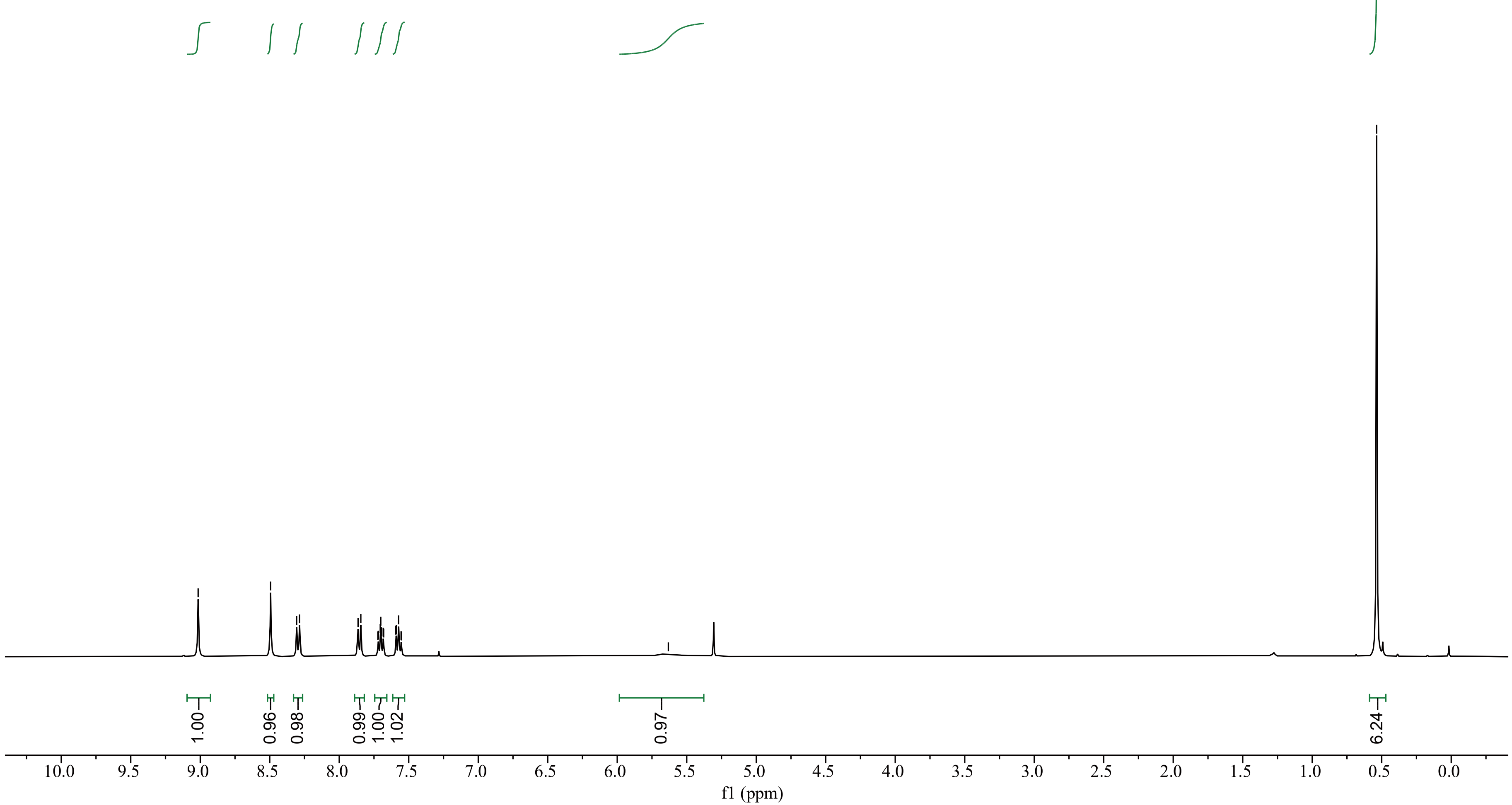

Compound **2bb** ^{13}C NMR

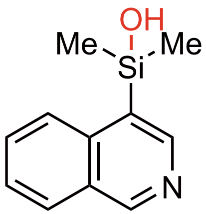

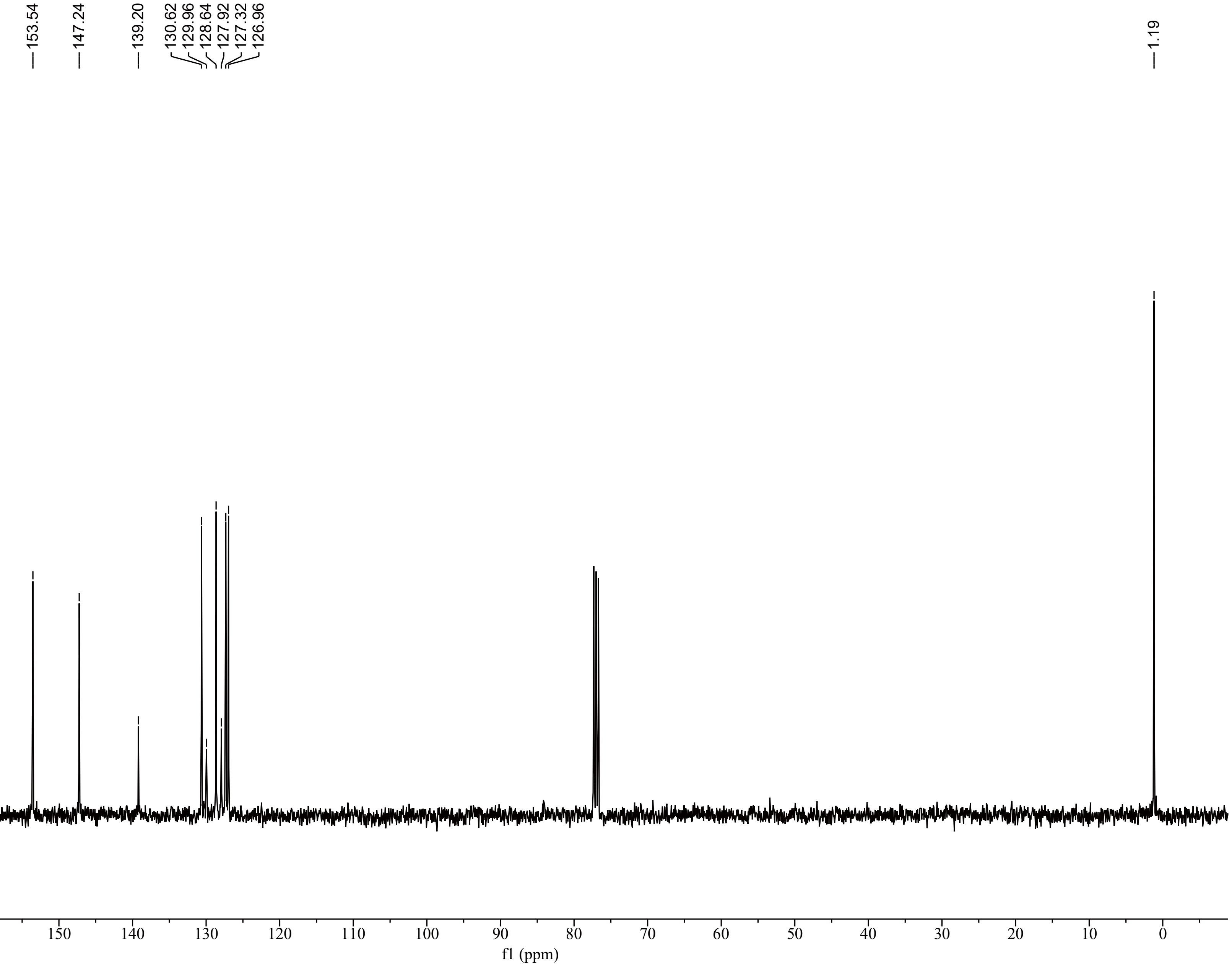

Compound **2bc** ^{1}H NMR

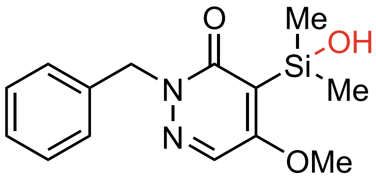

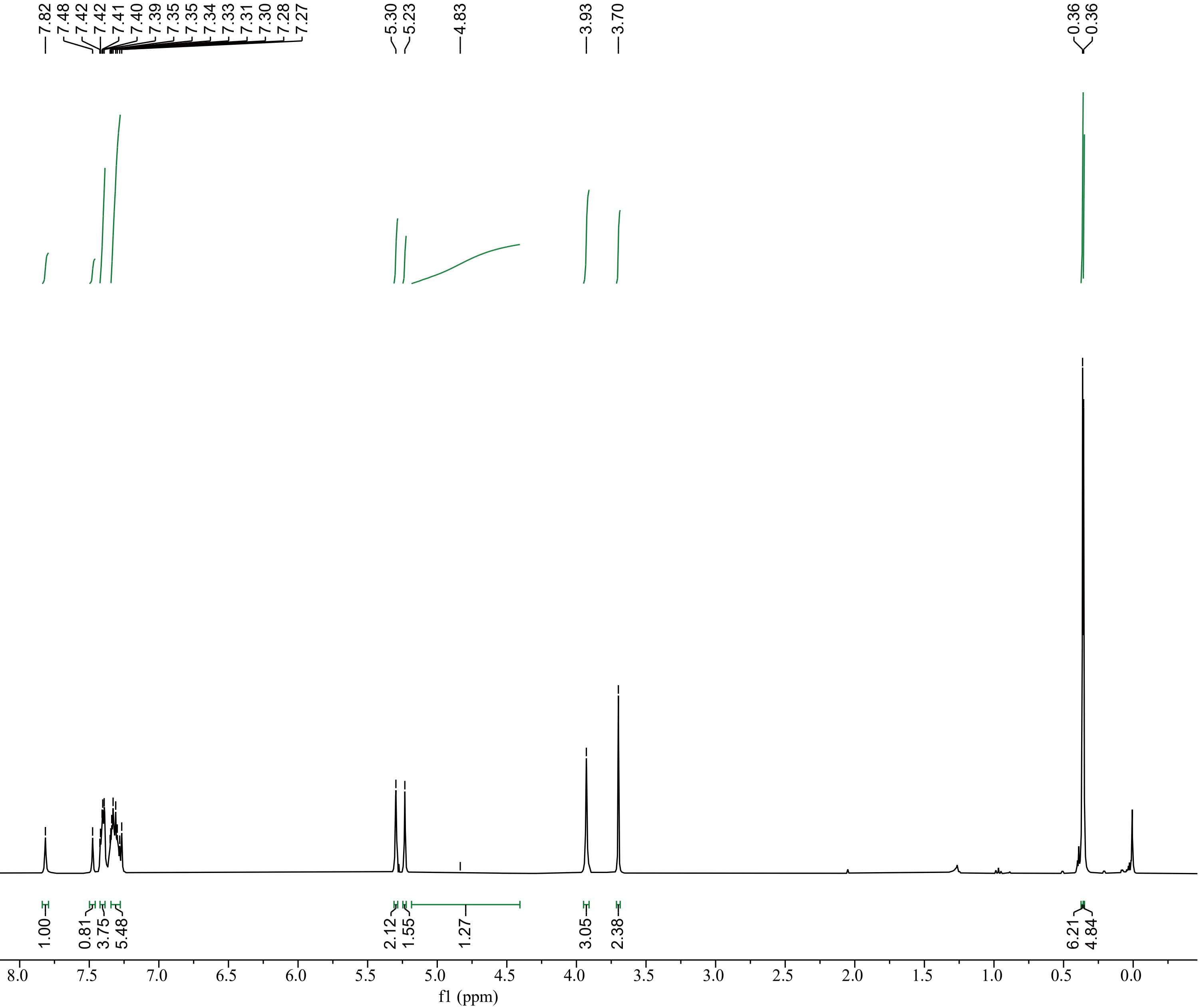

Compound **2bc** ^{13}C NMR

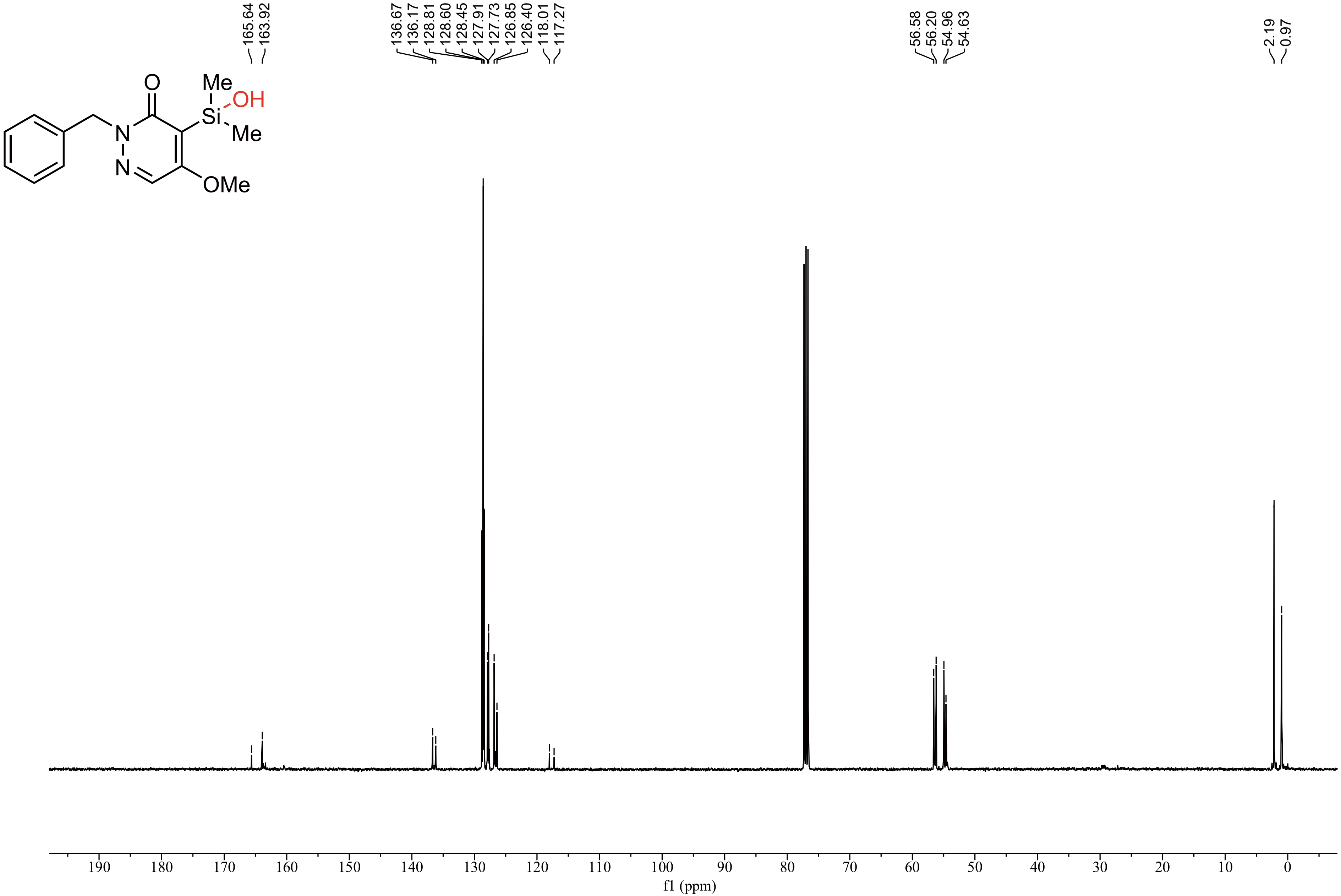

Compound **2bd** ^{1}H NMR

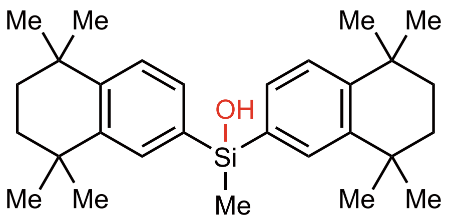

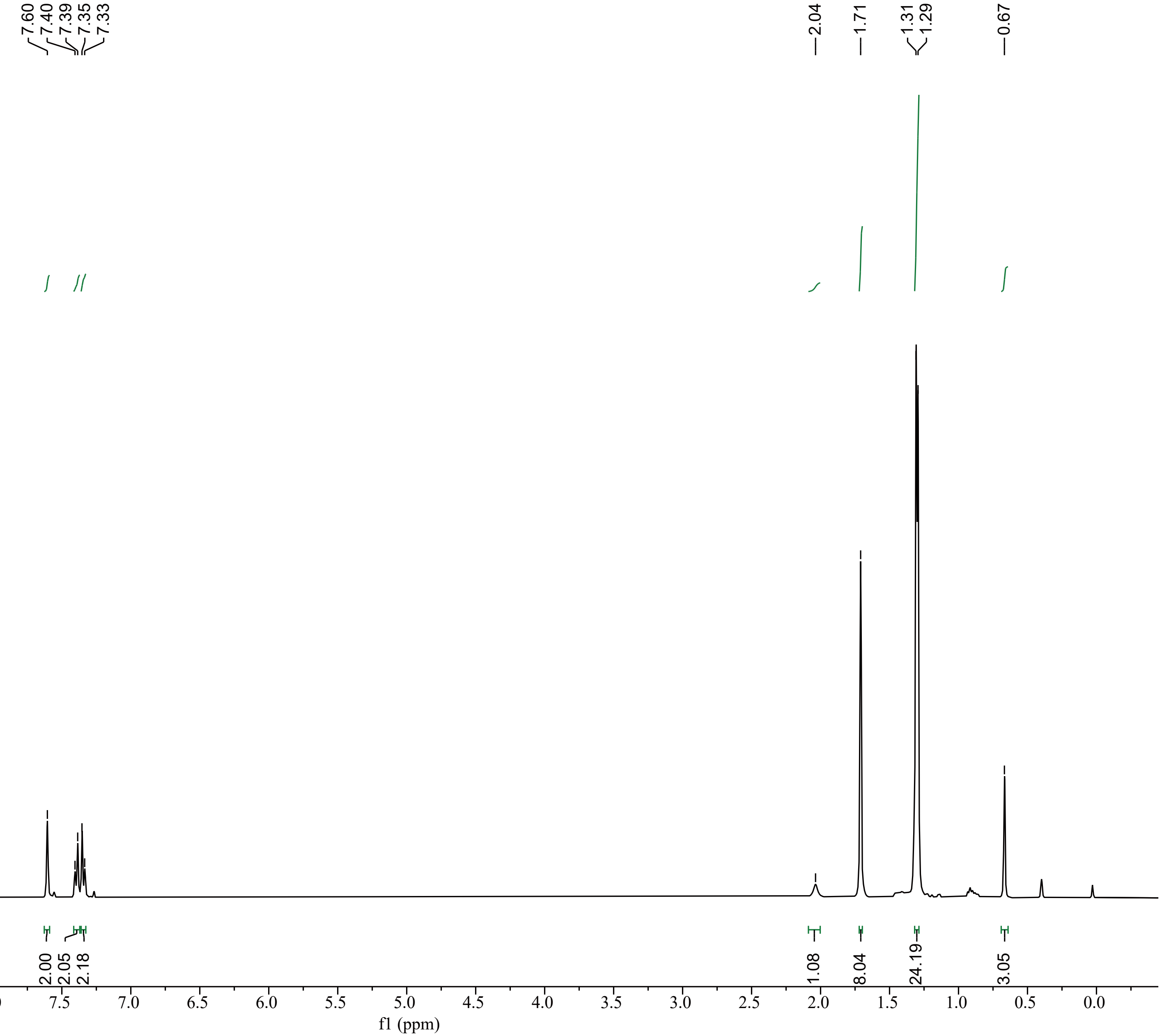

Compound **2bd** ^{13}C NMR

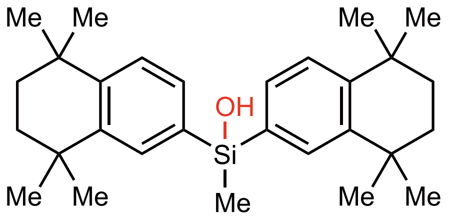

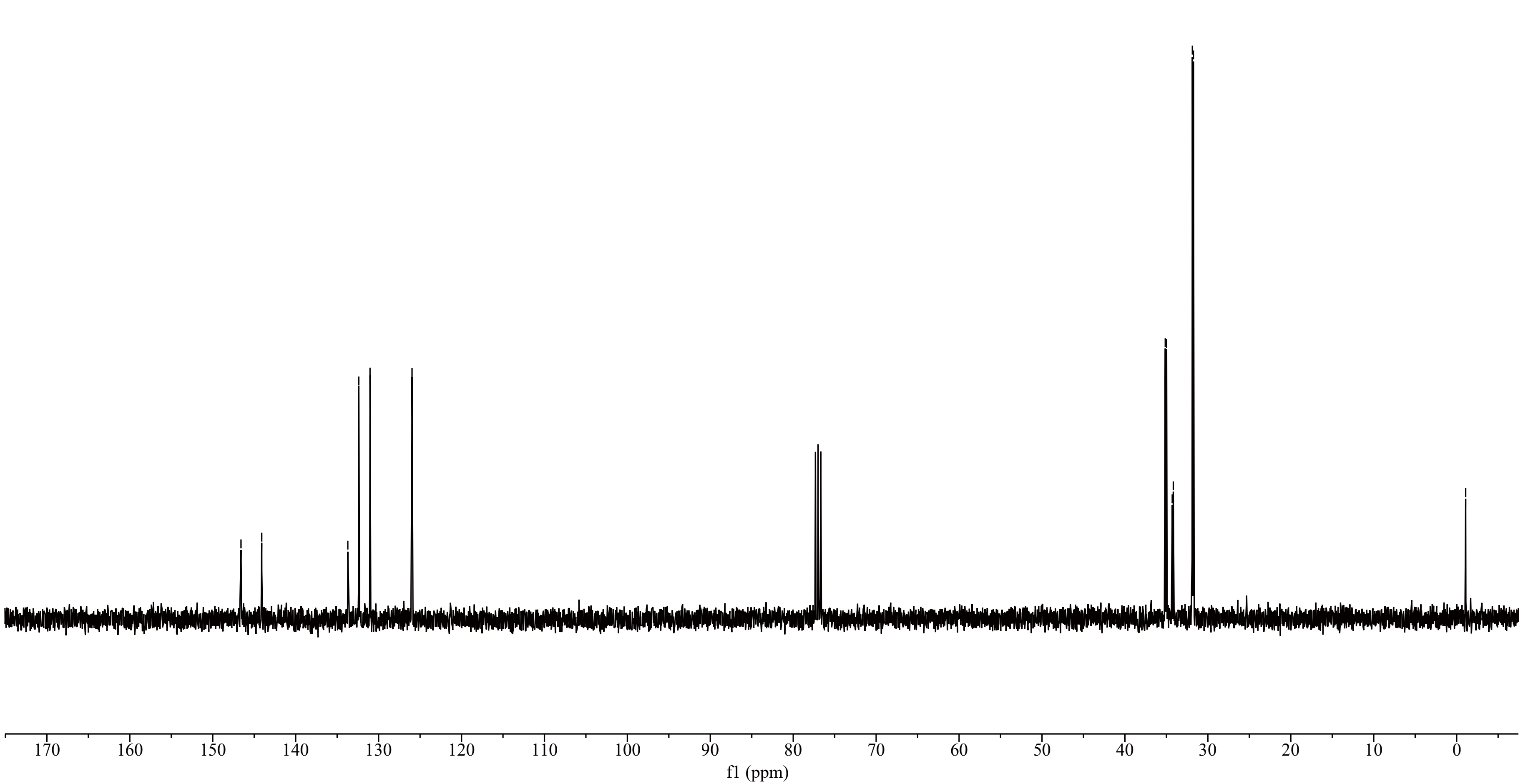

Compound **2be** ^{1}H NMR

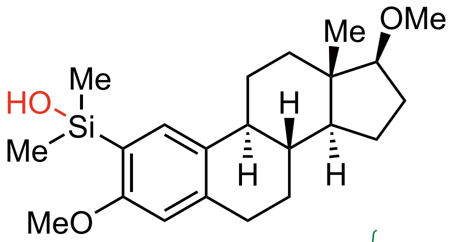

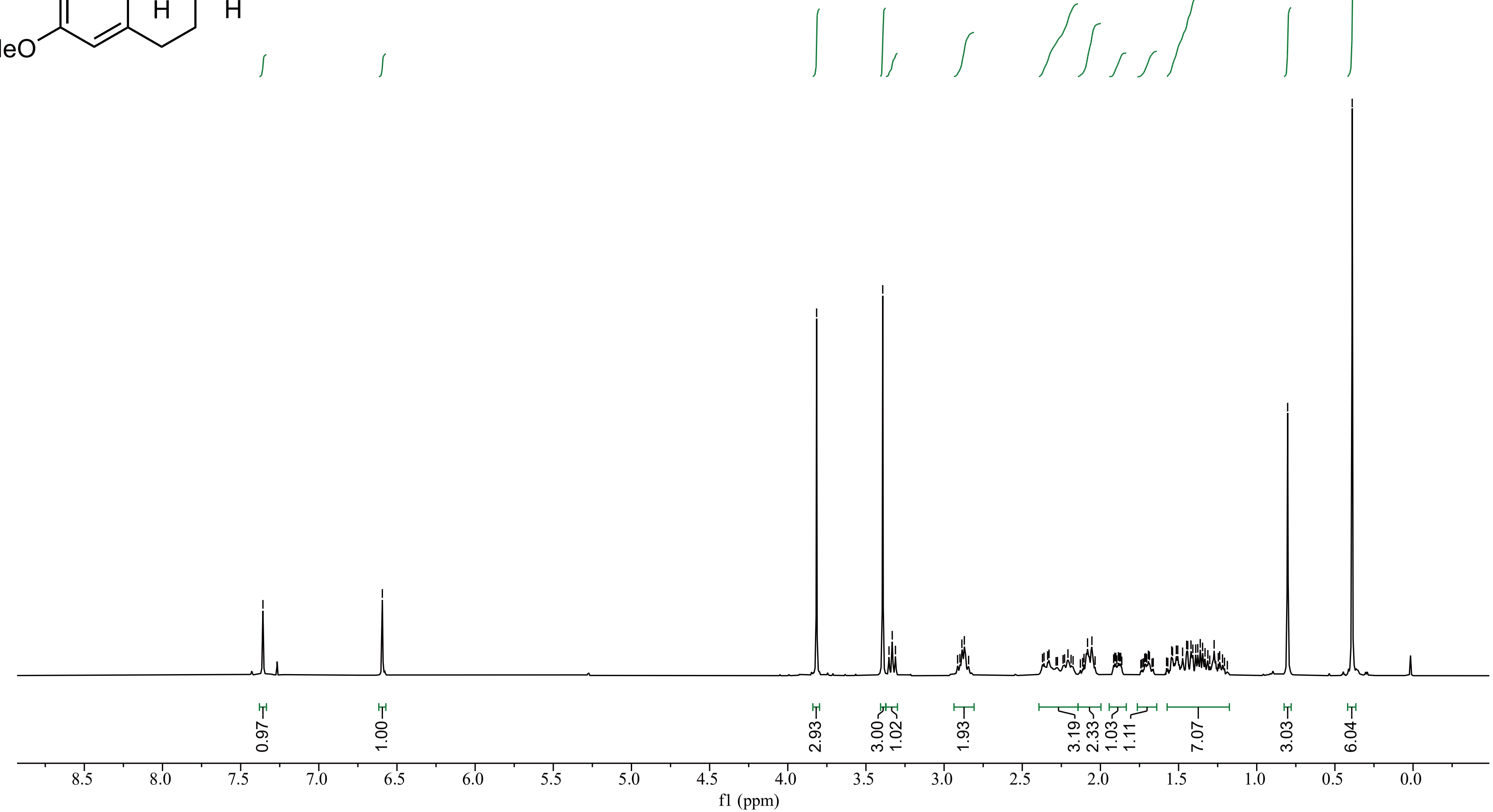

Compound **2be** ^{13}C NMR

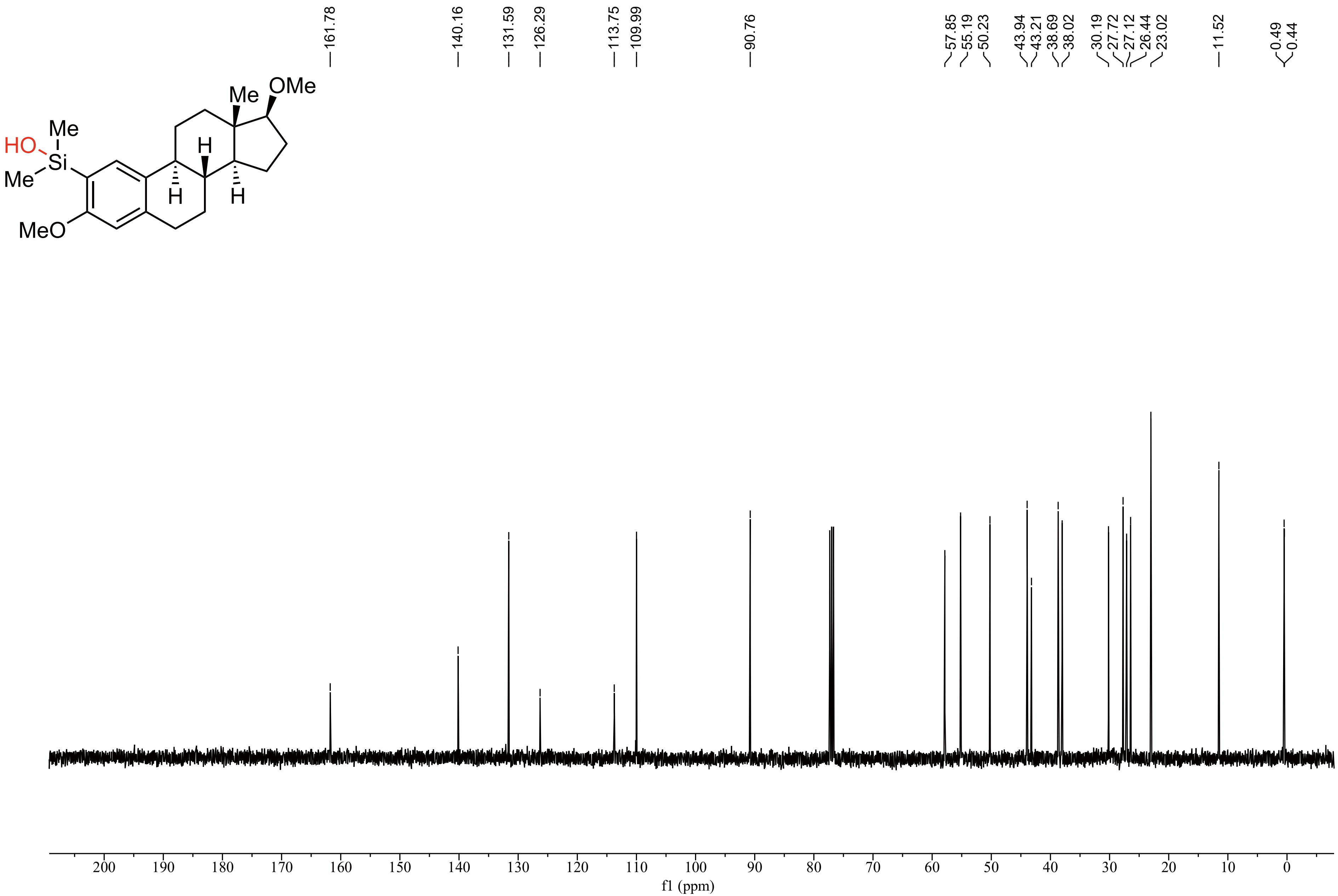

Compound **2bf** ^{1}H NMR

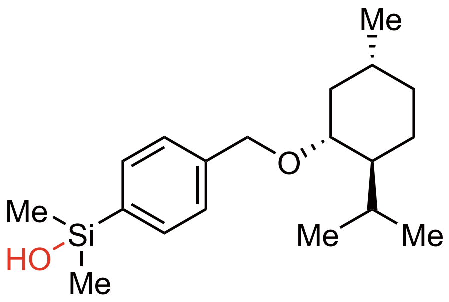

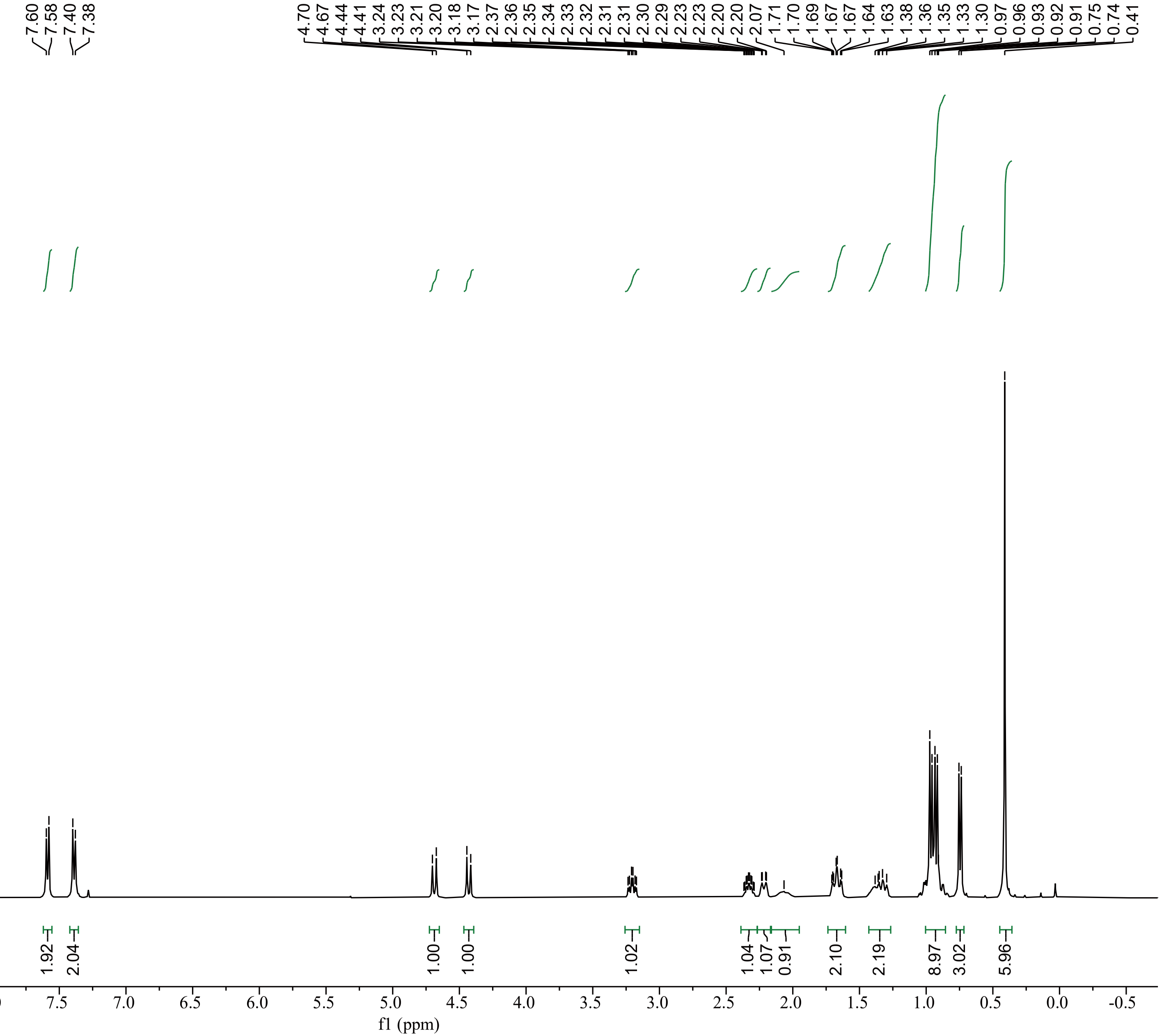

Compound **2bf** ^{13}C NMR

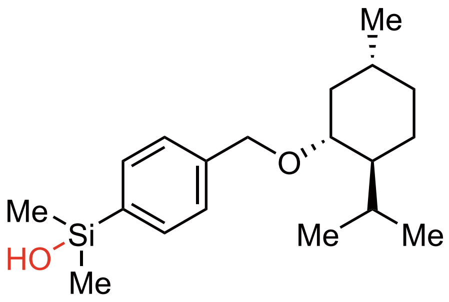

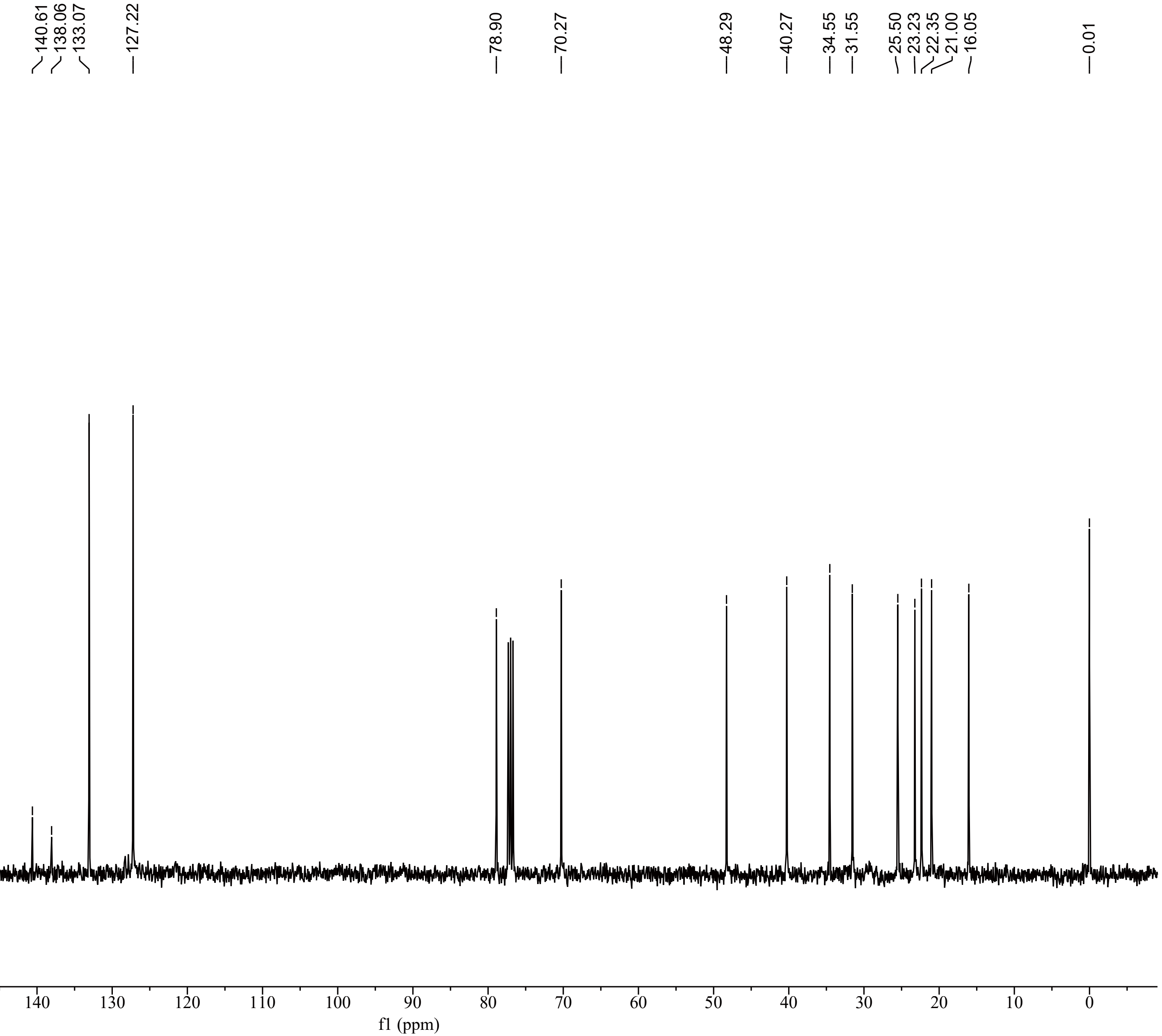

Compound **2bg** ^{1}H NMR

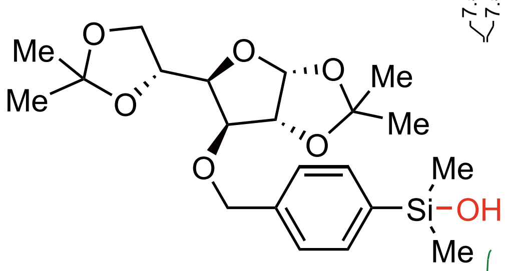

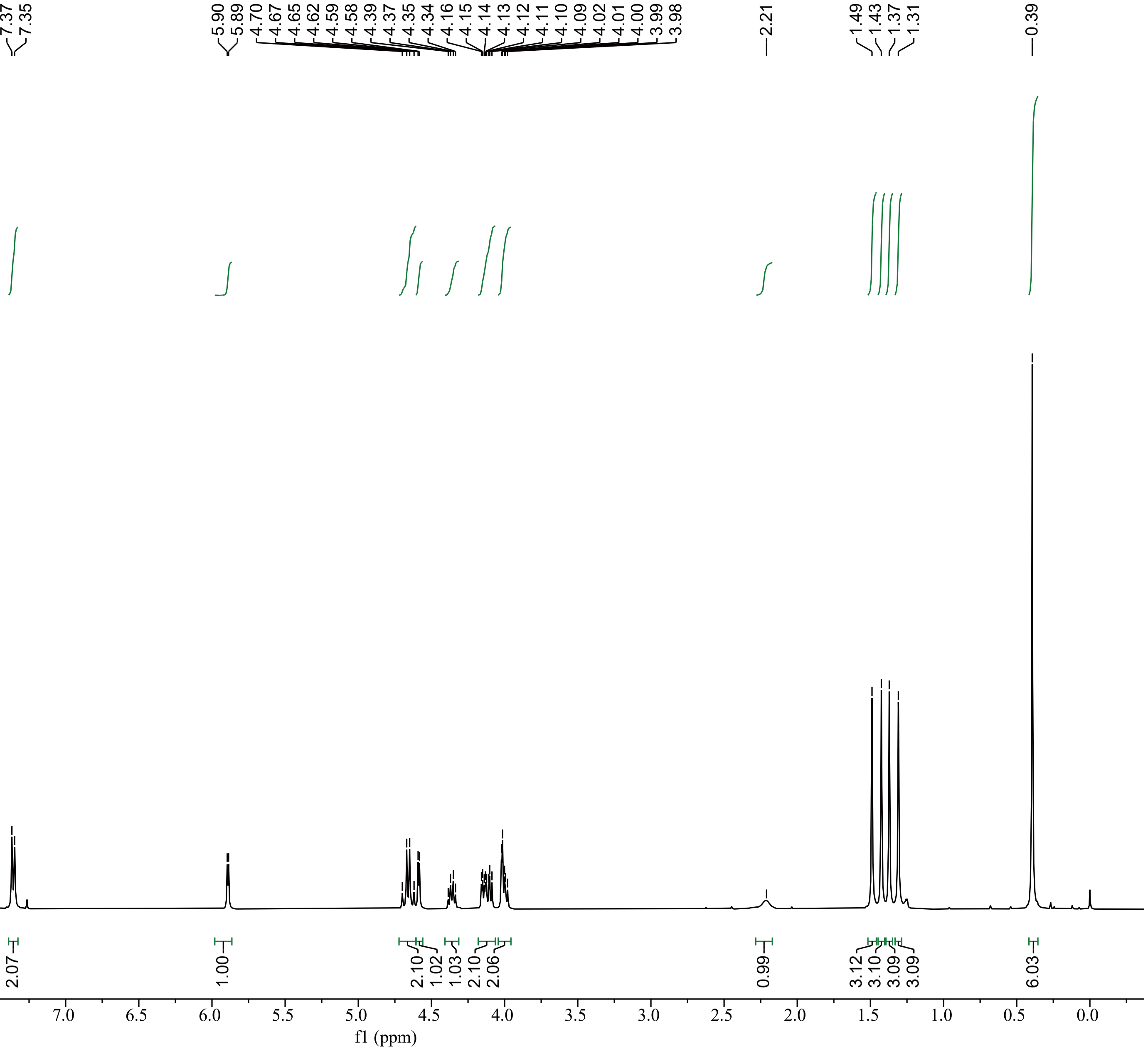

Compound **2bg** ^{1}H NMR

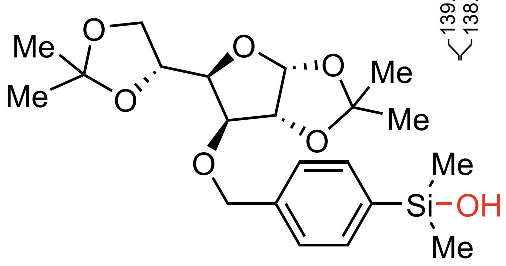

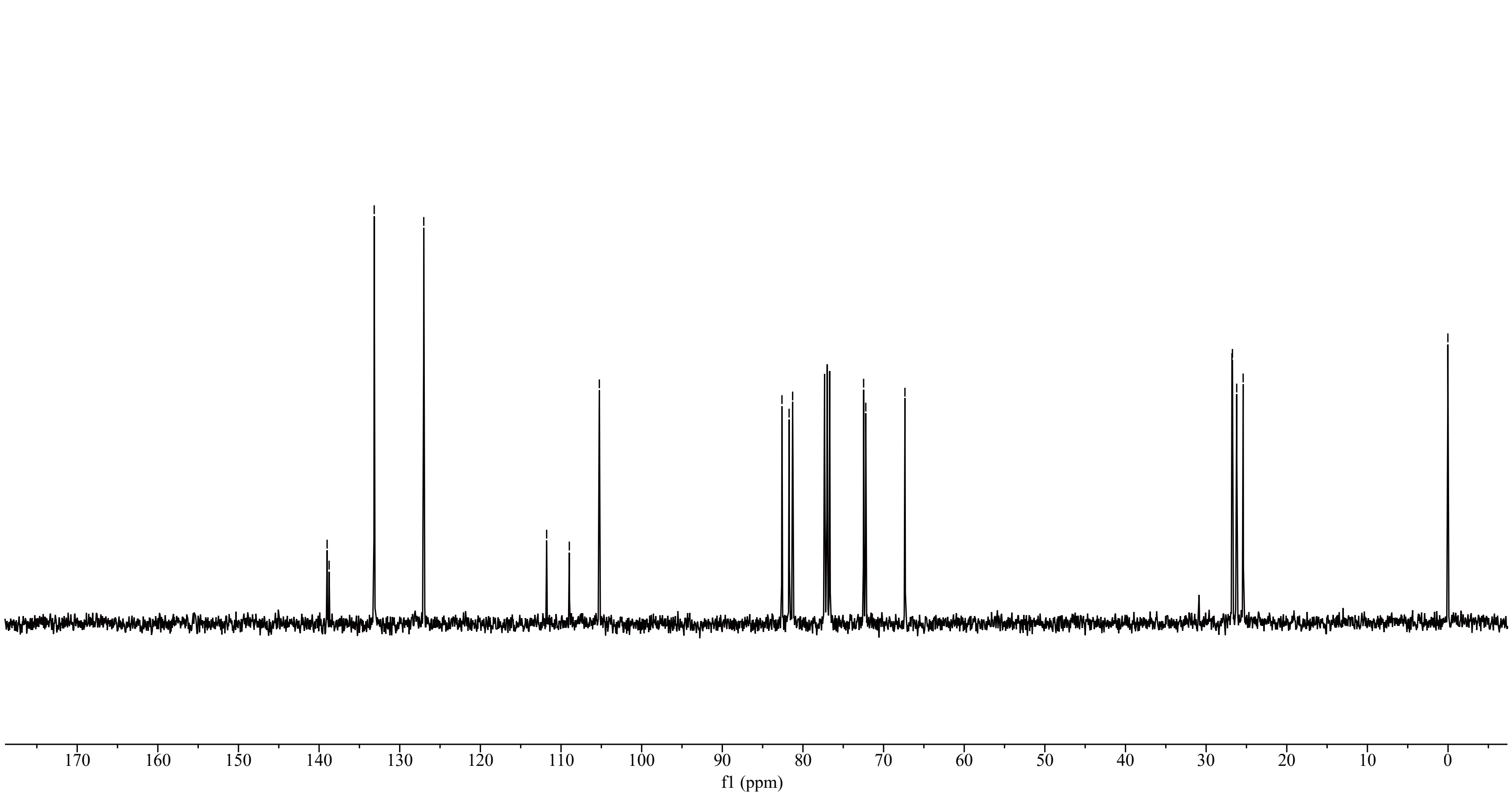

Compound **2bh** ^{1}H NMR

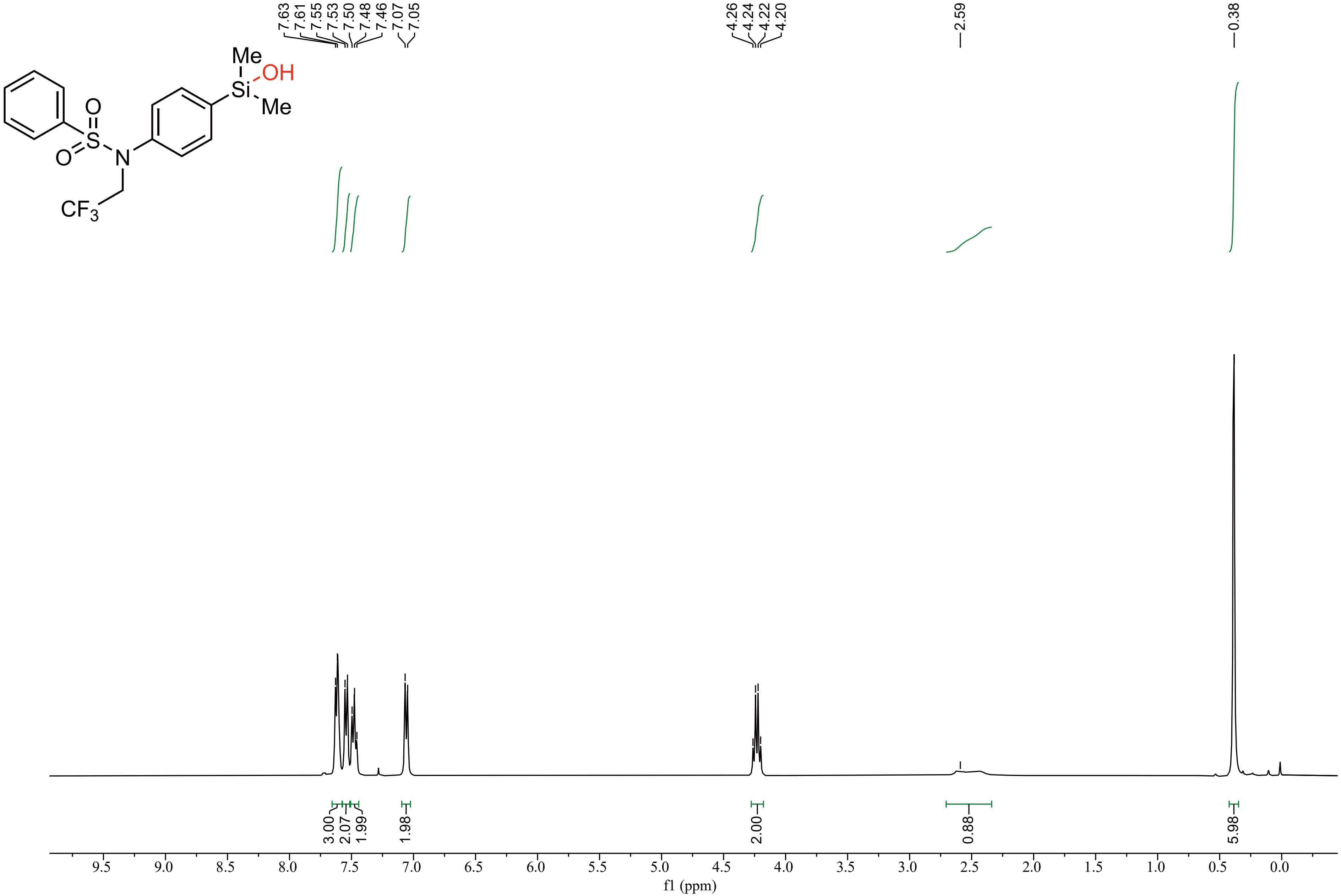

Compound **2bh** ^{13}C NMR

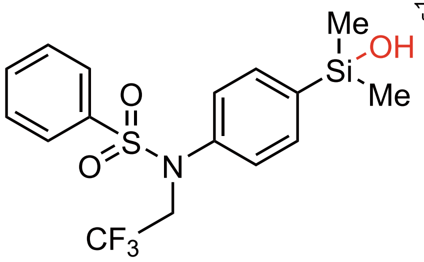

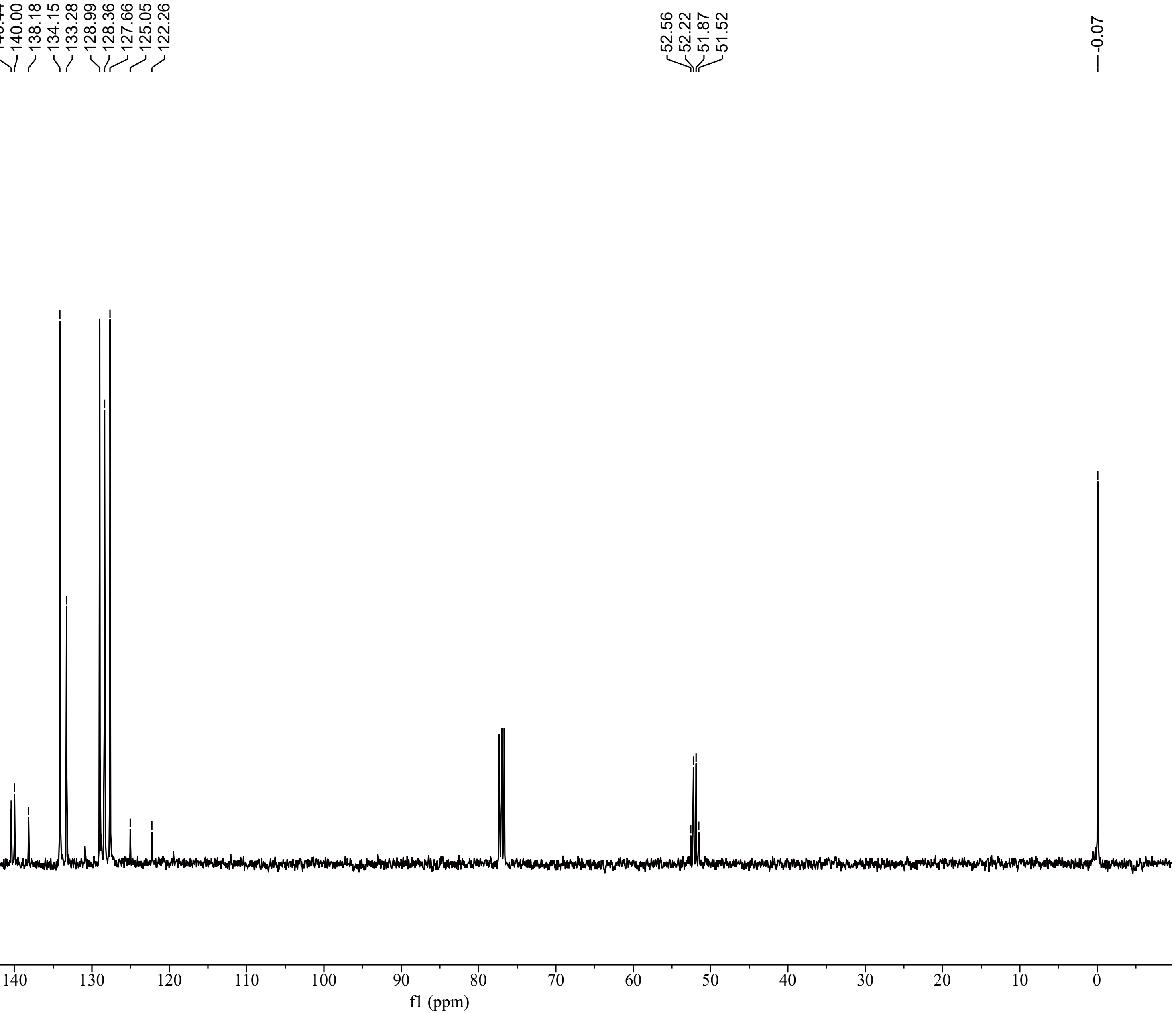

Compound **2bh** ^{19}F NMR

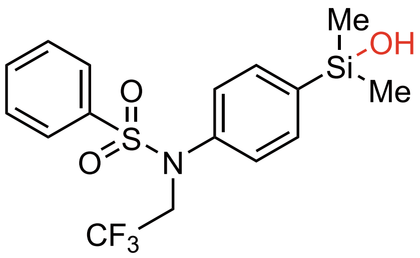

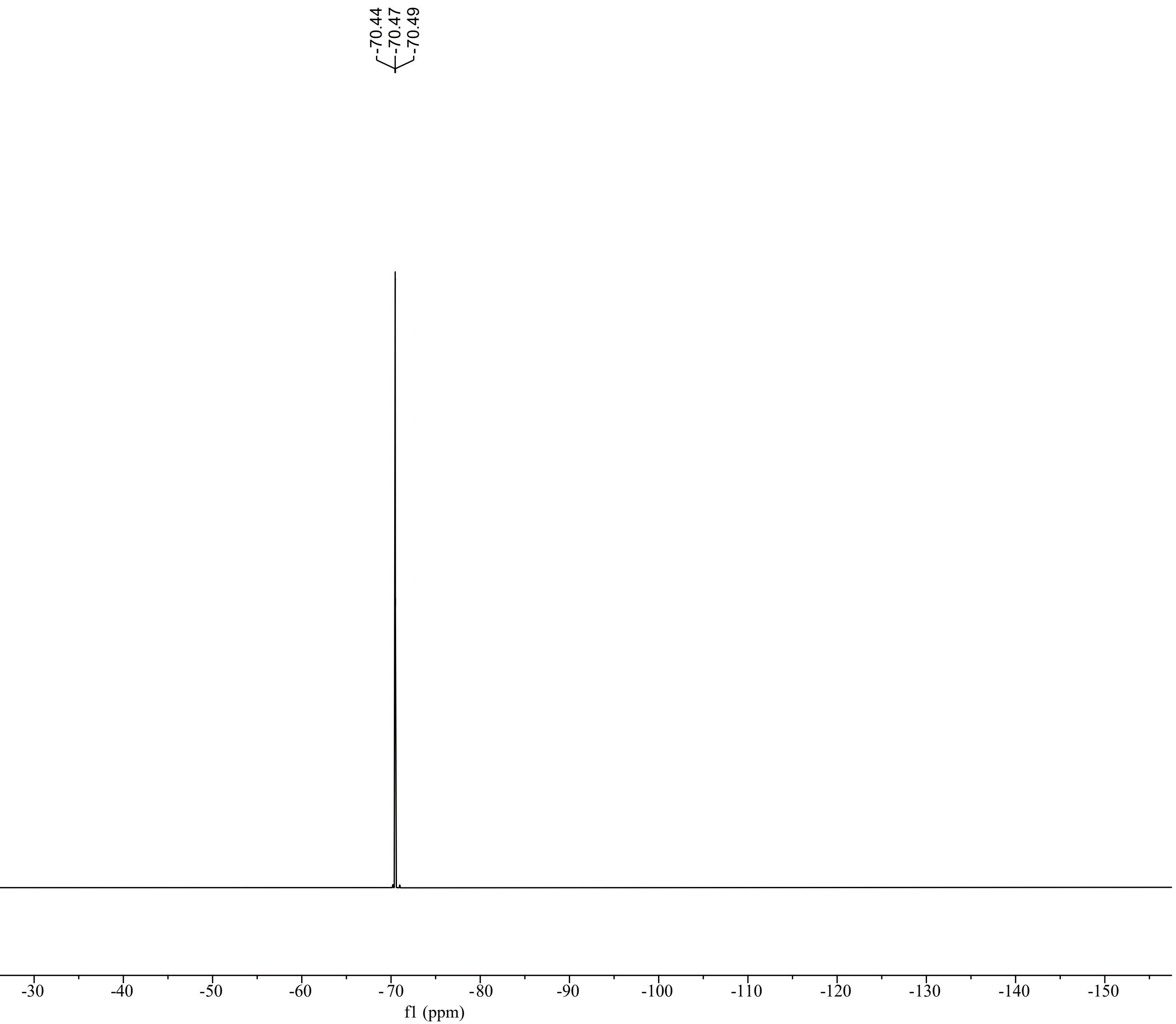

Compound **2bi** ^{1}H NMR

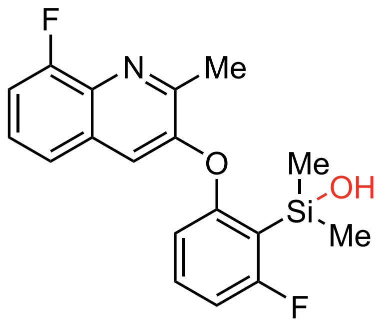

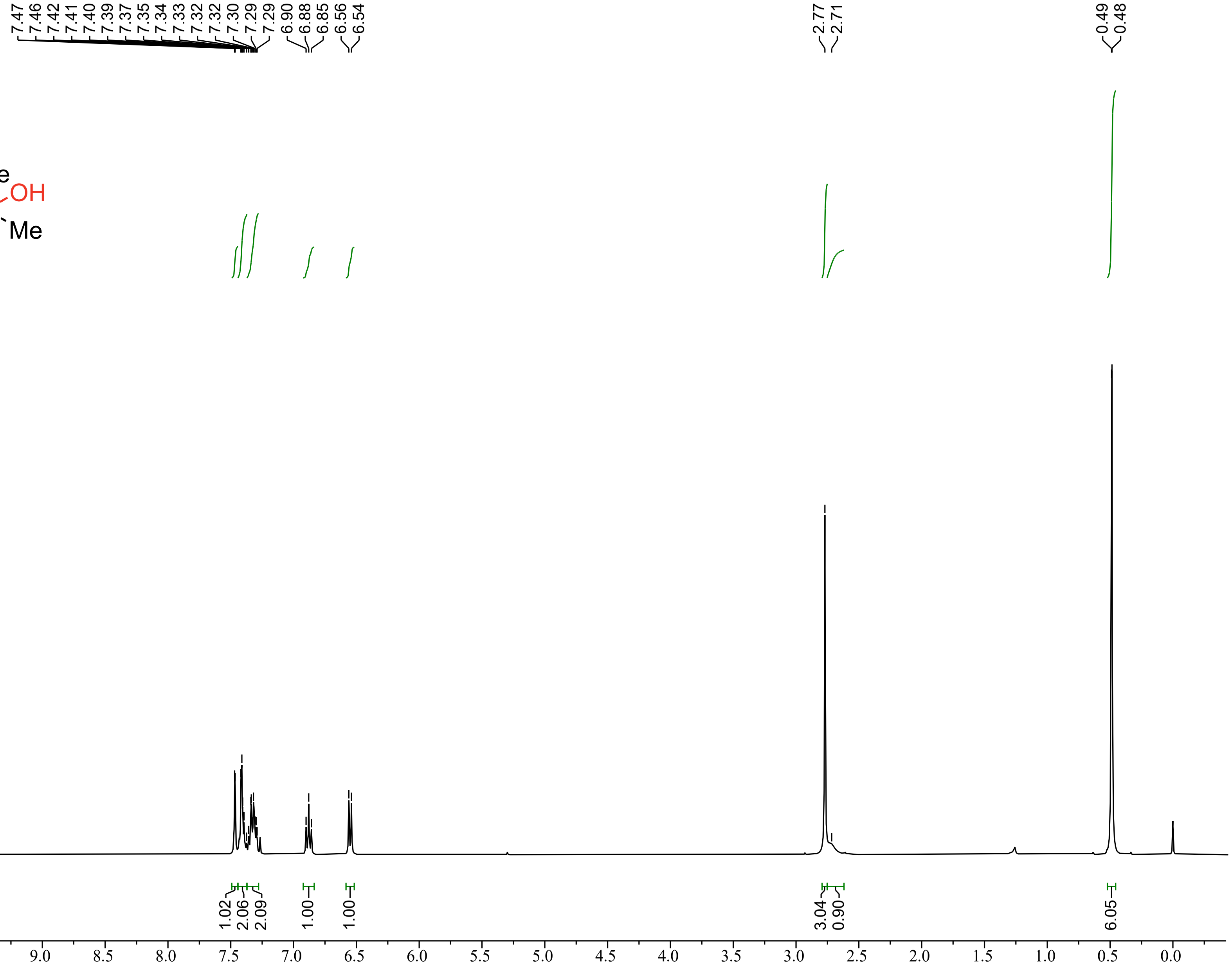

Compound **2bi** ^{13}C NMR

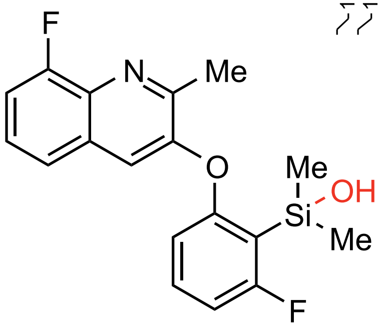

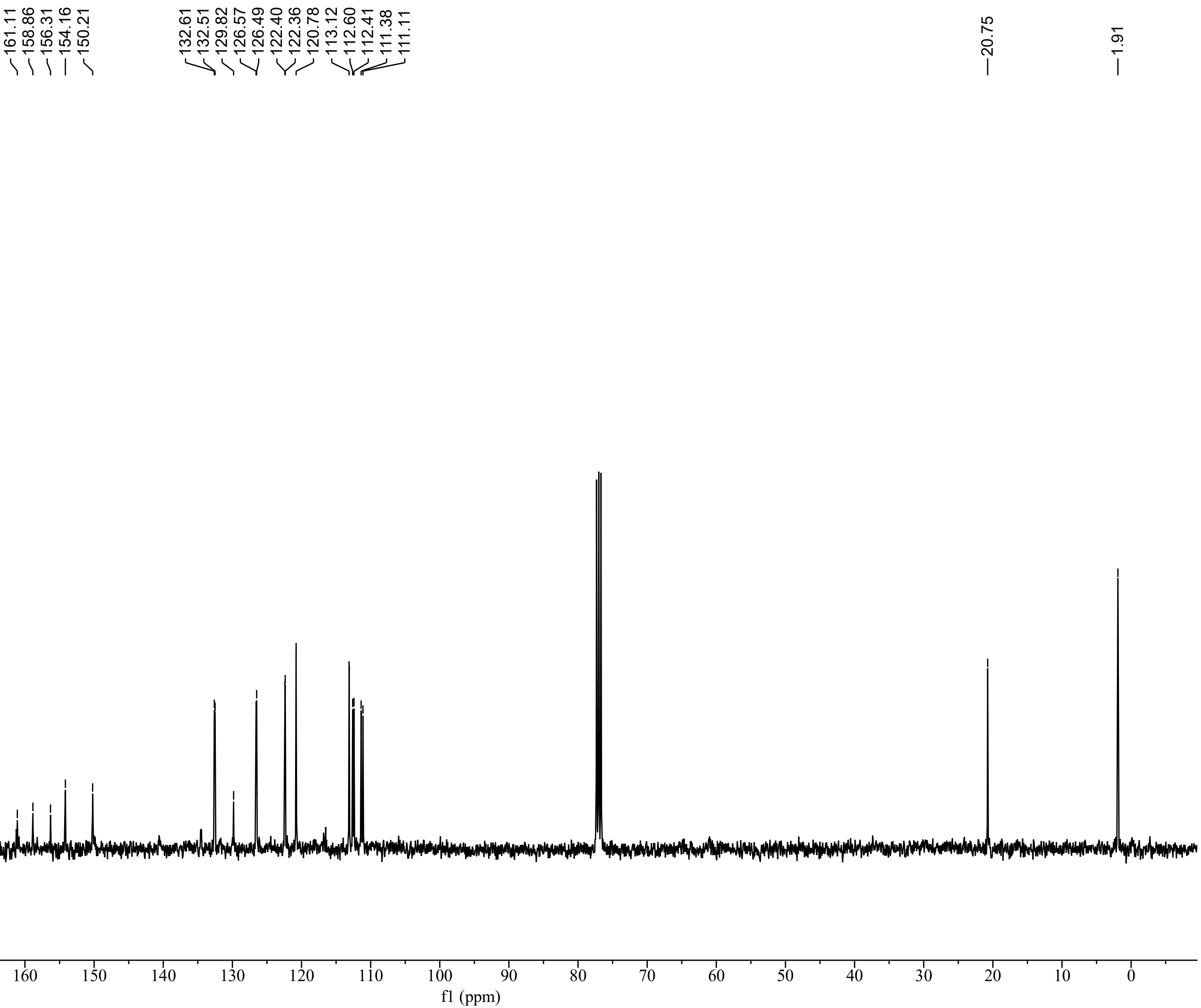

Compound **2bi** ^{19}F NMR

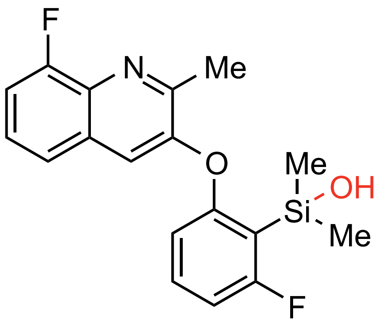

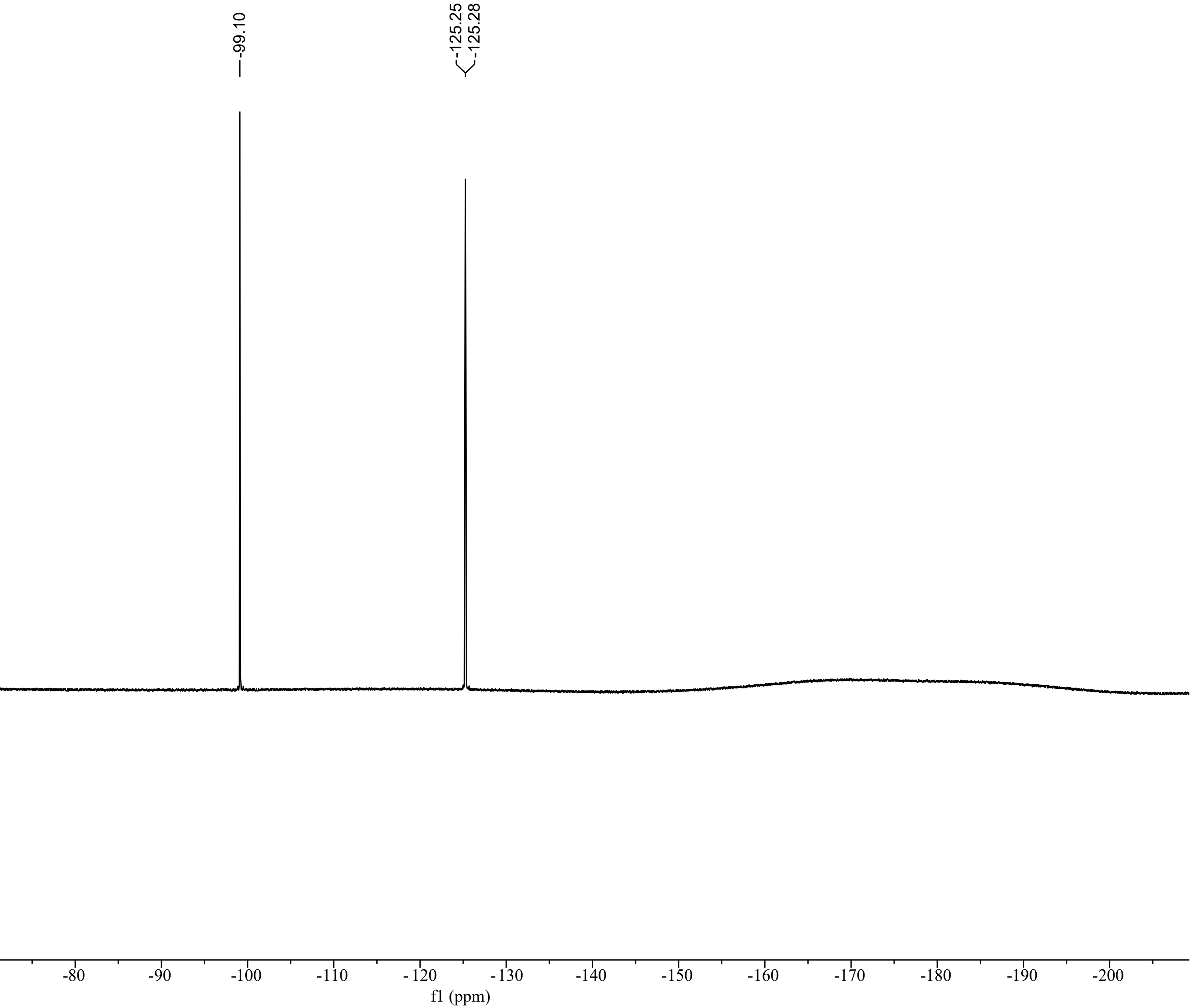

Compound **2bj** [1]H NMR

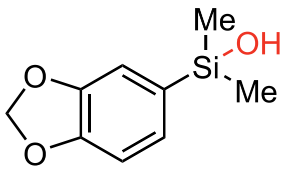

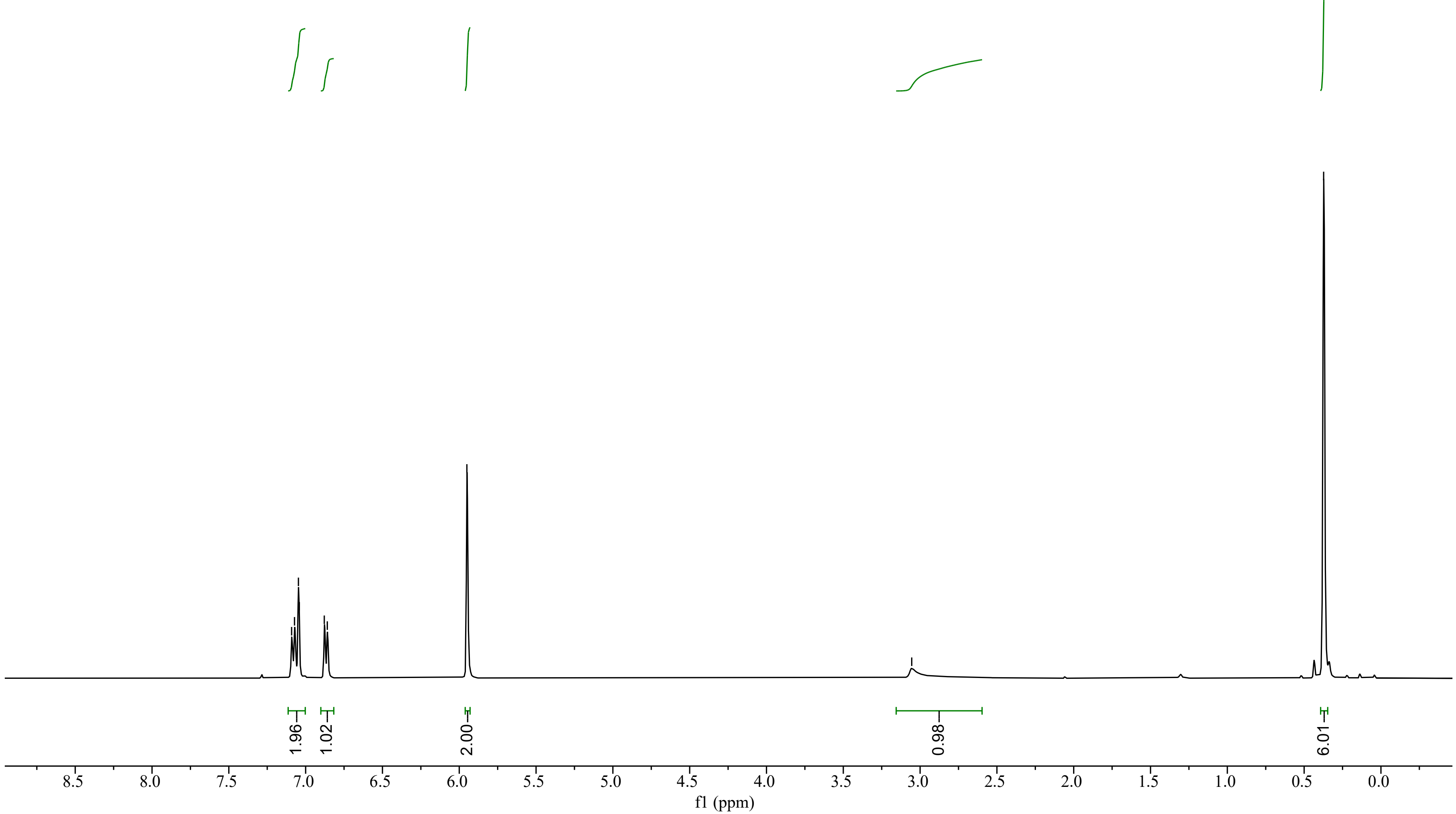

Compound **2bj** ^{13}C NMR

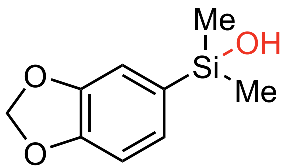

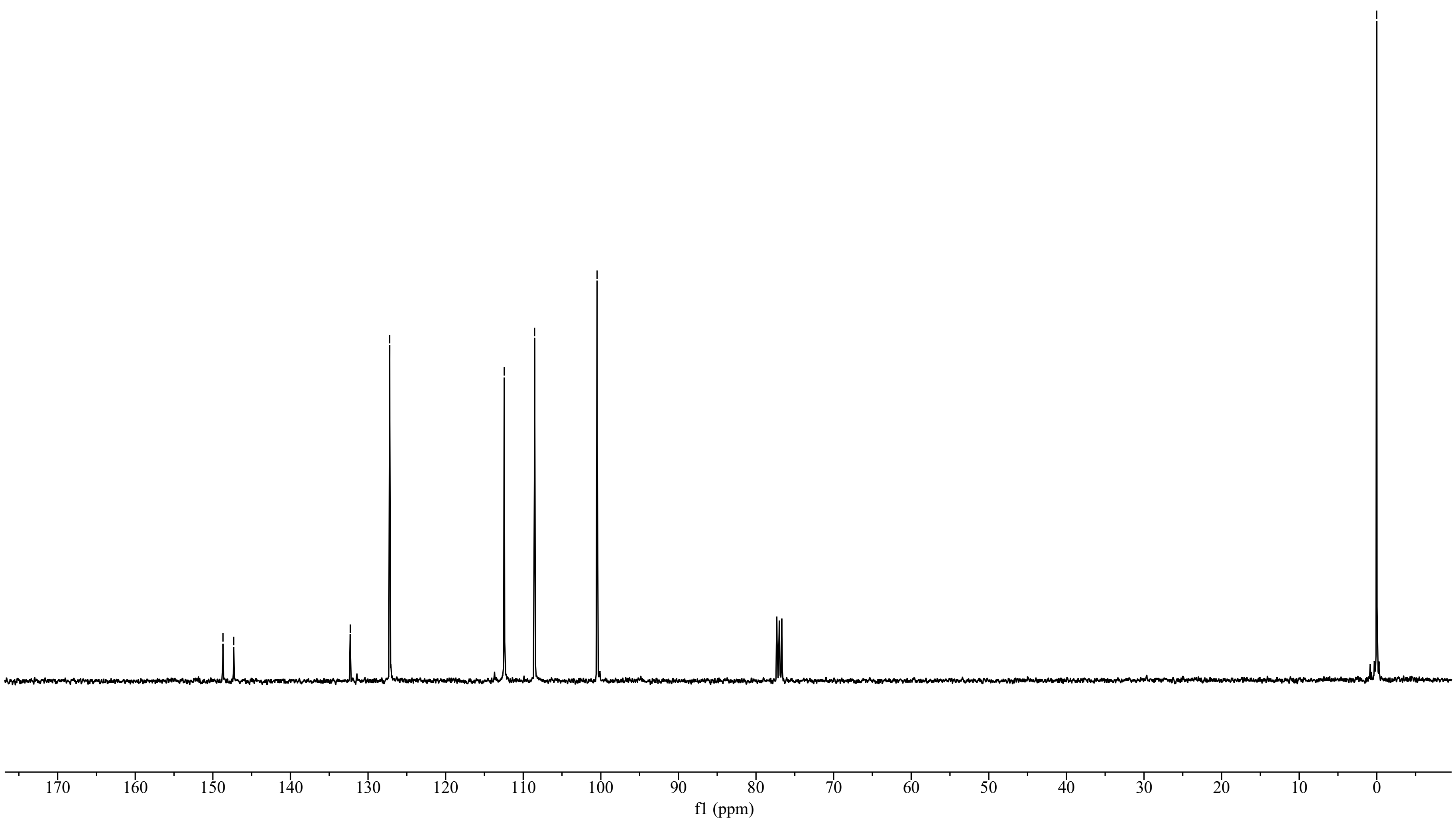

Compound **2bk** ^{1}H NMR

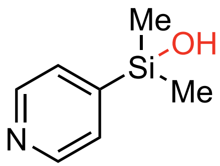

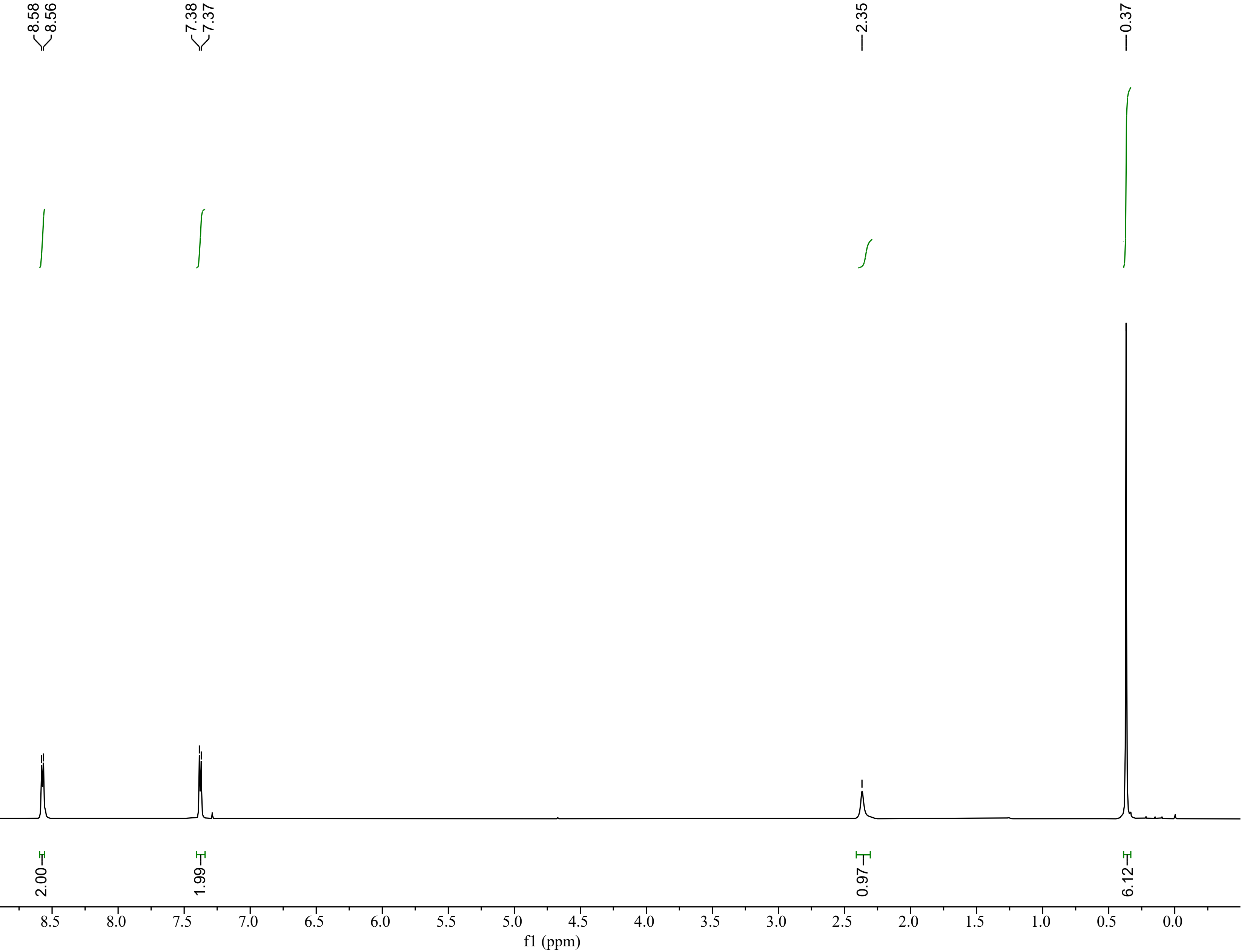

Compound **2bk** ^{13}C NMR

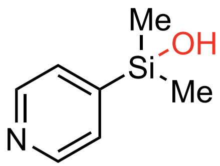

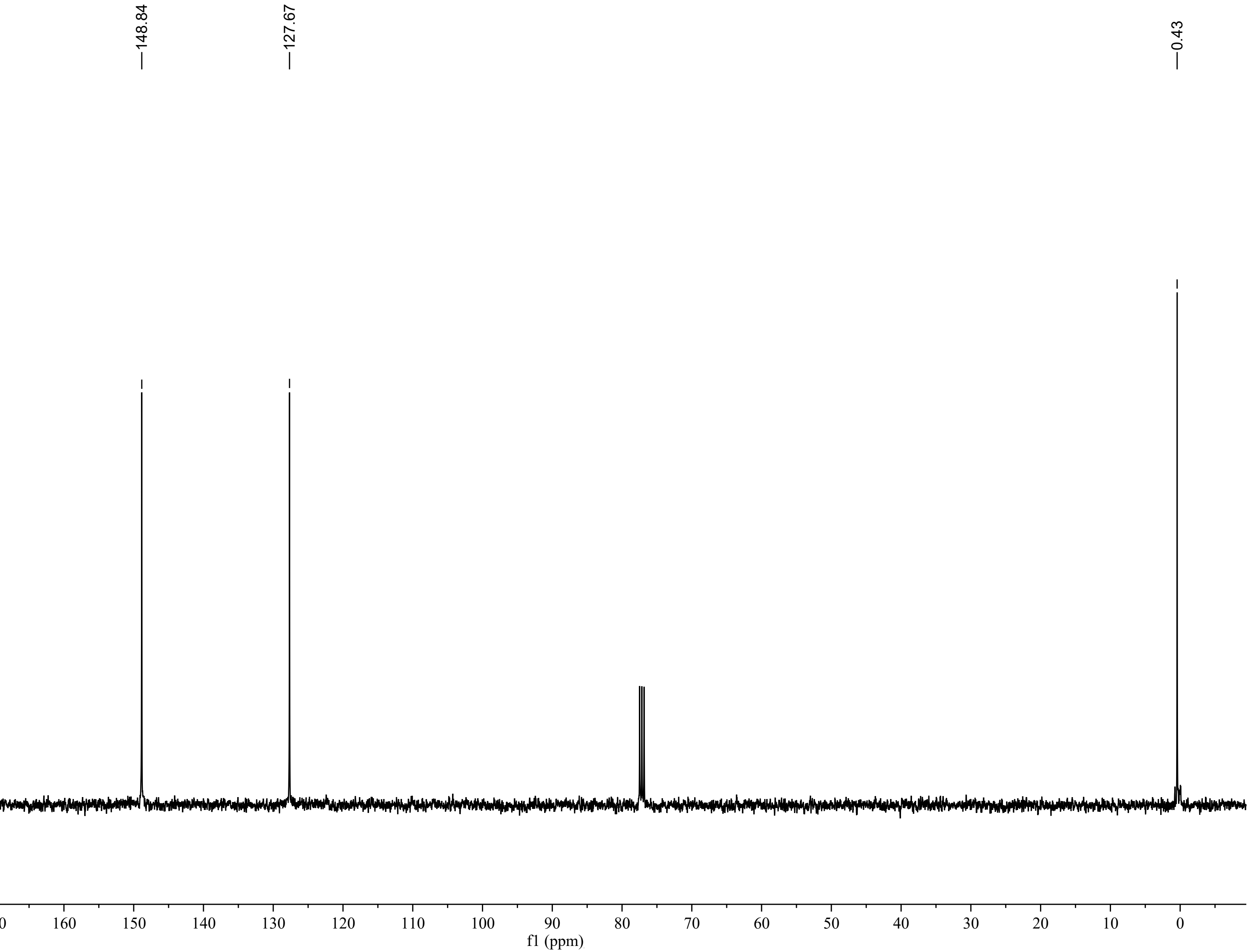

Compound **2bl** ^{1}H NMR

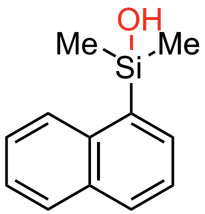

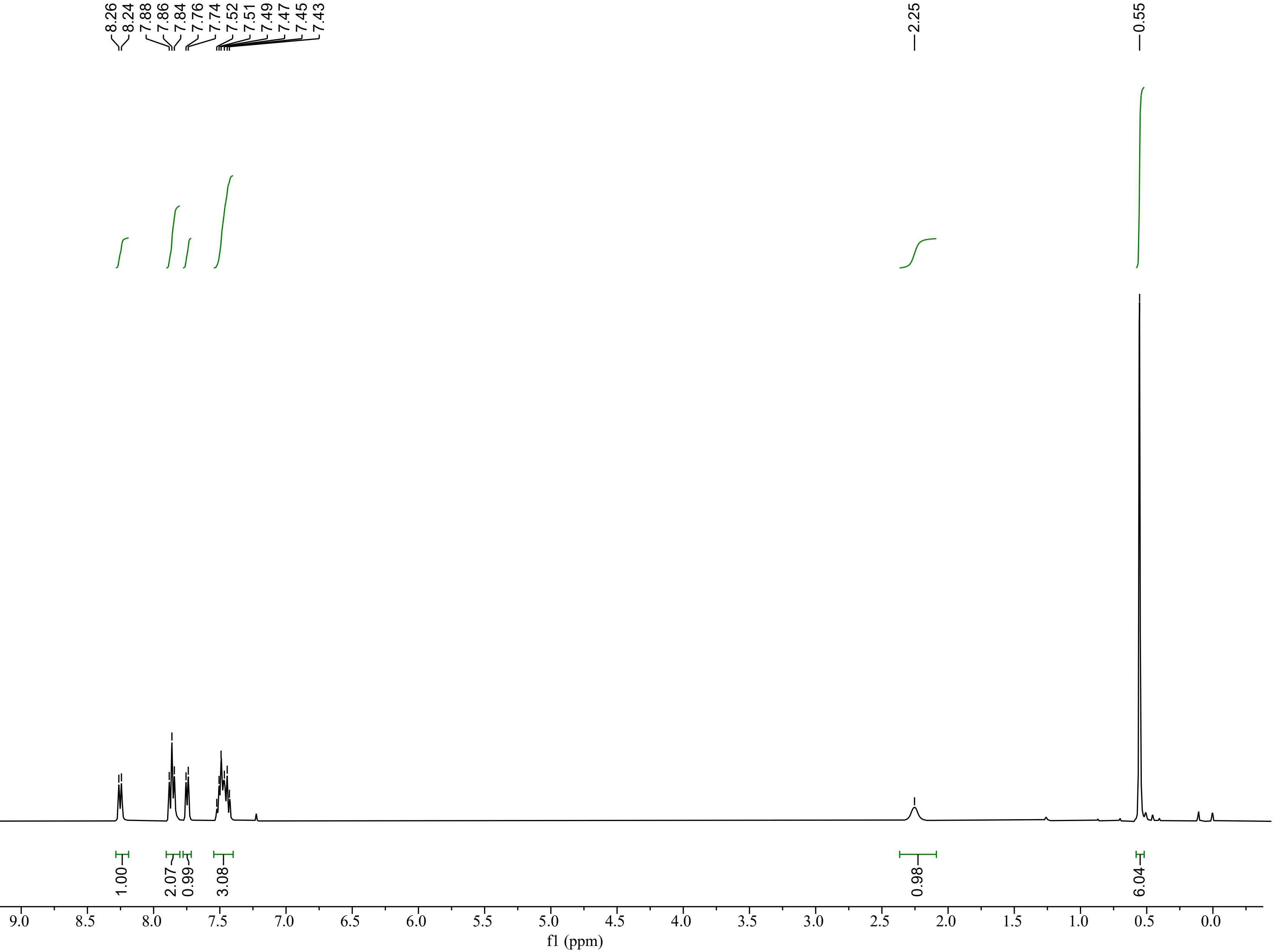

Compound **2bl** ^{13}C NMR

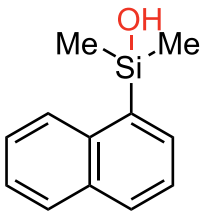

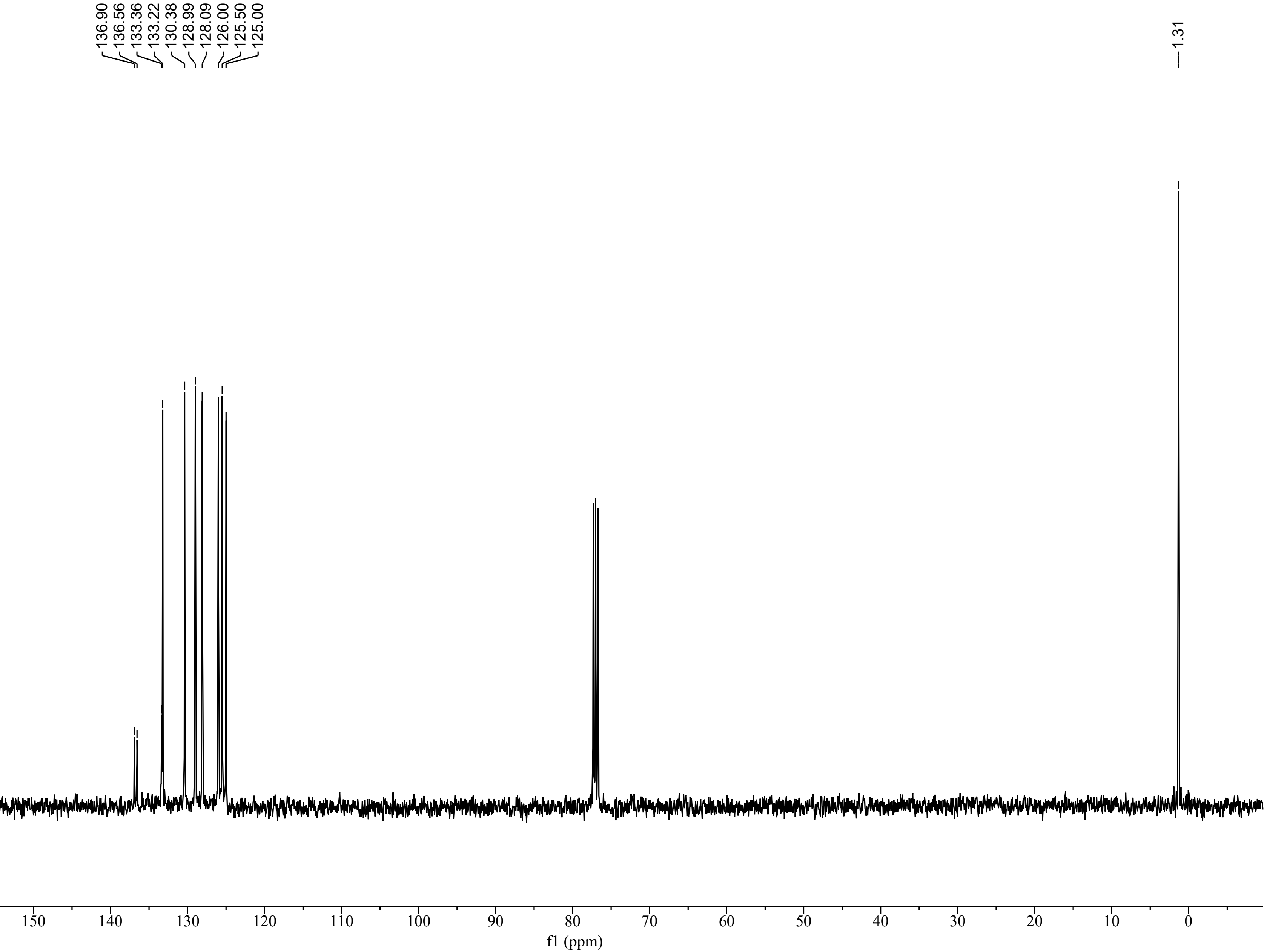

Compound **2bm** ^{1}H NMR

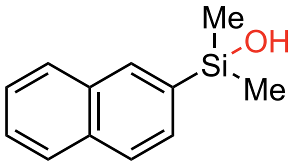

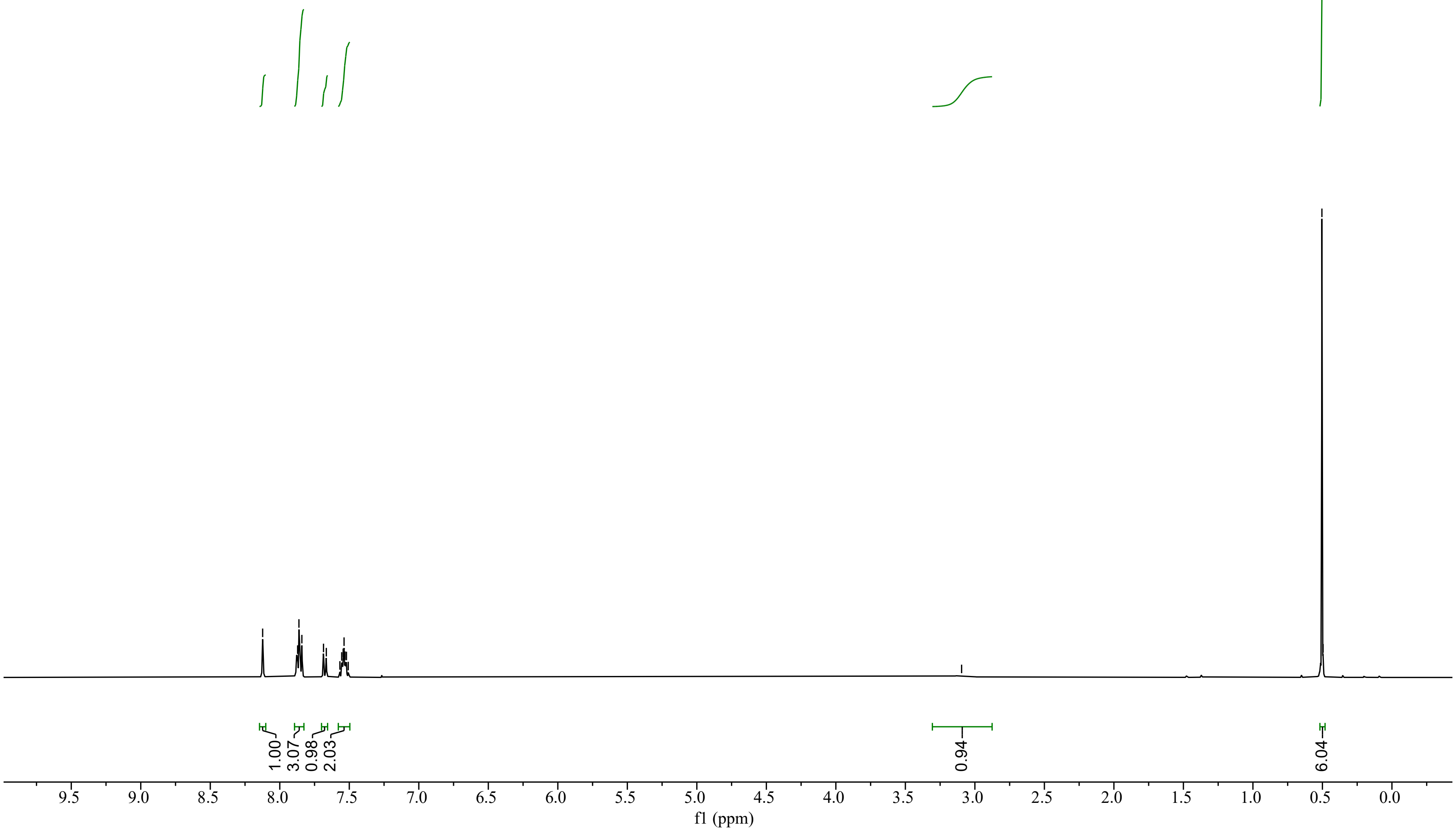

Compound **2bm** ^{13}C NMR

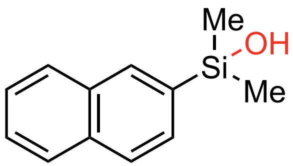

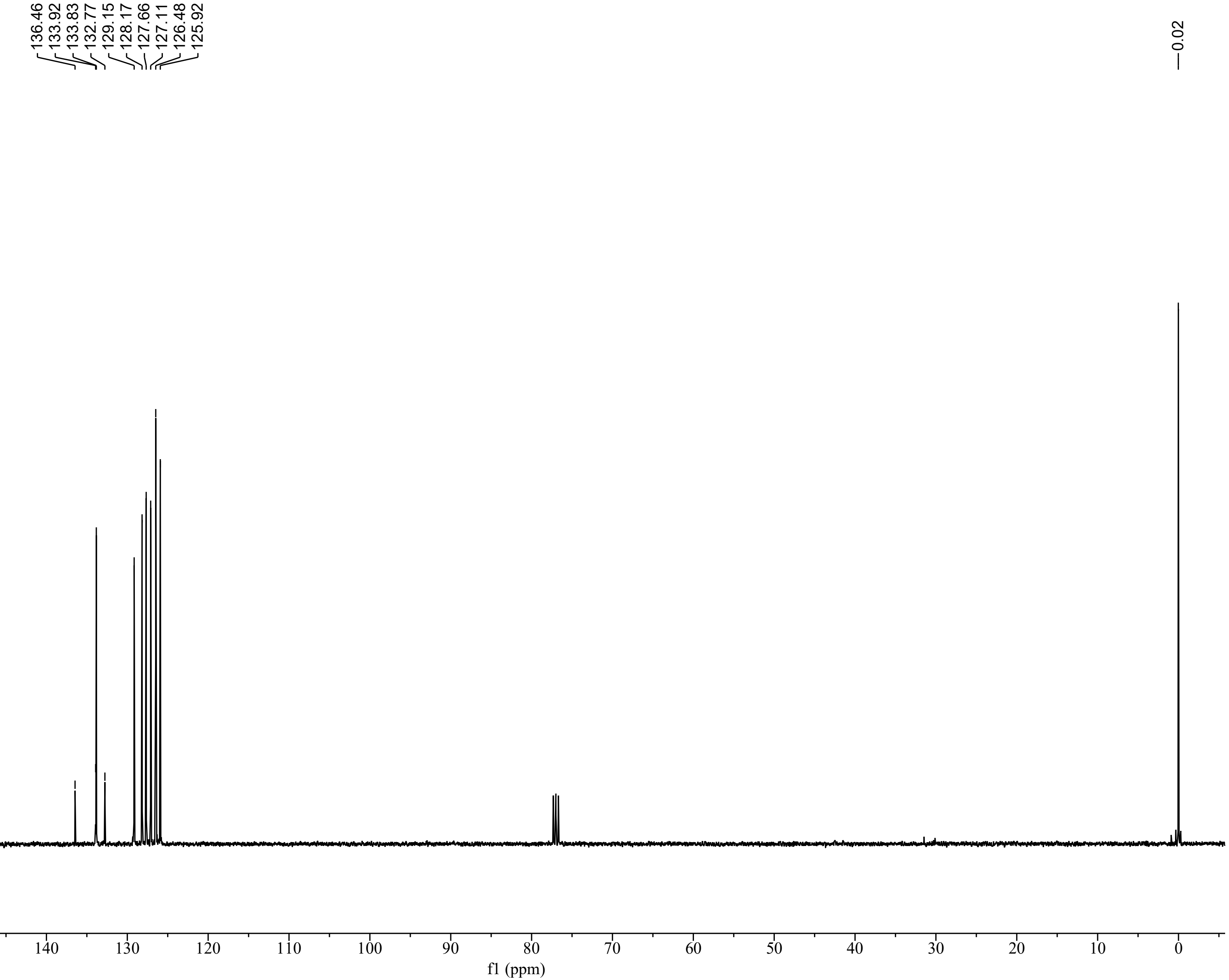

Compound **2bn** ^{1}H NMR

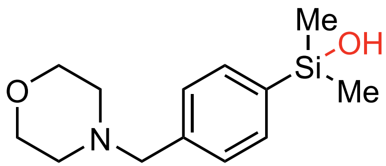

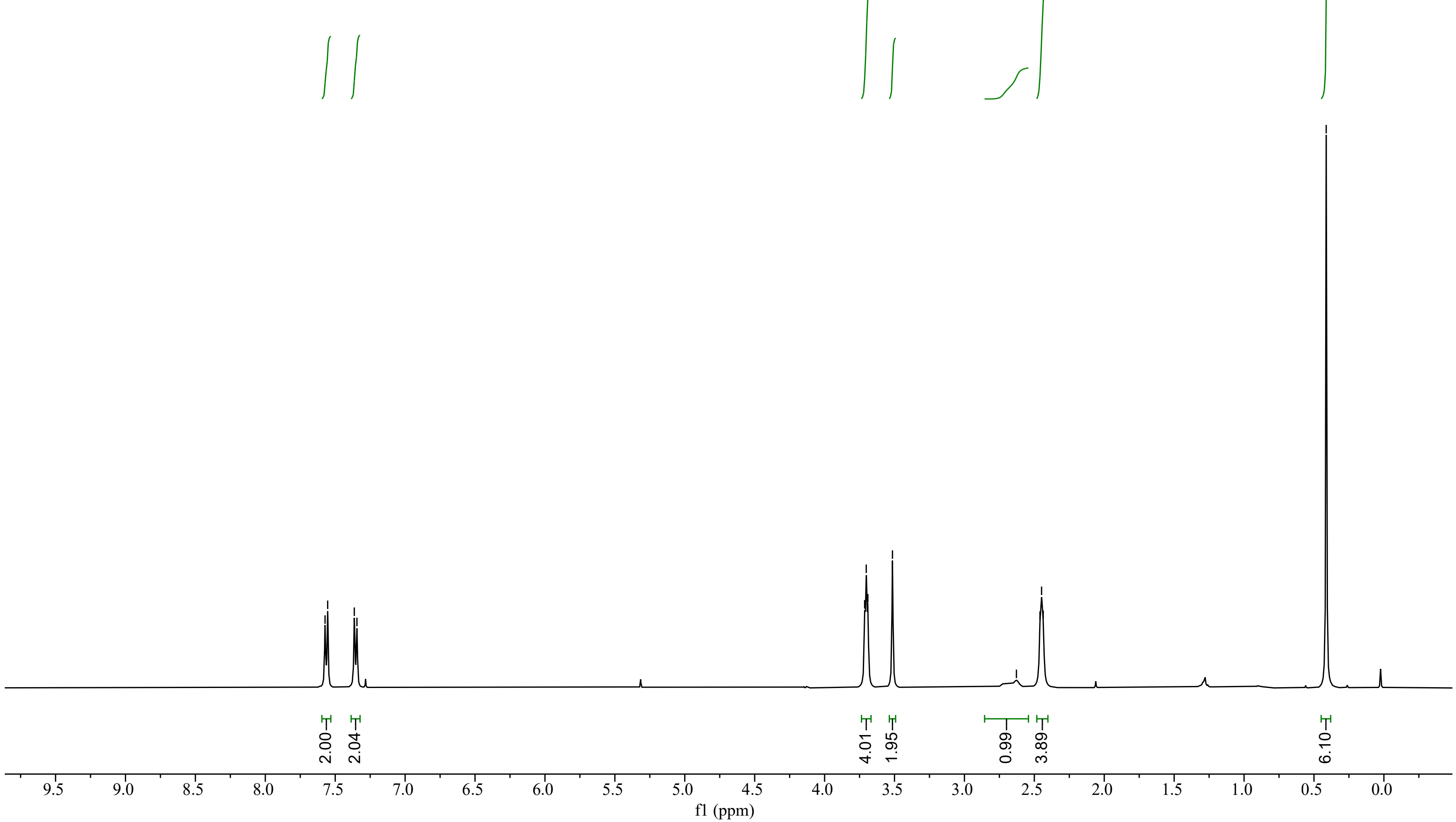

Compound **2bn** ^{13}C NMR

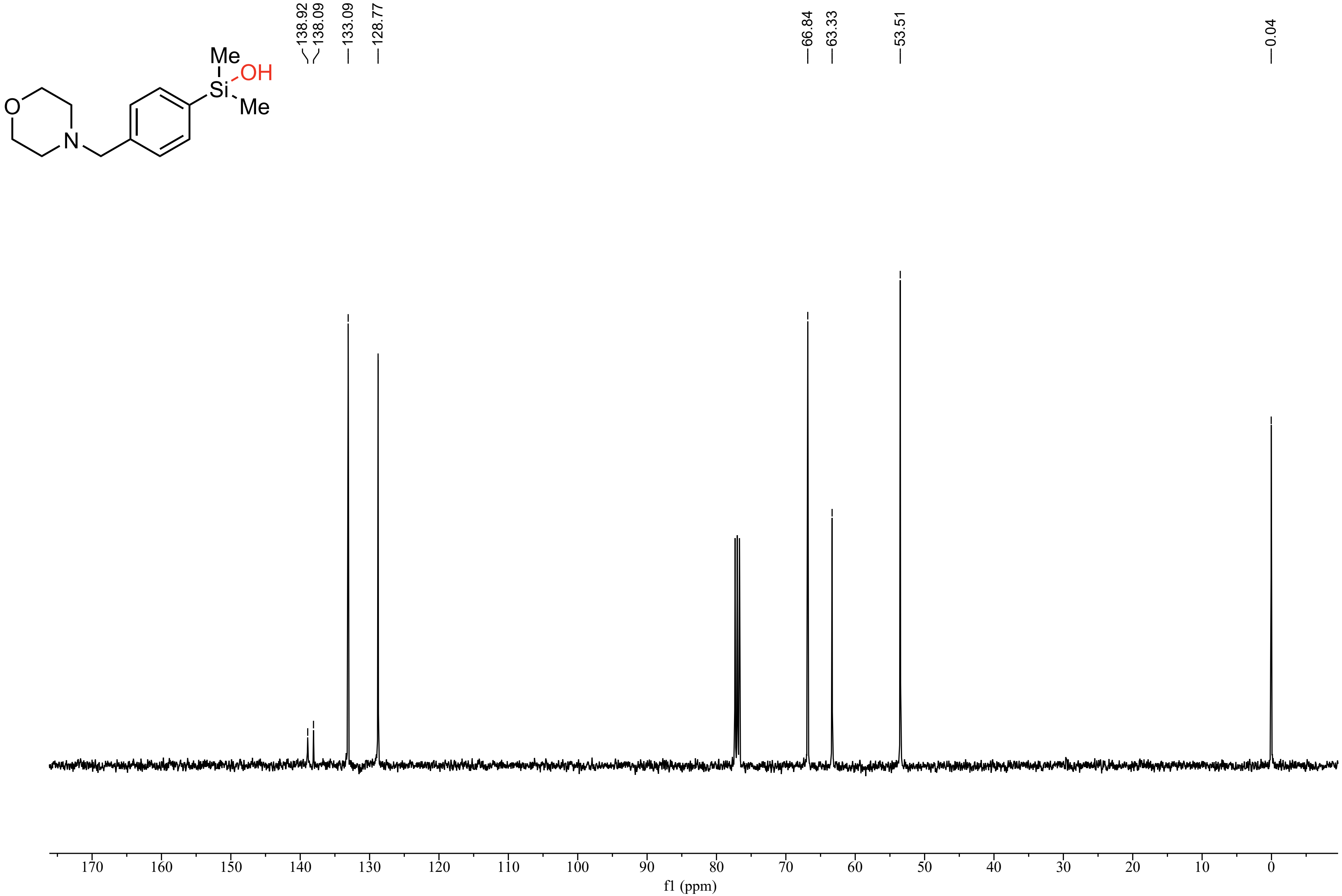

Compound **2bo** ^{1}H NMR

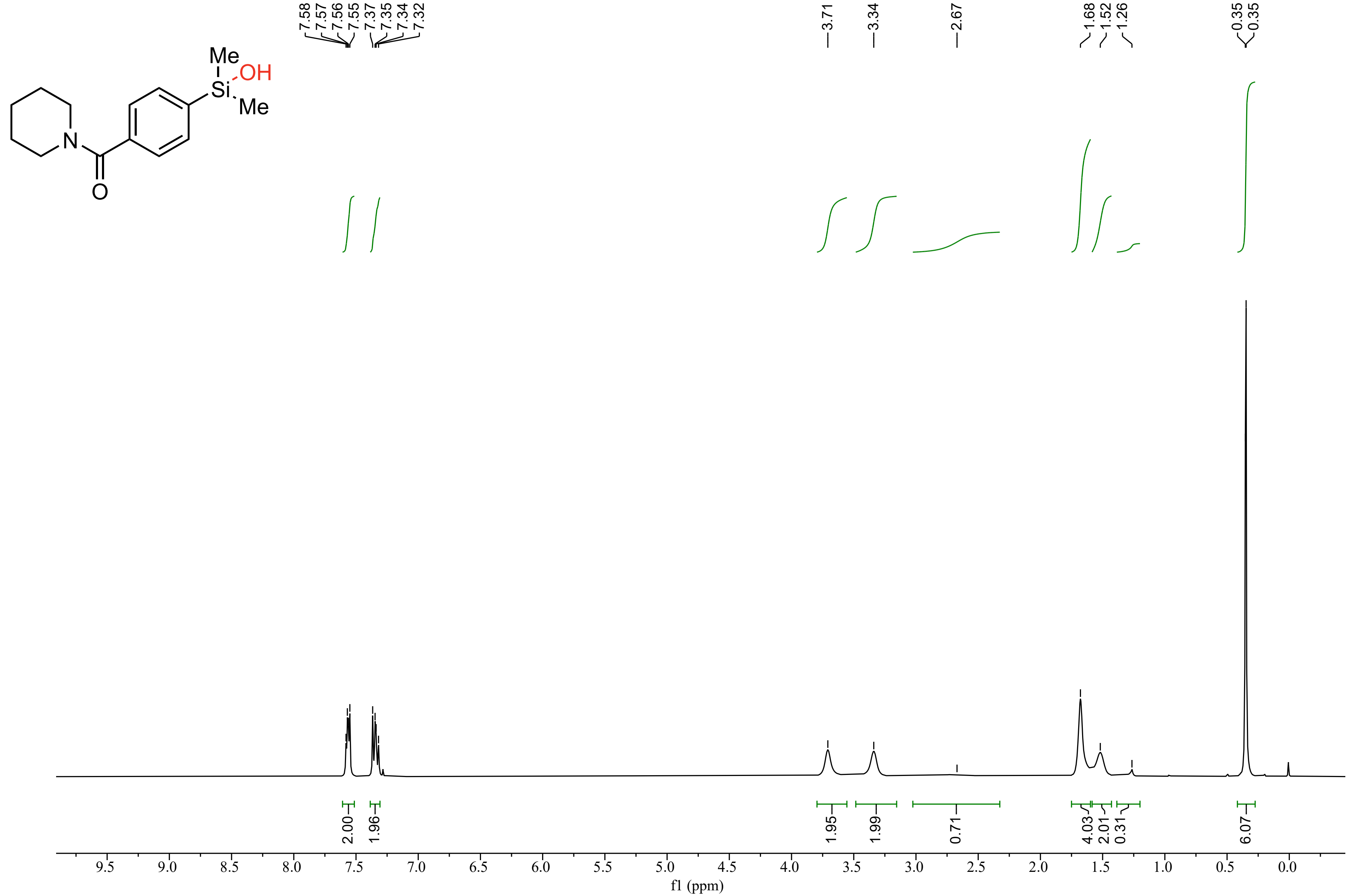

Compound **2bo** ^{13}C NMR

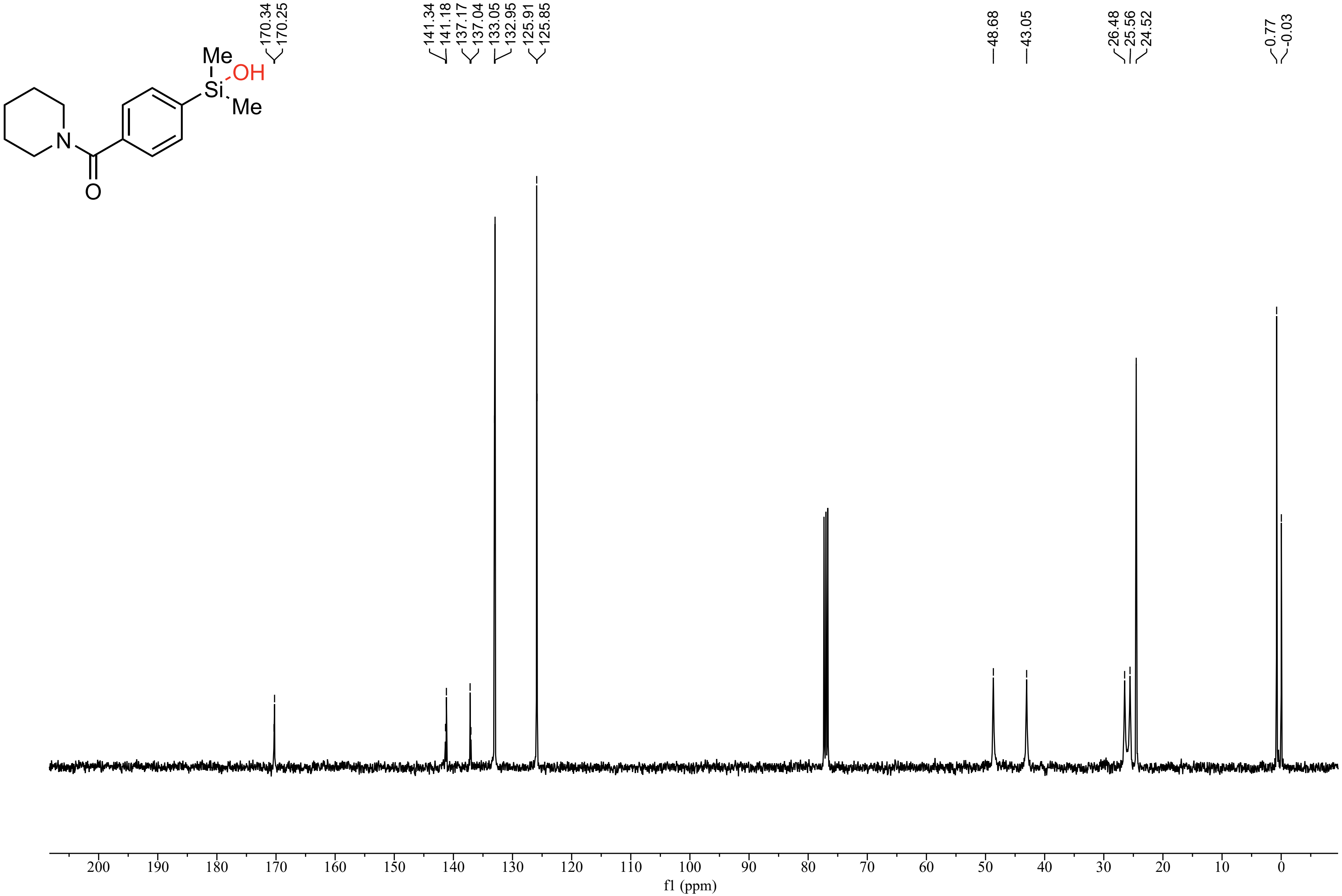

Compound **2bp** ^{1}H NMR

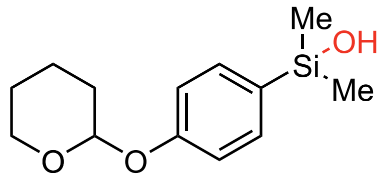

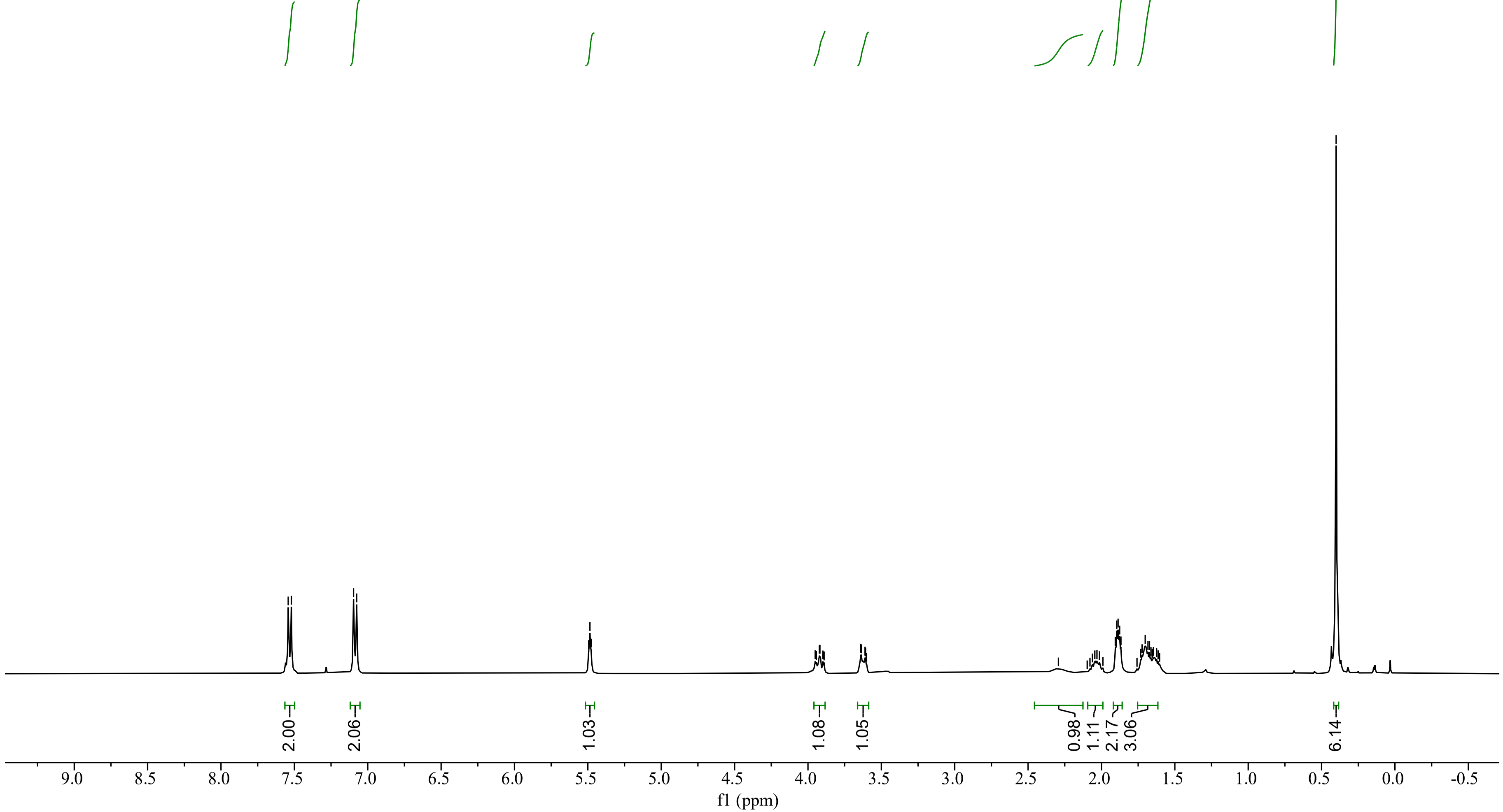

Compound **2bp** ^{13}C NMR

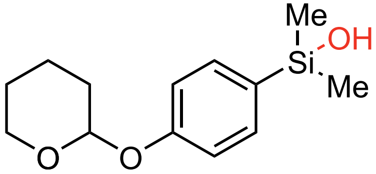

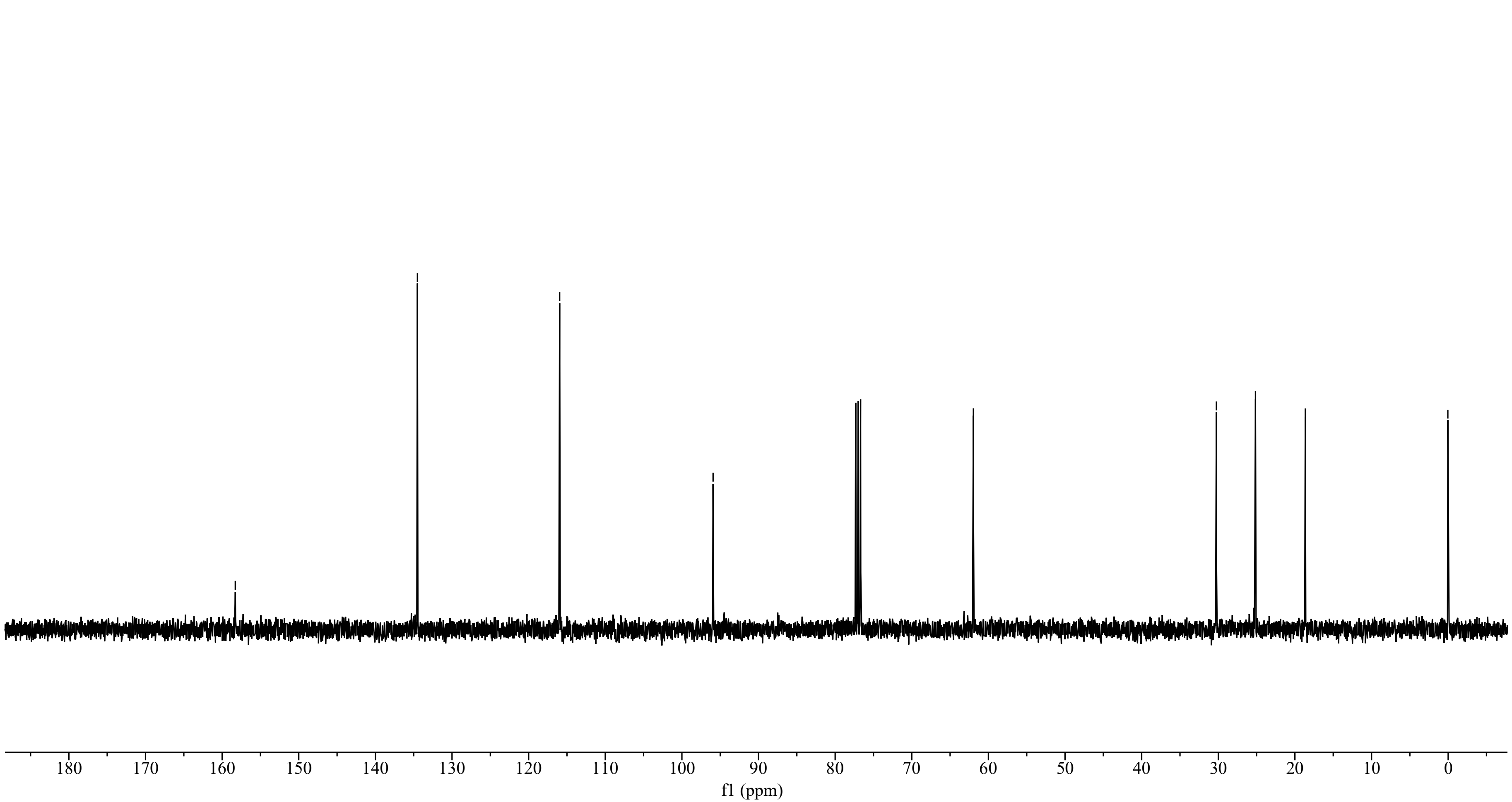

Compound **2bq** ^{1}H NMR

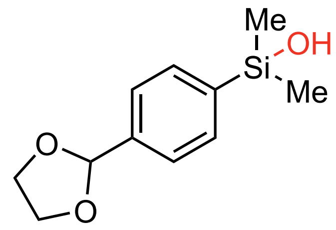

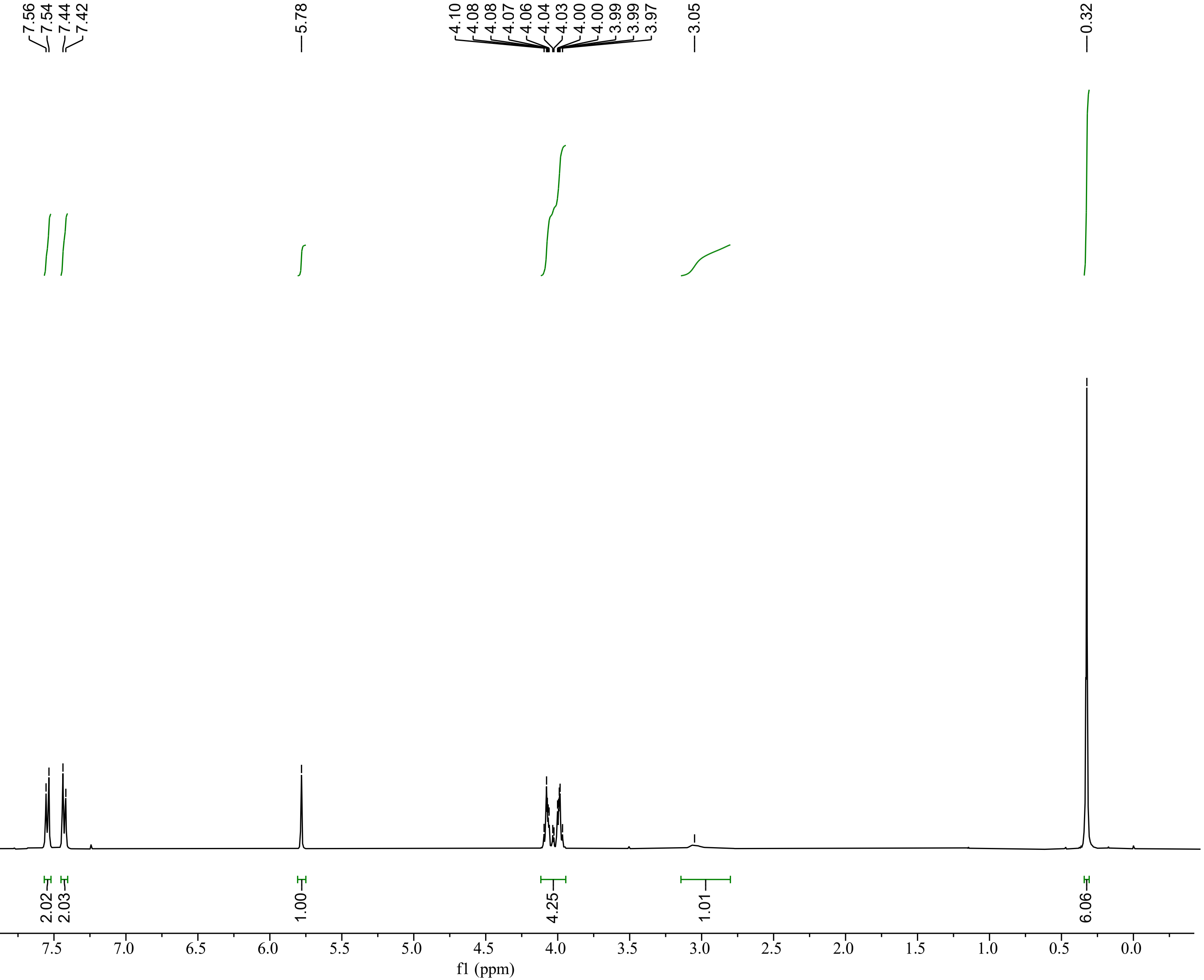

Compound **2bq** ^{13}C NMR

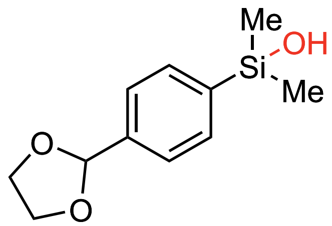

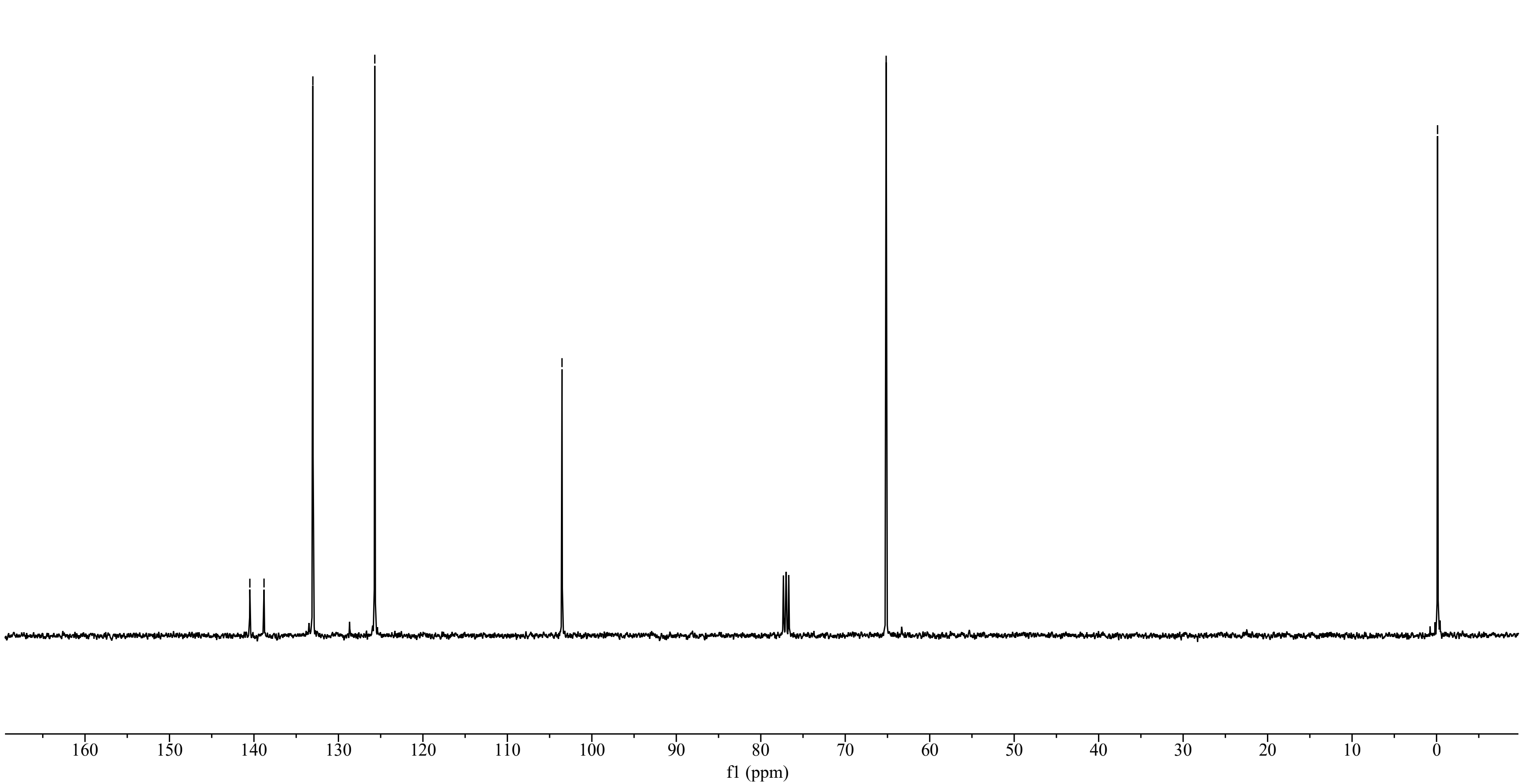

Compound **2br** [1]H NMR

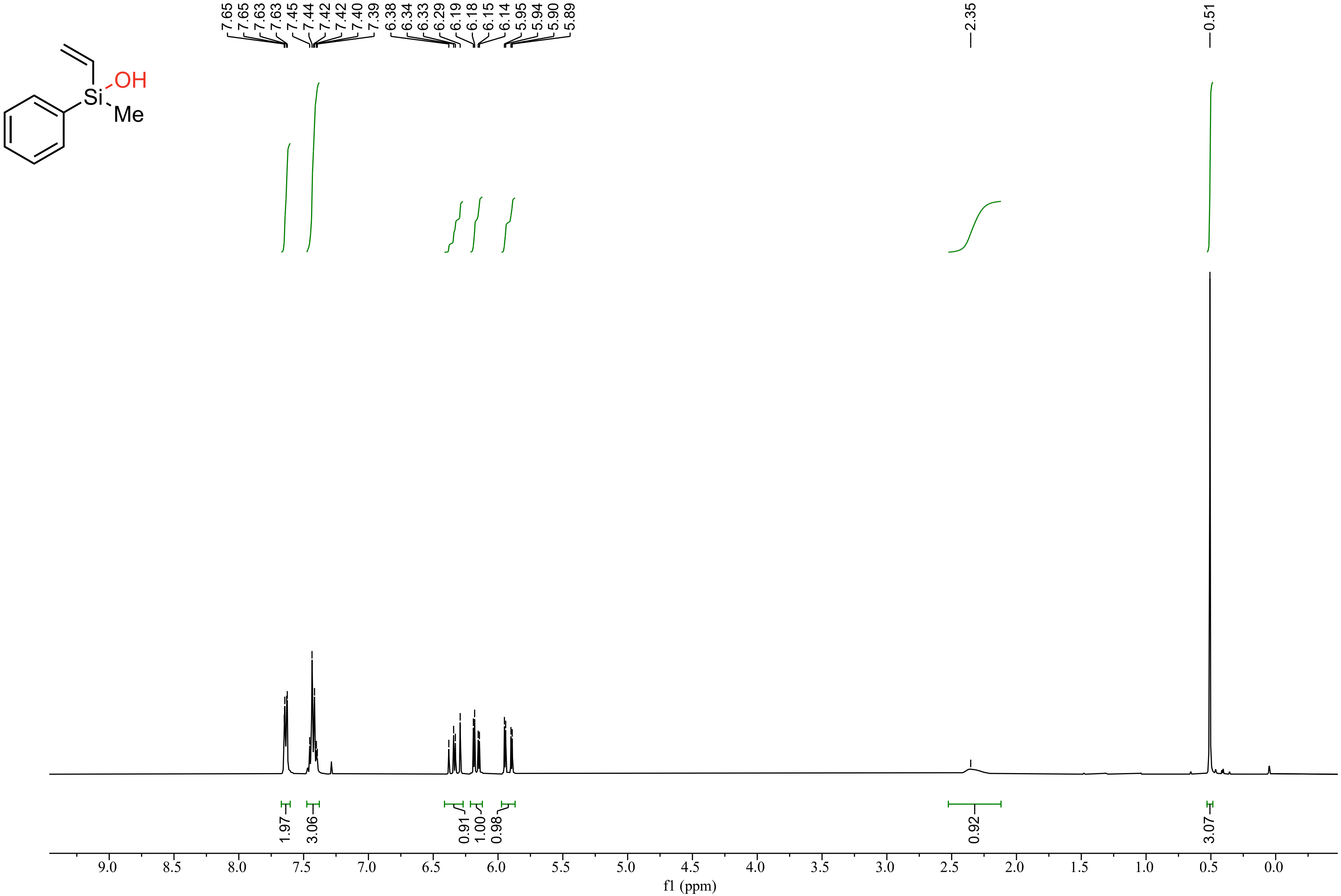

Compound **2br** ^{13}C NMR

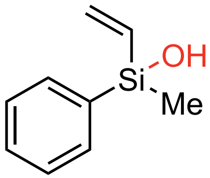

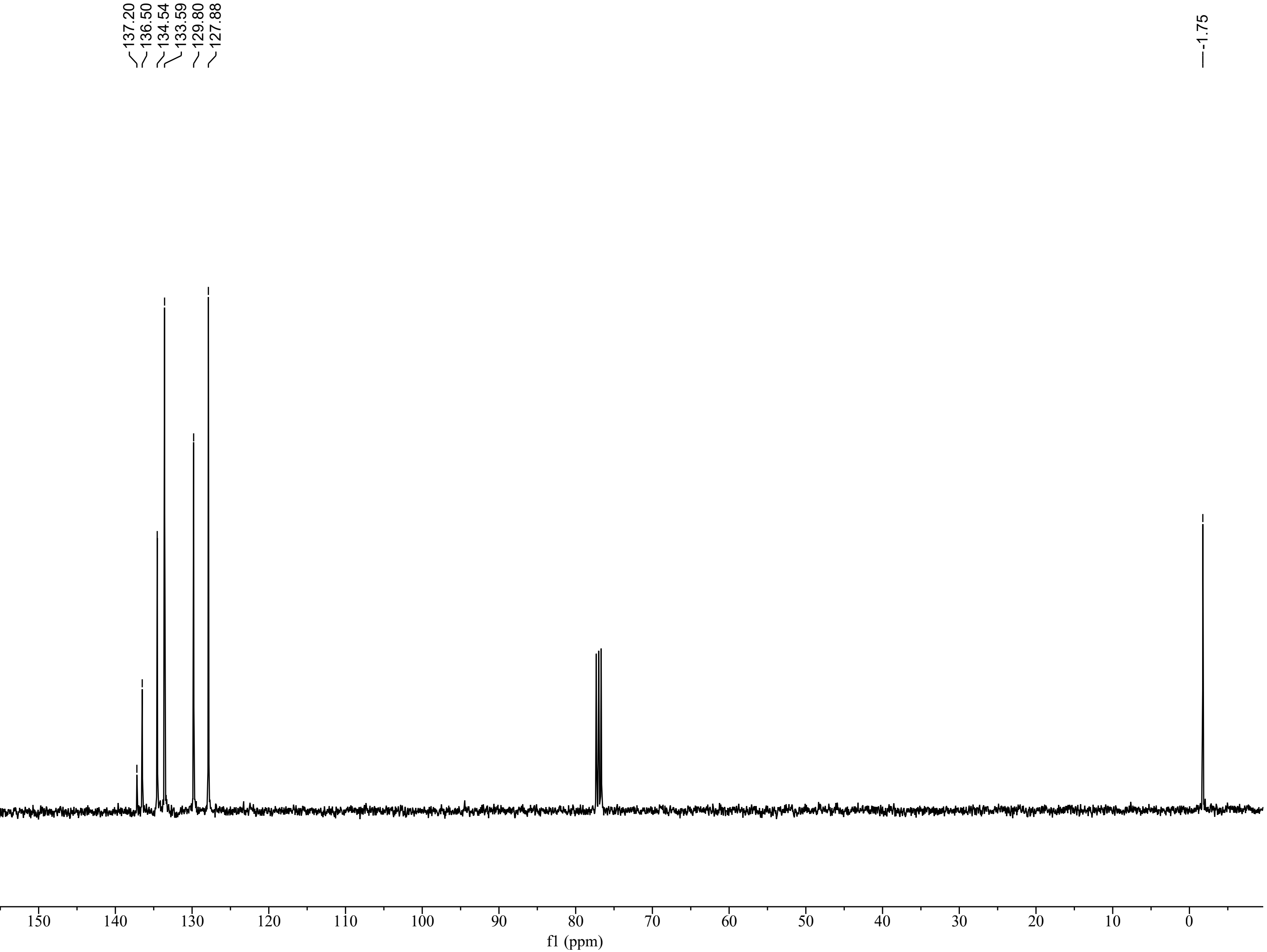

Compound **2bs** ^{1}H NMR

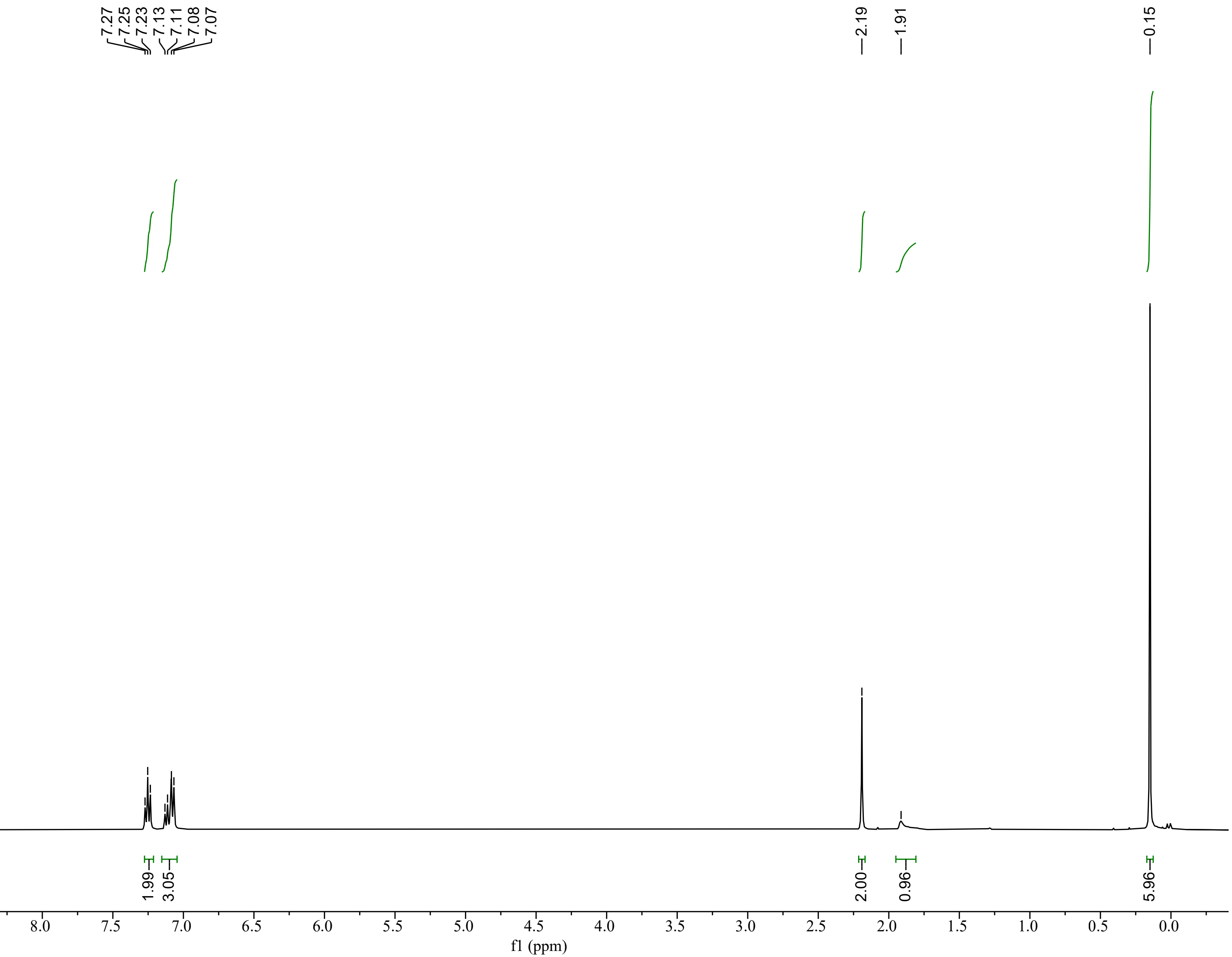

Compound **2bs** ^{13}C NMR

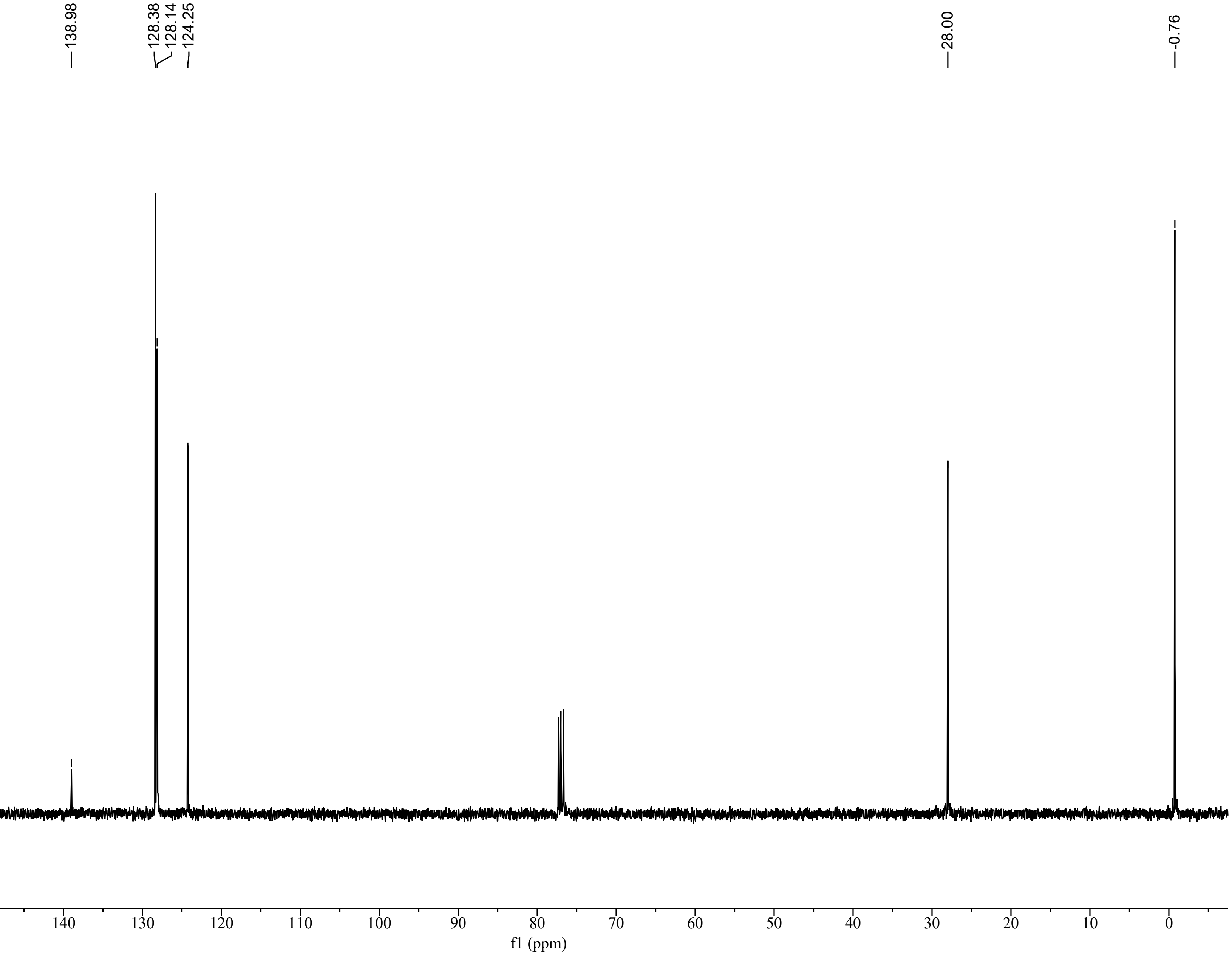

Compound **2bt** ^{1}H NMR

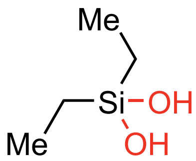

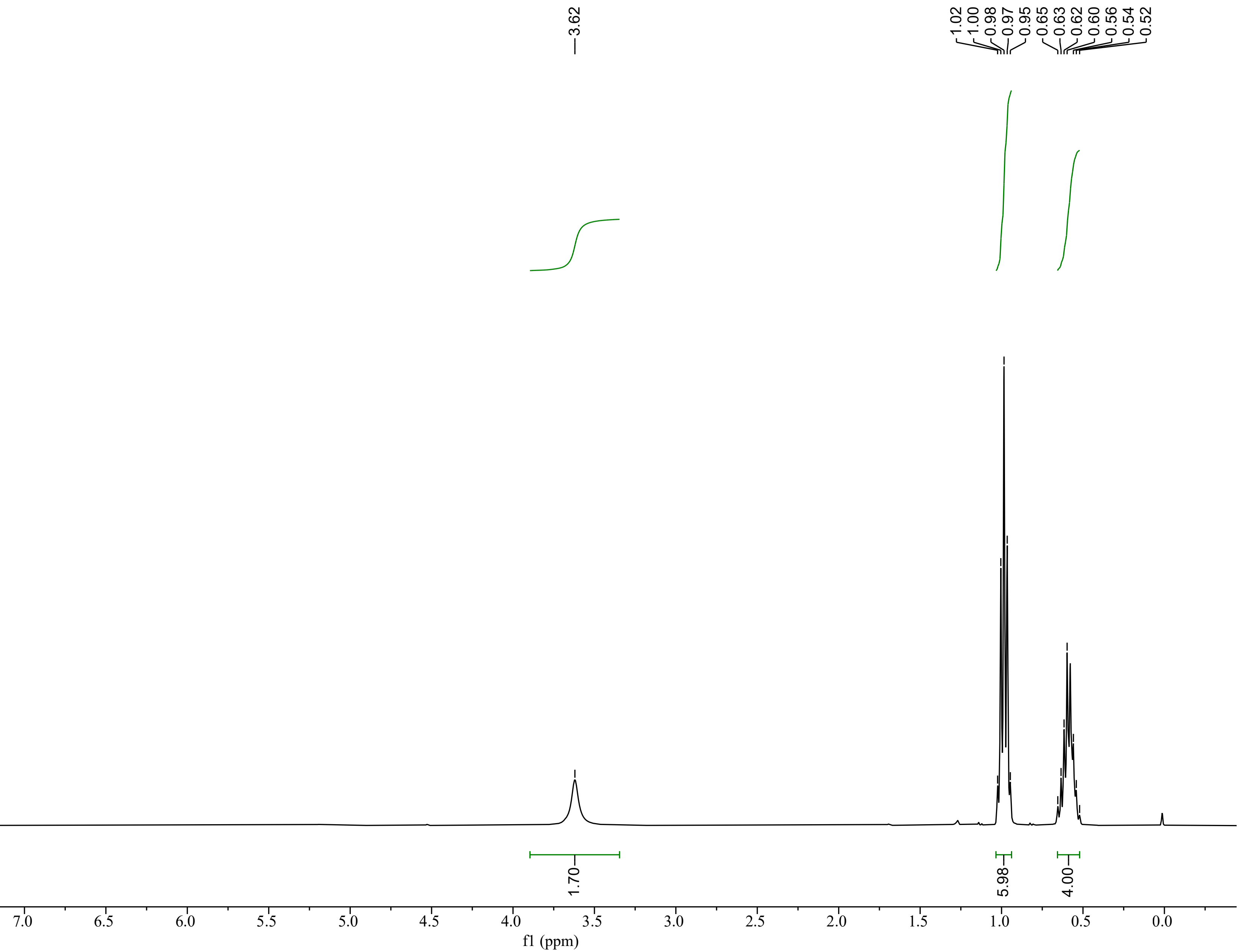

Compound **2bt** ^{13}C NMR

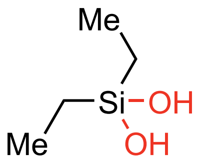

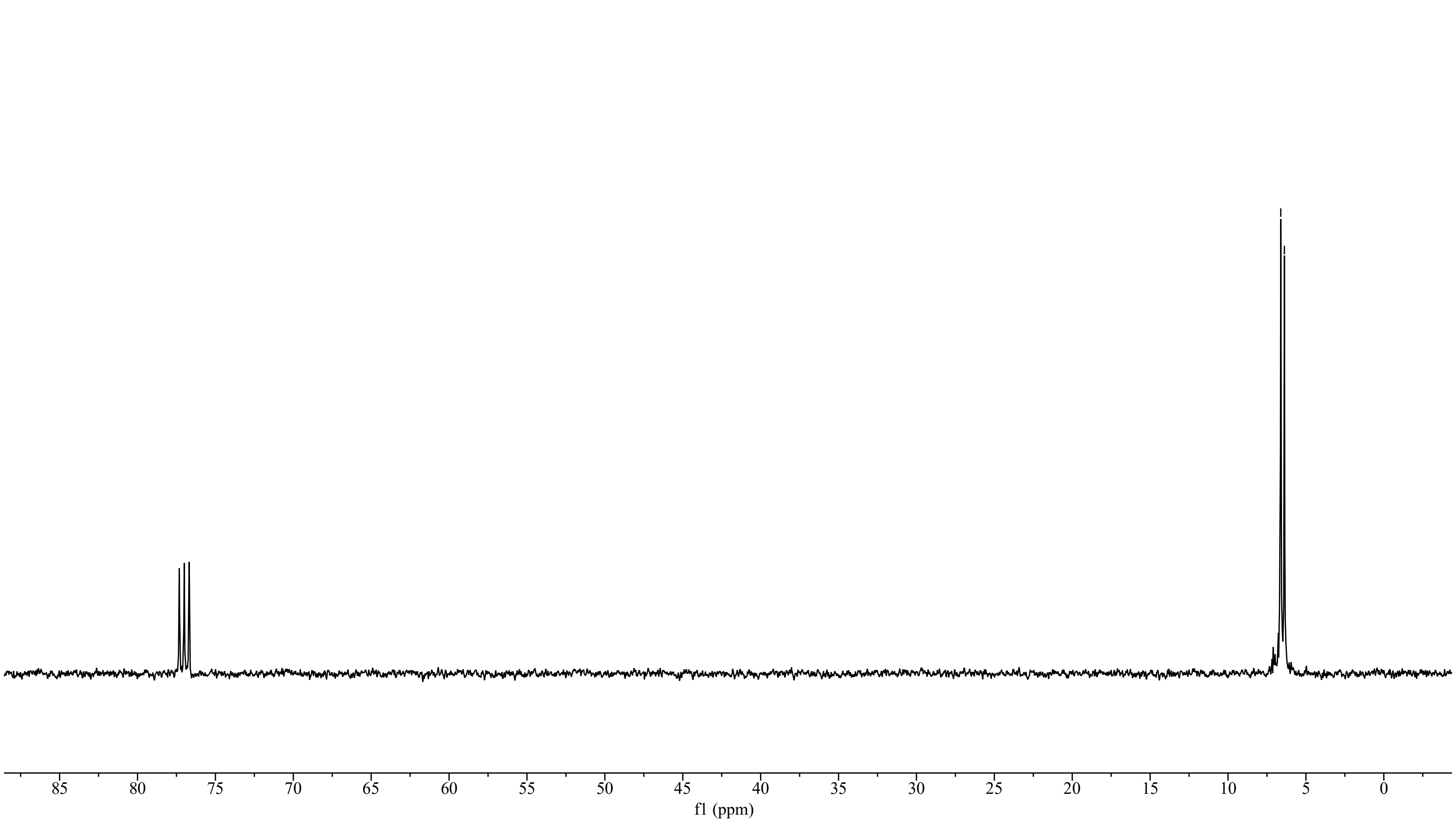

Compound **4a** ^{1}H NMR

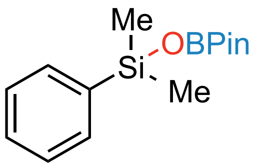

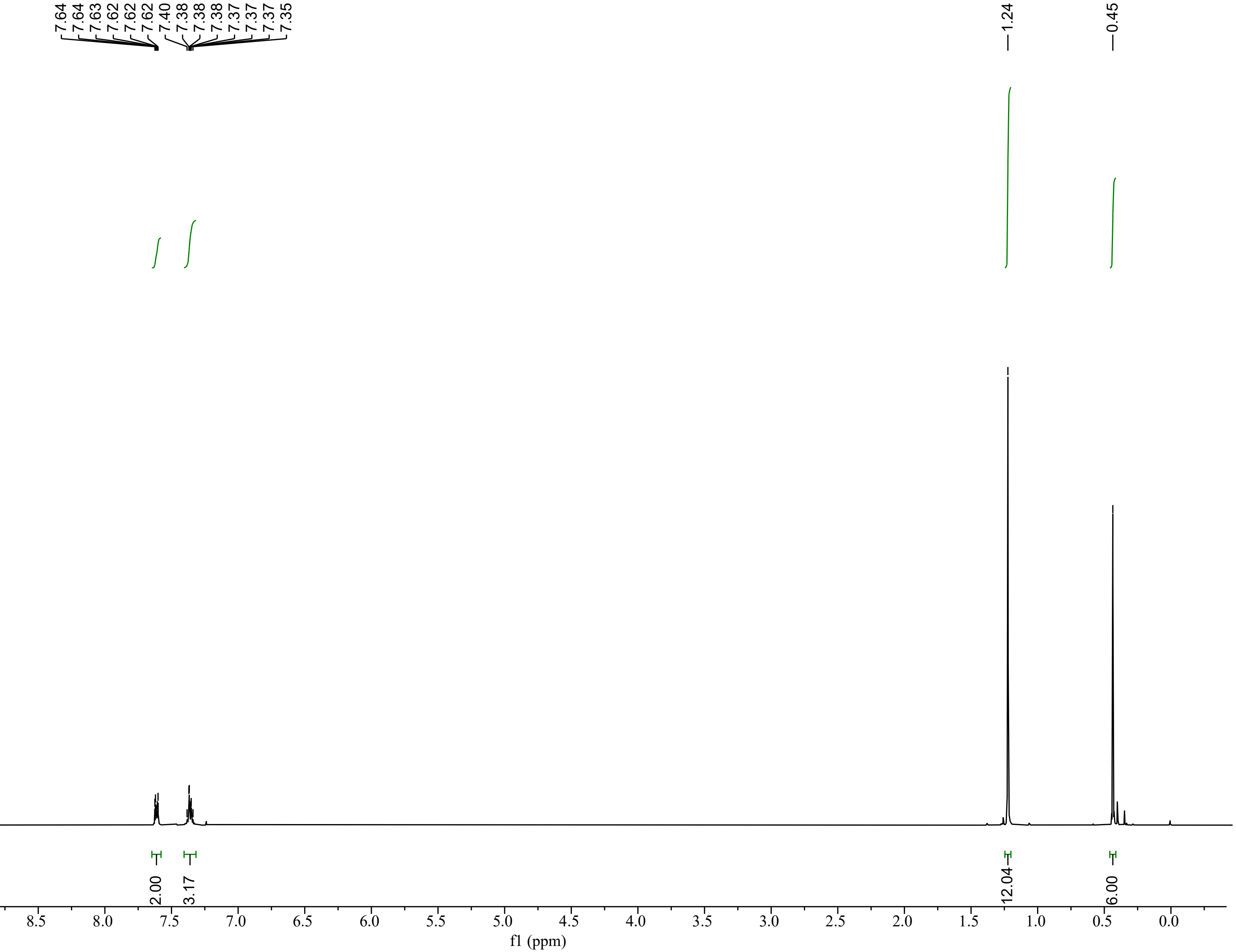

Compound **4a** ^{13}C NMR

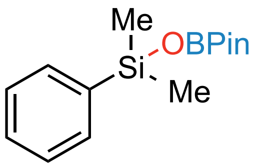

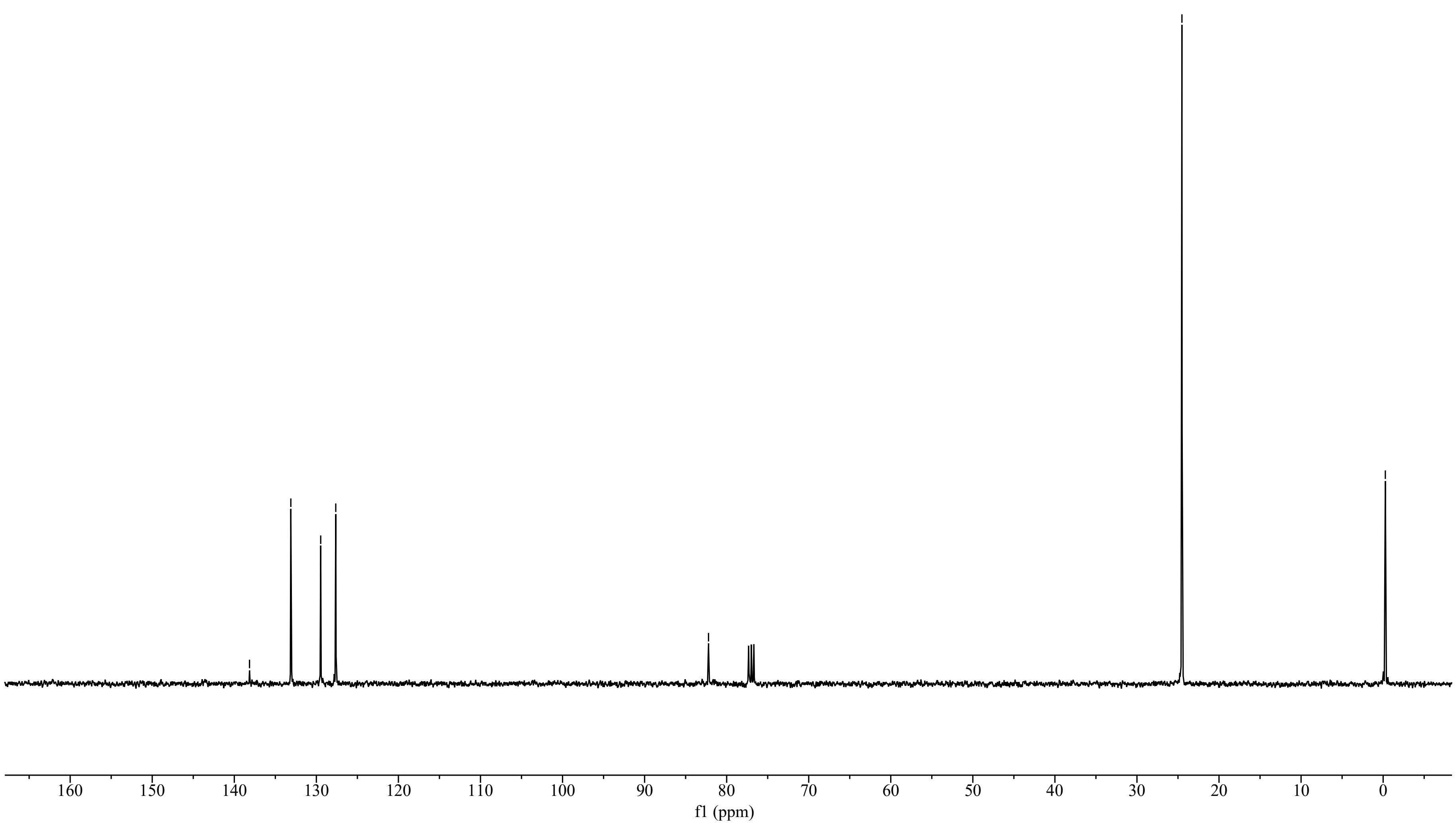

Compound **4b** ^{1}H NMR

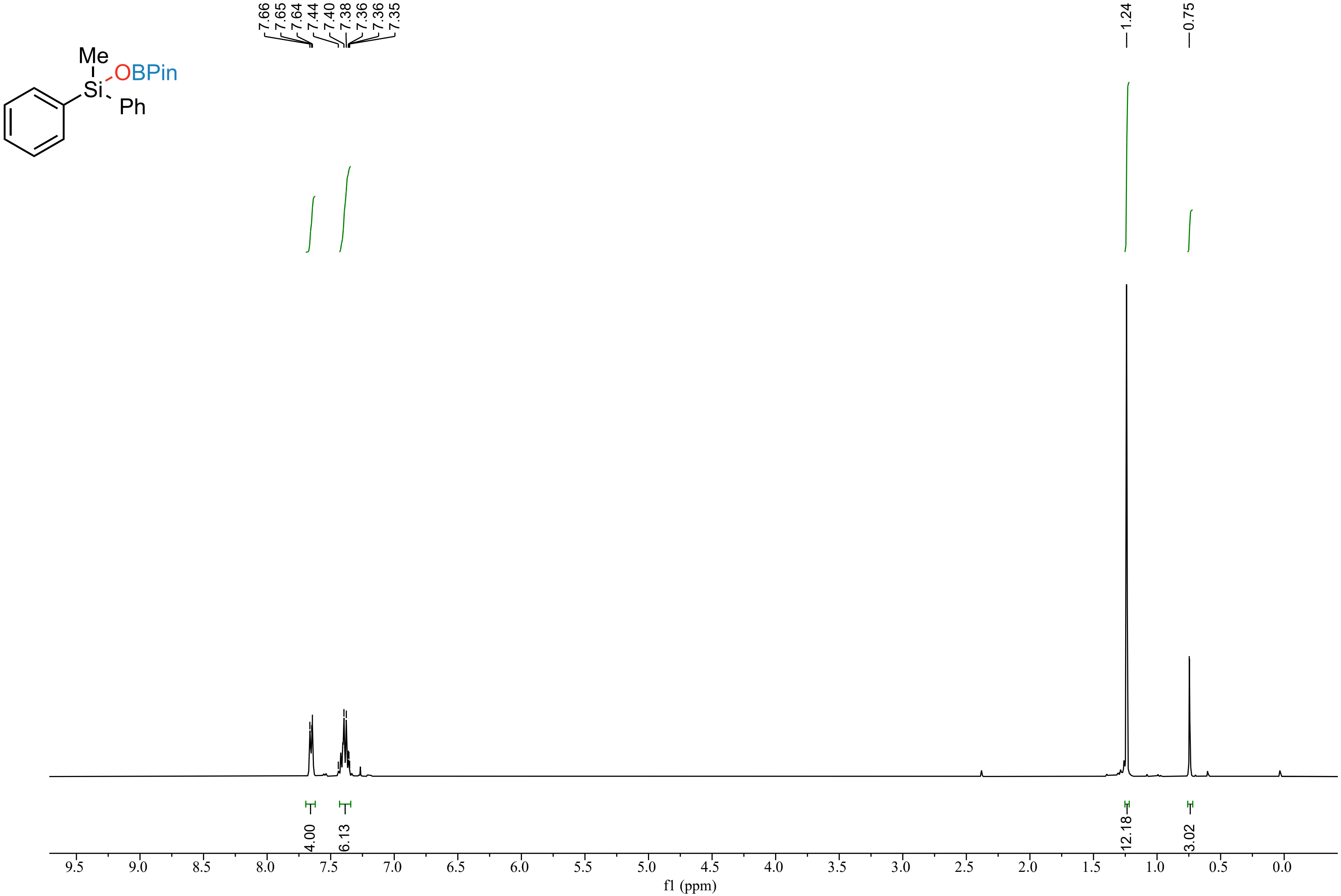

Compound **4b** ^{13}C NMR

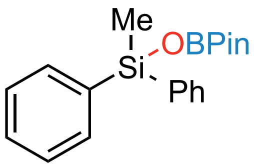

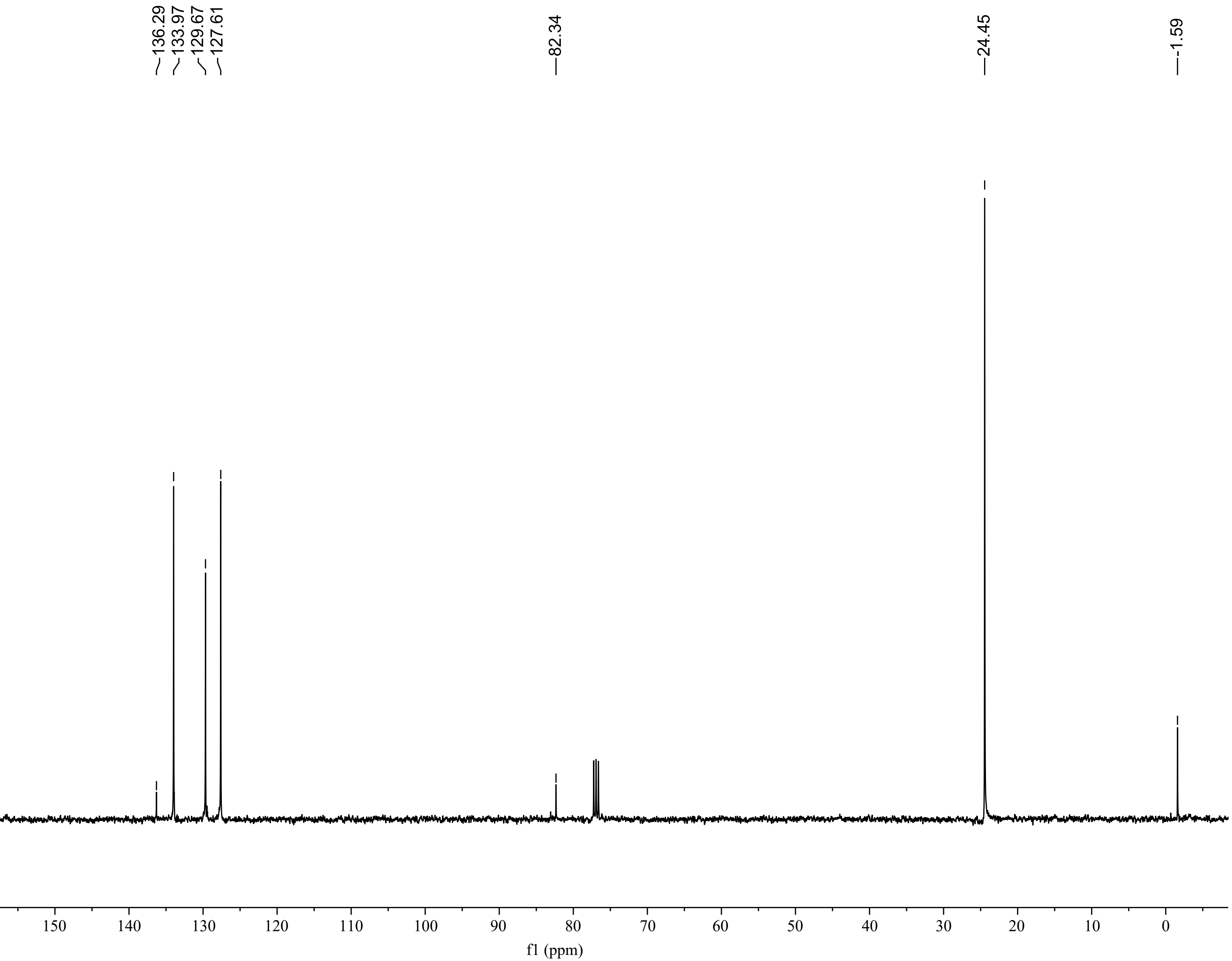

Compound **4c** ^{1}H NMR

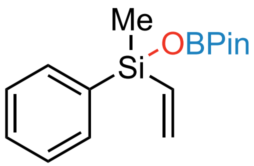

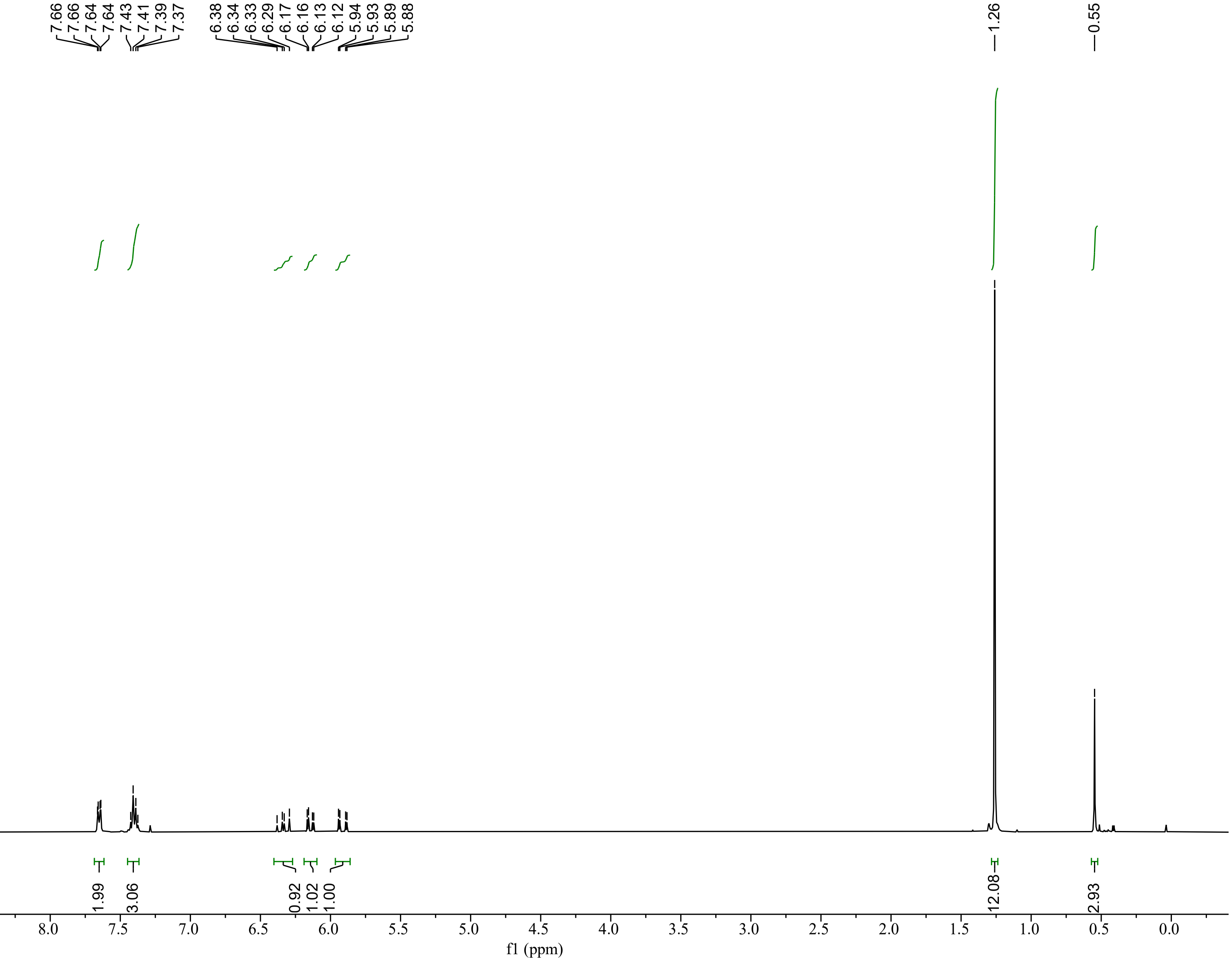

Compound **4c** ^{13}C NMR

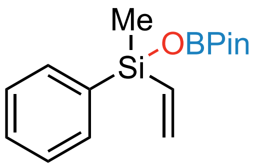

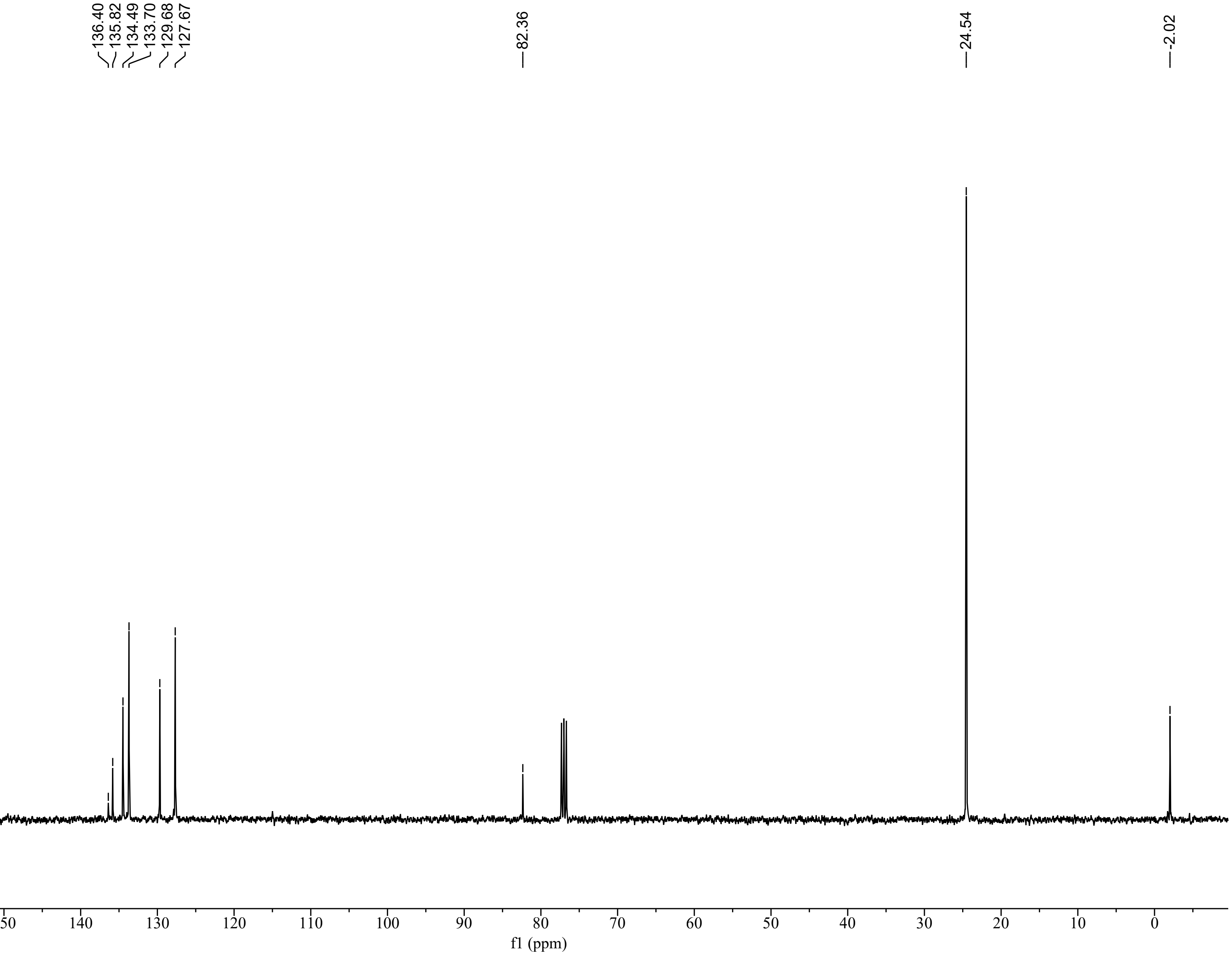

Compound **4d** ^{1}H NMR

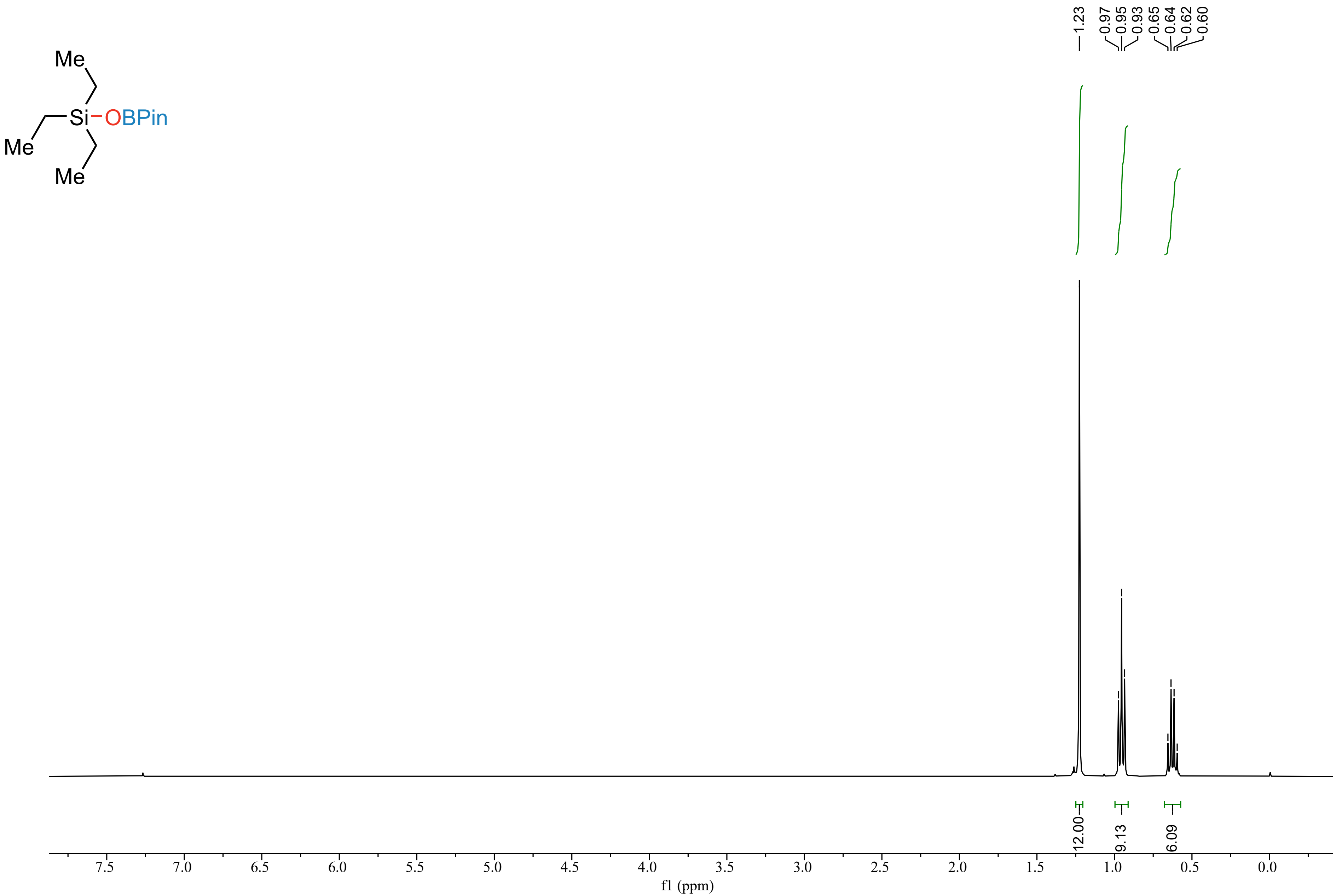

Compound **4d** ^{13}C NMR

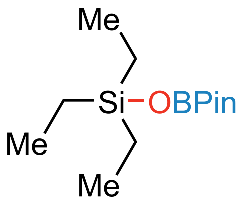

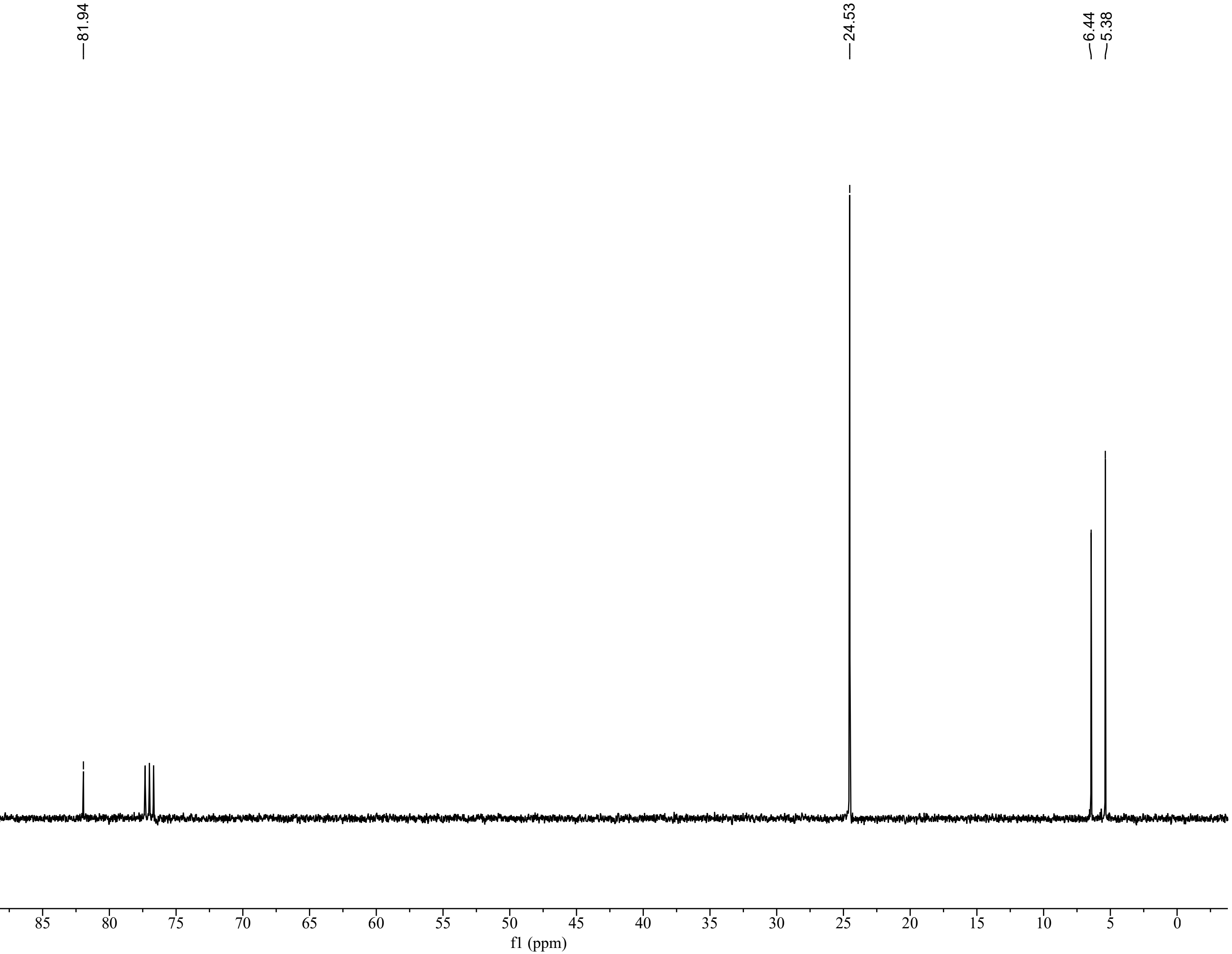

Compound **4e** [1]H NMR

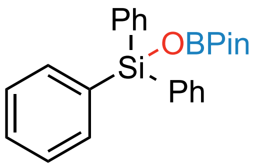

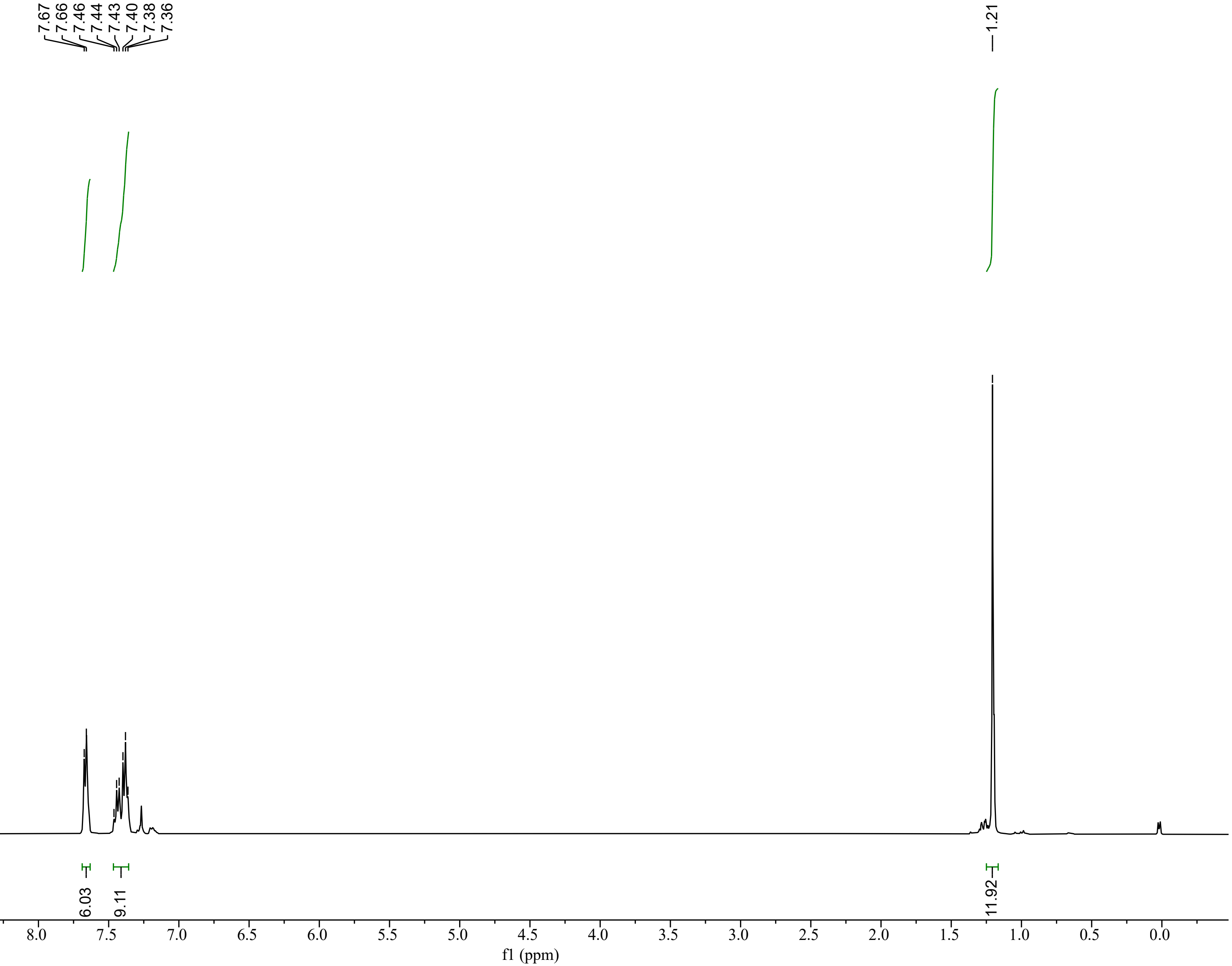

Compound **4e** ^{13}C NMR

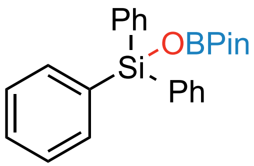

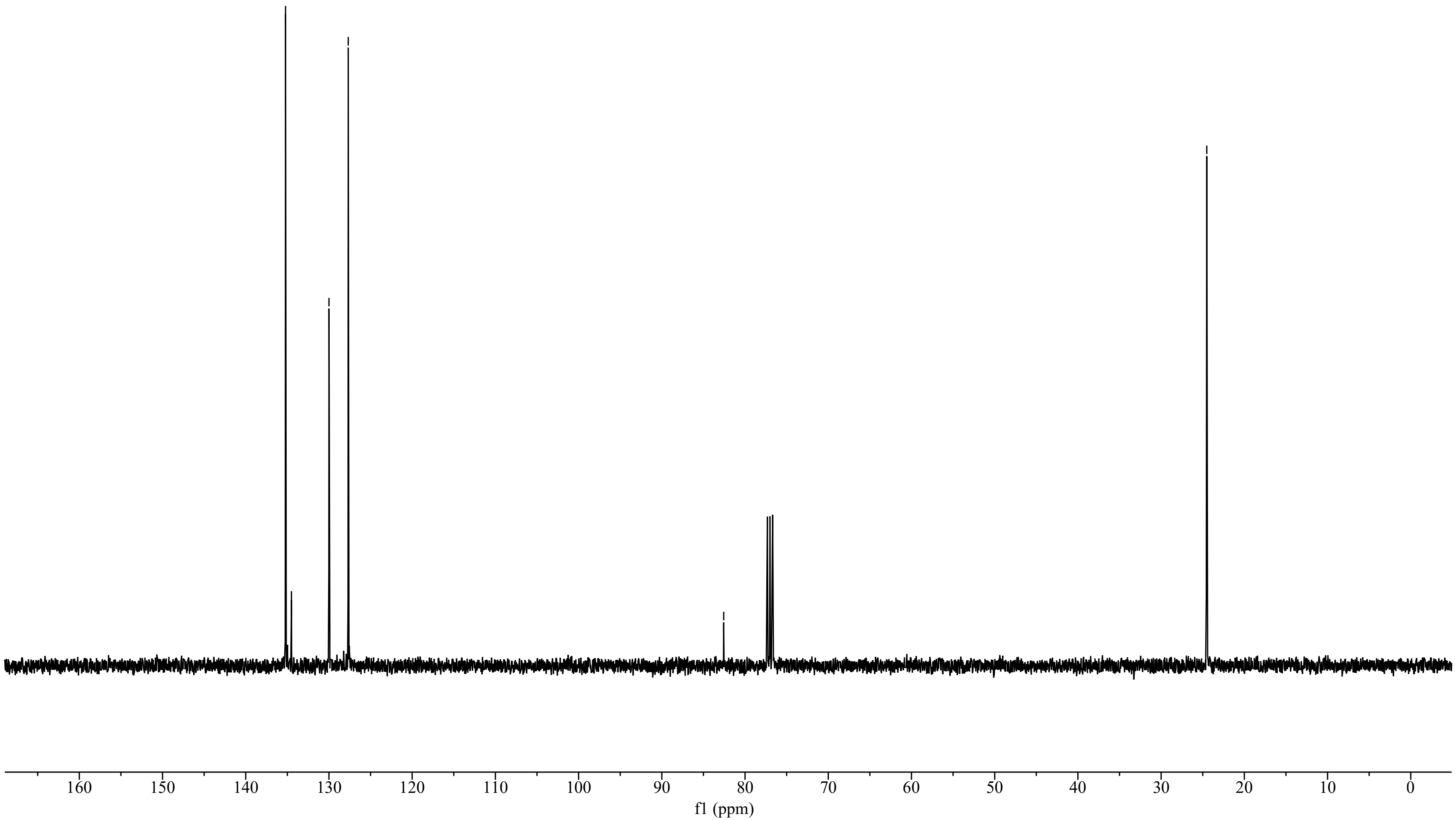

Compound **4f** ^{1}H NMR

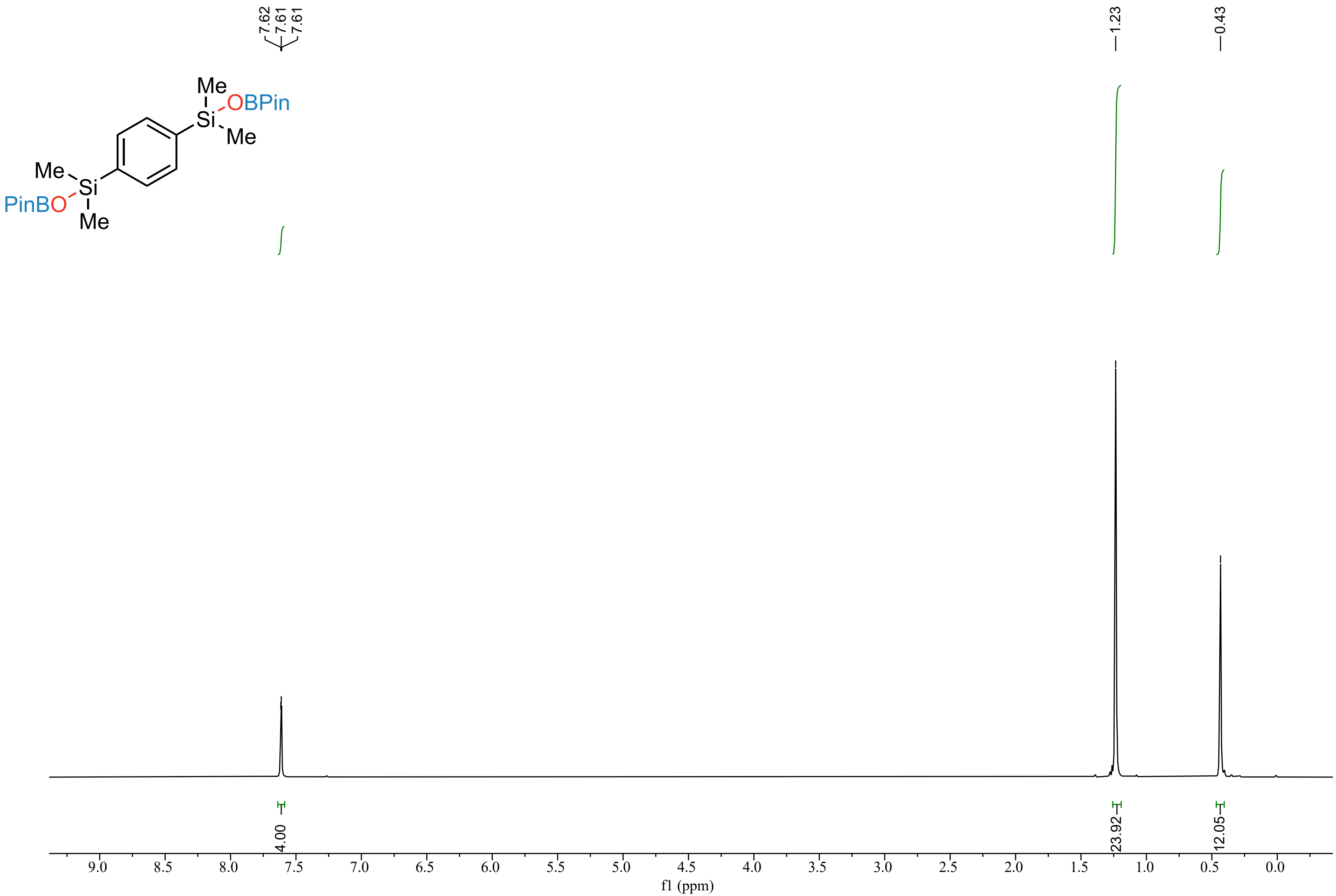

Compound **4f** ^{13}C NMR

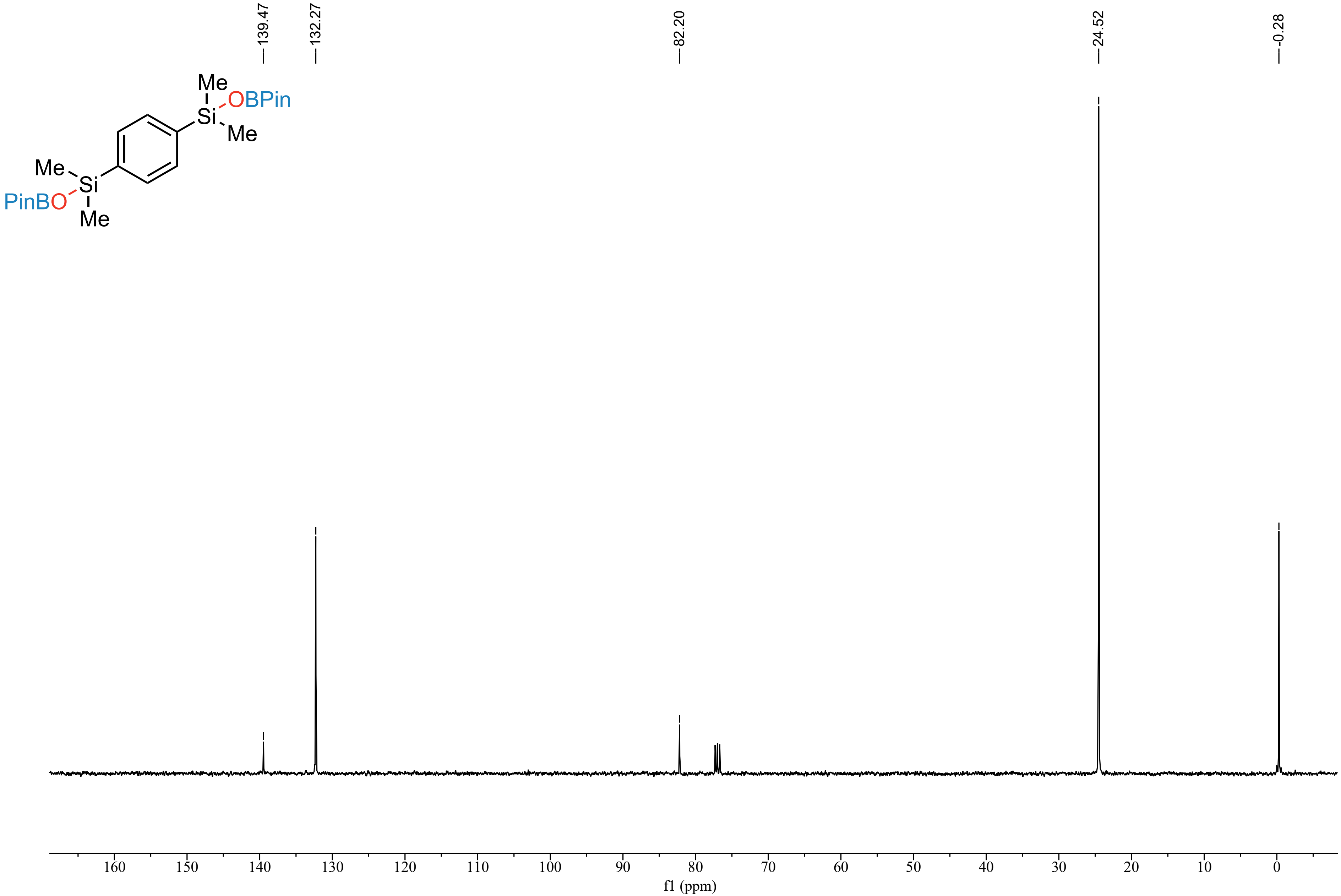

Compound **4g** ^{1}H NMR

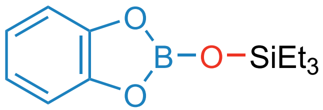

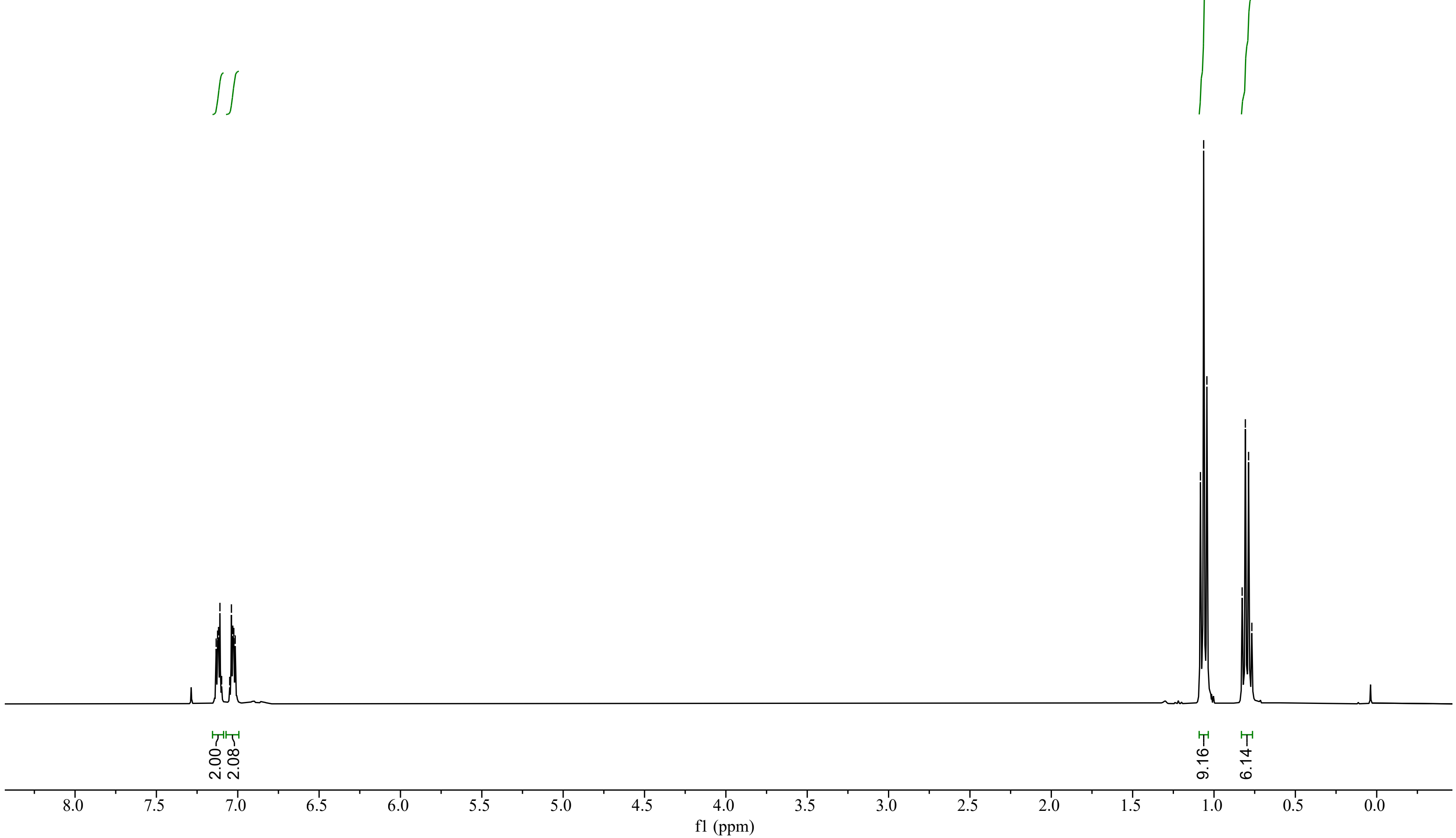

Compound **4g** ^{13}C NMR

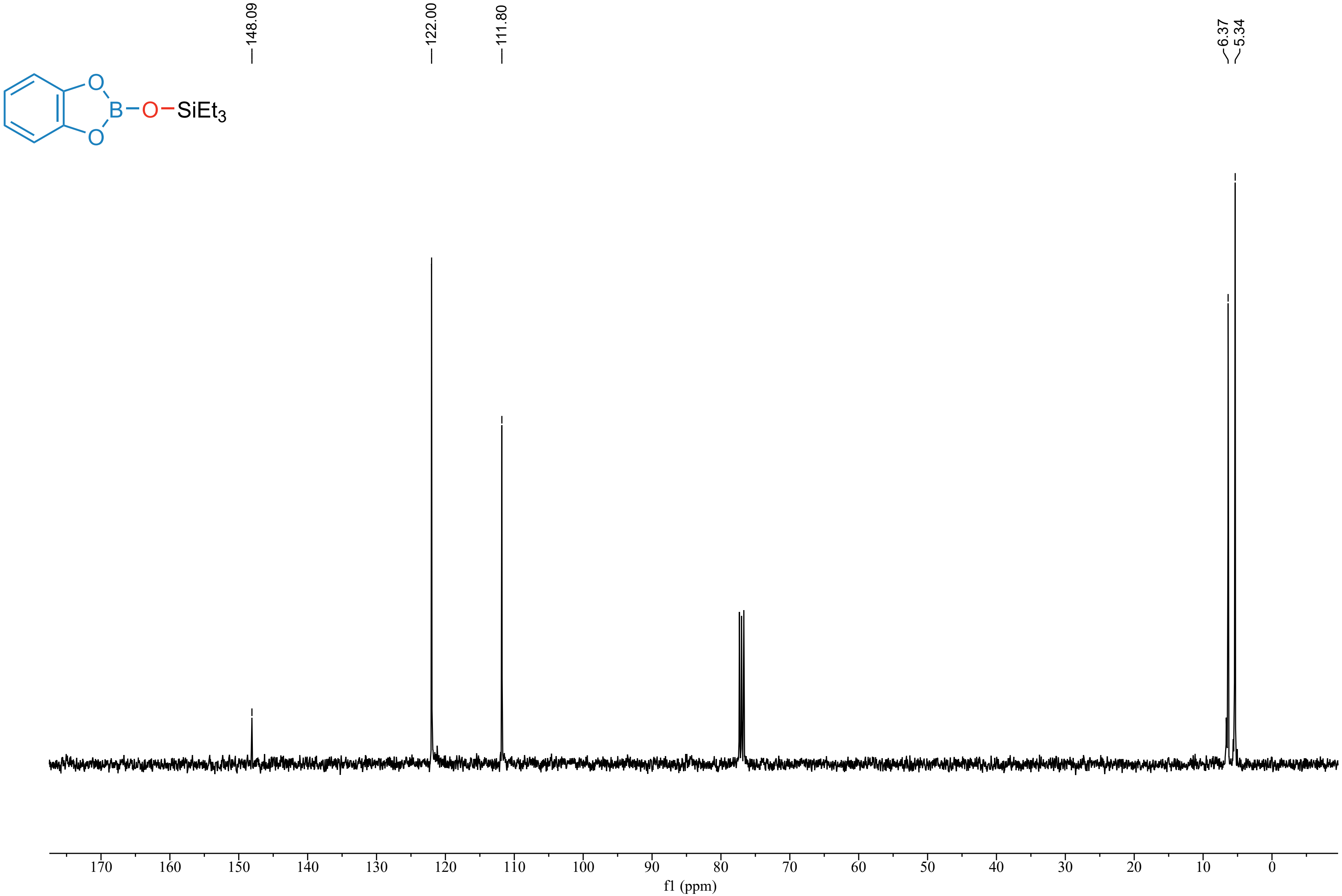

Compound **4h** ^{1}H NMR

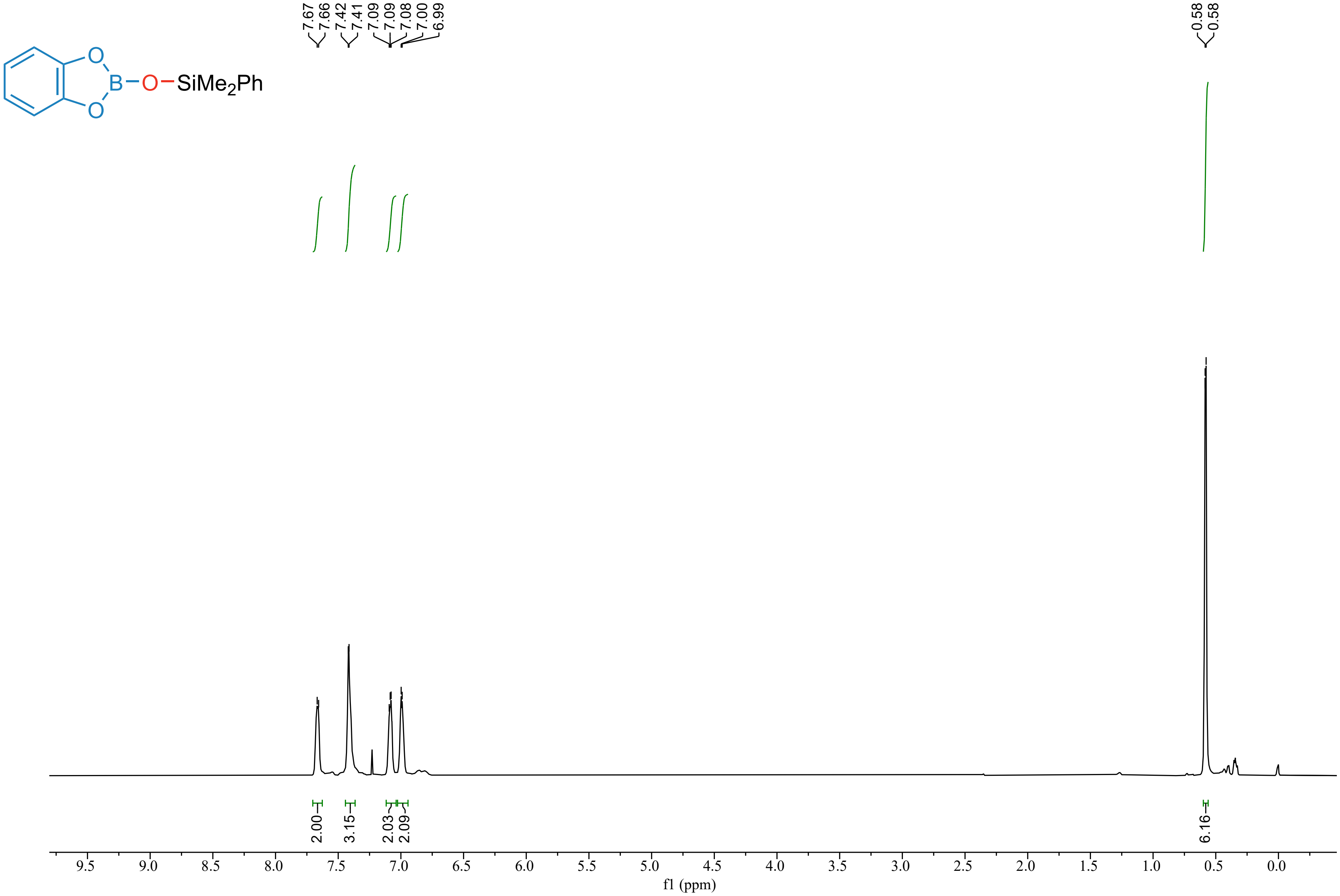

Compound **4h** ^{13}C NMR

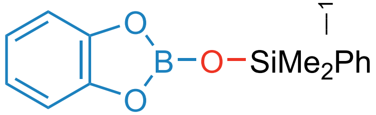

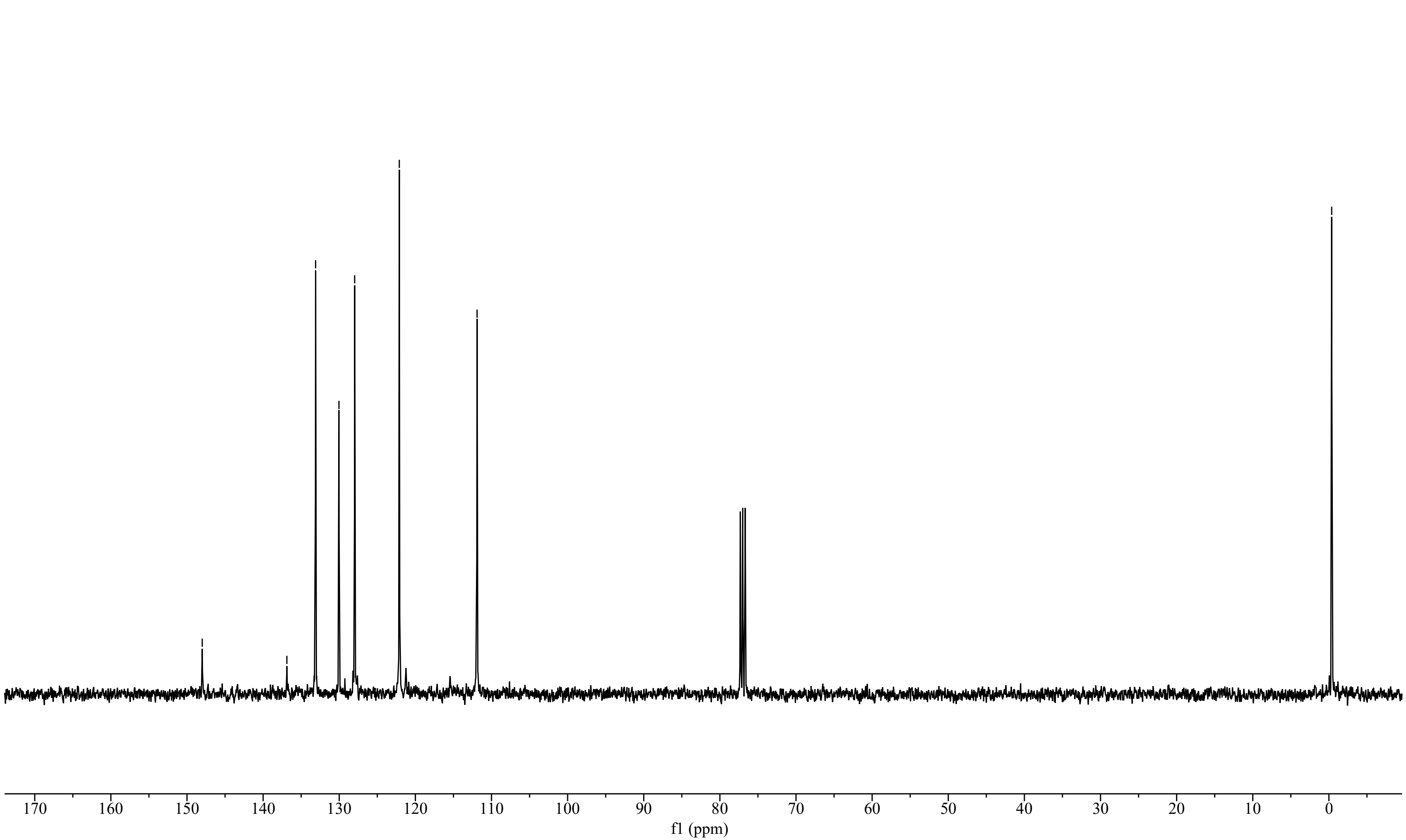

Compound **4i** ^{1}H NMR

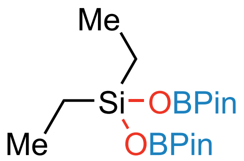

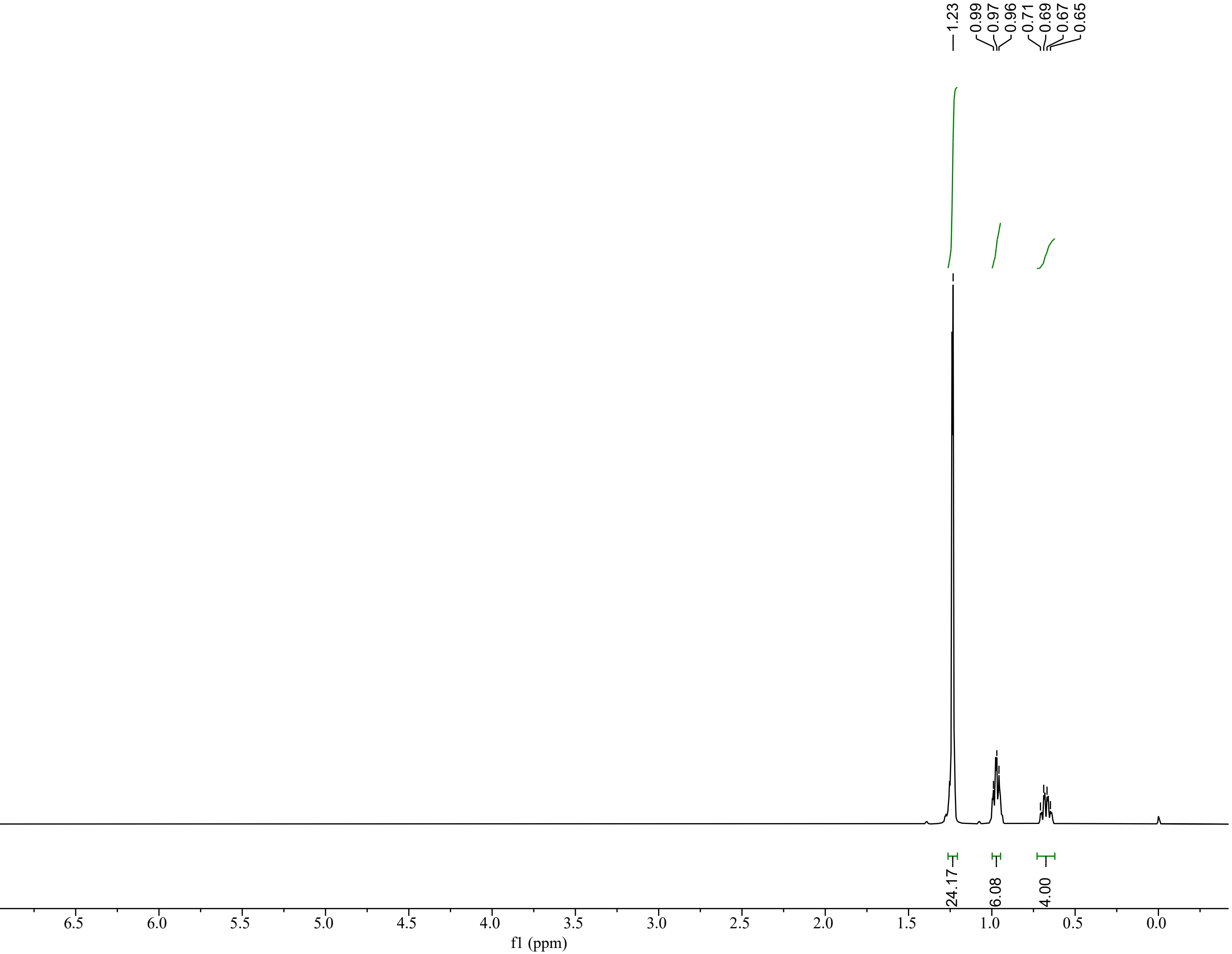

Compound **4i** ^{13}C NMR

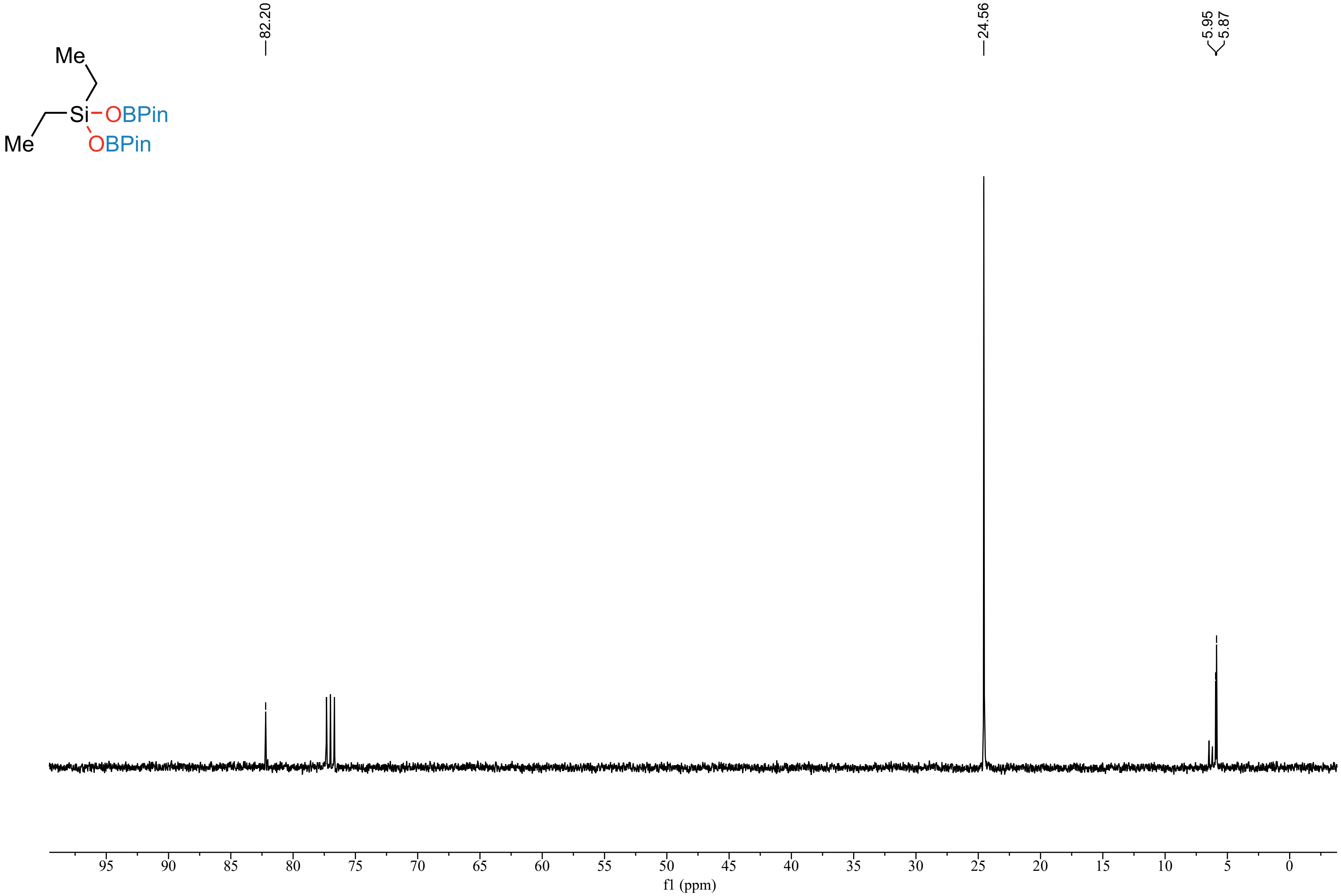

Compound **4j** [1]H NMR

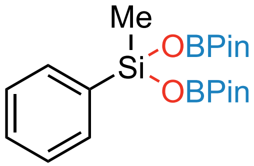

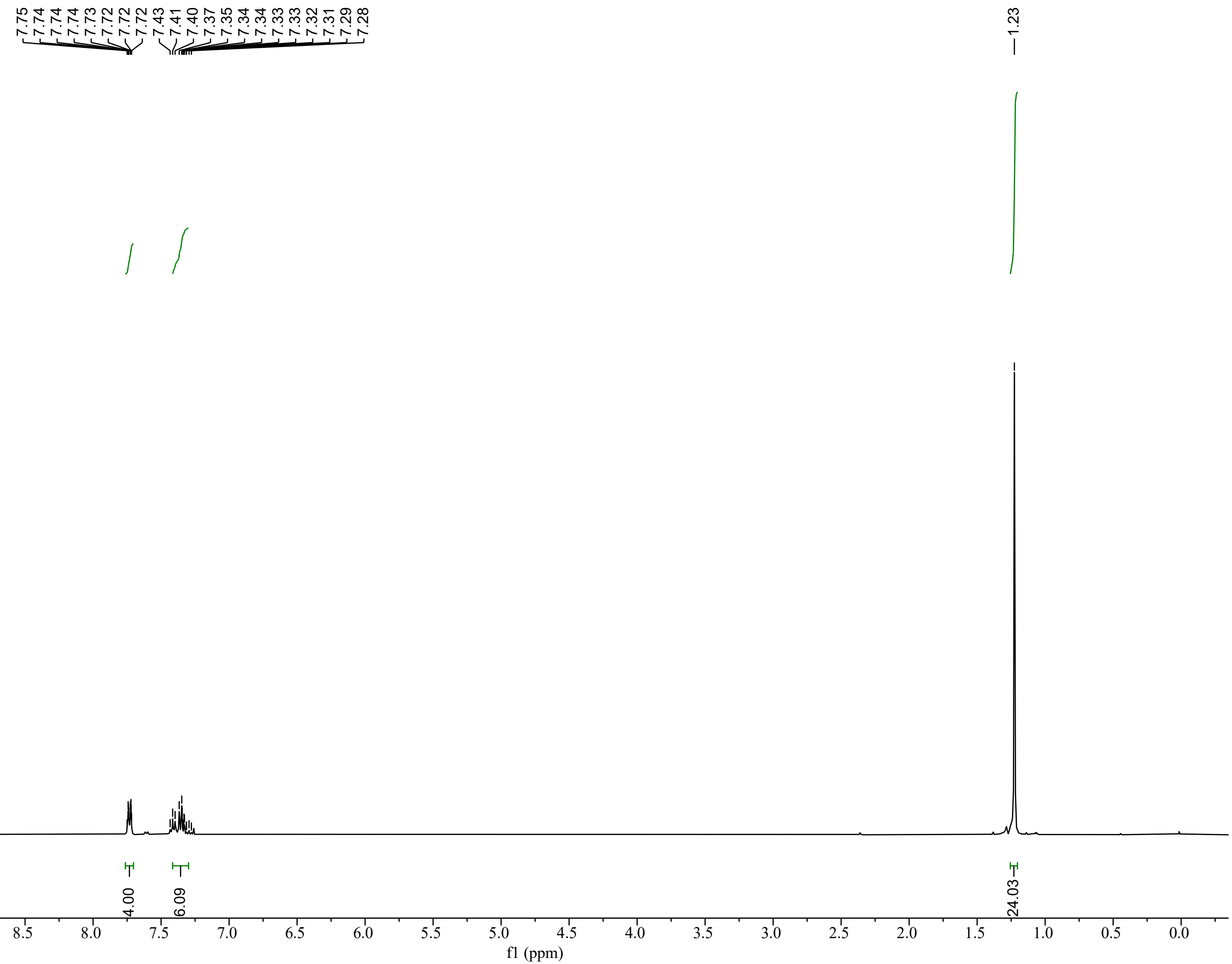

Compound **4j** ^{13}C NMR

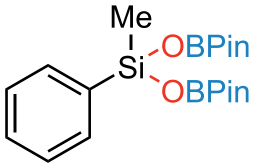

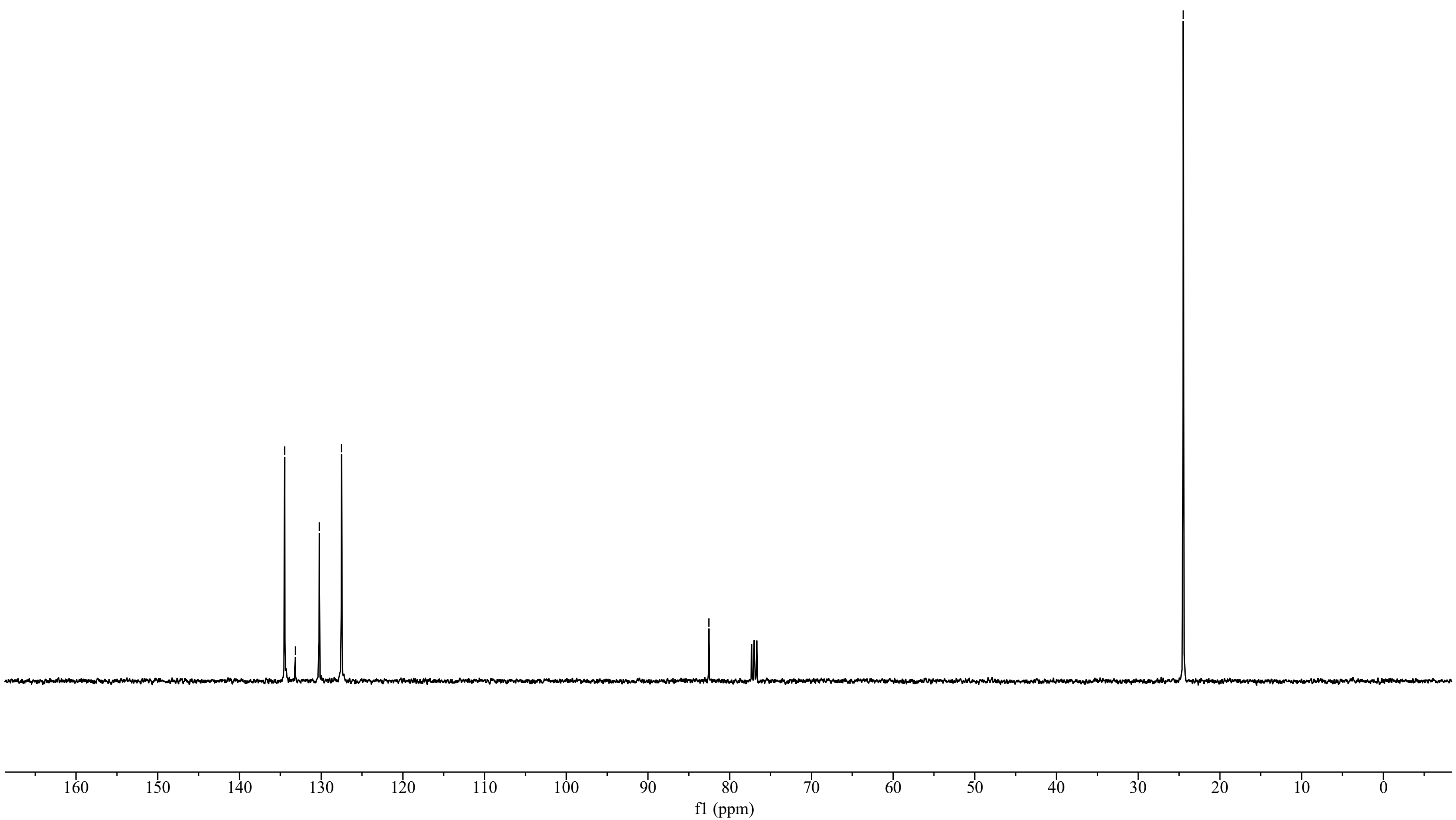

Compound **6a** ^{1}H NMR

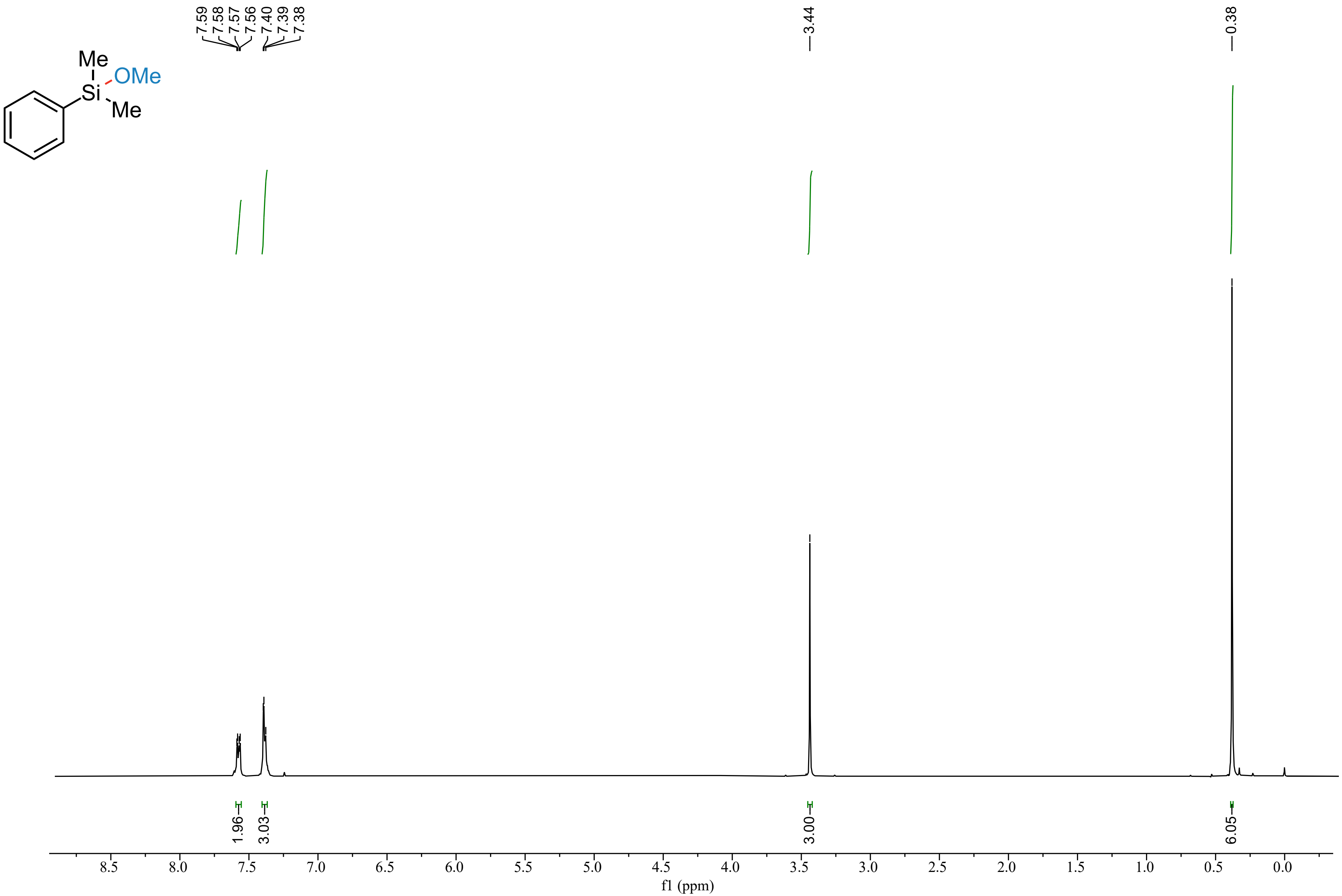

Compound **6a** ^{13}C NMR

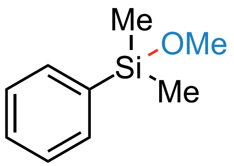

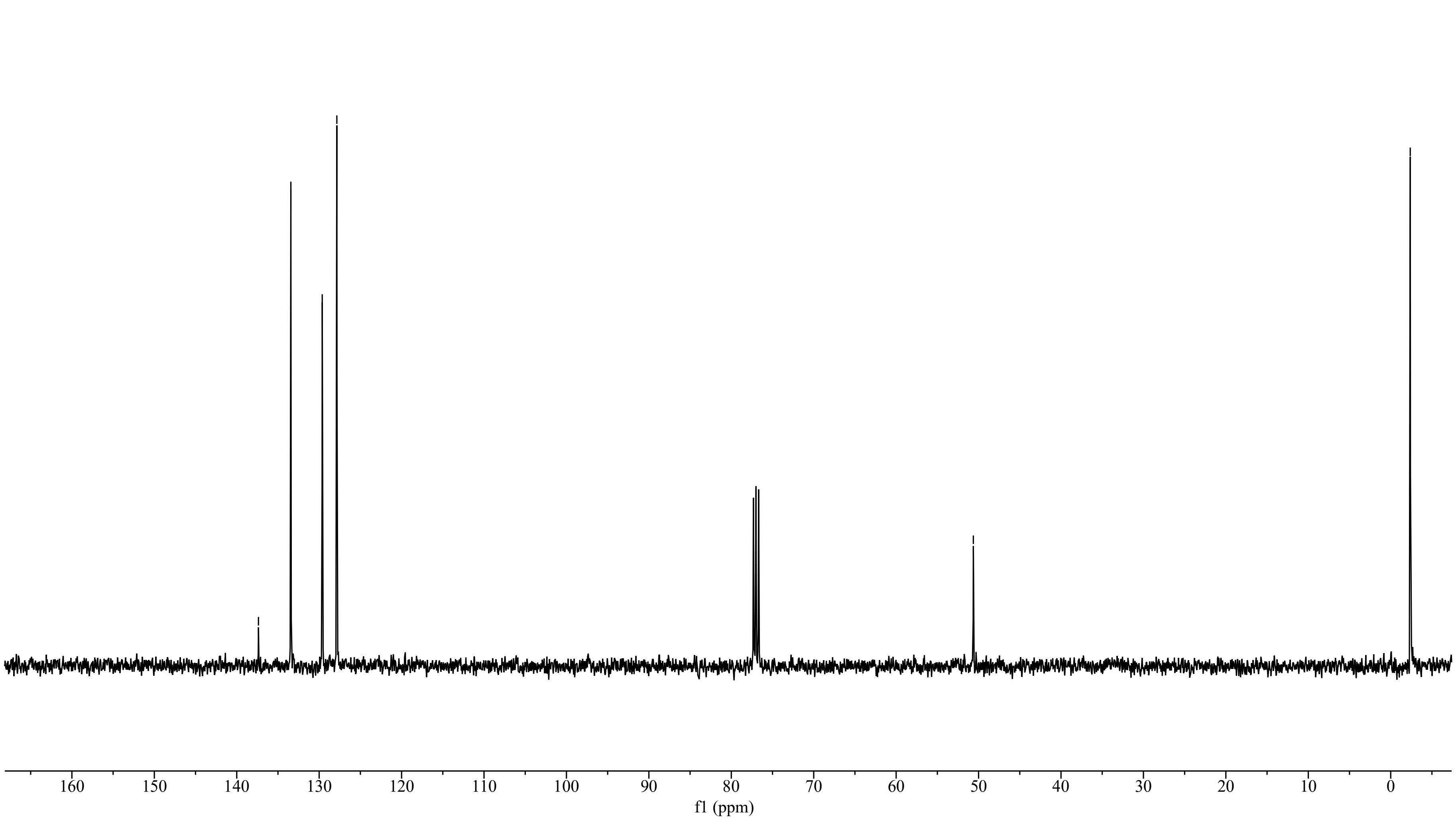

Compound **6b** ^{1}H NMR

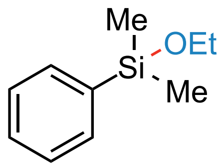

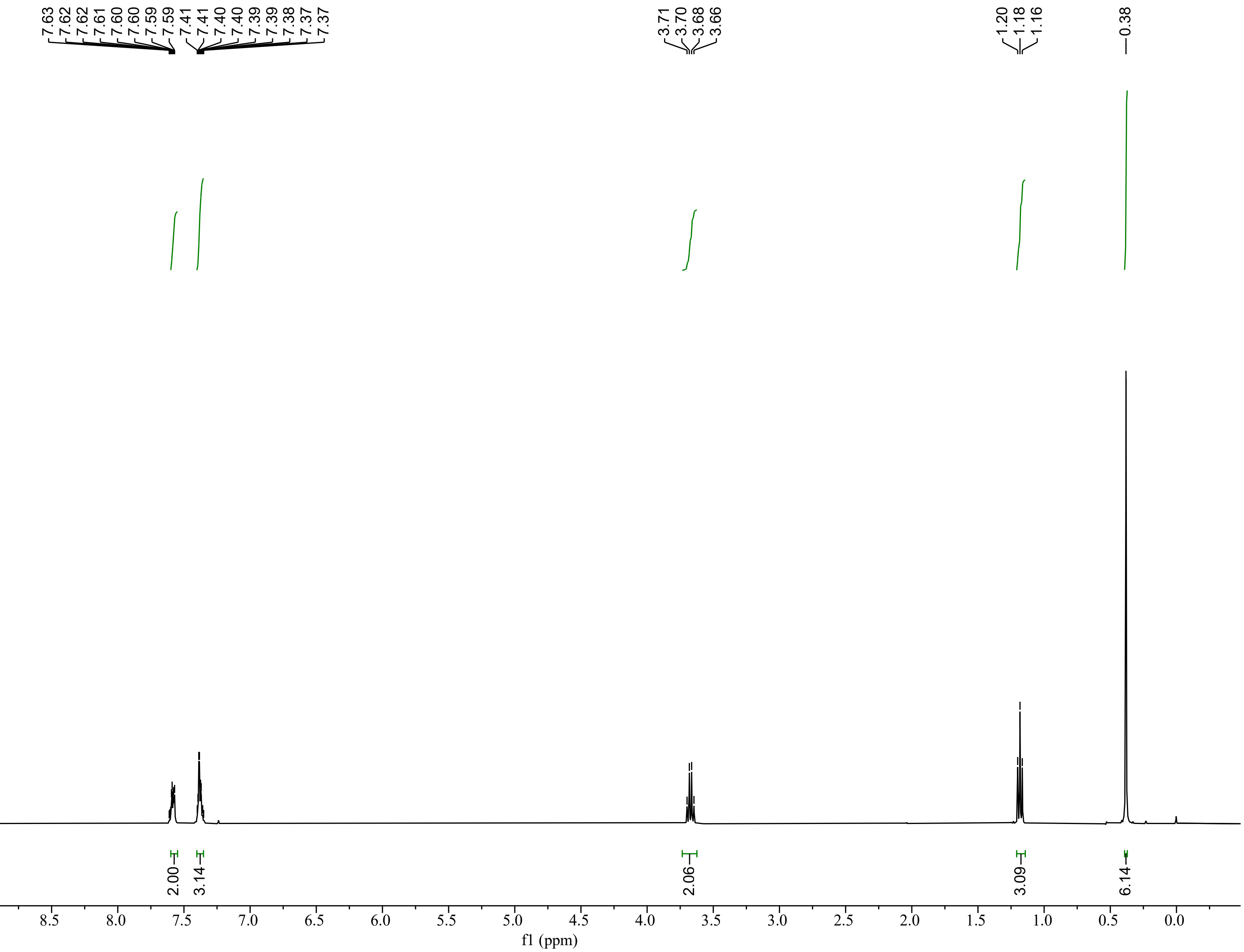

Compound **6b** ^{13}C NMR

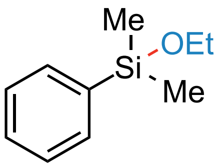

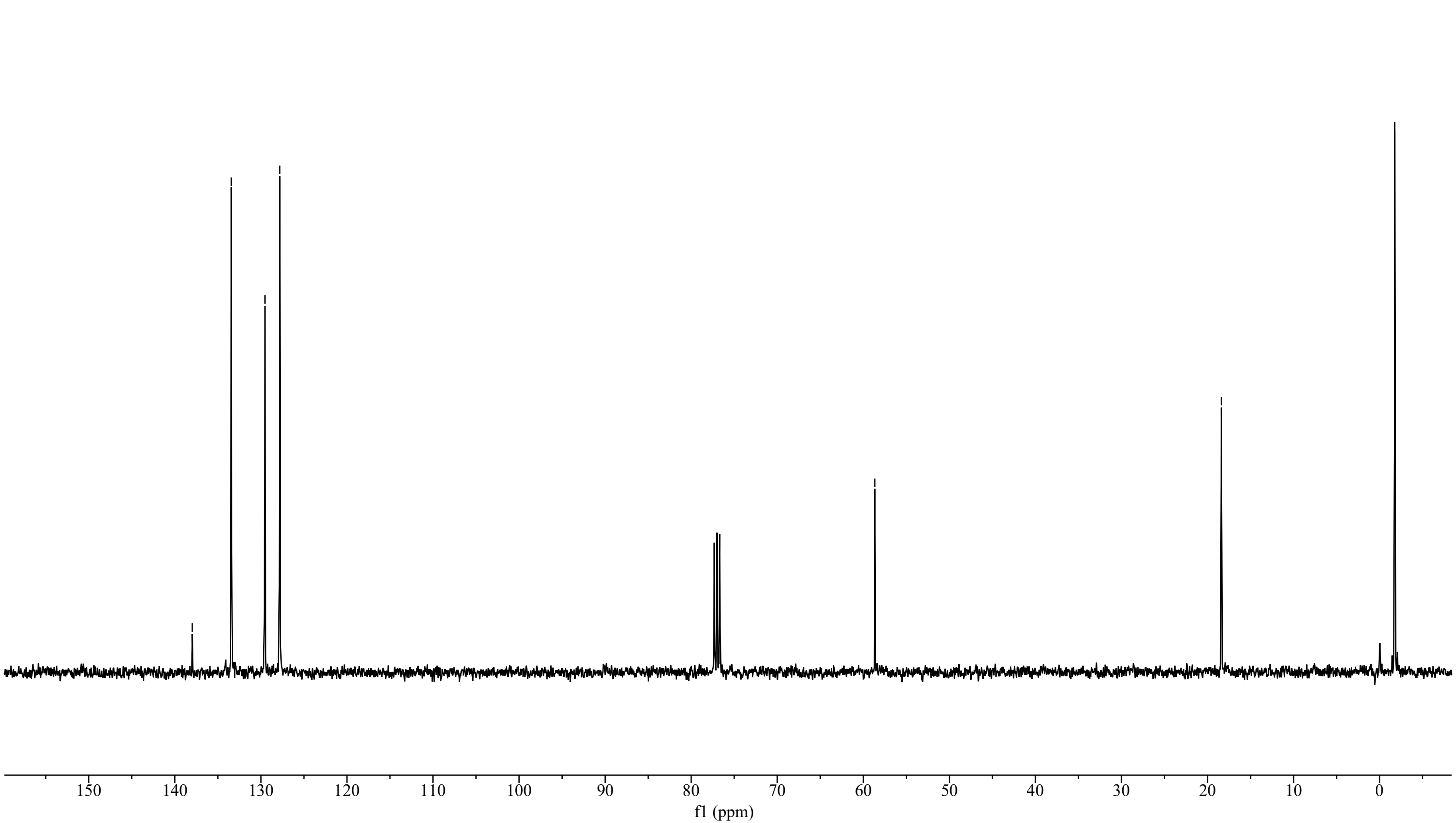

Compound **6c** ^{1}H NMR

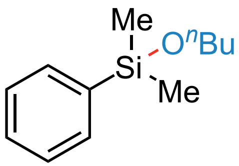

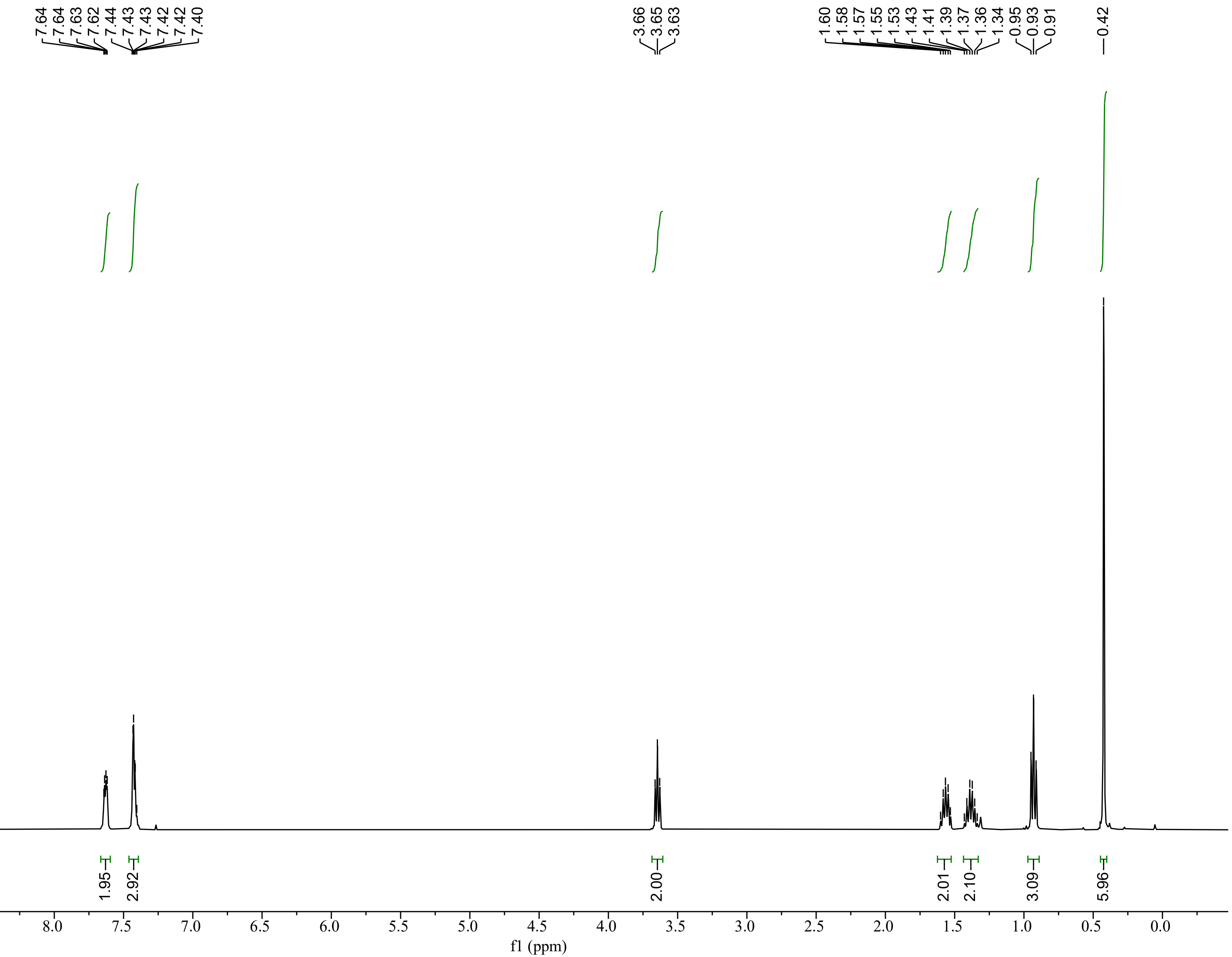

Compound **6c** ^{13}C NMR

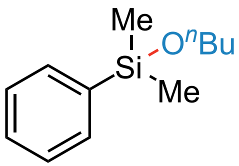

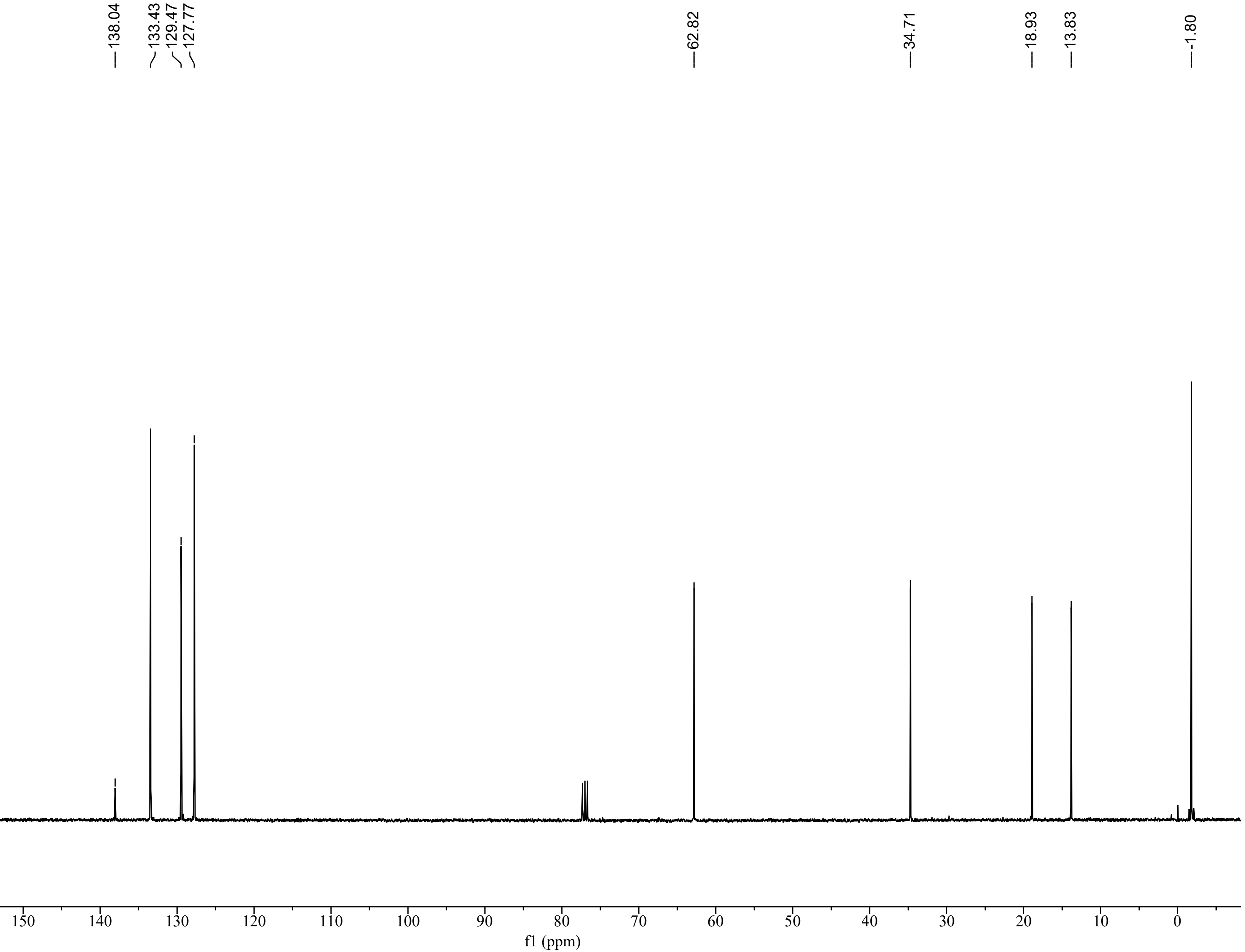

Compound **6d** ^{1}H NMR

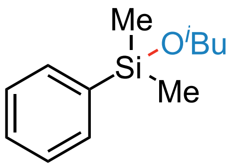

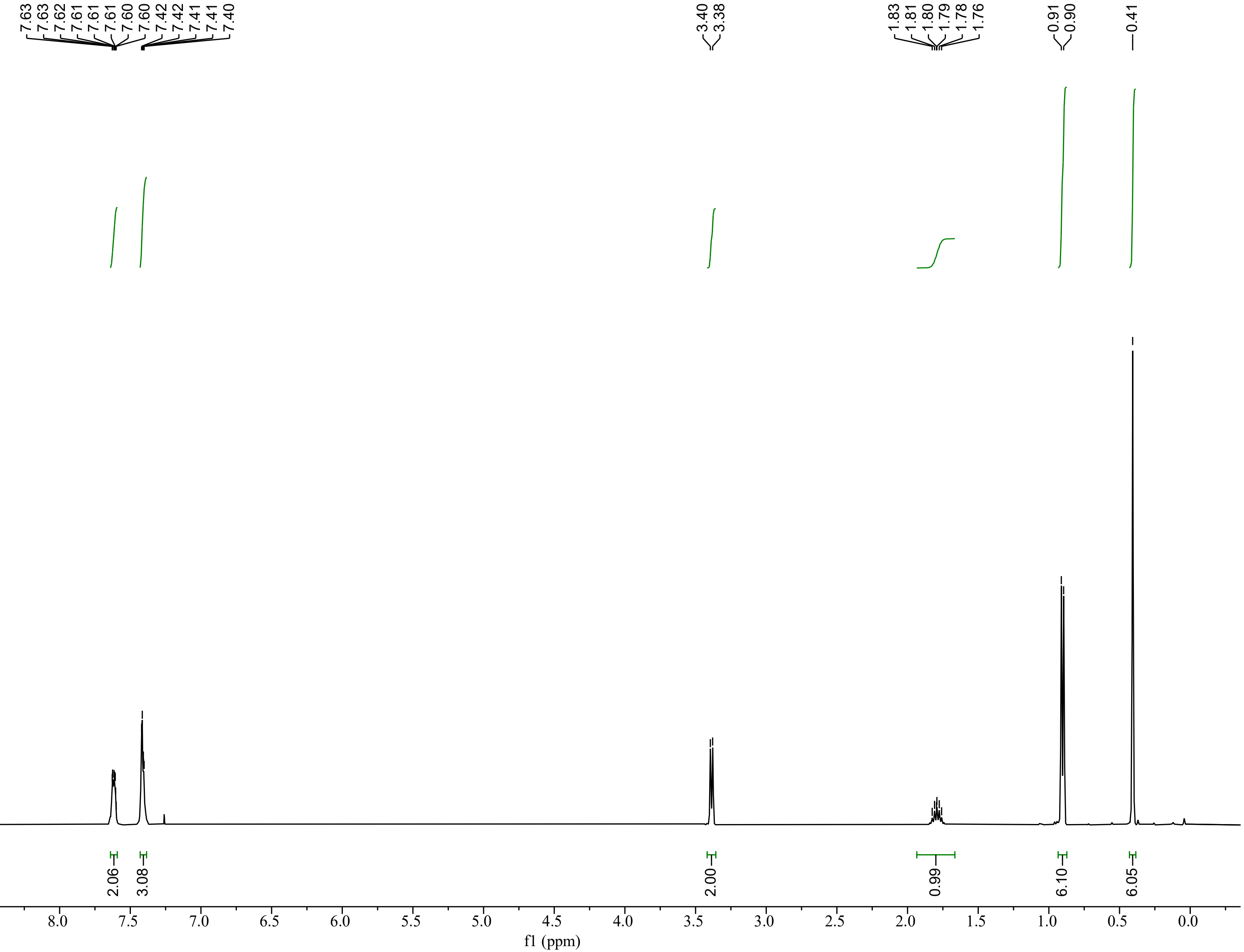

Compound **6d** ^{13}C NMR

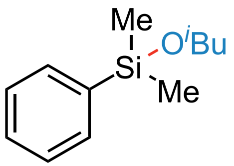

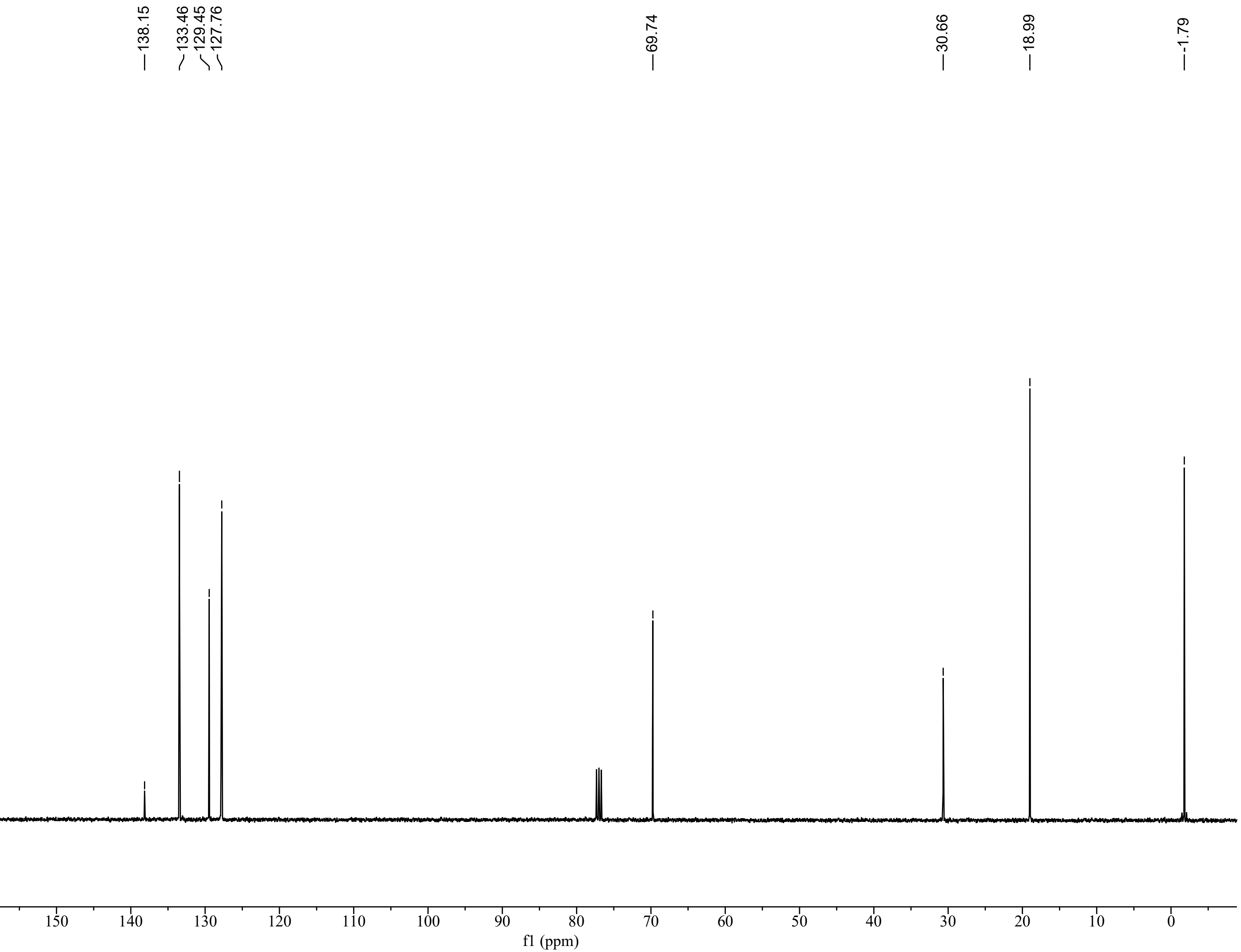

Compound **6e** ^{1}H NMR

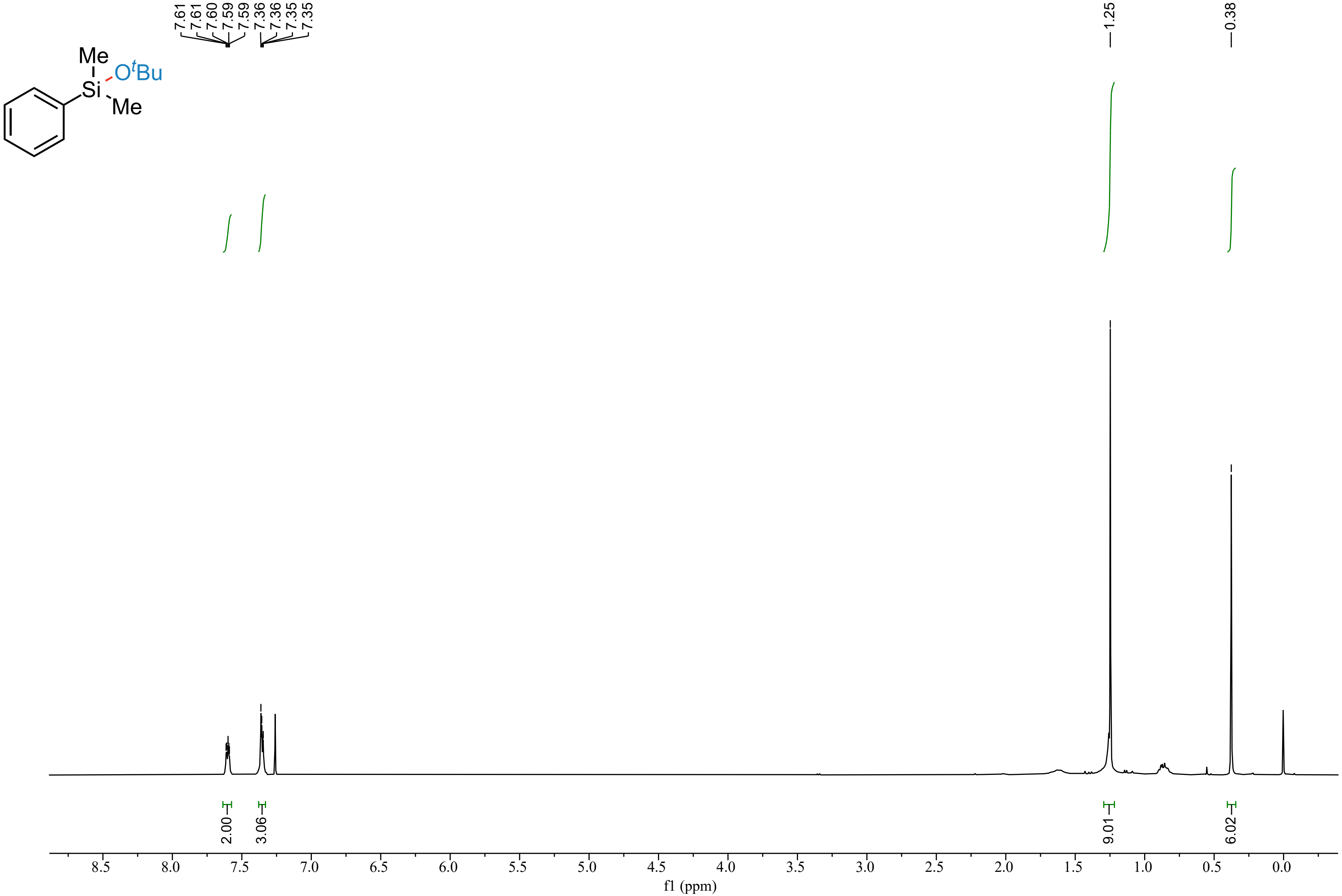

Compound **6e** ^{13}C NMR

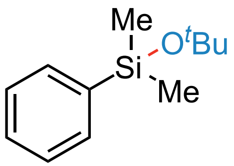

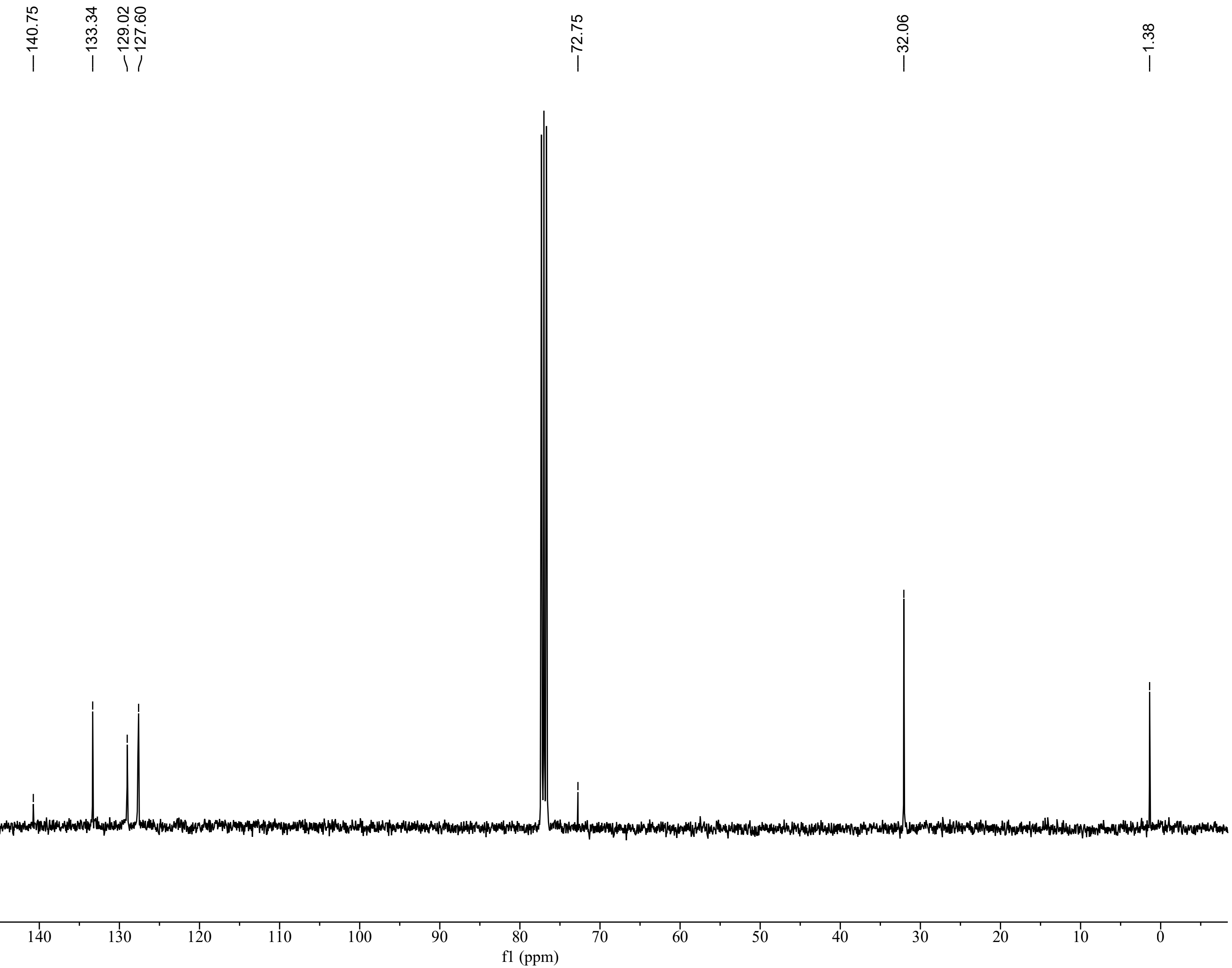

Compound **6f** ^{1}H NMR

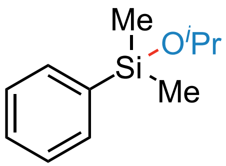

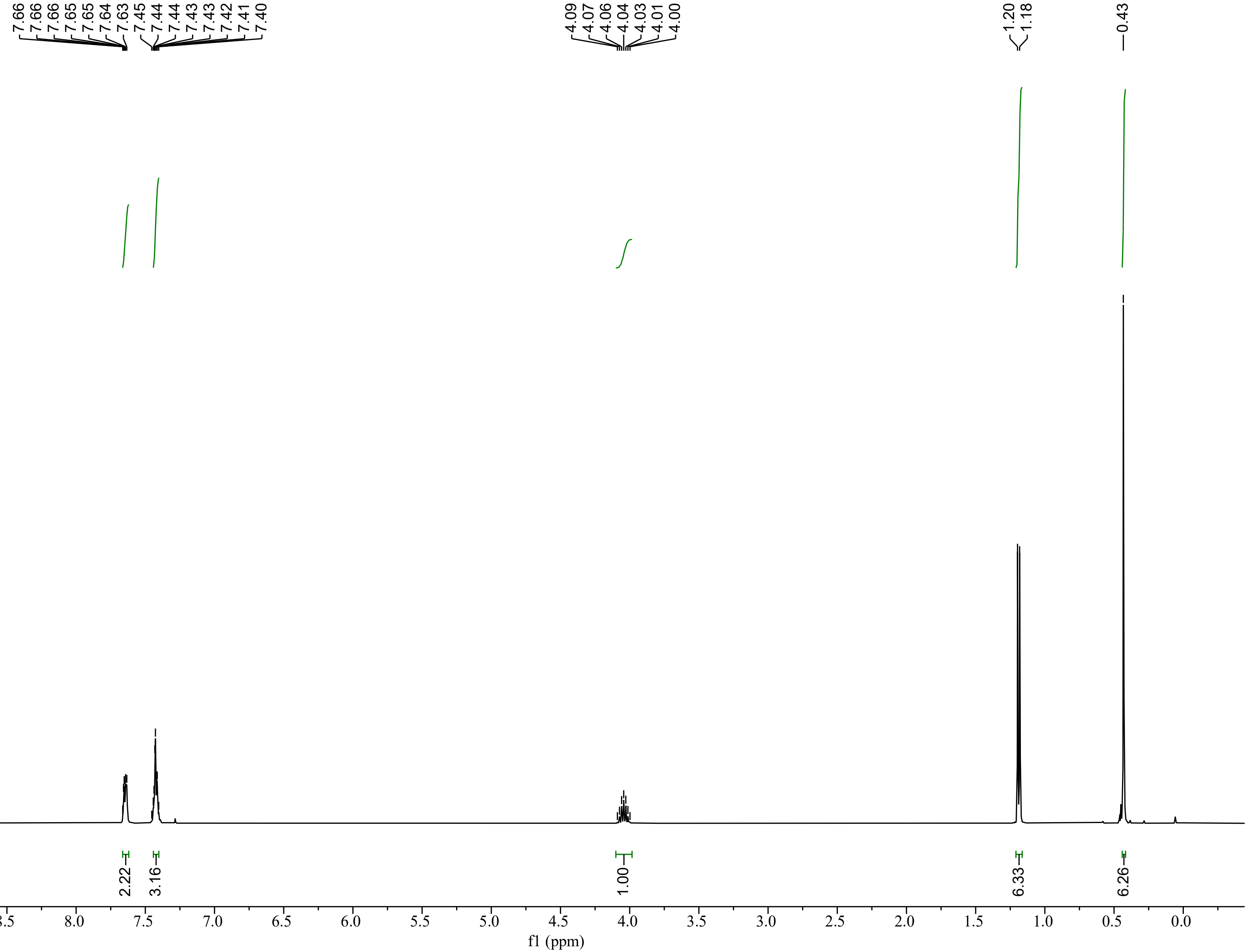

Compound **6f** ^{13}C NMR

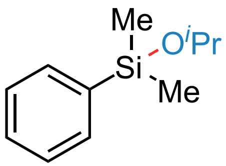

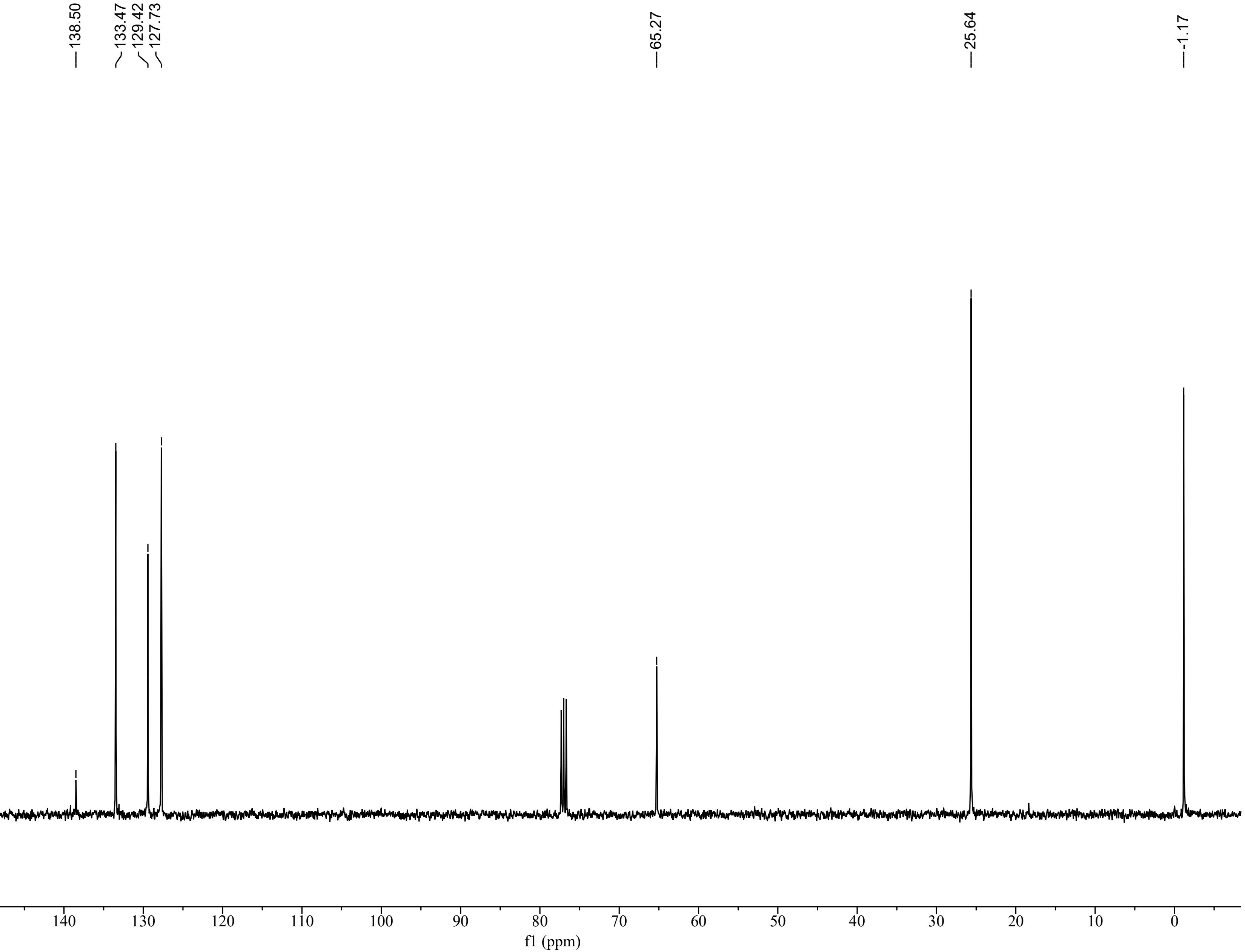

Compound **6g** [1]H NMR

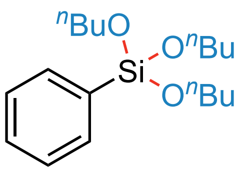

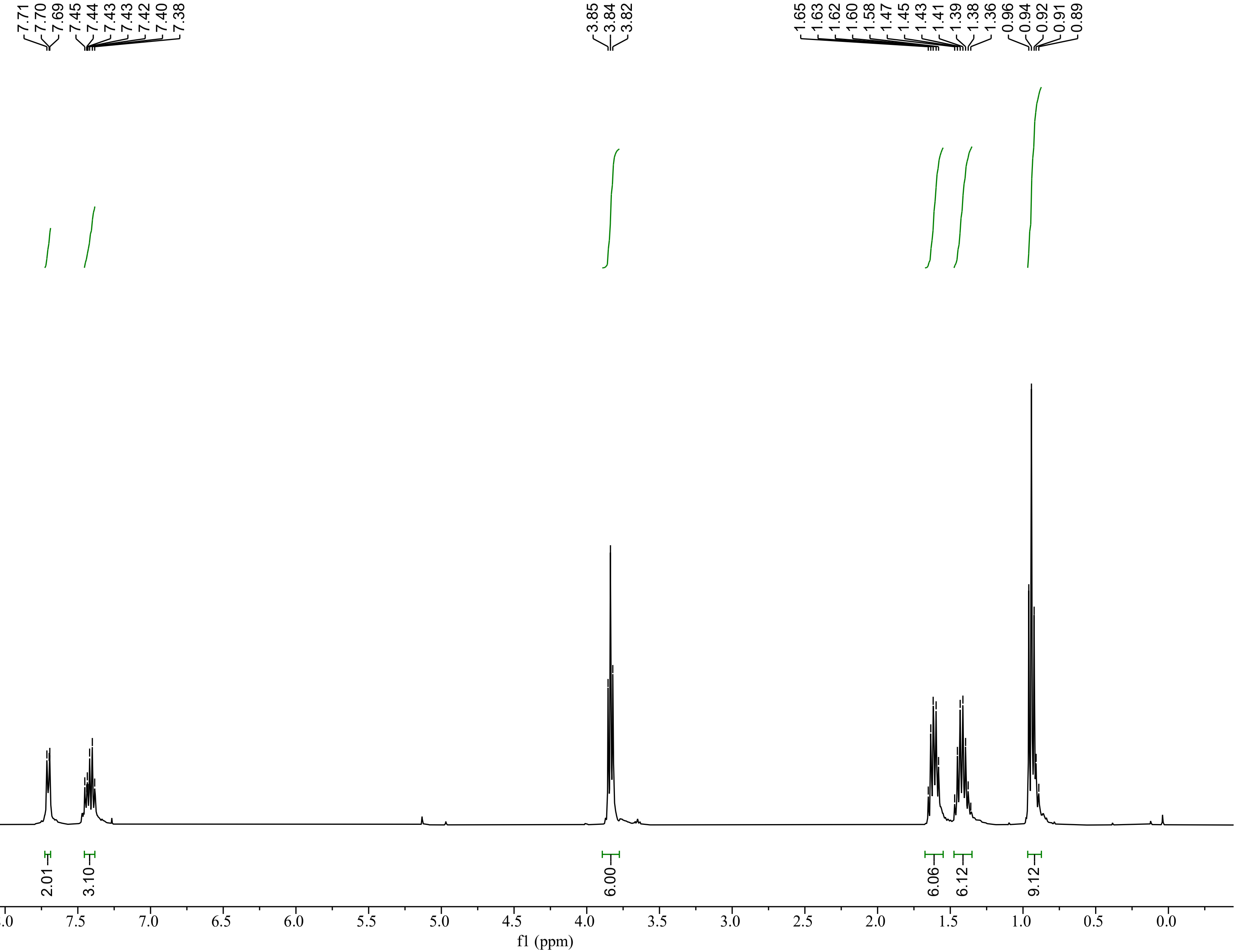

Compound **6g** ^{13}C NMR

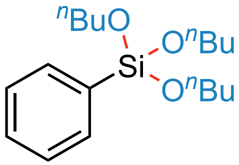

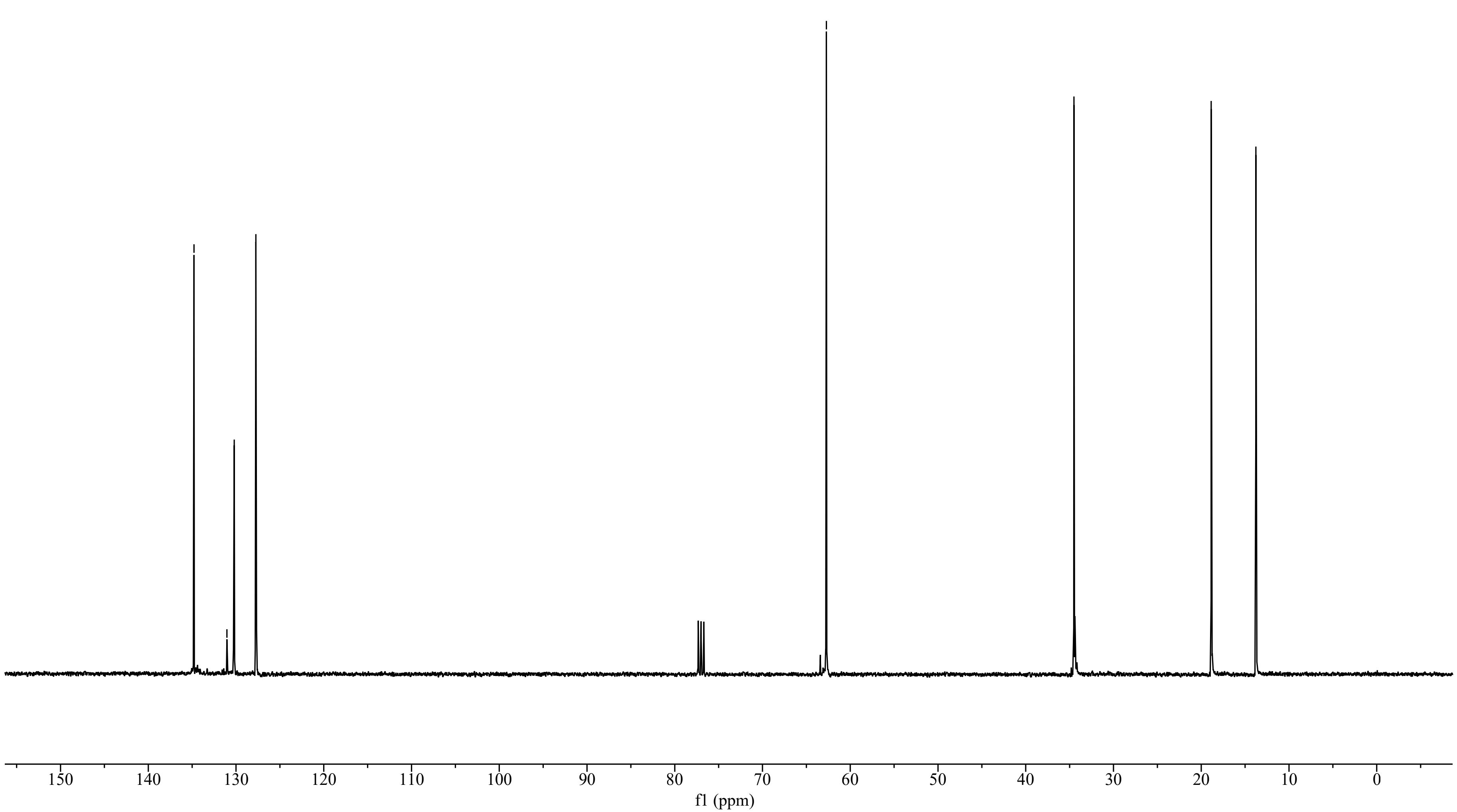

Compound **6h** ^1H NMR

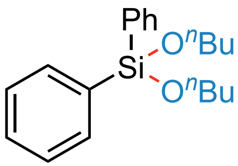

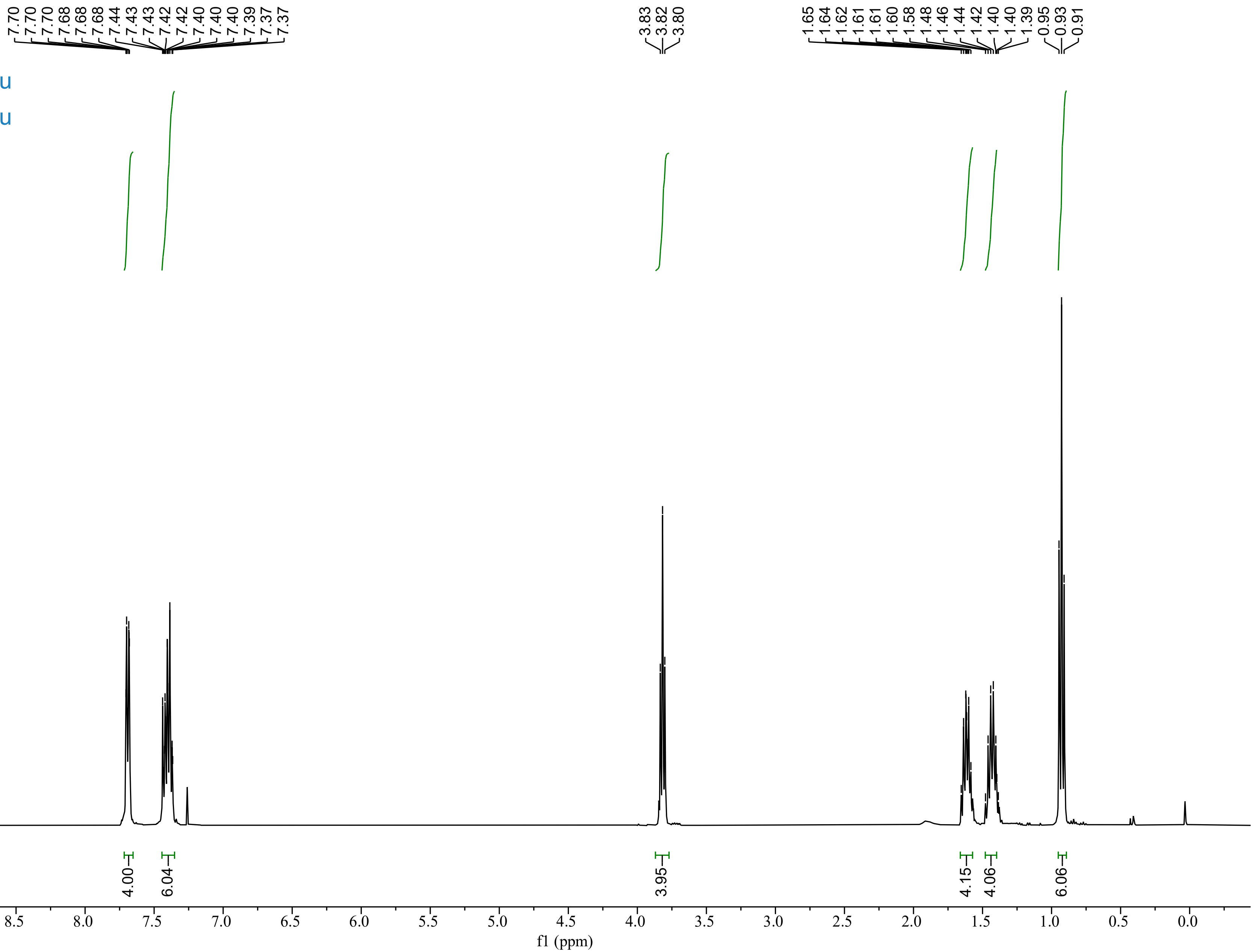

Compound **6h** ^{13}C NMR

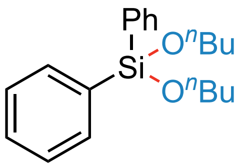

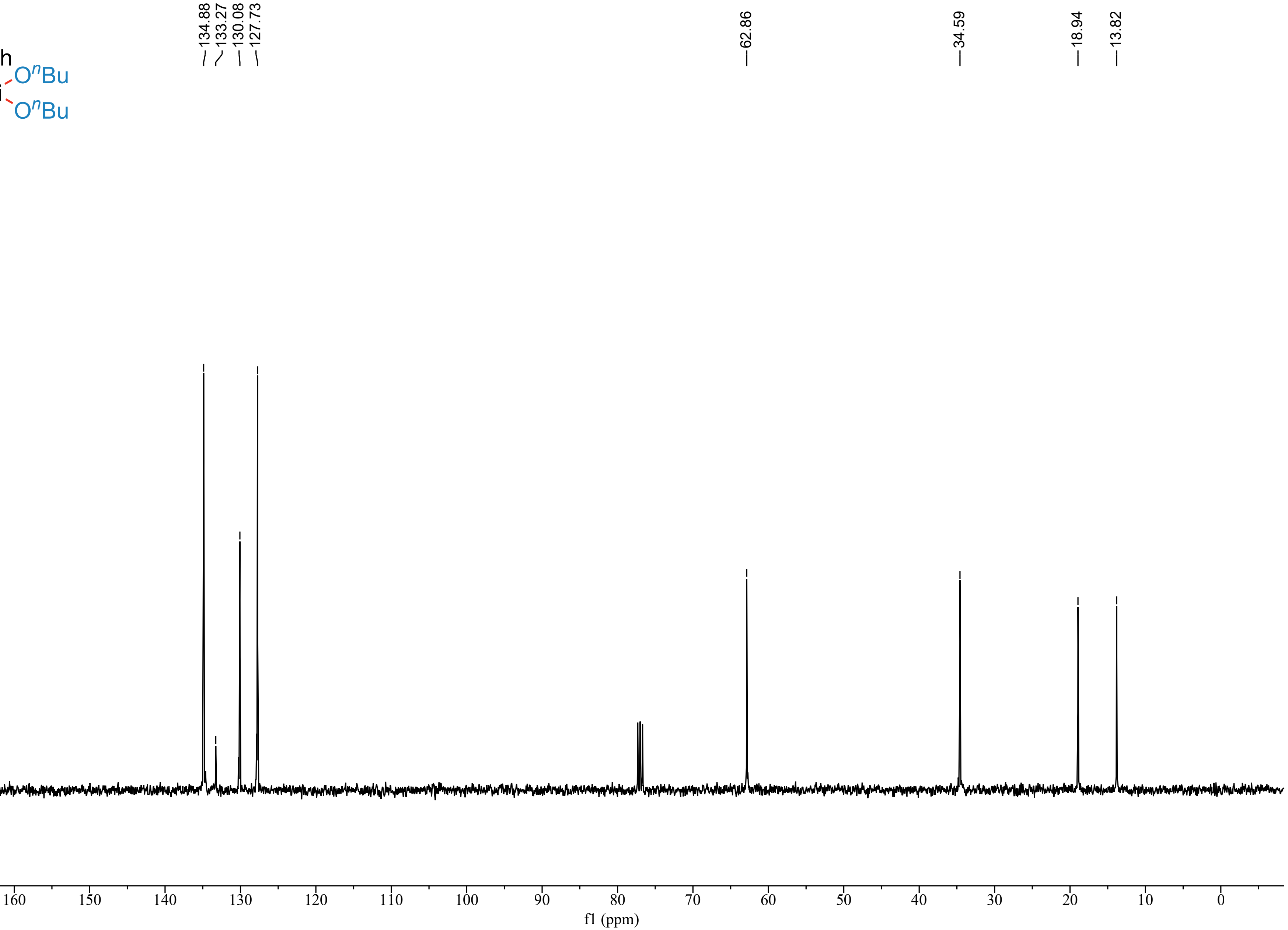

Compound **6i** ^{1}H NMR

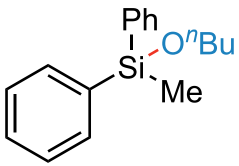

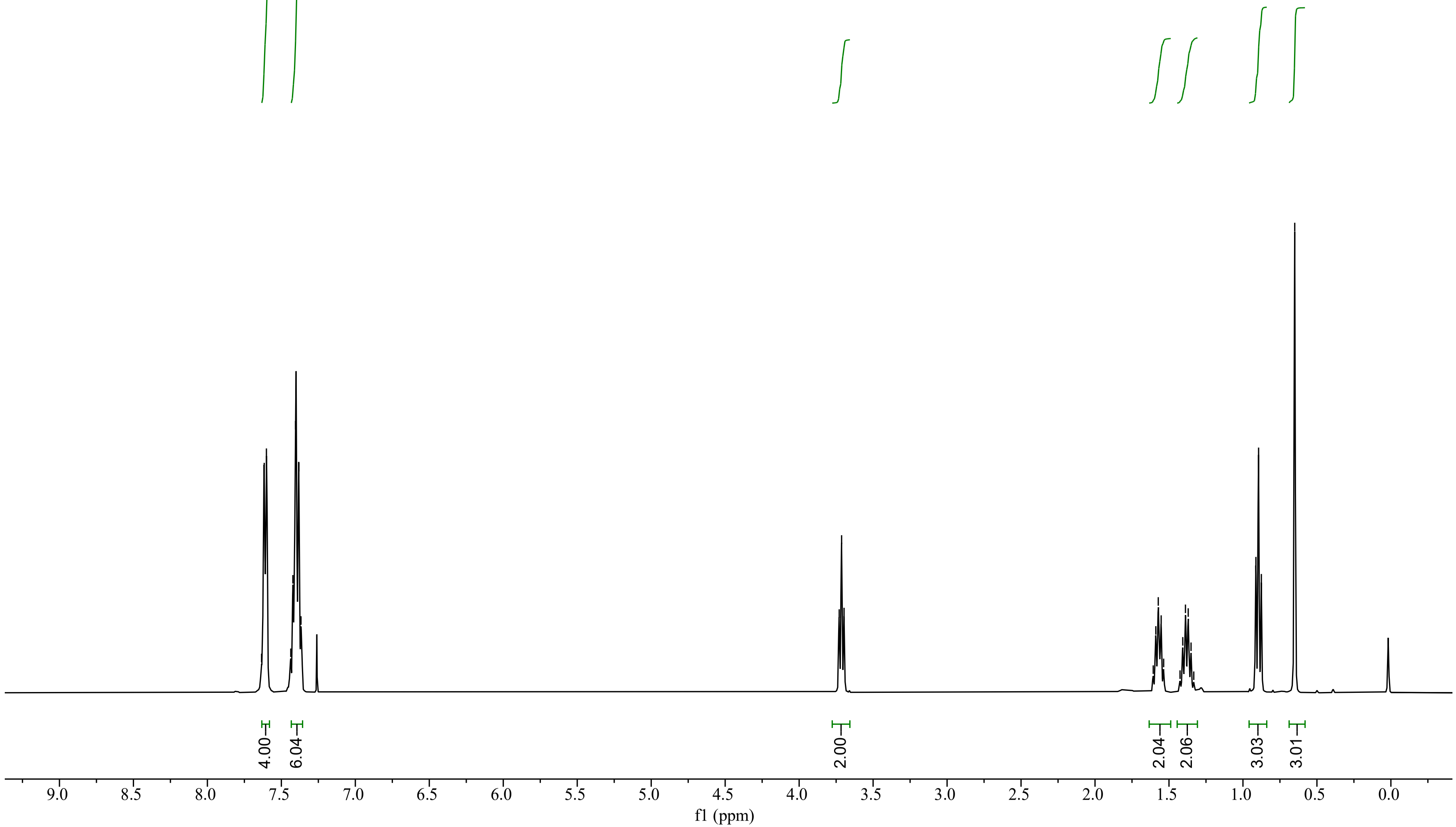

Compound **6i** ^{13}C NMR

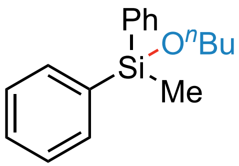

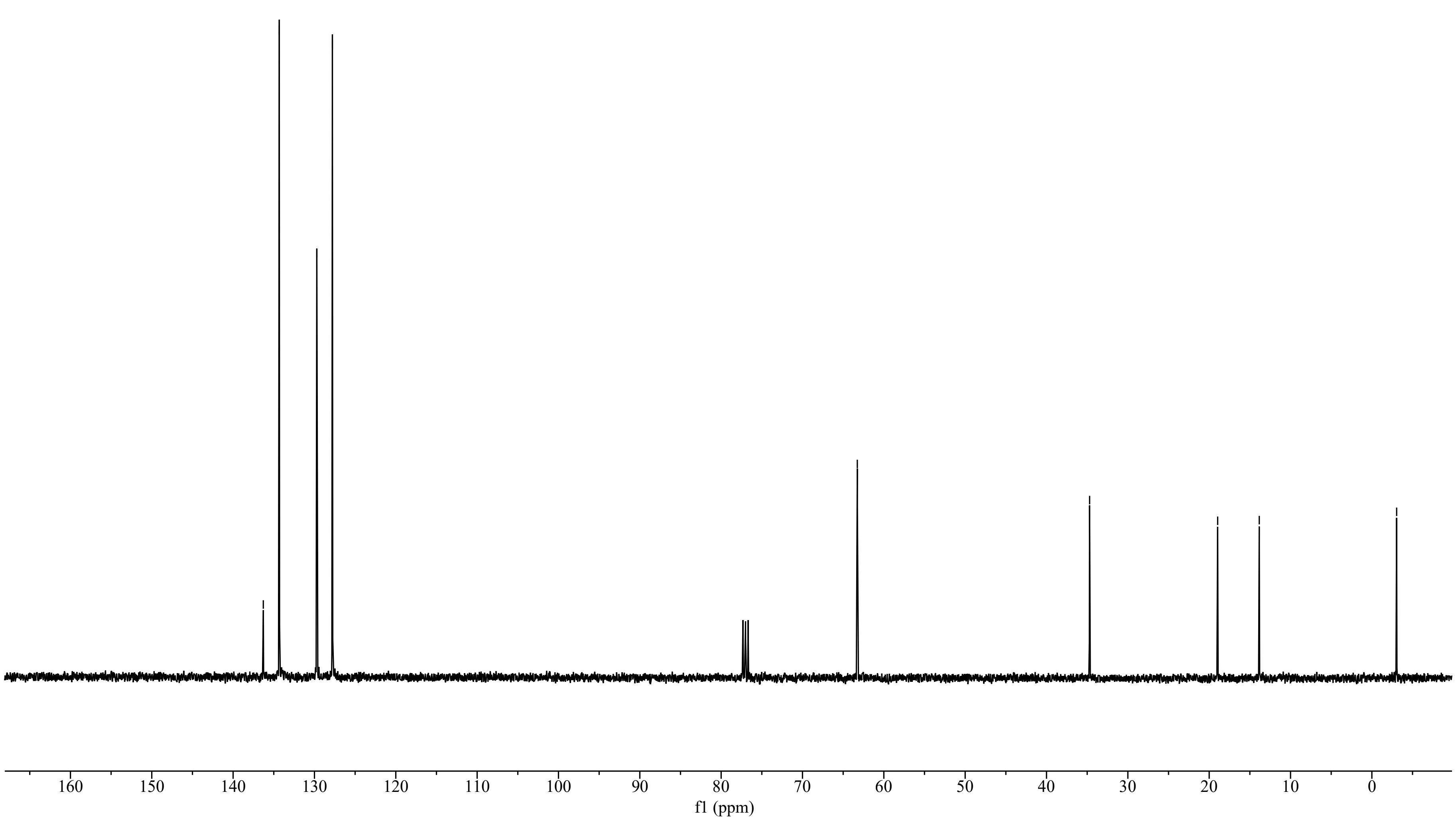

Compound **6j** ^{1}H NMR

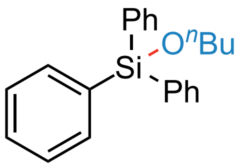

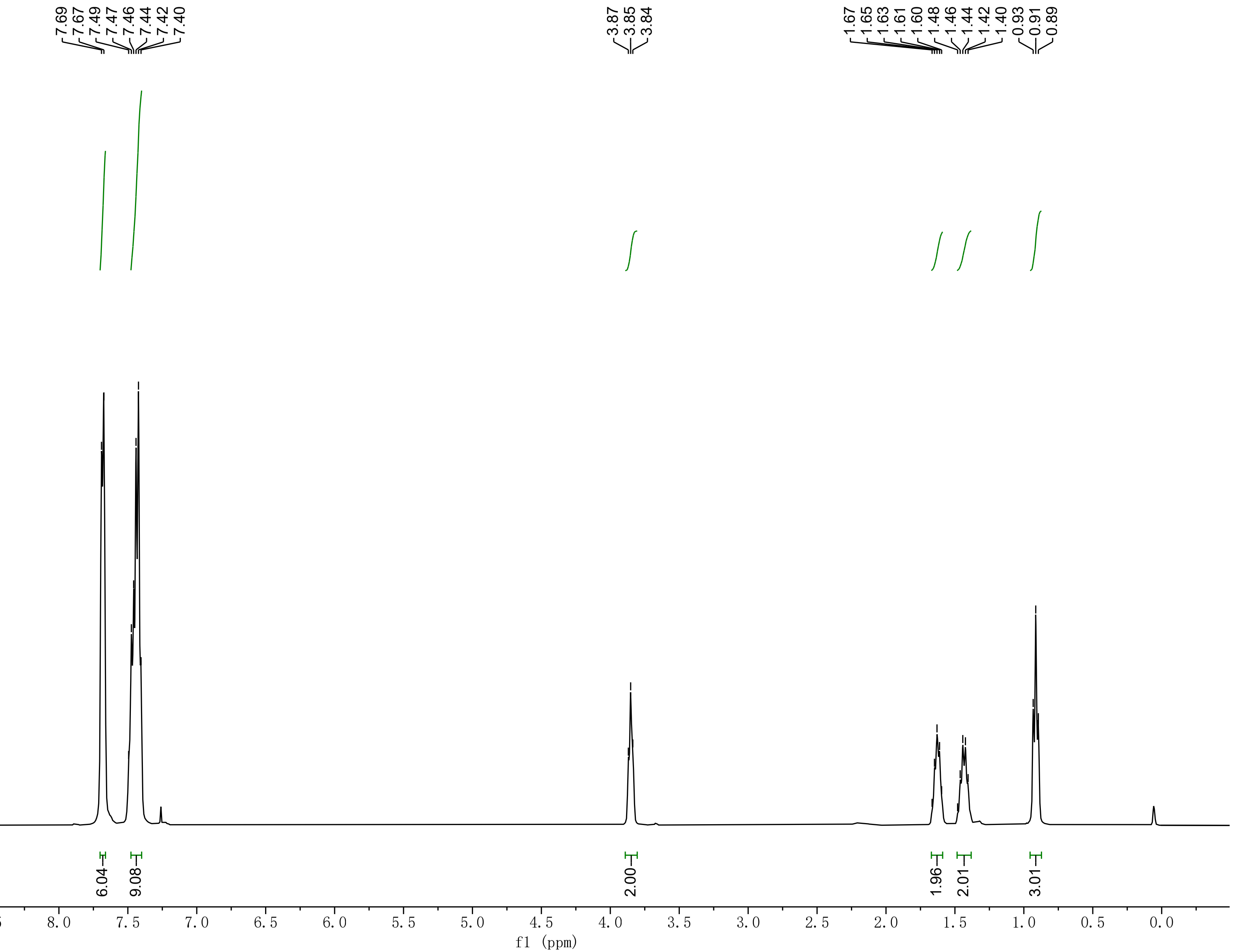

Compound **6j** ^{13}C NMR

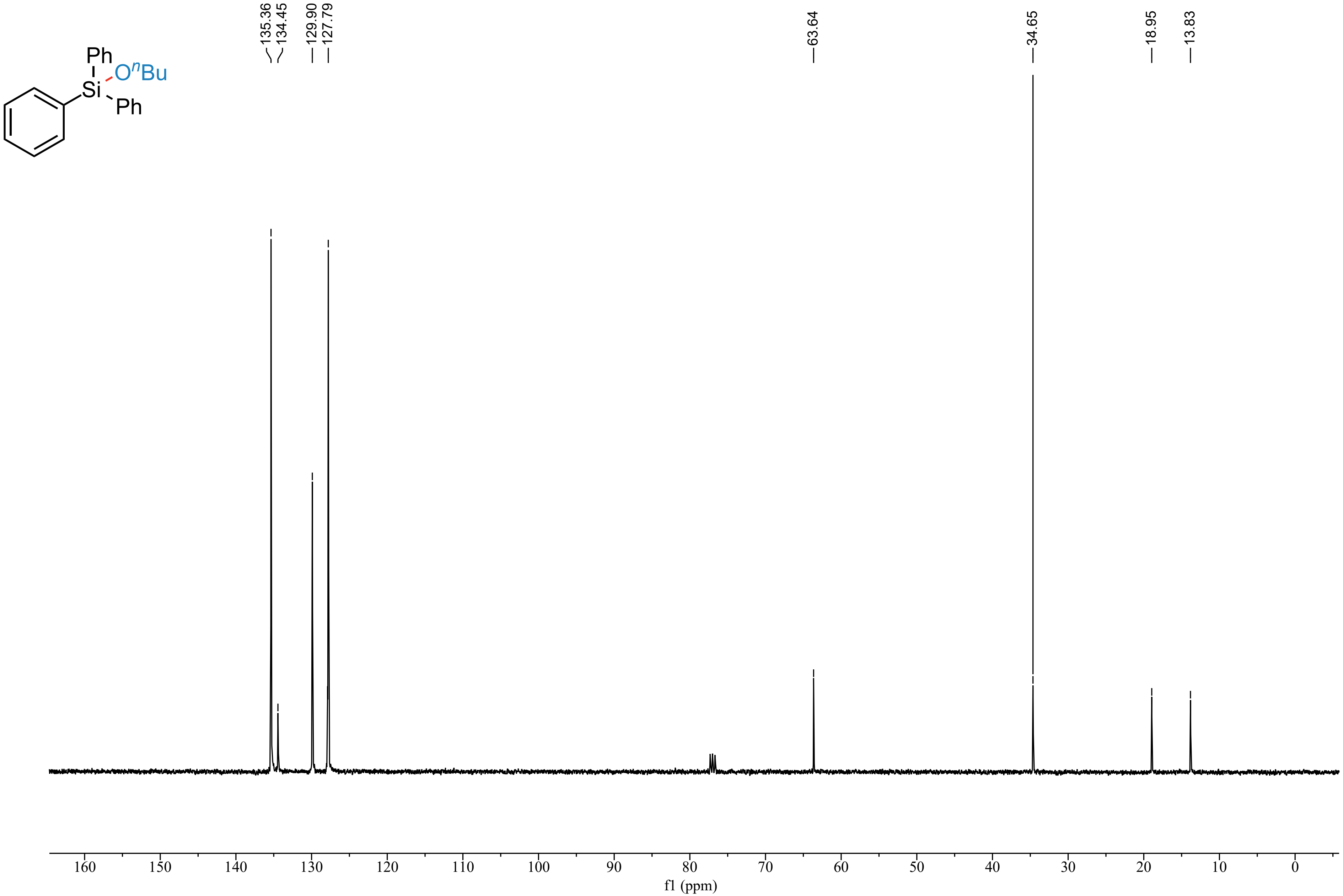

Compound **6k** ^{1}H NMR

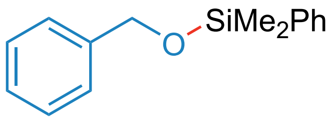

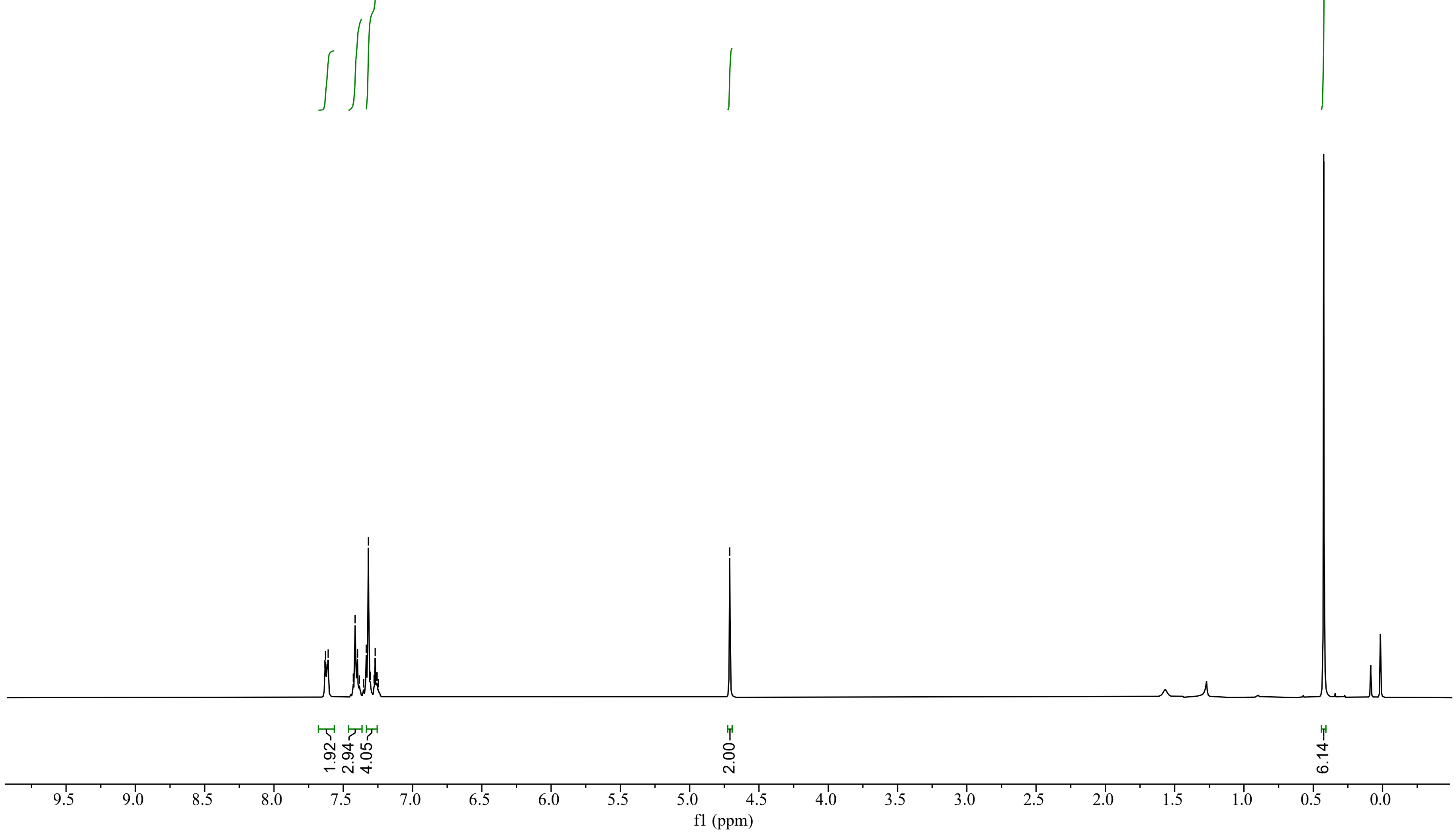

Compound **6k** ^{13}C NMR

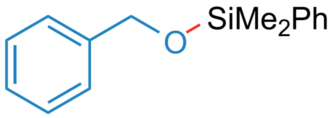

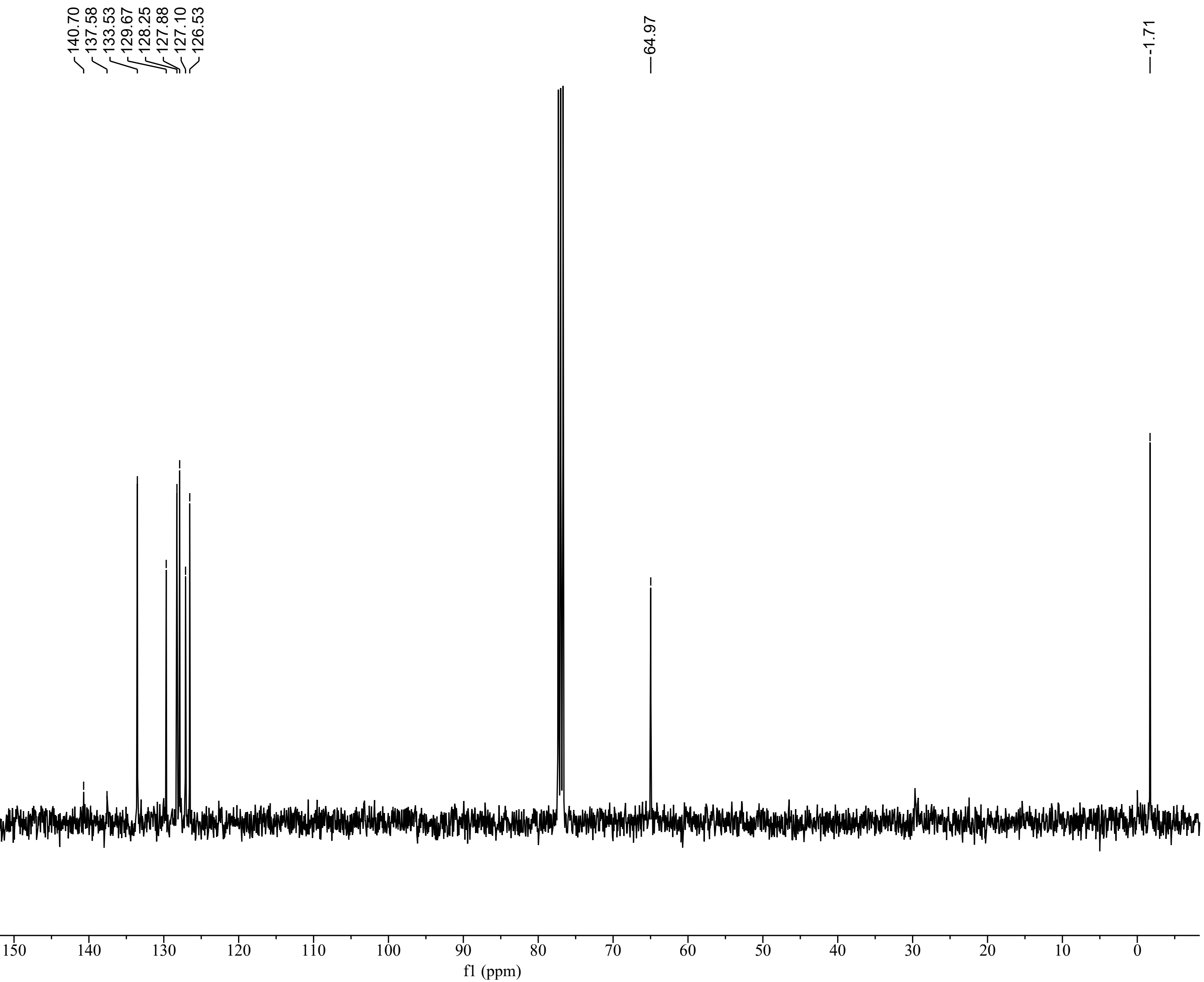

Compound **6l** ^{1}H NMR

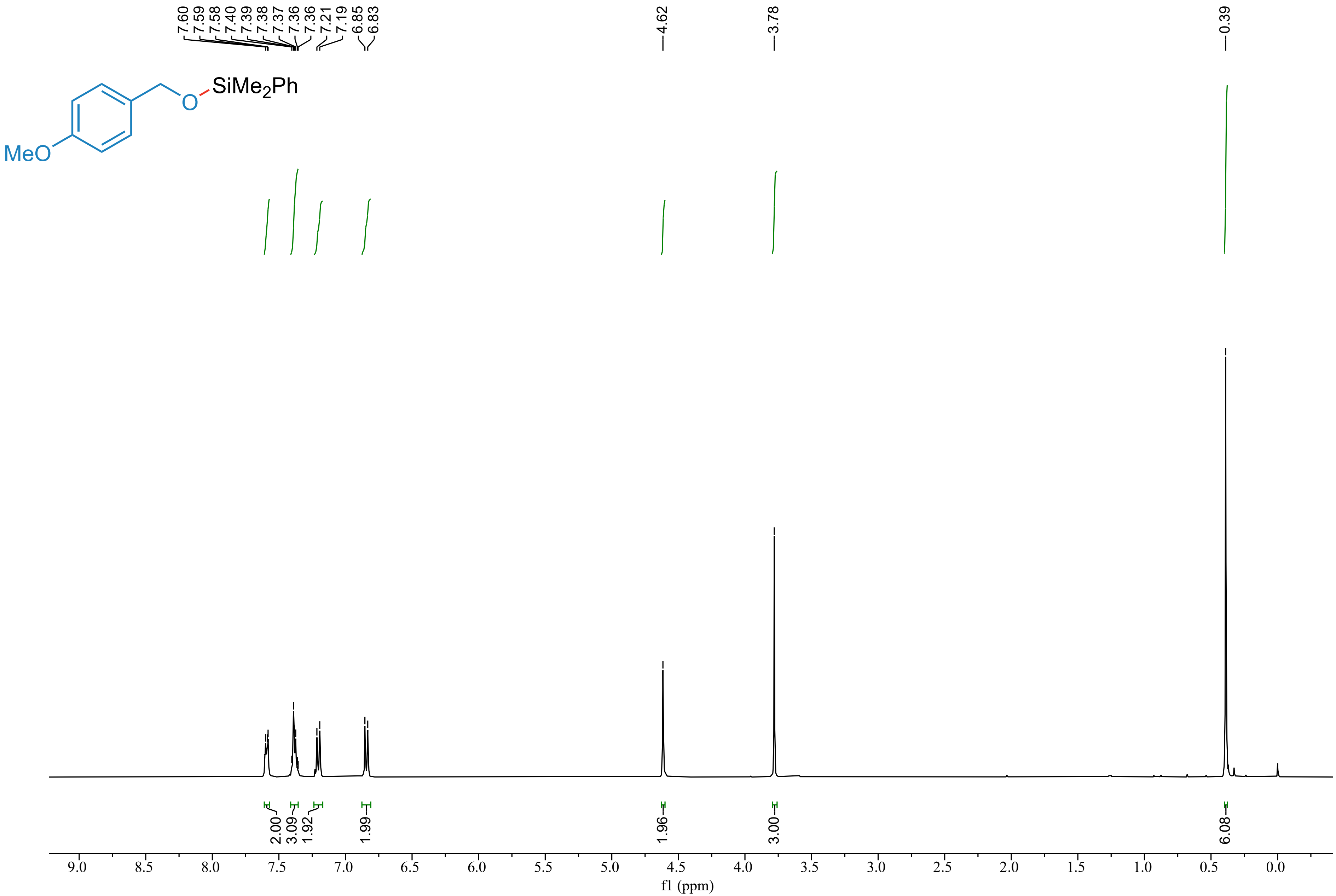

Compound **6l** ^{13}C NMR

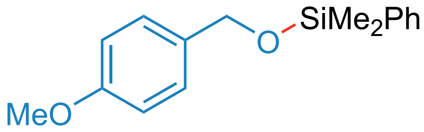

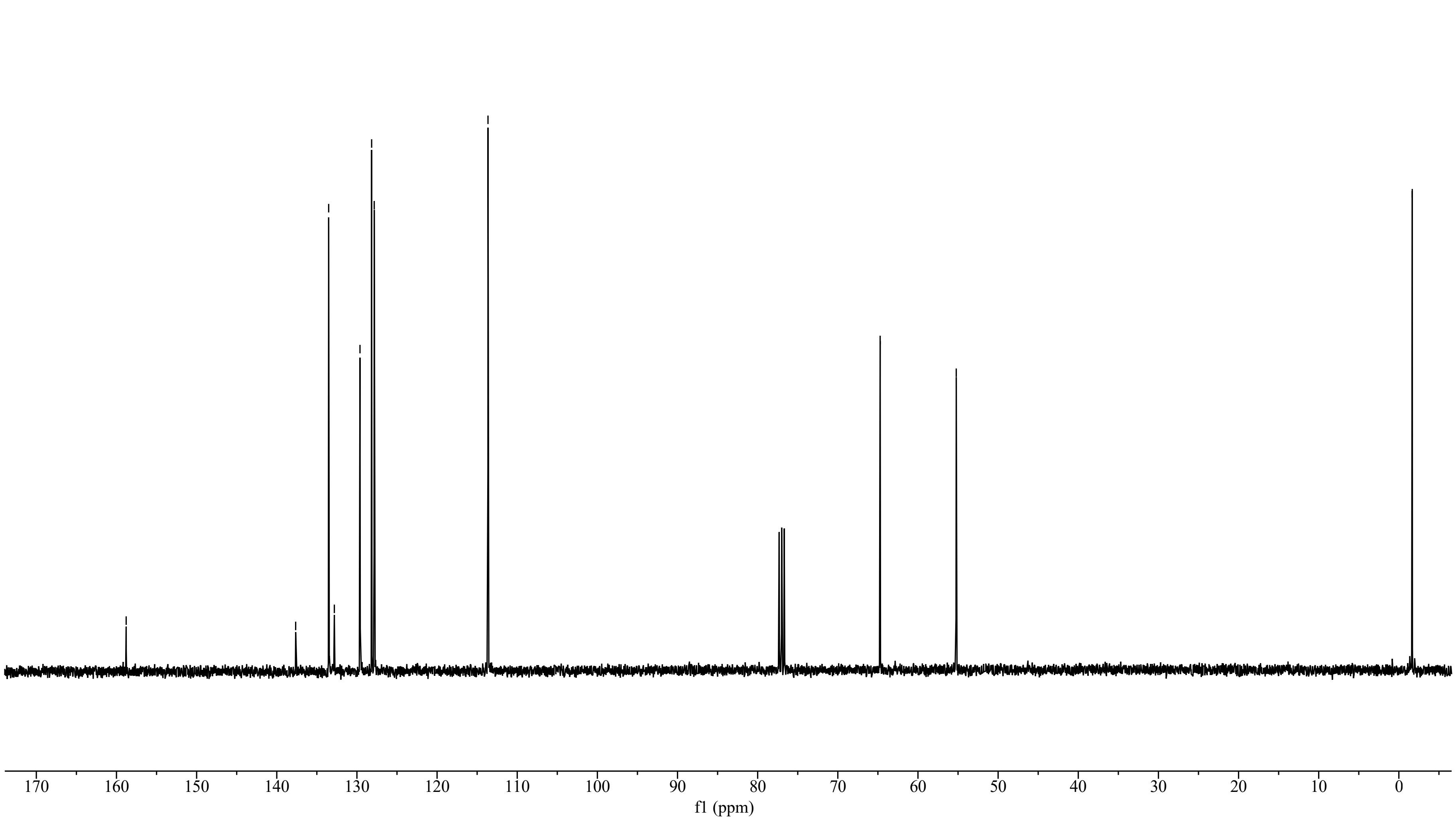

Compound **6m** ^{1}H NMR

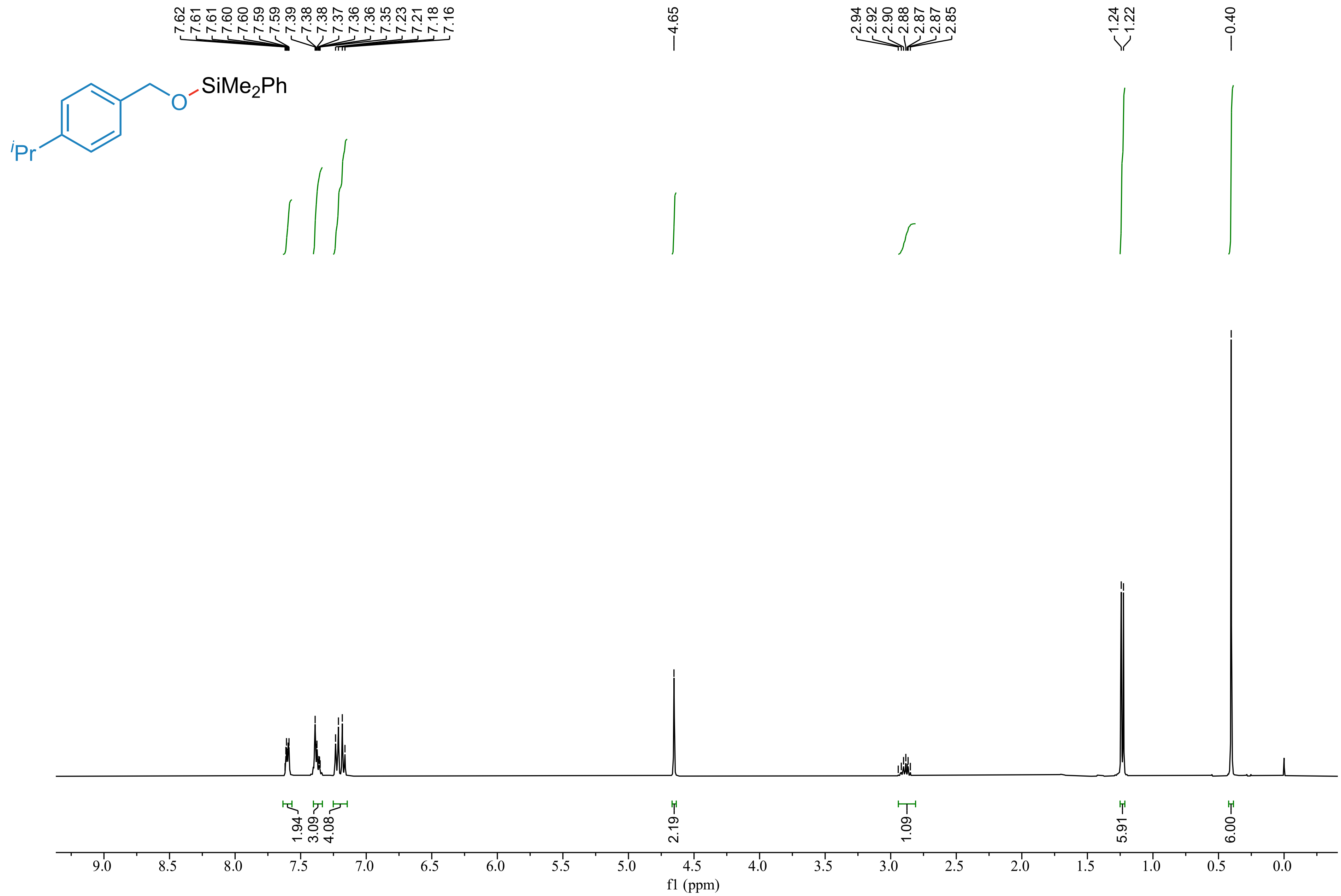

Compound **6m** ^{13}C NMR

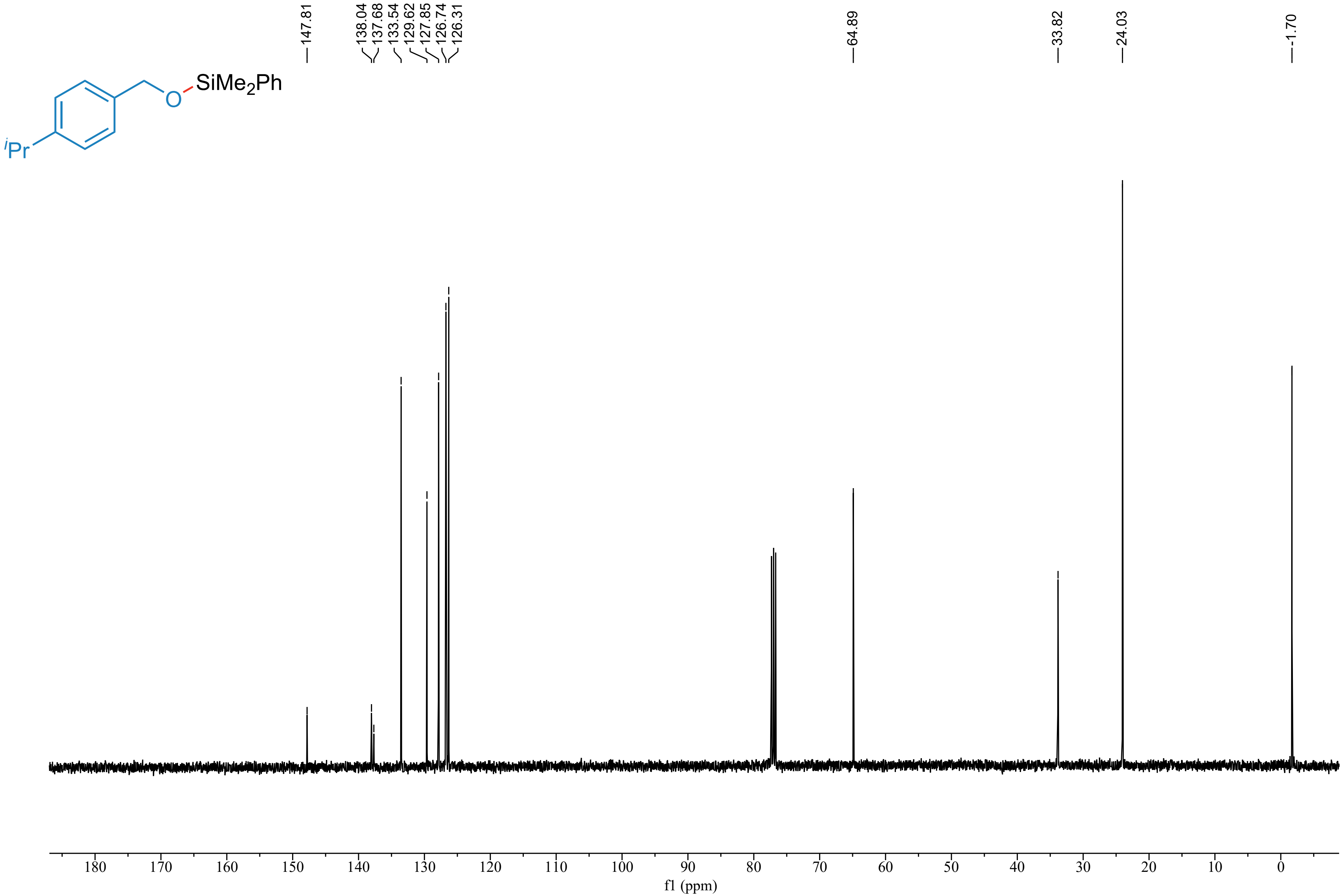

Compound **6n** ^{1}H NMR

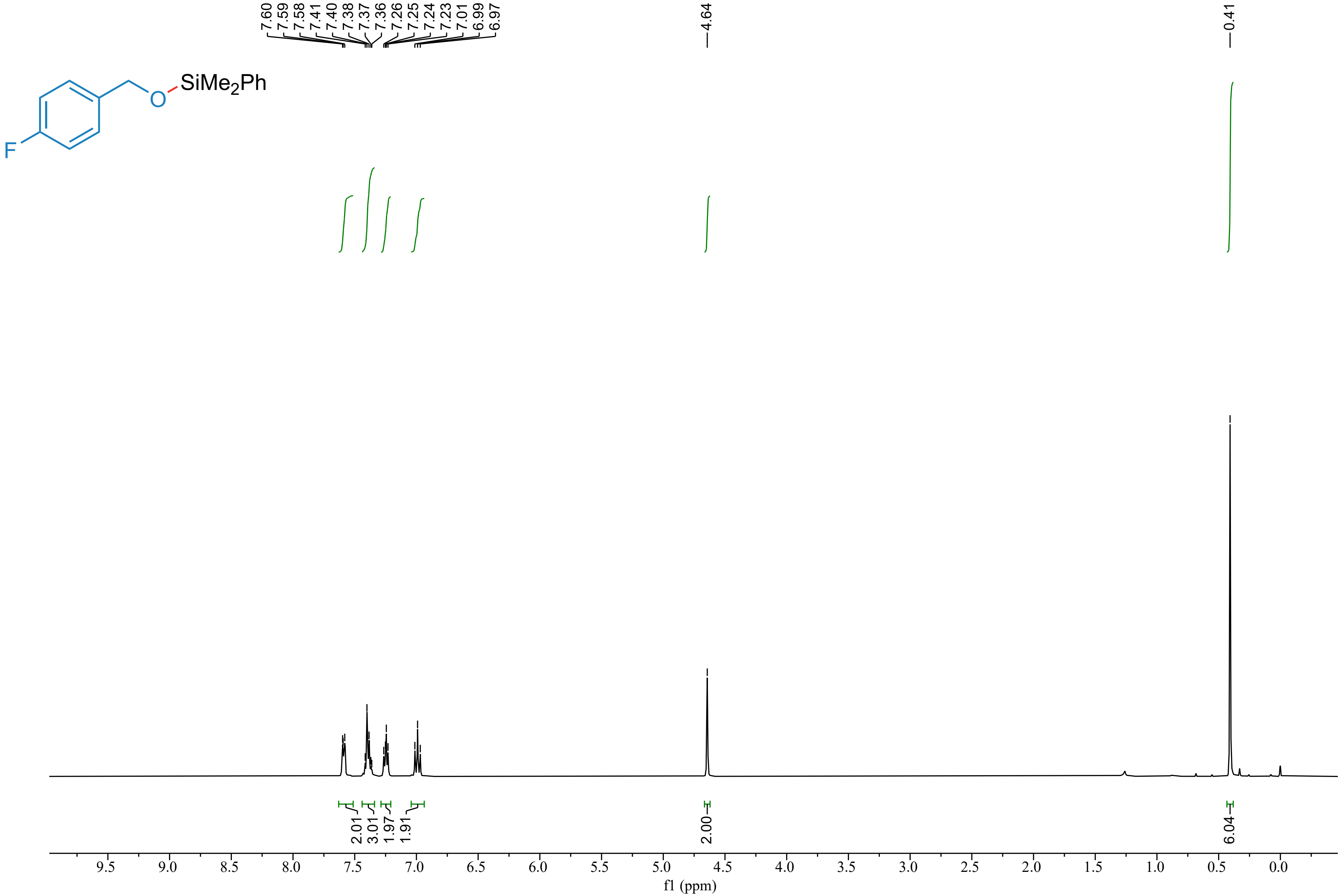

Compound **6n** ^{13}C NMR

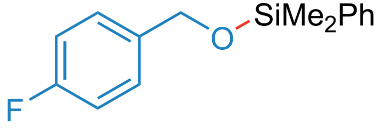

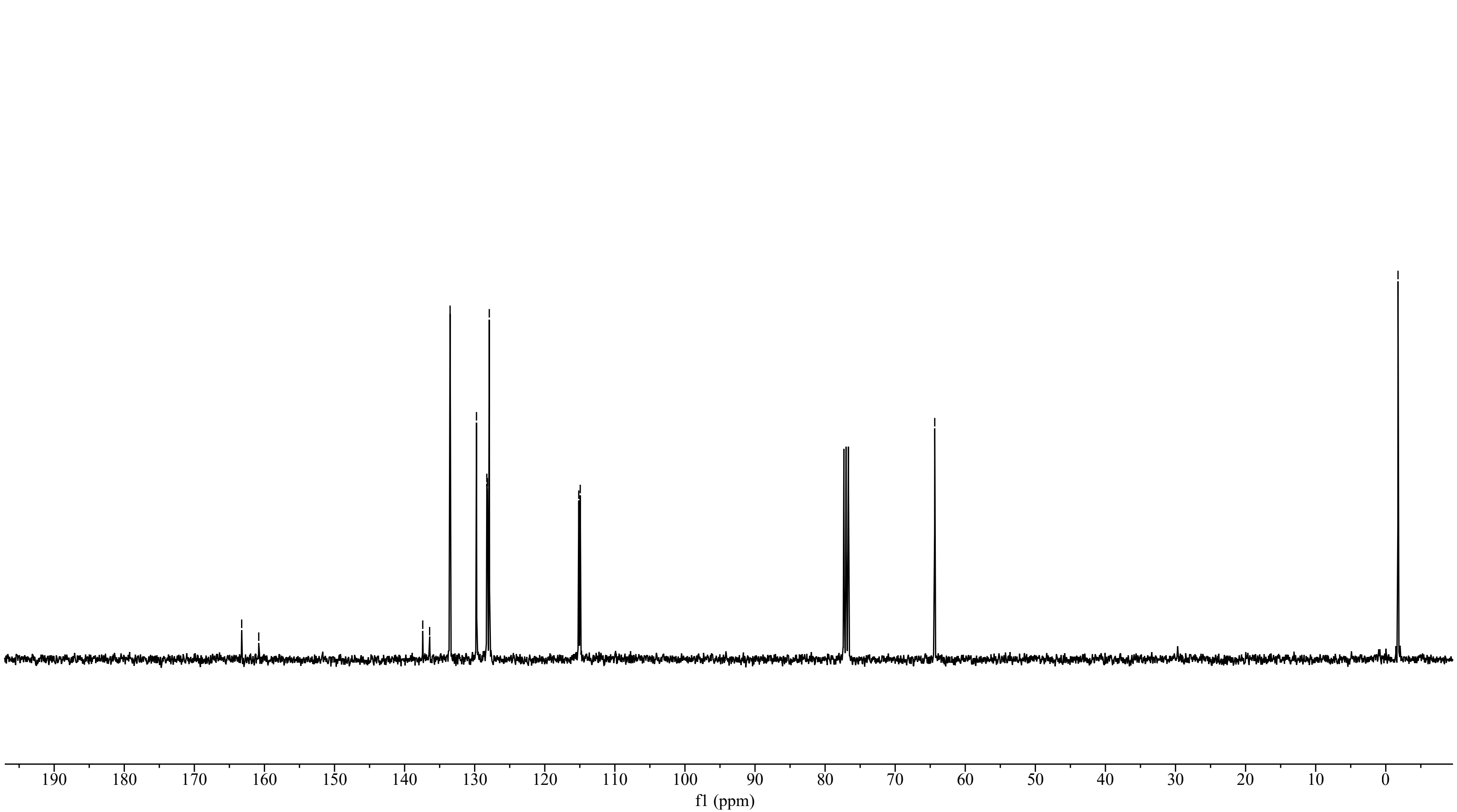

Compound **6n** ^{19}F NMR

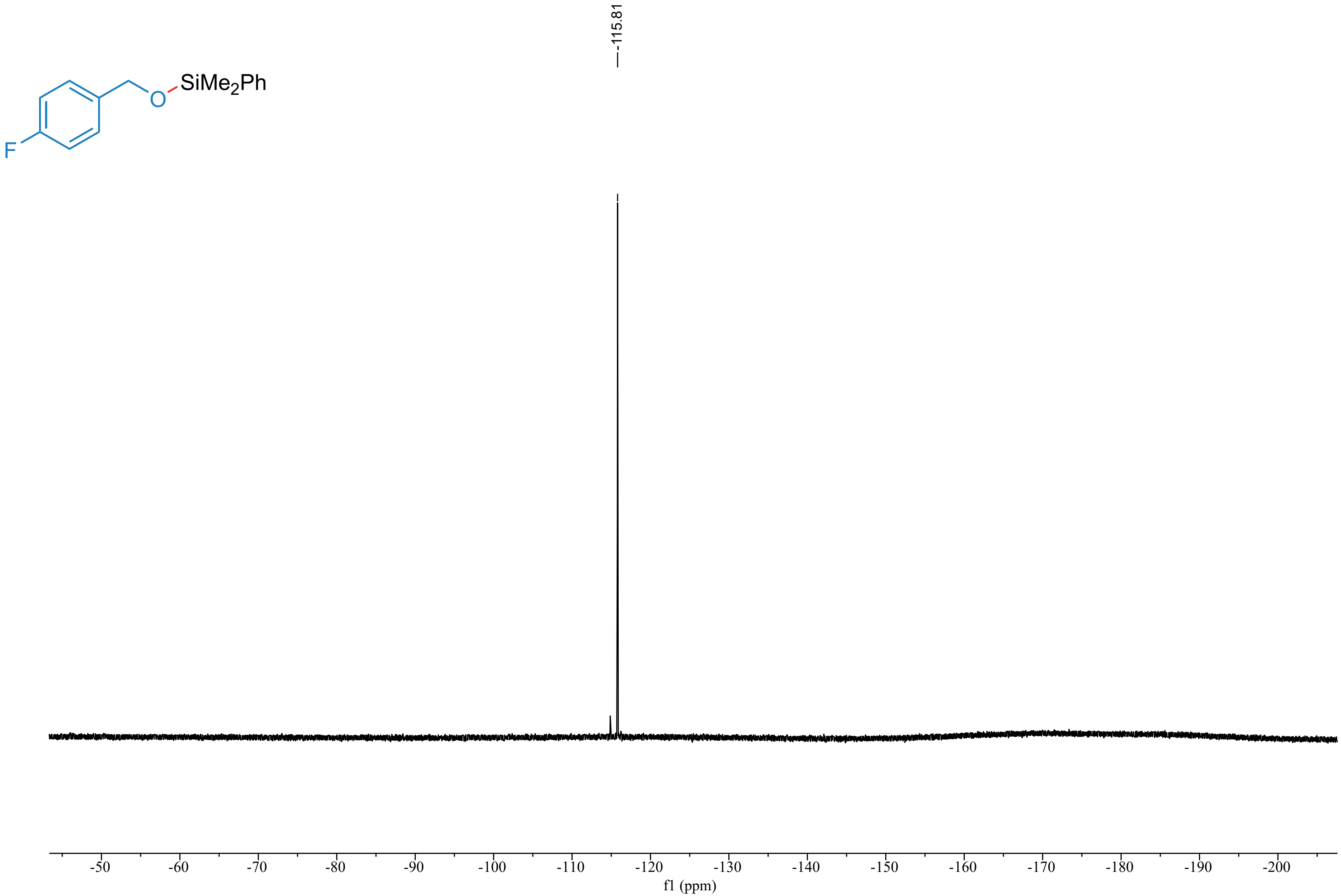

Compound **6o** ^{1}H NMR

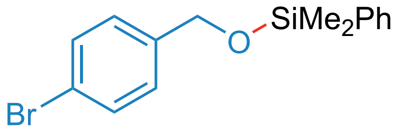

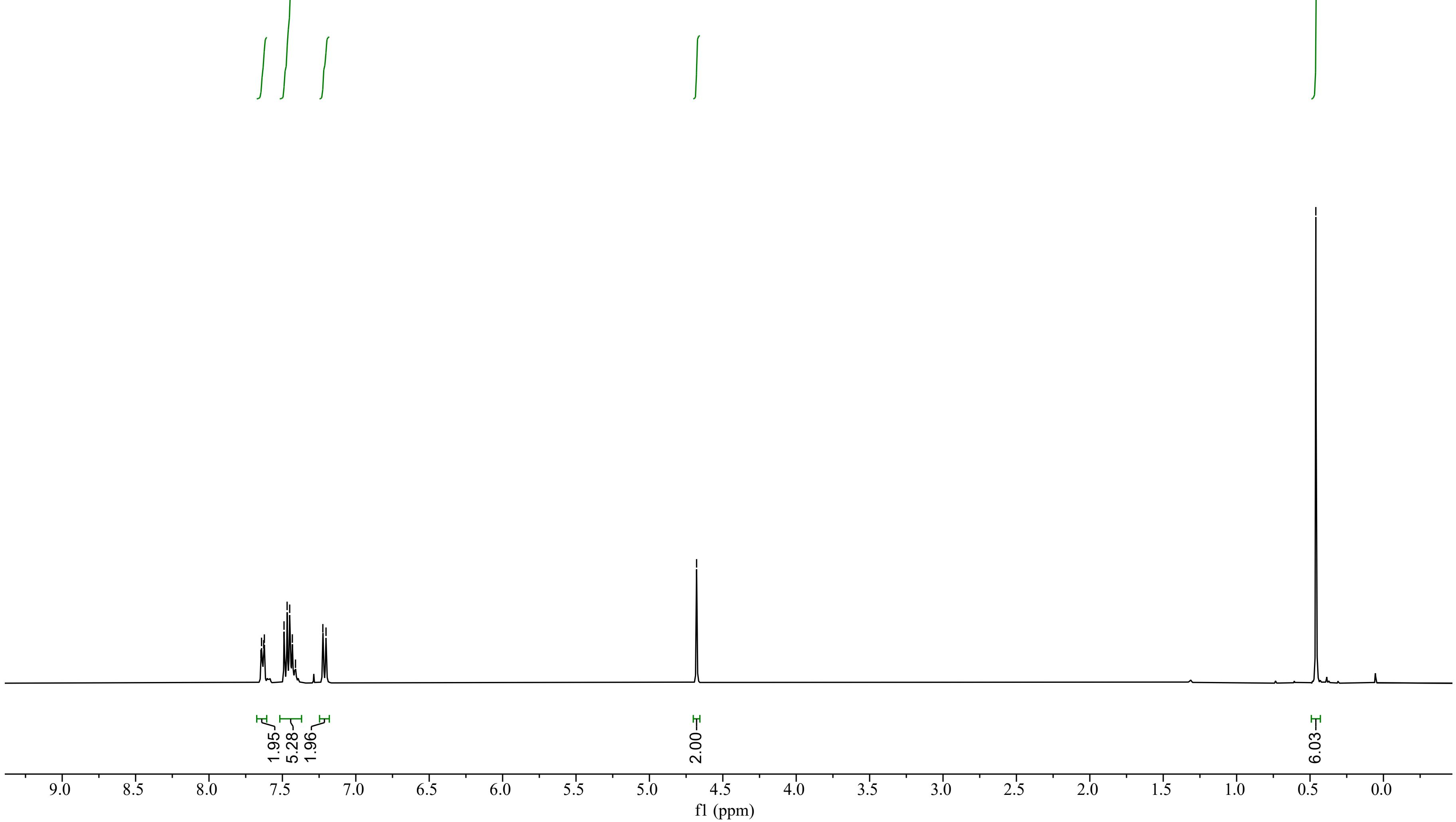

Compound **6o** ^{13}C NMR

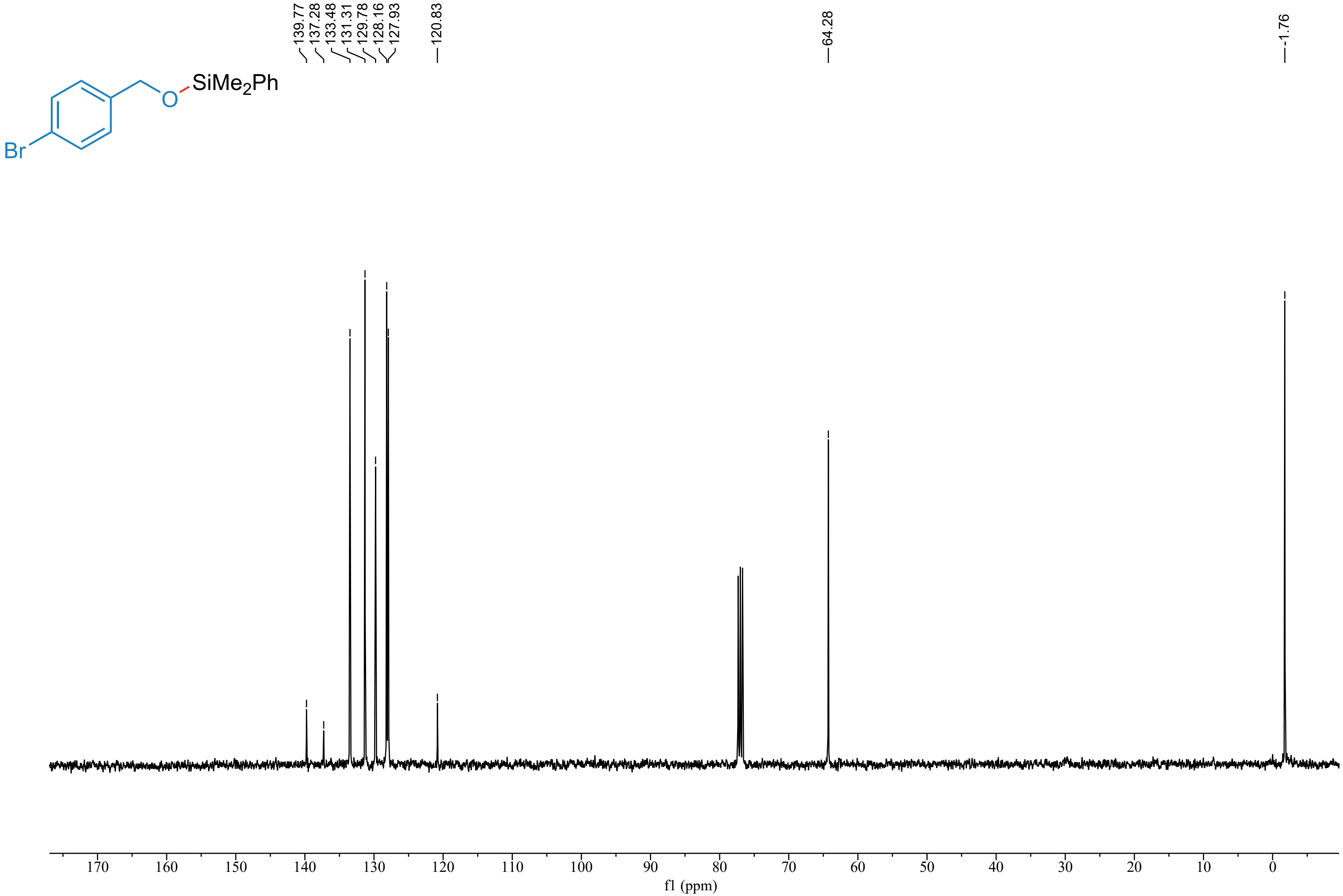

Compound **6p** ^{1}H NMR

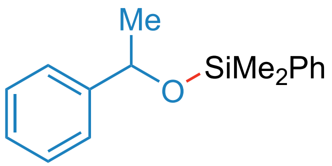

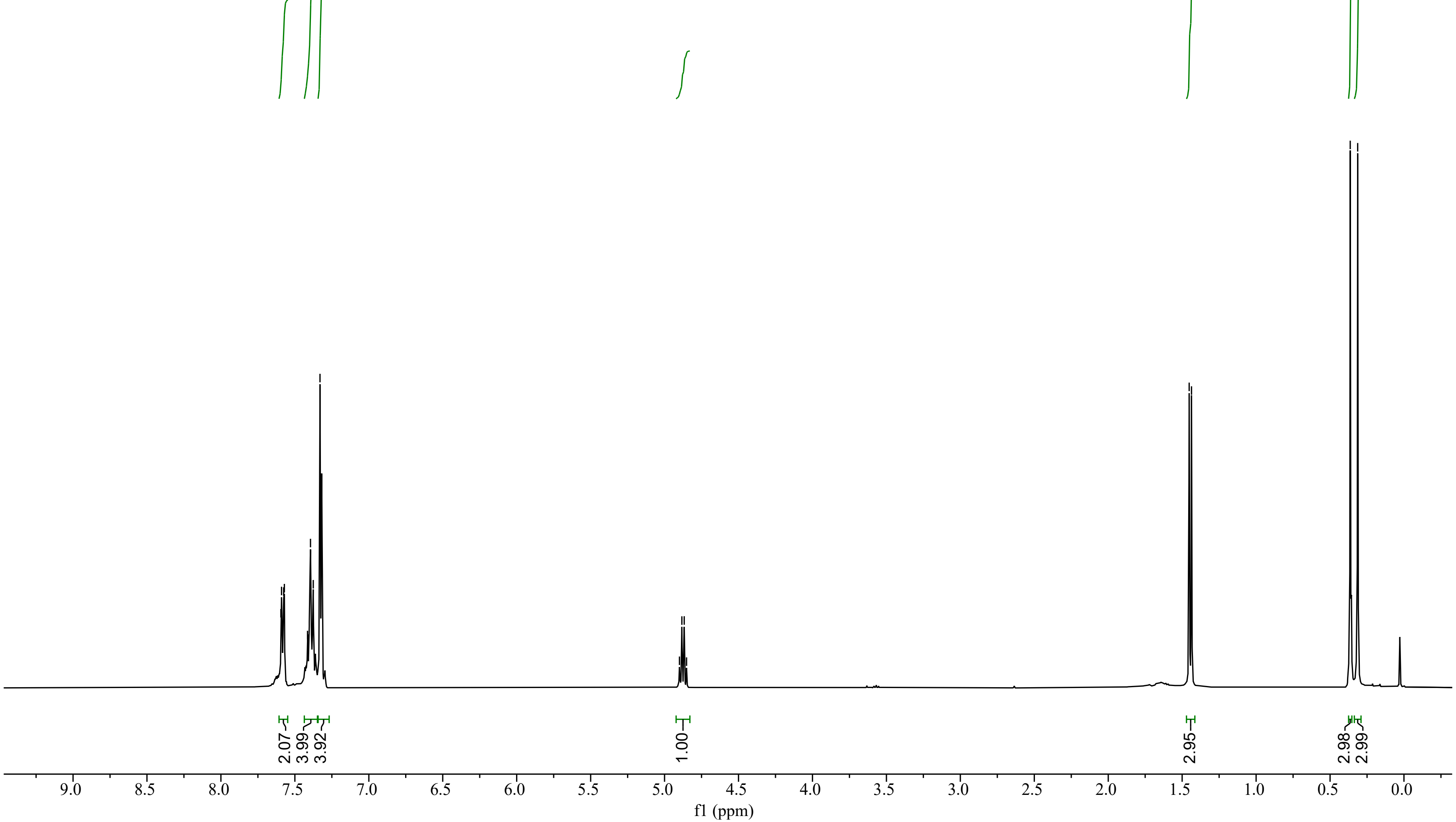

Compound **4p** ^{13}C NMR

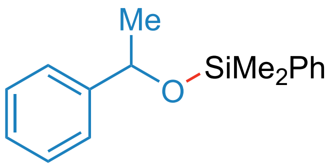

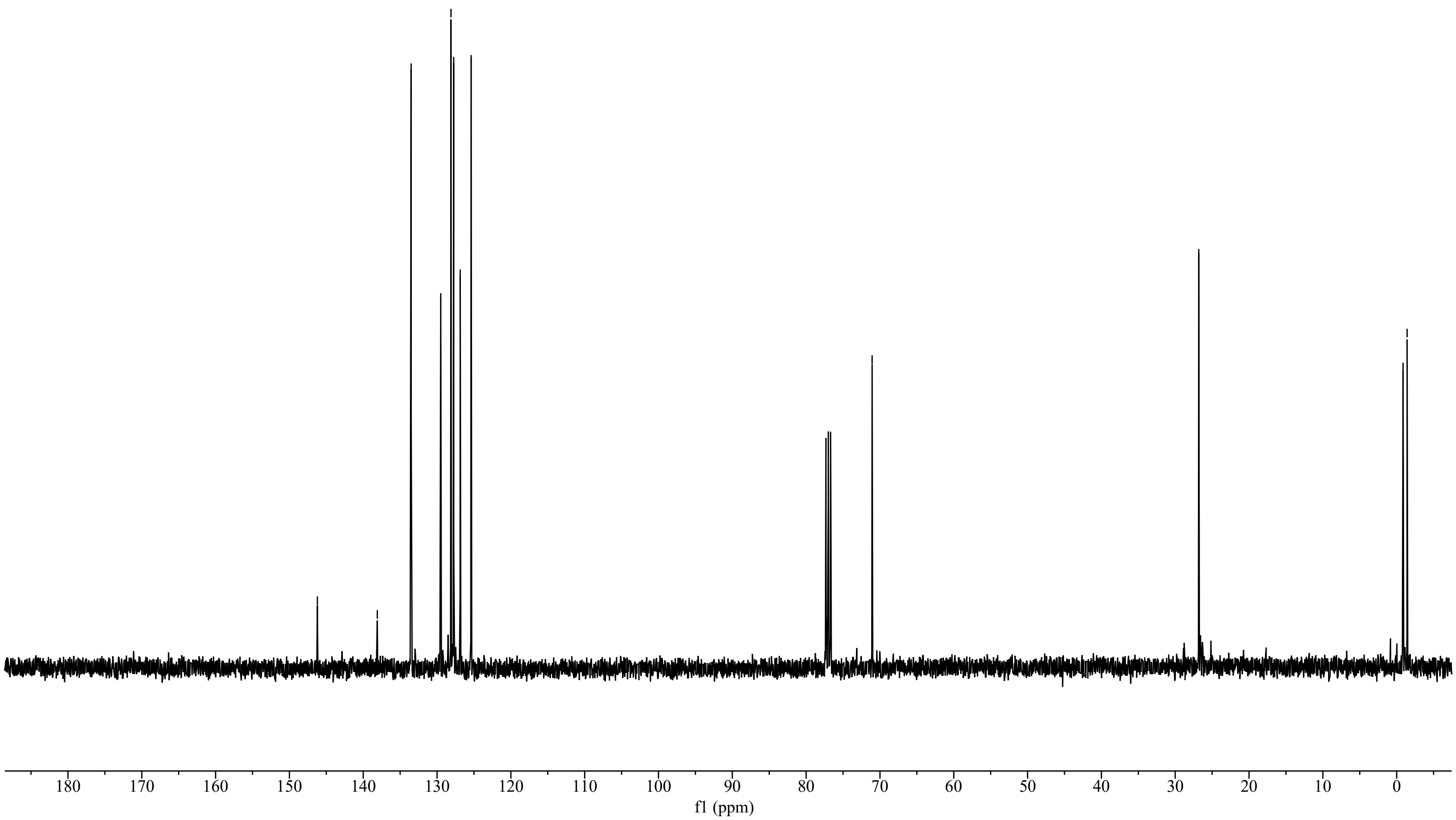

Compound **6q** ^{1}H NMR

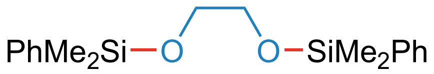

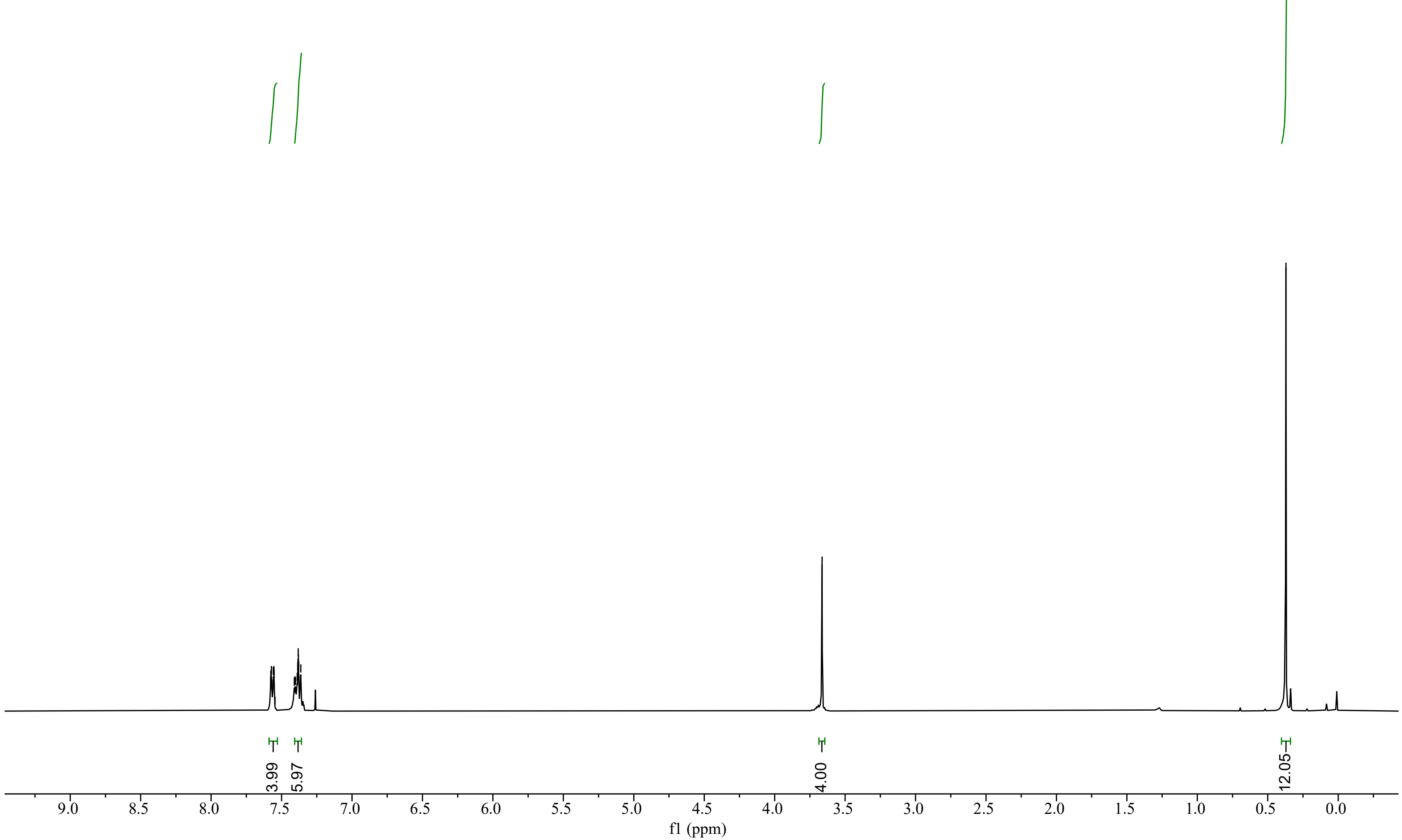

Compound **6q** ^{13}C NMR

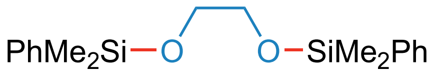

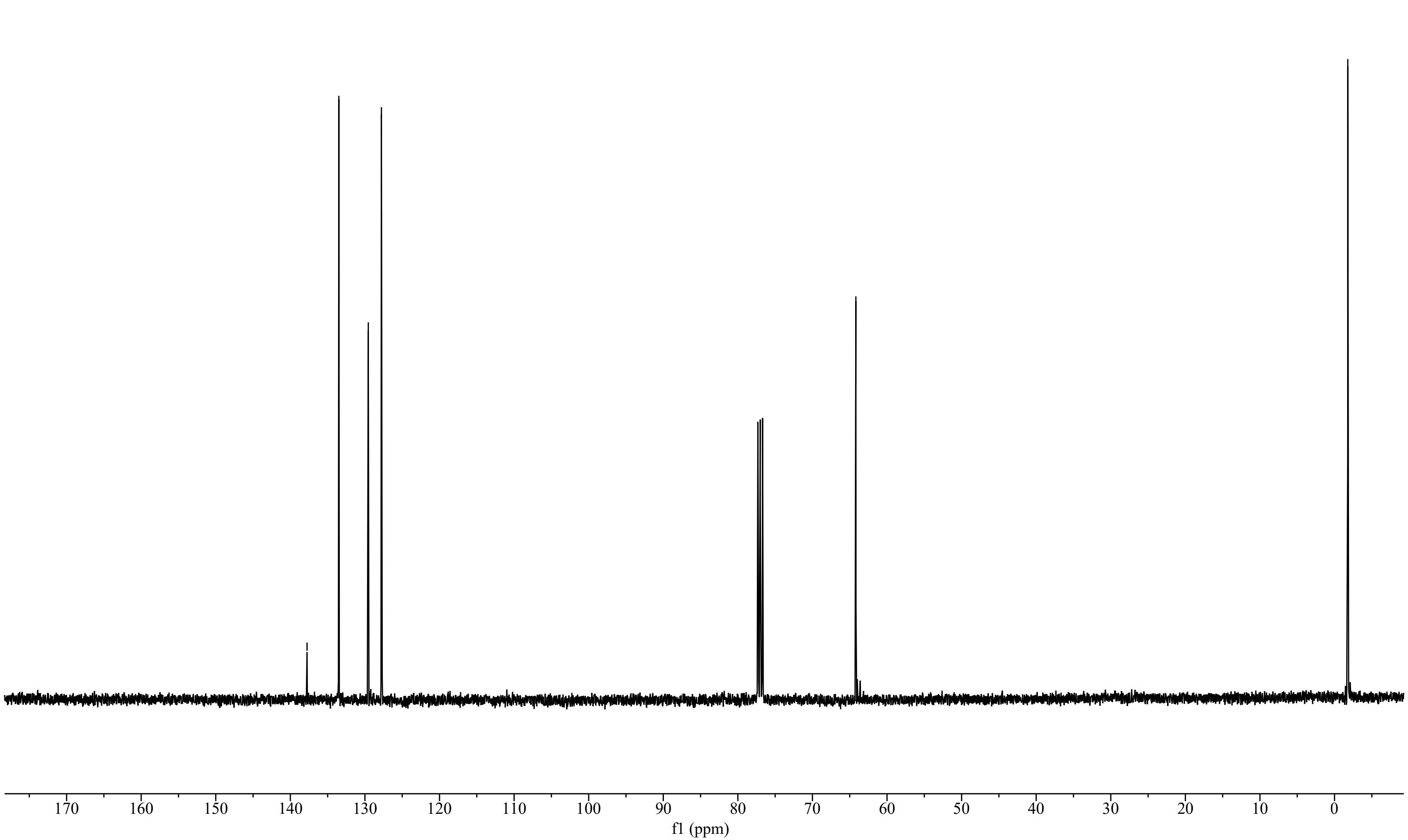

Compound **6r** ^{1}H NMR

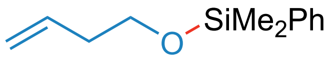

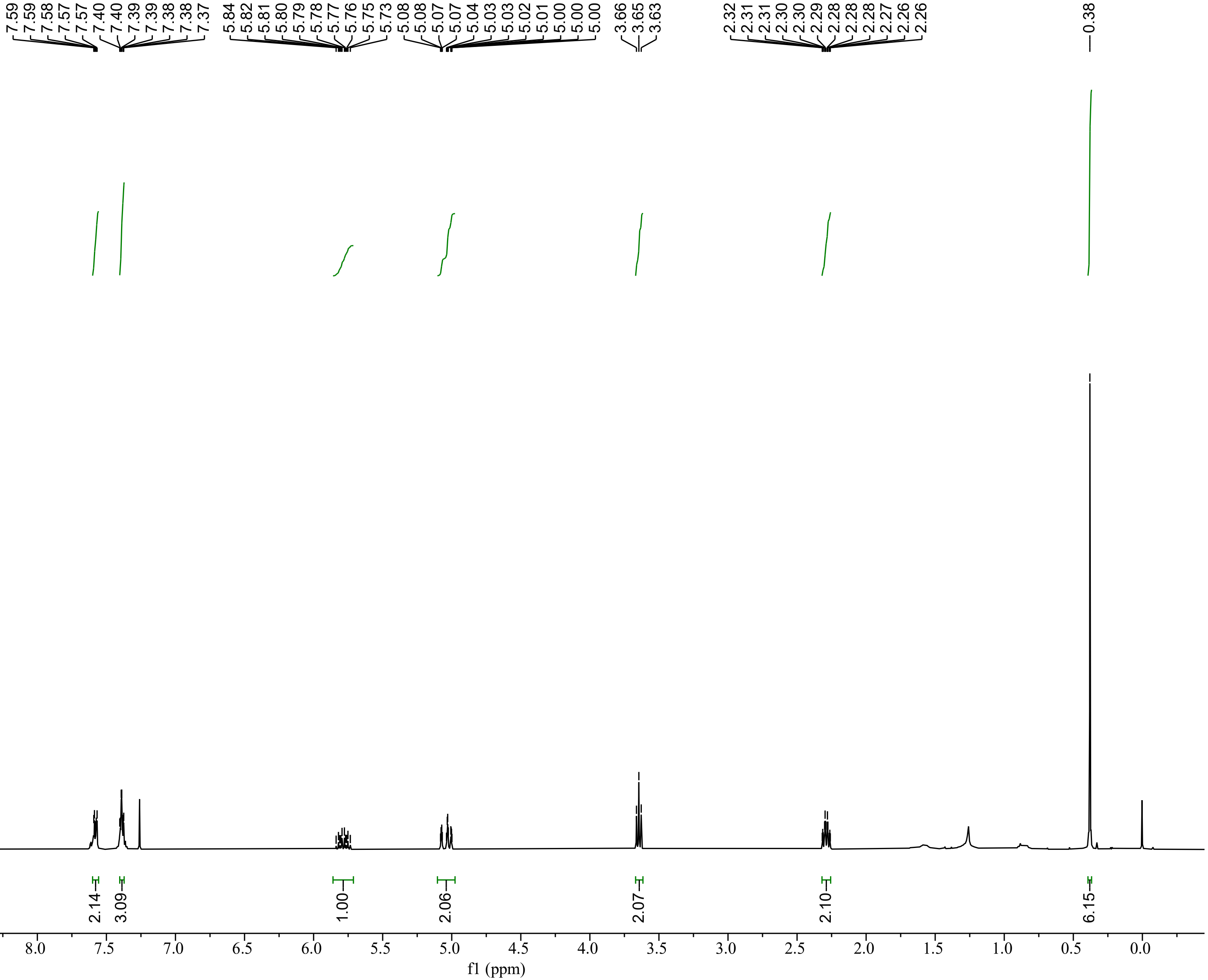

Compound **6r** ^{13}C NMR

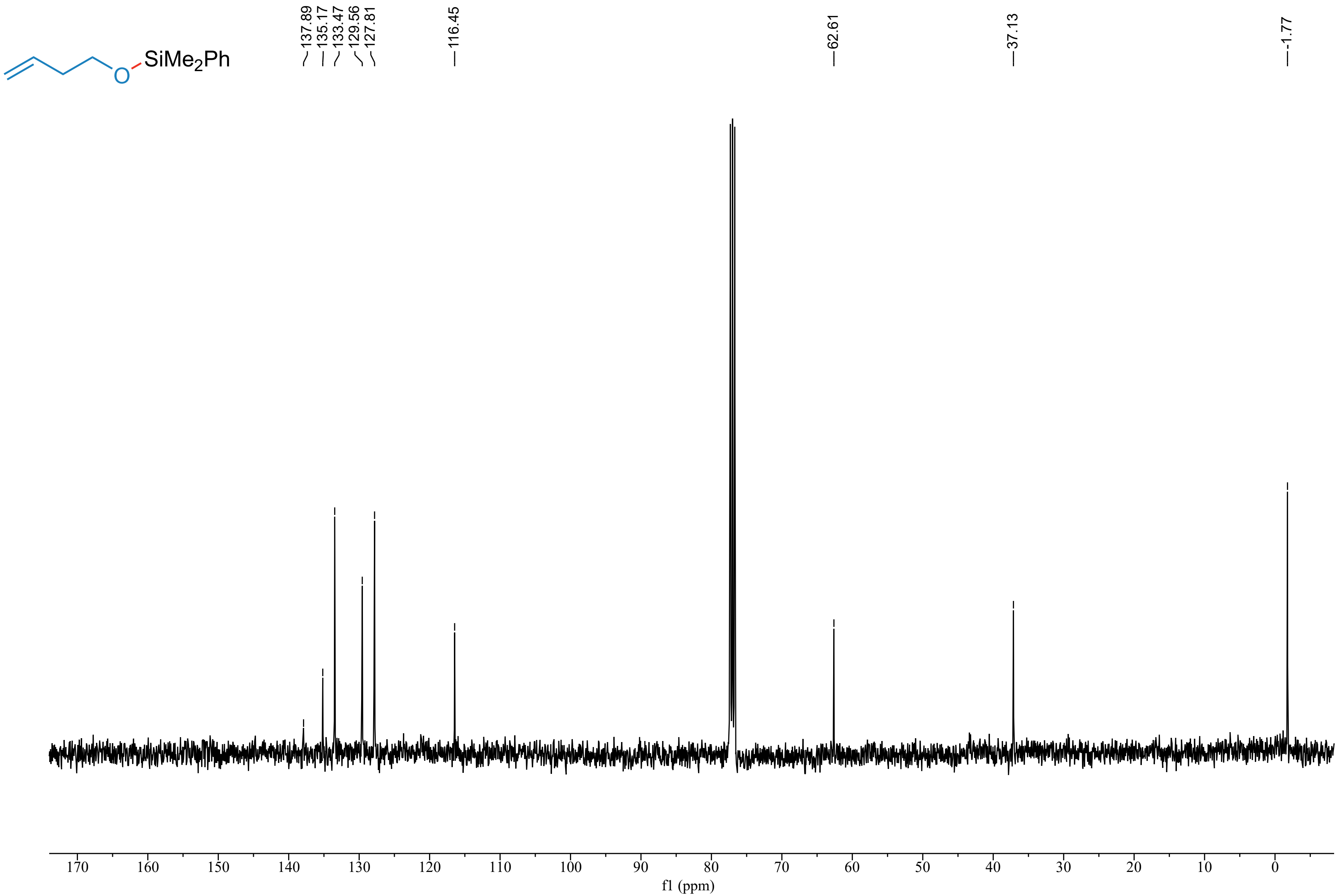

Compound **6s** ^{1}H NMR

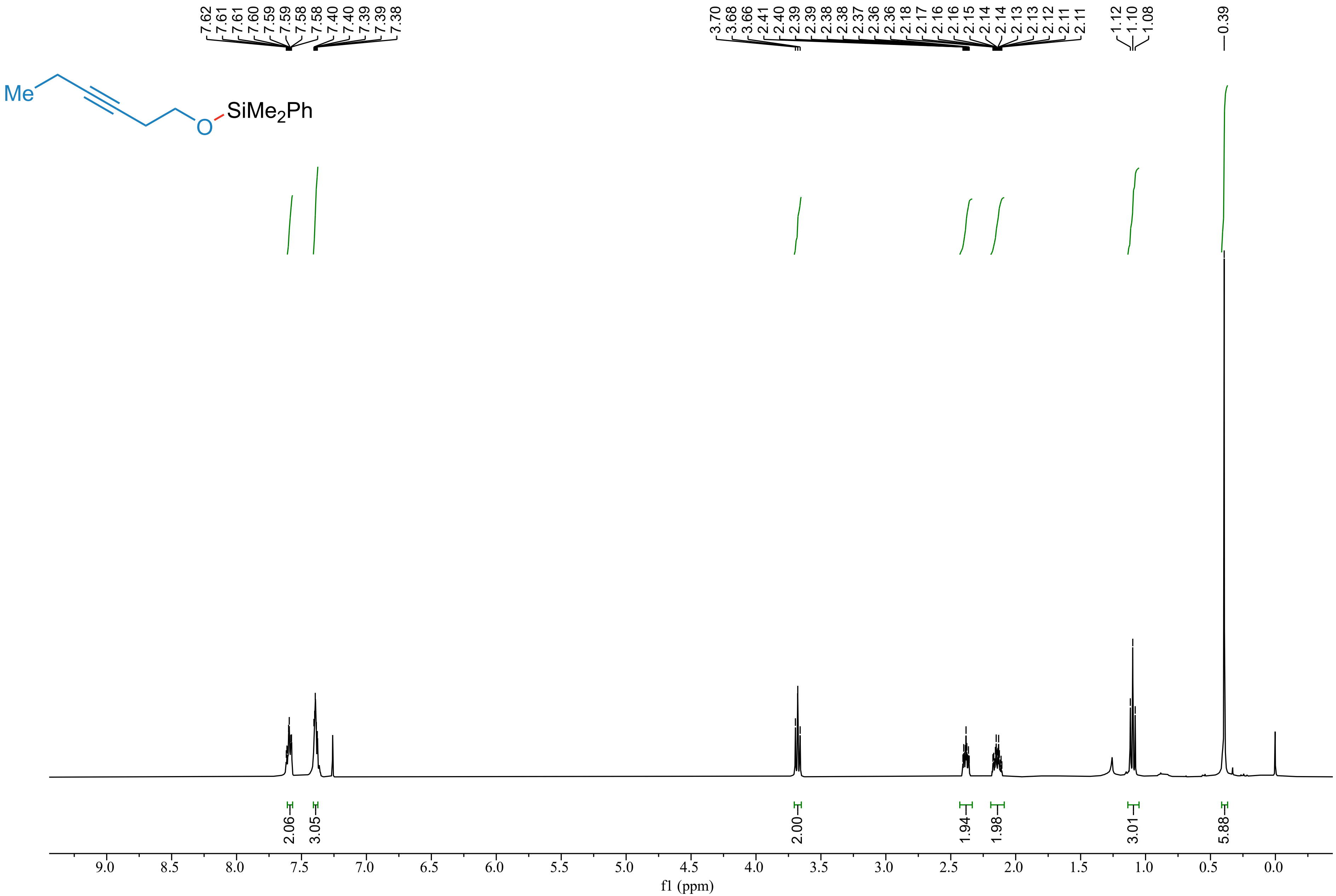

Compound **6s** ^{13}C NMR

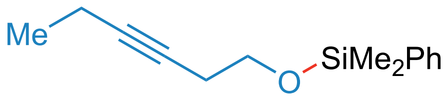

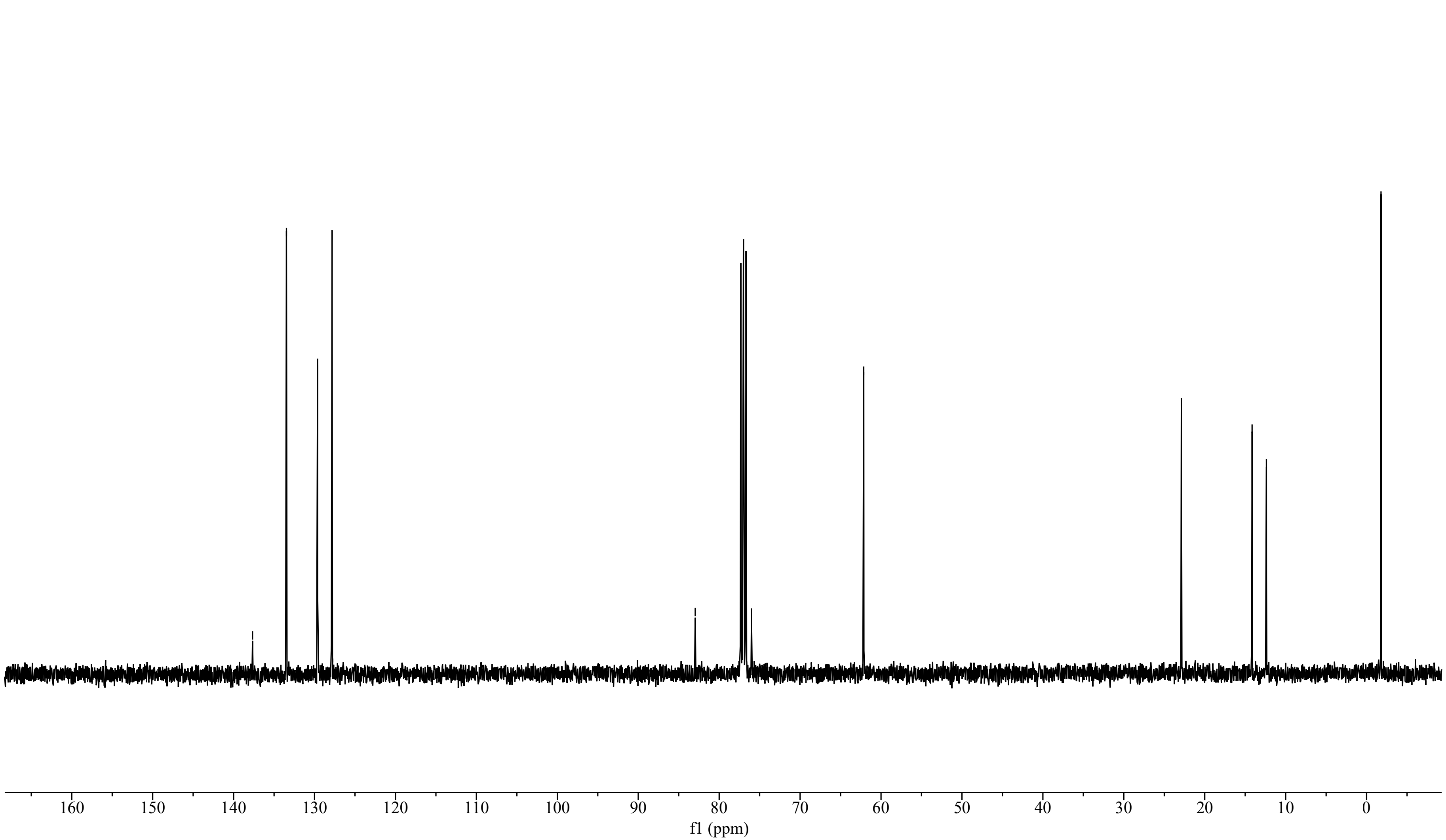

Compound **6t** ^{1}H NMR

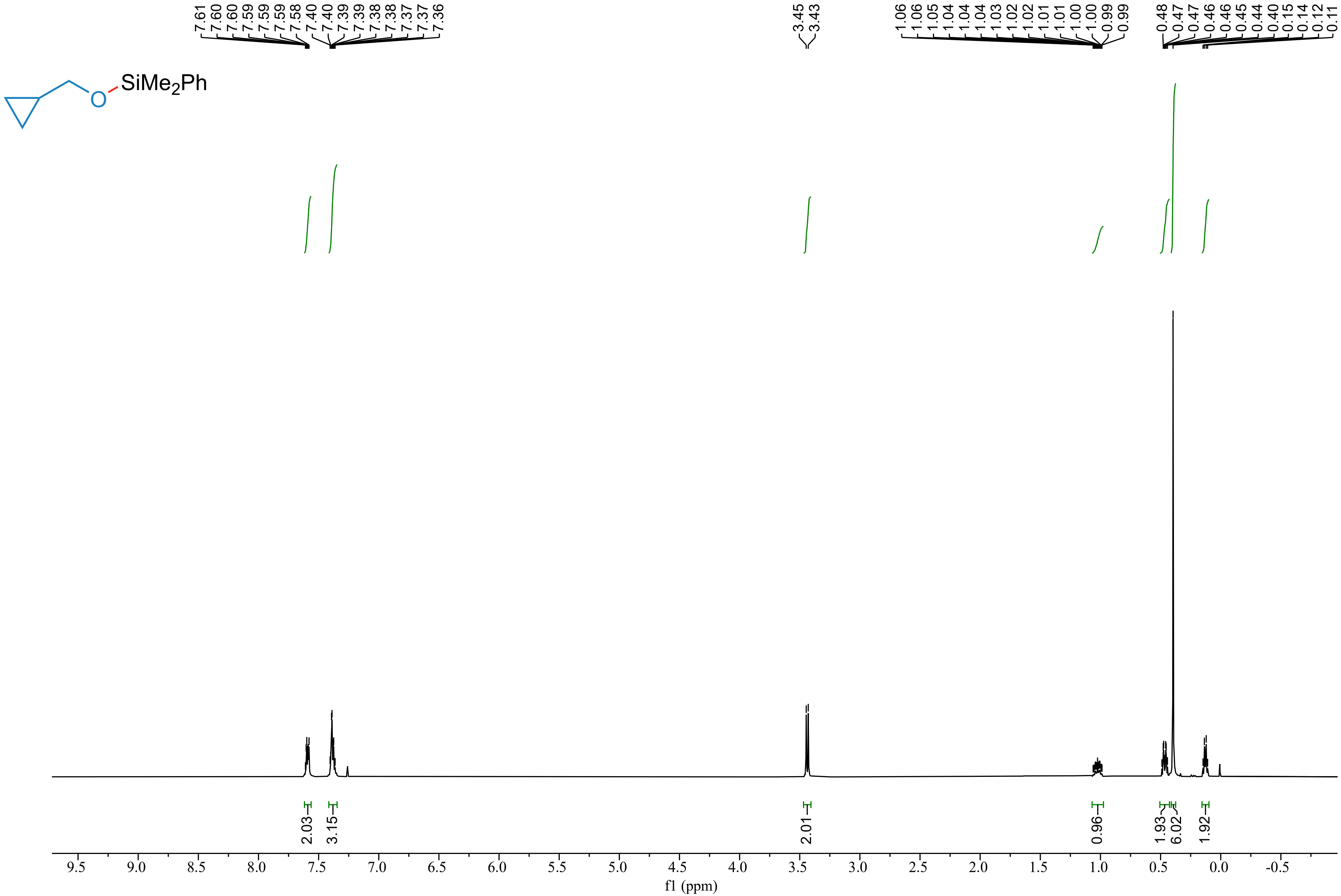

Compound **6t** ^{13}C NMR

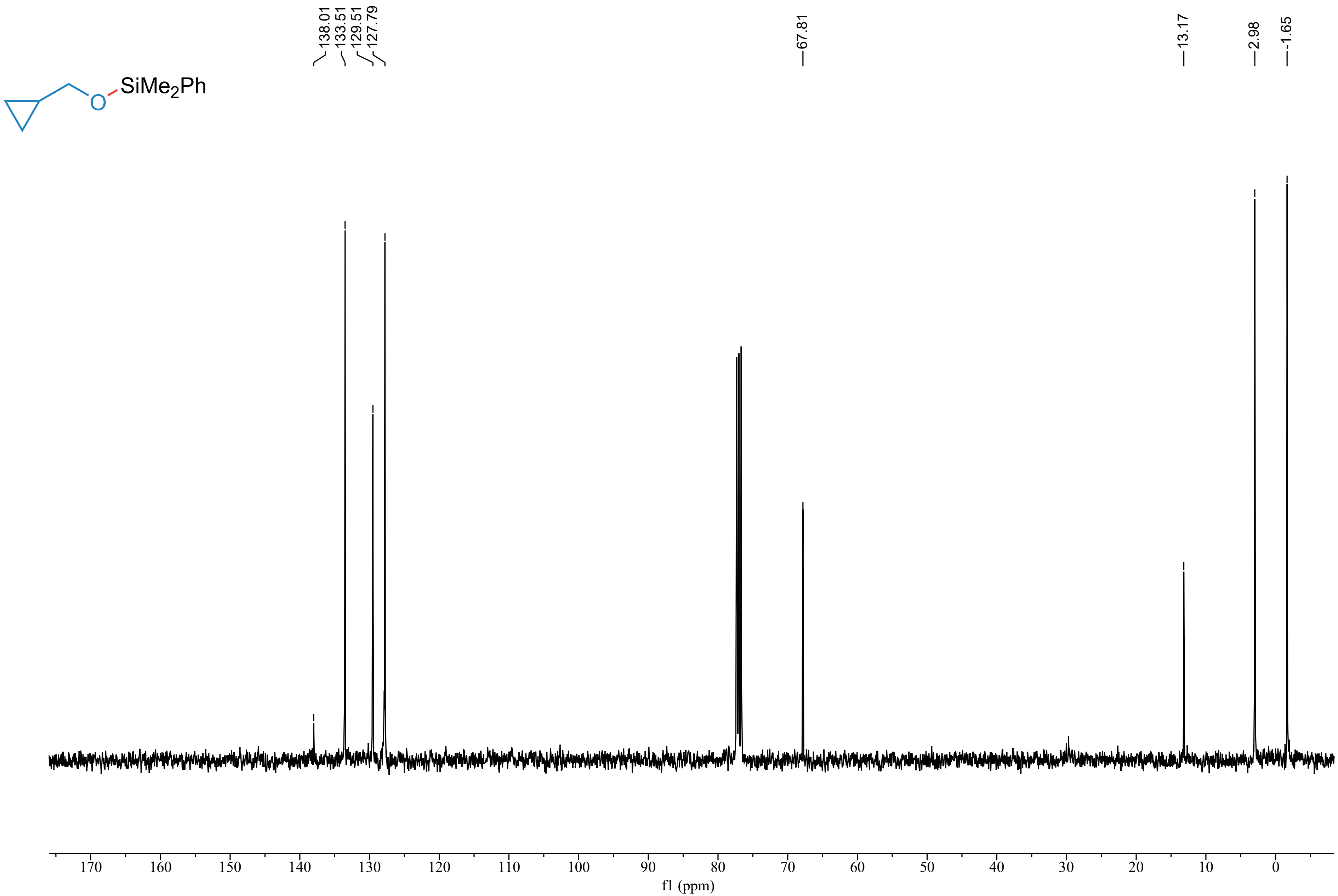

Compound **6u** ^{1}H NMR

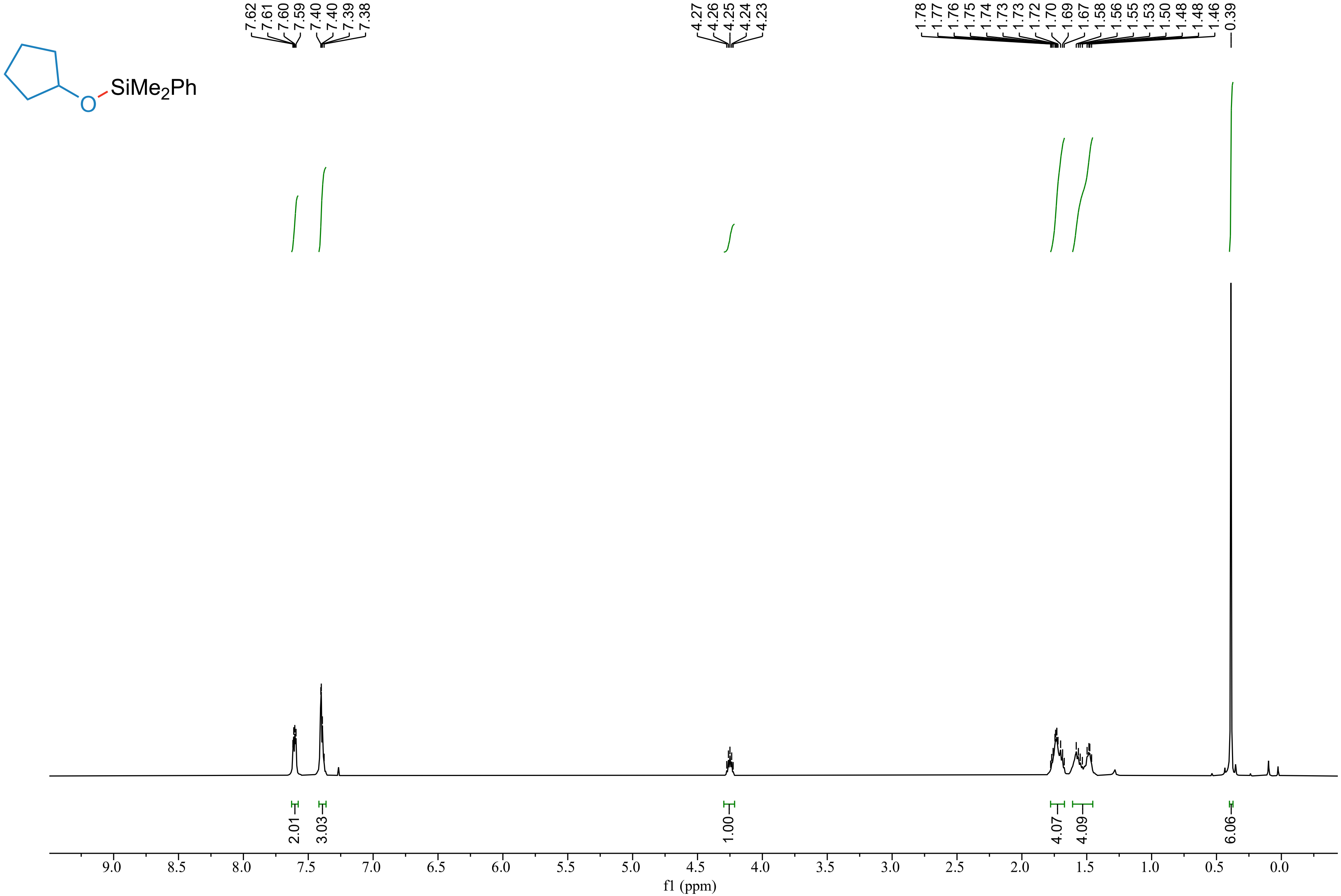

Compound **6u** ^{13}C NMR

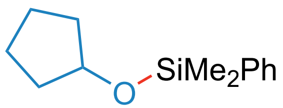

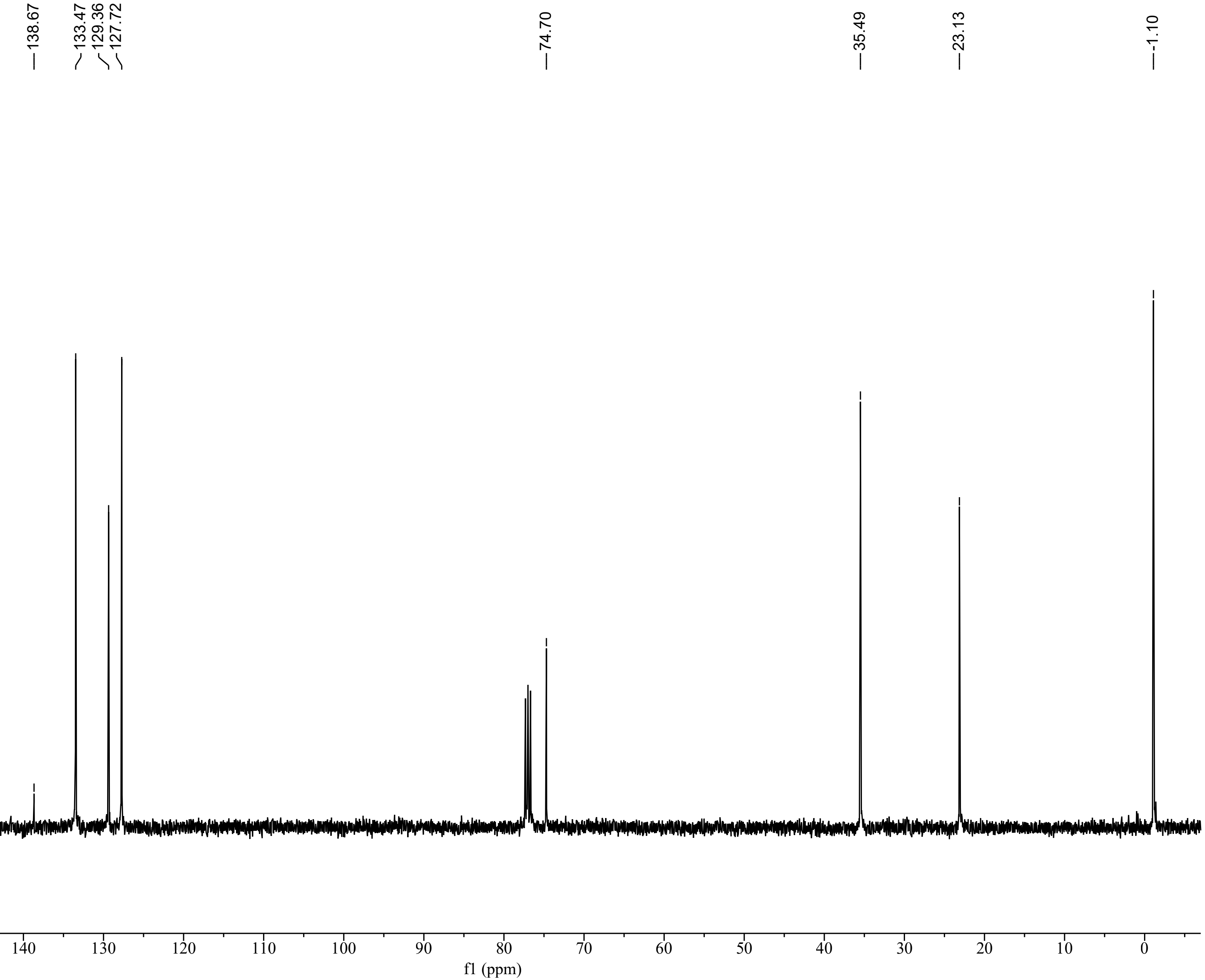

Compound **6v** ^{1}H NMR

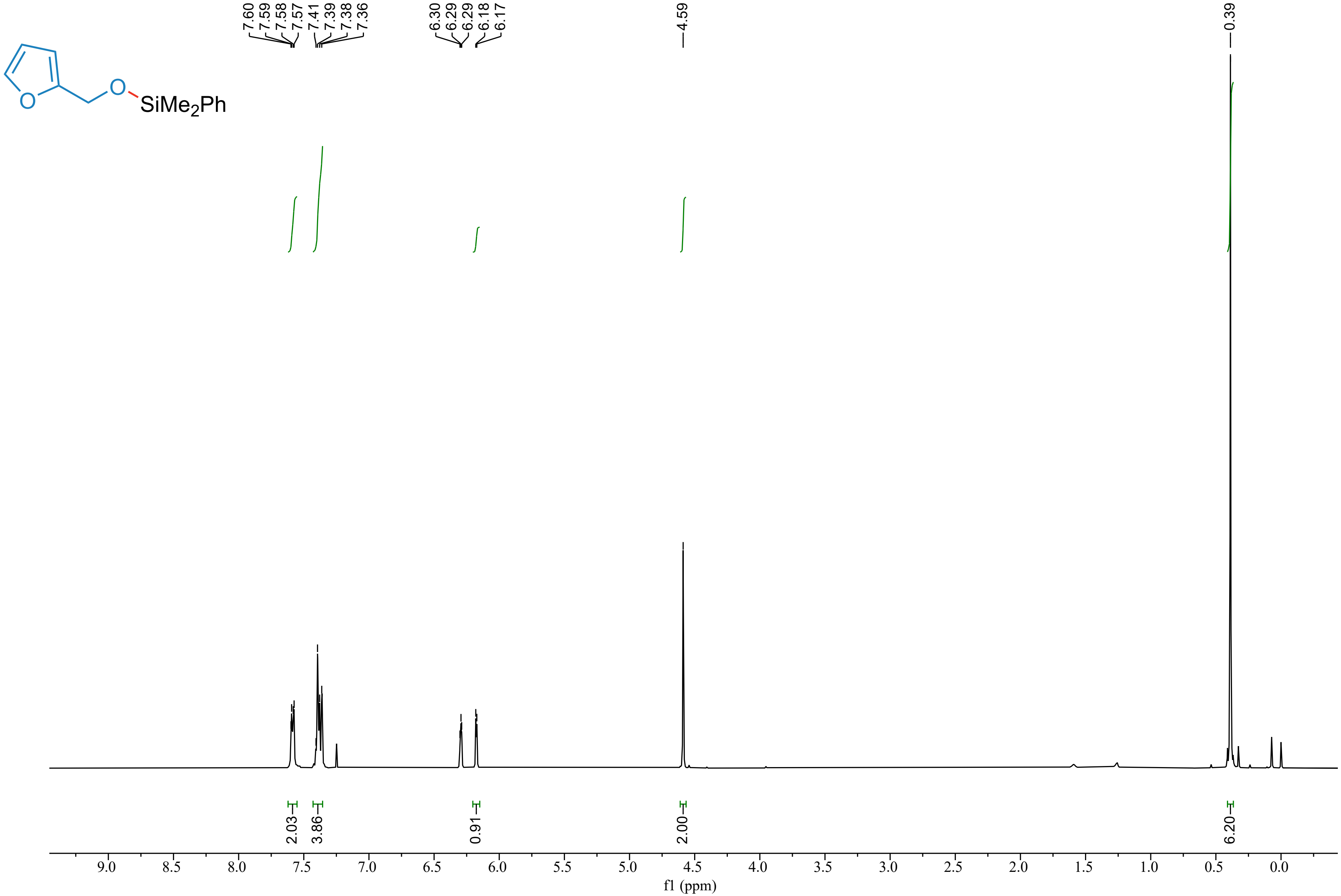

Compound **6v** ^{13}C NMR

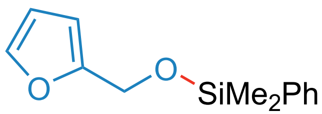

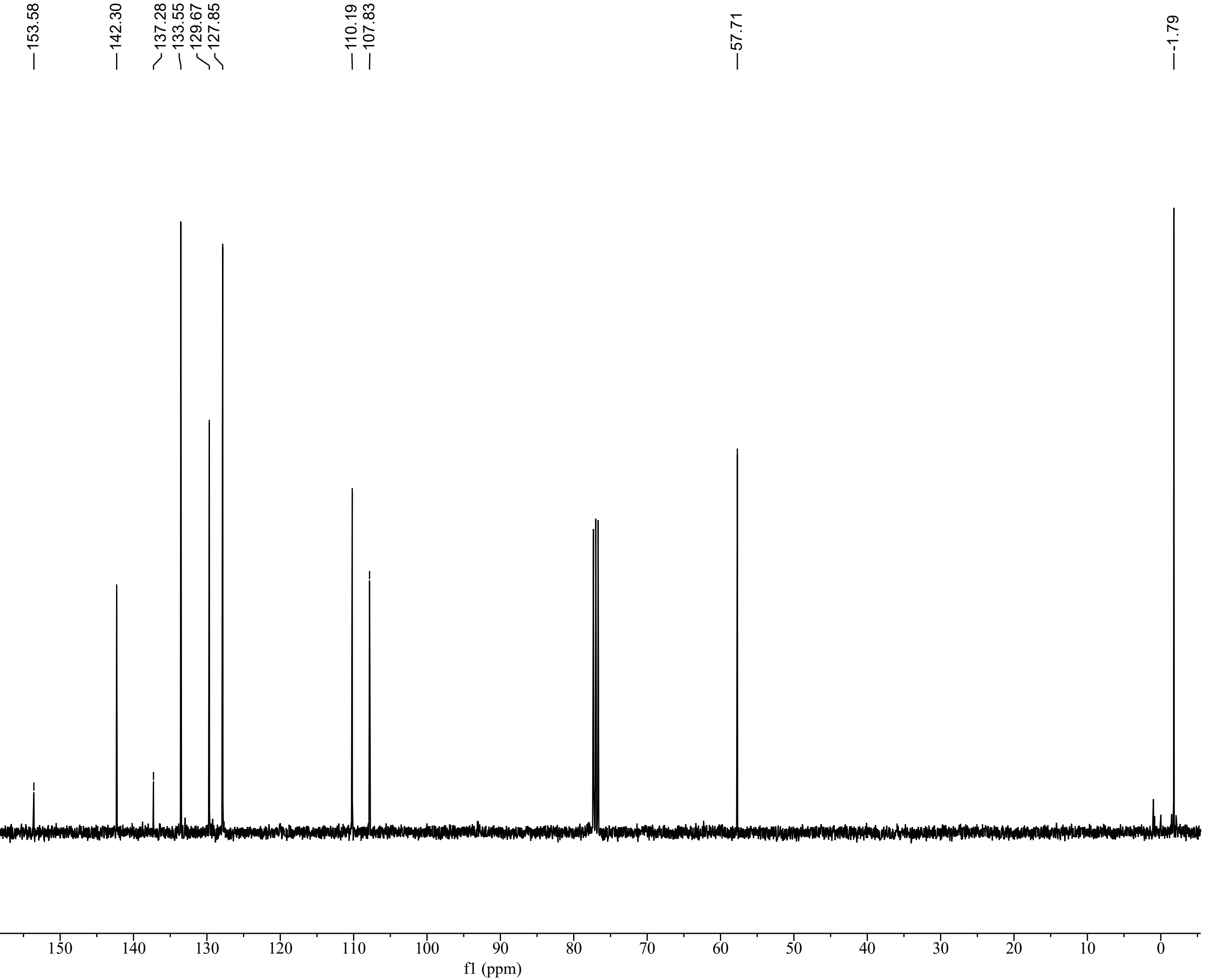

Compound **6w** [1]H NMR

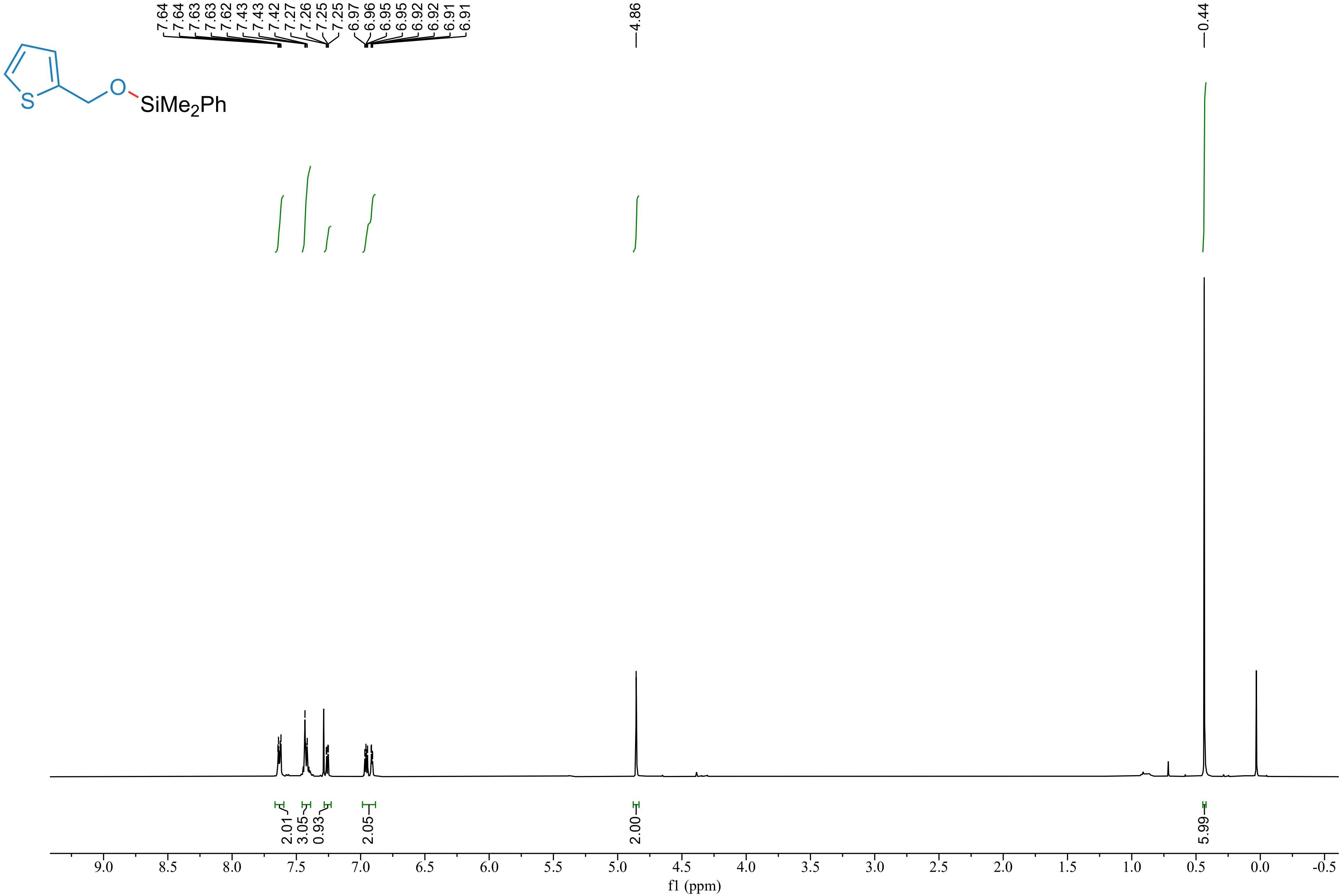

Compound **6w** ^{13}C NMR

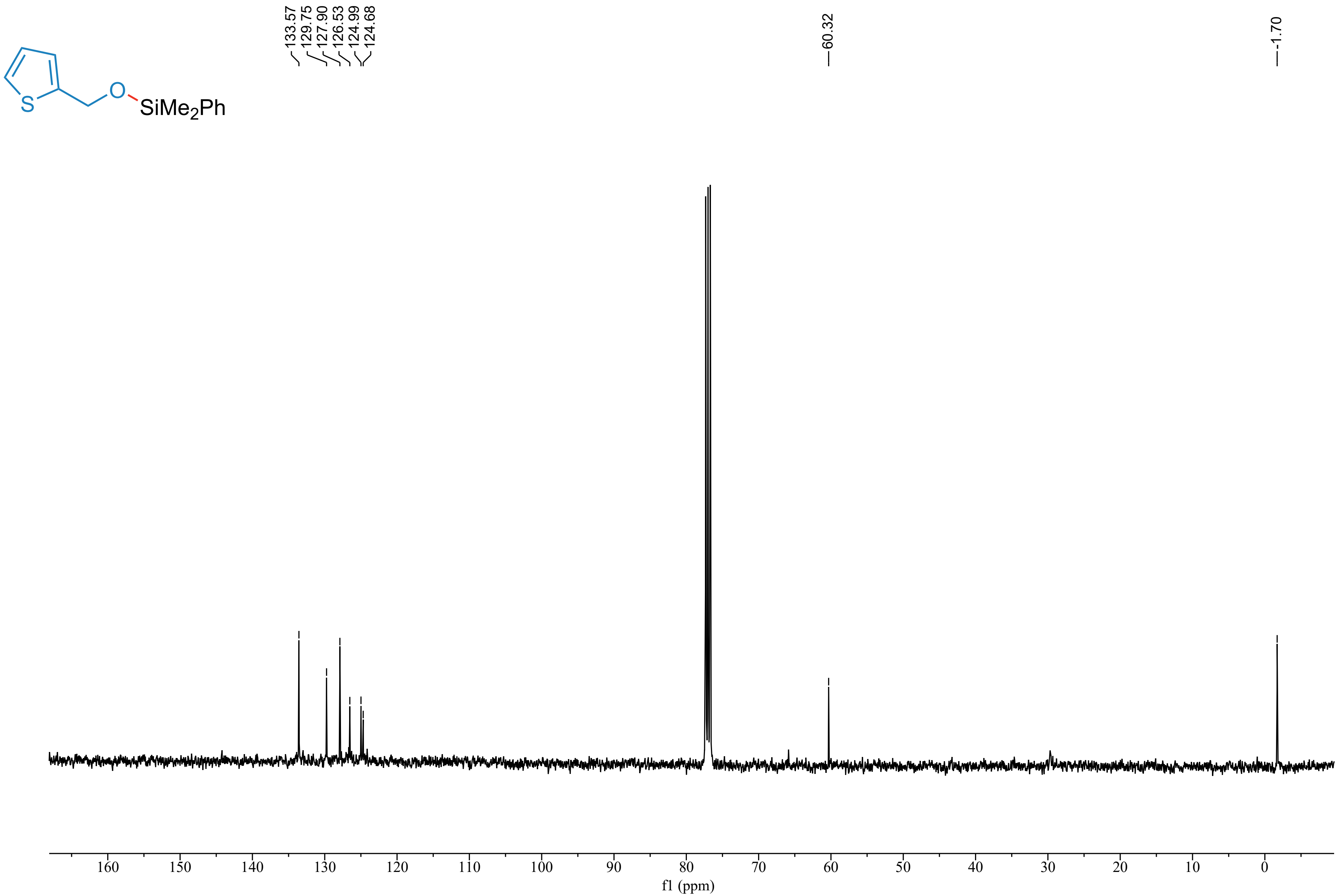

Compound **6x** ^{1}H NMR

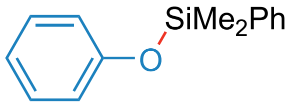

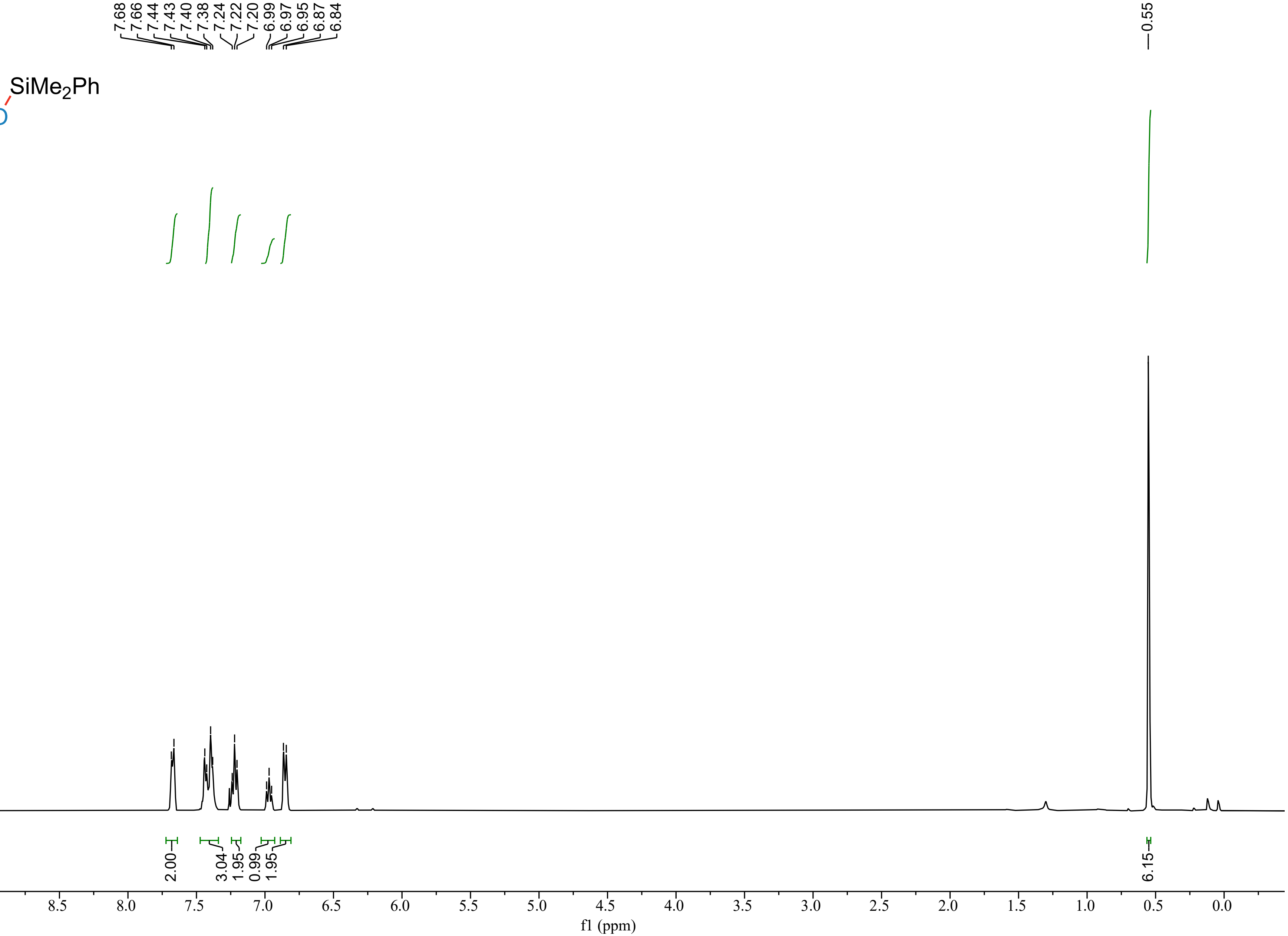

Compound **6x** ^{13}C NMR

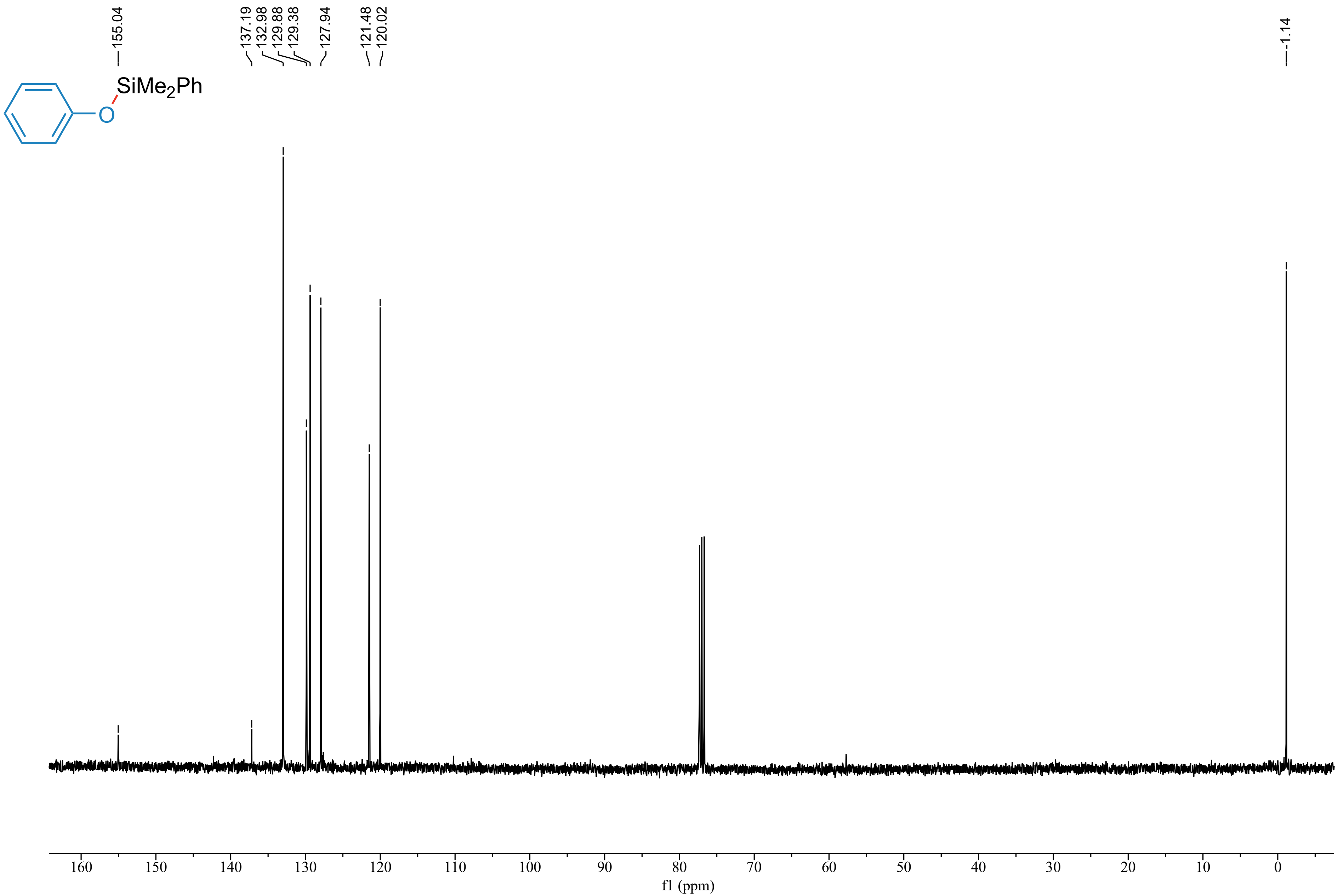

Compound **6y** ^{1}H NMR

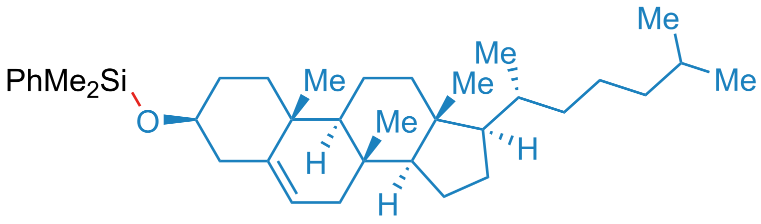

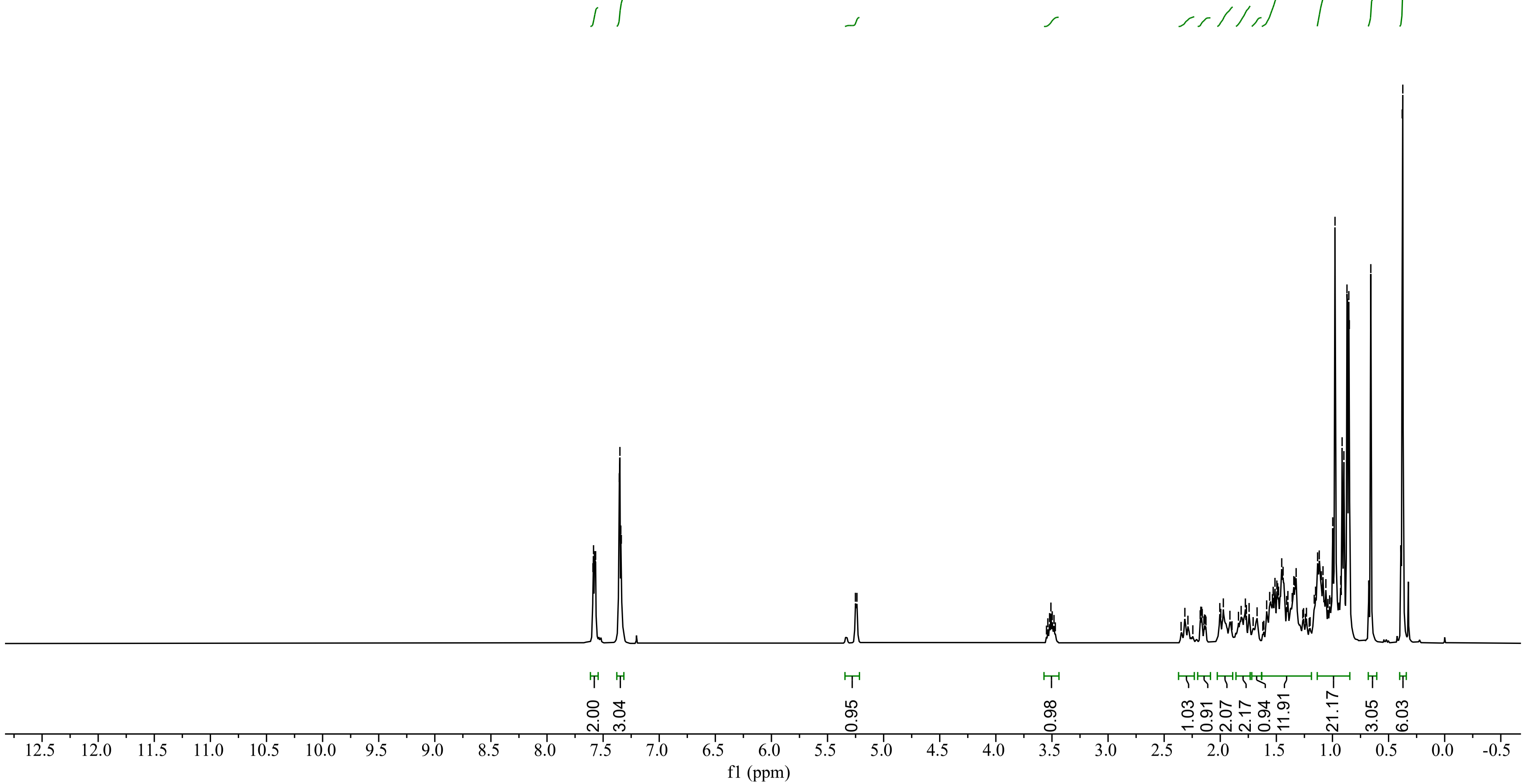

Compound **6y** ^{13}C NMR

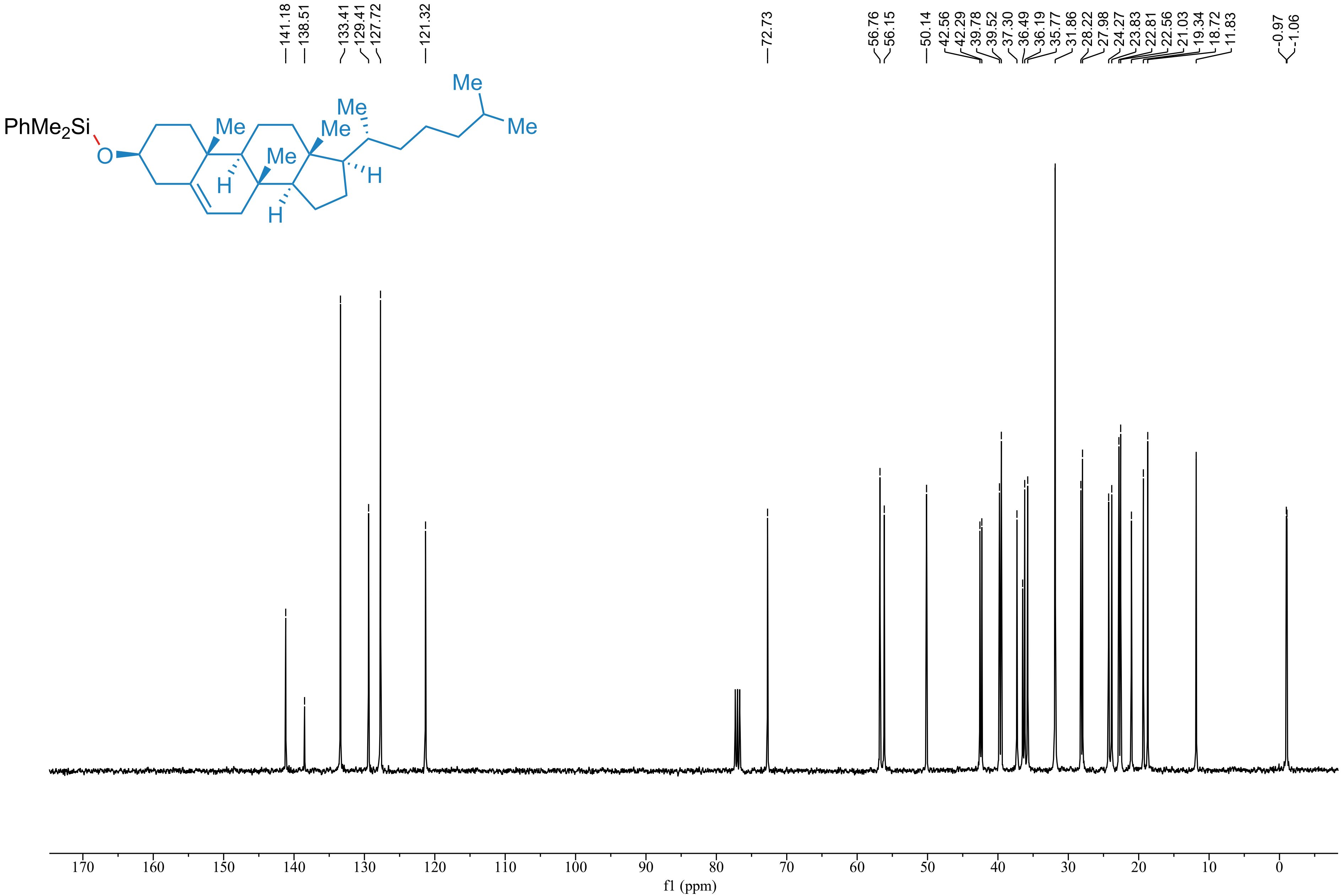

Compound **8** ^{1}H NMR

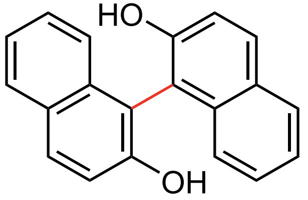

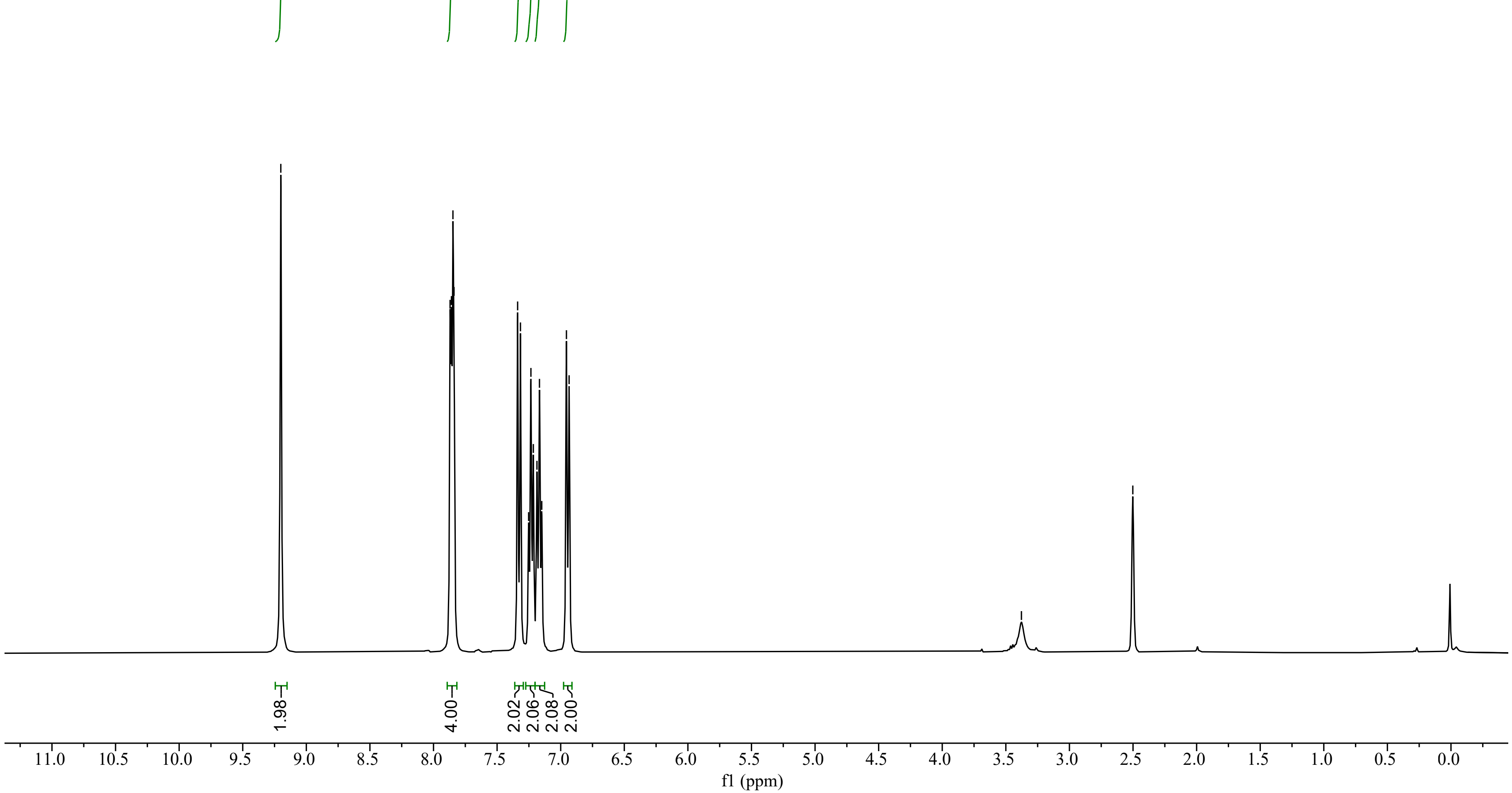

Compound **8** ^{13}C NMR

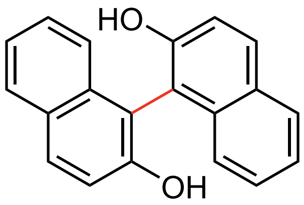

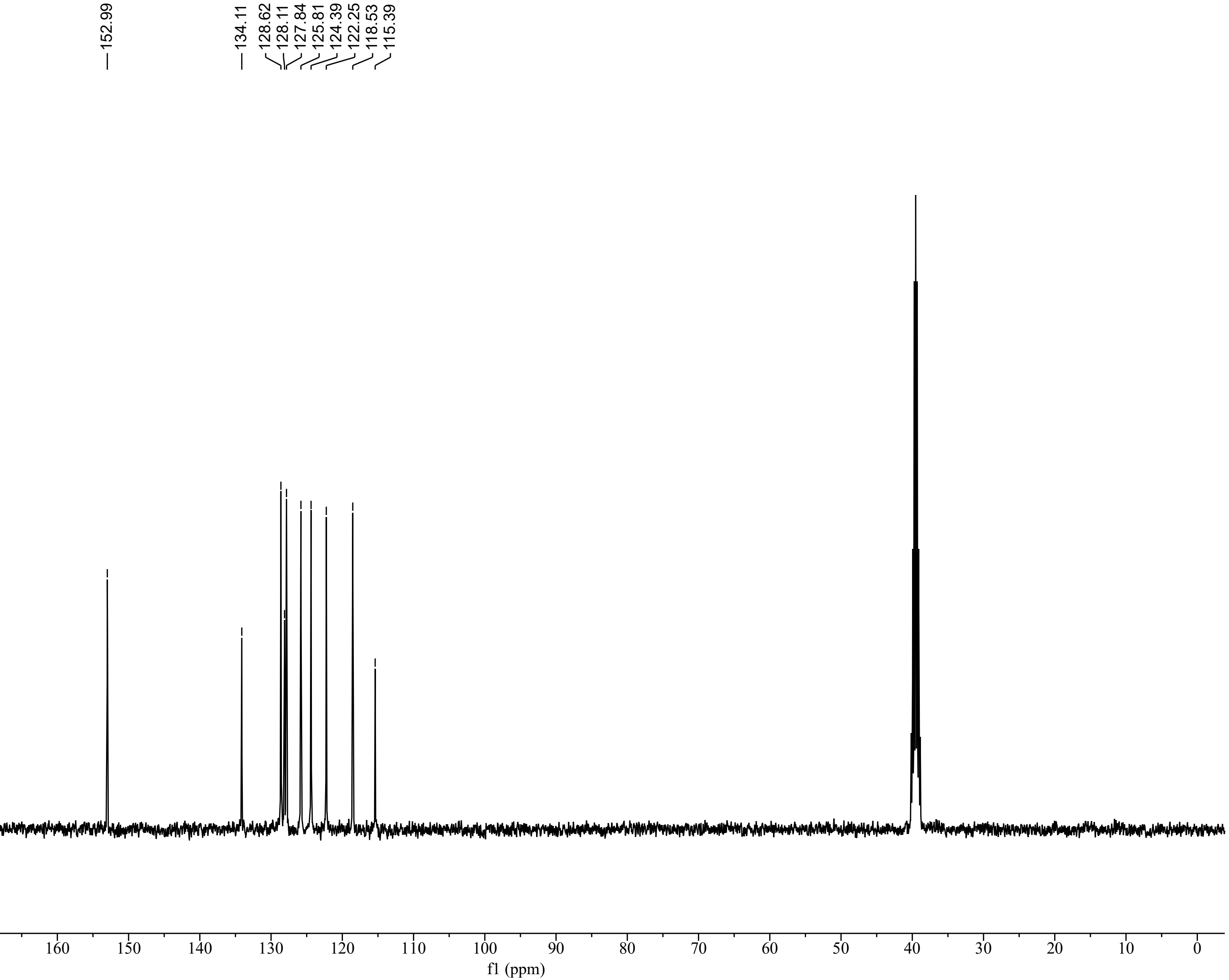

Compound **10** ^{1}H NMR

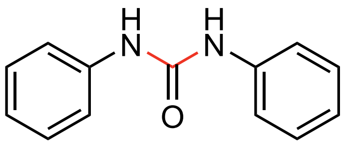

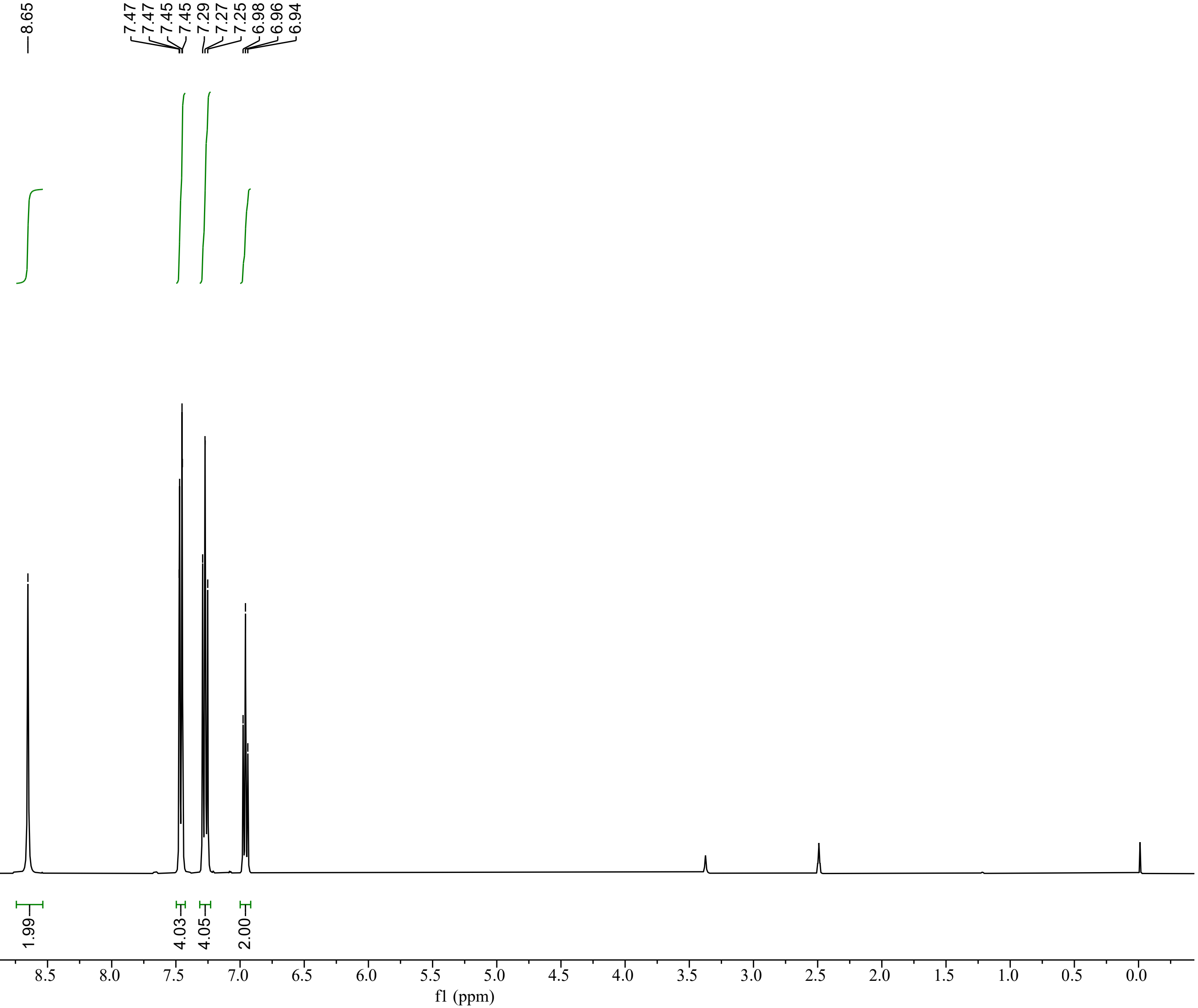

Compound **10** ^{13}C NMR

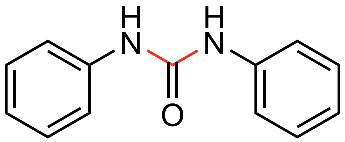

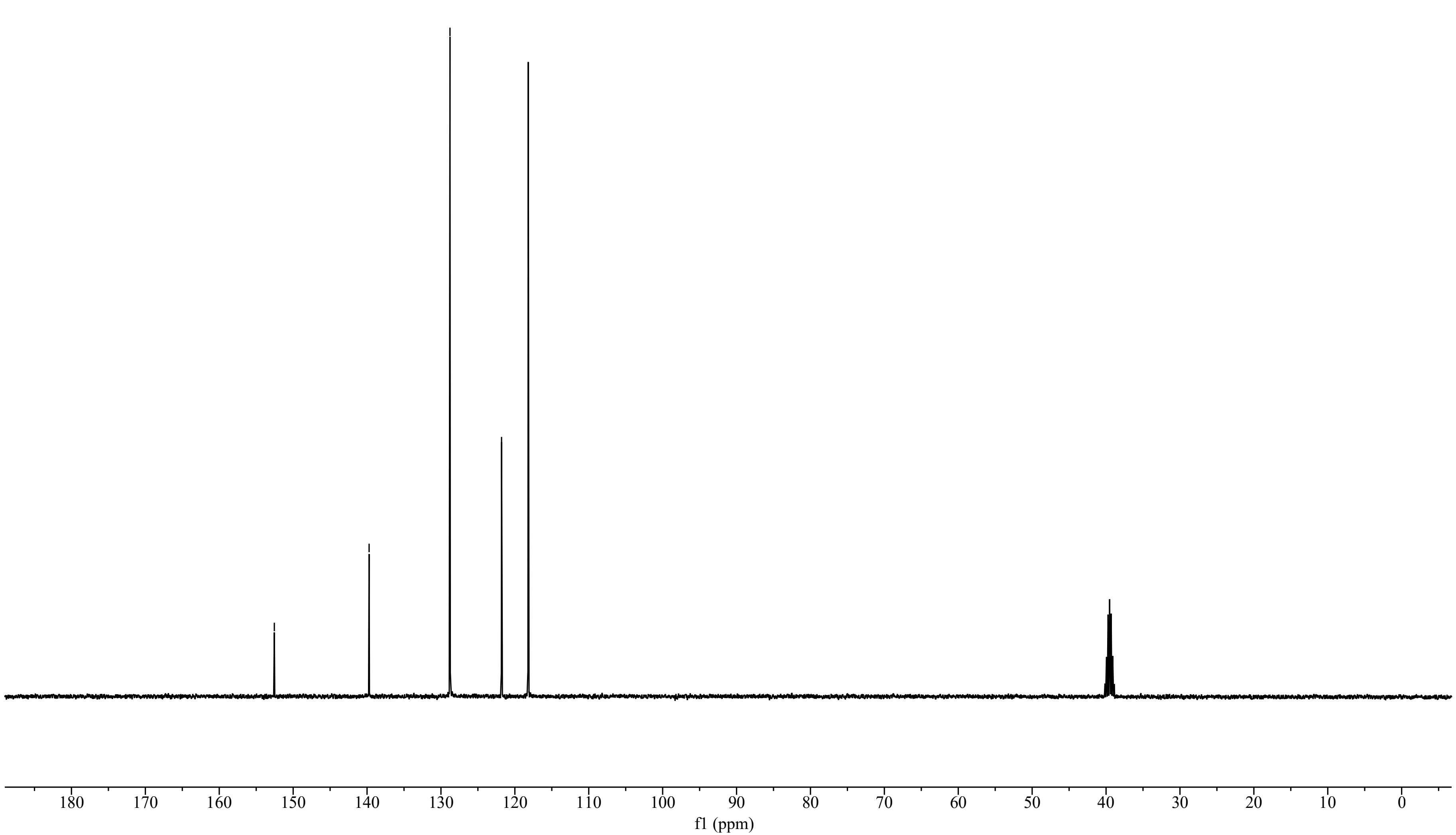

Compound **12** ^{1}H NMR

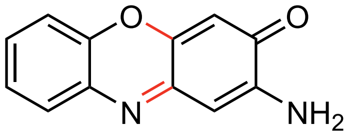

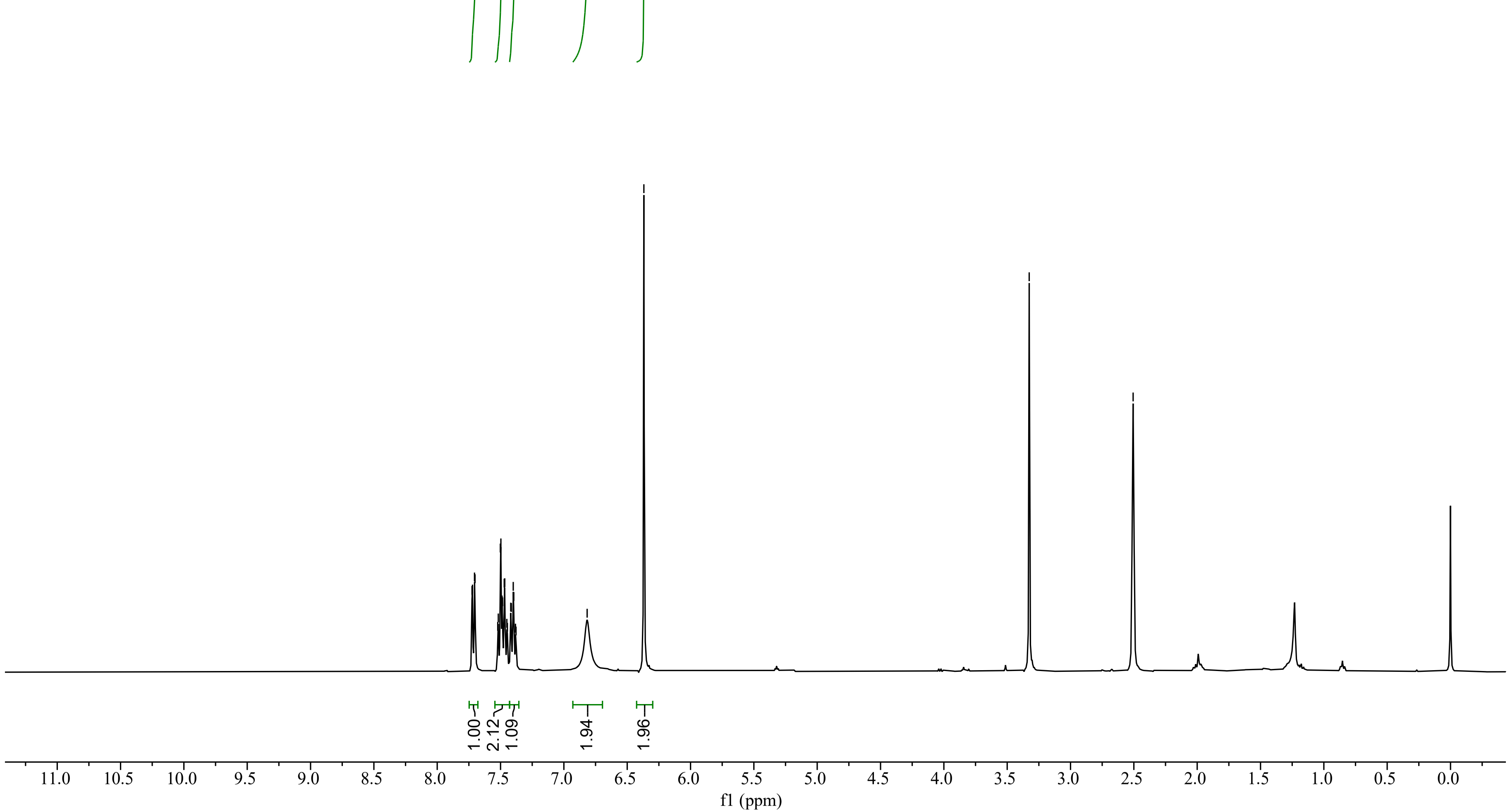

Compound **12** ^{13}C NMR

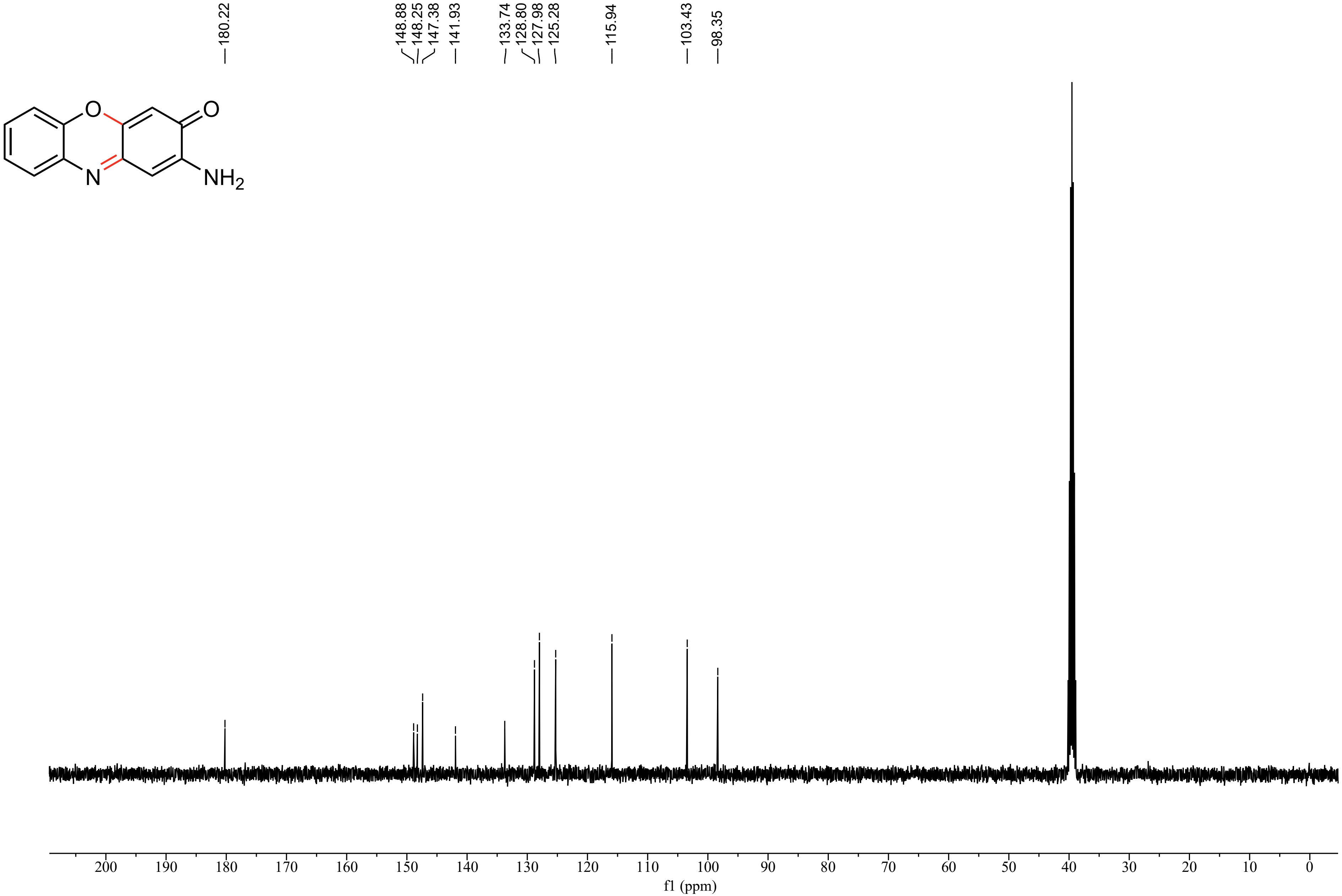

Geometries and Cartesian coordinates for optimized structures

CoN_4C_{10}

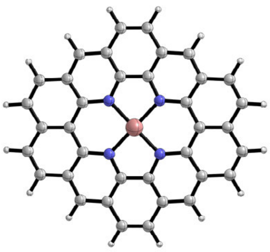

C	-1.41743346	-3.82388141	0.00127290
C	-0.72013507	-2.59846050	0.00227047
C	-2.66549138	-1.28399961	0.00441258
C	-3.44599112	-2.48950327	0.00436895
C	-2.80937259	-3.73449128	0.00249067
C	-3.33723943	0.00025896	0.00514144
C	-2.66528796	1.28441021	0.00347866
C	-0.71972332	2.59856066	0.00030994
C	-1.41682744	3.82409102	-0.00158598
C	-2.80878067	3.73492251	-0.00024603
C	-3.44559659	2.49003723	0.00257470
H	-3.41509270	-4.63846505	0.00218506
H	-3.41435744	4.63899185	-0.00120250
C	1.41681529	-3.82410608	0.00117415
C	0.71971127	-2.59857464	0.00221287
C	2.66527610	-1.28442211	0.00416795
C	3.44558470	-2.49004951	0.00409310
C	2.80876866	-3.73493661	0.00229091
C	3.33722781	-0.00027003	0.00478248
C	2.66547969	1.28398767	0.00314973
C	0.72012301	2.59844647	0.00021304
C	1.41742116	3.82386626	-0.00179276
C	2.80936042	3.73447713	-0.00065218
C	3.44597933	2.48949096	0.00210779
H	3.41434545	-4.63900638	0.00195476
H	3.41508028	4.63845050	-0.00170897
C	4.87497003	-2.42555444	0.00589697
H	5.43125218	-3.35926749	0.00612443
C	4.75034802	-0.00038139	0.00627911
C	4.87535445	2.42477077	0.00393757
H	5.43178459	3.35839551	0.00340777
C	5.50037729	1.22132114	0.00625461
H	6.58483248	1.15189256	0.00769951
C	-4.87536605	-2.42478168	0.00629852
H	-5.43179617	-3.35840655	0.00653469
C	-4.75035945	0.00037152	0.00679074
C	-4.87498171	2.42554361	0.00458750
H	-5.43126391	3.35925657	0.00416952
C	-5.50019502	1.22219295	0.00692244
H	-6.58466101	1.15293616	0.00849859
C	-5.50038871	-1.22133063	0.00776969
H	-6.58484374	-1.15190084	0.00927639
C	5.50018361	-1.22220242	0.00725163
H	6.58464977	-1.15294460	0.00865491
C	-0.67914746	-5.06512286	-0.00042204
C	0.67833242	-5.06523050	-0.00046531
H	1.24294520	-5.99359225	-0.00150151
C	-0.67834483	5.06521384	-0.00425322
C	0.67913505	5.06510618	-0.00435606
H	1.24389506	5.99337727	-0.00612382
H	-1.24295780	5.99357454	-0.00593582
H	-1.24390748	-5.99339509	-0.00142186
Co	-0.00000591	-0.00000608	0.00362087
N	1.31694761	-1.38944726	0.00344482
N	1.31716784	1.38922582	0.00236502
N	-1.31695956	1.38943466	0.00252705
N	-1.31717964	-1.38923849	0.00356650

CoPc

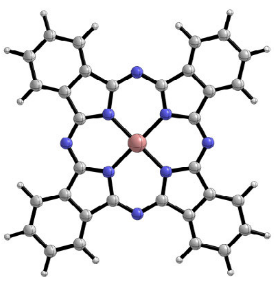

Co	0.00000000	0.00000000	-0.00013400
N	1.79560300	-0.71509500	-0.00321500
N	-0.71509100	-1.79560400	0.00296900
N	-1.79560300	0.71509500	-0.00322200
N	0.71509200	1.79560400	0.00296700
C	-0.00740900	2.96589300	0.02147500
C	3.06893600	5.81664200	0.09235800
C	1.77074400	6.33382500	0.10216300
C	-3.60391600	2.18916000	-0.04100900
C	-4.12269100	0.88670400	-0.05012700
C	-4.42371500	3.30415500	-0.06082100
C	-5.48475200	0.64157700	-0.08014600

C	-2.14912100	2.04292400	-0.01016200
C	-2.96589300	-0.00740700	-0.02163100
C	-2.04292000	-2.14911900	0.00995700
C	0.00741000	-2.96589400	0.02147700
C	2.14912100	-2.04292400	-0.01015100
C	2.04292100	2.14911900	0.00995300
C	2.96589300	0.00740700	-0.02163000
C	3.60391600	-2.18916100	-0.04099900
C	4.12269100	-0.88670400	-0.05012600
C	4.42371500	-3.30415500	-0.06081000
C	5.48475200	-0.64157700	-0.08015500
C	5.81666100	-3.06892700	-0.09205400
C	6.33384100	-1.77073200	-0.10177500
C	-0.88670400	-4.12268700	0.05012400
C	-2.18916000	-3.60390900	0.04093700
C	-0.64158500	-5.48474500	0.08038000
C	-3.30415800	-4.42369900	0.06088900
C	-1.77074500	-6.33382500	0.10215500
C	-3.06893700	-5.81664100	0.09235500
C	2.18916000	3.60391000	0.04093500
C	0.88670500	4.12268700	0.05012500
C	3.30415900	4.42370000	0.06088700
C	0.64158400	5.48474500	0.08038700

C	-5.81666100	3.06892700	-0.09205500
C	-6.33384100	1.77073300	-0.10176600
H	-5.88402800	-0.36685700	-0.08718900
H	-7.40804300	1.62529600	-0.12670300
H	-6.49670400	3.91343800	-0.10892000
H	-4.01983500	4.31072800	-0.05291700
H	-0.36684600	5.88402800	0.08752800
H	1.62531100	7.40802200	0.12730900
H	3.91345000	6.49667800	0.10934200
H	4.31072900	4.01981500	0.05291700
H	5.88402800	0.36685700	-0.08720600
H	7.40804200	-1.62529500	-0.12671900
H	6.49670400	-3.91343800	-0.10891900
H	4.01983500	-4.31072800	-0.05290000
H	0.36684600	-5.88402900	0.08751700
H	-1.62531200	-7.40802200	0.12729600
H	-3.91345100	-6.49667700	0.10933800
H	-4.31072900	-4.01981400	0.05292300
N	3.08919200	1.32985300	-0.00989800
N	-1.32985500	3.08919400	0.00972000
N	-3.08919100	-1.32985300	-0.00989200
N	1.32985500	-3.08919400	0.00972800

CoPc-16Cl

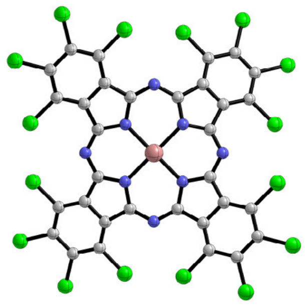

Co	-0.00000264	-0.00000335	0.14373554
N	-0.00845213	1.98236276	0.07754870
N	1.96860141	0.00836896	-0.03143203
N	0.00844950	-1.98236856	0.07753338
N	-1.96860858	-0.00837388	-0.03140425
C	-2.73275442	-1.12054916	0.20826450
C	-1.09387839	-2.74667343	-0.18432320
C	1.11718967	-2.73725106	-0.18461795
C	2.74222469	-1.09729180	0.20792466
C	2.73275072	1.12054295	0.20823662
C	1.09387034	2.74667200	-0.18431089
C	-2.74222737	1.09728439	0.20797351
C	-1.11719770	2.73724625	-0.18458236
C	0.68617254	4.07384270	-0.67208248
C	-0.72070531	4.06782437	-0.67231489
C	1.39776443	5.18715975	-1.07423581
C	-1.44166574	5.17499500	-1.07475030
C	0.66988798	6.32467344	-1.48045783
C	-0.72341812	6.31869190	-1.48074721
C	4.07007400	0.72096844	0.66924556
C	4.07611687	-0.68643774	0.66896014
C	5.18378037	1.44198651	1.05774424
C	5.19600436	-1.39801755	1.05709247
C	6.33027985	0.72416059	1.45050619
C	6.33629679	-0.67052701	1.45014445
C	-4.07611342	0.68642718	0.66902497

C	-6.33628185	0.67051116	1.45024282
C	-6.33026703	-0.72417617	1.45058842
C	-0.68618772	-4.07383906	-0.67211427
C	0.72069012	-4.06782424	-0.67235799
C	-1.39778569	-5.18715169	-1.07426933
C	1.44164454	-5.17499335	-1.07480850
C	-0.66991534	-6.32466448	-1.48050506
C	0.72339081	-6.31868576	-1.48080738
Cl	3.16258854	5.21406436	-1.09415443
Cl	1.54571766	7.77329240	-1.99869669
Cl	-1.61142678	7.75971564	-1.99942949
Cl	-3.20664930	5.18676793	-1.09534380
Cl	-5.22280166	3.16266596	1.07840173
Cl	-7.79069173	1.54492611	1.95379046
Cl	-7.77706328	-1.61083818	1.95464608
Cl	-5.19537833	-3.20681972	1.07984918
Cl	-3.16261001	-5.21405180	-1.09417322
Cl	-1.54575282	-7.77327825	-1.99874527
Cl	1.61139176	-7.75970742	-1.99950857
Cl	3.20662796	-5.18677022	-1.09541701
Cl	5.22281591	-3.16267899	1.07829338
Cl	7.79071626	-1.54494494	1.95365910
Cl	7.77708227	1.61081854	1.95455302
Cl	5.19538371	3.20680636	1.07981087
N	-2.34405902	-2.36610208	0.01017679
N	-2.36412967	2.34607367	0.00970734

C	-4.07007194	-0.72097890	0.66929571
C	-5.19599385	1.39800441	1.05718133
C	-5.18377353	-1.44199950	1.05780226
N	2.34405418	2.36609818	0.01016777
N	2.36412516	-2.34607959	0.00965504

Pyridinic N

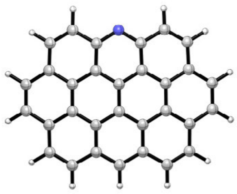

C	0.00000000	-3.60324703	-2.87676500
C	0.00000000	-3.66613767	-1.44049382
C	0.00000000	-2.45223136	-0.71573297
C	0.00000000	-1.21059742	-1.41358923
C	0.00000000	-1.16151668	-2.83816706
C	0.00000000	-2.41311963	-3.54737178
C	0.00000000	-2.45979895	0.70899464
C	0.00000000	0.00000000	-0.69646834
C	0.00000000	0.00000000	0.73418633
C	0.00000000	-1.22764742	1.43267436
C	0.00000000	1.22764742	1.43267436
C	0.00000000	2.45979895	0.70899464
C	0.00000000	2.45223136	-0.71573297
C	0.00000000	1.21059742	-1.41358923
C	0.00000000	1.16151668	-2.83816706
H	0.00000000	-4.54097389	-3.42918138
H	0.00000000	-2.38016495	-4.63462603
C	0.00000000	2.41311963	-3.54737178
C	0.00000000	3.60324703	-2.87676500
H	0.00000000	2.38016495	-4.63462603
H	0.00000000	4.54097389	-3.42918138
C	0.00000000	3.66613767	-1.44049382
C	0.00000000	4.88587446	-0.72019247
C	0.00000000	4.89734525	0.66135731
H	0.00000000	5.82173509	-1.27542221
H	0.00000000	5.84259015	1.20034703
C	0.00000000	3.69170212	1.40660761
C	0.00000000	3.66950525	2.84468229
H	0.00000000	4.62134205	3.37205198
C	0.00000000	2.49499753	3.53907199
H	0.00000000	2.49531321	4.62721916
C	0.00000000	1.22662671	2.85930234
C	0.00000000	0.00000000	3.54081675
H	0.00000000	0.00000000	4.63018958
C	0.00000000	-1.22662671	2.85930234
C	0.00000000	-2.49499753	3.53907199
H	0.00000000	-2.49531321	4.62721916
C	0.00000000	-3.66950525	2.84468229
C	0.00000000	-3.69170212	1.40660761
H	0.00000000	-4.62134205	3.37205198
C	0.00000000	-4.89734525	0.66135731
H	0.00000000	-5.84259015	1.20034703
C	0.00000000	-4.88587446	-0.72019247
H	0.00000000	-5.82173509	-1.27542221
N	0.00000000	0.00000000	-3.52483035

Pyrrolic N

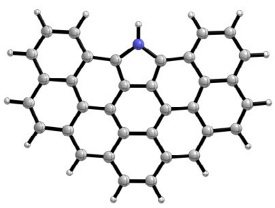

C	-2.65058216	-3.71418386	0.00000850
C	-1.21158151	-3.75892462	0.00000850
C	-0.52150653	-2.54802091	0.00000850
C	-1.29005112	-1.38278100	0.00000850
C	-2.66041411	-1.24564137	0.00000850
C	-3.42178534	-2.47914042	0.00000850
C	0.88288899	-2.43047320	0.00000850
C	-0.70311923	-0.12965379	0.00000850
C	0.68405282	0.02590506	0.00000850
C	1.49282454	-1.12823208	0.00000850
C	1.17251700	1.33123797	0.00000850
C	0.21691830	2.40806466	0.00000850
C	-1.22558020	2.20986097	0.00000850
C	-1.68575973	0.83529164	0.00000850
C	-2.05232639	3.34271243	0.00000850
C	-1.50829219	4.62848143	0.00000850
C	2.58993334	1.49758391	0.00000850
C	3.41699314	0.35435914	0.00000850
C	2.89867553	-0.96503135	0.00000850
H	4.49738993	0.49536598	0.00000850
C	3.67656348	-2.18777180	0.00000850
C	3.09484753	-3.42976275	0.00000850
H	4.76227327	-2.10721994	0.00000850
H	3.72802209	-4.31539492	0.00000850
C	1.65752093	-3.61495488	0.00000850
C	0.97575837	-4.85779205	0.00000850
C	-0.43196181	-4.95430455	0.00000850
H	1.55908890	-5.77804509	0.00000850
C	-4.82133577	-2.56925300	0.00000850
C	-5.46080622	-3.81032216	0.00000850
H	-5.40992452	-1.65382863	0.00000850
H	-6.54734091	-3.84926425	0.00000850

H	-3.13237994	3.20883631	0.00000850	C	-4.72818416	-4.99689991	0.00000850
H	-2.17396030	5.48810930	0.00000850	C	-3.32442051	-4.96723318	0.00000850
C	-0.12772509	4.82529686	0.00000850	H	-5.23838071	-5.95817807	0.00000850
C	0.74815405	3.72790530	0.00000850	C	-2.53598909	-6.18535134	0.00000850
H	0.28412738	5.83263680	0.00000850	C	-1.17310049	-6.19337972	0.00000850
C	2.18867949	3.90203860	0.00000850	H	-3.08324659	-7.12661459	0.00000850
C	3.06734914	2.86017995	0.00000850	H	-0.62748750	-7.13515031	0.00000850
H	2.56143021	4.92503624	0.00000850	N	-2.90586040	0.13803699	0.00000850
H	4.14012991	3.04393739	0.00000850	H	-3.82551711	0.56878005	0.00000850

Graphitic N

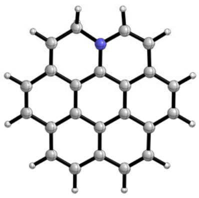

N	0.02242415	2.75754808	-0.03732670	H	-1.11316141	3.68858728	1.47319207
C	-2.42707198	2.80468260	-0.00563065	H	4.61743932	-1.28677745	-0.03805117
C	-2.45679028	1.44936053	-0.06696369	H	4.62010262	1.18850302	-0.19569244
C	-1.21330393	0.69113686	0.04251560	C	-3.68020055	0.67456643	-0.23083980
C	0.00073948	1.37278633	0.01188774	C	-3.67446225	-0.67908108	-0.17967129
C	-1.16773822	3.52318152	0.37965565	C	-2.44895863	-1.44278985	-0.03049346
C	-1.22303154	-0.73703128	0.04128456	H	-4.61373547	1.22167400	-0.35126709
C	1.24737815	0.66646705	-0.02721422	H	-4.60745355	-1.23464393	-0.26452128
C	1.23840097	-0.75536726	0.03930368	C	-2.43506636	-2.84939639	0.00226074
C	0.00016676	-1.46258134	0.07727770	C	-1.24725761	-3.56221910	0.08488550
C	2.46956210	-1.46563059	0.03968403	C	-0.00899422	-2.88664325	0.10703699
C	3.67735445	-0.73771071	-0.03792343	H	-3.38482785	-3.37996896	-0.04672415
C	3.68184194	0.64291960	-0.12509494	H	-1.25606314	-4.64993805	0.11029988
C	2.47159840	1.37051864	-0.12339405	C	2.43439679	-2.89803609	0.10365251
C	2.41387784	2.80597447	-0.21761732	H	3.38105168	-3.43523631	0.11622426
C	1.21430607	3.43703089	-0.15871335	C	1.25040408	-3.57698349	0.13694551
H	1.11746028	4.51818953	-0.19204103	H	1.23875861	-4.66480196	0.17481456
H	3.32768682	3.38291392	-0.32033411	H	-1.10315316	4.50888289	-0.09244792
H	-3.33655237	3.39151947	-0.11315890				

1a_CoPc_O_2

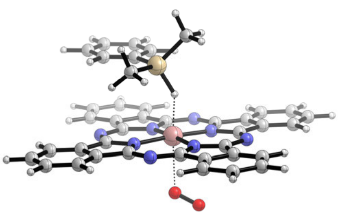

Co	0.44962190	0.04265487	-0.44750559	H	-3.07665696	-4.61262804	-1.27353141
N	-1.39433378	0.46438842	-0.83379503	C	-0.23094783	-6.48685235	-0.82587835
N	0.87155994	1.93031779	-0.39645475	H	1.77115343	-5.69930870	-0.44735252
N	2.32218919	-0.37614471	-0.19253280	H	-2.28472188	-6.99208093	-1.20614241
N	0.05326949	-1.83969232	-0.62111272	H	0.08579165	-7.52357209	-0.80263431
Si	-0.45778456	-0.47404903	2.66789078	C	4.31665612	-1.54574632	0.13087312
H	0.23525343	0.09906222	1.45848126	C	4.61010052	-0.17759375	0.22290164
C	0.94402256	-2.87865768	-0.50299015	C	5.29401782	-2.51548685	0.27553508
C	2.88011783	-1.63253581	-0.12540290	C	5.89371026	0.28148520	0.46394361
C	3.34165479	0.52026794	0.01980489	C	6.60891477	-2.06114997	0.52258921
C	2.10261095	2.49098743	-0.14671518	H	5.06506605	-3.57326686	0.20345666
C	-0.01904071	2.96993603	-0.51902714	C	6.90121897	-0.69758828	0.61448539

C	-1.95041838	1.71928026	-0.90498551	H	6.11874681	1.34018309	0.53462082
C	-1.18045382	-2.40182934	-0.86620166	H	7.40636067	-2.78601116	0.64285670
C	-2.41724114	-0.43225707	-1.03264455	H	7.92153120	-0.38347110	0.80447091
C	-3.38915120	1.63297541	-1.15166001	C	-0.04884522	-2.28548704	2.78843890
C	-3.68495265	0.26482365	-1.22637907	H	1.03573933	-2.44466559	2.71639237
C	-4.37246774	2.60148141	-1.25545657	H	-0.37982629	-2.67397922	3.76204611
C	-4.97760099	-0.19709455	-1.40743750	H	-0.53774940	-2.88452021	2.00917242
C	-5.69706219	2.14454507	-1.43897247	C	0.19568669	0.50941443	4.10639554
H	-4.14278721	3.65961185	-1.19072463	H	1.28426094	0.40154586	4.19875995
C	-5.99246247	0.78023041	-1.51297872	H	-0.03445850	1.57706366	3.99424293
H	-5.20477927	-1.25684927	-1.45412776	H	-0.26410624	0.15766984	5.04027906
H	-6.50053784	2.86813890	-1.52172066	C	-2.28247743	-0.18141029	2.41559003
H	-7.02068985	0.46478877	-1.65121022	C	-2.78249316	1.13900705	2.35719641
C	0.66025986	4.25383682	-0.35380535	C	-3.20160714	-1.24585436	2.30116721
C	2.00846458	3.94951566	-0.11647476	C	-4.15036653	1.38692523	2.19439756
C	0.20021419	5.55897408	-0.39326779	H	-2.09599704	1.98198283	2.44138577
C	2.95613965	4.93686366	0.09212431	C	-4.57169655	-1.00098478	2.14128419
C	1.15667300	6.57709439	-0.18113790	H	-2.84839503	-2.27472602	2.34221635
H	-0.84308174	5.79212040	-0.57676679	C	-5.04677671	0.31484548	2.08867019
C	2.50021131	6.27380155	0.05555063	H	-4.51574610	2.40886815	2.14852064
H	3.99852092	4.69944190	0.27543182	H	-5.26466392	-1.83326160	2.05954544
H	0.84055957	7.61404492	-0.20253810	H	-6.10860850	0.50560087	1.96308755
H	3.20821802	7.07958377	0.21427696	O	0.87513466	0.10043375	-2.99874159
C	-1.08495099	-3.85994594	-0.89416522	O	1.87846606	0.67659112	-3.33990935
C	0.26496944	-4.16283590	-0.66367226	N	2.24949480	-2.79304533	-0.26176949
C	-2.03321442	-4.84880264	-1.09452717	N	3.24839065	1.84670821	0.04653725
C	0.72636835	-5.46755105	-0.62397708	N	-1.32509243	2.88158258	-0.75048477
C	-1.57627415	-6.18521354	-1.05504932	N	-2.32777275	-1.76008839	-1.04746146

1a_CoPc-16Cl_O_2

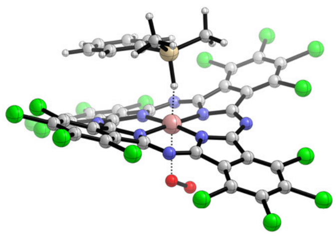

Co	-0.26186541	0.02549205	-0.29973551	H	-1.45929413	1.16607256	4.06426481
N	1.66237294	0.08374446	-0.51350209	H	0.07687706	1.21792669	4.95902431
N	-0.20471052	-1.90886150	-0.32788492	H	-0.13316302	2.20226055	3.49398672
N	-2.19735771	-0.03417979	-0.29423273	C	-0.26659681	-1.86811318	3.46675306
N	-0.32447315	1.95992886	-0.32004324	H	-1.36168034	-1.94846520	3.44841288
Si	0.27692350	-0.17482512	2.93127713	H	0.14653270	-2.64758664	2.81263968
H	-0.34638611	0.02962144	1.56543567	H	0.07306964	-2.07538964	4.49070886
C	-1.43908788	2.70951354	-0.08868871	C	2.11474613	-0.07254421	2.65252879
C	-3.02990650	1.04680961	-0.45696430	C	2.88159114	-1.23031217	2.40262142
C	-2.95801865	-1.16219391	-0.38780351	C	2.75520805	1.18245209	2.56243361
C	-1.26725357	-2.72358532	-0.02397955	C	4.23650456	-1.13832900	2.05529859
C	0.93342426	-2.65835861	-0.24024086	H	2.41334818	-2.21315301	2.45498698
C	2.46477308	-0.99548336	-0.79687705	C	4.10893071	1.27973164	2.21442997
C	0.77120530	2.77002407	-0.13520739	H	2.19092132	2.09571084	2.74926778
C	2.40761257	1.21165730	-0.69915879	C	4.84907933	0.11785650	1.95660629
C	3.77673614	-0.53783715	-1.27223181	H	4.80619773	-2.04173517	1.85225934
C	3.74489256	0.86545933	-1.20137636	H	4.57969527	2.25629827	2.13638127
C	4.91879550	-1.21209968	-1.65681729	H	5.89593962	0.19128391	1.67496010
C	4.85735874	1.62251372	-1.51346532	Cl	4.98808233	-2.97292608	-1.73409878
C	6.05719763	-0.44762924	-1.98400084	Cl	7.53820603	-1.27403646	-2.49112720
C	6.02693924	0.94335454	-1.91344470	Cl	7.47181822	1.87687288	-2.33179457
C	0.61797733	-4.00259556	0.26179943	Cl	4.85640660	3.38274534	-1.40683463
C	-0.78223423	-4.04637075	0.39343148	Cl	2.80679647	5.23573024	0.82757728

C	1.40605403	-5.07977645	0.61906033
C	-1.42191712	-5.17669034	0.86403178
C	0.76055544	-6.24059793	1.09354036
C	-0.62683332	-6.28828432	1.21230704
C	0.34356318	4.08739771	0.35122288
C	-1.06274029	4.05966848	0.35674356
C	1.04312314	5.20577142	0.76156044
C	-1.79685414	5.16429991	0.74609315
C	0.30225793	6.33749147	1.15829714
C	-1.09102631	6.31861823	1.14494728
C	-4.38400991	0.58922233	-0.79874332
C	-4.34042105	-0.81572256	-0.74789190
C	-5.54880719	1.25863903	-1.11983584
C	-5.46083789	-1.57752243	-1.01871507
C	-6.69742793	0.48930364	-1.39882677
C	-6.65452293	-0.90215853	-1.34766673
C	-0.36922981	1.23338503	3.95540391
Cl	1.16096053	7.79315617	1.68402237
Cl	-1.99419978	7.75675861	1.64454022
Cl	-3.56100343	5.16404231	0.76420501
Cl	-5.62490571	3.01932589	-1.20319171
Cl	-8.20546149	1.31118037	-1.82777256
Cl	-8.11056154	-1.84134874	-1.71016029
Cl	-5.43094242	-3.34103896	-0.97316974
Cl	-3.17459536	-5.25276616	1.05111124
Cl	-1.40851812	-7.75470798	1.82187610
Cl	1.73261102	-7.64647837	1.55289005
Cl	3.16743350	-5.02471622	0.52704899
O	-0.41468135	0.08158120	-2.99115704
O	-0.51917897	-0.96987181	-3.57230470
N	2.01760104	2.44551947	-0.40704041
N	-2.69056649	2.30653644	-0.26936175
N	-2.53954971	-2.39575413	-0.13982891
N	2.14686969	-2.25829389	-0.58807344

I

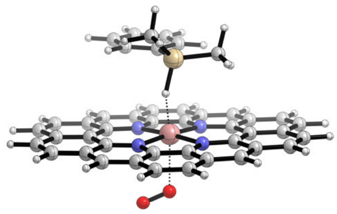

C	-0.11841285	-3.59075383	-1.32947617
C	0.06296837	-2.22449246	-1.02746905
C	-2.22152698	-1.81022969	-0.68568298
C	-2.48298104	-3.19719705	-0.94786624
C	-1.42922240	-4.06024408	-1.26794317
C	-3.32651350	-0.92005415	-0.39373636
C	-3.19948511	0.50346689	-0.15504013
C	-1.91623656	2.45972045	0.03417686
C	-3.02635077	3.29306651	0.28477682
C	-4.26924030	2.66218633	0.31818354
C	-4.37666417	1.28411878	0.10493146
H	-1.64658461	-5.10698184	-1.47139482
H	-5.17086130	3.23960826	0.51271642
C	2.49095938	-2.48424462	-1.34937700
C	1.38738348	-1.66269815	-1.03993668
C	2.67978809	0.27305361	-0.74364491
C	3.85560542	-0.50390230	-1.01906972
C	3.74009667	-1.86560594	-1.31806988
C	2.80942599	1.69129255	-0.47446432
C	1.70048842	2.59372267	-0.23649525
C	-0.59391028	3.02600333	0.00647249
C	-0.42017764	4.40792323	0.23073709
C	0.89567752	4.86910507	0.21308443
C	1.95878686	3.98838389	-0.01166296
H	4.64019256	-2.43898302	-1.53150286
H	1.10841210	5.92309290	0.38051160
C	5.14848458	0.10707146	-0.98929763
H	6.01573728	-0.51572643	-1.19273628
C	4.11230427	2.24001686	-0.46674414
C	3.30126054	4.48246845	-0.00695315
H	3.45734852	5.54274409	0.17380397
C	4.33740911	3.63425106	-0.22203573
H	5.36424303	3.98959810	-0.22197159
C	-3.81915015	-3.70460139	-0.88856520
H	-1.45929413	1.16607256	4.06426481
H	0.07687706	1.21792669	4.95902431
H	-0.13316302	2.20226055	3.49398672
C	-0.26659681	-1.86811318	3.46675306
H	-1.36168034	-1.94846520	3.44841288
H	0.14653270	-2.64758664	2.81263968
H	0.07306964	-2.07538964	4.49070886
C	2.11474613	-0.07254421	2.65252879
C	2.88159114	-1.23031217	2.40262142
C	2.75520805	1.18245209	2.56243361
C	4.23650456	-1.13832900	2.05529859
H	2.41334818	-2.21315301	2.45498698
C	4.10893071	1.27973164	2.21442997
H	2.19092132	2.09571084	2.74926778
C	4.84907933	0.11785650	1.95660629
H	4.80619773	-2.04173517	1.85225934
H	4.57969527	2.25629827	2.13638127
H	5.89593962	0.19128391	1.67496010
Cl	4.98808233	-2.97292608	-1.73409878
Cl	7.53820603	-1.27403646	-2.49112720
Cl	7.47181822	1.87687288	-2.33179457
Cl	4.85640660	3.38274534	-1.40683463
Cl	2.80679647	5.23573024	0.82757728
Cl	1.16096053	7.79315617	1.68402237
Cl	-1.99419978	7.75675861	1.64454022
Cl	-3.56100343	5.16404231	0.76420501
Cl	-5.62490571	3.01932589	-1.20319171
Cl	-8.20546149	1.31118037	-1.82777256
Cl	-8.11056154	-1.84134874	-1.71016029
Cl	-5.43094242	-3.34103896	-0.97316974
Cl	-3.17459536	-5.25276616	1.05111124
Cl	-1.40851812	-7.75470798	1.82187610
Cl	1.73261102	-7.64647837	1.55289005
Cl	3.16743350	-5.02471622	0.52704899

H	-3.97497014	-4.76209912	-1.08525229
C	-4.62389124	-1.47811936	-0.35061867
C	-5.66306613	0.65925988	0.14804923
H	-6.52939125	1.28161739	0.35636974
C	-5.77717105	-0.67439398	-0.06975646
H	-6.74488548	-1.16813736	-0.04376529
O	-0.41468135	0.08158120	-2.99115704
O	-0.51917897	-0.96987181	-3.57230470
N	2.01760104	2.44551947	-0.40704041
N	-2.69056649	2.30653644	-0.26936175
N	-2.53954971	-2.39575413	-0.13982891
N	2.14686969	-2.25829389	-0.58807344

TS(I-II)

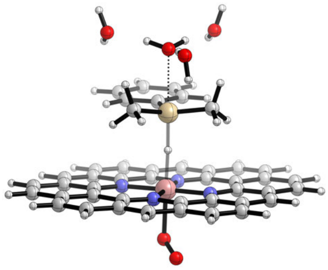

C	-2.51039597	-1.86136256	-2.40030057
C	-1.34582500	-1.22775346	-1.91639211
C	-2.41494392	0.81687107	-1.49528788
C	-3.64404302	0.23810876	-1.95994408
C	-3.66862717	-1.08731770	-2.40744835
C	-2.40240554	2.19317312	-1.04192894
C	-1.22676633	2.89633350	-0.56917091
C	1.05777205	2.97436243	-0.03931521
C	1.02125095	4.31645271	0.39669415
C	-0.21947730	4.94729413	0.32973121
C	-1.34451466	4.26208710	-0.14147197
H	-4.60775781	-1.51004541	-2.75904615
H	-0.32513681	5.98208168	0.64940633
C	-0.07909042	-3.31319086	-2.26496458
C	-0.11171717	-1.96457170	-1.84791416
C	2.15399779	-1.91002513	-1.24167700
C	2.26214794	-3.28831589	-1.62847984
C	1.14562329	-3.96324638	-2.13532366
C	3.32357940	-1.21766778	-0.73967559
C	3.34554299	0.17046230	-0.32510573
C	2.29172142	2.23712476	0.02935268
C	3.45465849	2.86741621	0.52234266
C	4.60223279	2.07899050	0.57353483
C	4.56944361	0.74261042	0.16147173
H	1.24605502	-5.00617320	-2.42929440
H	5.53768713	2.49651976	0.94056048
C	3.50936742	-3.97761020	-1.50658916
H	3.55032775	-5.02153460	-1.80601362
C	4.52851139	-1.94985063	-0.64388564
C	5.75895790	-0.04835065	0.23200959
H	6.66562635	0.42139331	0.60419892
C	5.73460777	-1.34723045	-0.15698169
H	6.62739844	-1.96500258	-0.10987828
C	-4.84986156	1.00676277	-1.96039757
H	-5.76048738	0.53168249	-2.31597312
C	-3.62494826	2.90217587	-1.06412955
C	-2.61007154	4.92719090	-0.18854001
H	-2.65936535	5.96136671	0.14178297
C	-3.70788855	4.26691978	-0.63339941
H	-4.67806611	4.75481375	-0.67583826
C	-4.83719744	2.29074896	-1.52318946
H	-5.74339132	2.89047720	-1.51355929
C	4.60035580	-3.32824911	-1.02944865
H	5.55673471	-3.83469754	-0.92924815
H	-1.22489061	-4.96882682	-3.09123517
C	2.22872486	4.94079806	0.88422786
C	3.39406233	4.24748953	0.94284096
H	4.30655635	4.70745611	1.31249543
H	2.17184845	5.97732444	1.20553340
H	-3.35793944	-3.69608783	-3.20734376
C	1.36364604	-1.09261589	2.54973876
H	2.08182494	-0.26805876	2.67427183
H	1.34636907	-1.68242339	3.47308789
H	1.74054895	-1.73051065	1.73655699
C	-0.93811547	1.21648859	2.70567637
H	-1.38304296	1.15468609	3.70519404
H	-0.12027520	1.95295220	2.72907192
H	-1.70143332	1.60131481	2.01329837
C	-1.57875153	-1.64883078	1.52296971
C	-1.20915806	-2.96578139	1.19235020
C	-2.92955104	-1.28039896	1.38946921
C	-2.16483395	-3.89511611	0.76869789
H	-0.16332118	-3.27241002	1.26840345
C	-3.88848337	-2.20627844	0.96581226
H	-3.24003477	-0.25939405	1.62008098
C	-3.50652440	-3.51625341	0.66065220
H	-1.86197610	-4.90945428	0.51755460
H	-4.92926534	-1.90424773	0.86937778
H	-4.25041667	-4.23751728	0.33063926
Co	0.46700411	0.50032985	-0.92062277
N	0.95262785	-1.29866380	-1.36100647
N	2.24408766	0.95306780	-0.37577524
N	-0.01343350	2.30386219	-0.50550421
N	-1.30152343	0.04978887	-1.49267485
H	0.12319304	0.10012209	0.66021752
Si	-0.29761284	-0.40895546	2.05340145
O	1.54929083	2.09196818	-3.05737481
O	0.91324863	1.04998743	-2.90886286
O	-0.97731302	-1.24501958	4.43474888
H	-1.94185591	-1.08422466	4.53878996
H	-0.84134199	-2.21895187	4.44409115
H	0.24300960	-0.10231792	5.24326767
O	-3.70617535	-0.72392127	4.52249061
O	-0.54752796	-3.98175028	4.23066259
O	0.90076807	0.53534012	5.58938610
H	-4.18164308	-1.18884132	3.81439251
H	-4.23599672	-0.82455744	5.32945822
H	-1.05398900	-4.35326200	3.48936069

C	-2.44603819	-3.23697661	-2.83483504
C	-1.28173082	-3.93175554	-2.77149314
H	-0.65818605	-4.58930442	4.97931778
H	1.21231466	1.03929005	4.82310503

II

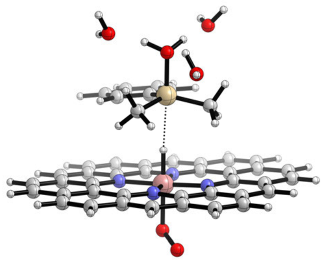

C	-1.94725983	-3.03797042	-1.89107826
C	-1.03080859	-2.00173037	-1.59943202
C	-2.68502404	-0.36152918	-1.37132979
C	-3.67855583	-1.36384263	-1.63543416
C	-3.29161040	-2.68317306	-1.89748611
C	-3.10139114	1.00489369	-1.13453265
C	-2.19498166	2.10817005	-0.89462953
C	-0.04130306	2.98431070	-0.62899867
C	-0.49039452	4.30866197	-0.42042796
C	-1.86639344	4.50127931	-0.45322672
C	-2.72952314	3.42324380	-0.68482686
H	-4.05671691	-3.42915128	-2.10296320
H	-2.28646755	5.49266206	-0.29589500
C	0.82557613	-3.61317109	-1.76341378
C	0.37498782	-2.29197726	-1.53905826
C	2.51908261	-1.43713088	-1.15214333
C	3.05107493	-2.75765814	-1.33851665
C	2.19446967	-3.82222562	-1.64320225
C	3.42413970	-0.34092815	-0.87744720
C	3.01122532	1.03384169	-0.68839771
C	1.36505510	2.69270002	-0.56693370
C	2.28422504	3.73544989	-0.30770692
C	3.62340663	3.36974593	-0.24214074
C	4.00519464	2.03577469	-0.42962831
H	2.61389177	-4.81568234	-1.78901199
H	4.38872869	4.11745639	-0.04415310
C	4.45701514	-2.99381154	-1.23036355
H	4.81910276	-4.00864767	-1.37290869
C	4.80460523	-0.63255455	-0.79048372
C	5.38831164	1.68246426	-0.35790166
H	6.10934444	2.47209235	-0.16323971
C	5.77045279	0.39233766	-0.53005751
H	6.81701106	0.10391257	-0.47814908
C	-5.06706219	-1.02327096	-1.63840542
H	-5.78741164	-1.81239917	-1.83761121
C	-4.48760982	1.28269242	-1.15111024
C	-4.14184002	3.64295891	-0.70720721
H	-4.50641326	4.65366881	-0.54291760
C	-4.98793757	2.60626893	-0.93024757
H	-6.06460809	2.75401442	-0.95220976
C	-5.45398827	0.25430028	-1.39802332
H	-6.50450977	0.53269560	-1.39502495
C	5.30018637	-1.96531072	-0.96399681
H	6.37239263	-2.12434627	-0.88192857
C	-1.45782979	-4.37389577	-2.13792685
C	-0.13090676	-4.64939276	-2.07480304
H	0.24663306	-5.65336897	-2.25010425
C	0.47246689	5.35802084	-0.17622436
C	1.79937590	5.08399970	-0.12235571
H	2.53055379	5.86570514	0.06552592
H	0.09774184	6.36793515	-0.03179319
H	-2.18558921	-5.14814681	-2.36596378
C	1.74038870	0.21439803	2.50266672
H	1.93688690	1.25390805	2.20827930
H	2.28899854	0.01872385	3.43402466
H	2.13782925	-0.44780442	1.72227408
C	-1.27371536	1.35466551	2.46292260
H	-1.75791041	1.64935113	3.40306792
H	-0.74041036	2.23280957	2.07601924
H	-2.05316911	1.07406428	1.74253704
C	-0.70239248	-1.69486325	2.14069524
C	0.18519976	-2.75771063	1.88528553
C	-2.08432332	-1.92904400	1.99666213
C	-0.29200594	-4.01725030	1.51056419
H	1.26229613	-2.60384768	1.97502804
C	-2.56398088	-3.18629942	1.62067460
H	-2.79653593	-1.12231141	2.17719934
C	-1.66676899	-4.23168996	1.37972718
H	0.40827832	-4.82629948	1.31397228
H	-3.63399071	-3.34954580	1.51236614
H	-2.03805671	-5.20972433	1.08244602
Co	0.16669815	0.35188790	-1.08122335
N	1.18079192	-1.25612626	-1.24637975
N	1.71157412	1.40614652	-0.73938916
N	-0.85374449	1.93797005	-0.85104428
N	-1.38215404	-0.72623134	-1.35704844
H	0.04626709	0.10958954	0.34506548
O	0.58291858	1.85892554	-3.39879121
O	0.31453293	0.63725623	-3.03655867
Si	-0.08317696	-0.04296534	2.73922694
O	-0.19456117	-0.27763889	4.52773931
H	-1.15213053	-0.36004420	4.87757030
H	0.37828026	-1.05701877	4.85441823
H	0.78078063	1.80496057	5.28981614
O	-2.65386713	-0.46464247	5.18381662
O	1.32277121	-2.26309648	5.05453952
O	0.77484513	2.50060198	4.61484615
H	-3.06740834	-1.34498867	5.16591158
H	-3.02228909	0.01648020	5.94459720
H	1.03100726	-3.12836273	4.71936416
H	1.77960713	-2.41106237	5.90001154
H	1.42460652	3.16024872	4.90137151

III

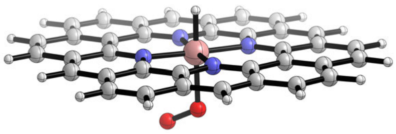

C	-1.39548453	-3.81688216	-0.10459466
C	-0.69472709	-2.59000577	-0.12829343
C	-2.63167658	-1.27726317	-0.16998673
C	-3.41493021	-2.48103318	-0.15996155
C	-2.78340578	-3.72909554	-0.12501290
C	-3.30358529	0.00577918	-0.18545123
C	-2.62843604	1.28705970	-0.16559126
C	-0.68818613	2.59476365	-0.11938387
C	-1.38584678	3.82331402	-0.09144007
C	-2.77398457	3.73909781	-0.11216404
C	-3.40865221	2.49275969	-0.15141709
C	1.43927500	-3.82025995	-0.09054170
C	0.74163672	-2.59150692	-0.11765525
C	2.68294559	-1.28400648	-0.13735501
C	3.46279444	-2.48969332	-0.12372503
C	2.82735278	-3.73620933	-0.09729669
C	3.35855140	-0.00269200	-0.14465893
C	2.68618086	1.28029040	-0.13292436
C	0.74817683	2.59260807	-0.10872728
C	1.44891151	3.81949579	-0.07734739
C	2.83677339	3.73196768	-0.08437240
C	3.46906882	2.48395157	-0.11511231
C	4.89123112	-2.42803383	-0.13590958
C	4.77168668	-0.00446143	-0.15232485
C	4.89734577	2.41873019	-0.12750078
C	5.52242134	1.21556944	-0.14955323
C	-4.84326531	-2.41584331	-0.18658532
C	-4.71591920	0.00759909	-0.20749193
C	-4.83714776	2.43126763	-0.17825848
C	-1.39548453	-3.81688216	-0.10459466
C	-5.46423541	1.22961642	-0.21008119
C	-5.46731674	-1.21250975	-0.21427318
C	5.51934054	-1.22638473	-0.15379347
C	-0.65786262	-5.05821591	-0.06769496
C	0.69858314	-5.05992200	-0.06181267
C	-0.64509810	5.06264877	-0.05023596
C	0.71134759	5.06091467	-0.04433236
H	3.44466868	4.63425382	-0.06721593
H	-3.39149779	-4.63136594	-0.11481016
H	-3.37980047	4.64285749	-0.09884450
H	3.43297021	-4.64008010	-0.08328027
H	5.44515559	-3.36320891	-0.12972907
H	5.45362832	3.35247737	-0.11807317
H	6.60692988	1.14559034	-0.15916737
H	-5.39978633	-3.34951151	-0.18329908
H	-5.39130956	3.36632127	-0.17175763
H	-6.54877705	1.16183846	-0.23069108
H	-6.55168381	-1.14192399	-0.23464466
H	6.60402214	-1.15910947	-0.16317723
H	1.26255808	-5.98849309	-0.03680458
H	1.27766133	5.98796862	-0.01609885
H	-1.20906178	5.99128147	-0.02667230
H	-1.22416559	-5.98549985	-0.04733986
Co	0.02092598	0.00148058	-0.12167586
N	1.33387294	-1.38421899	-0.14041780
N	1.33736625	1.38391673	-0.13565712
N	-1.28067129	1.38855887	-0.15884844
N	-1.28416962	-1.38218061	-0.16358600
O	0.04467241	-0.00199759	1.86068848
O	-1.13770327	-0.00074806	2.41998154

TS(III-IV)

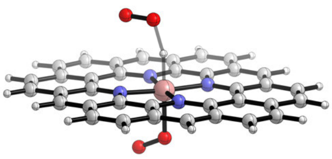

C	-1.46993200	-3.82436558	-0.02091936
C	-0.77830060	-2.59258472	-0.02521690
C	-2.72626754	-1.29364771	-0.05557761
C	-3.50064443	-2.50289703	-0.06260854
C	-2.85915469	-3.74622232	-0.04163563
C	-3.40706805	-0.01475371	-0.06344630
C	-2.74119789	1.27155533	-0.02952906
C	-0.80847998	2.59220127	0.02739447
C	-1.51440610	3.81550566	0.05660097
C	-2.90262732	3.72162830	0.03416546
C	-3.52960159	2.47160094	-0.01209310
H	-3.46031734	-4.65320762	-0.04513388
H	-3.51430996	4.62143685	0.04900479
C	1.36467636	-3.80771320	-0.01695450
C	0.65898854	-2.58423037	-0.02125275
C	2.59137185	-1.26236740	-0.05082774
C	3.37983994	-2.46268678	-0.05776054
C	5.41206114	1.25852455	-0.08912094
H	6.49673432	1.19578462	-0.11755170
C	-4.92929672	-2.44729052	-0.09441589
H	-5.47933987	-3.38472559	-0.10463107
C	-4.82009692	-0.02271396	-0.08956029
C	-4.95751385	2.40002500	-0.04517294
H	-5.51843299	3.33100792	-0.03640857
C	-5.57644209	1.19413844	-0.08672248
H	-6.66035013	1.11934347	-0.11271876
C	-5.56222537	-1.24809513	-0.11154441
H	-6.64693347	-1.18540994	-0.13615667
C	5.42627724	-1.18448135	-0.11389189
H	6.51014344	-1.10856047	-0.14091434
C	-0.72389872	-5.06092245	-0.00565004
C	0.63285834	-5.05285037	-0.00443662
H	1.20323781	-5.97783344	0.00241374
C	-0.78282108	5.06010295	0.09700779

C	2.75323520	-3.71312675	-0.03568496
C	3.25749321	0.02405744	-0.06347936
C	2.57646065	1.30212080	-0.02481651
C	0.62881159	2.60050799	0.03134444
C	1.32020597	3.83178898	0.06051359
C	2.70977117	3.75378197	0.04001905
C	3.35089658	2.51143020	-0.00732846
H	3.36486898	-4.61310945	-0.03818239
H	3.31087745	4.66069556	0.05583093
C	4.80817313	-2.39088950	-0.09237402
H	5.36892898	-3.32199667	-0.10137689
C	4.66908663	0.03256027	-0.09208140
C	4.77996426	2.45697641	-0.04322553
H	5.32984782	3.39453594	-0.03328528

C	0.57393810	5.06780905	0.09819269
H	1.13350721	5.99904356	0.12384606
H	-1.35319111	5.98477075	0.12159256
H	-1.28345871	-5.99247830	0.00011027
Co	-0.07081068	0.00495472	-0.09191043
N	1.24379302	-1.37213317	-0.03010224
N	1.22769128	1.39573317	-0.00201145
N	-1.39279854	1.38031415	-0.01068901
N	-1.37669197	-1.38706113	-0.03878353
H	-0.03191442	-0.01049891	1.44255368
O	0.43161974	-0.02133729	2.84580514
O	1.67363250	-0.01414419	2.88670007
O	-0.11353130	0.02489662	-2.08592646
O	1.05777670	0.03745765	-2.64117476

IV

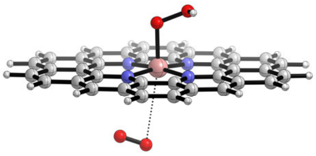

C	-1.41852723	-3.82607691	-0.01358450
C	-0.72289446	-2.59620475	-0.00386824
C	-2.66740150	-1.29200750	-0.02890420
C	-3.44681456	-2.49765817	-0.04156203
C	-2.80796584	-3.74333784	-0.03255662
C	-3.34283456	-0.00776087	-0.03738420
C	-2.67423094	1.27974207	-0.03420885
C	-0.73313163	2.59252717	-0.01070303
C	-1.43373419	3.81931971	-0.03294855
C	-2.82305498	3.73078720	-0.05482210
C	-3.45782842	2.48296554	-0.05664153
H	-3.41171022	-4.64874964	-0.03989257
H	-3.43002456	4.63393763	-0.07017412
C	1.41862966	-3.82025528	0.03630185
C	0.71746307	-2.59338107	0.02431510
C	2.65714988	-1.28165575	0.08033265
C	3.44156529	-2.48415940	0.09220872
C	2.80742726	-3.73215600	0.06957730
C	3.32628924	0.00590838	0.10290591
C	2.65185936	1.29066893	0.07823146
C	0.70709235	2.59466264	0.01875594
C	1.40332512	3.82428779	0.02201696
C	2.79258265	3.74181390	0.05582955
C	3.43147190	2.49653870	0.08448266
H	3.41459444	-4.63521801	0.08045774
H	3.39622362	4.64727091	0.06136856
C	4.86943057	-2.41628111	0.13292673
H	5.42850627	-3.34847657	0.14447347
C	4.73933058	0.00887154	0.13902936
C	4.85967903	2.43465225	0.12487033
H	5.41493549	3.36915983	0.13261249

C	5.48629825	1.23202606	0.15340287
H	6.57067813	1.16466706	0.18452871
C	-4.87582592	-2.43597641	-0.05993806
H	-5.43100483	-3.37057253	-0.06524928
C	-4.75548570	-0.01039244	-0.06142257
C	-4.88640526	2.41525348	-0.07724562
H	-5.44564010	3.34732212	-0.09041419
C	-5.50790879	1.20977679	-0.07802961
H	-6.59237118	1.13755350	-0.09290708
C	-5.50302324	-1.23354469	-0.06908081
H	-6.58778098	-1.16612499	-0.08341618
C	5.49131563	-1.21101750	0.15711230
H	6.57542125	-1.13917288	0.18809234
C	-0.67552034	-5.06551701	-0.00262257
C	0.68109100	-5.06287260	0.02052525
H	1.24707049	-5.99067350	0.02979576
C	-0.69552082	5.06155929	-0.03002580
C	0.66110307	5.06387844	-0.00390822
H	1.22364715	5.99379986	-0.00092107
H	-1.26091608	5.98958545	-0.04820099
H	-1.23757202	-5.99572983	-0.01209626
Co	-0.01348713	-0.00168532	0.13560172
N	1.30906265	-1.38496468	0.04270813
N	1.30320139	1.38824130	0.04349036
N	-1.32586633	1.38399208	-0.01032393
N	-1.31970118	-1.39069557	-0.01201432
O	-0.00253032	-0.00815811	2.15166170
O	-1.36396520	-0.05867954	2.64303130
H	-1.58915247	0.88251562	2.73271734
O	0.58506007	-0.00501753	-3.35875456
O	1.72388411	-0.00230928	-2.96150791

V

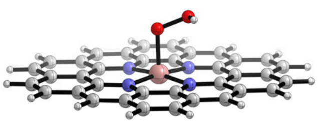

C	1.37699425	3.82541754	-0.16337556
C	0.67962757	2.59639631	-0.17054074

H	-5.46620518	-3.36118235	-0.07506432
C	-5.53533695	-1.22396914	-0.07176750

C	2.62257411	1.28982300	-0.17975145	H	-6.61989196	-1.15525785	-0.05144631
C	3.40364494	2.49445543	-0.17900806	C	4.83265367	2.43096108	-0.18285026
C	2.76639492	3.74092711	-0.16991942	H	5.38906369	3.36484055	-0.18068640
C	3.29655382	0.00471752	-0.18029686	C	4.70934511	0.00559421	-0.18685691
C	2.62634836	-1.28200568	-0.17957690	C	4.83749323	-2.42018832	-0.19013460
C	0.68358942	-2.59237316	-0.16538757	H	5.39576978	-3.35292325	-0.19197030
C	1.38307992	-3.82012430	-0.16538625	C	5.46041194	-1.21546171	-0.19106632
C	2.77259330	-3.73327025	-0.17583038	H	6.54506379	-1.14455662	-0.19460280
C	3.40874317	-2.48619455	-0.18355252	C	5.45842346	1.22777715	-0.18708664
H	3.37136042	4.64554588	-0.16662230	H	6.54319427	1.15900733	-0.18970203
H	3.37865188	-4.63715979	-0.17659375	C	-5.53742481	1.21896459	-0.07475687
C	-1.46036836	3.82302981	-0.14145768	H	-6.62187612	1.14851993	-0.05434753
C	-0.76093207	2.59532938	-0.15751924	C	0.63560168	5.06579618	-0.14934244
C	-2.70266894	1.28578807	-0.12728389	C	-0.72117666	5.06476474	-0.13953568
C	-3.48546260	2.48946853	-0.11589391	H	-1.28605564	5.99321183	-0.12783725
C	-2.84952673	3.73665361	-0.12355688	C	0.64353923	-5.06152849	-0.15306504
C	-3.37380844	-0.00061748	-0.10990148	C	-0.71327780	-5.06204012	-0.13937242
C	-2.70049758	-1.28593191	-0.12270183	H	-1.27692927	-5.99124288	-0.12908542
C	-0.75685509	-2.59263195	-0.15052651	H	1.20804763	-5.99026722	-0.15398053
C	-1.45424046	-3.82141572	-0.13677132	H	1.19895509	5.99526125	-0.14570028
C	-2.84364584	-3.73716184	-0.11806698	Co	-0.03499933	0.00313444	-0.05507391
C	-3.48135749	-2.49105985	-0.11048885	N	-1.35433966	1.38756212	-0.15408993
H	-3.45554430	4.64048154	-0.11218877	N	-1.35188129	-1.38534130	-0.14643463
H	-3.44828459	-4.64190478	-0.10721003	N	1.27767894	-1.38458922	-0.17227871
C	-4.91375719	2.42338390	-0.09012088	N	1.27492059	1.39022499	-0.18030009
H	-5.47172147	3.35626593	-0.08137357	O	-0.06660345	0.01495888	1.96429358
C	-4.78677815	-0.00180567	-0.08510438	O	1.28890957	0.06476792	2.47258901
C	-4.90982847	-2.42737354	-0.08507688	H	1.51192810	-0.87654183	2.56612340

VI

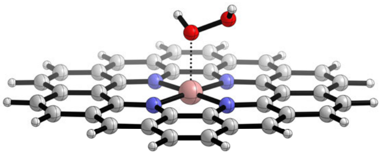

C	1.36669590	3.81378138	-0.16088701	C	-5.54557256	-1.23924154	-0.09763885
C	0.67083147	2.58657326	-0.15774484	H	-6.63000640	-1.17096458	-0.08111605
C	2.61618889	1.27571575	-0.17909810	C	4.82522426	2.41870081	-0.19056826
C	3.39576307	2.48175358	-0.18086085	H	5.38072086	3.35292568	-0.19093346
C	2.75817257	3.72660969	-0.17230025	C	4.70236013	-0.00667392	-0.19752146
C	3.28962499	-0.00812119	-0.18833322	C	4.83047560	-2.43193052	-0.20842954
C	2.61922093	-1.29357120	-0.19258392	H	5.38807086	-3.36488550	-0.21469258
C	0.67569423	-2.60825916	-0.18911783	C	5.45387206	-1.22769170	-0.20612530
C	1.37422154	-3.83404817	-0.19793959	H	6.53828935	-1.15689269	-0.21086719
C	2.76559739	-3.74414482	-0.20457957	C	5.45132875	1.21593479	-0.19749258
C	3.40116022	-2.49811727	-0.20213889	H	6.53588355	1.14752243	-0.20390066
H	3.36296327	4.63123546	-0.17407442	C	-5.54795892	1.20434200	-0.08300612
H	3.37200820	-4.64768131	-0.21114540	H	-6.63226307	1.13371540	-0.06755145
C	-1.46836014	3.81105141	-0.13438454	C	0.62640908	5.05408445	-0.15354114
C	-0.76951534	2.58576081	-0.14115494	C	-0.73090691	5.05295485	-0.14161511
C	-2.71365124	1.27029105	-0.12043158	H	-1.29635179	5.98083081	-0.13635421
C	-3.49539213	2.47485478	-0.11044298	C	0.63642035	-5.07588591	-0.19892427
C	-2.85967833	3.72075251	-0.11800404	C	-0.72087571	-5.07727747	-0.18866132
C	-3.38399544	-0.01524330	-0.11815674	H	-1.28451392	-6.00628422	-0.18856659
C	-2.71073491	-1.29945089	-0.14070828	H	1.20184343	-6.00377983	-0.20708194
C	-0.76478017	-2.60987125	-0.17654121	H	1.19002008	5.98310567	-0.15780559
C	-1.46090295	-3.83690108	-0.17577466	Co	-0.04489960	-0.01274742	-0.13026946
C	-2.85233455	-3.74996040	-0.15881859	N	-1.36513316	1.37610123	-0.13148024
C	-3.49039583	-2.50541039	-0.14041834	N	-1.36279128	-1.40226879	-0.16125396
H	-3.46619199	4.62418779	-0.11052089	N	1.27146469	-1.39942589	-0.18578311
H	-3.45694158	-4.65470016	-0.15778419	N	1.26842347	1.37861634	-0.16581216

C	-4.92445543	2.40861572	-0.09093148
H	-5.48194802	3.34158816	-0.08239952
C	-4.79687519	-0.01666950	-0.09866265
C	-4.91958706	-2.44206653	-0.11838265
H	-5.47526639	-3.37617057	-0.11863049
O	0.00029367	-0.11755008	2.13708921
O	1.34155690	0.07441721	2.57675740
H	1.47523850	-0.69978120	3.15871261
H	-0.48745126	0.59504437	2.59888465

Supplementary References

1. Achar, B. N., Fohlen, G. M., Parker, J. A. & Keshavayya, J. Synthesis and structural studies of metal(II) 4,9,16,23-phthalocyanine tetraamines. *Polyhedron* **6,** 1463–1467; 10.1016/S0277-5387(00)80910-9 (1987).
2. Alves, M. C. M., Dodelet, J. P., Guay, D., Ladouceur, M. & Tourillon, G. Origin of the electrocatalytic properties for oxygen reduction of some heat-treated polyacrylonitrile and phthalocyanine cobalt compounds adsorbed on carbon black as probed by electrochemistry and x-ray absorption spectroscopy. *J. Phys. Chem.* **96,** 10898–10905; 10.1021/j100205a054 (1992).
3. Chang, Q. *et al.* Determination of hydrogen peroxide with the aid of peroxidase-like Fe_3O_4 magnetic nanoparticles as the catalyst. *Microchim. Acta.* **165,** 299–305; 10.1007/s00604-008-0133-z (2009).
4. Kattel, S., Atanassov, P. & Kiefer, B. Catalytic activity of Co-N_x/C electrocatalysts for oxygen reduction reaction: A density functional theory study. *Phys. Chem. Chem. Phys.* **15,** 148–153; 10.1039/C2CP42609A (2013).
5. Wu, G. *et al.* Synthesis–structure–performance correlation for polyaniline–Me–C non-precious metal cathode catalysts for oxygen reduction in fuel cells. *J. Mater. Chem.* **21,** 11392; 10.1039/C0JM03613G (2011).
6. He, L., Weniger, F., Neumann, H. & Beller, M. Synthesis, characterization, and application of metal nanoparticles supported on nitrogen-doped carbon: Catalysis beyond electrochemistry. *Angew. Chem. Int. Ed.* **55,** 12582–12594; 10.1002/anie.201603198 (2016).
7. Chong, L. *et al.* Ultralow-loading platinum-cobalt fuel cell catalysts derived from imidazolate frameworks. *Science* **362,** 1276–1281; 10.1126/science.aau0630 (2018).
8. Zitolo, A. *et al.* Identification of catalytic sites in cobalt-nitrogen-carbon materials for the oxygen reduction reaction. *Nat. Commun.* **8,** 957; 10.1038/s41467-017-01100-7 (2017).
9. Li, J. *et al.* Atomically dispersed manganese catalysts for oxygen reduction in proton-exchange membrane fuel cells. *Nat. Catal.* **1,** 935–945; 10.1038/s41929-018-0164-8 (2018).
10. Weisz, P. B. & Prater, C. D. Interpretation of measurements in experimental catalysis. *Adv. Catal.* **6,** 143–196; 10.1016/S0360-0564(08)60390-9 (1954).
11. Vannice, M. A. *Kinetics of catalytic reactions* (Springer US, Boston, MA, 2005).
12. Ternan, M. The diffusion of liquids in pores. *Can. J. Chem. Eng.* **65,** 244–249; 10.1002/cjce.5450650208 (1987).
13. Chantong, A. & Massoth, F. E. Restrictive diffusion in aluminas. *AIChE J.* **29,** 725–731; 10.1002/aic.690290505 (1983).
14. Wilke, C. R. & Chang, P. Correlation of diffusion coefficients in dilute solutions. *AIChE J.* **1,** 264–270; 10.1002/aic.690010222 (1955).
15. Yaws, C. L. *Chemical properties handbook. Physical, thermodynamic, environmental, transport, safety, and health related properties for organic and inorganic chemicals* (McGraw-Hill, New York, London, 1999).
16. Yaws, C. L. *Thermophysical properties of chemicals and hydrocarbons* (William Andrew, Norwich, N.Y., 2008).
17. Fujita, M. & Hiyama, T. Fluoride ion-catalyzed reduction of aldehydes and ketones with hydrosilanes. Synthetic and mechanistic aspects and an application to the threo-directed reduction of .alpha.-substituted alkanones. *J. Org. Chem.* **53,** 5405–5415; 10.1021/jo00258a003 (1988).
18. Rayment, E. J., Summerhill, N. & Anderson, E. A. Synthesis of phenols via fluoride-free oxidation of

arylsilanes and arylmethoxysilanes. *J. Org. Chem.* **77,** 7052–7060; 10.1021/jo301363h (2012).

19. Ma, Y., Zhang, L., Luo, Y., Nishiura, M. & Hou, Z. $B(C_6F_5)_3$-catalyzed C-Si/Si-H cross-metathesis of hydrosilanes. *J. Am. Chem. Soc.* **139,** 12434–12437; 10.1021/jacs.7b08053 (2017).
20. Seyferth, D. & White, D. L. Acid-catalyzed isomerization of 1,2-bis(trimethylsilyl)benzene and related compounds. *J. Am. Chem. Soc.* **94,** 3132–3138; 10.1021/ja00764a040 (1972).
21. Wang, K. *et al.* Selective manganese-catalyzed oxidation of hydrosilanes to silanols under neutral reaction conditions. *Angew. Chem. Int. Ed.* **58,** 6380–6384; 10.1002/anie.201900342 (2019).
22. B. N. Kang, C. E. Ahn, J. C. Lee, H. B. Joo, S. S. Song, J. Y. Han. *Novel synthesis method of silane compound for packaging optical devices* (2015).
23. Cho, S. H. & Hartwig, J. F. Iridium-catalyzed diborylation of benzylic C–H bonds directed by a hydrosilyl group: Synthesis of 1,1-benzyldiboronate esters. *Chem. Sci.* **5,** 694–698; 10.1039/C3SC52824C (2014).
24. Nagai, Y., Ohtsuki, M., Nakano, T. & Watanabe, H. Correlaiton of Hammett σ constants with NMR parameters for substituted phenylsilanes, phenylmethylsilanes and phenyldimethylsilanes. *J. Organomet. Chem.* **35,** 81–90; 10.1016/S0022-328X(00)86885-0 (1972).
25. Lipowitz, J. Fluorine-19 substituent chemical shifts of fluorophenylsilanes. Substituent effects on silicon. *J. Am. Chem. Soc.* **94,** 1582–1589; 10.1021/ja00760a025 (1972).
26. Ohshita, J. *et al.* Polymeric organosilicon systems. XXIX. Thermal properties of poly[(disilanylene)oligophenylenes]. *J. Organomet. Chem.* **564,** 47–56; 10.1016/S0022-328X(98)00702-5 (1998).
27. Omann, L. & Oestreich, M. A catalytic S_EAr approach to dibenzosiloles functionalized at both benzene cores. *Angew. Chem. Int. Ed.* **54,** 10276–10279; 10.1002/anie.201504066 (2015).
28. Lee, M., Ko, S. & Chang, S. Highly selective and practical hydrolytic oxidation of organosilanes to silanols catalyzed by a ruthenium complex. *J. Am. Chem. Soc.* **122,** 12011–12012; 10.1021/ja003079g (2000).
29. Manson, B. W., Morrison, J. J., Coupar, P. I., Jaffrès, P.-A. & Morris, R. E. Synthesis of aldehyde functionalised polyhedral oligomeric silsesquioxanes. *J. Chem. Soc., Dalton Trans.* **2001,** 1123–1127; 10.1039/B100568P (2001).
30. Kan, S. B. J., Lewis, R. D., Chen, K. & Arnold, F. H. Directed evolution of cytochrome c for carbon-silicon bond formation: Bringing silicon to life. *Science* **354,** 1048–1051; 10.1126/science.aah6219 (2016).
31. Hevesi, L., Dehon, M., Crutzen, R. & Lazarescu-Grigore, A. Kinetic control in the cleavage of unsymmetrical disilanes. *J. Org. Chem.* **62,** 2011–2017; 10.1021/jo961131e (1997).
32. Beemelmanns, C., Husmann, R., Whelligan, D. K., Özçubukçu, S. & Bolm, C. Planar-chiral bis-silanols and diols as H-bonding asymmetric organocatalysts. *Eur. J. Org. Chem.* **2012,** 3373–3376; 10.1002/ejoc.201200548 (2012).
33. Chen, C.-H. *et al.* Controlling conformations in alternating dialkylsilylene-spaced donor-acceptor copolymers by a cooperative Thorpe-Ingold effect and polymer folding. *Chem. Eur. J.* **18,** 334–346; 10.1002/chem.201102032 (2012).
34. Naka, A. *et al.* Preparation of branched molecules by regioselective hydrosilation of tetrakis(ethynyldimethylsilyl)silanes and some of their properties. *J. Organomet. Chem.* **846,** 360–366; 10.1016/j.jorganchem.2017.07.015 (2017).
35. Moitra, N. *et al.* Surface functionalization of silica by Si-H activation of hydrosilanes. *J. Am. Chem. Soc.* **136,** 11570–11573; 10.1021/ja504115d (2014).

36. Itami, K., Mitsudo, K., Nishino, A. & Yoshida, J. Metal-catalyzed hydrosilylation of alkenes and alkynes using dimethyl(pyridyl)silane. *J. Org. Chem.* **67,** 2645–2652; 10.1021/jo0163389 (2002).
37. Sumida, Y., Harada, R., Sumida, T., Hashizume, D. & Hosoya, T. Hydrosilyl group-directed iridium-catalyzed peri-selective C–H borylation of ring-fused (hetero)arenes. *Chem. Lett.* **47,** 1251–1254; 10.1246/cl.180594 (2018).
38. Wiltse, H. R., Johnson, A. N., Durand, R. J., Brennessel, W. & Chin, R. M. Syntheses, characterization, and reactivity of diruthenium hydrido complexes. *Organometallics* **35,** 1079–1085; 10.1021/acs.organomet.6b00067 (2016).
39. Nielsen, L. & Skrydstrup, T. Sequential C-Si bond formations from diphenylsilane: Application to silanediol peptide isostere precursors. *J. Am. Chem. Soc.* **130,** 13145–13151; 10.1021/ja804720p (2008).
40. N. Kazuki, M. Nirmalya, K. Kazuyoshi, H. Toyoshi. *Method for producing surface-modified base material, method for producing joined body, new hydrosilane compound, surface treatment agent, surface treatment agent kit, and surface-modified base material* (2017).
41. Nakamura, M., Matsumoto, Y., Toyama, M., Baba, M. & Hashimoto, Y. Organosilicon compounds as adult T-cell leukemia cell proliferation inhibitors. *Chem. Pharm. Bull.* **61,** 237–241; 10.1248/cpb.c12-00839 (2013).
42. Rakita, P. E. & Worsham, L. S. ^{13}C NMR studies of organosilanes: IV. vinyl- and allyl-silanes. *J. Organomet. Chem.* **139,** 135–142; 10.1016/S0022-328X(00)85465-0 (1977).
43. Kim, Y. & Chang, S. Borane-catalyzed reductive α-silylation of conjugated esters and amides leaving carbonyl groups intact. *Angew. Chem. Int. Ed.* **55,** 218–222; 10.1002/anie.201508669 (2016).
44. Takale, B. S. *et al.* Exclusive chemoselective reduction of imines in the coexistence of aldehydes using AuNPore catalyst. *Org. Lett.* **16,** 2558–2561; 10.1021/ol500958p (2014).
45. Denmark, S. E. & Kallemeyn, J. M. Palladium-catalyzed silylation of aryl bromides leading to functionalized aryldimethylsilanols. *Org. Lett.* **5,** 3483–3486; 10.1021/ol035288m (2003).
46. Yoshida, H., Yamaryo, Y., Ohshita, J. & Kunai, A. Activator-free oxidative homocoupling of organosilanes catalysed by a palladium–DPPP complex. *Chem. Commun.* **2003,** 1510–1511; 10.1039/B303852A (2003).
47. Rayment, E. J., Mekareeya, A., Summerhill, N. & Anderson, E. A. Mechanistic study of arylsilane oxidation through ^{19}F NMR spectroscopy. *J. Am. Chem. Soc.* **139,** 6138–6145; 10.1021/jacs.7b00357 (2017).
48. Everson, D. A., Jones, B. A. & Weix, D. J. Replacing conventional carbon nucleophiles with electrophiles: Nickel-catalyzed reductive alkylation of aryl bromides and chlorides. *J. Am. Chem. Soc.* **134,** 6146–6159; 10.1021/ja301769r (2012).
49. Takeda, D., Oyama, R. & Yamada, S. A novel method for preparing silanols from silylmethanols. *Chem. Lett.* **38,** 532–533; 10.1246/cl.2009.532 (2009).
50. Denmark, S. E., Smith, R. C., Chang, W.-T. T. & Muhuhi, J. M. Cross-coupling reactions of aromatic and heteroaromatic silanolates with aromatic and heteroaromatic halides. *J. Am. Chem. Soc.* **131,** 3104–3118; 10.1021/ja8091449 (2009).
51. Koo, J., Kim, S. H. & Hong, S. H. Hydrogenation of silyl formates: Sustainable production of silanol and methanol from hydrosilane and carbon dioxide. *Chem. Commun.* **54,** 4995–4998; 10.1039/C8CC02276C (2018).
52. Igarashi, M., Matsumoto, T., Sato, K., Ando, W. & Shimada, S. Nonhydrolytic synthesis of silanols by the hydrogenolysis of benzyloxysilanes. *Chem. Lett.* **43,** 429–431; 10.1246/cl.131079 (2014).

53. Lyčka, A., Šnobl, D., Handlíř, K., Holeček, J. & Nádvorník, M. ^{29}Si and ^{13}C NMR spectra of some alkyldiphenylchlorosilanes, alkyldiphenylsilanoles and bis(alkyldiphenylsilyl)chromates. *Collect. Czech. Chem. Commun.* **47,** 603–612; 10.1135/cccc19820603 (1982).
54. Goncharova, I. K. *et al.* Aerobic Co-/N-hydroxysuccinimide-catalyzed oxidation of *p*-tolylsiloxanes to *p*-carboxyphenylsiloxanes: Synthesis of functionalized siloxanes as promising building blocks for siloxane-based materials. *J. Am. Chem. Soc.* **141,** 2143–2151; 10.1021/jacs.8b12600 (2019).
55. Korkin, S. *et al.* Phenylsilanetriol—synthesis, stability, and reactivity. *J. Organomet. Chem.* **686,** 313–320; 10.1016/S0022-328X(03)00721-6 (2003).
56. Missaghi, M. N., Galloway, J. M. & Kung, H. H. Bis(pyridyl)siloxane–Pd(II) complex catalyzed oxidation of alcohol to aldehyde: Effect of ligand tethering on catalytic activity and deactivation behavior. *Appl. Catal. A-Gen.* **391,** 297–304; 10.1016/j.apcata.2010.09.008 (2011).
57. Ito, M., Itazaki, M. & Nakazawa, H. Selective boryl silyl ether formation in the photoreaction of bisboryloxide/boroxine with hydrosilane catalyzed by a transition-metal carbonyl complex. *J. Am. Chem. Soc.* **136,** 6183–6186; 10.1021/ja500465x (2014).
58. Yoshimura, A. *et al.* A convenient and clean synthetic method for borasiloxanes by Pd-catalysed reaction of silanols with diborons. *Chem. Commun.* **53,** 5822–5825; 10.1039/C7CC02420G (2017).
59. Blandez, J. F., Primo, A., Asiri, A. M., Álvaro, M. & García, H. Copper nanoparticles supported on doped graphenes as catalyst for the dehydrogenative coupling of silanes and alcohols. *Angew. Chem. Int. Ed.* **53,** 12581–12586; 10.1002/anie.201405669 (2014).
60. Yuan, Y., Kumar, P. & Guo, S. Metal-Free ammonium iodide catalyzed oxidative dehydrocoupling of silanes with alcohols. *Synlett* **28,** 1620–1623; 10.1055/s-0036-1588816 (2017).
61. Mitsudome, T. *et al.* Highly efficient etherification of silanes by using a gold nanoparticle catalyst: Remarkable effect of O_2. *Chem. Eur. J.* **19,** 14398–14402; 10.1002/chem.201302807 (2013).
62. Toutov, A. A., Betz, K. N., Haibach, M. C., Romine, A. M. & Grubbs, R. H. Sodium hydroxide catalyzed dehydrocoupling of alcohols with hydrosilanes. *Org. Lett.* **18,** 5776–5779; 10.1021/acs.orglett.6b01687 (2016).
63. Dhiman, M., Chalke, B. & Polshettiwar, V. Organosilane oxidation with a half million turnover number using fibrous nanosilica supported ultrasmall nanoparticles and pseudo-single atoms of gold. *J. Mater. Chem. A* **5,** 1935–1940; 10.1039/C6TA09434A (2017).
64. Brown, C. A., Abrahamse, M. & Ison, E. A. Re-silane complexes as frustrated lewis pairs for catalytic hydrosilylation. *Dalton. Trans.* **49,** 11403–11411; 10.1039/D0DT02084B (2020).
65. Lorenz, C. & Schubert, U. An efficient catalyst for the conversion of hydrosilanes to alkoxysilanes. *Chem. Ber.* **128,** 1267–1269; 10.1002/cber.19951281220 (1995).
66. Gao, D. & Cui, C. N-heterocyclic carbene organocatalysts for dehydrogenative coupling of silanes and hydroxyl compounds. *Chem. Eur. J.* **19,** 11143–11147; 10.1002/chem.201301893 (2013).
67. Ojima, Y., Yamaguchi, K. & Mizuno, N. An efficient solvent-free route to silyl esters and silyl ethers. *Adv. Synth. Catal.* **351,** 1405–1411; 10.1002/adsc.200900230 (2009).
68. Wang, B. *et al.* Active cobalt catalyst for the cleavage of benzyl ether. *J. Org. Chem.* **76,** 9531–9535; 10.1021/jo2018284 (2011).
69. Ageshina, A. A. *et al.* Mixed er-NHC/phosphine Pd(II) complexes and their catalytic activity in the Buchwald-Hartwig reaction under solvent-free conditions. *Dalton. Trans.* **48,** 3447–3452; 10.1039/C9DT00216B (2019).
70. Xu, M. *et al.* Synthesis of urea derivatives from CO_2 and silylamines. *Angew. Chem. Int. Ed.* **58,** 5707–5711; 10.1002/anie.201900058 (2019).

71. Ferlin, F., Luque Navarro, P. M., Gu, Y., Lanari, D. & Vaccaro, L. Waste minimized synthesis of pharmaceutically active compounds via heterogeneous manganese catalysed C–H oxidation in flow. *Green Chem.* **22,** 397–403; 10.1039/C9GC02961C (2020).